haematologica

Journal of The Ferrata Storti Foundation

www.haematologica.org

ESH
EUROPEAN SCHOOL OF HAEMATOLOGY

**Connecting haematologists worldwide
through mentorship and lifelong learning**

UPCOMING ESH CONFERENCES

ESH plenary conference programmes are designed to place emphasis on leading-edge basic and clinical research and future perspectives. Ample time is deliberately provided for in-depth scientific discussion and interaction. Registered participants further benefit from a variety of opportunities for informal scientific interaction with the world's leading experts in their field, including during small Meet the Expert sessions and Mentored Posters Walks. ESH conference delegates are invited to submit abstracts. Selected abstracts are presented as brief oral communications or posters.

2020

HOW TO DIAGNOSE AND TREAT CONFERENCES
→ *emphasize clinical management, including future perspectives,
and use case-based lectures to stimulate interaction.*

MARCH 13-15, 2020 – Budapest, Hungary
2nd How to Diagnose and Treat **ACUTE LEUKAEMIA**
CHAIRS: H. Dombret, A. Ganser, J. Sierra, W. Stock
#ESHAL2020

NOVEMBER 6-8, 2020 – Paris, France
How to Diagnose and Treat **LYMPHOMA**
CHAIRS: C. Buske, C. Thieblemont, A. Younes
#ESHLYMPHOMA2020

TRANSLATIONAL RESEARCH CONFERENCES
→ *focus on leading-edge basic, clinical and therapeutic research and future perspectives.
The presentation of unpublished data is encouraged.*

MARCH 20-22, 2020 – Paris, France
1st Translational Research Conference **CHRONIC LYMPHOCYTIC LEUKAEMIA**
CHAIRS: J. Brown, P. Ghia, M. Hallek
#ESHCLL2020

APRIL 23-25, 2020 – Mandelieu-La Napoule, France
7th Translational Research Conference **MYELODYSPLASTIC SYNDROMES**
CHAIRS: P. Fenaux, U. Platzbecker, M. Sekeres
#ESHMDS2020

MAY 15-17, 2020 – Budapest, Hungary
9th Translational Research Conference **MYELOPROLIFERATIVE NEOPLASMS**
CHAIRS: J.J. Kiladjian, R. Levine, A. Vannucchi
#ESHMPN2020

OCTOBER 2-4, 2020 – Mandelieu-La Napoule, France
22nd Annual John Goldman Conference on
CHRONIC MYELOID LEUKEMIA: BIOLOGY AND THERAPY
CHAIRS: J. Cortes, T.P. Hughes, D.S. Krause
#ESHCML2020

OCTOBER 9-11, 2020 – Mandelieu-La Napoule, France
5th Translational Research Conference **MULTIPLE MYELOMA**
CHAIRS: K.C. Anderson, M.V. Mateos, P. Moreau
#ESHMM2020

NOVEMBER 13-15, 2020 – Paris, France
Translational Research Conference **BONE MARROW FAILURE DISORDERS**
CHAIRS: T. Brümmendorf, I. Dokal, C. Dufour, M.H.G.P. Raaijmakers,
R. Peffault de Latour, N. Young
#ESHBMFD2020

FOLLOW US, JOIN THE CONVERSATION AND CONNECT WITH YOUR PEERS:
twitter.com/ESHaematology
linkedin.com/company/european-school-of-haematology-esh/
youtube.com/channel/UCJ1_VblIFBXeSnPgvqPrCfQ
facebook.com/europeanschoolofhaematology
https://elearning.esh.org

haematologica
Journal of the Ferrata Storti Foundation

Table of Contents
Volume 105, Issue 3: March 2020

Errata Corrige

Letters to the Editor

Letters are available online only at www.haematologica.org/content/105/3.toc

Case Reports

Case Reports are available online only at www.haematologica.org/content/105/3.toc

100-YEAR OLD HAEMATOLOGICA IMAGES: DI GUGLIELMO DISEASE OR PURE ERYTHROID LEUKEMIA

Carlo L. Balduini

Ferrata-Storti Foundation, Pavia, Italy

E-mail: CARLO L. BALDUINI, - carlo.balduini@unipv.it

In 1917, Giovanni Di Guglielmo, at that time a young collaborator of Adolfo Ferrata at the University of Naples, Italy, described in *Folia Medica* a patient with an hematological disorder characterized by an increased number of granulocytes, erythrocytes and platelets and the presence of precursors of all these elements in circulation.[1] He classified this patient as affected by *eritroleucopiastrinemia* (erythro-leuko-thrombocythemia), a form that we would nowadays include in the context of myeloproliferative diseases. Until the description of this patient only leukemias characterized by proliferation of myeloid or lymphoid series were known, but the observation of this patient gave Di Guglielmo the idea that primitive bone marrow elements can abnormally proliferate not only along the myeloid line, but also along the erythropoietic and thrombopoietic lines. In particular, he hyphothesized that generalized erythroblastic proliferation throughout all organs of the body could be expected. Ten years later, he described in Haematologica two cases of what he had claimed would ultimately be found: *acute erythremic myelosis*.[2]

The image on the cover of this issue of Haematologica is one of the fine, hand-drawn color plates illustrating this article published in 1928 (Figure 1). Immature and atypical erythroid precursors were the dominant elements in peripheral blood and bone marrow of these severely anemic, neutropenic and thrombocytopenic patients. Abnormal erythroblasts were found also in the liver and spleen. The course of the disease was hyperacute and both patients died within a few weeks.

Old concepts are cast in cement and the idea of a leukemia of the erythroid line was new and unorthodox at that time and, therefore, Di Guglielmo was unable to convince anyone for a long time, his mentor Ferrata included,[3] that the proliferation of erythroblasts can not only have a reactive origin, but that it can also represent a genuine leukemia in rare cases. However, other similar cases were reported by Di Guglielmo himself and by other authors in subsequent decades and, eventually, most people accepted the idea that leukemia of the erythroid series really exists. In 1940, Dameshek proposed for this disorder the name of *Di Guglielmo disease*.[4] Then, the French-American-British (FAB) cooperative group, in their first proposal in 1976, included it within the Acute Myeloid Leukemia classification system as *erythroleukemia*, M6.[5] The 2016 revision to the World Health Organization classification of myeloid neoplasms and acute leukemia gave this disorder the name of *pure erythroid leukemia*,[6] a denomination that would have had full approval by Di Guglielmo.

In conclusion, the first patients with pure erythroid leukemia were described by Di Guglielmo in Haematologica in 1928.[7,8]
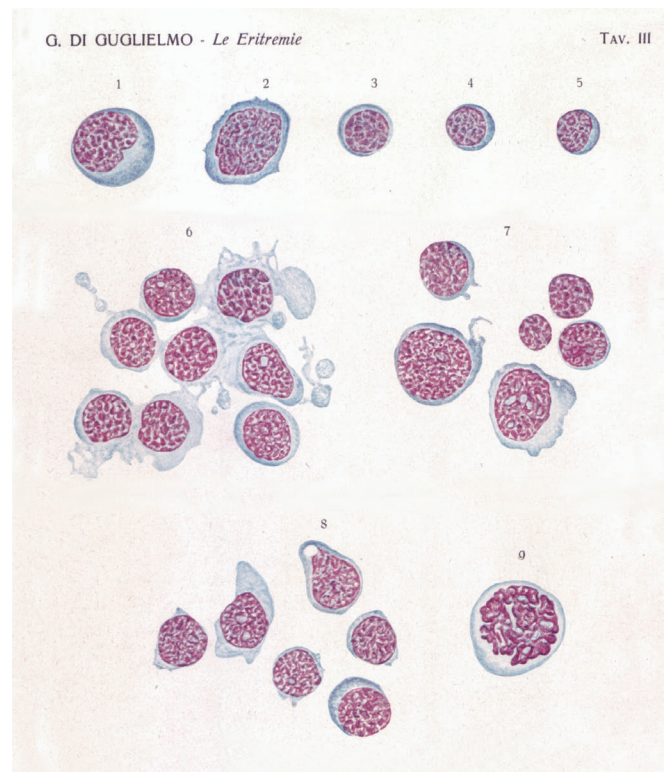
Figure 1. One of the figures of the Haematologica article describing for the first time *acute erythremic myelosis*, presently known as *pure erythroid leukemia*. According to the author's caption: "Images 1-5, erythroblastic elements in peripheral blood; Images 6- 8, groups of erythroblasts in the spleen (smear preparations) and Image 9, erythroblastic karyokinesis (spleen smear preparation)".

References

1. Di Guglielmo G. [Un caso di eritroleucemia]. Folia Med. 1917;13:386.
2. Di Guglielmo G. [Le eritremie]. Haematologica. 1928;9:301-347.
3. Wintrobe MM. The role of Giovanni Di Guglielmo in the history of hematology, in: Commemorazione di Giovanni di Guglielmo nel centenario della nascita. (E. Ascari, C.L. Balduini, M. Cazzola, M. Gobbi, A. Riccardi, G. Ucci EDS) Edizioni Medico Scientifiche Pavesi, Pavia (1986), pp 8-17.
4. Dameshek W. The Di Gugliemo syndrome. Blood. 1940;13:192
5. Bennett JM, Catovsky D, Daniel MT, et al. Proposals for the classification of the acute leukaemias. French-American-British (FAB) co-operative group. Br J Haematol. 1976;33(4):451-458.
6. Arber DA, Orazi A, Hasserjian R, et al. The 2016 revision to the World Health Organization classification of myeloid neoplasms and acute leukemia. Blood. 2016;127(20):2391-2405.
7. Boddu P, Benton CB, Wang W, Borthakur G, Khoury JD, Pemmaraju N. Erythroleukemia-historical perspectives and recent advances in diagnosis and management. Blood Rev. 2018;32(2):96-105.
8. Mazzarello P. One hundred years of Haematologica. Haematologica. 2020;105(1):12-21.

Genetic fingerprint defines hematopoietic stem cell pool size and function

Tatsuya Morishima[1,2] and Hitoshi Takizawa[1,3]

[1]Laboratory of Stem Cell Stress, International Research Center for Medical Sciences, Kumamoto University; [2]Laboratory of Hematopoietic Stem Cell Engineering, International Research Center for Medical Sciences, Kumamoto University and [3]Center for Metabolic Regulation of Healthy Aging, Kumamoto University, Kumamoto, Japan

E-mail: HITOSHI TAKIZAWA - htakizawa@kumamoto-u.ac.jp   or   TATSUYA MORISHIMA - tatsuyam@kumamoto-u.ac.jp

Hematopoietic stem cells (HSC) are at the apex of the hematopoietic tree, with self-renewal and multilineage differentiation potential. On the one hand, HSC can replenish the mature blood cells by differentiating into lineage-committed progenitor cells in response to the shortage of blood cells under both homeostatic and stressed conditions, such as bleeding and infection. On the other hand, HSC replicate themselves to maintain their number. This differentiation and self-renewal needs to be strictly regulated by gene expression regulation in order to maintain life-long hematopoiesis.[1] Gene expression is in general regulated by "cis- and trans-regulatory elements".[2] Trans-regulatory elements are defined as factors which regulate expression of distal genes (e.g. transcription factors), while cis-regulatory elements are defined as non-coding DNA sequences which regulate expression of proximal genes (e.g. promoter and enhancer regions). These cis-regulatory elements play important roles in evolution in which polymorphisms occur in cis-regulatory elements and contribute to phenotypic diversity of organisms within well-conserved genes.[3] Epigenetics plays important roles in HSC regulation, as epigenetic dysregulation in HSC is a key driver for HSC aging and hematopoietic malignancies.[4] Epigenetic regulation is also controlled by cis- and trans-regulatory elements. For example, histone modifications function as trans-regulatory elements, whereas DNA methylations function as cis-regulatory elements.

Phenotypic diversity is frequently caused by genetic variations such as single nucleotide polymorphism (SNP). It was reported that the size and function of the HSC pool vary between mice strains,[5-9] which suggests genetic background, such as SNP and copy number variations, define HSC homeostasis. In 2007, Liang *et al*. identified *latexin* (*Lxn*) as an HSC regulatory gene whose expression level is inversely correlated with HSC number.[10] Although a variation in *Lxn* gene expression and HSC number in different tested mouse strains was shown, the mechanism underlying regulation of *Lxn* gene expression and its variation between mice strains remained unknown.

In this issue of Haematologica, the same group who published the above-mentioned paper,[10] Zhang *et al*. identified the promoter region of the *Lxn* gene that controls the level of *Lxn* gene expression *via* both HMGB2, a chromatin protein, and genetic variations in the promoter region.[11] To study the transcriptional regulation of *Lxn*, the authors characterized the upstream region of the *Lxn* gene. Based on the natural variation of *Lxn* expression, they searched SNP with CpG island and identified a region with strong promoter activity in the upstream. Subsequently, DNA pulldown in combination with mass spectrometry analysis were performed to identify pro-

teins bound to this region, and HMGB2 was found to bind to the promoter region and to suppress *Lxn* gene promoter activity. To further confirm the regulatory role of HMGB2 in *Lxn* gene expression, Zhang *et al*. performed a gene knockdown experiment with EML cells, which share some of the characteristics of HSC.[12] This showed that HMGB2 knockdown suppresses EML cell growth and that additional *Lxn* gene knockdown could rescue this growth, suggesting that *Lxn* was one of the transcriptional targets of HMGB2. Consistent with the previous reports concerning the phenotype of cells over-expressing Lxn,[13,14] the HMGB2 knockdown cells showed enhanced apoptosis and cell cycle arrest, which could in part be rescued by *Lxn* gene knockdown. These data suggest HMGB2 positively regulates HSC survival and proliferation by suppressing expression of *Lxn* and *Lxn*-regulated apoptosis. Similar data were also shown in Lin$^-$Sca-1$^+$c-Kit$^+$ (LSK) cells primarily isolated from mouse bone marrow that contain HSC. HMGB2 knockdown in LSK cells showed suppressed proliferation, enhanced apoptosis and cell cycle arrest *in vitro*. In transplantation experiments, HMGB2 knockdown in LSK cells showed decreased reconstitution of whole peripheral blood cells and bone marrow LSK cells and long-term HSC in transplant recipients, indicating that HMGB2 plays an important role in HSC function *in vivo.*

The previous finding that *Lxn* expression level is correlated with HSC numbers[10] led the authors to hypothesize that the SNP in the promoter region of the *Lxn* gene may contribute to a variation in *Lxn* expression and HSC number. To test this, the authors introduced G to C mutation in the HMGB2 binding sequence in the *Lxn* gene promoter region and found that the G allele showed higher promoter activity for *Lxn* expression compared to the C allele. Furthermore, when *Lxn* gene expression and bone marrow HSC number were analyzed in different mouse strains carrying the G or C allele in this SNP region, the mice strain carrying the C allele showed relatively lower Lxn protein expression and higher HSC number compared to those carrying the G allele. These data suggest that a genetic variant in the *Lxn* gene promoter region defines the variation in *Lxn* gene expression level and HSC number.

Together, Zhang *et al*. revealed that the transcription of *Lxn* regulating HSC function, at least as far as apoptosis is concerned, was controlled by both trans-regulatory element, HMGB2, and cis-regulatory element, as genetic variation was observed in the *Lxn* gene promoter region (Figure 1). HMGB2 is known as a chromatin-associated protein which remodels chromatin structure and gene expression.[15] Although the molecular mechanism by which HMGB2 regulates *Lxn* gene transcription remains unclear, all the data provided in this study suggest *Lxn*
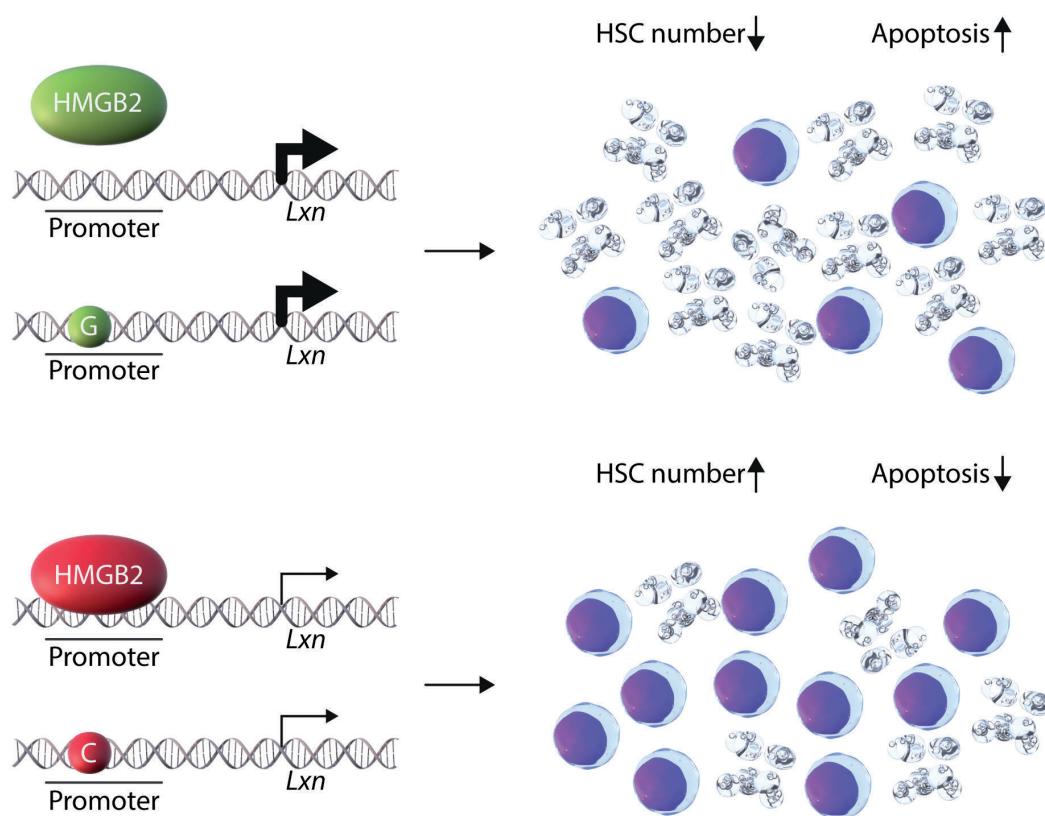
Figure 1. Cis- and trans-regulation of *Lxn* gene transcription modulates hematopoietic stem cell function. In trans-regulatory mechanisms of hematopoietic stem cell (HSC) function and number, HMGB2 protein binding to the *Lxn* gene promoter region positively regulates HSC by suppressing *Lxn* gene transcription and blocks apoptosis. In the cis-regulatory mechanism of HSC, the G allele in the SNP found in *Lxn* gene promoter region is associated with higher *Lxn* gene transcription and lower HSC number, whereas the C allele is associated with suppressed *Lxn* gene transcription and higher HSC number.

gene transcription may be regulated through epigenetic modification. HMGB2 is also known to regulate senescence-associated gene expression by orchestrating the chromatin landscape of the gene loci.[16] As the authors discussed, it would be interesting to study the role of *Lxn* gene regulation by HMGB2 in the context of HSC senescence and aging. The SNP identified in this study was in the CG-rich region. Although direct evidence was not shown, these data imply a functional role of the genetic variation, such as SNP, in *Lxn* gene regulation *via* DNA methylation. Taken together, this report suggests epigenetic regulation of HSC via *Lxn* gene transcriptional regulation. The molecular mechanism of how epigenetic regulation by HMGB2 protein and genetic variation in the *Lxn* gene promoter region work together needs to be better understood.

This report is the first demonstration that genetic variation, especially SNP, is a determinant for the variations among different mouse strains in HSC pool size and function. The authors also discussed a similar observation made in humans,[11] opening the possibility that the genetic variation in the *Lxn* gene promoter region may contribute to the pathogenesis of hematopoietic aplasia/neoplasia, such as bone marrow failure or leukemia. If epigenetic regulation of *Lxn* gene transcription is involved in these hematopoietic diseases, it could be a new therapeutic target for genetic correction/modification such as genome

editing. Since other genes that regulate HSC function, besides the *Lxn* gene, could undergo genetic variation through cis-regulatory elements, it would be interesting to characterize SNP in the regulatory region of HSC regulatory genes. This would help to develop therapeutic strategies for personalized medicine.

References

1. Orkin SH, Zon LI. Hematopoiesis: an evolving paradigm for stem cell biology. Cell. 2008;132(4):631-644.
2. Gilad Y, Rifkin SA, Pritchard JK. Revealing the architecture of gene regulation: the promise of eQTL studies. Trends Genet. 2008;24(8): 408-415.
3. Wittkopp PJ, Kalay G. Cis-regulatory elements: molecular mechanisms and evolutionary processes underlying divergence. Nat Rev Genet. 2011;13(1):59-69.
4. Beerman I, Rossi DJ. Epigenetic Control of Stem Cell Potential during Homeostasis, Aging, and Disease. Cell Stem Cell. 2015;16(6): 613-625.
5. Henckaerts E, Langer JC, Snoeck HW. Quantitative genetic variation

in the hematopoietic stem cell and progenitor cell compartment and in lifespan are closely linked at multiple loci in BXD recombinant inbred mice. Blood. 2004;104(2):374-379.

6. de Haan G, Nijhof W, Van Zant G. Mouse strain-dependent changes in frequency and proliferation of hematopoietic stem cells during aging: correlation between lifespan and cycling activity. Blood. 1997;89(5):1543-1550.

7. Geiger H, True JM, de Haan G, Van Zant G. Age- and stage-specific regulation patterns in the hematopoietic stem cell hierarchy. Blood. 2001;98(10):2966-2972.

8. de Haan G, Bystrykh LV, Weersing E, et al. A genetic and genomic analysis identifies a cluster of genes associated with hematopoietic cell turnover. Blood. 2002;100(6):2056-2062.

9. Cahan P, Li Y, Izumi M, Graubert TA. The impact of copy number variation on local gene expression in mouse hematopoietic stem and progenitor cells. Nat Genet. 2009;41(4):430-437.

10. Liang Y, Jansen M, Aronow B, Geiger H, Van Zant G. The quantitative trait gene latexin influences the size of the hematopoietic stem

11. Zhang C, Fondufe-Mittendorf YN, Wang C, et al. Latexin regulation by HMGB2 is required for hematopoietic stem cell maintenance. Haematologica. 2020;105(3):573-584.

12. Ye ZJ, Kluger Y, Lian Z, Weissman SM. Two types of precursor cells in a multipotential hematopoietic cell line. Proc Natl Acad Sci U S A. 2005;102(51):18461-18466.

13. You Y, Wen R, Pathak R, et al. Latexin sensitizes leukemogenic cells to gamma-irradiation-induced cell-cycle arrest and cell death through Rps3 pathway. Cell Death Dis. 2014;5:e1493.

14. Liu Y, Howard D, Rector K, et al. Latexin is down-regulated in hematopoietic malignancies and restoration of expression inhibits lymphoma growth. PLoS One. 2012;7(9):e44979.

15. Agresti A, Bianchi ME. HMGB proteins and gene expression. Curr Opin Genet Dev. 2003;13(2):170-178.

16. Aird KM, Iwasaki O, Kossenkov AV, et al. HMGB2 orchestrates the chromatin landscape of senescence-associated secretory phenotype gene loci. J Cell Biol. 2016;215(3):325-34.

cell population in mice. Nat Genet. 2007;39(2):178-188.

Staying hydrated is important also for erythroblasts

Anupama Narla[1] and Narla Mohandas[2]

[1]Department of Pediatrics, Stanford University, School of Medicine, Stanford, CA and [2]Laboratory of Red Cell Physiology, New York Blood Center, New York, NY, USA

E-mail: ANUPAMA NARLA - anunarla@stanford.edu or NARLA MOHANDAS - mnarla@nybc.org

In this edition of *Haematologica*, Caulier and colleagues provide new insights into the role of PIEZO1, a mechanosensitive ion channel, in regulating normal human erythropoiesis.[1] Defects in PIEZO1 have also been shown to lead to disordered erythropoiesis in hereditary xerocytosis, an inherited red cell disorder leading to red cell dehydration.[2,3] Using *in vitro* cellular models of human erythropoiesis, the authors documented that the chemical activation of PIEZO1 either in an erythroid cell line model or in normal human hematopoietic stem cells (HSC) repressed erythroid differentiation. Importantly, they further documented that there was delayed erythroid differentiation in HSC from patients with PIEZO1 mutations. These findings provide unexpected and novel insights into the role of ion channels in the regulation of human erythropoiesis.[1]

Anemia is a significant health problem that affects nearly two billion people around the world. The major causes of anemia are: (i) an increased rate of destruction of circulating red cells in disorders that include red cell membrane disorders, sickle cell disease, immune hemolytic anemia, nutritional anemias and malaria; (ii) acute blood loss or splenic sequestration; and (iii) decreased production of red cells in the bone marrow due to ineffective erythropoiesis,which includes thalassemias, inherited bone marrow failure syndromes, infiltrative processes such as myelodysplastic syndrome and acute myeloid leukemia and suppression of erythropoiesis due to infection and medications. While significant progress has been made over the years to improve our understanding of the contribution of increased red cell destruction to anemia, much less is known about the extent of the effect of ineffective erythropoiesis and its contribution to anemia in the various red cell disorders. This is particularly true in the case of inherited red blood cell membrane disorders. The lack

of progress has been due in part to a lack of an adequate and easily implementable methodology to study the complex process of human erythroid differentiation.

The generation of enucleated circulating human red cells is a complex biological process that begins in the bone marrow with the commitment of pluripotent HSC to the erythroid lineage (Figure 1). Subsequent stages of maturation include erythroid progenitors, burst-forming unit–erythroid and colony-forming unit–erythroid (CFU-E), which can be identified by their development into representative clonal colonies of red cells *in vitro*. The CFU-E then undergoes terminal differentiation, progressing through four to five morphological stages, each having characteristic light microscopic and ultrastructural features. During terminal erythroid differentiation there is an increasing amount of hemoglobin synthesis accompanied by nuclear chromatin condensation and in the final stage of differentiation there is nuclear extrusion to generate an anucleate reticulocyte which over 2 to 3 days matures, first in the marrow and then in the circulation, into the discoid erythrocyte.

Significant progress has been made during the last decade in developing culture systems to study the differentiation of human CD34 cells intto enucleate reticulocytes and using various cell surface markers to monitor the progression through all stages of erythroid differentiation.[4-7] These developments are enabling detailed characterization of normal and disordered human erythropoiesis.[8-13] Importantly, as a result of this progress it is now possible to obtain insights into at what stage of the complex process of erythroid differentiation various genes contribute to ineffective erythropoiesis.

Using these *in vitro* cellular models of human erythropoiesis, the study by Caulier and colleagues documented that the chemical activation of PIEZO1 either in an ery-
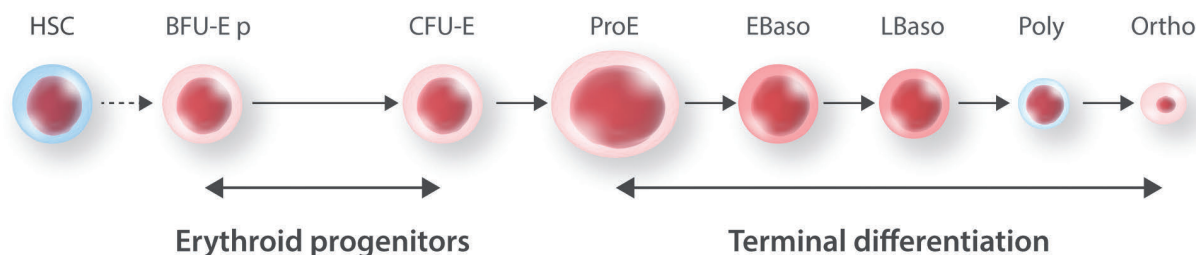
Figure 1. Schematic representation of the various developmental stages of hematopoietic stem cells during erythroid differentiation. The multipotent hematopoietic stem cell first commits to the erythroid lineage to generate erythroid progenitors, which are recognized by their ability to form erythroid colonies in a semisolid methylcellulose culture system in response to interleukin-3, stem cell factor and erythropoietin. They cannot be distinguished based on their morphology. It is estimated that hematopoietic stem cells undergo approximately eight to ten cell divisions prior to the generation of the first morphologically recognizable erythroid cell in the bone marrow, the proerythroblast. During terminal erythroid differentiation, the proerythroblast undergoes five mitoses to generate an orthochromatic erythroblast. This ordered progression during normal erythropoiesis may be disturbed at any of the different developmental stages in various pathological states, leading to ineffective erythropoiesis. HSC: hematopoietic stem cell; BFU-E: burst-forming unit–erythroid; CFU-E: colony-forming unit–erythroid; ProE: proerythroblast; EBaso: early basophilic erythroblast; LBaso: late basophilic erythroblast; Poly: polychromatic erythroblast; Ortho: orthochromatic erythroblast.

throid cell line model or in primary normal HSC repressed erythroid differentiation. Importantly, the authors also showed that there was delayed erythroid differentiation of HSC from patients carrying PIEZO1 mutations. Delayed erythroid differentiation due to PIEZO1 activation was shown to be dependent on calcium entry and transcriptional control through the phosphorylation of transcription factors NFAT, STAT5 and ERK1/2.

These findings provide unexpected and novel insights into the role of ion channels in regulating human erythropoiesis. Although the reported findings represent an important step in our understanding of the role of PIEZO1 in regulating human erythropoiesis and ineffective erythropoiesis in hereditary xerocytosis, a number of questions remain unanswered. The variability in the delayed erythoid differentiation among different patients has not been defined. Furthermore, while ineffective erythropoiesis has been documented to be a feature of terminally differentiating erythroblasts, it is less clear at what specific stage of terminal erythroid differentiation apoptosis dominates. There is also no information about whether ineffective erythropoiesis is a feature of erythroid progenitors. It is anticipated that these important issues will be pursued in future studies.

In spite of some of these unanswered questions, the studies by Caulier and colleagues are significant in that they provide new and previously unsuspected insights into the role of ion channels in regulating human erythropoiesis. These valuable insights expand our current understanding of the role not only of growth factors and cytokines but also of ion channels in human erythroid differentiation. It is likely that the experimental strategies used in the study will be useful in furthering our understanding of the regulation of human erythropoiesis

in general and the contribution of ineffective erythropoiesis to anemia in various human red cell disorders.

References

1. Caulier A, Jankovsky N, Demont Y, et al. PIEZO1 activation delays erythroid differentiation of normal and hereditary xerocytosis-derived human progenitor cells. Haematologica. 2020;105(3):610-622.
2. Zarychanski R, Schulz VP, Houston BL, et al. Mutations in the mechanotransduction protein PIEZO1 are associated with hereditary xerocytosis. Blood. 2017;120(9):1908-1915.
3. Picard V, Guitton C, Thuret I, et al. Clinical and biological features in PIEZO1-hereditary xerocytosis and Gardos-channelopathy: a retrospective series of 126 patients. Haematologica. 2019;104(8):1554-1564.
4. Anstee DJ, Gampel A, Toye AM. Ex-vivo generation of human red cells for transfusion. Curr Opin Hematol. 2012;19(3):163-169.
5. Hu J, Liu J, Xue F, et al. Isolation and functional characterization of human erythroblasts at distinct stages: implications for understanding of normal and disordered erythropoiesis in vivo. Blood. 2013;121(16):3246-3253.
6. Li J, Hale J, Bhagia P, et al. Isolation and transcriptome analysis of human erythroid progenitors. Blood. 2014;124(24):3636-3645.
7. Yan H, Hale J, Jaffray J, et al. Developmental differences between neonatal and adult human erythropoiesis. Am J Hematol. 2018;93(4):494-503.
8. Liang L, Peng Y, Zhang J, et al. Deubiquitylase USP7 regulates human terminal erythroid differentiation by stabilizing GATA1. Haematologica. 2019;104(11):2178-2188.
9. Yan H, Wang Y, Qu X, et al. Distinct roles for TET family proteins in regulating human erythropoiesis. Blood. 2017;129(14): 2002-2012.
10. Rio S, Gastou M, Karboul N, et al. Regulation of globin-heme balance in Diamond-Blackfan anemia by HSP70/GATA1. Blood. 2019;133(12):1358-1370.
11. Ali AM, Huang Y, Pinheiro RF, et al. Severely impaired terminal erythrod differentiation as an independent prognostic marker in myelodysplastic syndromes. Blood Adv. 2018;2(12):1393-1402.
12. Gastou M, Rio S, Dussiot M, et al. The severe phenotype of Diamond Blackfan anemia is modulated by heat shock protein 70. Blood Adv. 2017;1(12):1959-1976.
13. Dulmovits BM, Appiah-Kubi AO, Papoin J, et al. Pomalidomide reverses γ-globin silencing through the transcriptional reprogramming of adult hematopoietic progenitors. Blood. 2016;127(11):1481-1492.

Are next-generation sequencing results knocking on Heaven's door for transplantation planning in chronic myelomonocytic leukemia?

Guillermo F. Sanz,[1,2,3,4] Mariam Ibañez[1,2,4,5] and Elvira Mora[1,2]

[1]Department of Hematology, Hospital Universitario y Politécnico La Fe, Valencia; [2]Instituto de Investigación Sanitaria La Fe, Valencia [3]Department of Medicine, University of Valencia, Valencia; [4]Centro de Investigación Biomédica en Red de Cáncer, CIBERONC, Instituto de Salud Carlos III, Madrid and [5]Departamento de Ciencias Biomédicas, Facultad de Ciencias de la Salud, Universidad CEU Cardenal Herrera, Valencia, Spain

E-mail: GUILLERMO SANZ - sanz_gui@gva.es

Chronic myelomonocytic leukemia (CMML) is a heterogeneous malignant myeloid disorder included in the 2016 revision to the World Health Organization (WHO) classification of myeloid neoplasms and acute leukemia in the category of myelodysplastic syndromes/myeloproliferative neoplasms. CMML patients show a diverse biological, clinical picture and heterogeneous prognosis, with short overall survival (OS) and increased risk of progression to acute myeloid leukemia. The diagnosis of CMML requires a monocytosis, defined as an absolute monocyte count above $1x10^9$/L that should represent >10% of the white blood count (WBC) differential, which persists for more than 3 months and for which other causes of reactive monocytosis have been excluded. The current World Health Organization classification includes three CMML groups, divided on the basis of blast counts, for better prognostication: CMML-0 [<2% peripheral blood (PB) and <5% bone marrow (BM) blasts]; CMML-1 (2-4% PB and/or 5-9% BM blasts); and CMML-2 (5-19% PB and/or 10-19% BM blasts). The classical French-American-British classification, still widely used, divides CMML into so-called "dysplastic" CMML (WBC ≤13x10^9/L) and "myeloproliferative" CMML (WBC >13 x10^9/L).

Cytogenetic abnormalities and somatic mutations are found in, respectively, 25-30% and up to 95% of CMML patients and both have a strong influence on OS. The validated CMML-specific cytogenetic risk classification recognizes three risk categories: low-risk (normal karyotype or loss of the Y chromosome as a single anomaly; ~78%), high-risk (trisomy 8 or abnormalities of chromosome 7, or complex karyotype; ~12%), and intermediate-risk (all other abnormalities; ~9%).[1] The most frequently mutated genes in CMML affect epigenetic regulation and DNA methylation (ASXL1 and TET2), RNA splicing (SRSF2), and transcription (RUNX1) and signaling pathways (RAS).[2-4] Frameshift and nonsense ASXL1 mutations confer an adverse prognosis,[2-4] aggravated when EZH2 and ASXL1 mutations co-occur.[5] DNMT3A and TP53 mutations, although less common in CMML, have also been associated with poorer OS.[6,7] It is noteworthy that the number of mutations also influences patients' outcomes, as recently demonstrated in a study in which a shorter OS was observed in CMML patients with three or more concomitant mutations.[7]

Specific prognostic scoring systems for individual risk assessment are essential in order to provide risk-adapted treatment. The most commonly used are the CMML-specific prognostic scoring system (CPSS),[8] the MD Anderson Cancer Center prognostic score (MDAPS)[9] and the revised International Prognostic Scoring System (IPSS-R)[10] (the last only being applicable to "dysplastic" CMML). More recent scoring systems that also include somatic mutations are those by the Groupe Français des Myélodysplasies (GFM),[2] the Mayo Clinic[3], and the molecular CPSS.[4] All these molecular prognostic scoring systems consider ASXL1 mutations; the molecular CPSS also takes into account mutations in NRAS, SETBP1, and RUNX1.

Allogeneic hematopoietic cell transplant (HCT) is the only potentially curative therapy for patients with CMML but the number of transplant-eligible patients is low because of these individuals' advanced age, comorbidities, and frailty. A recent multicenter retrospective study with 1,656 CMML patients of whom 89 received an allogeneic HCT demonstrated the benefit of HCT for patients with higher-risk disease as determined by the CPSS[11] and multiple retrospective studies have documented a 3-year OS rate of 30-40%.[12-15] For high-risk transplant-ineligible and/or lower-risk patients the most widely used therapies are hydroxyurea, hypomethylating agents, and best supportive care. Recent evidence suggests that hypomethylating agents might be superior to hydroxyurea.[11]

Many studies have evaluated the prognostic factors for transplantation outcomes in CMML patients, with contradictory results.[16] As would be expected, patients transplanted in complete remission[13] as well as those with <5% blasts at transplantation[14] had better outcomes in comparison to those with more advance disease at transplantation. The favorable effect of using hypomethylating agents before transplantation over intensive chemotherapy is debatable.[14-16] In a large study by the Center for International Blood and Marrow Transplantation Research (CIBMTR), the CPSS score at the time of HCT strongly influenced OS after transplantation.[15] Table 1 shows the predictive factors for increased relapse or reduced OS evidenced in major studies on allogenic HCT for CMML.

In this issue of Haematologica, Woo and colleagues, analyze long-term outcomes after allogeneic HCT in 129 patients with CMML from a single institution and evaluate clinical and molecular risk factors associated with outcomes.[17] Of note, this study is the first to evaluate the impact of somatic mutations determined by next-generation sequencing (NGS) on allogeneic HCT outcomes in a large and homogeneous series of patients from a single institution. In a subcohort of 52 patients in whom a NGS panel of 75 genes was used, 85% of patients had at least one mutation, congruent with previous reports on

Table 1. Predictive factors for overall survival after allogeneic hematopoietic cell transplantation in relevant series of patients with chronic myelomonocytic leukemia.

	EBMT {Symeonidis:2015[13]}	MDACC {Kongtim:2016[14]}	CIBMTR {Liu:2017[15]}	FHCRC {Woo:2019[17]}
Study period	1988-2009	1991-2013	2001-2012	1986-2017
N. of patients	513	83	209	129
Median age, years (range)	53 (18-75)	57 (18-78)	57 (23-74)	55 (7-74)
Disease at HCT (CMML/AML, %)	56 / 44	57 / 43	100 / 0	71 / 29
Factors predicting OS				
Complete remission at HCT	Favorable	Favorable	NA	No effect
Higher-risk categories by CPSS/MDAPS	NA	NA	Unfavorable/NA	Unfavorable/Unfavorable
Performance Status (KPS≥90)	NA	No effect	Favorable	NA
HCT-CI ≥4	NA	NA	NA	Unfavorable
High-risk CMML-specific cytogenetics	No effect	No effect	NA	Unfavorable
Graft source (peripheral blood)	No effect	NA	Favorable	No effect
Transplant from matched related donors	No effect	Favorable	NA	No effect
Prior HMA treatment	No effect	Favorable	No effect	No effect
Molecular profile	NA	NA	NA	Increased relapse: -Mutations in NRAS, ATRX, WT1 - ≥10 gene mutations - ≥4 mutations in epigenetic regulators
Conditioning intensity	No effect	No effect	NA	No
Development of chronic GvHD	No effect	Favorable	NA	NA
Age	No effect	No effect	NA	No effect
Year of transplant	No effect	No effect	NA	No effect

EBMT: European Society for Blood and Marrow Transplantation; MDACC: MD Anderson Cancer Center; CIBMTR: Center for International Blood and Marrow Transplantation Research; FHCRC: Fred Hutchinson Cancer Research Center; HCT.: hematopoietic cell transplant; CMML; chronic myelomonocytic leukemia; AML: acute myeloid leukemia; OS: overall survival; CPSS: CMML-specific prognostic scoring system; MDAPS: MD Anderson prognostic scores; KPS: Karnofsky Performance Score; HCT-CI: Hematopoietic Cell Transplant-Comorbidity Index; PB: peripheral blood; HMA: hypomethylating agents, GvHD: graft-versus-host disease; NA: information not available.;

CMML. The most commonly mutated genes were *ASXL1* (52%), *TET2* (42%), and *SRSF2* (25%). Other frequently encountered mutations were evident for WT1 (27%), *RUNX1* (17%), *DNMT3A* (17%), *SMC1A* (17%), *EZH2* (12%), and *ATRX* (12%), highly likely because most patients had intermediate-2 or high-risk disease according to the CPSS.[17]

In the study by Woo *et al.*, mutations in *NRAS* were associated with an increased relapse risk whereas mutations in *ATRX* and *WT1*, conferred both a higher relapse risk and inferior OS. Moreover, this study showed that a high overall mutation burden (≥10 mutations) as well as the presence of four or more mutated epigenetic regulatory genes were linked to a higher risk of relapse. Unsupervised clustering revealed two higher-risk groups with specific associations between mutations and clinical features. The presence of a higher mutation burden was closely related to a longer period between diagnosis and transplantation but not with complex chromosomal abnormalities or an excess of blasts. The currently published recommendation of an international expert panel is to use the CPSS for considering a patient as a candidate for allogeneic HCT and to transplant those CMML patients belonging to the intermediate-2/high CPSS risk groups.[18] Whether the better outcomes observed with lower CPSS scores and the lower mutational burden observed in less advanced disease could argue in favor of

transplanting patients with CMML earlier in the course of their disease (e.g., extending transplantation to patients with intermediate-1 CPSS risk score) is debatable and can only be properly answered by a carefully designed study.

As previously reported in other HCT series on CMML, in the study by Woo *et al.*, relapse risk was also significantly associated with adverse cytogenetics, higher-risk CPSS and MDAPS scores, and measurable residual disease by cytogenetics at transplantation. A higher mortality was seen in patients with high-risk cytogenetics and a high HCT Comorbidity Index. Of interest, neither disease status at transplantation (complete remission *vs.* non-complete remission) nor pre-transplant therapy (intensive chemotherapy or hypomethylating agents) nor conditioning intensity had a clear and independent impact on transplant outcomes. Additionally, the year of transplant did not affect the risk of relapse or OS, clearly indicating that newer transplant strategies are needed to improve those outcomes.[17]

In summary, this study has identified both clinical and novel molecular risk factors for outcomes after allogeneic HCT that add relevant information which could be taken into account when planning transplantation for CMML patients. Table 2 illustrates the clinical and molecular risk factors for allogeneic HCT outcome in CMML patients, among whom different groups of higher-risk patients amenable to transplantation can be detected at different

Table 2. Schematic representation of the relationships between clinical and hematologic characteristics, cytogenetics, somatic mutations, prognostic scoring systems and transplant outcomes in patients with chronic myelomonocytic leukemia.

	FEATURES														
	Prognostic Scoring System		Mutational Burden		Age	ECOG & PS	Peripheral Counts				Bone Marrow Blasts		Cytogenetics		
	CPSS score Higher-risk	MDAPS score Higher-risk	≥10 total mutations	≥4 mutations in epigenetic modifying genes	> 60 years	2 - 3	RBC transfusion dependence and / or low Hb	High WBC counts (x 10^9/L) > 13	>20	Low platelet count	Excess of Blasts (%) 5 - 10	> 10	High-Risk Trisomy 8	Complex karyotype (>2)	Abn chr 7
CPSS score Risk															
MDAPS score Risk															
Mutational Profiling															
Delayed time from Diagnosis to HCT															
Overall Survival															
Relapse Risk after HCT															

ECOG: Eastern Cooperative Oncology Group; PS: Performance Status; CPSS: CMML-specific prognostic scoring system; MDAPS: MD Anderson prognostic score; RBC: red blood cells; Hb: hemoglobin; WBC: white blood cells; Abn: abnormalities; Chr: chromosome; HCT: hematopoietic cell transplant

time points of the course of the disease.

However, even though NGS studies could therefore be used to select a group of high-risk CMML patients for transplantation, our view is that it might still be premature to incorporate the results of NGS techniques into the decision-making process for CMML patients undergoing allogeneic HCT. The main reasons are that NGS techniques and results are not well standardized, their reproducibility is unproven, the characterization of allele variants as pathogenic is not homogenously defined, and the variant allele frequency threshold used to define the presence of mutations is widely variable (5% in the series by Woo *et al.*) Furthermore, the impact of co-occurring mutations on prognosis is still unclear.[19] Additionally, the value of molecular profiling for treatment decision-making in CMML patients is diminished by the limited number of treatment alternatives and because there is no single somatic mutation that favors the use of a particular treatment approach.[19]

In conclusion, molecular profiling will likely emerge in the near future as highly valuable for planning transplantation in CMML patients, adding up to other well-recognized patient and disease characteristics such as higher-risk CPSS and MDAPS categories and HCT-Cormorbidity Index. Prospective cooperative studies focused on NGS

results before and after transplantation and involving large numbers of patients will be eventually required to improve the cure rate afforded by allogeneic HCT in CMML.

References

1. Such E, Cervera J, Costa D, et al. Cytogenetic risk stratification in chronic myelomonocytic leukemia. Haematologica. 2011;96(3):375-383.
2. Itzykson R, Kosmider O, Renneville A, et al. Prognostic score including gene mutations in chronic myelomonocytic leukemia. J Clin Oncol. 2013;31(19):2428-2436.
3. Patnaik MM, Itzykson R, Lasho TL, et al. ASXL1 and SETBP1 muta-

tions and their prognostic contribution in chronic myelomonocytic leukemia: a two-center study of 466 patients. Leukemia. 2014;28(11):2206-2212.

4. Elena C, Gallì A, Such E, et al. Integrating clinical features and genetic lesions in the risk assessment of patients with chronic myelomonocytic leukemia. Blood. 2016;128(10):1408-1417.

5. Patnaik MM, Vallapureddy R, Lasho TL, et al. EZH2 mutations in chronic myelomonocytic leukemia cluster with ASXL1 mutations and their co-occurrence is prognostically detrimental. Blood Cancer J. 2018;8(1):12.

6. Patnaik MM, Barraco D, Lasho TL, et al. DNMT3A mutations are associated with inferior overall and leukemia-free survival in chronic myelomonocytic leukemia. Am J Hematol. 2017;92(1):56-61.

7. Montalban-Bravo G, Takahashi K, Patel K, et al. Impact of the number of mutations in survival and response outcomes to hypomethylating agents in patients with myelodysplastic syndromes or myelodysplastic/myeloproliferative neoplasms. Oncotarget. 2018;9(11):9714-9727.

8. Such E, Germing U, Malcovati L, et al. Development and validation of a prognostic scoring system for patients with chronic myelomonocytic leukemia. Blood. 2013;121(15):3005-3015.

9. Onida F, Kantarjian HM, Smith TL, et al. Prognostic factors and scoring systems in chronic myelomonocytic leukemia: a retrospective analysis of 213 patients. Blood. 2002;99(3):840-849.

10. Greenberg PL, Tuechler H, Schanz J, et al. Revised international prognostic scoring system for myelodysplastic syndromes. Blood. 2012;120(12):2454-2465.

11. Pleyer L, Leisch M, Kourakli A, et al. Effects of the therapeutic armamentarium on survival and time to next treatment in CMML subtypes: an international analysis of 950 cases coordinated by the AGMT study group. Blood. 2019;134(Suppl 1):844-844.

12. Park S, Labopin M, Yakoub-Agha I, et al. Allogeneic stem cell transplantation for chronic myelomonocytic leukemia: a report from the Societe Francaise de Greffe de Moelle et de Therapie Cellulaire. Eur J Haematol. 2013;90(5):355-364.

13. Symeonidis A, van Biezen A, de Wreede L, et al. Achievement of complete remission predicts outcome of allogeneic haematopoietic stem cell transplantation in patients with chronic myelomonocytic leukaemia. A study of the Chronic Malignancies Working Party of the European Group for Blood and Marrow Trans. Br J Haematol. 2015;171(2):239-246.

14. Kongtim P, Popat U, Jiménez A, et al. Treatment with hypomethylating agents before allogeneic stem cell transplant improves progression-free survival for patients with chronic myelomonocytic leukemia. Biol Blood Marrow Transplant. 2016;22(1):47-53.

15. Liu HD, Ahn KW, Hu Z-H, et al. Allogeneic hematopoietic cell transplantation for adult chronic myelomonocytic leukemia. Biol Blood Marrow Transplant. 2017;23(5):767-775.

16. Sanz GF. A Lot to learn about allogeneic hematopoietic cell transplantation for chronic myelomonocytic leukemia. Biol Blood Marrow Transplant. 2017;23(5):713-714.

17. Woo J, Ro Choi D, Storer BE, et al. Impact of clinical, cytogenetic, and molecular profiles on long-term survival after transplantation in patients with chronic myelomonocytic leukemia. Haematologica. 2020;105(3):652-660.

18. de Witte T, Bowen D, Robin M, et al. Allogeneic hematopoietic stem cell transplantation for MDS and CMML: recommendations from an international expert panel. Blood. 2017;129(13):1753-1762.

19. Sanz GF, Ibáñez M, Such E. Do next-generation sequencing results drive diagnostic and therapeutic decisions in MDS? Blood Adv. 2019;3(21):3454-3460.

Leukemia stem cell gene expression signatures contribute to acute myeloid leukemia risk stratification

Katherine L. B. Knorr and Aaron D. Goldberg

Division of Hematologic Malignancies, Department of Medicine, Memorial Sloan Kettering Cancer Center, New York, NY, USA

E-mail: AARON D. GOLDBERG - goldbera@mskcc.org

The majority of patients with acute myeloid leukemia (AML) will die of their disease. Nevertheless, the prognosis of AML varies widely. Some AML patients may be cured by chemotherapy alone, while others require approaches such as allogeneic stem cell transplantation to have the best chance of long-term survival. As physicians, we are often asked by our AML patients: "How likely is this treatment going to work, and how long do I have to live?"[1]

Prognostication in AML has evolved over time. Initially, models for prediction of response to therapy were based on patient's parameters such as age and performance status in combination with cell characteristics such as morphology and chromosomal karyotype. With technological advancements, our understanding of disease biology has evolved and factors including molecular mutations and minimal residual disease have been integrated into prognostication schemes. Recently, an international expert panel on behalf of the European LeukemiaNet (ELN) published a revised version of a widely utilized prognostication scheme that categorizes AML patients into three risk groups (Favorable, Intermediate, and Adverse) based on genetic abnormalities (incorporating chromosomal karyotype and specific molecular mutations).[2] These AML risk groups have profound clinical implications, particularly with regard to post-remission therapy for younger fit patients. In general, fit Favorable-risk AML patients who achieve a first complete remission after induction chemotherapy go on to consolidation chemotherapy with curative intent. However, even fit patients with Adverse- and Intermediate-risk AML are unlikely to be cured by chemotherapy alone, and therefore it is reasonable to consider allogeneic stem cell transplantation for Intermediate- and Adverse-risk patients upon achievement of first complete remission.

Why is AML so often resistant to chemotherapy? The biology of AML chemoresistance is complex. However, at a basic level, adverse-risk AML cells are more likely to evade conventional chemotherapeutics that target the cell cycle. It has therefore been hypothesized that one powerful driver of adverse prognosis in AML may be the properties of the leukemia stem cell (LSC), a type of cell that exhibits cell cycle quiescence, self-renewal, and chemoresistance.[3-6] Although AML LSC remain challenging to isolate, assessment of AML LSC gene expression signatures has been proposed as a method to further refine prognosis – with LSC-like AML phenotypes contributing to adverse risk.
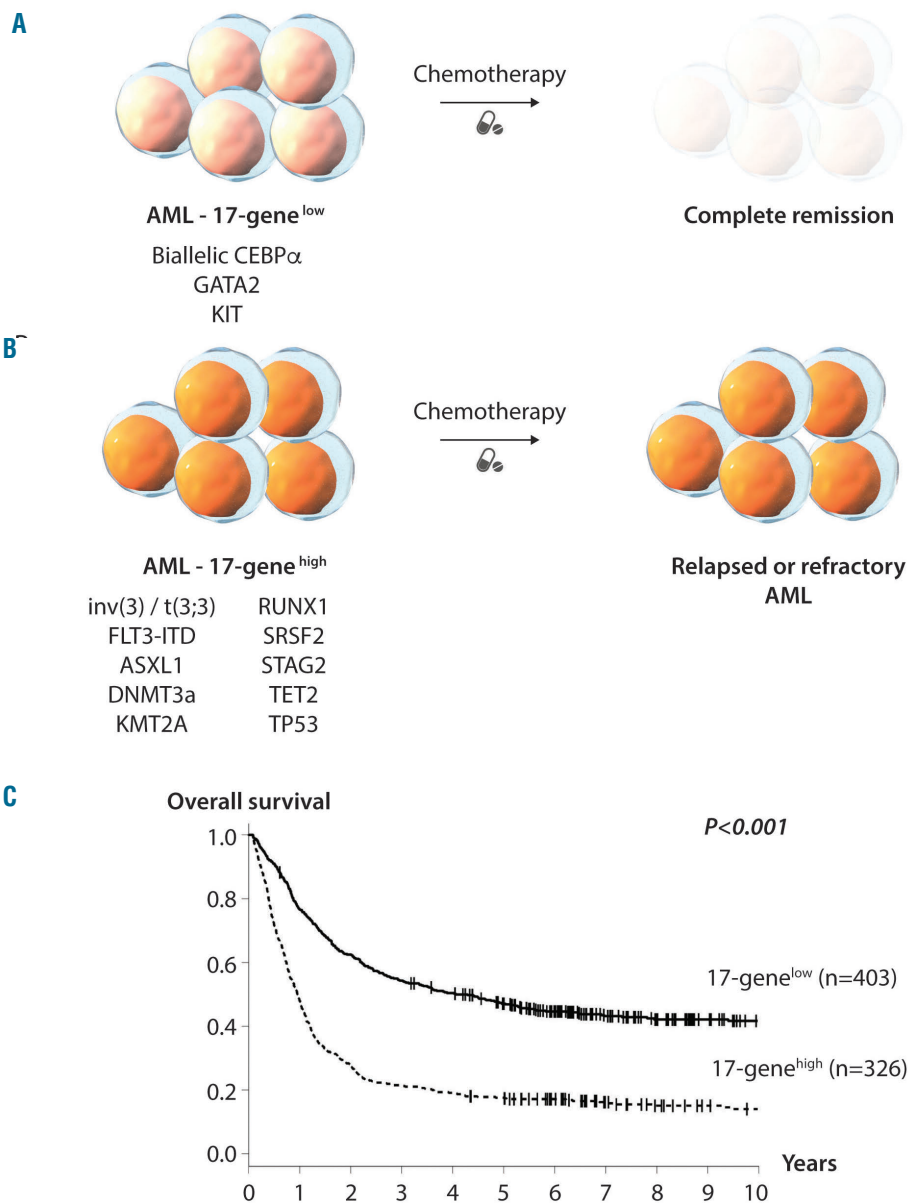
Figure 1. The 17-gene leukemia stem cell score refines prognosis in acute myeloid leukemia beyond that afforded by the European LeukemiaNet risk categories. (A) Patients with acute myeloid leukemia (AML) with a 17-gene[low] leukemia stem cell (LSC) score more frequently have biallelic *CEBPA*, *GATA2*, and *KIT* mutations and are more sensitive to chemotherapy. (B) Patients with AML with a 17-gene[high] LSC score more frequently have unfavorable molecular abnormalities and are more resistant to chemotherapy. (C) The 17-gene LSC score has a powerful prognostic impact, particularly in younger adult AML patients (aged <60 years).

A study by Ng *et al.* recently defined a list of genes differentially expressed between LSC and non-LSC fractions (validated by xenotransplantation) from 78 AML patients.[7] The list of genes highly expressed in LSC was subjected to statistical regression analysis to relate the expression profile to patients' survival, which yielded an optimal "17-gene LSC score" prognostic signature. When the scoring algorithm was applied to five cohorts of AML patients, high scores consistently correlated with poor prognostic factors such as older age, higher initial white blood cell count, and unfavorable cytogenetics. High scores also correlated with resistance to standard induc-

tion chemotherapy, higher rates of relapse, and poor outcomes including inability to achieve complete response, decreased overall survival, and shorter event-free and relapse-free survival. Ng *et al.* proposed that this scoring tool could be applied to guide selection of initial therapy in newly diagnosed patients, specifically to identify high-risk patients not likely to benefit from standard induction chemotherapy.

In this issue of *Haematologica*, Bill *et al.* provide an impressive validation of the 17-gene LSC scoring system using RNA-sequencing data from a large number of patients treated in cooperative group (CALGB) trials.[8]

This work confirms and expands upon the insights published in 2016 by Ng *et al.*, showing the prognostic value of LSC gene expression signatures in an independent large cohort of AML patients. Here, Bill *et al.* apply the 17-gene LSC score to 934 *de novo* AML patients and report the association of the 17-gene LSC score with prognostic clinical parameters, specific AML mutations, and ELN risk classification.

Using unsorted pre-treatment bone marrow and/or peripheral blood specimens, the group conducted transcriptome analysis via RNA-sequencing. The 17-gene LSC score was calculated as the weighted sum of the normalized expression values of the 17 genes included in the signature panel defined by Ng *et al.* The scores derived were then divided into two groups using the median as the cutoff to define "17-gene^high" (more LSC-like) and "17-gene^low" (less LSC-like) (Figure 1A, B).

Consistent with prior data, allocation into the 17-gene-^high and 17-gene^low groups correlated with known prognostic factors. 17-gene^low patients were more often younger (age <60 years) and predominantly had favorable cytogenetic profiles. Bill *et al.* also correlated the 17-gene score with known AML mutations.[8] Favorable mutations in genes such as *CEBPA*, *GATA2*, and *KIT* were more frequent in patients with a 17-gene^low score (Figure 1A) while unfavorable mutations in genes including *ASXL1*, *RUNX1*, and *TP53* occurred more frequently in patients with a 17-gene^high score (Figure 1B). Patients with extremely high-risk *EVI1* rearrangements inv(3)/t(3;3) were exclusively found in the 17-gene^high score group. With respect to mutation burden, more LSC-like AML harbored slightly more mutations, with a median of two among patients with a 17-gene^low score and of three among those with a 17-gene^high score.

Next, Bill *et al.* assessed outcomes in the groups with 17-gene^low and 17-gene^high scores. Both groups followed known associations for favorable and poor outcomes (complete remission rate, longer disease-free and overall survival) in, respectively, the younger (Figure 1C) and older cohorts of patients. In addition to validating the prognostic impact of the 17-gene LSC score in a large independent cohort and adding correlations with AML mutations, Bill *et al.* also compared the 17-gene LSC score to AML ELN risk stratification.[8]

When patients were classified according to the ELN stratification into Favorable-, Intermediate-, and Adverse-risk groups, there were significant differences in ELN risk distribution between the 17-gene^low and 17-gene^high LSC score patients of different ages. In younger patients with a 17-gene^low score, most (66%) were classified as having Favorable-risk, with 14% and 17% classified as having Intermediate- and Adverse-risk, respectively. However, younger patients with a 17-gene^high score were spread across the ELN classification: Adverse-risk (41%), Intermediate-risk (32%), and Favorable-risk (26%). In older patients with a 17-gene^low score, only 36% were classified in the Favorable-risk group, while 24% had an Intermediate risk and 40% an Adverse risk. By comparison, older patients with a 17-gene^high score clustered mainly into the Adverse-risk group (63%), with fewer in the Intermediate- (18%), and Favorable-risk (18%) groups.

When assessing outcomes, the 17-gene LSC score failed to add significant prognostic information to ELN classification in older AML patients, in whom prognosis remains poor across prognostic groups with conventional chemotherapy.

Intriguingly, the data suggest that the 17-gene LSC score can provide additional prognostic value particularly for younger patients who may be currently misclassified as having a favorable risk. Younger patients with an ELN Favorable-risk classification with a high 17-gene LSC score (20% of ELN Favorable-risk patients) have a worse prognosis than would otherwise be expected from the ELN classification alone. This unexpectedly high-risk group of patients epitomizes the rationale for using refined prognostication schemes such as the 17-gene scoring tool, with the goal of tailoring first-line therapy more precisely and identifying populations of patients in need of prospective clinical trials.

The comprehensive RNA-sequencing approach described by Bill *et al.* does have some limitations. From a practical point of view, while pre-treatment cytogenetics as well as genomic profiling for mutations in specific genes have become standards of care for patients with AML, it is premature to recommend universal pre-treatment RNA-sequencing. Future studies in adult AML may validate the prognostic significance of pre-treatment profiling of a limited list of LSC-related genes using more targeted gene expression analysis, as was recently shown using Nanostring technology in pediatric AML.[9]

In a broader perspective, prognosis in any disease is shaped by the efficacy of available therapy. All patients evaluated in the current study by Bill *et al.* received cytarabine/anthracycline-based induction chemotherapy.[8] Although AML prognosis has traditionally been evaluated in response to cytotoxic chemotherapy, the prognostic impact of ELN genetic risk classification and LSC gene expression signatures will need to be re-evaluated in the context of novel and more targeted therapeutics.

Recently, the BCL-2 inhibitor venetoclax in combination with hypomethylating agents has become a new standard of care for adult patients with AML who are unfit, by virtue of age or comorbidities, to receive intensive chemotherapy.[10] Although many patients still relapse, this combination shows activity in disease often refractory to standard induction chemotherapy, including secondary AML, therapy-related AML, and AML with high-risk cytogenetic and mutation profiles. One explanation for the relatively mutation-agnostic efficacy of venetoclax + azacitidine is the combination's suppression of oxidative phosphorylation and disruption of energy metabolism in LSC.[11] The impact of LSC gene expression signatures on prognosis in patients treated with hypomethylating agents + venetoclax has yet to be determined. Similarly, the impact of LSC gene expression signatures on prognosis in *FLT3*-mutated patients may also need to be re-evaluated, as more effective and specific FLT3 inhibitors enter clinical practice.[12] In general, as more effective therapies are developed that target the fundamental biology of AML, prognostic factors and even post-remission therapies will need to be re-examined.

References

1. Liesveld J. Management of AML: who do we really cure? Leuk Res. 2012;36(12):1475-1480.
2. Dohner H, Estey E, Grimwade D, et al. Diagnosis and management of AML in adults: 2017 ELN recommendations from an international expert panel. Blood. 2017;129(4):424-447.
3. Thomas D, Majeti R. Biology and relevance of human acute myeloid leukemia stem cells. Blood. 2017;129(12):1577-1585.
4. Lapidot T, Sirard C, Vormoor J, et al. A cell initiating human acute myeloid leukaemia after transplantation into SCID mice. Nature. 1994;367(6464):645-648.
5. Shlush LI, Zandi S, Mitchell A, et al. Identification of pre-leukaemic haematopoietic stem cells in acute leukaemia. Nature. 2014;506(7488):328-333.
6. Pollyea DA, Gutman JA, Gore L, Smith CA, Jordan CT. Targeting acute myeloid leukemia stem cells: a review and principles for the development of clinical trials. Haematologica. 2014;99(8):1277-1284.
7. Ng SW, Mitchell A, Kennedy JA, et al. A 17-gene stemness score for rapid determination of risk in acute leukaemia. Nature. 2016;540(7633):433-437.
8. Bill M, Nicolet D, Kohlschmidt J, et al. Mutations associated with a 17-gene leukemia stem cell score and the score's prognostic relevance in the context of the European LeukemiaNet classification for acute myeloid leukemia. Haematologica.2020;105(3):721-729.
9. Duployez N, Marceau-Renaut A, Villenet C, et al. The stem cell-associated gene expression signature allows risk stratification in pediatric acute myeloid leukemia. Leukemia. 2019;33(2):348-357.
10. DiNardo CD, Pratz K, Pullarkat V, et al. Venetoclax combined with decitabine or azacitidine in treatment-naive, elderly patients with acute myeloid leukemia. Blood. 2019;133(1):7-17.
11. Pollyea DA, Stevens BM, Jones CL, et al. Venetoclax with azacitidine disrupts energy metabolism and targets leukemia stem cells in patients with acute myeloid leukemia. Nat Med. 2018;24(12):1859-1866.
12. Perl AE, Martinelli G, Cortes JE, et al. Gilteritinib or chemotherapy for relapsed or refractory FLT3-mutated AML. N Engl J Med. 2019;381(18):1728-1740.

Thrombopoietin receptor agonists for the treatment of inherited thrombocytopenia

Michael Makris[1,2]

[1]Department of Infection, Immunity and Cardiovascular disease, University of Sheffield, and [2]Sheffield Haemophilia and Thrombosis Centre, Royal Hallamshire Hospital, Sheffield, UK

E-mail: m.makris@sheffield.ac.uk

The inherited thrombocytopenias are a heterogeneous group of increasingly recognized disorders, which can be associated with bleeding of variable severity. Their prevalence has been estimated to be around 1 in 100,000 of the population,[1] but it is likely that this is an underestimate due to many individuals being undiagnosed, wrongly diagnosed or not recorded on registries after a correct diagnosis. More recently, it has been reported that the prevalence of MYH9-related disorders can be as frequent as 1 in 20,000 of the population.[2]

The inherited nature of the thrombocytopenias has been recognized for decades, with the main disorders being the May-Hegglin anomaly, and the Sebastien, Fechtner and Epstein syndromes. These disorders were associated with a variable degree of renal impairment, deafness and cataracts. Although initially believed to be different disorders, when the genes responsible were identified, it became clear that all of these syndromes were variants of defects in the same *MYH9* gene encoding for non-muscle myosin heavy chain A.[3] The nomenclature was subsequently changed to reflect this, and they are now known as the *MYH9*-related disorders (MYH9-RD).

The recent introduction of high throughput sequencing (HTS), together with the formation of consortia with large numbers of clinicians caring for inherited thrombocytopenia patients, has led to a dramatic increase in the number of genes responsible for the disorder. Inherited thrombocytopenias can be syndromic, predisposing to renal failure, hearing loss and cataracts, as in *MYH9-RD*, while others, such as the *RUNX1*, *ANKRD26* and *ETV6*, can be associated with predisposition to hematologic malignancy.[4,5]

In contrast to the major advances in the genetic basis of inherited thrombocytopenia, the management of these disorders has hardly changed, with the main therapeutic decision being whether to transfuse platelets or not. Part of the difficulty is the variability in the number of platelets, as well as the bleeding tendency which is often not directly proportional to the platelet count. A possible explanation for this is the variable and often large size of the platelets in some of these disorders; since hemostatic reactions take place on the cell surface, disorders associated with larger platelets would be expected to be associated with less bleeding. Treatment is usually required when patients are actively bleeding, or to prevent bleeding prior to surgery or invasive procedures.

Platelet transfusions, however, can be problematic because of the potential for adverse events. They carry the risk of transfusion-transmitted infection, alloimmunization with production of platelet specific or HLA antibodies, allergic reactions and transfusion-related acute lung injury (TRALI). As a result, the use of platelet transfusions tends to be avoided if possible, and clinicians use tranexamic acid, sometimes with desmopressin, as non-specific hemostatic agents to treat these patients.

Thrombopoietin receptor agonists have been available for the treatment of immune thrombocytopenia in adults and children for some time. The two products with the longest availability are eltrombopag, which is given orally, and romiplostim, which is administered subcutaneously. In the UK, eltrombopag is available for use in patients with thrombocytopenia of at least six months duration whilst romiplostim is approved for ITP of 12 months duration or more.

In an important initial publication from 2010, Pecci *et al.* showed that eltrombopag could increase the platelet count of patients with *MYH9*-related thrombocytopenia.[6] Twelve patients with a platelet count of <50x10⁹/L were

treated with 50mg eltrombopag for three weeks, and those who did not achieve a platelet count of >100x10⁹/L received an additional three weeks of treatment at 75mg once daily. Five patients achieved a platelet count of >100x10⁹/L with the 50mg dose and an additional three achieved this with the 75mg dose. Overall, 67% of patients achieved a platelet count of >100x10⁹/L, 25% achieved a minor response, and a single patient did not respond. The treatment was well tolerated, and the bleeding symptoms resolved in 8 of 10 patients who presented these at study entry.[6]

Since it is known that in most forms of inherited thrombocytopenia the megakaryocytes respond to TPO receptor agonists,[7] the next logical step was to investigate these agents for the treatment of other forms of inherited thrombocytopenia, and this is what Zaninetti *et al.* have done.[8] In this issue of the Journal, they report on their multicenter prospective investigation of eltrombopag in patients with five different types of inherited thrombocytopenia. A total of 24 patients with *MYH9*-related disease, *ANKRD26*-related thrombocytopenia, X-linked/Wiskott-Aldrich syndrome, monoallelic Bernard-Soullier syndrome, and *ITGB3*-related thrombocytopenia were included. Patients awaiting procedures received an escalating dose of 50-75mg eltrombopag for 3-6 weeks, while individuals with active bleeding received an escalating dose of 25-75mg for up to 16 weeks (Figure 1). The responses varied between the different defects, but overall 48% of the patients responded, achieving a platelet count of over 100x10⁹/L. All four patients who were experiencing mucosal bleeding on entry, stopped bleeding following the eltrombopag treatment. The treatment with eltrombopag was well tolerated, but one patient with Wiskott Aldrich syndrome discontinued the treatment due to deterioration of his eczema.[8]

The trial by Zanetti *et al.* excluded some patients with inherited thrombocytopenia and predisposition to hematologic malignancy, such as those with mutations in the *RUNX1* (previously known as *AML1*) and *ETV6* genes; *ANKRD26* patients were, however, included. The evidence that TPO receptor agonists accelerate disease progression is controversial. A study of the use of the TPO
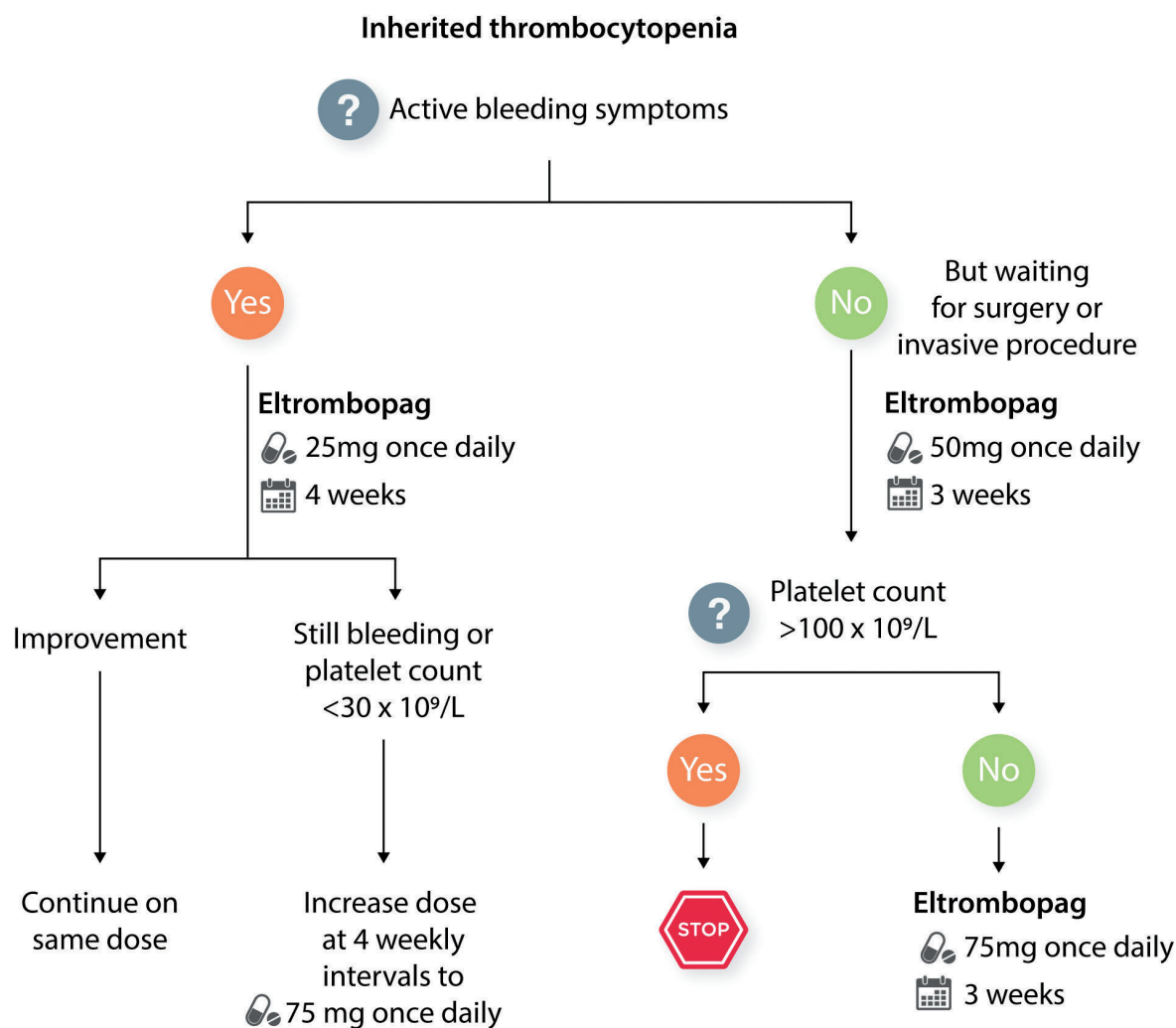
Figure 1. Outline of the phase II clinical trial using eltrombopag in patients with inherited thrombocytopenia.

receptor agonist romiplostim in patients with myelodysplasia and thrombocytopenia was halted early despite leading to an increase in the platelet count and improvement in bleeding symptoms because of concern regarding progression to acute myeloid leukemia (AML). In the final analysis, however, the AML progression risk was not significant, with a hazard ratio of 1.20 and a 95% confidence interval of 0.38-3.84.[9] No such concern was observed in a subsequent trial of eltrombopag monotherapy in similar settings.[10]

As mentioned before, there are at least 40 different genes associated with inherited thrombocytopenia.[11] At this stage, it is not known whether patients with other gene mutations will respond to eltrombopag in the same way, or whether any of these disorders will respond to the other TPO receptor agonists such as romiplostim; while the answer to both of these questions is likely to be yes, this is still speculation and needs to be confirmed in clinical trials or case series.

Considering the rarity and variety of the inherited thrombocytopenias, as well as the brief period for which most of these individuals require treatment to improve their platelet count, it is unlikely that a pharmaceutical manufacturer will perform the required trials to get approval of their drug for this indication.

The study by Zanetti *et al.* is important because it establishes eltrombopag as a therapeutic entity in the treatment of inherited thrombocytopenia. At this stage, we do not know if patients with mutations in other genes, or even different mutations in the same gene, will respond the same way, if at all. In view of this, it would be sensible to offer patients soon after diagnosis a 3-week therapeutic trial of 50mg of eltrombopag daily with the option of another three weeks at 75mg daily in the non- or poor-responders. In this way, at moments of possible future need, it will already be known whether they are eltrombopag responders or not, in which case they are likely to require platelet transfusions. I believe that, for elective procedures, the use of eltrombopag as a first-line agent is a very reasonable proposition, even when the drug is not licensed for this indication.

Although in many countries there are national registries of patients with inherited bleeding disorders, these tend to be for individuals with clotting factor deficiencies and do not include persons with inherited thrombocytopenia. I believe that all patients with inherited thrombocytopenia should be entered in registries so that the natural history, as well as the response to TPO receptor agonist treatment for all the different genetic defects, can be established. It is unlikely that this will be achieved for most of the disorders without international collaboration.

References

1. Balduini CL, Pecci A, Noris P. Diagnosis and management of inherited thrombocytopenias. Semin Thromb Hemost. 2013;39(2):161-171.
2. Fernandez-Prado R, Carriazo-Julio SM, Torra R, Ortiz A, Perez-Gomez MV. MYH9-related disease: it does exist, may be more frequent than you think and requires specific therapy. Clin Kidney J. 2019;12(4):488-493.
3. Kelley MJ, Jawien W, Ortel TL, Korczak JF. Mutation of MYH9, encoding for non-muscle myosin heavy chain A, in May-Hegglin anomaly. Nat Genet. 2000;26(1):106-108.
4. Noris P, Pecci A. Hereditary thrombocytopenias: a growing list of disorders. Hematology Am Soc Hematol Educ Program. 2017;2017(1):385-399.
5. Galera P, Dulau-Florea A, Calvo KR. Inherited thrombocytopenia and platelet disorders with germline predisposition to myeloid neoplasia. Int J Lab Hematol. 2019;41 Suppl 1:131-141.
6. Pecci A, Gresele P, Klersy C, et al. Eltrombopag for the treatment of the inherited thrombocytopenia deriving from MYH9 mutations. Blood. 2010;116(26):5832-5837.
7. Pecci A. Pathogenesis and management of inherited thrombocytopenias: rationale for the use of thrombopoietin-receptor agonists. Int J Hematol. 2013;98(1):34-47.
8. Zaninetti C, Gresele P, Bertomoro A, et al. Eltrombopag for the treatment of inherited thrombocytopenias: a phase 2 clinical trial. Haematologica. 2020;105(3):820-828.
9. Giagounidis A, Mufti GJ, Fenaux P, et al. Results of a randomized double-blind study of romiplostim versus placebo in patients with low/intermediate-1-risk myelodysplastic syndrome and thrombocytopenia. Cancer. 2014;120(12):1838-1846.
10. Mittelman M, Platzbecker U, Afanasyev B, et al. Eltrombopag for advanced myelodysplastic syndromes or acute myeloid leukaemia and severe thrombocytopenia (ASPIRE): a randomised, placebo-controlled, phase 2 trial. Lancet Haematol. 2018;5(1):e34-e43.
11. Almazni I, Stapley R, Morgan NV. Inherited Thrombocytopenia: Update on genes and genetic variants which may be associated with bleeding. Front Cardiovasc Med. 2019;6:80.

Hemolytic transfusion reactions in sickle cell disease: underappreciated and potentially fatal

Ferrata Storti Foundation

Swee Lay Thein,[1] France Pirenne,[2,3] Ross M. Fasano,[4,5] Anoosha Habibi,[3,6] Pablo Bartolucci,[6] Satheesh Chonat,[5] Jeanne E. Hendrickson[7] and Sean R. Stowell[4]

[1]National Heart, Lung and Blood Institute, National Institutes of Health, Bethesda, MA, USA; [2]Etablissement Français du Sang, INSERM U955, Université Paris Est Créteil, Créteil, France; [3]Laboratoire d'Excellence GR-Ex, Paris, France; [4]Center for Transfusion Medicine and Cellular Therapies, Department of Laboratory Medicine and Pathology, Emory University School of Medicine, Atlanta, GA, USA; [5]Aflac Cancer and Blood Disorders Center, Department of Pediatrics, Emory University School of Medicine, Atlanta, GA, USA; [6]Sickle Cell Referral Center, Department of Internal Medicine, Henri-Mondor University Hospital–UPEC, AP-HP, Créteil, France and [7]Departments of Laboratory Medicine and Pediatrics, Yale University School of Medicine, New Haven, CT, USA

Introduction

Patients with sickle cell disease (SCD) often receive red blood cell (RBC) transfusion support for the prevention and management of many acute and chronic disease complications.[1-3] The beneficial effects of transfusion therapy observed in recent clinical studies, and the lack of effective treatments for this population of patients, have led to an increased use of blood.[4] While RBC transfusions may be life-saving, we are concerned about their expanding use and would like to raise awareness of RBC alloimmunization, a major complication of transfusion, particularly in patients with SCD in whom the incidence is much higher than in other groups of patients.[5] Hemolytic transfusion reactions, which primarily occur in RBC alloimmunized patients, are often under-recognized in patients with SCD, in particular because the symptoms mimic those of acute vaso-occlusive crises, and serological markers of new alloantibodies may be equivocal.[6,7] In addition to increasing the risk of potentially fatal acute or delayed-type hemolytic transfusion reactions (DHTR),[8-10] the development of RBC alloantibodies can also significantly delay the procurement of compatible RBC for future transfusions.[11]

Currently, there is a lack of evidence in this area to inform best practice, and management is often based on anecdotal case reports. While there have been reports of a variety of cases illustrating the challenges associated with recognizing and treating hemolytic transfusion reactions in patients with SCD,[12,13] the potential reasons for the higher incidence of RBC alloantibodies in SCD patients merit discussion. Here, we share our experience in managing alloimmunized patients and hemolytic transfusion reactions, and challenge the medical community to consider lessons learned from diagnostic criteria and mitigation policies for transfusion-related acute lung injury (TRALI) in order to minimize the morbidity and mortality associated with transfusion in patients with SCD.

Why are patients with sickle cell disease at high risk of red blood cell alloimmunization?

One possible reason for the relatively high incidence of alloimmunization observed in patients with SCD is the mismatch in RBC antigens expressed in the donor pool (primarily Northern European descent) and patients with SCD (mainly of African descent).[8] Mismatch of RBC antigens is not the only reason, however, as a significant proportion of patients with SCD who receive phenotypically matched blood from exclusively ethnically matched donors still become alloimmunized.[9] Molecular analyses of the *RH* genes in patients with SCD and African-American donors reveal remarkable *RH* allelic diversity in this population, with mismatch between serological Rh phenotype and *RHD* or *RHCE* genotype due to variant *RH* alleles in a large proportion of the individuals.[10] Thus, *RH* genotyping in addition to serological typing may be required to identify the most compatible RBC, though it is not yet known if such an approach completed prospectively instead of reactively (after antibodies against alloantigens in the *RH* family form) will decrease RBC alloimmunization, and whether it will be possible to source rarer *RH* genotypes on a regular basis for patients on a transfusion program. The clinical context of RBC transfusion in SCD may also contribute to the higher rate of alloimmunization; the

risk of alloimmunization in SCD is increased when patients are transfused for acute complications, such as acute chest syndrome, acute pain and acute multi-system organ failure, which are clinical complications marked by significant inflammation. Thus, unique aspects of transfusion therapy in patients with SCD, in conjunction with other possible immune perturbations, appear to place such patients at a particular risk of RBC alloimmunization.[5,14-17]

Definitions of acute and delayed hemolytic transfusion reactions and hyperhemolysis

While acute hemolytic transfusion reactions can largely be avoided by stringent alloantibody investigations prior to transfusion, DHTR, which typically occur days or weeks following the implicated transfusion episode of seemingly compatible RBC,[7] are more difficult to avoid. The delayed nature of DHTR is thought to reflect the recrudescence of an alloantibody not detected at the time of the RBC compatibility testing just prior to transfusion.[6,18,19] The inability to detect RBC alloantibodies at the time of transfusion presumably reflects evanescence of a prior alloantibody response to a level below the detection threshold in routine clinical assays. Following re-exposure to the implicated alloantigen, immunological memory generated during the primary encounter facilitates an amnestic immune response that results in the rapid production of alloantibodies against the transfused unit (Figure 1). This in turn causes destruction of the transfused RBC, which is often accompanied by clinical symptoms associated with accelerated hemolysis.[18,19] DHTR
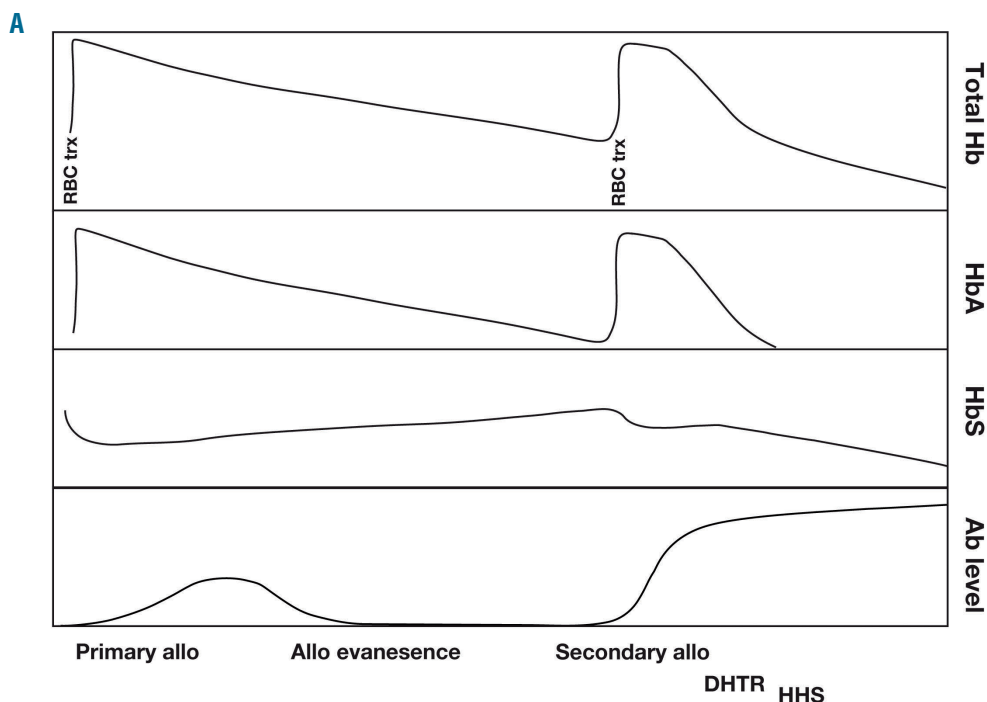
Figure 1. Delayed-type hemolytic transfusion reactions. (A) Exposure to a red blood cell (RBC) alloantigen through transfusion or pregnancy can result in the development of alloantibodies (allo) that quickly evanescence over time, possibly preventing their detection prior to a subsequent transfusion. Re-exposure to RBC expressing the same alloantigen can induce an amnestic alloantibody response, which can cause accelerated clearance of the transfused RBC, resulting in hemolysis and a delayed-type transfusion reaction (DHTR). Alloantibody-induced clearance of transfused RBC can occasionally result in hyperhemolysis, otherwise known as hyperhemolytic syndrome (HHS), which is signified by the accelerated clearance of the patient's own RBC and which can be particularly fatal. (B). Alloantibodies that develop in response to exposure to alloantigens can lead to direct clearance of RBC through a variety of antibody effector mechanisms, including complement activation. Sometimes patients will experience a DHTR in the absence of a detectable alloantibody; an alloantibody may be present and simply be below the detection threshold of clinical assays or an alloantibody may be absent entirely, with the DHTR possibly reflecting heme-mediated complement activation and RBC hemolysis. Regardless of the mode of hemolysis experienced by transfused RBC in the setting of a DHTR, heme released may activate complement, thereby potentially contributing to the development of hyperhemolysis. Trx: transfusion; Hb: hemoglobin.
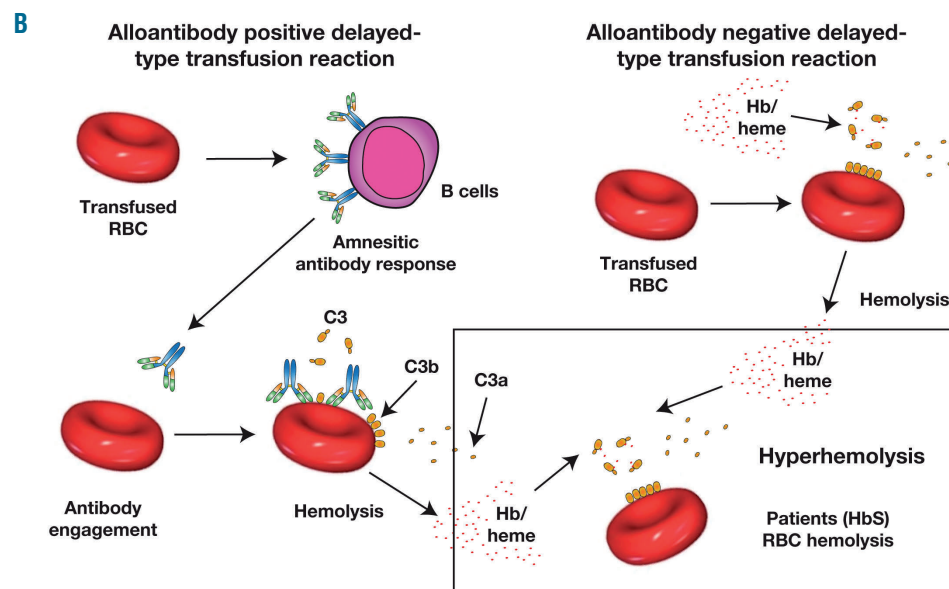
can be further complicated by bystander hemolysis or hyperhemolysis, a process that results in the accelerated clearance of both the transfused RBC and the patient's own RBC[20,21] (Figure 1). Such hyperhemolysis can be particularly fatal in patients with SCD for reasons that remain incompletely understood.

Attention to a high incidence of delayed hemolytic transfusion reactions

While DHTR can be life-threatening, unawareness of their frequency and lack of severity of these transfusion reactions have likely resulted in too little attention regarding their potential impact on overall SCD morbidity and mortality. For years, the overall incidence of DHTR per transfusion in SCD was estimated to be around 1:1000.[22-24] making it a relatively uncommon transfusion reaction in this population of patients. However, newer reports suggest that these data may be misleading. As mentioned previously, given the similarities between the clinical presentation of DHTR and the more common complications of vaso-occlusive crises, DHTR can be easily missed.[6,7,25] Unless an alloantibody screen is performed, an amnestic alloantibody response will not be detected and a diagnosis of DHTR may not be entertained. Furthermore, as some reports suggest that as many as 30% of DHTR can be alloantibody-negative,[14,26] clinicians must rely on HbA measurements obtained within 48 h of the implicated transfusion and at the time of a presumptive DHTR in order to make a reliable diagnosis of DHTR[12,27] (Figure 1). Unfortunately, alloantibody screens and HbA values are not routinely ordered following transfusion or in recently transfused patients admitted for acute pain, raising the possibility that the incidence of DHTR in patients with SCD may be much higher than previously appreciated.[27]

In an effort to assess the incidence of DHTR more accurately, a recent prospective study evaluated adult patients after transfusion using total Hb, HbA and HbS quantification within 48 h after all transfusions and defined DHTR as a significant decrease in HbA (>50%) and/or in total Hb levels (>30%) within 25 days of a trigger transfusion along with hemoglobinuria, symptoms of a vaso-occlusive crisis, and/or worsening symptoms of anemia.[27] Using this approach, a DHTR was found to occur following 4.2% of episodic transfusions,[27] over ten times more frequently than previously speculated, making DHTR the single most common adverse event following episodic transfusion in patients with SCD. Nearly 11% of all patients with DHTR died,[27] suggesting that these reactions are not only more common than previously suggested, but also likely to affect SCD mortality significantly. These results provide one possible explanation for the recent observation that alloimmunized patients with SCD have a much higher mortality rate than non-alloimmunized individuals with SCD.[28]

Comparison of delayed hemolytic transfusion reactions with transfusion-related acute lung injury

There are resemblances between the underappreciated incidence and impact of DHTR in patients with SCD and the history of other transfusion reactions with fatal outcomes.[29] Until relatively recently, TRALI was a rarely recognized complication of primarily platelet and plasma transfusion defined by acute lung injury within 6 h of transfusion in the presence of hypoxia, with radiographic evidence of bilateral infiltrates in the absence of circulatory overload.[30] Because patients who are susceptible to TRALI often have significant comorbidities, changes in pulmonary function that accompanied transfusion were historically attributed to other etiologies.[31] However, once the impact of TRALI was recognized and regulatory agencies heightened hemovigilance efforts, TRALI quickly became identified as the most common cause of transfusion-related mortality in the USA and Europe.[32] Epidemiological studies found associations between blood products donated from multiparous women and other donor factors that increased the likelihood that a recipient would develop TRALI.[32] In particular, anti-HLA and other anti-leukocyte alloantibodies that may bind and activate leukocytes intravascularly became implicated in the pathogenesis of TRALI.[33-35] Implementation of manufacturing practices that excluded multiparous females and other donors who appeared to increase the risk of TRALI in transfusion recipients has resulted in a significant reduction in TRALI cases.[36,37] Thus, TRALI provides a key example of an underappreciated transfusion complication that can result in significant morbidity and mortality and that, upon additional study, improved diagnostic criteria and changes in clinical practice, has dramatically reduced in incidence over time.[31]

Strategies to prevent delayed hemolytic transfusion reactions

The most effective way to prevent a DTHR is to avoid unnecessary RBC transfusion. When transfusion avoidance is not feasible, provision of the most compatible RBC units is recommended. In an effort to reduce the risk of DHTR, transfusion services keep records of previously identified alloantibodies in order to reduce the risk of re-exposure to a particular alloantigen once an alloantibody has been detected. Using this approach, hospital transfusion services provide RBC that are negative for the particular alloantigens against which a patient has previously made alloantibodies. However, when patients seek care in multiple healthcare systems this information is often not available.[38,39] In this setting, transfusion services can only rely on transfusion histories at the presenting facility or other facilities if obtainable, which are often either not obtained or incomplete.[38,39] As this approach often results in inadequate alloimmunization histories,[40] multiple encounters in different healthcare systems place patients with SCD at a significantly high risk of DHTR.[38] Furthermore, transfusions are often initiated when patients present with acute complications at centers where providers may not be familiar with SCD management, including transfusion complications. Implementation of healthcare-wide acute care plans for patients with SCD that include consideration of possible transfusion complications may provide the type of guidance needed to increase awareness among all providers within a healthcare system.

Nonetheless, despite effective communication between healthcare systems, alloantibodies may not be detected if antibody evaluations are not routinely completed following transfusion episodes that are at a higher risk of inducing alloantibodies. This reflects the ability of newly formed alloantibodies to fall below the level of detection prior to a subsequent transfusion evaluation, which may occur months to years later.[41] Thus, RBC alloantibody evanescence can contribute significantly to the risk of DHTR in the absence of systematic post-transfusion sero-

logical evaluation. To avoid these challenges, routine serological testing should be considered for all SCD patients 1 to 3 months after each transfusion episode.[42] Even with such a policy in place, up to 30% of DHTR with bystander hemolysis occur in the absence of any detectable alloantibody,[14,26] making it particularly difficult to predict and prevent these transfusion reactions fully.

Shared laboratory data between hospital systems is critical

Significant barriers to laboratory information exchange exist in many healthcare systems in many countries, and efforts that allow alloantibody identification histories of all patients (including those with SCD) to be shared between such systems must become a priority. This critical patient safety initiative would facilitate antibody identification in a patient's sample, would decrease the burden of identifying optimal RBC units when working with incomplete transfusion histories, would increase the timely provision of fully compatible RBC units, and would decrease the incidence of DHTR.[38,39] Currently, the lack of such data sharing prevents many transfusion services from knowing the transfusion requirements of newly encountered patients with SCD at the time of a transfusion request,[40] or from knowing the availability of compatible RBC once alloantibodies have been characterized.[11,43] If complex alloantibody profiles were known *a priori* and corresponding donor databases were available, compatible donor units could be readily identified, allowing transfusion requirements to be addressed in a more timely and safe manner.[38,39,44]

Routine post-transfusion antibody screening and HbA quantification should be considered to improve identification of red blood cell alloantibodies and delayed hemolytic transfusion reactions

Although additional studies are certainly needed to establish the incidence of DHTR in various hospital settings, more uniform detection of these reactions is important if future DHTR are to be avoided and if effective treatment strategies are to be implemented.[45] While patients may experience accelerated clearance of transfused RBC in the absence of clinical systems, to facilitate detection of clinically meaningful DHTR, we recommend that patients with SCD with a history of transfusion in the preceding 21 days who present with any complication requiring medical attention should be evaluated with an antibody screen regardless of whether or not another RBC transfusion is warranted. Using this approach, a higher percentage of alloantibodies that form as a result of a recent transfusion should be identified. However, as nearly 30% of DHTR have been reported to occur in the absence of detectable alloantibodies,[14,26] evaluation for DHTR will also require acquisition of HbA values following transfusion and at the time of clinical presentation of any complication requiring medical attention.[27] As episodic transfusions are much more likely to be initiated during acute complications and result in DHTR,[6,7,27] polices that include obtaining HbA values within 48 h following an episodic transfusion may be particularly helpful when interpreting a HbA value at the time of suspected DHTR. Thus, we recommend considering routine HbA measurements following any episodic RBC transfusion and an antibody screen and HbA measurement at the time of any hospital presentation within 21 days of the most recent episodic transfusion (Table 1).

Therapeutic options for ongoing delayed hemolytic transfusion reactions

In addition to facilitating more accurate diagnoses of DHTR, routine approaches aimed at identifying DHTR will allow consideration of more effective therapeutic options for ongoing DTHR; these therapies are particularly important to consider for DHTR involving hyperhemolysis. Erythropoietin and intravenous iron are often given to boost endogenous RBC production in a setting of severe anemia.[12] Plasmapheresis has also been attempted

---

Table 1. Recommendations for better prevention, more accurate diagnosis and improved treatment of delayed-type hemolytic transfusion reactions in sickle cell disease.

Prevention:
National and International
  1) RBC alloimmunization databases
  2) RBC donor databases

Institutional
  1) Reduce RBC alloimmunization through prophylactic matching for Rh (C/c, E/e) and K antigens.
  2) Judicious use of RBC transfusions
  3) Routine alloantibody evaluation for all patients with SCD within 1 to 3 months after each episodic transfusion (while rare, some alloantibodies may not be detectable within 3 months after transfusion)

Diagnosis:
Institutional
  1) Alloantibody screen for any SCD exacerbation within 21 days of transfusion (regardless of whether another transfusion is being considered)
  2) HbA quantification within 48 h following episodic transfusion and at the time of any SCD exacerbation occurring within 21 days of a transfusion

Treatment:
Institutional
  1) Supportive care (including erythropoietin and iron)
  2) Intravenous immunoglobin and corticosteroids
  3) Consideration of treatment with complement inhibitors in cases of severe DHTR (including those with hyperhemolysis)
  4) Consider rituximab prophylaxis in cases with a history of severe DHTR and only "least incompatible" blood can be sourced for transfusion.

RBC: red blood cell; SCD: sickle cell disease; HbA: hemoglobin A.

to reduce heme levels,[46] although the level of anemia and inability to transfuse may prevent this from becoming a realistic option in many patients. Intravenous immunoglobulin and corticosteroids may further reduce hemolysis in the setting of DHTR.[47] While characteristics of the transfused unit, such as RBC storage, may have an impact on transfusion outcomes in SCD,[48] recent studies suggest that exuberant complement activation may account for the most severe DHTR with accompanying hyperhemolysis.[49] Consistent with this, treatment of patients experiencing DHTR-associated hyperhemolysis with eculizumab, an anti-C5 complement-blocking antibody, has been shown to reverse complement activation, reduce hemolysis, and result in rapid clinical improvement.[49,50] While additional studies are needed, these reports hold promise and suggest that more effective treatment options that could significantly improve patients' care may be on the horizon (Table 1).

Avoiding additional RBC transfusion at the time of an ongoing DHTR with bystander hemolysis is recommended, as transfusion of even seemingly compatible RBC that are negative for all alloantigens that the patient is known to be alloimmunized against may worsen the ongoing hemolysis. If the alloantibody in question cannot be identified or if it is identified but compatible units cannot be allocated, alloantibody function tests can be ordered to assess the clinical significance of a patient's alloantibodies. This test typically involves evaluation of monocyte engulfment of antibody-coated cells *in vitro* as a read out of alloantibody function.[51] However, this approach is time-consuming, and may not provide timely results in an acute setting.[51] Should the clinical status of the patient necessitate consideration of a "least incompatible" RBC transfusion, rituximab prophylaxis has been described to reduce DHTR in small case reports.[52,53]

Summary

In conclusion, RBC alloantibodies and DHTR are not uncommon in patients with SCD. They are underappreciated and, in our opinion, are the single leading cause of transfusion-associated morbidity and mortality in this vulnerable population of patients. Many of the challenges associated with preventing and treating DTHR can be addressed by developing international and national RBC alloantibody databases, limiting RBC transfusions to situations that are evidence-based, implementing more accurate diagnostic strategies (through routine use of HbA quantification and standard antibody screening), better understanding the pathophysiology, and formally testing additional prophylactic and treatment approaches to prevent and treat these reactions. We urge our colleagues in hematology, transfusion medicine (from donor centers to transfusion services), laboratory information technology, funding agencies, and regulatory agencies to view RBC alloimmunization and DTHR in patients with SCD with a similar urgency as TRALI was viewed in past decades. Such a heightened awareness, and subsequent industry changes, are predicted to directly reduce the significant transfusion-associated complications that contribute to the current morbidity and mortality of patients with SCD.

Acknowledgments

References

1. Adams RJ, McKie VC, Hsu L, et al. Prevention of a first stroke by transfusions in children with sickle cell anemia and abnormal results on transcranial Doppler ultrasonography. N Engl J Med. 1998;339(1):5-11.
2. Platt OS. Prevention and management of stroke in sickle cell anemia. Hematology Am Soc Hematol Educ Program. 2006:54-57.
3. Howard J. Sickle cell disease: when and how to transfuse. Hematology Am Soc Hematol Educ Program. 2016;2016(1):625-31.
4. Drasar E, Igbineweka N, Vasavda N, et al. Blood transfusion usage among adults with sickle cell disease - a single institution experience over ten years. Br J Haematol. 2011;152(6):766-770.
5. Yazdanbakhsh K, Ware RE, Noizat-Pirenne F. Red blood cell alloimmunization in sickle cell disease: pathophysiology, risk factors, and transfusion management. Blood. 2012;120(3):528-537.
6. Vidler JB, Gardner K, Amenyah K, Mijovic A, Thein SL. Delayed haemolytic transfusion reaction in adults with sickle cell disease: a 5-year experience. Br J Haematol. 2015;169(5):746-53.
7. Habibi A, Mekontso-Dessap A, Guillaud C, et al. Delayed hemolytic transfusion reaction in adult sickle-cell disease: presentations, outcomes, and treatments of 99 referral center episodes. Am J Hematol. 2016;91(10):989-994.
8. Nickel RS, Hendrickson JE, Fasano RM, et al. Impact of red blood cell alloimmunization on sickle cell disease mortality: a case series. Transfusion. 2016;56(1):107-114.
9. Pirenne F, Yazdanbakhsh K. How I safely transfuse patients with sickle-cell disease and manage delayed hemolytic transfusion reactions. Blood. 2018;131(25):2773-2781.
10. Dean CL, Maier CL, Chonat S, et al. Challenges in the treatment and prevention of delayed hemolytic transfusion reactions with hyperhemolysis in sickle cell disease patients. Transfusion. 2019;59(5):1698-1705.
11. Vichinsky EP, Earles A, Johnson RA, Hoag MS, Williams A, Lubin B. Alloimmunization in sickle cell anemia and transfusion of racially unmatched blood. N Engl J Med. 1990;322(23):1617-1621.
12. Chou ST, Jackson T, Vege S, Smith-Whitley K, Friedman DF, Westhoff CM. High prevalence of red blood cell alloimmunization in sickle cell disease despite transfusion from Rh-matched minority donors. Blood. 2013;122(6):1062-1071.
13. Chou ST, Evans P, Vege S, et al. RH genotype matching for transfusion support in sickle cell disease. Blood. 2018;132(11):1198-1207.
14. Chou ST, Fasano RM. Management of patients with sickle cell disease using transfusion therapy: guidelines and complications. Hematol Oncol Clin North Am. 2016;30(3):591-608.
15. Fasano RM, Booth GS, Miles M, et al. Red blood cell alloimmunization is influenced by recipient inflammatory state at time of transfusion in patients with sickle cell disease. Br J Haematol. 2015;168(2):291-300.
16. Yazdanbakhsh K. Immunoregulatory networks in sickle cell alloimmunization. Hematology Am Soc Hematol Educ Program. 2016;2016(1):457-461.
17. Platt OS. Sickle cell anemia as an inflammatory disease. J Clin Invest. 2000;106(3):337-8.
18. Williams LA, 3rd, Lorenz RG, Tahir A, Pham HP, Marques MB. High percentage of evanescent red cell antibodies in patients with sickle cell disease highlights need for a National Antibody Database. South Med J. 2016;109(9):588-591.
19. Siddon AJ, Kenney BC, Hendrickson JE, Tormey CA. Delayed haemolytic and serologic transfusion reactions: pathophysiology, treatment and prevention. Curr Opin Hematol. 2018;25(6):459-467.
20. King KE, Shirey RS, Lankiewicz MW, Young-Ramsaran J, Ness PM. Delayed hemolytic transfusion reactions in sickle cell disease: simultaneous destruction of recipients' red cells. Transfusion. 1997;37(4):376-381.
21. Ibanez C, Habibi A, Mekontso-Dessap A, et

al. Anti-HI can cause a severe delayed hemolytic transfusion reaction with hyperhemolysis in sickle cell disease patients. Transfusion. 2016;56(7):1828-1833.

22. Talano JA, Hillery CA, Gottschall JL, Baylerian DM, Scott JP. Delayed hemolytic transfusion reaction/hyperhemolysis syndrome in children with sickle cell disease. Pediatrics. 2003;111(6 Pt 1):e661-665.

23. Michot JM, Driss F, Guitton C, et al. Immunohematologic tolerance of chronic transfusion exchanges with erythrocytapheresis in sickle cell disease. Transfusion. 2015;55(2):357-363.

24. Aygun B, Padmanabhan S, Paley C, Chandrasekaran V. Clinical significance of RBC alloantibodies and autoantibodies in sickle cell patients who received transfusions. Transfusion. 2002;42(1):37-43.

25. Diamond WJ, Brown FL Jr, Bitterman P, Klein HG, Davey RJ, Winslow RM. Delayed hemolytic transfusion reaction presenting as sickle-cell crisis. Ann Intern Med. 1980;93(2): 231-234.

26. Chadebech P, Habibi A, Nzouakou R, et al. Delayed hemolytic transfusion reaction in sickle cell disease patients: evidence of an emerging syndrome with suicidal red blood cell death. Transfusion. 2009;49(9):1785-1792.

27. Narbey D, Habibi A, Chadebech P, et al. Incidence and predictive score for delayed hemolytic transfusion reaction in adult patients with sickle cell disease. Am J Hematol. 2017;92(12):1340-1348.

28. Telen MJ, Afenyi-Annan A, Garrett ME, Combs MR, Orringer EP, Ashley-Koch AE. Alloimmunization in sickle cell disease: changing antibody specificities and association with chronic pain and decreased survival. Transfusion. 2015;55(6 Pt 2):1378-1387.

29. Carson JL, Triulzi DJ, Ness PM. Indications for and adverse effects of red-cell transfusion. N Engl J Med. 2017;377(13): 1261-1272.

30. Yomtovian R, Kline W, Press C, et al. Severe pulmonary hypersensitivity associated with passive transfusion of a neutrophil-specific antibody. Lancet. 1984;1(8371):244-246.

31. Shaz BH, Stowell SR, Hillyer CD. Transfusion-related acute lung injury: from bedside to bench and back. Blood. 2011;117(5):1463-1471.

32. Silliman CC, Boshkov LK, Mehdizadehkashi Z, et al. Transfusion-related acute lung injury: epidemiology and a prospective analysis of etiologic factors. Blood. 2003;101(2):454-462.

33. Looney MR, Su X, Van Ziffle JA, Lowell CA, Matthay MA. Neutrophils and their Fc gamma receptors are essential in a mouse model of transfusion-related acute lung injury. J Clin Invest. 2006;116(6):1615-1623.

34. Kapur R, Kim M, Rebetz J, Hallstrom B, et al. Gastrointestinal microbiota contributes to the development of murine transfusion-related acute lung injury. Blood Adv. 2018;2(13):1651-1663.

35. Semple JW, Rebetz J, Kapur R. Transfusion-associated circulatory overload and transfusion-related acute lung injury. Blood. 2019;133(17):1840-1853.

36. Chapman CE, Stainsby D, Jones H, et al. Ten years of hemovigilance reports of transfusion-related acute lung injury in the United Kingdom and the impact of preferential use of male donor plasma. Transfusion. 2009;49 (3):440-452.

37. Murphy MF, Navarrete C, Massey E. Donor screening as a TRALI risk reduction strategy. Transfusion. 2009;49(9):1779-1782.

38. Unni N, Peddinghaus M, Tormey CA, Stack G. Record fragmentation due to transfusion at multiple health care facilities: a risk factor for delayed hemolytic transfusion reactions. Transfusion. 2014;54(1):98-103.

39. Harm SK, Yazer MH, Monis GF, Triulzi DJ, Aubuchon JP, Delaney M. A centralized recipient database enhances the serologic safety of RBC transfusions for patients with sickle cell disease. Am J Clin Pathol. 2014;141(2):256-261.

40. Fasano RM, Branscomb J, Lane PA, Josephson CD, Snyder AB, Eckman JR. Transfusion service knowledge and immunohaematological practices related to sickle cell disease and thalassemia. Transfus Med. 2019;29(3):185-192.

41. Stack G, Tormey CA. Detection rate of blood group alloimmunization based on real-world testing practices and kinetics of antibody induction and evanescence. Transfusion. 2016;56(11):2662-2667.

42. Castro O, Oneal P, Medina A, Onojobi G, Gordeuk VR. Preventing delayed hemolytic transfusion reactions in sickle cell disease. Transfusion. 2016;56(11):2899-2900.

43. Dean CL, Maier CL, Roback JD, Stowell SR. Multiple hemolytic transfusion reactions misinterpreted as severe vaso-occlusive crisis in a patient with sickle cell disease. Transfusion. 2019;59(29):448-453.

44. Hauser RG, Hendrickson JE, Tormey CA. TRIX with treats: the considerable safety benefits of a transfusion medicine registry. Transfusion. 2019;59(8):2489-2492.

45. Mekontso Dessap A, Pirenne F, Razazi K, et al. A diagnostic nomogram for delayed hemolytic transfusion reaction in sickle cell disease. Am J Hematol. 2016;91(12):1181-1184.

46. Hayes C, Shafi H, Mason H, Klapper E. Successful reduction of plasma free-hemoglobin using therapeutic plasma exchange: a case report. Transfus Apher Sci. 2016;54(2): 253-255.

47. Gardner K, Hoppe C, Mijovic A, Thein SL. How we treat delayed haemolytic transfusion reactions in patients with sickle cell disease. Br J Haematol. 2015;170(6):745-756.

48. Karafin MS, Carpenter E, Pan A, Simpson P, Field JJ. Older red cell units are associated with an increased incidence of infection in chronically transfused adults with sickle cell disease. Transfus Apher Sci. 2017;56(3):345-351.

49. Dumas G, Habibi A, Onimus T, et al. Eculizumab salvage therapy for delayed hemolysis transfusion reaction in sickle cell disease patients. Blood. 2016;127(8):1062-1064.

50. Chonat S, Quarmyne MO, Bennett CM, et al. Contribution of alternative complement pathway to delayed hemolytic transfusion reaction in sickle cell disease. Haematologica. 2018;103(10):e483-e485.

51. Tong TN, Cen S, Branch DR. The monocyte monolayer assay: past, present and future. Transfus Med Rev. 2019;33(1):24-28.

52. Noizat-Pirenne F, Bachir D, Chadebech P, et al. Rituximab for prevention of delayed hemolytic transfusion reaction in sickle cell disease. Haematologica. 2007;92(12):e132-135.

53. Noizat-Pirenne F, Habibi A, Mekontso-Dessap A, et al. The use of rituximab to prevent severe delayed haemolytic transfusion reaction in immunized patients with sickle cell disease. Vox Sang. 2015;108(3): 262-267.

Hemophilia therapy: the future has begun

Pier Mannuccio Mannucci

Fondazione IRCCS Ca' Granda Ospedale Maggiore Policlinico, Angelo Bianchi Bonomi Hemophilia and Thrombosis Center, Milan, Italy

Ferrata Storti Foundation

ABSTRACT

The success story of hemophilia care first began in the 1970s, when the availability of plasma-derived concentrates of coagulation factor VIII (FVIII) and factor IX (FIX) provided efficacious treatment of bleeding in patients with hemophilia A and B. This positive scenario was consolidated in terms of greater safety and availability in the 1990s, when the first recombinant coagulation factors were produced. This meant that, instead of only treating episodic bleeding events, prophylaxis regimens could be implemented as a preventive measure. Following the demonstration of its superiority in the frame of two randomized clinical trials, prophylaxis became evidence-based standard of care. In high-income countries, these achievements have led to a patients' life expectancy being extended to close to that of the general male population. Alongside this, the last decade has witnessed further spectacular therapeutic progress, such as the availability of coagulation factors with a longer plasma half-life that allow for wider intervals between treatment. Moreover, new therapeutic products based on new mechanisms other than the replacement of the deficient factor, have become available (emicizumab) or are at an advanced stage of development. This review celebrates the success story of hemophilia care, while also discussing current limitations, issues and as yet unmet needs. The prospects of cure by means of gene therapy are also outlined.

Introduction

Among the more than 6,000 human diseases caused by single gene defects,[1] the plasma deficiencies of coagulation proteins are of great importance to the hematologist, entailing as they do a lifelong bleeding tendency with important morbidity and mortality if not adequately managed. Inherited coagulation deficiencies are rare diseases according to the definitions adopted in the United States (less than 200,000 cases nationwide) and Europe (less than 5 cases per 10,000 persons in the general population).[2] The hemophilias are clinically relevant rare diseases: hemophilia A (HA), which results from the deficiency or dysfunction of coagulation factor VIII (FVIII), and hemophilia B (HB) of factor IX (FIX). Both are due to mutations in genes located on chromosome X and thus largely affect males, with bleeding symptoms roughly proportional to the degree of factor deficiency in plasma. The main sites of spontaneous bleeding are joints and muscles, which, if inadequately treated, cause chronic damage to the musculoskeletal system resulting in severe handicaps and disability. Furthermore, trauma and surgical interventions are accompanied by uncontrolled bleeding.

A recent report on the worldwide distribution[3] shows that the hemophilias are more frequent than previously estimated: 17.1 cases per 100,000 males with HA for all degrees of FVIII deficiency, 3.8 cases per 100,000 of HB, with a prevalence of 6 per 100,000 for HA and 1.1 per 100,000 for HB of cases with complete plasma factor deficiency, and thus a more severe clinical phenotype (Table 1).[3] Inherited coagulation disorders are much rarer. These are due to defects in genes encoding other factors, such as fibrinogen, prothrombin, factors V, VII, X, XI and XIII.[4] The defective genes are transmitted with an autosomal recessive pattern of inheritance and thus affect both sexes at similar rates. Prevalence rates in the general population range between 1 case per 500,000 for the more frequent factor VII deficiency and 1 in 2-3 million for the rarest prothrombin and factor XIII deficiencies (Table 1).[4]

The natural history and clinical phenotype of rarer coagulopathies are less accu-

rately established than for the hemophilias, but, in general, they tend to be less clinically severe at the same level of plasma deficiency.[4,5] The inherited bleeding disorder von Willebrand disease (vWD) is not included among coagulation disorders because the primary defect is in the gene encoding the huge multimeric protein von Willebrand factor (vWF), essential for platelet-vessel wall interactions and the formation of the primary hemostatic plug.[6] However, in vWD, there is often the additional deficiency of coagulation FVIII secondary to the primary defect of vWF that functions as a physiological stabilizer of FVIII to which is complexed in blood, and thus explains mechanistically the secondary coagulation defect.[6] vWF is encoded by a large gene on chromosome 12 (band 12p13.31), and vWD is transmitted as an autosomal dominant trait or as a recessive trait in the most severe and rarest type 3 (prevalence: 1 in 1-2 million).[6] The prevalence in the general population of clinically relevant cases is similar to that of HA,[7] although mild vWF deficiencies of little clinical significance are much more frequent in the frame of population studies.[8] In general, most patients with vWD are less severely affected clinically than those with the hemophilias, but they suffer more frequently from bleeding from mucosal tracts, such as epistaxis, menorrhagia, and gastrointestinal bleeding.[6] Soft tissue bleeding, such as hemarthrosis and postoperative hemorrhages, is only frequent in cases associated with moderately severe FVIII deficiency, i.e. type 3 vWD.[6]

Besides this general background on the inherited coagulation disorders, in this article it will be emphasized that, in the last decade, there has been tremendous progress in the available therapeutic armamentarium, particularly for patients with the hemophilias. Recent review articles show the progress regarding rare coagulation disorders and vWD.[5,9]

Early therapeutic progress in hemophilia

One hundred years ago, at the time when Haematologica was first published, there was practically no treatment for the hemophilias or for the other inherited coagulation disorders. Whole blood was the only treatment approach available and this was of poor clinical efficacy (Figure 1), such that the life expectancy of hemophiliacs was 10-15 years, even in the most favorable circumstances. The few cases that survived were compromised by severe musculoskeletal damage that confined them to bed or to a wheelchair, and ice, analgesics and splinting were the only measures that could be used to alleviate

Table 1. Prevalence of inherited deficiencies of coagulation proteins and corresponding encoding genes and chromosomes.

Protein	Case prevalence in the general population*	Gene and chromosome
Fibrinogen	1 in 1 million	*FGA, FGB* (4q31.3), *FGG* (4q32.1)
Prothrombin	1 in 2 million	*F2* (11p11.2)
Factor V	1 in 1 million	*F5* (1q24.2)
Factor VII	1 in 500,000	*F7* (13q34)
Factor VIII	6 in 100,000 males	*F8* (x928)
Factor IX	1 in 100,000 males	*F9* (x927.1)
Factor X	1 in million	*F10* (13q34)
Factor XI	1 in 1 million	*F11* (4q35.2)
Factor XIII	1 in 3 million	*F13A1* (6p25.1) *F13B* (1q31.3)

*Prevalences refer to the severe forms of the diseases due to homozygous or compound heterozygous gene mutations.

- Ice
- Splinting
- Bed rest

Blood transfusion

Plasma

Cryo-precipitate

- Plasma derived FVIII and FIX concentrates
- DDAVP

- Viral inactivation or removal
- Cloning of FIX and FVIII genes

- APCC
- rFVIII
- rFIX
- rFVIIa

Consolidation decade

- Extended half life FVIII & FIX
- Non-factor replacement therapies
- Gene therapy in development

1920s 1930s 1940s 1950s 1960s 1970s 1980s 1990s 2000s 2010s

rFVIII = recombinant FVIII; **rFIX** = recombinant FIX; **rFVIIa** = activated recombinant FVII; **APCC** = activated prothrombin complex concentrates.

Figure 1. Progress in hemophilia therapy. Each decade of the last and current century features the main weapons available at the time for the treatment of patients with hemophilia. Each column represents a decade.

pain and other symptoms associated with joint and muscle bleeding (Figure 1). The second World War and related combat casualies were triggers for the improved preparation of plasma, that contains all the coagulation factors (Figure 1). However, this form of replacement therapy was not widely available and of limited clinical efficacy. So, even until the 1960s, the life expectancy of patients with hemophilia was no more than 20-30 years.

A first step forward was the demonstration in 1964 by Judith Pool that cryoprecipitation of fresh-frozen plasma was able to concentrate FVIII (and also vWF and fibrinogen) in the pellet (Figure 1). But the most significant advance was seen in the 1970s with the industrial manufacturing and commercial availability of freeze-dried plasma concentrates of FVIII for HA and of the coagulation factors (II, VII, IX, X) of the so called prothrombin complex (PCC) for HB and the corresponding rare coagulopathies (Figure 1). The main advantages of these products was storage in simple refrigerators, reconstitution in small amounts of fluid, and no need for a drip to administrate blood, plasma and cryoprecipitate. Their availability, at least in European and North American countries and Japan, was the success story of the 1970s because they allowed home care and self-treatment. Some countries, such as Sweden, were also pioneers in using these products to develop prophylactic treatment of hemorrhages instead of only treating episodic bleeding events.[10] Our demonstration in 1977 that the synthetic drug desmopressin (DDVP) was clinically efficacious as a non-transfusional form of FVIII replacement in mild HA and vWD contributed to further progress in the field.[10]

However, the 1980s threw a dramatic shadow on this favorable scenario when a large proportion of patients treated with factor produced from very large plasma pools developed serious or fatal blood-borne viral infections such as hepatitis and HIV/AIDS.[11] Fortunately, this gloomy decade was accompanied by rapid progress in molecular medicine that not only clarified the genetic basis of the coagulation defects but also, and most importantly, led to the therapeutic production in the 1990s of recombinant coagulation FVIII and IX (Figure 1). Moreover, the addition of virucidal or virus-removal steps to the manufacturing process made plasma-derived coagulation products safer, such that no bloodborne viral infections have been reported since the late 1980s - early 1990s.[11] The wider availability of safer and more effective therapies for hemophilia care attracted more attention among researchers and resulted in progress in what had so far been the rather hopeless management of a dire complication of HA: the development in at least one-third of patients of alloantibodies that make them refractory to replacement therapy, because the coagulant activity contained in FVIII replacement products is neutralized by specific inhibitors (and more rarely for FIX).[11,12] In the late 1990s, plasma concentrates of activated factors of the prothrombin complex (APCC), as well as the production of activated factor VII (rFVIIa) by recombinant DNA technology, offered novel ways to bypass the coagulation defect associated with FVIII inhibitors, and thus to improve the management of acute bleeding and surgical interventions (Figure 1).[11,13] It was also demonstrated that inhibitory alloantibodies could be eradicated in approximately two-thirds of cases through the induction of immune tolerance (ITI) by means of the long-lasting and highly expensive administration of large doses of plasma-derived or recombinant FVIII prod-

ucts, so that successful patients could resume replacement therapy and prophylaxis with efficacious outcomes.[14,15] All this progress improved not only the pattern and quality of patients' lives, but also led to substantial changes in their life expectancy, achieving figures very close to those of males without hemophilia in the general population;[16-18] the figures are particularly encouraging if the ravages of the early years of uncontrolled HIV infection and AIDS are excluded.[3,17] The late 1990s and the whole first decade of the third millennium were years of consolidation and relatively slow progress (Figure 1), mainly characterized by the refinement of recombinant factors. There was a continuous improvement in the purity of these products, and the use of animal and human proteins during manufacturing and in the final formulation was avoided.

With this optimistic scenario of hemophilia care and of patients' life-expectancy, particularly in comparison with other monogenic diseases such as cystic fibrosis, thalassemia and muscular dystrophy, in the first decade of the new millennium efforts were mainly addressed to the formidable and still unresolved challenges of the global availability and affordability of replacement therapy and to the more widespread implementation of prophylaxis.[19-21] On the other hand, relatively little effort has been made to develop new therapeutic products. In contrast, multiple new therapies designed to address the challenges and the gaps in the standard treatments are now being developed.

Recent progress in hemophilia therapy

Prophylaxis as standard of care

Primary prophylaxis of bleeding episodes became the evidence-based standard of care following the randomized clinical trial of Manco-Johnson *et al.*,[22] who demonstrated that this preventive regimen was clearly superior to the episodic management of bleeds, because it reduced the rate of their occurrence and also achieved a marked reduction in joint damage. A subsequent randomized study by Gringeri *et al.*[23] confirmed and strengthened this evidence, so that prophylaxis became the undisputed standard of care in countries that could afford it. Additional and important advantages were a much improved patient quality of life, including less hospitalizations and days lost from school and work, and an improved social life. However, the implementation of prophylaxis met some obstacles,[20,21] in addition to that of affordability.[24] The degree of adherence was often less than optimal, particularly in children and adolescents, owing to the burden created by the need of 2-3 or more weekly intravenous injections. This not only interfered with the patients' quality of life, but also created problems of vein access, with the related frequent need to resort to ports or other central venous access devices.[20,21]

Extended plasma half-life coagulation factors

Frequent intravenous injections are necessary due to the relatively short plasma half-life of replaced coagulation factors (range 10-14 hours for FVIII, 18-22 hours for FIX). Thus, starting from the 2010s, attempts were made to engineer these factors by recombinant technology, with the goal of obtaining medications that remained in the circulation longer and thus reducing the number of intravenous injections. Two main techniques were introduced: (i) coagulation factor fusion to proteins like the Fc part of

IgG1 or albumin;[25,26] and (ii) conjugation with chemicals such as polyethylene glycol (PEG).[27,28] The mechanism whereby albumin and Fc fusion prolongs the plasma half-life of coagulation factors is through the neonatal Fc receptor,[25,29] which recycles them in plasma and thereby prolongs their effective circulation.[29] PEG, attached randomly or site-specifically to coagulation factors, acts by slowing their degradation and renal elimination.[27,28]

Two extended half-life (EHL) recombinant coagulation factors were licensed in 2014: the Fc-fused FIX eftrenonacog alfa and the Fc-fused FVIII efmoroctocog alfa.[30,31] Subsequently, other EHL FVIII and FIX products were clinically evaluated, licensed and marketed (Tables 2 and 3), so that three pegylated FVIII products plus an albumin fusion and a pegylated FIX product, in addition to the two Fc- fusion products, are now available.[32-40] FIX products can prolong the plasma half-life by from 4- to 5-fold (Table 3), whereas the half-life of FVIII can still be prolonged by no more than 1.5-1.7 fold (Table 2) due to its dependence on the half-life of its chaperone vWF to which it is complexed in blood. Pivotal clinical studies, conducted in highly selected adults and children, showed that these products were efficacious in stopping or preventing bleeding in the frame of episodic and prophylactic treatment regimens, and that they could also be used to safely manage surgical interventions.[32-40]

The median annualized bleeding rate (ABR), the parameter most commonly used to evaluate the clinical efficacy of antihemophilic products, ranged from 1 to 4 episodes, accumulating all the different prophylactic dosing regimens evaluated clinically for FVIII products.[41] These ABR values compare favorably with those much higher values obtained with episodic regimens, ranging from 18 to 41.[41] For EHL FIX products, the ABR had a similar range of values with different prophylaxis regimens.[31,40] In practice, EHL FVIII products can be effectively administered twice instead of thrice weekly, but most patients are not satisfactorily protected from bleeds with weekly dosing regimens.[41] EHL FIX products are much more satisfactory, because they can be given every 10 or even 15 days,[42] and thus allow a lower annual burden of intravenous injections, the average reduction being more prominent (~60%) than for FVIII products (~30%) (Figure 2). Furthermore, higher trough levels of both FVIII (2-3%) and FIX (5-10%) could be achieved than with SHL products,[41,42] and there was, in general, a lower annual consumption in units of EHL products.[41,42] From a practical clinical standpoint these considerations broadly apply to all the different products, and these may be considered equivalent in terms of efficacy at a time when no face-to-face comparative clinical study is available. The market price of all these products is usually higher, but there are exceptions in countries where the price per unit of EHL FVIII is very close to that of SHL FVIII.

A few limitations warrant our attention. Despite higher trough plasma factor levels, the ideal goal of avoiding all

Table 2. Extended half-life factor VIII products.

Engineered protein	Year of first licensing	Manufacturer	Plasma half-life (hours)	Half-life prolongation*
Efmoroctocog alfa	2014	Biogen/Sobi	19	1.5-1.7
Rurioctocog alfa pegol	2015	Baxalta/Takeda	14.3	1.3-1.5
Danoctocog alfa pegol	2018	Bayer	19	1.6
Turoctocog alfa pegol	2019	Novo Nordisk	18.4	1.6

*Calculated from an average plasma half-life of standard coagulation FVIII of approximately 12 hours.

Table 3. Extended half-life factor IX products.

Engineered protein	Year of first licensing	Manufacturer	Plasma half-life (hours)	Half-life prolongation*
Efrenonacog alfa	2014	Biogen/Sobi	82	4.3
Albutrepenonacog alfa	2016	CSL Behring	101	5.3
Nonacog beta pegol	2017	Novo Nordisk	93	4.9

*Calculated from an average plasma half-life of standard FIX products of approximately 19 hours.

FVIII products	FIX products
Reduction of infusion number: **30%**	Reduction of infusion number: **60%**
Trough levels: **2-3 IU/dL** *Patients with severe hemophilia A are converted to a moderate phenotype*	Trough levels: **5-10 IU/dL** *Patients with severe hemophilia B are converted to a mild phenotype*
Half-life: **1.3-1.7 fold increase**	Half-life: **4-6 fold increase**
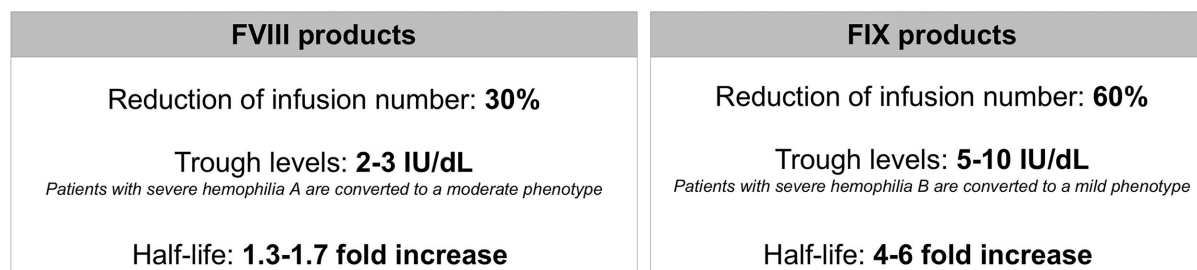
Figure 2. Summary features of Factor VIII and Factor IX products with an extended half-life. Comparative main characteristics of the extended half-life coagulation factor products (left FVIII, right FX), including the percentage reduction of the annual infusion number compared with the standard half-life products, trough plasma factor levels that can be achieved, expected changes in the clinical phenotype the range of increase of plasma half-life.

spontaneous bleeds was achieved in no more than 30-40% of cases in the prophylaxis dosing regimens evaluated in the pivotal studies, even though higher rates of zero bleeding were often obtained in the extension studies through the personalization of the dosing regimens.[41] Because these products have only been marketed for six years or less, no evaluation of long-term, real-life experience has yet been made. No theoretical concerns regarding a higher rate of inhibitor development with these highly engineered coagulation factors were raised in the pivotal studies,[41] although only previously-treated patients at low risk of developing this complication were enrolled. It remains to be seen whether or not this risk is smaller, equal or higher than that of the SHL recombinant or plasmatic products in high-risk patients, i.e. those not previously treated with any source of FVIII and thus with no tolerance of this moiety. Finally, four of the seven currently marketed EHL products use an exogenous chemical such as PEG. Pegylation has been safely used to prolong the length of time medication remains in the circulation in several products, e.g. epoietin, interferon, the human growth factor, and many others.[28] The amount of PEG used to prolong the half-life of FVIII, present in tiny amounts in plasma, is the smallest among all the pegylated medications, but, as yet, this does not apply for FIX.[43] On the other hand, none of the currently licensed pegylated medications is administered lifelong from birth, a unique situation for antihemophilic factors. For the moment, in contrast to the US Food and Drug Administration (FDA), the European Medicines Agency (EMA) has chosen to restrict the use of most pegylated coagulation factors to patients over the age of 12 years.

Non-factor therapies

In spite of the progress made with the availability of EHL factors, unmet needs remained. In HA patients without inhibitors, the reduction in the frequency of intravenous injections was not considered satisfactory,[41,42] and therapy still based on the need for a venous access continued to be unattractive. HA patients with FVIII inhibitors remained poor candidates for prophylaxis that could only be provided by bypassing products such as APCC and rFVIIa that are very expensive[44] and difficult to administer on a regular preventive basis. With these drawbacks in mind, therapeutic approaches that were not based on the replacement of the deficient factor were developed. This took place in two main ways: (i) for HA, by mimicking the coagulant activity of FVIII; and (ii) for both HA and HB, by increasing defective thrombin formation through the inhi-

bition of the naturally occurring anticoagulants (antithrombin, tissue factor pathway inhibitor, and activated protein C). For the moment, only the monoclonal antibody emicizumab that mimics FVIII activity has been licensed and marketed. The approach of quenching the anticoagulant pathways, potentially applicable not only to both the hemophilias but also to all the inherited coagulation disorders, is currently undergoing an advanced stage of clinical development, but since no product has been licensed yet, here this will receive less attention than emicizumab.

Emicizumab

This bispecific monoclonal antibody supports the spatial interaction between activated FIX (FIXa) and factor X, and thereby promotes thrombin formation by mimicking FVIIIa activity regardless of FVIII deficiency and the presence of FVIII inhibitors.[45] Administered subcutaneously, this drug reaches a steady state with a long plasma half-life that allows well-spaced dosing intervals of at least every week or even every two weeks.[46,47] It was first licensed in 2017 in the USA, and then in Europe and Japan, for the prophylaxis of bleeding in adults and pediatric patients with HA, with and without inhibitors. The first two pivotal studies were carried out in patients with FVIII inhibitors: HAVEN 1 in adults and adolescents,[48] and HAVEN 2 in pediatric patients under 12 years of age.[49] Using various dosing regimens and intervals between the subcutaneous injections, both the studies found that the ABR ranged between 0.2 and 2.9, values that compare favorably with those observed in inhibitor patients not on prophylaxis (Table 4). The rate of zero bleeding events ranged between 63% and 90%, the highest rate being obtained in HAVEN 2 when the medication was given at a dosage of 3 mg/Kg of body weight every two weeks (Table 4). These results are impressive if one considers that, until now, HA patients with FVIII inhibitors have been poor candidates for a feasible prophylaxis of bleeding, because attempts to use aPCC or rFVIII were jeopardized by the need for very frequent intravenous injections, let alone the very high costs.[44] Following the striking results obtained in HAVEN 1 and 2, emicizumab has also been evaluated in HA patients without inhibitors.[50,51] In the HAVEN 3 study, previously treated adult patients were assigned to subcutaneous emicizumab administered weekly or even every two weeks; study participants had much lower ABR than those not on prophylaxis (1.5 and 1.3 *vs.* 38.2) and much higher rates of zero bleeds (50% and 40% *vs.* 0%) (Table 4).

Table 4. Bleeding rates observed with different emicizumab dosing regimen(s) in patients with hemophilia A with and without inhibitors in the context of the HAVEN studies.

STUDY	DOSING REGIMEN	ABR (MEDIAN)	ZERO BLEEDING RATES
HAVEN 1	1×W prophylaxis (1.5 mg/kg) (n = 35)	2.9	63%
	No prophylaxis (n = 18)	23.3	6%
HAVEN 2	1×W prophylaxis (1.5 mg/kg) (n = 68)	0.3	76.9%
	E2W prophylaxis (3.0 mg/kg) (n = 10)	0.2	90%
	E4W prophylaxis (6 mg/kg) (n = 10)	2.2	60%
HAVEN 3	1×W prophylaxis (1.5 mg/kg) (n = 36)	1.5	50%
	E2W prophylaxis (3.0 mg/kg) (n = 35)	1.3	40%
	No prophylaxis (n = 18)	38.2	0
HAVEN 4	E4W prophylaxis (6 mg/kg) (n = 41)	4.5[a]	NR

ABR: annualized bleeding rate; NR: not reported; 1×W: once weekly; E2W: every 2 weeks; E4W: every 4 weeks. [a]Median ABR during the expansion phase.

All in all, the main benefit of this first non-factor replacement antihemophilic medication is the feasibility of regular prophylaxis in patients with inhibitors, using the advantageous and user-friendly subcutaneous administration route at weekly intervals or even less frequently. The high cost of emicizumab is an issue, but all the products used so far to manage patients with inhibitors are very expensive, including the traditional bypassing agents and immune tolerance inductions (ITI). Furthermore, the licensing of emicizumab also for HA patients without inhibitors is an important alternative to the currently available options of SHL and EHL coagulation factors, with the advantage of the subcutaneous instead of the intravenous route of administration. Efficacy parameters, such as the ABR and the zero bleeding rates, appear to be better than those obtained with the EHL FVIII products, but since there have still not been any face-to-face comparison studies between replacement and non-replacement products, this impression stems from indirect data.

A potential but still unexplored approach is the use of this non-FVIII product in young, previously untreated patients (PUP) with severe HA who, at high risk of developing inhibitors following exposure to FVIII replacement, might be able to avoid this complication. Another definite advantage is the subcutaneous route of administration, which would promote early prophylaxis without the need for venous ports. Emicizumab may also help to prevent the intracranial hemorrhages that are relatively frequent in the early years of life. Potential disadvantages may materialize in cases in which FVIII replacement is required to prevent or treat breakthrough bleeds, because the delayed FVIII inhibitors may develop in dangerous, high-risk circumstances, such as at the time of major trauma or surgery. Thus, the use of emicizumab in PUP is still a subject of debate and warrants a specific study to evaluate the forementioned advantages and disadvantages of this approach.

Other unanswered questions and causes for concern remain (Table 4). It is still not known whether or not the FVIII-mimicking activity of emicizumab provides the same physiological benefits of the bona fide coagulation factor, such as the long-term preservation of joint and bone health and the optimal support of wound healing.[52] In pivotal studies, a few patients developed thrombotic microangiopathies and other thromboses when inhibitor patients had a bleeding episode and were concomitantly treated with large and frequent doses of APCC.[48] At least 23 deaths have been associated with the use of emicizumab, mostly in patients with inhibitors, but also in some without. The deaths occurred both in the context of the pivotal clinical studies and as a result of the expanded access, compassionate and post marketing use, as reported by the manufacturer[53] and by the FDA Adverse Events Reporting System (FEARS).[54] As emphasized by Aledort,[55] more information on causality or chance association is needed to dissipate the uncertainty that surrounds these cases among consumers and care-givers.

Other non-factor therapies

Medications with mechanisms of actions other than that of emicizumab, and also mainly administered subcutaneously, are currently at an advanced stage of clinical development. Concizumab, a monoclonal antibody against the anticoagulant protein TFPI, increases the potential for thrombin generation.[56,57] A trend towards lower bleeding rates was observed in patients with HA and HB with and without inhibitors, but the cases were too few to provide robust evidence of efficacy. Another anti-TFPI monoclonal antibody is PF-06741086, currently undergoing a phase II trial (NCT02974855).[58] Fiturisan is a compound that interferes with RNA, and that decreases the plasma concentrations of antithrombin.[59,60] In early clinical studies, this agent, given subcutaneously at progressively higher dosages and even at monthly intervals, was accompanied by the progressive decrease in plasma antithrombin paralleled by an increase in thrombin generation and reduction of the ABR. Phase III studies of fiturisan in patients with severe HA and HB with and without inhibitors are at the advanced phase of development,[61,62] but the drug is as yet not licensed for clinical use. A fatal thrombotic event that occurred in 2017 in a patient with severe HA during a phase II study[63] led to the FDA temporarily stopping the study, but some protocol and guideline changes have allowed it to be restarted and to move this product forward to phase III studies; these are currently ongoing. On the whole, it is still too early to truly understand the role of these additional non-factor products in the scenario of hemophilia care, but potential advantages are their use not only in HA but also in HB and other inherited coagulation disorders, with or without inhibitors. Another advantage is that they can be administered at intervals that are as widely spaced as once a month.[59,60]

Gene therapy

As we have seen, within the already positive scenario that developed at the beginning of the third millennium in terms of almost normal life expectancy, a new era of huge innovation in hemophilia therapy is currently underway.[64] A recent study attempted to identify the main players involved in this almost miraculous progress. These include outstanding and dedicated physician-scientists, patient advocates and consumer organizations, but also more and more pharmaceutical companies involved in the hemophilia market.[64] With this background, are there still reasons and incentives for further progress? The main thrust stems from patients, who want to be cured! For them, cure means to be free of spontaneous bleeds, because the ideal zero rate has not been fully achieved with the available weaponry.[65] Thus, the ideal goal is gene therapy, preferably with a single therapeutic intervention of life-long duration.

The first vector associated with curative gene transfer in animal models of hemophilia was the adeno-associated virus (AAV), and, so far, AAV vectors are the only tools used to achieve therapeutic levels of FVIII and IX in hemophilia patients.[66-70] Historically, the first study involved ten patients with severe HB at the Royal Free Hospital in London, UK, who received single but increasing doses of an AAV8 vector, some of them with a current follow up of 9-10 years.[71,72] They continue to have stable expression of the transgene, with plasma levels ranging from 2% to 5%, and a 90% reduction in bleeding episodes.[72] Among the six additional ongoing studies in HB,[73] impressive results were obtained in the SPK-9001 phase I-II study, of particular interest because it used an AAV8 vector expressing the gain-of-function FIX Padua gene mutation.[74] The 15 patients who received a single infusion of this vector attained mean plasma levels of FIX of 33.7% (range 14.3-76.8%) over a period of at least 52 weeks.[74] According to

the manufacturers, in the SPK-9001 study, a single vector infusion was accompanied by a 98% reduction in the ABR;[75] this has led to a pivotal phase II study, which is currently undergoing.[76] Satisfactory plasma FIX levels were also obtained in the phase I-II studies BAX335 and AMT-060, using an AAV8 vector.[76-78] In both studies, FIX levels remained stable for 2-3 years and ABR were reduced, such that a phase III AMT-061 study has begun. On the whole, at least 56 HB patients have been treated with various serotypes of AAV vectors (mainly AAV5 and AAV8), and long-term expression of the transgene was obtained after a single intravenous infusion of the vector.[73]

The use of gene transfer was initially slower in HA, due to the much larger size of the FVIII gene that made it difficult to pack the corresponding cDNA in AAV vectors. This problem was tackled by using a B-domain delated human FVIII cDNA endowed with a liver-specific promoter.[79,80] Striking clinical results in HA were first published in 2017 using increasing dosages of the vector AAV5-hFVIII-SQ (valoctogene roxaparvovec).[81] One year after a single administration, median FVIII in plasma was 77% and ranged from 19 to as high as 164%.[81] Importantly, the mean ABR decreased by 97% from previous values. According to a recent update of the results obtained in 13 patients at year 2 after gene transfer,[82] two of them had normal plasma FVIII levels (52% and 86%), ten had values within the range of mild HA (from 6% to 38%), and one had levels (4%) compatible with moderate HA. All these patients had experienced a dramatic reduction in the incidence of bleeds, in spite of the fact that they had stopped FVIII prophylaxis. These excellent results were substantially maintained in the eight patients who were also evaluated at year 3 after gene transfer.[82] Additional patients are currently being recruited into a phase III trial, which has set three ambitious goals: (i) enrollment of 130 patients; (ii) to obtain stable FVIII levels of at least 40%; and (iii) to demonstrate superiority over the traditional therapies. At least five additional trials of gene therapy for HA are currently ongoing using various AAV serotypes as vectors. The results available so far confirm the efficiency and durability of AAV-mediated gene therapy. However, at the moment, maximum follow up is no longer than 1.5 years,[73] and, as for all new therapeutic developments, long-term follow up is still required to firmly consolidate the safety profile.

There are still important problems and issues that need to be resolved before licensing procedures and availability of gene therapy for the hemophilias can be carried forward. Only adult patients have been enrolled in studies so far, because in pediatric patients, the active dividing hepatocytes of children mean that there is no guarantee of achieving a persistent expression of a non-integrating vector, such as AAV. On the other hand, the long-term expression that followed a single vector infusion in the first UK-based FIX-deficient patients is surprising, because, according to the physiological turnover rate of hepatocytes (10% per year in adults), a transgene expression drop by 50% should have occurred within the first five years of treatment. Thus, some degree of integration of the transgene has perhaps taken place in the host DNA, with a theoretical risk of genotoxicity and cancer development.[83,84] Only liver biopsies can truly establish the fate of the AAV genome, and to what extent it is episomal or DNA integrated.[85,86] Liver biopsies would also be useful to establish the histological consequences of the most significant adverse effect observed so far in practically all the gene transfer studies, that is, a dose-dependent increase in transaminases that was controlled by means of short periods of corticosteroid administration.[73,87] It remains to be established whether or not these flares of hepatocyte cell necrosis, called inappropriately "transaminitis", are causing chronic liver damage. Normally in the context of AAV only a small percentage of the hepatocytes are stably transduced and responsible for long-term expression (in a serotype and dose-dependent manner). However, liver biopsies are not necessary informative on the either acute (transient transaminitis) or histological changes if the results are "normal" or negative. Moreover, follow up beyond 2-3 years is still awaited for most studies, so it is not clear how long transgene expression is going to be maintained. This is important, because immune reactions to the AAV capsid lead to the formation of neutralizing antibodies that prevent effective repeat of vector delivery, at least with the same AAV serotype.[73,87] Moreover, there are still no models of payment for gene therapy in hemophilia. BioMarin, the California-based pharmaceutical company that sponsored the forementioned study of gene transfer in HA,[81,82] recently declared to the Wall Street Journal that, once licensed, they are planning to price their product (brand name: Valrox) between 2 and 3 million dollars. This would make it the most expensive medication in the world, even more expensive than the current 'leader' Zolgensma, priced at 2.1 million dollars for patients with spinal muscular dystrophy.

Once these challenges to gene therapy in the hemophilias are solved, for a number of reasons, this is likely to become the treatment of choice. Despite the major advances in prophylaxis obtained with EHL factor products and non-factor therapies, breakthrough bleeding has still not been fully eliminated, and treatment is still invasive, both physically and psychologically, even when the subcutaneous route of administration is used. Patients with severe hemophilia live with the risk of bleeding every day of their lives, and no repeated dosing regimen will be able to replace the advantages of a one-off lifetime cure. Finally, we should not forget that 70% of patients worldwide have no treatment, either because nothing is available or because they cannot afford it; life expectancy at birth for these patients is still only ten years or less! The World Federation of Hemophilia has been attempting to tackle this formidable problem since its foundation in 1967, but despite great progress in medium-income countries, the great majority of low-income countries are still in the same situation they were in 100 years ago: ice, splinting, bed rest, and blood transfusions when available!

References

1. Jackson M, Marks L, May GHW, Wilson JB. The genetic basis of disease. Essays Biochem. 2018;62(5):643-723.
2. Khosla N, Valdez R. A compilation of national plans, policies and government actions for rare diseases in 23 countries. Intractable Rare Dis Res. 2018;7(4):213-222.
3. Iorio A, Stonebraker JS, Chambost H, et al. Establishing the prevalence and prevalence at birth of hemophilia in males: a meta-analytic approach using national registries. Ann Intern Med. 2019;171:540-546.
4. Palla R, Peyvandi F, Shapiro AD. Rare bleeding disorders: diagnosis and treatment. Blood. 2015;125(13):2052-2061.
5. Menegatti M, Peyvandi F. Treatment of rare factor deficiencies other than hemophilia. Blood. 2019;133(5):415-424.
6. Leebeek FW, Eikenboom JC. Von

Willebrand's disease. N Engl J Med. 2016; 375(21):2067-2080.

7. Sadler JE, Mannucci PM, Berntorp E. Impact, diagnosis and treatment of von Willebrand disease. Thromb Haemost. 2000;84(2):160-174.

8. Rodeghiero F, Castaman G, Dini E. Epidemiological investigation of the prevalence of von Willebrand's disease. Blood. 1987;69(2):454-459.

9. Mannucci PM. New therapies for von Willebrand disease. Blood Adv. 2019;3(21): 3481-3487.

10. Mannucci PM, Ruggeri ZM, Pareti FI, Capitanio A. 1-Deamino-8-d-arginine vasopressin: a new pharmacological approach to the management of haemophilia and von Willebrands' diseases. Lancet. 1977 23;1 (8017):869-872

11. Peyvandi F, Garagiola I, Young G. The past and future of haemophilia: diagnosis, treatments, and its complications. Lancet. 2016;388(10040):187-197.

12. Wight J, Paisley S. The epidemiology of inhibitors in haemophilia A: a systematic review. Haemophilia. 2003;9(4):418-435.

13. Rocino A, Franchini M, Coppola A. Treatment and prevention of bleeds in haemophilia patients with inhibitors to factor VIII/IX. J Clin Med. 2017;6(4): E46.

14. DiMichele DM, Hoots WK, Pipe SW, Rivard GE, Santagostino E. International workshop on immune tolerance induction: consensus recommendations. Haemophilia. 2007;13 (Suppl 1):1-22.

15. Hay CR, DiMichele DM; International Immune Tolerance Study. The principal results of the International Immune Tolerance Study: a randomized dose comparison. Blood. 2012;119(6):1335-1344.

16. Plug I, Van Der Bom JG, Peters M, et al. Mortality and causes of death in patients with hemophilia, 1992-2001: a prospective cohort study. J Thromb Haemost. 2006;4(3): 510-516.

17. Darby SC, Kan SW, Spooner RJ, et al. Mortality rates, life expectancy, and causes of death in people with hemophilia A or B in the United Kingdom who were not infected with HIV. Blood. 2007;110(3):815-825.

18. Tagliaferri A, Rivolta GF, Iorio A, et al. Mortality and causes of death in Italian persons with haemophilia, 1990-2007. Haemophilia. 2010;16(3):437-446.

19. Carcao MD, Aledort L. Prophylactic factor replacement in hemophilia. Blood Rev. 2004;18(2):101-113.

20. Bolton-Maggs PH. Optimal haemophilia care versus the reality. Br J Haematol. 2006; 132(6):671-682.

21. Saxena K. Barriers and perceived limitations to early treatment of hemophilia. J Blood Med. 2013;4:49-56.

22. Manco-Johnson MJ, Abshire TC, Shapiro AD, et al. Prophylaxis versus episodic treatment to prevent joint disease in boys with severe hemophilia. N Engl J Med. 2007;357 (6):535-544.

23. Gringeri A, Lundin B, von Mackensen S, Mantovani L, Mannucci PM; ESPRIT Study Group. A randomized clinical trial of prophylaxis in children with hemophilia A (the ESPRIT Study). J Thromb Haemost. 2011;9 (4):700-710.

24. Chen SL. Economic costs of hemophilia and the impact of prophylactic treatment on patient management. Am J Manag Care. 2016;22(5 Suppl):s126-133.

25. Dumont JA, Liu T, Low SC, et al. Prolonged activity of a recombinant factor VIII-Fc fusion protein in hemophilia A mice and

dogs. Blood. 2012;119(13):3024-3030.

26. Schulte S. Innovative coagulation factors: albumin fusion technology and recombinant single-chain factor VIII. Thromb Res 2013;131 (Suppl. 2):s2-s6

27. Ivens IA, Baumann A, McDonald TA, et al. PEGylated therapeutic proteins for haemophilia treatment: a review for haemophilia caregivers. Haemophilia. 2013;19(1):11-20.

28. Swierczewska M, Lee KC, Lee S. What is the future of PEGylated therapies? Expert Opin Emerg Drugs. 2015;20(4):531-536.

29. Roopenian DC, Akilesh S. FcRn: the neonatal Fc receptor comes of age. Nat Rev Immunol. 2007;7(9):715-725.

30. Powell JS, Josephson NC, Quon D, et al. Safety and prolonged activity of recombinant factor VIII Fc fusion protein in hemophilia A patients. Blood. 2012;119(13):3031-3037.

31. Shapiro AD, Ragni MV, Valentino LA, et al. Recombinant factor IX-Fc fusion protein (rFIXFc) demonstrates safety and prolonged activity in a phase 1/2a study in hemophilia B patients. Blood. 2012;119(3):666-672.

32. Mahlangu J, Powell JS, Ragni MV, et al. Phase 3 study of recombinant factor VIII Fc fusion protein in severe hemophilia A. Blood. 2014;123(3):317-325.

33. Konkle BA, Stasyshyn O, Chowdary P, et al. Pegylated, full-length, recombinant factor VIII for prophylaxis and on-demand treatment of severe hemophilia A. Blood. 2015;126(9):1078-1085.

34. Mullins ES, Stasyshyn O, Alvarez-Román MT, et al. Extended half-life pegylated, full-length recombinant factor VIII for prophylaxis in children with severe haemophilia A. Haemophilia. 2017;23(2):238-246.

35. Reding MT, Ng HJ, Poulsen LH, et al. Safety and efficacy of BAY 94-9027, a prolonged-half-life factor VIII. J Thromb Haemost. 2017;15(3):411-419.

36. Santagostino E, Lalezari S, Reding MT, et al. Safety and efficacy of BAY 94-9027, an extended-half-life factor VIII, during surgery in patients with severe hemophilia A: Results of the PROTECT VIII clinical trial. Thromb Res. 2019;183:13-19.

37. Giangrande P, Andreeva T, Chowdary P, et al. Clinical evaluation of glycoPEGylated recombinant FVIII: Efficacy and safety in severe haemophilia A. Thromb Haemost. 2017;117(2):252-261.

38. Meunier S, Alamelu J, Ehrenforth S, et al. Safety and efficacy of a glycoPEGylated rFVIII (turoctocog alpha pegol, N8-GP) in paediatric patients with severe haemophilia A. Thromb Haemost. 2017;117(9):1705-1713.

39. Gruppo R, López-Fernández MF, Wynn TT, Engl W, Sharkhawy M, Tangada S. Perioperative haemostasis with full-length, PEGylated, recombinant factor VIII with extended half-life (rurioctocog alfa pegol) in patients with haemophilia A: Final results of a multicentre, single-arm phase III trial. Haemophilia. 2019;25(5):773-781.

40. Santagostino E, Negrier C, Klamroth R, et al. Safety and pharmacokinetics of a novel recombinant fusion protein linking coagulation factor IX with albumin (rIX-FP) in hemophilia B patients. Blood. 2012;120(12): 2405-2411.

41. Aledort L, Mannucci PM, Schramm W, Tarantino M. Factor VIII replacement is still the standard of care in haemophilia A. Blood Transfus 2019;17:479-486

42. Mancuso ME, Santagostino E. Outcome of clinical trials with new extended half-life

FVIII/IX concentrates. J Clin Med. 2017;6: E39.

43. Baumann A, Piel I, Hucke F, Sandmann S, Hetzel T, Schwarz T. Pharmacokinetics, excretion, distribution, and metabolism of 60-kDa polyethylene glycol used in BAY 94-9027 in rats and its value for human prediction. Eur J Pharm Sci. 2019 Mar 15;130:11-20.

44. Gringeri A, Mantovani LG, Scalone L, Mannucci PM; COCIS Study Group. Cost of care and quality of life for patients with hemophilia complicated by inhibitors: the COCIS Study Group. Blood. 2003;102(7): 2358-2363.

45. Kitazawa T, Igawa T, Sampei Z, et al. A bispecific antibody to factors IXa and X restores factor VIII hemostatic activity in a hemophilia A model. Nat Med. 2012;18(10): 1570-1574.

46. Uchida N, Sambe T, Yoneyama K, et al. A first-in-human phase 1 study of ACE910, a novel factor VIII-mimetic bispecific antibody, in healthy subjects. Blood. 2016;127(13):1633-1641.

47. Shima M, Hanabusa H, Taki M, et al. Factor VIII-mimetic function of humanized bispecific antibody in hemophilia A. N Engl J Med. 2016;374(21):2044-2053.

48. Oldenburg J, Mahlangu JN, Kim B, et al. Emicizumab prophylaxis in hemophilia A with inhibitors. N Engl J Med. 2017;377 (9):809-818.

49. Young G, Liesner R, Sidonio R, et al. Emicizumab Prophylaxis Provides Flexible and Effective Bleed Control in Children with Hemophilia with Inhibitors: Results from the HAVEN 2 Study. Paper presented at: American Society of Hematology Annual Meeting; December 1 4, 2018; San Diego

50. Mahlangu J, Oldenburg J, Paz-Priel I, et al. Emicizumab prophylaxis in patients who have hemophilia A without inhibitors. N Engl J Med. 2018;379(9):811-822.

51. Pipe SW, Shima M, Lehle M, et al. Efficacy, safety, and pharmacokinetics of emicizumab prophylaxis given every 4 weeks in people with haemophilia A (HAVEN 4): a multicentre, open-label, non-randomised phase 3 study. Lancet Haematol. 2019;6(6):e295-e305.

52. Samuelson Bannow B, Recht M, Négrier C, et al. Factor VIII: long-established role in haemophilia A and emerging evidence beyond haemostasis. Blood Rev. 2019;35:43-50.

53. Fatalities in emicizumab-kxwh clinical trials, expanded access, compassionate use, and the postmarketing setting. South San Francisco, CA: Genentech, 2018 (https://www.emicizumabinfo.com/content/dam/gene/emicizumabinfo/hcp/pdfs/fatalities.pdf).

54. FDA adverse events reporting system (FAERS) public dashboard: FAERS cases 14455349 and 16262656. Rockville, MD: Food and Drug Administration (https://fis.fda.gov/sense/app/d10be6bb-494e-4cd2-82e4-0135608ddc13/sheet/33a0f68e-45c-48e2-bc81-8141c6aaf772/state/ analysis).

55. Aledort LM. Deaths associated with emicizumab in patients with hemophilia A. N Engl J Med. 2019;381(19):1878-1879.

56. Chowdary P, Lethagen S, Friedrich U, et al. Safety and pharmacokinetics of anti-TFPI antibody (concizumab) in healthy volunteers and patients with hemophilia: a randomized first human dose trial. J Thromb Haemost. 2015;13(5):743-754.

57. Eichler H, Angchaisuksiri P, Kavakli K, et al. A randomized trial of safety, pharmacoki-

netics and pharmacodynamics of concizum-ab in people with hemophilia A. J Thromb Haemost. 2018;16(11):2184-2195.

58. Gu JM, Zhao XY, Schwarz T, et al. Mechanistic modeling of the pharmacody-namic and pharmacokinetic relationship of tissue factor pathway inhibitor-neutralizing antibody (BAY 1093884) in cynomolgus monkeys. AAPS J. 2017;19(4):1186-1195.

59. Pasi KJ, Rangarajan S, Georgiev P, et al. Targeting of antithrombin in hemophilia A or B with RNAi therapy. N Engl J Med. 2017;377(9):819-828.

60. Ragni MV, Georgiev P, Mant T, et al. Fitusiran, an investigational RNAi therapeu-tic targeting antithrombin for the treatment of hemophilia: updated results from a phase 1 and phase 1/2 extension study in patients without inhibitors [abstract]. Blood. 2016;128(22):2572.

61. ClinicalTrials.gov. A Study study of fitusiran (ALN-AT3SC) in severe hemophilia A and B patients with inhibitors (ATLAS-INH). Identifier: NCT03417102. 2018. https://clin-icaltrials.gov/ct2/show/NCT03417102. Accessed February, 2019.

62. Clinicaltrials.gov. A study of fitusiran (ALN-AT3SC) in severe hemophilia A and B patients without inhibitors. Identifier: NCT03417245. 2018. https://clinicaltrials.gov/ct2/show/NCT034 17245. Accessed June, 2019.

63. Alnylam. Alnylam provides pipeline update on fitusiran and givosiran investigational RNAi therapeutic programs. 2017. http://investors.alnylam.com/news-releas-es/news-release-details/alnylam-provides-pipeline-update-fitusiran-and-givosiran. Accessed February, 2019.

64. Mannucci PM. Miracle of haemophilia drugs: Personal views about a few main players. Haemophilia. 2018;24:557-562.

65. von Mackensen S, Kalnins W, Krucker J, et al. Haemophilia patients' unmet needs and their expectations of the new extended half-life factor concentrates. Haemophilia. 2017;23:566-574.

66. Wang L, Takabe K, Bidlingmaier SM, Ill CR, Verma IM. Sustained correction of bleeding disorder in hemophilia B mice by gene ther-apy. Proc Natl Acad Sci U S A. 1999;96: 3906 3910.

67. Chao H, Mao L, Bruce AT, Walsh CE. Sustained expression of human factor VIII in mice using a parvovirus based vector. Blood. 2000;95:1594 1599.

68. Mount JD, Herzog RW, Tillson DM, et al. Sustained phenotypic correction of hemo-philia B dogs with a factor IX null mutation by liver directed gene therapy. Blood. 2002;99:2670 2676.

69. Sarkar R, Mucci M, Addya S, et al. Long term efficacy of adeno associated virus serotypes 8 and 9 in hemophilia A dogs and mice. Hum Gene Ther. 2006;17:427 439.

70. Snyder RO, Miao C, Meuse L, et al. Correction of hemophilia B in canine and murine models using recombinant adeno associated viral vectors. Nat Med. 1999;5:64 70.

71. Nathwani AC, Tuddenham E, Rangarajan S, et al. Adenovirus associated virus vector mediated gene transfer in hemophilia B. N Engl J Med. 2011;365:2357 2365.

72. Nathwani AC, Reiss UM, Tuddenham E, et al. Long term safety and efficacy of factor IX gene therapy in hemophilia B. N Engl J Med. 2014;371:1994 2004.

73. Peyvandi F, Garagiola I. Clinical advances in gene therapy updates on clinical trials of gene therapy in haemophilia. Haemophilia. 2019;25(5):738-746.

74. George LA, Sullivan SK, Giermasz A, et al. Hemophilia B gene ther apy with a high specific activity factor IX variant. N Engl J Med. 2017;377:2215 2227.

75. http://ir.sparktx.com/news releases/news-release details/spark therapeutics and pfiz-er announce data 15 participants.

76. Chapin J, Rottensteiner H, Scheiflinger F, Monahan PE. An analysis of bleeding rates and factor IX consumption in the phase I/II BAX 335 gene therapy trial in subjects with hemophilia B. Abstracts of the XXVI Congress of the International Society on Thrombosis and Haemostasis. Res Pract Thromb Haemost. 2017;1(Suppl. 1):144.

77. Miesbach W, Meijer K, Coppens M, et al. Gene therapy with adenoassociated virus vector 5 human factor IX in adults with hemophilia B. Blood. 2018;131:1022 1031.

78. Leebeek F, Meijer K, Coppens M, et al Reduction in annualized bleeding and factor IX consumption up to 2.5 years in adults with severe or moderate severe hemophilia B treated with AMT 060 (AAV5 hFIX) gene therapy. Blood. 2018;132 (Suppl. 1): 3476.

79. Ward NJ, Buckley S, Waddington SN, et al. Codon optimization of human factor VIII cDNAs leads to high level expression. Blood. 2011;117:798 807.

80. Siner JI, Iacobelli NP, Sabatino DE, et al. Minimal modification in the factor VIII B domain sequence ameliorates the murine hemophilia A phenotype. Blood. 2013;121: 4396 4403.

81. Rangarajan S, Walsh L, Lester W, et al. AAV5 Factor VIII gene transfer in severe hemophilia A. N Engl J Med. 2017;377: 2519 2530.

82. Pasi KJ, Rangarajan S, Mitchell N, et al. Multiyear Follow-up of AAV5-hFVIII-SQ gene therapy for hemophilia A. N Engl J Med. 2020;382:29-40 .

83. Donsante A, Miller DG, Li Y, et al. AAV vec-tor integration sites in mouse hepatocellular carcinoma. Science. 2007;317(5837):477.

84. Nault JC, Datta S, Imbeaud S, et al. Recurrent AAV2-related insertional mutage-nesis in human hepatocellular carcinomas. Nat Genet. 2015;47:1187-1193.

85. Manno CS, Pierce GF, Arruda VR, et al. Successful transduction of liver in hemophil-ia by AAV-Factor IX and limitations imposed by the host immune response. Nat Med. 2006;12:342-347.

86. Kaeppel C, Beattie SG, Fronza R, et al. A largely random AAV integration profile after LPLD gene therapy. Nat Med. 2013;19:889-891.

87. D'Avola D, López-Franco E, Sangro B, et al. Phase I open label liver-directed gene thera-py clinical trial for acute intermittent por-phyria. J Hepatol. 2016;65(4):776-783.

Ferrata Storti Foundation

An international registry of patients with plasminogen deficiency (HISTORY)

Amy D. Shapiro,[1] Marzia Menegatti,[2] Roberta Palla,[3] Marco Boscarino,[2] Christopher Roberson,[1] Paolo Lanzi,[4] Joel Bowen,[5] Charles Nakar,[1] Isaac A. Janson[1] and Flora Peyvandi[2,3]

[1]Indiana Hemophilia & Thrombosis Center, Indianapolis, IN, USA; [2]Fondazione IRCCS Ca' Granda Ospedale Maggiore Policlinico, Angelo Bianchi Bonomi Hemophilia and Thrombosis Center and Fondazione Luigi Villa, Milan, Italy; [3]Università degli Studi di Milano, Department of Pathophysiology and Transplantation, Milan, Italy; [4]Misto s.r.l., Milan, Italy and [5]Rho, Inc., Durham, NC, USA

ABSTRACT

Plasminogen deficiency is an ultra-rare multisystem disorder characterized by the development of fibrin-rich pseudomembranes on mucous membranes. Ligneous conjunctivitis, which can result in vision impairment or loss, is the most frequent symptom reported. Affected systems may also include the respiratory tract, oropharynx, female reproductive tract, gingiva, middle ear, renal collecting system, skin and central nervous system. Untreated, plasminogen deficiency may result in significant reduction in quality of life and morbidity with potential life-threatening complications. Non-specific therapies are inadequate and plasminogen concentrates are not commercially available. The current understanding of plasminogen deficiency and management of disease symptoms and its progression are based on case reports/series and two small clinical trials. To date there has never been a comprehensive, international study to examine the natural history or optimal therapeutic intervention; knowledge gaps include identification of contributing factors and triggers of disease manifestations, inability to predict disease course, and insufficient real-world data for use of therapeutics. We have created an international, observational study (HISTORY) in a large cohort of persons with plasminogen deficiency and first-degree family members to address these gaps and to advance knowledge and care. HISTORY will build upon the established relationship between the Indiana Hemophilia and Thrombosis Center and the Fondazione Angelo Bianchi Bonomi, IRCCS Ca' Granda Ospedale Maggiore Policlinico - University of Milan and will utilize a modified version of the Prospective Rare Bleeding Disorders Database (PRO-RBDD). A biorepository containing samples from subjects with plasminogen deficiency will be established. This article describes the rationale behind the study and efforts towards its goals.

Introduction

Diseases are defined as rare if they affect fewer than 200,000 people in the United States of America (USA) or fewer than 1 in 2,000 in the European Union; there are estimated to be approximately 6,500 clinically distinct rare diseases across all medical specialties.[1] Given the large number of diseases meeting this broad classification, the term 'ultra-rare disease' has emerged to describe the rarest of these disorders; this phrase is not well defined, but in the United Kingdom (UK) it has come to mean fewer than 1,000 patients in that country (approximately 1 in 65,000). These diseases pose unique considerations for the researcher, clinician and patient; these range from an understanding of the natural history of the disease and accurate diagnosis, to safe and effective treatment options and availability of knowledgeable specialists.

Randomized and large prospective clinical trials are often not feasible for ultra-rare diseases as the limited number of eligible patients and phenotypic hetero-

geneity affect recruitment, interpretation of data and applicability of conclusions to the larger real-world population of patients; in many cases it may not be possible to design a clinical trial accurately because of insufficient knowledge of the disease.[2] Instead clinicians have often relied on personal experience, case studies/series and patient registries to understand the natural history of these diseases and to collect data on therapeutic interventions and patient outcomes. Patient registries may be national, regional or international, each with its own advantages and disadvantages. The value of international patient registries in rare diseases has long been recognized; however, given the large number of rare diseases and the small number of affected patients, funding opportunities are frequently limited, particularly for long-term maintenance.[1]

Some diseases are so rare that many clinicians may never see a case; for example, plasminogen deficiency (PLGD) is an ultra-rare disease with an estimated prevalence of approximately 1.6 per million population. Most commonly it presents as ligneous conjunctivitis, an extravascular accumulation of fibrin-rich, woody (ligneous) pseudomembranes on the mucous membrane of the eye; it can also manifest on other mucous membranes, and as a life-long, systemic disease impacting multiple systems either intermittently or continuously. No specific therapies are approved by the Food and Drug Administration or European Medicines Agency and non-specific treatments are inadequate.

Current knowledge of PLGD stems from case reports and small series; systematic prospective data collection coupled with serial biological samples collected from persons with PLGD and first-degree family members has not been performed. Knowledge gaps include identification of contributing factors to and triggers of disease manifestations, inability to predict disease course, and insufficient real-world data for individualized use of potential new therapeutics. To address unmet needs, a retrospective and prospective data collection system of a large cohort of people with PLGD and their family members has been developed to define the natural history of PLGD and is entitled *Hypoplasminogenemia: An International RetroSpecTive and PrOspective CohoRt StudY* (HISTORY). HISTORY addresses key gaps in the knowledge about the natural history of PLGD and builds on the productivity/infrastructure of the established collaborative efforts of research teams at the Indiana Hemophilia and Thrombosis Center (IHTC), the Fondazione Angelo Bianchi Bonomi, IRCCS Ca' Granda Ospedale Maggiore Policlinico of Milan (IRCCS) and the University of Milan (UNIMI). Phenotypic data combined with genetic and advanced laboratory testing will be used to investigate disease course predictors and evaluate/elucidate phenotypic relationships. A specimen biorepository will serve as a resource for further analyses. Overarching study goals are to analyze phenotypic heterogeneity, to identify markers to predict disease course, and to develop improved methods to utilize new therapeutics.

Plasminogen deficiency

Congenital PLGD is an autosomal recessive disorder caused by mutations in *PLG* that result in functionally deficient and/or reduced levels of circulating plasminogen.[3] An epidemiological study performed in the UK observed a 0.26% prevalence of asymptomatic heterozygous PLGD;[4-6] similar prevalences of heterozygous PLGD have been reported in other countries.[7-9] The UK data suggest that the prevalence of individuals with symptomatic PLGD (homozygous/compound heterozygous) is 1.6 per million population;[10,11] there are estimated to be 500 symptomatic people with PLGD in the USA and 12,000 worldwide. Based on experience with other rare bleeding disorders, a higher prevalence of PLGD is likely to occur in regions where consanguineous marriages are more common;[11,12] for this reason, a national study would likely misstate the true prevalence and phenotypic diversity of the disease. An increased number of females are reported to be symptomatic compared to males (ratio of 1.27-1.88:1).[12,13]

People with PLGD may exhibit a multi-organ systemic disease that commonly manifests as the extravascular accumulation of fibrin-rich, woody (ligneous) pseudomembranes on mucous membranes. PLGD is a lifelong disease, although the most severe symptoms are observed in infants and children.[3,14] Ligneous conjunctivitis is the most common disease symptom (81% prevalence);[3] pseudomembrane growth may be triggered by a local infection or injury and can result in impairment or loss of vision if untreated and/or persistent.[3,11] Approximately one-third of people with PLGD have corneal involvement with potential for blindness,[11,12] and 30% present with ligneous gingivitis resulting in periodontal destruction and tooth loss.[3,12,13] Other common symptom locations include the respiratory tract (20%), ears (14%), female genitourinary tract (9%), and kidneys (4%).[3,11,15-18]

Lesions are often inflamed and painful and can compromise organ function, resulting in life-threatening conditions including renal and respiratory failure (e.g., tracheobronchial lesions).[11,18] Central nervous system complications have been noted, including Dandy-Walker malformation and occlusive hydrocephalus[12] in 14% of children due to fibrin deposition in the cerebral ventricular system; shunts used to drain cerebrospinal fluid are prone to occlusion or poor peritoneal absorption, leading some neurosurgeons to recommend ventriculocholecystic shunts.[19] In women, dysmenorrhea, abnormal menses, dyspareunia, and infertility have been reported.[15] Wound healing may be severely impaired.[20] Lesions in the middle ear may result in hearing loss.[11] Although the initial case of PLGD was documented in a patient with recurrent venous thromboembolism, an association between PLGD and increased thrombotic risk has not been demonstrated.[10,21] Patients may suffer substantial morbidity and mortality and experience reduced quality of life and education/work potential.[14]

Surgical removal of lesions often results in accelerated pseudomembrane regrowth compounding clinical morbidity.[22] Case reports describing use of topical or systemic heparin, corticosteroids, cyclosporine, azathioprine, hyaluronidase, α-chymotrypsin, oral contraceptives, warfarin, and amniotic membrane placement have been published; these approaches show inconsistent success (examples of therapies utilized are shown Table 1).[13,23-29] Fresh-frozen plasma has been reported to be successful in some cases when eye drops, subconjunctival injection and/or intravenous infusions are utilized;[30,31] however, as fresh-frozen plasma contains low concentrations of plasminogen, volume overload may occur when the intra-

venous route of administration is used. Infusion reactions, time required for administration and need for repeated infusions may also limit intravenous use of fresh-frozen plasma.

Several case studies have reported on topical ophthalmological application of plasminogen for the treatment of ligneous conjunctivitis. Watts *et al.* noted that following surgical removal of pseudomembranes, plasminogen eye drops administered every 2 h prevented regrowth; a maintenance dose every 6 h prevented symptoms for over 1 year.[32] Similarly, Pons *et al.* reported resolution of ligneous conjunctivitis with administration of plasminogen eye drops; in this patient, multisystem manifestations subsequently developed that could not be treated.[33] An interim analysis of a phase II/III clinical trial studying ophthalmological plasminogen (2 drops, 4-12 times daily) was reported by Nakar *et al.*[34] Ten out of 11 subjects (91%) experienced full regression of ophthalmological lesions and/or absence of recurrence following surgical excision (the 11th subject was withdrawn because of non-compliance). This clinical trial (NCT01554956) is ongoing.

Shapiro *et al.* have reported results from a phase II/III clinical trial (NCT02690714) investigating the use of an intravenous plasma-derived plasminogen concentrate (6.6 mg/kg iv, every 2-4 days depending on individual pharmacokinetic profile).[14] All 14 subjects achieved trough plasminogen levels at least 10% above baseline; all preexisting clinical manifestations of PLGD (including lesions on the conjunctiva, gingiva, nasopharynx, bronchus, colon, kidney, cervix, and vagina) resolved or improved. An amended biologics license application is expected to be filed with the Food and Drug Administration for this product in the first half of 2020.

The rarity of PLGD results in frequent mis- and delayed diagnoses by professionals lacking specialist knowledge. Difficulty with diagnosis and disease rarity have contributed to an inability to document the natural history, develop clinical guidelines, and optimize treatment regimens. An exclusively USA-based registry would be of limited value as this would restrict recruitment and might fail to identify the full spectrum of the disorder. Therefore, an international effort has been undertaken to gain unique and broad insights into the disease, its progression and optimal treatment.

Registries in rare coagulation disorders

Hemophilia A and B are two of the more common rare coagulation disorders; they affect approximately 1:5,000 and 1:30,000 persons, respectively. Our current understanding of hemophilia and the wide availability of specialized care and therapeutic options are a result of the many clinical trials and patient registries that have been developed over the years.

Patient registries in hemophilia may be national, regional or international. O'Mahony *et al.* noted that 27/35 European countries had their own national hemophilia patient registry and some countries have multiple national registries operated by different organizations with little consideration given to interoperability.[35,36] This lack of interoperability and the variability in inclusion/exclusion criteria for enrolled subjects, definitions utilized, data collected, and different goals of these

Table 1. Examples of published therapies for the most common manifestations of plasminogen deficiency, ligneous conjunctivitis and ligneous gingivitis.

Therapy*	LC [reference]	LG [reference]
Fresh-frozen plasma	[31]	[22]
Plasminogen concentrate	[14,34]	[14]
Anticoagulants		
Heparin	[23]	
Warfarin		[28]
Argatroban	[33]	
Immunosuppressants		
Corticosteroids	[23]	[10]
Azathioprine	[11]	
Cyclosporine A	[24,25]	
Oral contraceptives	[27]	
Thrombolytic		
Anistreplase	[10]	
Hyaluronidase	[26]	
Alpha chymotrypsin	[26]	
Mast cell stabilizer		
Cromoglicic acid	[11]	
Anti-proliferative agent		
Mitomycin C	[11]	

LC: ligneous conjunctivitis; LG: ligneous gingivitis. *Not all reported therapeutic results have been shown to be reproducible.

national registries all limit the pooling of data to the detriment of all stakeholders. One example of the issues associated with multiple registries pursuing similar goals may be observed in those that examined the determinants of hemophilic inhibitor development and predictors of immune tolerance induction success: different registries reported different conclusions based on the patients enrolled and the data collected.[37] Ideally, collaboration between registries and harmonization of data collection are necessary to achieve minimal datasets for advancement of shared clinical goals in these rare disorders.[38,39]

Advantages and disadvantages of national, regional and international registries are highlighted in the following examples.

The American Thrombosis and Hemostasis Network

The American Thrombosis and Hemostasis Network (ATHN) collects data on patients in the USA with rare coagulation disorders. The centralized database and standardized definitions for data entry enhance research and clinical goals; these include the generation of the largest genetic hemophilia repository (My Life, Our Future) and the surveillance of over 80,000 persons with rare coagulation disorders (Community Counts).[40,41] Despite these successes, Gupta *et al.* noted limitations in data collection; for example, of the known 3,626 patients with an ultra-rare coagulation disorder, less than 11% had been included in the Community Counts registry.[39] Furthermore, the strictly USA-centric dataset may limit wider applicability of results to other countries with different medical resources and population diversity. These limitations highlight why efforts to create a comprehensive ultra-rare coagulation disorder registry in a single country may be less successful than desired.

European Network of Rare Bleeding Disorders

The Rare Bleeding Disorders Database (RBDD) project was established at UNIMI in 2004 to organize and analyze clinical, genetic and treatment data on rare bleeding disorders, including deficiencies of fibrinogen and factors II, V, combined V and VIII, VII, X, XI and XIII. In 2007, this database was modified to include the use of a web-based application to create the retrospective European Network of Rare Bleeding Disorders (EN-RBD) project.[42] Data on 592 patients from 11 European countries were included. These data led to the first authoritative understanding of the relationship between coagulation factor activity level and clinical bleeding severity in ultra-rare bleeding disorders; in turn this resulted in the development of a new severity classification system for bleeding symptoms.[43]

Prospective Rare Bleeding Disorders Database

To overcome limitations of retrospective data collection, EN-RBD was subsequently modified to incorporate prospective data on patients. This registry, the Prospective Rare Bleeding Disorders Database (PRO-RBDD), enrolled patients from 62 centers in Europe, Asia, the Middle East, the Americas, Africa, and Oceania.[44] The greatly expanded international network of participating centers was considered essential for a registry focusing on diseases for which the prevalence may approach 1 per million population; this extended outreach may permit increased and more rapid enrollment, and greater phenotypic and genetic diversity.

The aims of PRO-RBDD are a more accurate determination of the prevalence of rare bleeding disorders, the incidence of bleeding episodes, the use of treatment products, and the optimization of clinical management. Currently, subjects with deficiencies in fibrinogen and factors V, V/VIII, XI and XIII are being enrolled in PRO-RBDD with phenotype/genotype evaluation performed at a central laboratory to ensure consistency. Initial results have helped define minimal factor XIII plasma levels (15 IU/dL) necessary to prevent spontaneous major bleeding in people with factor XIII deficiency;[45] this observation highlights the importance of registry data to clinical practice.

The plasminogen deficiency registry (HISTORY project)

HISTORY is an extension of PRO-RBDD; it is an observational cross-sectional study that will contain both retrospective and prospective data from an international population of people with PLGD and their immediate family members. PRO-RBDD was selected as the ideal infrastructure for HISTORY as previously gained experience, proven track-record and established collaborations should ensure timely and efficient achievement of study goals. Retrospective data will be collected for 1 year prior to study entry; prospective data will be collected for each subject for a 3-year on-study period.

The overarching goals driving data analysis are development of disease severity categories, disease course predictors and need for specific surveillance in particular subpopulations, and treatment algorithms and recommendations to guide clinical care and management. As such, the registry design will allow collection of general information about each subject's health, with specific details regarding: original diagnosis (age, reason for screening); phenotype and genotype analysis; type, site and number of clinical manifestations indicative of pseudomembrane formation; detailed information on type, intensity, and duration of any prophylactic treatment, frequency and dose; type, frequency and dose of therapy administered to treat acute or chronic pseudomembranes; laboratory parameters; use of concomitant therapy; detailed information of management of surgical procedures; obstetric data; and complications associated with treatment.

The coordinating centers for this study are the IHTC and IRCCS/UNIMI. The IHTC is enrolling subjects from North, South and Central America and IRCCS/UNIMI is enrolling subjects from the rest of the world. The database will be located at UNIMI and specimens will be stored at the IHTC and/or IRCCS/UNIMI biorepositories. Safeguards have been implemented to protect confidential medical information to meet national regulations; all clinical information and biological samples will be stored in accordance with the Health Insurance Portability and Accountability Act of 1996 or General Data Protection Regulation in the USA and Europe, respectively.

Clinical study protocols and laboratory manuals have been developed and approved by local institutional review boards. HISTORY will be conducted in compliance with Good Clinical Practice as stated in the Declaration of Helsinki; it is registered at clinicaltrials.gov (NCT03797495).

Patient recruitment and study visits

There is currently no authoritative natural history study for PLGD; HISTORY is a 4-year study (Figure 1A) that will be the first international effort to define the natural history of this disorder by reviewing retrospective and prospective data from up to 100 probands and their first-degree family members (approximately 500 subjects in total). Asymptomatic family members will be recruited in addition to symptomatic individuals. Asymptomatic family members are not routinely tested for PLGD; study testing will provide a unique opportunity to prospectively monitor any newly diagnosed patients to investigate the deficiency prior to symptom development. The inclusion of heterozygous family members may additionally reveal the relationship between minimal plasminogen activity levels and natural history. Inclusion and exclusion criteria are listed in Table 2.

The registry will include a minimum of seven data entry points per subject (baseline and every 6 months for 3 years) with data also collected at other non-scheduled visits (Figure 1B and Table 3). Retrospective baseline data (demographic and clinical history for 1 year prior to enrollment) will be collected at each study site, with prospective follow-up data acquired by telephone if an in-person visit is not required. In-person evaluation will occur in cases of suspected clinical manifestations indicative of pseudomembranes or other intermittent medical events including pregnancy. Laboratory evaluation and physical examination will be performed at baseline and at study termination.

To accelerate recruitment and meet the study objectives efficiently, PLGD patients/families/providers held within an IHTC tracking system (~50 probands) will be contacted to determine interest in the study, as will authors of published literature on cases/series of PLGD. Advertisements will be placed in scientific journals that focus on diseases for which clinicians may interface with people with PLGD. Furthermore, an outreach program using social media, a

dedicated website (*www.plgdeficiency.com*), presentations at international meetings, and direct contact with interested colleagues will be pursued. Study coordinators at IRCCS/UNIMI will contact their established treatment center network throughout the world. In addition to hematologists, specialists including gynecologists and ophthalmologists will also be contacted; these healthcare professionals may be the first to observe a patient with PLGD. A multidisciplinary approach including such specialists is essential to improve overall awareness and understanding of the disorder; it may also prevent the loss of patients to follow-up by a hematologist as some patients may continue treatment outside of a specialist hematology center. As PLGD may affect different systems throughout life, the investigators are enrolling subjects across a wide range of ages, countries, phenotypes and genotypes. People with PLGD are motivated to participate in studies to advance PLGD understanding as few study opportunities exist.

To date, 26 centers from 12 countries have agreed to participate in HISTORY; 51 subjects (24 probands and 27 first-degree family members) are currently enrolled in the study. Demographic data for these 51 subjects are shown in Table 4. Initial results have identified asymptomatic siblings with PLGD; these subjects are being monitored to understand the factors that trigger initial symptom development.

Therapeutic interventions

Regular monitoring and individualization of therapy is required for people with PLGD as there is currently no compelling evidence that a patient's clinical course can be predicted from their plasminogen activity level or genetic defect.[12] Similarly, if a patient presents with ligneous conjunctivitis, the likelihood of developing multisystem disease cannot be predicted; it is unknown what routine scans should be performed, what surveillance methods

A   **Overall study timeline**
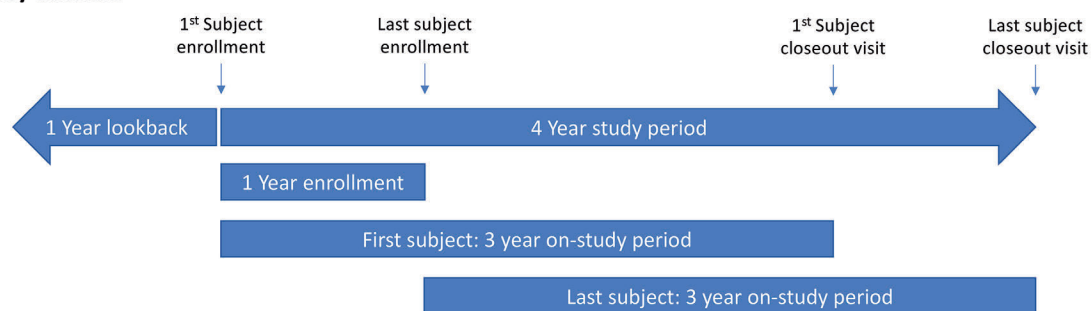
B   **Subject visits & data collection**
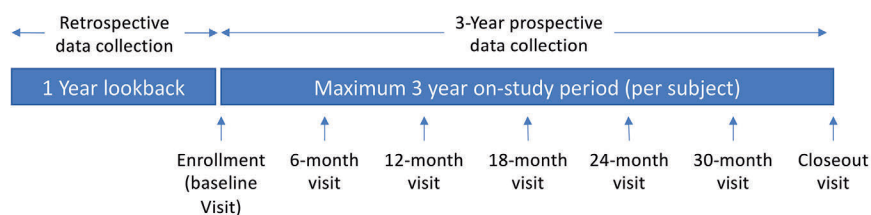
Figure 1. Overall study timeline and scheduled study visits. (A) The 4-year study plan includes a 1-year enrollment period and a maximum 3-year on-study period for each subject enrolled. Retrospective clinical data for 1 year prior to study enrollment will also be collected. (B) The initial baseline visit will include informed consent, demographics, screening, laboratory investigations, genetic testing, medical examination and history, and a 1-year retrospective collection of relevant clinical data. Subsequent study visits will occur every 6 months and will include a medical history review; the closeout visit will occur at the 3-year time point. See also Table 3.

Table 2. Inclusion and exclusion criteria for enrollment in HISTORY

Inclusion criteria	Exclusion criteria
Males or females with plasminogen deficiency diagnosed locally with plasminogen activity levels <50% OR first-degree family members of a person diagnosed with plasminogen deficiency (to include parents, siblings, half-siblings)	Any psychiatric disorder, other mental disorder, or any other medical disorder that impairs the subject's ability to give informed consent or to comply with the requirements of the study protocol (unless a caregiver or authorized representative is willing to provide consent/assent)
All ages eligible	Previous organ transplant recipient
Available clinical history and treatment for at least 1 year prior to entry except for infants <1 year of age	Refusal to provide informed consent
Willingness to provide samples for analysis including DNA, plasma etc.	Special patient populations, including prisoners or those who are deemed medically or cognitively unsuitable for research by their treating physician
Willingness to participate in prospective follow-up for up to 3 years	Inability to obtain a blood sample due to poor or limited venous access

Table 3. Details of the study visits.

Assessments	Baseline	Year One 6 months	Year One 12 months	Year Two 18 months	Year Two 24 months	Year Three 30 months	Year Three 36 months	Unscheduled*
Informed consent	X							
Re-consent (if minor reaches 18 years)								X
Eligibility criteria	X							
Demographics	X							
Laboratory investigations								
Plasminogen antigen level	X						X	
Plasminogen activity level	X						X	X
Genetic testing	X							
Family history	X						X	
Medical history								
Initial comprehensive history/review of systems	X							
Medical history since last visit (procedures, pregnancy, treatment, other symptoms or complications, etc.)		X	X	X	X	X	X	X
Concurrent medications	X	X	X	X	X	X	X	X

*Additional data will be collected at the time of an unscheduled visit for re-consent, illness, pregnancy (plasminogen activity level and banked plasma will be collected at confirmation of pregnancy, during the third trimester and at delivery), and development of lesions.

should be used, or how frequently clinical visits should occur to monitor for symptoms to ensure early intervention and prevent sequelae. Furthermore, it is unknown if treatment should be lifelong, intermittent, or may be withdrawn over time and how this varies by patient, disease severity, and affected system.

All non-specific therapeutic interventions to treat acute and chronic manifestations of PLGD will be recorded, along with efficacy, safety and complications. Specific treatments, including ophthalmological plasminogen drops and systemic intravenous plasminogen replacement therapy are currently under clinical investigation;[14,34] any use of these investigational agents will also be recorded. Currently, data to support wider real-world optimal therapeutic regimens are lacking. There are no standard dosing regimens for intravenous plasminogen replacement therapy and the required minimal plasminogen plasma levels to treat or prevent specific manifestations are unknown; treatment for each patient must be individualized based on their pharmacokinetic profile.[14] HISTORY will explore development of a population pharmacokinetic model[46] for the investigational intravenous plasminogen concentrate[14] to estimate plasma levels and adjust doses if symptoms emerge.

Factors that correlate with disease expression and severity

No screening test for PLGD exists; specific plasminogen activity/antigen levels are required, but assays are not uniformly available. This study will collect methodological details of locally performed tests to review their diagnostic utility; testing will be repeated centrally to confirm diagnosis and local assay utility. Peyvandi *et al.* demonstrated that clotting level activity in some rare bleeding disorders does not correlate with clinical bleeding severity.[43] Published data suggest that this may also be true for PLGD; therefore, global coagulation assays (including thrombin generation, thromboelastography, simultaneous thrombin/plasmin generation and fibrinolytic potential)[47-50] will be performed to evaluate their utility in phenotypic prediction and clinical management.

Table 4. Demographics of the initial 51 enrolled subjects.

Demographics	Subjects with plasminogen deficiency	Unaffected family members
Gender		
Male	9	11
Female	15	16
Age		
<18 years	14	8
≥18 years	10	19
Ethnicity		
White	21	22
Hispanic/Latino	3	5
Consanguineous parentage		
Yes	0	0
No	22	27
Unknown	2	0
Endogenous plasminogen activity		
Median (%)	18.5	n/a
Range (%)	1 - 42	n/a
Endogenous plasminogen antigen		
Median (mg/dL)	3.4	n/a
Range (mg/dL)	1 - 12	n/a

n/a: not applicable.

The true prevalence of PLGD is not well established and likely depends on the population in any particular region or country; similarly, the genetic alterations influencing disease expression and severity are not well defined. A genome-wide association study conducted by Ma *et al.* determined genetic modifiers of plasminogen levels in normal adults;[51] the study revealed that four single nucleotide polymorphisms were associated with variations in plasminogen levels. How these variations affect the severity or progression of PLGD is unknown. The *PLG*(K38E) mutation is known to result in a milder clinical course;[12,13] conversely, other mutations are known to not be predictive (for example, in one family with the conserved W597C mutation, one member was asymptomatic, another had ligneous periodontitis, and a third had

ligneous conjunctivitis).[12] HISTORY will record the prevalence of different mutations in the affected and heterozygote population and attempt to determine the relationship between mutation and clinical penetrance heterogeneity; it will also examine polymorphisms that may influence fibrinolytic capacity (e.g., in fibrinogen Aα and plasminogen activator inhibitor 1).[52] The enrollment of relatives of people with PLGD may enable a refinement of plasminogen activity levels observed in heterozygotes.

The registry will also incorporate environmental and host-specific factors that may modify plasminogen levels and/or disease symptoms. A study in healthy subjects found that smoking contributes to plasma plasminogen levels;[51] it is not known whether this and other environmental factors affect plasminogen plasma levels in patients with PLGD. It is also not clear whether an environmental trigger is required for symptom development and/or disease expression, or whether and, if so, how specific plasminogen antibodies develop. HISTORY will address some of these unknown environmental/host factors.

Plasminogen deficiency biorepository

Research involving human genetic or genomic information analyzed in conjunction with personal or health data has become increasingly important for untangling genetic, lifestyle and environmental disease determinants. A biorepository containing DNA, plasma, and serum will be created; samples will be stored for up to 15 years. If planned analyses are not revealing, stored samples will be utilized to explore other biomarkers to elucidate a correlation/prediction of phenotypic heterogeneity (e.g., polymorphisms in inflammatory markers, whole genome analyses).

Data analyses

To understand the impact of specific data on disease expression, all collected data will be analyzed. Clinical data on people with PLGD will be evaluated for categorical characterization (i.e., asymptomatic, intermittently symptomatic, and continuously symptomatic). The probands' age in each category will be analyzed to evaluate age as a variable for symptom expression. Categories will be modeled and analyzed against a range of variables including gender, environmental factors, genetic studies, laboratory coagulation parameters including specific and exploratory global assays, and treatment administration. Subjects with clinical symptoms will be evaluated for the presence of individual affected sites *versus* multiple/systemic symptoms, and also analyzed based on prior listed variables. A descriptive analysis of symptoms reported by physiological system will be performed and modeled against study variables (levels, genetics, global assays, and exploratory investigations) to determine whether any of them are predictive. Symptoms and data will be reviewed to determine whether severity categories can be established. Urine analysis will be performed, as unpublished data suggest that PLGD may be associated with microalbuminuria; its prevalence in the wider PLGD population is unknown. Data will be collected on subjects who receive nonspecific and/or specific treatments if available; they will be analyzed for therapeutic response, disease control, and recurrence or emergence on therapy.

Further details of the methods, procedures, and planned analyses are reported in the *Online Supplementary Material*.

Conclusions

There is currently no central repository to collect and analyze data from people with PLGD; clinicians rely on case reports and individual experience to diagnose and treat patients, resulting in treatment variability and less than optimal outcomes. The HISTORY study may play a substantial role in addressing these deficits by collecting clinical, genetic, and laboratory data which will be analyzed to identify potential markers that can assist in disease course prediction and understanding heterogeneity in phenotypic expression. This study may also enable the development of standardized assays, the identification of at-risk groups, and guidelines for non-specific and specific therapies.

To date, no other international team of dedicated experts has been assembled to investigate the natural history of PLGD and fill knowledge gaps; HISTORY provides the first comprehensive effort to address this ultra-rare disease. It is not possible for one center or country to singlehandedly complete this study; all interested parties are therefore strongly encouraged to view the study website (*www.plgdeficiency.com*), participate if they know of or care for anyone with PLGD or contact the authors directly to discuss potential involvement in this registry. Full enrollment and patient diversity will benefit all those with this disorder.

References

1. Forrest CB, Bartek RJ, Rubinstein Y, Groft SC. The case for a global rare-diseases registry. Lancet. 2011;377(9771):1057-1059.
2. Jansen-van der Weide MC, Gaasterland CMW, Roes KCB, et al. Rare disease registries: potential applications towards impact on development of new drug treatments. Orphanet J Rare Dis. 2018;13(1):154.
3. Schuster V, Hugle B, Tefs K. Plasminogen deficiency. J Thromb Haemost. 2007;5(12):2315-2322.
4. Tait RC, Walker ID, Conkie JA, et al. Plasminogen levels in healthy volunteers--influence of age, sex, smoking and oral contraceptives. Thromb Haemost. 1992;68(5):506-510.
5. Tait RC, Walker ID, Conkie JA, Islam SI, McCall F. Isolated familial plasminogen deficiency may not be a risk factor for thrombosis. Thromb Haemost. 2018;76(6):1004-1008.
6. Tefs K, Tait CR, Walker ID, Pietzsch N, Ziegler M, Schuster V. A K19E missense mutation in the plasminogen gene is a common cause of familial hypoplasminogenaemia. Blood Coagul Fibrinolysis. 2003;14(4):411-416.
7. Dykes D, Polesky H. Incidence of the PLG* QO allele in human populations. In: Mayr WR, ed. Advances in Forensic Haemogenetics: Springer-Verlag Berlin Heidelberg, 1988:261-264.
8. Okamoto A, Sakata T, Mannami T, et al. Population-based distribution of plasminogen activity and estimated prevalence and relevance to thrombotic diseases of plasminogen deficiency in the Japanese: the Suita study. J Thromb Haemost. 2003;1(11):2397-2403.
9. Weidinger S, Patutschnick W,

Schwarzfischer F. Further evidence of a silent plasminogen (PLG) allele in two paternity cases. Z Rechtsmed. 1988;101(2):99-104.

10. Mehta R, Shapiro AD. Plasminogen deficiency. Haemophilia. 2008;14(6):1261-1268.

11. Schuster V, Seregard S. Ligneous conjunctivitis. Surv Ophthalmol. 2003;48(4):369-388.

12. Klammt J, Kobelt L, Aktas D, et al. Identification of three novel plasminogen (PLG) gene mutations in a series of 23 patients with low PLG activity. Thromb Haemost. 2011;105(3):454-460.

13. Tefs K, Gueorguieva M, Klammt J, et al. Molecular and clinical spectrum of type I plasminogen deficiency: a series of 50 patients. Blood. 2006;108(9):3021-3026.

14. Shapiro AD, Nakar C, Parker JM, et al. Plasminogen replacement therapy for the treatment of children and adults with congenital plasminogen deficiency. Blood. 2018;131(12):1301-1310.

15. Pantanowitz L, Bauer K, Tefs K, et al. Ligneous (pseudomembranous) inflammation involving the female genital tract associated with type-1 plasminogen deficiency. Int J Gynecol Pathol. 2004;23 (3):292-295.

16. Chi AC, Prichard E, Richardson MS, Rasenberger KP, Weathers DR, Neville BW. Pseudomembranous disease (ligneous inflammation) of the female genital tract, peritoneum, gingiva, and paranasal sinuses associated with plasminogen deficiency. Ann Diagn Pathol. 2009;13(2):132-139.

17. Cohen J, Cohen S, Cymberknoh MC, Gross M, Hirshoren N, Shoseyov D. Laryngeal obstruction in congenital plasminogen deficiency. Pediatr Pulmonol. 2012;47(9):923-925.

18. Ciftci E, Ince E, Akar N, Dogru U, Tefs K, Schuster V. Ligneous conjunctivitis, hydrocephalus, hydrocele, and pulmonary involvement in a child with homozygous type I plasminogen deficiency. Eur J Pediatr. 2003;162(7-8):462-465.

19. Weinzierl MR, Collmann H, Korinth MC, Gilsbach JM, Rohde V. Management of hydrocephalus in children with plasminogen deficiency. Eur J Pediatr Surg. 2007;17(2):124-128.

20. Schott D, Dempfle CE, Beck P, et al. Therapy with a purified plasminogen concentrate in an infant with ligneous conjunctivitis and homozygous plasminogen deficiency. N Engl J Med. 1998;339(23):1679-1686.

21. Martin-Fernandez L, Marco P, Corrales I, et al. The unravelling of the genetic architecture of plasminogen deficiency and its relation to thrombotic disease. Sci Rep. 2016;6:39255.

22. Hidayat AA, Riddle PJ. Ligneous conjunctivitis. A clinicopathologic study of 17 cases. Ophthalmology. 1987;94(8):949-959.

23. De Cock R, Ficker LA, Dart JG, Garner A, Wright P. Topical heparin in the treatment of ligneous conjunctivitis. Ophthalmology. 1995;102(11):1654-1659.

24. Holland EJ, Chan CC, Kuwabara T, Palestine AG, Rowsey JJ, Nussenblatt RB. Immunohistologic findings and results of treatment with cyclosporine in ligneous conjunctivitis. Am J Ophthalmol. 1989;107(2):160-166.

25. Shimabukuro M, Iwasaki N, Nagae Y, et al. Ligneous conjunctivitis: a case report. Jap J Ophthalmol. 2001;45(4):375-377.

26. Firat T. Ligneous conjunctivitis. Am J Ophthalmol. 1974;78(4):679-688.

27. Sartori MT, Saggiorato G, Pellati D, et al. Contraceptive pills induce an improvement in congenital hypoplasminogenemia in two unrelated patients with ligneous conjunctivitis. Thromb Haemost. 2003;89(01):86-91.

28. Fine G, Bauer K, Al-Mohaya M, Woo SB. Successful treatment of ligneous gingivitis with warfarin. Oral Surg Oral Med Oral Pathol Oral Radiol Endod. 2009;107(1):77-80.

29. Barabino S, Rolando M. Amniotic membrane transplantation in a case of ligneous conjunctivitis. Am J Ophthalmol. 2004;137 (4):752-753.

30. Tabbara KF. Prevention of ligneous conjunctivitis by topical and subconjunctival fresh frozen plasma. Am J Ophthalmol. 2004;138 (2):299-300.

31. Kizilocak H, Ozdemir N, Dikme G, et al. Treatment of plasminogen deficiency patients with fresh frozen plasma. Pediatr Blood Cancer. 2018;65(2):e26779.

32. Watts P, Suresh P, Mezer E, et al. Effective treatment of ligneous conjunctivitis with topical plasminogen. Am J Ophthalmol. 2002;133(4):451-455.

33. Pons V, Olivera P, Garcia-Consuegra R, et al. Beyond hemostasis: the challenge of treating plasminogen deficiency. A report of three cases. J Thromb Thrombolysis. 2016;41 (3):544-547.

34. Nakar CT, Caputo R, Price FW, et al. Safety & efficacy of human plasma derived plasminogen ophthalmic drops for treatment of ligneous conjunctivitis: report of phase 2/3 clinical trial. Blood. 2015;126(23):2288.

35. O'Mahony B, Noone D, Giangrande PL, Prihodova L. Haemophilia care in Europe - a survey of 35 countries. Haemophilia. 2013;19(4):e239-247.

36. Keipert C, Hesse J, Haschberger B, et al. The growing number of hemophilia registries: quantity vs. quality. Clin Pharmacol Ther. 2015;97(5):492-501.

37. Osooli M, Berntorp E. Inhibitors in haemophilia: what have we learned from registries? A systematic review. J Intern Med. 2015;277(1):1-15.

38. European Medicines Agency. Report on Haemophilia Registries; Workshop 8 June 2018; Patient Registries Initiative. [cited September 23, 2019]; Available from: https://www.ema.europa.eu/en/documents/report/report-haemophilia-registries-workshop_en.pdf

39. Gupta S, Acharya S, Roberson C, Lail A, Soucie JM, Shapiro A. Potential of the Community Counts registry to characterize rare bleeding disorders. Haemophilia. 2019;25(6):1045-1050.

40. Konkle BA, Johnsen JM, Wheeler M, et al. Genotypes, phenotypes and whole genome sequence: approaches from the My Life Our Future haemophilia project. Haemophilia. 2018;24 Suppl 6:87-94.

41. Centers for Disease Control and Prevention. Community Counts. [cited September 24, 2019]; Available from: https://www.cdc.gov/ncbddd/hemophilia/communitycounts/data-reports/2018-9/table-1-patient-characteristics-by-calendar.html

42. Peyvandi F, Palla R, Menegatti M, et al. Coagulation factor activity and clinical bleeding severity in rare bleeding disorders: results from the European Network of Rare Bleeding Disorders. J Thromb Haemost. 2012;10(4):615-621.

43. Peyvandi F, Di Michele D, Bolton-Maggs PH, et al. Classification of rare bleeding disorders (RBDs) based on the association between coagulant factor activity and clinical bleeding severity. J Thromb Haemost. 2012;10(9):1938-1943.

44. European Association for Haemophilia and Allied Disorders. Prospective Rare Bleeding Disorders Database (PRO-RBDD). [cited September 23, 2019]; Available from: http://eahad.org/prospective-rare-bleeding-disorders-database-pro-rbd/

45. Menegatti M, Palla R, Boscarino M, et al. Minimal factor XIII activity level to prevent major spontaneous bleeds. J Thromb Haemost. 2017;15(9):1728-1736.

46. Iorio A, Keepanasseril A, Foster G, et al. Development of a Web-Accessible Population Pharmacokinetic Service-Hemophilia (WAPPS-Hemo): study protocol. JMIR Res Protoc. 2016;5(4):e239.

47. Hemker HC, Giesen P, Al Dieri R, et al. Calibrated automated thrombin generation measurement in clotting plasma. Pathophysiol Haemost Thromb. 2003;33 (1):4-15.

48. Chitlur M, Sorensen B, Rivard GE, et al. Standardization of thromboelastography: a report from the TEG-ROTEM working group. Haemophilia. 2011;17(3):532-537.

49. van Geffen M, Loof A, Lap P, et al. A novel hemostasis assay for the simultaneous measurement of coagulation and fibrinolysis. Hematology. 2011;16(6):327-336.

50. Colucci M, Binetti BM, Tripodi A, Chantarangkul V, Semeraro N. Hyperprothrombinemia associated with prothrombin G20210A mutation inhibits plasma fibrinolysis through a TAFI-mediated mechanism. Blood. 2004;103(6):2157-2161.

51. Ma Q, Ozel AB, Ramdas S, et al. Genetic variants in PLG, LPA, and SIGLEC 14 as well as smoking contribute to plasma plasminogen levels. Blood. 2014;124(20):3155-3164.

52. Li JF, Lin Y, Yang YH, et al. Fibrinogen Aalpha Thr312Ala polymorphism specifically contributes to chronic thromboembolic pulmonary hypertension by increasing fibrin resistance. PLoS One. 2013;8 (7):e69635.

Ferrata Storti Foundation

Seronegative antiphospholipid syndrome: refining the value of "non-criteria" antibodies for diagnosis and clinical management

Pasquale Pignatelli,[1,2*] Evaristo Ettorre,[3*] Danilo Menichelli,[1] Arianna Pani,[4,5] Francesco Violi,[1,2**] and Daniele Pastori[1**]

[1]I Clinica Medica, Department of Internal Medicine and Medical Specialties, Sapienza University of Rome, Rome; [2]Mediterranea Cardiocentro, Naples; [3]Department of Cardiovascular, Respiratory, Nephrologic, Anesthesiologic and Geriatric Sciences, Division of Gerontology, Sapienza University, Rome; [4]Department of Oncology and Onco-Hematology, University of Milan, Milan and [5]Clinical Pharmacology Unit, ASST Grande Ospedale Metropolitano Niguarda, Milan, Italy

*PP and EE contributed equally to this work.
**FV and DP contributed equally to this work as co-senior authors.

ABSTRACT

Antiphospholipid syndrome (APS) is a systemic autoimmune disease characterized by arterial and venous thrombotic manifestations and/or pregnancy-related complications in patients with persistently high antiphospholipid antibodies (aPL), the most common being represented by anticardiolipin antibodies (aCL), anti-beta 2 glycoprotein-I (aβ2GPI), and lupus anticoagulant (LAC). A growing number of studies have showed that, in some cases, patients may present with clinical features of APS but with temporary positive or persistently negative titers of aPL. For these patients, the definition of seronegative APS (SN-APS) has been proposed. Nevertheless, the negativity to classic aPL criteria does not imply that other antibodies may be present or involved in the onset of thrombosis. The diagnosis of SN-APS is usually made by exclusion, but its recognition is important to adopt the most appropriate anti-thrombotic strategy to reduce the rate of recurrences. This research is in continuous development as the clinical relevance of these antibodies is far from being completely clarified. The most studied antibodies are those against phosphatidylethanolamine, phosphatidic acid, phosphatidylserine, phosphatidylinositol, vimentin/cardiolipin complex, and annexin A5. Moreover, the assays to measure the levels of these antibodies have not yet been standardized. In this review, we will summarize the evidence on the most studied non-criteria aPL, their potential clinical relevance, and the antithrombotic therapeutic strategies available in the setting of APS and SN-APS.

Correspondence:

PASQUALE PIGNATELLI
pasquale.pignatelli@uniroma1.it.

Check the online version for the most updated information on this article, online supplements, and information on authorship & disclosures: www.haematologica.org/content/105/3/562

Introduction

The prevalence of antiphospholipid antibodies (aPL) in the general population is difficult to estimate due to the lack of population-based studies. The most frequently detectable aPL are anticardiolipin antibodies (aCL), antiβ2-glycoprotein I antibodies (anti-β2-GPI), and lupus anticoagulant (LAC).[1] A large review of the literature in 2013 estimated that the prevalence of aPL positivity is 6% among women with pregnancy complications, 10% among patients with deep venous thrombosis (DVT), 11% among patients with myocardial infarction, and 17% among patients with juvenile stroke (<50 years of age). As acknowledged by the Authors, this prevalence should be considered with caution, because 60% of the papers were published before 2000, all three criteria aPL tests were performed in only 11% of the papers, and 36% of papers used a low-titer aCL cut off.[2]

Subjects carrying aPL who develop thrombotic complications are diagnosed with the antiphospholipid syndrome (APS), which was first described in 1983 by Hughes, who initially defined it as "anticardiolipin syndrome".[3] This definition was derived from clinical observation of recurrent miscarriages, central nervous system

disease, and recurrent venous thromboembolism (VTE) in patients with systemic lupus erythematosus (SLE) and serum positivity for anticardiolipin antibodies (aCL) and lupus anticoagulant (LAC).[3] Recently, Duarte-Garcia *et al.* found an annual incidence of APS of 2.1 per 100,000 per year, with a prevalence of 50 APS patients per 100,000, equally distributed between males and females.[4]

A more clinically challenging scenario is represented by patients with a clinical history characterized by episodes of thrombosis (especially if recurrent) without cardiovascular risk factors, and more in general, in absence of an identifiable cause of thrombosis, suggestive of a thrombophilic condition, such as APS, but in absence of any positivity of aPL. For these patients, the definition of seronegative APS (SN-APS) was proposed.[5] In the context of SN-APS, several non-criteria aPL have been investigated with divergent results.

In this review, we will discuss criteria for defining the SN-APS, the new potential non-criteria antibodies implied in SN-APS and its clinical management.

Antiphospholipid syndrome

Diagnosis of antiphospholipid syndrome

Antiphospholipid syndrome is a systemic autoimmune disorder characterized by arterial and venous thrombotic manifestations and/or pregnancy morbidity in patients with persistently high levels of aPL.[6] APS may be classified as primary or secondary, the latter being present in 30-40% of patients with SLE.[7] The 2006 Sapporo criteria are those currently recommended to diagnose APS.[8] They include the presence of one clinical criterion and high values of at least one aPL among IgM/IgG aCL in serum or plasma, IgM/IgG anti-β2 glycoprotein-I (aβ2GPI) antibodies in serum or plasma, and LAC in plasma. Clinical and laboratory criteria are listed in Figure 1.[7]

The persistence of high antibody values should be tested at least 12 weeks apart, and, in addition, the antibody titers should be dosed at least 12 weeks after the thrombotic event but no more than five years afterwards.[7,8] Of note, not all patients remain positive over time, and factors associated with persistence of aPL positivity are not well known, but may include inflammation and oxidative stress.[9]

Subjects positive for aPL have a low risk of developing thrombotic events (<1%/year), but after a first episode, the risk of recurrence increases by 10-67%.[10] This finding was supported by a recent study performed by Kearon *et al.*,[11] in which 307 patients with a first unprovoked VTE were tested for aPL. In this study, the persistence of aPL on ≥2 occasions was associated with an increased risk of recurrent thrombosis, despite negative D-Dimer values (HR 4.5: 95%CI: 1.5-13.0; *P*=0.006).[11]

Clinical presentation of antiphospholipid syndrome

Antiphospholipid syndrome can be broadly classified in venous, arterial or obstetric APS, which are, however, not mutually exclusive. In a retrospective analysis of a cohort of 160 patients with a definite APS, VTE was the most common manifestation (47.5%), followed by arterial thromboembolism (43.1%), while obstetrical complications was found in only 9.7% of patients; in this study, catastrophic APS (C-APS) represented 2.5% of the cases.[12]

Stroke and transient ischemic attack often involve APS patients, but also lower limb ischemia and myocardial infarction can occur.[12] In this context, the relationship between aPL and myocardial infarction seems to be bidi-
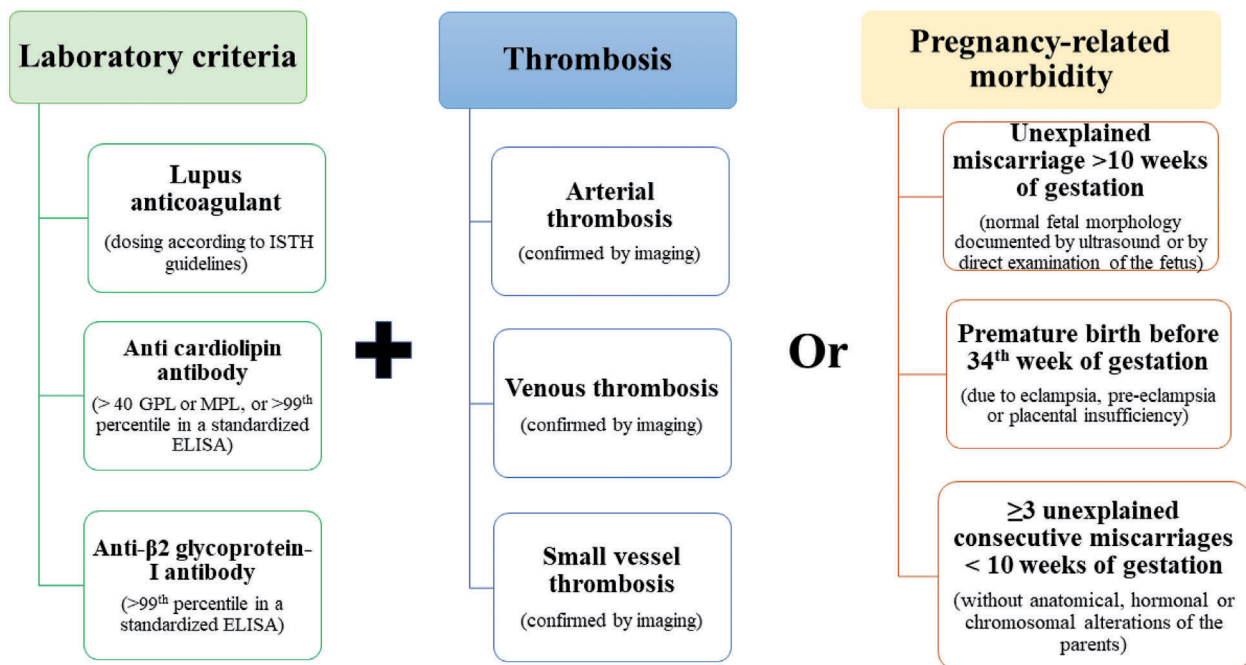
Figure 1. Summary of criteria for antiphospholipid syndrome (APS) diagnosis according to Sapporo criteria. GPL: glycopeptidolipid; MPL: monophosphoryl lipid A.

rectional. Therefore, patients carrying aPL have an increased risk of ischemic heart disease, and conversely, after a first coronary artery disease event, patients positive for aPL showed twice the risk of recurrent major adverse cardiovascular events at 12 and 24 months.[13] This risk was also evident in subjects with juvenile myocardial infarction in absence of cardiovascular risk factors.[13]

Concerning obstetric complications, fetal loss, especially after 10th week of gestation and premature birth due to eclampsia or placental insufficiency are frequent complications in APS women.[14] In young women with a history of multiple miscarriage, the immunological study for aPL should be considered.

Finally, catastrophic APS (C-APS) is a severe and life-threatening manifestation characterized by simultaneous venous or/and arterial thrombosis, often triggered by infections and surgical procedures. C-APS involves multiple organs and systems due to excess of proinflammatory cytokines, coagulation cascade, and platelet activation, leading to thrombosis and microangiopathic hemolytic anemia.[15]

In addition to the above described signs and symptoms, the clinical presentation of patients with APS may be more heterogeneous, involving thrombosis of medium and small vessels (Table 1).[6,7,16-18] The relevance in clinical practice of non-conventional APS criteria was investigated during the 14th Congress on Antiphospholipid Antibodies, in which each relevant clinical manifestation was analyzed and each evidence was evaluated by the GRADE system. This system also considers the balance of patient-important outcomes, the overall quality of the evidence for each outcome, and any uncertainty about values.[18]

The most commonly affected sites are the kidney, the skin, and the cardiovascular and nervous systems. In the kidney, it is possible to find an acute thrombotic microangiopathy or a chronic pattern of vaso-occlusive lesions such as cortical ischemic lesions, arterial fibrous intimal hyperplasia or interstitial fibrosis.[6] APS nephropathy can be identified with a urine test associated with a 24-hour investigation of proteinuria. A biopsy is mandatory in cases where the cause is not clearly identifiable, as in patients with concomitant diabetes, uncontrolled arterial hypertension or other autoimmune diseases such as SLE.

Concerning the skin, livedo reticularis can be found, and recurrent ulcerations called livedoid vasculopathy have also been described.[8] To evaluate skin abnormalities, a clinical examination is often adequate, and there is usually no need for skin biopsy.

Cardiac abnormalities include valve leaflet thickening,[6] and diastolic dysfunction, especially of the right ventricle.[19] Heart valve disease and diastolic dysfunction can be investigated by resting transthoracic echocardiography and by cardiac magnetic resonance imaging (MRI) if a myocardial involvement is suspected (i.e. myocarditis). Pericardium may also be involved, especially in patients with APS and SLE.

Finally, APS is associated with an increased risk of dementia, seizures, multiple sclerosis-like illness, migraine, myelitis transversa and chorea, due to vascular damage and a direct action of antibodies on neurons and ependymal cells.[7,20,21] However, unlike other neurological disorders, seizure is not considered a non-conventional criterion due to lack of strength of evidence.[18] To identify critical illness such as neurological disorders, instrumental

examinations are mandatory. An MRI and an electroencephalogram could be useful in recognizing brain atrophy associated with dementia and seizures, and could identify more elusive symptoms such as chorea and migraine if associated with an accurate physical examination.

Other blood alterations include thrombocytopenia (commonly mild with platelet count between $50x10^9$/L and $150x10^9$/L, but also severe with platelet counts $<20x10^9$/L often associated with microangiopathy) and hemolytic anemia with the possible presence of schistocytes.[6] In particular, thrombocytopenia is common in APS, affecting 20-46% of patients and could paradoxically be associated with an increased risk of thrombosis.[18] Thrombocytopenia may be the result of an increased activation and destruction of platelets by an immune-mediated mechanism involving aPL or by thrombotic microangiopathy.[22]

After the exclusion of a pseudo-thrombocytopenia, and performing a Coombs test to ascertain the autoimmune nature of thrombocytopenia, corticosteroids, immunosuppressive agents, immunoglobulins and new drugs such as Mammalian target of rapamycin (mTOR) inhibitors and monoclonal antibodies could be helpful in patients with autoimmune thrombocytopenia.[23]

Definition of seronegative antiphospholipid syndrome and non-criteria antiphospholipid antibodies

The first definition of SN-APS was given in 2003 by Hughes and Khamashta[5] who described patients with clinical manifestations highly suggestive of APS in absence of the laboratory criteria such as LAC, aCL and aβ2GPI antibodies.

Seronegative APS is usually a diagnosis of exclusion and should be suspected in patients with a clinical history suggestive of APS, such as those with recurrent arterial venous thrombotic events, recurrent miscarriage, or unexplained thrombocytopenia, with persistent negativity of aPL tested on at least two occasions, and when other causes of throm-

Table 1. "Extra-criteria" manifestations of antiphospholipid syndrome.

Nervous system
Dementia
Seizures
Multiple sclerosis–like illness
Chorea
Myelitis
Skin
Livedo reticularis
Livedoid vasculopathy
Heart
Valve vegetations or thickening (Libman-Sacks Endocarditis)
Diastolic dysfunction
Blood
Thrombocytopenia
Hemolytic anemia
Kidney
Microangiopathy
Chronic vaso-occlusive lesions (atherosclerosis, glomerular ischemia, interstitial fibrosis, arterial fibrous intimal hyperplasia)

bosis are excluded, such as genetic thrombophilia (factor V and II mutations), active cancer, trauma, major surgery, or prolonged bed rest. This is particularly evident in young patients without established cardiovascular risk factors (i.e. obesity, diabetes, hypertension, dyslipidemia). Most importantly, other forms of coagulopathy should be excluded first, including Protein C and S and anti-thrombin deficiency. In addition, the patient's personal medical history should be carefully investigated to exclude previous positivity to aPL.

To better characterize the entity of SN-APS, antibodies against different phospholipids or protein co-factors have been investigated in patients negative to conventional aPL (Table 2).

The antibodies that have been most studied so far are those directed against: 1) a zwitterionic phospholipid, namely phosphatidylethanolamine (PE); 2) negatively charged phospholipids other than cardiolipin, including phosphatidic acid (PA), phosphatidylserine (PS), phosphatidylinositol (PI); 3) vimentin (forming a complex with

Table 2. Summary of positivity for extra-criteria antibodies in each study of seronegative antiphospholipid syndrome (SN-APS).

Authors (year)	Study typology P=prospective; R=retrospective CS=cross-sectional CaS= case series	Population studied		aPL positivity in SN-APS (n)						Main findings
		APS (n)	SN-APS (n)	IgA aPL	aPE	NCP	AVA/CL	aPS/PT	aANX	
Sanmarco[39] (2001)	CS	67	18	-	18	-	-	-	-	
Sanmarco[40] (2007)	CS	-	25	-	25	-	-	-	-	25 of the 40 aPE-positive patients (63%) were negative for the APS laboratory criteria
Kumar[83] (2009)	CaS	-	5	5	-	-	-	-	-	
Ortona[47] (2010)	CS	40	29	-	-	-	27	-	-	Vimentin seems to be positive in a large number of mainly SN-APS patients.
Conti[49] (2013)	CS	25	24	-	-	-	11	1	1	SN-APS were positive for 11/24 (45.8%) for anti-vimentin/cardiolipin antibodies, 3/24 (12.5%) for anti-prothrombin antibodies, and 1/24 (4.2%) for anti-annexin V antibodies.
Ruiz-García[35] (2014)	CS	22	35	35	-	-	-	-	-	Isolated IgA aβ2GPI antibodies were found in 22% of patients. Patients with arterial thrombosis were positive only for IgA aβ2GPI.
Cousins[32] (2015)	CS	40	40	1	-	-	-	-	-	IgA aCL or IgA aβ2GPI antibodies, were present in a significant proportion of patients with APS, and in a small proportion of SN-APS.
Mekinian[27] (2016)	CS	83	96	-	47	-	-	5	57	68% of patients with obstetrical SN-APS have non-conventional aPL
Zohoury[24] (2017)	CS	107	68	-	8	-	11	8	-	1/3 of SN-APS patients showed reactivity to 1 or more non-criteria markers
Tortosa[36] (2017)	R	-	38	38	-	-	-	-	-	The presence of IgA aβ2GPI in people with no history of APS-events is the main independent risk factor for the development of these types of events, mainly arterial thrombosis
Litvinova[25] (2018)	CS	41	17	-	-	5	-	4	4	87 patients: 41 APS, 11 aPL carriers, 17 SN-APS. <1% of patients with thrombotic/obstetrical SN-APS had non-conventional aPL Anti-PS/PT antibodies were correlated with LA. APS triple patients were also positive for anti-PS/PT antibodies
Truglia[50] (2018)	CS	-	61	-	-	-	33	-	-	Non-conventional tests, mainly aCL/Vim and aCL seem to be the most sensitive approaches for identifying aPL in patients with obstetric SN-APS
Billoir[84] (2019)	R	-	23	-	23	-	-	-	-	aPE persists in 23 patients (10%): 15 with a thrombotic event, 6 with obstetrical morbidity and 2 with a combined event
Ganapati[61] (2019)	R	58	12	-	-	-	-	7	-	Addition of aPS/PT to current APS criteria to SN-APS patients led to reclassification of additional 12.1% patients as APS overall and 42.8% in obstetric APS category

aANX: Annexin A5 antibody; aPE: phosphatidylethanolamine; aPL: antiphospholipid antibodies; APS: antiphospholipid syndrome; aPS/PT antiphosphatidylserine/prothrombin; AVA/CL: anti vimentin/cardiolipin complex; LA: lupus anticoagulant; NCP: negatively charged phospholipids (phosphatidic acid, phosphatidylserine and phosphatidylinositol); SN-APS: seronegative APS.

cardiolipin); 4) prothrombin (forming complex with PS – anti-PS/PT); and 5) the anticoagulant protein Annexin A5 (Table 2). In addition, the IgA isotype aβ2GPI is under investigation in APS and SN-APS patients.

A collaborative USA/UK study analyzed a comprehensive panel of 'non-criteria' aPL tests in a series of 175 consecutive patients matching the criteria for APS and 68 SN-APS patients with clinical manifestations suggestive of APS but having negative serology. The Authors found that one-third of the 'seronegative' sera gave positive results.[24] The study concluded that patients with clinical features of APS, but negative for conventional criteria markers, should undergo additional testing for non-criteria biomarkers.[24]

A recent study evidenced that positivity for the extra-criteria aPL was <1% in SN-APS (thrombotic or obstetric); however, the lack of clear inclusion and exclusion criteria does not allow a precise estimation of the prevalence to be made.[25]

Similarly, non-criteria antibodies were detected in 18.8% of SN-APS patients also in a Chinese cohort composed of APS and patients with only clinical criteria for APS.[26] This is also confirmed in obstetric SN-APS patients, in whom 68% were positive for non-conventional aPL.[27]

Here we will provide an overview of current evidence on the most studied non-criteria aPL that, although not validated in large cohort studies, may have a potential role in the pathogenesis of APS.

IgA antibody isotype anti-β 2 glycoprotein-I and anticardiolipin antibodies

There is a growing body of evidence to suggest a potential usefulness of IgA in the context of APS.[28] Very recent evidence suggested that, while IgG/M isotypes recognize an epitope in domain 1, the epitopes recognized by IgA are the domains 3, 4 and 5.[29] However, as reported by the 13th International Congress on Antiphospholipid Antibodies, testing for IgA-aβ2GPI should be considered only in patients negative for IgG and IgM isotypes with APS symptoms.[30]

Studies investigating the prevalence of IgA aPL reported a variable prevalence ranging from 14% to 72% according to different reports;[28] however, these studies have a retrospective design, used different assays to measure IgA aPL, and used different cut-off values to define aPL positivity.[31,32]

A large study including 5,892 patients (803 with SLE and 5,089 from the Antiphospholipid Standardization Laboratory sent for evaluation for APS) found that IgA aβ2GPI isotype was positive in 255 (4.3%) patients, in 198 cases in association with other aPL, while only aPL was detectable in 57.[33] Isolated IgA aβ2GPI positivity was associated with an increased risk of arterial thrombosis (*P*<0.001), venous thrombosis (*P*=0.015), and all thrombosis (*P*<0.001).[33]

A second study evaluated, in addition to IgM and IgG, the positivity and predictivity of IgA aCL and IgA aβ2GPI in 430 patients: 111 with APS, 119 with SLE, and 200 healthy controls.[34] Positivity for IgA aCL was 38%; IgA aβ2GPI was 46% in patients with APS. All three antibody isotypes (IgM, IgG and IgA) were significantly associated with a diagnosis of APS, with high specificity but not good sensitivity, based on receiver operating characteristic (ROC) analysis. Looking at likely hazard ratios, the IgA aβ2GPI (HR 33.9, 95%CI: 10.5-109.5) was similarly asso-

ciated to APS as compared to IgG aβ2GPI (HR 33.4, 95%CI: 13.0-86.1), but showed a higher association compared to IgM aβ2GPI (HR 9.2, 95%CI: 4.6-18.4) and was associated with thrombotic but not obstetric complications in patients with APS.[34]

Indeed, IgA aβ2GPI levels seem to be associated with thrombotic events in patients without other aPL.[33,35] Thus, a case-control study including 244 asymptomatic patients screened for aPL and positive only for IgA aβ2GPI and 221 negative patients followed for five years showed that the presence of IgA aβ2GPI was associated with an increased risk for developing clinical thrombotic APS events (OR 5.15; *P*<0.001).[36]

Although attractive, these data were not confirmed by another study evaluating the presence of IgA aβ2GPI antibodies in SN-APS.[25]

Based on this evidence, it is not clear whether testing for IgA aCL and IgA aβ2GPI antibodies in addition to the routine tests may improve thrombotic risk stratification. Thus, the use of IgA antibodies to identify a SN-APS needs to be further investigated.

Antibodies to phosphatidylethanolamine

Phosphatidylethanolamine is mainly found in the inner leaflets of plasma membranes and contributes to 20-50% of total phospholipids. It works as an anticoagulant by enhancing activated protein C (APC) activity. Other investigators have demonstrated that PE inhibits coagulation activity interfering with the factor Xa-prothrombin system.[37]

Several studies reported that antibodies against PE (aPE) are significantly associated with major clinical events such as fetal loss and/or thrombosis, and are mainly present in the absence of the laboratory criteria of APS. Bérard *et al.* showed that aPE were the only aPL found in 6 of 34 patients suffering from thrombotic events and with a negative screening for antibodies to anionic phospholipids, including LA.[38] A second study focused on patients with unexplained thrombosis and no criteria for APS. Thus, in 98 patients with unexplained thrombosis, 142 with thrombophilia, 67 with APS, 75 with hereditary hemostatic defects and 110 without thrombosis, the authors found that aPE prevalence was significantly higher both in patients with APS (43%; *P*<0.0001) and in those with unexplained thrombosis (18%; *P*=0.001) compared to patients without thrombosis.[39] Subsequently, in a large multicenter study including 317 patients with deep venous thrombosis and 52 with arterial events, aPE were found in 15% of the thrombotic patients, most of whom were only positive for aPL.[40] Some interesting data were also reported regarding the association between aPE and obstetric complications. Gris *et al*. measured various aPL in a large cohort of 518 women with unexplained or explained early fetal losses and a control group of healthy mothers. IgM-aPE were found to be independent risk factors for unexplained early fetal loss.[41]

A retrospective study on 228 SN-APS demonstrated a positivity for aPE in 10% of the patients.[42] In contrast, a recent study on a Chinese population composed of APS and patients with only clinical criteria for APS failed to demonstrate any aPE positivity in SN-APS.[26]

The above reported results suggest that aPE could be considered as markers of a variant of APS when they are associated with thrombosis and a potential tool to define the SN-APS subjects.

Antibodies against phosphatidic acid, phosphatidylserine and phosphatidylinositol

In an effort to expand the panel of aPL to other negatively-charged phospholipids, antibodies against phosphatidic acid (PA), phosphatidylserine (PS), and phosphatidylinositol (PI), which fall under the category of anionic phospholipids, were proposed.[43] Anti-PS antibodies inhibited the development and invasion of the trophoblast, decreased hCG levels, and retarded the formation of syncytiotrophoblast in *in vitro* models.[44] Few clinical studies have investigated this issue. In a first study on 866 women with recurrent pregnancy loss (RPL), the authors found that 87 of 866 women who were negative for aCL had a positivity for one of the other aPL.[42] In a second study on 872 women with RPL, 49 (3.6%) were negative for both aCL and LA but positive for aPS.[46] In this second study, the presence of aPS had a positive correlation with the number of consecutive pregnancy losses.[46] This result was not confirmed when the same author analyzed a larger population of 1,020 woman with RPL.[46] Moreover, Zhang *et al.* did not find any positivity for aPE, aPS or aPI in an evaluation study of 288 subjects (86 patients with APS, 30 patients with non-APS thrombosis, 32 patients with non-APS pregnancy-related morbidity, 42 patients with SLE, and 39 healthy controls).[26]

Based on the current evidence, testing for aPA, aPI and aPS is not recommended, as these antibodies appeared to overlap with the accepted diagnostic markers of APS. Nonetheless, the results obtained on RPL with a seronegative profile suggest a potential role for aPA, aPI and aPS in defining SN-APS in this particular setting.

Anti-vimentin/cardiolipin complex

Vimentin is the most abundant type III intermediate filament of the cytoskeletal system and it was recently localized on the surface of apoptotic neutrophils and T cells, activated macrophages, platelets, and vascular endothelial cells. After becoming antigenic with a still unexplained mechanism, Vimentin is exposed and could be bound by anti-vimentin antibodies (AVA).[47,48] Vimentin could also electrically interact with cardiolipin on the surface of apoptotic cells generating the vimentin/cardiolipin complex. Antibodies against this complex (vimentin/cardiolipin antibodies, AVA/CL) show a prothrombotic effect. Thus, Ortona *et al.* demonstrated an AVA/CL-mediated activation of the TLR4/IRAK/Nf-kB molecular pathway that leads to the release of pro-inflammatory and procoagulant factors by endothelial cells.[47] Hence, AVA/CL could play a role in arterial thrombosis by inducing platelet and coagulation cascade activation.

The role of AVA/CL in SN-APS has been investigated only in a few clinical studies. Thus, Ortona *et al.*[47] analyzed serum IgG AVA/CL antibodies detected by ELISA in 29 SN-APS, 40 APS, 30 patients with SLE, 30 with rheumatoid arthritis, and 32 healthy controls. They found a positivity for AVA/CL in almost all APS patients (92%), and also in a large proportion of SN-APS (55%); interestingly, this positivity was persistent in almost all cases. Similarly, Conti *et al.* found AVA/CL positivity in 24 SN-APS patients.[49] Moreover, in a retrospective analysis of 61 obstetric SN-APS, 76% resulted positive for AVA/CL.[50] However, the overlapping presence of AVA/CL antibodies in SLE and APS weakens the specificity of such a diagnostic marker. Hence, the observation by Ortona *et al.*[47] needs to be confirmed by larger prospective clinical studies in order to better define the role of AVA/CL in SN-APS.

Anti-prothrombin and antiphosphatidylserine/prothrombin antibodies

Prothrombin is a plasma glycoprotein involved in the coagulation cascade converted to thrombin by extrinsic thromboplastin during the second stage of blood clotting.[51] A large amount of data, obtained from various, mainly retrospective, studies gave contrasting evidence concerning the clinical significance of anti-prothrombin antibody (aPT). Thus, in a comparison between 106 subjects who experienced either a non-fatal myocardial infarction or cardiac death and 106 subjects without coronary disease, Vaarala *et al.* found that a high level of aPT (highest tertile of distribution) predicted a 2.5-fold increase in the risk of cardiovascular events.[52] Conversely, Atsumi *et al.* did not find any correlation between clinical manifestation of aPT and APS in an evaluation of 265 APS patients.[53] More recently, two prospective studies validated the role of aPT in predicting the first or recurrent risk of thrombosis in patients with APS.[54,55] Considering a group of 142 LA positive patients, Forastiero *et al.* found that a higher rate of thrombosis in patients with positive anti-PT compared with patients without anti-PT (8.6% *vs.* 3.5% per patient year). The highest incidence of thrombosis was detected in patients positive for both aβ2GPI and aPT (8.4% per patient year).[54] Moreover, a 15-year longitudinal prospective study by Bizzaro *et al.* identified IgG aPT antibody as the most useful thrombosis predictor in SLE patients.[55]

Another intriguing issue is represented by the different potential role of IgG/IgM antiphosphatidylserine/prothrombin (aPS/PT) compared to aPT. Indeed, a high correlation between APS classical antibody panel and aPS/PT IgG/IgM suggests that this marker may be useful in the evaluation of APS.[56] The clinical significance of aPT and aPS-PT was evaluated by testing for the presence of these antibodies in 212 SLE patients and in 100 healthy individuals. Results show that aPT and aPS-PT were found in 47% of the patients (aPT in 31% and aPS-PT in 31%). Their presence did not correlate with that of aCL, aβ2GPI, LA and/or anti-protein S. IgG but not IgM aPT were more frequently found in patients with thrombosis than in those without. IgG and IgM aPS-PT were also more frequent in patients with thrombosis (venous and/or arterial) than in those without. Levels of IgG aPT and IgG and IgM aPS-PT were higher in patients with thrombosis than in those without. More significantly, 48% of the patients with aPL-related clinical features who were negative for standard tests had aPT.[57] Recently, the clinical significance of aPS/PT antibodies was prospectively evaluated in a cohort of 191 aPL carriers:[58] IgG aPS/PT antibodies were detected in 40 (20.9%) and IgM aPS/PT in 102 (53.4%) of the carriers. The cumulative incidence rate of thrombotic events was significantly higher in the IgG aPS/PT positive (*P*=0.035) but not in the IgM aPS/PT positive carriers. Similar results were obtained in a second study evaluating 152 patients with a previous thrombosis of whom 90 were SN-APS; 10% of SN-APS patients in this study were positive for aPS/PT.[59] Of note, aPS/PT are associated with recurrent early or late abortions and with premature delivery irrespective of other aPL.[60]

Based on the above studies, aPT and aPS/PT can be

potentially used as confirmatory diagnostic markers and as indicators of the risk of thrombosis. Recently, the presence of IgG and IgM aPS/PT was also detected in 9 of 17 SN-APS.[25] Similar, and even stronger evidence was provided by two retrospective studies on SN-APS patients that found approximately 50% of subjects were positive for aPS/PT.[61,62] Nonetheless, further studies must be undertaken before these antibodies can be included in the diagnostic criteria of SN-APS.

Annexin A5 antibody

Annexin A5 is a glycoprotein that binds to negative phospholipids such as PS. It has been proposed that annexin A5 forms a protective anticoagulant shield on vascular endothelial cells and that aβ2GPI antibodies in complex with ß2GPI may disturb the shield and hence predispose to thrombosis. Due to this marked heterogeneity, it remains controversial whether anti-annexin A5 antibodies (aANX) are associated with clinical manifestations. In a comparison of 112 APS patients with 40 healthy controls, Singh *et al.* found aANX positivity in 69 APS and in only 3 controls.[63] On the contrary, de Laat *et al.* found no association between aANX and history of thrombosis in 198 patients with primary APS, SLE or lupus-like disease.[64] aANX was also found to be predictive for fetal loss in a study of three groups (total 518 women) of patients with unexplained primary recurrent early fetal loss, patients with explained episodes, and mothers with no previous obstetric incident, respectively.[41]

Annexin A5 resistance was proposed as a mechanism for APS. The annexin A5 resistance (A5R) assay identifies patients with an antibody-mediated disruption of annexin A5 on endothelial surfaces. This is demonstrated by the resistance to the annexin A5 anticoagulant effects (i.e. annexin A5 resistance) *in vitro*. This test was validated in 750 patients with a history of thrombosis, pregnancy complications, and controls.[65] The authors found a reduction in A5 anticoagulant ratios in aPL antibody-positive patients with thrombosis and/or pregnancy complications compared with aPL antibody-negative patients and controls. This suggests that reduced A5R could identify patients with a propensity for thrombosis or pregnancy complications.[65]

Very recently, a case report described the presence of multiple annexin autoantibodies in a patient with recurrent miscarriages, fulminant stroke, and SN-APS.[66] Hence, although attractive, the evaluation of aANX or A5R in clinical practice for the management of SN-APS requires larger prospective studies.

From risk assessment to antithrombotic treatment

The first step in the assessment of thrombotic risk in APS and SN-APS patients is represented by antibody characterization and evaluation of cardiovascular risk factors. Thus, the thrombotic risk varies according to aPL positivity and antibody titers. For example, a retrospective study on 3,088 APS patients demonstrated that single positivity for aCL or aβ2GPI was associated with low risk of event [odds ratio (OR) <5], while LA positivity alone conferred a medium risk of event (OR 5-9); this risk increased in patients with double or triple positivity (OR >9).[67]

Some scores have also been proposed to stratify the risk of events in APS patients; the APL Score has no clinical items and is based exclusively on the antibody titers (Table 3).[68] An aPL score of ≥30 was an independent risk factor for thrombosis (hazard ratio 3.144, 95%CI: 1.383-7.150; *P*=0.006) in patients with autoimmune diseases.[69]

Another score is the Global Anti-Phospholipid Syndrome Score (GAPSS), which was developed in a cross-sectional study on a cohort of 211 patients with SLE. The score includes traditional cardiovascular risk factors such as hypertension and hyperlipidemia and the presence / absence of aPL70 (Table 3). Of note, both scores also include one non-criteria aPL, such as aPS/PT.

These scores, although potentially useful in clinical practice, require further prognostic validation.

The thrombotic risk stratification is more challenging in patients with SN-APS. It is important to identify and characterize the presence of non-criteria aPL, as they seem to be associated with different thrombotic complications (Table 4). Thus, aPS/PT and antibodies to vimentin/CL complex increase the risk of arterial thrombosis, while pregnancy-related complications are associated with the presence of PE, PA, PS and PI antibodies (Table 4).

Table 3. Scores for risk stratification in antiphospholipid syndrome.

APL Score - ITEMS	CUT-OFF	POINTS
APTT mixing >49 sec	5	
CONFIRMATION TEST, ratio	>1.3	2
	>1.1	1
KCT mixing >29 sec.	8	
DRVVT mixing	>45 sec.	4
CONFIRMATION TEST, ratio	>1.3	2
	>1.1	1
IgG ACL, GPL.		
High titers	>30	20
Medium/low titers	>18.5	4
IgM ACL, MPL	>7	2
IgG Anti-β2GPI		
High titers >15 U	20	
Medium/low titers	>2.2 U	6
IgM anti-β2GPI	>6 U	1
IgG aPS/PT		
High titers >10 U	20	
Medium/low titers	>2 U	13
IgM aPS/PT >9.2 U	8	

GAPSS	Item	Points
CLINICAL	Hyperlipidemia	3
	Arterial hypertension	1
LABORATORY	aCL IgG/IgM	5
	Anti β2GPI IgG/IgM	4
	aPS/PT IgG/IgM	3
	LA	4
	Total	20

APTT: activated partial thromboplastin time; KCT: kaolin clotting time; dRVVT: dilute Russell's viper venom time; aCL: anticardiolipin antibodies; β2GPI: β2-glicoprotein I; aPS/PT: phosphatidylserine prothrombin complex; aPL: antiphospholipid antibody; GPL: IgG phospholipid units; MPL: IgM phospholipid units; LA: lupus anticoagulant.

Primary and secondary prevention strategies

Antiphospholipid antibody carriers

In subjects with positivity for aPL in the absence of clinical thrombotic events, primary prevention strategy includes cardiovascular risk factors such as arterial hypertension, diabetes, dyslipidemia and cigarette smoking (Figure 2). Treatment with low-dose aspirin (LDA, 75-100 mg/die) is still controversial[6] and could be considered in patients at high risk, such as those with triple positivity or persistent positivity with medium-high titer of aCL.[71,72] Recently, the positivity for IgG aPS/PT has been suggested as a marker of thrombotic risk in aPL carriers in addition to triple positivity (Figure 2).[58] Regarding oral anticoagulation, with or without LDA, the quality of evidence is too low to demonstrate benefit or harm of anticoagulant use in aPL carriers.[73]

In women with a high-risk aPL profile but no history of thrombosis or pregnancy complications, treatment with LDA (75-100 mg daily) during pregnancy should be considered according to 2019 European League Against Rheumatism (EULAR) recommendations.

Secondary antiphospholipid syndrome

In APS patients with previous arterial or venous thromboembolism, use of unfractionated or low molecular weight heparins (LMWH) is recommended in the acute phase[6] followed by long-term treatment with warfarin, with an international normalized ratio (INR) range between 2-3.[8,74]

Warfarin therapy in APS has several critical points. Indeed, a recent study[10] showed that, in the APS population, the management of anticoagulant therapy is more problematic compared to a population of patients with

Table 4. Suggested extra-criteria antibodies in seronegative antiphospholipid syndrome and its clinical manifestations.

Extra-critera antibodies	Clinical manifestations
Anti-prothrombin/phosphatidylserine antibodies	Thrombosis
Anti-annexin V antibodies/annexin A5 resistance	Thrombosis and/or pregnancy complications
Antibodies to vimentin/CL complex	Arterial thrombosis
Phosphatidylethanolamine	Fetal loss and/or thrombosis
Phosphatidic acid	Fetal loss
Phosphatidylserine	Fetal loss
Phosphatidylinositol	Fetal loss
IgA aCL and aβ2GPI antibodies	Thrombosis

CL:cardiolipin; aβ2GPI: anti- β2 Glycoprotein I.

aPL carriers	• Management of cardiovascular risk factors • Consider LDA in high-risk patients (triple positivity or high titers aCL)
Secondary prevention of VTE (APS and SN-APS)	• LMWH or UFH • Warfarin (INR range 2.0-3.0), If recurrence under warfarin, add on statin, LDA or hydroxychloroquine
Secondary prevention in arterial thrombosis (APS and SN-APS)	• LDA/Clopidogrel • Warfarin (INR range 2.0-3.0). Consider LDA association in patients with recurrent arterial thrombosis and low risk of bleeding. • Add statin if indicated
Prevention of pregnancy complications* (APS and SN-APS) *EULAR 2019	• First pregnancy with no history of thrombosis: consider LDA • History of ≥3 recurrent spontaneous miscarriages <10th week of gestation and/or fetal loss (≥10th week of gestation): LDA + prophylactic heparin • History of delivery <34 weeks of gestation: LDA or LDA + prophylactic heparin. • Patients with clinical 'non-criteria' obstetric APS, treatment with LDA alone or in combination with heparin might be considered

Figure 2. Summary of antithrombotic treatment options in patients with antiphospholipid syndrome and seronegative antiphospholipid syndrome.[72] APS: antiphospholipid syndrome; aPL: antiphospholipid antibodies; aCL: anticardiolipin antibodies; VTE: venous thromboembolism; LDA: low-dose aspirin, LMWH: low molecular weight heparin, UFH: unfractionated heparin; INR: international normalized ratio; EULAR: European League Against Rheumatism.

atrial fibrillation (AF). Thus, APS patients had a shorter time within the therapeutic range than those with AF (53.5% *vs.* 68%; *P*=0.001) and needed a higher mean weekly dose of warfarin to reach the therapeutic range.[10]

In the case of low-quality therapy with warfarin or recurrent thrombosis, two possible therapeutic approaches could be considered. The first is to adopt a higher intensity warfarin therapy with target INR 3-4, which is, however, not current practice given its association with a reduced risk of thrombosis in the majority of patients.[6,72,75] A second approach is represented by the addition of LDA to anticoagulation, which should, however, be reserved for high-risk patients, particularly after an arterial thrombotic event.[6,76]

More recently, non-vitamin K antagonist oral anticoagulants (NOAC) have been investigated in patients with APS with divergent results.[77] Following the results from the Trial on Rivaroxaban in AntiPhospholipid Syndrome (TRAPS),[78] which included triple positive thrombotic APS, rivaroxaban is contraindicated in APS patients with triple aPL positivity.[72] An analysis from the RE-COVER/RE-COVER II and RE-MEDY trials showed similar safety and efficacy of dabigatran in patients with thrombophilia and previous venous thromboembolic events, in whom APS represented the second most common inherited disorders, accounting for 20% of all patients.[79] These results need to be confirmed in real-world studies. A randomized trial investigating the efficacy and safety of apixaban in APS patients is currently ongoing;[80] this study will include patients with both venous and arterial thrombosis. Laboratory testing of NOAC may be useful in patients with APS as no pre-clinical data in this patient population are available.

Recently, new drugs have been administered in APS patients with thrombotic events. A first example is represented by mTOR inhibitors; these were found to reduce the onset of new vascular lesions after transplantation in patients with APS nephropathy.[81] Monoclonal antibodies such as rituximab[82] (anti-CD20 agent) and eculizumab[23] (anti-C5 agent) are currently administrated to manage non-criteria symptoms refractory to standard therapy and to add-on in catastrophic APS and kidney transplantation in APS patients, respectively. Despite these findings, the use of these drugs should be avoided due to lack of strong evidence in APS patients; their use could be considered in patients with refractory C-APS, as suggested by EULAR guidelines.[72]

Obstetric antiphospholipid syndrome

Women who are diagnosed with confirmed APS should be treated with antepartum administration of prophylactic or intermediate dose of unfractionated heparin or prophylactic LMWH combined with LDA (75-100 mg/day), according to the 2012 American College of Cardiology (ACC) guidelines.[74]

Recent 2019 EULAR recommendations suggest that women: 1) with a history of obstetric APS, such as a history of ≥3 recurrent spontaneous miscarriages <10th week of gestation and in those with a history of fetal loss (≥10th week of gestation); and 2) with a history of delivery <34 weeks of gestation due to eclampsia/severe pre-eclampsia or due to placental insufficiency, should be started on a combined therapy including LDA and prophylactic heparin during pregnancy.[72]

Heparin at prophylactic dose should be maintained for six weeks after delivery to avoid maternal thrombosis. Finally, heparin should be increased to therapeutic doses, in addition to LDA, in women with a history of thrombotic APS.

Conclusions

The diagnosis of SN-APS should be formulated only after the exclusion of other causes of inherited and acquired thrombophilic conditions. Although several different antibodies to a number of antigens are involved in SN-APS, the routine testing of these non-criteria antibodies is not recommended, but may be considered in patients with a high clinical suspicion of APS, such as those presenting with recurrent unexplained thrombosis, thrombosis at unusual sites, or women with recurrent pregnancy-related complications. The assessment and interpretation of these non-conventional antibodies should be performed by specialized centers of hemostasis and thrombosis to reduce laboratory variability.

The detection of non-criteria aPL may help guide antithrombotic strategies in SN-APS patients with arterial or venous thrombosis. As an example, patients treated with NOAC for recurrent VTE events, who become positive for non-criteria aPL, may be switched to VKA or LMWH, especially in cases of a recurrent thrombotic events. Moreover, in case of an unprovoked DVT, and among patients who could be withdrawn from anticoagulation, the positivity for a non-criteria aPL may help decide whether or not to continue long-term anticoagulation.

In conclusion, there is growing evidence to suggest a role for non-criteria aPL in those patients defined as "seronegative".

References

1. Meroni PL, Borghi MO, Raschi E, Tedesco F. Pathogenesis of antiphospholipid syndrome: understanding the antibodies. Nat Rev Rheumatol. 2011;7(6):330-339.
2. Andreoli L, Chighizola CB, Banzato A, et al. Estimated frequency of antiphospholipid antibodies in patients with pregnancy morbidity, stroke, myocardial infarction, and deep vein thrombosis: a critical review of the literature. Arthritis Care Res (Hoboken). 2013;65(11):1869-1873.
3. Hughes GR. Thrombosis, abortion, cerebral disease, and the lupus anticoagulant. Br Med J (Clin Res Ed). 1983;287(6399):1088-1089.
4. Duarte-Garcia A, Pham MM, Crowson CS, et al. The Epidemiology of Antiphospholipid Syndrome. A Population-Based Study. Arthritis Rheumatol. 2019;71 (9):1545-1552.
5. Hughes GR, Khamashta MA. Seronegative antiphospholipid syndrome. Ann Rheum Dis. 2003;62(12):1127.
6. Garcia D, Erkan D. Diagnosis and Management of the Antiphospholipid Syndrome. N Engl J Med. 2018;378(21): 2010-2021.
7. Limper M, de Leeuw K, Lely AT, et al. Diagnosing and treating antiphospholipid syndrome: a consensus paper. Neth J Med. 2019;77(3):98-108.
8. Miyakis S, Lockshin MD, Atsumi T, et al. International consensus statement on an update of the classification criteria for definite antiphospholipid syndrome (APS). J Thromb Haemost. 2006;4(2):295-306.
9. Lopez-Pedrera C, Barbarroja N, Jimenez-Gomez Y, et al. Oxidative stress in the pathogenesis of atherothrombosis associated with anti-phospholipid syndrome and systemic lupus erythematosus: new therapeutic approaches. Rheumatology (Oxford). 2016;55(12):2096-2108.

10. Pastori D, Parrotto S, Vicario T, et al. Antiphospholipid syndrome and anticoagulation quality: a clinical challenge. Atherosclerosis. 2016;244:48-50.

11. Kearon C, Parpia S, Spencer FA, et al. Antiphospholipid antibodies and recurrent thrombosis after a first unprovoked venous thromboembolism. Blood. 2018;131(19): 2151-2160.

12. Pengo V, Ruffatti A, Legnani C, et al. Clinical course of high-risk patients diagnosed with antiphospholipid syndrome. J Thromb Haemost. 2010;8(2):237-242.

13. Pastori D, Bucci T, Triggiani M, et al. Immunoglobulin G (IgG) anticardiolipin antibodies and recurrent cardiovascular events. A systematic review and Bayesian meta-regression analysis. Autoimmun Rev. 2019;18(5):519-525.

14. Uthman I, Noureldine MHA, Ruiz-Irastorza G, Khamashta M. Management of antiphospholipid syndrome. Ann Rheum Dis. 2019;78(2):155-161.

15. Espinosa G, Rodriguez-Pinto I, Cervera R. Catastrophic antiphospholipid syndrome: an update. Panminerva Med. 2017;59(3): 254-268.

16. Espinosa G, Cervera R. Current treatment of antiphospholipid syndrome: lights and shadows. Nat Rev Rheumatol. 2015;11(10): 586-596.

17. Schreiber K, Radin M, Sciascia S. Current insights in obstetric antiphospholipid syndrome. Curr Opin Obstet Gynecol. 2017;29(6):397-403.

18. Abreu MM, Danowski A, Wahl DG, et al. The relevance of "non-criteria" clinical manifestations of antiphospholipid syndrome: 14th International Congress on Antiphospholipid Antibodies Technical Task Force Report on Antiphospholipid Syndrome Clinical Features. Autoimmun Rev. 2015;14(5):401-414.

19. Tektonidou MG, Ioannidis JP, Moyssakis I, et al. Right ventricular diastolic dysfunction in patients with anticardiolipin antibodies and antiphospholipid syndrome. Ann Rheum Dis. 2001;60(1):43-48.

20. Roldan JF, Brey RL. Neurologic manifestations of the antiphospholipid syndrome. Curr Rheumatol Rep. 2007;9(2):109-115.

21. Bucci T, Menichelli D, Pignatelli P, et al. Relationship of Antiphospholipid Antibodies to Risk of Dementia: A Systematic Review. J Alzheimers Dis. 2019;69(2):561-576.

22. Artim-Esen B, Diz-Kucukkaya R, Inanc M. The significance and management of thrombocytopenia in antiphospholipid syndrome. Curr Rheumatol Rep. 2015;17(3):14.

23. Chighizola CB, Meroni PL. Thrombosis and Anti-phospholipid Syndrome: a 5-Year Update on Treatment. Curr Rheumatol Rep. 2018;20(7):44.

24. Zohoury N, Bertolaccini ML, Rodriguez-Garcia JL, et al. Closing the Serological Gap in the Antiphospholipid Syndrome: The Value of "Non-criteria" Antiphospholipid Antibodies. J Rheumatol. 2017;44(11):1597-1602.

25. Litvinova E, Darnige L, Kirilovsky A, et al. Prevalence and Significance of Non-conventional Antiphospholipid Antibodies in Patients With Clinical APS Criteria. Front Immunol. 2018;9:2971.

26. Zhang S, Wu Z, Zhang W, et al. Clinical performance of non-criteria antibodies to phospholipids in Chinese patients with antiphospholipid syndrome. Clin Chim Acta. 2019;495:205-209.

27. Mekinian A, Bourrienne MC, Carbillon L, et al. Non-conventional antiphospholipid antibodies in patients with clinical obstetrical APS: Prevalence and treatment efficacy in pregnancies. Semin Arthritis Rheum. 2016;46(2):232-237.

28. Brusch A. The Significance of Anti-Beta-2-Glycoprotein I Antibodies in Antiphospholipid Syndrome. Antibodies (Basel). 2016;5(2).

29. Serrano M, Martinez-Flores JA, Norman GL, et al. The IgA Isotype of Anti-beta2 Glycoprotein I Antibodies Recognizes Epitopes in Domains 3, 4, and 5 That Are Located in a Lateral Zone of the Molecule (L-Shaped). Front Immunol. 2019;10:1031.

30. Lakos G, Favaloro EJ, Harris EN, et al. International consensus guidelines on anticardiolipin and anti-beta2-glycoprotein I testing: report from the 13th International Congress on Antiphospholipid Antibodies. Arthritis Rheum. 2012;64(1):1-10.

31. Meijide H, Sciascia S, Sanna G, Khamashta MA, Bertolaccini ML. The clinical relevance of IgA anticardiolipin and IgA anti-beta2 glycoprotein I antiphospholipid antibodies: a systematic review. Autoimmun Rev. 2013;12(3):421-425.

32. Cousins L, Pericleous C, Khamashta M, et al. Antibodies to domain I of beta-2-glycoprotein I and IgA antiphospholipid antibodies in patients with 'seronegative' antiphospholipid syndrome. Ann Rheum Dis. 2015;74(1):317-319.

33. Murthy V, Willis R, Romay-Penabad Z, et al. Value of isolated IgA anti-beta2 -glycoprotein I positivity in the diagnosis of the antiphospholipid syndrome. Arthritis Rheum. 2013;65(12):3186-3193.

34. Pericleous C, Ferreira I, Borghi O, et al. Measuring IgA Anti-beta2-Glycoprotein I and IgG/IgA Anti-Domain I Antibodies Adds Value to Current Serological Assays for the Antiphospholipid Syndrome. Plos One. 2016;11(6):e0156407.

35. Ruiz-Garcia R, Serrano M, Martinez-Flores JA, et al. Isolated IgA anti- beta2 glycoprotein I antibodies in patients with clinical criteria for antiphospholipid syndrome. J Immunol Res. 2014;2014:704395.

36. Tortosa C, Cabrera-Marante O, Serrano M, et al. Incidence of thromboembolic events in asymptomatic carriers of IgA anti ss2 glycoprotein-I antibodies. PloS One. 2017;12(7): e0178889.

37. Sanmarco M, Boffa MC. Antiphosphatidylethanolamine antibodies and the antiphospholipid syndrome. Lupus. 2009;18 (10):920-923.

38. Berard M, Chantome R, Marcelli A, Boffa MC. Antiphosphatidylethanolamine antibodies as the only antiphospholipid antibodies. I. Association with thrombosis and vascular cutaneous diseases. J Rheumatol. 1996;23(8):1369-1374.

39. Sanmarco M, Alessi MC, Harle JR, et al. Antibodies to phosphatidylethanolamine as the only antiphospholipid antibodies found in patients with unexplained thromboses. Thromb Haemost. 2001;85(5):800-805.

40. Sanmarco M, Gayet S, Alessi MC, et al. Antiphosphatidylethanolamine antibodies are associated with an increased odds ratio for thrombosis. A multicenter study with the participation of the European Forum on antiphospholipid antibodies. Thromb Haemost. 2007;97(6):949-954.

41. Gris JC, Quere I, Sanmarco M, et al. Antiphospholipid and antiprotein syndromes in non-thrombotic, non-autoimmune women with unexplained recurrent primary early foetal loss. The Nimes Obstetricians and Haematologists Study--NOHA. Thromb Haemost. 2000;84(2):228-236.

42. Billoir P, Miranda S, Abboud J, et al. [Which place of antiphosphatidylethanolamine antibodies research in seronegative antiphospholipid syndrome suspicion?]. Rev Med Interne. 2019;40(6):351-354.

43. Bertolaccini ML, Amengual O, Atsumi T, et al. 'Non-criteria' aPL tests: report of a task force and preconference workshop at the 13th International Congress on Antiphospholipid Antibodies, Galveston, TX, USA, April 2010. Lupus. 2011;20(2):191-205.

44. Katsuragawa H, Kanzaki H, Inoue T, et al. Monoclonal antibody against phosphatidylserine inhibits in vitro human trophoblastic hormone production and invasion. Biol Reprod. 1997;56(1):50-58.

45. Yetman DL, Kutteh WH. Antiphospholipid antibody panels and recurrent pregnancy loss: prevalence of anticardiolipin antibodies compared with other antiphospholipid antibodies. Fertil Steril. 1996;66(4):540-546.

46. Jaslow CR, Carney JL, Kutteh WH. Diagnostic factors identified in 1020 women with two versus three or more recurrent pregnancy losses. Fertil Steril. 2010;93(4): 1234-1243.

47. Ortona E, Capozzi A, Colasanti T, et al. Vimentin/cardiolipin complex as a new antigenic target of the antiphospholipid syndrome. Blood. 2010;116(16):2960-2967.

48. Musaelyan A, Lapin S, Nazarov V, et al. Vimentin as antigenic target in autoimmunity: A comprehensive review. Autoimmun Rev. 2018;17(9):926-934.

49. Conti F, Capozzi A, Truglia S, et al. The mosaic of "seronegative" antiphospholipid syndrome. J Immunol Res. 2014;2014: 389601.

50. Truglia S, Capozzi A, Mancuso S, et al. A Monocentric Cohort of Obstetric Seronegative Anti-Phospholipid Syndrome. Front Immunol. 2018;9:1678.

51. Sciascia S, Sanna G, Murru V, et al. Anti-prothrombin (aPT) and anti-phosphatidylserine/prothrombin (aPS/PT) antibodies and the risk of thrombosis in the antiphospholipid syndrome. A systematic review. Thromb Haemost. 2014;111(2):354-364.

52. Vaarala O, Puurunen M, Manttari M, et al. Antibodies to prothrombin imply a risk of myocardial infarction in middle-aged men. Thromb Haemost. 1996;75(3):456-459.

53. Atsumi T, Ieko M, Bertolaccini ML, et al. Association of autoantibodies against the phosphatidylserine-prothrombin complex with manifestations of the antiphospholipid syndrome and with the presence of lupus anticoagulant. Arthritis Rheum. 2000;43(9): 1982-1993.

54. Forastiero R, Martinuzzo M, Pombo G, et al. A prospective study of antibodies to beta2-glycoprotein I and prothrombin, and risk of thrombosis. J Thromb Haemost. 2005;3(6): 1231-1238.

55. Bizzaro N, Ghirardello A, Zampieri S, et al. Anti-prothrombin antibodies predict thrombosis in patients with systemic lupus erythematosus: a 15-year longitudinal study. J Thromb Haemost. 2007;5(6):1158-1164.

56. Heikal NM, Jaskowski TD, Malmberg E, et al. Laboratory evaluation of anti-phospholipid syndrome: a preliminary prospective study of phosphatidylserine/prothrombin antibodies in an at-risk patient cohort. Clin Exp Immunol. 2015;180(2):218-226.

57. Bertolaccini ML, Atsumi T, Koike T, Hughes GR, Khamashta MA. Antiprothrombin anti-

bodies detected in two different assay systems. Prevalence and clinical significance in systemic lupus erythematosus. Thromb Haemost. 2005;93(2):289-297.

58. Tonello M, Mattia E, Favaro M, et al. IgG phosphatidylserine/prothrombin antibodies as a risk factor of thrombosis in antiphospholipid antibody carriers. Thromb Res. 2019;177:157-160.

59. Bardin N, Alessi MC, Dignat-George F, et al. Does the anti-prothrombin antibodies measurement provide additional information in patients with thrombosis? Immunobiology. 2007;212(7):557-565.

60. Zigon P, Perdan Pirkmajer K, Tomsic M, et al. Anti-Phosphatidylserine/Prothrombin Antibodies Are Associated with Adverse Pregnancy Outcomes. J Immunol Res. 2015;2015:975704.

61. Ganapati A, Goel R, Kabeerdoss J, et al. Study of clinical utility of antibodies to phosphatidylserine/prothrombin complex in Asian-Indian patients with suspected APS. Clin Rheumatol. 2019;38(2):545-553.

62. Zigon P, Podovsovnik A, Ambrozic A, et al. Added value of non-criteria antiphospholipid antibodies for antiphospholipid syndrome: lessons learned from year-long routine measurements. Clin Rheumatol. 2019;38(2):371-378.

63. Singh NK, Yadav DP, Gupta A, Singh U, Godara M. Role of anti-annexin A5 in pathogenesis of hypercoagulable state in patients with antiphospholipid syndrome. Int J Rheum Dis. 2013;16(3):325-330.

64. de Laat B, Derksen RH, Mackie IJ, et al. Annexin A5 polymorphism (-1C-->T) and the presence of anti-annexin A5 antibodies in the antiphospholipid syndrome. Ann Rheum Dis. 2006;65(11):1468-1472.

65. Wolgast LR, Arslan AA, Wu XX, et al. Reduction of annexin A5 anticoagulant ratio identifies antiphospholipid antibody-positive patients with adverse clinical outcomes. J Thromb Haemost. 2017;15(7):1412-1421.

66. Scholz P, Auler M, Brachvogel B, et al. Detection of multiple annexin autoantibodies in a patient with recurrent miscarriages, fulminant stroke and seronegative antiphospholipid syndrome. Biochem Med (Zagreb). 2016;26(2):272-278.

67. Sciascia S, Cosseddu D, Montaruli B, Kuzenko A, Bertero MT. Risk Scale for the diagnosis of antiphospholipid syndrome. Ann Rheum Dis. 2011;70(8):1517-1518.

68. Otomo K, Atsumi T, Amengual O, et al. Efficacy of the antiphospholipid score for the diagnosis of antiphospholipid syndrome and its predictive value for thrombotic events. Arthritis Rheum. 2012;64(2):504-512.

69. Oku K, Amengual O, Atsumi T. Antiphospholipid scoring: significance in diagnosis and prognosis. Lupus. 2014;23 (12):1269-1272.

70. Sciascia S, Sanna G, Murru V, et al. GAPSS: the Global Anti-Phospholipid Syndrome Score. Rheumatology. 2013;52(8):1397-1403.

71. Ruiz-Irastorza G, Cuadrado MJ, Ruiz-Arruza I, et al. Evidence-based recommendations for the prevention and long-term management of thrombosis in antiphospholipid antibody-positive patients: report of a task force at the 13th International Congress on antiphospholipid antibodies. Lupus. 2011;20(2):206-218.

72. Tektonidou MG, Andreoli L, Limper M, et al. EULAR recommendations for the management of antiphospholipid syndrome in adults. Ann Rheum Dis. 2019;78(10):1296-1304.

73. Bala MM, Paszek E, Lesniak W, et al. Antiplatelet and anticoagulant agents for primary prevention of thrombosis in individuals with antiphospholipid antibodies. Cochrane Database Syst Rev. 2018;7: CD012534.

74. Guyatt GH, Akl EA, Crowther M, et al. Executive summary: Antithrombotic Therapy and Prevention of Thrombosis, 9th ed: American College of Chest Physicians Evidence-Based Clinical Practice Guidelines. Chest. 2012;141(2 Suppl):7S-47S.

75. Crowther MA, Ginsberg JS, Julian J, et al. A comparison of two intensities of warfarin for the prevention of recurrent thrombosis in patients with the antiphospholipid antibody syndrome. N Engl J Med. 2003;349 (12):1133-1138.

76. Keeling D, Mackie I, Moore GW, et al. Guidelines on the investigation and management of antiphospholipid syndrome. Br J Haematol. 2012;157(1):47-58.

77. Cohen H, Efthymiou M, Isenberg DA. Use of direct oral anticoagulants in antiphospholipid syndrome. J Thromb Haemost. 2018;16(6):1028-1039.

78. Pengo V, Denas G, Zoppellaro G, et al. Rivaroxaban vs warfarin in high-risk patients with antiphospholipid syndrome. Blood. 2018;132(13):1365-1371.

79. Goldhaber SZ, Eriksson H, Kakkar A, et al. Efficacy of dabigatran versus warfarin in patients with acute venous thromboembolism in the presence of thrombophilia: Findings from RE-COVER(R), RE-COVER II, and RE-MEDY. Vasc Med. 2016;21(6):506-514.

80. Woller SC, Stevens SM, Kaplan DA, et al. Apixaban for the Secondary Prevention of Thrombosis Among Patients With Antiphospholipid Syndrome: Study Rationale and Design (ASTRO-APS). Clin Appl Thromb Hemost. 2016;22(3):239-247.

81. Canaud G, Bienaime F, Tabarin F, et al. Inhibition of the mTORC pathway in the antiphospholipid syndrome. N Engl J Med. 2014;371(4):303-312.

82. Erkan D, Aguiar CL, Andrade D, et al. 14th International Congress on Antiphospholipid Antibodies: task force report on antiphospholipid syndrome treatment trends. Autoimmun Rev. 2014;13(6):685-696.

83. Kumar S, Papalardo E, Sunkureddi P, et al. Isolated elevation of IgA anti-beta2glycoprotein I antibodies with manifestations of antiphospholipid syndrome: a case series of five patients. Lupus. 2009;18(11):1011-1014.

84. Billoir P, Miranda S, Abboud J, et al. [Which place of antiphosphatidylethanolamine antibodies research in seronegative antiphospholipid syndrome suspicion?]. Rev Med Interne. 2019;40(6):351-354.

Latexin regulation by HMGB2 is required for hematopoietic stem cell maintenance

Cuiping Zhang,[1] Yvonne N Fondufe-Mittendorf,[2] Chi Wang,[3] Jin Chen,[4] Qiang Cheng,[4] Daohong Zhou,[5] Yi Zheng,[6] Hartmut Geiger[6,7] and Ying Liang[1]

[1]Departments of Toxicology and Cancer Biology, University of Kentucky, Lexington, KY, USA; [2]Department of Molecular and Cellular Biochemistry, University of Kentucky, Lexington, KY, USA; [3]Department of Cancer Biostatistics, University of Kentucky, Lexington, KY, USA; [4]Department of Internal Medicine and Computer Science, University of Kentucky, Lexington, KY, USA; [5]Department of Pharmacodynamics, University of Florida, Gainesville, FL, USA; [6]Cincinnati Children's Hospital Medical Center, Experimental Hematology and Cancer Biology, Cincinnati, OH, USA and [7]Institute for Molecular Medicine, University of Ulm, Ulm, Germany

ABSTRACT

Hematopoietic stem cells provide life-long production of blood cells and undergo self-renewal division in order to sustain the stem cell pool. Homeostatic maintenance of hematopoietic stem cell pool and blood cell production is vital for the organism to survive. We previously reported that latexin is a negative regulator of hematopoietic stem cells in mice. Its natural variation in the expression is inversely correlated with hematopoietic stem cell number. However, the molecular mechanisms regulating latexin transcription remain largely unknown, and the genetic factors contributing to its natural variation are not clearly defined. Here we discovered a chromatin protein, high-mobility group protein B2, as a novel transcriptional suppressor of latexin by using DNA pull-down and mass spectrometry. High-mobility group protein B2 knockdown increases latexin expression at transcript and protein levels, and decreases hematopoietic stem cell number and regeneration capacity *in vivo*. Concomitant blockage of latexin activation significantly reverses these phenotypic changes, suggesting that latexin is one of the downstream targets and functional mediators of high-mobility group protein B2. We further identified a functional single nucleotide polymorphism, rs31528793, in the latexin promoter that binds to high-mobility group protein B2 and affects the promoter activity. G allelic variation in rs31528793 associates with the higher latexin expression and lower hematopoietic stem cell number, whereas C allele indicates the lower latexin expression and higher stem cell number. This study reveals for the first time that latexin transcription is regulated by both trans-acting (high-mobility group protein B2) and cis-acting (single nucleotide polymorphism rs31528793) factors. It uncovers the functional role of naturally occurring genetic variants, in combination with epigenetic regulator, in determining differential gene expression and phenotypic diversity in the hematopoietic stem cell population.

Introduction

Stem cells are key to the homeostatic maintenance of mature and functional cells in a variety of tissues and organs. They have the unique ability to perpetuate themselves through self-renewal and to replenish dying or damaged cells through multi-lineage differentiation. The balance between self-renewal and differentiation is critical for tissue homeostasis, and any disruption in this balance could lead to serious problems such as tissue degeneration and development of cancer.[1] Probably the best-studied adult stem cells are hematopoietic stem cells (HSC), which are responsible for life-long production of all hematopoietic lineages.[2-4] The total number of HSC is kept constant under steady-state conditions, but it also changes in response

to stress or injury. The flexibility of stem cells to adapt to physiological needs is achieved by precise regulation of self-renewal and differentiation. Many molecules and signaling pathways have been found to be involved in this process.[3] However, identification of the collection of genes contributing to critical stem cell functions is far from complete.

Hematopoietic stem cell number and function exhibit natural variation among humans as well as among different mouse strains.[5-8] The natural variation is largely attributed to DNA variants in the genome that function as regulatory elements to control gene expression.[9] The genetic diversity is a powerful but underused tool for unraveling the critical gene networks in stem cell regulation. Using genome-wide association studies, increasing numbers of gene regulatory variants have been strongly implicated in hematologic phenotypes and diseases in humans, such as fetal hemoglobin-associated genetic variants in patients with sickle cell disease (SCD) and β-thalassemia.[10,11] Recently, several reports have revealed an important yet previously unrecognized role of genetic variants in regulating epigenetics.[9,12-15] For example, DNA variations may affect the recruitment and binding affinity of transcription factors, which in turn lead to histone tail modifications.
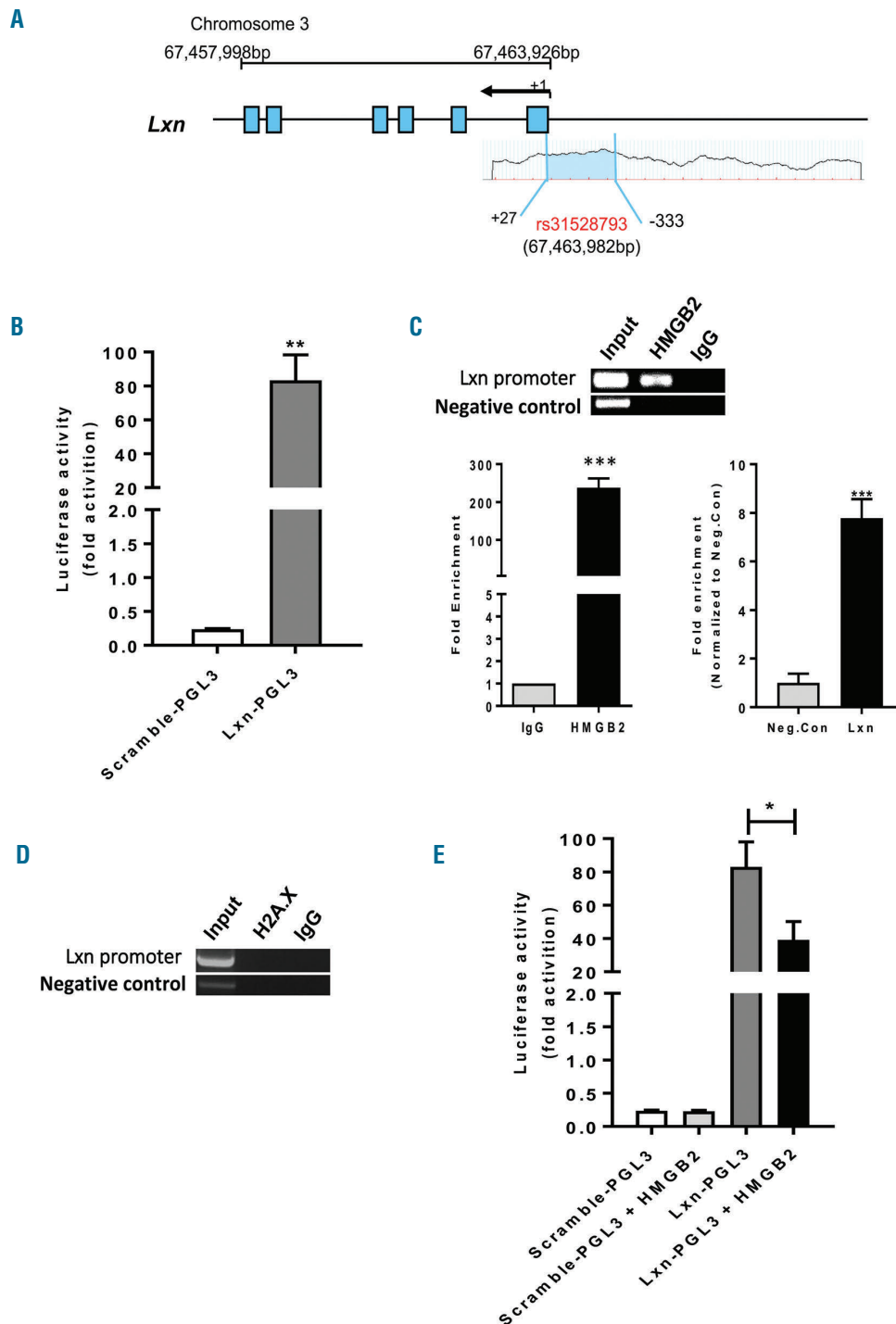
Figure 1. HMGB2 suppresses *Lxn* promoter activity. (A) *Lxn* promoter sequence spans from 333 nucleotides upstream of the transcription start site (+1) of *Lxn* gene to 27 nucleotides into the first exon. The chromosomal positions for *Lxn* gene and SNP rs31528793 are indicated. (B) Lxn promoter sequence has strong promoter activity. Luciferase activity was determined in HEK cells transduced with luciferase reporter construct containing either *Lxn* promoter sequence (Lxn-PGL3) or control vector (PGL3). (C) HMGB2 specifically binds to *Lxn* promoter sequence. Cromatin immunoprecipitation (ChIP) assay was performed with an HMGB2 polyclonal antibody (HMGB2) or IgG control (IgG). The genomic sequence in the 500 base pairs downstream of the *Lxn* promoter region were used as the negative sequence control to determine the HMGB2 binding specificity (Negative control). *Lxn* promoter sequence was amplified and quantified by real-time polymerase chain reaction (PCR) (top). The fold enrichment of HMGB2 in the *Lxn* promoter was quantified by normalization to either IgG control (bottom left) or negative sequence control (bottom right). (D) H2A.X does not bind to *Lxn* promoter. ChIP assay was performed with an H2A.X polyclonal antibody (H2A.X) or IgG control (IgG). The genomic sequence in the 500 base pairs downstream of the *Lxn* promoter region were used as the negative sequence control to determine the H2A.X binding specificity (Negative control). *Lxn* promoter sequence was amplified and quantified by real-time PCR. (E) HMGB2 suppresses *Lxn* promoter activity. Luciferase activity was determined in HEK cells transduced with luciferase reporter construct containing either Lxn promoter sequence (Lxn-PGL3) or control vector with scramble sequence (Scramble-PGL3) without or with HMGB2 plasmid (Scramble-PGL3 + HMGB2, and Lxn-PGL3 + HMGB2). Data are the average of three independent experiments with triplicates in each experiment (n=9). *P<0.05; **P<0.01; ***P<0.001.

Such variations in the epigenetic environment result in significant variations in gene expression, which collectively manifest as a phenotypic trait. Despite these advances, the precise molecular mechanisms underlying the association between the genetic variants and hematopoietic phenotypes remain largely unknown.

Inbred mouse strains provide a model system for exploring the myriad of regulatory gene network contributing to hematologic diversity.[10,16] We carried out a comparative study of two inbred strains, C57BL/6 (B6) and DBA/2 (D2), in which we documented large natural variation in a number of stem cell traits.[5-8] One of the most significant traits is the natural size of the HSC population, i.e. young B6 mice have 3- to 8-fold fewer stem cells in bone marrow (BM) than D2 mice, depending on the assay used for stem cell quantification. We further identified *Lxn* as the regulatory gene whose expression is negatively correlated with HSC number.[17,18] *Lxn* regulates HSC in a cell-autonomous manner through concerted mechanisms of decreased self-renewal and increased apoptosis. Even though we identified several genetic variants that might be associated with the differential expression of *Lxn* in B6 and D2 stem cells, there is no direct evidence of how these variants regulate *Lxn* transcription and whether they have any functional effects.

In this study, we report for the first time that a chromatin protein, HMGB2, binds to *Lxn* promoter and plays an important role in the transcriptional regulation of *Lxn*. Knockdown of HMGB2 increases *Lxn* expression at both transcript and protein levels, suggesting a suppressive role of HMGB2 in *Lxn* transcription. HMGB2 knockdown decreases the number of functional HSC by promoting apoptosis and reducing proliferation. Concomitant knockdown of *Lxn* reverses these functional effects, suggesting that *Lxn* is one of the downstream targets of HMGB2. Moreover, we discovered that a functional polymorphism, SNP rs31528793, is associated with the differential expression of *Lxn* in different mouse strains, including B6 and D2. This study, for the first time, reveals the genetic and epigenetic regulation of *Lxn* transcription, suggesting that both trans- and cis-elements (HMGB2 and SNP, respectively) contribute to the differential gene expression and phenotypic diversity in the HSC population

Methods

Luciferase reporter assay

Lxn promoter activity and HMGB2 transcription activity were measured by luciferase reporter assay with a Tropix TR717 luminometer using a dual luciferase assay kit.

Identification of *Lxn* promoter binding proteins

Lxn promoter binding proteins were isolated by µMACSTM FactorFinder Kit (Miltenyi Biotec Inc., Auburn, CA, USA). The high purity double-strand DNA oligonucleotides containing SNP rs31528793 was used as the DNA bait for protein pull-down. The associated proteins were determined by mass spectrometry at the Mass Spectrometry and Proteomics Facility at Ohio State University.

Protein-DNA binding assays

Chromatin immunoprecipitation: chromatin immunoprecipitation (ChIP) assay was performed on LK (Lin- c-KIT+) cells using ChIP assay kit (Sigma Aldrich, #CHP1) with HMGB2 polyclonal anti-

Table 1. Lxn promoter binging protein.

Lxn promoter sequence containing SNP rs31528793	
Histone H2A type 1- F	(H2A1F)
Histone H2A type 2- A	(H2A2A)
Protein S100-A9	(S10A9)
Protein S100-A8	(S10A8)
Histone H2A.X	(H2A.X)
High mobility group protein B2	(HMGB2)
Histone H2B type 1- H	(H2B1H)
Histone H2AV	(H2AV)
Histone H1.3	(H1.3)
Peptidyl-prolyl cis-trans isomerase A	(PPIA)
Eosinophil cationic protein 1 precursor	(ECP1)
Myeloperoxidase precursor	(PERM)
Histone H1.1	(H11)
Histone H1.5	(H15)
Coronin-1A	(COF1)

Double-strand DNA oligonucleotides containing single nucleotide polymorphism (SNP rs31528793) were used as "bait" to capture associated proteins from bone marrow cell lysate of C57BL/6 mouse. Proteins binding to Lxn promoter sequences were isolated by µMACSTM FactorFinder Kit (Miltenyi Biotec Inc., Auburn, CA, USA) and identified by Mass Spectrometry. Proteins with a Mascot score of 100 or higher with a minimum of two unique peptides from one protein having a –b or –y ion sequence tag of five residues or better were considered significant.

bodies (ab67282), H2A.X antibody (ab11175), or Rabbit IgG control (ab171870) (Abcam, Cambridge, MA, USA). HMGB2 binding affinity was determined by SYBR green quantitative polymerase chain reaction (qPCR).

Electrophoretic mobility shift assay: electrophoretic mobility shift assays (EMSA) were performed in 293T cells transduced with HMGB2 lentivirus using the LightShift™ Chemiluminescent EMSA Kit (Thermo Scientific™).

Gene knockdown and expression measurement

EML or c-KIT+ (LSK) cells were transduced with HMGB2 shRNA (MSH027321-LVRU6GP, GeneCopoeia), *Lxn* Mission shRNA (Sigma-Aldrich) virus. Gene expression was measured by real-time PCR with commercially available primer/probe mix for *Hmgb2* or *Lxn* in ABI PRISM 7700 (Applied Biosystems, Foster City, CA, USA). Protein expression was measured by western blot with anti-Hmgb2 antibody (ab67282), goat polyclonal anti-*Lxn* antibodies (ab59521, Abcam), or mouse monoclonal anti-β-actin antibody (A5441, Sigma).

Immunostaining and flow cytometry

Hematopoietic stem cells and hematopoietic progenitor cells: young (8-12 week) female C57BL/6, DBA2, 129X1/SvJ, A/J and CD45.1 mice (Jackson Laboratories, Bar Harbor, ME, USA) were used for HSC/hematopoietic progenitor cell isolation (HPC). HSC/HPC were defined as Lin−, Sca-1+ (clone E13-161.7) and c-KIT+ (LSK) cells. Long-term HSC (LT-HSC) were identified as LSK plus CD34 and FLT3 negative cells.

Cell cycle: cell cycle was analyzed by BrdU incorporation using BrdU Flow Kit.

Apoptosis: apoptosis was evaluated by Annexin V staining.

Active caspase 3 analysis: active caspase 3 analysis was analyzed using PE Active Caspase-3 Apoptosis Kit. All kits are from BD Pharmingen™. Flow cytometry was performed on a FacsAria II (Becton Dickinson) and the data were analyzed with FlowJo software (Tree Star, Ashland, OR, USA).
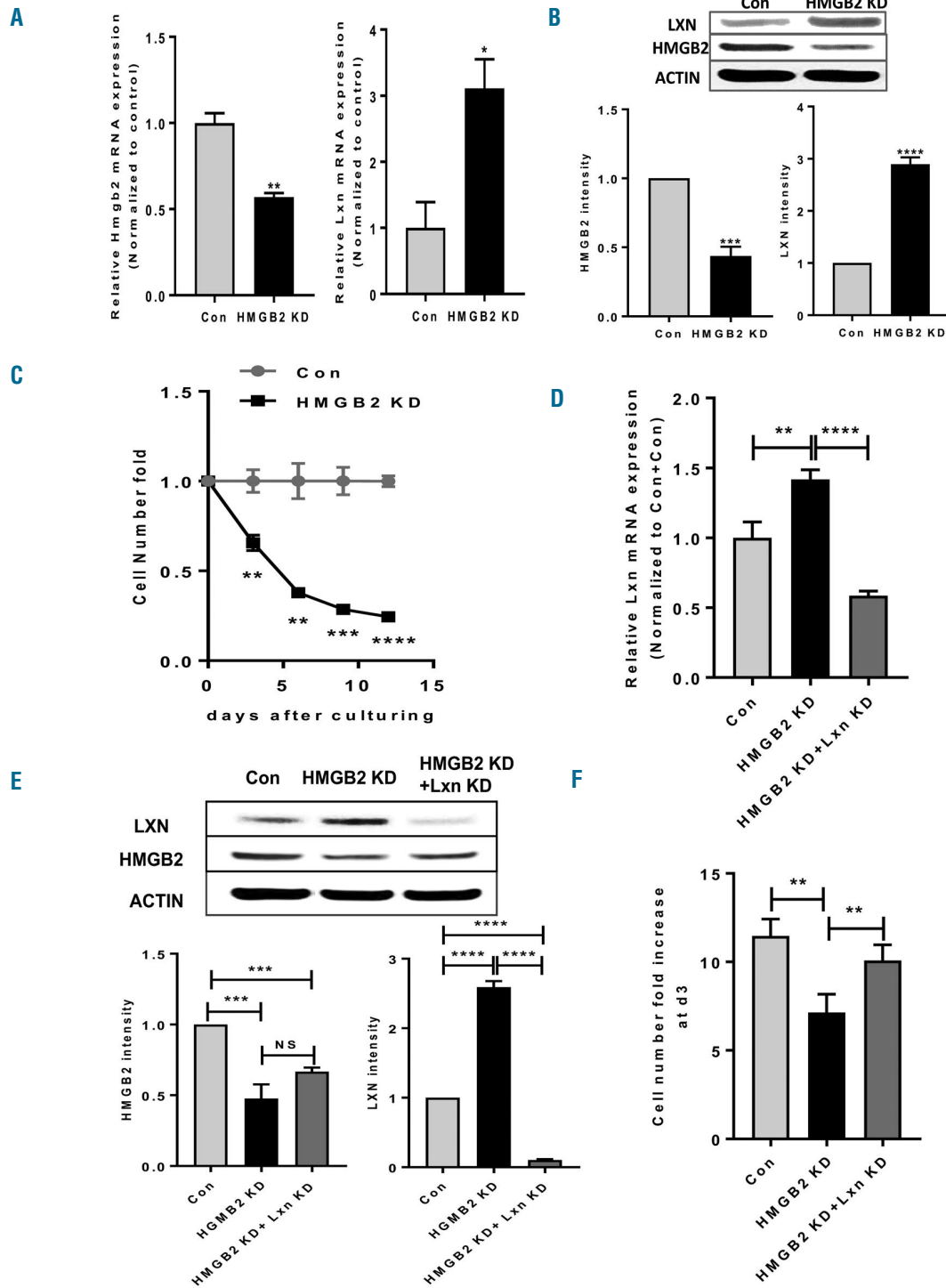
Figure 2. HMGB2 knockdown increases *Lxn* expression and decreases the number of hematopoietic stem cell (HSC) cell line. (A) Knockdown of HMGB2 in EML cells increases *Lxn* mRNA expression. EML cells were infected by control lentivirus (Con) or HMGB2 knockdown shRNA (HMGB2 KD). HMGB2 and *Lxn* mRNA levels were measured by quantitative real-time polymerase chain reaction (PCR). Glyceraldehyde-3-phosphate dehydrogenase (GAPDH) was the endogenous control for mRNA expression normalization. (B) Knockdown of HMGB2 in EML cells increases *Lxn* protein expression. EML cells were infected by control lentivirus (Con) or HMGB2 knockdown shRNA (HMGB2 KD). HMGB2 and *Lxn* protein levels were measured by western blot. Actin was the normalization control. (Top) Representative western blot out of three independent experiments. (Bottom) Quantification of intensity of HMGB2 (left) and *Lxn* (right) proteins. (C) HMGB2 knockdown decreases EML cell number. EML cells infected with empty (Con) or HMGB2 shRNA (HMGB2 KD) were cultured for 12 days and counted at different time points. (D) *Lxn* mRNA was decreased in HMGB2-knockdown EML cells with simultaneous knockdown of *Lxn*. HMGB2-knockdown EML cells (HMGB2 KD) were co-transfected with *Lxn* shRNA lentiviral vector (HMGB2 KD + *Lxn* KD). *Lxn* mRNA and protein was measured by real-time PCR and western blot. (E) *Lxn* protein was decreased in HMGB2-knockdown EML cells with simultaneous knockdown of *Lxn*. HMGB2-knockdown EML cells (HMGB2 KD) were co-transfected with *Lxn* shRNA lentiviral vector (HMGB2 KD + *Lxn* KD). HMGB2 and *Lxn* protein levels were measured by western blot. Actin was the normalization control. (Top) Representative western blot out of three independent experiments. (Bottom) Quantification of intensity of HMGB2 (left) and *Lxn* (right) proteins. (F) *Lxn* knockdown restores the number of HMGB2-knockdown EML cells to a level comparable to control group. Data shown are EML cell number at day 3 of cell culture. All data are the average of three independent experiments with triplicates in each experiment (n=9). *$P<0.05$; **$P<0.01$; ***$P<0.001$; ****$P<0.0001$.
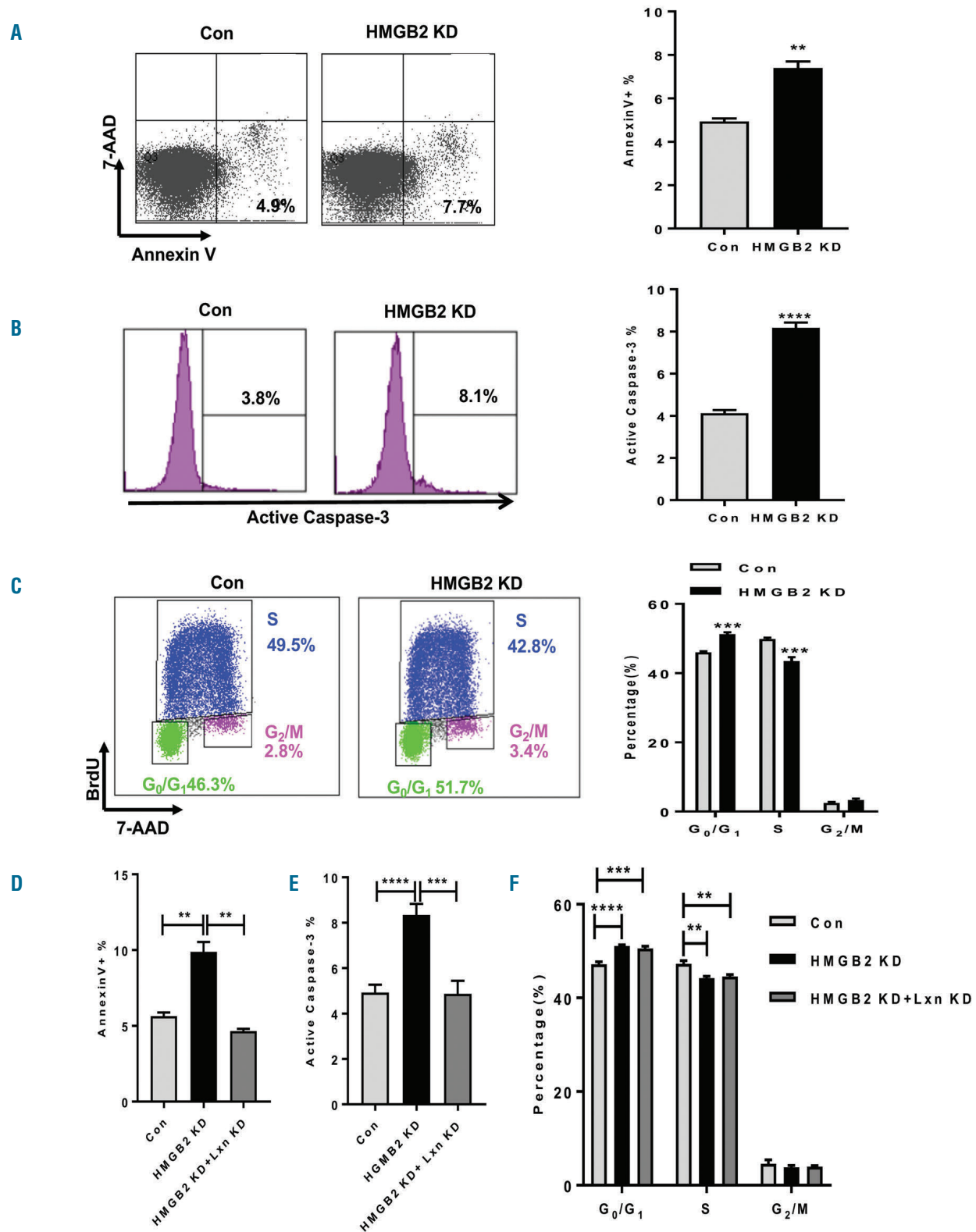
Figure 3. HMGB2 knockdown increases apoptosis and decreases proliferation. (A) HMGB2 knockdown increases apoptosis of EML cells. Representative FACS plots (left) and quantification (right) of Annexin V+ and 7AAD- apoptotic EML cells transduced with control-shRNA (Con) or HMGB2 knockdown shRNA lentivirus (HMGB2 KD). (B) HMGB2 knockdown increases the percentage of active caspase 3 positive EML cells. Representative flow cytometry profile (left) and quantification (right) of active caspase 3 immnuofluorescence signal in EML cells. (C) HMGB2 knockdown decreases proliferation of EML cells. Representative FACS plots showing the G0/G1 (BrdU- and 7AAD-), S (BrdU+), and G2/M (BrdU- and 7AAD+) phages of cell cycle in EML cells (left). (Right) Frequencies of each phase. (D) *Lxn* knockdown (HMGB2 KD + *Lxn* KD) restores the percentage of apoptotic (Annexin V+) HMGB2-knockdown EML cells (HMGB2 KD) to a level comparable to control group (Con). (E) *Lxn* knockdown (HMGB2 KD + *Lxn* KD) restores the percentage of active caspase-3 positive HMGB2-knockdown EML cells (HMGB2 KD) to a level comparable to control group (Con). (F) *Lxn* knockdown (HMGB2 KD + *Lxn* KD) did not restore the cell cycle status of HMGB2-knockdown EML cells (HMGB2 KD) to control group level (Con). Data presented as the average±Standard Deviation of six measurements from two independent experiments. *$P<0.05$; **$P<0.01$; ***$P<0.001$.

Functional analysis of hematopoietic stem cells and hematopoietic progenitor cells

Colony forming cell assay: colony forming cell (CFC) assay was performed in complete MethoCult media (Stem Cell Technologies, Vancouver, Canada), and colony was counted on day 14.

Cobblestone area forming cell (CAFC) assay: cobblestone area forming cell (CAFC) assay was performed as described previously.[17] The most primitive HSC showed cobblestones at day 35 of culture, and their frequency was calculated by using L-Calc Limiting Dilution Analysis Software (Stem Cell Technologies, Vancouver, Canada).

In vivo transplantation assay: *in vivo* transplantation assay, 3×10^5 transduced cells (GFP+ cells) plus 2×10^5 competitor B6.SJL/BoyJ BM cells were injected into B6.SJL/BoyJ mice after 24 hours of transduction, and GFP+ chimerism in peripheral blood (PB) and BM was measured at 16 weeks post transplantation.

Statistical analysis

Data were examined for homogeneity of variances (F-test), then
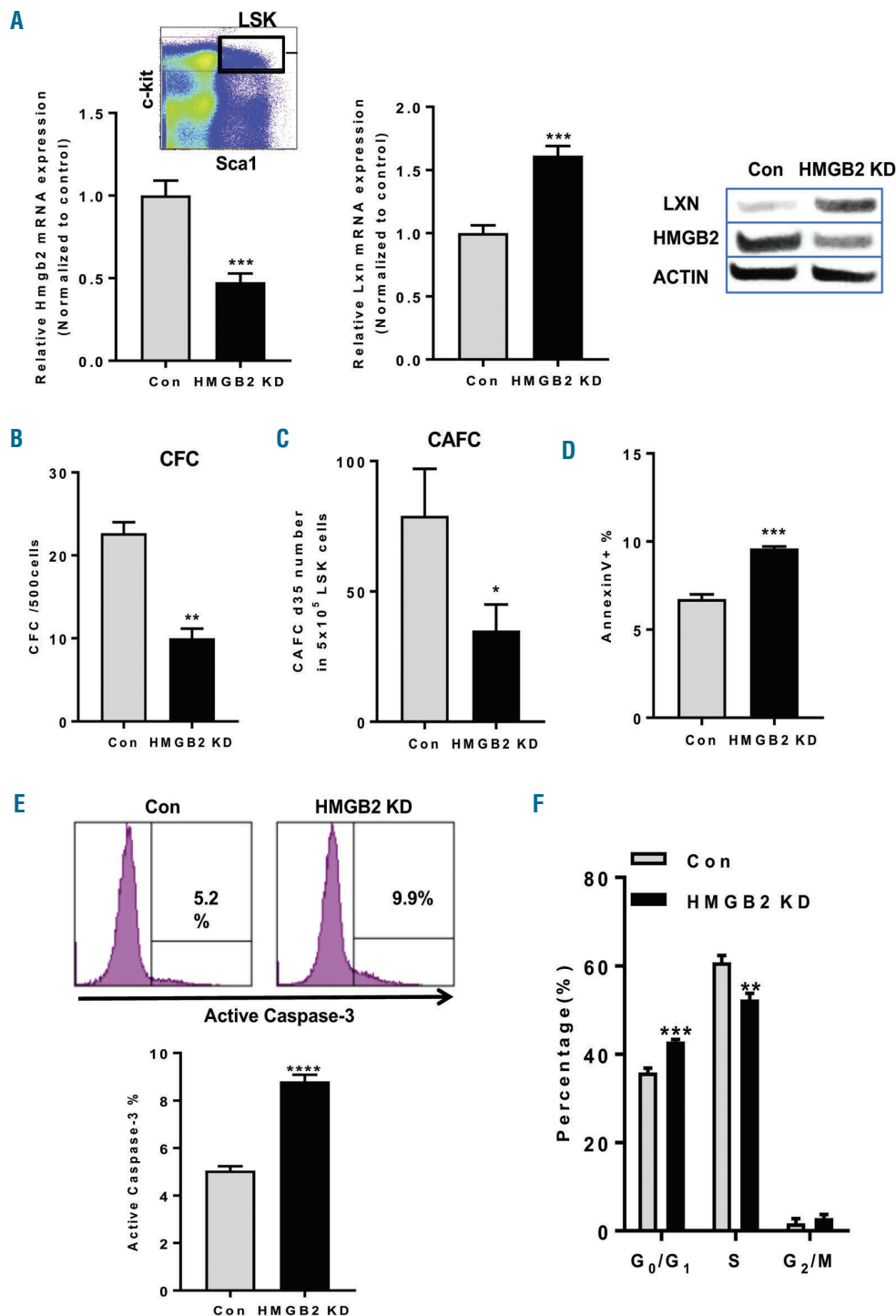
Figure 4. HMGB2 knockdown increases *Lxn* expression and decreases the number and function of bone marrow hematopoietic stem cells. (A) HMGB2 knockdown increases *Lxn* expression in hematopoietic stem and progenitor cells. HMGB2 knockdown (HMGB2 KD) in bone marrow LSK cells (left) increases *Lxn* mRNA (middle) and protein expression (right) compared to control group (Con). *Lxn* mRNA and protein levels were measured by quantitative real-time polymerase chain reaction and western blot. Glyceraldehyde-3-phosphate dehydrogenase (GAPDH) was the endogenous control for mRNA expression normalization. Actin was the control for protein normalization. (B) HMGB2 knockdown decreases the number of clonogenic and functional hematopoietic progenitor and (C) stem cells. LSK cells transduced with control and knockdown lentivirus were sorted, and the numbers of progenitor and stem cells were measured by colony forming cell (CFC) and cobblestone area forming cell assay (CAFC), respectively. (D) HMGB2 knockdown increases apoptosis (Annexin V+) of LSK cells. (E) HMGB2 knockdown increases the proportion of active caspase-3 positive LSK cells. The representative histogram of active capase-3 flow cytometry profile (top) and the quantification of positive cell proportion (bottom) are shown. (F) HMGB2 knockdown decreases proliferation of LSK cells. The apoptosis and proliferation were determined with the same way as in EML cells. Values are the mean±Standard Deviation from three independent experiments. *$P<0.05$; **$P<0.01$; ***$P<0.001$.

analyzed by Student's *t*-test or One-way ANOVA using Tukey's test. *P<0.05* was considered statistically significant. All statistical analyses were conducted with Graphpad Prism.[7]

All animal work and experiments were performed under the guideline of approved Institutional Review Board and Ethics Committee, Biosafety Committee, and Animal Care and Use Committee protocols at the University of Kentucky.

Results

HMGB2 binds to *Lxn* promoter and suppresses its activity

The transcriptional regulation of the *Lxn* gene remains largely unknown. We used two criteria to identify the potential promoter in the upstream regulatory region of *Lxn*. First, we looked for the regions containing SNP because the natural variation of *Lxn* expression is mainly caused by genetic variants. Secondly, we and others have shown that promoter hypermethylation is involved in the downregulation of *Lxn* in several types of cancer cells, including leukemia stem cells.[19-24] This prompted us to search for regions enriched with CG dinucleotides (CpG island). We thus analyzed the mouse *Lxn* upstream puta-

tive promoter sequence (*http://www.methprimer.com*) and identified a CG-enriched region that contains a SNP rs31528793 (Figure 1A). Using the NCBI SNP database (*https://www.ncbi.nlm.nih.gov/SNP/snp_ref.cgi?rs=rs3152879 3*) search, we confirmed the presence of this polymorphism. This region spans from the canonical 5' promoter (-333 nucleotide, nt) to the transcription start site (+1 nt), and extends through the first exon (+27 nt). We next amplified and sequenced this region, confirming the existence of this SNP (*data not shown*). To determine whether it has promoter activity, we performed *in vitro* luciferase reporter assay and found that this sequence in *Lxn* upstream regulatory region had a strong promoter activity (Figure 1B).

We next performed *in silico* analyses to search for the potential transcription factors in the *Lxn* promoter region by using the transcription factor prediction program, TRANSFAC (*www.cbrc.jp/research/db/TFSEARCH.html*). Results from this analysis showed that SNP rs31528793 falls within the consensus binding motif for the transcription factors, *Adr-1* and *Ets-1*. Our previous microarray data showed that only *Ets-1* was expressed in HSC (*data not shown*). We thus only evaluated the binding of *Ets-1* to *Lxn* promoter with chromatin immunoprecipitation (ChIP)

A

Donor
CD45.2
HMGB2 KD or WT
LSK cells (3x10^5)

Competitor
CD45.1
(2x10^5)

Recipients   9Gy
CD45.1

PB, BM LSK and LT-HSC chimerism

B

GFP % of whole PB

C

LSK GFP+% in BM

D

LT-HSC GFP+% in BM
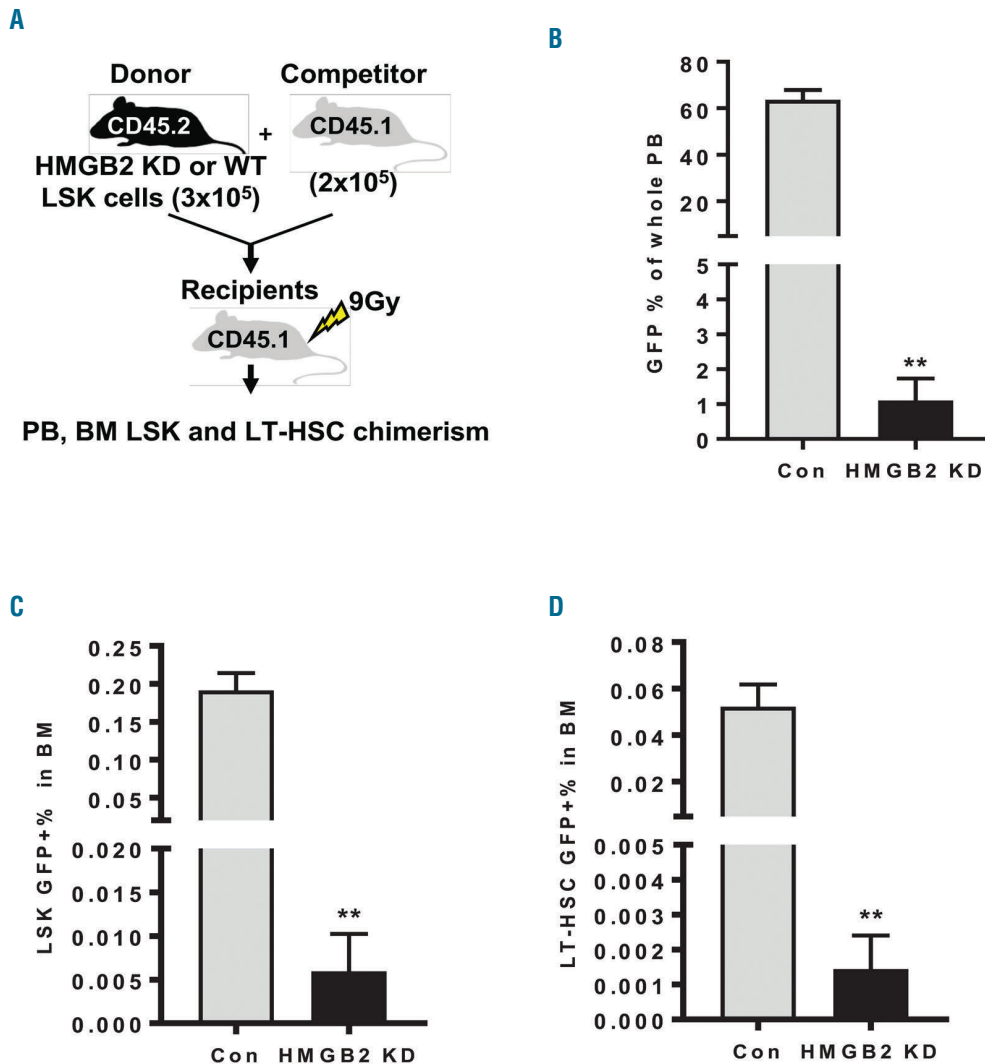
Figure 5. HMGB2 knockdown decreases hematopoietic stem cell (HSC) regenerative capacity. (A) Experimental scheme for competitive repopulation assay. Donor cells were 3x10^5 LSK cells transduced with HMGB2 shRNA (HMGB2 KD) or control vector (Con), and transplanted into myeloablated recipient mice along 2x10^5 competitor cells. Donor derived cells were determined by CD45.2 markers in the peripheral blood (PB), bone marrow (BM) LSK cells and long-term HSCs (LT-HSC) at 16 weeks post-transplantation. Long-term HSC were determined by the markers lineage-Sca-1$^+$c-kit$^+$flk2$^-$CD34$^-$. (B) Frequencies of HMGB2 KD or control (CD45.2)-derived leukocytes, (C) BM LSK cells, and (D) LT-HSC. Data are the average±Standard Deviation pooled from two independent experiments with five recipients in each group per experiment (n=10 per donor group). **P<0.01.
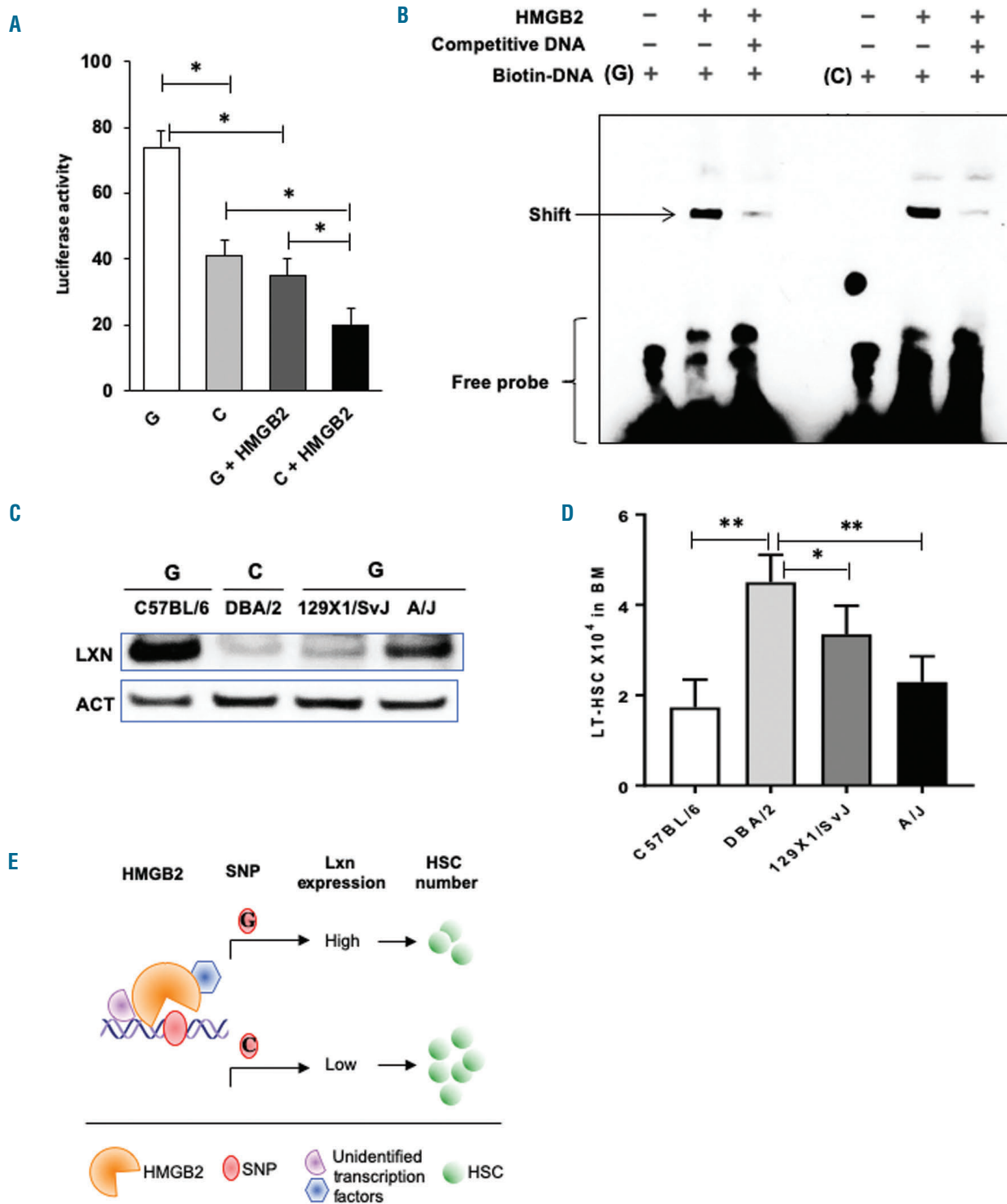
Figure 6. SNP rs31528793 associates with *Lxn* promoter activity and hematopoietic stem cell (HSC) number. (A) SNP rs31528793 affects *Lxn* promoter activity. G allele is associated with the higher promoter activity whereas C allele lowers its activity. HMGB2 has transcription suppressor activity in both alleles. The luciferase reporter assay was performed on G or C containing vectors (G or C) and on the vectors co-transfected with HMGB2 plasmids (G+ HMGB2; or C+ HMGB2). The average values of three independent experiments are shown with standard deviation (SD) (n=12). (B) HMGB2 binds to G/C containing *Lxn* promoter. Electrophoretic mobility shift assay (EMSA) was performed with HMGB2 polyclonal antibody and biotin labeled oligonucleotides containing G or C allele. One representative experiment shown out of three independent experiments. (C) G/C allele in SNP rs31528793 indicates LXN protein level. Western blot measured LXN protein in bone marrow cells of different mouse strains carrying either G or C allele. One representative experiment shown out of three independent experiments. (D) G/C allele in SNP rs31528793 indicates HSC number. Long-term HSC and frequency (%) were determined by the markers lineage-Sca-1+c-kit+flk2-CD34-. Results are average (± 1 Standard Deviation) of nine mice from three independent experiments. *P<0.05; **P<0.01. (E) Model of transcriptional regulation of *Lxn* by HMGB2 and the effect of SNP rs31528793 on the natural variation of *Lxn* expression and HSC number. HMGB2 binds to the *Lxn* promoter and acts as a transcriptional suppressor. SNP rs31528793 in the *Lxn* promoter sequence causes the differential promoter activity in which G allele is associated with higher *Lxn* expression and lower HSC number whereas C allele is associated with higher *Lxn* expression and lower HSC number. HMGB2 is involved in *Lxn* transcriptional regulation either by itself or by modifying chromatin structure in the *Lxn* promoter region, thereby facilitating access of other transcription factors to the region.

and found that *Ets-1* did not bind to *Lxn* promoter (*data not shown*). These results prompted us to use the "DNA-pull down" and mass spectrometry to directly look for proteins that bind to this region. We found 15 candidate binding proteins (Table 1). HMGB2 and H2A.X are of particular interest because of the involvement of their family members in the regulation of stem cell function and differentiation as the chromatin modifiers.[25-34] We thus focused on these two proteins and examined their role in *Lxn* transcriptional regulation.

We performed ChIP-qPCR assay to measure the binding and occupancy of HMGB2 and H2A.X to the *Lxn* promoter. The result showed that HMGB2, but not H2A.X, were significantly enriched at the *Lxn* promoter region in comparison to IgG control and to the control region at the downstream 500 bps of the promoter (Figure 1C and D). This result supports the idea of the specific binding of HMGB2 to *Lxn* promoter. We next performed luciferase assay, and found that HMGB2 suppressed *Lxn* promoter activity (Figure 1E). Altogether, to our knowledge, this is the first time HMGB2 has been identified as a novel transcription suppressor of *Lxn* gene.

HMGB2 knockdown increases *Lxn* expression and changes the function of a HSC cell line

We next examined the regulatory role of HMGB2 in *Lxn* transcription and its effects on EML cells. EML is the only known hematopoietic cell line with both lympho and myelo-erythroid differentiation potential, and is considered to represent HSC.[35-37] Knockdown HMGB2 in EML cells significantly increased *Lxn* expression at both mRNA and protein level (Figure 2A and B, respectively), reinforcing the finding of transcriptional suppression of HMGB2 on *Lxn* expression. We previously reported *Lxn* as a negative regulator of HSC number,[17] we thus hypothesized that knockdown of HMGB2 would decrease EML cell number *via* upregulation of *Lxn*. We therefore monitored the growth of EML cells with HMGB2 knockdown for two weeks, and found that HMGB2 knockdown led to a dramatic decrease in the cell number compared to control group (Figure 2C). Since HMGB2 is a chromatin binding protein, its effect on EML number may not act solely through *Lxn* upregulation. We simultaneously knocked down *Lxn* in HMGB2 shRNA-transduced cells, and determined whether blocking *Lxn* upregulation could attenuate HMGB2-induced growth inhibition. We confirmed that the expression of *Lxn* mRNA and protein in HMGB2-shRNA transduced EML cells was reduced by the co-transduction with *Lxn*-shRNA (Figure 2D and E). Figure 2F shows that HMGB2 knockdown significantly decreased EML cell number, and the concomitant *Lxn* knockdown reversed this change, resulting in an increase in the cell number to the level comparable to control group. These data imply that *Lxn* is one of the downstream transcriptional targets of HMGB2, and that HMGB2 suppresses *Lxn* transcription which in turn increases EML number.

We previously reported that *Lxn* negatively regulates HSC function through increasing apoptosis and decreasing proliferation,[23,38,39] we hypothesized that HMGB2 inhibition may have similar effects on EML cells. Indeed, we found that knocking down HMGB2 significantly increased the percentage of apoptotic EML cells (Figure 3A). The change was further confirmed by the increased proportion of active caspase 3 positive cells (Figure 3B).

Moreover, knocking down HMGB2 significantly decreased the percentage of cells in the S phase in the cell cycle (Figure 3C). The concomitant increase in apoptosis and decrease in proliferation by HMGB2 inhibition may contribute to the decreased cell number (Figure 2B). We next tested whether apoptosis and proliferation could be rescued by blocking *Lxn* upregulation in HMGB2 knockdown condition (see also Figure 2E and F). The results showed that *Lxn* knockdown on the top of HMGB2 knockdown decreased apoptosis (Figure 3D) and the proportion of active caspase 3 positive cells (Figure 3E), and restored their changes to the level of control group. However, the cell cycle changes were not fully restored (Figure 3F), suggesting that *Lxn* may be a major player in regulating apoptosis, and other downstream targets of HMGB2 might be involved in cell cycle regulation that counteract *Lxn* function. Overall, these data suggest that HMGB2 positively regulates HSC function *via* the suppression of *Lxn* expression.

HMGB2 knockdown increases *Lxn* expression in bone marrow hematopoietic stem cells and decreases their number and regenerative function

Because of the observed effect of HMGB2 on *Lxn* expression and EML function, we next asked whether HMGB2 plays a similar role in primary HSC. We knocked down HMGB2 in bone marrow lineage- Sca-1+ c-Kit+ (LSK) cells (Figure 4A, left), which are enriched with HSC and hematopoietic progenitor cells (HPC), and then determined the effect of HMGB2 knockdown on *Lxn* expression and HSC and HPC cell numbers, apoptosis and cell cycling. We found that knockdown HMGB2 in LSK cells also led to a significant increase in *Lxn* expression at both transcript and protein levels (Figure 4A, middle and right). We next performed *in vitro* short-term CFC and long-term CAFC assays to determine functional HPC and HSC, respectively. The result showed that the numbers of HPC and HSC in HMGB2-knockdown cells were nearly 2-fold lower than those in control cells (Figure 4B and C). Moreover, HMGB2 knockdown led to an increase in apoptosis (Figure 4D) and the proportion of active caspase 3 positive cells (Figure 4E), and a decrease in proliferation in LSK cells (Figure 4F), similar to those seen in the EML cells. These data confirm that HMGB2 also regulates *Lxn* transcription in primary HSC, and thereby affects the number and clonality of HSC and HPC.

We next performed a more stringent transplantation experiment to determine the effect of HMGB2 inhibition on HSC regenerative capacity *in vivo*. Donor cells are LSK cells that were transduced with either HMGB2 shRNA or control shRNA. They were next transplanted into the myeloablated recipient mice with helper cells, and blood and BM regeneration were examined at 16 weeks post transplantation (Figure 5A). The results showed that HMGB2 knockdown resulted in significant decreases in the regeneration of blood cells, BM HSC/HPC-enriched LSK cells, and the most primitive long-term HSC with unlimited self-renewal capacity (Figure 5B-D). These results suggest that HMGB2 inhibition impairs HSC regenerative functionality. Altogether, our data obtained from the EML cell line and primary HSC strongly support the idea that the HMGB2 suppresses *Lxn* expression, which in turn affects HSC and HPC number and function.

SNP rs31528793 affects *Lxn* promoter activity and hematopoietic stem cell number

The level of a given mRNA transcript is controlled by trans-acting factors and/or cis-acting modulators. Our data suggest that HMGB2 might act as a trans-acting modulator to regulate *Lxn* transcription. Since we previously reported that several SNP identified by us may contribute to the natural variation of *Lxn* expression,[17] we next asked whether any of these SNP is associated with *Lxn* expression as a cis-acting regulator. SNP rs31528793 is the only genetic variant in the *Lxn* promoter region (Figure 1A), we thus asked whether it affects the *Lxn* promoter activity. We made a G to C mutation in the luciferase reporter construct containing the *Lxn* promoter sequence and performed the luciferase reporter assay. The G to C change decreased the promoter activity by more than 2-fold (Figure 6A), suggesting a potential suppressive role of this polymorphism in *Lxn* transcription (Figure 6A, left two columns). Since HMGB2 binds to this region, we next examined whether G/C variant affects HMGB2 binding. The result showed that HMGB2 further suppresses *Lxn* promoter activity, and C allele still causes nearly 2-fold decrease of the promoter activity. We next performed the EMSA assay and further confirmed the interaction of HMGB2 with the *Lxn* promoter containing SNP rs31528793 (Figure 6B). These results indicate that SNP rs31528793 influences *Lxn* promoter activity, with the G allele conferring a high activity, while the C allele is associated with a low activity. Therefore, the genetic variants of the *Lxn* promoter add another layer of regulatory mechanism of *Lxn* transcription.

We previously reported that *Lxn* is differentially expressed in HSC of C57BL/6 (B6) and DBA2 (D2) mice, and its expression level is inversely correlated with HSC number.[17] It is known that B6 mice carry G allele whereas D2 mice have C allele. We therefore hypothesized that the G allele is associated with the higher promoter activity, high *Lxn* expression and low HSC numbers, whereas the C allele has the opposite effect. Next, we examined *Lxn* expression and HSC numbers in B6, D2 and the other two mouse strains, 129X1/SvJ and A/J that carry G allele at the SNP rs31528793 position (*http://www.informatics.jax.org/snp/rs31528793*). We found that D2 mouse strain had the lowest expression of *Lxn* and highest HSC number, whereas all the other three strains showed higher *Lxn* expression and lower HSC number (Figure 6C and D), suggesting that G/C allelic variant could be indicative of *Lxn* expression level and HSC number variation. It is noted that *Lxn* expression level varies in strains carrying G allele suggesting that other SNP outside of the *Lxn* promoter region may contribute to such variation.

Discussion

Lxn plays an important role in regulating HSC function.[17,38] It was originally identified *via* the natural variation of HSC numbers between B6 and D2 inbred mouse strains in which B6 mice have fewer HSC than D2 mice at a young age. The expression of *Lxn* is inversely correlated to the size of HSC population, i.e. its level in B6 is higher than that in D2 cells. Therefore, *Lxn* is a negative regulator of HSC number and its mode of action is primarily through increasing HSC apoptosis and decreasing HSC regenerative capability and proliferation. However, nothing is known about how *Lxn* is transcriptionally regulated in HSC and other stem cells, or why it is differentially expressed in different inbred mouse strains.

Here, we identified a *Lxn* upstream regulatory sequence with a strong promoter activity. More importantly, the SNP (rs31528793) in this region significantly affects its promoter activity, and the G allele carried in B6, 129X1/SvJ and A/J mouse strains confers the promoter a stronger activity than the C allele in D2 strain. Genetic variants have been recently identified to play an important role in transcriptional regulation and thereby resulting in gene expression and phenotype variation.[9,13-15,40] We thus proposed that the G/C containing promoter might be involved in *Lxn* transcriptional regulation. Using DNA pull-down and mass spectrometry, we, for the first time, identified a chromatin binding protein, HMGB2, as a novel transcriptional suppressor of *Lxn* expression. HMGB2 binding was validated by ChIP-qPCR assay in which the endogenous HMGB2 demonstrated a stronger affinity to the *Lxn* specific promoter sequence. HMGB2 knockdown increases *Lxn* expression and decreases HSC numbers in both HSC cell line and BM-derived primary LSK cells. This effect was abrogated when the increased level of *Lxn* was blocked, indicating that *Lxn* is one of the downstream targets and functional mediators of HMGB2 in HSC. Altogether, these results suggest that both cis- and trans-factors are involved in the regulation of *Lxn* transcription (Figure 6E). In trans-regulating mode, HMGB2 acts as a suppressor for *Lxn* transcription. In *cis*-regulating mode, G allele at SNP rs31528793 is associated with stronger promoter activity, a high level of *Lxn* expression, and a small size of HSC pool. In contrast, the C allelic variant attenuates these effects and *Lxn* transcription is less responsive to HMGB2, which leads to a lower *Lxn* expression and an increased stem cell number. Therefore, our work not only identified HMGB2 as a novel transcription regulator of *Lxn*, but also provides a potential functional significance of SNP rs31528793 in contributing to natural variations in *Lxn* expression and HSC number. Despite these findings, how H2MGB2 regulates *Lxn* transcription requires further investigation. We cannot exclude the possibility that HMGB2 directly regulates *Lxn* transcription as the transcription factor. But it is also likely that HMGB2 acts as a chromatin adaptor or modifier to recruit other transcription factors for the initiation of the transcription process (Figure 6E). This mode of action was shown in the GFI1b transcription during erythroid differentiation process in which the binding of HMGB2 to GFI1b promoter enhances the binding of other factors, such as Oct-1, GATA-1 and NF-Y, which collectively activates Gfi1b transcription.[32] In addition, the relationship of HMGB2 binding site to SNP rs31528793, and how they co-ordinately or independently regulate *Lxn* transcription requires further investigation. However, our current data provide more support for the independent regulatory mechanism because of the following observations. Firstly, the suppression extent of HMGB2 on G-containing promoter (ratio of "G+ HMGB2" to "G" is 0.47) is similar to that on C-containing promoter (ratio of "C+ HMGB2" to "C" is 0.48) (Figure 6A). These data suggest that suppression of HMGB2 on *Lxn* promoter activity is independent of allelic variant. Secondly, results of EMSA also show the similar intensity of shifted bands, suggesting that G/C variant does not affect HMGB2 binding (Figure 6B). Lastly, to further confirm binding of HMGB2 to the *Lxn* promoter

and determine the effect of SNP rs31528793 on HMGB2 binding *in vivo*, we performed ChIP-qPCR assay on BM cells of C57BL/6 and DBA/2 mice which naturally carry the SNP. The binding affinity of HMGB2 was quantitatively measured by real-time PCR with primers spanning the promoter sequence containing G/C SNP (see also Figure 1C). We did not detect any difference in the binding affinity, suggesting that the G/C allelic variant does not cause differential binding of HMGB2 to *Lxn* promoter (*data not shown*). Altogether, this evidence strongly suggests that HMGB2 and SNP rs31528793 act independently to regulate *Lxn* transcription.

HMGB2 is a member of the high mobility group family proteins. It is a non-histone chromatin-binding protein that remodels chromatin architecture, therefore affecting gene expression. HMGB2 has been shown to play an important role in maintaining stem cell population in a tissue-specific manner. For example, in the nervous system, HMGB2 deletion leads to the increased neural stem/progenitor cells by increasing their proliferation.[41] However, in articular cartilage, loss of HMGB2 reduces the regenerative capacity of mesenchymal stem cells by increasing apoptosis.[42] Similarly, knockdown of HMGB2 decreased the number of muscle stem (satellite) cells by inhibiting proliferation and stimulating differentiation, thereby leading to the impaired muscle regeneration.[43] Our study showed that the functional effects of HMGB2 on HSC and the blood system are similar to those in mesenchymal and muscle stem cells. Knockdown of HMGB2 decreased HSC number and blood regeneration by increasing apoptosis and decreasing proliferation. These effects are mediated, at least in part, *via* the upregulation of *Lxn*, which is a negative regulator of HSC function. HMGB2 has also been shown to play an important role in cellular senescence and aging.[44,45] It binds to the chromosome loci of key senescence-associated secretory phenotype (SASP) genes and prevents their incorporation into transcriptionally repressive heterochromatin environment during senescence, thereby inducing *SASP* gene expression. Since we found that *Lxn* is one of the transcriptional targets of HMGB2, whether *Lxn* is involved in senescence and aging remains a subject of great interest and remains to be determined. Our unpublished data show that *Lxn* expression increases with aging, and old HSC with *Lxn* depletion have the increased regenerative capacity that is comparable to young HSC. Thus, inhibition of *Lxn* may rejuvenate old HSC.

Natural genetic variation is associated with a variety of hematologic phenotypes in humans. Genome-wide association studies have revealed DNA variants that are implicated in hematologic traits such as fetal hemoglobin levels, hematocrit, cell counts and sizes of different types of blood cells, as well as in disease susceptibility.[10] One of the best examples of the functional effect of genetic variation is a regulatory SNP that causes the blood disorder α-thalassemia. This SNP creates a new transcriptional promoter that interferes with normal transcription of α-globin genes and leads to disease development.[11] However, very few genes underlying the vast majority of these DNA variants have been uncovered and very little is known about how they contribute to the phenotypic diversity in the population.[9] *Lxn* is the first stem cell regulatory gene reported that accounts for the natural diversity of HSC function.[17] Here, also for the first time, we discovered that SNP rs31528793 is one of the DNA variants that are associated with the differential expression of *Lxn* in mouse. The *Lxn* gene is evolutionarily conserved. Since it is identified by the genetic diversity that arises through natural selection, it may physiologically regulate a function in other natural populations, such as humans. In fact, our preliminary data have indicated that there is also a negative correlation between *Lxn* level and the number of HSC and HPC in healthy humans (*C Zhang et al., 2019, unpublished data*). Therefore, *Lxn* may be involved in human hematopoiesis and there might be polymorphisms in human genome that are functionally similar to mouse SNP rs31528793. Interestingly, a recent report has shown that a SNP rs6441224 in *Lxn* promoter is associated with its expression level in humans.[46] So it would be very interesting to determine whether HMGB2 binds to this SNP-containing promoter region and regulates human *Lxn* and HSC function. These would become very useful genetic markers for screening of transplantation donors with a larger stem cell reservoir or for prediction of better recovery of cancer patients from the therapy-induced BM and stem cell suppression.

References

1. Warr MR, Pietras EM, Passegue E. Mechanisms controlling hematopoietic stem cell functions during normal hematopoiesis and hematological malignancies. Wiley Interdiscip Rev Syst Biol Med. 2011;3(6):681-701.

2. Ema H, Morita Y, Suda T. Heterogeneity and hierarchy of hematopoietic stem cells. Exp Hematol. 2014;42(2):74-82.

3. Rossi L, Lin KK, Boles NC, et al. Less is more: unveiling the functional core of hematopoietic stem cells through knockout mice. Cell Stem Cell. 2012;11(3):302-317.

4. Orkin SH, Zon LI. Hematopoiesis: an evolving paradigm for stem cell biology. Cell. 2008;132(4):631-644.

5. Henckaerts E, Langer JC, Snoeck HW. Quantitative genetic variation in the hematopoietic stem cell and progenitor cell compartment and in lifespan are closely linked at multiple loci in BXD recombinant inbred mice. Blood. 2004;104(2):374-379.

6. de Haan G, Bystrykh LV, Weersing E, et al. A genetic and genomic analysis identifies a cluster of genes associated with hematopoietic cell turnover. Blood. 2002; 100(6):2056-2062.

7. Geiger H, True JM, de Haan G, et al. Age- and stage-specific regulation patterns in the hematopoietic stem cell hierarchy. Blood. 2001;98(10):2966-2972.

8. de Haan G, Nijhof W, Van Zant G. Mouse strain-dependent changes in frequency and proliferation of hematopoietic stem cells during aging: correlation between lifespan and cycling activity. Blood. 1997; 89(5):1543-1550.

9. Furey TS, Sethupathy P. Genetics. Genetics driving epigenetics. Science. 2013;

342(6159):705-706.

10. Sankaran VG, Orkin SH. Genome-wide association studies of hematologic phenotypes: a window into human hematopoiesis. Curr Opin Genet Dev. 2013;23(3):339-344.

11. De Gobbi M, Viprakasit V, Hughes JR, et al. A regulatory SNP causes a human genetic disease by creating a new transcriptional promoter. Science. 2006;312(5777):1215-1217.

12. McVicker G, van de Geijn B, Degner JF, et al. Identification of genetic variants that affect histone modifications in human cells. Science. 2013;342(6159):747-749.

13. Kilpinen H, Waszak SM, Gschwind AR, et al. Coordinated effects of sequence variation on DNA binding, chromatin structure, and transcription. Science. 2013; 342(6159):744-747.

14. Kasowski M, Kyriazopoulou-Panagiotopoulou S, Grubert F, et al. Extensive variation in chromatin states across humans. Science. 2013; 342(6159):750-752.

15. Heinz S, Romanoski CE, Benner C, et al. Effect of natural genetic variation on enhancer selection and function. Nature. 2013;503(7477):487-492.

16. Van Zant G, Liang Y. Natural genetic diversity as a means to uncover stem cell regulatory pathways. Ann N Y Acad Sci. 2009; 1176:170-177.

17. Liang Y, Jansen M, Aronow B, et al. The quantitative trait gene latexin influences the size of the hematopoietic stem cell population in mice. Nat Genet. 2007;39(2):178-188.

18. de Haan G. Latexin is a newly discovered regulator of hematopoietic stem cells. Nat Genet. 2007;39(2):141-142.

19. Scadden DT. Nice Neighborhood: Emerging Concepts of the Stem Cell Niche. Cell. 2014;157(1):41-50.

20. Muthusamy V, Premi S, Soper C, et al. The hematopoietic stem cell regulatory gene latexin has tumor-suppressive properties in malignant melanoma. J Invest Dermatol. 2013;133(7):1827-1833.

21. Abd Elmageed ZY, Moroz K, Kandil E. Clinical significance of CD146 and latexin during different stages of thyroid cancer. Mol Cell Biochem. 2013;381(1-2):95-103.

22. Mitsunaga K, Kikuchi J, Wada T, el al. Latexin regulates the abundance of multiple cellular proteins in hematopoietic stem cells. J Cell Physiol. 2012;227(3):1138-1147.

23. Liu Y, Howard D, Rector K, et al. Latexin is down-regulated in hematopoietic malignancies and restoration of expression inhibits lymphoma growth. PLoS One. 2012;7(9):e44979.

24. Li Y, Basang Z, Ding H, et al. Latexin expression is downregulated in human gastric carcinomas and exhibits tumor suppressor potential. BMC Cancer. 2011; 11:121.

25. Jin C, Zang C, Wei G, et al. H3.3/H2A.Z double variant-containing nucleosomes mark 'nucleosome-free regions' of active promoters and other regulatory regions. Nat Genet. 2009;41(8):941-945.

26. Creyghton MP, Markoulaki S, Levine SS, et al. H2AZ is enriched at polycomb complex target genes in ES cells and is necessary for lineage commitment. Cell. 2008; 135(4):649-661.

27. Andang M, Hjerling-Leffler J, Moliner A, et al. Histone H2AX-dependent GABA(A) receptor regulation of stem cell proliferation. Nature. 2008;451(7177):460-464.

28. Lee MG, Villa R, Trojer P, et al. Demethylation of H3K27 regulates polycomb recruitment and H2A ubiquitination. Science. 2007;318(5849):447-450.

29. Gevry N, Chan HM, Laflamme L, et al. p21 transcription is regulated by differential localization of histone H2A.Z. Genes Dev. 2007;21(15):1869-1881.

30. Pusterla T, de Marchis F, Palumbo R, et al. High mobility group B2 is secreted by myeloid cells and has mitogenic and chemoattractant activities similar to high mobility group B1. Autoimmunity. 2009; 42(4):308-310.

31. Pfannkuche K, Summer H, Li O, et al. The high mobility group protein HMGA2: a co-regulator of chromatin structure and pluripotency in stem cells? Stem Cell Rev. 2009;5(3):224-230.

32. Laurent B, Randrianarison-Huetz V, Marechal V, et al. High-mobility group protein HMGB2 regulates human erythroid differentiation through trans-activation of GFI1B transcription. Blood. 2010; 115(3):687-695.

33. Nishino J, Kim I, Chada K, et al. Hmga2 promotes neural stem cell self-renewal in young but not old mice by reducing p16Ink4a and p19Arf Expression. Cell. 2008;135(2):227-239.

34. Yanai H, Ban T, Wang Z, et al. HMGB proteins function as universal sentinels for nucleic-acid-mediated innate immune responses. Nature. 2009;462(7269):99-103.

35. Ye ZJ, Kluger Y, Lian Z, et al. Two types of precursor cells in a multipotential hematopoietic cell line. Proc Natl Acad Sci USA. 2005;102(51):18461-18466.

36. Lemieux ME, Cheng Z, Zhou Q, et al. Inactivation of a single copy of Crebbp selectively alters pre-mRNA processing in mouse hematopoietic stem cells. PloS One. 2011;6(8):e24153.

37. Kutlesa S, Zayas J, Valle A, et al. T-cell differentiation of multipotent hematopoietic cell line EML in the OP9-DL1 coculture system. Exp Hematol. 2009;37(8):909-923.

38. Liu Y, Zhang C, Li Z, et al. Latexin Inactivation Enhances Survival and Long-Term Engraftment of Hematopoietic Stem Cells and Expands the Entire Hematopoietic System in Mice. Stem Cell Rep. 2017;8(4):991-1004.

39. You Y, Wen R, Pathak R, et al. Latexin sensitizes leukemogenic cells to gamma-irradiation-induced cell-cycle arrest and cell death through Rps3 pathway. Cell Death Dis. 2014;5:e1493.

40. Consortium GT, Laboratory DA. Coordinating Center -Analysis Working G, Statistical Methods groups-Analysis Working G, Enhancing Gg, Fund NIHC, et al. Genetic effects on gene expression across human tissues. Nature. 2017; 550(7675):204-213.

41. Abraham AB, Bronstein R, Reddy AS, et al. Aberrant neural stem cell proliferation and increased adult neurogenesis in mice lacking chromatin protein HMGB2. PLoS One. 2013;8(12):e84838.

42. Taniguchi N, Carames B, Ronfani L, et al. Aging-related loss of the chromatin protein HMGB2 in articular cartilage is linked to reduced cellularity and osteoarthritis. Proc Natl Acad Sci U S A. 2009;106(4):1181-1186.

43. Zhou X, Li M, Huang H, et al. HMGB2 regulates satellite-cell-mediated skeletal muscle regeneration through IGF2BP2. J Cell Sci. 2016;129(22):4305-4316.

44. Aird KM, Iwasaki O, Kossenkov AV, et al. HMGB2 orchestrates the chromatin landscape of senescence-associated secretory phenotype gene loci. J Cell Biol. 2016; 215(3):325-334.

45. Nacarelli T, Liu P, Zhang R. Epigenetic Basis of Cellular Senescence and Its Implications in Aging. Genes (Basel). 2017;24;8(12).

46. Kloth M, Goering W, Ribarska T, et al. The SNP rs6441224 influences transcriptional activity and prognostically relevant hypermethylation of RARRES1 in prostate cancer. Int J Cancer. 2012;131(6):E897-904.

Pro-inflammatory cytokine blockade attenuates myeloid expansion in a murine model of rheumatoid arthritis

Giovanny Hernandez,[1] Taylor S. Mills,[1] Jennifer L. Rabe,[1] James S. Chavez,[1] Susan Kuldanek,[1] Gregory Kirkpatrick,[2] Leila Noetzli,[2] Widian K. Jubair,[3] Michelle Zanche,[4] Jason R. Myers,[4] Brett M. Stevens,[1] Courtney J. Fleenor,[5,6] Biniam Adane,[1] Charles A. Dinarello,[7] John Ashton,[4] Craig T. Jordan,[1] Jorge Di Paola,[2] James R. Hagman,[5,6] V. Michael Holers,[3] Kristine A. Kuhn[3] and Eric M. Pietras[1,6]

[1]Division of Hematology, University of Colorado Anschutz Medical Campus, Aurora, CO; [2]Department of Pediatrics, University of Colorado Anschutz Medical Campus, Aurora, CO; [3]Division of Rheumatology, University of Colorado Anschutz Medical Campus, Aurora, CO; [4]Genomics Research Center, University of Rochester, Rochester, NY; [5]Department of Biomedical Research, National Jewish Health, Denver, CO; [6]Department of Immunology & Microbiology, University of Colorado Anschutz Medical Campus, Aurora, CO and [7]Division of Infectious Disease, University of Colorado Anschutz Medical Campus, Aurora, CO, USA

ABSTRACT

Rheumatoid arthritis (RA) is a debilitating autoimmune disease characterized by chronic inflammation and progressive destruction of joint tissue. It is also characterized by aberrant blood phenotypes including anemia and suppressed lymphopoiesis that contribute to morbidity in RA patients. However, the impact of RA on hematopoietic stem cells (HSC) has not been fully elucidated. Using a collagen-induced mouse model of human RA, we identified systemic inflammation and myeloid overproduction associated with activation of a myeloid differentiation gene program in HSC. Surprisingly, despite ongoing inflammation, HSC from arthritic mice remain in a quiescent state associated with activation of a proliferation arrest gene program. Strikingly, we found that inflammatory cytokine blockade using the interleukin-1 receptor antagonist anakinra led to an attenuation of inflammatory arthritis and myeloid expansion in the bone marrow of arthritic mice. In addition, anakinra reduced expression of inflammation-driven myeloid lineage and proliferation arrest gene programs in HSC of arthritic mice. Altogether, our findings show that inflammatory cytokine blockade can contribute to normalization of hematopoiesis in the context of chronic autoimmune arthritis.

Check the online version for the most updated information on this article, online supplements, and information on authorship & disclosures: www.haematologica.org/content/105/3/585

Introduction

Rheumatoid arthritis (RA) is a chronic, systemic inflammatory autoimmune disease affecting up to 1% of the population.[1] RA is associated with significant morbidity and mortality, and substantial healthcare-related costs.[2] While the pathogenesis of RA is most often associated with breaking of central tolerance and activation of autoimmune T and B lymphocytes, all types of blood cells contribute to the RA disease process. Platelets and myeloid cells, such as neutrophils and macrophages, have been shown to infiltrate the joint synovia, damaging tissue and presenting antigens that initiate autoimmunity.[3] RA is also associated with co-morbid hematologic manifestations including chronic anemia, impaired production of naïve T cells, autoimmune cytopenias and leukocytosis during disease 'flares'.[4-7] In addition, RA is associated with elevated levels of pro-inflammatory cytokines including interleukin-1 (IL-1), tumor necrosis factor (TNF) and interferon (IFN)-γ.[4] Therapeutic blockade of these factors has been used with success to alleviate the symptoms of inflammatory arthritis in patients, underscoring the importance of pro-inflammatory cytokines in the pathogenesis of RA.[5]

Maintenance of the blood system requires a carefully orchestrated interaction between blood-forming hematopoietic stem cells (HSC) and cell-extrinsic signals provided by their microenvironment in the bone marrow (BM).[6] Such signals regulate HSC quiescence and/or direct HSC differentiation into lineage-biased multipotent progenitors (MPP) and mature blood cells.[7] Pro-inflammatory cytokines can activate 'emergency' gene programs in HSC associated with overproduction of myeloid- and platelet-biased MPP subsets that, in turn, overproduce myeloid cells and platelets at the expense of other lineages.[8-10] Along these lines, hematopoietic defects in RA patients have been ascribed to pro-inflammatory cytokines.[11] However, the underlying molecular mechanism(s) and impact of therapeutic intervention on HSC function have not been well characterized.

Here, we used the type II collagen-induced arthritis (CIA) mouse model of human RA to identify the impact of chronic autoimmune arthritis on HSC function. We found that CIA leads to expansion of myeloid progenitors in the BM and overproduction of myeloid cells. HSC from CIA mice activated a myeloid gene program, although they retained their quiescence and long-term repopulating function. Interestingly, HSC quiescence was associated with a proliferation arrest program, characterized by downregulation of cell cycle and mRNA translation genes, which may serve to limit spurious HSC activation. Notably, we showed that pharmacological cytokine blockade using the recombinant IL-1 receptor antagonist anakinra alleviated inflammatory arthritis and myeloid expansion in the blood and BM of mice with CIA. In addition, anakinra treatment reduced activation of inflammation-induced myeloid and proliferation arrest gene programs in HSC. Taken together, our findings suggest that anti-inflammatory therapies such as cytokine blockade can restore hematopoietic function in the context of chronic inflammatory diseases such as RA.

Methods

The methods are described in detail in the *Online Supplement.*

Mice and *in vivo* treatments

Male, 6- to 12-week old C57BL/6J (strain #000664) and B10.RIII (strain #000457) mice from The Jackson Laboratory (Bar Harbor, ME, USA) were maintained in a temperature- and light-controlled environment with irradiated chow and water *ad libitum* for all experiments. Arthritis was induced by intradermal injection of type II chicken (for C57BL/6J mice) or bovine (for B10.RIII mice) collagen (Sigma-Aldrich) emulsified in Complete Freund Adjuvant (CFA; Sigma-Aldrich).[12] Anakinra (Swedish Orphan Biovitrum) was administered daily at a dose of 50 mg/kg via subcutaneous injection. All animal procedures were approved by the University of Colorado Denver Anschutz Medical Campus Institutional Animal Care and Use Committee (IACUC).

Flow cytometry and hematopoietic stem cell isolation

BM was flushed from femora and tibiae with Hank's balanced salt solution (HBSS) without calcium or magnesium salts but containing 2% heat-inactivated fetal bovine serum (FBS). BM cells were depleted of red blood cells using ACK lysis except for the erythroblast analysis. Next, 1×10^7 cells were stained for hematopoietic stem and progenitor cells or 1×10^6 for mature BM

cells and were analyzed on a BD FACSCelesta or LSRII instrument. For HSC isolation, posterior limb, anterior limb and pelvic bones were crushed in HBSS + 2% FBS, treated with ACK, placed on a Histopaque 1119 gradient and enriched in c-Kit cells using anti-c-Kit microbeads (Miltenyi) and separation on an AutoMACS Pro (Miltenyi). Cells were double-sorted to purity on a FACSAria IIu or FACSAria Fusion (Becton Dickenson) at 20 psi using a 100 μm nozzle.

Hematopoietic stem cell and bone marrow transplantation assays

Lethally irradiated (11 Gy, split dose 3 h apart) CD45.1+ Boy/J congenic recipient mice were transplanted with either 250 CD45.2+ donor HSC plus 5×10^5 CD45.1+ Sca-1 depleted cells, or 5×10^5 unfractionated BM cells, via the retro-orbital vein in a 100 μL volume of HBSS + 2% FBS. Recipient mice were maintained on autoclaved water containing Bactrim for 4 weeks following transplantation, and donor blood chimerism was assessed every 4 weeks up to 16 weeks via bleeding from the tail vein or retro-orbital sinus.

Gene expression analyses

RNA-sequencing analysis was performed on three biological replicate pools of 4×10^3 to 1×10^4 HSC isolated from groups of two mice per condition (control and CIA). DESeq2-1.12.3 within R-3.3.0 was used for data normalization and differential expression analysis with an adjusted *P*-value threshold of 0.05. Fluidigm analyses were performed using commercially designed DeltaGene primer sets on a Biomark instrument (Fluidigm). Relative gene expression was calculated using the ΔCt method. Data were normalized to *Actb*.

Cytokine analysis

Serum cytokine levels were determined using a Luminex 36-analyte ProCartaPlex cytokine array (Thermo Fisher) according to the manufacturer's instructions.

Statistical analysis

Statistical analyses were performed using Prism 7 software (GraphPad). *P*-values were determined using a Mann-Whitney *U*-test or one-way analysis of variance. *P*-values ≤0.05 were considered statistically significant.

Results

Aberrant blood system in mice with collagen-induced arthritis

The CIA system is the most commonly studied model of RA, and faithfully recapitulates several disease features, including B- and T-cell-driven autoimmunity and chronic production of pathogenic cytokines.[12] To assess the impact of RA on the blood system, C57BL/6 mice were injected intradermally at the base of the tail twice 21 days apart with an emulsion of CFA and type II collagen (Figure 1A). Non-arthritic control mice were injected with CFA alone on the same treatment schedule. After the second (boost) injection, mice rapidly developed polyarthritis characterized by swelling and erythema of the front and rear paws, metatarsals and/or ankles within a week of the boost injection (Figure 1A, *Online Supplementary Figure S1A*). Peripheral blood parameters in CIA mice 21 days after the boost injection showed a significant increase in neutrophils, while lymphocyte and platelet numbers were not

significantly different (Figure 1B). While the overall number of BM cells in the femora and tibiae of CIA mice were unchanged, (Figure 1C), Mac-1+Gr1hi BM granulocytes were significantly increased in CIA mice while the numbers of Mac-1+Gr1intLy6C- immature granulocytes and Mac-1+Gr1intLy6C+ monocytes were unchanged (Figure 1D and *Online Supplementary Figure S1B*). On the other hand, the numbers of CD19+IgM+ immature B cells and CD19+ IgM- B cells were significantly decreased, as were the numbers of CD4+ and CD8+ T cells (Figure 1D-F and *Online Supplementary Figure S1B*). CIA mice were anemic, with significantly decreased hematocrit and hemoglobin levels (Figure 1G). CIA BM was also pale, with decreased basophilic erythroblasts (population II) (Figure 1H, I and *Online Supplementary Figure S1B*). Altogether, CIA mice exhibited myeloid expansion, consistent with previously published studies using the KRN×G7 genetic autoimmune arthritis model.[13] Importantly our findings mirror features of human RA, such as leukocytosis, anemia and immunosenescence.[14,15]
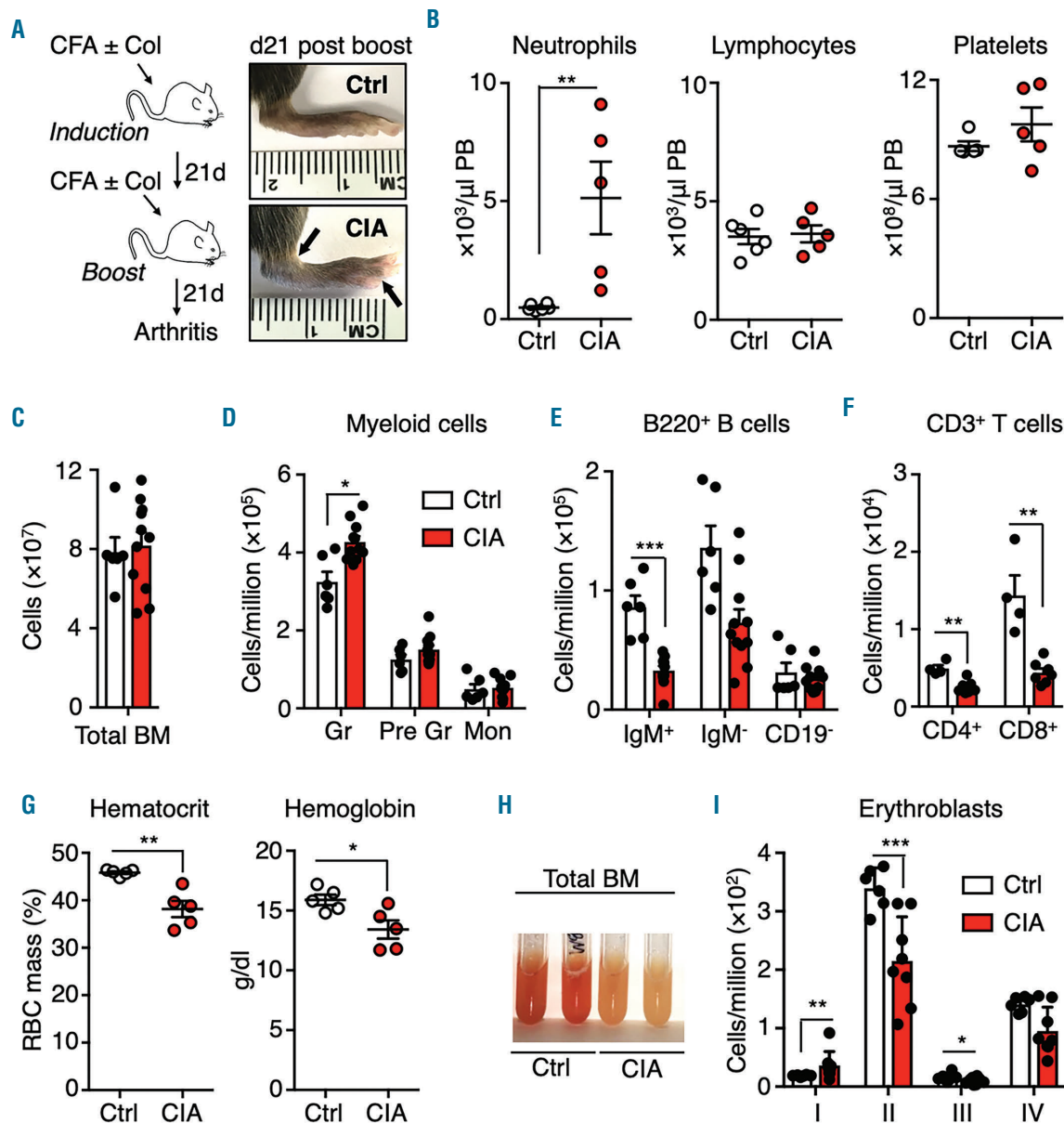
Figure 1. Altered blood system in mice with collagen-induced arthritis. (A) The strategy for producing collagen-induced arthritis (CIA) and representative images showing swelling and anklyosis in the hind paws of a CIA mouse and a control (Ctrl) mouse 21 days after disease induction. (B) Peripheral blood (PB) parameters, determined by a complete blood count, of Ctrl and CIA mice (n=5 per group). (C) Total bone marrow (BM) cellularity of hind legs, and (D-F) numbers of the indicated populations (see *Online Supplementary Figure S1* for FACS gating and surface marker definitions) expressed as number per million BM cells (n=6 Ctrl and 11 CIA). (G) Red blood cell parameters in PB (n=5 per group). (H) Representative image of flushed BM. (I) Erythroblast number per million BM cells (n=6 Ctrl and 11 CIA. *P<0.05; **P<0.01 ***P<0.001, as determined by the Mann-Whitney *U*-test. The data were compiled from three independent experiments. CFA: complete Freund adjuvant; Gr: mature granulocytes; Pre-Gr: immature granulocytes; Mon: monocytes; RBC: red blood cells.
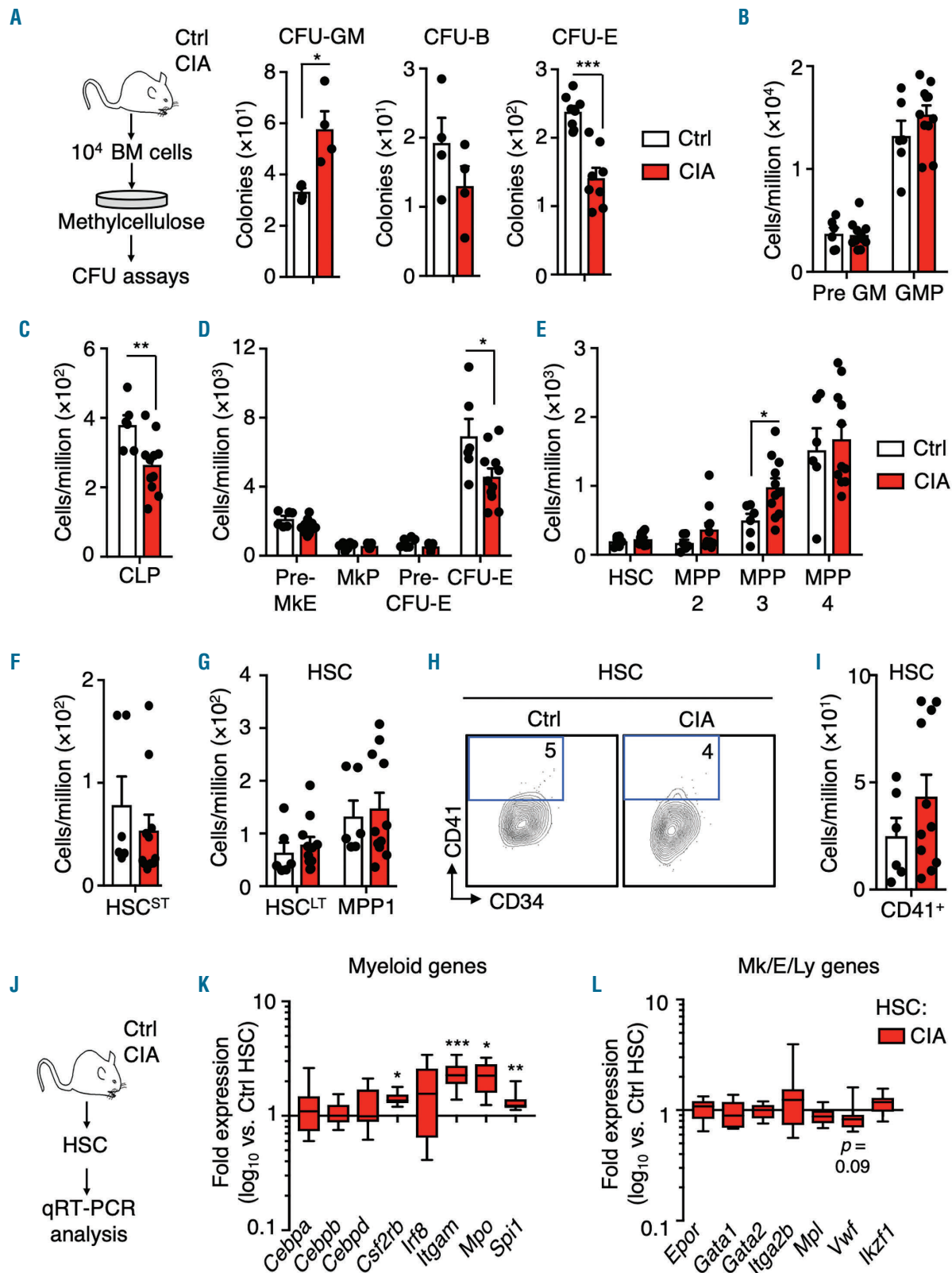
Figure 2. Myeloid expansion in the bone marrow of mice with collagen-induced arthritis. (A) Experimental design and numbers of colony-forming units (CFU)-granulocyte-macrophage (GM), CFU-burst (CFU-B) (n=4 per group) and CFU-erythroid (CFU-E) (n=8/group) in unfractionated bone marrow cells from control mice (Ctrl) and mice with collagen-induced arthritis (CIA). (B-I) Numbers of the indicated populations (see *Online Supplementary Figure S1* for FACS gating and surface marker definitions) expressed as number per million cells. (H) Representative FACS plots showing the gating strategy for identifying the CD41⁺ fraction of hematopoietic stem cells (HSC) (n=6 Ctrl and 11 CIA). The data were compiled from three independent experiments. (J) Experimental design and (K, L) Fluidigm gene expression analysis of HSC from Ctrl and CIA mice showing (K) myeloid and (L) megakaryocyte (Mk), erythroid (E) and lymphoid (Ly) lineage genes. The data are presented as $\log_{10}$ fold expression in CIA HSC *versus* Ctrl HSC. Ct values were normalized to *Actb* (n=8-16 per group). Data are compiled from two independent experiments. *$P<0.05$; **$P<0.01$ ***$P<0.001$, as determined by the Mann-Whitney U-test. BM: bone marrow; Pre GM: precursor granulocyte-macrophage; GMP: granulocyte-macrophage progenitors, CLP; common lymphoid progenitors; Pre MkE: precursor megakaryocyte/erythroid; MkP: megakaryocyte progenitors; MPP: multipotent progenitors; qRT-PCR: real-time quantitative polymerase chain reaction.

Collagen-induced arthritis leads to myeloid expansion and activation of a myeloid gene program in hematopoietic stem cells

We next assessed BM lineage potential using methylcellulose-based colony-forming unit (CFU) assays (Figure 2A). Strikingly, the numbers of granulocyte-macrophage colonies (CFU-GM) (Figure 2A) were significantly increased, whereas erythroid colony formation was impaired (Figure 2A). CFU-GM were also significantly increased in the spleens of CIA mice alongside a significant increase in splenocyte numbers, indicative of extramedullary hematopoiesis[16] (*Online Supplementary Figure S2A-C*). While granulocyte-macrophage progenitors (GMP; Lin⁻c-Kit⁺CD41⁻CD150⁻FcγR⁺) were unchanged in the BM, common lymphoid progenitors (CLP; Lin⁻Flk2⁺IL7R⁺c-Kit^int^Sca1^int^) and phenotypic CFU-E cells (Lin⁻c-Kit⁺CD41⁻FcγR⁻CD150⁻CD105⁺) were significantly reduced (Figure 2B-D and *Online Supplementary Figure S1C*). Recently, distinctive lineage-biased MPP populations downstream of HSC were identified and termed MPP2, MPP3 and MPP4, (LSK Flk2⁻CD48⁺CD150⁺, LSK Flk2⁻CD48⁺CD150⁻, and LSK Flk2⁺, respectively); these populations exhibit megakaryocyte/erythroid, myeloid and lymphoid lineage priming, respectively.[7] CIA mice exhibited expansion of myeloid-biased MPP3 in the BM (Figure 2E and *Online Supplementary Figure S1C*), consistent with myeloid overproduction. Within the phenotypic LSK Flk2⁻CD48⁻CD150⁺ compartment, hereafter referred to in the text as HSC, the distribution of CD34⁻ long-term HSC (HSC^LT^) and metabolically-activated CD34⁺ MPP1 subsets was unchanged (Figure 2G and *Online Supplementary Figure S1C*). Despite some heterogeneity between individual mice, we also did not observe a significant increase in the abundance of CD41-expressing (CD41⁺) HSC, which rapidly differentiate into megakaryocytes in the context of inflammation (Figure 2H, I).[17,18] Likewise, the numbers of short-term HSC (HSC^ST^; LSK Flk2⁻CD48⁻CD150⁻) were unchanged (Figure 2F and *Online Supplementary Figure S1C*). Since remodeling of BM stroma occurs in RA patients and animal models,[19] we analyzed stromal cell populations comprising the endosteal HSC niche[6] and observed a significant decrease in bone-forming mesenchymal stromal cells (MSC), consistent with reduced bone-forming activity in a genetic mouse model of RA (*Online Supplementary Figure S2D, E*).[19,20] Lastly, we confirmed activation of a myeloid lineage gene program in HSC from CIA mice using custom Fluidigm real-time quantitative polymerase chain reaction (qRT-PCR) assays (Figure 2J). Consistent with prior reports,[21] expression of myeloid genes was increased in HSC from CIA mice, including the myeloid master regulator *Spi1/PU*.1 and its target genes *Itgam1* and *Csf2rb*, as well as *Mpo* (Figure 2K). On the other hand, other lineage determinant genes were minimally altered (Figure 2L). Altogether, these data identify aberrant activation of an 'emergency' myeloid differentiation pathway in CIA mice, characterized by BM remodeling, myeloid expansion and activation of a myeloid gene program in HSC.

Impact of collagen-induced arthritis on long-term reconstitution of hematopoietic stem cells

We and others previously showed that chronic inflammation impairs HSC long-term reconstitution capacity.[8] To interrogate long-term HSC potential, we transplanted purified CD45.2⁺ HSC from control and CIA donor mice into lethally-irradiated (11 Gy) CD45.1⁺ recipient mice (Figure 3A and *Online Supplementary Figure S3A*). Strikingly, overall reconstitution capacity of HSC from CIA mice 16 weeks after transplantation was not significantly different from that of controls (Figure 3B), consistent with short-term CFU assays on purified HSC (*Online Supplementary Figure S3B*). Interestingly myeloid lineage output at week 16 was significantly increased (Figure 3C), with a significantly increased proportion of CIA donor-derived phenotypic MPP3, consistent with a myeloid biased phenotype (*Online Supplementary Figure S3C, D*). In parallel, we assessed HSC function independently of surface markers via transplantation of unfractionated BM cells from control and CIA mice (Figure 3D). We observed no defect in reconstitution, save for a slight myeloid bias (Figure 3E-F) and a decreased frequency of CIA donor-derived phenotypic HSC, likely related to a decreased frequency of HSC in the BM of CIA mice (*Online Supplementary Figures S1D* and *S3E, F*). These results suggest that long-term HSC potential is not compromised, although a degree of myeloid bias is present, consistent with prior published results in the KRN×G7 arthritis model.[21] Likewise, expression of genes associated with HSC identity and self-renewal was largely unchanged (Figure 3G-I) except for an increase in *Cd48* expression, suggesting that HSC from CIA mice may be primed toward differentiation into MPP (Figure 3I). However, at the protein level CD48 and other key surface markers associated with lineage bias or differentiation, such CD150, were unchanged,[22] suggesting that such MPP priming could be restricted primarily to the mRNA level (*Online Supplementary Figure S4A, B*). In addition, reactive oxygen species, which accompany differentiation and can impair HSC function if chronically elevated,[23,24] were unchanged in HSC from CIA mice (*Online Supplementary Figure S4C*). Taken together, these data indicate that, apart from myeloid priming, the functional and molecular properties of HSC are largely unperturbed in CIA mice.

A proliferation arrest gene program is associated with quiescence in hematopoietic stem cells from mice with collagen-induced arthritis

To gain additional insight into the impact of CIA on HSC molecular regulation, we performed RNA-sequencing analysis on HSC isolated from control and CIA mice (Figure 4A). Differential expression analysis identified 292 significantly downregulated genes and 237 upregulated genes based on an adjusted *P*-value (P_{adj}) of >0.05 (Figure 4B and *Online Supplementary Table S1*). To uncover potential mechanisms regulating HSC function in CIA mice, we used the Upstream Regulator analysis function in Ingenuity Pathway Analysis (IPA) software. Strikingly, few regulatory pathways were significantly activated in HSC from CIA mice, most notably APC and PTEN, which both suppress HSC activity and enforce quiescence (Figure 4C and *Online Supplementary Table S2*).[25] On the other hand, pathways activated in response to inflammatory and mitogenic cues were downregulated, including ERK, MYC and IL-1/NF-κB (Figure 4C and *Online Supplementary Table S2*).[26] In parallel, gene ontology (GO) analysis[27] identified enrichment of downregulated genes involved in protein translation initiation, G1/S cell cycle transition, positive regulation of gene expression and transcription (Figure 4D and *Online Supplementary Table S3*). Conversely, significantly upregulated genes in HSC from CIA mice

were enriched for cell cycle arrest, negative regulation of transcription, and regulation of cell proliferation categories (Figure 4E and *Online Supplementary Table S4*). Reinforcing these findings, gene set enrichment analysis identified significant (false discovery rate<0.1) enrichment of downregulated genes related to mRNA translation initiation, elongation and termination in HSC from CIA mice (*Online Supplementary Table S5*), whereas only two gene sets were significantly enriched, both related to mitochondrial ribosome function (*Online Supplementary Table S6*). The GEO

accession number for the RNA-sequencing data reported in this paper is GSE129511.

Using Fluidigm qRT-PCR to validate our RNA-sequencing analyses, we found decreased expression of *Myc*, *Mycn*, *Ccnd1* and *Ccnd2*, which are all required for HSC cell cycle entry (Figure 4F). Conversely, cyclin-dependent kinase inhibitors (CKI) *Cdkn1a* (*p21*) and *Cdkn1c* (*p57*), which enforce HSC quiescence, were significantly upregulated in HSC from CIA mice (Figure 4G). In addition, *Eif4b*, which is required for Eif4a activity during mRNA
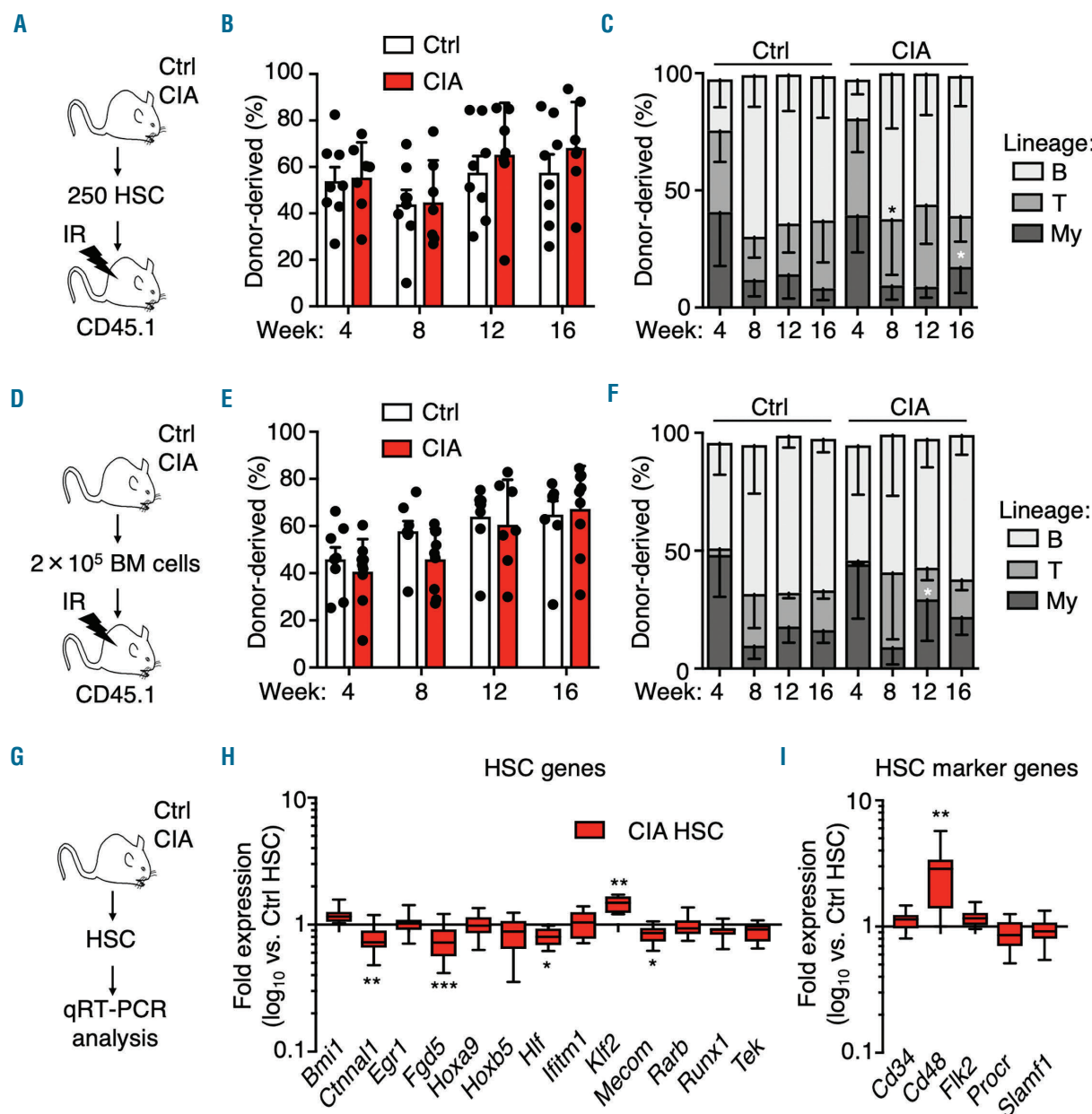
Figure 3. Hematopoietic stem cells from mice with collagen-induced arthritis retain reconstituting capacity. (A-C) Long-term engraftment of purified hematopoietic stem cells (HSC) isolated from control mice (Ctrl) and mice with collagen-induced arthritis (CIA). (A) Experimental design. (B) Donor chimerism and (C) lineage distribution in peripheral blood of recipient mice over time (n=8 Ctrl and 7 CIA recipient mice). (D-F) Long-term engraftment of unfractionated bone marrow isolated from Ctrl and CIA mice. (D) Experimental design. (E) Donor chimerism and (F) lineage distribution in peripheral blood of recipient mice over time (n=10 Ctrl and 9 CIA recipient mice). The data are representative of one of two independent experiments. (G) Experimental design and (H-I) Fluidigm gene expression analysis of HSC from Ctrl and CIA mice showing (H) HSC genes and (I) HSC surface marker genes. The data are presented as $\log_{10}$ fold expression in CIA HSC *versus* Ctrl HSC. Ct values were normalized to *Actb* (n=8-16 per group). *$P<0.05$, as determined by the Mann-Whitney *U*-test. The data were compiled from two independent experiments.
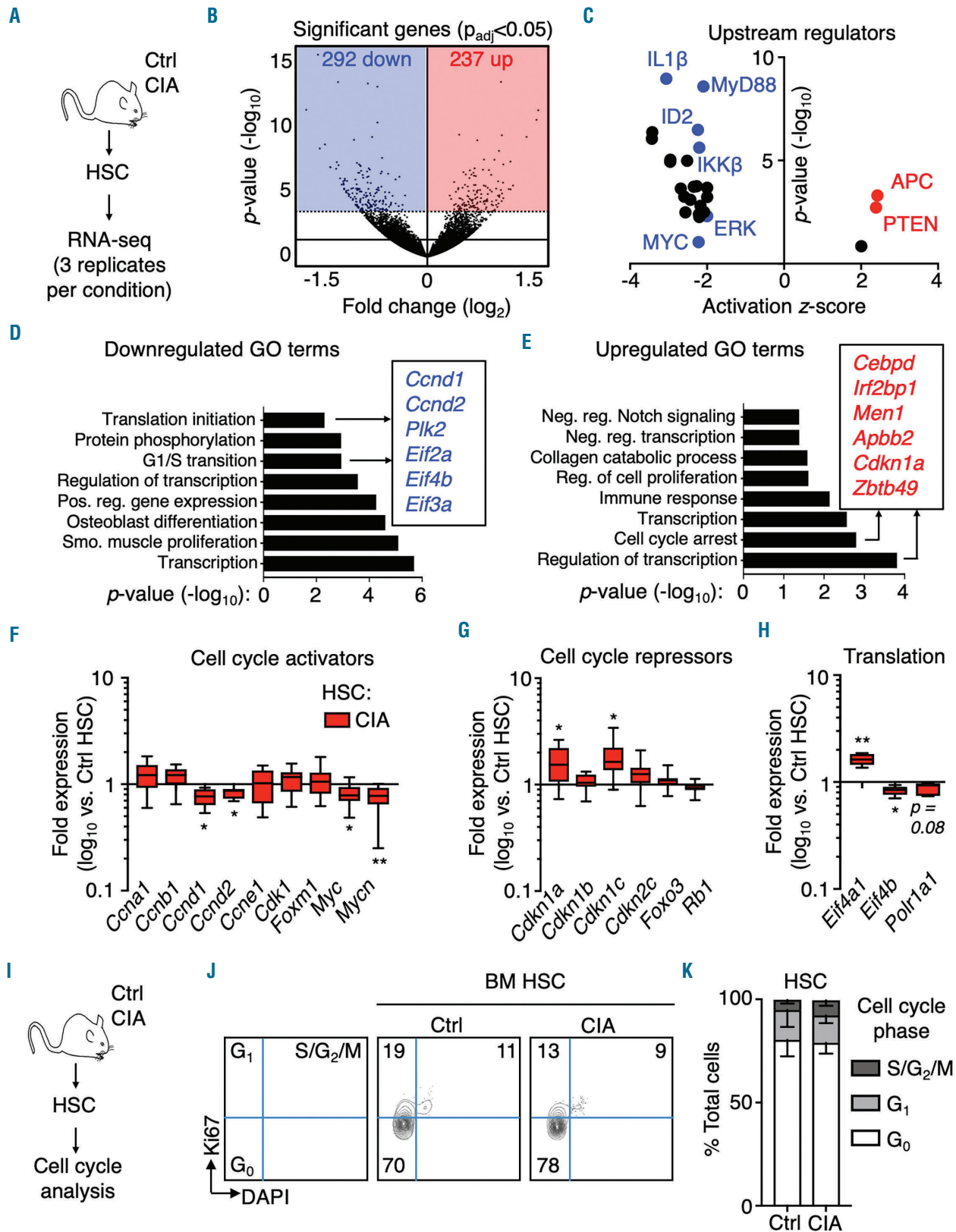
Figure 4. Activation of a proliferation arrest gene program in hematopoietic stem cells from mice with collagen-induced arthritis. (A) Experimental design. (B) Volcano plot showing significantly differentially expressed genes (shaded areas) based on P_{adj} <0.05 (n=3 per group); hematopoietic stem cell (HSC) pools were sorted from three independent sets of mice. (C) Significantly differentially activated upstream regulators as determined by Ingenuity Pathway Analysis. (D, E) Gene ontology (GO) analysis of significantly differentially (D) downregulated and (E) upregulated gene sets. (F-H) Fluidigm gene expression analysis of HSC from control mice (Ctrl) and mice with collagen-induced arthritis showing (F) cell cycle activator genes; (G) cell cycle repression genes; (H) mRNA translation genes. The data are presented as log_{10} fold expression in CIA HSC *versus* Ctrl HSC. Ct values were normalized to *Actb* (n=8-16 per group). The data were compiled from two independent experiments. (I) Experimental design. (J) Representative FACS plots and (K) cell cycle distribution of HSC in Ctrl and CIA mice (n=8 Ctrl and 7 CIA mice). The data were compiled from two independent experiments. See also *Online Supplementary Tables S1-S6*. *P<0.05; **P<0.01 ***P<0.001, as determined by the Mann-Whitney *U*-test.

translation, was decreased (Figure 4H). Collectively, these data identify a global downregulation of HSC activation pathways despite chronic inflammation.

To identify the functional impact, we analyzed the cell cycle distribution of HSC in control and CIA mice (Figure 4I). Strikingly, HSC from CIA mice retained a quiescent cell cycle phenotype (Figure 4J-K). Likewise, the cell cycle distribution of phenotypic MPP or Lin⁻cKit⁺Sca-1⁻CD34⁺ myeloid progenitors (MyPro) was unaltered (*Online Supplementary Figure S5E*). This suggests that myeloid expansion in CIA mice likely arises from preferential differentiation into myeloid-biased progenitors from HSC and/or MPP, rather than from increased proliferative activity. Thus, despite ongoing inflammatory arthritis, HSC retain a quiescent phenotype associated with a proliferation arrest gene program that could serve to prevent cell cycle entry during chronic inflammatory stress.

Systemic pro-inflammatory cytokine production in mice with collagen-induced arthritis

RA-associated cytokines, such as IL-1, TNF, IFN-γ, and myeloid growth factors, such as granulocyte-colony stimulating factor (G-CSF), can activate myeloid gene programs in hematopoietic stem and progenitor cells, leading to altered blood lineage output.[8,10] We therefore used a Luminex-based 36-plex array to analyze cytokine levels in the serum of control and CIA mice (Figure 5A, *Online Supplementary Figure S6*). Several cytokines were increased in the serum of CIA mice, including TNF, G-CSF and IFN-γ. On the other hand, IL-1β, which is often produced locally at the joint synovia in RA patients,[28] was not detected

(Figure 5B). Using qRT-PCR, we found IFN target genes unchanged in HSC from CIA mice, consistent with unchanged Sca-1 surface expression (Figure 5C, *Online Supplementary Figure S4A, B*).[16] In contrast, IL-1 receptor (*Il1r1*), which is a target of multiple cytokines including IL-1 itself, was increased in HSC from CIA mice (Figure 5D). These data suggest that systemic production of pro-inflammatory cytokines is a feature of CIA mice, similar to human RA patients.

Impact of cytokine blockade on myeloid expansion in mice with collagen-induced arthritis

Cytokine blockade therapy, particularly against IL-1 and TNF, is efficacious in reducing inflammatory arthritis. It can also normalize blood parameters in RA patients,[29] although its impact on hematopoiesis is not well described. We used anakinra, a recombinant form of human IL-1 receptor antagonist (IL-1Ra) that is approved for treatment of RA in human patients and is considered a paradigm for cytokine blockade therapy.[30] We induced CIA in C57BL/10.RIII (B10.RIII) mice (Figure 6A), a C57BL/6-related strain that develops a severe and highly penetrant autoimmune arthritis following CIA induction.[31] These mice are thus ideal for testing therapeutic interventions. Consistent with prior mouse studies, anakinra treatment significantly reduced arthritis severity based on clinical scoring of paw swelling (Figure 6B).[32] Strikingly, anakinra normalized peripheral blood neutrophil and, to a lesser extent, red blood cell counts (Figure 6C, *Online Supplementary Figure S7A*). Anakinra treatment also normalized granulocyte and B-cell numbers in the BM, with a
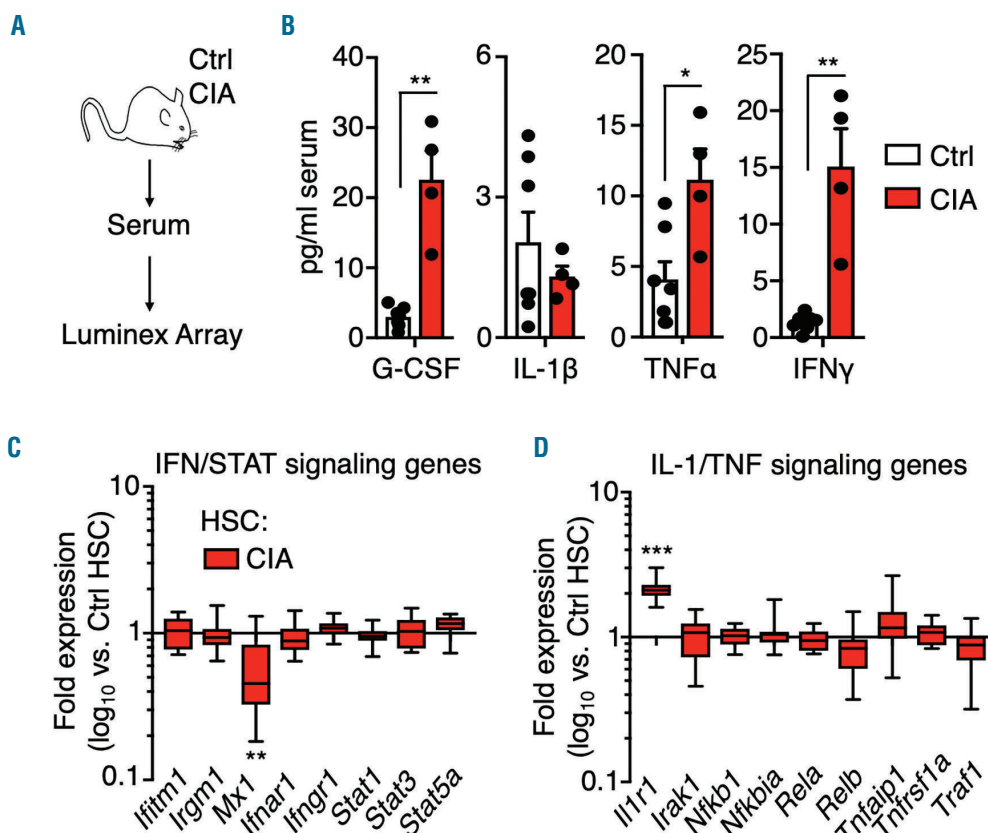
Figure 5. Systemic inflammation in mice with collagen-induced arthritis. (A) Experimental design. (B) Cytokine levels in serum from control mice (Ctrl) and mice with collagen-induced arthritis (CIA) (n=7 Ctrl and 4 CIA). Serum sample data were compiled from two independent experiments. (C,D) Gene expression analysis of hematopoietic stem cells (HSC) from Ctrl and CIA mice showing (C) IFN/STAT signaling genes and (D) IL-1/TNF signaling genes. The data are presented as log₁₀ fold expression in CIA HSC *versus* Ctrl HSC. (n=14-16 per group) *P<0.05; **P<0.01, as determined by the Mann-Whitney *U*-test.

slight but statistical increase in immature granulocytes in anakinra-treated mice, perhaps reflecting slowed differentiation of these cells into mature granulocytes (Figure 6D, E). While the numbers of common lymphoid progenitors were not restored, anakinra treatment modestly reduced GMP and MPP3 expansion in CIA mice to a point below statistical significance relative to controls, suggesting reduced activation of myeloid differentiation pathways (Figure 6F-H). On the other hand, HSC^{LT} and MPP1 numbers were unchanged in all conditions (Figure 6I). Altogether, these data indicate that pro-inflammatory cytokine blockade can at least partially alleviate myeloid expansion and neutrophilia associated with CIA.

Cytokine blockade reverses inflammation-driven gene programs in hematopoietic stem cells from mice with collagen-induced arthritis

Given the impact of anakinra treatment on hematopoiesis, we next assessed the effect of anakinra on cell cycle activity in HSC, MPP and MyPro in CIA mice. We found their cell cycle distribution remained unchanged (Figure 7A-C), indicating that anakinra treatment does not alter cell cycle distribution in these populations. Nonetheless, anakinra treatment partially normalized expression of *Ccnd1* and almost completely normalized expression of the cell cycle inhibitors *Cdkn1b*, *Cdkn2c* and *Rb1* (Figure 7D). Strikingly, anakinra also significantly
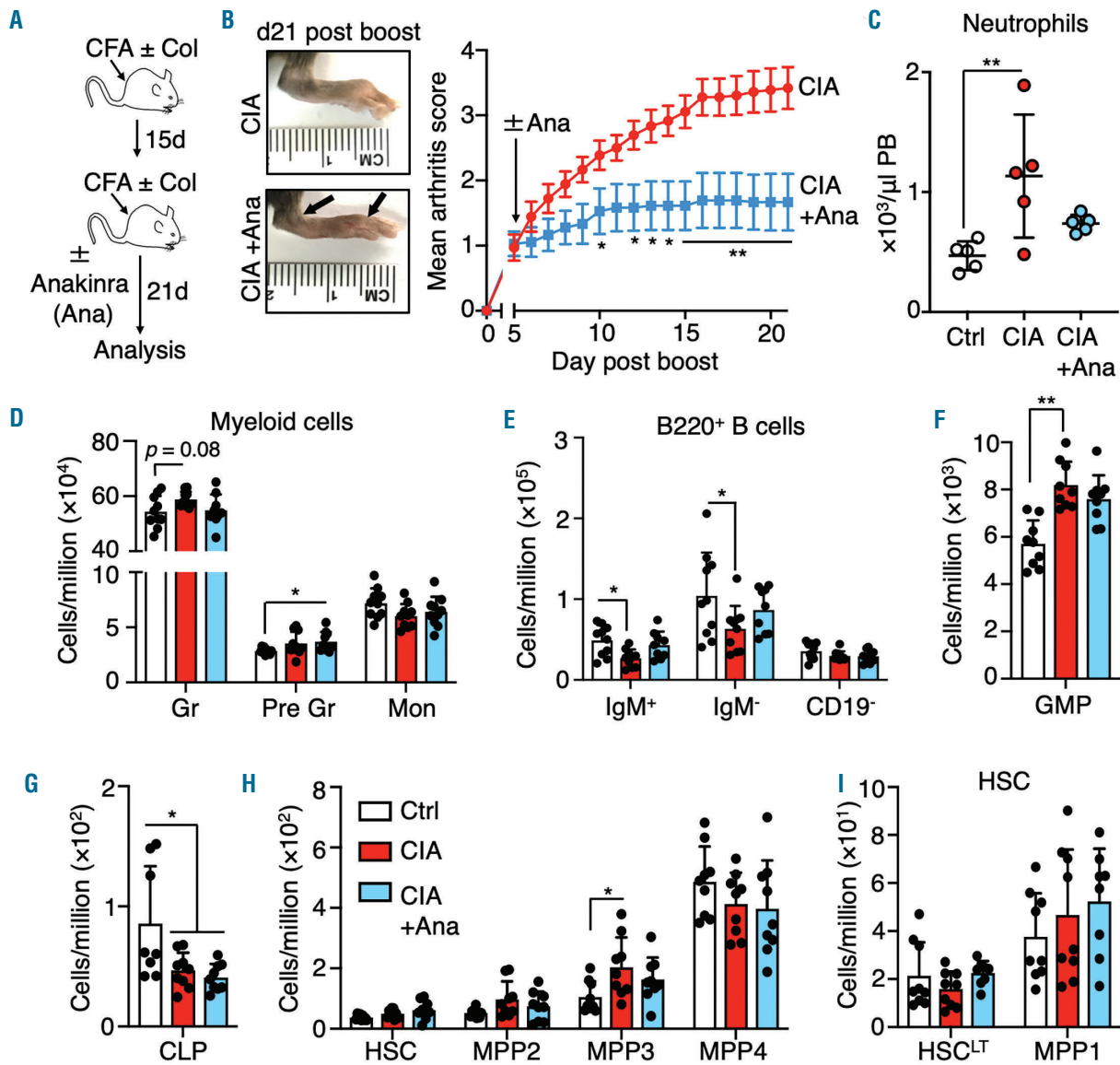
Figure 6. Cytokine blockade reduces myeloid expansion in mice with collagen-induced arthritis. (A) Induction of collagen-induced arthritis (CIA) and anakinra (Ana) treatment strategy in B10.RIII mice. (B) Representative images showing swelling and anklyosis in the hind paws of mice 17 days after disease induction (top left, CIA mice not treated with Ana; bottom left, CIA mice treated with Ana) and impact of Ana treatment on arthritis score (right) (n=9 per group). (C) Peripheral blood neutrophil count and (D-I) number of the indicated bone marrow populations expressed as number per million BM cells of control, CIA and CIA+Ana mice (n=9 per group). The data were compiled from two independent experiments. *P<0.05; **P<0.01 ***P<0.001, as determined by one-way analysis of variance or the Mann-Whitney *U*-test. CFA: complete Freund adjuvant; Col: collagen; Ctrl: control; PB: peripheral blood; Gr: mature granulocytes; Pre Gr: immature granulocytes; Mon: monocytes, GMP: granulocyte-macrophage progenitors, CLP; common lymphoid progenitors; MPP: multipotent progenitors.

decreased expression of aberrantly activated myeloid lineage genes in HSC from CIA mice, including PU.1 and targets such as *Csfr2b*, *Itgam*, as well as *Il1r1* and the myeloid transcription factor *Irf8* (Figure 7E), consistent with reduced myeloid expansion in anakinra-treated CIA mice. Taken together, these data indicate that inflammation-driven myeloid and proliferation arrest gene programs in HSC are at least partially reversible, and can be alleviated by cytokine blockade therapy.

Discussion

Human RA is associated with deregulations in the blood system that can contribute to disease pathogenesis and patient morbidity.[14,15,33] Here, we used the CIA mouse model of human RA to better understand the impact of disease and therapeutic intervention on the hematopoietic system. We found that CIA induced a profoundly myeloid-skewed hematopoietic hierarchy characterized
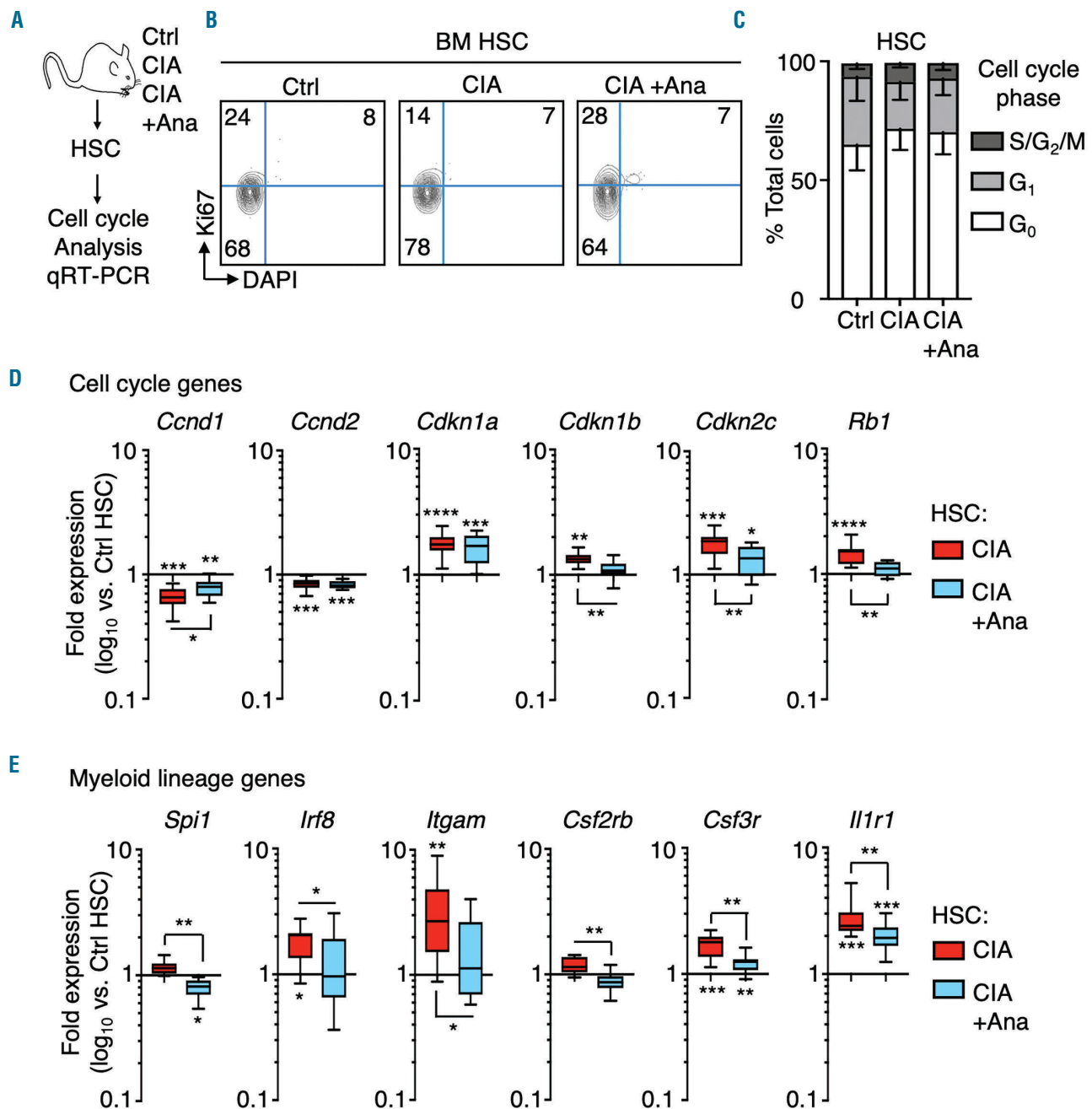
Figure 7. Cytokine blockade attenuates inflammation-induced hematopoietic stem cell gene programs. (A) Experimental design. (B) Representative FACS plots and (C) cell cycle distribution of hematopoietic stem cells (HSC) from control mice (Ctrl), mice with collagen-induced arthritis (CIA) and CIA mice treated with anakinra (+Ana) (n=5 per group). (D) Fluidigm analysis of proliferation arrest gene programs in HSC from Ctrl, CIA and CIA +Ana mice. The data are presented as $\log_{10}$ fold expression *versus* Ctrl HSC (n=12-16 per group). (E) Fluidigm analysis of myeloid gene expression in HSC from Ctrl, CIA and CIA +Ana mice. The data are presented as $\log_{10}$ fold expression *versus* Ctrl HSC. Ct values were normalized to *Actb* (n=12-16 per group). The data are presented as $\log_{10}$ fold expression *versus* Ctrl HSC (n=12-16 per group). The data were compiled from two independent experiments. *$P<0.05$; **$P<0.01$ ***$P<0.001$, ****$P<0.0001$ as determined by one-way analysis of variance or the Mann-Whitney U-test. BM: bone marrow.

by selective expansion of myeloid progenitors and mature myeloid cells and activation of myeloid lineage genes in HSC. Despite chronic inflammation, HSC from CIA mice retained their long-term potential and maintained a quiescent cell cycle state associated with the induction of a proliferation arrest gene program. Strikingly, we found that cytokine blockade therapy was able to attenuate these effects (Figure 8).

Myeloid expansion, chronic anemia of inflammation and immunosenescence are well-documented hematopoietic phenotypes in human RA patients, although the precise causes remain elusive and may be multifactorial.[14,15,33] Strikingly, myeloid expansion in CIA mice closely resembles that in other models of chronic inflammation including those induced by lipopolysaccharide, IL-1, IFN and pathogen infection.[8,10,34] Pro-inflammatory signals can directly activate myeloid transcription factors including *Spi1/PU*.1 and C/EBP family members, which 'override' competing lineage programs and drive expansion of myeloid-biased progenitors.[35-37] In line with this, we observed increased expression of *Spi1/PU.1* and its target genes in HSC from CIA mice. In addition, transplantation of purified CIA HSC revealed an increased proportion of donor-derived myeloid cells and phenotypic MPP3, suggesting that BM inflammation primes HSC to differentiate preferentially into myeloid-lineage progenitors. Given that *PU.1* activation in HSC and myeloid expansion are features of both our CIA and chronic IL-1 models, they are likely stereotypical responses to ongoing inflammation rather than a disease-specific mechanism, wherein PU.1 could serve as a central 'node' that activates a myeloid gene program in HSC following a variety of inflammatory insults. Newly developed pharmacological

inhibitors of PU.1[38] could thus provide therapeutic benefit by blocking this 'node' independently of cytokines in an inflammatory disease.

In the literature, inflammation is often associated with increased HSC proliferation, typically in response to acute challenges.[8,10] On the other hand, we previously found that HSC can maintain quiescence in the context of ongoing chronic type I IFN signaling.[16] Likewise, here we showed that HSC quiescence, phenotypic pool size and long-term repopulating capacity are maintained in CIA mice. Quiescence protects HSC by preventing excessive apoptosis, differentiation, or replicative 'aging' associated with proliferation, and HSC lacking quiescence maintenance genes, such as *Ckdn1a* and *Cdkn1c*, become exhausted in response to stress.[25] Notably, we found that HSC maintained a quiescent state despite ongoing BM remodeling, including decreased phenotypic endosteal MSC. MSC are required for HSC maintenance and quiescence,[6] and there is evidence that MSC function may be degraded in the context of RA.[13,33] Our data suggest there are mechanism(s) that may limit HSC proliferation in response to 'emergency' inflammatory signals and/or BM niche remodeling. Indeed, HSC from CIA mice activated a proliferation arrest gene program characterized by downregulation of genes including *Myc* and *Ccnd1/2*, alongside upregulation of *Cdkn1a*, *Cdkn1b* and *Cdkn1c*. Likewise, *MYC* and *CCND2* are downregulated in CD34^{+} hematopoietic stem and progenitor cells from human RA patients.[39] Such a program could protect HSC pool integrity by increasing the threshold necessary for HSC cell cycle entry, thereby compensating for impaired BM niche function and/or elevated levels of pro-inflammatory cytokines. The functional significance of this gene program
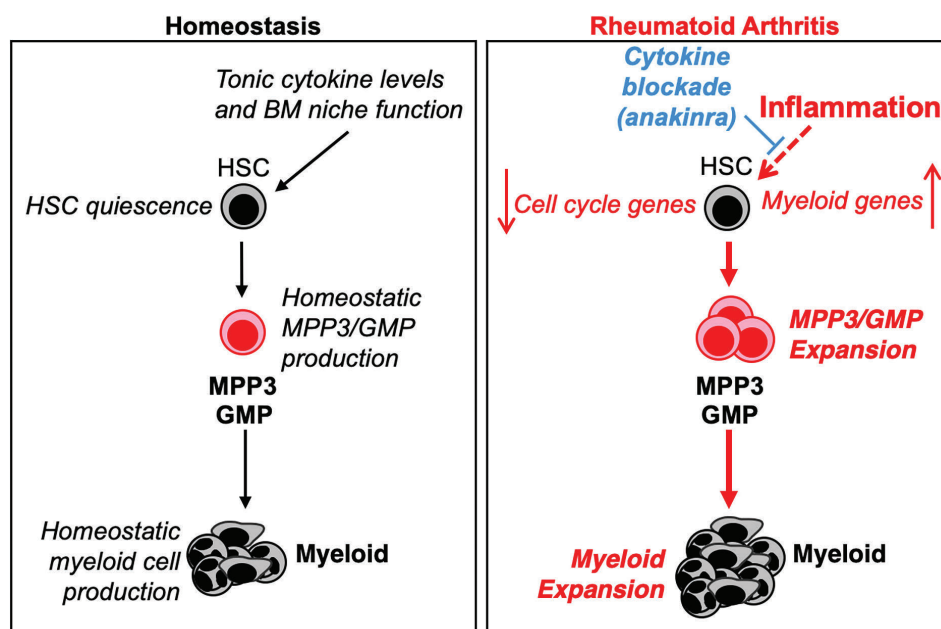
Figure 8. Model of inflammation-driven hematopoietic alterations in mice with collagen-induced arthritis. Under homeostatic conditions, hematopoietic stem cells (HSC) are largely quiescent but occasionally enter the cell cycle and give rise to lineage-biased multipotent progenitor (MPP) subsets, leading to a balanced lineage output and nominal HSC self-renewal capacity. In mice with collagen-induced arthritis (CIA), chronic inflammation leads to expansion of myeloid-biased MPP3 and granulocyte-macrophage progenitors (GMP), resulting in increased myeloid cell production. Concurrently, inflammation induces a myeloid lineage gene program in HSC that may bias HSC toward further overproduction of MPP3. Despite ongoing inflammation, HSC are maintained in a quiescent state characterized by repression of cell cycle and mRNA translation genes alongside induction of cell cycle inhibitor genes. Notably, pro-inflammatory cytokine blockade, here using anakinra, attenuates myeloid expansion and altered gene expression in HSC. These data indicate that chronic inflammation drives aberrant hematopoiesis in rheumatoid arthritis, and this phenotype can be attenuated by cytokine-blocking therapy.

could be further addressed by determining whether HSC from CIA mice fail to proliferate in response to a concurrent inflammatory stimulus. Future studies could also address the functional significance of disease-induced changes in key BM niche populations such as MSC in hematopoiesis.

Interestingly, these results are distinct from the increased HSC cell cycle activity and HSC depletion observed in a model of chronic *M. avium* infection.[40] The difference could be due to ongoing consumption of mature immune cells (particularly granulocytes) during the active infection that drives continuous HSC proliferation. Notably, serum levels of IFN-γ in mice infected with *M. avium* are also over 20-fold higher than those in our mice with CIA, which may be sufficient to activate HSC and overwhelm quiescence-enforcing mechanisms. While we found elevated serum IFN-γ levels in CIA mice, these did not translate into activation of IFN target genes in HSC, suggesting that either the IFN-γ level was not sufficiently high to activate HSC, or or HSC had become refractory to such signals. Altogether, our data suggest that chronic inflammation could actually induce protection of the HSC pool (at least up to a point) by activating stress response mechanisms that maintain quiescence. Such a model is in line with an emerging body of work showing that pro-inflammatory signaling can play a positive role in hematopoiesis.[8] This model could explain the rarity of BM failure in RA patients despite some increased risk of myelodysplastic syndrome,[41] as well as the rarity of graft failure in RA patients undergoing autologous BM transplantation.[42]

While concurrent activation of myeloid differentiation and proliferation arrest gene programs in HSC seems paradoxical, cell cycle arrest is crucial for myeloid differentiation by promoting accumulation of factors needed for differentiation.[43] Myeloid transcription factors, including PU.1, promote cell cycle arrest via induction of cell cycle inhibitors such as *Cdkn1a* while repressing cell cycle activators like *Ccnd1*.[43,44] Thus, induction of myeloid gene programs could serve a dual purpose during chronic inflammation: protecting the HSC pool from excess proliferation while promoting myeloid differentiation of actively cycling hematopoietic progenitor cells. In this way, HSC may participate minimally in day-to-day blood system maintenance[45] during chronic inflammation, with occasional HSC divisions nonetheless leading to preferential myeloid progenitor production. On the other hand, telomere attrition has been identified in CD34+ hematopoietic stem and progenitor cells from human RA patients.[46] RA is typified by years of ongoing disease, including 'flares' and therapies which could induce premature replicative 'aging' in the HSC compartment.[11] Further analyses should clarify the extent to which HSC are affected by telomere attrition and whether such effects are due to increased proliferation *versus* impaired telomere maintenance. Divisional tracing approaches, such as H2B-GFP labeling[47] in mouse models including the CIA model, could therefore provide valuable insights into the long-term impact of inflammatory disease on HSC proliferation.

Cytokine blockade therapies, including anakinra, have been used for over a decade to treat chronic inflammatory disorders, such as RA.[5] Anakinra can correct aberrant blood parameters in RA patients.[29] However, the impact of cytokine blockade on hematopoiesis in the BM has not been closely studied. Here, we show that anakinra treatment reduces myeloid progenitor expansion in mice with CIA, characterized by partial reduction of MPP3 and GMP.

It should be noted that MPP3 is not a transient population; clonal analyses and transplantation assays have shown that MPP3 can persist in mice and continue to produce GMP for weeks if not months. Hence, it is possible that the impact of cytokine blockade on hematopoiesis is gradual, with further reduction in MPP3 and GMP numbers as these populations turn over and are not replaced due to reduced activity of 'emergency' differentiation pathways in HSC. Indeed, anakinra reduced activation of myeloid and proliferation arrest gene programs activated in HSC from CIA mice. This suggests that HSC molecular responses to inflammation are reversible and may be regulated in proportion to the level of inflammatory signaling and/or BM remodeling in the individual.

Our data are agnostic as to whether anakinra acts directly on HSC, or orthogonally by reducing inflammation at the joints, which in turn translates into less systemic inflammation. Indeed, we did not detect increased IL-1 levels in the serum of CIA mice, consistent with studies in human patients indicating that IL-1 production is often localized to the joint synovia.[28] On the other hand, we found increased *Il1r1* expression in HSC from CIA mice, suggesting that HSC could be sensitized to tonic IL-1 production in the BM, even if IL-1 levels themselves do not increase. Along these lines, anakinra treatment reduces expression of *IL1R1* and other IL-1 target genes in blood cells from breast cancer patients.[48] Hence, anakinra could also contribute to restored HSC function by breaking a feedback loop between IL-1 and *Il1r1* expression in HSC from CIA mice. Future studies could determine the extent to which anakinra reduces the effects of inflammation on HSC via direct *versus* indirect mechanisms such as reduction in downstream cytokine production. Notably, other cytokine blocking drugs, such as the TNF inhibitor etanercept, also alleviate the symptoms of inflammatory arthritis in RA patients.[49] It is therefore possible that blockade of other cytokines elicits a similar restoration of hematopoiesis. In addition, blockade of multiple inflammatory cytokines may further normalize hematopoiesis in RA and other diseases, although such interventions could also increase the risk of infection or cytopenia in patients.[50] Taken together, our findings show that pro-inflammatory cytokine blocking treatment can reverse inflammatory-induced changes in hematopoiesis and HSC gene regulation, with the degree of impact likely related to the duration of treatment and/or the extent to which inflammatory arthritis is alleviated in the patient. Our data thus provide further rationale for the use of anti-cytokine therapies to redirect HSC fate and restore normal hematopoiesis in patients with RA and, potentially, other chronic inflammatory diseases.

References

1. Myasoedova E, Crowson CS, Kremers HM, Therneau TM, Gabriel SE. Is the incidence of rheumatoid arthritis rising?: results from Olmsted County, Minnesota, 1955-2007. Arthritis Rheum. 2010;62(6):1576-1582.

2. Birnbaum H, Pike C, Kaufman R, Marynchenko M, Kidolezi Y, Cifaldi M. Societal cost of rheumatoid arthritis patients in the US. Curr Med Res Opin. 2010;26(1):77-90.

3. Papadaki G, Kambas K, Choulaki C, et al. Neutrophil extracellular traps exacerbate Th1-mediated autoimmune responses in rheumatoid arthritis by promoting DC maturation. Eur J Immunol. 2016;46(11):2542-2554.

4. Firestein GS, Malnnes IB. Immunopathogenesis of rheumatoid arthritis. Immunity. 2017;46(2):183-196.

5. Dinarello CA. Anti-inflammatory agents: present and future. Cell. 2010;140(6):935-950.

6. Morrison SJ, Scadden DT. The bone marrow niche for haematopoietic stem cells. Nature. 2014;505(7483):327-334.

7. Pietras EM, Reynaud D, Kang Y-A, et al. Functionally distinct subsets of lineage-biased multipotent progenitors control blood production in normal and regenerative conditions. Cell Stem Cell. 2015;17(1):35-46.

8. Pietras EM. Inflammation: a key regulator of hematopoietic stem cell fate in health and disease. Blood. 2017;130(15):1693-1698.

9. Manz MG, Boettcher S. Emergency granulopoiesis. Nat Rev Immunol. 2014;14(5):302-314.

10. King KY, Goodell MA. Inflammatory modulation of HSCs: viewing the HSC as a foundation for the immune response. Nat Rev Immunol. 2011;11(10):685-692.

11. Colmegna I, Weyand CM. Haematopoietic stem and progenitor cells in rheumatoid arthritis. Rheumatology (Oxford). 2011;50(2):252-260.

12. Brand DD, Latham KA, Rosloniec EF. Collagen-induced arthritis. Nat Protoc. 2007;2(5):1269-1275.

13. Ma YD, Park C, Zhao H, et al. Defects in osteoblast function but no changes in long-term repopulating potential of hematopoietic stem cells in a mouse chronic inflammatory arthritis model. Blood. 2009;114(20):4402-4410.

14. Papadaki HA, Kritikos HD, Valatas V, Boumpas DT, Eliopoulos GD. Anemia of chronic disease in rheumatoid arthritis is associated with increased apoptosis of bone marrow erythroid cells: improvement following anti-tumor necrosis factor-alpha antibody therapy. Blood. 2002;100(2):474-482.

15. Koetz K, Bryl E, Spickschen K, O'Fallon WM, Goronzy JJ, Weyand CM. T cell homeostasis in patients with rheumatoid arthritis. Proc Natl Acad Sci U S A. 2000;97(16):9203-9208.

16. Pietras EM, Lakshminarasimhan R, Techner J-M, et al. Re-entry into quiescence protects hematopoietic stem cells from the killing effect of chronic exposure to type I interferons. J Exp Med. 2014;211(2):245-262.

17. Haas S, Hansson J, Klimmeck D, et al. Inflammation-induced emergency megakaryopoiesis driven by hematopoietic stem cell-like megakaryocyte progenitors. Cell Stem Cell. 2015;17(4):422-434.

18. Gekas C, Graf T. CD41 expression marks myeloid-biased adult hematopoietic stem cells and increases with age. Blood. 2013;121(22):4463-4472.

19. Shaw AT, Gravallese EM. Mediators of inflammation and bone remodeling in rheumatic disease. Semin Cell Dev Biol. 2016;49:2-10.

20. Schepers K, Campbell TB, Passegué E. Normal and leukemic stem cell niches: insights and therapeutic opportunities. Cell Stem Cell. 2015;16(3):254-267.

21. Oduro KA, Liu F, Tan Q, Kim CK, et al. Myeloid skewing in murine autoimmune arthritis occurs in hematopoietic stem and primitive progenitor cells. Blood. 2012;120(11):2203-2213.

22. Challen GA, Boles NC, Chambers SM, Goodell MA. Distinct hematopoietic stem cell subtypes are differentially regulated by TGF- 1. Cell Stem Cell. 2010;6(3):265-278.

23. Chen C, Liu Y, Liu Y, Zheng P. The axis of mTOR-mitochondria-ROS and stemness of the hematopoietic stem cells. Cell Cycle. 2009;8(8):1158-1160.

24. Ludin A, Gur-Cohen S, Golan K, et al. Reactive oxygen species regulate hematopoietic stem cell self-renewal, migration and development, as well as their bone marrow microenvironment. Antioxid Redox Signal. 2014;21(11):1605-1619.

25. Pietras EM, Warr MR, Passegué E. Cell cycle regulation in hematopoietic stem cells. J Cell Biol. 2011;195 (5):709-20.

26. Wilson A, Murphy MJ, Oskarsson T, et al. c-Myc controls the balance between hematopoietic stem cell self-renewal and differentiation. Genes Dev. 2004;18(22):2747-2763.

27. Huang DW, Sherman BT, Lempicki RA. Systematic and integrative analysis of large gene lists using DAVID bioinformatics resources. Nat Protoc. 2009;4(1):44-57.

28. Rooney M, Symons JA, Duff GW. Interleukin 1 beta in synovial fluid is related to local disease activity in rheumatoid arthritis. Rheumatol Int. 1990;10(5):217-219.

29. Karanikolas G, Charalambopoulos D, Vaiopoulos G, et al. Adjunctive anakinra in patients with active rheumatoid arthritis despite methotrexate, or leflunomide, or cyclosporin-A monotherapy: a 48-week, comparative, prospective study. Rheumatology (Oxford). 2008;47(9):1384-1388.

30. Joosten LA, Helsen MM, Saxne T, van De Loo FA, Heinegard D, van Den Berg WB. IL-1 alpha beta blockade prevents cartilage and bone destruction in murine type II collagen-induced arthritis, whereas TNF-alpha blockade only ameliorates joint inflammation. J Immunol. 1999;163(9):5049-5055.

31. Myers LK, Miyahara H, Terato K, Seyer JM, Stuart JM, Kang AH. Collagen-induced arthritis in B10.RIII mice (H-2r): identification of an arthritogenic T-cell determinant. Immunology. 1995;84(4):509-513.

32. van Den Berg WB, Joosten LA, van De Loo FA. TNF alpha and IL-1 beta are separate targets in chronic arthritis. Clin Exp Rheumatol. 1999;17(6 Suppl 18):S105-114.

33. Papadaki HA, Marsh JCW, Eliopoulos GD. Bone marrow stem cells and stromal cells in autoimmune cytopenias. Leuk Lymphoma. 2002;43(4):753-760.

34. Takizawa H, Fritsch K, Kovtonyuk LV, et al. Pathogen-induced TLR4-TRIF innate immune signaling in hematopoietic stem cells promotes proliferation but reduces competitive fitness. Cell Stem Cell. 2017;21(2):225-225.

35. Pietras EM, Mirantes-Barbeito C, Fong S, et al. Chronic interleukin-1 exposure drives haematopoietic stem cells towards precocious myeloid differentiation at the expense of self-renewal. Nat Cell Biol. 2016;18(6):607-618.

36. Hirai H, Zhang P, Dayaram T, et al. C/EBPbeta is required for "emergency" granulopoiesis. Nat Immunol. 2006;7(7):732-739.

37. Libregts SF, Gutiérrez L, de Bruin AM, et al. Chronic IFN- production in mice induces anemia by reducing erythrocyte life span and inhibiting erythropoiesis through an IRF-1/PU.1 axis. Blood. 2011;118(9):2578-2588.

38. Antony-Debré I, Paul A, Leite J, et al. Pharmacological inhibition of the transcription factor PU.1 in leukemia. J Clin Invest. 2017;127(12):4297-4313.

39. Colmegna I, Pryshchep S, Oishi H, Goronzy JJ, Weyand CM. Dampened ERK signaling in hematopoietic progenitor cells in rheumatoid arthritis. Clin Immunol. 2012;143(1):73-82.

40. Matatall KA, Jeong M, Chen S, et al. Chronic infection depletes hematopoietic stem cells through stress-induced terminal differentiation. Cell Rep. 2016;17(10):2584-2595.

41. Wolach O, Stone R. Autoimmunity and inflammation in myelodysplastic syndromes. Acta Haematol. 2016;136 (2):108-117.

42. Bingham SJ, Snowden J, McGonagle D, et al. Autologous stem cell transplantation for rheumatoid arthritis--interim report of 6 patients. J Rheumatol Suppl. 2001;64:21-24.

43. Kueh HY, Champhekar A, Champhekhar A, Nutt SL, Elowitz MB, Rothenberg EV. Positive feedback between PU.1 and the cell cycle controls myeloid differentiation. Science. 2013;341(6146):670-673.

44. Staber PB, Zhang P, Ye M, Welner RS, et al. Sustained PU.1 levels balance cell-cycle regulators to prevent exhaustion of adult hematopoietic stem cells. Mol Cell. 2013;49(5):934-946.

45. Sun J, Ramos A, Chapman B, Johnnidis JB, Le L, Ho Y-J, et al. Clonal dynamics of native haematopoiesis. Nature. 2014;514(7522):322-327.

46. Colmegna I, Diaz-Borjon A, Fujii H, Schaefer L, Goronzy JJ, Weyand CM. Defective proliferative capacity and accelerated telomeric loss of hematopoietic progenitor cells in rheumatoid arthritis. Arthritis Rheum. 2008;58(4):990-1000.

47. Foudi A, Hochedlinger K, Van Buren D, et al. Analysis of histone 2B-GFP retention reveals slowly cycling hematopoietic stem cells. Nat Biotechnol. 2008;27(1):84-90.

48. Wu T-C, Xu K, Martinek J, et al. IL1 receptor antagonist controls transcriptional signature of inflammation in patients with metastatic breast cancer. Cancer Res. 2018;78(18):5243-5258.

49. Brennan FM, Mcinnes IB. Evidence that cytokines play a role in rheumatoid arthritis. J Clin Invest. 2008;118(11):3537-3545.

50. Ridker PM, MacFadyen JG, Thuren T, et al. Effect of interleukin-1 inhibition with canakinumab on incident lung cancer in patients with atherosclerosis: exploratory results from a randomised, double-blind, placebo-controlled trial. Lancet. 2017;390(10105):1833-1842.

CRISPR/Cas9-mediated *ELANE* knockout enables neutrophilic maturation of primary hematopoietic stem and progenitor cells and induced pluripotent stem cells of severe congenital neutropenia patients

Masoud Nasri,[1] Malte Ritter,[1*] Perihan Mir,[1*] Benjamin Dannenmann,[1*] Narges Aghaallaei,[1] Diana Amend,[1] Vahagn Makaryan,[2] Yun Xu,[1] Breanna Fletcher,[2] Regine Bernhard,[1] Ingeborg Steiert,[1] Karin Hähnel,[1] Jürgen Berger,[3] Iris Koch,[3] Brigitte Sailer,[3] Katharina Hipp,[3] Cornelia Zeidler,[4] Maksim Klimiankou,[1] Baubak Bajoghli,[1] David C. Dale,[2] Karl Welte[1,5,§] and Julia Skokowa[1,§]

[1]Department of Oncology, Hematology, Immunology, Rheumatology and Clinical Immunology, University Hospital Tübingen, Tübingen, Germany; [2]Department of Medicine, University of Washington, Seattle, WA, USA; [3]Max Planck Institute for Developmental Biology, Tübingen, Germany; [4]Department of Oncology, Hematology, Immunology and Bone Marrow Transplantation, Hannover Medical School, Hannover, Germany and [5]University Children's Hospital Tübingen, Tübingen, Germany

*MR, PM and BD are co-second authors.

§KW and JS are co-senior authors.

ABSTRACT

Autosomal-dominant *ELANE* mutations are the most common cause of severe congenital neutropenia. Although the majority of congenital neutropenia patients respond to daily granulocyte colony stimulating factor, approximately 15 % do not respond to this cytokine at doses up to 50 μg/kg/day and approximately 15 % of patients will develop myelodysplasia or acute myeloid leukemia. "Maturation arrest," the failure of the marrow myeloid progenitors to form mature neutrophils, is a consistent feature of *ELANE* associated congenital neutropenia. As mutant neutrophil elastase is the cause of this abnormality, we hypothesized that *ELANE* associated neutropenia could be treated and "maturation arrest" corrected by a CRISPR/Cas9-sgRNA ribonucleoprotein mediated *ELANE* knockout. To examine this hypothesis, we used induced pluripotent stem cells from two congenital neutropenia patients and primary hematopoietic stem and progenitor cells from four congenital neutropenia patients harboring *ELANE* mutations as well as HL60 cells expressing mutant *ELANE*. We observed that granulocytic differentiation of *ELANE* knockout induced pluripotent stem cells and primary hematopoietic stem and progenitor cells were comparable to healthy individuals. Phagocytic functions, ROS production, and chemotaxis of the *ELANE* KO (knockout) neutrophils were also normal. Knockdown of *ELANE* in the mutant *ELANE* expressing HL60 cells also allowed full maturation and formation of abundant neutrophils. These observations suggest that *ex vivo* CRISPR/Cas9 RNP based *ELANE* knockout of patients' primary hematopoietic stem and progenitor cells followed by autologous transplantation may be an alternative therapy for congenital neutropenia.

Introduction

Autosomal dominant *ELANE* mutations encoding neutrophil elastase (NE) are the most common cause of severe congenital neutropenia (CN), an inherited bone marrow failure syndrome.[1-3] Patients with CN suffer from severe life-threatening bacterial infections starting early after birth due to the absence or very low numbers of neutrophils in the peripheral blood (usually less than 500 cells per μL[3]).

Hematopoietic stem and progenitor cells (HSPC) of CN patients fail to differentiate into mature neutrophils. This differentiation defect can be partially restored with daily or alternate-day subcutaneous injections of recombinant human granulocyte colony stimulating factor (rhG-CSF) in supra-physiological concentrations.[4] Although rhG-CSF therapy improves the life expectancy and quality of life of CN patients, a subgroup does not respond to rhG-CSF. Additionally, about 15 % of CN patients developed myelodysplastic syndrome (MDS) or acute myeloid leukemia (AML) till now.[3] There is a positive correlation between a rhG-CSF dose required to achieve acceptable neutrophil counts and a cumulative incidence to develop MDS or AML in CN patients.[5] Therefore, CN patients, especially patients who either require high rhG-CSF dosages (above 50 μg/kg/day) and those who do not respond at all, need alternative therapeutic options. Hematopoietic stem cell transplantation (HSCT) would be a treatment of choice in CN patients, but it is associated with many adverse events, *e.g.* acute or chronic graft-*versus*-host-disease (GvHD), life-threatening infections, graft failure or graft rejection. Indeed, the overall survival of CN patients after HSCT is approximately 80 % only.

Recently established new technologies of CRISPR/Cas9-mediated gene editing in mammalian cells[6,7] offer novel therapeutic options, especially for inherited monogenic disorders, including *ELANE* mutations associated CN. In this case, CRISPR/Cas9-mediated gene correction or knockout of the mutant gene in patient`s HSPC *ex vivo* followed by autologous transplantation of the corrected HSPC might be a better treatment than high dose rhG-CSF or allogeneic stem cell transplantation.

ELANE mutations induce unfolded protein response (UPR) and endoplasmic reticulum (ER) stress in HSPC of CN patients that leads to increased apoptosis and defective granulocytic differentiation.[8-11] Therefore, inactivation of *ELANE* using CRISPR/Cas9-mediated knockout may abrogate UPR and ER stress caused by mutated *ELANE* with subsequent restoration of granulocytic differentiation. In support of this hypothesis, we recently identified a β-lactam-based inhibitor of human neutrophil elastase (NE), MK0339, which restored defective granulocytic differentiation of induced pluripotent stem cells (iPSC) and HL60 cells expressing mutated NE.[12] In addition, a recent report by Nayak *et al*. demonstrated the restoration of the *in vitro* granulopoiesis of *ELANE*-CN patient-derived iPSC upon treatment with Sivelestat, another NE-specific small-molecule inhibitor.[12,13] Moreover, the fact that individuals showing mosaicism of inherited *ELANE* mutations have a higher proportion of *ELANE* mutated mature neutrophils hematopoietic cells in the bone marrow than in the blood[14,15] supports the hypothesis that inactivation of *ELANE* mutations will improve neutrophil differentiation.

Another possibility to correct the disease phenotype is the direct correction of the specific gene mutation by the activation of homology-directed repair (HDR) of the mutated gene allele after cutting by CRISPR/Cas9 and co-transfection with a repair template. Most CN patients harbor inherited autosomal dominant missense or frameshift *ELANE* mutations that are distributed throughout all five exons and two introns.[16] Therefore, CRISPR/Cas9-mediated correction of *ELANE* mutations would need to be patient/mutation specific. Since mutated *ELANE* may induce UPR and ER stress in edited cells, the introduction of new indels in the *ELANE* gene during the process of

CRISPR/Cas9 based editing may be not beneficial for the integrity of the hematopoietic stem cell (HSC) pool.

The first pre-clinical CRISPR/Cas9-based gene therapy study of common inherited blood disorders, sickle cell disease, and β-thalassemia, was reported.[17,18] In these settings, the β-globin gene locus was inactivated by the introduction of deletions in autologous HSPC by CRISPR/Cas9-mediated gene editing. This was done to mimic the hereditary persistence of fetal hemoglobin mutations in HSC.[17,18]

Here, we describe a CRISPR/Cas9 mediated *ELANE* KO by electroporation of HSPC and iPSC with *ELANE* specific CRISPR/Cas9-sgRNA ribonucleoprotein (RNP) complexes. *ELANE* KO induces granulocytic differentiation of HSPC and iPSC of CN patients harboring *ELANE* mutations without affecting their phagocytic functions. These results suggest that it may be possible to use CRISPR/Cas9 based *ELANE* KO in autologous HSCT as a therapy for *ELANE* associated neutropenia.

Methods

Patients

Three healthy donors and five severe congenital neutropenia patients harboring *ELANE* mutations (*ELANE*-CN) were used in the study. Bone marrow and peripheral blood samples from patients were collected in association with an annual follow-up recommended by the Severe Chronic Neutropenia International Registry. Study approval was obtained from the Ethical Review Board of the Medical Faculty, University of Tübingen. Informed written consent was obtained from all participants of this study.

Cell culture

Human CD34+ HSPC were isolated from bone marrow mononuclear cell fraction using Ficoll gradient centrifugation followed by magnetic bead separation using Human CD34 Progenitor Cell Isolation Kit, (Miltenyi Biotech, #130-046-703). CD34+ cells were cultured in a density of 2 x 10^5 cells/mL in Stemline II Hematopoietic Stem Cell Expansion medium (Sigma Aldrich, #50192) supplemented with 10 % FBS, 1 % penicillin/streptomycin, 1 % L-Glutamine and a cytokine cocktail consisting of 20 ng/mL IL-3, 20 ng/mL IL-6, 20 ng/mL TPO, 50 ng/ml SCF and 50 ng/mL FLT-3L (all cytokines were purchased from R&D Systems). Human induced pluripotent stem cells (iPSC) were cultured on Geltrex LDEV-free reduced growth factor basement membrane matrix (Thermo Fisher Scientific, #A1413201) coated plates in a density of 2 x 10^5 cells/mL in StemFlex medium (Thermo Fisher Scientific, #A3349401) supplemented with 1 % penicillin/streptomycin. HL60 cells were maintained in RPMI-1640 supplemented with 10 % fetal bovine serum (FBS) (Gemini Bio Products, West Sacramento, CA, USA), 2 mM L-glutamine, and 1 % penicillin/streptomycin (Thermo Fisher Scientific) at 37°C and 5 % CO2.

Design of the *ELANE*-specific guide RNA (gRNA)

Specific CRISPR-RNA (crRNA) for the knockout of the ELANE gene (cut site: chr19 [CTGCGCGGAGGC-CACTTCTG, +852,969 : -852,969], NM_001972.3 Exon 2, 161 bp; NP_001963.1 p.F54) was designed using the CCTop website.[19]

CRISPR/Cas9-gRNA RNP mediated *ELANE* KO in iPSC and HSPC

Electroporation was carried out using the Amaxa nucleofection system (P3 primary kit, #V4XP-3024) according to the manufacturer's instructions. 1x10⁶ human iPSC or CD34⁺ HSPC were electroporated with assembled gRNA (8 μg) and Cas9 (15 μg) protein (Integrated DNA Technologies).

Isolation of single cell iPSC clones

8 x 10³ human iPSC were plated on Geltrex-coated 10-cm dish in StemFlex medium (Thermo Fisher Scientific, #A3349401) and RevitaCell supplement (Thermo Fisher Scientific, #A2644501). The medium was changed every 24 hours without RevitaCell supplement. On day 7, single iPSC colonies were picked and transferred to the Geltrex-coated 96-well plates (one clone/well).

Colony Forming Unit (CFU) assay

CD34⁺ cells were resuspended in IMDM supplemented with 2 % FBS (Stemcell Technologies, #07700) and enriched Methocult (Stemcell Technologies, #H4435). The cell suspension was plated on 3.5 cm dishes (3x10³ cells/dish) for 14 days.

In vitro phagocytosis assay

Cells were incubated with or without fluorescein-conjugated *Staphylococcus aureus* BioParticles (Invitrogen, #S2851) at a ratio of 100 particles per cell for two hours at 37°C, washed twice with PBS/ 2 % BSA, resuspended in 300 μL FACS buffer and analyzed by flow cytometry.

Statistical analysis

Differences in mean values between groups were analyzed using two-sided, unpaired Student's *t*-tests using GraphPad Prism software.

Additional Material and Methods are available in the *Online Supplementary Material and Methods*.

Results

Inhibition of *ELANE* expression restored defective granulocytic differentiation of HL60 cell lines expressing endogenous *ELANE* mutations

We created CRISPR/Cas9 edited mutant *ELANE* knock-in HL60 human promyelocytic cell lines expressing either p.P139L or p.C151Y *ELANE* mutations. All-trans retinoic acid (ATRA) induced differentiation of wild-type and
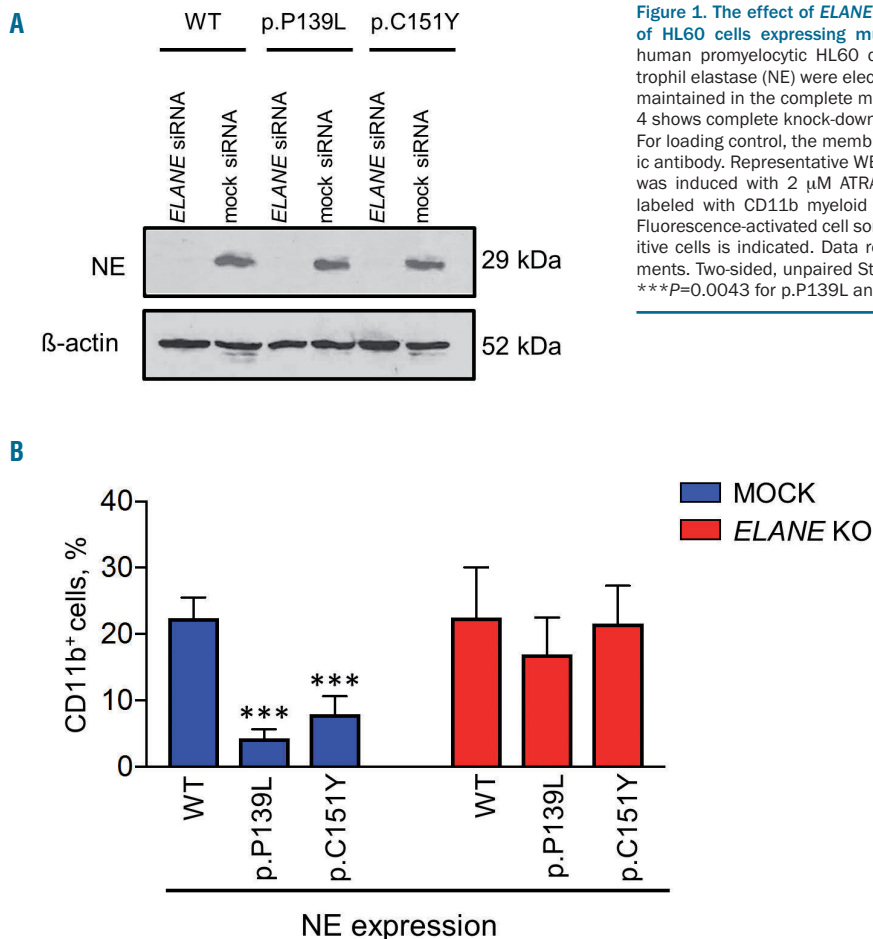
Figure 1. The effect of *ELANE* knock-down on the impaired myeloid differentiation of HL60 cells expressing mutant neutrophil elastase. (A) CRISPR/Cas9 edited human promyelocytic HL60 cells expressing p.P139L and p.C151Y mutant neutrophil elastase (NE) were electroporated with scrambled and anti-*ELANE* siRNA and maintained in the complete medium for five days. Western blot (WB) analysis at day 4 shows complete knock-down of NE detected with an anti-NE monoclonal antibody. For loading control, the membrane was stripped and re-probed with a β-actin-specific antibody. Representative WB membranes are depicted. (B) Myeloid differentiation was induced with 2 μM ATRA (all-trans retinoic acid). After five days, cells were labeled with CD11b myeloid differentiation surface marker and examined using Fluorescence-activated cell sorting (FACS) analysis. The proportion of CD11b-PE positive cells is indicated. Data represent means ± SD from four independent experiments. Two-sided, unpaired Student's *t*-test *P*-values are shown, ***P<0.0001 and ***P=0.0043 for p.P139L and p.C151Y respectively compared to wild-type (WT).

mutant HL60 clones revealed a typical impairment of granulocytic differentiation capacities in both mutant cell lines, as assessed by the significantly lower proportion of cells expressing CD11b granulocytic differentiation marker in p.P139L and p.C151Y mutant cell lines compared to the wild-type ($P<0.0001$ and $P=0.00043$, respectively) on day 5 of differentiation (Figure 1A-B and *Online Supplementary Figure S1A-C*). These findings are consistent with *ELANE* associated neutropenia patients phenotype.

As a proof-of-principle experiment, we have used RNA interference (RNAi) technology to knock down the expression of the *ELANE* gene in these cell lines. Thereby, we investigated the biological effects of inhibition of mutant NE on the granulocytic differentiation. Indeed, transfection of commercially available siRNA against the exon 4 of *ELANE*, completely knocked down the expression of NE in all cell lines. Production of CD11b positive cells was significantly restored in both mutant cell lines ($P=0.00041$ for p.P139L and $P=0.00048$ for p.C151Y), but not in wild-type cells (Figure 1A-B and *Online Supplementary Figure S1A-C*).

Design and validation of sgRNA targeting *ELANE*

We further generated guide RNA (gRNA) specifically targeting exon 2 of *ELANE* by annealing CRISPR-RNA (crRNA) with trans-activating crRNA (tracrRNA). gRNA was incubated with recombinant Cas9 protein to generate CRISPR/Cas9-gRNA RNP complexes. The gRNA targeting exon 2 of *ELANE* (cut site: chr19[+852.969:-852.969], Figure 2A) was selected to introduce stop-codon mutations and to induce nonsense-mediated mRNA decay (NMD) of *ELANE* mRNA, which is caused by stop-codon or frameshift mutations at the beginning of *ELANE* mRNA. Based on our experimental analysis, the selected gRNA has high on-target activity with low off-target score (*data not shown*). To evaluate inhibition of NE expression by CRISPR/Cas9 RNP mediated targeting of exon 2 of *ELANE*, we generated an *ELANE* KO myeloid cell line
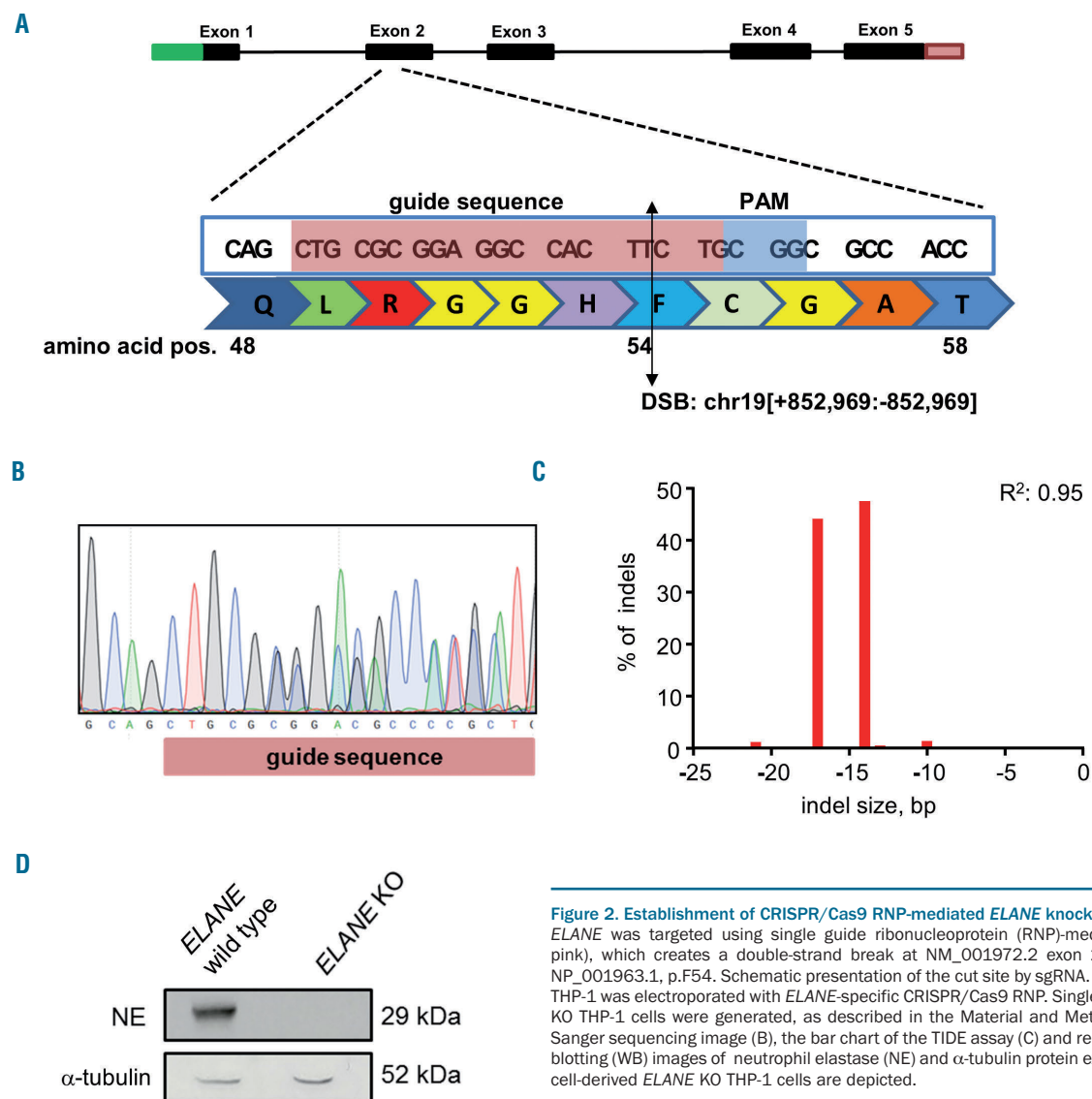
Figure 2. Establishment of CRISPR/Cas9 RNP-mediated *ELANE* knockout in THP-1 cells. (A) *ELANE* was targeted using single guide ribonucleoprotein (RNP)-mediated (highlighted in pink), which creates a double-strand break at NM_001972.2 exon 2, 161 bp after ATG; NP_001963.1, p.F54. Schematic presentation of the cut site by sgRNA. (B-D) Myeloid cell line THP-1 was electroporated with *ELANE*-specific CRISPR/Cas9 RNP. Single cell clones of *ELANE* KO THP-1 cells were generated, as described in the Material and Methods. Representative Sanger sequencing image (B), the bar chart of the TIDE assay (C) and representative Western blotting (WB) images of neutrophil elastase (NE) and α-tubulin protein expression (D) in single cell-derived *ELANE* KO THP-1 cells are depicted.
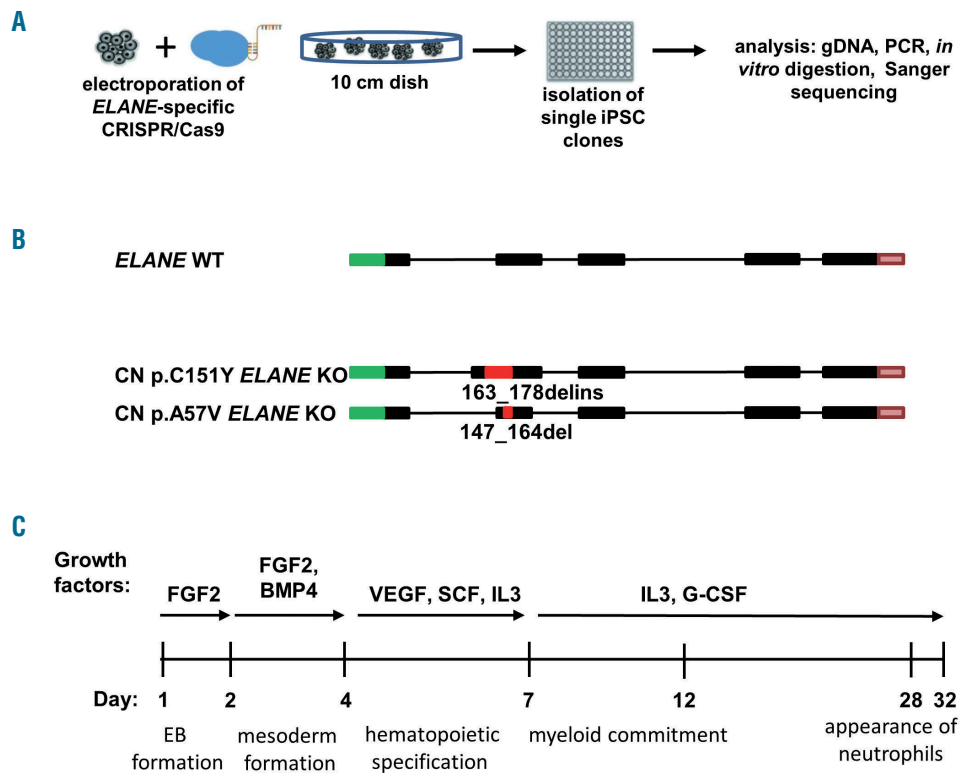
Figure 3. Generation of *ELANE* KO CN iPSC clones. (A) Scheme of the *ELANE*-specific CRISPR/Cas9-gRNA ribonucleoprotein electroporation of induced pluripotent stem cells (iPSC) and generation of *ELANE* KO iPSC clones. Generation of single *ELANE* knockout iPSC clones was made by seeding single iPSC, subsequent picking of each clone and transferring them into 96 well plates. Screening of each iPSC clone was done by Cas9 *in vitro* digestion and Sanger sequencing. (B) Scheme of CRISPR/Cas9 introduced modifications in the *ELANE* gene in iPSC clones of congenital neutropenia (CN) patients. Red inserts show positions of indels in *ELANE* mRNA (NM_001972.2) and numbers refer to bp position after ATG. (C) Scheme of the EB-based hematopoietic/neutrophilic differentiation of iPSC.

THP-1, which has high basal expression levels of *ELANE* and NE. The efficiency of *ELANE* knockout in the total population of edited THP-1 cells was 77 %, as assessed by Sanger sequencing and tracking of indels by decomposition (TIDE) analysis (*data not shown*). The pure *ELANE* KO THP-1 cell clone has compound heterozygosity of 14 and 17 bp deletions on each allele (Figure 2B-C). The NE expression was completely absent in the pure *ELANE* KO THP-1 cell clone, as determined by Western blotting (WB) using anti-NE antibody against the C-terminus of NE protein (Figure 2D, *Online Supplementary Figure S2A-B*). These data suggest that sgRNA targeting *ELANE* that we designed led to a complete loss of NE protein.

Restoration of the *in vitro* granulocytic differentiation in *ELANE*-CN iPSC clones after *ELANE* knockout

We generated iPSC from peripheral blood mononuclear cells (PB MNC) of two *ELANE*-CN patients, harboring *ELANE* mutations p.C151Y or p.A57V (CN p.C151Y iPSC and CN p.A57V iPSC, respectively). Additionally, iPSC of one healthy control (healthy ctrl iPSC) were evaluated. All three iPSC lines expressed elevated mRNA and protein levels of pluripotent stem cell-specific factors, displayed alkaline phosphatase activity and expression of pluripotent embryonic stem cell surface markers (*Online Supplementary Figure 3A-C*).

Next, we used electroporation of iPSC clones with *ELANE*-specific CRISPR/Cas9-sgRNA RNP to generate pure *ELANE* KO CN iPSC clones. For this, electroporated iPSC were seeded on a geltrex coated culture dish and single-cell derived iPSC clones were isolated transferred to geltrex coated 96 well-plates for the subsequent selection of *ELANE* knockout clones (Figure 3A). Confirmed *ELANE* knockout iPSC clones have followed *ELANE* modifica-

tions: 274 bp del/ins in CN p.C151Y *ELANE* KO iPSC, and 17 bp del in CN p.A57V *ELANE* KO iPSC (Figure 3B). The editing efficiency of healthy ctrl iPSC was 97 % (*Online Supplementary Figure S4A*), therefore, we used the total population of gene-edited healthy control (ctrl) iPSC for further analysis. We did not detect any off-target activity of the gRNA for the selected cDNA sites in all studied iPSC, as assessed using Sanger sequencing (*Online Supplementary Figure S4B* and *Tables S1, S2*).

Applying a slightly modified *in vitro* embryoid body (EB)-based iPSC differentiation method that allows generation of hematopoietic cells and mature myeloid cells for approximately 30 days,[22,23] we found an increase in the percentage of CD15+CD16+CD45+ granulocytes in *ELANE* KO CN-iPSC cell culture, as compared to CN-iPSC. The generation of granulocytes from *ELANE* KO CN-iPSC was comparable to iPSC generated from a healthy donor (Figure 3C, 4A, and *Online Supplementary Figure S5A*). Generation of immature hematopoietic cells (CD34+KDR+, CD34+CD43+, CD45−CD235+CD41a+ and CD45+CD34+ cells) and CD45+CD33+ myeloid progenitor cells in *ELANE* KO CN- and CN-iPSC lines were similar or increased, in comparison to corresponding MOCK treated iPSC lines (*Online Supplementary Figure S6A*).

A CFU assay was performed with *ELANE*-/- iPSC-derived CD34+ cells from CN patients and showed elevated levels of CFU-G but reduced CFU-M colony numbers, as compared to CD34+ cells derived from MOCK treated CN iPSC clones (Figure 4C). These data suggest that *ELANE* knockout restores granulocytic differentiation in CN.

We did not observe any significant defects in *in vitro* granulocytic differentiation of *ELANE* KO iPSC generated from a healthy donor, as compared to MOCK treated cells (Figure 4A-C, *Online Supplementary Figures S5 and S6*).

ELANE knockout in HSPC of *ELANE*-CN patients restores diminished granulocytic differentiation

To further evaluate the clinical applicability of *ELANE* KO as a treatment option of *ELANE*-associated CN, we performed CRISPR/Cas9 RNP-mediated gene editing in primary bone marrow CD34⁺ HSPC of four *ELANE*-CN patients (Table 1) and three healthy donors and differentiated the cells towards neutrophils. *ELANE* knockout in CD34⁺HSPC was performed by electroporation of human CD34⁺ HSPC with assembled *ELANE* specific sgRNA and Cas9 protein (Figure 5A). The editing efficiency varied between 27 % and 94 % (Figure 5B, *Online Supplementary Figure S7*). As expected, NE levels in neutrophils differentiated from the total population of edited cells were markedly reduced (Figure 5C-D, *Online Supplementary Figure S8A-B*). Moreover, *ELANE* KO leads to elevated granulocytic differentiation, as assessed by the percentage of CD15⁺CD11b⁺CD45⁺ cells (Figure 6A, *Online Supplementary Figure S9A-B*) and morphological examination of cytospin preparations of mature granulocytes generated on day 14 of the *in vitro* granulocytic differentiation using liquid culture (Figure 6B). At the same time, the ratio of *ELANE* KO cells increased from day 7 to day 14 of differentiation (Figure 5B). Simultaneously, the percentage of CD34⁺CD45⁺ cells was reduced in *ELANE* KO cells of CN patients, but not in healthy donor cells (*Online Supplementary Figure S10A*). In one patient (CN I120F), no difference in the percentage of CD15⁺CD11b⁺CD45⁺ cells between MOCK and *ELANE* KO samples was observed, but a clear improvement of granulocytic differentiation was detected in cytospin slides. This finding may be explained by relative mild neutropenia (*Online Supplementary Table 3*) and possible expression of CD15 in not fully mature myeloid cells in this patient.

Scanning and transmission electron microscopy revealed that *ELANE* KO cells of both healthy control and one CN patient showed no significant differences in morphology or intracellular structures, compared with MOCK cells of a healthy donor (Figure 6C-D).

Altogether, these data suggest that *ELANE* KO cells have a differentiation advantage over the HSPC carrying mutated *ELANE*.

Neutrophils generated from *ELANE* KO HSPC exhibited unaffected ROS production, phagocytosis and chemotaxis upon activation *in vitro*

We further evaluated *in vitro* activation of neutrophils generated from *ELANE* KO HSPCs in liquid culture for 14 days. We first performed an assessment of H_2O_2 levels (ROS) in fMLP-activated *ELANE* KO neutrophils generated from a healthy donor. We detected no differences between *ELANE* WT and *ELANE* KO neutrophils (Figure 7A).

Phagocytosis was evaluated by incubation of cells with fluorescein-conjugated *Staphylococcus aureus* BioParticles for two hours. Percentage of GFP⁺ granulocytes that engulfed bacteria were assessed by FACS using gating on granulocyte population in the dot plot of forward-scatter light (FSC) *versus* side-scatter light (SSC) channels. We did not detect any significant differences in phagocytosis of *ELANE* KO neutrophilic granulocytes, as compared to control MOCK cells (Figure 7B). As an independent evaluation of phagocytosis kinetics, we performed live cell imaging of neutrophils incubated with pHrodo Green *E. coli* Bioparticles Conjugate using IncuCyte ZOOM system and observed similar phagocytosis behavior of

MOCK and *ELANE* KO neutrophils generated from a healthy donor or one CN patient (Figure 7C).

Chemotactic activity of fMLP-treated neutrophils was also comparable between MOCK and *ELANE* KO groups (Figure 7D).
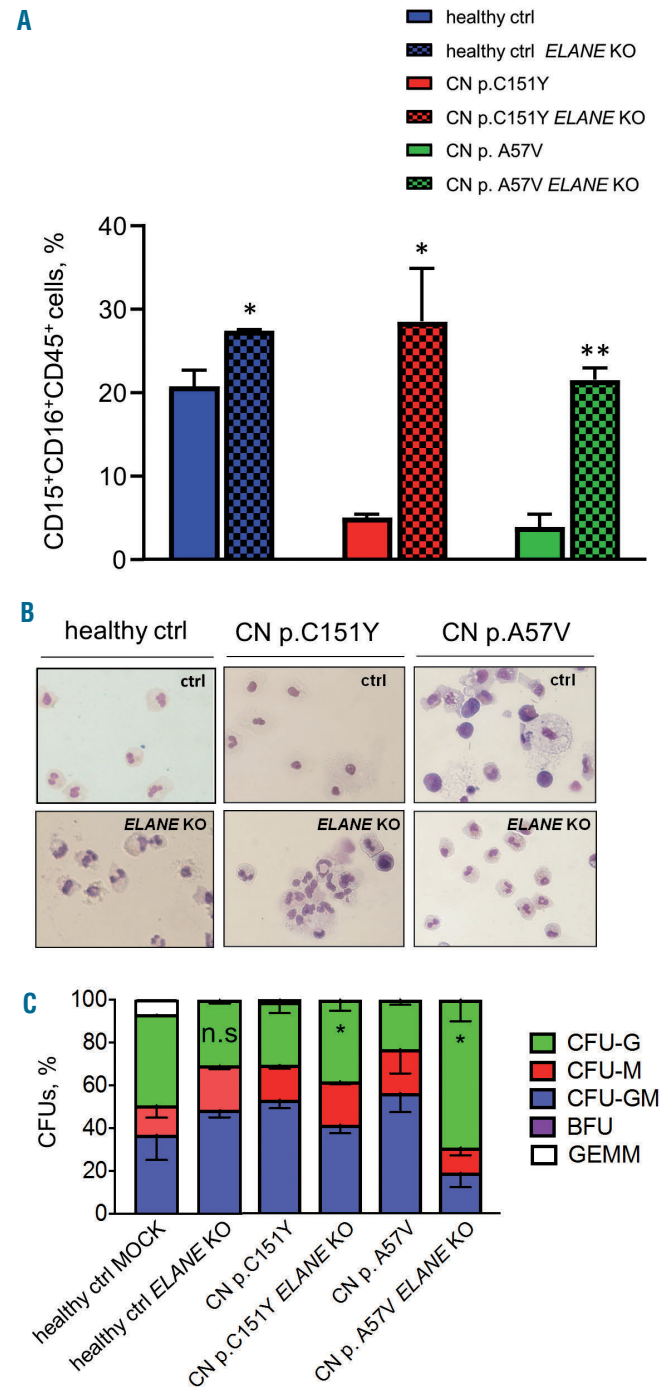
Figure 4. *ELANE* knockout restored granulocytic differentiation of *ELANE*-CN iPSC. (A) Flow cytometry analysis of suspension cells harvested from embryoid body (EB)-based granulocytic cell culture of respective iPSC clones on day 28 or 32 of differentiation. Data represent means ± standard deviation (SD) from two independent experiments. *P<0.05, **P<0.01. (B) Wright-Giemsa staining of cytospin preparations of suspension myeloid cells harvested from iPSC culture at day 28 or 32 of differentiation. Representative images are depicted. (C) Colony-forming unit (CFU) assay of CD34⁺ cells harvested from EB-based iPSC culture on day 14 of differentiation. Data represent means ± SD from two independent experiments. *P<0.05.

Unaffected phagocytic activity of *ELANE* KO PMN in zebrafish embryos

To evaluate the phagocytic activity of *ELANE* KO PMN *in vivo*, we transplanted fluorescently labeled polymorphonuclear leukocytes (PMN) generated from *ELANE* KO HD into zebrafish embryos (Figure 8A). PMN were injected into the duct of Cuvier, a wide circulation channel on the yolk sac connecting the heart to the trunk vasculature. Subsequently, Alexa-594-conjugated *Staphylococcus aureus* BioParticles were injected locally in the tail fin close to the caudal vein. Live imaging showed that human neutrophils migrated into the caudal hematopoietic tissue (CHT), which is equivalent to the fetal liver in mammals and provides a human-compatible environment.[24,25] Confocal imaging of this region revealed that most of the *ELANE* KO neutrophils were found inside the perivascular pocket (Figure 8B) and many of them have engulfed bacteria (white arrows in Figure 8B and 8C, *Online Supplementary Movie S1*). Time-lapse *in vivo* imaging of the xenotrans-

planted embryos also revealed that human *ELANE* KO PMN have the capability to form surface protrusion within the perivascular region (Figure 8D, *Online Supplementary Movie S2*). We could not detect a difference between transplanted human *ELANE* KO and control MOCK PMN in zebrafish embryos (*data not shown*). These observations indicate that human *ELANE* KO PMN are able to migrate and phagocyte *in vivo*.

ELANE KO restores deregulated expression of UPR gene BiP and anti-apoptotic factor Bcl-xl in *ELANE* KO iPSC derived cells of CN patients

We further evaluated the effects of *ELANE* KO on the expression of UPR gene BiP and anti-apoptotic factor Bcl-xl (*Online Supplementary Figure S11*). We analyzed pure *ELANE* KO HSPC (for Bcl-xl) or neutrophils (for BiP) generated from iPSC of two CN patients. We found that *ELANE* KO HSPC express elevated mRNA levels of Bcl-xl and BiP expression was markedly reduced in *ELANE* KO

A
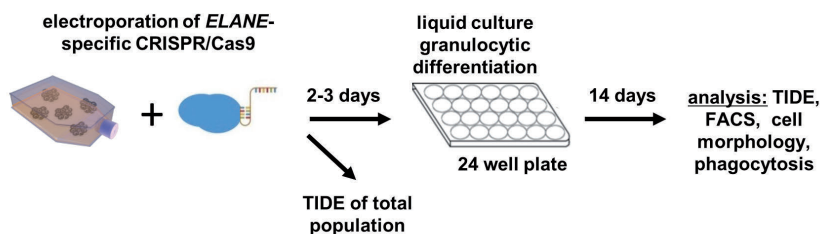
B

Sample, *ELANE* mutation position	Exon	Indel Efficiency, %	
		day 7	day 14
healthy ctrl 1	-	71	69
healthy ctrl 2	-	57	46
healthy ctrl 3	-	86	94
CN p.A57V	Exon 2	52	63
CN p.I120F	Exon 3	81	90
CN p.S126L	Exon 4	45	57
CN p.C223AfsX17	Exon 5	27	37

C

D
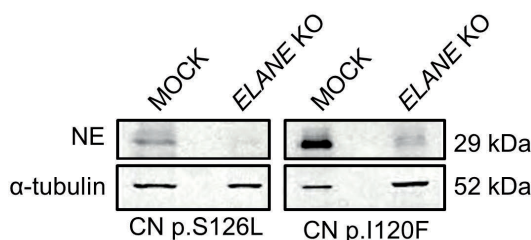
Figure 5. Efficient CRISPR/Cas9 RNP-based *ELANE* knockout in HSPC. (A) Scheme of the generation of *ELANE* KO HSPC using electroporation with *ELANE*-specific CRISPR/Cas9-gRNA ribonucleoprotein (RNP). (B) TIDE results of edited CD34⁺ HSPC at day 7 and 14 of liquid culture differentiation. (C and D) Hematopoietic stem and progenitor cells (HSPC) of healthy controls (C), or two CN patients (D) were electroporated with *ELANE*-specific CRISPR/Cas9 RNP, on day 14 of culture, cells were lysed in Laemmli buffer and Western blotting (WB) analysis using anti-neutrophil elastase (NE) antibody against C-terminus of NE was performed, staining with α-tubulin antibody was used as loading control. Representative WB images of cells from two independent experiments are depicted.

PMN, compared to cells carrying mutated *ELANE*. As expected, *ELANE* mRNA levels were severely diminished in *ELANE* KO cells (*Online Supplementary Figure S11*).

Discussion

The majority of patients suffering from congenital neutropenia respond well to daily treatment with rhG-CSF leading to a normal quality of life. However, in the last 25 years, we learned that CN is a preleukemic syndrome and that approximately 15 % of patients do not respond to even ultra-high dosages (>50 µg/kg/d) of rhG-CSF. Therefore, we are searching for other treatment modalities for CN patients that may prevent leukemic transformation and may be useful for those who are requiring high dosages of rhG-CSF or not responding at all to rhG-CSF. For these patients, the only available treatment is stem cell transplantation with the risk of transplant-associated adverse events such as acute or chronic GvHD.

In the present study, we described for the first time the establishment of an *in vitro* cellular model of CRISPR/Cas9 mediated gene therapy of CN associated with autosomal dominant *ELANE* mutations, the most frequent cause of
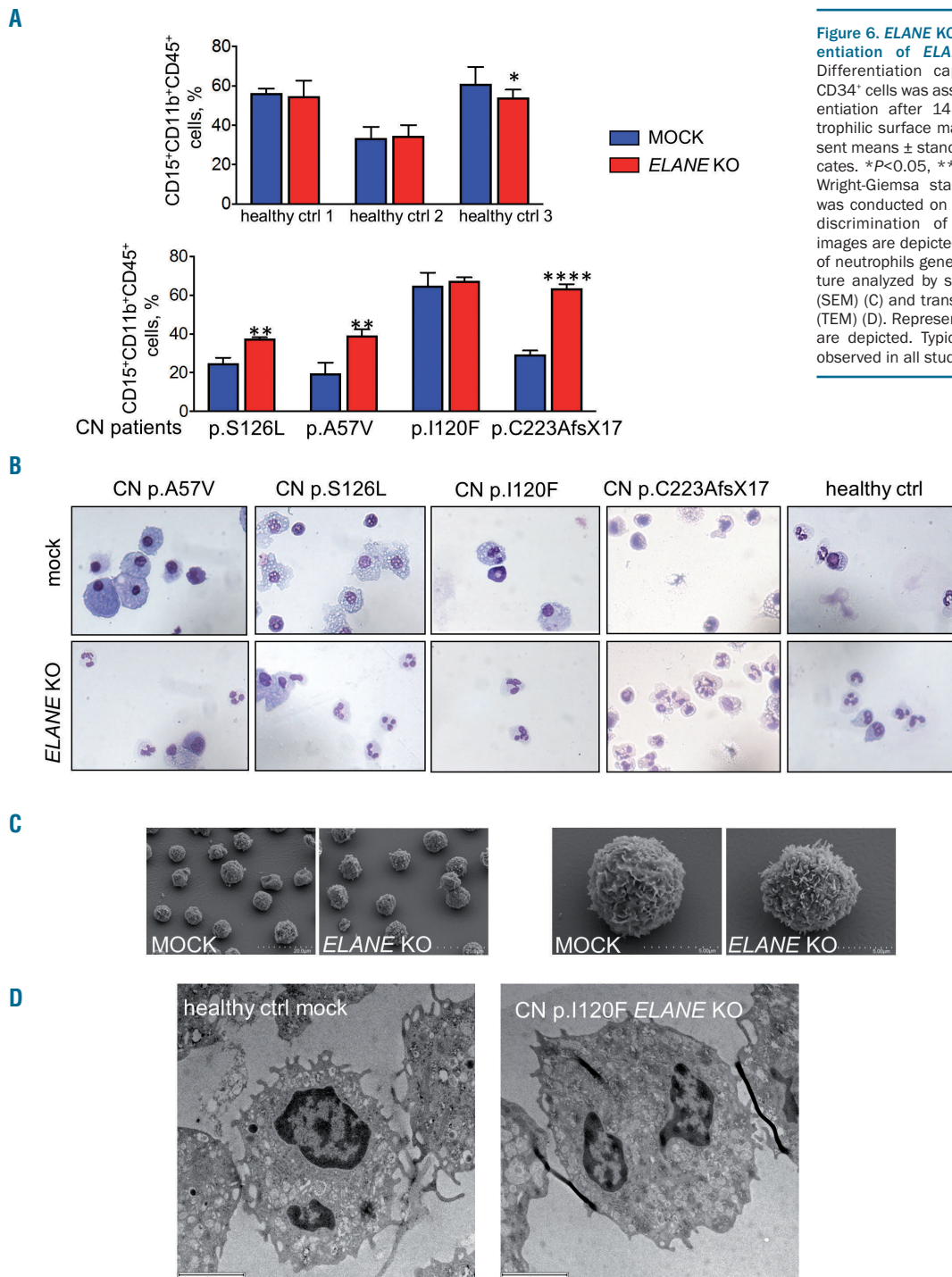
Figure 6. *ELANE* KO restored granulocytic differentiation of *ELANE*-CN primary HSPC. (A) Differentiation capacity of *ELANE* knockout CD34+ cells was assessed by liquid culture differentiation after 14 days by investigating neutrophilic surface marker expression. Data represent means ± standard deviation (SD) from triplicates. *$P<0.05$, **$P<0.01$, ****$P<0.0001$. (B) Wright-Giemsa staining of differentiated cells was conducted on day 14 allowing morphologic discrimination of the cells. Representative images are depicted. (C-D) Electron micrographs of neutrophils generated on day 14 of liquid culture analyzed by scanning electron microscopy (SEM) (C) and transmission electron microscopy (TEM) (D). Representative SEM and TEM images are depicted. Typical neutrophil morphology is observed in all studied samples.

CN. We tested *ex vivo* CRISPR/Cas9 RNP-based *ELANE* knockout in HSPC of CN patients that may be used for autologous transplantation as a therapeutic approach for *ELANE*-CN patients. Virus- and DNA-free application of CRISPR/Cas9 RNP markedly increases gene editing efficiency and simultaneously decreases the probability and frequency of off-target effects, because CRISPR/Cas9 RNP activity is preserved in cells for only approximately 48 hours. We recently reported the establishment of the fluorescent labeling of CRISPR/Cas9 RNP complexes for gene editing of primary hematopoietic stem cells and subsequent sorting of gene-modified cells for further applications.[26] Implementation of this method will improve the efficiency of gene knockout or gene correction in HSPC, including *ELANE* knockout or correction of *ELANE* mutations.

In case of *ELANE* KO, different combinations of the *ELANE* gene editing are expected: we may generate unedited, monoallelic edited (of mutated or WT allele), or bi-allelic edited HSPC. Since we did not use any selection marker for edited HSPC, we were not able to estimate the proportion of HSPC with inactivation of the mutated *ELANE* allele. The fact that the proportion of *ELANE* KO cells was elevated upon granulocytic differentiation strongly argues for the differentiation advantage of the edited cells lacking *ELANE* (including loss of the mutated allele).

There are several potential unforeseen consequences of the *ELANE* gene knockout strategy. For example, Tidwell *et al.* reported the presence of two in-frame ATG codons in exon 2 and exon 4 of *ELANE*.[27] They showed that the internal translation of NE can be initiated when the canon-
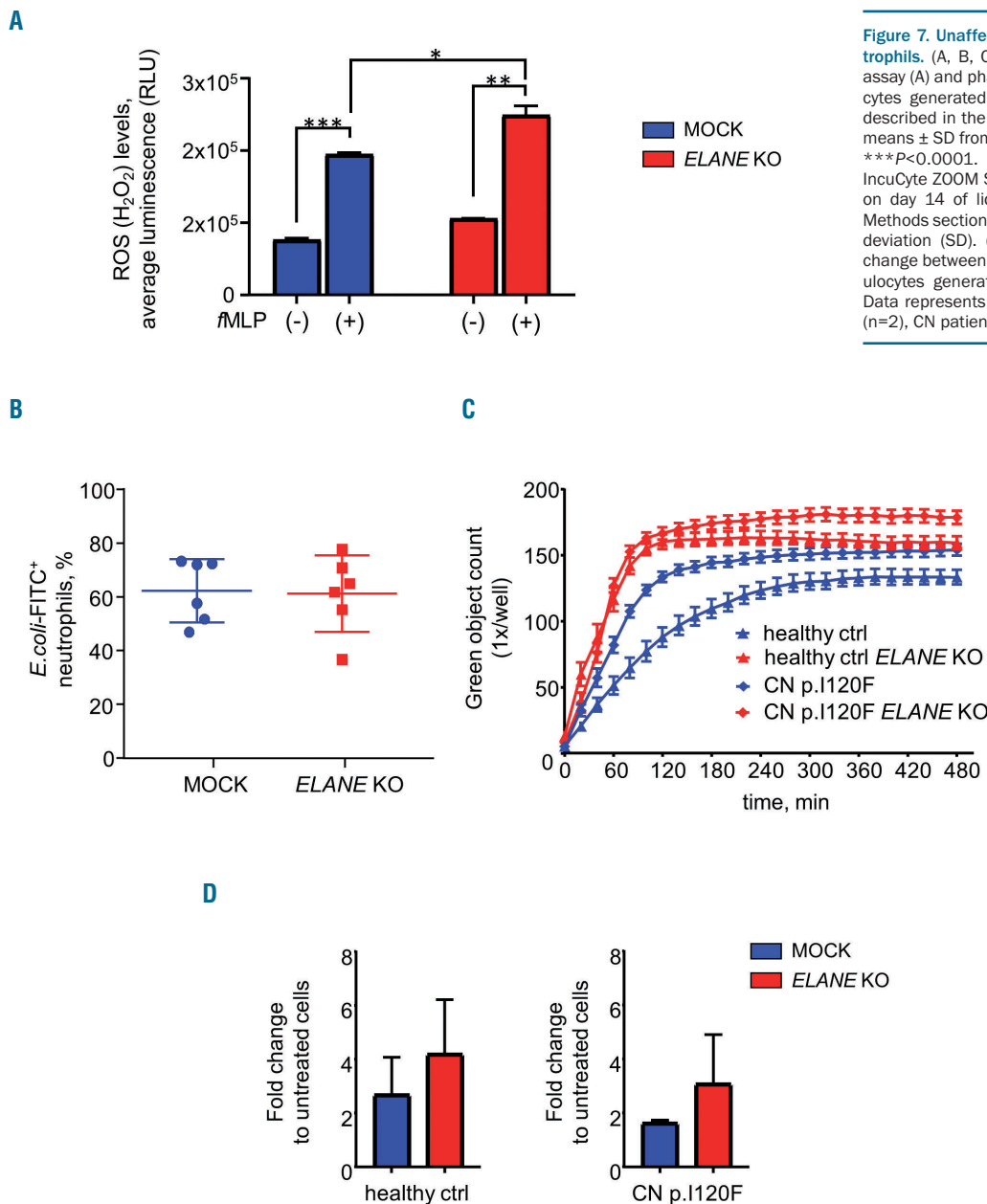
Figure 7. Unaffected functions of *ELANE* KO neutrophils. (A, B, C) Reactive oxygen species (ROS) assay (A) and phagocytosis assay (B, C) of granulocytes generated on day 14 of liquid culture, as described in the *Methods* section. Data represent means ± SD from duplicates. *$P<0.05$, **$P<0.01$, ***$P<0.0001$. (C) Phagocytosis Kinetic using IncuCyte ZOOM System of granulocytes generated on day 14 of liquid culture as described in the Methods section. Data represent mean ± standard deviation (SD). (D) Chemotaxis depicted as fold change between fMLP-treated and untreated granulocytes generated on day 14 of liquid culture. Data represents mean ± SD, healthy control (ctrl) (n=2), CN patient (n=1).

ical translational start site and/or internal start sites in exon 2 are disrupted and that expression of internally-initiated *ELANE* is pathogenic. We found a marked reduction of *ELANE* mRNA, most probably due to the induction of nonsense-mediated mRNA decay (NMD) of *ELANE* mRNA after exposure of cells to *ELANE*-specific CRISPR/Cas9 sgRNA RNP. We also did not detect any additional NE protein bands on WB analysis of edited cells using antibody recognizing C-terminus of NE. Based on these observations, we concluded that our sgRNA is inducing loss of NE protein without activation of the pathogenic *ELANE* forms from the internal ATG.

We did not detect off-target activity in edited cells, but recent results from Alan Bradley have suggested that the introduction of CRISPR/Cas9 editing can cause multiple genomic changes far beyond the actual target.[28] Therefore,

for clinical applications, evaluation of the off-target activity of CRISPR/Cas9 on whole genome level using next-generation sequencing should be performed. In addition, it would be important to evaluate that the editing of *ELANE* occurred in the repopulating hematopoietic stem cell population and that these cells maintained their ability to engraft immunodeficient mice *in vivo*. Since most probably HSC are not expressing NE, we will not expect any damaging effects of the *ELANE* KO on the functions and integrity of HSC.

We demonstrated here, that CRISPR/Cas9 mediated *ELANE* KO in HSPC and iPSC of CN patients induces granulocytic differentiation and *in vitro* generated *ELANE* KO neutrophils have no defects in the phagocytic activity, ROS production, and chemotaxis. NE is a proteolytic enzyme of the neutrophil serine protease (NSP) family,
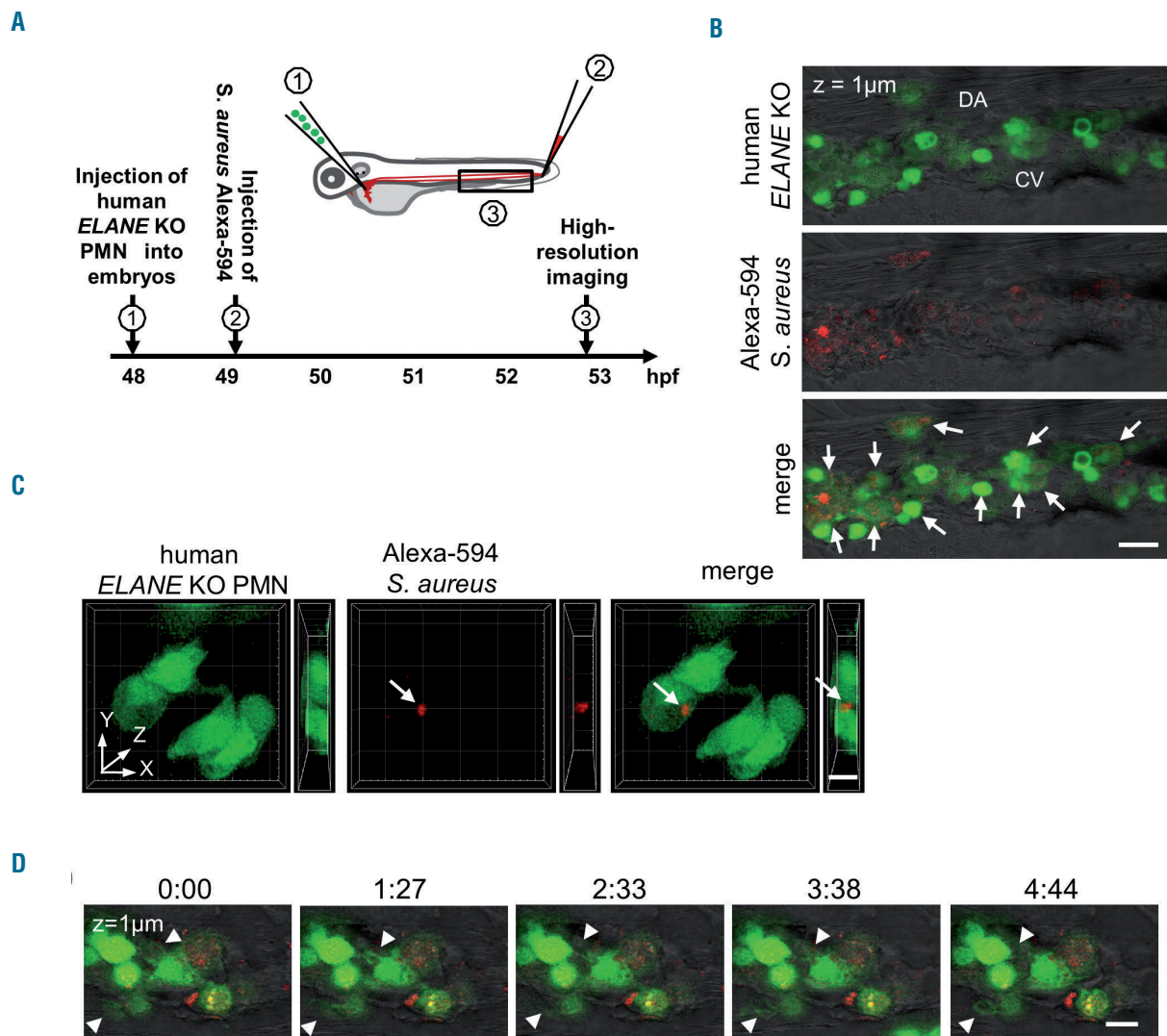
Figure 8. Human *ELANE* KO PMN are capable to migrate and to phagocyte *S. aureus* BioParticles in zebrafish embryos *in vivo*. (A) The scheme of *in vivo* phagocytosis assay in zebrafish embryos xenotransplanted with human fluorescently labeled polymorphonuclear leukocytes (PMN). (B) A representative confocal image highlighting the presence of transplanted human *ELANE* KO PMN in the caudal hematopoietic site of a zebrafish embryo at 53 hpf. White arrows indicate *S. aureus* BioParticles phagocytosed by human *ELANE* KO PMN. CV: caudal vein; DA: dorsal aorta. Scale bar: 20 μm. (C) Three-dimensional rendering of a z-stacks of 12 μm illustrating human *ELANE* KO PMN, one of them has engulfed *S. aureus* BioParticles (white arrow). Scale bar: 10 μm. (D) Still photographs from a time-lapse recording illustrating the phagocytic activity of transplanted human *ELANE* KO PMN in the zebrafish embryo. Arrowheads indicate the formation of neutrophil protrusions. Numbers indicate time in minutes. Scale bar: 10 μm.

including also cathepsin G (CG), proteinase 3 (PR3) and azurocidin (AZU1). NSP are stored in cytoplasmic granules, can be secreted into the extra- and peri-cellular space upon cellular activation and considered to be crucially involved in bacterial defense. NE and PR3 are very similar in their substrate specificity supporting a potentially redundant function for these two enzymes. *Elane*^{-/-} mice have normal neutrophil counts, but there are conflicting results regarding the effect of NE-deficiency on neutrophil extravasation to sites of inflammation, phagocytosis, and neutrophil extracellular traps in mice. NE may or may not be essential for these processes.[29-33] Papillon-Lefevre Syndrome (PLS) is the only human disorder known to cause NE deficiency. This rare autosomal recessive disease is due to loss-of-function mutations in the DPPI gene locus with the loss of the lysosomal cysteine protease cathepsin C/dipeptidyl peptidase I (DPPI). The activation of NSP, including NE, depends on the N-terminal processing activity of DPPI. Therefore, PLS patients exhibit a severe reduction in the activity and stability of all three NSP including NE. Intriguingly, patients with PLS have no defects in their ability to kill bacteria *e.g. Staphylococcus aureus* or *E.coli*, suggesting that redundancies in the neutrophil's bactericidal mechanisms negate the necessity for serine proteases for killing common bacteria.[34] Moreover, since the other serine proteases including CG, PR3 and neutrophil serine protease 4 remain intact, we do not expect for the resultant cells to develop any neutrophil-specific functional anti-bacterial or immunodeficiency phenotype in *ELANE* KO cells. Based on these observations, at this juncture, we believe that CRISPR/Cas9 based knockout of *ELANE* in HSPC of CN patients may restore defective granulopoiesis in CN patients without seriously impairing neutrophil functions. Further studies, including gene expression analysis to understand which pathways are affected by *ELANE* mutations and verifying that these pathways are indeed restored by *ELANE* KO, are essential to justify the therapeutic applications of *ELANE* KO technology in the future. It will also contribute to the understanding of the pathophysiology of the CN caused by *ELANE* mutations. Our first attempts to investigate intracellular signaling pathways affected by mutated *ELANE* revealed the restoration of mRNA expression of anti-apoptotic Bcl-xl factor that is downregulated in CN myeloid progenitor cells.[35] Moreover, we found downregulation of mRNA levels of the key UPR player BiP, normally upregulated in HSPC of CN patients harboring *ELANE* mutations.[8-10]

CRISPR/Cas9 technology also allowed correction of the specific gene mutations. We selected the *ELANE* knockout approach since *ELANE* mutations are heterozygous gain-of-function gene defects that are distributed throughout all five exons and two introns of *ELANE* and specific *ELANE* mutations correction would require specific settings for each patient based on the mutation position. In addition, the requirement of the introduction of the donor repair template DNA in a gene correction approach requires the activation of HDR making it difficult to achieve efficient correction in primary HSPC. We and other investigators have reported that *ELANE* mutations induce UPR and ER stress.[8-11] We also described deregulated signaling pathways in HSPC of CN patients downstream of *ELANE* mutations, such as diminished expression of transcription factors LEF-1, and C/EBPα,[36–39] abrogated expression and phosphorylation of the adaptor protein HCLS1,[40] elevated apoptosis[35] and hyperactivated NAMPT/sirtuins.[41] These intracellular defects may lead to the elevated fragility of HSPC during *ex vivo* gene manipulations and may affect gene correction efficiency. Moreover, gene editing strategy directed to the correction of *ELANE* mutations may lead to the creation of novel missense or frameshift mutations that may result in the novel mutant NE protein with damaging functions and potential generation of the pre-leukemic HSPC clones with proliferative advantage and possible leukemic transformation. Adeno-associated virus (AAV)-based vector may be used for the delivery of the donor repair template and is considered safer than retroviral constructs. Two groups recently published successful gene deletions as a gene therapy approach to cure sickle cell disease, a common inherited blood disorder.[17,18] It should be noted that AAV-based expression constructs may induce anti-viral host immune responses and may non-specifically integrate into the host genome.

In summary, we report here for the first time a method of CRISPR/Cas9 mediated *ELANE* gene deletion in hematopoietic stem cells and iPSC from CN patients harboring *ELANE* mutations. The *ELANE* gene deletion resulted in the increase of granulocytic differentiation to functional normal mature neutrophils in these patients *in vitro*. Therefore, CRISPR/Cas9 based gene knockout of *ELANE* in CN patients harboring *ELANE* mutation might be a useful treatment option especially in patients requiring high G-CSF dosages or do not responding to G-CSF at all. In addition, it remains to be investigated in subsequent clinical studies whether, in CN patients harboring *ELANE* mutations, the *ELANE* gene knockout would also abrogate the leukemogenesis.

References

1. Dale DC, Person RE, Bolyard AA, et al. Mutations in the gene encoding neutrophil elastase in congenital and cyclic neutropenia. Blood. 2000; 96(7):2317-2322.

2. Skokowa J, Germeshausen M, Zeidler C, Welte K. Severe congenital neutropenia: inheritance and pathophysiology. Curr Opin Hematol. 2007; 14(1):22-28.

3. Skokowa J, Dale DC, Touw IP, Zeidler C, Welte K. Severe congenital neutropenias.

Nat Rev Dis Primers. 2017;3:17032.

4. Welte K, Gabrilove J, Bronchud MH, Platzer E, Morstyn G. Filgrastim (r-metHuG-CSF): the first 10 years. Blood. 1996;88(6):1907-1929.

5. Rosenberg PS, Zeidler C, Bolyard AA, et al.

Stable long-term risk of leukaemia in patients with severe congenital neutropenia maintained on G-CSF therapy. Br J Haematol. 2010;150(2):196-199.

6. Jinek M, Chylinski K, Fonfara I, Hauer M, Doudna JA, Charpentier E. A programmable dual-RNA-guided DNA endonuclease in adaptive bacterial immunity. Science. 2012;337(6096):816-821.

7. Ran FA, Hsu PD, Wright J, Agarwala V, Scott DA, Zhang F. Genome engineering using the CRISPR-Cas9 system. Nat Protoc. 2013;8(11):2281-2308.

8. Grenda DS, Murakami M, Ghatak J, et al. Mutations of the ELA2 gene found in patients with severe congenital neutropenia induce the unfolded protein response and cellular apoptosis. Blood. 2007;110(13): 4179-4187.

9. Nanua S, Murakami M, Xia J, et al. Activation of the unfolded protein response is associated with impaired granulopoiesis in transgenic mice expressing mutant Elane. Blood.2011;117(13):3539-3547.

10. Nustede R, Klimiankou M, Klimenkova O, et al. ELANE mutant-specific activation of different UPR pathways in congenital neutropenia. Br J Haematol. 2016;172(2):219-227.

11. Kollner I, Sodeik B, Schreek S, et al. Mutations in neutrophil elastase causing congenital neutropenia lead to cytoplasmic protein accumulation and induction of the unfolded protein response. Blood. 2006;108(2):493-500.

12. Makaryan V, Kelley ML, Fletcher B, Bolyard AA, Aprikyan AA, Dale DC. Elastase inhibitors as potential therapies for ELANE-associated neutropenia. J Leukoc Biol. 2017;102(4):1143-1151.

13. Nayak RC, Trump LR, Aronow BJ, et al. Pathogenesis of ELANE-mutant severe neutropenia revealed by induced pluripotent stem cells. J Clin Invest. 2015;125(8):3103-3116.

14. Ancliff PJ, Gale RE, Watts MJ, et al. Paternal mosaicism proves the pathogenic nature of mutations in neutrophil elastase in severe congenital neutropenia. Blood. 2002;100(2): 707-709.

15. Benson KF, Horwitz M. Possibility of somatic mosaicism of ELA2 mutation overlooked in an asymptomatic father transmitting severe congenital neutropenia to two offspring. Br J Haematol. 2002;118(3):923; author reply -4.

16. Makaryan V, Zeidler C, Bolyard AA, et al. The diversity of mutations and clinical outcomes for ELANE-associated neutropenia. Curr Opin Hematol. 2015;22(1):3-11.

17. Ye L, Wang J, Tan Y, et al. Genome editing using CRISPR-Cas9 to create the HPFH genotype in HSPCs: An approach for treating sickle cell disease and beta-thalassemia. Proc Natl Acad Sci U S A. 2016;113(38): 10661-10665.

18. Traxler EA, Yao Y, Wang YD, et al. A genome-editing strategy to treat beta-hemoglobinopathies that recapitulates a mutation associated with a benign genetic condition. Nat Med. 2016;22(9):987-990.

19. Stemmer M, Thumberger T, Del Sol Keyer M, Wittbrodt J, Mateo JL. CCTop: an intuitive, flexible and reliable CRISPR/Cas9 target prediction tool. PLoS One. 2015; 10(4):e0124633.

20. Brinkman EK, Chen T, Amendola M, van Steensel B. Easy quantitative assessment of genome editing by sequence trace decomposition. Nucleic Acids Res. 2014;42(22):e168.

21. Bajoghli B, Kuri P, Inoue D, et al. Noninvasive in toto imaging of the thymus reveals heterogeneous migratory behavior of developing T cells. J Immunol. 2015; 195(5):2177-2186.

22. Lachmann N, Ackermann M, Frenzel E, et al. Large-scale hematopoietic differentiation of human induced pluripotent stem cells provides granulocytes or macrophages for cell replacement therapies. Stem Cell Reports. 2015;4(2): 282-296.

23. Dannenmann B, Zahabi A, Mir P, et al. Human iPSC-based model of severe congenital neutropenia reveals elevated UPR and DNA damage in CD34(+) cells preceding leukemic transformation. Exp Hematol. 2019;71-51-60.

24. Hamilton N, Sabroe I, Renshaw SA. A method for transplantation of human HSCs into zebrafish, to replace humanised murine transplantation models. F1000Res. 2018; 7:594.

25. Staal FJ, Spaink HP, Fibbe WE. Visualizing human hematopoietic stem cell trafficking in vivo using a zebrafish xenograft model. Stem Cells Dev. 2016;25(4):360-365.

26. Nasri M, Mir P, Dannenmann B, et al. Fluorescent labeling of CRISPR/Cas9 RNP for gene knockout in HSPCs and iPSCs reveals an essential role for GADD45b in stress response. Blood Adv. 2019;3(1):63-71.

27. Tidwell T, Wechsler J, Nayak RC, et al. Neutropenia-associated ELANE mutations disrupting translation initiation produce novel neutrophil elastase isoforms. Blood. 2014;123(4):562-569.

28. Kosicki M, Tomberg K, Bradley A. Repair of double-strand breaks induced by CRISPR-Cas9 leads to large deletions and complex rearrangements. Nat Biotechnol. 2018;36(8):765-771.

29. Allport JR, Lim YC, Shipley JM, et al. Neutrophils from MMP-9- or neutrophil elastase-deficient mice show no defect in transendothelial migration under flow in vitro. J Leukoc Biol. 2002;71(5):821-828.

30. Martinod K, Witsch T, Farley K, Gallant M, Remold-O'Donnell E, Wagner DD. Neutrophil elastase-deficient mice form neutrophil extracellular traps in an experimental model of deep vein thrombosis. J Thromb Haemost. 2016;14(3):551-558.

31. Hirche TO, Atkinson JJ, Bahr S, Belaaouaj A. Deficiency in neutrophil elastase does not impair neutrophil recruitment to inflamed sites. Am J Resp Cell Mol Biol. 2004;30(4):576-584.

32. Young RE, Thompson RD, Larbi KY, et al. Neutrophil elastase (NE)-deficient mice demonstrate a nonredundant role for NE in neutrophil migration, generation of proinflammatory mediators, and phagocytosis in response to zymosan particles in vivo. J Immunol. 2004;172(7):4493-4502.

33. Belaaouaj A, McCarthy R, Baumann M, et al. Mice lacking neutrophil elastase reveal impaired host defense against gram negative bacterial sepsis. Nat Med. 1998;4(5):615-618.

34. Pham CT, Ivanovich JL, Raptis SZ, Zehnbauer B, Ley TJ. Papillon-Lefevre syndrome: correlating the molecular, cellular, and clinical consequences of cathepsin C/dipeptidyl peptidase I deficiency in humans. J Immunol. 2004;173(12):7277-7281.

35. Cario G, Skokowa J, Wang Z, et al. Heterogeneous expression pattern of pro- and anti-apoptotic factors in myeloid progenitor cells of patients with severe congenital neutropenia treated with granulocyte colony-stimulating factor. Br J Haematol. 2005;129(2):275-278.

36. Skokowa J, Cario G, Uenalan M, et al. LEF-1 is crucial for neutrophil granulocytopoiesis and its expression is severely reduced in congenital neutropenia. Nat Med. 2006;12(10): 1191-1197.

37. Skokowa J, Welte K. LEF-1 is a decisive transcription factor in neutrophil granulopoiesis. Ann N Y Acad Sci. 2007;1106:143-151.

38. Skokowa J, Welte K. Dysregulation of myeloid-specific transcription factors in congenital neutropenia. Ann N Y Acad Sci. 2009;1176:94-100.

39. Skokowa J, Welte K. Defective G-CSFR signaling pathways in congenital neutropenia. Hematol Oncol Clin North Am. 2013;27(1): 75-88, viii.

40. Skokowa J, Klimiankou M, Klimenkova O, et al. Interactions among HCLS1, HAX1 and LEF-1 proteins are essential for G-CSF-triggered granulopoiesis. Nat Med. 2012;18 (10):1550-1559.

41. Skokowa J, Lan D, Thakur BK, et al. NAMPT is essential for the G-CSF-induced myeloid differentiation via a NAD(+)-sirtuin-1-dependent pathway. Nat Med. 2009;15 (2):151-158.

PIEZO1 activation delays erythroid differentiation of normal and hereditary xerocytosis-derived human progenitor cells

Alexis Caulier,[1,2][*] Nicolas Jankovsky,[1][*] Yohann Demont,[3] Hakim Ouled-Haddou,[1] Julien Demagny,[4] Corinne Guitton,[5] Lavinia Merlusca,[2] Delphine Lebon,[1,2] Pascal Vong,[1] Aurélien Aubry,[1] Agnès Lahary,[6] Christian Rose,[7] Sandrine Gréaume,[8] Emilie Cardon,[1] Jessica Platon,[1] Halima Ouadid-Ahidouch,[9] Jacques Rochette,[1,10] Jean-Pierre Marolleau,[1,2] Véronique Picard[11] and Loïc Garçon[1,4,10]

[1]EA4666 HEMATIM, Université Picardie Jules Verne, Amiens; [2]Service des Maladies du Sang, CHU Amiens, Amiens; [3]Unité de Thérapie Cellulaire, CHU Amiens, Amiens; [4]Service d'Hématologie Biologique, CHU Amiens; [5]Service de Pédiatrie Générale, CHU Bicêtre, AP-HP, Le Kremlin-Bicêtre; [6]Laboratoire d'Hématologie, CHU Rouen, Rouen; [7]Service d'Oncologie et d'Hématologie, Hôpital Saint Vincent de Paul, Lille; [8]Etablissement Français du Sang (EFS) de Normandie, Bois-Guillaume; [9]EA4667 Laboratoire de Physiologie Cellulaire et Moléculaire, Université Picardie Jules Verne, Amiens; [10]Laboratoire de Génétique Moléculaire, CHU Amiens, Amiens and [11]Laboratoire d'Hématologie, AP-HP, Le Kremlin-Bicêtre, France

*AC and NJ contributed equally to this work.

ABSTRACT

Hereditary xerocytosis is a dominantly inherited red cell membrane disorder caused in most cases by gain-of-function mutations in PIEZO1, encoding a mechanosensitive ion channel that translates a mechanic stimulus into calcium influx. We found that PIEZO1 was expressed early in erythroid progenitor cells, and investigated whether it could be involved in erythropoiesis, besides having a role in the homeostasis of mature red cell hydration. In UT7 cells, chemical PIEZO1 activation using YODA1 repressed glycophorin A expression by 75%. This effect was PIEZO1-dependent since it was reverted using specific short hairpin-RNA knockdown. The effect of PIEZO1 activation was confirmed in human primary progenitor cells, maintaining cells at an immature stage for longer and modifying the transcriptional balance in favor of genes associated with early erythropoiesis, as shown by a high *GATA2/GATA1* ratio and decreased *α/β-globin* expression. The cell proliferation rate was also reduced, with accumulation of cells in G0/G1 of the cell cycle. The PIEZO1-mediated effect on UT7 cells required calcium-dependent activation of the NFAT and ERK1/2 pathways. In primary erythroid cells, PIEZO1 activation synergized with erythropoietin to activate STAT5 and ERK, indicating that it may modulate signaling pathways downstream of erythropoietin receptor activation. Finally, we studied the *in-vitro* erythroid differentiation of primary cells obtained from 14 *PIEZO1*-mutated patients, from 11 families, carrying ten different mutations. We observed a delay in erythroid differentiation in all cases, ranging from mild (n=3) to marked (n=8). Overall, these data demonstrate a role for PIEZO1 during erythropoiesis, since activation of PIEZO1 - both chemically and through activating mutations - delays erythroid maturation, providing new insights into the pathophysiology of hereditary xerocytosis.

Introduction

PIEZO proteins were identified as a family of mechanically activated transductors, first described in neuronal cell lines, which convert mechanical forces into biological signals.[1] PIEZO1 is a large, three-blade propeller-shaped protein displaying 38 transmembrane-helix domains, and is encoded by the broadly

expressed *FAM38A* gene[2,3] (GTEx Project) (*https://gtexportal.org/home/gene/PIEZO1*). Activation of the mechanosensitive ion channel PIEZO1 has a significant effect on red blood cell physiology. Under physiological conditions, PIEZO1 regulates ATP release from human mature erythrocytes,[4] and has been shown to control red blood cell volume and hydration homeostasis through ion balance.[5] PIEZO1 induces a cationic current that develops quickly after activation of the protein by a mechanical stress; this activation is followed by a rapid inactivation determined by the C-terminal extracellular domain and the inner pore helix.[6] PIEZO1 is a non-selective channel although it presents a preferential conductance of monovalent cations, and a significant permeability to calcium (Ca^{2+}).[1,7] *PIEZO1* gain-of-function mutations have been associated with most cases of hereditary xerocytosis (HX), leading to either a slower inactivation or altered channel kinetics.[8–11] These mutations induce excessive Ca^{2+} influx and secondary activation of the Gardos channel in red cells, thereby causing potassium (K^+) leakage, water loss, and erythrocyte dehydration.[12,13]

So far, the role of PIEZO1 during erythropoiesis has only been described in mature erythrocytes. However, it is also expressed earlier in human erythroid progenitors.[8,14] In many cell types such as epithelial, urothelial and endothelial cells, PIEZO1 has been involved in regulation of the cell cycle, proliferation and differentiation.[15-18] Prompted by a recent report that a PIEZO1 mutation could mimic myelodysplastic syndrome with megaloblastic features,[19] we performed an extensive and comprehensive investigation of PIEZO1 expression and function using primary human erythroid progenitor cells. We investigated consequences of its activation either by the selective activator YODA1 in normal human erythroid progenitors or by activating mutations in HX–derived hematopoietic progenitors from 14 patients carrying ten different mutations. We observed that PIEZO1 activation in our models modified the kinetics of erythropoiesis, inducing a delay in terminal erythroid differentiation. Our results suggest that PIEZO1 plays a key role during human erythroid differentiation.

Methods

The primary cell culture protocol, multiparametric flow cytometry (MFC), live imaging flow cytometry (IFC), western blot, immunofluorescence, quantitative reverse transcriptase polymerase chain reaction (RT-qPCR) analysis and reagents are detailed in the *Online Supplementary Methods.*

Cell lines culture

The UT7 cell line was maintained in α-minimum essential medium (Dominique Dutscher) supplemented with 10% fetal calf serum (Eurobio) and cytokines. Two subclones were used: the UT7/GM clone and the UT7/EPO clone. The UT7/GM clone was used as a model of erythropoietin (EPO)-driven differentiation, proliferating under 5 ng/mL recombinant human granulocyte-macrophage colony-stimulating factor (GM-CSF; Miltenyi) and differentiating under 5 U/mL EPO after GM-CSF had been removed by two washes in 1x phosphate-buffered saline.[20] The UT7/EPO clone (a gift from Dr. Y.Zermati, Institut Cochin, Paris, France) was used as a model of EPO-driven proliferation, and cultured with 2 U/mL EPO (*Online Supplementary Figure S1*).[21]

Patients' samples and primary cell cultures

HX hematopoietic cells were obtained from blood samples collected into EDTA or from phlebotomy bags after patients' informed consent in accordance with the Helsinki declaration. This study was conducted in compliance with French legislation on non-interventional studies. Patients' data were collected directly from their medical records or through the HX French Cohort registry, approved by the National Commission on Informatics and Liberty. The diagnosis of HX was based on clinical and biological features and a typical osmotic gradient ektacytometry curve before genetic testing. Thirteen of the patients in this study were recently extensively described.[22] Control samples were obtained from blood or mobilized peripheral blood mononuclear cells (MNC) of healthy subjects. The MNC were isolated using density gradient-centrifugation (Ficoll-Paque PLUS, GE Healthcare) and CD34^{+} cells were sorted by magnetic microbead separation on MACS columns (AutoMACS Separator). The complete protocol for erythroid differentiation is described in *Online Supplementary Figures S1 and S2* and detailed in the *Online Supplementary Methods.*

Lenti/retroviral production and cell infection

Four short hairpin (Sh) RNA against *PIEZO1* (Sh-PIEZO1) and one control scrambled ShRNA (Sh-SCR) cloned in pLKO.1-CMV-tGFP vector were designed using the Mission® shRNA tool and purchased from Sigma-Aldrich (detailed sequences are provided in *Online Supplementary Table S1*). Specific anti-PIEZO1 targeting was verified using an online alignment research tool (nucleotide BLAST®, NCBI). Viral production was ensured in the HEK293T cell line, after transfection using Lipofectamine® LTX with Plus™ reagent (Thermo Fisher Scientific) in antibiotic-free, high-glucose Dulbecco modified Eagle medium (Dominique Dutscher). Lentiviral supernatant was harvested from day 2 to 4, and filtered through a 0.45 µM polyvinylidene fluoride membrane (Millex-HV 0.45 µM 33 mm, Merck-Millipore) before ultracentrifugation on day 4 (100,000 g for 90 min at 4°C, Optima L-80XP, Beckman-Coulter). We used a mix of the four ShRNA to knockdown *PIEZO1* in the UT7/EPO cell line. Infection was performed overnight with 8 µg/mL polybrene (Sigma-Aldrich). In UT7/EPO cells, 10 µL of each supernatant were used to infect $5x10^5$ cells, and were sufficient to induce >90% GFP, both with the Sh-SCR and Sh-PIEZO1 mix. Forty-eight hours after transduction, cells were washed in 50 mL 1x phosphate-buffered saline and cultured for an additional 3 days in the presence of dimethylsulfoxide (DMSO) or YODA1 before MFC staining. The retroviral MigR vector containing dominant-negative MEK was a generous gift from Prof. S. Giraudier (Hôpital Saint-Louis, Paris, France).

Statistical analysis

Statistical analyses were performed using two-tailed *P* values and parametric tests. The α value for statistical significance was set at 0.05. For quantitative variables we used a Student *t*-test for paired or unpaired samples depending on the experiment under consideration. All numerical values are expressed as mean values ± standard deviation.

Results

PIEZO1 is expressed at an early stage during *in vitro* erythropoiesis of human CD34^{+} cells

We first assessed *PIEZO1* expression during synchronized human *in vitro* erythroid differentiation as described in *Online Supplementary Figure S2B*. *PIEZO1* mRNA was

preferentially expressed in CD34^{+} cells and in early stages of erythropoiesis from day 4 to 10 (corresponding to burst-forming unit-erythroid/colony-forming unit-erythroid/proerythroblast in our culture system) then decreased during terminal maturation (Figure 1A). This was in agreement with previously published RNA-sequencing analyses on erythroid precursors.[14,23,24]

Expression of glycophorin A (*GPA*) was measured in parallel as a positive marker of erythroid differentiation (Figure 1B). Similar results were observed at the protein level using MFC (Figure 1C, D). The specificity of PIEZO1 antibody staining using MFC was verified by western blot and immunofluorescence assays (*Online Supplementary Figure S4*).
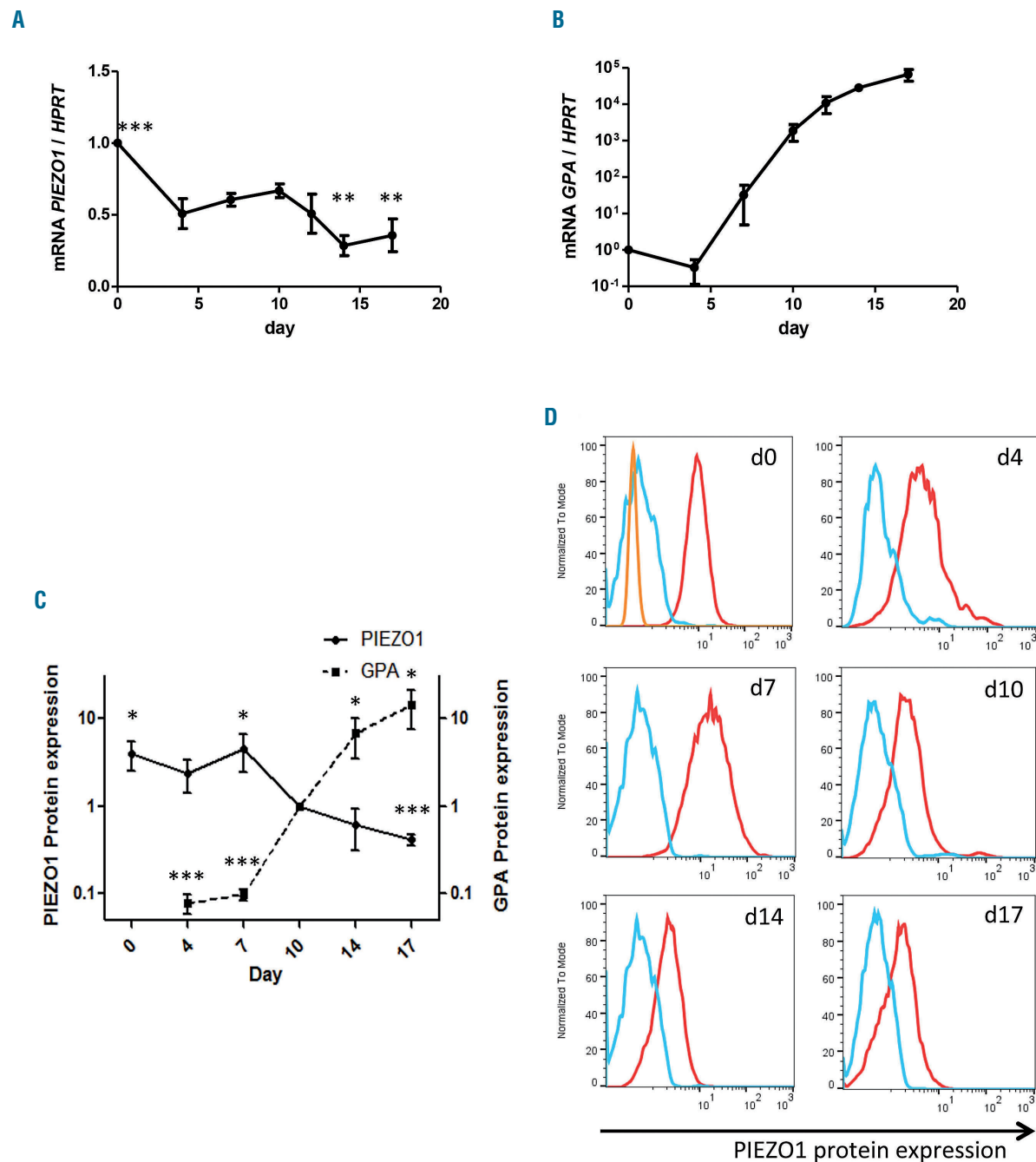
Figure 1. PIEZO1 expression during human *in vitro* erythroid differentiation. PIEZO 1 expression was assessed at day 4 in CD45^{low}/CD123^{-}/CD34^{+}/CD36^{-} cells, and at day 7 in CD36^{+} cells, for both the gene and protein expression experiments. (A) *PIEZO1* mRNA expression (determined by quantitative reverse transcriptase polymerase chain reaction, RT-qPCR) relative to *HPRT* expression, during synchronized erythroid differentiation. Differential expression relative to day 0. Statistical analysis was made compared to day 10. No significant change was seen at days 4, 7, and 12. (B) Glycophorin A (*GPA*) mRNA expression (determined by RT-qPCR) relative to *HPRT* expression, during synchronized erythroid differentiation. Reference was day 0. (C) Kinetics of relative PIEZO1 protein expression during *in-vitro* erythroid differentiation, in parallel to relative GPA membrane expression. For both, expression at each time point was assessed by multiparametric flow cytometry (MFC) (mean fluorescence intensity at the time point relative to that at day 10.) (D) MFC histograms of PIEZO1 protein expression assessed at different culture time points (red). We used both the secondary antibody alone (blue) and a non-specific rabbit anti HLA-DR1 antibody (orange) as controls. (n=3 for all experiments). ***$P<0.001$; **$P<0.01$; * $P<0.05$.

YODA1 inhibits cell proliferation and blocks erythroid differentiation in a PIEZO1-dependent manner in UT7 cells

The UT7/GM cell line was used as a model of EPO-induced erythroid differentiation. Indeed, these cells expressed a low level of GPA under exposure to GM-CSF, and acquired GPA in the presence of EPO (*Online Supplementary Figure S1A-C*). We tested YODA1, a specif-

ic PIEZO1 activator,[25] at increasing concentrations and selected 5 μM for further experiments in these cells (*Online Supplementary Figure S3A, B*). At this concentration, YODA1 decreased cell proliferation (Figure 2A) and increased the percentage of cells in the G0/G1 phase (Figure 2B). No difference in cell mortality or apoptosis rate was noted (*Online Supplementary Figure S3C, D*). Under the differentiation condition using 5 U/mL EPO,
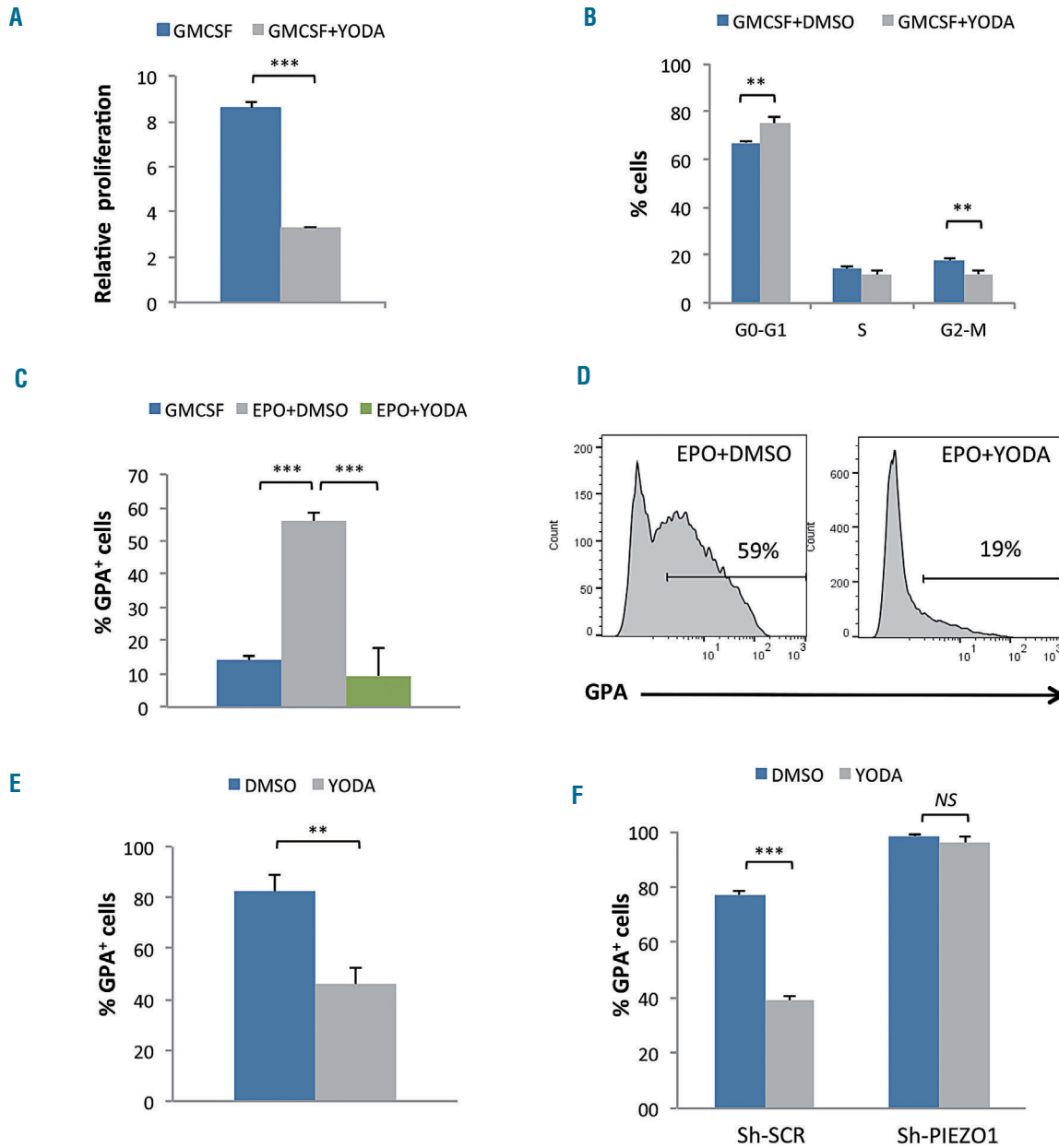
Figure 2. Effect of PIEZO1 chemical activation on the proliferation and differentiation of UT7 cells. Glycophorin A (GPA) expression and cell proliferation were assessed after 72 h of culture in medium containing granulocyte-macrophage colony-stimulating factor (GMCSF) or erythropoietin (EPO). (A) In the UT7/GM cell line, stimulation with 5 μM YODA1 reduced cell expansion compared to that induced by dimethylsulfoxide (DMSO) (2.6 fold). (B) In the UT7/GM cell line exposure to 5 μM YODA1 in GMCSF-containing medium led to cell accumulation in the G0/G1 phase of the cycle (67±1% with DMSO *vs.* 75±3% with YODA1), and a significant decrease in cells in the G2/M phase (18±1% with DMSO vs. 12±2% with YODA1). (C) Stimulation with 5 U/mL EPO induced partial erythroid differentiation in UT7/GM cells, as shown by GPA acquisition (56±3% *vs.* 14±2% in GMCSF-containing medium), which was strongly inhibited after PIEZO1 chemical activation using 5 μM YODA1 (9±8% with YODA1 *vs.* 56±3% with EPO+DMSO). (D) Representative multiparametric flow cytometry histograms showing the repression of EPO-mediated GPA expression after exposure to YODA1 in UT7/GM cells. (E) GPA repression was also observed in UT7/EPO cells after exposure to 5 μM YODA1 for 3 days (82±6% *vs.* 46±7% with DMSO). (F) In UT7/EPO cells transduced with Sh-SCR, YODA1 repressed GPA expression (39±1.8% *vs.* 77±1.1% with DMSO) whereas infection with a mixture of four different Sh-PIEZO1 abolished the YODA1-mediated inhibition of GPA (96±2% with YODA1 *vs.* 98±0.4%, *P=NS*). (n=3 for all experiments, ***P<0.001; **P<0.01).

YODA1 significantly repressed GPA induction (Figure 2C, D), and this effect was dose-dependent (*Online Supplementary Figure S3A*). Using the UT7/EPO cell line that proliferates in the presence of EPO and expresses a high level of GPA at baseline (*Online Supplementary Figure S1A, right*), we observed a similar dose-dependent GPA downregulation after exposure to YODA1 (Figure 2E and *Online Supplementary Figure S3B, E*). We ruled out any YODA1 off-target effect using a Sh-RNA lentiviral strategy that specifically knocks down PIEZO1. Transduction efficiency was >90%, as assessed by GFP expression. The Sh-RNA-mediated *PIEZO1* decrease was 65% at the RNA level (*Online Supplementary Figure S4A*). At the protein level, the decrease was 50% as assessed by MFC (*Online Supplementary Figure S4B*) in comparison to the level in cells transduced with a Sh-scrambled control (Sh-SCR). The PIEZO1 decrease was confirmed using western blotting and immunofluorescence (*Online Supplementary Figure S4C, D*). Following exposure to YODA1, GPA expression decreased in Sh-SCR-transduced cells but not in cells transduced with Sh-PIEZO1 (Figure 2F). The effect was related to GFP intensity, being weaker in cells expressing Sh-PIEZO1 at a lower level (*Online Supplementary Figure S4E*). Sh-PIEZO1 had the opposite effect of YODA1 on GPA expression since it enhanced erythroid differentiation by increasing the percentage of GPA+ cells compared to the control Sh-SCR. (Figure 2F and *Online Supplementary Figure S4E*). Sh-PIEZO1 did not revert the decreased proliferation induced by YODA1 exposure, and induced a reduced proliferation rate by itself in comparison to Sh-SCR (*Online Supplementary Figure S4F*).

PIEZO1 activation delays erythroid differentiation in human CD34+-derived erythroid cells

We then investigated whether the erythroid blockage induced by YODA1 in leukemic cell lines was confirmed in human primary cells. Sorted CD34+ cells were driven into erythroid differentiation (*Online Supplementary Figure S2A*). A dose of 1 μM YODA1 was selected for drug exposure based on dose-escalation data (*Online Supplementary Figure S5A*). Erythroid differentiation was assessed on day 10 by MFC and cytology. YODA1 reduced cell amplification without increasing cell death or apoptosis (*Online Supplementary Figure S5B-D*). Importantly, it led to a drastic delay in GPA acquisition, with accumulation of immature CD36+/CD117+ erythroblasts and a decrease in CD71+/GPA^{High} mature cells (Figure 3A-D). These results were confirmed by cytology, which showed an increase in immature erythroid precursors after exposure to YODA1 (Figure 3E, F). To investigate the timing of the YODA1 effect more precisely, we synchronized the cell culture (*Online Supplementary Figure S2B*). CD36+/GPA- colony-forming unit-erythroid cells were sorted on day 7 and exposed sequentially to 1 μM YODA1 or DMSO from day 7, 10, or 13 to the end of the culture. Red cell terminal differentiation was evaluated as the mean percentage of enucleated cells on day 21. The YODA1 effect was maximal when cells were exposed early, from day 7 to 10, as shown by the significant decrease in the Hoechst negative fraction at day 21 (*Online Supplementary Figure S6A, B*). A decrease in the ratio of enucleated cells was also observed on cytological analyses after early exposure, with the effect being weaker when YODA1 was administered on day 13 (*Online Supplementary Figure S6C*). We showed here that erythroid differentiation was delayed but not blocked

after PIEZO1 activation, since precursors reached final enucleation, but at a slower rate. Taken together, these data argue for a YODA1 effect at the transition between the GPA^{low} and GPA^{high} stages, corresponding to the beginning of the differentiation of erythroid precursors.[26]

PIEZO1 activation delays erythroid differentiation through transcriptional control

Using RT-qPCR we investigated whether the YODA1-induced delay in erythroid differentiation was driven by global transcriptional control. In human primary erythroid cells, EPO-mediated *GPA* mRNA induction was inhibited by YODA1, indicating that the GPA repression occurred at the transcriptional level. PIEZO1 activation also reduced EPO-mediated *α-* and *β-globin* mRNA induction (Figure 4A). Since *GATA2* expression during erythropoiesis is associated with the early proliferative stage while *GATA1* is the key protagonist of terminal differentiation, we evaluated the *GATA2/GATA1* mRNA ratio after exposure to YODA1. It increased significantly in comparision with the ratio after exposure to DMSO (Figure 4B). A broader analysis of erythroid gene expression confirmed that primary erythroblasts exposed to YODA1 displayed an immature erythroid profile, with higher expression of *BMI1* and *STAT5A* mRNA and lower *ALAS2, EPOR, AHSP* and *SLC4A1* mRNA expression (Figure 4C).

YODA1-induced inhibition of erythroid differentiation is Ca²⁺-dependent and does not require activation of the Gardos channel

PIEZO1-mediated red cell dehydration in HX is Ca²⁺-dependent; since PIEZO1 is a non-selective cation channel, we next evaluated whether this was also the case during erythropoiesis. In UT7/GM cells, YODA1 caused a strong dose-dependent increase in cytosolic Ca²⁺ (Figure 5A). This effect was abolished in Ca²⁺-free medium, consistent with YODA1 causing a strong Ca²⁺ influx from the extracellular to the intracellular compartment (Figure 5A, B). Ca²⁺ chelation using 2 mM ethylene glycol tetra-acetic acid (EGTA) totally blocked the YODA1-mediated decrease of GPA; this was rescued by addition of 2 mM calcium chloride (Figure 5C). The same effect was observed after intracellular Ca²⁺ chelation using BAPTA-AM (*data not shown*). Since red cell dehydration in PIEZO1-HX involves a Ca²⁺-dependent secondary activation of the Gardos channel,[20] we investigated whether the effect of PIEZO1 on erythroblasts was also Gardos-dependent. As shown in Figure 5D, in UT7/GM cells, Senicapoc, a selective Gardos channel inhibitor, did not revert the YODA1-associated blockade of GPA, indicating that YODA1-induced inhibition of erythroid differentiation did not require secondary activation of the Gardos channel.

PIEZO1 effect on erythroid differentiation involves modulation of NFAT, ERK1/2, and STAT5 pathways in UT7 cells and human primary erythroblasts

We next investigated Ca²⁺-dependent signaling pathways activated downstream PIEZO1 in erythroid cells. Since NFAT is a well-known target of Ca²⁺-signaling in many cell types,[27] we evaluated whether it was involved in erythroid cells. Calcineurin inhibition using 5 μM tacrolimus completely blocked the YODA1-induced GPA repression in UT7/EPO cells (Figure 6A). Moreover, exposure to YODA1 led to substantial nuclear translocation of NFATc1, significantly increasing the similarity score value

compared to DMSO (Figure 6B, C, and *Online Supplementary Figure S7A*). These data argue for a role of the PIEZO1/Ca^{2+}/NFAT pathway in the control of erythroid differentiation. We also tested whether the main transduction pathways associated with EPO signaling were involved. We used a strategy based on: (i) protein

phosphorylation measurements after stimulation with YODA1 and/or cytokines in cell lines and primary cells and (ii) chemical inhibitors, assuming that inhibition of any pathway downstream of PIEZO1 would revert the YODA1-mediated phenotype. We tested two main pathways: ERK1/2 and STAT5. The phospho-ERK inhibitor
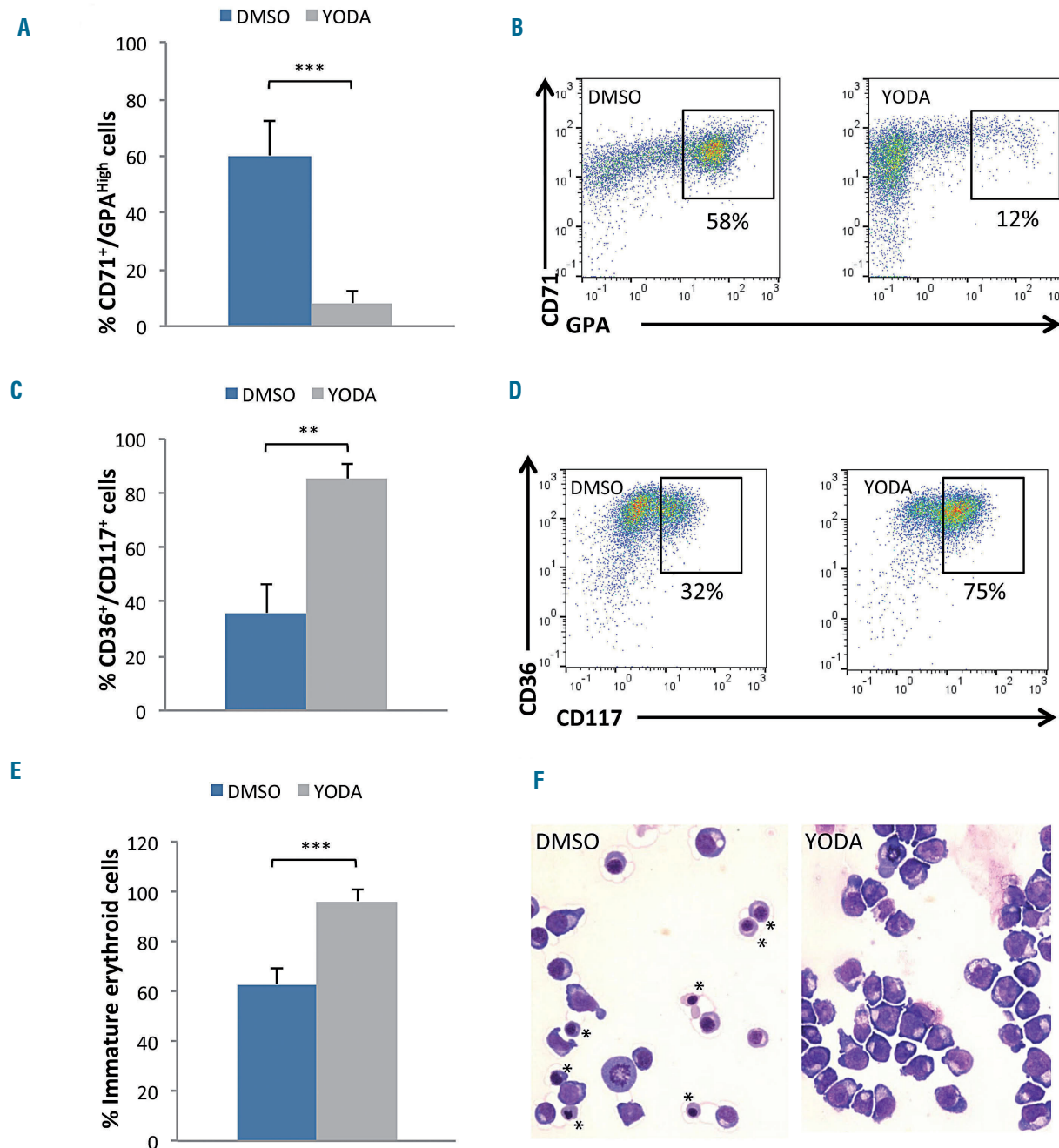
Figure 3. PIEZO1 chemical activation delayed erythroid differentiation of human primary CD34$^+$-derived cells. (A) Exposure to 1 μM YODA1 for 3 days decreased the mature erythroblastic population expressing CD71 and GPA^{High} [8±4% vs. 60±12% with dimethylsulfoxide (DMSO)]: multiparametric flow cytometry (MFC) at day 10. (B) Representative MFC plots showing the decrease in the CD71$^+$/GPA^{High} population due to YODA1 (right) compared to the effect of DMSO (left), at day 10. (C) Exposure to 1 μM YODA1 increased the immature erythroblastic population expressing CD36 and CD117 (85±5%) compared to that following exposure to DMSO (36±11%). (D) Representative MFC plots showing the increase in CD36$^+$/CD117$^+$ population due to YODA1 (right) compared to that due to DMSO (left), at day 10. (E) Excess of immature erythroid cells, i.e., proerythroblasts and basophilic erythroblastsb upon exposure to YODA1 compared to exposure to DMSO, assessed by cytology after May-Grünwald-Giemsa (MGG) staining (96±5% vs. 63±6%). (F) Representative cytology after MGG staining at day 10 of *in vitro* erythroid differentiation showing a heterogeneous population of erythroblasts at all stages of maturation including the orthochromatic (*) stage in the control (left) compared to a more homogeneous population of immature erythroblasts in the presence of 1 μM YODA (right). (n=4 in experiment E, n=3 in all other experiments). ***$P<0.001$; **$P<0.01$; *$P<0.05$.

UO126 induced spontaneous GPA expression in the absence of EPO, showing that ERK activation was necessary to maintain UT7/GM cells in an undifferentiated GPA[low] state. YODA1 did not revert the high GPA expression induced by ERK1/2 inactivation (Figure 6D). The same results were observed using a retrovirus containing a MEK dominant-negative form (*Online Supplementary Figure S7B*). This indicated that the effect of YODA1 required a functional ERK pathway. Phospho-Flow experiments showed that YODA1 induced strong ERK phosphorylation in UT7/GM cells (Figure 6E). This was confirmed by western blot analysis (*data not shown*). ERK phosphorylation was Ca^{2+}-dependent, since it decreased strongly in the presence of EGTA (Figure 6E), and PIEZO1-dependent, since it was abrogated in cells transduced with Sh-PIEZO1 lentivirus (Figure 6F). In human primary erythroid progenitors, no p-ERK1/2 was detected in the absence of EPO. In the presence of EPO, YODA1 synergized with EPO for ERK phosphorylation, consistent with a role for PIEZO1 in the modulation of EPO-dependent ERK signaling in primary cells (Figure 6G). This effect was confirmed by western blot analysis (*Online Supplementary Figure S7C*). We

observed a similar synergistic effect in EPO-induced STAT5 phosphorylation in primary erythroid cells (Figure 6H), also confirmed by western blotting (*Online Supplementary Figure S7D*). Of note, no effect of YODA1 on STAT5 phosphorylation was seen in UT7/GM cells, in which STAT5-phopshorylation is not EPO-dependent (*Online Supplementary Figure S7E*). Taken together, these data argue for a role of PIEZO1 in modulating ERK and STAT5 signaling pathways downstream of EPO-receptor activation in human progenitor cells.

PIEZO1 gain-of-function mutations in hereditary xerocytosis delay erythroid differentiation and mimic the effect of chemical activation

Since most HX patients have *PIEZO1* gain-of-function mutations, we tested whether the same phenotype could be observed during *in vitro* erythroid differentiation from PIEZO1-HX progenitors. Fourteen patients from 11 families (HX #1 to #11) carrying ten different *PIEZO1* mutations were tested (HX#3: 2 siblings; HX#10: 3 siblings). The patients' characteristics are shown in Table 1. Nine phlebotomy samples from five patients [3 families, HX#1
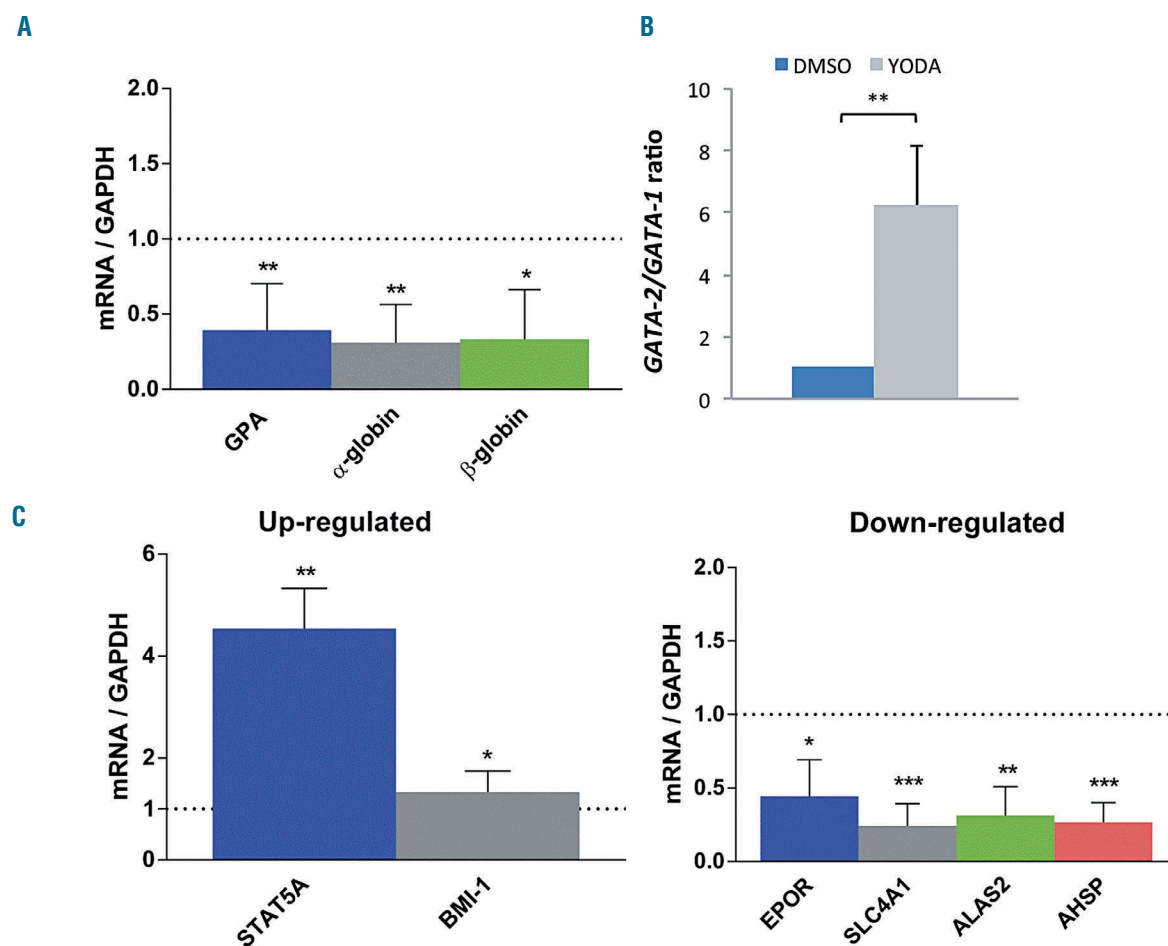
Figure 4. Effect of PIEZO1 activation on the transcriptional program of erythroid differentiation in primary human CD34$^+$-derived cells, assessed by quantitative reverse transcriptase polymerase chain reaction. For all experiments, primary cells were cultured for 10 days, with 1 μM YODA1 or dimethylsulfoxide (DMSO) stimulation from day 3 to 10. Gene expression was assessed relative to *GAPDH* expression. (A) Compared to exposure to DMSO, exposure to 1 μM YODA1 decreased *GPA* mRNA expression (x0.49±0.17), *β-globin* RNA expression (x0.4±0.26) and *α-globin* RNA expression (x0.3±0.24). (B) Compared to exposure to DMSO, exposure to 1 μM YODA1 increased the *GATA2/GATA1* mRNA ratio (x6.2±1.9). (C) Stimulation with 1 μM YODA1 increased *STAT5A* and *BMI-1* expression, and decreased *EPOR*, *SLC4A1*, *ALAS2*, and *AHSP* mRNA expression. (n=3 for all experiments); ***P<0.001; **P<0.01; *P<0.05.

(n=3), HX#2 (n=3), and HX#10(n=3)] were used; CD34+ cells were sorted and cultured in erythroid medium. Alternatively, for nine non-phlebotomized patients, MNC were purified from 12 blood samples and were grown directly in the same medium. For controls, we used magnetically sorted CD34+ cells from mobilized peripheral blood MNC (n=5), and MNC from healthy control blood samples (n=9). At day 10, we observed a clear delay in erythroid differentiation for seven of the ten *PIEZO1*-HX mutations (8/14 patients), as shown by a decrease in mature CD71+/GPA^{High} cells (Figure 7A from sorted CD34+ cells and 7B from MNC). A moderate but visible delay

was observed for the three other *PIEZO1*-HX mutations (6/14 patients). The intensity of the phenotype was heterogeneous from one mutation to another (Figure 7B), but was reproducible for a given mutation (Figure 7A). For one patient (HX#1), MNC and CD34+ cells were cultured in parallel and a similar phenotype was observed (one representative dot plot is shown Figure 7C). Cytological analyses after staining with May-Grünwald-Giemsa performed in triplicate for this patient confirmed the delayed erythroid differentiation, showing accumulation of immature erythroblasts (Figure 7D, E). MFC data for all HX mutations and controls are shown in *Online Supplementary*
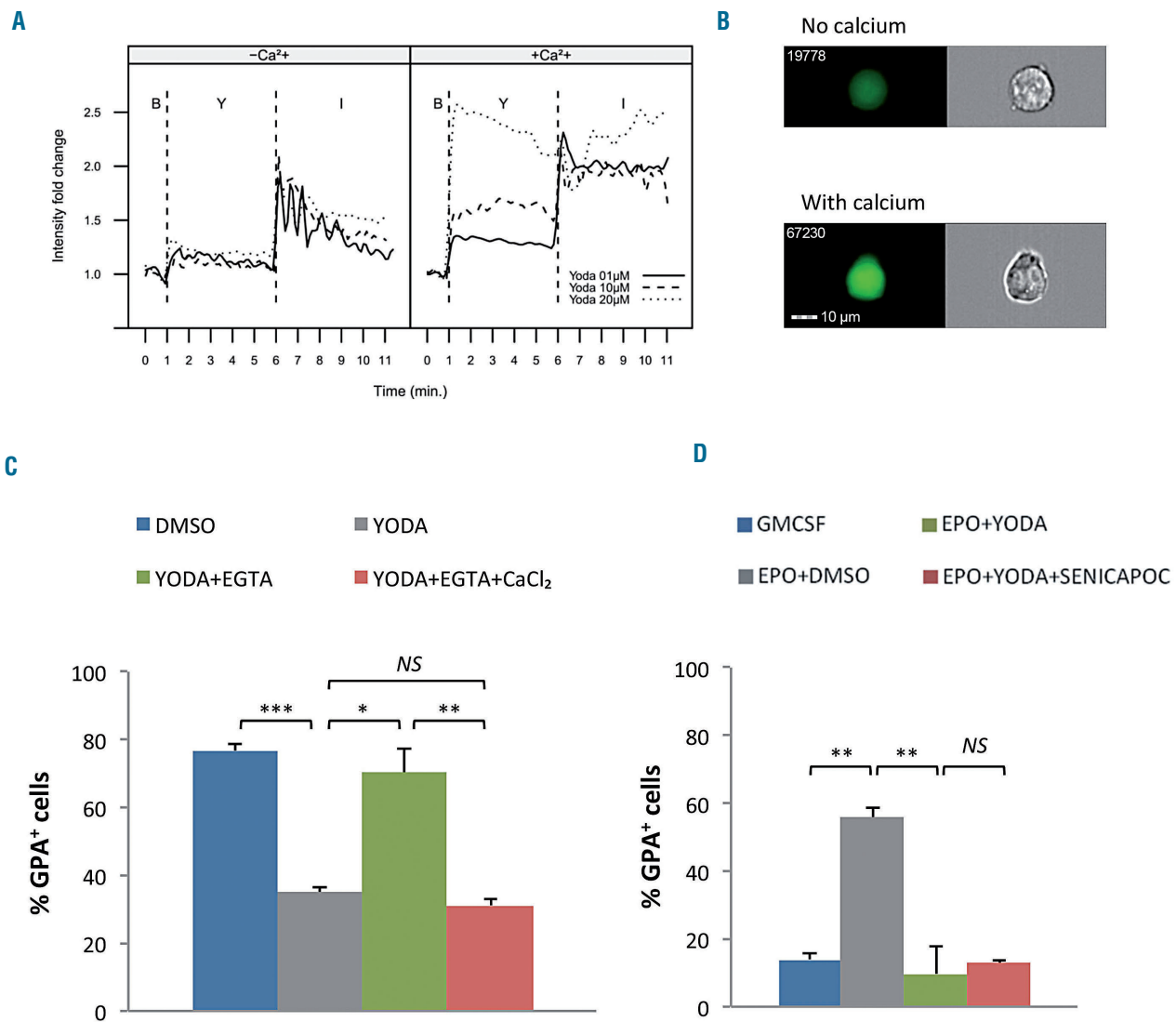
Figure 5. The effect of PIEZO1 activation on erythroid differentiation is calcium-dependent but does not involve a secondary activation of the Gardos channel. (A and B) Cells were incubated with Fluo4-AM for 30 min before stimulation with 5 μM YODA1. (C and D) UT7/EPO cells were cultured for 72 h after drug stimulation. (A) YODA1 stimulation caused a dose-dependent increase in cytosolic calcium concentration in a calcium-containing medium (+Ca^{2+}, right panel). No effect was seen in a calcium-free medium (-Ca^{2+}, left panel). YODA1 stimulation ("Y") was performed 60 s after the baseline recording ("B"), before recording for 300 s. The YODA1 concentration was 1 μM (solid line), 10 μM (dashed line), or 20 μM (dotted line). The positive control for an intracellular Ca^{2+} increase was stimulation with 1 μM ionomycin ("I") recording for 300 s. The image shown here is representative of three identical experiments. (B) Image of intracellular Ca^{2+} content assessed by ImageStreamX using Fluo4-AM cell permeant, after stimulation with 20 μM YODA1 in Ca^{2+}-containing (lower panel) or Ca^{2+}-free (upper panel) medium. (C) In UT7/EPO cells, exposure to 5 μM YODA1 decreased glycophorin A (GPA) expression (35±1.4%) compared to the expression following exposure to dimethylsulfoxide (DMSO) (77±2%). Extracellular Ca^{2+} chelation using 2 mM ethylene glycol tetra-acetic acid (EGTA) prevented the GPA decrease due to YODA1 (70±7%), and the effect was rescued by adding 2 mM extra calcium chloride (31±2%). (D) Co-exposure with 4 μM Senicapoc, a selective Gardos channel inhibitor, did not block the GPA decrease (13±1%) due to YODA1 stimulation (10±8%, *P=NS*) in erythropoietin (EPO)-containing medium, compared to DMSO (56±3%). (n=3 for all experiments; ***$P<0.001$; **$P<0.01$; *$P<0.05$). GMCSF: granulocyte-macrophage colony-stimulating factor.
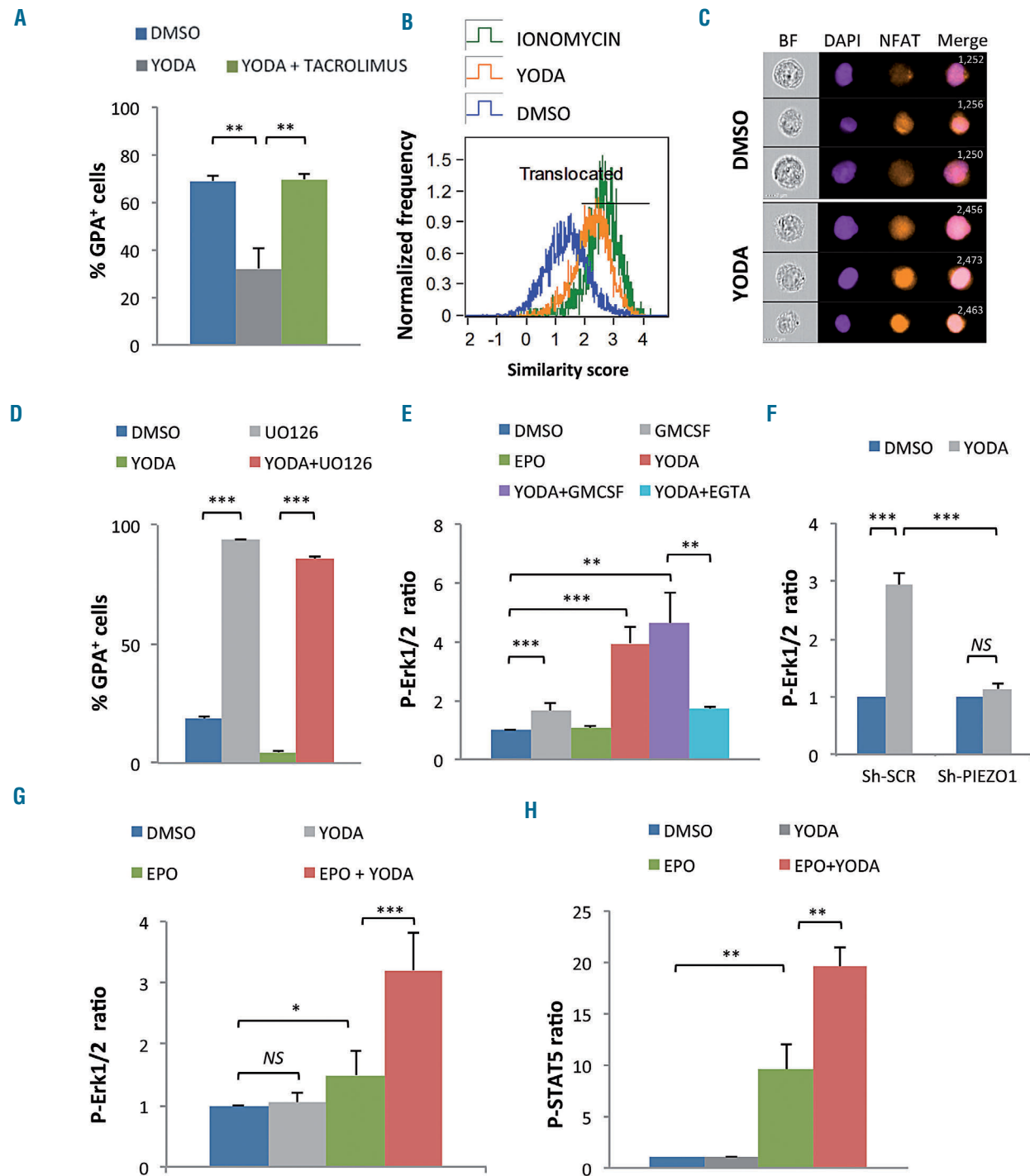
Figure 6. YODA1 activates NFAT, ERK and STAT5 pathways in erythroid cells. (A) The decrease in glycophorin A (GPA) in UT7/EPO cells after exposure to 5 μM YODA1 was blocked by concomitant exposure to 5 μM tacrolimus (32±8% *vs.* 70±2.5%). (B) NFAT nuclear translocation secondary to exposure to 10 μM YODA1, assessed on ImageStream®X by the similarity score (SS) value in UT7/EPO cells, after overnight starvation of serum and erythropoietin (EPO). The SS is a mathematical tool used in Amnis IDEAS® software to assess the co-localization of a fluorescent signal (NFATc1-PE) and 4',6-diamidino-2-phenylindole (DAPI) nuclear staining. A high SS value means a highly translocated state. (C) Images of NFATc1 cellular localization using live imaging flow cytometry. After exposure to dimethylsulfoxide (DMSO), NFATc1 was preferentially localized in the cytosol, whereas 10 μM YODA1 increased NFATc1 nuclear translocation. Images were extracted from Amnis IDEAS® software for mean SS values of each condition. (D) In UT7/GM cells, 10 μM UO126 induced high glycophorin A (GPA) expression (94±0.2%) compared to that following exposure to DMSO (18±2%) in medium containing granulocyte-monocyte colony-stimulating factor (GMCSF), and reverted the YODA1-mediated GPA repression when EPO was added (86±1%). Cells were incubated with UO126 for 30 min before stimulation with 5 μM YODA1, then cultured for 72 h. (E) ERK phosphorylation assessed by PhosphoFlow in UT7/GM cells. Values shown are the p-ERK ratio relative to DMSO alone. GMCSF induced mild ERK phosphorylation (x1.65±0.27) whereas 10 U/mL EPO did not (x1.06±0.1, *P=NS*). YODA1 (10 μM) induced strong ERK phosphorylation (x3.96±0.581), an effect that was markedly inhibited by 2 mM ethylene glycol tetra-acetic acid (EGTA) (x1.71±0.05). (F) ERK phosphorylation assessed by PhosphoFlow in UT7/EPO cells. Sh-RNA-mediated PIEZO1 knockdown inhibited the 10 μM YODA1-induced ERK phosphorylation (fold P-ERK increase in Sh-SCR-transduced cells: *x*2.93±0.2; in Sh-PIEZO1-transduced cells: x1.13±0.1). (G) ERK phosphorylation assessed by PhosphoFlow in primary human CD34+-derived erythroid cells. YODA1 did not induce ERK phosphorylation (x1.04±0.16, *P=NS*), whereas 5 U/mL EPO did moderately (x1.49±0.4). YODA1 synergized with EPO to induce ERK phosphorylation (x3.21±0.62). (H) STAT5 phosphorylation assessed by PhosphoFlow in primary human CD34+-derived erythroid cells. Compared to DMSO, YODA1 did not induce STAT5 phosphorylation (x1.03±0.09, *P=NS*), whereas EPO did (x9.6±2.4), and YODA1 enhanced EPO-driven STAT5 phosphorylation (x19.6±1.9). (n=3 in A and D, and n=4 in all other experiments); ***P<0.001 ; **P<0.01; *P<0.05

Figures S8 and *S9*. Cultures of cells from four patients could be driven beyond day 10 and showed progressive terminal maturation and enucleation, but at a heterogeneous rate, confirming that erythroid differentiation was delayed but not totally blocked (*Online Supplementary Figure S10*).

Discussion

The mechanotransductor PIEZO1 has a well-described role in regulating hydration and volume of mature erythrocytes.[12,28] Indeed, activating mutations are responsible for most HX cases and, recently, a frequent polymorphism (E756del) has been associated with resistance to malaria in African populations,[29,30] although its influence on red cell hydration status is still controversial.[31] *PIEZO1* expression during erythropoiesis has been previously studied using RNA-sequencing analysis, the results of which were in agreement with our data that *PIEZO1* is expressed in early progenitors[14] and decreases during terminal maturation.[23] These findings were confirmed at a protein level by extensive proteomic analyses of human erythroid differentiation.[24] Whether PIEZO1 has a specific role during erythropoiesis is not known, although evoked in recent case reports.[19,32] Our data show for the first time that PIEZO1 is expressed and functional in erythroid progenitors, and that its activation influences erythroid differentiation, both in leukemic cell lines and primary erythroid cells. Indeed, PIEZO1 activation maintained cells at an immature GPA^{low} stage for longer and tilted the transcriptional balance in favor of genes associated with an immature stage, such as *GATA2* and *BMI1*, at the expense of genes associated with terminal differentiation, such as *GATA1*, *GPA*, *ALAS2* or *α* and *β globin* without myeloid bias.[33,34] Of

note, we used the chemical activator YODA1 to evaluate the effects of PIEZO1 on erythropoiesis.[25] The phenotype was dependent on PIEZO1 since it was abrogated after Sh-RNA mediated *PIEZO1* knockdown, and was also confirmed in erythroid cells from HX patients carrying *PIEZO1* gain-of-function mutations. Interestingly, we observed that *PIEZO1* knockdown using a Sh-RNA strategy enhanced erythroid differentiation in UT7 cells. Since PIEZO1 activation was associated with an undifferentiated state in UT7 cells, we may assume that a low PIEZO1 level at the cell surface could lead to a lower "basal" activation rate and favor cell differentiation at the expense of cell proliferation. Of note, it was intriguing that a 50% reduction of PIEZO1 expression was sufficient to revert the YODA1-mediated effects. Although the GFP intensity determined the strength of YODA1 blockade, Sh-PIEZO1 significantly - but not totally - blocked the effects of YODA1 in GFP intermediate cells. This may argue for a threshold effect of PIEZO1, which could be further confirmed in patch-clamp experiments.

PIEZO1 is known as a non-selective cation channel.[7] We showed that the effect of PIEZO1 activation on erythropoiesis was Ca^{2+}-dependent, as described in mature red cells as well as in many other 'PIEZO1-sensitive' cells such as endothelial, urothelial, and epithelial cells.[5,15–17] However, the consequences of a PIEZO1-mediated increase in intracellular Ca^{2+} may depend on the cell type. In mature red cells, the observed phenotype (i.e., red cell dehydration) occurs because of a secondary activation of the Gardos channel, which in turn exports K$^+$ and induces loss of water.[13] The effects of PIEZO1 on erythropoiesis seem not to occur through this pathway, since the Gardos inhibitor Senicapoc could not revert the phenotype. Ca^{2+} influx has previously been shown to be involved during erythropoiesis. Notably, it has been suggested that EPO

Table 1. Characteristics of the 14 patients, 11 families and 10 *PIEZO1* mutations, number of patients and family per mutation and main hematologic features.

Mutation Id	Patient n/ Family n	Exon	*PIEZO1* mutation cDNA	Protein	Age	Hb (g/L)	MCV (fL)	Reticulocytes x10⁹/L	Ferritin (μg/L)	MRI (μmol/g)	N. of experiments	Erythroid phenotype
HX#1	1/1	14	c.1792G>A	p.Val598Met	43	144	107	404	828	190	N=3	High
HX#2	2/2	18 18	c.2344G>A c.2423G>A	p.Gly782Ser p.Arg808Gln	55	142	101	441	613	95	N=3	High
HX#3	3/3 4/3	42 42	c.6058G>A* c.6058G>A*	p.Ala2020Thr p.Ala2020Thr	31 61	146 174	85 91	173 293	30 980	NA 104	N=1 N=1	Mild/moderate Mild/moderate
HX#4	5/4	42	c.6007G>A c.7471C>T	p.Ala2003Thr p.Arg2491Trp	24	118	99	451	86	NA	N=3	High
HX#5	6/5	51	c.7391A>C	p.His2464Pro	36	181	87	205	71	NA	N=1	High
HX#6	7/6	16	c.2152G>A c.7463G>A#	p.Gly718Ser p.Arg2488Gln	51	152	93	167	119	34	N=1	Mild/moderate
HX#7	8/7	51	c.7529C>T	p.Pro2510Leu	43	112	83	183	NA	NA	N=1	High
HX#8	9/8	16	c.2042T>C	p.Phe681Ser	44	145	102	248	86	15	N=1	High
HX#9	10/9	51	c.7367G>A*	p.Arg2456His	63	112	120	288	535	200	N=2	High
HX#10	11/10 12/10 13/10	16	c.2005G>T c.2005G>T c.2005G>T	p. Asp669Tyr p. Asp669Tyr p. Asp669Tyr	62 39 35	141 142 149	98 104 107	249 496 290	1000 889 507	330 NA 180	N=1 N=1 N=1	Mild/moderate Mild/moderate Mild/moderate
HX#11	14/11	51	c.7367G>A*	p.Arg2456His	78	129	85	221	600	NA	N=1	High

*Functional studies showing slower PIEZO1 inactivation kinetics.[8,12] #: Functional studies showing a lower PIEZO1 activation threshold.[8] Ferritin assays and magnetic resonance imaging evaluation of iron liver content were performed at diagnosis or before iron chelation/phlebotomy. Patients HX#9 and HX#11, from two different families, had the same *PIEZO1* mutation. Id: identity; Hb: hemoglobin; MCV: mean corpuscular volume; MRI: magnetic resonance imaging.

could indirectly regulate Ca^{2+} currents by modulating Ca^{2+}-channel expression at the cell surface.[35,36] However, consequences on erythroid maturation remain largely unknown. Ca^{2+} signaling is required during enucleation in mice,[37] but we did not observe any effect on enucleation rate when PIEZO1 was activated in the last step of differentiation (*data not shown*). In contrast, we did observe that Ca^{2+} influx through PIEZO1 had an early effect on erythro-

poiesis and noticed that NFAT, ERK1/2 and STAT5 were activated by PIEZO1-dependent Ca^{2+} entry in erythroid cells. In particular, we found that ERK was strongly phosphorylated by YODA1. ERK phosphorylation was inhibited after *PIEZO1* knockdown, a result contrasting with a recent study showing that YODA1 phosphorylated ERK in endothelial cells in a PIEZO1-independent manner.[38] However, this observation was made using chemical
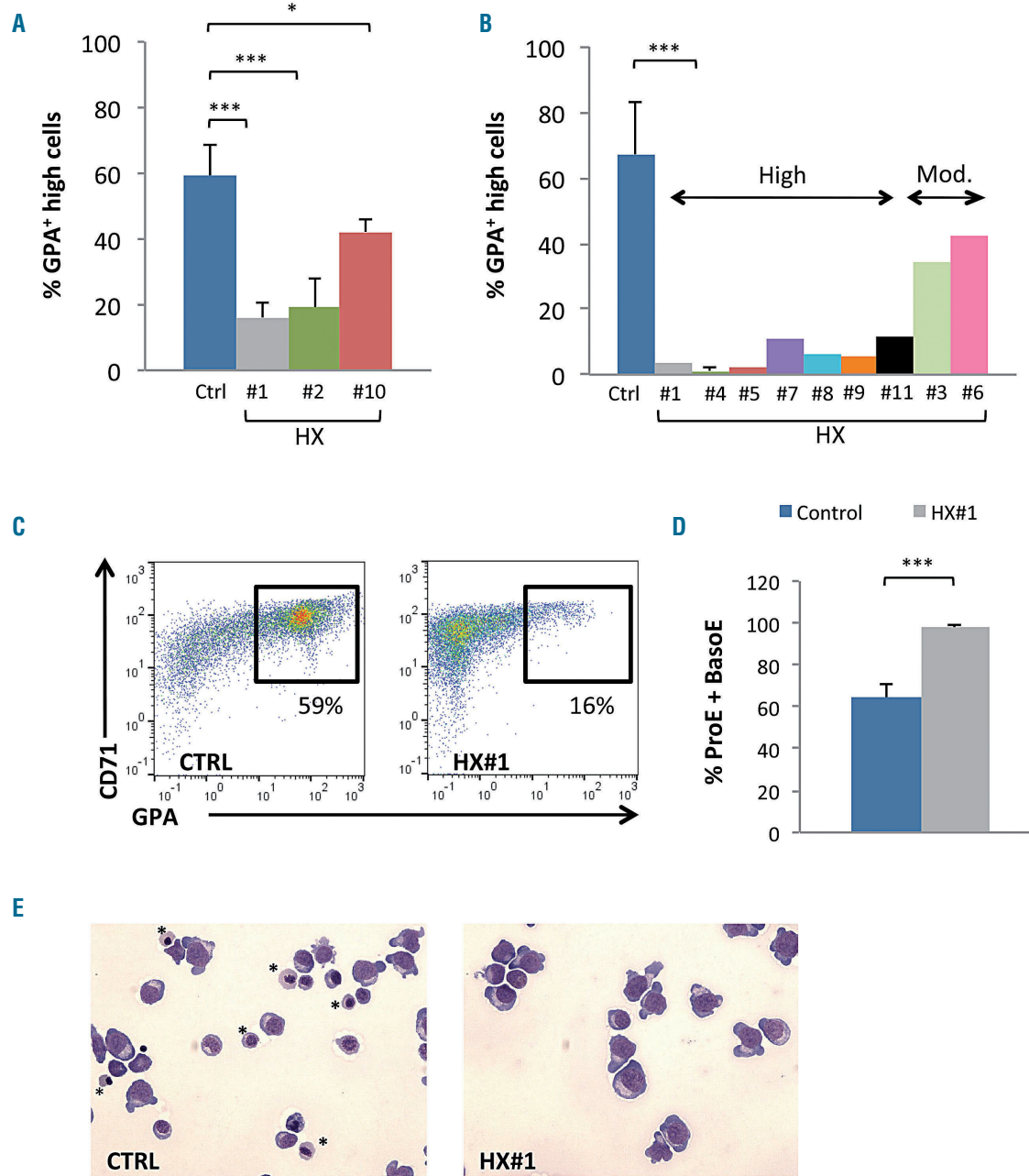
Figure 7. Delay in erythroid differentiation of progenitor cells obtained from patients with *PIEZO1*-mutated hereditary xerocytosis. (A) Culture of CD34+-derived erythroid cells from patients with hereditary xerocytosis (HX); differentiation was assessed at day 10 by multiparametric flow cytometry (MFC). The mean percentage of CD71+/GPA^High cells was 59±9% in control samples, 16±5% in HX#1 (*P*<0.001), 19±9% in HX#2 (*P*<0.01), and 42±4% in HX#10 (P<0.05). (n=5 for control samples; n=3 for HX#1, 2 and 10). (B) Culture of mononuclear cells from HX patients; differentiation assessed on day 10 by MFC (n=9 for control samples; n=3 for HX#4; n=1 for HX#1-11). The mean percentage of CD71+/GPA^High cells was 71±17% in the control group, and ranged from 0.3% to 11.7% in the "high delay" group and from 22.5% to 44% in the "moderate delay" group. (C) Illustrative CD71/GPA MFC plots at day 10 of erythroid differentiation of CD34+ cells obtained from patient HX#1 (right) and from one representative control sample (left). (D) Cytological analysis after staining with May-Grünwald-Giemsa (MGG): count of immature erythroblasts [proerythroblasts (ProE) and basophilic erythroblasts (BasoE)] on day 10, x200 magnification. Immature erythroblasts were 64.2±6.2% in control samples *vs.* 97.7±1.5% in HX#1 (n=6 control samples; n=3 for patient HX#1). (E) Example of cytology on day 10 for patient HX#1 (right) and for a control sample (left), MGG staining, x200 magnification. *show orthochromatic erythroblasts. ***P<0.001; **P<0.01; *P<0.05.

PIEZO1 inhibitors, which are much less specific than a Sh-RNA based strategy. The PIEZO1-Ca²⁺-ERK axis has been described in epithelial cells, in which it regulated the cell cycle and survival.[15] Whether Ca²⁺ entry into erythroblasts through PIEZO1 was sufficient to activate the ERK pathway by itself or whether it triggered secondary pathways is under investigation. ERK1/2 activation has been shown to promote early human progenitor cell expansion and its constitutive activation in mice blocked differentiation of fetal liver erythroid progenitor cells.[39-41] Alternatively, ERK activation through EPO has been shown to promote erythroid differentiation in a MASL1-dependent manner.[42] This discrepancy in the role of ERK1/2 in erythroid differentiation may depend on its activation level. Our results showed that PIEZO1 activation synergized both EPO-dependent ERK and STAT5 phosphorylation in primary erythroblasts, suggesting that PIEZO1 may act as a modulator of EPO signaling during human erythropoiesis. Previous data suggested that erythroid regulation involved balanced STAT5 and ERK1/2 phosphorylation, and we assume that PIEZO1 may modify this equilibrium to delay erythroid terminal differentiation.[43] Of note, YODA1-sustained ERK1/2 activation in UT7/GM cells did not promote cell proliferation, in contrast to other cell types, but instead led to accumulation in the G0/G1 phase of the cell cycle.[41,44] This may be due to the fact that YODA1 phosphorylated ERK1/2 but not STAT5 in UT7/GM cells in which proliferation was mainly dependent on STAT5. Alternatively, PIEZO1 activation could modulate cell cycle regulators as previously shown in canine epithelial cells.[6] This highlights the heterogeneous role of PIEZO1 activation, which differs depending on the type of cell. We also showed that the effects of YODA1 required NFAT activation and nuclear translocation, which have been involved in mice erythropoiesis.[45] Whether this pathway also depends on EPO signaling is under investigation.

Erythroid cells from HX patients carrying *PIEZO1* gain-of-function mutations had a similar phenotype as the one observed after PIEZO1 chemical activation. This highlights the pathophysiological relevance of this ion channel, proving that how PIEZO1 is activated (i.e., constitutive mutation *vs.* chemical activation) is not critical. Moreover, it suggests that the HX erythroid phenotype may involve a certain degree of impaired erythropoiesis, as evoked in two recent case reports, which may participate in the high rate of iron overload described in these patients.[8,19,22,32] However, the delay in erythroid differentiation does not translate into anemia since most patients have a totally compensated hemolysis. First, dyserythropoiesis may be mild *in vivo*. Second, it has been suggested that *PIEZO1*-HX red blood cells have an increased hemoglobin affinity for oxygen.[46] Therefore, hemoglobin level could represent a balance between factors that tend to decrease it (hemolysis, dyserythropoiesis) and factors that tend to increase it (hemoglobin hyperaffinity). We were unable to find a clear correlation between *in vivo* erythrocyte parameters in HX patients and the *in vitro* erythroid phenotype. This may be due to different mechanisms involved, since mature red cell dehydration is known to be Gardos-dependent while the YODA1-induced erythroid delay was insensitive to Senicapoc. However, it would be of great interest to correlate, for each mutation, the intensity of the erythroid phenotype with functional tests such as high-throughput patch clamping on red cells.[47] Alternatively, modeling the different HX mutations through viral transduction in normal erythroid progenitors would represent an interesting way to better understand the disease heterogeneity and to highlight the potential role of other genetic factors that may modulate the phenotype.

In summary, we describe here a role for PIEZO1 during human erythroid differentiation, in erythroleukemic cell lines, in normal primary erythroblasts after exposure to YODA1, and in primary cells from HX patients carrying an activating *PIEZO1* mutation. We observed a delay in terminal erythroid maturation which depended on Ca²⁺ entry, and NFAT, STAT5 and ERK1/2 pathway activation. We observed that PIEZO1 could synergize with EPO-signaling during human erythropoiesis and that its constitutive activation in HX led to impairment in proliferation and differentiation of erythroid progenitors, highlighting a new pathophysiological mechanism in this rare disorder.

References

1. Coste B, Mathur J, Schmidt M, et al. Piezo1 and Piezo2 are essential components of distinct mechanically activated cation channels. Science. 2010;330(6000):55-60.
2. Saotome K, Murthy SE, Kefauver JM, Whitwam T, Patapoutian A, Ward AB. Structure of the mechanically activated ion channel Piezo1. Nature. 2018;554(7693):481-486.
3. Zhao Q, Zhou H, Chi S, et al. Structure and mechanogating mechanism of the Piezo1 channel. Nature. 2018;554(7693):487-492.
4. Cinar E, Zhou S, DeCourcey J, Wang Y, Waugh RE, Wan J. Piezo1 regulates mechanotransductive release of ATP from human RBCs. Proc Natl Acad Sci U S A. 2015;112(38):11783-11788.
5. Cahalan SM, Lukacs V, Ranade SS, Chien S, Bandell M, Patapoutian A. Piezo1 links mechanical forces to red blood cell volume. Elife. 2015;4.
6. Wu J, Young M, Lewis AH, Martfeld AN, Kalmeta B, Grandl J. Inactivation of mechanically activated Piezo1 ion channels is determined by the C-terminal extracellular domain and the inner pore helix. Cell Rep. 2017;21(9):2357-2366.
7. Gnanasambandam R, Bae C, Gottlieb PA, Sachs F. Ionic selectivity and permeation properties of human PIEZO1 channels. PLoS One. 2015;10(5):e0125503.
8. Andolfo I, Alper SL, De Franceschi L, et al. Multiple clinical forms of dehydrated hereditary stomatocytosis arise from mutations in PIEZO1. Blood. 2013;121(19):3925-3935.
9. Zarychanski R, Schulz VP, Houston BL, et al. Mutations in the mechanotransduction protein PIEZO1 are associated with hereditary xerocytosis. Blood. 2012;120(9):1908-1915.
10. Albuisson J, Murthy SE, Bandell M, et al. Dehydrated hereditary stomatocytosis linked to gain-of-function mutations in mechanically activated PIEZO1 ion channels. Nat Commun. 2013;4:1884.
11. Bae C, Gnanasambandam R, Nicolai C, Sachs F, Gottlieb PA. Xerocytosis is caused by mutations that alter the kinetics of the mechanosensitive channel PIEZO1. Proc Natl Acad Sci U S A. 2013;110(12):E1162-1168.

12. Glogowska E, Schneider ER, Maksimova Y, et al. Novel mechanisms of PIEZO1 dysfunction in hereditary xerocytosis. Blood. 2017;130(16):1845-1856.
13. Rapetti-Mauss R, Picard V, Guitton C, et al. Red blood cell Gardos channel (KCNN4): the essential determinant of erythrocyte dehydration in hereditary xerocytosis. Haematologica. 2017;102(10):e415-e418.
14. Li J, Hale J, Bhagia P, et al. Isolation and transcriptome analyses of human erythroid progenitors: BFU-E and CFU-E. Blood. 2014;124(24):3636-3645.
15. Gudipaty SA, Lindblom J, Loftus PD, et al. Mechanical stretch triggers rapid epithelial cell division through Piezo1. Nature. 2017;543(7643):118-121.
16. Miyamoto T, Mochizuki T, Nakagomi H, et al. Functional role for Piezo1 in stretch-evoked Ca2+ influx and ATP release in urothelial cell cultures. J Biol Chem. 2014;289(23):16565-16575.
17. Li J, Hou B, Tumova S, et al. Piezo1 integration of vascular architecture with physiological force. Nature. 2014;515(7526):279-282.
18. Del Mármol JI, Touhara KK, Croft G, MacKinnon R. Piezo1 forms a slowly-inactivating mechanosensory channel in mouse embryonic stem cells. Elife. 2018;7.
19. Park J, Jang W, Han E, et al. Hereditary dehydrated stomatocytosis with splicing site mutation of PIEZO1 mimicking myelodysplastic syndrome diagnosed by targeted next-generation sequencing. Pediatr Blood Cancer. 2018;65(7):e27053.
20. Garçon L, Lacout C, Svinartchouk F, et al. Gfi-1B plays a critical role in terminal differentiation of normal and transformed erythroid progenitor cells. Blood. 2005;105(4):1448-1455.
21. Walrafen P, Verdier F, Kadri Z, Chrétien S, Lacombe C, Mayeux P. Both proteasomes and lysosomes degrade the activated erythropoietin receptor. Blood. 2005;105(2):600-608.
22. Picard V, Guitton C, Thuret I, et al. Clinical and biological features in PIEZO1-hereditary xerocytosis and Gardos-channelopathy: a retrospective series of 126 patients. Haematologica. 2019;104(8):1554-1564.
23. An X, Schulz VP, Li J, et al. Global transcriptome analyses of human and murine terminal erythroid differentiation. Blood. 2014;123(22):3466-3477.
24. Gautier E-F, Ducamp S, Leduc M, et al. Comprehensive proteomic analysis of human erythropoiesis. Cell Rep. 2016;16(5):1470-1484.
25. Syeda R, Xu J, Dubin AE, et al. Chemical activation of the mechanotransduction channel Piezo1. Elife. 2015;4.
26. Hu J, Liu J, Xue F, et al. Isolation and functional characterization of human erythroblasts at distinct stages: implications for understanding of normal and disordered erythropoiesis in vivo. Blood. 2013;121(16):3246-3253.
27. Hogan PG. Transcriptional regulation by calcium, calcineurin, and NFAT. Genes Dev. 2003;17(18):2205-2232.
28. Gallagher PG. Disorders of erythrocyte hydration. Blood. 2017;130(25):2699-2708.
29. Caulier A, Rapetti-Mauss R, Guizouarn H, Picard V, Garçon L, Badens C. Primary red cell hydration disorders: pathogenesis and diagnosis. Int J Lab Hematol. 2018;40 (Suppl 1):68-73.
30. Ma S, Cahalan S, LaMonte G, et al. Common PIEZO1 allele in African populations causes RBC dehydration and attenuates Plasmodium infection. Cell. 2018;173(2):443-455.e12.
31. Rooks H, Brewin J, Gardner K, et al. A gain of function variant in PIEZO1 (E756del) and sickle cell disease. Haematologica. 2019;104(3):e91-e93.
32. Paessler M, Hartung H. Dehydrated hereditary stomatocytosis masquerading as MDS. Blood. 2015;125(11):1841.
33. Moriguchi T, Yamamoto M. A regulatory network governing Gata1 and Gata2 gene transcription orchestrates erythroid lineage differentiation. Int J Hematol. 2014;100(5):417-424.
34. Hattangadi SM, Wong P, Zhang L, Flygare J, Lodish HF. From stem cell to red cell: regulation of erythropoiesis at multiple levels by multiple proteins, RNAs, and chromatin modifications. Blood. 2011;118(24):6258-6268.
35. Cheung JY, Zhang XQ, Bokvist K, Tillotson DL, Miller BA. Modulation of calcium channels in human erythroblasts by erythropoietin. Blood. 1997;89(1):92-100.
36. Chu X, Cheung JY, Barber DL, et al. Erythropoietin modulates calcium influx through TRPC2. J Biol Chem. 2002;277(37):34375-34382.
37. Wölwer CB, Pase LB, Russell SM, Humbert PO. Calcium signaling is required for erythroid enucleation. PLoS ONE. 2016;11(1):e0146201.
38. Dela Paz NG, Frangos JA. Yoda1-induced phosphorylation of Akt and ERK1/2 does not require Piezo1 activation. Biochem Biophys Res Commun. 2018;497(1):220-225.
39. Sui X, Krantz SB, You M, Zhao Z. Synergistic activation of MAP kinase (ERK1/2) by erythropoietin and stem cell factor is essential for expanded erythropoiesis. Blood. 1998;92(4):1142-1149.
40. Zhang J, Socolovsky M, Gross AW, Lodish HF. Role of Ras signaling in erythroid differentiation of mouse fetal liver cells: functional analysis by a flow cytometry-based novel culture system. Blood. 2003;102(12):3938-3946.
41. Zhang J, Lodish HF. Constitutive activation of the MEK/ERK pathway mediates all effects of oncogenic H-ras expression in primary erythroid progenitors. Blood. 2004;104(6):1679-1687.
42. Kumkhaek C, Aerbajinai W, Liu W, et al. MASL1 induces erythroid differentiation in human erythropoietin-dependent CD34+ cells through the Raf/MEK/ERK pathway. Blood. 2013;121(16):3216-3227.
43. Arcasoy MO, Jiang X. Co-operative signalling mechanisms required for erythroid precursor expansion in response to erythropoietin and stem cell factor. Br J Haematol. 2005;130(1):121-129.
44. Marshall CJ. Specificity of receptor tyrosine kinase signaling: transient versus sustained extracellular signal-regulated kinase activation. Cell. 1995;80(2):179-185.
45. Giampaolo S, Wójcik G, Klein-Hessling S, Serfling E, Patra AK. NFAT-mediated defects in erythropoiesis cause anemia in Il2-/- mice. Oncotarget. 2018;9(11):9632-9644.
46. Kiger L, Guitton C, Ghazal K, et al. Physiopathology of hereditary xerocytosis: Piezo gain of function mutations impact hemoglobin oxygen. Haematologica. 2017;102(s2):446.
47. Rotordam GM, Fermo E, Becker N, et al. A novel gain-of-function mutation of Piezo1 is functionally affirmed in red blood cells by high-throughput patch clamp. Haematologica. 2019;104(5):e179-e183.

A novel, highly potent and selective phosphodiesterase-9 inhibitor for the treatment of sickle cell disease

James G. McArthur,[1] Niels Svenstrup,[2] Chunsheng Chen,[3] Aurelie Fricot,[4] Caroline Carvalho,[4] Julia Nguyen,[3] Phong Nguyen,[3] Anna Parachikova,[2] Fuad Abdulla,[3] Gregory M. Vercellotti,[3] Olivier Hermine,[4] Dave Edwards,[5] Jean-Antoine Ribeil,[6] John D. Belcher[3] and Thiago T. Maciel[4]

[1]Imara Inc., 2nd Floor, 700 Technology Square, Cambridge, MA, USA; [2]H. Lundbeck A/S, Ottiliavej 9, 2500 Valby, Denmark; [3]Department of Medicine, Division of Hematology, Oncology and Transplantation, University of Minnesota, Minneapolis, MN, USA; [4]INSERM UMR 1163, CNRS ERL 8254, Imagine Institute, Laboratory of Excellence GR-Ex, Paris Descartes - Sorbonne Paris Cité University, Paris, France; [5]Kinexum, 8830 Glen Ferry Drive, Johns Creek, GA, USA and [6]Departments of Biotherapy, Necker Children's Hospital, Assistance Publique-Hôpitaux de Paris (AP-HP), Paris Descartes-Sorbonne Paris Cité University, Paris, France

ABSTRACT

The most common treatment for patients with sickle cell disease (SCD) is the chemotherapeutic hydroxyurea, a therapy with pleiotropic effects, including increasing fetal hemoglobin (HbF) in red blood cells and reducing adhesion of white blood cells to the vascular endothelium. Hydroxyurea has been proposed to mediate these effects through a mechanism of increasing cellular cGMP levels. An alternative path to increasing cGMP levels in these cells is through the use of phosphodiesterase-9 inhibitors that selectively inhibit cGMP hydrolysis and increase cellular cGMP levels. We have developed a novel, potent and selective phosphodiesterase-9 inhibitor (IMR-687) specifically for the treatment of SCD. IMR-687 increased cGMP and HbF in erythroid K562 and UT-7 cells and increased the percentage of HbF positive erythroid cells generated *in vitro* using a two-phase liquid culture of CD34+ progenitors from sickle cell blood or bone marrow. Oral daily dosing of IMR-687 in the Townes transgenic mouse SCD model, increased HbF and reduced red blood cell sickling, immune cell activation and microvascular stasis. The IMR-687 reduction in red blood cell sickling and immune cell activation was greater than that seen with physiological doses of hydroxyurea. In contrast to other described phosphodiesterase-9 inhibitors, IMR-687 did not accumulate in the central nervous system, where it would inhibit phosphodiesterase-9 in neurons, or alter rodent behavior. IMR-687 was not genotoxic or myelotoxic and did not impact fertility or fetal development in rodents. These data suggest that IMR-687 may offer a safe and effective oral alternative for hydroxyurea in the treatment of SCD.

Introduction

Sickle cell disease (SCD) is a genetic disease arising from a point mutation in the *HBB* gene that leads to the polymerization of hemoglobin S (HbS) during deoxygenation.[1-5] HbS forms long chains of polymers that deform red blood cells (RBC) into a sickle shape, which impairs RBC transit in smaller blood vessels and renders them prone to hemolysis.[6,7] Increased RBC lysis and release of free HbS scavenges nitric oxide (NO) and promotes vasoconstriction, which further alters vascular biology.[8-10] This process in turn promotes the activation and mobilization of white blood cells (WBC), increasing their adhesiveness to activated endothelium.[11-16] These pathological manifestations in RBC and WBC in SCD ultimately result in painful vaso-occlusive crises, end-organ damage, and, in many cases, premature death.[17-19]

Hydroxyurea (HU) was the first approved disease modifying therapy for SCD.[20-24] HU was originally developed as a chemotherapeutic agent, and is believed to mitigate disease pathology and organ damage sequelae by increasing RBC expression of fetal hemoglobin (HbF) and reducing WBC counts.[8,23,25-27] HU has been proposed to stimulate soluble guanyl cyclase, resulting in the elevation of cellular cGMP levels and activation of protein kinase G, which ultimately induces HbF expression.[26] HU may also indirectly affect NO biology as a result of these activities, or directly increase NO levels. Despite its activity on multiple pathways that can improve SCD pathophysiology, HU is under-used in patients with SCD and often underdosed.[28,29] Use of HU is challenged by responder effects and the careful safety monitoring required due to its myelosuppressive properties, and by concerns about toxicities, including HU impact on fertility and long-term carcinogenic potential.[30-35] As a result of these risks, female and male patients are advised to discontinue HU therapy when trying to conceive or during pregnancy.

The cGMP specific phosphodiesterase 9 (PDE9) enzyme degrades cGMP and therefore PDE9 inhibitors (PDE9i) increase intracellular cGMP levels recapitulating the HbF induction mechanism of HU.[36-38] PDE9 is highly expressed in erythropoietic cells, and is further elevated in neutrophils and reticulocytes from patients with SCD.[39] A PDE9i originally developed for the treatment of neurodegenerative diseases (BAY73-6691) has been shown to increase HbF transcripts in K562 cells.[38] BAY73-6691 also reduced WBC adhesion to endothelial cells, the adhesion of patient-derived neutrophils to immobilized fibronectin, leukocyte recruitment to the microvasculature, and, in conjunction with HU, it reduced the lethality of TNF-α induced vaso-occlusion in a mouse model of SCD.[38,40]

We describe here a novel, potent, and selective phosphodiesterase 9A inhibitor (IMR-687) that induced cGMP and HbF in the erythroid cell line K562 and increased HbF expression in erythroid cells derived from multiple SCD patients. In murine SCD models, IMR-687 increased plasma cGMP levels and HbF expression in RBC and impacted a number of disease-relevant features of SCD, including reducing lung inflammation, RBC sickling, and occlusion of micro-vessels. Furthermore, unlike PDE9i that was developed for neurodegenerative diseases, IMR-687 did not alter cognition in mice and, unlike HU, did not induce myelosuppression. In summary, IMR-687 demonstrated disease-relevant improvements in several aspects of SCD with comparable efficacy to HU.

Methods

Phosphodiesterase enzyme inhibition

Phosphodiesterase enzyme (PDE) inhibition IC50 values were determined for IMR-687 using recombinant human PDE enzymes in a radiometric assay.[41]

K562 and UT-7 erythroid cells

Human erythroleukemic K562 and UT-7 cells (American Type Culture Collection) were cultured as described in the *Online Supplementary Methods*. Terminal cell viability was determined by use of a trypan-blue exclusion technique (Thermo Fisher Scientific, France), ATP-based assays (Cell-Titer Glo, Promega), or automated cell counts (Countess Automated Cell Counter, Life Technologies). Apoptosis was assessed by Annexin V FACS assay (Biolegend).

Fetal hemoglobin quantification

K562 cells (5x10^{6}) supernatants were assayed using an ELISA kit for HbF (Cloud Clone Corp, CEA996Hu) (see *Online Supplementary Methods*). Permeabolized cells were stained with PE-mouse anti-human HbF and the percentage of HbF+ cells (% HbF) and the HbF levels (MFI) determined by flow cytometry (see *Online Supplementary Methods*).

Sickle cell disease patient cells

Blood was collected from five adult patients with severe SCD, aged 19-33 years (median age 32 years), admitted to the Biotherapy Department of Necker Hospital for an exchange transfusion. All samples used in this study were obtained from patients who signed informed consent forms approved by the ethical committee of Necker Hospital on 11th September 2015 (study IMNIS2015-01). CD34+ cells were were cultured in the presence of 15% BIT 9500 [mixture of bovine serum albumin (BSA) + insulin + transferrin from Stem Cell Technologies], 100 U/mL penicillin-streptomycin, 2 mM L-glutamine, 10 ng/mL recombinant human (rh) IL-3 (Peprotech), 100 ng/mL rhIL-6 (Peprotech), and 100 ng/mL rhSCF (Peprotech) for seven days and then CD36+ cells, isolated and cultured in media containing 100 ng/mL rhSCF, 10 ng/mL rhIL-3 and 2 UI/mL erythropoetin (Cilag, France) supplemented with dimethyl sulfoxide (DMSO), 30 µM HU or 10 µM IMR-687 for five days, at which point the HbF+ erythroid cells (LD−/GPA+/Band3+) was determined by FACS.

Animals

Townes model. HbSS-Townes mice[42] on a 129/B6 background (Jackson Laboratory, Bar Harbor, ME, USA; 10-12 weeks old, n=7 per group) were dosed daily by gavage with vehicle (polyethylene glycol in water 1:3), 50 or 25 mg/kg of HU, or 30 mg/kg of IMR-687. On day 30, mice were anesthetized and blood counts, spleen weights, and plasma bilirubin, LDH, nitrite, HbF and free Hb determined (see *Online Supplementary Methods*).

Table 1. Phosphodiesterase enzyme (PDE) selectivity of IMR-687.

Enzyme	IC50 (µM)	Enzyme	IC50 (µM)
PDE1A3	88.4	PDE4D4	NI
PDE1B	8.48	PDE4D5	NI
PDE1C	12.2	PDE4D7	NI
PDE2A3	NI	PDE5A1	>100
PDE3A	NI	PDE5A2	81.9
PDE3B	NI	PDE5A3	>100
PDE4A1	>100	PDE6AB	NI
PDE4A4	>100	PDE6C	NI
PDEA10	NI	PDE7A	NI
PDE4B1	NI	PDE7B	>100
PDE4B2	>100	PDE8A1	NI
PDE4B3	>100	PDE8B	NI
PDE4C2	NI	PDE9A1	0.008
PDE4D1	>100	PDE9A2	0.010
PDE4D2	>100	PDE10A2	>100
PDE4D3	NI	PDE11A1	NI

Enzyme inhibition by IMR-687 on human recombinant PDE was demonstrated to be more selective to PDE9 by 1,000-10,000-fold over PDE1A3, 1B, 1C, and PDE5A2 isoforms. No measurable inhibition was observed in PDE2A3, 3A, 3B, 4A1, 4A4, 4A10, 4B1, 4B2, 4B3, 4C2, 4D1, 4D2, 4D3, 4D4, 4D5, 4D7, 5A1, 5A3, 6AB, 6C, 7A, 7B, 8A1, 8B, 10A1, 10A2 or 11A1 at doses up to 100 uM. NI: no inhibition detected.

Lung homogenate myeloperoxide (MPO) and arginase were also determined (see *Online Supplementary Methods*).

Hemoglobin S-Townes vaso-occlusive crisis model. HbSS-Townes mice[42] (6-17 weeks old, n=3 per group) were treated with vehicle (0.08% w/v methyl cellulose), 100 mg/kg of HU, 10 or 30 mg/kg of IMR-687, or 100 mg/kg HU + 30 mg/kg IMR-687 in their drinking water. On day 7 of treatment, the mice were implanted with dorsal skin-fold chambers (DSFC). Three days later, on day 10 of treatment, mice with DSFC were anesthetized, placed on a special intravital microscopy stage, and 20-23 flowing subcutaneous venules in the DSFC window were selected and mapped. Mice were then placed in a hypoxic atmosphere chamber (7% O_2/ 93% N2) for 1 hour (h), after which they were returned to room air. All the selected venules were re-examined after 1 and 4 h of re-oxygenation in room air, and the number of static (no flow) venules was counted and expressed as percent stasis. After this, mice were euthanized and plasma hematocrit, bilirubin, Hb and heme were measured and WBC, RBC, sickled RBC and HbF+ RBC quantified (see *Online Supplementary Methods*).

Results

Phosphodiesterase enzyme selectivity

To determine the selectivity of IMR-687 for the phosphodiesterase 9A, 33 recombinant human PDE were incubated *in vitro* with increasing concentrations of IMR-687 and their activity determined. The IC50 of IMR-687 for PDE9A1 and PDE9A2 were 8.19 nM and 9.99 nM, respectively. IMR-687 inhibited PDE9A with more than 800-fold greater potency than PDE1A3, PDE1B, PDE1C, PDE5A2, with IC50 values of 88.4 μM, 8.48 μM, 12.2 μM, and 81.9 μM, respectively (Table 1). Significant inhibition of the other 27 PDE enzymes tested, including PDE4 and PDE10, was not observed (Table 1).

cGMP and fetal hemoglobin induction in erythroid cells

To determine if IMR-687 would increase cGMP levels in an erythroid cell line, actively growing K562 cells were cultured in media containing increasing concentrations of IMR-687 or HU. cGMP levels were assessed using a non-
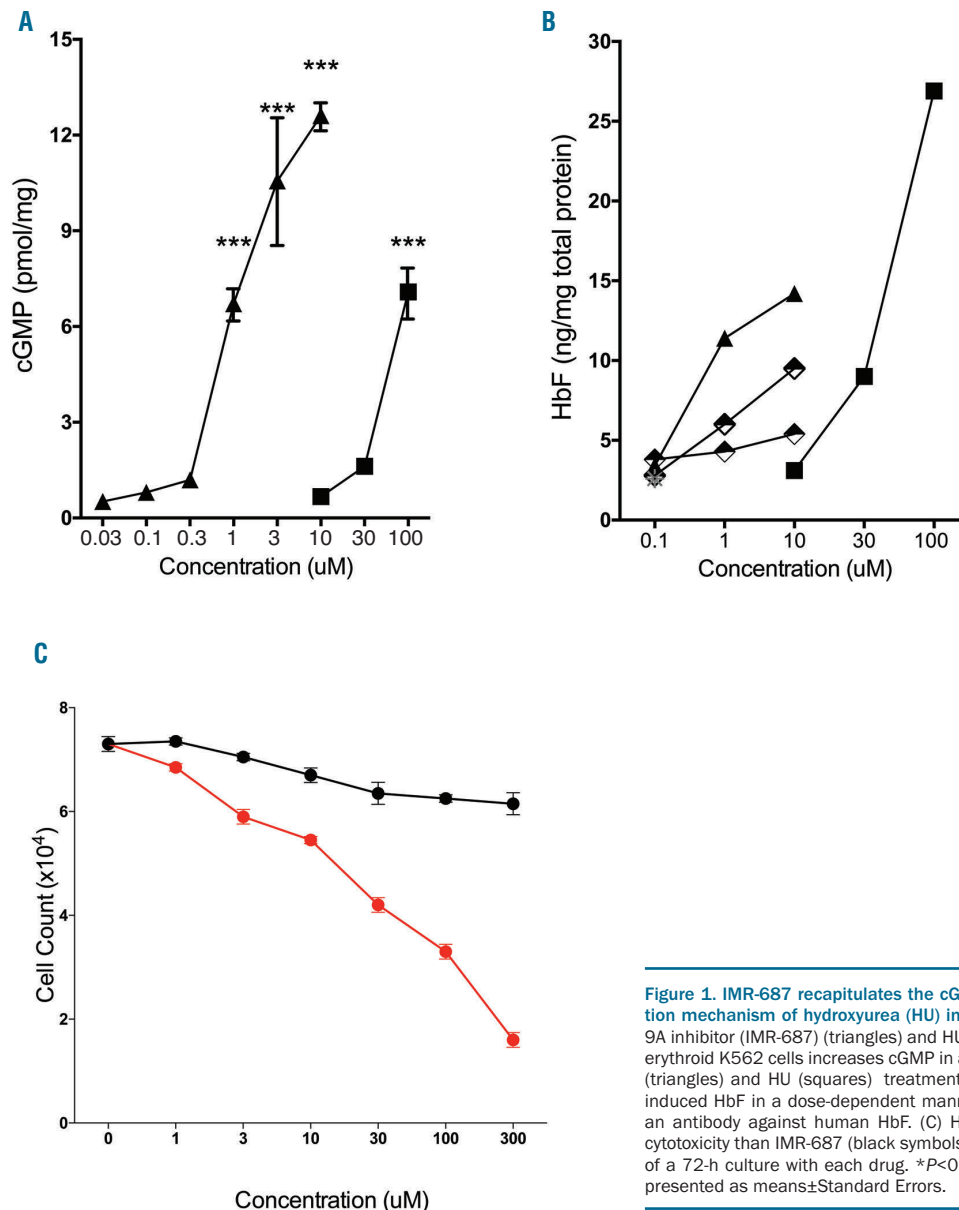
Figure 1. IMR-687 recapitulates the cGMP and fetal hemoglobin (HbF) induction mechanism of hydroxyurea (HU) in erythroid cells. (A) Phosphodiesterase 9A inhibitor (IMR-687) (triangles) and HU (squares) treatment for 6 hours (h) in erythroid K562 cells increases cGMP in a dose-dependent manner. (B) IMR-687 (triangles) and HU (squares) treatment in erythroid K562 cells for 72 h also induced HbF in a dose-dependent manner, evaluated by an ELISA assay using an antibody against human HbF. (C) HU (red symbols) demonstrates greater cytotoxicity than IMR-687 (black symbols) as assessed by cell counts at the end of a 72-h culture with each drug. *$P<0.05$; **$P<0.01$; ***$P<0.001$. Data are presented as means±Standard Errors.

radioactive cGMP enzyme immunoassay (ENZO Life Sciences, France) with the acetylation protocol and protein levels were quantified by the BCA assay (Pierce, France). IMR-687 incubated for 6 h induced cGMP in a dose-dependent manner at a dose that was well tolerated (Figure 1A).

Almeida *et al.* reported that exposure to the PDE9i BAY73-6691 and the sGC activator BAY 41-2271, increased HbF mRNA expression in K562 cells.[38] To confirm this finding with IMR-687, actively growing K562 cells were exposed to increasing concentrations of IMR-687 or HU, and HbF expression was assessed by ELISA after 72 h. IMR-687 dose-dependently induced more HbF than either BAY73-6691 or BAY 41-2271 and was 4.6
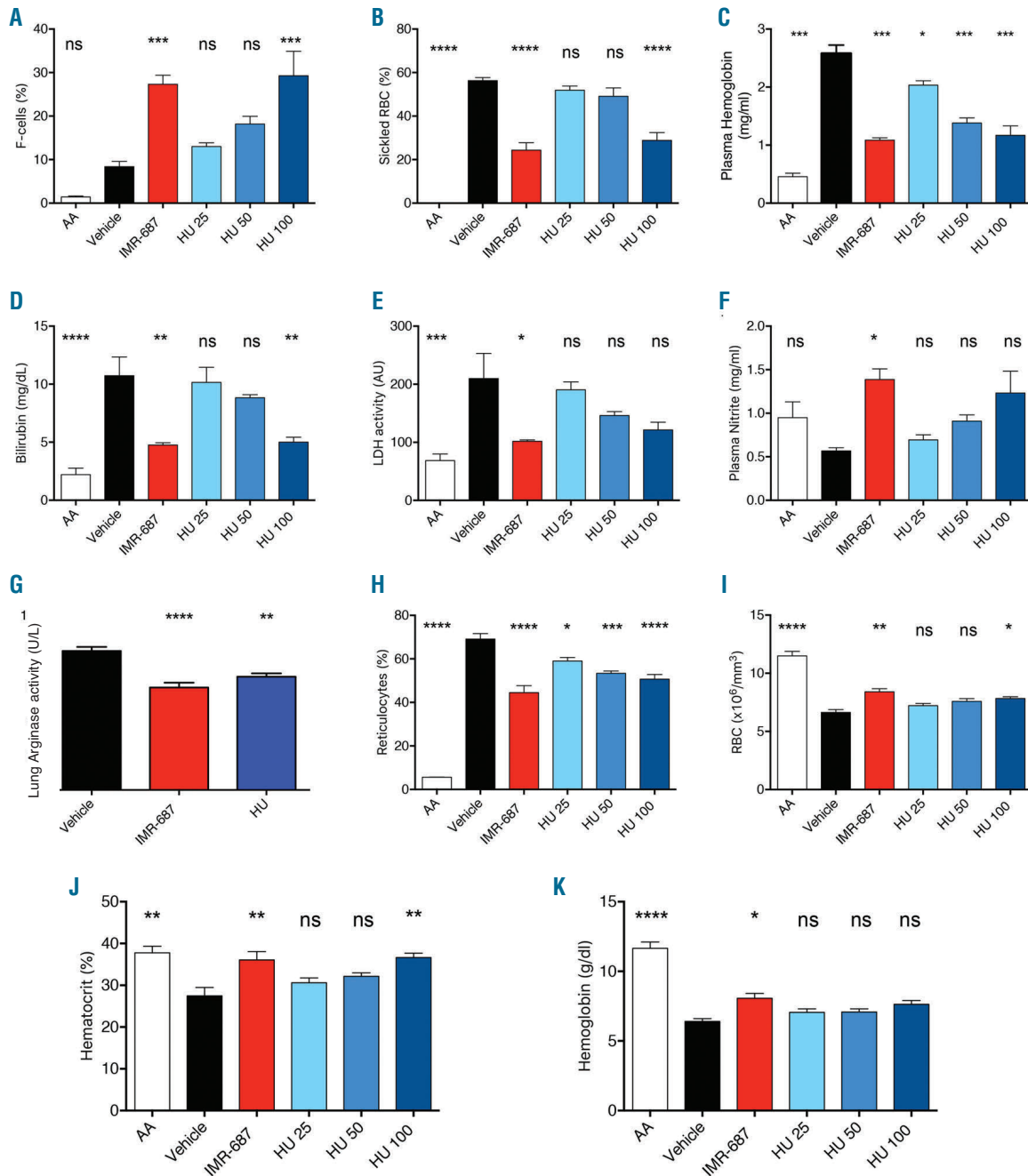
Figure 2. Treatment of phosphodiesterase 9A inhibitor (IMR-687) in sickle mice for 30 days results in fetal hemoglobin (HbF) induction, reduced hemolysis and reduced reticulocytosis. Townes-HbSS mice were dosed orally for 30 days with IMR-687 at 30 mg/kg or hydroxyurea (HU) at 25, 50 or 100 mg/kg. Treatment with IMR-687, or HU at the highest dose resulted in an increase in HbF (A) in Ter-119⁺ red blood cells (RBC), reduction in the percentage of RBC with a sickle shape observed on blood smear (B), and a reduction in hemolysis as indicated by reduced plasma free hemoglobin (C), plasma bilirubin levels (D), and lactate dehydrogenase (LDH) levels (E), and indirectly with an increase in plasma nitrate levels (F) and reduction in lung arginase levels (G). Commensurate with these changes there was a reduction in evidence of reticulocytosis including reduced reticulocyte counts (H), increased mature RBC counts (I), increased hematocrit (J) and hemoglobin (K). Statistical significance was calculated for each agent and dose compared to a vehicle-treated control (n=7). *P<0.05; **P<0.01; ***P<0.001; ns: not significant (P>0.05). Data are presented as means±Standard Errors.

times more potent at 10 μM than a dose of HU that demonstrated cytotoxicity (Figure 1B). Induction of HbF by IMR-687 was observed with the GM-CSF dependent erythroid line UT-7 (*data not shown*). While HU produced more HbF at higher concentrations, the induction was accompanied by cytotoxicity which was not observed with IMR-687 (Figure 1C).

Improved sickle cell disease phenotypes *in vivo* in murine model of sickle cell disease

We next tested the impact of IMR-687 and HU on F-cells, RBC sickling and markers of hemolysis in HbSS-Townes mice. After 30 days of treatment at 30 mg/kg/day of IMR-687, we observed a greater than 3-fold increase in the percent of HbF[+] F-cells (8.4% in vehicle treated and 27.3% in IMR-687 treated; *P*<0.001) (Figure 2A) and a corresponding 2-fold decrease in sickled RBC (56.3% in vehicle treated and 24.4% in IMR-687 treated; *P*<0.0001) (Figure 2B). We saw a similar induction of HbF and reduction in sickled RBC with mice treated with HU doses of 100 mg/kg/day (29.3% F cells and 28.8% sickled RBC). This dose, which resulted in mortality in mice, was higher than the dose employed in patients. At HU doses that were tolerated in mice, the induction of HbF was modest and not significant compared to vehicle control (25 and 50 mg/mL/day increased F-cells to 13% and 18% compared to 8.4% for vehicle). There was a minimal decrease in the percent of sickled RBC with 25-50 mg/kg/day of HU compared to vehicle control (percentage of sickled RBC was decreased to 52% and 49%, respectively, compared to 56% for vehicle) (Figure 2A and B).

The significant reduction in the RBC sickling by IMR-687 produced a corresponding decrease in markers of hemolysis. This was seen in a reduction of free plasma Hb (Figure 2C) where IMR-687 reduced plasma free Hb levels over 55%. HU treatment also reduced free Hb levels in a dose-dependent fashion with the highest dose, 100 mg/kg, reducing levels by approximately 55%.

Consistent with the reduction in hemolysis and reduction in free Hb, plasma bilirubin levels and LDH activity, markers of hemolysis[46] were significantly increased in vehicle treated SS mice compared to AA mice and reduced over 2-fold in IMR-687 treated mice (4.7 mg/dL, *P*<0.01 and 102 AU, *P*<0.05) (Figure 2D and E). The impact of the 100 mg/kg HU treatment was less pronounced, reducing bilirubin levels to 5 mg/dL (*P*<0.01) and LDH levels to 121 AU (not significant). HU dosed at 25 and 50 mg/kg did not produce a significant reduction in either marker of hemolysis.

Red cell lysis results in the release of Hb which consumes the plasma pool of NO and increases the vasculopathy associated with SCD7 nitrite generated in the plasma from an excess of NO produced by endothelial NO synthase (eNOS), can be converted back to NO as levels drop, acting as a biochemical reserve for NO.[47] In HbSS-Townes mice, plasma nitrate levels are 41% lower than those in control AA mice (0.56 mg/mL *vs.* 0.95 mg/mL) (Figure 2F). Hemolysis results in the release of Hb and heme, which acts as a scavenger of NO. Treatment of SS mice with 30 mg/kg of IMR-687 increased plasma nitrite levels almost 2.5-fold to 1.39 mg/mL (*P*<0.05). HU in a dose-dependent manner increased nitrite levels as well, with a peak of 1.23 mg/mL in the 100 mg/kg dose group; however, these changes were not significant and were modest at therapeutic doses of HU. The difference in

plasma nitrite levels in IMR-687 and 100 mg/kg HU treated mice were not significantly different.

Hemolysis also results in the release of arginase which reduces NO bioavailability and is correlated with SCD mortality.[10] IMR-687 reduced lung arginase 25% (*P*<0.0001) (Figure 2G) compared to vehicle controls. This effect was less pronounced in the mice treated with 100 mg/kg of HU.

Reticulocytosis reflects the bone marrow's response to anemia due to hemolysis. IMR-687 treated mice demon-
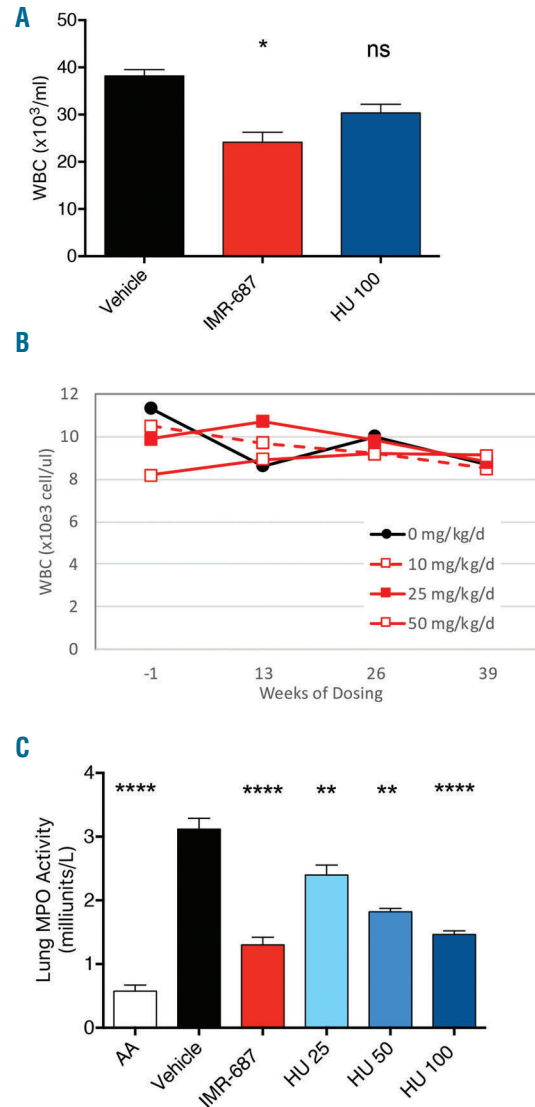
Figure 3. Treatment of phosphodiesterase 9A inhibitor (IMR-687) in sickle mice for 30 days results in reduced immune cell activity. White blood cell (WBC) counts are elevated in Townes-HbSS mice above normal controls (A). Townes-HbSS mice were dosed orally for 30 days with IMR-687 at 30 mg/kg or hydroxyurea (HU) at 100 mg/kg. Treatment with IMR-687 or HU reduced circulating WBC counts (A) (n=3). NS: not significant; *P>0.05. Data are presented as means±Standard Errors. This decrease in WBC counts is not seen in normal mice, rats or dogs dosed with IMR-687, including long-term 9-month toxicology studies in dogs dosed orally daily with 10, 25, or 50 mg/kg of IMR-687 (B). Along with the reduction in circulating WBC levels in IMR-687-treated Townes mice, there was a significant reduction in lung myeloperoxidase activity (C) (n=7). **P<0.01; ***P<0.001; ns: not significant (P>0.05). Data are presented as means±Standard Errors. MPO: myeloperoxide.

strated significant changes in all measures of reticulocytosis including a 36% reduction in reticulocyte counts (Figure 2H), a 27% increase in mature RBC (Figure 2I), a 10% increase in hematocrit (Figure 2J), and a 1.5g/dL increase in Hb (Figure 2K). HU at a dose of 100 mg/kg produced smaller changes in reticulocyte counts, RBC, hematocrit and Hb; the changes in Hb were not significant. At HU doses of 25 and 50 mg/kg, only the change in reticulocyte counts was significant.

Townes mice have elevated circulating WBC counts, the major component of which are neutrophils. WBC were 36% lower in IMR-687 (24.1x10^9/L *vs.* 38.2x10^9/L; *P*<0.05) and 21% lower in 100 mg/kg HU treatment groups (30.4x10^9/L *vs.* 38.2x10^9/L) (Figure 3A). While the reduction in WBC with HU treatment can result from the myelotoxicity of HU, the IMR-687 reduction in peripheral WBC was not due to myelotoxicity as demonstrated in long-term toxicology studies conducted in normal rats (*data not shown*) and dogs (Figure 3B) treated with IMR-687 for up to 6 and 9 months, respectively. In these studies, super-physiological doses of IMR-687 did not result in any reduction in peripheral WBC counts. Furthermore, a histological examination of bone marrow smears from IMR-687-treated rats and dogs did not demonstrate any myelotoxicity (*data not shown*). This reduction in WBC counts with IMR-687 treatment likely reflects reduced WBC activation or mobilization in this sickle cell model.

Not only were peripheral WBC counts increased in Townes mice, but soluble WBC-derived factors were elevated, including lung-associated myeloperoxidase (MPO), which is released by activated neutrophils, reduces plasma NO, and contributes to vascular damage.[48] MPO levels were elevated over 5-fold in HbSS-Townes mice compared to control mice (3.1 mU/L *vs.* 0.57 mU/L in control mice; *P*<0.0001) (Figure 3C). MPO levels were reduced 2.3-fold in IMR-687-treated mice and 2.1-fold in 100 mg/kg HU-treated mice (1.3 mU/L and 1.5 mU/L, respectively; *P*<0.0001). Lower doses of HU also reduced MPO levels in the lungs.

Reduced vaso-occlusion in hemoglobin S-Townes mice

Occlusion of vessels by sickled RBC and adhesive WBC
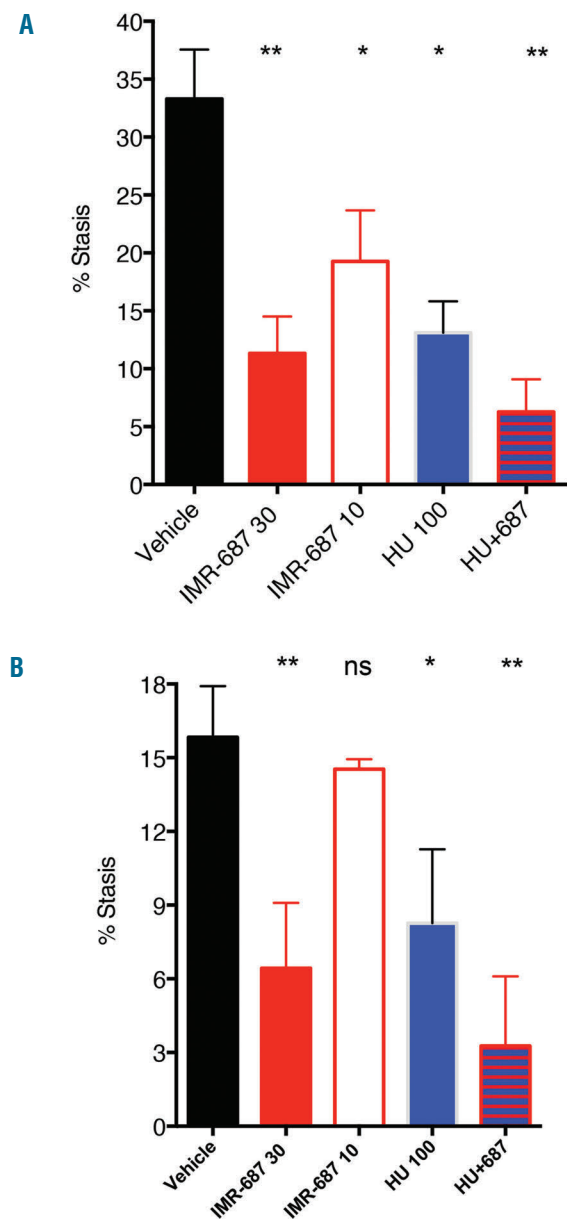
Figure 4. Treatment with phosphodiesterase 9A inhibitor (IMR-687) reduces vessel-occlusion in the Townes-HbSS sickle cell disease model. Townes-HbSS mice were dosed orally for 30 days with IMR-687 at 30 or 10 mg/kg or hydroxyurea (HU) at 100 mg/kg or 30 mg/kg IMR-687 in combination with 100 mg/kg HU. After ten days of treatment, animals were exposed to hypoxic conditions for quantification of microvessel occlusion *via* dorsal skin-fold chambers implanted on day 7 of treatment. On day 10 of treatment, 20-23 flowing venules in the chamber window were selected and mapped. Mice were then exposed to 1 h of hypoxia (7% O$_2$) and then returned to room air. The same venules were re-examined at 1 h (A) and 4 h (B) post hypoxia for blood flow, and static (no flow) venules were counted and the data expressed as percent stasis. Data are presented as means±Standard Deviations. Statistical significance was calculated for each agent and dose compared to a vehicle-treated control. *P*<0.05; **P*<0.01; ns: not significant (*P*>0.05). Data are presented as means±Standard Errors.

Figure 5. IMR-687 increases F-cells in patient-derived sickle cell disease (SCD) CD36$^+$ cells. CD36$^+$ cells derived from CD34$^+$ adult SCD peripheral blood cells were cultured as described in the *Methods* section. Increase in the percentage of F-cells for each treatment is shown. Statistical significance was calculated for each agent compared to a vehicle-treated control (n=9). **P*<0.01; ns: not significant (*P*>0.05). Errors are presented as Standard Error.

in SCD leads to multi-organ pathology. To assess the impact of IMR-687 on vessel occlusion, HbSS-Townes mice were exposed to 1 h of hypoxia (7% O_2/ 93% N2) and the percentage of static venules (no blood flow) was quantified after return to normoxic conditions using a DSFC and intravital microscopy. After vehicle-treated mice were returned to normoxia, microvascular stasis was 33% and 16% after 1 h (Figure 4A) and 4 h (Figure 4B), respectively. Treatment with IMR 687 for ten days decreased stasis to 12% ($P<0.01$ *vs.* vehicle) and 7% ($P<0.01$) at 30 mg/kg/day and 20% ($P<0.05$) and 14% (ns) at 10 mg/kg/day after 1 h and 4 h in normoxia. Treatment of SS mice with HU at 100 mg/kg/day for ten days decreased microvascular stasis to 13% ($P<0.05$) and 8% ($P<0.05$) after 1 h and 4 h, respectively. When mice were given the combination of IMR 687 (30 mg/kg/day) and HU (100 mg/kg/day), stasis was 7% ($P<0.01$) and 4% ($P<0.01$) at 1 h and 4 h, respectively, suggesting a potential synergistic effect of the two agents.

Fetal hemoglobin induction in sickle cell disease patient erythroblasts

Erythroblasts were generated *in vitro* using two-phase liquid culture from CD34^{+} progenitors from nine SCD blood or bone marrow (SCD patients undergoing hip replacement for osteonecrosis) donors. These cells were treated with IMR-687 to determine if the drug could increase HbF expression in patient-derived erythrocytes.

F-cells were determined by their expression of HbF in the LiveDead-GPA[+]Band3^{+} population (Figure 5) by FACS. The mean for the DMSO control group (n=9) was 13.3% HbF positive. IMR-687 increased the percentage of F-cells to 21.9% ($P<0.01$, n=9). HU increased the percentage of F-cells to 22.2% ($P<0.01$, n=7, due to cytotoxicity induced by HU in 2 cultures). HU had a greater impact on the

intensity of HbF staining in blood-derived CD34^{+} cells, increasing the MFI of the cells to 9744±2805 compared to 6073±1217 in control cells ($P=0.041$, n=7, due to cytotoxicity in 2 cultures), while IMR-687 significantly increased the MFI to 7813±1374 ($P<0.01$, n=9). This difference may be due in part to the greater cytotoxic stress of culturing the cells in 30 μM HU, evidenced by the loss of 2 of the 9 HU cultures.

Phosphodiesterase 9 inhibitor IMR-687 demonstrated low central nervous system accumulation and did not alter behavior

Many PDE9i were originally developed for neurological diseases.[49-55] In contrast, IMR-687 is a novel PDE9i selected specifically for low CNS exposure to reduce the potential impact of neuronal PDE9 inhibition on cognitive development and function. C57Bl/6J mice were dosed with IMR-687 at 10 mg/kg/day for five days or a CNS-active PDE9i, PF-04447943, originally developed for the treatment of neurological disorders. Plasma concentrations of the two PDE9i were very similar, while the brain exposure levels of IMR-687 were 5-fold lower than those seen with PF-04447943 (Figure 6A). Comparing the brain/plasma exposure profiles of the two drugs confirmed a very low concentration of IMR-687 in the CNS (7% brain/plasma ratio) compared to the PF-04447943, (41% brain/plasma ratio). Not unexpectedly, given its low brain exposure, IMR-687 showed no effect on locomotor activity or behavioral responses in toxicology studies (*data not shown*) nor in a classical fear conditioning mouse model of learning and memory (Figure 6B) (see *Online Supplementary Methods*). In contrast, the brain penetrant PF-04447943 significantly increased conditioned fear responses in mice at a similar dose. Besides confirming the lack of CNS activity of IMR-687, this finding suggests that brain-penetrant PDE9i treat-
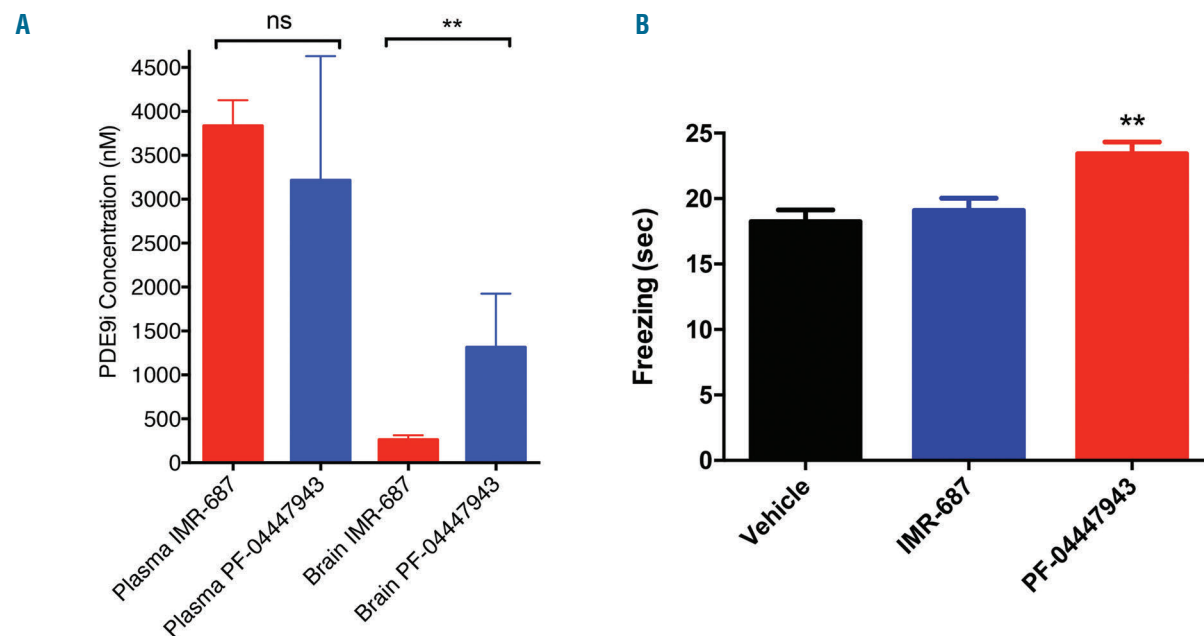
Figure 6. A brain-penetrant phosphodiesterase-9 inhibitor (PDE9i), but not IMR-687, increases fear responses in a model of learning and memory. (A) Fear conditioning responses are increased and persistent in mice treated with a brain-penetrant PDE9i compared to vehicle-treated or IMR-687-treated mice. (B) Drug exposure of the brain-penetrant PDE9i is 5-fold greater than that of IMR-687. Errors are presented as Standard Error. ns: not significant.

ment could trigger cognitive modulation of unknown consequences with chronic therapy.

Discussion

Previous groups have described that reticulocytes and neutrophils from SCD patients express elevated levels of PDE9 and that exposure to a PDE9 inhibitor reduced the adhesive properties and extravagation of neutrophils in sickle cell models.[38,39] They also reported the ability of this PDE9i to increase HbF mRNA levels in K562 cells. We describe a novel non-brain penetrant PDE9i, IMR-687, and its ability to increase HbF protein expression in human cell lines, patient-derived cells, and mouse models of SCD, and reduce many of the associated disease pathologies, including reduced RBC sickling and hemolysis, and normalization of WBC counts. Normalization of hemolysis is one of the major key improvements in SCD pathophysiology, having the potential to impact hemolytic-related complications. This is the first demonstration of the reduction in hemolysis by a PDE9i. IMR-687 treatment was also efficacious in a model of vaso-occlusive crisis, preventing *in vivo* microvascular occlusion following a transient hypoxic insult. These effects were similar to the benefits seen with a high dose of HU, associated with mortality in the mouse model that was associated with some lethality in mice and cellular toxicity *in vitro*.

Hydroxyurea has been associated with activity in multiple pathways beyond cGMP, including cAMP, c-Jun kinases, epigenetic modification, and regulation of miRNA.[56] It is, therefore, intriguing that many of the beneficial RBC and WBC effects of HU therapy in models of SCD are recapitulated by inhibitors to a PDE9 enzyme at daily doses that were safe and well tolerated. This suggests that an optimized dose of IMR-687 may be useful as a single agent therapy for SCD. That said, IMR-687 may also have a role in combination with low-dose HU in refractory patients. This may open the way for a new group of patients to see the full benefits of HU. Data in the Townes mouse model suggested that IMR-687 and HU together had an additive effect in reducing vaso-occlusion. This effect did not seem to be mediated by an additive effect on induction of HbF or reduction in RBC sickling. It may have been through an additive effect in NO modulation; this remains hypothetical, although not unexpected, given the robust reduction in hemolysis seen with IMR-687 which would reduce the release of heme, an NO scavenger. Clinically, IMR-687 is being tested in adult SCD patients both as a solo therapy and in those taking HU.

IMR-687 was purposefully developed for SCD, selected not only for its potency and selectivity, but also its low brain exposure to avoid concerns about modulating cognitive function, especially in children with SCD. The data presented in this report indicate that, in the context of SCD models, IMR-687 has many of the beneficial *in vitro* and *in vivo* properties of HU without its attendant toxicities. Furthermore, many of the positive changes associated with HU are sufficiently recapitulated by selective targeting of the PDE9 pathway, which acts through increases in cGM, culminates in increased HbF and ameliorates RBC pathology. This offers significant advantages over drugs that increase cGMP systemically, impacting cells that are not necessarily suitable targets, and mediating side effects such as hypotension. The clinical development of a safe, well-tolerated, orally available drug like IMR-687, with low CNS exposure, acting through the PDE9 pathway, may offer an improved single treatment option for patients living with SCD. In the light of these findings, clinical studies are underway to determine if IMR-687 might offer a safe, well-tolerated and efficacious alternative to HU therapy for SCD patients.

References

1. Ingram VM. A specific chemical difference between the globins of normal human and sickle-cell anaemia haemoglobin. Nature. 1956;178(4537):792-794.
2. Bertles JF, Rabinowitz R, Dobler J. Hemoglobin interaction: modification of solid phase composition in the sickling phenomenon. Science. 1970;169(3943):375-377.
3. Ross PD, Hofrichter J, Eaton WA. Thermodynamics of gelation of sickle cell deoxyhemoglobin. J Mol Biol. 1977;115(2):111-134.
4. Platt OS, Brambilla DJ, Rosse WF, et al. Mortality in sickle cell disease. Life expectancy and risk factors for early death. N Engl J Med. 1994;330(23):1639-1644.
5. Ware RE, de Montalembert M, Tshilolo L, Abboud MR. Sickle cell disease. Lancet. 2017;390(10091):311-323.
6. Berger SA, King WS. The flow of sickle-cell blood in the capillaries. Biophys J. 1980; 29(1):119-148.
7. Kato GJ, Gladwin MT, Steinberg MH. Deconstructing sickle cell disease: reappraisal of the role of hemolysis in the development of clinical subphenotypes. Blood Rev. 2007;21(1):37-47.
8. Gladwin MT, Schechter AN, Ognibene FP, et al. Divergent nitric oxide bioavailability in men and women with sickle cell disease. Circulation. 2003;107(2):271-278.
9. Reiter CD, Wang X, Tanus-Santos JE, et al. Cell-free hemoglobin limits nitric oxide bioavailability in sickle-cell disease. Nat Med. 2002;8(12):1383-1389.
10. Morris CR, Kato GJ, Poljakovic M, et al. Dysregulated arginine metabolism, hemolysis-associated pulmonary hypertension, and mortality in sickle cell disease. JAMA. 2005;294(1):81-90.
11. Belcher JD, Marker PH, Weber JP, Hebbel RP, Vercellotti GM. Activated monocytes in sickle cell disease: potential role in the activation of vascular endothelium and vaso-occlusion. Blood. 2000;96(7):2451-2459.
12. Hebbel RP, Boogaerts MA, Eaton JW, Steinberg MH. Erythrocyte adherence to endothelium in sickle-cell anemia. A possible determinant of disease severity. N Engl J Med. 1980;302(18):992-995.
13. Hebbel RP, Yamada O, Moldow CF, Jacob HS, White JG, Eaton JW. Abnormal adherence of sickle erythrocytes to cultured vascular endothelium: possible mechanism for microvascular occlusion in sickle cell disease. J Clin Invest. 1980;65(1):154-160.
14. Turhan A, Weiss LA, Mohandas N, Coller BS, Frenette PS. Primary role for adherent leukocytes in sickle cell vascular occlusion: a new paradigm. Proc Natl Acad Sci U S A. 2002;99(5):3047-3051.
15. Zennadi R, Chien A, Xu K, Batchvarova M, Telen MJ. Sickle red cells induce adhesion of lymphocytes and monocytes to endothelium. Blood. 2008;112(8):3474-3483.
16. Frenette PS. Sickle cell vaso-occlusion: multistep and multicellular paradigm. Curr Opin Hematol. 2002;9(2):101-106.
17. Nath KA, Hebbel RP. Sickle cell disease: renal manifestations and mechanisms. Nat Rev Nephrol. 2015;11(3):161-171.
18. Thornburg CD, Dixon N, Burgett S, et al. A pilot study of hydroxyurea to prevent chronic organ damage in young children

with sickle cell anemia. Pediatr Blood Cancer. 2009;52(5):609-615.

19. Kassim AA, DeBaun MR. Sickle cell disease, vasculopathy, and therapeutics. Annu Rev Med. 2013;64:451-466.

20. Charache S, Terrin ML, Moore RD, et al. Effect of hydroxyurea on the frequency of painful crises in sickle cell anemia. Investigators of the Multicenter Study of Hydroxyurea in Sickle Cell Anemia. N Engl J Med. 1995;332(20):1317-1322.

21. Heeney MM, Ware RE. Hydroxyurea for children with sickle cell disease. Pediatr Clin North Am. 2008;55(2):483-501, x.

22. Maier-Redelsperger M, de Montalembert M, Flahault A, et al. Fetal hemoglobin and F-cell responses to long-term hydroxyurea treatment in young sickle cell patients. The French Study Group on Sickle Cell Disease. Blood. 1998;91(12):4472-4479.

23. Platt OS, Orkin SH, Dover G, Beardsley GP, Miller B, Nathan DG. Hydroxyurea enhances fetal hemoglobin production in sickle cell anemia. J Clin Invest. 1984; 74(2):652-656.

24. Wang WC, Ware RE, Miller ST, et al. Hydroxycarbamide in very young children with sickle-cell anaemia: a multicentre, randomised, controlled trial (BABY HUG). Lancet. 2011;377(9778):1663-1672.

25. Erard F, Dean A, Schechter AN. Inhibitors of cell division reversibly modify hemoglobin concentration in human erythroleukemia K562 cells. Blood. 1981; 58(6):1236-1239.

26. Cokic VP, Smith RD, Beleslin-Cokic BB, et al. Hydroxyurea induces fetal hemoglobin by the nitric oxide-dependent activation of soluble guanylyl cyclase. J Clin Invest. 2003;111(2):231-239.

27. Odievre MH, Bony V, Benkerrou M, et al. Modulation of erythroid adhesion receptor expression by hydroxyurea in children with sickle cell disease. Haematologica. 2008;93(4):502-510.

28. Stettler N, McKiernan CM, Melin CQ, Adejoro OO, Walczak NB. Proportion of adults with sickle cell anemia and pain crises receiving hydroxyurea. JAMA. 2015; 313(16):1671-1672.

29. Adams-Graves P, Bronte-Jordan L. Recent treatment guidelines for managing adult patients with sickle cell disease: challenges in access to care, social issues, and adherence. Expert Rev Hematol. 2016;9(6):541-552.

30. Sheehan VA, Luo Z, Flanagan JM, et al. Genetic modifiers of sickle cell anemia in the BABY HUG cohort: influence on laboratory and clinical phenotypes. Am J Hematol. 2013;88(7):571-576.

31. Steinberg MH. Determinants of fetal hemoglobin response to hydroxyurea. Semin Hematol. 1997;34(3 Suppl 3):8-14.

32. Dover GJ, Humphries RK, Moore JG, et al. Hydroxyurea induction of hemoglobin F production in sickle cell disease: relationship between cytotoxicity and F cell production. Blood. 1986;67(3):735-738.

33. Lanzkron S, Haywood C, Jr., Hassell KL, Rand C. Provider barriers to hydroxyurea use in adults with sickle cell disease: a survey of the Sickle Cell Disease Adult Provider Network. J Natl Med Assoc. 2008; 100(8):968-973.

34. Meyappan JD, Lampl M, Hsu LL. Parents' assessment of risk in sickle cell disease treatment with hydroxyurea. J Pediatr Hematol Oncol. 2005;27(12):644-650.

35. Berthaut I, Guignedoux G, Kirsch-Noir F, et al. Influence of sickle cell disease and treatment with hydroxyurea on sperm parameters and fertility of human males. Haematologica. 2008;93(7):988-993.

36. Soderling SH, Bayuga SJ, Beavo JA. Identification and characterization of a novel family of cyclic nucleotide phosphodiesterases. J Biol Chem. 1998; 273(25): 15553-15558.

37. Soderling SH, Bayuga SJ, Beavo JA. Cloning and characterization of a cAMP-specific cyclic nucleotide phosphodiesterase. Proc Natl Acad Sci U S A. 1998;95(15):8991-8996.

38. Almeida CB, Scheiermann C, Jang JE, et al. Hydroxyurea and a cGMP-amplifying agent have immediate benefits on acute vaso-occlusive events in sickle cell disease mice. Blood. 2012;120(14):2879-2888.

39. Almeida CB, Traina F, Lanaro C, et al. High expression of the cGMP-specific phosphodiesterase, PDE9A, in sickle cell disease (SCD) and the effects of its inhibition in erythroid cells and SCD neutrophils. Br J Haematol. 2008;142(5):836-844.

40. Miguel LI, Almeida CB, Traina F, et al. Inhibition of phosphodiesterase 9A reduces cytokine-stimulated in vitro adhesion of neutrophils from sickle cell anemia individuals. Inflamm Res. 2011;60(7):633-642.

41. Thompson WJ, Appleman MM. Multiple cyclic nucleotide phosphodiesterase activities from rat brain. Biochemistry. 1971; 10(2):311-316.

42. Ryan TM, Townes TM, Reilly MP, et al. Human sickle hemoglobin in transgenic mice. Science. 1990;247(4942):566-568.

43. EC L. Peripheral Blood Smear. In: Walker HK HW, Hurst JW, ed. Clinical Methods: The History, Physical, and Laboratory Examinations. Boston: Butterworths; 1990.

44. Kleihauer E, Braun H, Betke K. [Demonstration of fetal hemoglobin in erythrocytes of a blood smear]. Klin Wochenschr. 1957;35(12):637-638.

45. Fairbanks VF, Ziesmer SC, O'Brien PC. Methods for measuring plasma hemoglobin in micromolar concentration compared. Clin Chem. 1992;38(1):132-140.

46. Kato GJ, McGowan V, Machado RF, et al. Lactate dehydrogenase as a biomarker of hemolysis-associated nitric oxide resistance, priapism, leg ulceration, pulmonary hypertension, and death in patients with sickle cell disease. Blood. 2006;107(6):2279-2285.

47. Dezfulian C, Raat N, Shiva S, Gladwin MT. Role of the anion nitrite in ischemia-reperfusion cytoprotection and therapeutics. Cardiovasc Res. 2007;75(2):327-338.

48. Zhang H, Xu H, Weihrauch D, et al. Inhibition of myeloperoxidase decreases vascular oxidative stress and increases vasodilatation in sickle cell disease mice. J Lipid Res. 2013;54(11):3009-3015.

49. da Silva FH, Pereira MN, Franco-Penteado CF, De Nucci G, Antunes E, Claudino MA. Phosphodiesterase-9 (PDE9) inhibition with BAY 73-6691 increases corpus cavernosum relaxations mediated by nitric oxide-cyclic GMP pathway in mice. Int J Impot Res. 2013;25(2):69-73.

50. Hutson PH, Finger EN, Magliaro BC, et al. The selective phosphodiesterase 9 (PDE9) inhibitor PF-04447943 (6-[(3S,4S)-4-methyl-1-(pyrimidin-2-ylmethyl)pyrrolidin-3-yl]-1-(tetrahydro-2H-py ran-4-yl)-1,5-dihydro-4H-pyrazolo[3,4-d]pyrimidin-4-one) enhances synaptic plasticity and cognitive function in rodents. Neuropharmacology. 2011;61(4):665-676.

51. Vardigan JD, Converso A, Hutson PH, Uslaner JM. The selective phosphodiesterase 9 (PDE9) inhibitor PF-04447943 attenuates a scopolamine-induced deficit in a novel rodent attention task. J Neurogenet. 2011;25(4):120-126.

52. van der Staay FJ, Rutten K, Barfacker L, et al. The novel selective PDE9 inhibitor BAY 73-6691 improves learning and memory in rodents. Neuropharmacology. 2008;55(5): 908-918.

53. Prickaerts J, Heckman PRA, Blokland A. Investigational phosphodiesterase inhibitors in phase I and phase II clinical trials for Alzheimer's disease. Expert Opin Investig Drugs. 2017;26(9):1033-1048.

54. Heckman PR, Wouters C, Prickaerts J. Phosphodiesterase inhibitors as a target for cognition enhancement in aging and Alzheimer's disease: a translational overview. Curr Pharm Des. 2015;21(3):317-331.

55. Saavedra A, Giralt A, Arumi H, Alberch J, Perez-Navarro E. Regulation of hippocampal cGMP levels as a candidate to treat cognitive deficits in Huntington's disease. PLoS One. 2013;8(9):e73664.

56. Pule GD, Mowla S, Novitzky N, Wiysonge CS, Wonkam A. A systematic review of known mechanisms of hydroxyurea-induced fetal hemoglobin for treatment of sickle cell disease. Expert Rev Hematol. 2015;8(5):669-679.

Ferrata Storti Foundation

Impact of red blood cell transfusion dose density on progression-free survival in patients with lower-risk myelodysplastic syndromes

Louise de Swart,[1] Simon Crouch,[2] Marlijn Hoeks,[1,3] Alex Smith,[2] Saskia Langemeijer,[1] Pierre Fenaux,[4] Argiris Symeonidis,[5] Jaroslav Čermák,[6] Eva Hellström-Lindberg,[7] Reinhard Stauder,[8] Guillermo Sanz,[9] Moshe Mittelman,[10] Mette Skov Holm,[11] Luca Malcovati,[12] Krzysztof Mądry,[13] Ulrich Germing,[14] Aurelia Tatic,[15] Aleksandar Savic,[16] Antonio Medina Almeida,[17] Njetočka Gredelj-Šimec,[18] Agnes Guerci-Bresler,[19] Odile Beyne-Rauzy,[20] Dominic Culligan,[21] Ioannis Kotsianidis,[22] Raphael Itzykson,[4] Corine van Marrewijk,[1] Nicole Blijlevens,[1] David Bowen[23] and Theo de Witte,[24] on behalf of the EUMDS Registry Participants

[1]Department of Hematology, Radboud University Medical Center, Nijmegen, the Netherlands; [2]Epidemiology and Cancer Statistics Group, Department of Health Sciences, University of York, York, UK; [3]Center for Clinical Transfusion Research, Sanquin Research, Leiden, the Netherlands; [4]Service d'Hématologie, Hôpital Saint-Louis, Assistance Publique des Hôpitaux de Paris and Université Paris 7, Paris, France; [5]Department of Medicine, Division of Hematology, University of Patras Medical School, Patras, Greece; [6]Department of Clinical Hematology, Institute of Hematology & Blood Transfusion, Praha, Czech Republic; [7]Department of Medicine, Division of Hematology, Karolinska Institutet, Stockholm, Sweden; [8]Department of Internal Medicine V (Hematology and Oncology), Innsbruck Medical University, Innsbruck, Austria; [9]Department of Hematology, Hospital Universitario y Politécnico La Fe, Valencia, Spain; [10]Department of Medicine A, Tel Aviv Sourasky (Ichilov) Medical Center and Sackler Medical Faculty, Tel Aviv University, Tel Aviv, Israel; [11]Department of Hematology, Aarhus University Hospital, Aarhus, Denmark; [12]Department of Hematology Oncology, Fondazione IRCCS Policlinico San Matteo, University of Pavia, Pavia, Italy; [13]Department of Hematology, Oncology and Internal Medicine, Warsaw Medical University, Warsaw, Poland; [14]Department of Hematology, Oncology and Clinical Immunology, Universitätsklinik Düsseldorf, Düsseldorf, Germany; [15]Center of Hematology and Bone Marrow Transplantation, Fundeni Clinical Institute, Bucharest, Romania; [16]Clinic of Hematology - Clinical Center of Vojvodina, Faculty of Medicine, University of Novi Sad, Novi Sad, Serbia; [17]Department of Clinical Hematology, Hospital da Luz, Lisbon, Portugal; [18]Department of Internal Medicine, Division of Hematology, Merkur University Hospital, Zagreb, Croatia; [19]Service d'Hématologie, Centre Hospitalier Universitaire (CHU) Brabois Vandoeuvre, Nancy, France; [20]Service de Médecine Interne, IUCT-Oncopole, CHU Toulouse, Toulouse, France; [21]Department of Haematology, Aberdeen Royal Infirmary, Aberdeen, UK; [22]Department of Hematology, Democritus University of Thrace Medical School, University Hospital of Alexandroupolis, Alexandroupolis, Greece; [23]St. James's Institute of Oncology, Leeds Teaching Hospitals, Leeds, UK and [24]Department of Tumor Immunology - Nijmegen Center for Molecular Life Sciences, Radboud University Medical Center, Nijmegen, the Netherlands

ABSTRACT

Progression-free survival (PFS) of patients with lower-risk myelodysplastic syndromes (MDS) treated with red blood cell transfusions is usually reduced, but it is unclear whether transfusion dose density is an independent prognostic factor. The European MDS Registry collects prospective data at 6-monthly intervals from newly diagnosed lower-risk myelodysplastic syndromes patients in 16 European countries and Israel. Data on the transfusion dose density - the cumulative dose received at the end of each interval divided by the time since the beginning of the interval in which the first transfusion was received - were analyzed using proportional hazards regression with time-varying co-variates, with death and progression to higher-risk MDS/acute myeloid leukemia as events. Of the 1,267 patients included in the analyses, 317 died without progression; in 162 patients the disease had progressed. PFS was significantly associated with age, EQ-5D index, baseline World Health Organization classification, bone marrow blast count, cytogenetic risk category, number of cytopenias, and country. Transfusion dose density was inversely associated with PFS

($P<1x10^{-4}$): dose density had an increasing effect on hazard until a dose density of 3 units/16 weeks. The transfusion dose density effect continued to increase beyond 8 units/16 weeks after correction for the impact of treatment with erythropoiesis-stimulating agents, lenalidomide and/or iron chelators. In conclusion, the negative effect of transfusion treatment on PFS already occurs at transfusion densities below 3 units/16 weeks. This indicates that transfusion dependency, even at relatively low dose densities, may be considered as an indicator of inferior PFS. This trial was registered at *www.clinicaltrials.gov as #NCT00600860.*

Introduction

Red blood cell transfusions (RBCT) are the major component of the supportive care of patients with myelodysplastic syndromes (MDS). The life expectancy of MDS patients treated with RBCT is usually shorter than that of untransfused patients,[1,2] but whether the impaired outcome is a result of intrinsic deterioration of the underlying disease or a result of external factors related to transfusion per se (for example the iron toxicity induced by RBCT) remains an open question. Since 2007, the European MDS (EUMDS) Registry has prospectively collected observational data on patients with MDS classified as low and intermediate-1 risk according to the International Prognostic Scoring System (IPSS),[3] collectively defined as lower-risk MDS.[4] The majority of lower-risk MDS patients become transfusion dependent (51% in the EUMDS Registry),[4] usually within 6 months after diagnosis. With an expected median survival of 2.4 to 11.8 years, these patients might be prone to long-term accumulation of iron due to RBCT.[3,5-8] The toxic effects of iron overload in other iron-loading diseases, such as hereditary hemochromatosis[9] and the thalassemia syndromes,[10] are well known, but the consequences in MDS patients require further clarification. MDS patients are generally older than patients with other iron-loading disorders.[11] Their exposure to RBCT may not be long enough to develop classical tissue damage due to iron overload, but they may suffer from oxidative stress caused by toxic iron species, including non-transferrin bound iron (NTBI) and labile plasma iron (LPI), which have been suggested to serve as early indicators of iron toxicity in iron-loading anemias, such as thalassemia syndromes.[8,12] Biomarkers of oxidative stress have been found to be increased in patients with MDS and iron overload.[4,13-16] Data from a recently completed study of the EUMDS Registry[17] showed that elevated LPI levels - in contrast to elevated NTBI levels and transferrin saturation - are associated with decreased survival. The risk of dying prematurely in patients with detectable LPI levels occurred too early in this study to be explained by classical iron overload with organ toxicity (lungs, liver and heart) after long term transfusions, and this may suggest a direct effect associated with elevated LPI levels.

The aim of this analysis was to assess the effect of RBCT dose density on progression-free survival (PFS) of patients with lower-risk MDS. The hypothesis is that transfusional iron may be toxic and associated with oxidative stress, which may lead to bone marrow failure, genetic damage, increased risk for progression or premature death. Two countervailing forces may play a role in this analysis: (i) patients with symptomatic anemia are more likely to receive more frequent RBCT; and (ii) higher RBCT doses may lead to faster deterioration of lower-risk MDS or to a higher risk of complications by co-morbidities.

Methods

Patients with lower-risk MDS (IPSS risk: low or intermediate-1)[3] from 16 European countries and Israel were included in the EUMDS Registry, after providing signed informed consent, within 100 days of their initial diagnosis of a MDS which was made according to the World Health Organization (WHO) 2001 criteria.[18] Patients with an IPSS intermediate-2 or high risk, or with therapy-related MDS were excluded, but MDS-specific treatment, started before registration within 100 days after diagnosis, was not a reason for exclusion. Data were collected at baseline and at each 6-monthly outpatient routine follow-up visit. Clinical information was collected on: demographics, anthropometrics, co-morbidities, performance status, quality of life (EQ-5D), concomitant medication, laboratory parameters, diagnostics including information on bone marrow morphology, histology, cytogenetics, RBCT episodes, total number of transfused units and simultaneous therapeutic interventions. All subjects were followed prospectively by full reports every 6 months until death, progression to high risk MDS or leukemia, loss to follow-up or withdrawal of informed consent. The Registry was approved by each institution's ethics committee in accordance with national legislation.

Transfusion data available in the EUMDS Registry consists of the number of units received between each reported visit, usually at 6-month intervals. In order to assess the association between transfusions received and PFS, proportional hazards regression with time-varying covariates was employed, adjusting the effect of transfusions by appropriate baseline and time-varying variables. For the purposes of the time-to-event analyses, time was measured from the date of diagnosis with MDS to the date of disease progression or date of death. Progression is defined as an increase to either refractory anemia with excess blasts-2 or to acute leukemia. Patients without disease progression and still alive at the time of the analyses were censored at the date of their last visit.

In order to avoid problems with simultaneity of cause and effect assumed by the proportional hazards approach to survival analysis a "dose density" variable was defined, in the following way, for blood transfusions received. The cumulative total of units of blood received at the end of each inter-visit time interval was calculated. This was then divided by the time since the beginning of the time interval in which the first post-diagnosis transfusion was received, giving a dose-density measurement. This dose-density was then assigned to each time interval. The value of this variable at each point in time represents the average rate at which the patient has been receiving units of blood since they started transfusions.

Adjusted baseline variables included age at diagnosis, number of cytopenias and number of units of blood received before diagnosis. Adjusted time-varying variables (with the intention of adjusting for the condition of the patient over time) were bone marrow blast count, EQ-5D index, revised IPSS cytogenetic category, and platelet and neutrophil counts. Additional analyses were adjusted for the effect of treatment with erythropoiesis-stimulating agents (ESA), iron chelation therapy and lenalidomide, taking these treatments to be confounding factors. Finally, a sensitivity

analysis was performed in the survival regressions to take into account that the population was not homogeneous but distributed over different centers in several countries, using a random effects frailty term. The random effect, called "frailty", is the term that describes the common risk or the individual heterogeneity, acting as a factor on the hazard function. Missing values in adjustment variables were imputed with last observation carried forward or next observation carried backward.

Results

Patients' characteristics

The EUMDS Registry contained data from 2,192 patients diagnosed between December 3, 2007 and March 14, 2017 of whom 1,504 patients had data recorded from three or more visits (visit 3 = landmark at the 1-year follow-up). Two patients with refractory anemia with excess blasts-2 were excluded, resulting in the inclusion of 1,502 patients. An additional 235 patients were excluded, as one or more of the following variables had never been measured or the test failed throughout the study: cytogenetics (n=112), EQ-5D (n=101), blast count (n=60), platelet count (n=1), and neutrophil count (n=2). The final cohort consisted of 1,267 patients, unselected for any type of treatment. In 162 patients the disease had progressed to higher-risk MDS or acute myeloid leukemia and 317 patients had died without progression. The median survival after disease progression was 5.3 months [95% confidence interval (95% CI); 3.2- 9.8 months]. Full details of the

Table 1. Baseline characteristics of the included patients from time of diagnosis and progression-free survival, stratified according to transfusion status at the visit 3 landmark.

	Total N. (%)	Hazard ratio (95% CI)	Adjusted hazard ratio* (95% CI)	Transfusion status at landmark	
				No	Yes
Total	1267 (100.0)			751 (100.0)	516 (100.0)
Median age at diagnosis, years (range)	73.0 (18.0 - 95.0)	1.03 (1.02 - 1.04)	1.03 (1.02 - 1.04)	73.0 (18.0 - 91.0)	73.0 (21.0 - 95.0)
Sex					
Male	757 (59.7)	1	1	445 (59.3)	312 (60.5)
Female	510 (40.3)	0.84 (0.70 - 1.01)	0.76 (0.62 - 0.92)	306 (40.7)	204 (39.5)
WHO diagnosis:					
RA	218 (17.2)	0.84 (0.64 - 1.10)	0.78 (0.59 - 1.03)	139 (18.5)	79 (15.3)
RARS	214 (16.9)	0.73 (0.56 - 0.96)	0.59 (0.45 - 0.78)	123 (16.4)	91 (17.6)
RCMD	492 (38.8)	1	1	296 (39.4)	196 (38.0)
RCMD-RS	86 (6.8)	1.03 (0.72 - 1.46)	0.91 (0.64 - 1.30)	47 (6.3)	39 (7.6)
RAEB-1	133 (10.5)	1.58 (1.20 - 2.07)	1.86 (1.41 - 2.46)	78 (10.4)	55 (10.7)
MDS-U	41 (3.2)	0.64 (0.34 - 1.22)	0.68 (0.36 - 1.29)	27 (3.6)	14 (2.7)
Deletion 5q	83 (6.6)	0.61 (0.40 - 0.92)	0.54 (0.35 - 0.83)	41 (5.5)	42 (8.1)
MDS Comorbidity Index					
Low	782 (61.7)	1	1	482 (64.2)	300 (58.1)
Intermediate	411 (32.4)	1.24 (1.02 - 1.50)	1.08 (0.88 - 1.31)	232 (30.9)	179 (34.7)
High	71 (5.6)	1.55 (1.08 - 2.22)	1.30 (0.90 - 1.89)	35 (4.7)	36 (7.0)
Not known	3 (0.2)	-	-	2 (0.3)	1 (0.2)
Karnofsky status					
80-100	881 (69.5)	1	1	543 (72.3)	338 (65.5)
50-70	210 (16.6)	1.72 (1.38 - 2.15)	1.40 (1.10 - 1.77)	93 (12.4)	117 (22.7)
10-40	10 (0.8)	2.04 (0.76 - 5.48)	1.89 (0.69 - 5.15)	3 (0.4)	7 (1.4)
Not known	166 (13.1)	1.08 (0.80 - 1.45)	0.99 (0.73 - 1.34)	112 (14.9)	54 (10.5)
Quality of life					
Visual analog score, mean (SD)	70.5 (19.7)	0.99 (0.98 - 0.99)	0.99 (0.99 - 1.00)	73.1 (18.9)	66.8 (20.2)
IPSS category					
Low	680 (53.7)	1	1	460 (61.3)	220 (42.6)
Intermediate	557 (44.0)	1.95 (1.62 - 2.34)	1.71 (1.39 - 2.11)	274 (36.5)	283 (54.8)
Cytogenetics not done	30 (2.4)	0.83 (0.43 - 1.62)	0.74 (0.38 - 1.45)	17 (2.3)	13 (2.5)
Revised IPSS category					
Very low	386 (30.5)	1	1	310 (41.3)	76 (14.7)
Low	571 (45.1)	1.80 (1.41 - 2.29)	1.85 (1.45 - 2.37)	309 (41.1)	262 (50.8)
Intermediate	204 (16.1)	3.19 (2.41 - 4.22)	3.40 (2.55 - 4.52)	89 (11.9)	115 (22.3)
High	39 (3.1)	4.27 (2.72 - 6.71)	4.59 (2.91 - 7.22)	11 (1.5)	28 (5.4)
Very high	3 (0.2)	3.15 (0.78 - 12.82)	4.65 (1.13 - 19.15)	1 (0.1)	2 (0.4)
Not known	64 (5.1)	1.69 (1.07 - 2.68)	1.76 (1.11 - 2.80)	31 (4.1)	33 (6.4)

*Hazard ratio adjusted for all other variables in the table. 95% CI: 95% confidence Interval; WHO: World Health Organization; RA: refractory anemia; RARS: refractory anemia with ring sideroblasts; RCMD: refractory cytopenia with multilineage dysplasia; RCMD-RS: refractory cytopenia with multilineage dysplasia & ring sideroblasts; RAEB: refractory anemia with excess blasts; MDS-U: myelodysplastic syndrome, unclassifiable; MDS: myelodysplastic syndrome; SD: standard deviation; IPSS: International Prognostic Scoring System.

exclusions are provided in the *Online Supplementary Data*. Table 1 and *Online Supplementary Table S1* show the patients' baseline demographics. For the landmark analysis patients were defined as untransfused if they had never received a transfusion from diagnosis until the end of the study period (death or progression), or if they had received transfusion only once (n=751). Patients were defined as transfused if they had received multiple transfusions (n=516) within the first year of follow-up (visit 3 = landmark). Regular transfusions were usually initiated during the first 6 months. Using visit 3 as the landmark ensured that the majority of patients who received more than one transfusion were correctly identified.

Distribution of transfusion dose density

The distribution of non-zero dose densities at the third visit (the landmark visit) is shown in Figure 1. Mean dose density among those who had received a transfusion at 1 year of follow-up was 1.24 units per month, with a median of 0.88 units per month (interquartile range, 0.31 – 1.85). Dose densities of the transfused patients declined on approach to the final recorded interval, if the patient died or progressed to higher-risk MDS during the last interval (*Online Supplementary Figure S1*). This implies that patients received fewer transfusions per month in the interval during which death occurred than in the preceding intervals. Presumably, the treatment focus switches to palliative care at home on the approach to death. Patients alive at the last recorded visit and with no signs of progression did not show an increase of transfusion density over time (*Online Supplementary Figure S1*).

Outcome of patients stratified according to transfusion status at the landmark 1 year after registration

The patients' characteristics at the time of the landmark visit 3 stratified according to transfusion status are shown in *Online Supplementary Table S2*. One hundred forty-five subjects untransfused at visit 3 went on to have transfusions after the landmark visit. Out of 516 transfused by the time of the landmark, 288 subjects were not reported to have received any further transfusions, but of these 288, 125 subjects did not have any further visits and another 91 had only one additional visit. Of the 163 subjects who had one or more additional visits (91+72, respectively), 73 received treatment with ESA, 19 with lenalidomide, ten with hypomethylating agents, two with hydroxycarbamide, and three with iron chelators. Unadjusted PFS stratified by transfusion status (transfused n=516, untransfused n=751) at the third visit is presented in Figure 2A. The overall PFS of the untransfused patients at visit 3 was significantly better (*P*<0.0001) than that of the transfused patients.

Transfused patients were divided into those receiving above (high density) or below (low density) the median value (0.87 units per month) of non-zero dose densities. Unadjusted PFS stratified by transfusion status and dose density (untransfused n=751, low dose density n=258, high dose density=258) at the third visit is presented in Figure 2B. The overall PFS of the three groups of patients, stratified according to the dose density at visit 3, was significantly different (*P*<0.0001). We evaluated the time to progression in the three groups of patients by censoring those who died before progression (Figure 2C). The hazard ratios for the patients in the low and high density

groups were 1.85 (95% CI: 1.24-2.76), and 3.79 (95% CI: 2.65-5.42) relative to the non-transfused group. The recently revised International Working Group (IWG) hematologic response criteria for patients with MDS refined RBCT burden by dividing patients into three categories (non-transfused patients, patients with a low transfusion burden (0.75-2 units per month) and those with a high transfusion burden (≥2 units per month).[19] We therefore repeated the analysis, subdividing the patients into four groups: no transfusions, >0 to <0.75 (low transfusion burden), 0.75 to 1.75 (mid transfusion burden) and >1.75 (high transfusion burden). The results are shown in Figure 2D. The main effect occurred for low dose densities, such that the outcomes of the mid and high transfusion density groups were similar. The low transfusion burden group of Figure 2D (density >0 - <0.75 units per month) is almost identical to the low burden group (density <0.89 units pwer month) of Figure 2B. MDS-related causes of death increased from 28% in the non-transfused group to 39% and 48% in the mid and high transfusion burden groups, respectively (*data not shown*).

Impact of individual prognostic factors

The univariate effect of various covariates on outcome was investigated in order to discover the appropriate functional form for the covariates (i.e., to discover whether a linear or non-linear form was best) and to discover appropriate ways of adjusting for confounding covariates. Increasing RBCT dose density was associated with inferior PFS ($P<1\times10^{-4}$). The functional form is shown in Figure 3A. The effect of the dose density increased until a dose density of about 1 unit per month; thereafter, the effect was flat. Baseline age (as a continuous variable) was strongly associated with PFS ($P<1\times10^{-4}$) in univariate regression analyses, as were baseline MDS diagnosis ($P<1\times10^{-4}$), quality of life measured by the EQ-5D Index ($P<1\times10^{-4}$), country of origin ($P=0.002$), bone marrow blast count ($P<1\times10^{-4}$), number of cytopenias ($P<1\times10^{-4}$), revised IPSS cytogenetic category ($P<1\times10^{-4}$), hemoglobin concentration ($P<1\times10^{-4}$), neutrophil count ($P<1\times10^{-4}$) and platelet count ($P<1\times10^{-4}$). No difference in
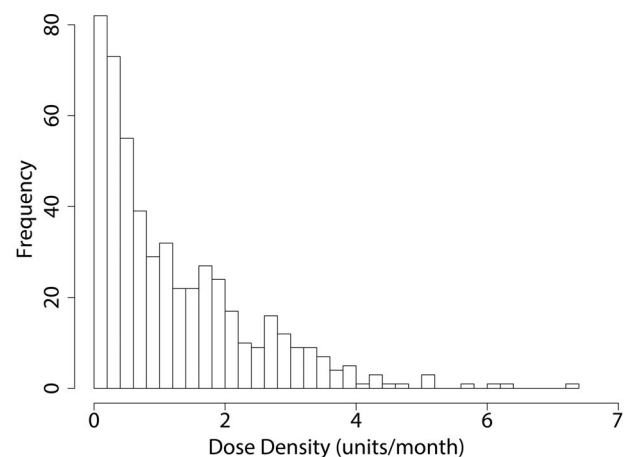
Figure 1. Distribution of dose densities of all transfused patients in the interval preceding the 1-year landmark. Frequency: number of patients in each dose density ranging from >0 to 0.2 units per month to >6 units per mont.

PFS was detected by sex (*P*=0.1), but PFS in females was superior in the multivariate analyses.

Progression-free survival using time-varying covariates proportional hazards regression analysis

Variables used for adjustment at baseline included age at diagnosis, sex, country of origin, number of cytopenias (and their corresponding blood counts), and number of units of blood received before registration. Time-varying variables measured longitudinally included: dose density, EQ-5D Index, components of the IPSS-R, and receipt of ESA, iron chelators and lenalidomide.

In multivariate analysis, not adjusting for the effects of ESA, iron chelation and lenalidomide therapy, all variables entered in the regression retained statistical significance. The functional form of the dose density effect (*P*<10⁻⁴) is shown in Figure 3B. With a frailty term added for the sub-

jects' country of origin, all previously significant variables, including the dose density, retained statistical significance, with a dose density *P*-value of <10⁻⁴.

Impact of therapeutic interventions on red blood cell transfusion densities

Treatment with ESA, lenalidomide and iron chelators may improve erythropoiesis and reduce the need for RBCT. Reduction of the RBCT rate results in a gradual decrease of the subsequent RBCT dose densities in intervals during the response period. We therefore investigated how many of the transfused patients had been treated with these interventions and calculated the average treatment duration and the number of patients with reduced transfusion densities after starting the intervention. In our cohort of 1,267 patients, 679 received treatment with an ESA and 151 had reduced transfusion densities in the first
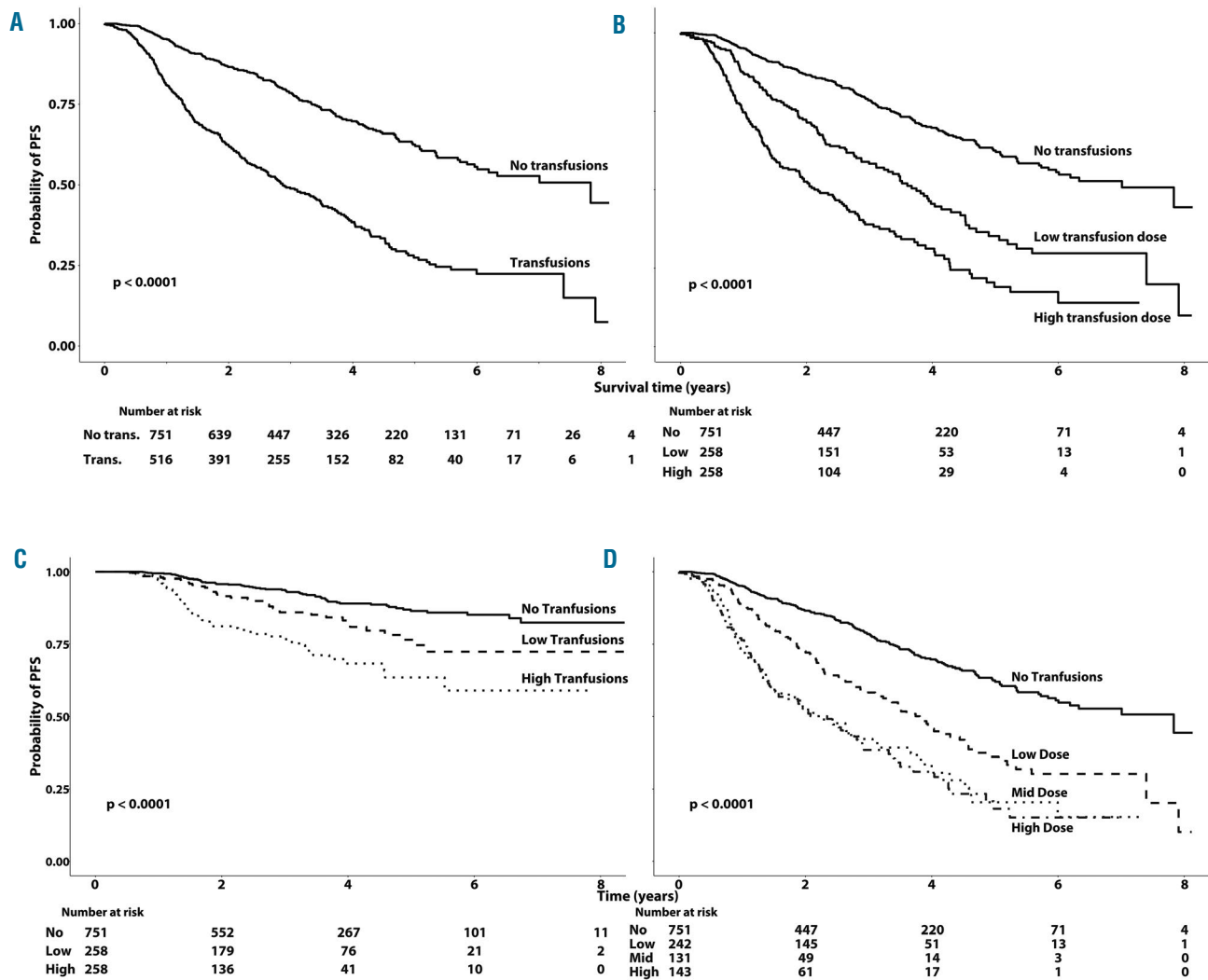
Figure 2. Progression-free survival and risk of progression according to transfusion status at the landmark of visit 3 (1 year after registration). (A) Kaplan-Meier plot of progression-free survival (PFS) of patients who did or did not receive transfusions by the landmark (visit 3). (B) Kaplan-Meier plot of PFS of patients who received transfusions at a low density (<0.87 units/month) or at a high density (>0.87 units/month) by the landmark *versus* PFS of patients who did not receive transfusions; (C) Kaplan-Meier plot of time to progression of patients surviving until progression subdivided according to transfusion burden or not as in panel B; (D) Kaplan-Meier plot of PFS of patients receiving transfusions at densities according to the revised International Working Group criteria: low dose density: >0- <0.75 units per month; mid dose density: 0.75 - 1.75 units per month; high dose density >1.75 units per month.

visit after starting ESA treatment. *Online Supplementary Figure S2* gives the individual dose density over time during ESA treatment of the 151 responding patients. Overall, 100 patients received treatment with lenalidomide: of these, 53 patients had a reduced transfusion density in the first visit after starting lenalidomide treatment; *Online Supplementary Figure S3* shows the individual dose density over time during lenalidomide treatment of the 53 responding patients. Within our study group 186 patients received treatment with iron chelators and 75 patients had a response leading to reduced transfusion densities in the first interval after starting of iron chelation treatment (*Online Supplementary Figure S4*). In contrast to the dose densities over time during ESA and lenalidomide treatment, the longer-term dose densities during iron chelation appeared to show a more stable pattern: subjects receiving a certain level of blood transfusion dose density when they first received iron chelation appeared to maintain that level of dose density. The decline of the dose density was less pronounced, but this might be a reflection of the longer transfusion period before starting chelation treatment when compared with the other two interventions.

The observed patterns of dose density trajectories suggest that receiving ESA, lenalidomide or iron chelation therapy modulates the dose density and we, therefore, included these variables in the regression model. This analysis resulted in an effect for the dose density similar to that of the previous analyses (Figure 3B), with a *P*-value of <0.0001. Indeed all variables entered in the regression retained statistical significance, except for platelet count (*P*=0.47) and neutrophil count (*P*=0.24). However, the dose density effect continued to increase beyond 1 unit per month after correction for the three interventions (ESA, iron chelation and lenalidomide) up until a dose of 6 units per month (Figure 3C).

Some patients received more than one intervention simultaneously, including 25 patients who received chelation and lenalidomide and 88 patients who received ESA and chelation. However, no additional impact could be detected over and above the impact of the two individual interventions.

Discussion

This large prospective, observational study confirmed the reported association of transfusion dose density with reduced PFS in patients with lower-risk MDS.[20] More surprisingly, we showed in this study that this negative association already occurred at a low transfusion rate. In addition, we showed that the risk of progression increased both in the low and high transfusion burden groups when compared to the non-transfused patients. We were even able to show that the deleterious effect of transfusions occurred at a very low transfusion burden (<0.75 units per month or <3 units per 16 weeks as defined by the revised IWG criteria), when the patients were subdivided according to the revised IWG hematological response criteria.[19] These patients with a very low transfusion burden are considered as untransfused patients using the revised IWG response criteria.[19]

The main focus of our study was to analyze the association of transfusion rate with outcome, assuming that regularly transfused patients may be exposed to the postulated toxicity of RBCT at a lower transfusion burden than

generally accepted. Several studies have addressed this question using various definitions of transfusion rate. The initial publications describing the impact of RBCT on outcome in MDS compared RBCT-dependent patients with RBCT-independent patients, using RBCT dependency as a time-dependent variable.[1,21] These studies were based on various definitions of RBCT dependency,[22,23] including a study using a rigid criterion, which implied a RBCT rate of at least 1 unit per month during a period of 2 months.[24] In this last study, transfusion dependency occurred in a minority of the patients (35% to 44%). The use of this
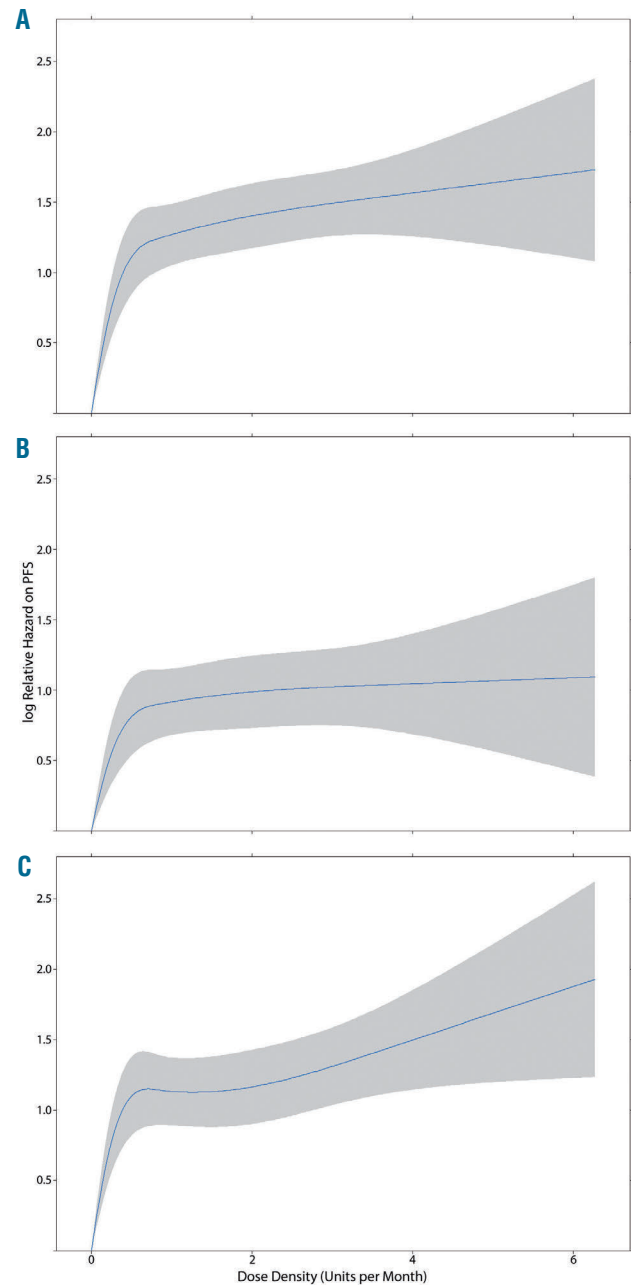
Figure 3. Influence of dose density on progression-free survival. (A) Dose density effect on progression-free survival (PFS) in an univariate analysis. (B) Dose density effect on PFS in a multivariate regression model unadjusted for the three treatment variables. (C) Dose density effect on PFS in a multivariate regression model adjusted for treatment with either erythropoiesis-stimulating agent, Iron chelation or lenalidomide.

definition implies that patients regularly receiving fewer than 3 units per 16 weeks are defined as RBCT-independent, but these patients might also be subject to the deleterious association with RBCT. In addition, patients may respond to therapeutic interventions, such as ESA, lenalidomide or iron chelators and become RBCT-independent again. The conclusion was that the severity of anemia was the leading cause of impaired survival rather than RBCT dependency.[24] However, the definition of severe anemia (<9 g/dL in males and <8 g/dL in females) implies that the majority of these patients were regularly transfused, as confirmed in the study.[24] This study also showed that the transfusion rate was significantly associated with an increased risk of cardiac complications. The risk of cardiac complications was significantly higher in patients with a RBCT intensity of >3 units per month compared to that in patients transfused with <1 unit per month.[24] In an open forum discussion RBCT dependency was even defined much higher, at 2 units per month in a 3-month interval.[25] In a Spanish study of 191 transfused patients with MDS, the interval between each transfusion was used to calculate the transfusion intensity.[26] It was concluded that high transfusion intensity was associated with decreased survival and increased risk of development of acute myeloid leukemia, in concordance with our study. Interestingly, the cumulative transfusion burden was not a prognostic factor when the transfusion intensity was included in the model.[26]

The traditional evaluations of the prognostic impact of factors influencing outcome have used standard time-to-event methods based on variables at diagnosis; however, many variables in MDS may change over time. This aspect can be addressed by using proportional hazards regression with time-varying covariates. The EUMDS Registry is collecting its observational data at registration of each new patient (within 100 days after diagnosis) and follow-up data at 6-monthly intervals. This practice leads to regular visit intervals of 6 months. For many patients in this dataset, the value of the recorded transfusion rate varied strongly over time, as shown in the *Online Supplementary Files*. We therefore calculated the RBCT rate at each reported visit during all preceding visit intervals between the date of the first RBCT and the date of the last visit, leading to a "smoothed" variable, defined as dose density. This reflects an average rate of receiving transfusions during the whole observation period with transfusions. The relatively low number of red cell units transfused per month can be explained by the remarkable variation of the transfusion rate over time, even when using interval visit reports of 6 months' duration.

Baseline age, bone marrow percentage category, number of cytopenias, and the EQ-5D Index retained their significant prognostic impact in the proportional hazards regression with time-varying explanatory variables. The non-linear component of the dose density effect was also retained ($P<1x10^{-4}$). The unfavorable effect of the dose density increased until a dose density of about 2 units per month and leveled off thereafter. A similar form and effect was observed when using the cumulative dose of RBCT units over time in an identical multivariate regression model with the same variables (*data not shown*). The negative impact of the cumulative RBCT dose started already at the time of administering the first RBCT and did not increase any further beyond 30 units received (*data not shown*).

Many patients showed a (temporary) decrease of the RBCT dose density, reflecting response to ESA,[27] lenalidomide,[28] and/or iron chelators[12] in 22%, 53% and 40% of the treated patients, respectively. The observed patterns of dose density trajectories suggest that receipt of ESA, lenalidomide and/or iron chelation modulates the dose density and we therefore included these variables as confounding variables in the regression model. This analysis showed that the impact of the dose density remained similar to that in the previous analyses, but in contrast to the previous analyses there is some evidence that the dose density effect continued to increase beyond 2 units per month after correction for the three interventions.

Red blood cells are usually transfused after a certain period of storage, but the survival of stored red blood cells depends on this period.[29,30] Transfusion of stored red cells leads to pro-inflammatory reactions, associated with a higher risk of infection and increased levels of circulating iron and, in particular, NTBI species, which enhance bacterial growth *in vitro*.[31,32] Infusion of autologous red blood cells from healthy volunteers after prolonging storage up to 6 weeks resulted in increased extravascular hemolysis, decreased red cell survival, elevated NTBI and ferritin levels in units transfused after 6 weeks compared to units transfused after shorter shortage.[33] Excess toxic iron species, including NTBI and especially its component LPI,[34] catalyze the cellular generation of reactive oxygen species. Oxidative stress may lead to pro-inflammatory responses and to oxidation of lipids, proteins and DNA causing cell and tissue damage.[35,36] Elevated NTBI levels after a single unit of RBC stored for 6 weeks normalize within 24 hours.[37] However, in multi-transfused patients (cumulative number of units ≥10) with MDS, NTBI and LPI remained elevated until the next transfusion.[17]

In conclusion, the negative association of transfusions on PFS already occurs at low RBCT dose densities below 3 units per 16 weeks. This indicates that the RBCT dependency in patients transfused at relatively low rates, who are usually considered as untransfused patients, may be considered as an indicator of poor prognosis for PFS. This poor prognosis in transfusion-dependent patients might be the result of direct toxicity of iron radicals resulting from the RBCT or the result of concomitant disease progression, including hematopoietic impairment. Data from our group provide support for the direct toxicity of RBCT density on outcome, because patients had a better outcome if treated with chelators, which remove toxic iron radicals effectively. Future studies, including interventional studies, are needed to confirm our observations, which may lead to adaptions of the current recommendations.

References

1. Cazzola M, Malcovati L. Myelodysplastic syndromes--coping with ineffective hematopoiesis. N Engl J Med. 2005;352 (6):536-538.

2. Malcovati L, Porta MG, Pascutto C, et al. Prognostic factors and life expectancy in myelodysplastic syndromes classified according to WHO criteria: a basis for clinical decision making. J Clin Oncol. 2005;23 (30):7594-7603.

3. Greenberg P, Cox C, LeBeau MM, et al. International scoring system for evaluating prognosis in myelodysplastic syndromes. Blood. 1997;89(6):2079-2088.

4. de Swart L, Smith A, Johnston TW, et al. Validation of the revised international prognostic scoring system (IPSS-R) in patients with lower-risk myelodysplastic syndromes: a report from the prospective European LeukaemiaNet MDS (EUMDS) registry. Br J Haematol. 2015;170(3):372-383.

5. Zipperer E, Post JG, Herkert M, et al. Serum hepcidin measured with an improved ELISA correlates with parameters of iron metabolism in patients with myelodysplastic syndrome. Ann Hematol. 2013;92(12):1617-1623.

6. Santini V, Girelli D, Sanna A, et al. Hepcidin levels and their determinants in different types of myelodysplastic syndromes. PLoS One. 2011;6(8):e23109.

7. Cuijpers ML, Raymakers RA, Mackenzie MA, de Witte TJ, Swinkels DW. Recent advances in the understanding of iron overload in sideroblastic myelodysplastic syndrome. Br J Haematol. 2010;149(3):322-333.

8. Shenoy N, Vallumsetla N, Rachmilewitz E, Verma A, Ginzburg Y. Impact of iron overload and potential benefit from iron chelation in low-risk myelodysplastic syndrome. Blood. 2014;124(6):873-881.

9. Ambaglio I, Malcovati L, Papaemmanuil E, et al. Inappropriately low hepcidin levels in patients with myelodysplastic syndrome carrying a somatic mutation of SF3B1. Haematologica. 2013;98(3):420-423.

10. Rund D, Rachmilewitz E. Beta-thalassemia. N Engl J Med. 2005;353(11):1135-1146.

11. Gattermann N, Rachmilewitz EA. Iron overload in MDS-pathophysiology, diagnosis, and complications. Ann Hematol. 2011;90 (1):1-10.

12. Gattermann N, Finelli C, Della Porta M, et al. Hematologic responses to deferasirox therapy in transfusion-dependent patients with myelodysplastic syndromes. Haematologica. 2012;97(9):1364-1371.

13. Ghoti H, Amer J, Winder A, Rachmilewitz E, Fibach E. Oxidative stress in red blood cells, platelets and polymorphonuclear leukocytes from patients with myelodysplastic syndrome. Eur J Haematol. 2007;79 (6):463-467.

14. De Souza GF, Ribeiro HL, Jr., De Sousa JC, et al. HFE gene mutation and oxidative damage biomarkers in patients with myelodysplastic syndromes and its relation to transfusional iron overload: an observational cross-sectional study. BMJ Open. 2015;5(4): e006048.

15. Saigo K, Takenokuchi M, Hiramatsu Y, et al. Oxidative stress levels in myelodysplastic syndrome patients: their relationship to serum ferritin and haemoglobin values. J Int Med Res. 2011;39(5):1941-1945.

16. Bulycheva E, Rauner M, Medyouf H, et al. Myelodysplasia is in the niche: novel concepts and emerging therapies. Leukemia. 2015;29(2):259-268.

17. de Swart L, Reiniers C, Bagguley T, et al. Labile plasma iron levels predict survival in patients with lower-risk myelodysplastic syndromes. Haematologica. 2018;103(1):69-79.

18. Vardiman JW, Harris NL, Brunning RD. The World Health Organization (WHO) classification of the myeloid neoplasms. Blood. 2002;100(7):2292-2302.

19. Platzbecker U, Fenaux P, Ades L, et al. Proposals for revised IWG 2018 hematological response criteria in patients with MDS included in clinical trials. Blood. 2018;133(10):1020-1030.

20. Goldberg SL, Chen E, Corral M, et al. Incidence and clinical complications of myelodysplastic syndromes among United States Medicare beneficiaries. J Clin Oncol. 2010;28(17):2847-2852.

21. Hiwase DK, Singhal D, Strupp C, et al. Dynamic assessment of RBC-transfusion dependency improves the prognostic value of the revised-IPSS in MDS patients. Am J Hematol. 2017;92(6):508-514.

22. Malcovati L, Germing U, Kuendgen A, et al. Time-dependent prognostic scoring system for predicting survival and leukemic evolution in myelodysplastic syndromes. J Clin Oncol. 2007;25(23):3503-3510.

23. Waszczuk-Gajda A, Madry K, Machowicz R, et al. Red blood cell transfusion dependency and hyperferritinemia are associated with impaired survival in patients diagnosed with myelodysplastic syndromes: results from the first Polish MDS-PALG registry. Adv Clin Exp Med. 2016;25(4):633-641.

24. Malcovati L, Della Porta MG, Strupp C, et al. Impact of the degree of anemia on the outcome of patients with myelodysplastic syndrome and its integration into the WHO classification-based Prognostic Scoring System (WPSS). Haematologica. 2011;96 (10):1433-1440.

25. Gale RP, Barosi G, Barbui T, et al. What are RBC-transfusion-dependence and -independence? Leuk Res. 2011;35(1):8-11.

26. Pereira A, Nomdedeu M, Aguilar JL, et al. Transfusion intensity, not the cumulative red blood cell transfusion burden, determines the prognosis of patients with myelodysplastic syndrome on chronic transfusion support. Am J Hematol. 2011;86 (3):245-250.

27. Hellstrom-Lindberg E, Negrin R, Stein R, et al. Erythroid response to treatment with G-CSF plus erythropoietin for the anaemia of patients with myelodysplastic syndromes: proposal for a predictive model. Br J Haematol. 1997;99(2):344-351.

28. Fenaux P, Giagounidis A, Selleslag D, et al. A randomized phase 3 study of lenalidomide versus placebo in RBC transfusion-dependent patients with low-/intermediate-1-risk myelodysplastic syndromes with del5q. Blood. 2011;118(14):3765-3776.

29. Luten M, Roerdinkholder-Stoelwinder B, Schaap NP, de Grip WJ, Bos HJ, Bosman GJ. Survival of red blood cells after transfusion: a comparison between red cells concentrates of different storage periods. Transfusion. 2008;48(7):1478-1485.

30. van de Watering L, Lorinser J, Versteegh M, Westendord R, Brand A. Effects of storage time of red blood cell transfusions on the prognosis of coronary artery bypass graft patients. Transfusion. 2006;46(10):1712-1718.

31. Hod EA, Zhang N, Sokol SA, et al. Transfusion of red blood cells after prolonged storage produces harmful effects that are mediated by iron and inflammation. Blood. 2010;115(21):4284-4292.

32. McQuilten ZK, French CJ, Nichol A, Higgins A, Cooper DJ. Effect of age of red cells for transfusion on patient outcomes: a systematic review and meta-analysis. Transfus Med Rev. 2018;32(2):77-88.

33. Rapido F, Brittenham GM, Bandyopadhyay S, et al. Prolonged red cell storage before transfusion increases extravascular hemolysis. J Clin Invest. 2017;127(1):375-382.

34. de Swart L, Hendriks JC, van der Vorm LN, et al. Second international round robin for the quantification of serum non-transferrin-bound iron and labile plasma iron in patients with iron-overload disorders. Haematologica. 2016;101(1):38-45.

35. Rachmilewitz EA, Weizer-Stern O, Adamsky K, et al. Role of iron in inducing oxidative stress in thalassemia: can it be prevented by inhibition of absorption and by antioxidants? Ann N Y Acad Sci. 2005;1054: 118-123.

36. Hershko C, Link G, Cabantchik I. Pathophysiology of iron overload. Ann N Y Acad Sci. 1998;850:191-201.

37. Hod EA, Brittenham GM, Billote GB, et al. Transfusion of human volunteers with older, stored red blood cells produces extravascular hemolysis and circulating non-transferrin-bound iron. Blood. 2011;118(25):6675-6682.

Impact of treatment with iron chelation therapy in patients with lower-risk myelodysplastic syndromes participating in the European MDS registry

Marlijn Hoeks,[1,2] Ge Yu,[3] Saskia Langemeijer,[4] Simon Crouch,[3]
Louise de Swart,[4] Pierre Fenaux,[5] Argiris Symeonidis,[6] Jaroslav Čermák,[7]
Eva Hellström-Lindberg,[8] Guillermo Sanz,[9] Reinhard Stauder,[10]
Mette Skov Holm,[11] Moshe Mittelman,[12] Krzysztof Mądry,[13] Luca Malcovati,[14]
Aurelia Tatic,[15] Antonio Medina Almeida,[16] Ulrich Germing,[17]
Aleksandar Savic,[18] Njetočka Gredelj Šimec,[19] Dominic Culligan,[20]
Raphael Itzykson,[5] Agnes Guerci-Bresler,[21] Borhane Slama,[22]
Arjan van de Loosdrecht,[23] Corine van Marrewijk,[4] Jackie Droste,[4]
Nicole Blijlevens,[4] Marian van Kraaij,[24] David Bowen,[25] Theo de Witte[26] and
Alex Smith[3] on behalf of the EUMDS Registry Participants

[1]Centre for Clinical Transfusion Research, Sanquin Research, Leiden, the Netherlands;
[2]Department of Clinical Epidemiology, Leiden University Medical Center, Leiden,
the Netherlands; [3]Epidemiology and Cancer Statistics Group, Department of Health
Sciences, University of York, York, USA; [4]Department of Hematology, Radboud University
Medical Center, Nijmegen, the Netherlands; [5]Service d'Hématologie, Hôpital Saint-Louis,
Assistance Publique des Hôpitaux de Paris and Université Paris 7, Paris, France;
[6]Department of Medicine, Division of Hematology, University of Patras Medical School,
Patras, Greece; [7]Department of Clinical Hematology, Institute of Hematology and Blood
Transfusion, Praha, Czech Republic; [8]Department of Medicine, Division of Hematology,
Karolinska Institutet, Stockholm, Sweden; [9]Department of Haematology, Hospital
Universitario y Politécnico La Fe, Valencia, Spain; [10]Department of Internal Medicine V
(Haematology and Oncology), Innsbruck Medical University, Innsbruck, Austria;
[11]Department of Haematology, Aarhus University Hospital, Aarhus, Denmark;
[12]Department of Medicine A, Tel Aviv Sourasky (Ichilov) Medical Center and Sackler
Medical Faculty, Tel Aviv University, Tel Aviv, Israel; [13]Department of Haematology,
Oncology and Internal Medicine, Warszawa Medical University, Warszawa, Poland;
[14]Department of Hematology Oncology, Fondazione Istituto Di Ricovero e Cura a
Carettere Scientifico, Policlinico San Matteo, University of Pavia, Pavia, Italy; [15]Center of
Hematology and Bone Marrow Transplantation, Fundeni Clinical Institute, Bucharest,
Romania; [16]Department of Hematology, Hospital da Luz, Lisbon, Portugal; [17]Department
of Haematology, Oncology and Clinical Immunology, Universitätsklinik Düsseldorf,
Düsseldorf, Germany; [18]Clinic of Hematology - Clinical Center of Vojvodina, Faculty of
Medicine, University of Novi Sad, Novi Sad, Serbia; [19]Department of Internal Medicine,
Division of Hematology, Merkur University Hospital, Zagreb, Croatia; [20]Department of
Haematology, Aberdeen Royal Infirmary, Aberdeen, UK; [21]Service d'Hématologie, Centre
Hospitalier Universitaire Brabois Vandoeuvre, Nancy, France; [22]Service d'Hématologie,
Centre Hospitalier d'Avignon, Avignon, France; [23]Department of Hematology – Cancer
Center Amsterdam VU University Medical Center, Amsterdam, the Netherlands; [24]Unit
Transfusion Medicine, Sanquin Blood Bank, Amsterdam, the Netherlands; [25]St. James's
Institute of Oncology, Leeds Teaching Hospitals, Leeds, UK and [26]Department of Tumor
Immunology - Nijmegen Center for Molecular Life Sciences, Radboud University Medical
Center, Nijmegen, the Netherlands

ABSTRACT

Iron overload due to red blood cell (RBC) transfusions is associated with morbidity and mortality in lower-risk myelodysplastic syndrome (MDS) patients. Many studies have suggested improved survival after iron chelation therapy (ICT), but valid data are limited. The aim of this study was to assess the effect of ICT on overall survival and hematologic improvement in lower-risk MDS patients in the European MDS registry. We compared chelated patients with a contemporary, non-chelated control group within the European MDS registry, that met the eligibility criteria for starting iron chelation. A Cox proportional hazards model was used to assess overall survival (OS), treating receipt of chelation as a time-varying variable. Additionally, chelated and non-chelated patients were compared

using a propensity-score matched model. Of 2,200 patients, 224 received iron chelation. The hazard ratio and 95% confidence interval for OS for chelated patients, adjusted for age, sex, comorbidity, performance status, cumulative RBC transfusions, Revised-International Prognostic Scoring System (IPSS-R), and presence of ringed sideroblasts was 0.50 (0.34-0.74). The propensity-score analysis, matched for age, sex, country, RBC transfusion intensity, ferritin level, comorbidity, performance status, and IPSS-R, and, in addition, corrected for cumulative RBC transfusions and presence of ringed sideroblasts, demonstrated a significantly improved OS for chelated patients with a hazard ratio of 0.42 (0.27-0.63) compared to non-chelated patients. Up to 39% of chelated patients reached an erythroid response. In conclusion, our results suggest that iron chelation may improve OS and hematopoiesis in transfused lower-risk MDS patients. This trial was registered at *clinicaltrials.gov identifier: 00600860*.

Introduction

Myelodysplastic syndromes (MDS) comprise a heterogeneous group of clonal hematopoietic stem cell disorders characterized by abnormal differentiation and maturation of hematopoietic cells, bone marrow (BM) failure and genetic instability, with an enhanced risk of progressing to acute myeloid leukemia (AML).[1] Iron overload (IOL), as a consequence of frequently administered red blood cell transfusions (RBCT) and/or ineffective erythropoiesis, is a common finding in MDS. The effects of toxic iron species in other iron loading diseases, such as primary hemochromatosis, thalassemia and sickle cell anemia are well known, but the consequences in MDS are less clear.[2-4] With an expected median survival of 2.4-11.8 years in lower risk MDS (LR-MDS) patients,[5] these patients are prone to long-term accumulation of iron due to RBCT as well as direct iron toxicity due to the formation of reactive oxygen species (ROS).[6]

Several studies have reported beneficial effects of iron chelation therapy (ICT) on overall survival (OS) and other clinical outcomes in MDS patients with IOL.[7-10] However, valid data on the effect of ICT are limited, as most studies are carried out in small or highly selected patient groups, or suffer from serious methodological problems such as confounding by indication. Performing a randomized, controlled trial to explore this is cumbersome due to patients' widespread belief in the beneficial effects of ICT and also the personal opinion of many treating physicians, which may negatively affect enrollment. Likewise, patients included in a randomized, controlled trial do not generally reflect the actual LR-MDS patient group, which is usually made up of elderly patients with multiple comorbidities.

In addition to the possible beneficial effects of ICT on OS, there is increasing evidence to indicate hematologic improvement in patients during treatment with iron chelators.[11-16] Alongside improvement in hemoglobin, platelet, and neutrophil levels, transfusion independence is achieved in a minority of chelated patients.[11,12,14] The underlying mechanisms are still unclear.[17]

The aim of this study was to evaluate the effect of ICT on OS, hematologic improvement, and ferritin levels in lower risk MDS patients in the European MDS (EUMDS) Registry.

Methods

The EUMDS registry prospectively collects observational data on LR-MDS patients from 142 centers in 16 countries in Europe and Israel. Patients were included within 100 days of MDS diagnosis according to the World Health Organization 2001 classification, restricted to patients with a low or intermediate-1 score according to the International Prognostic Scoring System (IPSS).[18] IPSS was the current prognostic indicator at the start of the registry, in accordance with the currently used prognostic score; the Revised-IPSS (IPSS-R) was reconstructed afterwards. The ethics committees of all participating centers approved the protocol and all patients provided written informed consent. Data were collected at baseline and at each 6-monthly routine outpatient follow-up visit. Data were collected on: comorbidity, transfusion history, use of iron chelators (agent, time frame; no drug doses or schedules were collected), peripheral blood values, conventional iron parameters (e.g. serum ferritin), bone marrow pathology, and progression to higher-risk MDS or AML. Subjects were prospectively followed until death, loss to follow up, or withdrawal of informed consent.

In Europe, three iron chelators are available for treatment of secondary IOL, but availability varies between countries. We analyzed all patients, chelated or non-chelated, who are eligible for receiving ICT based on at least one criterion for starting ICT (cumulative ≥15 RBC units, RBCT intensity of ≥1 unit/month during a 6-month period, or serum ferritin level >1000 µg/L), thereby preventing immortal time bias. As chelated and non-chelated patients may differ in characteristics that affect outcome, two different approaches were performed in order to control for potential bias: 1) analysis of all eligible chelated and non-chelated patients using receipt of ICT as a time-varying co-variate, adjusting for co-variates related to both receiving ICT and OS: sex, age, comorbidity, performance status, RBCT intensity, number of units transfused, IPSS-R, and presence of ringed sideroblasts; 2) Propensity Score (PS), i.e. conditional probability for being treated with ICT on the basis of patient characteristics, matching of the same group. Variables included in the PS were: age, sex, country, RBCT intensity, ferritin level, MDS comorbidity index, performance status, and IPSS-R. A 3-to-1 nearest neighbor matching method with replacement and caliper (0.2) was applied.[19] In addition, we used a robust sandwich estimator to correct for intra-individual correlation of multiply used controls. Further details on the PS matching are provided in the *Online Supplementary Methods*.[20-22] OS was defined as the time from eligibility for ICT to death; subjects still alive were censored at the last follow-up date. Cox proportional hazards regression models and Kaplan-Meier survival curves were applied and hazard ratios (HR) with 95% confidence intervals (95%CI) were reported.[23]

Erythroid responses were defined as a reduction in RBCT density (number of RBCT over time; see *Online Supplementary Methods* for definition and details) or as transfusion independency at least once as the transfusion density was reduced to zero, platelet responses were assessed according to the modified

International Working Group (IWG) criteria.[24] Ferritin responses were defined as a decrease of ≥1000 μg/L or a drop of the serum ferritin value below 1000 μg/L.

All analyses were undertaken in Stata 15 (StataCorp, College Station, TX, USA).

Results

Patient population

Data were extracted from the EUMDS registry on July 5th 2017, 2,200 patients, diagnosed between December 3rd

Table 1. Baseline characteristics of non-chelated and chelated patients at the check-up prior to reaching the eligibility criteria and estimates of overall survival.

	Non-chelated	Chelated	Deferasirox	Deferoxamine	Deferiprone
Total	490	199	150	36	13
N. of countries with chelated patients	17 / 17	17 / 17	14 / 17	9 / 17	6 / 17
Mean age at eligible (SD)	76 (10)	70 (9)	70 (9)	72 (9)	70 (10)
Time from diagnosis (months)					
Inclusion, median (p10-p90)	7 (0 - 35)	8 (0 - 32)	9 (0 - 36)	6 (0 - 30)	7 (0 - 33)
Inclusion, mean (SD)	14 (16)	13 (15)	14 (16)	9 (11)	12 (13)
Chelation median (p10-p90)	NA	17 (4 - 46)	17 (4 - 47)	13 (2 - 39)	22 (5 - 51)
Chelation mean (SD)	NA	21 (17)	21 (18)	17 (13)	26 (18)
Number of units transfused					
Median (range)	4.0 (1.0 – 33.0)	2.0 (0.0 – 28.0)	2.5 (0.0 – 28.0)	3.0 (0.0 – 18.0)	2.0 (0.0 – 8.0)
Median at start of chelation (range)	NA	13.0 (2.0 – 91.0)	12.0 (2.0 – 75.0)	10.5 (2.0 – 75.0)	24.5 (2.0 – 91.0)
Ferritin (μg/L)					
Median (p10-p90)	547.0	675.0	683.0	682.0	525.0
	(116.0 – 1384.0)	(256.0 – 1573.0)	(264.0 – 1600.0)	(256.0 – 1920.0)	(190.5 – 918.1)
Median at start of chelation (p10-p90)	NA	1221.0	1210.0	1173.0	2202.0
		(475.8 – 3000.0)	(449.3 – 2832.0)	(335.0 – 3000.0)	(475.8 – 4900.0)
Comorbidity (MDSCI)					
Low risk	308 63.2%	150 75.8%	118 79.2%	23 63.9%	9 69.2%
Intermediate risk	149 30.6%	43 21.7%	28 18.8%	11 30.6%	4 30.8%
High risk	30 6.2%	5 2.5%	3 2.0%	2 5.6%	0 0.0%
Performance status					
Unable to care for self	8 2.0%	1 0.6%	1 0.8%	0 0.0%	0 0.0%
Unable to work	132 32.3%	36 20.2%	21 15.9%	12 34.3%	3 27.3%
Able to work and normal activity	269 65.8%	141 79.2%	110 83.3%	23 65.7%	8 72.7%
Prognostic indicator (IPSS-R)					
Reaching criteria (LOCF***)					
Very low	48 13.4%	22 13.5%	18 14.6%	2 6.9%	2 18.2%
Low	199 55.6%	95 58.3%	66 53.7%	21 72.4%	8 72.7%
Intermediate	111 31.0%	46 28.2%	39 31.7%	6 20.7%	1 9.1%
High	38 10.6%	9 5.5%	6 4.9%	3 10.3%	0 0.0%
Very high	3 0.8%	1 0.6%	1 0.8%	0 0.0%	0 0.0%
Duration of treatment with chelation (months)					
Median (p10-p90)	NA	13 (3 - 41)	14 (3 - 41)	9 (1 - 34)	13 (2 - 30)
Ever received ESA					
No	312 63.7%	115 57.8%	85 56.7%	22 61.1%	8 61.5%
Yes	178 36.3%	84 42.2%	65 43.3%	14 38.9%	5 38.5%
Ever received hypomethylating					
No	460 93.9%	184 92.5%	136 90.7%	36 100.0%	12 92.3%
Yes	30 6.1%	15 7.5%	14 9.3%	0 0.0%	1 7.7%
Ever received lenalidomide					
No	467 95.3%	179 89.9%	136 90.7%	33 91.7%	10 76.9%
Yes	23 4.7%	20 10.1%	14 9.3%	3 8.3%	3 23.1%
Overall Survival (OS)*					
Unadjusted	1	0.57 (0.45 – 0.73)	1	1.99 (1.18 – 3.35)	0.42 (0.10 – 1.71)
Adjusted**	1	0.50 (0.34 – 0.74)	1	2.46 (1.12 – 5.41)	0.30 (0.02 – 3.58)

*Hazard Ratios (HR) and 95% Confidence Intervals (CI) were estimated using receipt of chelation as a time-varying co-variate. ** Adjusted by age at eligibility, sex, comorbidity, Performance Status, number of units transfused, Revised-International Prognostic Scoring System (IPSS-R), and ringed sideroblasts present. ***LOCF: last observation carried forward (only for cytogenetics and bone marrow blasts); SD: Standard Deviation; RBCT: red blood cell transfusion; MDSCI: Myelodysplastic Syndrome Specific Comorbidity Index; ESA: erythropoiesis stimulating agents; NA: not applicable.

2007 and April 25th 2017, had been registered, of which 1,161 patients received at least one RBCT and 224 patients received iron chelation therapy (ICT) (Figure 1). A small proportion of patients had received ICT without being transfused or prior to starting RBCT, these subjects generally had a high ferritin level and were excluded from subsequent analyses. Of the 1,161 transfused patients, 850 patients had been transfused for a duration of ≥2 months. Out of these 850 patients, 689 met the eligibility criteria. *Online Supplementary Figure S1* summarizes the number of patients who reached each criterion. At the time of analysis, 236 patients were deceased (154 non-chelated, 82 chelated) and nine patients progressed to high-risk MDS or AML (4 non-chelated, 5 chelated).

Comparing outcome of chelated *versus* non-chelated patients using iron chelation therapy as a time-dependent variable

Table 1 shows the characteristics of the 689 patients at the check-up prior to meeting one of the eligibility criteria; the date of this check-up is when the patients entered this analysis. Mean age of the 199 chelated patients was 70 years and these patients were younger than the non-chelated patients (mean age was 76 years). Median time from date of diagnosis to date of meeting the eligibility criteria was seven months in the non-chelated and eight months in the chelated subjects. The median follow-up period from study entry for chelated and non-chelated patients was 39.4 months (range 4.1-106.6 months) and 27.1 months (range 2.5-105.6 months), respectively. Non-chelated subjects had a higher number of cumulative units transfused than chelated subjects (4 *vs.* 2 units) at time of inclusion and, on average, chelated patients had 13 units transfused prior to commencing ICT. The latter had a higher median ferritin level recorded at baseline (675 μg/L *vs.* 547 μg/L), and this had increased to 1,221 μg/L prior to start of ICT. While non-chelated and chelated subjects had similar IPPS-R scores, chelated patients had fewer co-morbidities as measured by the MDS-CI score and a better performance status as measured by Karnofsky

Performance Status. OS was estimated using receiving ICT as a time-dependent variable, hence the number of patients reported in the risk table in Figure 2 reflects the time when a subject commences ICT. The hazard ratio for OS in the univariate analysis was 0.57 (95%CI: 0.45-0.73) (Table 1 and Figure 2). This benefit increased when adjusted for the factors in Table 1 and the following variables: sex, RBCT intensity, and the presence of ringed sideroblasts (HR: 0.50, 95%CI: 0.34-0.74). No statistically significant interactions were detected when using a sophisticated prediction-type model. When we restricted the analysis to patients who were treated with deferasirox (the largest group), thereby excluding possible differences between patients using different chelators, the crude HR for OS was 0.53 (95%CI: 0.40-0.69) and the adjusted HR for OS was 0.38 (95%CI: 0.24-0.60). Out of the 199 chelated patients, 150 received deferasirox as the initial chelator, 36 deferoxamine, and 13 deferiprone, and differences were seen in the baseline characteristics by type of chelator with deferasirox-treated patients being younger and fitter. Twenty-two patients switched from one chelator to another, or were treated with all three chelators consecutively (*Online Supplementary Table S1*), but usually the treatment period of the second chelator was shorter than the treatment period of the first chelator. The median time on chelation for all 199 patients was 13 months (range 3-41 months) and patients who were initially treated with deferoxamine had inferior OS compared to deferasirox-treated patients (adjusted HR: 2.46, 95%CI: 1.12-5.41) (Table 1). The OS of the deferoxamine-treated patients was similar to non-chelated patients (adjusted HR: 0.98, 95%CI: 0.52-1.86).

Matching of chelated and non-chelated patients by propensity scores

The variables used in the propensity score matching are described in *Online Supplementary Table S2* for all eligible patients by chelation status, initially excluding any missing variables and then after multiple imputation (MI). Along with the factors already shown in Table 1, there
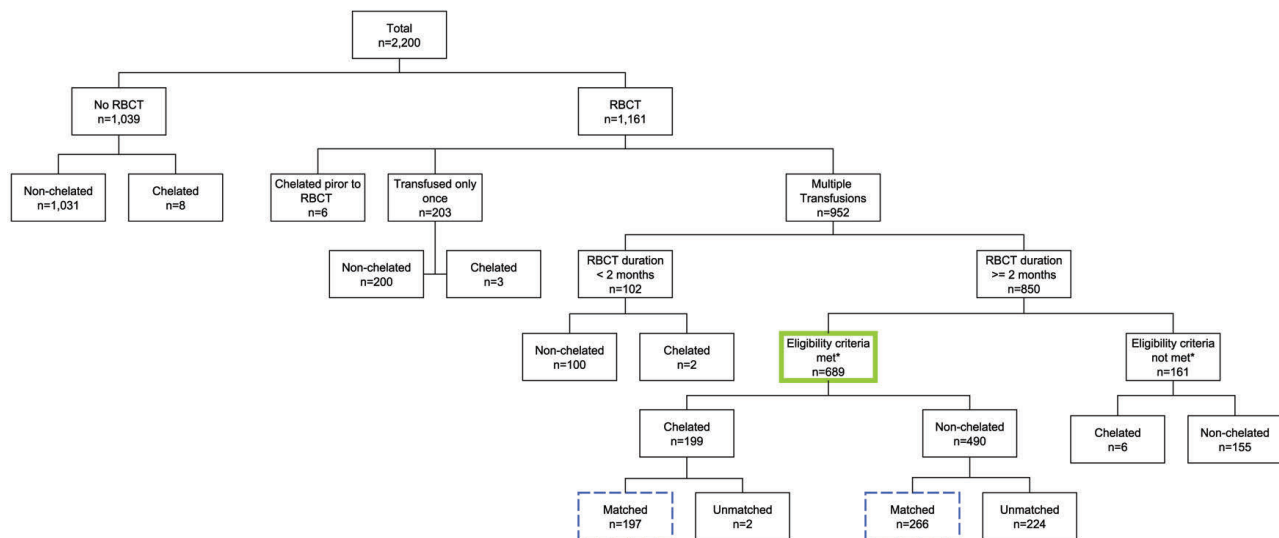
Figure 1. Number of registry patients by transfusion and chelation status. *Cumulative red blood cell transfusion (RBCT) units >15 or RBCT intensity of >1 RBC unit/month or serum ferritin >1000 μg/L.

was a difference by country as to whether a patient was treated with ICT; patients in the UK were less likely to be treated.

The overlap of propensity scores of both groups (chelated and non-chelated), which is essential for PS matching, was good for the majority of the patients (*Online Supplementary Figure S2*). The matched MI dataset included 197 of 199 chelated cases and identified 591 non-chelated controls. There were no differences by sex, RBCT intensity, cumulative RBCT units, serum ferritin levels, comorbidity, performance status, IPSS-R, presence of ringed sideroblasts, quality of life (QoL), and country between both groups (Table 2). Figure 3 shows the unadjusted survival plot by ICT status with receiving ICT as a time-dependent variable for the matched patients. A multivariate Cox proportional hazard model was used to

adjust for potential confounders (age, sex, comorbidity, performance status, monthly RBCT intensity, number of RBC units transfused, IPSS-R, and presence of ringed sideroblasts). The estimated crude and adjusted hazard ratios were 0.70 (95% CI: 0.51-0.95) and 0.42 (0.27-0.63), respectively (Table 2) and the adjusted survival curve is shown in Figure 4. When we again restricted the analysis to the deferasirox-treated patients, the crude HR for OS was 0.63 (95%CI: 0.45-0.88) and the adjusted HR was 0.34 (95%CI: 0.22-0.53).

The distribution of erythropoiesis-stimulating agent (ESA) and lenalidomide-treated patients among chelated and non-chelated patients at time of eligibility were similar in the unmatched and matched sample. A sensitivity analysis excluding the treatment of ESA and lenalidomide showed similar results.

Unmatched sample

Number at risk	0	6	12	18	24	30	36	42	48	54	60
Non−chelated	612	548	389	280	191	138	105	71	42	26	16
Chelated	77	101	128	118	117	101	72	58	47	34	24

P<0.001
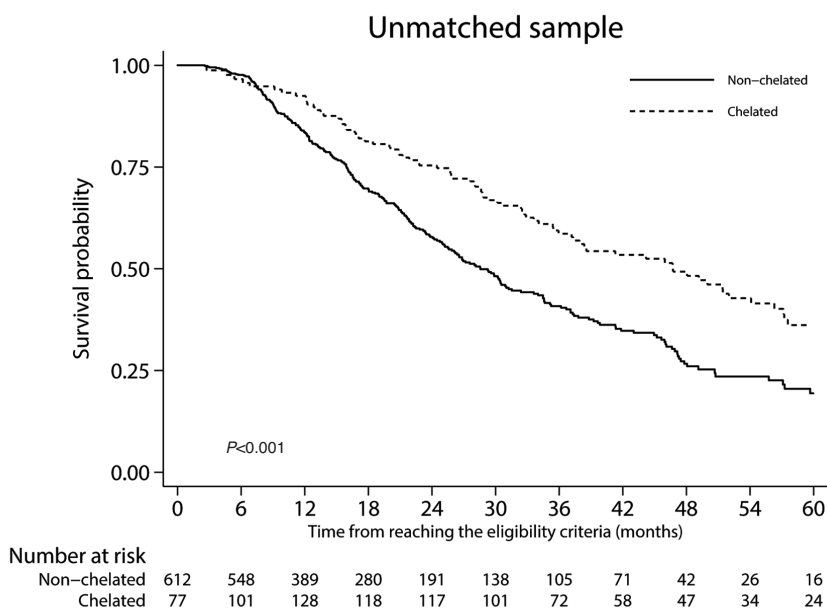
Figure 2. Overall survival by iron chelation therapy as a time-dependent variable in unmatched patients.

3 to 1 matched sample

Number at risk	0	6	12	18	24	30	36	42	48	54	60
Non−chelated	713	638	434	333	227	172	137	92	69	49	25
Chelated	75	101	128	118	117	101	73	58	47	34	24

P<0.001
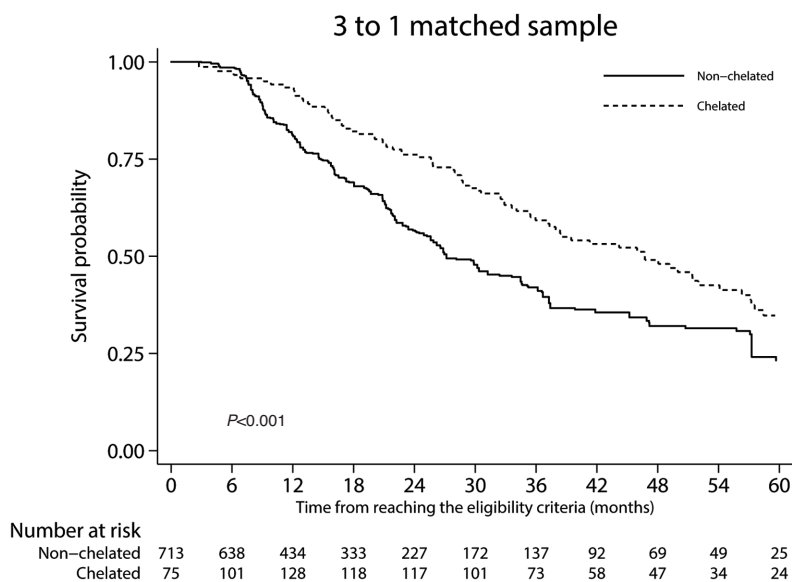
Figure 3. Overall survival by iron chelation therapy as a time-dependent variable in matched patients.

Table 2. Baseline characteristics for all matched subjects included in the propensity analyses

Co-variates	Matched* data with imputations**			
	Non-chelated N = 591	Chelated N = 197	P	Standardized differences***
Age (years)	71 (11)	70 (9)	0.364	-0.077
Sex			0.797	-0.021
Female	210 35.5%	72 36.5%		
Male	381 64.5%	125 63.5%		
RBCT Intensity (per month)	0.7 (1.0)	0.6 (1.0)	0.484	-0.058
Cumulative RBCT units	4.5 (4.9)	4.3 (4.7)	0.570	-0.047
Ferritin level (µg/L, median, p25-p75)	730.6 (494.6-977.3)	683.6 (504-915.5)	0.328	-0.086
Comorbidity (MDSCI)			0.965	-0.004
Low risk	440 74.5%	150 76.1%		
Intermediate risk	145 24.5%	42 21.3%		
High risk	6 1.0%	5 2.5%		
Performance status			0.279	0.090
Unable to care for self	4 0.7%	1 0.5%		
Unable to work	135 22.8%	38 19.3%		
Able to work and normal activity	452 76.5%	158 80.2%		
Prognostic indicator (IPSS-R)			0.914	0.009
Very low	83 14.0%	22 11.2%		
Low	337 57.0%	120 60.9%		
Intermediate	134 22.7%	45 22.8%		
High	34 5.8%	9 4.6%		
Very high	3 0.5%	1 0.5%		
Ring-sideroblast present			0.445	0.062
Yes	419 70.9%	134 68.0%		
No	172 29.1%	63 32.0%		
Platelet level (10x^9/L, median, p25-p75)	162.5 (99.2-294)	224.0 (121-324)	0.086	0.148
Hemoglobin level (g/dL, median, p25-p75)	8.8 (8.2-9.8)	8.4 (7.7-9.5)	0.021	-0.194
Quality of Life (EQ-5D)				
Index (mean, SD)	0.7 (0.2)	0.7 (0.2)	0.186	0.125
VAS (mean, SD)	64.8 (21.0)	68.1 (19.9)	0.083	0.165
Country			0.140	-0.122
Austria	25 4.2%	10 5.1%		
Croatia	9 1.5%	1 0.5%		
Czech Republic	58 9.8%	25 12.7%		
Denmark	15 2.5%	8 4.1%		
France	113 19.1%	40 20.3%		
Germany	23 3.9%	8 4.1%		
Greece	80 13.5%	23 11.7%		
Israel	11 1.9%	5 2.5%		
Italy	11 1.9%	5 2.5%		
the Netherlands	17 2.9%	7 3.6%		
Poland	22 3.7%	8 4.1%		
Portugal	2 0.3%	1 0.5%		
Romania	34 5.8%	11 5.6%		
Republic of Serbia	8 1.4%	2 1.0%		
Spain	11 1.9%	5 2.5%		
Sweden	97 16.4%	20 10.2%		
UK	55 9.3%	18 9.1%		
Overall Survival (OS)				
Unadjusted	1.0	0.70 (0.51 – 0.95)		
Adjusted****	1.0	0.42 (0.27 – 0.63)		

Continuous variables are reported as mean (Standard Deviation), while categorical variables are reported as number (%). *Matched by age, gender, country, red blood cell transfusion (RBCT) intensity, ferritin level, comorbidity, performance status, and Revised-International Prognostic Scoring System (IPSS-R) at eligibility. **Multiple imputations in RBCT intensity, ferritin level, comorbidity, Performance Status, and IPSS-R at eligibility for non-chelated patients. ***The standardized difference in percent is the mean difference as a percentage of the average standard deviation. ****Adjusted by age, sex, comorbidity, performance status, RBCT intensity, number of units transfused, IPSS-R, and RS present. MDSCI: myelodysplastic syndrome specific comorbidity index; EQ-5D: European Quality of Life - 5 dimensions.

Impact of iron chelation therapy on hematopoiesis and ferritin levels

Figure 5 shows the changes in transfusion density over eight visits in chelated and non-chelated patients. Forty-eight (62.3%) of the 77 responding patients were treated with ESA and 16 (20.8%) were treated with lenalidomide during chelation therapy. Compared to first check-up, 61 of the 197 chelated patients (31.0%) had a reduction in transfusion density, i.e. an absolute decrease, during at least one interval between check-ups, two patients (1.0%) maintained the same density throughout, and 134 (68.0%) never had a reduction in transfusion density. For those patients who showed a reduction, the average value in the monthly rate was -1.63 units per month (SD: 2.12, median: -0.96) compared to first check-up. Figure

6A shows the monthly RBC transfusion density for chelated patients with and without an erythroid response and non-chelated patients. In terms of becoming transfusion independent, 35 (17.8%) of the 197 treated patients had at least one interval between check-ups of approximately six months during which they had not received any further transfusions and 19 (9.6%) of the 197 patients were transfusion independent during more than one interval between check-ups after starting chelation therapy. In total, 54 patients (27.4%) became (temporarily) transfusion independent. In total, 77 chelated patients had an erythroid response: 61 patients had a reduction in transfusion density, and 16 patients who did not have a reduction in transfusion density became transfusion independent during at least one interval between check-ups.
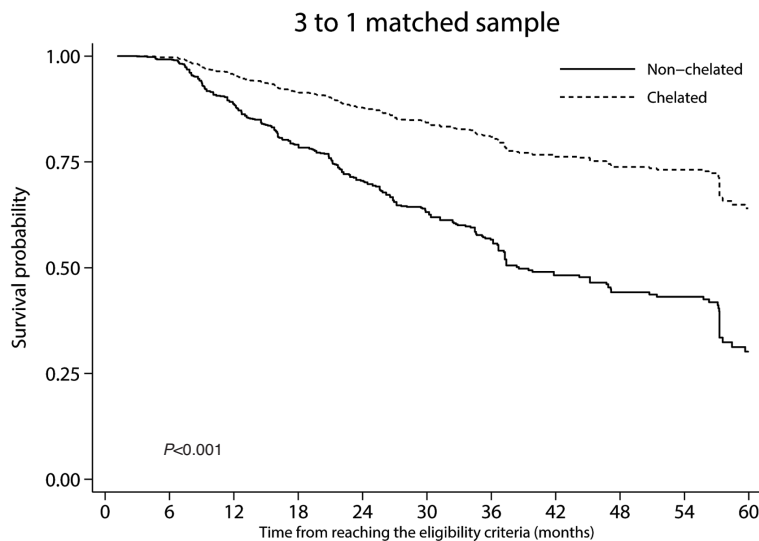
Figure 4. Adjusted overall survival by iron chelation therapy as a time-dependent variable in matched patients.
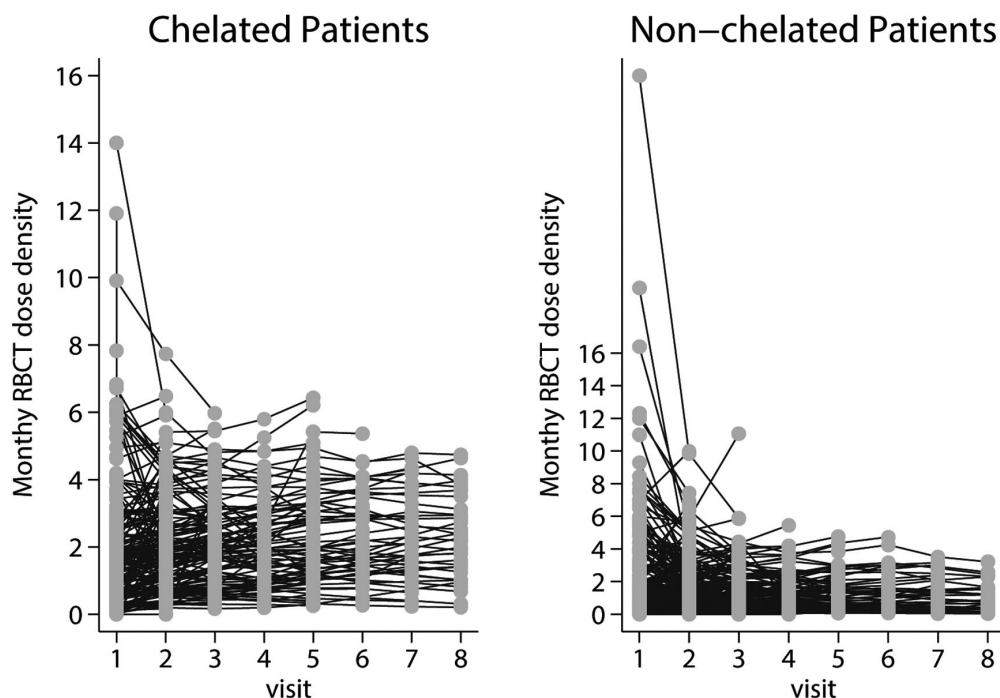
Figure 5. Changes in transfusion density over time in chelated and non-chelated patients. Time: eight 6-monthly visits.

We observed hematologic responses with all chelating agents.

A subgroup of chelated patients had an at least temporary platelet response (22.9%) over time. Median platelet counts were in the normal range in both the chelated and non-chelated group.

Figure 6B demonstrates ferritin levels of chelated patients with and without a ferritin response and non-chelated patients. Fifteen (51.7%) of the 29 responding patients were treated with ESA and five (17.2%) were treated with lenalidomide. A subgroup of patients had a ferritin response (5.6-23.5%) over time. Responding patients showed ongoing mean serum ferritin levels of approximately 1000 μg/L, whereas non-responding chelated patients had mean ferritin values of approximately 2100 μ/L.

Chelated patients follow up

On average, chelated patients did not start therapy until 17 months after diagnosis (Table 1). Of the 199 chelated patients, at the time of the analysis, follow up was ongoing for 148 patients, for seven patients their disease had progressed to higher risk MDS/AML, 29 patients had died, and four have missing values of treatment dates (these four patients are still ongoing), nine patients had withdrawn from the study (four of these because of disease progression and five after starting intensive treatment such as an allogeneic stem cell transplantation), and six were lost to follow up. Most patients (101 of the 148 ongoing patients) were receiving chelation at the time of the last report. Twenty of the 199 chelated patients switched from deferasirox to another chelating agent.
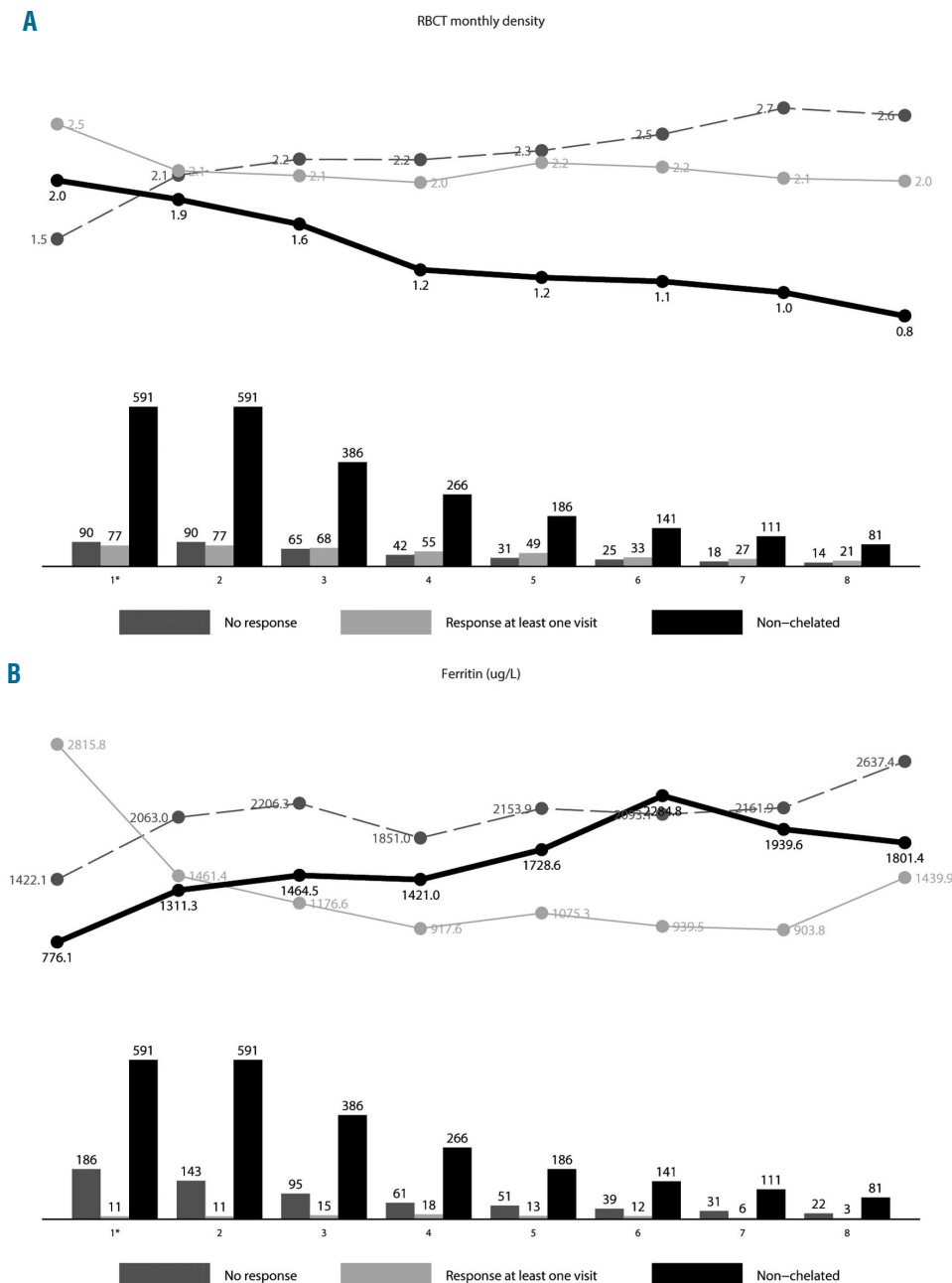
Figure 6. Trajectory analysis in chelated patients with and without response and for non-chelated patients. (A) Monthly red blood cell transfusion density for chelated patients with and without an erythroid response and for non-chelated patients. (B) Ferritin levels of patients with and without a ferritin response, defined as a decrease of ≥1000 μg/L or a drop of the serum ferritin value below 1000 μg/L, and for non-chelated patients.
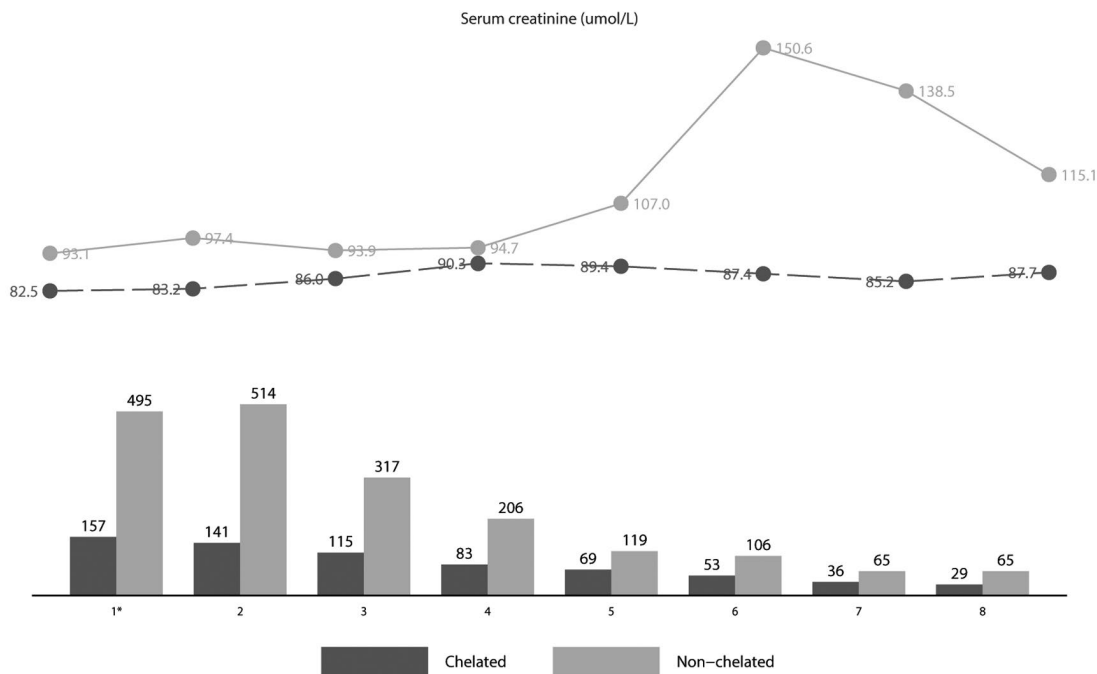
Figure 7. Serum creatinine levels (μmol/L) in chelated and non-chelated patients per check-up.

Reasons for cessation of iron chelation therapy

Information on reasons of cessation of ICT was not routinely recorded in the study. However, information about the deferasirox-treated patients was available for seven patients: fatigue and diarrhoea (1 patient), physician's choice (1 patient), economic reasons (1 patient), renal failure (1 patient), no effect (1 patient), dyspepsia (1 patient), and lower limb cramps and dosage change (1 patient).

Renal function

Non-chelated patients had slightly higher median creatinine values compared to chelated patients at time of eligibility [non-chelated: median 86 μmol/L (p10-p90: 61-135); chelated: median 79 μmol/L (p10-p90: 59-107)]. Forty-four chelated patients had higher serum creatinine levels at the first visit after discontinuing chelation compared with creatinine levels at time of eligibility (P=0.02 for all chelating agents and P=0.03 for deferasiox-treated patients). Renal function in non-chelated patients increased similarly over time (Figure 7).

Discussion

The results of this study indicate that ICT may improve OS in transfusion-dependent lower-risk MDS patients (LR-MDS). Our results are in line with several previously reported studies.[7-10,12,25-28] Some of these studies attempted to correct for confounding factors, but still suffered from confounding by indication. This generally results in an overestimation of the beneficial effect of ICT on OS in LR-MDS patients. So far, one randomized controlled trial has been reported on this subject. The randomized, placebo-controlled, TELESTO trial[29] evaluated the event-free survival (EFS) (a composite outcome, including non-fatal events related to cardiac and liver function, and transfor-

mation to AML or death) and safety of deferasirox *versus* placebo in low- and intermediate-1-risk MDS patients. This study demonstrated an EFS risk reduction of 36.4% in the deferasirox arm (P=0.015). However, there was no difference in median OS in the deferasirox-treated arm (HR 0.83, 95%CI: 0.54-1.28, P=0.200) when compared with placebo, but more than 50% of the placebo-treated patients switched to ICT after study treatment discontinuation (the placebo drug). The results of the TELESTO study are in line with our results. However, the included patients may not represent 'real-life' elderly MDS patients with multiple comorbidities, as reflected by the mean age of 61 years old of the patients included in TELESTO study compared to the mean age of 70 years in the EUMDS Registry study. Furthermore, low accrual rates and the crossover to ICT after cessation of the placebo, affected the statistical power of the TELESTO study.

Meanwhile, well-designed prospective observational data, reflecting, 'real-life' data, contribute to the better understanding of the effect of ICT on OS in LR-MDS patients. Recently, a study from the Canadian MDS registry demonstrated a superior OS for 83 chelated patients compared to non-chelated patients (5.2 *vs.* 2.1 years; P<0.001).[30] The patients in this study were selected at the onset of transfusion dependency. Chelated patients became transfusion-dependent at a much longer interval from diagnosis than non-chelated patients (median 18 *vs.* 6 months) and OS was calculated from the time of becoming transfusion-dependent. Even after matching, some incomparability between the two groups remained in factors like concurrent treatment, presence of ringed sideroblasts, and ferritin levels. Therefore, confounding cannot be excluded in this study. Nevertheless, their conclusions are in accordance with our findings, supporting the probable beneficial effect of ICT on OS in LR-MDS patients.

The mechanisms by which ICT influences OS after a relatively short exposure to iron chelation therapy (median duration of 13 months) are not completely understood. A recently published study of the EUMDS Registry, as well as the follow-up data of this study, demonstrated detectable labile plasma iron (LPI) levels to be associated with inferior OS in LR-MDS patients.[31,32] The risk of dying prematurely in patients with detectable LPI levels occurred too early in this study to explain this risk by classical IOL due to organ toxicity (e.g. liver and heart) after long-term transfusions, but this indicates a direct toxic effect associated with elevated LPI levels.[31]

Likewise, there is increasing evidence that increased LPI levels may be a general predictor of an increased non-relapse mortality during and after hematopoietic stem cell transplantion.[33]

Toxic iron species are known to catalyze the cellular generation of ROS, which play a key role in cellular damage.[34,35] ROS damage (mitochondrial) DNA, with potential consequent genomic instability, mutagenesis, and cell death. ROS are associated with leukemic transformation of the MDS clone.[6] Moreover, ICT is associated with a decrease in LPI and ROS.[6,16] Overall, the present study indicates that ICT may partly counteract the unfavorable consequences of secondary IOL.

In up to 31.0% of chelated patients a reduction in transfusion density was observed during at least one interval between check-ups. Likewise, 27.4% of the responding patients became, at least temporarily, transfusion independent. Platelet responses were less frequently observed. However, platelet count in this context was less relevant because the platelet counts in both groups were within the normal range, and will not likely lead to severe bleeding complications. Contemporary treatment with ESA and/or lenalidomide may have enhanced these responses.

Several previous studies recorded hematologic responses to ICT.[11-16] While the percentage of patients with hematologic responses in these studies are in line with the present study, none of the former studies included a control group in their analyses. One of the key factors is the relatively short period of ICT (median 13 months) in this study. The duration of ICT may improve by the introduction of a better tolerated formulation of deferasirox.[36] ICT is usually prescribed relatively late after detection of signs of IOL. Earlier initiation of ICT may prevent or decrease the occurrence of transfusional iron toxicity on hematopoiesis. Moreover, we recorded data only at 6-monthly intervals. Short duration hematologic responses in between check-ups may be missed by this approach. But on the other hand, short-term responses may not be clinically relevant.

Pre-clinical studies have shown a beneficial effect of ICT on hematopoiesis.[35,37] Inhibition of the transcription factor NF-κB, involved in many cellular processes, and modulation of mammalian target of rapamycin (M-TOR) signaling, a major regulator of cell death and proliferation, have been proposed to play a role.[17] Future studies should address this issue appropriately.

In the trajectory analyses, ferritin responses occurred in up to 23.5% of the chelated patients. Serum ferritin levels have frequently been reported to be a prognostic marker in LR-MDS patients, but serum ferritin is an imprecise surrogate marker for secondary IOL and toxicity.[38,39] This is reflected by the observation that a relatively small proportion of chelated patients have a considerable decrease in serum ferritin levels, while these patients show a significant survival benefit. Serum ferritin levels are influenced by the stage of MDS and by concurrent infection and inflammation, which is common in LR-MDS patients.[38] In addition, there is no convincing evidence regarding its use for monitoring secondary IOL in MDS patients.[38,40] Tissue biopsy and MRI T2* are currently regarded to be the most specific and sensitive diagnostic tests for detecting IOL.[38] However, the clinical utility of these assays remains unclear in MDS and invasiveness (biopsy), unavailability, and expense (MRI T2*) hamper their general use in clinical practice. As discussed above, LPI is associated with inferior survival in LR-MDS patients.[31,32] Future studies are warranted to evaluate the effect of ICT on LPI levels as a measure of iron toxicity. Measurement of oxidative stress, including malondialdehyde, a long-lasting lipid peroxidation product, formed as a consequence of oxidative stress from IOL, are also possible future markers to detect and monitor the biological consequences of secondary IO in LR-MDS patients, should they be proven to correlate with clinical outcomes.[41,42]

Analysis of renal function demonstrated that ICT is associated with an increase in creatinine levels. In some patients, this will be clinically relevant and/or a reason to stop or lower the dose of ICT. In other patients, an increase in creatinine levels will not affect cessation of ICT.

This large cohort, with prospectively collected 'real-life' data from diagnosis, provides a unique opportunity to study the effect of ICT in a large number of lower-risk MDS patients in daily practice. An important strength of the study is that the results can be widely generalized to this, mostly elderly, patient population with multiple comorbidities, who are typically excluded from clinical trials. The variation in iron chelation practice across the different countries, due to variable interpretation of the poor quality outcome data for ICT in MDS, made it possible to compare the effects of ICT on OS to a non-chelated control group. In Europe, unlike in the United States, socio-economic status does not influence the prescription of ICT (either deferoxamine or deferasirox) because the costs are covered by the national health systems.

Since conventional statistical modeling is limited by the number of co-variates to be added to a model, propensity-score matched analysis is able to incorporate more confounding factors in the model, including country-specific effects. Confounding by indication, a common problem in observational studies, is maximally reduced by using the propensity-score matched method and is, therefore, a major strength of this study. To our knowledge, we are the first to apply this method in order to adequately deal with confounding in this setting.

Limitations of our study include the moderate sample size of the deferoxamine and deferiprone groups. In addition, our analysis could not consider differences in dosing schemes and therapy compliance. This prevented us from drawing definitive conclusions of the effect of the separate iron chelators on OS. Data were collected at the scheduled 6-monthly intervals. Subtle changes in patient-related factors in the intervening 6-month period may have been missed. Not all patients can be matched by the propensity score approach. This might introduce selection bias. However, the same magnitude and direction of

the results were seen in the analysis of the unmatched samples. Therefore, in this case, propensity-score matching will probably not have led to significant selection bias. Finally, despite using a large control group, eligible for using ICT, and a propensity-score matched analysis corrected for many known and measured confounders, we cannot exclude residual confounding. Considering the size of the effect, it is unlikely that residual confounding would explain the difference found between chelated and non-chelated patients.

In summary, the results of this study suggest that ICT may improve OS and hematopoiesis in transfused LR-MDS patients.

References

1. Nimer SD. Myelodysplastic syndromes. Blood. 2008;111(10):4841-4851.
2. Porter J, Garbowski M. Consequences and management of iron overload in sickle cell disease. Hematology Am Soc Hematol Educ Program. 2013;2013:447-456.
3. Olivieri NF, Brittenham GM. Iron-chelating therapy and the treatment of thalassemia. Blood. 1997;89(3):739-761.
4. Powell LW, Seckington RC, Deugnier Y. Haemochromatosis. Lancet. 2016; 388(10045):706-716.
5. Greenberg P, Cox C, LeBeau MM, et al. International scoring system for evaluating prognosis in myelodysplastic syndromes. Blood. 1997;89(6):2079-2088.
6. Porter JB, de Witte T, Cappellini MD, et al. New insights into transfusion-related iron toxicity: Implications for the oncologist. Crit Rev Oncol Hematol. 2016;99:261-271.
7. Rose C, Brechignac S, Vassilief D, et al. Does iron chelation therapy improve survival in regularly transfused lower risk MDS patients? A multicenter study by the GFM (Groupe Francophone des Myélodysplasies). Leuk Res. 2010; 34(7):864-870.
8. Raptis A, Duh MS, Wang ST, et al. Treatment of transfusional iron overload in patients with myelodysplastic syndrome or severe anemia: data from multicenter clinical practices. Transfusion. 2010;50(1):190-199.
9. Neukirchen J, Fox F, Kündgen A, et al. Improved survival in MDS patients receiving iron chelation therapy - a matched pair analysis of 188 patients from the Düsseldorf MDS registry. Leuk Res. 2012; 36(8):1067-1070.
10. Delforge M, Selleslag D, Beguin Y, et al. Adequate iron chelation therapy for at least six months improves survival in transfusion-dependent patients with lower risk myelodysplastic syndromes. Leuk Res. 2014;38(5):557-563.
11. Messa E, Biale L, Castiglione A, et al. Erythroid response during iron chelation therapy in a cohort of patients affected by hematologic malignancies and aplastic anemia with transfusion requirement and iron overload: a FISM Italian multicenter retrospective study. Leuk Lymphoma. 2017;58(11):2752-2754.
12. Angelucci E, Santini V, Di Tucci AA, et al. Deferasirox for transfusion-dependent patients with myelodysplastic syndromes: safety, efficacy, and beyond (GIMEMA MDS0306 Trial). Eur J Haematol. 2014;92(6):527-536.
13. Nolte F, Höchsmann B, Giagounidis A, et al. Results from a 1-year, open-label, single arm, multi-center trial evaluating the efficacy and safety of oral Deferasirox in patients diagnosed with low and int-1 risk myelodysplastic syndrome (MDS) and transfusion-dependent iron overload. Ann Hematol. 2013;92(2):191-198.
14. Jensen PD, Heickendorff L, Pedersen B, et al. The effect of iron chelation on haemopoiesis in MDS patients with transfusional iron overload. Br J Haematol. 1996;94(2):288-299.
15. List AF, Baer MR, Steensma DP, et al. Deferasirox reduces serum ferritin and labile plasma iron in RBC transfusion-dependent patients with myelodysplastic syndrome. J Clin Oncol. 2012;30(17):2134-2139.
16. Gattermann N, Finelli C, Della Porta M, et al. Hematologic responses to deferasirox therapy in transfusion-dependent patients with myelodysplastic syndromes. Haematologica. 2012;9(9):1364-1371.
17. Breccia M, Voso MT, Aloe Spiriti MA, et al. An increase in hemoglobin, platelets and white blood cells levels by iron chelation as single treatment in multitransfused patients with myelodysplastic syndromes: clinical evidences and possible biological mechanisms. Ann Hematol. 2015;94(5):771-777.
18. Bennett JM. World Health Organization classification of the acute leukemias and myelodysplastic syndrome. Int J Hematol. 2000;72(2):131-133.
19. Caliendo M, Kopeinig S. SOME PRACTICAL GUIDANCE FOR THE IMPLEMENTATION OF PROPENSITY SCORE MATCHING. Journal of Economic Surveys. 2008;22(1):31-72.
20. Rosenbaum PR, Rubin DB. Constructing a Control Group Using Multivariate Matched Sampling Methods That Incorporate the Propensity Score. The American Statistician. 1985;39(1):33-38.
21. Stürmer T, Joshi M, Glynn RJ, et al. A review of the application of propensity score methods yielded increasing use, advantages in specific settings, but not substantially different estimates compared with conventional multivariable methods. J Clin Epidemiol. 2006;59(5):437-447.
22. Schafer JL. Analysis of Incomplete Multivariate Data: Taylor & Francis, 1997.
23. Schultz LR, Peterson EL, Breslau N. Graphing survival curve estimates for time-dependent covariates. Int J Methods Psychiatr Res. 2002;11(2):68-74.
24. Cheson BD, Greenberg PL, Bennett JM, et al. Clinical application and proposal for modification of the International Working Group (IWG) response criteria in myelodysplasia. Blood. 2006;108(2):419-425.
25. Zeidan AM, Hendrick F, Friedmann E, et al. Deferasirox therapy is associated with reduced mortality risk in a medicare population with myelodysplastic syndromes. J Comp Eff Res. 2015;4(4):327-340.
26. Mainous AG, Tanner RJ, Hulihan MM, et al. The impact of chelation therapy on survival in transfusional iron overload: a meta-analysis of myelodysplastic syndrome. Br J Haematol. 2014;167(5):720-723.
27. Remacha Á, Arrizabalaga B, Villegas A, et al. Evolution of iron overload in patients with low-risk myelodysplastic syndrome: iron chelation therapy and organ complications. Ann Hematol. 2015;94(5):779-787.
28. Lyons RM, Marek BJ, Paley C, et al. Relation between chelation and clinical outcomes in lower-risk patients with myelodysplastic syndromes: Registry analysis at 5 years. Leuk Res. 2017;56:88-95.
29. Angelucci E, Li J, Greenberg PL, et al. Safety and efficacy, including event-free survival, of deferasirox versus placebo in iron-overloaded patients with low- and intermediate-1-risk myelodysplastic syndromes (MDS): outcomes from the randomized, double blind Telesto study. Blood, annual meeting abstracts. 2018;132(S1):abstract 234.
30. Leitch HA, Parmar A, Wells RA, et al. Overall survival in lower IPSS risk MDS by receipt of iron chelation therapy, adjusting for patient-related factors and measuring from time of first red blood cell transfusion dependence: an MDS-CAN analysis. Br J Haematol. 2017;179(1):83-97.
31. de Swart L, Reiniers C, Bagguley T, et al. Labile plasma iron levels predict survival in patients with lower-risk Myelodysplastic syndromes. Haematologica. 2018; 103(1):69-79.
32. Hoeks M, Bagguley T, Roelofs R, et al. Elevated labile plasma iron (LPI) levels in patients with lower-risk myelodysplastic syndromes (MDS) are associated with

decreased quality of life and reduced overall survival. Blood, annual meeting abstracts. 2018;132(S1):abstract 4392.

33. Wermke M, Eckholdt J, Götze KS, et al. Enhanced labile plasma iron and outcome in acute myeloid leukaemia and myelodysplastic syndrome after allogeneic haemopoietic cell transplantation (ALLIVE): a prospective, multicentre, observational trial. Lancet Haematol. 2018; 5:e201-210.

34. Hershko C, Link G, Cabantchik I. Pathophysiology of iron overload. Ann N Y Acad Sci. 1998;850:191-201.

35. Pilo F, Angelucci E. A storm in the niche: Iron, oxidative stress and haemopoiesis. Blood Rev. 2018;32(1):29-35.

36. Taher AT, Saliba AN, Kuo KH, et al. Safety and Pharmacokinetics of the Oral Iron Chelator SP-420 in β-thalassemia. Am J Hematol. 2017;92(12):1356-1361.

37. Hartmann J, Braulke F, Sinziq U, et al. Iron overload impairs proliferation of erythroid progenitors cells (BFU-E) from patients with myelodysplastic syndromes. Leuk Res. 2013;37(3):327-332.

38. Cazzola M, Della Porta MG, Malcovati L. Clinical relevance of anemia and transfusion iron overload in myelodysplastic syndromes. Hematology Am Soc Hematol Educ Program. 2008:166-175.

39. Malcovati L, Porta MG, Pascutto C, et al. Prognostic factors and life expectancy in myelodysplastic syndromes classified according to WHO criteria: a basis for clinical decision making. J Clin Oncol. 2005; 23(30):7594-7603.

40. Greenberg PL, Attar E, Bennett JM, et al. NCCN Clinical Practice Guidelines in Oncology: myelodysplastic syndromes. J Natl Compr Canc Netw. 2011;9(1):30-56.

41. Pimková K, ChrastinováL, Suttnar J, et al. Plasma levels of aminothiols, nitrite, nitrate, and malondialdehyde in myelodysplastic syndromes in the context of clinical outcomes and as a consequence of iron overload. Oxid Med Cell Longev. 2014 Jan; DOI 10.1155/2014/416028.

42. de Souza GF, Barbosa MC, Santos TE, et al. Increased parameters of oxidative stress and its relation to transfusion iron overload in patients with myelodysplastic syndromes. J Clin Pathol. 2013;66(11):996-998.

Ferrata Storti Foundation

Impact of clinical, cytogenetic, and molecular profiles on long-term survival after transplantation in patients with chronic myelomonocytic leukemia

Janghee Woo,[1,2] Dae Ro Choi,[1] Barry E. Storer,[1] Cecilia Yeung,[1,2] Anna B. Halpern,[1,2] Rachel B. Salit,[1,2] Mohamed L. Sorror,[1,2] David W. Woolston,[1] Tim Monahan,[1] Bart L. Scott[1,2] and H. Joachim Deeg[1,2]

[1]Fred Hutchinson Cancer Research Center and [2]University of Washington School of Medicine, Seattle, WA, USA

Correspondence:

H. JOACHIM DEEG
jdeeg@fredhutch.org

ABSTRACT

Chronic myelomonocytic leukemia (CMML) is a heterogeneous group of clonal hematopoietic malignancies with variable clinical and molecular features. We analyzed long-term results of allogeneic hematopoietic cell transplantation in patients with CMML and determined clinical and molecular risk factors associated with outcomes. Data from 129 patients, aged 7-74 (median 55) years, at various stages of the disease and transplanted from related or unrelated donors were analyzed. Using a panel of 75 genes somatic mutations present before hematopoietic cell transplantation were identified In 52 patients. The progression-free survival rate at 10 years was 29%. The major cause of death was relapse (32%), which was significantly associated with adverse cytogenetics (hazard ratio, 3.77; P=0.0002), CMML Prognostic Scoring System (hazard ratio, 14.3, P=0.01), and MD Anderson prognostic scores (hazard ratio, 9.4; P=0.005). Mortality was associated with high-risk cytogenetics (hazard ratio, 1.88; P=0.01) and high Hematopoietic Cell Transplantation Comorbidity Index (score ≥4: hazard ratio, 1.99; P=0.01). High overall mutation burden (≥10 mutations: hazard ratio, 3.4; P=0.02), and ≥4 mutated epigenetic regulatory genes (hazard ratio 5.4; P=0.003) were linked to relapse. Unsupervised clustering of the correlation matrix revealed distinct high-risk groups with unique associations of mutations and clinical features. CMML with a high mutation burden appeared to be distinct from high-risk groups defined by complex cytogenetics. New transplant strategies must be developed to target specific disease subgroups, stratified by molecular profiling and clinical risk factors.

Introduction

Chronic myelomonocytic leukemia (CMML) can present either as a myeloproliferative type (MP-CMML) or a myelodysplastic type (MD-CMML), with leukocyte counts of ≥13 × 10⁹/L and <13 × 10⁹/L, respectively, and is therefore classified by the World Health Organization (WHO) as a myelodysplastic/myeloproliferative neoplasm (MDS/MPN).[1] The clinical course in terms of survival and risk of evolution into acute myeloid leukemia (AML) varies.[2] Prognosis tends to be worse with MP-CMML than with MD-CMML.[3] The blast percentage (in blood and bone marrow) has clear prognostic implications.[4,5] CMML-0 allows for <2% blasts in peripheral blood or <5% blasts in the bone marrow or both; CMML-1 refers to cases with 2% to 4% blasts in the peripheral blood or 5% to 9% in bone marrow or both; and CMML-2 refers to cases with 5% to 19% blasts in peripheral blood, 10% to 19% in bone marrow, or the presence of Auer rods.

The highly heterogeneous nature of CMML has led to the development of various prognostic scoring systems in an attempt to assign individual patient risk.[6-8] These systems have incorporated hematologic indices, cytogenetic abnormalities, and transfusion dependency. More recently, recurrent somatic mutations have been identified in genes associated with signaling pathways (*RAS, CBL, CSF3R,* and

JAK2), DNA methylation (*DNMT3A*, *IDH1*, *IDH2*, and *TET2*), transcription (*RUNX1*), epigenetic regulation (*ASXL1*, *EZH2*, and *SETBP1*), and splicing (*SF3B1*, *SRSF2*, *U2AF1*, and *ZRSR2*).[9-11] *TET2* and *SRSF2* mutations are the most prevalent in CMML.[12,13] Patients with MP-CMML have a higher propensity for alterations in signaling pathways,[14] whereas patients with MD-CMML predominantly have mutations associated with epigenetics.[15] Recognition of associations between somatic mutations and clinical features has improved the risk stratification of CMML (molecular CMML Prognostic Scoring System, m-CPSS).[16] Mutations in *RUNX1*, *NRAS*, *SETBP1*, and *ASXL1* appear to be associated with unfavorable outcomes.[16,17]

Treatment of CMML with chemotherapy alone only infrequently results in prolonged remission. A randomized trial comparing oral etoposide and hydroxyurea showed superior survival with hydroxyurea.[18] Treatment with hypomethylating agents results in less toxicity than associated with conventional chemotherapy; but again, remissions tend to be of short duration.[19,20] The only therapeutic modality with proven curative potential is allogenic hematopoietic cell transplantation (HCT).[21-27] Published data indicate that the major factors determining long-term relapse-free survival and overall survival are cytogenetic risk category, comorbidities, patient's age and achievement of complete remission.[21,25-27] In the present study, we analyzed long-term outcomes after allogenic HCT for patients with CMML and, in a subcohort, carried out a comprehensive mutation analysis of 75 genes implicated in myeloid malignancies to define the relationship between somatic mutations and previously established risk factors.

Methods

Patients

Between May 1986 and September 2017, 129 patients with CMML underwent HCT at the Fred Hutchinson Cancer Research Center. All provided informed consent for enrollment in investigational protocols and for long-term follow-up as required by the institutional review board of the Center. The characteristics of the patients and their diseases are summarized in Table 1. Patients were 7-74 (median, 55) years of age. The diagnosis and stratification of CMML, and determination of AML transformation were based on WHO 2016 criteria for all cases.[1] The disease was also risk-categorized by cytogenetics,[28] the MD Anderson Prognostic Score (MDAPS),[6] the CMML-specific Prognostic Scoring System (CPSS),[8] and the revised International Prognostic Scoring System (IPSS-R).[29] The HCT Comorbidity Index (HCT-CI) scores were 0-1 in 35 patients, 2-3 in 49 patients, and 4-11 in 45 patients.[30]

Donor and transplant characteristics

Donor and transplant characteristics are summarized in Table 2. All patients (and donors) were HLA genotyped, following institutional standards. Genotyping was carried out retrospectively in patients transplanted before the routine use of molecular typing. Donors for 42 patients (33%) were related (38 HLA-identical siblings, 4 HLA-mismatched family members), whereas 87 patients (67%) had unrelated donors (68 HLA-matched, 19 HLA mismatched, including 2 cord blood transplants). The stem cell source was bone marrow in 34 (26%) patients, peripheral blood stem cells in 93 (72%) and cord blood in two. Reduced-intensity conditioning regimens were used in 19% of patients and high-intensity (myeloablative) regimens in 81% of patients. Graft-*versus*-host disease (GvHD) prophylaxis consisted of a calcineurin inhibitor-based regimen in all patients. The severity of any acute and chronic GvHD was assessed and the conditions were treated as described previously.[31,32]

Mutation analysis

Mutation analysis was performed on DNA from bone marrow mononuclear cells collected prior to transplantation in 52 patients. DNA was extracted using a DNeasy Blood & Tissue Kit (Qiagen, Valencia, CA, USA), following the manufacturer's protocol. Next-generation sequencing libraries were prepared from 400 ng genomic DNA using the Archer VariantPlex Myeloid 75 gene

Table 1. Patient and disease characteristics.

Variable	N. of patients	%
Patients	129	
Age (years)	7-74 (median, 55)	
Gender		
Male	85	65.9
Female	44	34.1
Diagnosis		
WHO		
CMML-0	21	16.3
CMML-1	31	24.0
CMML-2	38	29.5
CMML-T*	37	28.7
CMML-nonspecified	2	1.6
Subgroup		
Myelodyplastic (MD)	88	68.2
Myeloproliferative (MP)	40	31.0
Indeterminate	1	0.8
Cytogenetic risk†		
Low	72	55.8
Intermediate	22	17.1
High	30	23.3
Not available‡	5	3.9
CPSS		
Low	1	0.8
Intermediate-1	16	12.4
Intermediate-2	74	57.4
High	30	23.3
Not determined‡	8	6.2
MDAPS		
Low	29	22.5
Intermediate-1	34	26.4
Intermediate-2	46	35.7
High	15	11.6
Not determined‡	5	3.9
IPSS-R for myelodysplastic-CMML		
Very low	8	9.1
Low	10	11.4
Intermediate	26	29.5
High	20	22.7
Very high	20	22.7
Not determined‡	4	4.5
HCT-CI		
0-1	35	27.1
2-3	49	38.0
≥4	45	34.9

*Progressed to blasts ≥20% with a previous history of CMML. †According to Such E, *et al.*[28] ‡Due to failed cell growth in cytogenetic study. WHO: World Health Organization; CMML; chronic myelomonocytic leukemia; CPSS: CMML Prognostic Scoring System; MDAPS, MD Anderson Prognostic Score; IPSS-R: Revised International Prognostic Scoring System; HCT-CI: Hematopoietic Cell Transplantation Comorbidity Index.

panel (ArcherDX, Boulder, CO, USA) following the manufacturer's instructions. We employed highly sensitive and specific targeted sequencing methods, exploiting unique molecular barcodes by anchored multiplex polymerase chain reaction (PCR) chemistry to tag the starting DNA material before PCR amplification.[33] These methods significantly enhance the sensitivity and specificity of variant detection by filtering out duplicate reads and PCR errors. We followed variant calling procedures as previously reported.[34] Pairwise associations between mutations and clinical parameters were evaluated by the Fisher exact test and Pearson correlation, corrected for the testing of multiple hypotheses. Hierarchical clustering of associations was performed by in-house scripts in R/Bioconductor. The Euclidean distance between variables was calculated, and the final partition of variables was obtained by the hclust function in the R package 'stat' with complete linkage as the argument. Details are provided in the *Online Supplementary Methods*.

Statistical analysis

Survival was defined as the time from transplantation to death or date of last contact. Relapse-free survival was defined as the time from transplantation to relapse or death from causes other than relapse. Non-relapse mortality (NRM) was defined as death without prior relapse. Estimates of the probability of overall and relapse-free survival were obtained by the Kaplan-Meier method,

and estimates of the probability of relapse, NRM, and GvHD were summarized using cumulative incidence estimates. NRM was considered a competing risk for relapse, and death without chronic GvHD a competing risk for chronic GvHD. Associations of various factors with the cause-specific hazards of failure for each of these endpoints were assessed using Cox regression. All *P*-values are two-sided and do not incorporate adjustment for multiple comparisons; however, because of the large number of individual mutations considered, we report only associations significant at the 0.01 level of significance, unless the mutation is considered of interest based on prior studies.

Results

Conventional risk classification

As shown in Table 1, according to WHO criteria, 21 patients (16%) had CMML-0, 31 (24%) had CMML-1, 38 (30%) had CMML-2, and 37 patients (29%) had CMML-T (progressed to a blast count ≥20% with previous history of CMML). In two patients, the staging was inconclusive. In 88 patients (68%), the white blood cell count was <13 × 10^9/L, thus qualifying as MD-CMML, and 40 patients (31%) had MP-CMML with a white cell count ≥13 × 10^9/L. In one patient, the white blood cell count from the pre-HCT period was not available. Among 124 patients with cytogenetic data, 72 (56%) were considered low risk, 22 (17%) intermediate risk, and 30 (23%) high risk according to the CMML-specific cytogenetic classification.[28] More than 80% of patients were "higher" risk according to the CPSS classification (i.e., 30 were high risk and 74 intermediate-2 risk), while 50% of patients were "higher" risk according to the MDAPS (i.e., 15 were high risk and 46 intermediate-2 risk).

Engraftment and graft-*versus*-host disease

One hundred twenty patients (93%) achieved sustained engraftment, as defined by absolute neutrophil counts of ≥0.5 × 10^5/μL for three or more consecutive days. Seven of the remaining nine patients had donor cell engraftment, as determined by chimerism analysis, but died before day 100 without achieving an absolute neutrophil count ≥0.5 × 10^5/μL, while two patients died with recurrent CMML. Of the 126 patients evaluable for GvHD (surviving beyond day 28 with donor cell engraftment), acute GvHD of grades II-IV developed in 93 (74%) and grades III–IV in 32 (25%). Chronic GvHD occurred in 57 patients within 2 years, for a cumulative incidence of 45%.

Relapse

Relapse or disease progression occurred in 40 patients between 7 and 2,490 (median 154) days after transplantation. The estimated probability of relapse or disease progression was 28% at 3 years, and 32% at 10 years (Figure 1A).

Survival

With a median follow-up of 9.3 (range 0.4-25.2) years, 39 patients are alive while 90 patients have died. The overall survival rates at 3 and 10 years were 38% and 28%, respectively, while the relapse-free survival rates at the corresponding times were 37% and 29% (Figure 1A).

Clinical determinants of post-transplant outcomes

The results of the univariate analyses are summarized in Table 3. Relapse incidence was significantly increased

Table 2. Donor and transplant characteristics.

Variable	N. of patients	%
Donor		
Related	42	32.6
HLA-matched	38	29.5
HLA-mismatched	4	3.1
Unrelated	87	67.4
HLA-matched	68	52.7
HLA-mismatched*	19	14.7
Cell source		
Bone marrow	34	26.4
Peripheral blood	93	72.1
Cord blood	2	1.6
Conditioning regimen		
Myeloablative conditioning		
BU (16 mg/kg) / CY (120 mg/kg) ± ATG	41	31.8
FLU (120 mg/m²) / BU (16 mg/kg)	13	10.1
TBI (2 Gy) / I-131-antiCD45	12	9.3
BU (7 mg/kg) / TBI (12 Gy)	11	8.5
BU (7 mg/kg) / CY (50 mg/kg) / TBI (12Gy)	10	7.8
CY (120 mg/kg) / TBI (14.4 or 13.2 Gy)	10	7.8
TREO (42 g/m²) / FLU (150 mg/m²) / TBI (2 Gy)	9	7.0
Reduced-intensity conditioning		
FLU (90 mg/m²) / TBI (2-3 Gy)	21	16.3
Others†	2	1.6
GvHD prophylaxis		
CSP/MTX	43	33.3
CSP/MMF	36	27.9
TAC/MTX	35	27.1
TAC/MMF	6	4.7
CSP/MMF/MTX	2	1.6
CSP/others	7	5.4

*Includes two cord blood transplants. †FLU (175 mg/m²) / CY (50 mg/kg) / TBI (3 Gy), FLU (125 mg/m²) / melphalan (140 mg/m²). HLA: human leukocyte antigen; BU: busulfan; CY: cyclophosphamide; ATG: antithymocyte globulin; FLU: fludarabine; TBI: total-body irradiation; TREO: treosulfan; I-131-antiCD45, iodine-131 monoclonal antibody BC8; GvHD, graft-*versus*-host disease; CSP, cyclosporine; MMF, mycophenolate mofetil; TAC, tacrolimus; MTX, methotrexate.

with higher-risk cytogenetics [hazard ratio (HR), 3.77; 95% confidence interval (95% CI): 1.9-7.5; P=0.0002)] (Figure 1B) and the presence of measurable residual disease by cytogenetics at HCT (HR, 2.55; 95% CI: 1.3-5.0; P=0.007) (Figure 1C). Classification of CMML by WHO criteria was associated with relapse only with progression to ≥20% blasts (HR, 3.61; 95% CI: 1.2-10.5; P=0.02) (*Online Supplementary Figure S1A*). Stratification for MDAPS and CPSS showed statistically significant associations with relapse. Specifically, high risk by MDAPS criteria was associated with relapse incidence [HR, 5.24 (P=0.03), 7.15 (P=0.008) and 9.41 (P=0.005) for intermediate-1 (n=34), intermediate-2 (n=46) and high-risk patients (n=15), respectively] (Figure 1D). Similarly, patients who were classified as high risk by CPSS (n=30; 25%) had a incidence of relapse than that of lower-risk patients (HR, 14.3; 95% CI: 1.9-108; P=0.01) (Figure 1E). Among patients with leukocyte counts <13 × 10⁹/L (MD-CMML), the very high-risk group, as determined by the IPSS-R (n=20), was associated with a higher relapse incidence (HR, 7.82; 95% CI: 1.7-35; P=0.007) (*Online Supplementary Figure S1B*).

In multivariate analysis the two strongest factors for relapse determined in univariate analysis, cytogenetic risk and MDAPS classification, remained statistically significant (Table 4).

Overall mortality increased with high-risk cytogenetics (HR, 1.88; 95% CI: 1.2-3.0; P=0.01) (Figure 1F), the presence of measurable residual disease as determined by cytogenetics (HR, 1.65; 95% CI: 1.1-2.6; P=0.02) (Figure 1G), and a high HCT-CI [HCT-CI ≥4 (n=45): HR, 1.99; 95% CI: 1.2-3.4; P=0.01) (Figure 1H), primarily due to increased NRM (HCT-CI ≥4: HR, 3.39; 95% CI: 1.5-7.5; P=0.003) (Figure 1I). Bone marrow blast counts ≥20% at HCT also had a negative impact on survival, although the effect did not reach statistical significance (HR, 1.67; 95% CI: 0.9-3.2; P=0.13) (*Online Supplementary Figure S1C*). Risk stratification by the prognostic scoring systems was generally less predictive of survival, likely due to a high incidence of NRM (*Online Supplementary Figure S1D-F*). Survival after reduced intensity conditioning was not different from that after myeloablative conditioning (HR, 1.1; 95% CI: 0.7-1.9; P=0.71) (*Online Supplementary Figure S1G, H*). Pre-transplant therapy and disease status at transplant (complete remission *vs.* non-complete remission) did not significantly affect overall survival. However, there was a
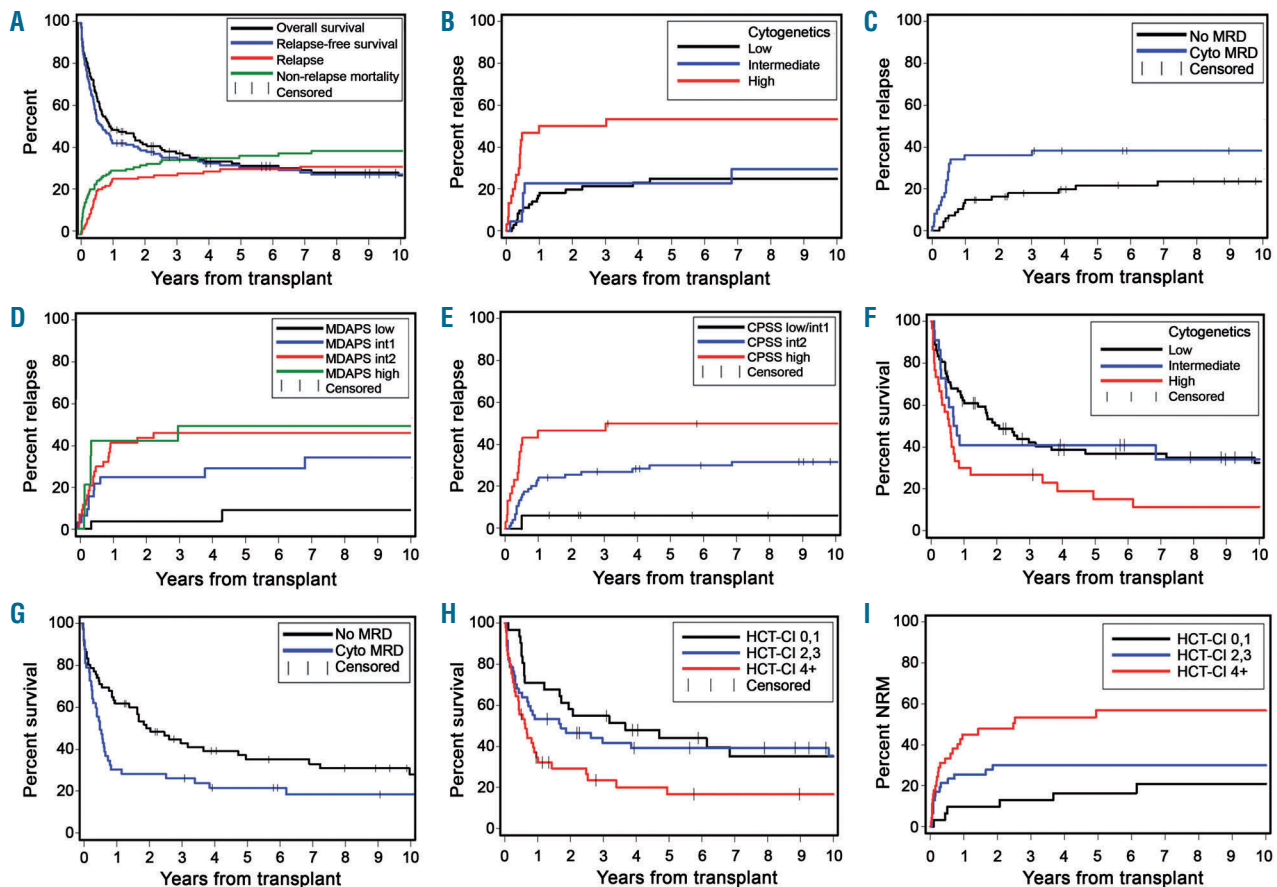
Figure 1. Clinical risk factors associated with relapse and overall mortality/survival in patients with chronic myelomonocytic leukemia following hematopoietic cell transplantation. Overall and relapse-free survival (RFS) and the probabilities of relapse and non-relapse mortality (NRM) are shown for all 129 patients. Tick marks indicate censored patients. (A) Survival, RFS, relapse and NRM for all patients. (B) Relapse by cytogenetic risk. (C) Relapse by measurable residual disease (MRD) at transplantation as indicated by cytogenetics. (D) Relapse by MD Anderson Prognostic Score (MDAPS) and (E) by CMML-specific Prognostic Scoring System (CPSS) risk group. (F) Overall survival dependent upon cytogenetic risk and (G) MRD by cytogenetics. (H) NRM and (I) overall survival by Hematopoietic Cell Transplantation-Comorbidyt Index (HCT-CI).

trend toward higher relapse incidence in patients given pre-HCT intensive cytotoxic chemotherapy and hypomethylating agents, and toward lower relapse incidence with achievement of complete remission at transplant (Table 3). Year of transplant did not have an influence on relapse incidence, overall survival (Table 3), or NRM (for years 2000-2010: HR, 0.7; 95% CI: 0.38-1.50; *P*=0.57; for years after 2010: HR, 1.05; 95% CI: 0.49-2.25; *P*=0.60).

Mutational landscape

In a subcohort of 52 patients for whom pre-transplant bone marrow samples were available, we carried out a mutational analysis of 75 genes. At least one somatic mutation was identified in 44 of the 52 patients (85%) (median number/patient = 5; range, 0–21) (*Online Supplementary Figure S2* and *Online Supplementary Tables S1* and *S2*). The most common mutations were those in *ASXL1* (52%), *TET2* (42%), and *SRSF2* (25%), consistent

Table 3. Univariate regression analyses.

Parameter	N.	Overall survival (mortality)		Relapse/progression	
		HR (95% CI)	*P*	HR (95% CI)	*P*
Conditioning by intensity					
Myeloablative conditioning	103	1			
Reduced-intensity conditioning	23	1.10 (0.7–1.9)	0.71	1.32 (0.6–2.8)	0.46
Age at transplant					
<55 years	62	1		1	
55+ years	67	1.13 (0.7–1.7)	0.57	0.95 (0.5–1.8)	0.88
CMV serostatus					
Recipient –ve and Donor –ve	32	1		1	
Recipient +ve or Donor +ve	95	1.11 (0.7–1.8)	0.67	0.92 (0.5–1.8)	0.81
Sex match					
Others	90	1		1	
Female to male	37	0.94 (0.6–1.5)	0.78	0.48 (0.2–1.1)	0.07
HCT-CI					
0, 1	31	1		1	
2, 3	47	1.10 (0.6–1.9)	0.73	0.94 (0.4–2.0)	0.87
4+	45	1.99 (1.2–3.4)	0.01	1.08 (0.5–2.4)	0.84
Interval (diagnosis to transplant)					
< 6 months	29	1		1	
6–18 months	66	1.02 (0.6–1.7)	0.95	0.97 (0.4–2.2)	0.93
> 18 months	34	1.34 (0.7–2.4)	0.33	1.72 (0.7–4.1)	0.22
Pre-transplant therapy†					
Supportive care	32	1		1	
Low intensity	34	1.01 (0.6–1.8)	0.99	1.87 (0.7–5.1)	0.22
Induction chemo ± HMA	38	1.31 (0.7–2.3)	0.36	2.23 (0.9–5.9)	0.09
HMA	25	1.37 (0.7–2.6)	0.32	2.28 (0.8–6.4)	0.12
Status at transplant					
Non-complete remission	64	1		1	
Complete remission	64	1.00 (0.7–1.5)	0.99	0.58 (0.3–1.1)	0.1
Individual mutations					
ASXL1	27	1.4 (0.7–2.8)	0.33	1.1 (0.4–3.0)	0.89
TET2	22	1.8 (0.9–3.6)	0.10	1.6 (0.6–4.6)	0.40
RUNX1	9	1.1 (0.4–2.6)	0.90	1.9 (0.6–6.1)	0.29
SETBP1	5	0.8 (0.2–2.6)	0.67	0.6 (0.1–4.3)	0.54
NRAS	6	1.9 (0.7–5.1)	0.22	4.7 (1.4–16)	0.03
WT1	10	4.3 (1.7–11)	0.004	6.3 (1.6–24)	0.01
ATRX	6	4.9 (1.8–13)	0.005	17.3 (4.1–73)	0.0005
Total number of mutations					
≥10	15	1.5 (0.7–3.2)	0.30	3.4 (1.2–9.6)	0.02
Functional groups‡					
Epigenetic					
Trend over 0, 1, 2, 3, 4, 5+ mutations	16, 11, 12, 3, 4, 6	1.2 (1.0–1.5)	0.09	1.5 (1.1–2.0)	0.02
≥ 4	10	1.5 (0.7–3.4)	0.33	5.4 (1.9–16)	0.003
Tumor suppressor					
Presence	7	2.3 (0.9–5.9)	0.09	3.1 (0.8–11)	0.13
Signaling					
Trend over 0, 1, 2, 3, 4, 5+ mutations	16, 11, 10, 4, 4, 7	1.1 (0.9–1.3)	0.58	1.1 (0.8–1.5)	0.57

*According to Such E, *et al.*[28] †Supportive care includes transfusion, treatment with granulocyte colony-stimulating factor and erythropoiesis-stimulating agents. Low intensity treatments include hydroxyurea, lenalidomide, steroids, azathioprine, imatinib, and ruxolitinib. Hypomethylating agents include azacitidine and decitabine. ‡According to *Online Supplementary Table S1*. HR: hazard ratio; 95% CI: 95% confidence interval; CMV: cytomegalovirus; HCT-CI: Hematopoietic Cell Transplantation - Comorbidity Index; HMA: hypomethylating agents.

with previous reports on mutation profiles in patients with CMML.[16,17] Among the mutations in *ASXL1*, 67% were nonsense mutations, while the remainder were either frameshift or stop/gain mutations. Mutations were also frequent in *WT1* (27%), *RUNX1* (17%), *DNMT3A* (17%), *SMC1A* (17%), *EZH2* (12%), and *ATRX* (12%), the high frequency presumably being related to the fact that more than 85% of our cohort (104 of 129 patients) had intermediate-2 or high-risk disease according to the CPSS (Table 1).

Incorporation of mutations into the overall analysis

Among mutations with prognostic weight reported in previous studies,[16] such as *ASXL1*, *NRAS*, *RUNX1*, and *SETBP1*, only mutations in *NRAS* (n=6) were significantly associated with relapse (HR, 4.7; 95% CI: 1.4-16; *P*=0.03). In addition, mutations in *ATRX* (n=6) and in the *WT1* gene (n=10) were significantly associated with relapse (HR, 17.3; 95% CI: 4.1-73; *P*=0.0005; and HR, 6.3; 95% CI: 1.6-24; *P*=0.01, respectively) and inferior survival (HR, 4.9; 95% CI: 1.8-13; *P*=0.005; and HR, 4.3; 95% CI: 1.7-11; *P*=0.004, respectively).

The impact of mutations was not affected by adjustment in the multivariate analysis, and results remained unchanged.

We then grouped mutations and clinical parameters that co-occurred by unbiased clustering of a correlation matrix across individual mutations and clinical features, including prognostic scoring systems (MDAPS, CPSS, and the CMML-specific cytogenetic classification), leukocyte counts (MP-CMML), and blast counts (Figure 2 and *Online Supplementary Figure S3*). This approach identified two groups: group 1 mainly included mutations in signaling pathways (e.g. *RAS* or *JAK2*) and *TP53*, associated with high-risk cytogenetics and blasts (Figure 2A and *Online Supplementary Figure S3A*), while group 2 included mutations in epigenetic regulatory genes and splicing factors (Figure 2A). Within this group, mutations in *DNMT3A*, *SETBP1*, and *EZH2* tended to co-occur, and mutations in *TET2* and *WT1* were associated with mutations in *ATRX*. The total number of mutations [≥10 mutations (n=15): HR, 3.4; 95% CI: 1.2-9.6; *P*=0.02] and greater number of mutations in genes regulating epigenetic processes [≥4 mutations (n=10): HR, 5.4; 95% CI: 1.9-16; *P*=0.003], but not mutations in signaling pathways and tumor suppressor genes (*TP53* and *PPM1D*), were associated with relapse (Figure 2B, C, Table 3, and *Online Supplementary Table S1*). When cytogenetics, total number of mutations, established prognostic scoring systems and mutations in epigenetic processes and signaling pathways were considered for their impact on relapse (Figure 2D and *Online Supplementary Figure S3B*), mutations in epigenetic processes [≥4 mutations; odds ratio (OR)=8.8], high blast count (≥20%; OR=4.7), high-risk MDAPS (OR=4.0) and high-risk cytogenetics (OR=3.2) were the major factors contributing to the probability of relapse (details in *Online Supplementary Table S3*). Pairwise association analysis showed that high blast counts, high-risk by CPSS, and high-risk cytogenetics were closely associated, and mutations in epigenetic regulators tended to occur predominantly in disease classified as high-risk by the MDAPS (Figure 2D and *Online Supplementary Table S3*). The m-CPSS risk model did not allow for further differentiation of risk groups as virtually all patients became classified as intermediate-2 or high risk. All patients were upgraded to

higher risk groups due to their prevalent high-risk mutations. (*Online Supplementary Figure S3B*). As illustrated in Figure 2E, the delay between diagnosis and HCT was longer (median, 536 days) among patients with higher numbers of mutations than among those with fewer mutations (median delay, 309 days), including epigenetic regulators (522 *vs*. 344 days), but not mutations in signaling pathways (475 *vs*. 366 days). These observations were consistent with a previous report on non-transplanted patients showing increasing mutations with longer disease duration.[15] Overall, the data indicate that molecular annotation uncovered distinct subgroups of CMML that were not distinguished by conventional risk classification. Specifically, a very high-risk group (independent of high-risk cytogenetics and high blast counts) with a long delay to HCT was characterized by a higher number of mutations in epigenetic regulators.

Discussion

We analyzed the long-term outcomes of allogeneic HCT in 129 patients with CMML in relation to clinical, pathological, and molecular characteristics. The results confirm the curative potential of HCT, since transplanted patients had 3- and 10 -year relapse-free survival rates of 37%, and 29%, respectively. The outcomes were superior in lower-risk patients, who had survival probabilities of 40% to 50% at 10 years. However, the relapse incidence and NRM rates were high. As in our previous studies[21] and in reports from other centers,[25,26,35] high-risk cytogenetics, disease transformation (to CMML-T), and risk classification in scoring systems such as IPSS-R, CPSS and MDAPS, were strongly correlated with post-transplant relapse. As in earlier analyses,[36] there was a suggestion that intensive cytotoxic therapy prior to HCT was associated with inferior outcome, presumably related to the fact that patients considered to be at high risk were more likely to receive induction-type chemotherapy. Nevertheless, it was of note that the intensity of conditioning did not significantly affect overall transplant outcome, although it must be noted that a broad spectrum of conditioning regimens was given to this cohort. Furthermore, as in a previous analysis[21] and in other trials in patients with myeloid malignancies,[37] patients with high HCT-CI scores had inferior survival, although the probability of relapse was not altered. The source of stem cells did not affect outcome significantly, and results with related and unrelated donors were similar.

The present results indicate that providing HCT at an earlier disease stage and in patients with a low comorbidity burden who have not received cytotoxic therapy results in superior transplant outcomes, as also suggested by others.[5] These three parameters are likely interrelated as prolonged pre-HCT observation and therapy tend to be associated with the acquisition of new co-morbidities, and likely new mutations, a concept supported by results in our subcohort of patients with mutational data. However, disease characteristics such as high-risk cytogenetics and evidence of measurable residual disease by cytogenetics, still had a profound impact on relapse and survival, even with high-intensity conditioning regimens.

We hypothesize that mutational profiling assists in defining prognosis more narrowly. The analysis of mutations in 75 genes uncovered distinct risk groups defined by

mutations and disease phenotype which differed for HCT outcomes. In particular, the total number of mutations and more mutations in epigenetic regulators were significantly associated with relapse and with inferior survival. Reminiscent of observations in patients with MPN or MDS,[15,38] patients with more mutations experienced a higher incidence of relapse, especially when the mutations occurred in genes involved in epigenetic regulation. Those

mutations occurred predominantly in patients with dysplastic CMML, as also observed by others.[15] Of note, however, our unsupervised clustering analysis uncovered a previously unrecognized group of high-risk patients with a higher mutation burden involving epigenetic regulators. This group of patients was not closely associated with high-risk disease as determined by cytogenetics, suggesting independent mechanisms and heterogeneity in the dis-
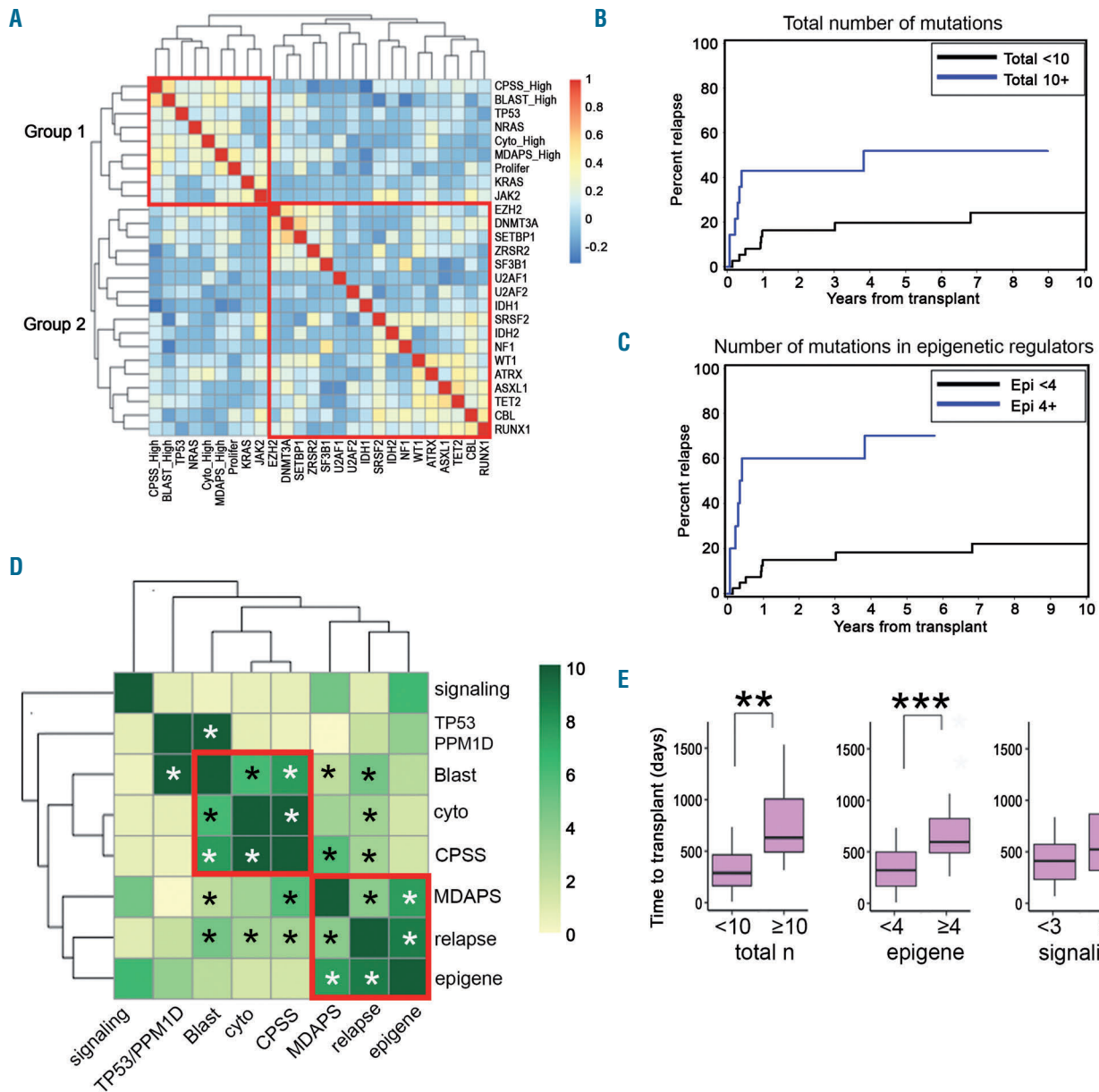
Figure 2. Molecular profiling and risk factors associated with hematopoietic cell transplantation outcomes in patients with chronic myelomonocytic leukemia. (A) Unsupervised hierarchical clustering of a correlation matrix between mutations and clinical parameters. Group 1 consists of mutations in mitotic signaling pathways, myeloproliferative type of chronic myelomonocytic leukemia (CMML) (Prolifer), mutations in *TP53*, and high-risk disease by cytogenetics and prognostic scoring systems. Group 2 consists of mutations in epigenetic pathways, methylation, and splicing regulation. (B) Increased relapse following hematopoietic cell transplantation in patients with high mutation burden, stratified by total number of mutations (≥10 *vs.* <10), and (C) stratified by number of mutations in epigenetic regulators (≥4 *vs.* <4; classified in *Online Supplementary Table S1*). (D) Unsupervised clustering of association (odds ratio, corresponding to the scaling bar) between groups of mutations (signaling pathways, epigenetic regulators, and tumor suppressors), high-risk cytogenetics (cyto), risk stratification systems (CPSS, MDAPS) and relapse. CMML with a high mutation burden in epigenetic regulators (epigene) was distinct from previously recognized high-risk diseases by cytogenetic abnormalities, blast count, and mutations in tumor suppressors (red boxes). (E) Time from diagnosis to transplant. High mutation burden (≥10), in particular, in epigenetic processes (≥4), was associated with a longer interval from diagnosis to transplant, consistent with the concept of disease evolution and acquisition of more mutations (in epigenetic but less so in signaling pathways) with disease duration *P<0.05 (individual values in *Online Supplementary Table S3*). **P=0.01, ***P=0.03.

ease process. Mutations in *TP53* were less frequent in patients with CMML (<10%) than previously reported for MDS[39] and were not strongly correlated with unfavorable outcomes, underscoring the biological differences between MDS and CMML. The difference may be related to the fact that CMML is infrequently a "secondary disease" (1 of 129 patients in the present series), whereas about 30% of MDS patients transplanted at our Center present with treatment-related or secondary disease.[40] The data need to be interpreted with caution, in view of the limited sample size.

The present mutational data suggest a significant association of *ATRX* and *WT1* with post-transplant relapse and overall mortality in patients with CMML. Although the numbers of cases with these mutations were limited, most mutations occurred in important functional protein domains, suggesting that the mutations would be of functional relevance.[41] Somatic mutations in *ATRX* are also seen in up to 43% of patients with MDS with unexplained microcytosis[42] and in a rare subtype of MDS associated with thalassemia (ATMDS).[43] Previous studies in CMML have not included *ATRX* in their mutation panels,[16,17] and additional investigations are warranted to confirm this association of *ATRX* mutations with CMML. *WT1* mutations are common in patients with high-risk MDS and AML[38] where they are associated with relapse.[39,44] *WT1* mutations in the present study occurred in or adjacent to loci that have been shown to be mutated in AML.[44] Our CMML cohort was predominantly composed of high-risk patients as determined by CPSS and m-CPSS criteria, which, in turn, might be responsible for the prevalence of *WT1* mutations and unfavorable transplant outcomes. Although there was a suggestive association of each individual mutation with relapse and survival, the biological impact of these mutations in a limited cohort of CMML patients must be assessed cautiously. Mutations co-occur with other mutations and rarely work as a single dominant factor. Cooperation with other mutations is likely.

Functional data in the right context (e.g., the exact identical mutation at the endogenous locus in hematopoietic cells) are often lacking. The functional consequences of the frequent mutations in *ATRX* or *WT1* will need to be tested in hematopoietic cells to confirm the proposed biological impact of these mutations.

In conclusion, this analysis adds mutational risk factors to previously identified clinical risk factors for post-HCT outcome in patients with CMML, such as comorbidity, cytogenetic risk, and high-risk disease according to the CPSS and MDAPS. Molecular profiling identified distinct high-risk disease groups with high mutation burden, particularly in epigenetic processes that characterized disease entities distinct from the conventional high-risk groups defined by cytogenetics. Of note, the data also show that these high-risk features are only incompletely overcome by HCT, and relapse and NRM rates remain high. This study confirms the clinical and molecular heterogeneity of CMML which significantly affects the outcome following HCT. New transplant strategies that target specific disease subgroups must be developed. Furthermore, early transplantation should be considered for patients with intermediate-risk disease and lower HCT-CI. Vigilant surveillance and early enrollment in clinical trials for post-transplant relapse must be planned for patients with high-risk disease as defined by complex cytogenetics and high mutation burden.

References

1. Arber DA, Orazi A, Hasserjian R, et al. The 2016 revision to the World Health Organization classification of myeloid neoplasms and acute leukemia. Blood. 2016;127(20):2391-2405.

2. Germing U, Strupp C, Knipp S, et al. Chronic myelomonocytic leukemia in the light of the WHO proposals. Haematologica. 2007;92(7):974-977.

3. Cervera N, Itzykson R, Coppin E, et al. Gene mutations differently impact the prognosis of the myelodysplastic and myeloproliferative classes of chronic myelomonocytic leukemia. Am J Hematol. 2014;89(6):604-609.

4. Schuler E, Schroeder M, Neukirchen J, et al. Refined medullary blast and white blood cell count based classification of chronic myelomonocytic leukemias. Leuk Res. 2014;38(12):1413-1419.

5. Patnaik MM, Pierola AA, Vallapureddy R, et al. Blast phase chronic myelomonocytic leukemia: Mayo-MDACC collaborative study of 171 cases. Leukemia. 2018;32(11):2512-2518.

6. Onida F, Kantarjian HM, Smith TL, et al. Prognostic factors and scoring systems in chronic myelomonocytic leukemia: a retrospective analysis of 213 patients. Blood. 2002;99(3):840-849.

7. Patnaik MM, Padron E, LaBorde RR, et al. Mayo prognostic model for WHO-defined chronic myelomonocytic leukemia: ASXL1 and spliceosome component mutations and outcomes. Leukemia. 2013;27(7):1504-1510.

8. Such E, Germing U, Malcovati L, et al. Development and validation of a prognostic scoring system for patients with chronic myelomonocytic leukemia. Blood. 2013;121(15):3005-3015.

9. Kohlmann A, Grossmann V, Klein HU, et al. Next-generation sequencing technology reveals a characteristic pattern of molecular mutations in 72.8% of chronic myelomonocytic leukemia by detecting frequent alterations in TET2, CBL, RAS, and RUNX1. J Clin Oncol. 2010;28(24):3858-3865.

10. Papaemmanuil E, Gerstung M, Malcovati L, et al. Clinical and biological implications of driver mutations in myelodysplastic syndromes. Blood. 2013;122(22):3616-3627; quiz 3699.

11. Piazza R, Valletta S, Winkelmann N, et al. Recurrent SETBP1 mutations in atypical chronic myeloid leukemia. Nat Genet. 2013;45(1):18-24.

12. Kosmider O, Gelsi-Boyer V, Ciudad M, et al. TET2 gene mutation is a frequent and adverse event in chronic myelomonocytic leukemia. Haematologica. 2009;94(12):1676-1681.

13. Meggendorfer M, Roller A, Haferlach T, et al. SRSF2 mutations in 275 cases with chronic myelomonocytic leukemia (CMML). Blood. 2012;120(15):3080-3088.

14. Ricci C, Fermo E, Corti S, et al. RAS mutations contribute to evolution of chronic myelomonocytic leukemia to the proliferative variant. Clin Cancer Res. 2010;16(8):2246-2256.

15. Itzykson R, Kosmider O, Renneville A, et al. Clonal architecture of chronic myelomonocytic leukemias. Blood. 2013;121(12):2186-2198.

16. Elena C, Galli A, Such E, et al. Integrating clinical features and genetic lesions in the risk assessment of patients with chronic myelomonocytic leukemia. Blood. 2016;128(10):1408-1417.

17. Itzykson R, Kosmider O, Renneville A, et al. Prognostic score including gene mutations in chronic myelomonocytic leukemia. J Clin Oncol. 2013;31(19):2428-2436.

18. Wattel E, Guerci A, Hecquet B, et al. A randomized trial of hydroxyurea versus VP16 in adult chronic myelomonocytic leukemia. Groupe Francais des Myelodysplasies and European CMML Group. Blood. 1996;88(7):2480-2487.

19. Solary E, Itzykson R. How I treat chronic myelomonocytic leukemia. Blood. 2017;130(2):126-136.

20. Zandberg DP, Huang TY, Ke X, et al. Treatment and outcomes for chronic myelomonocytic leukemia compared to myelodysplastic syndromes in older adults. Haematologica. 2013;98(4):584-590.

21. Eissa H, Gooley TA, Sorror ML, et al. Allogeneic hematopoietic cell transplantation for chronic myelomonocytic leukemia: relapse-free survival is determined by karyotype and comorbidities. Biol Blood Marrow Transplant. 2011;17(6):908-915.

22. Elliott MA, Tefferi A, Hogan WJ, et al. Allogeneic stem cell transplantation and donor lymphocyte infusions for chronic myelomonocytic leukemia. Bone Marrow Transplant. 2006;37(11):1003-1008.

23. Itonaga H, Aoki K, Aoki J, et al. Prognostic impact of donor source on allogeneic hematopoietic stem cell transplantation outcomes in adults with chronic myelomonocytic leukemia: a nationwide retrospective analysis in Japan. Biol Blood Marrow Transplant. 2018;24(4):840-848.

24. Kerbauy DM, Chyou F, Gooley T, et al. Allogeneic hematopoietic cell transplantation for chronic myelomonocytic leukemia. Biol Blood Marrow Transplant. 2005;11(9):713-720.

25. Liu HD, Ahn KW, Hu ZH, et al. Allogeneic hematopoietic cell transplantation for adult chronic myelomonocytic leukemia. Biol Blood Marrow Transplant. 2017;23(5):767-775.

26. Motohashi K, Fujisawa S, Doki N, et al. Cytogenetic risk stratification may predict

allogeneic hematopoietic stem cell transplantation outcomes for chronic myelomonocytic leukemia. Leuk Lymphoma. 2018;59(6):1332-1337.

27. Symeonidis A, van Biezen A, de Wreede L, et al. Achievement of complete remission predicts outcome of allogeneic haematopoietic stem cell transplantation in patients with chronic myelomonocytic leukaemia. A study of the Chronic Malignancies Working Party of the European Group for Blood and Marrow Transplantation. Br J Haematol. 2015;171(2):239-246.

28. Such E, Cervera J, Costa D, et al. Cytogenetic risk stratification in chronic myelomonocytic leukemia. Haematologica. 2011;96(3):375-383.

29. Greenberg PL, Tuechler H, Schanz J, et al. Revised international prognostic scoring system for myelodysplastic syndromes. Blood. 2012;120(12):2454-2465.

30. Sorror ML. How I assess comorbidities before hematopoietic cell transplantation. Blood. 2013;121(15):2854-2863.

31. Martin P, Nash R, Sanders J, et al. Reproducibility in retrospective grading of acute graft-versus-host disease after allogeneic marrow transplantation. Bone Marrow Transplant. 1998;21(3):273-279.

32. Przepiorka D, Weisdorf D, Martin P, et al. 1994 Consensus Conference on acute GVHD grading. Bone Marrow Transplant. 1995;15(6):825-828.

33. Peng Q, Vijaya Satya R, Lewis M, Randad P, Wang Y. Reducing amplification artifacts in high multiplex amplicon sequencing by using molecular barcodes. BMC Genomics. 2015;16:589.

34. Woo J, Howard NP, Storer BE, et al. Mutational analysis in serial marrow samples during azacitidine treatment in patients with post-transplant relapse of acute myeloid leukemia or myelodysplastic syndromes. Haematologica. 2017;102(6):e216-e218.

35. de Witte T, Bowen D, Robin M, et al. Allogeneic hematopoietic stem cell transplantation for MDS and CMML: recommen-

dations from an international expert panel. Blood. 2017;129(13):1753-1762.

36. Zang DY, Deeg HJ, Gooley T, et al. Treatment of chronic myelomonocytic leukaemia by allogeneic marrow transplantation. Br J Haematol. 2000;110(1):217-222.

37. Barba P, Ratan R, Cho C, et al. Hematopoietic cell transplantation comorbidity index predicts outcomes in patients with acute myeloid leukemia and myelodysplastic syndromes receiving CD34(+) selected grafts for allogeneic hematopoietic cell transplantation. Biol Blood Marrow Transplant. 2017;23(1):67-74.

38. Makishima H, Yoshizato T, Yoshida K, et al. Dynamics of clonal evolution in myelodysplastic syndromes. Nat Genet. 2017;49(2):204-212.

39. Lindsley RC, Saber W, Mar BG, et al. Prognostic mutations in myelodysplastic syndrome after stem-cell transplantation. N Engl J Med. 2017;376(6):536-547.

40. Deeg HJ, Scott BL, Fang M, et al. Five-group cytogenetic risk classification, monosomal karyotype, and outcome after hematopoietic cell transplantation for MDS or acute leukemia evolving from MDS. Blood. 2012;120(7):1398-1408.

41. Shi J, Wang E, Milazzo JP, Wang Z, Kinney JB, Vakoc CR. Discovery of cancer drug targets by CRISPR-Cas9 screening of protein domains. Nat Biotechnol. 2015;33(6):661-667.

42. Herbaux C, Duployez N, Badens C, et al. Incidence of ATRX mutations in myelodysplastic syndromes, the value of microcytosis. Am J Hematol. 2015;90(8):737-738.

43. Steensma DP, Higgs DR, Fisher CA, Gibbons RJ. Acquired somatic ATRX mutations in myelodysplastic syndrome associated with alpha thalassemia (ATMDS) convey a more severe hematologic phenotype than germline ATRX mutations. Blood. 2004;103(6):2019-2026.

44. Rampal R, Figueroa ME. Wilms tumor 1 mutations in the pathogenesis of acute myeloid leukemia. Haematologica. 2016;101(6):672-679.

Multilevel defects in the hematopoietic niche in essential thrombocythemia

Ferrata Storti Foundation

Ting Sun,[1,3] Mankai Ju,[1,3] Xinyue Dai,[1] Huan Dong,[1] Wenjing Gu,[1] Yuchen Gao,[1] Rongfeng Fu,[1,3,4,5] Xiaofan Liu,[1,3,4,5] Yueting Huang,[1,3,4,5] Wei Liu,[1,3,4,5] Ying Ch,[1,3,4,5] Wentian Wang,[1,3,4,5] Huiyuan Li,[1,3,4,5] Yuan Zhou,[1,4,7] Lihong Shi,[1,4,6,7] Renchi Yang,[1,2,3,4,5,6] and Lei Zhang[1,2,3,4,5,6,7]

[1]State Key Laboratory of Experimental Hematology; [2]National Clinical Research Center for Blood Diseases; [3]Institute of Hematology & Blood Diseases Hospital, Chinese Academy of Medical Sciences & Peking Union Medical College, Tianjin; [4]Tianjin Laboratory of Blood Disease Gene Therapy; [5]CAMS Key Laboratory of Gene Therapy for Blood Diseases; [6]CAMS Center for Stem Cell Medicine and [7]PUMC Department of Stem Cell and Regenerative Medicine, Tianjin, China

ABSTRACT

The role of the bone marrow niche in essential thrombocythemia (ET) remains unclear. Here, we observed multilevel defects in the hematopoietic niche of patients with *JAK2V617F*-positive ET, including functional deficiency in mesenchymal stromal cells (MSC), immune imbalance, and sympathetic-nerve damage. Mesenchymal stromal cells from patients with *JAK2V617F*-positive essential thrombocythemia had a transformed transcriptome. In parallel, they showed enhanced proliferation, decreased apoptosis and senescence, attenuated ability to differentiate into adipocytes and osteocytes, and insufficient support for normal hematopoiesis. Additionally, they were inefficient in suppressing immune responses. For instance, they poorly inhibited proliferation and activation of CD4-positive T cells and the secretion of the inflammatory factor soluble CD40-ligand. They also poorly induced formation of mostly immunosuppressive T-helper 2 cells (Th2) and the secretion of the anti-inflammatory factor interleukin-4 (IL-4). Furthermore, we identified WDR4 as a potent protein with low expression and which was correlated with increased proliferation, reduced senescence and differentiation, and insufficient support for normal hematopoiesis in MSC from patients with *JAK2V617F*-positive ET. We also observed that loss of WDR4 in MSC cells downregulated the interleukin-6 (IL-6) level through the ERK–GSK3β–CREB signaling based on our *in vitro* studies. Altogether, our results show that multilevel changes occur in the bone marrow niche of patients with *JAK2V617F*-positive ET, and low expression of WDR4 in MSC may be critical for inducing hematopoietic related changes.

Correspondence:

LEI ZHANG
zhanglei1@ihcams.ac.cn

RENCHI YANG
rcyang@ihcams.ac.cn

LIHONG SHI
shilihongxys@ihcams.ac.cn

Check the online version for the most updated information on this article, online supplements, and information on authorship & disclosures: www.haematologica.org/content/105/3/661

Introduction

In ET with the acquired *JAK2V617F* mutation, neoplastic clones take over the BM niche, and consequently normal hematopoiesis fails.[1] Multiple mechanisms may be involved in this process; however, the specific mechanisms leading to the replacement of normal hematopoietic stem/progenitor cells (HSPC) by mutant HSPC remain unclear.

Hematopoiesis is a parenchymal process that takes place in the BM, wherein it is tightly regulated by a complex communication network involving various factors that collectively form the niche for hematopoiesis. All blood cells are derived from HSPC that are primarily present in the perivascular niche, along with mesenchymal stromal cells (MSC) that synthesize various factors promoting HSPC maintenance and/or quiescence.[2,3] Perivascular stromal cells marked by nestin (NES) in the BM are closely associated with HSPC and can regulate the proliferation, differentiation, and long-term hematopoietic capacity of HSPC *via* direct or indirect pathways. Importantly, these NES-positive cells maintain HSPC in the BM, and when ectopi-

cally transplanted, they help to reconstitute hematopoietic activity in the host region.[4] Although malignant hematopoiesis is mainly caused by genetic abnormalities of the mutant stem cells themselves, increasing evidence has shown that abnormal regulation of the hematopoietic niche in the BM has also significant effects.[5,6] Recently, several studies have shown that genetic and physiological changes in MSC may accompany hematopoietic disorders, such as myelodysplastic syndrome, and leukemia.[7-9] However, little is known about BM-derived MSC (BM-MSC) in patients with ET.

Perivascular NES-positive MSC are extensively innervated by sympathetic nerve fibers that play vital roles in hematopoiesis and cancer progression by targeting HSPC, MSC, and osteoblasts *via* the b3 and b2 adrenergic receptor (B3AR and B2AR) signaling pathways.[4,10,11] The nervous system also regulates immunity and inflammation in the BM, which have long been known to extensively participate in regulation of hematopoiesis.[12] Both T-helper 1 cells (Th1) and Th2 cells produce granulocyte-macrophage colony-stimulating factor (GM-CSF), which promotes the differentiation of macrophages from hematopoietic stem cells.[13] Th2 cells also produce lineage-specific cytokines, such as IL-4, which can increase production of granulocytes and monocytes from mature unipotential hematopoietic progenitor cells, while contributing to thrombocytopenia *via* inhibitory effects throughout the process of megakaryopoiesis.[14,15] Emerging reports have shown that T-cell imbalance in the BM and abnormal secretion of inflammatory factors can impair normal hematopoiesis while accelerating the proliferation of malignant clones that carry mutations.[16,17] Moreover, the inflammatory microenvironment can impair sympathetic nerve maintenance and regeneration.[18] Recently, neuropathy and inflammation have been reported in a mouse model of *JAK2V617F*-positive myeloproliferative neoplasms (MPN), which tends to exhibit abnormal hematopoiesis.[19] Nonetheless, the sympathetic and inflammatory environment in the BM of patients with ET has not been widely examined.

IL-6 is a multifunctional and pleiotropic cytokine that plays critical roles in the immune system and in a variety of biological processes including hematopoiesis. It is secreted by numerous cell types, including monocytes, dendritic cells, macrophages, T cells, B cells, fibroblasts, osteoblasts, endothelial cells, and particularly MSC.[20-23] IL-6 has both pro- and anti-inflammatory properties and is involved in the pathogenesis of nearly all inflammatory diseases. It has been reported that mice homozygous for a mutation in the IL-6 receptor signaling subunit glycoprotein 130 (gp130Y757F/Y757F) develop a wide range of hematopoietic abnormalities, including splenomegaly, lymphadenopathy, neutrophilia, and thrombocytopenia in addition to elevated myelopoiesis and megakaryopoiesis in the BM.[24,25] These mice show glycoprotein 130-dependent signal transduction and hyperactivation of the transcriptional activator STAT3. IL-6 also participates in the pathogenesis of various blood disorders by increasing the number of early pluripotent precursor cells and committed myeloid precursors in the BM.[22,26,27] The ERK–GSK3β–CREB signaling pathway has been demonstrated to be involved in regulating IL-6; however, to date, its role in BM-MSC remains unclear.[28-30]

WDR4, located in human chromosomal region 21q22.3, codes for a member of the WD repeat protein family, which has been shown to participate in various cellular processes, such as differentiation, apoptosis, cell cycle progression, and stem cell self-renewal by regulating a wide range of signaling pathways *via* epigenetic regulation of gene expression, or ubiquitin-mediated degradation of proteins.[31,32] *WDR4* is involved in the regulation of an prometastatic and immunosuppressive microenvironment in lung cancer.[33] Downregulation of *WDR4* has been detected in the megakaryocytes and platelets of patients with ET, as shown in the GEO Profiles (GEO numbers: GSE2006 and GSE567). However, the role of WDR4 in ET has not been evaluated.

In the present study, we compared the normal BM niche with that of *JAK2V617F*-positive ET patients to have a comprehensive insight into the changes that occur in the BM microenvironment, and to identify the factors correlated with them.

Methods

Patients and samples

Ninety-one untreated ET patients and fifty healthy donors (HD) were included in this study. The characteristics of the subjects are detailed in the *Online Supplementary Table S1*. This study was approved by the hospital-based ethics committee.

Isolation, expansion, and characterization of MSC

BM-MSC were isolated and expanded *in vitro*, and their cell morphology, immunophenotype, proliferation, cell cycle, apoptosis, differentiation, and senescence were evaluated. Additional information on the experimental design is provided in the *Online Supplementary Material and Methods.*

Transcriptomics and quantitative real-time PCR (qPCR) analyses

Total RNA was isolated from MSC at passage four and used for transcriptomic and qPCR analyses. Detailed information is provided in the *Online Supplementary Material and Methods*.

Measurement of cytokine levels

Luminex assay (R&D Systems, Minneapolis, MN, USA) was performed on the supernatants obtained from the BM extracts to assess for inflammatory factors according to the manufacturer's instructions. Enzyme-linked immunosorbent assay (ELISA) was performed on the supernatants obtained from the BM extracts or from the MSC cultures. A list of the ELISA kits is provided in the *Online Supplementary Table S3*.

Colony-forming unit (CFU) assay

To evaluate the capacity of MSC to sustain normal hematopoiesis, a CFU assay was performed according to the manufacturer's instructions. Detailed information is provided in the *Online Supplementary Material and Methods*.

Results

Gene expression profiles of BM-MSC derived from HD and patients with *JAK2V617F*-positive ET

First, we performed RNA sequencing on MSC of HD or patients with *JAK2V617F*-positive ET. A total of 766 upregulated and 429 downregulated genes were detected in the patient samples (Figure 1A). Gene Ontology analysis revealed changes in the gene sets related to cell cycle, differentiation, proliferation, cell death, and aging (Figure
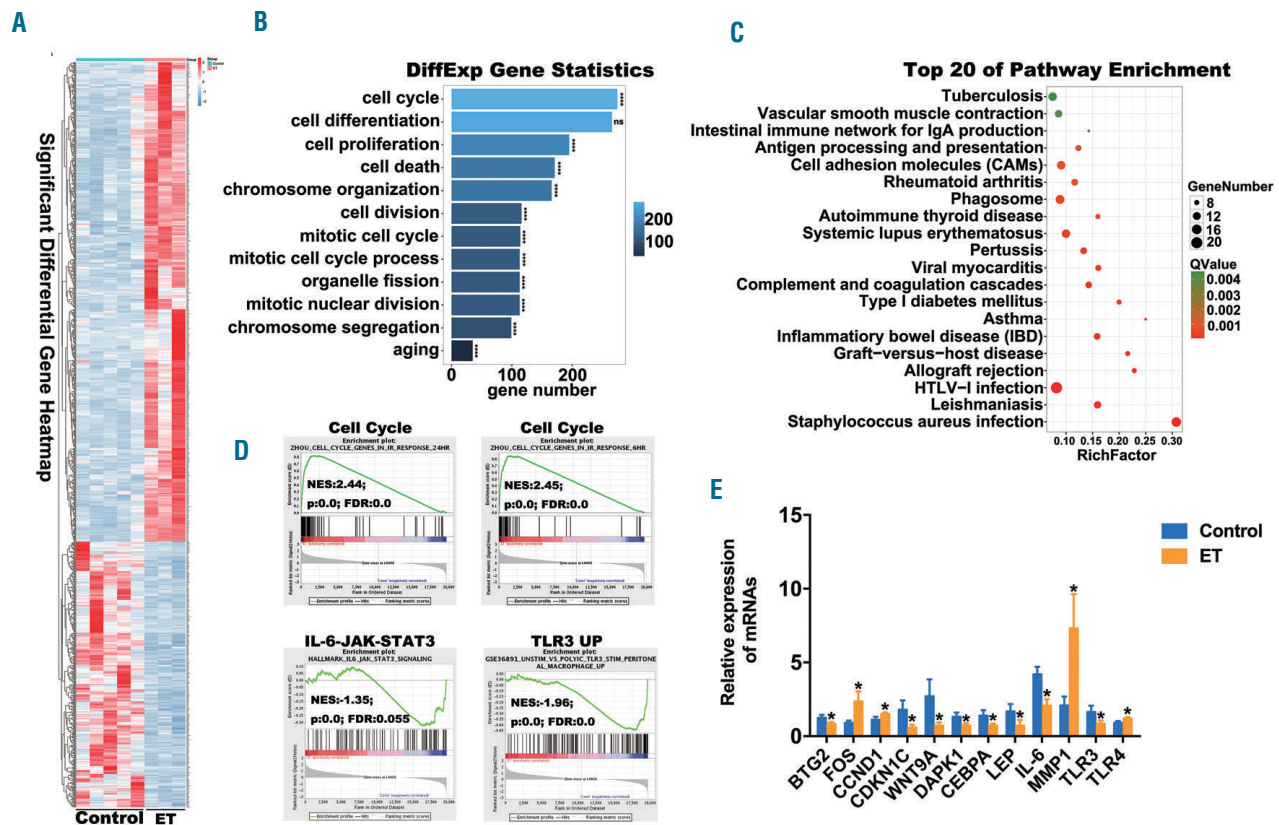
Figure 1. Transcriptomic analysis revealed multiple abnormalities in bone marrow derived mesenchymal stromal cells (BM-MSC) from patients with *JAK2V617F*-positive essential thrombocythemia (ET). A. Heatmap of transcriptomic analysis from eight MSC samples (control, n=5; untreated patients with *JAK2V617F*-positive ET, n=3) demonstrated that MSC from patients with *JAK2V617F*-positive ET differed from those isolated from HD. Briefly, 1,195 genes were identified with a cut-off of greater than 2.0-fold for gene expression change and *P*<0.05. B. GO analysis of genes enriched in terms of different function showed changes in gene sets related to the cell cycle, cell differentiation, proliferation, death, and aging. C. KEGG analysis was carried out to identify differential pathway enrichment between ET and control. Rich factor refers to the ratio of the number of genes differentially expressed in the pathway entry to the total number of genes in the pathway entry. A larger rich factor indicates a higher degree of enrichment. The q-value is the *P*-value after multiple-hypothesis test corrections, ranging from 0 to 1 (a value closer to zero indicates a more significant enrichment). The figure is plotted with the top 20 paths sorted according to the q value from small to large and shows enrichment of genes of inflammation pathways. D. GSEA using MSigDB identified differential gene enrichment between ET and the control. NES, Normal p and FDR q-values for each gene set are shown. The results revealed differential expression of genes involved in cell cycle, inflammatory responses, and hematopoietic support. E. qPCR validation of relevant genes (control, n=16; untreated patients with *JAK2V617F*-positive ET, n=16). MSC used for gene analysis were isolated and expanded *in vitro* and identified according to the minimal criteria for defining multipotent mesenchymal stromal cells stated by the International Society for Cellular Therapy position at passage four.[50] *P< 0.05; **P<0.01, ***P<0.001; ****P<0.0001. Data are presented as the mean or mean ± SEM. ET: essential thrombocythemia; HD: healthy donors; GO: Gene Ontology; KEGG: Kyoto Encyclopedia of Genes and Genomes; GSEA: gene set enrichment analysis; MsigDB: Molecular Signatures Database; NES: normalized enrichment score; qPCR: quantitative real-time PCR; n: number of unique donors in each group; ns: not significant; SEM: standard error of mean.

1B). Further analysis showed a prominent abundance of gene signatures associated with inflammation (Figure 1C). Gene Set Enrichment (GSEA) analysis confirmed significant enrichment of dysregulated genes involved in the cell cycle, inflammatory responses, and hematopoietic support (Figure 1D). These changes, confirmed by qPCR (Figure 1E), suggested multiple functional defects in MSC of patients with *JAK2V617F*-positive ET.

BM-MSC from patients with *JAK2V617F*-positive ET show enhanced proliferation and attenuated apoptosis, senescence, and differentiation

To verify the results of the gene expression analyses, we performed Cell Counting Kit 8 (CCK-8) assays, which revealed that the MSC of the patients had higher proliferative capacity than the MSC of the HD (Figure 2A). Furthermore, the apoptosis (Figure 2B) and senescence rates (Figure 2C) of the MSC derived from the patients

were lower. The adipogenic and osteogenic differentiation potentials of the ET MSC were also significantly lower (Figure 2D). In line with the above results, the majority of the ET MSC were in S and G2 phases (Figure 2E). Additionally, we detected an increase in the level of NES mRNA (Figure 2F) and the number of NES-positive cells (Figure 2 G-H) in the BM of the patients. No difference in immunophenotype or morphology was detected between the MSC of the HD and those of the patients (*Online Supplementary Figure S1 A-B*).

BM-MSC from patients with *JAK2V617F*-positive ET show insufficient capacity to support normal hematopoiesis

To assess the capacity of MSC to support hematopoiesis, we established a coculture setting involving normal CD34-positive cells and MSC derived from the HD or patients with *JAK2V617F*-positive ET. The recov-

ered CD34-positive cells after seven or 14 days of coculture were plated in a semisolid medium containing methylcellulose or agar in the presence of a cytokine cocktail, and their hematopoietic potential was estimated by determining the number of CFU. We thereby observed that CD34-positive cells had fewer CFU in total (CFU-Total), particularly for granulocytes and macrophages (CFU-GM), when cocultured with the ET MSC relative to

those obtained with the HD MSC. There was no significant difference in the number of CFU for megakaryocytes (CFU-MK) between the two co-cultures (Figure 3A-B). These results indicated that BM-MSC from patients with *JAK2V617F*-positive ET were deficient in the maintenance of normal hematopoiesis.

Many cytokines influence hematopoiesis. To identify the effectors, we performed ELISA on the supernatants of

Figure 2. Bone marrow derived mesenchymal stromal cells (BM-MSC) from patients with *JAK2V617F*-positive essential thrombocythemia (ET) show enhanced proliferation and attenuated apoptosis, senescence, and differentiation. A. Growth curves of BM-MSC isolated from HD (n=12) and patients with *JAK2V617F*-positive ET (n=12). The ET MSC grew progressively faster than controls. B. Decreased apoptosis of BM-MSC derived from patients with *JAK2V617F*-positive ET as determined by flow cytometry (control, n=16; ET, n=16). C. The number of β-galactosidase–positive cells were lower in BM-MSC derived from patients with *JAK2V617F*-positive ET compared to those from control patients (control, n=16; ET, n=16). D. Differentiation potentials of MSC toward adipocytes, osteocytes, and chondrocytes were assessed by Oil Red O, Alizarin Red, and Alcian Blue staining, respectively, after induction for 14–21 days. Representative micrographs of BM-MSC derived from HD, and patients with *JAK2V617F*-positive ET are shown. Variations in the differentiation between HD (n=12) and ET samples (n=16) were quantified by the staining index described in the Methods section. E. Cell cycle status was determined by flow cytometry. Patients with *JAK2V617F*-positive ET had less MSC in the G1 phase and more in the S and G2 phases relative to those in the HD controls (control, n=12; ET, n=12). F. NES mRNA expression in BM cells of the controls (n=17) and patients with *JAK2V617F*-positive ET (n=16). G. NES-positive cells in the bone marrow of an HD control (n =1) and patient with *JAK2V617F*-positive ET (n=1) shown by immunofluorescence. H. BM sections of the controls and patients with *JAK2V617F*-positive ET immunostained with NES (brown). (control, n=8; ET, n=37; upper panels); BM sections of the controls and patients with *JAK2V617F*-positive ET immunostained with NES (red) and CD34 (brown). (control, n=8; ET, n=37; lower panels). MSC used in each assay were at passage four (except for those immunostained with NES or NES and CD34). *P<0.05; **P<0.01, ***P<0.001; Data are presented as the mean ± SEM. ET: essential thrombocythemia; HD: healthy donors; n: number of unique donors in each group; IF: immunofluorescence; ns: not significant; SEM: standard error of mean.

the MSC cultures. We thereby observed that ET MSC secreted less IL-6, leptin, and GM-CSF than HD MSC (Figure 3C).

BM-MSC from patients with *JAK2V617F*-positive ET show an impaired immunomodulatory capacity

CD4-positive T cells from patients with *JAK2V617F*-positive ET showed enhanced proliferation and activation compared to normal controls (Figure 4A-B). No changes were observed in the levels of GATA3, T-bet, ROR-γt, or FOXP3 (Figure 4C). Notably, Th2 cell counts were significantly decreased in patients with *JAK2V617F*-positive ET (Figure 4D). The level of the anti-inflammatory factor IL-4 was lower in the patient samples, while pro-inflammatory factors, such as IL-1β, and sCD40L, were upregulated. No difference was observed in IL-6 levels between the patient and healthy samples (Figure 4E).

We next evaluated whether MSC play a role in the immune disorder mentioned above. We observed that CD4-positive T-cell proliferation and activation were remarkably enhanced, and Th2 cell counts were significantly lower when cocultured with ET MSC relative to those observed with HD MSC (Figure 4 F-H). Additionally, IL-4 was downregulated and sCD40L was upregulated with the ET MSC coculture (Figure 4I).

Downregulation of WDR4 is correlated with enhanced proliferation, decreased senescence, and impaired differentiation in BM-MSC of patients with *JAK2V617F*-positive ET

WDR4 was one of the differentially expressed genes according to our RNA sequencing results and was recently reported to regulate the immunosuppressive microenvironment of solid tumors.[25] Downregulation of *WDR4*
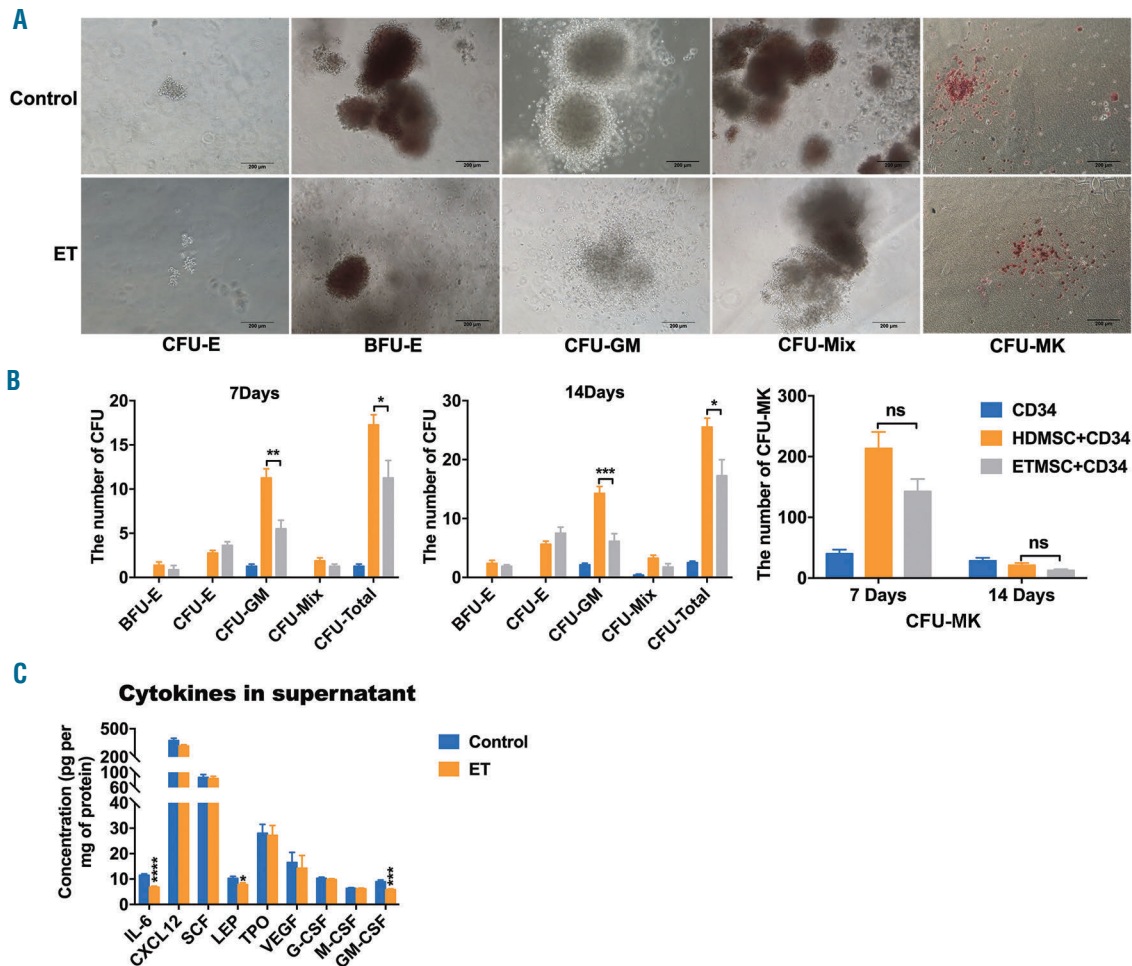
Figure 3. Bone marrow derived mesenchymal stromal cells (BM-MSC) from patients with *JAK2V617F*-positive essential thrombocythemia (ET) show insufficient ability to support normal hematopoiesis. A. Representative micrographs of CFU formed by purified normal CD34-positive cells in the presence of BM-MSC from HD (n=12) and patients with *JAK2V617F*-positive ET (n=16). B. Numbers of BFU-E, CFU-E, CFU-GM, CFU-Mix, CFU-Total, and CFU-MK formed by purified normal CD34-positive cells after coculture with BM-MSC from HD (n=12) or from patients with *JAK2V617F*-positive ET (n=16) for 7 or 14 days. After 7 or 14 days of coculture of purified normal CD34-positive cells and MSC from patients with *JAK2V617F*-positive ET, the numbers of CFU-GM and CFU-Total were significantly lower, with no significant changes in the numbers of BFU-E, CFU-E, CFU-Mix, and CFU-MK. C. Cytokines secreted by BM-MSC into the culture medium analyzed by ELISA (control, n=16; *JAK2V617F*-positive ET, n=16). MSC used in each assay were at passage four. *$P<0.05$; **$P<0.01$; ***$P<0.001$; ****$P<0.0001$. Data are presented as the mean ± SEM. ET: essential thrombocythemia; HD: healthy donors; ELISA: enzyme-linked immunosorbent assay; n: number of unique donors in each group; ns: not significant; BFU-E: burst-forming unit-erythroid; CFU-E: colony-forming unit-erythroid; CFU-GM: colony-forming unit-granulocyte and macrophage; CFU-Mix: colony-forming units mixed; CFU-Total: total colony-forming units; CFU-MK: colony-forming unit-megakaryocyte; SEM: standard error of mean.

expression was confirmed by qPCR and Western blotting in MSC derived from patients with *JAK2V617F*-positive ET (Figure 5 A-B). To further evaluate the function of WDR4 in BM-MSC, we used lentiviruses carrying the WDR4 cDNA (LV-WDR4) or a specific shRNA targeting WDR4 (LV-shWDR4). LV-shWDR4–infected MSC had significantly lower WDR4 mRNA and protein levels than those in the control groups, and LV-WDR4 effectively increased the WDR4 level in BM-MSC (Figure 5 C-D). We next established coculture systems between normal mononuclear or CD4-positive T cells from the BM, and WDR4 knockdown or overexpressing MSC. Among the subgroups that had different levels of *WDR4* expression, no changes were observed in terms of CD4-positive T-cell proliferation and activation, inflammatory cytokine secretion, or Th2-cell subtype counts (*Online Supplementary Figure S2*). We next examined the role of *WDR4* in BM-MSC regarding functions besides

immunoregulation. In HD MSC infected with LV-shWDR4, we observed biological characteristics similar to those in ET MSC, including enhanced proliferation (Figure 5E), decreased senescence (Figure 5F), and an impaired ability to differentiate into adipocytes, osteocytes, and chondrocytes (Figure 5G). Conversely, when ET MSC were infected with LV-WDR4, the previously detected abnormal biological properties were partially reversed (Figure 5 E–G) except for apoptosis (*Online Supplementary Figure S3*).

Insufficient action of the WDR4–IL-6 axis decreases hematopoiesis-supporting activities of BM-MSC from *JAK2V617F*-positive ET patients

We next investigated whether WDR4 affected the hematopoiesis-supporting function of BM-MSC. Hematopoiesis was studied by analyzing CFU. After 14 days of coculture of normal CD34-positive cells with HD

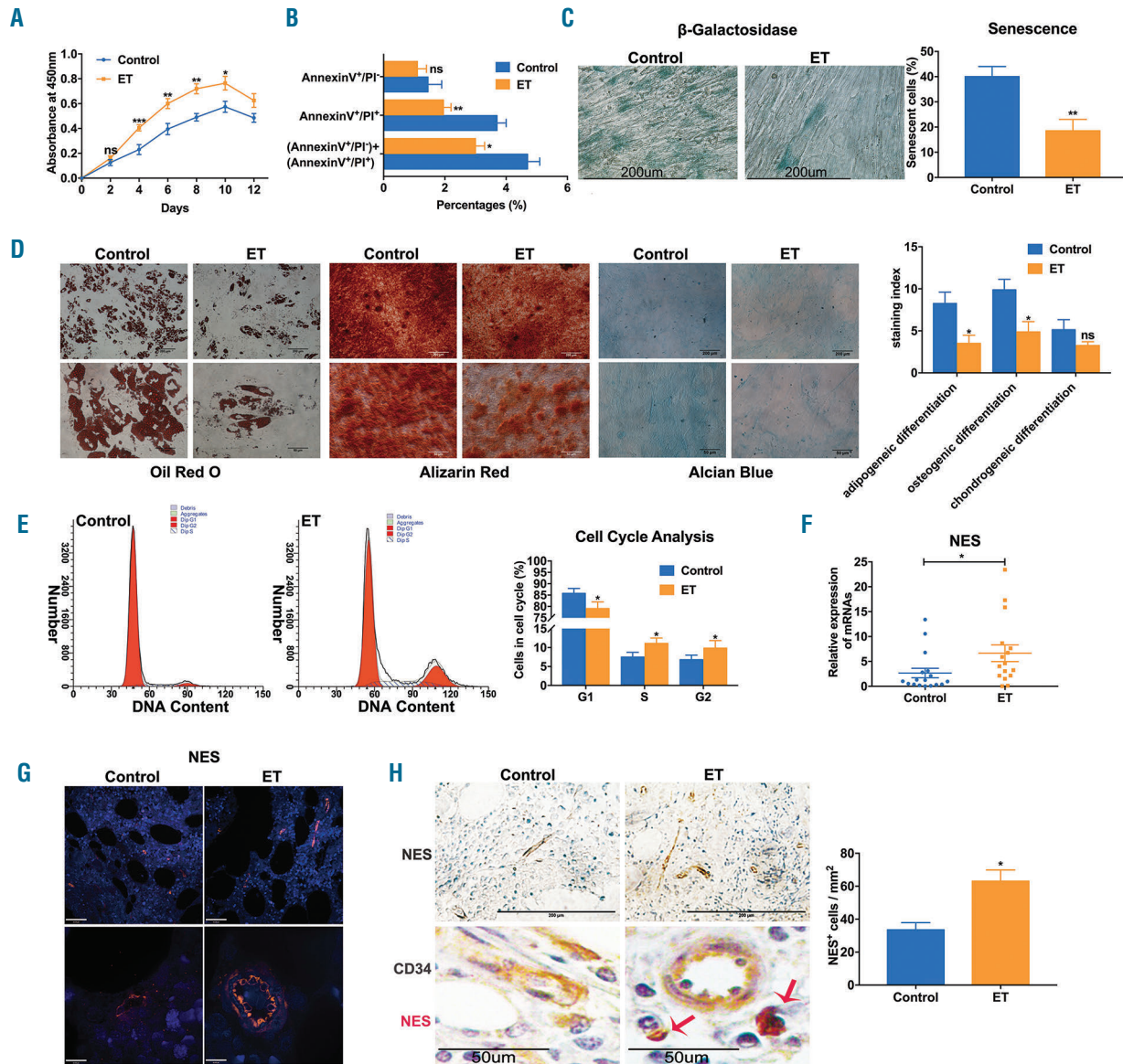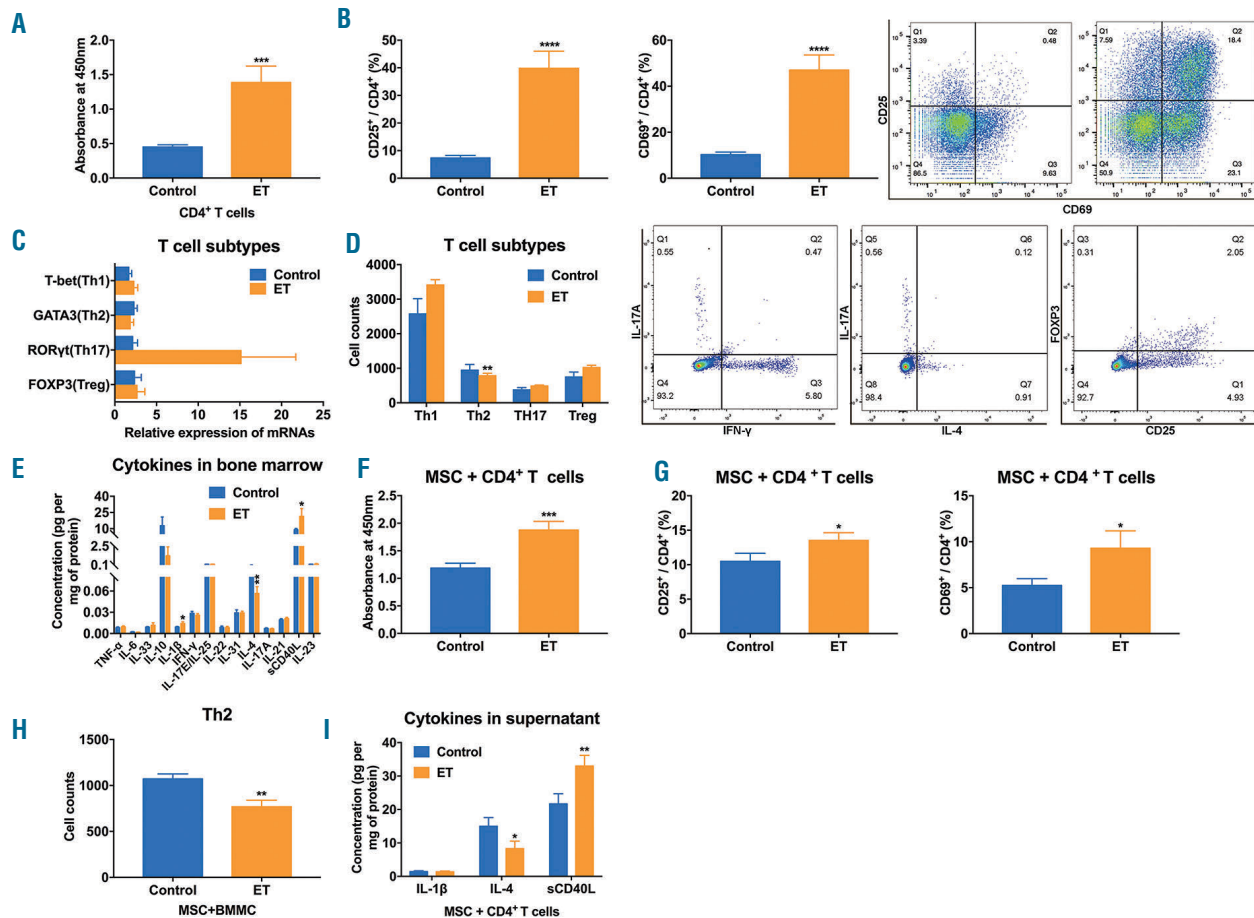**Figure 4. Bone marrow derived mesenchymal stromal cells (BM-MSC) from patients with *JAK2V617F*-positive essential thrombocythemia (ET) have an impaired immunomodulatory capacity.** A–B. Proliferation (A) and activation (B) of CD4-positive T cells from HD (n=12) and patients with *JAK2V617F*-positive ET (n=12). C. Expression of T-cell subset transcription factors in bone marrow mononuclear cells (BMMC) derived from HD (n=12) and patients with *JAK2V617F*-positive ET (n=12). T-cell–expressed transcription factors T-bet, GATA-3, RORγt, and FOXP3, representing Th1, Th2, Th17, and Treg cells, respectively. D. Flow-cytometric analysis of the T-cell subset in the bone marrow of HD (n=16) and patients with *JAK2V617F*-positive ET (n=16). CD4-positive cells were sorted into Th1, Th2, Th17, and Treg subsets according to the expression of IFN-γ, IL-4, IL-17 and FOXP3 with CD25. The number of the Th2 subset in patients with *JAK2V617F*-positive ET was lower relative to that in the control group. E. A Luminex assay performed using the supernatant of bone marrow extract from HD (n=20) and from patients with *JAK2V617F*-positive ET (n=24), revealed a decreased level of IL-4 and elevated IL-1β and sCD40L levels in ET. F–G. Proliferation (F) and activation (G) of normal CD4-positive T cells were higher after coculture with BM-MSC from patients with *JAK2V617F*-positive ET (n=8) relative to those observed with HD MSC (n=8). H. Flow-cytometric analysis of T-cell subsets showed lower number of Th2 cells formed from normal BMMC after coculture with BM-MSC from patients with *JAK2V617F*-positive ET (n = 12) relative to those with HD MSC (n=12). I. Decreased level of IL-4 and increased level of sCD40L were found in the supernatant of cell coculture medium of normal CD4-positive T cells and BM-MSC isolated from patients with *JAK2V617F*-positive ET, as determined by ELISA (control, n=12; ET, n=12). MSC used in each assay were at passage four. *P<0.05; **P<0.01; ***P<0.001; ****P<0.0001. Data are presented as the mean ± SEM. ET: essential thrombocythemia; HD: healthy donors; BMMC: bone marrow mononuclear cells; ELISA: enzyme-linked immunosorbent assay; n: number of unique donors in each group; SEM: standard error of mean.
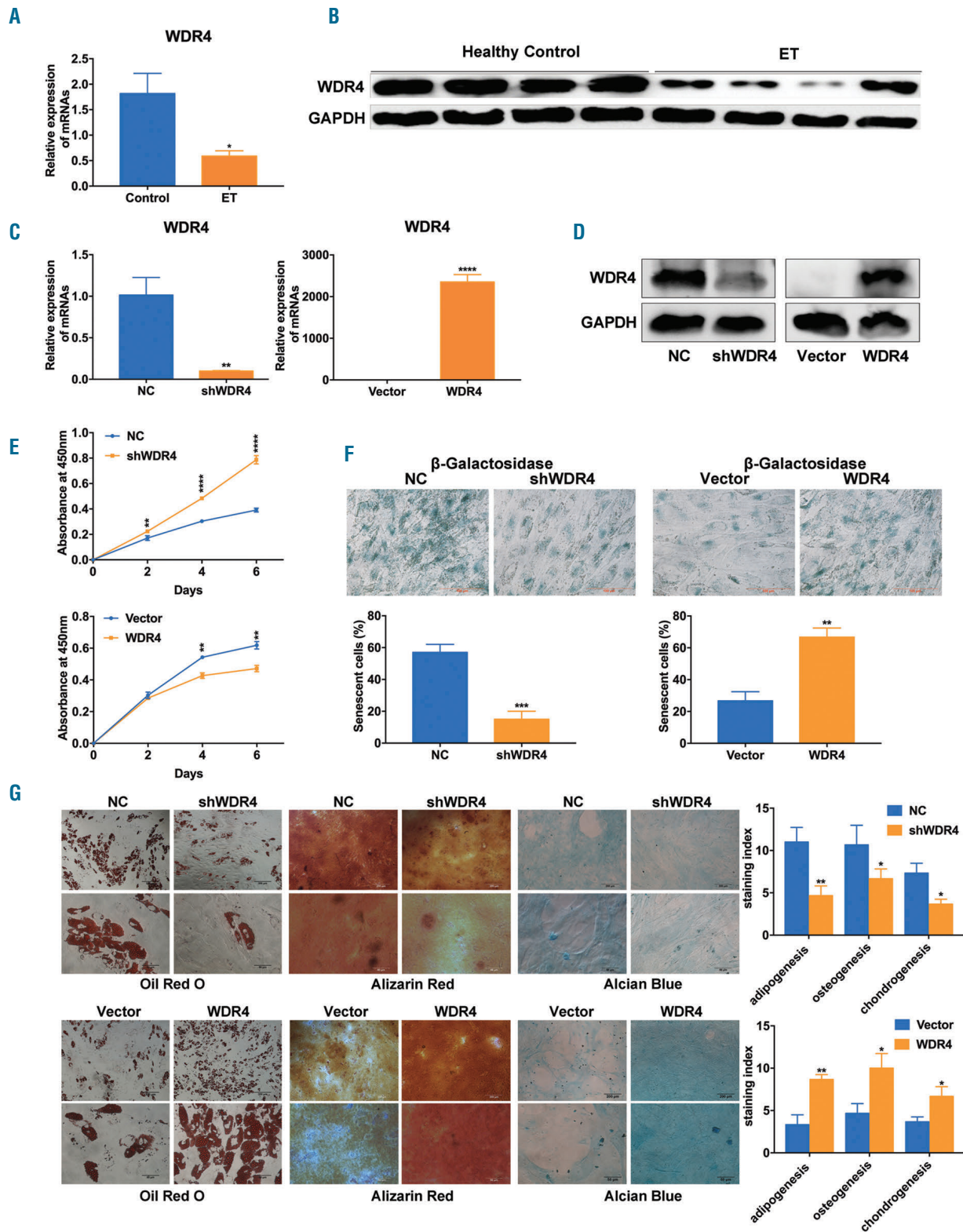
Figure 5. Low expression of WDR4 is correlated with enhanced proliferation, decreased senescence, and impaired differentiation of bone marrow derived mesenchymal stromal cells (BM-MSC) isolated from patients with *JAK2V617F*-positive essential thrombocythemia (ET). A. WDR4 mRNA expression in BM-MSC isolated from the controls (n=20) and patients with *JAK2V617F*-positive ET (n=15).B. WDR4 protein expression in BM-MSC isolated from the controls (n=4) and patients with *JAK2V617F*-positive ET (n= 4). C–D. WDR4 shRNA and cDNA decreased or increased WDR4 expression in BM-MSC efficiently, as determined by qPCR (C) and Western blotting (D). E. WDR4 cDNA treatment decreased the proliferative capacity of BM-MSC, while WDR4 shRNA treatment increased the proliferation of BM-MSC, as measured by the CCK-8 assay. F. WDR4 cDNA increased senescence of BM-MSC as measured by β-galactosidase staining while WDR4 shRNA had the opposite effect. G. WDR4 increased the differentiation potential of BM-MSC into adipocytes, osteocytes, and chondrocytes as indicated by Oil Red O, Alizarin Red, and Alcian Blue staining, respectively. MSC used in each assay were at passage four. All the experiments (except for the quantitation of WDR4 mRNA and WDR4 protein expression in clinical samples) were repeated at least three times. *P<0.05; **P<0.01; ***P<0.001; ****P<0.0001. Data are presented as the mean ± SD (except for mRNA expression of WDR4 in clinical samples, mean ± SEM). ET: essential thrombocythemia; CCK-8: Cell Counting Kit 8; n: number of unique donors in each group; NC: normal control; SD: standard deviation; SEM: standard error of mean.
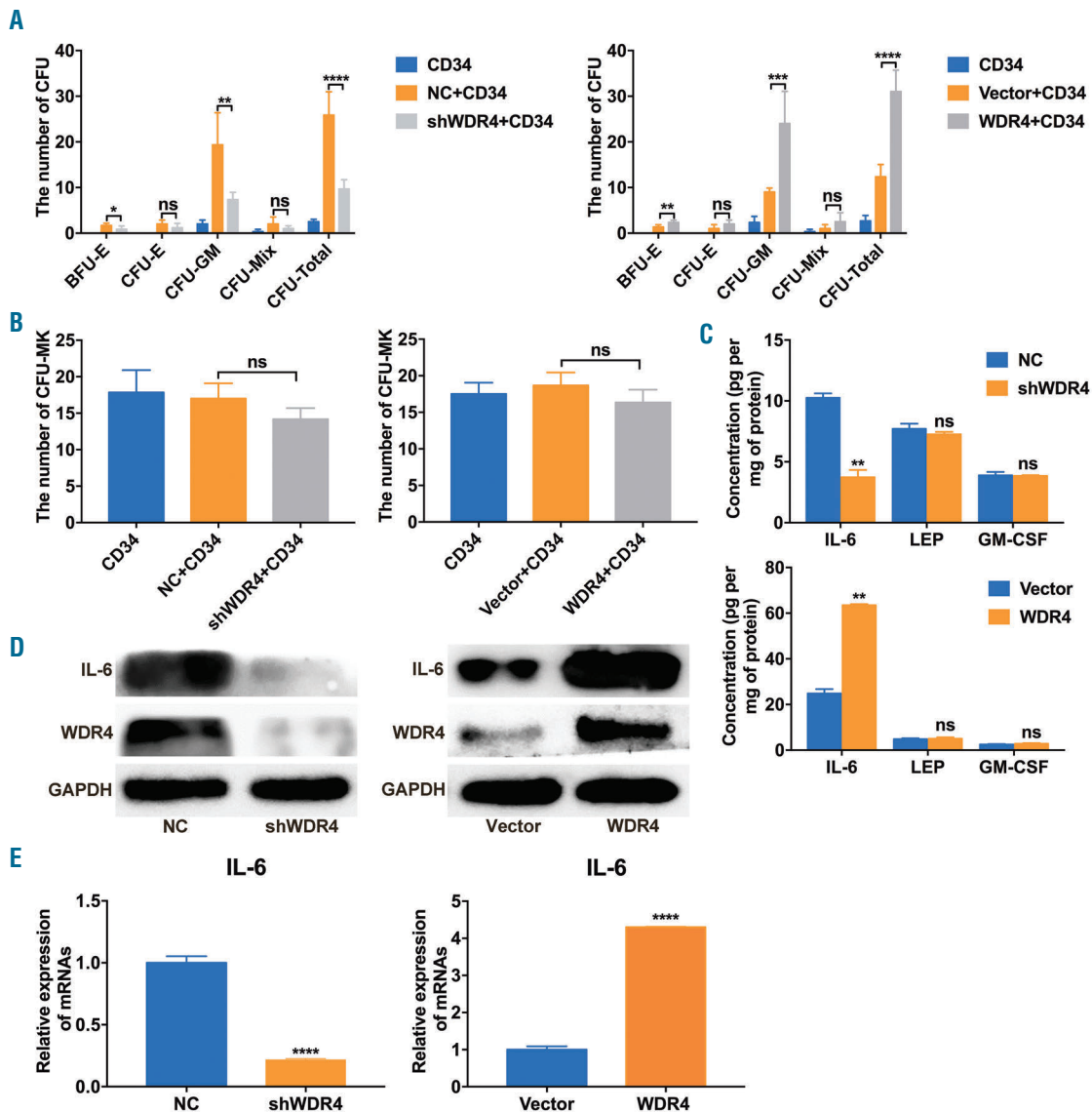
Figure 6. Insufficient action of the WDR4–IL-6 axis decreases hematopoiesis-supportive activities of bone marrow derived mesenchymal stromal cells (BM-MSC) from patients with *JAK2V617F*-positive ET. A–B. Numbers of BFU-E, CFU-E, CFU-GM, CFU-Mix, and CFU-MK formed by purified normal CD34-positive cells after coculture with BM-MSC infected with LV-shWDR4, or LV-WDR4. WDR4 increased the number of BFU-E, CFU-GM, and CFU-Total formed by normal CD34-positive cells (A). No changes were observed in the number of CFU-MK (B). C. WDR4 increased the secretion of IL-6 from BM-MSC as determined by ELISA on the supernatant obtained from the MSC cultures. D–E. WDR4 increased the intracellular expression of IL-6 in BM-MSC as determined by Western blotting (D) and qPCR (E). MSC used in each assay were at passage four. All the experiments were repeated at least three times. *P 0.05; **$P<0.01$; ***$P<0.001$; ****$P<0.0001$. Data are presented as the mean ± SD. qPCR: quantitative real-time polymerase chain reaction; CFU-E: colony-forming unit-erythroid; CFU-GM: colony-forming unit-granulocyte and macrophage; CFU-Total: total colony-forming units; CFU-MK: colony-forming unit-megakaryocyte; n: number of unique donors in each group; ns: not significant; NC: normal control; SD: standard deviation.

MSC infected with LV-shWDR4, the numbers of erythroid burst-forming units (BFU-E), CFU-GM, and CFU-Total were significantly lower than those in the control groups (Figure 6A). In contrast, increasing WDR4 expression corrected the ET MSC-mediated defects, as evidenced by higher numbers of BFU-E, CFU-GM, and CFU-Total relative to those in the control groups (Figure 6A). No changes were observed in the CFU-MK number (Figure 6B).

We next examined whether WDR4 regulated the hematopoietic cytokines mentioned above that were differentially produced between the two MSC samples. The results revealed a link between IL-6 and WDR4 (Figure 6C). We next performed qPCR and Western blotting to assess

whether IL-6 expression was affected by WDR4. In WDR4 knock-down HD MSC, intracellular IL-6 protein (Figure 6D) and mRNA levels (Figure 6E) were decreased. Furthermore, in the ET MSC, restoration of WDR4 expression alleviated the decrease in IL-6 levels (Figure 6 D–E). Taken together, these results indicate that WDR4 promotes the intracellular expression and secretion of IL-6 by BM-MSC.

WDR4 acts through the ERK–GSK3β–CREB pathway to increase IL-6 expression and secretion by BM-MSC

To identify candidate kinases through which WDR4 may act on IL-6, we evaluated the levels of 43 phosphorylated kinases in HD MSC infected with LV-shWDR4 rela-
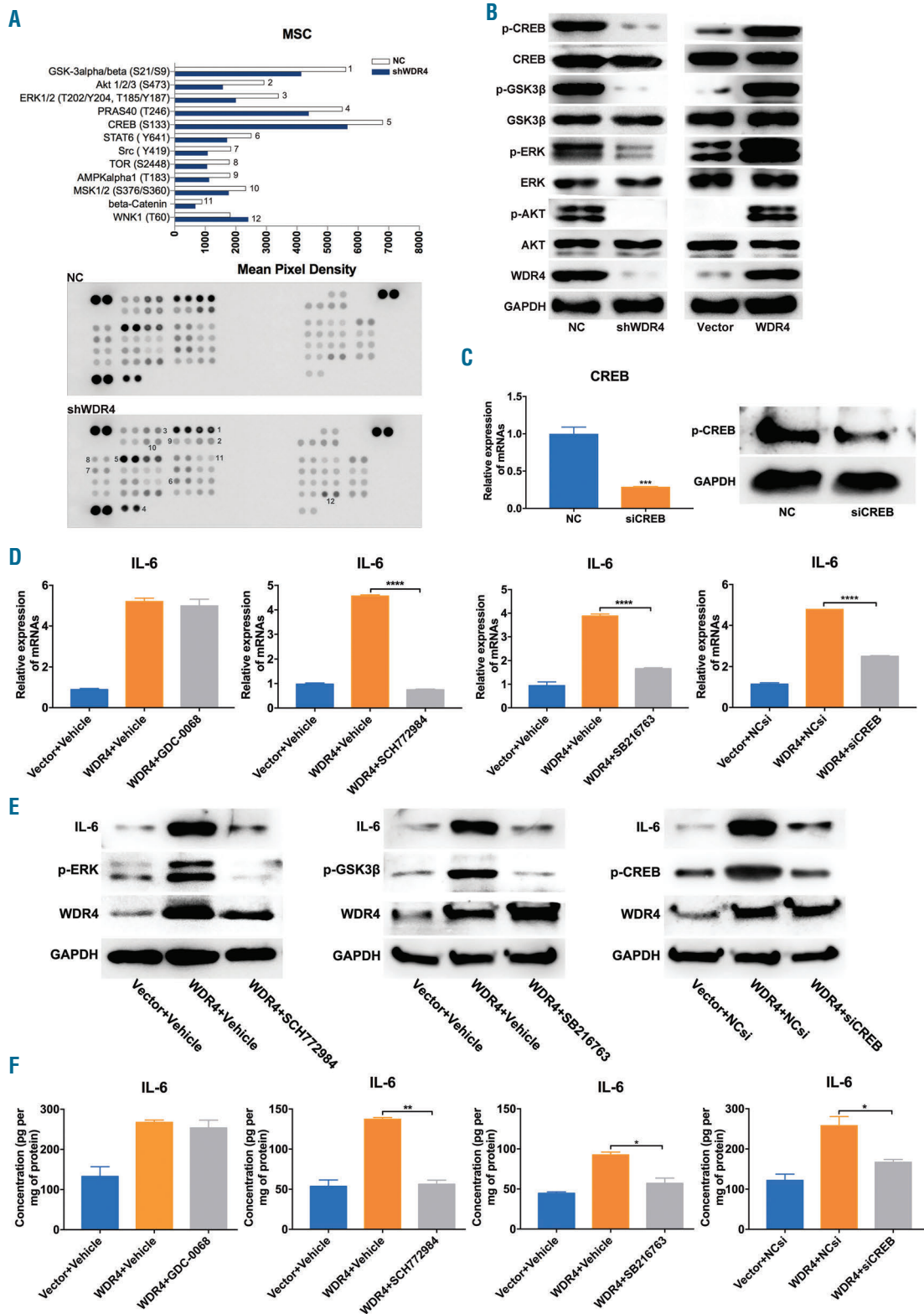
Figure 7. WDR4 acts through the ERK−GSK3β−CREB pathway to enhance IL-6 expression and secretion by bone marrow derived mesenchymal stromal cells (BM-MSC). A. Graphic representation of the quantification of 12 proteins with the most significant difference in phosphorylation status between MSC infected with LV-shWDR4 and MSC in the control group, as measured by a phospho-kinase array of 43 phosphorylated kinases. B. Western blot analysis of phosphorylation levels of GSK3β (S9), AKT1/2/3 (S472/S473/S474), ERK1/2 (T202/Y204, T185/Y187), and CREB (S133) in MSC infected with LV-shWDR4 or LV-WDR4 and their respective controls. C. CREB-specific siRNA decreased CREB expression in BM-MSC efficiently, as determined by qPCR and Western blotting. D–F. IL-6 induction by WDR4 over-expression was at least partially suppressed by an ERK1/2 inhibitor (SCH772984), GSK3 inhibitor (SB216763), or CREB-specific siRNA as determined by qPCR (D), Western blotting (E), and ELISA (F). MSC used in each assay were at passage four. All the experiments were repeated at least three times. *P<0.05; **P<0.01; ***P<0.001; ****P<0.0001. Data are presented as the mean ± SD. qPCR: quantitative real-time polymerase chain reaction; ELISA: enzyme-linked immunosorbent assay; NC: normal control; SD: standard deviation.

tive to those in the controls. Among the kinases that were affected by LV-shWDR4 infection, GSK3β, AKT, ERK, and CREB are known to be upstream of IL-6 (Figure 7A). We next validated the results by Western blotting. Phosphorylation levels of GSK3β (S9), AKT1/2/3 (S472/S473/S474), ERK1/2 (T202/Y204, T185/Y187), and CREB (S133) significantly decreased with WDR4 knockdown in HD MSC and increased with WDR4-overexpression in ET MSC (Figure 7B).

To determine which kinases are involved in WDR4-mediated IL-6 upregulation, we used kinase inhibitors specific for AKT1/2/3 (GDC-0068), ERK1/2 (SCH772984), and GSK3β (SB216763), and an siRNA specific for CREB in ET MSC infected with LV-WDR4. We thereby found that inhibition of ERK1/2, GSK3β, or CREB could at least partially suppress WDR4-induced IL-6 upregulation, while

inhibition of AKT1, -2, or -3 caused no significant effect as assessed with qPCR (Figure 7D), Western blotting (Figure 7E), and ELISA (Figure 7F). These findings indicate that WDR4 promotes IL-6 expression and secretion *via* the ERK–GSK3β–CREB signaling pathway in BM-MSC.

Neuropathy and aberrant expression of IL-1β in the BM of patients with *JAK2V617F*-positive ET

Markedly lower numbers of sympathetic nerve fibers and insheathing Schwann cells were found in the BM of patients with *JAK2V617F*-positive ET (Figure 8A). Norepinephrine, which is mainly secreted by sympathetic nerve fibers, was also significantly downregulated in ET BM (Figure 8C). Additionally, B3AR, a norepinephrine receptor, and IL-1β levels were upregulated in the BM of patients with *JAK2V617F*-positive ET (Figure 8B-D).
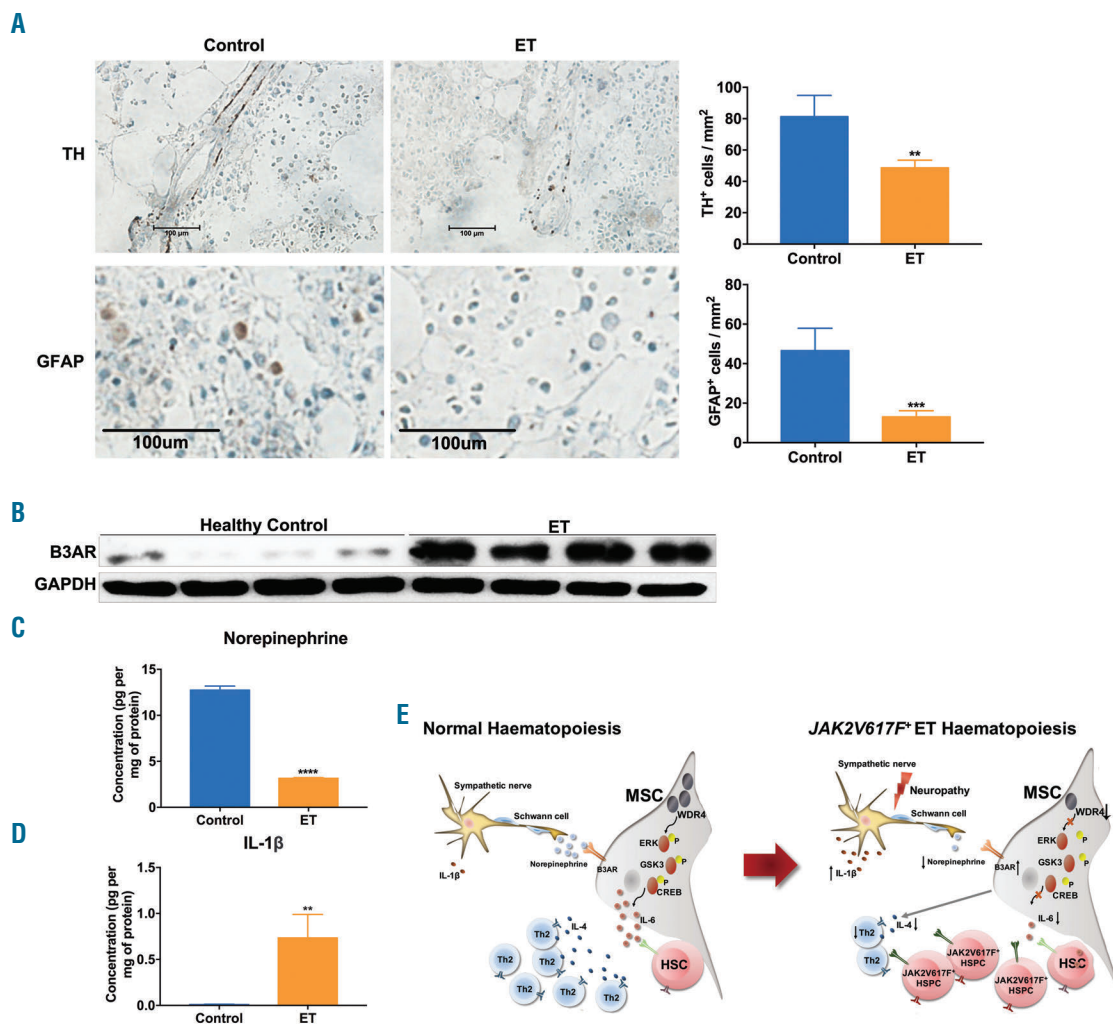
Figure 8. Neuropathy and aberrant expression of IL-1β in the bone marrow (BM) of patients with *JAK2V617F*-positive essential thrombocythemia (ET). A. Sympathetic nerve fibers quantitated with the help of an anti-TH antibody (control, n=9; ET, n=42), and Schwann cells visualized using an anti-GFAP antibody (control, n=9; ET, n=40) decreased in the BM of patients with *JAK2V617F*-positive ET relative to those in the HD, as determined by immunohistochemistry. B. Increased expression of B3AR in the BM of patients with *JAK2V617F*-positive ET (n=4) relative to the HD (n=4) as determined by Western blotting. C–D. Lower NE levels (C) (control, n=20; ET, n=20) and higher IL-1β levels (D) (control, n=20; ET, n=20) in the BM of patients with *JAK2V617F*-positive ET relative to the control, as measured by ELISA on the supernatant of the BM aspirates. E. A model illustrating BM hematopoietic dysfunction in *JAK2V617F*-positive ET. *P<0.05; **P<0.01; ***P<0.001; ****P<0.0001. Data are presented as the mean ± SEM. ET: essential thrombocythemia; HD: healthy donors; n: number of unique donors in each group; TH: tyrosine hydroxylase; GFAP: glial fibrillary acidic protein; NE: norepinephrine; B3AR: β3 adrenoceptor; SEM: standard error of mean.

Discussion

In the present study, we observed transcriptional and functional abnormalities in the hematopoietic niche of patients with *JAK2V617F*-positive ET, including functional deficiency in MSC, immune imbalance, and sympathetic neuropathy, relative to those in HD controls. BM-MSC from patients with *JAK2V617F*-positive ET showed an altered transcriptome, faster proliferation, attenuated apoptosis and senescence, decreased potential to differentiate into adipocytes and osteocytes, and insufficient support for normal hematopoiesis. These findings partially agree with those found in previous studies of the myelodysplastic syndrome, leukemia, and MPN by other groups, but differ from the conclusions obtained from an MPN mouse model and patients.[7-9,19,34] NES-positive cells have been reported to be heterogeneous populations comprising mesenchymal cells and endothelial cells in the BM.[4] We co-stained bone marrow samples with NES and CD34 (endothelial cell marker), and found that patients with *JAK2V617F*-positive ET showed higher numbers of NES-positive mesenchymal cells in the BM relative to those in the HD controls. This observation contradicts the results obtained from the MPN mouse model and patients mentioned above but is consistent with the results obtained in patients with ET, polycythemia vera (PV), and primary myelofibrosis (PMF) by other group.[34] NES⁻/leptin receptor⁻/CXCL12⁺ MSC subpopulations have been reported to be essential for the maintenance of HSC in mouse models.[35] Furthermore, in BM sections from patients with myelodysplastic syndrome, HSC are mostly in close contact with CD271⁺/NES⁻ MSC.[36] Hock *et al*. confirmed that HSC with elevated proliferation rates were functionally compromised.[37] Therefore, given that MSC of patients with *JAK2V617F*-positive ET showed enhanced proliferation, we hypothesize that functional deficits are also present in these MSC. These studies, as well as our data, may explain the poor ability of the expanded MSC isolated from patients with *JAK2V617F*-positive ET to support normal hematopoiesis. Regarding the paradox with the mouse models of MPN, it is possible that the heterogeneity of the patients with MPN contributed to the observed discrepancy since our study involved only patients with *JAK2V617F*-positive ET as subjects, but not those with PV or PMF. Because of the low number of the primitive non-passaged BM-MSC (0.08% of BM mononuclear cells), MSC used for functional analysis were expanded *ex vivo* in the present work. It is possible that this process caused changes that were not completely consistent with the most primitive state *in vivo*.[38] Additionally, although mouse models are powerful tools for studying MSC *in vivo*, animals may not fully recapitulate the medical conditions in humans, and inter-species differences in structure, function, and immunophenotype may have contributed to the contradictory results. Additionally, *JAK2V617F* mutation is detected in approximately 95% of patients with PV and 50% of patients with ET and PMF, and mouse models of *JAK2V617F* show a tendency to develop a PV phenotype more often than ET.[39-40] Furthermore, the hematopoietic niches of different MPN phenotypes may differ to some extent. Therefore, both animal models and clinical specimens help us to better understand the intrinsic state of MSC under medical conditions in humans. The ratio of mutant to wild-type *JAK2* has been proved to be critical for the phenotypic manifes-

tation.[41] Nonetheless, a successful model that accurately recapitulates the human manifestations of *JAK2*-positive ET is currently not available for us. Collectively, the present *in vitro* findings revealed a perturbed transcriptome and aberrant biological characteristics of BM-MSC of patients with *JAK2V617F*-positive ET.

It has been reported that expansion of BM CD4-positive T cells can lead to exhaustion of hematopoietic cells.[42] In this study, we found that MSC of patients with *JAK2V617F*-positive ET showed reduced inhibition of CD4-positive T-cell proliferation and activation, and secretion of the inflammatory cytokine sCD40L. In addition, they showed decreased induction of mostly immunosuppressive and antineoplastic Th2 cell formation, and secretion of the anti-inflammatory cytokine IL-4. Th2 formation is highly dependent on the activation of signal transducers and activators of transcription 6 by IL-4.[43] Thus, low secretion of IL-4 may be both the cause and consequence of blockage of the Th2 response. These results are mostly compatible with the results of previous studies.[14,15,42] Attenuated senescence of MSC from patients with *JAK2V617F*-positive ET was observed in the present study. Thus, one paradox arises, given that decreased senescence of MSC is typically linked to their anti-inflammatory status. The concept that MSC are highly plastic and the local inflammatory environment thus can shape the immunomodulatory effects of MSC may help to improve the understanding of the state of MSC in pathological processes. Specific inflammatory signals prompt MSC to switch between the proinflammatory and anti-inflammatory phenotypes.[44] One possible explanation for the contradiction between aging and their inflammatory phenotype is that aging-related changes may be compensated to some extent by the local inflammatory milieu. Additionally, MSC can be polarized by downstream Toll-like receptor (TLR) signaling into two homogenous phenotypes. TLR4-primed MSC mostly produce pro-inflammatory cytokines, while TLR3-primed MSC express mostly immunosuppressive cytokines.[45] TLR4 has been confirmed to inhibit senescence via epigenetic silencing of senescence-related genes.[46] Thus, another possible explanation is that upregulation of TLR4 and downregulation of TLR3 polarize the MSC from patients with *JAK2V617F*-positive ET to a proinflammatory phenotype with an anti-senescence effect. Collectively, these results indicate that MSC contribute at least partially to the immune imbalance in the BM of ET patients.

The changes mentioned above provide a possible link between the alterations in hematopoietic niches to the pathophysiology of *JAK2V617F*-positive ET in humans. Nonetheless, the underlying mechanisms remain unclear. In this study, we determined a mechanism whereby WDR4 deficiency impairs the ability of BM-MSC to support normal differentiation of hematopoietic progenitors in patients with *JAK2V617F*-positive ET. This effect occurs due to decreased IL-6 expression and secretion through suppression of the ERK–GSK3β–CREB pathway. Overall patients with MPN have been described to have higher IL-6 levels in the BM and there is published data on the oncogene-dependent mechanisms of fibroblasts expansion and IL-6 upregulation in fibroblasts in patients with *JAK2V617F*-positive MPN.[47] Nonetheless, in the present study, a prominent reduction in IL-6 levels was found in the supernatants of the culture medium of BM-MSC from patients with *JAK2V617F*-positive ET, with no obvi-

ous changes in IL-6 levels in the BM extract. This may be the case because the myelofibrosis grade of the patients enrolled in this study was 0-1. The significance of the hematopoiesis-supporting role of IL-6 has been well-documented.[24-27] Most HSPC are in contact with MSC in the BM, forming a highly sophisticated interaction network through direct contact and paracrine effects.[2] Thus, one possible explanation is that IL-6 levels in MSC contribute to the regulation of hematopoietic progenitors through local signals. Interestingly, our CFU assays showed that although some types of colonies depended on WDR4-IL6 axis, CFU-MK did not. *JAK2V617F* leads to increased HSC survival and biased differentiation to the lineages that signal through JAK2, including MK-platelets.[41] Therefore, it is reasonable to hypothesize that these *JAK2V617F* CFU-MK would outgrow other lineages that are more dependent on the WDR4-IL6 axis in the BM of ET patients. Further work is required. In the present study, CD34-positive cells cultured with MSC infected with LV-shWDR4 showed a different phenotype to those with ET MSC in terms of BFU-E. We observed a trend towards BFU-E reduction in patients with ET, but the difference was not significant. The difference is likely related to the diversity between these groups. Both groups treated with WDR4 shRNA or control shRNA showed similar characteristics in terms of clinical or laboratory features, while an overlap existed between BFU-E levels in patients and control samples, possibly because of the heterogeneity of clinical specimens and variable disease progression of the patients. Together these findings indicate that dysregulation of the WDR4-IL6 axis is involved in most dysfunctions in ET MSC.

Neuropathy was detected in the present study in BM sections of patients with *JAK2V617F*-positive ET. Although 10 μm sections are not optimal for accurate identification and quantification of BM fibers, no thicker sections were approved due to the scarcity of the clinical specimens. Aberrant expression of NE and B3AR were also detected in the BM of the patients. IL-1β, secreted by hematopoietic progenitors and many types of stromal cells, has been shown to mediate neuropathy in the BM of *JAK2V617F*-positive MPN mice and patients.[19] We also found elevated IL-1β levels in the BM extract of patients with *JAK2V617F*-positive ET, which may explain why neuropathy was detected. Neuropathy has been linked to the loss of NES-positive cells in MPN mice and patients,[19] while denervation of the BM in HD or patients with acute myeloid leukemia can lead to increased numbers of NES-positive cells.[9] A higher number of NES-positive cells was estimated in this study when thinner sections (5 μm) were used. Given that combining data derived from sections with different thickness may introduce significant bias,

further studies are required to understand the relevance between neuropathy and NES-positive cells. IL-1β has previously been reported to upregulate NES,[48] suggesting that immune cues are involved in altering both the sympathetic nervous system and MSC. NE inhibits nuclear factor-κB activity and pro-inflammatory cytokine release by binding to B2AR and B3AR on MSC and other immune cells.[12,18] The decreased production of NE, possibly caused by increased neurotoxic inflammatory cytokines, in ET can facilitate the formation of an inflammatory environment. Further studies are required to elucidate the connection between MSC, immunity, and sympathetic nerves.

In summary, this study revealed multilevel defects in the hematopoietic microenvironment of patients with *JAK2V617F*-positive ET and demonstrated that one of the differentially expressed genes, WDR4, underlies most dysfunctions in ET MSC *via* downregulation of IL-6 expression and secretion through suppression of the ERK–GSK3β–CREB pathway. Activation of the JAK-STAT3 pathway through IL-6 binding and its receptor is essential for maintaining normal hematopoiesis. A study recently revealed that IL-6 stimulated JAK2-STAT3 signaling in PV and PMF, but suppressed this signaling in ET.[49] Our results, alongside with those of previous studies, provide a compelling rationale for exploring the in vivo effect of the WDR4-IL-6 axis against ET in the future. Due to technical limitations, we also suggested a number of hypotheses and potential explanations for the paradoxes with other groups and future work is required for their validation.

References

1. Vainchenker W, Kralovics R. Genetic basis and molecular pathophysiology of classical myeloproliferative neoplasms. Blood. 2017; 129(6):667-679.
2. Crane GM, Jeffery E, Morrison SJ. Adult haematopoietic stem cell niches. Nat Rev Immunol. 2017;17(9):573-590.
3. Cordeiro Gomes A, Hara T, Lim VY, et al. Hematopoietic stem cell niches produce lineage-instructive signals to control multi-

potent progenitor differentiation. Immunity. 2016;45(6):1219-1231.
4. Xie L, Zeng X, Hu J, Chen Q. Characterization of Nestin, a selective marker for bone marrow derived mesenchymal stem cells. Stem Cells Int. 2015;2015:762098.
5. Korn C, Mendez-Ferrer S. Myeloid malignancies and the microenvironment. Blood. 2017;129(7):811-822.
6. Himburg HA, Termini CM, Schlussel L, et al. Distinct bone marrow sources of pleiotrophin control hematopoietic stem

cell maintenance and regeneration. Cell Stem Cell. 2018;23(3):370-381.e5.
7. Manso BA, Zhang H, Mikkelson MG, et al. Bone marrow hematopoietic dysfunction in untreated chronic lymphocytic leukemia patients. Leukemia. 2019;33(3):638-652.
8. Ping Z, Chen S, Hermans SJF, et al. Activation of NF-kappaB driven inflammatory programs in mesenchymal elements attenuates hematopoiesis in low-risk myelodysplastic syndromes. Leukemia. 2019;33(2):536-541.
9. Hanoun M, Zhang D, Mizoguchi T, et al.

Acute myelogenous leukemia-induced sympathetic neuropathy promotes malignancy in an altered hematopoietic stem cell niche. Cell Stem Cell. 2014;15(3):365-375.

10. Hanoun M, Maryanovich M, Arnal-Estape A, Frenette PS. Neural regulation of hematopoiesis, inflammation, and cancer. Neuron. 2015;86(2):360-373.

11. Maestroni GJM. Adrenergic modulation of haematopoiesis. J. Neuroimmune. Pharmacol. 2019 Feb 14. [Epub ahead of print].

12. Pavlov VA, Chavan SS, Tracey KJ. Molecular and functional neuroscience in immunity. Annu Rev Immunol. 2018; 36:783-812.

13. Broxmeyer HE, Bruns HA, Zhang S, et al. Th1 cells regulate hematopoietic progenitor cell homeostasis by production of oncostatin M. Immunity. 2002;16(6):815-825.

14. Gao A, Gong Y, Zhu C, et al. Bone marrow endothelial cell-derived interleukin-4 contributes to thrombocytopenia in acute myeloid leukemia. Haematologica. 2019 Feb 21. [Epub ahead of print].

15. Keller U, Aman MJ, Derigs G, Huber C, Peschel C. Human interleukin-4 enhances stromal cell-dependent hematopoiesis: costimulation with stem cell factor. Blood. 1994;84(7):2189-2196.

16. Agarwala S, Tamplin OJ. Neural crossroads in the hematopoietic stem cell niche. Trends Cell Biol. 2018;28(12):987-998.

17. Tripodo C, Burocchi A, Piccaluga PP, et al. Persistent immune stimulation exacerbates genetically driven myeloproliferative disorders via stromal remodeling. Cancer Res. 2017;77(13):3685-3699.

18. Buttner R, Schulz A, Reuter M, et al. Inflammaging impairs peripheral nerve maintenance and regeneration. Aging Cell. 2018;17(6):e12833.

19. Arranz L, Sanchez-Aguilera A, Martin-Perez D, et al. Neuropathy of haematopoietic stem cell niche is essential for myeloproliferative neoplasms. Nature. 2014;512(7512):78-81.

20. Jones SA, Jenkins BJ. Recent insights into targeting the IL-6 cytokine family in inflammatory diseases and cancer. Nat Rev Immunol. 2018;18(12):773-789.

21. Verboogen DRJ, Revelo NH, Ter Beest M, van den Bogaart G. Interleukin-6 secretion is limited by self-signaling in endosomes. J Mol Cell Biol. 2019;11(2):144-157.

22. Csaszar E, Wang W, Usenko T, et al. Blood stem cell fate regulation by Delta-1-mediated rewiring of IL-6 paracrine signaling. Blood. 2014;123(5):650-658.

23. Jiang C, Zhang Q, Shanti RM, et al. Mesenchymal stromal cell-derived interleukin-6 promotes epithelial-mesenchymal transition and acquisition of epithelial stem-like cell properties in ameloblastoma epithelial cells. Stem Cells. 2017;35(9):2083-2094.

24. Jenkins BJ, Roberts AW, Najdovska M, Grail D, Ernst M. The threshold of gp130-dependent STAT3 signaling is critical for normal regulation of hematopoiesis. Blood. 2005;105(9):3512-3520.

25. Jenkins BJ, Roberts AW, Greenhill CJ, et al. Pathologic consequences of STAT3 hyperactivation by IL-6 and IL-11 during hematopoiesis and lymphopoiesis. Blood. 2007;109(6):2380-2388.

26. Chiba Y, Mizoguchi I, Hasegawa H, et al. Regulation of myelopoiesis by proinflammatory cytokines in infectious diseases. Cell Mol Life Sci. 2018;75(8):1363-1376.

27. Maeda K, Mehta H, Drevets DA, Coggeshall KM. IL-6 increases B-cell IgG production in a feed-forward proinflammatory mechanism to skew hematopoiesis and elevate myeloid production. Blood. 2010;115(23):4699-4706.

28. Li R, Xin T, Li D, Wang C, Zhu H, Zhou H. Therapeutic effect of Sirtuin 3 on ameliorating nonalcoholic fatty liver disease: The role of the ERK-CREB pathway and Bnip3-mediated mitophagy. Redox Biol. 2018; 18:229-243.

29. Rodionova E, Conzelmann M, Maraskovsky E, et al. GSK-3 mediates differentiation and activation of proinflammatory dendritic cells. Blood. 2007; 109(4):1584-1592.

30. Yun MR, Choi HM, Kang HN, et al. ERK-dependent IL-6 autocrine signaling mediates adaptive resistance to pan-PI3K inhibitor BKM120 in head and neck squamous cell carcinoma. Oncogene. 2018;37(3):377-388.

31. Lin S, Liu Q, Lelyveld VS, Choe J, Szostak JW, Gregory RI. Mettl1/Wdr4-mediated m(7)G tRNA methylome is required for normal mRNA translation and embryonic stem cell self-renewal and differentiation. Mol Cell. 2018;71(2):244-255.e5.

32. Schapira M, Tyers M, Torrent M, Arrowsmith CH. WD40 repeat domain proteins: a novel target class? Nat Rev Drug Discov. 2017;16(11):773-786.

33. Wang YT, Chen J, Chang CW, et al. Ubiquitination of tumor suppressor PML regulates prometastatic and immunosuppressive tumor microenvironment. J Clin Invest. 2017;127(8):2982-2997.

34. Avanzini MA, Bernardo ME, Novara F, et al. Functional and genetic aberrations of in vitro-cultured marrow-derived mesenchymal stromal cells of patients with classical Philadelphia-negative myeloproliferative neoplasms. Leukemia. 2014;28(8):1742-1745.

35. Greenbaum A, Hsu YM, Day RB, et al. CXCL12 in early mesenchymal progenitors is required for haematopoietic stem-cell maintenance. Nature. 2013;495(7440):227-230.

36. Flores-Figueroa E, Varma S, Montgomery K, Greenberg PL, Gratzinger D. Distinctive contact between CD34+ hematopoietic progenitors and CXCL12+ CD271+ mesenchymal stromal cells in benign and myelodysplastic bone marrow. Lab Invest. 2012;92(9):1330-1341.

37. Hock H, Hamblen MJ, Rooke HM, et al. Gfi-1 restricts proliferation and preserves functional integrity of haematopoietic stem cells. Nature. 2004;431(7011):1002-1007.

38. Moravcikova E, Meyer EM, Corselli M, Donnenberg VS, Donnenberg AD. Proteomic profiling of native unpassaged and culture-expanded mesenchymal stromal cells (MSC). Cytometry A. 2018;93(9):894-904.

39. Lacout C, Pisani DF, Tulliez M, Gachelin FM, Vainchenker W, Villeval JL. JAK2V617F expression in murine hematopoietic cells leads to MPD mimicking human PV with secondary myelofibrosis. Blood. 2006;108(5):1652-1660.

40. Akada H, Yan D, Zou H, Fiering S, Hutchison RE, Mohi MG. Conditional expression of heterozygous or homozygous Jak2V617F from its endogenous promoter induces a polycythemia vera-like disease. Blood. 2010;115(17):3589-3597.

41. Tiedt R, Hao-Shen H, Sobas MA, et al. Ratio of mutant JAK2-V617F to wild-type Jak2 determines the MPD phenotypes in transgenic mice. Blood. 2008;111(8):3931-3940.

42. Pinto AI, Brown N, Preham O, Doehl JSP, Ashwin H, Kaye PM. TNF signalling drives expansion of bone marrow CD4+ T cells responsible for HSC exhaustion in experimental visceral leishmaniasis. PLoS Pathog. 2017;13(7):e1006465.

43. Nemeth K, Keane-Myers A, Brown JM, et al. Bone marrow stromal cells use TGF-beta to suppress allergic responses in a mouse model of ragweed-induced asthma. Proc Natl Acad Sci USA. 2010;107(12):5652-5657.

44. Mounayar M, Kefaloyianni E, Smith B, et al. PI3kalpha and STAT1 interplay regulates human mesenchymal stem cell immune polarization. Stem Cells. 2015;33(6):1892-1901.

45. Le Blanc K, Mougiakakos D. Multipotent mesenchymal stromal cells and the innate immune system. Nat. Rev. Immunol. 2012;12(5):383-396.

46. Kim SJ, Shan P, Hwangbo C, et al. Endothelial toll-like receptor 4 maintains lung integrity via epigenetic suppression of p16(INK4a). Aging Cell. 2019:e12914.

47. Hoermann G, Cerny-Reiterer S, Herrmann H, et al. Identification of oncostatin M as a JAK2 V617F-dependent amplifier of cytokine production and bone marrow remodeling in myeloproliferative neoplasms. FASEB J. 2012;26(2):894-906.

48. Li Y, Wang L, Pappan L, Galliher-Beckley A, Shi J. IL-1beta promotes stemness and invasiveness of colon cancer cells through Zeb1 activation. Mol Cancer. 2012;11:87.

49. Suboticki T, Mitrovic Ajtic O, Beleslin-Cokic BB, et al. IL-6 stimulation of DNA replication is JAK1/2 mediated in cross-talk with hyperactivated ERK1/2 signaling. Cell Biol. Int. 2019;43(2):192-206.

50. Dominici M, Le Blanc K, Mueller I, et al. Minimal criteria for defining multipotent mesenchymal stromal cells. The International Society for Cellular Therapy position statement. Cytotherapy. 2006; 8(4):315-317.

Ferrata Storti Foundation

Human BCR/ABL1 induces chronic myeloid leukemia-like disease in zebrafish

Mengchang Xu,[1] Yin Ye,[2] Zhi'an Ye,[1] Song'en Xu,[1] Wei Liu,[2] Jin Xu,[2] Yiyue Zhang,[2] Qifa Liu,[3] Zhibin Huang,[2] and Wenqing Zhang[1,2]

[1]Key Laboratory of Zebrafish Modeling and Drug Screening for Human Diseases of Guangdong Higher Education Institutes, Department of Developmental Biology, School of Basic Medical Sciences, Southern Medical University; [2]Division of Cell, Developmental and Integrative Biology, School of Medicine, South China University of Technology and [3]Department of Hematology, Nanfang Hospital, Southern Medical University, Guangzhou, China

ABSTRACT

Chronic myeloid leukemia (CML) is induced by the *BCR/ABL1* oncogene, which encodes a protein tyrosine kinase. We examined the effect of direct overexpression of the human p210$^{BCR/ABL1}$ oncoprotein in zebrafish. Humanized p210$^{BCR/ABL1}$ protein was detectable in *Tg(hsp70:p210$^{BCR/ABL1}$)* transgenic zebrafish embryos and adult kidney marrow. Transgenic zebrafish developed CML, which could be induced *via* cells transplanted into recipients. The expression of human *BCR/ABL1* promoted myeloid lineages in *Tg(hsp70:p210$^{BCR/ABL1}$)* transgenic embryos. A total of 77 of 101 (76.24%) *Tg(hsp70:p210$^{BCR/ABL1}$)* adult transgenic zebrafish (age 6 months-1 year) developed CML. CML in zebrafish showed a triphasic phenotype, similar to that in humans, involving a chronic phase predominantly characterized by neutrophils in various degrees of maturation, an accelerated phase with an increase in blasts and immature myeloid elements, and a blast phase with >90% blasts in both the peripheral blood and kidney marrow. Tyrosine kinase inhibitors, as the standard drug treatment for human CML, effectively reduced the expanded myeloid population in *Tg(hsp70:p210$^{BCR/ABL1}$)* transgenic embryos. Moreover, we screened a library of 171 compounds and identified ten new drugs against BCR/ABL1 kinase-dependent or -independent pathways that could also reduce *lcp1$^+$* myeloid cell numbers in *Tg(hsp70:p210$^{BCR/ABL1}$)* transgenic embryos. In summary, we generated the first humanized zebrafish CML model that recapitulates many characteristics of human CML. This novel *in vivo* model will help to elucidate the mechanisms of CML disease progression and allow high-throughput drug screening of possible treatments for this disease.

Correspondence:

WENQING ZHANG
mczhangwq@scut.edu.cn

ZHIBIN HUANG
huangzhb1986@scut.edu.cn

Check the online version for the most updated information on this article, online supplements, and information on authorship & disclosures: www.haematologica.org/content/105/3/674

Introduction

Chronic myeloid leukemia (CML) is a malignant bone marrow proliferative tumor originating from hematopoietic stem cells (HSC), with an annual incidence of 1-2/100,000 and accounting for 15-20% of all adult leukemias.[1] CML is characterized by uncontrolled proliferation of myeloid cells and their progenitors in the peripheral blood (PB) and bone marrow (BM).[2] The development of CML progresses from a chronic phase (CP) to an accelerated phase (AP), and finally to a blast phase (BP). Most patients in the CML-CP are clinically asymptomatic, but are diagnosed with leukocytosis characterized by mature granulocytes in the PB and BM. Disease progression to AP and BP is accompanied by a severe reduction in cellular differentiation, with immature blasts displacing mature cells.[3] The final transformation phase can result in both lymphoblastic (25%) and myeloblastic (50%) subtypes, with a further 25% manifesting biphenotypic or undifferentiated phenotypes.[4]

The presence of the Philadelphia chromosome (Ph$^+$) is an important diagnostic indicator for CML.[5] It is generated by a reciprocal translocation between chromosomes 9 and 22, referred to as t(9;22)(q34;q11).[6] This translocation results in the *BCR/ABL1* fusion gene, which is translated to the p210$^{BCR/ABL1}$ oncoprotein in almost

all patients with CML.[7,8] This fusion protein is a constitutively active tyrosine kinase that persistently activates various signaling pathways regulating cell proliferation, transformation, and survival, thereby promoting leukemogenesis.[9] Further research and exploration are needed to recognize the blast crisis of CML since the specific mechanism leading to it is not yet fully understood.

The therapeutic use of tyrosine kinase inhibitors (TKI), such as imatinib, dasatinib, and bosutinib, has transformed the management of CML, largely turning a lethal disorder into a chronic condition. However, conventional TKI therapy for CML still presents challenges, including the appearance of TKI-resistant BCR/ABL1 mutants[10] and the relative resistance of CML leukemia stem cells (LSC)[11] to TKI. In addition, all TKI have a similar spectrum of toxic effects[4] that can negatively affect the patient's quality of life. Furthermore, CML and other malignancies include a population of cancer stem cells (CSC) that is able to regenerate or self-renew, resulting in therapeutic resistance and disease progression, and the inability to eradicate these CSC remains a significant obstacle to curing these diseases.

Biomedical research requires suitable animal disease models in which to study the mechanisms responsible for the cellular and molecular pathologies, and for testing certain therapeutic methods. There are high levels of conservation in terms of genomics, histoembryology, physiology, cardiac electrophysiology, and drug metabolic pathways between zebrafish and humans,[12] and zebrafish thus represent a possible model for studying hematopoietic development and for high-throughput drug screening. However, there is currently no zebrafish CML model. The construction of a zebrafish CML model would expand our ability to study this disease and to develop new drugs that could benefit CML patients.

Methods

Zebrafish husbandry

All experiments involving zebrafish were carried out in accordance with the guidelines set by the Institutional Animal Care and Use Committee of Southern Medical University, Guangzhou, China. Zebrafish were raised, bred, and staged according to standard protocols.[13,14] The following strains were used: AB (wild-type strain, WT) and *Tg(lyz:DsRed)*.[15]

Generation of the pToL *hsp70*:p210[BCR/ABL1] construct and of *Tg(hsp70:p210[BCR/ABL1])* transgenic zebrafish

The transgenic construct consisted of the zebrafish heat shock protein (Hsp) 70 promoter, human *BCR/ABL1* (h*BCR/ABL1*) (b3a2) cDNA, Tol2 elements, and the SV40 polyA sequence. We cloned *hsp70* promoter elements by polymerase chain reaction (PCR) using *hsp70*-specific primers 5′-GTATCGATTCAGGGGT-GTCGCTTGGT-3′ and 5′-CCGATATCACCGGTCT-GCAGGAAAAAAAAAC-3′. The h*BCR/ABL1* (b3a2) cDNA fragment was isolated from the plasmid NGFR P210[16] (Addgene) after digestion with EcoRI. The *hsp70* promoter sequence was then placed upstream of the h*BCR/ABL1* (b3a2) cDNA and subcloned into the pToL vector with minimal Tol2 elements and an SV40 polyA sequence to form the pToL *hsp70*:p210[BCR/ABL1] construct. The transgenic line was generated by injecting 50 pg of the pToL *hsp70*:p210[BCR/ABL1] construct together with Tol2 transposase mRNA into zebrafish embryos at the one-cell stage. Founders were identified by PCR confirmation of the transgene.

Western blot

Protein was extracted from whole embryos at 6 days post-fertilization (dpf) or from blood cells from the kidney marrow (KM) of 1-year-old *Tg(hsp70:p210[BCR/ABL1])* and age-matched WT controls. Proteins were quantified, and assessed by western blot analysis. Protein lysates were probed with rabbit anti-c-Abl antibody (1:1000 dilution, Cell Signaling Technology). Mouse anti-glyceraldehyde 3-phosphate dehydrogenase (GAPDH) antibody (1:5000 dilution, Cell Signaling Technology) was included as an internal control.

Cell proliferation assay

Wild-type (WT) and *Tg(hsp70:p210[BCR/ABL1])* embryos at 3 dpf and 1-year old adults were incubated in 10 mM BrdU (Sigma-Aldrich) for 2 hours (h) and 4 h, respectively. The embryos and KM blood cells were stained with mouse-anti-BrdU antibody (Roche) and rabbit-anti-Lcp1 antibody (gift from Dr. Zilong Wen),[17] followed by Alexa Fluor 555-anti-mouse antibody (Invitrogen) and Alexa Fluor 488-anti-rabbit antibody (Invitrogen) for fluorescent visualization.

Terminal deoxynucleotidyl transferase dUTP nick end labeling assay

Transferase dUTP nick end labeling (TUNEL) assay was carried out using an *In Situ* Cell Death Detection Kit (TMR red, Roche), followed by rabbit anti-Lcp1 antibody and Alexa Fluor 488-anti-rabbit antibody (Invitrogen) for fluorescent visualization.

Transplantation

Whole KM cell suspensions were prepared from *Tg(lyz:DsRed)* and *Tg(hsp70:p210[BCR/ABL1]-lyz:DsRed)* (CML-like) fish. Three days after receiving a sublethal dose of radiation (25 Gy), 0.2 million cells were injected intracardially into irradiated WT recipients using a glass capillary needle (World Precision Instruments).

Drug treatment

Embryos were soaked in egg water containing 1‰ dimethylsulfoxide (DMSO) (Sigma-Aldrich), 20 μmol/L imatinib (Selleck), 5 μmol/L dasatinib (Selleck), 10 μmol/L bosutinib (Selleck), 20 μmol/L LY364947 (MedChemExpress), 2.5 μmol/L FTY720 (MedChemExpress), 0.5 μmol/L BEZ235 (MedChemExpress), or compounds from a compound library (TargetMol) for drug treatment.

Statistical analysis

Data were analyzed using SPSS software (version 20). Differences between two groups were analyzed using Student t-tests and differences among multiple groups by one-way analysis of variance (ANOVA) with Tukey's adjustment. Significance was accepted when $P<0.05$. Data were expressed as mean±Standard Error of Mean (SEM).

Details of other methods used are available in the *Online Supplementary Appendix.*

Results

Transient expression of humanized BCR/ABL1 increased the number of myeloid cells in zebrafish larvae

The *BCR/ABL1* fusion gene is present in nearly all cases of CML. Protein sequence comparisons revealed that zebrafish Bcr and Abl1 shared around 71% and 73% identities, respectively, with their human counterparts and contained a highly conserved kinase domain on Abl1

(Ensembl GRCh37 release 92). We evaluated the function of the hBCR/ABL1 oncoprotein in zebrafish by over-expressing h*BCR/ABL1* mRNA encoding the p210$^{BCR/ABL1}$ oncoprotein. We then detected the numbers of myeloid cells during embryonic hematopoietic development by

lcp1, lyz, mpx whole-mount *in situ* hybridization (WISH), and Sudan Black B (SB) cytochemical staining (Figure 1). *lcp1*, also named *l-plastin*, is a pan-myeloid marker that identifies all myeloid subsets, including macrophages and neutrophils. Numbers of *lcp1*⁺ cells were significantly
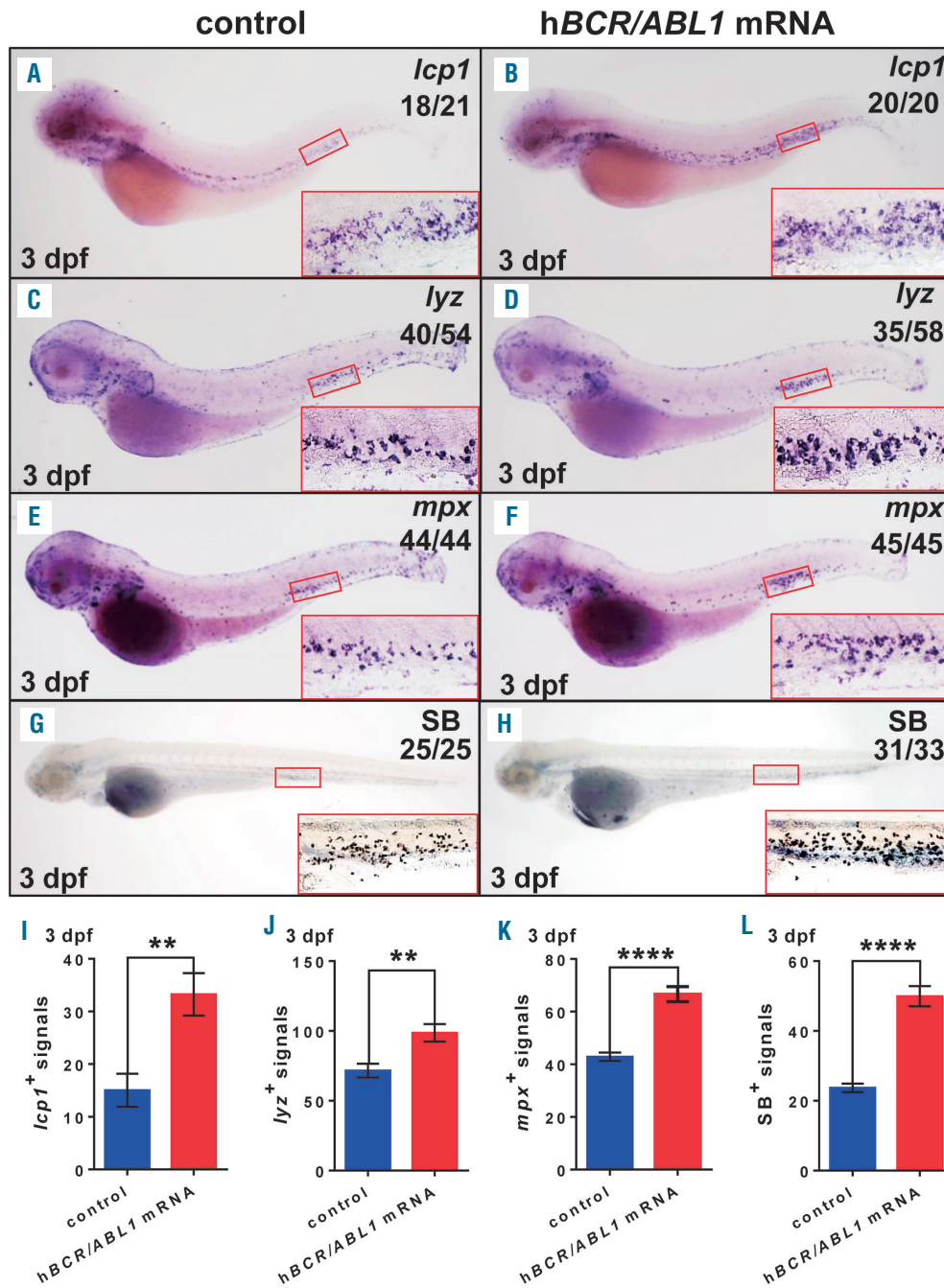
Figure 1. Expression levels of myeloid markers (*lcp1, lyz, mpx* and SB) increased after transient expression of humanized *BCR/ABL1* (h*BCR/ABL1*) in zebrafish larvae. Whole mount *in situ* hybridization (WISH) of *lcp1* (A and B), *lyz* (C and D), and *mpx* (E and F) expressions in wild-type (WT) zebrafish larvae after transient over-expression of h*BCR/ABL1* mRNA (right) were higher than controls (left) at 3 dpf. (G and H) The number of SB⁺ cells in WT zebrafish larvae after transient overexpression of h*BCR/ABL1* mRNA (right) was higher than controls (left) at 3 dpf. n/n: number of zebrafish larvae showing representative phenotype/total number of zebrafish larvae examined. Original magnification ×32 (A-H). Red rectangles in each panel indicate the signals in PBI region, and the regions were enlarged at the lower right (original magnification ×200). (I-L) Statistical analysis. *lcp1*⁺ signals (I), *lyz*⁺ signals (J), *mpx*⁺ signals (K), and SB⁺ signals (L) in PBI region after injection were calculated and compared at 3 dpf (Student *t*-tests, mean±Standard Error of Mean, **P<0.01; ****P<0.0001).

increased after overexpression of hBCR/ABL1 compared with the control group. Expression levels of markers of more mature neutrophils, such as *lyz, mpx,* and SB, also increased significantly. Patients with CML typically develop a highly characteristic differential white blood cell (WBC) count with high concentrations of myelocytes and segmented neutrophils. The current results implied that hBCR/ABL1 expression in zebrafish may promote myelocytes and may be capable of inducing myeloid leukemia *in vivo*.

hBCR/ABL1 was inherited in Tg(hsp70:p210^BCR/ABL1) transgenic zebrafish

Tg(hsp70:p210^BCR/ABL1) transgenic zebrafish were created using a construct (Figure 2A) expressing h*BCR/ABL1 under* the control of the zebrafish heat shock-inducible *hsp70* promoter.[18,19] The construct was designed to integrate the complete coding sequence into the host genome using the Tol2 transposition system, allowing the generation of multiple lines of transgenic zebrafish. *Tg(hsp70:p210^BCR/ABL1)* transgenic zebrafish founders were confirmed by PCR (Figure 2B). Stable F1 *Tg(hsp70:p210^BCR/ABL1)* transgenic zebrafish were obtained by intercrossing founder fish and were confirmed by sequencing (*data not shown*). F2 and the offsprings were obtained by mating F1 fish with WT fish. The temporospatial expression of h*BCR/ABL1* in *Tg(hsp70:p210^BCR/ABL1)* transgenic zebrafish was evaluated by WISH (Figure 2C). h*BCR/ABL1* expression was apparent throughout the body of *Tg(hsp70:p210^BCR/ABL1)* embryos at 3 dpf after heat shock treatment. Further detection by real-time-quantitative (RT-q)-PCR showed that levels of h*BCR/ABL1* mRNA were significantly elevated after heat shock treatment in both *coro1a*:GFP^+ blood cells from *Tg(hsp70:p210^BCR/ABL1)* transgenic zebrafish embryos and hematopoietic progenitors and myelocytes in KM blood cells from *Tg(hsp70:p210^BCR/ABL1)* transgenic zebrafish adults (*Online Supplementary Figure S1*). The h*BCR/ABL1* oncogene encoding the p210^BCR/ABL1 protein was also detected in *Tg(hsp70:p210^BCR/ABL1)* transgenic zebrafish embryos and adult kidneys (Figure 2D). The molecular weight of p210^BCR/ABL1 measured *in vitro* (*Online Supplementary Figure S2*) confirmed that the weight of the fusion protein generated was as expected. The p210^BCR/ABL1 protein was highly expressed in *Tg(hsp70:p210^BCR/ABL1)* transgenic zebrafish after heat-shock treatment.

Inducible hBCR/ABL1 expression in Tg(hsp70:p210^BCR/ABL1) transgenic zebrafish promoted myeloid lineage in zebrafish embryos

Expression of p210^BCR/ABL1 induces leukemia and myeloproliferative disorders, indicating a direct, causal role of BCR/ABL in CML.[9,20-23] We established *Tg(hsp70:p210^BCR/ABL1)* transgenic zebrafish with expression of p210^BCR/ABL1 and stable inheritance. To further explore the function of p210^BCR/ABL1 in zebrafish, we observed its influence on hematopoietic development in zebrafish embryos using WISH and cytochemical staining with lineage-specific markers (Figure 2E). The numbers of *lcp1*^+ pan-myeloid cells, *lyz*^+ neutrophils, SB^+ neutrophils, and *mfap4*^+ macrophages were significantly increased in *Tg(hsp70:p210^BCR/ABL1)* transgenic zebrafish larvae at 3 dpf compared with WT controls. This suggested that h*BCR/ABL1* expressed in zebrafish could either promote the production of HSC or their differentiation into each

hematopoietic lineage. To distinguish between these possibilities, we detected the HSC marker (*cmyb*), erythrocyte marker (*βe1*), and lymphocyte marker (*rag1*). There was no difference in the number of *cmyb*^+ HSCs between *Tg(hsp70:p210^BCR/ABL1)* transgenic zebrafish and WT controls at 36 hpf, but the number was significantly increased in transgenic zebrafish at 60 hpf (*Online Supplementary Figure S3A-D, I and J*). Numbers of *βe1*^+ erythrocytes and *rag1*^+ lymphocytes were significantly decreased in the transgenic zebrafish compared with the WT control zebrafish at 5 dpf (*Online Supplementary Figure S3E-H*). These findings suggest that h*BCR/ABL1* may promote myeloid differentiation.

Inducible hBCR/ABL1 expression in Tg(hsp70:p210^BCR/ABL1) adult zebrafish created phenotype resembling human CML

The natural progression of untreated CML is bi- or triphasic, with the initial CP followed by AP, BP, or both. CP is characterized by leukocytosis in both the PB and BM, and a preponderance of granulocytes in various degrees of maturation. However, blasts account for <2% of the peripheral WBC and <5% of the nucleated cells in the BM.[24] As the disease progresses, patients enter the AP followed by the BP, during which there is hematopoietic differentiation arrest, allowing immature blasts to accumulate in the BM and spill into the circulation. A level of 10-19% of blasts in the PB or BM marks the transition from CP to AP, along with a predominance of promyelocytes. A level of at least 20% PB or BM blasts indicates the progression to the BP.[24] To explore the possibility of developing leukemia-like hematologic disorders in *Tg(hsp70:p210^BCR/ABL1)* adult fish, PB and KM cells were collected from *Tg(hsp70:p210^BCR/ABL1)* and WT fish at 6 months to 1-year old and subjected to cytological and WBC analyses (Table 1 and Figure 3A and B). Seventy-seven of 101 (76.24%) *Tg(hsp70:p210^BCR/ABL1)* adult zebrafish developed CML-like disease, including 68 with a CML-CP phenotype, marked by massive leukocytosis in the PB or KM, including increased percentages of myelocytes and myeloid precursors. In the early stage of CML-CP, the increased leukocytes were primarily neutrophils in various degrees of maturation. Myelocytes accounted for >15% in the PB or >50% in the KM, with blasts usually accounting for <2% of the PB and <5% of the KM during this phase. We referred to this period as CML-CP1 (Table 2). Differentiation was then interrupted in the late stage of CML-CP as the condition progressed towards CML-AP. The increased leukocytes were primarily myeloid precursors and blasts, with myeloid precursors >10% and blasts >2% in the PB, and myeloid precursors >15% and blasts >5% in the KM. We referred to this period as CML-CP2 (Table 2). Eight of the 77 CML-like *Tg(hsp70:p210^BCR/ABL1)* transgenic zebrafish showed CML-AP phenotype including significant 2- to 10-fold increases in the percentages of blasts and myeloid precursors, with blasts >10% in the PB or KM. Amongst the 77 CML-like *Tg(hsp70:p210^BCR/ABL1)* adult zebrafish, one progressed to CML-BP with >90% blasts expanding in both the PB and KM. We also identified some phenotypes accompanying these CML-like *Tg(hsp70:p210^BCR/ABL1)* adult zebrafish, including eosinophilia, lymphocytosis and thrombocytosis (Figure 3C). Six of 77 (7.79%) CML-like *Tg(hsp70:p210^BCR/ABL1)* adult zebrafish presented with eosinophilia, with eosinophils accounting for >0.1% of
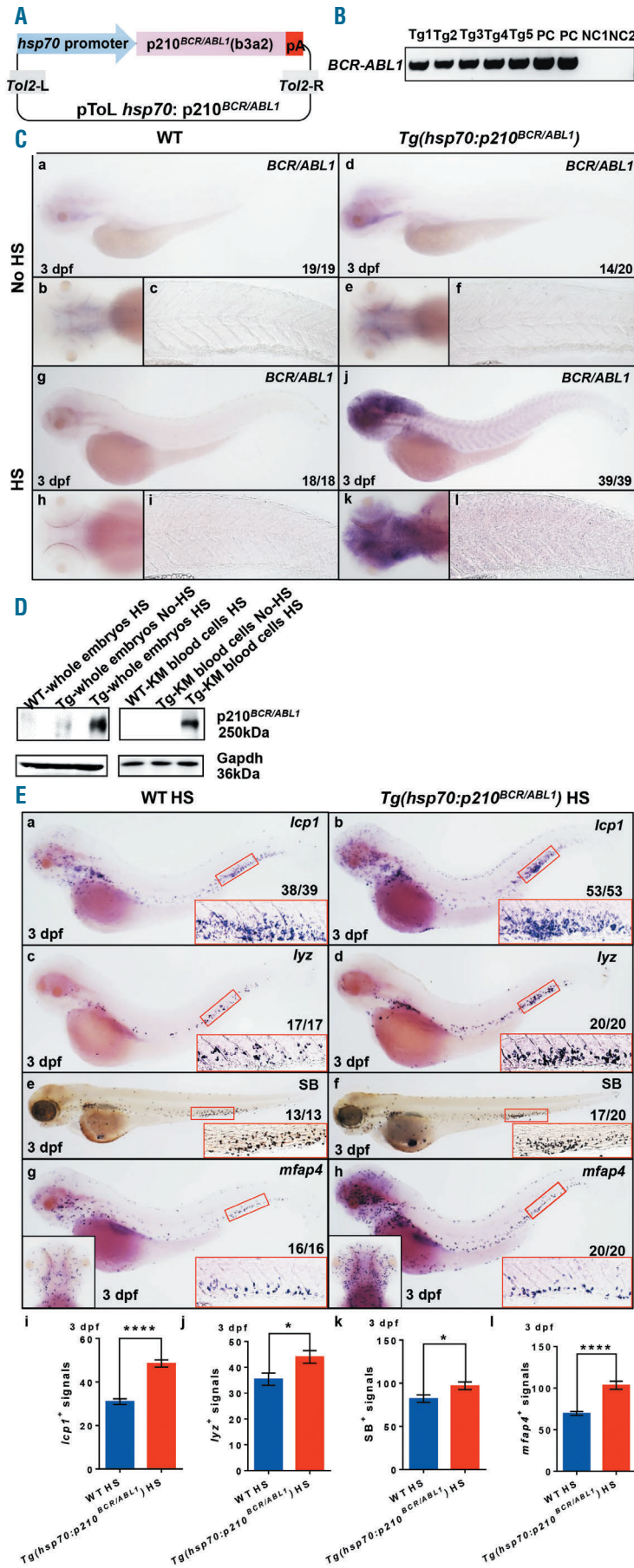
Figure 2. Expression of h*BCR/ABL1* in *Tg(hsp70:p210^{BCR/ABL1})* transgenic zebrafish. (A) Structure of pToL *hsp70*:p210^{BCR/ABL1}. (B) Detection of the hBCR/ABL1 cDNA sequence integrated into the wild-type (WT) zebrafish genome using the specific polymerase chain reaction (PCR) amplifying a 466 bp fragment within the h*BCR/ABL1* fusion section. Tg: *Tg(hsp70:p210^{BCR/ABL1})* founder individuals; PC: pToL *hsp70*:p210^{BCR/ABL1} plasmid as the positive control; NC1: ddH$_2$O as the negative control; NC2: genomic DNA of WT fish as the negative control. (C) Whole mount *in situ* hybridization (WISH) of h*BCR/ABL1* mRNA temporospatial expression in 3 dpf WT and *Tg(hsp70:p210^{BCR/ABL1})* zebrafish embryos without (a-f) or with (g-l) heat-shock treatment. Original magnification x32 (a, d, g and j). Signals in head (b, e, h, k) and tail (c, f, i, l) region under 100× and 200× magnification, respectively. n/n: number of zebrafish embryos showing representative phenotype/total number of zebrafish embryos examined. (D) Expression of p210^{BCR/ABL1} expressed in embryos (n=200) and kidney marrow (KM) blood cells (approx. 2x10^6 cells) of *Tg(hsp70:p210^{BCR/ABL1})* adult zebrafish assessed by western blot. GAPDH as the loading control. Tg: *Tg(hsp70:p210^{BCR/ABL1})* transgenic zebrafish; No-HS: T*Tg(hsp70:p210^{BCR/ABL1})* transgenic zebrafish without heat-shock treatment; HS: *Tg(hsp70:p210^{BCR/ABL1})* transgenic zebrafish with heat-shock treatment. (E) WISH of *lcp1* (a-b), *lyz* (c-d), and *mfap4* (g-h) expressions in HS *Tg(hsp70:p210^{BCR/ABL1})* (right) were higher than WT controls (left) at 3 dpf. (e-f) The number of SB positive cells in HS *Tg(hsp70:p210^{BCR/ABL1})* (right) was higher than WT controls (left) at 3 dpf. n/n: number of zebrafish larvae showing representative phenotype/total number of zebrafish larvae examined. Original magnification ×32 (a-h). Red rectangles in each panel indicate the signals in PBI region and the regions were enlarged at the lower right (original magnification ×200). Black rectangles in the panel indicate the signals in the brain region (vertical view, original magnification ×50). (i-l) Statistical analysis. *lcp1*$^+$ signals (i), *lyz*$^+$ signals (j), *mfap4*$^+$ signals (l), and SB$^+$ signals (k) in PBI region were calculated and compared at 3 dpf. Student *t*-tests, mean±Standard Error of Mean; *$P<0.05$; ****$P<0.0001$.

the PB cell count compared with approximately 0.01±0.00% in WT adult zebrafish (n=55) (*Online Supplementary Table S1*). This was similar to the "Ph-positive eosinophilic/basophilic CML" described by Goh *et al.*[24] Large numbers of lymphocytes accumulated in the PB in 8 of 77 (10.39%) CML-like *Tg(hsp70:p210^BCR/ABL1)* adult zebrafish, accounting for >5% of the PB cell count compared with around 1.80±0.23% in WT adult zebrafish (n=55) (*Online Supplementary Table S1*), similar to the lymphocytosis[25] observed in CML patients. Thrombocytosis[26] is present in approximately half of all newly diagnosed CML patients. Thirteen of the 77 (16.88%) CML-like *Tg(hsp70:p210^BCR/ABL1)* adult zebrafish presented with thrombocytosis, with platelets accounting for >0.5% of the PB cell count compared with around 0.11±0.04% in WT adult zebrafish (n=55) (*Online Supplementary Table S1*). Histological examination of the spleen in CML-like *Tg(hsp70:p210^BCR/ABL1)* demonstrated expansion of the splenic red pulp, predominantly by granulocytic myeloid cells (Figure 3D). In addition, the morbidity of CML-like disease in heat-shock-treated *Tg(hsp70:p210^BCR/ABL1)* adult zebrafish was higher than in non-induced *Tg(hsp70:p210^BCR/ABL1)* adult zebrafish. The ratios of individuals in CML-CP2 and CML-AP were increased among heat-shock-treated *Tg(hsp70:p210^BCR/ABL1)* compared with untreated *Tg(hsp70:p210^BCR/ABL1)* adult zebrafish (Figure 3E). This result suggests that overexpression of BCR/ABL1 is an important factor in accelerating the course of CML.

Tg(hsp70:p210^BCR/ABL1) transgenic fish displayed abnormal myeloid cell expansion resulting from increased proliferation and inhibition of apoptosis

The above results indicated that myeloid cells accumulated in *Tg(hsp70:p210^BCR/ABL1)* fish from the embryonic stage to the adult, which could be caused by accelerated proliferation or reduced apoptosis. To clarify the cellular mechanisms responsible for myeloid cell expansion in *Tg(hsp70:p210^BCR/ABL1)* fish, we monitored myeloid cell proliferation and death by BrdU incorporation and TUNEL assay, respectively. BrdU incorporation was significantly increased in *Tg(hsp70:p210^BCR/ABL1)* larvae and adult KM compared with WT controls, indicating that myeloid cell expansion in *Tg(hsp70:p210^BCR/ABL1)* fish was the result of increased proliferation (Figure 4A, B, E and F). However, myeloid cell apoptosis was also significantly decreased in *Tg(hsp70:p210^BCR/ABL1)* larvae and adult KM compared with WT controls, suggesting that the expansion of myeloid cells *Tg(hsp70:p210^BCR/ABL1)* was also caused by reduced apoptosis (Figure 4C, D, G and H).

Tg(hsp70:p210^BCR/ABL1) transgenic cells with induced CML-like disease were transplantable

To determine the aggressiveness of the leukemia induced by *Tg(hsp70:p210^BCR/ABL1)* activity, whole KM blood cells from *Tg(hsp70:p210^BCR/ABL1)* fish were transplanted into γ-irradiated WT adult hosts and the resulting fish were tested to determine if the CML-like phenotype developed in the *Tg(hsp70:p210^BCR/ABL1)* fish could be transplanted into the WT fish. We used 1-year old *Tg(hsp70:p210^BCR/ABL1)-lyz:DsRed)* CML-like donors and *Tg(lyz:DsRed)* control donors, in which the granulocytes were marked by red fluorescence. Each irradiated WT fish received 0.2 million KM blood cells from donors and were then raised under normal conditions. All four surviving recipients of *Tg(hsp70:p210^BCR/ABL1)-lyz:DsRed)* CML-like donor cells developed CML-like disease within 2-3 weeks of transplantation with whole KM blood cells, indicated by infiltration of DsRed⁺ granulocytes into the periphery (Figure 5A) and the robust expansion of myeloid cells in both the PB and KM (Figure 5B). In contrast, no control fish showed signs of a CML-like phenotype. We collected leukemia cells from the PB and KM and showed that these inflated cells were *BCR/ABL1*⁺ by PCR (Figure 5C). We concluded that the myeloid cells that accumulated in *Tg(hsp70:p210^BCR/ABL1)* fish could proliferate autonomously and could cause CML-like disease in a WT host.

Tg(hsp70:p210^BCR/ABL1) transgenic leukemic model responded to chemotherapeutic drug treatment

Recent studies demonstrated that zebrafish shares 82% of disease-associated targets and numerous drug metabolism pathways with humans.[12] To determine if the pharmacological mechanism in *Tg(hsp70:p210^BCR/ABL1)* transgenic zebrafish was also conserved compared with CML patients, we treated the WT and *Tg(hsp70:p210^BCR/ABL1)* embryos with the widely used anti-CML drugs, imatinib, dasatinib, and bosutinib, to the maximum teratogenic doses, with DMSO as a placebo (*Online Supplementary*

Table 1. Hemogram and classification of Tg(hsp70:p210BCR/ABL1) fish at 6-12 months

Classification	Group	Number	Percentages in PB (%)				Percentages in KM (%)				Leukemia cell types
			Blasts	Myeloid precursors	Myelocytes	Lymphocytes	Blasts	Myeloid precursors	Myelocytes	Lymphocytes	
WT	Normal	55	0.06 ± 0.04	1.68 ± 0.39	8.09 ± 1.45	90.17 ± 1.55	4.41 ± 0.56	12.56 ± 0.76	46.89 ± 1.29	36.14 ± 1.21	
Tg(hsp70:p210BCR/ABL1)	CML-CP	68	0.40 ± 0.12	2.99 ± 0.59	8.88 ± 1.24	87.73 ± 1.45	3.37 ± 0.51	12.16 ± 0.92	50.48 ± 1.39*	34.00 ± 0.98	Neutrophils and myeloid precursors
	CML-AP	8	1.75 ± 0.82	19.00 ± 3.95†	14.20 ± 3.06	65.05 ± 5.86	10.36 ± 1.32‡	18.54 ± 1.51†	36.29 ± 2.98	34.82 ± 2.47	Myeloid precursors and blasts
	CML-BP	1	99.28§	0.26	0.13	0.33	90.25§	1.96	4.56	3.23	Blasts

The White blood cell counts were obtained by identifying at least 500 cells per kidney marrow (KM) preparation and at least 1500 cells per peripheral blood (PB) preparation. The percentages were indicated by mean ± SEM. Adult Tg(hsp70:p210BCR/ABL1) fish characterized by myelocytes > 15% in PB or > 50% in KM were divided into CML-CP, blasts usually account for < 2% in PB or < 5% in KM. Adult Tg(hsp70:p210BCR/ABL1) fish characterized by blasts > 10% in PB or KM were divided into CML-AP. Adult Tg(hsp70:p210BCR/ABL1) fish characterized by blasts > 90% in both PB and KM were divided into CML-BP. * Indicates myelocytes in PB or KM increased > 15% or 50%. † Indicates myeloid precursors in PB or KM increased > 10% or >15%. ‡ Indicates blasts in PB or KM increased > 10%. § Indicates blasts in PB or KM increased > 90%.
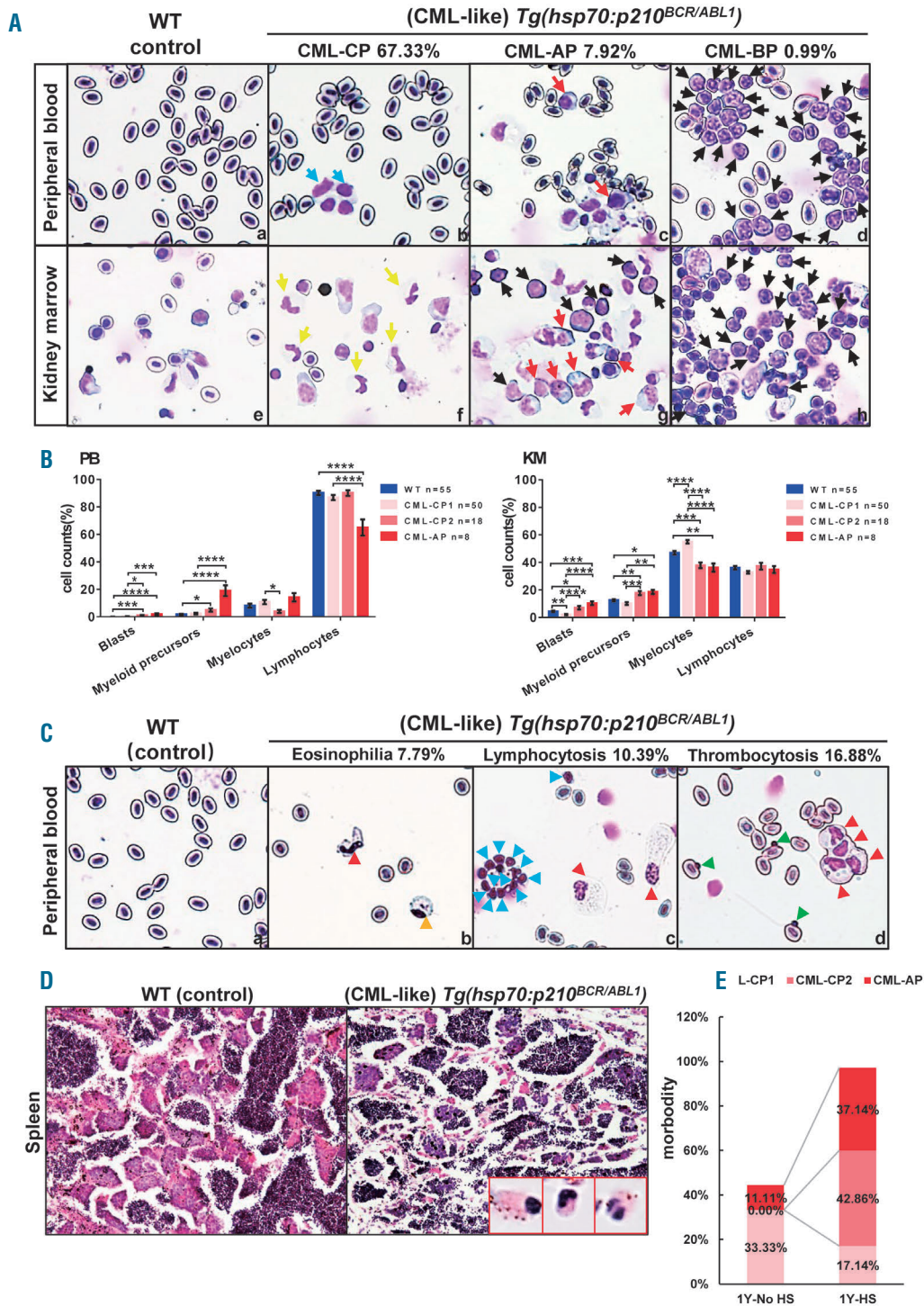
Figure 3. *Tg(hsp70:p210BCR/ABL1)* **adult fish display abnormal myeloid cell expansion resembled chronic myeloid leukemia (CML)-like phenotypes.** (A) May-Grunwald-Giemsa staining of peripheral blood (PB) cells (top) and kidney marrow (KM) blood cells (bottom) were obtained from wild-type (WT) (a, e) (n=55) and *Tg(hsp70:p210BCR/ABL1)* (b-d, f-h) (n=101) adult zebrafish. Blue arrows indicate accumulated promyelocytes in CML-chronic phase (CP)-like fish. Yellow arrows indicate neutrophils in CML-CP-like fish. Red arrows indicate myeloid precursors in CML accelerated phase (AP)-like fish. Black arrows indicate blasts in both CML-AP-like fish and CML-BP-like fish. The percentages indicate the ratio that number of fish with leukemia-like phenotype in total number of fish. Original magnification x400. (B) Statistical analysis. Blood cell counts of PB and KM were calculated manually based on their morphology. ANOVA; mean±Standard Error of Mean; *P<0.05; **P<0.01; ***P<0.001; ****P<0.0001. (C) Large numbers of eosinophils (b, yellow arrow), lymphocytes (c, blue arrow), and platelets (d, green arrow) accumulated in CML-like *Tg(hsp70:p210BCR/ABL1)* adult fish PB compared with WT controls (a, n=55). The percentages indicate the ratio that number of abnormal cells accumulated in total number of CML-like *Tg(hsp70:p210BCR/ABL1)* adult fish. Red arrows indicate neutrophils. Original magnification x400. Stains were May-Grunwald-Giemsa. (D) Histology of the spleen from CML-like *Tg(hsp70:p210BCR/ABL1)* adult fish showing disruption of the spleen architecture and massive invasion by hematopoietic cells compared with WT controls. Original magnifications x200 for each panel. Inset (red rectangles): granulocytic myeloid cells at higher magnification x1000. Stains were Hematoxylin & Eosin. (E) The morbidity rate of CML was higher in 1 Y-HS *Tg(hsp70:p210BCR/ABL1)* adult fish (n=35) compared with 1 Y-No HS *Tg(hsp70:p210BCR/ABL1)* adult fish (n=18), 97.14% and 44.44%, respectively. 1Y-No HS: 1-year-old *Tg(hsp70:p210BCR/ABL1)* adult fish without heat shock treatment. 1Y-HS: 1-year-old *Tg(hsp70:p210BCR/ABL1)* adult fish with heat shock treatment. The morbidity rates of *Tg(hsp70:p210BCR/ABL1)* transgenic fish in the HS group developing into CML-CP 1 phase was 17.14%, while that in the No-HS treatment group was 33.33%. The morbidity rate of *Tg(hsp70:p210BCR/ABL1)* transgenic fish in the heat shock treatment group developing into CML-CP 2 phase and CML-AP phase were 42.86% and 37.14%, compared with 0.00% and 11.11%, respectively, in the No-HS *Tg(hsp70:p210BCR/ABL1)* adult fish.

Figure S4). After incubation with these TKI for 48 h, we calculated the numbers of *lcp1*⁺ myeloid cells in WT and *Tg(hsp70:p210^{BCR/ABL1})* larvae in the posterior blood island (PBI) region at 5 dpf (Figure 6A and B). All the TKI significantly reduced the number of *lcp1*⁺ myeloid cells in *Tg(hsp70:p210^{BCR/ABL1})* larvae compared with the DMSO control group. In addition, lower concentrations (20 and 40 μmol/L) of imatinib significantly reduced the expanded *lcp1*⁺ myeloid population in *Tg(hsp70:p210^{BCR/ABL1})* larvae, but the number of *lcp1*⁺ myeloid cells was also significantly reduced in WT larvae at higher concentrations (80 μmol/L) compared with DMSO (*Online Supplementary Figure S5*). These results suggest that high doses of imatinib may affect normal myelopoiesis, which may be associated with more adverse events or unpredictable off-target effects. Further studies are needed to clarify these effects and to support the clinical treatment of patients with CML.

We screened a library of 171 compounds in 3 dpf WT and *Tg(hsp70:p210^{BCR/ABL1})* embryos to examine their ability to reverse the disease phenotype. We reduced the incubation time to 24 h to speed up the screening process, and then calculated the numbers of *lcp1*⁺ myeloid cells in WT and *Tg(hsp70:p210^{BCR/ABL1})* larvae in the PBI region at 4 dpf. Ten inhibitors, including the natural compound, icaritin, as well as CC-223, BEZ235, AZD3759, icotinib, DB07268, NQDI-1, selonsertib (GS-4997), LY364947 and ciliobrevin A (HPI-4) effectively reduced the expanded *lcp1*⁺ myeloid population in *Tg(hsp70:p210^{BCR/ABL1})* embryos compared with DMSO-treated controls (Figure 6C).

Discussion

We constructed a new germline of transgenic zebrafish expressing the hBCR/ABL1 fusion protein. Expression of hBCR/ABL1 in *Tg(hsp70:p210^{BCR/ABL1})* transgenic zebrafish altered hematopoiesis by up-regulating myeloid genes, as detected in larvae at 3 dpf. Adult *Tg(hsp70:p210^{BCR/ABL1})* transgenic zebrafish developed CML characterized by clonal myelocytic blasts, representing the first zebrafish model of hBCR/ABL1-induced CML. As the disease progressed, hematopoietic differentiation was interrupted, and immature blasts and myeloid precursors accumulated in the BM and spilled into the circulation in this zebrafish model, closely resembling the natural course of human CML progression without treatment. The most accurate CML animal model to date is the SCLtTA/BCR-ABL mouse line[21] established by Koschmieder *et al*. in 2005. However, these mice only survive for 4-17 weeks, while adult *Tg(hsp70:p210^{BCR/ABL1})* transgenic zebrafish could survive for from 12 to >18 months, with or without heat shock, which was longer than all previous mouse models. The incidence of CML in the *Tg(hsp70:p210^{BCR/ABL1})* transgenic model was increased by hBCR/ABL1 heat shock. This *Tg(hsp70:p210^{BCR/ABL1})* transgenic model may thus provide insights into the mechanism that drives the transition from CML-CP to CML-AP or CML-BP.

Tyrosine kinase inhibitors (imatinib, dasatinib, and bosutinib) effectively reduced the expanded myeloid population in *Tg(hsp70:p210^{BCR/ABL1})* embryos, suggesting that the pharmacological pathways in this model were similar to those in human CML. The discovery of imatinib has greatly improved the longevity and quality of life of patients with CML; however, some patients develop resistance to TKI and may even progress toward CML-AP or CML-BP of the disease despite TKI therapy. Second- and third-generation TKI were developed to treat patients in whom imatinib fails, with up to 40-87% of patients achieving durable complete cytogenetic remission.[4] However, more serious side-effects have recently been associated with these second- and third-generation TKI. Understanding the underlying cause of resistance and screening for novel targeted drugs with low toxicity and high efficiency thus remain important steps in combating CML. Further studies are planned to generate site-directed mutations of the ABL1 kinase domain in *Tg(hsp70:p210^{BCR/ABL1})* transgenic zebrafish using gene-editing technology (such as CRISPR/Cas9). The ABL1 kinase domain is frequently mutated in clinical cases, and examination of these mutants may thus help to elucidate the mechanism responsible for TKI resistance.

In the present study, we screened a compound library and discovered 10 new targeted drugs that reduced the

Table 2. Hemogram and classification of *Tg(hsp70:p210^{BCR/ABL1})* fish in chronic myeloid leukemia chronic phase.

Classification	Group	Number	Percentages in PB (%)				Percentages in KM (%)				Location	Leukemia cell types
			Blasts	Myeloid precursors	Myelocytes	Lymphocytes	Blasts	Myeloid precursors	Myelocytes	Lymphocytes		
Normal		55	0.06 ± 0.04	1.68 ± 0.39	8.09 ± 1.45	90.17 ± 1.55	4.41 ± 0.56	12.56 ± 0.76	46.89 ± 1.29	36.14 ± 1.21		
CML-CP 1	I	27	0.00 ± 0.00	1.29 ± 0.42	4.09 ± 1.16	94.62 ± 1.36	1.42 ± 0.42	8.15 ± 0.49	58.75 ± 0.90*	31.68 ± 1.04	KM	Neutrophils in various degrees of maturation
	II	4	0.15 ± 0.15	3.27 ± 1.53	20.11 ± 7.08*	76.46 ± 8.51	2.57 ± 0.93	10.68 ± 2.16	43.93 ± 3.51	42.82 ± 3.86	PB	
	III	19	0.38 ± 0.22	3.48 ± 1.52	17.79 ± 2.38*	78.36 ± 2.63	2.79 ± 0.83	12.82 ± 2.38	52.06 ± 2.34*	32.32 ± 1.59	KM and PB	
CML-CP 2	IV	15	0.78 ± 0.31	3.40 ± 0.86	3.03 ± 0.67	92.79 ± 1.26	8.35 ± 1.24‡	19.07 ± 1.47†	37.61 ± 2.36	34.98 ± 2.17	KM	Myeloid precursors
	V	3	2.45 ± 1.31‡	12.22 ± 3.83†	8.26 ± 5.07	77.07 ± 7.69	0.71 ± 0.57	11.47 ± 4.02	39.07 ± 3.72	48.75 ± 8.09	PB	

White blood cell counts were obtained by identifying at least 500 cells per kidney marrow (KM) preparation and at least 1,500 cells per peripheral blood (PB) preparation. The percentages were indicated by mean±Standard Error of Mean. Chronic myeloid leukemia-chronic phase (CML-CP) 1: blasts <2%, myeloid precursors <10% in PB or blasts <5%, myeloid precursors <15% in KM. CML-CP 2: blasts >2%, myeloid precursors >10% in PB or blasts >5%, myeloid precursors >15% in KM. CML-CP 1-Group I: myelocytes increased in KM. CML-CP 1-Group II: myelocytes and myeloid precursors increased in PB. CML-CP 1-Group III: myelocytes increased in both PB and KM, myeloid precursors increased in PB. CML-CP 2-Group IV: myeloid precursors and blasts increased in KM. CML-CP 2-Group V: myeloid precursors and blasts increased in PB. *Indicates myelocytes in PB or KM increased by >15% or 50%. †Indicates myeloid precursors in PB or KM by >10% or >15%. ‡Indicates blasts in PB or KM increased by >2% or >5%.
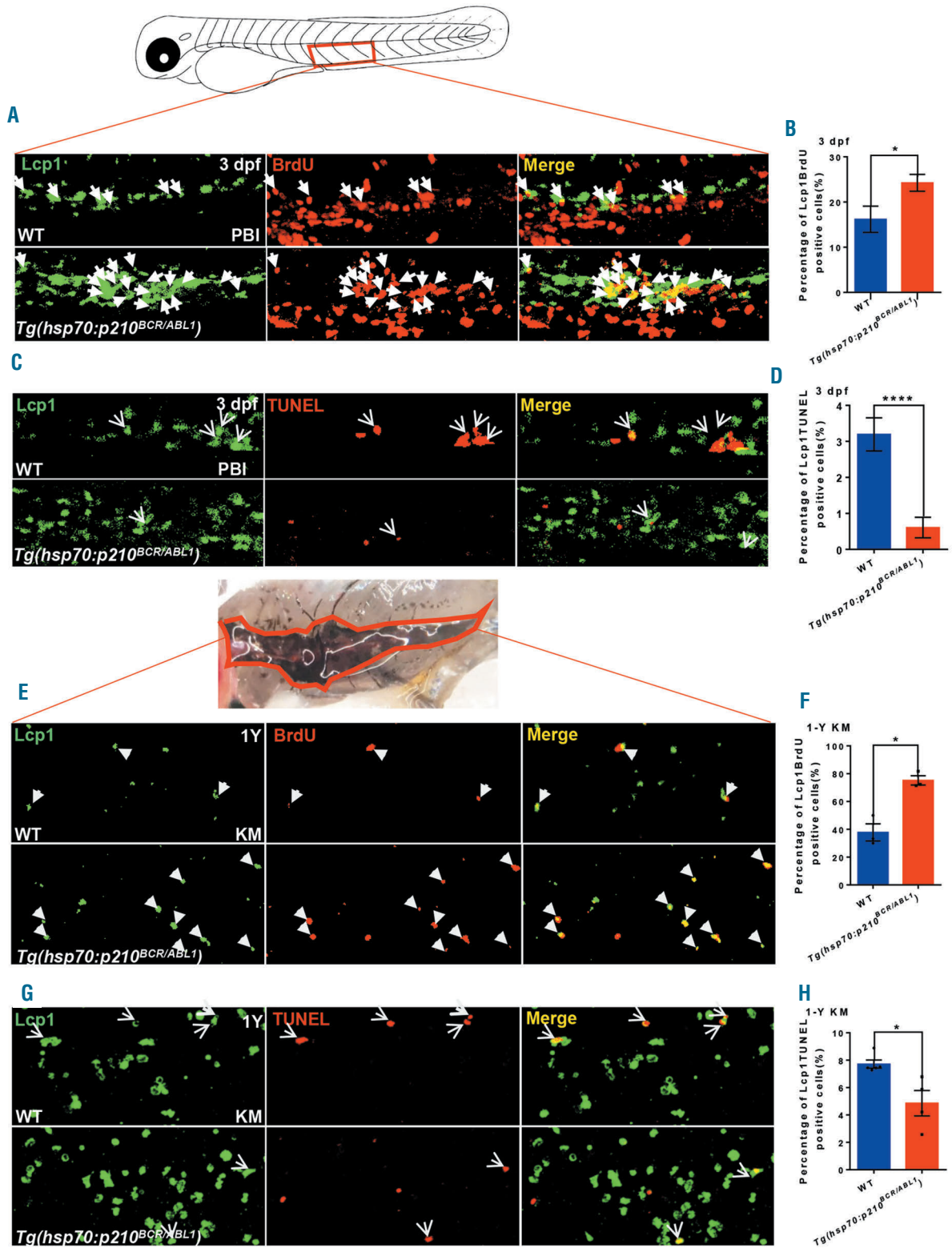
Figure 4. The abnormal myeloid cell expansion in *Tg(hsp70:p210^BCR/ABL1)* fish caused by proliferation and apoptosis perturbation. Lcp1 and BrdU antibody immunofluorescence double staining indicates a significant increase in the myeloid cells proliferation in the PBI region of 3 dpf HS *Tg(hsp70:p210^BCR/ABL1)* larvae (n=28) compared with the wild-type (WT) controls (n=18) (A and B) and kidney marrow (KM) Lcp1⁺ cells in 1-year *Tg(hsp70:p210^BCR/ABL1)* adults (n=3) compared with the WT controls (n=3) (E and F). Lcp1 antibody and transferase dUTP nick end labeling (TUNEL) assay co-staining were used to detect the apoptosis. The number of Lcp1⁺ cells in the PBI region (C and D)/KM (G and H) in 3 dpf/1-year HS *Tg(hsp70:p210^BCR/ABL1)* (n=27/n=4) significantly decreased compared with WT (n=19/n=5). Arrows indicate Lcp1BrdU/Lcp1TUNEL double-positive cells. Original magnification x100 (A, C, E, G). Percentage of the PBI region and KM localized Lcp1⁺ myeloid cells that incorporate BrdU/TUNEL in Lcp1+ myeloid cells in 3 dpf or 1-year HS WT and *Tg(hsp70:p210^BCR/ABL1)* fish. Student *t*-test; mean±Standard Error of Mean; *P<0.05; ****P<0.0001.
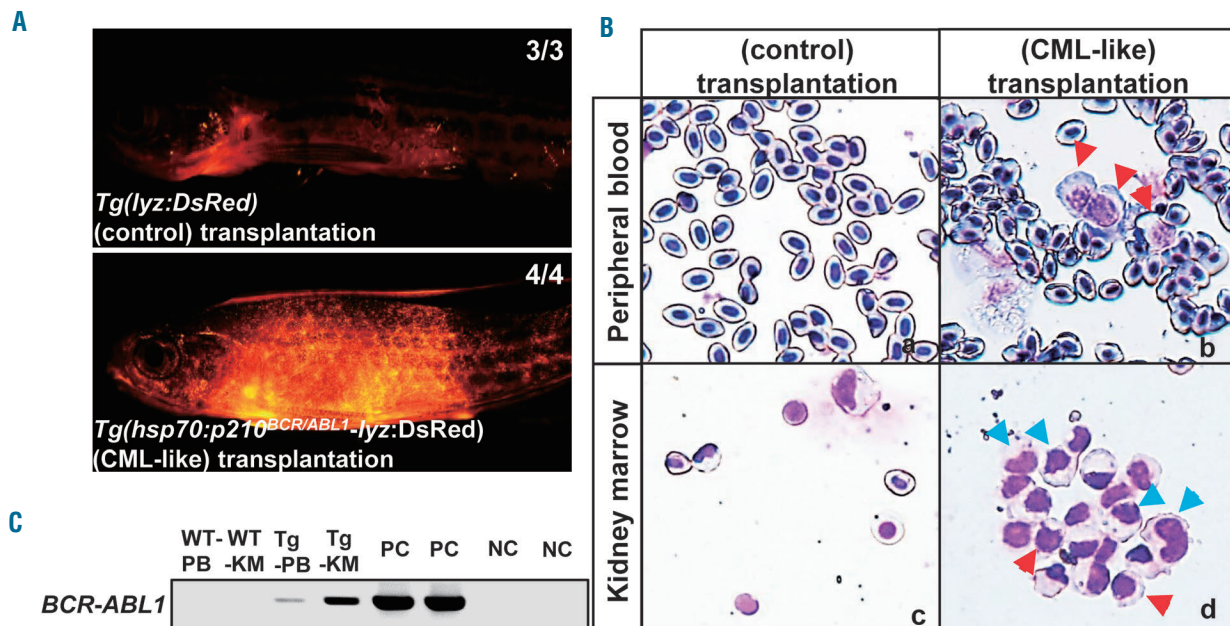
Figure 5. Wild-type (WT) fish transplanted with chronic myeloid leukemia (CML)-like leukemic cells show myeloid expansion in the early stage. Of 43 and 65 recipients transplanted with *Tg(lyz:DsRed)* control and CML-like *Tg(hsp70:p210^BCR/ABL1^-lyz:DsRed)* kidney marrow (KM) cells, three and four survived, respectively. (A) DsRed positive cells repopulated in recipients within 2-3 weeks after transplantation of *Tg(lyz:DsRed)* control (left) and CML-like *Tg(hsp70:p210^BCR/ABL1^-lyz:DsRed)* (right) KM blood cells. (B) All survived recipients were stained by May-Grunwald-Giemsa. Myelocytes (d, blue arrows) increased in KM of WT fish after transplanted with CML-like *Tg(hsp70:p210^BCR/ABL1^-lyz:DsRed)* KM cells. Myeloid precursors (b and d, red arrows) increased in both peripheral blood (PB) and KM of WT fish after being transplanted with CML-like *Tg(hsp70:p210^BCR/ABL1^-lyz:DsRed)* KM blood cells. Original magnification x400. (C) h*BCR/ABL1^+^* cDNA fragments detected in PB and KM cells of WT fish after being transplanted with *Tg(lyz:DsRed)* control (WT-PB/WT-KM) and CML-like *Tg(hsp70:p210^BCR/ABL1^-lyz:DsRed)* KM cells (Tg-PB/Tg-KM) assessed by polymerase chain reaction. PC: pToL *hsp70:p210^BCR/ABL1^* as the positive control. NC: ddH$_2$O as the negative control.

expanded myeloid population in *Tg(hsp70:p210^BCR/ABL1^)* transgenic zebrafish embryos. Icaritin is a natural flavonoid derived from the traditional Chinese medicine Epimedium. Icaritin was previously shown to inhibit the growth of leukemic cell lines, including imatinib-resistant *BCR/ABL1^+^* blast cells and BCR/ABL1-T315I mutant cells *via* mechanisms involved in MAPK and JAK/STAT signaling.[27-29] The current results show that icaritin could reduce the expanded *lcp1^+^* myeloid population in *Tg(hsp70:p210^BCR/ABL1^)* embryos, consistent with these previous findings. Overactivation of PI3K/AKT/mTOR is known to play a pivotal role in many human cancers, thus providing strong support for the therapeutic anticancer application of PI3K/Akt/mTOR inhibitors.[30,31] Sadovnik *et al.* found that escape of CML LSC was disrupted by the addition of PI3K/mTOR blockers.[32] Furthermore, the PI3K/mTOR dual inhibitor BEZ235 had beneficial effects on a variety of tumors *in vivo* and *in vitro*, including lymphoid malignancies[33] and myeloid malignancies.[34,35] Bendell also identified the active-site inhibitor CC-223, which targets both mTORC1 and mTORC2 through mTOR kinase activity to inhibit activation of AKT and 4EBP1, as a promising therapeutic agent with activity against many non-Hodgkin lymphoma and solid tumor cell lines.[36] In the current study, the *Tg(hsp70:p210^BCR/ABL1^)* embryonic zebrafish model responded well to both BEZ235 and CC-223. Overall, these results suggest that targeting the PI3K/Akt/mTOR signaling pathway may be an effective strategy for overcoming CML therapy resistance. Unexpectedly, however,

Tg(hsp70:p210^BCR/ABL1^) larvae did not respond well to the sphingosine 1-phosphate antagonist, FTY720, and the number of *lcp1^+^* myeloid cells in WT zebrafish conversely increased after treatment with FTY720. Previous studies reported that the FTY720-mediated PP2A reactivation could markedly reduce the survival and self-renewal of CML-quiescent HSC through BCR-ABL1 kinase-independent and PP2A-mediated inhibition of JAK2 and β-catenin.[37] We therefore hypothesized that, although sphingosine 1-phosphate may play a role in hematopoietic regulation, further studies are needed to determine its precise mechanism. LY364947,[38,39] ciliobrevin A,[40] DB07268,[41] selonsertib,[42] NQDI-1,[43] AZD3759,[44] and icotinib[45] have recently been shown to target key factors and signaling pathways essential for the survival of CML LSC and other CSC, including transforming growth factor β,[39] Hedgehog,[46] c-Jun N-terminal kinases,[47] apoptosis signal-regulating kinase 1,[48] and epidermal growth factor receptor.[49] The *Tg(hsp70:p210^BCR/ABL1^)* transgenic zebrafish embryos in the current study also responded well to these compounds. Our findings, therefore, suggest that inhibition of BCR/ABL1 kinase-dependent or kinase-independent pathways (Figure 6D) might offer potential for overcoming resistance to TKI and thus eradicate LSC, thereby paving the way for the development of novel, more effective LSC-eradicating treatment strategies for CML.

In conclusion, the *Tg(hsp70:p210^BCR/ABL1^)* transgenic model represents a phenotype-based, cost-effective, *in vivo* model of CML suitable for high-throughput chemical screening. This model may improve our understanding of
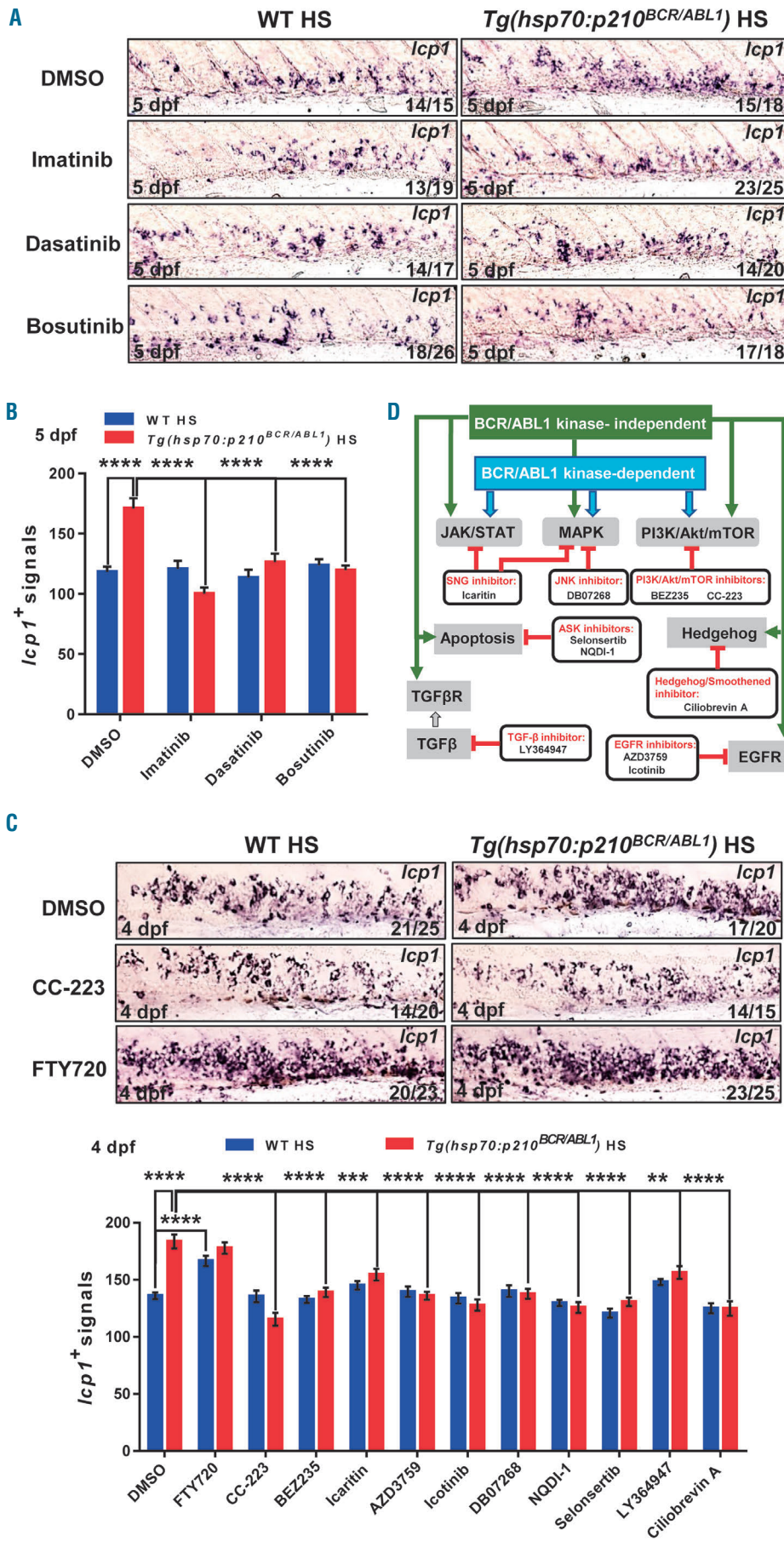
Figure 6. *Tg(hsp70:p210^BCR/ABL1^)* transgenic zebrafish model responds to chemotherapy. (A and B) TKI treatment in zebrafish larvae. 3 dpf HS WT (left panels) and *Tg(hsp70:p210^BCR/ABL1^)* (right panels) larvae treated for 48 hours with 1‰ DMSO control, 20 μmol/L imatinib, 5 μmol/L dasatinib and 10 μmol/L bosutinib. (A) WISH of *lcp1* expression in the drug treated larvae at 5 dpf. n/n, number of zebrafish larvae showing representative phenotype/total number of zebrafish larvae examined. Original magnification, x200. (Bottom): statistical analysis. Enumeration of *lcp1⁺* signals shown in (A). Average numbers of *lcp1⁺* cells per larva with drug treatment. ANOVA; mean ± SEM; ****P<0.0001. (C) Drug screening. Upper: WISH of *lcp1* expression in *Tg(hsp70:p210^BCR/ABL1^)* (right) larvae and WT controls (left) at 4 dpf after treatment (1‰ DMSO, 20 μmol/L CC-223, 2.5 μmol/L FTY720) for 24 hours. n/n, number of zebrafish larvae showing representative phenotype/total number of zebrafish larvae examined. Original magnification, x200. Under: Statistical analysis. 3 dpf HS WT and *Tg(hsp70:p210^BCR/ABL1^)* larvae (n=25 and n=20, n=23 and n=25, n=20 and n=15, n=22 and n=24, n=20 and n=21, n=14 and n=24, n=19 and n=19, n=20 and n=19, n=19 and n=18, n=23 and n=24, n=23 and n=17, n=16 and n=15, respectively) were treated for 24 hours with drugs (1‰ DMSO, 2.5 μmol/L FTY720, 20 μmol/L CC-223, 0.5 μmol/L BEZ235, 40 μmol/L icaritin, 20 μmol/L AZD3759, 80 μmol/L icotinib, 40 μmol/L DB07268, 80 μmol/L NQDI-1, 40 μmol/L selonsertib, 20 μmol/L LY364947, 1 μmol/L ciliobrevin A, respectively). Average numbers of *lcp1⁺* cells per larva with drug treatment. ANOVA; mean ± SEM; **P<0.01; ***P<0.001; ****P<0.0001. (D) Sketch map of inhibitors target BCR/ABL1 kinase-dependent or kinase-independent pathways. JNK: the c-Jun N-terminal kinase. ASK: apoptosis signal-regulating kinase. TGF-β, the transforming growth factor β. EGFR: the epidermal growth factor receptor.

the protein functions, pharmacological mechanisms, and toxicology of novel targeted drugs, thus improving the cure rate for patients with CML.

References

1. von Bubnoff N, Pleyer L, Neureiter D, Faber V, Duyster J. Chronic myelogenous leukemia (CML). In: Greil R, Pleyer L, Faber V, Neureiter D, eds. Chronic Myeloid Neoplasias and Clonal Overlap Syndromes: Epidemiology, Pathophysiology and Treatment Options. Vienna: Springer Vienna, 2010:117-152.

2. Champlin RE, Golde DW. Chronic myelogenous leukemia: recent advances. Blood. 1985;65(5):1039-1047.

3. Cotta CV, Bueso-Ramos CE. New insights into the pathobiology and treatment of chronic myelogenous leukemia. Ann Diag Pathol. 2007;11(1):68-78.

4. Apperley JF. Chronic myeloid leukaemia. Lancet. 2015;385(9976):1447-1459.

5. Rowley JD. Letter: A new consistent chromosomal abnormality in chronic myelogenous leukaemia identified by quinacrine fluorescence and Giemsa staining. Nature. 1973;243(5405):290-293.

6. Melo JV. The diversity of BCR-ABL fusion proteins and their relationship to leukemia phenotype. Blood. 1996;88(7):2375-2384.

7. Shtivelman E, Lifshitz B, Gale RP, Roe BA, Canaani E. Alternative splicing of RNAs transcribed from the human abl gene and from the bcr-abl fused gene. Cell. 1986; 47(2):277-284.

8. Ben-Neriah Y, Daley GQ, Mes-Masson AM, Witte ON, Baltimore D. The chronic myelogenous leukemia-specific P210 protein is the product of the bcr/abl hybrid gene. Science. 1986;233(4760):212-214.

9. Ren R. Mechanisms of BCR-ABL in the pathogenesis of chronic myelogenous leukaemia. Nat Rev Cancer. 2005;5(3):172-183.

10. An X, Tiwari AK, Sun Y, Ding P-R, Ashby CR, Jr., Chen Z-S. BCR-ABL tyrosine kinase inhibitors in the treatment of Philadelphia chromosome positive chronic myeloid leukemia: A review. Leuk Res. 2010;34(10):1255-1268.

11. Ross TS, Mgbemena VE. Re-evaluating the role of BCR/ABL in chronic myelogenous leukemia. Mol Cell Oncol. 2014;1(3): e963450-e963450.

12. MacRae CA, Peterson RT. Zebrafish as tools for drug discovery. Nat Rev Drug Discov. 2015;14(10):721-731.

13. Westerfield M. The Zebrafish Book. A Guide for the Laboratory Use of Zebrafish (Danio rerio). University of Oregon Press, Eugene., 2000.

14. Kimmel CB, Ballard WW, Kimmel SR, Ullmann B, Schilling TF. Stages of embryonic development of the zebrafish. Dev Dyn. 1995;203(3):253-310.

15. Hall C, Flores MV, Storm T, Crosier K, Crosier P. The zebrafish lysozyme C promoter drives myeloid-specific expression in transgenic fish. Bmc Dev Biol. 2007;7:42.

16. He YP, Wertheim JA, Xu LW, et al. The coiled-coil domain and Tyr177 of bcr are required to induce a murine chronic myelogenous leukemia-like disease by bcr/abl. Blood. 2002;99(8):2957-2968.

17. Jin H, Sood R, Xu J, et al. Definitive hematopoietic stem/progenitor cells manifest distinct differentiation output in the zebrafish VDA and PBI. Development. 2009;136(4):647-654.

18. Adam A, Bartfai R, Lele Z, Krone PH, Orban L. Heat-inducible expression of a reporter gene detected by transient assay in zebrafish. Exp Cell Res. 2000;256(1):282-290.

19. Halloran MC, Sato-Maeda M, Warren JT, et al. Laser-induced gene expression in specific cells of transgenic zebrafish. Development. 2000;127(9):1953-1960.

20. Roumiantsev S, de Aos IE, Varticovski L, Ilaria RL, Van Etten RA. The Src homology 2 domain of Bcr/Abl is required for efficient induction of chronic myeloid leukemia-like disease in mice but not for lymphoid leukemogenesis or activation of phosphatidylinositol 3-kinase. Blood. 2001;97(1):4-13.

21. Koschmieder S, Gottgens B, Zhang P, et al. Inducible chronic phase of myeloid leukemia with expansion of hematopoietic stem cells in a transgenic model of BCR-ABL leukemogenesis. Blood. 2005; 105(1):324-334.

22. Honda H, Oda H, Suzuki T, et al. Development of acute lymphoblastic leukemia and myeloproliferative disorder in transgenic mice expressing p210(bcr/abl): A novel transgenic model for human Ph-1-positive leukemias. Blood. 1998;91(6):2067-2075.

23. Huettner CS, Koschmieder S, Iwasaki H, et al. Inducible expression of BCR/ABL using human CD34 regulatory elements results in a megakaryocytic myeloproliferative syndrome. Blood. 2003;102(9):3363-3370.

24. Sabattini E, Bacci F, Sagramoso C, Pileri SA. WHO classification of tumours of haematopoietic and lymphoid tissues in 2008: an overview. Pathologica. 2010;102(3):83-87.

25. Dowding C, Th'ng KH, Goldman JM, Galton DA. Increased T-lymphocyte numbers in chronic granulocytic leukemia before treatment. Exp Hematol. 1984;12(10):811-815.

26. Mason JE Jr, DeVita VT, Canellos GP. Thrombocytosis in chronic granulocytic leukemia: incidence and clinical significance. Blood. 1974;44(4):483-487.

27. Zhu JF, Li ZJ, sen Zhang G, et al. Icaritin Shows Potent Anti-Leukemia Activity on Chronic Myeloid Leukemia In Vitro and In Vivo by Regulating MAPK/ERK/JNK and JAK2/STAT3/AKT Signalings. Plos One. 2011;6(8): e23720.

28. Zhu S, Wang Z, Li Z, et al. Icaritin suppresses multiple myeloma, by inhibiting IL-6/JAK2/STAT3. Oncotarget. 2015;6(12):10460-10472.

29. Chen M, Turhan AG, Ding H, Lin Q, Meng K, Jiang X. Targeting BCR-ABL(+) stem/progenitor cells and BCR-ABL-T315I mutant cells by effective inhibition of the BCR-ABL-Tyr177-GRB2 complex. Oncotarget. 2017;8(27):43662-43677.

30. Xia P, Xu X-Y. PI3K/Akt/mTOR signaling pathway in cancer stem cells: from basic research to clinical application. Am J Cancer Res. 2015;5(5):1602-1609.

31. Polivka J Jr, Janku F. Molecular targets for cancer therapy in the PI3K/AKT/mTOR pathway. Pharmacol Ther. 2014;142(2):164-175.

32. Sadovnik I, Hoelbl-Kovacic A, Herrmann H, et al. Identification of CD25 as STAT5-Dependent Growth Regulator of Leukemic Stem Cells in Ph+ CML. Clin Cancer Res. 2016;22(8):2051-2061.

33. Wong J, Welschinger R, Hewson J, Bradstock KF, Bendall LJ. Efficacy of dual PI-3K and mTOR inhibitors in Vitro and in Vivo in acute lymphoblastic leukemia. Oncotarget. 2014;5(21):10460-10472.

34. Deng L, Jiang L, Lin X-H, et al. The PI3K/mTOR dual inhibitor BEZ235 suppresses proliferation and migration and reverses multidrug resistance in acute myeloid leukemia. Acta Pharmacol Sin. 2017;38(3):382-391.

35. Xin P, Li C, Zheng Y, et al. Efficacy of the dual PI3K and mTOR inhibitor NVP-BEZ235 in combination with imatinib mesylate against chronic myelogenous leukemia cell lines. Drug Des Deve Ther. 2017;11:1115-1126.

36. Bendell JC, Kelley RK, Shih KC, et al. A Phase I dose-escalation study to assess safety, tolerability, pharmacokinetics, and preliminary efficacy of the dual mTORC1/mTORC2 kinase inhibitor CC-223 in patients with advanced solid tumors or multiple myeloma. Cancer. 2015; 121(19):3481-3490.

37. Neviani P, Harb JG, Oaks JJ, et al. PP2A-activating drugs selectively eradicate TKI-resistant chronic myeloid leukemic stem cells. J Clin Invest. 2013;123(10):4144-4157.

38. Pellicano F, Holyoake TL. Assembling defenses against therapy-resistant leukemic stem cells: Bcl6 joins the ranks. J Exp Med. 2011;208(11):2155-2158.

39. Naka K, Hoshii T, Muraguchi T, et al. TGF-beta-FOXO signalling maintains leukaemia-initiating cells in chronic myeloid leukaemia. Nature. 2010; 463(7281):676-680.

40. Xiang W, Jiang T, Guo F, et al. Hedgehog pathway inhibitor-4 suppresses malignant properties of chondrosarcoma cells by disturbing tumor ciliogenesis. Oncol Rep. 2014;32(4):1622-1630.

41. Liu M, Wang S, Clampit JE, et al. Discovery of a new class of 4-anilinopyrimidines as potent c-Jun N-terminal kinase inhibitors: Synthesis and SAR studies. Bioorg Med Chem Lett. 2007;17(3):668-672.

42. Lin JH, Zhang JJ, Lin S-L, Chertow GM. Design of a Phase 2 Clinical trial of an ASK1 inhibitor, GS-4997, in patients with diabetic kidney disease. Nephron. 2015; 129(1):29-33.

43. Volynets GP, Chekanov MO, Synyugin AR, et al. Identification of 3H-Naphtho 1,2,3-de quinoline-2,7-diones as inhibitors of apoptosis signal-regulating kinase 1 (ASK1). J Med Chem. 2011;54(8):2680-2686.

44. Zeng Q, Wang J, Cheng Z, et al. Discovery and evaluation of clinical candidate AZD3759, a potent, oral active, central nervous system-penetrant, epidermal growth factor receptor tyrosine kinase Inhibitor. J Med Chem. 2015;58(20):8200-8215.

45. Tan F, Shen X, Wang D, et al. Icotinib (BPI-2009H), a novel EGFR tyrosine kinase inhibitor, displays potent efficacy in preclinical studies. Lung Cancer. 2012; 76(2):177-182.

46. Hyman JM, Firestone AJ, Heine VM, et al. Small-molecule inhibitors reveal multiple strategies for Hedgehog pathway blockade. Proc Natl Acad Sci U S A. 2009; 106(33): 14132-14137.

47. Redig AJ, Vakana E, Platanias LC. Regulation of mammalian target of rapamycin and mitogen activated protein kinase pathways by BCR-ABL. Leuk Lymphoma. 2011;52 suppl 1:45-53.

48. Bellazzo A, Di Minin G, Collavin L. Block one, unleash a hundred. Mechanisms of DAB2IP inactivation in cancer. Cell Death Differ. 2017;24(1):15-25.

49. Corrado C, Saieva L, Raimondo S, Santoro A, De Leo G, Alessandro R. Chronic myelogenous leukaemia exosomes modulate bone marrow microenvironment through activation of epidermal growth factor receptor. J Cell Mol Med. 2016;20(10): 1829-1839.

The novel Isatin analog KS99 targets stemness markers in acute myeloid leukemia

Charyguly Annageldiyev,[1,2] Krishne Gowda,[2,3] Trupti Patel,[4]
Priyanjali Bhattacharya,[4] Su-Fern Tan,[5] Soumya Iyer,[6] Dhimant Desai,[2,3]
Sinisa Dovat,[6] David J. Feith,[5,7] Thomas P. Loughran Jr.,[5,7] Shantu Amin,[2,3] David
Claxton[1,2] and Arati Sharma[1,2,3]

[1]Department of Medicine, Division of Hematology and Oncology, Pennsylvania State
University College of Medicine, Hershey, PA, USA; [2]Penn State Hershey Cancer Institute,
Pennsylvania State University College of Medicine, Hershey, PA, USA; [3]Department of
Pharmacology, Pennsylvania State University College of Medicine, Hershey, PA, USA;
[4]Department of Integrative Biotechnology, SBST, VIT Vellore, Tamilnadu, India;
[5]Department of Medicine, Division of Hematology and Oncology, University of Virginia
School of Medicine, Charlottesville, VA, USA; [6]Department of Pediatrics, Pennsylvania
State University College of Medicine, Hershey, PA, USA and [7]University of Virginia Cancer
Center, Charlottesville, VA, USA

ABSTRACT

Leukemic stem cells are multipotent, self-renewing, highly proliferative cells that can withstand drug treatments. Although currently available treatments potentially destroy blast cells, they fail to eradicate leukemic progenitor cells completely. Aldehyde dehydrogenase and STAT3 are frequently up-regulated in pre-leukemic stem cells as well as in acute myeloid leukemia (AML) expressing the $CD34^+CD38^-$ phenotype. The Isatin analog, KS99 has shown anticancer activity against multiple myeloma which may, in part, be mediated by inhibition of Bruton's tyrosine kinase activation. Here we demonstrate that KS99 selectively targets leukemic stem cells with high aldehyde dehydrogenase activity and inhibits phosphorylation of STAT3. KS99 targeted cells co-expressing CD34, CD38, CD123, TIM-3, or CD96 immunophenotypes in AML, alone or in combination with the standard therapeutic agent cytarabine. AML with myelodysplastic-related changes was more sensitive than *de novo* AML with or without *NPM1* mutation. KS99 treatment reduced the clonogenicity of primary human AML cells as compared to normal cord blood mononuclear cells. Downregulation of phosphorylated Bruton's tyrosine kinase, STAT3, and aldehyde dehydrogenase was observed, suggesting interaction with KS99 as predicted through docking. KS99 with or without cytarabine showed *in vivo* preclinical efficacy in human and mouse AML animal models and prolonged survival. KS99 was well tolerated with overall negligible adverse effects. In conclusion, KS99 inhibits aldehyde dehydrogenase and STAT3 activities and causes cell death of leukemic stem cells, but not normal hematopoietic stem and progenitor cells.

Introduction

Acute myeloid leukemia (AML) is a heterogeneous disease with treatment relying primarily on traditional cytotoxic agents and hematopoietic stem cell transplantation. AML arises from hematopoietic stem and progenitor cells (HSPC) through various alterations in stem cells.[1] During blast transformation, mutant progenitors undergo stepwise genetic, epigenetic and clonal changes, and give rise to pre-leukemia stem cells (pre-LSC) as well as fully transformed leukemia stem cells (LSC).[2] These cells are frequently chemo-resistant, and their division leads to clonally aggressive AML.[1] Thus, effective therapies are warranted to destroy AML stem cells selectively, but not normal HSPC. While LSC were initially defined as cells with $CD34^+CD38^-$ phenotype with ability to engraft in mouse models,[2-5] recent data have demonstrated $CD34^+CD38^+$ AML cells also have an engraftment poten-

tial in animal models.[4,6-8] After relapse, numbers of LSC increase dramatically and CD34⁻ cells often acquire engraftment potential.[6,9]

Inclusion of additional AML-specific LSC surface antigens, including CD123, CD96 and TIM-3, can help identify and target resistant leukemic cells.[10-13] It has been suggested that the self-renewal capacity of otherwise quiescent AML-LSC is supported by upregulation of the surface marker T-cell immunoglobulin mucin-3 (TIM-3). TIM-3 is not expressed in normal HSC, suggesting that the TIM-3⁺ population may contain the great majority of functional LSC in most types of AML.[14] These markers play a role in activating the inactive LSC for the purpose of self-renewal and disease maintenance, thus facilitating relapse with minimal to moderate survival benefit.[12-16]

Stem cells protect themselves by upregulation of aldehyde dehydrogenase (ALDH), a cytosolic enzyme that guards them against the DNA damage induced by reactive oxygen species and reactive aldehydes.[17] A population of CD34⁺CD38⁻ leukemic cells with moderate ALDH activity has been shown to contribute to relapse in AML.[18] Targeting intracellular markers including ALDH and signal transducer and activator of transcription 3 (STAT3) in LSC marked by additional surface markers like CD34, CD123, TIM-3 or CD96 may validate therapeutic targets more efficiently. Despite substantial advances in the understanding of LSC markers, so far, no agents have been made available in the clinic to selectively target these progenitors. Cytarabine (Ara-C) and anthracyclines (7+3) are the current standard induction and consolidation therapy for AML, but these regimes only provide moderate therapeutic benefit.[19] The recent approval of novel agents including venetoclax, gilteritinib, and midostaurin has advanced therapy.

In this study, we identify the unexplored anti-LSC activity of the recently published small molecule Isatin analog, KS99. Earlier studies had established KS99 as an anti-microtubule agent with a dual role as Bruton's tyrosine kinase (BTK) inhibitor in multiple myeloma (MM).[20] Since BTK has a role in the maturation and regulation of dendritic cells (DC) *via* interleukin 10 (IL-10) and Signal transducer and activator of transcription 3 (STAT3), blocking BTK carefully modulates the STAT3.[21] Modulation of STAT3 is important in prolonging survival of AML patients, especially considering that upstream mutations result in the activation of STAT3 and the protein per se is not mutated in this condition.[22] STAT3 activity in LSC is associated with a poor prognosis in AML patients, possibly because it contributes to resistance to chemotherapy.[22,23] ALDH has been identified as a potential biomarker and therapeutic target in chemoresistant AML.[24-26] Here, we report that, besides BTK inhibition, KS99 targets stemness markers, STAT3, and ALDH, in putative LSC expressing surface CD34, CD123, TIM-3, and CD96. We demonstrate that KS99 is active against AML as a single agent or in combination with standard of care Ara-C.

Methods

The *Online Supplementary Appendix* contains detailed information on experimental methods and materials.

Cell lines and cell culture

Details of the acute myeloid leukemia cell line culture conditions are provided in the *Online Supplementary Appendix*.

Acute myeloid leukemia patient and healthy donor cells

Bone marrow (BM) aspirates or peripheral blood (PB) samples were obtained from AML patients, and cord blood (CB) samples were obtained from the freshly delivered placenta of healthy donors after informed consent using protocols approved by the Penn State College of Medicine Institutional Review Board (IRB) (#2000-186). Mononuclear cells (MNC) were isolated by density gradient separation (Ficol-Paque, GE Healthcare Life Sciences, Pittsburgh, PA, USA) and frozen for later use. Details are provided in the *Online Supplementary Appendix*.

Cell viability and Annexin V assay

Cell viability and apoptosis were determined using MTS [3-(4,5-dimethylthiazol-2-yl)-5-(3-carboxymethoxyphenyl)-2-(4-sulfophenyl)-2H-tetrazolium, inner salt] assay (CellTiter 96 AQueous One Solution Cell Proliferation Assay, Promega, Madison, WI, USA) and Muse Annexin V & Dead Cell Kit (MCH100105, Millipore, Burlington, MA, USA). Details are provided in the *Online Supplementary Appendix*.

Colony-forming assay

Cryopreserved human AML patient samples and cord blood mononuclear cells were thawed and washed with RPMI 1640 (10% FBS) and used for the colony formation assay. Details are provided in the *Online Supplementary Appendix*.

Western blot analysis

Acute myeloid leukemia cells were treated with indicated concentrations of KS99 or DMSO. Cells were collected, washed with cold PBS, and whole cell lysates were harvested. Further details are provided in the *Online Supplementary Appendix*.

Flow cytometry

To detect apoptosis in LSC, DMSO, KS99 or Ara-C-treated cells were washed and stained with various markers; anti-human CD45 conjugated with APC-Cy7, CD34-FITC, CD38-APC, CD123-APC, TIM-3-PE-Cy7, or CD96-BV711 monoclonal antibodies for 30 minutes on ice, followed by Annexin V-BV421 and 7AAD staining. Further details are provided in the *Online Supplementary Appendix*.

Aldehyde dehydrogenase assay

The enzyme activity of ALDH was measured by using ALDE-FLUOR kit (StemCell Technologies, Vancouver, Canada), as described in the manufacturer's protocol. It is a fluorescent-based assay that detects ALDH1A1 isoform, which is highly expressed in stem cells. Further details are provided in the *Online Supplementary Appendix*.

Animal studies

Acute myeloid leukemia cell transplantable models luciferase-expressing human AML cell lines (U937 and MV4-11) and murine AML cell line (C1498) were used to investigate the efficacy of KS99. In addition, the pharmacokinetics of the drug were examined to determine the circulating levels of KS99 in the blood. Further details are provided in the *Online Supplementary Appendix*.

In silico docking of KS99 with ALDH1A1, BTK, and STAT3

Details are provided in the *Online Supplementary Appendix*.

Statistical analysis

The statistical analysis methodology is described in the *Online Supplementary Appendix*.
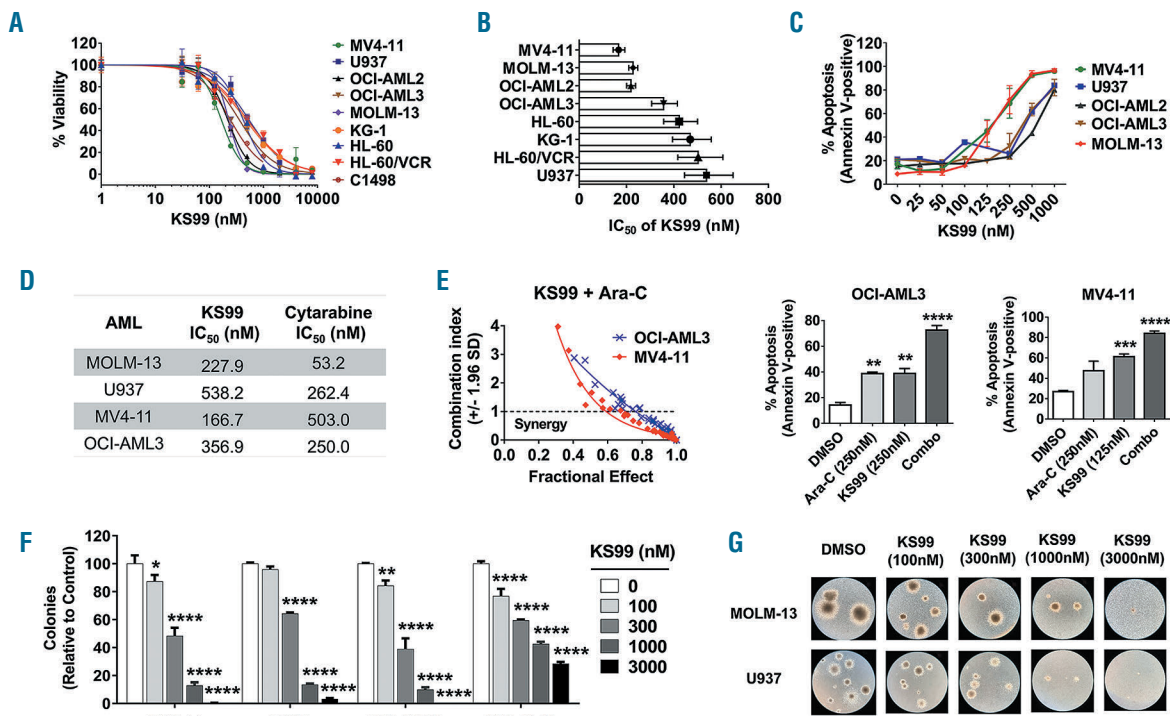
Figure 1. KS99 inhibits cell proliferation and clonogenicity and induces apoptosis in human acute myeloid leukemia (AML) cell lines. (A) Cell viability of AML cell lines after the treatment with KS99. (B) IC_{50} values for AML cell lines were plotted with 95% confidence intervals. (C) Induction of apoptosis with KS99 was determined as the percentage of Annexin V-positive cells. (D) The sensitivity of human AML cell lines to KS99 or Cytarabine (Ara-C) alone. (E) OCI-AML3 and MV4-11 cells were treated with increasing doses of KS99, Ara-C or combination. (E, left) Combination Index (CI) values of KS99 and Ara-C co-treatment were calculated by CalcuSyn. Synergy CI<0.9. (E, right) Apoptosis was determined as the percentage of Annexin V-positive cells. (F and G) KS99 reduced the colony-forming ability of AML cell lines. The representative colony microscopy images (4X) are shown as indicated. Data are the mean±standard error of the mean. *$P<0.05$; **$P<0.01$; ***$P<0.001$; ****$P<0.0001$; one-way ANOVA.

Results

KS99 induces apoptosis and reduces cell survival of human acute myeloid leukemia cell lines

To assess the effect of KS99 on AML cells *in vitro*, a panel of human leukemic cell lines [MOLM-13, MV4-11, OCI-AML2, OCI-AML3, HL-60, vincristine resistant HL-60 (HL-60/VCR), U937, and KG-1], and mouse leukemia C1498 cells were selected. Cell viability was measured after treatment with KS99 (10 nM-10 μM) for 48 hours (h). For most of the cell lines, KS99 treatment led to a decrease in the viability in the nanomolar (nM) range (Figure 1A). The half inhibitory concentration (IC_{50}) values for all the human cell lines were between 100 nM and 600 nM. Specifically, MV4-11, MOLM-13, and OCI-AML2 manifested higher sensitivity with lower IC_{50} values of 166 nM, 228 nM, and 218 nM, respectively. The other cell lines showed relatively higher IC_{50} values (300-600 nM) (Figure 1B). Similarly to human AML cells, mouse C1498 cells were sensitive to KS99 with an IC_{50} of 217 nM.

Furthermore, flow cytometry demonstrated apoptosis on selected cell lines. KS99 induced apoptosis within the nanomolar range (100-500 nM) in a dose-dependent manner (Figure 1C). MOLM-13 cells were chosen for time-dependent survival, and the outcome showed an early decrease in cell proliferation at 6-8 h with a prominent decline in viability post 24-48 h of treatment (*Online Supplementary Figure S1A*). Simultaneously, apoptosis was evident as early as 4 h of treatment with maximum effect at 48 h (*Online Supplementary Figure S1B*). These time points were considered when further functional assays were conducted. Chemotherapeutics are clinically often used in combination to achieve complete remission (CR) in AML patients. Hence, we decided to compare and combine KS99 to Ara-C to evaluate an increase in efficacy of Ara-C. The sensitivity of AML cell lines to KS99 and Ara-C is shown in Figure 1D. For the synergy studies, OCI-AML3 and MV4-11 cells were treated with Ara-C (0.062-4 μM) and KS99 (0.03125-2 μM) for 72 h, and the combination index (CI) was calculated. KS99 significantly increased cytotoxic responses, in combination with Ara-C, and showed synergy (CI<0.9) in both cell lines (Figure 1E, left panel). Furthermore, subtoxic KS99 concentrations (lower than IC_{50}) reduced IC_{50} of Ara-C by a median of 2-3-fold (*Online Supplementary Figure S1C*). Similarly, KS99 augmented the pro-apoptotic effect of Ara-C in OCI-AML3 and MV4-11 cells (Figure 1E, right panel). Next, the inhibitory effect of KS99 on colony forming ability of human AML cell lines was determined. The treatment of KS99 led to a decrease in the number and size of colonies across the selected range and cell lines (Figure 1F and G). These results show that KS99 is active in AML and can be combined with Ara-C to enhance anti-leukemic activity.

KS99 exerts a cytotoxic effect in primary human acute myeloid leukemia and favors cases with poor prognosis

The pro-apoptotic activity of KS99 was tested on newly diagnosed and untreated primary human AML patients (n=21). Cells were treated with increasing concentrations of KS99 (0.1-6 μM) for the 48 h. The IC_{50} values were cal-
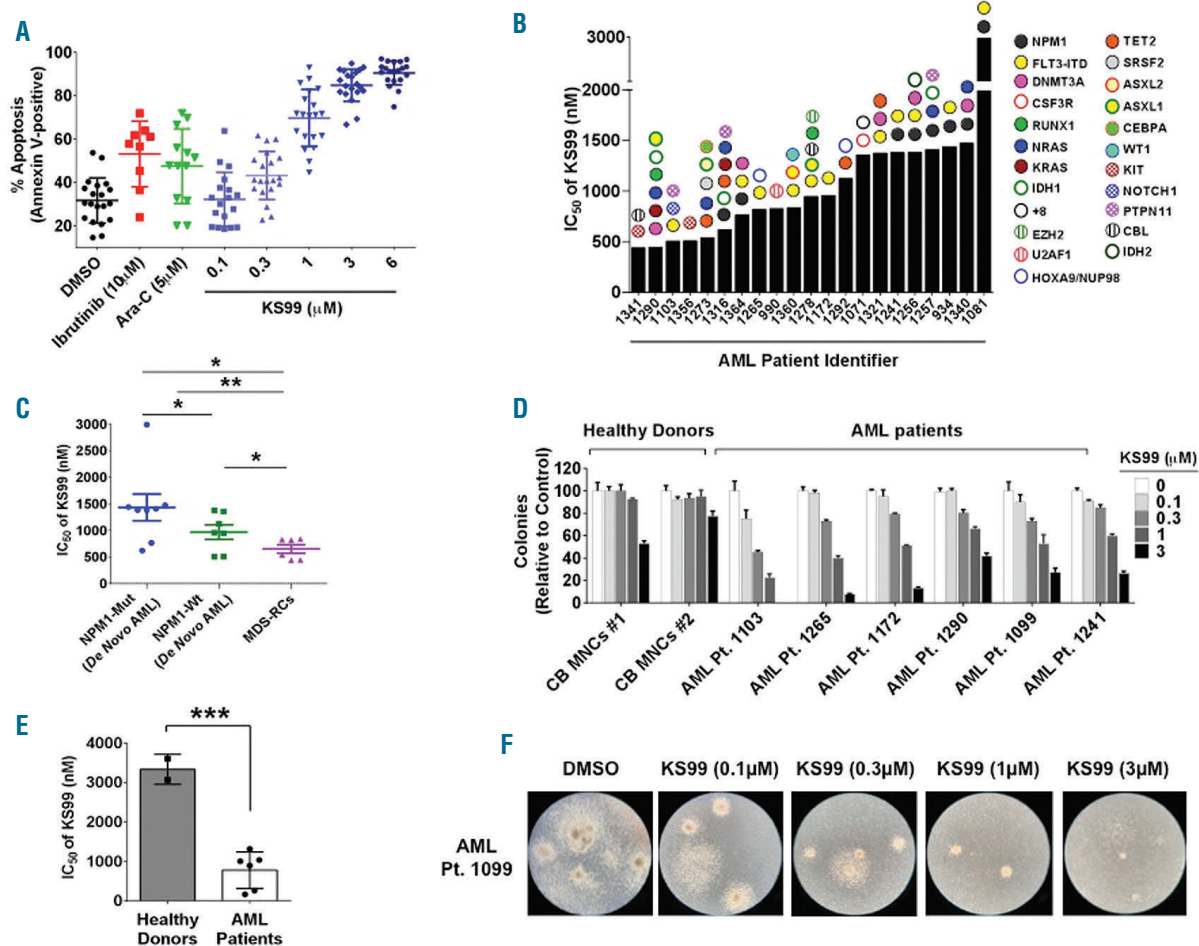
Figure 2. KS99 induces apoptosis and inhibits clonogenicity in primary human acute myeloid (AML) leukemia cells. Sensitivity of primary human AML cells to KS99 (n=21), Cytarabine (Ara-C) (n=13) or ibrutinib (n=9) after 48 hours (h) treatment. (A) Apoptosis was determined as the percentage of Annexin V-positive cells. (B) The IC$_{50}$ values of KS99 for primary human AML cells, based on the number of viable cells (i.e. Annexin V$^-$/7AAD$^-$). Individual genetic mutations are indicated by colored points. (C) Comparison of IC$_{50}$ values of KS99 for AML subgroups. AML with myelodysplastic-related changes (MDS-RC) was compared to *de novo* AML (*NPM1* mutant *vs.* wild type). (D-F) Primary human AML samples and cord blood mononuclear cells (CB MNC) obtained from healthy donors were treated with indicated concentrations of KS99 and colonies were counted after 10-14 days. Data represent triplicate wells (n=3). (D) Bar graphs show the dose-dependent response of KS99. (E) Bar graph shows a comparison of IC$_{50}$ values of KS99 for AML patient samples and CB MNC in the colony-forming assay. (F) Representative microscopy images (4X) of AML Patient 1099 colonies after KS99 treatment. Data are the mean±standard error of the mean (SEM) *P<0.05; **P<0.01; ***P<0.001; ****P<0.0001; unpaired *t*-test.

culated on the basis of Annexin-V/7AAD signals determined by flow cytometry. The sensitivity of primary human AML cells to KS99 was compared to AML standard of care agent, Ara-C. Since KS99 has been reported earlier by our group as BTK inhibitor,[20,27,28] a known BTK inhibitor, ibrutinib[27] was also included in this study for comparative purposes. Interestingly, almost all the primary cells from AML patients were quite sensitive to KS99 at a lower micromolar range (0.3-3 μM) (Figure 2A). The effectiveness of 5 μM Ara-C or 10 μM ibrutinib was equivalent to 0.3-1 μM KS99, defining the potential of relatively low doses of KS99 on patient samples (Figure 2A). We next tested whether sensitivity to KS99 is correlated with the mutational status of primary AML samples. The sensitivity of AML patient samples (n=21) with individual mutation status is shown in Figure 2B. Clinical and genetic data for AML patient samples are shown in *Online Supplementary Table S1*. It is important to note that cases associated with poor prognosis had lower IC$_{50}$ values and thus higher sensitivity to KS99 (left to right of Figure 2B). *NPM1*/FLT-3-ITD status seems to be resistant (found in 4

of 6 with highest IC$_{50}$). The AML subset, AML with myelodysplastic-related changes (MDS-RC), were more sensitive than *de novo* AML cases (*P*=0.0077) with or without an *NPM1* mutation (*P*=0.012, *P*=0.045, respectively) (Figure 2C). Within the *de novo* AML, *NPM1* wild-type cases were more sensitive than *NPM1* mutant cases (*P*=0.02) (Figure 2C).

KS99 targets leukemic progenitor cells while sparing normal hematopoietic stem and progenitor cells

Primary human AML cases (n=6) with various cytogenetic and molecular status (*Online Supplementary Table S1*) were selected to test the anti-leukemic activity of KS99 in colony-forming assay. Normal cord blood mononuclear cells (CB-MNC) (n=2) were used as HSPC controls to demonstrate the selectivity of KS99 towards LSC. The colony-forming capacity of primary human AML cases was significantly reduced in the presence of KS99, while normal CB-MNC were much less sensitive (Figure 2D). CB-MNC had significantly higher IC50 values (4.2-fold) as compared to primary human AML cases (Figure 2E).
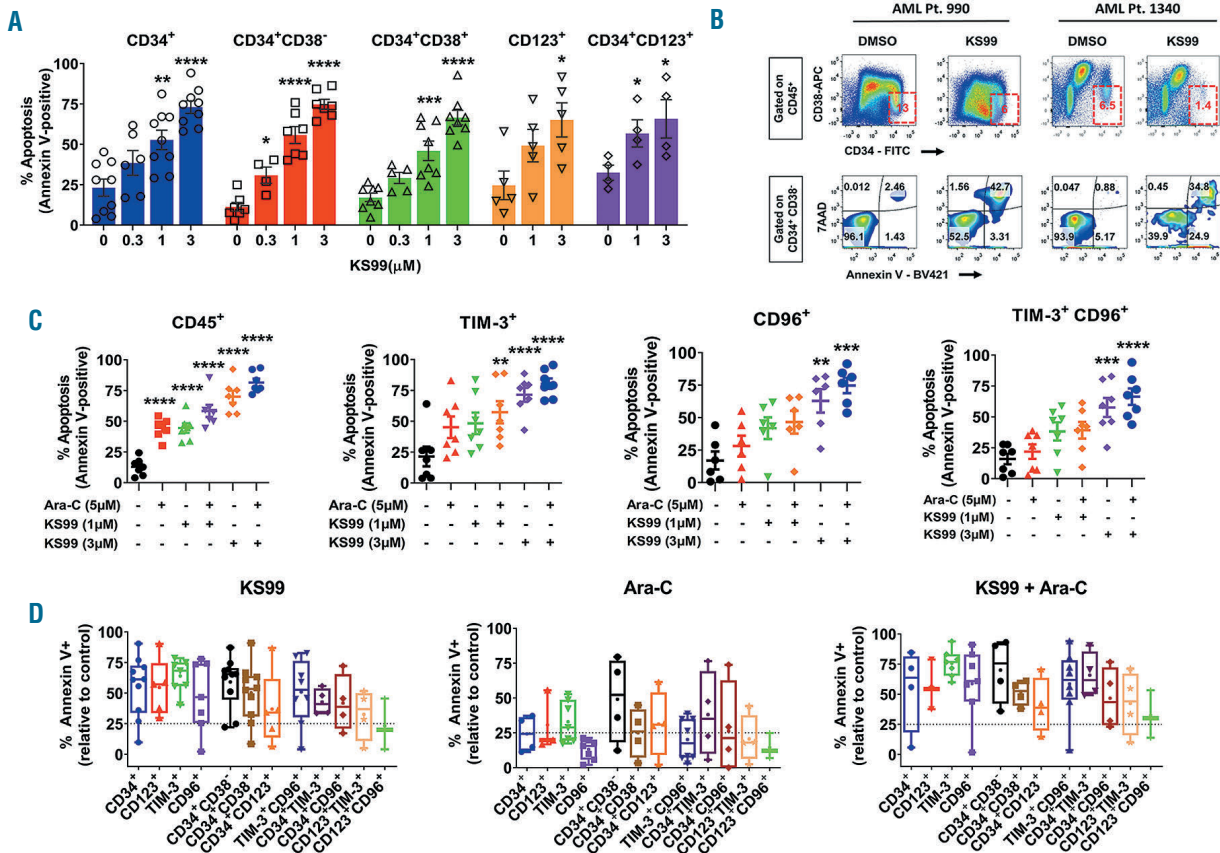
Figure 3. KS99 induces apoptosis in leukemic stem cells (LSC). (A) Dose-dependent apoptotic response of KS99 in primary human leukemic stem cells (LSC) identified as CD34+, CD34+CD38−, CD34+CD38+, CD123+, or CD34+CD123+ cells. Error bars are mean±standard error of the mean (SEM). (B) Representative flow cytometric analysis of cell death in LSC. (C) Apoptosis in CD45+, TIM-3+, CD96+, or TIM-3+CD96+ cells after the treatment with KS99 and Cytarabine (Ara-C). Error bars are mean±SEM. (D) Apoptotic response of KS99, Cytarabine (Ara-C) or combination in primary human AML cells expressing or co-expressing LSC immunophenotypes; CD34, CD38, CD123, TIM-3, and CD96. Data were normalized to DMSO-treated cells. Error bars represent maximum and minimum values. *$P<0.05$; **$P<0.01$; ***$P<0.001$; ****$P<0.0001$; unpaired t-test.

KS99-treated cells formed smaller AML blast colonies than the control treatment, as shown in Figure 2F and *Online Supplementary Figure S3*. Overall, these results showed that KS99 targets clonogenicity of leukemic cells as monotherapy while sparing normal HSPC. Since clonogenic activity is an indicator of pre-LSC, LSC and HSPC,[29] these observations were followed by flow cytometric analysis for cell surface markers of LSC.

KS99 induces apoptosis in primary human leukemic stem cells

To validate the anti-LSC activity of KS99, primary human AML cells were treated with increasing concentrations of KS99 (0.3 μM, 1 μM or 3 μM), Ara-C (5 μM), or combinations of KS99 with Ara-C for 24 h under the LSC culture conditions described by Pabst *et al.*[27] Since there is no one perfect LSC marker, we studied multiple well reported markers.[30,31] LSC were phenotypically defined by gating on CD45+ followed by CD34+C-D38−/CD38+, CD123+, TIM-3+, or CD96+. Induction of apoptosis was observed in CD123+ and CD34+CD123+ cells with KS99 treatment in a dose-dependent manner (Figure 3A). CD34+CD38− and CD34+CD38+ cells were analyzed to see whether KS99 has a pro-apoptotic activity in subpopulations of CD34+ cells, and we found that CD34+ cells were

sensitive to KS99 regardless of CD38 status (Figure 3A and B). We also observed that KS99 selectively targeted blast-like cells as compared to granulocyte-like or lymphocyte-like cells in causing reduction of CD34+ cells (*Online Supplementary Figure S2*). Next, KS99 was compared and combined with Ara-C in CD45+, TIM-3+, CD96+ or TIM-3+CD96+ human AML cells. Cells showed similar sensitivity to KS99 as observed in CD34+ and CD123+ cells (Figure 3C). When KS99 was added to Ara-C, it increased Ara-C's pro-apoptotic activity, especially in CD96+ or TIM-3+CD96+ cells (Figure 3C). Furthermore, we extended our analysis by evaluating the pro-apoptotic activity of KS99 alone and in combination with Ara-C in LSC co-expressing CD34, CD38, CD123, TIM-3, or CD96 immunophenotypes (Figure 3D). Interestingly, cells coexpressing CD123 and TIM-3 or CD96 immunophenotypes were less sensitive to Ara-C or KS99 compared to other co-expressions. However, their sensitivity was increased with combination treatment (Figure 3D, right panel). Overall, these results show that KS99 induces apoptosis not only in CD45+ or CD34+ human AML cells, but also in TIM-3+, CD96+, or cells co-expressing various LSC phenotypes. In addition, it also has the potential to enhance the activity of Ara-C in AML stem cells, given that most cells of each phenotype are sensitive to the combination.
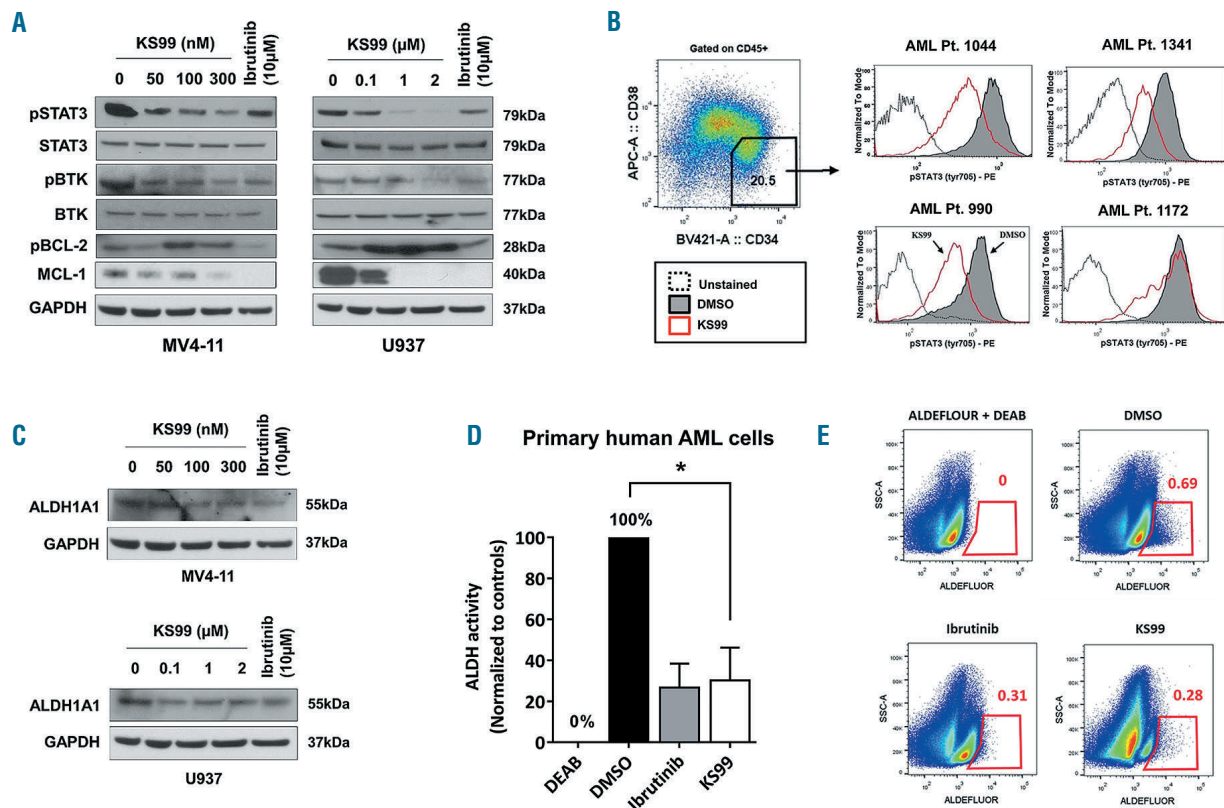
Figure 4. KS99 down-regulates pBTK, pSTAT3 and inhibits aldehyde dehydrogenase (ALDH) activity. (A) Immunoblot analysis of the whole MV4-11 and U937 cell lysates after the treatment either with DMSO, increasing concentrations of KS99 or ibrutinib (10 μM) for 24 hours (h). GAPDH was used as a loading control. (B) Flow cytometric detection of pSTAT3 in LSC of primary human acute myeloid leukemia (AML) samples (n=4). (C) Immunoblotting of whole-cell lysates of KS99 or ibrutinib-treated MV4-11 and U937 cells with ALDH1A1. GAPDH was used as a loading control. (D and E) Primary human AML samples were treated either with DMSO, KS99 (3 μM) or ibrutinib (10 μM) for 48 h. ALDH activity was measured by ALDEFLOUR assay kit *via* flow cytometry. Results are mean±standard error of the mean. n=3. *$P<0.05$ was assessed by unpaired *t*-test.

KS99 interacts with BTK, STAT3, and ALDH1A1

A molecular docking approach was used to examine the interaction of KS99 with BTK, STAT3, and ALDH1A1 (isoform) at the atomic level. For ALDH1A1, STAT3 and BTK, the lowest binding energies were -9.65 kcal/mol, -6.76 kcal/mol, and -9.31 kcal/mol, respectively (*Online Supplementary Figure S4*). The inhibition constant values for the aforesaid proteins was 84.19 nM, 11.14 μM, and 150.61 nM, respectively, suggesting that KS99 interacts with them. It should be noted that the lower energy scores correlate with a higher binding affinity,[32] i.e. better for ALDH1A1 and BTK, followed, in this case, by STAT3. KS99 binds poorly with the developed structure of STAT3 with higher binding energy and inhibition constant as compared to ALDH1A1 and BTK. The phosphotyrosine 48 amino acid binding pocket of STAT3 interacted with KS99 at comparatively higher binding energy and inhibition constant than other proteins docked in this study. Further details are provided in *Online Supplementary Table S2*.

KS99 mediated downregulation of pBTK and pSTAT3 with reduced aldehyde dehydrogenase activity in acute myeloid leukemia cell lines and primary human acute myeloid leukemia cells

To extend studies of KS99 from earlier observations, we examined BTK and STAT3 signaling in AML cell lines by western blotting and in primary AML cells by flow cytom-

etry. Western blot results confirmed that KS99 significantly inhibits phosphorylation of BTK, and STAT3 in a dose-dependent manner in MV4-11 and U937 cells (Figure 4A). Moreover, the degree of inhibition of pSTAT3 and pBTK with 10 μM ibrutinib was achieved with low nanomolar concentrations of KS99 in both cell lines. As reported previously for MM cells,[20] KS99 up-regulated BCL-2 phosphorylation and down-regulated MCL-1 in AML cells (Figure 4A). We did not observe BCL-2 phosphorylation with ibrutinib treatment but did see MCL-1 downregulation.

We obtained comparable results in primary human AML samples using flow cytometry. KS99 or vehicle-treated (DMSO) primary human AML cells were initially gated on the 7AAD-negative population (live cells) followed by CD45^{+} and CD34^{+}CD38^{−}, respectively. pSTAT3 was reduced by KS99 treatment in 3 out of 4 of the CD34^{+}CD38^{−} subpopulation of tested primary human AML cases (Figure 4B). Overall, these results suggest that KS99 down-regulates pBTK and pSTAT3.

Earlier studies have shown that LSC exhibit ALDH activity and it associates with drug resistance.[17] Western blot data showed downregulation of ALDH1A1, an isoform of ALDH with KS99 treatment in a dose-dependent manner in MV4-11 cells, whereas, in U937 cells, all the concentrations showed the same degree of downregulation (Figure 4C). Ibrutinib also down-regulated ALDH1A1, as reported previously for ovarian cancers.[33-35] ALDH activ-
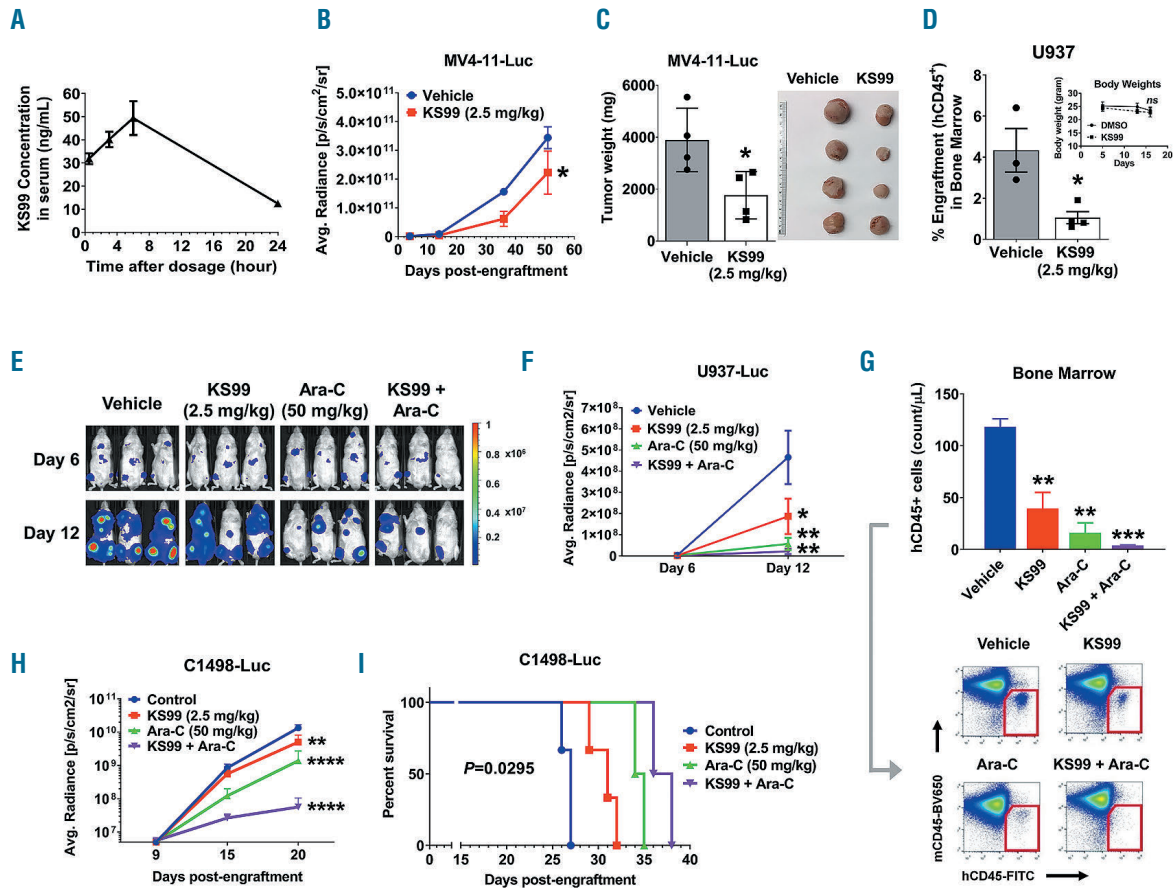
Figure 5. Preclinical efficacy of KS99 in acute myeloid leukemia (AML) mouse models. (A) Pharmacokinetics of KS99 (2.5 mg/kg body weight) concentration in plasma of NSG mice (n=3 per time point) measured after 0.5, 3, 6 and 24 hours (h) of treatment. Results are mean±standard error of the mean (SEM). (B) Mice engrafted with luciferase-expressing MV4-11 (MV4-11-Luc) cells subcutaneously were treated either with vehicle control (DMSO) or KS99 (2.5 mg/kg). Bioluminescence imaging (BLI) and quantification of radiance as a surrogate for tumor of mice (n=4) over the time course of the study were assessed. (C) Tumors were isolated and weighed at the termination of the study. (D) U937-bearing NSG mice (n=3-4) were treated either with vehicle control (DMSO) or KS99 (2.5 mg/kg). Bar graph indicates the percentage of human CD45$^+$ cells in the bone marrow of mice. The insert is the body weight of mice throughout the study. Points represent individual mice (mean±SEM). (E-G) Luciferase-expressing U937 (U937-Luc)-bearing NRG mice (n=3) were treated either with vehicle control (DMSO), KS99 (2.5 mg/kg), Cytarabine (Ara-C, 50 mg/kg) or combination of KS99 and Ara-C. (E and F) Bioluminescence imaging signals of mice over the time course of the study. (G) Bar graph depicts a number of human CD45$^+$ cells in the bone marrow of mice as detected using flow cytometry (top) and representative flow cytometric analysis of bone marrow cells (bottom). *$P<0.05$; **$P<0.01$; ***$P<0.001$ were assessed by two-way ANOVA analysis. (H and I) Luciferase-expressing C1498 (C1498-Luc)-bearing albino C57BL/6 mice (n=3) were treated either with vehicle control (DMSO), KS99 (2.5 mg/kg), Cytarabine (Ara-C, 50 mg/kg) or a combination. (H) Quantification of BLI signals of mice over the time course of the study. (I) Kaplan-Meier survival analysis of animals. Results are mean±SEM. NS: not significant; *$P<0.05$; **$P<0.01$; ***$P<0.001$; ****$P<0.0001$, unpaired t-test.

ity in primary human AML cells was tested by ALDE-FLOUR assay as described above. Briefly, cells were treated with DMSO, ibrutinib (10 μM) or KS99 (3 μM) for 48 h, harvested and subjected to flow cytometer. Both KS99 and ibrutinib treatments caused a decrease in the ALDH$^+$ subpopulation in all primary human AML cases studied (Figure 4D and E).

KS99 reduces the leukemic burden in preclinical acute myeloid leukemia animal models and improves the survival of animals

The study by Pandey *et al*. has shown the efficacy of KS99 at 1 mg/kg body weight in multiple myeloma.[20] In the current work, we determined the maximum-tolerated dose (MTD) of KS99 in NSG mice to be 2.5 mg/kg *via* an intraperitoneal (i.p.) route. Next, a single dose pharmacokinetic (PK) study was performed in NSG mice. Mice were injected with KS99 (2.5 mg/kg), sacrificed at various time

points post-dosing (n=3), and plasma levels were analyzed by LC-MS/MS. PK data showed a maximum of 49 ng/mL (105.1 nM) plasma drug concentration and rapid elimination from the systemic circulation after 8 h (Figure 5A).

To evaluate the preclinical efficacy of KS99 *in vivo*, subcutaneous (s.c.) and disseminated xenograft mouse models were used. For the subcutaneous xenograft model, MV4-11-Luc cells were injected subcutaneously into NSG mice. Once visible tumors had been established, mice were treated with either vehicle control or KS99 (2.5 mg/kg) three times a week (*Online Supplementary Figure S5A*). Data showed a 65% decrease in bioluminescent signals in KS99-treated mice compared to the vehicle. Tumor sizes and weight (approx. 70%) were lower than vehicle-treated animals (Figure 5C).

To extend our findings in a subcutaneously implanted AML xenograft model, the efficacy of KS99 was further evaluated in a disseminated mouse model using human

AML U937 cells. Leukemia-bearing mice were randomized into treatment groups according to body weight and treated as above, followed by the treatment regimen shown in *Online Supplementary Figure S5B*. Analysis of bone marrow (BM) at termination showed an approximate 76% reduction of hCD45+ cells in the KS99-treated group compared to the vehicle-treated group (*P*<0.05) (Figure 5D). Overall, KS99 treatment at 2.5 mg/kg was well tolerated by animals, as evidenced by no significant changes in body weight, suggesting negligible drug-associated toxicity (Figure 5D, see insert).

Next, KS99 was compared and combined with Ara-C in U937-Luc-bearing NOD.Cg-Rag1tm1Mom Il2rgtm1 Wjl/SzJ (NRG) mice. The treatment was initiated with vehicle control, KS99, Ara-C (50 mg/kg, IP) or combination (*Online Supplementary Figure S5C*). Although single-agent treatments KS99 (approx. 2.5 fold) or Ara-C (approx. 8.2-fold) showed a decrease in the progression of AML, co-treatment (approx. 22.2-fold decrease) was more effective at suppressing AML than either drug alone, as assessed by BLI (Figure 5E and F). Furthermore, efficacy was confirmed by flow cytometric analysis of bone marrow cells at the time of termination (Figure 5G). Mice treated with KS99, or Ara-C monotherapy exhibited a decrease of approximately 66% or approximately 86% in hCD45+ cells, respectively (Figure 5G). Interestingly, almost complete eradication (approx. 96%) of the leukemic burden was noticed in the combined treatment (KS99 + Ara-C) group (Figure 5G).

The above observations in human AML animal models were validated in an immunocompetent syngeneic animal model of AML. As for the above results, treatment with KS99, Ara-C or combination in C1498-Luc-bearing albino C57BL/6 mice showed a reduction in leukemia progression analyzed by BLI (*P*<0.01, *P*<0.0001, and *P*<0.0001, respectively) (Figure 5H). Moreover, KS99 improved overall survival of mice (*P*=0.0295) (Figure 5I). Mice treated with both agents survived longer than single agent-treated mice (Figure 5I).

Overall these results show that KS99 reduces the leukemic burden in AML xenograft models and improves animal survival. Efficacy can be further improved by combining KS99 with Ara-C or other AML chemotherapeutics.

Discussion

Current first-line cytotoxic chemotherapy for AML shows limited success, with 50% of younger patients and 80% of older patients succumbing to the disease.[36] Unfortunately, these therapies have dose-limiting normal HSPC toxicity, which is one of the major obstacles in the treatment of AML.[37] It is well established that cancer stem cells have a major role in the initiation, progression, and relapse of solid tumors.[38] In AML, the leukemic stem cells have a similar role, and these cells acquire resistance to conventional chemotherapeutic drugs upon the accumulation of molecular mutations post-primary chemotherapy.[39] The LSC within AML are responsible for tumor growth and maintenance.[38] Relapse is frequently observed, and is largely attributed to acquired resistance of LSC to chemotherapeutic agents.[2,3,37] Therefore, eradication of the LSC is likely necessary to increase survival of AML patients.[40] Our studies here focus on small molecule KS99,

a novel Isatin derivative which we show has the potential to target LSC. KS99 inhibited cell growth, induced apoptosis, and suppressed survival in both human AML cell lines and primary human AML cells.

Studies have shown that BTK is highly expressed and remains an important target in AML.[41] BTK inhibitors, ibrutinib and CG-806, are proving to be promising AML agents [27,42,43] Our previous studies showed that KS99 is a dual inhibitor of BTK/tubulin in multiple myeloma.[20] However, its role in targeting the LSC which control the poor prognosis of AML have remained undiscovered until now. BTK functions by initiating a cascade of downstream transcriptional factors that increase cell proliferation in cancer and favor cell survival.[20] While ibrutinib blocks the BTK and causes apoptosis of cancer cells, the fact that the LSC are functional may lead to relapse in some cases. Our data show that KS99 inhibits the BTK-driven STAT3 phosphorylation, which is an empirical player of LSC signaling.[44,45] Various reports have clarified the role of STAT3 signaling in pre-LSC and have associated it to poor prognosis in multiple cancers, including AML.[22,46-48] The effect of KS99 in CD34+CD38− LSC has shown decreased levels of phosphorylated STAT3, which leads to reduced expression of MCL-1 against increased phosphorylated BCL, probably due to BTK inhibition. This observation corroborates with MM and earlier studies.[20,22,46-48] *In silico* analysis shows binding of KS99 to STAT3 and emphatically to the phosphotyrosine-containing SH2 domain of STAT3. This further proves that the interaction between KS99 and BTK has a major role in down-regulating STAT3.

Aldehyde dehydrogenase, a detoxifying enzyme, is expressed in both normal progenitor cells and AML stem cells.[17,25,33-35] In colony-forming assays, KS99 illustrates the reduction in the colony-forming capacity of AML progenitor cells but mostly spares normal HSPC. This finding, with a specific selectivity of KS99, is further supported by a reduction in ALDH activity. Our western blot and flow cytometry data showed a significant decrease in ALDH expression and activity. Furthermore, the data are supported by docking studies which predict the strong binding affinity of KS99 to ALDH1A1 isoform at very low predictive inhibition constant. Collectively, our data suggest that KS99 induces apoptosis by inhibiting the STAT3 and ALDH activation in LSC. *In silico* data described here also support the effective binding of KS99 to ALDH1A1 at an inhibitory constant of 84.19 nM, suggesting that the molecule has a role in directly inhibiting the activity of ALDH and further inhibiting growth and survival of AML cells. The amino acid residues involved in the probable KS99-ALDH hydrophobic interaction likely increase binding affinity, stabilizing the ligand at its binding site and further affecting ALDH activity.

We showed that KS99 is highly active in CD34+, CD34+CD38− or CD34+CD38+ expressing cells in AML patient samples. However, a number of previous studies have shown that LSC in AML can also reside within CD123+, TIM-3+ or CD96+ cells.[12-16] We, therefore, extended our studies to these cells and were able to show that primary human AML cells expressing or co-expressing CD123, TIM-3 or CD96 were also sensitive to KS99. These results are consistent with colony-forming and ALDH observations. Furthermore, the combination of KS99 helped to augment the pro-apoptotic efficacy of Ara-C in LSC, especially in TIM-3+ cells co-expressing CD34 or

CD123. Altogether, it indicated that KS99 targets LSC in AML.

Study of 21 primary human AML cases with KS99 showed a higher sensitivity of cases with mutations associated with poor prognosis compared to cases with favorable prognosis. NPM1 mutation is linked to better prognosis and responds well to traditional chemotherapy, but is relatively insensitive *in vitro* to KS99. In contrast, AML with poor prognosis MDS-RC[49-54] were killed by KS99 at lower concentrations. AML with MDS-RC represents 25-35% of all AML, and, given its poor prognosis, calls for better therapies. Currently, experimental and investigational agents are available to target different subgroups of AML, but few address AML with MDS-RC. Our study suggests that KS99 not only targets LSC, but has potential activity against AML with MDS-RC.

Finally, our preclinical animal data are clear evidence of the therapeutic potential of KS99 in immunocompromised and immunocompetent AML xenograft models. In addition, KS99 augmented the efficacy of standard of care agent, Ara-C. Although KS99 has shown *in vivo* AML inhibitory potential in this study, the activity has been modest. We believe that these findings are expected given the PK profile of this agent. The plasma concentrations achievable at the MTD were well below the IC_{50} determined from *in vitro* studies and, together with the relatively rapid decay in these levels, provide data explaining less than robust *in vivo* activity. Current efforts are directed at the study of different formulations for drug delivery and structural variants of KS99 which may yield similar *in vitro* activity with improved toxicity and pharmacokinetic characteristics.

In summary, we demonstrate that KS99 inhibits ALDH, pSTAT3, and pBTK in AML and decreases cell proliferation and clonogenicity while increasing apoptosis. BTK phosphorylation is also inhibited, though the evidence presented here suggests that this may not be the primary target of drug inhibition. We believe that *in silico* data suggest that ALDH may be such a primary target. Almost all human AML cases, including those with MDS-RC, have been sensitive to KS99. This agent targets LSC and progenitors with limited toxicity towards normal HSPC. Our study offers a comparative validation of KS99 to the standard agent Ara-C in specific targeting of AML-LSC. This study advances KS99 alone or in combination as a candidate agent for therapeutic development after reformulation or chemical modification of KS99 or its derivatives which may prove active in clinical trials of AML.

References

1. Pandolfi A, Barreyro L, Steidl U. Concise review: preleukemic stem cells: molecular biology and clinical implications of the precursors to leukemia stem cells. Stem Cells Transl Med. 2013;2(2):143-150.
2. Bonnet D, Dick JE. Human acute myeloid leukemia is organized as a hierarchy that originates from a primitive hematopoietic cell. Nat Med. 1997;3(7):730-737.
3. Lapidot T, Sirard C, Vormoor J, et al. A cell initiating human acute myeloid leukaemia after transplantation into SCID mice. Nature. 1994;367(6464):645-648.
4. Pollyea DA, Gutman JA, Gore L, Smith CA, Jordan CT. Targeting acute myeloid leukemia stem cells: a review and principles for the development of clinical trials. Haematologica. 2014;99(8):1277-1284.
5. Sarry JE, Murphy K, Perry R, et al. Human acute myelogenous leukemia stem cells are rare and heterogeneous when assayed in NOD/SCID/IL2Rgammac-deficient mice. J Clin Invest. 2011;121(1):384-395.
6. Ho TC, LaMere M, Stevens BM, et al. Evolution of acute myelogenous leukemia stem cell properties after treatment and progression. Blood. 2016;128(13):1671-1678.
7. Taussig DC, Miraki-Moud F, Anjos-Afonso F, et al. Anti-CD38 antibody-mediated clearance of human repopulating cells masks the heterogeneity of leukemia-initiating cells. Blood. 2008;112(3):568-575.
8. Civin CI, Almeida-Porada G, Lee MJ, et al. Sustained, retransplantable, multilineage engraftment of highly purified adult human bone marrow stem cells in vivo. Blood. 1996;88(11):4102-4109.
9. Dick JE. Absence of CD34 on some human SCID-repopulating cells. Ann N Y Acad Sci. 1999;872:211-217; discussion 217-219.
10. Ding Y, Gao H, Zhang Q. The biomarkers of leukemia stem cells in acute myeloid leukemia. Stem Cell Investig. 2017;4:19.
11. Sato N, Caux C, Kitamura T, et al. Expression and factor-dependent modulation of the interleukin-3 receptor subunits on human hematopoietic cells. Blood. 1993;82(3):752-761.
12. Testa U, Pelosi E, Frankel A. CD 123 is a membrane biomarker and a therapeutic target in hematologic malignancies. Biomark Res. 2014;2(1):4.
13. Jin L, Lee EM, Ramshaw HS, et al. Monoclonal antibody-mediated targeting of CD123, IL-3 receptor alpha chain, eliminates human acute myeloid leukemic stem cells. Cell Stem Cell. 2009;5(1):31-42.
14. Kikushige Y, Shima T, Takayanagi S, et al. TIM-3 is a promising target to selectively kill acute myeloid leukemia stem cells. Cell Stem Cell. 2010;7(6):708-717.
15. Hosen N, Park CY, Tatsumi N, et al. CD96 is a leukemic stem cell-specific marker in human acute myeloid leukemia. Proc Natl Acad Sci U S A. 2007;104(26):11008-11013.
16. Iwasaki M, Liedtke M, Gentles AJ, Cleary ML. CD93 Marks a Non-Quiescent Human Leukemia Stem Cell Population and Is Required for Development of MLL-Rearranged Acute Myeloid Leukemia. Cell Stem Cell. 2015;17(4):412-421.
17. Yang X, Yao R, Wang H. Update of ALDH as a Potential Biomarker and Therapeutic Target for AML. Biomed Res Int. 2018;2018:9192104.
18. Gerber JM, Smith BD, Ngwang B, et al. A clinically relevant population of leukemic CD34(+)CD38(-) cells in acute myeloid leukemia. Blood. 2012;119(15):3571-3577.
19. Robak T, Wierzbowska A. Current and emerging therapies for acute myeloid leukemia. Clin Ther. 2009;31 Pt 2:2349-2370.

20. Pandey MK, Gowda K, Sung SS, et al. A novel dual inhibitor of microtubule and Bruton's tyrosine kinase inhibits survival of multiple myeloma and osteoclastogenesis. Exp Hematol. 2017;53:31-42.

21. Kawakami Y, Inagaki N, Salek-Ardakani S, et al. Regulation of dendritic cell maturation and function by Bruton's tyrosine kinase via IL-10 and Stat3. Proc Natl Acad Sci U S A. 2006;103(1):153-158.

22. Redell MS, Ruiz MJ, Alonzo TA, Gerbing RB, Tweardy DJ. Stat3 signaling in acute myeloid leukemia: ligand-dependent and -independent activation and induction of apoptosis by a novel small-molecule Stat3 inhibitor. Blood. 2011;117(21):5701-5709.

23. Kanna R, Choudhary G, Ramachandra N, et al. STAT3 inhibition as a therapeutic strategy for leukemia. Leuk Lymphoma. 2018;59(9):2068-2074.

24. Blume R, Rempel E, Manta L, et al. The molecular signature of AML with increased ALDH activity suggests a stem cell origin. Leuk Lymphoma. 2018;59(9):2201-2210.

25. Gasparetto M, Smith CA. ALDHs in normal and malignant hematopoietic cells: Potential new avenues for treatment of AML and other blood cancers. Chem Biol Interact. 2017;276:46-51.

26. Bogen A, Buske C, Hiddemann W, Bohlander SK, Christ O. Variable aldehyde dehydrogenase activity and effects on chemosensitivity of primitive human leukemic cells. Exp Hematol. 2017;47:54-63.

27. Rushworth SA, Murray MY, Zaitseva L, Bowles KM, MacEwan DJ. Identification of Bruton's tyrosine kinase as a therapeutic target in acute myeloid leukemia. Blood. 2014;123(8):1229-1238.

28. Li X, Yin X, Wang H, et al. The combination effect of homoharringtonine and ibrutinib on FLT3-ITD mutant acute myeloid leukemia. Oncotarget. 2017;8(8):12764-12774.

29. Dicke KA, Spitzer G, Scheffers PH, et al. In vitro colony growth of acute myelogenous leukemia. Hamatol Bluttransfus. 1976;19:63-77.

30. Pollyea DA, Jordan CT. Therapeutic targeting of acute myeloid leukemia stem cells. Blood. 2017;129(12):1627-1635.

31. Thomas D, Majeti R. Biology and relevance of human acute myeloid leukemia stem cells. Blood. 2017;129(12):1577-1585.

32. Du X, Li Y, Xia YL, et al. Insights into Protein-Ligand Interactions: Mechanisms, Models, and Methods. Int J Mol Sci. 2016; 17(2).

33. Smith C, Gasparetto M, Humphries K, et al. Aldehyde dehydrogenases in acute myeloid leukemia. Ann N Y Acad Sci. 2014; 1310:58-68.

34. Hoang VT, Hoffmann I, Borowski K, et al. Identification and separation of normal hematopoietic stem cells and leukemia stem cells from patients with acute myeloid leukemia. Methods Mol Biol. 2013;1035:217-230.

35. Kastan MB, Schlaffer E, Russo JE, et al. Direct demonstration of elevated aldehyde dehydrogenase in human hematopoietic progenitor cells. Blood. 1990;75(10):1947-1950.

36. Lowenberg B, Rowe JM. Introduction to the review series on advances in acute myeloid leukemia (AML). Blood. 2016; 127(1):1.

37. Dick JE. Stem cell concepts renew cancer research. Blood. 2008;112(13):4793-4807.

38. Tan BT, Park CY, Ailles LE, Weissman IL. The cancer stem cell hypothesis: a work in progress. Lab Invest. 2006;86(12):1203-1207.

39. Lacerda L, Pusztai L, Woodward WA. The role of tumor initiating cells in drug resistance of breast cancer: Implications for future therapeutic approaches. Drug Resist Updat. 2010;13(4-5):99-108.

40. Wang JC, Dick JE. Cancer stem cells: lessons from leukemia. Trends Cell Biol. 2005;15(9):494-501.

41. Krause DS, Van Etten RA. Right on target: eradicating leukemic stem cells. Trends Mol Med. 2007;13(11):470-481.

42. Gu TL, Nardone J, Wang Y, et al. Survey of activated FLT3 signaling in leukemia. PLoS One. 2011;6(4):e19169.

43. Tomasson MH, Xiang Z, Walgren R, et al. Somatic mutations and germline sequence variants in the expressed tyrosine kinase genes of patients with de novo acute myeloid leukemia. Blood. 2008; 111(9):4797-4808.

44. Oellerich T, Mohr S, Corso J, et al. FLT3-ITD and TLR9 use Bruton tyrosine kinase to activate distinct transcriptional programs mediating AML cell survival and proliferation. Blood. 2015;125(12):1936-1947.

45. Smith CI, Baskin B, Humire-Greiff P, et al. Expression of Bruton's agammaglobulinemia tyrosine kinase gene, BTK, is selectively down-regulated in T lymphocytes and plasma cells. J Immunol. 1994;152(2):557-565.

46. Rezvani K, Barrett J. STAT3: the "Achilles" heel for AML? Blood. 2014;123(1):1-2.

47. Steensma DP, McClure RF, Karp JE, et al. JAK2 V617F is a rare finding in de novo acute myeloid leukemia, but STAT3 activation is common and remains unexplained. Leukemia. 2006;20(6):971-978.

48. Benekli M, Xia Z, Donohue KA, et al. Constitutive activity of signal transducer and activator of transcription 3 protein in acute myeloid leukemia blasts is associated with short disease-free survival. Blood. 2002;99(1):252-257.

49. Verhaak RG, Goudswaard CS, van Putten W, et al. Mutations in nucleophosmin (NPM1) in acute myeloid leukemia (AML): association with other gene abnormalities and previously established gene expression signatures and their favorable prognostic significance. Blood. 2005;106(12):3747-3754.

50. Gale RE, Green C, Allen C, et al. The impact of FLT3 internal tandem duplication mutant level, number, size, and interaction with NPM1 mutations in a large cohort of young adult patients with acute myeloid leukemia. Blood. 2008;111(5):2776-2784.

51. Thiede C, Koch S, Creutzig E, et al. Prevalence and prognostic impact of NPM1 mutations in 1485 adult patients with acute myeloid leukemia (AML). Blood. 2006; 107(10):4011-4020.

52. Schnittger S, Schoch C, Kern W, et al. Nucleophosmin gene mutations are predictors of favorable prognosis in acute myelogenous leukemia with a normal karyotype. Blood. 2005;106(12):3733-3739.

53. Dohner K, Schlenk RF, Habdank M, et al. Mutant nucleophosmin (NPM1) predicts favorable prognosis in younger adults with acute myeloid leukemia and normal cytogenetics: interaction with other gene mutations. Blood. 2005;106(12):3740-3746.

54. Suzuki T, Kiyoi H, Ozeki K, et al. Clinical characteristics and prognostic implications of NPM1 mutations in acute myeloid leukemia. Blood. 2005;106(8):2854-2861.

Concomitant targeting of BCL2 with venetoclax and MAPK signaling with cobimetinib in acute myeloid leukemia models

Lina Han,[1,2] Qi Zhang,[1] Monique Dail,[3] Ce Shi,[2] Antonio Cavazos,[1] Vivian R. Ruvolo,[1] Yang Zhao,[4] Eugene Kim,[3] Mohamed Rahmani,[5,6] Duncan H. Mak,[1] Sha S. Jin,[7] Jun Chen,[7] Darren C. Phillips,[7] Paul Bottecelli Koller,[1] Rodrigo Jacamo,[1] Jared K. Burks,[1] Courtney DiNardo,[1] Naval Daver,[1] Elias Jabbour,[1] Jing Wang,[4] Hagop M. Kantarjian,[1] Michael Andreeff,[1] Steven Grant,[6] Joel D. Leverson,[7] Deepak Sampath[8] and Marina Konopleva[1]

[1]Department of Leukemia, The University of Texas MD Anderson Cancer Center, Houston, TX, USA; [2]Department of Hematology, First Affiliated Hospital, Harbin Medical University, Harbin, China; [3]Department of Oncology Biomarkers, Genentech, South San Francisco, CA, USA; [4]Department of Bioinformatics and Computational Biology, The University of Texas MD Anderson Cancer Center, Houston, TX, USA; [5]College of Medicine, Sharjah Institute for Medical Research, University of Sharjah, Sharjah, UAE; [6]Division of Hematology/Oncology, Department of Internal Medicine, Virginia Commonwealth University, Richmond, VA, USA; [7]AbbVie Inc., North Chicago, IL, USA and [8]Department of Translational Oncology, Genentech, South San Francisco, CA, USA

ABSTRACT

The pathogenesis of acute myeloid leukemia (AML) involves serial acquisition of mutations controlling several cellular processes, requiring combination therapies affecting key downstream survival nodes in order to treat the disease effectively. The BCL2 selective inhibitor venetoclax has potent anti-leukemia efficacy; however, resistance can occur due to its inability to inhibit MCL1, which is stabilized by the MAPK pathway. In this study, we aimed to determine the anti-leukemia efficacy of concomitant targeting of the BCL2 and MAPK pathways by venetoclax and the MEK1/2 inhibitor cobimetinib, respectively. The combination demonstrated synergy in seven of 11 AML cell lines, including those resistant to single agents, and showed growth-inhibitory activity in over 60% of primary samples from patients with diverse genetic alterations. The combination markedly impaired leukemia progenitor functions, while maintaining normal progenitors. Mass cytometry data revealed that BCL2 protein is enriched in leukemia stem/progenitor cells, primarily in venetoclax-sensitive samples, and that cobimetinib suppressed cytokine-induced pERK and pS6 signaling pathways. Through proteomic profiling studies, we identified several pathways inhibited downstream of MAPK that contribute to the synergy of the combination. In OCI-AML3 cells, the combination downregulated MCL1 protein levels and disrupted both BCL2:BIM and MCL1:BIM complexes, releasing BIM to induce cell death. RNA sequencing identified several enriched pathways, including MYC, mTORC1, and p53 in cells sensitive to the drug combination. *In vivo*, the venetoclax-cobimetinib combination reduced leukemia burden in xenograft models using genetically engineered OCI-AML3 and MOLM13 cells. Our data thus provide a rationale for combinatorial blockade of MEK and BCL2 pathways in AML.

Introduction

Acute myeloid leukemia (AML) is characterized by the uncontrolled proliferation and arrested differentiation of abnormal stem and progenitor cells. Standard induction chemotherapy induces a high rate of complete remission but fails to improve overall survival especially in elderly patients with AML.[1,2] Genes significantly mutated in AML can be organized into several functional categories that are associated with enhanced proliferation, impaired differentiation, deregulated chromatin modification, and DNA methylation.[1,3] Therefore, co-targeting downstream pathways that contribute to

leukemogenesis may deliver the greatest clinical efficacy.

The anti-apoptotic protein BCL2 has been studied extensively for its role in leukemic transformation and chemoresistance. BCL2 is highly expressed in AML leukemia stem cells (LSC) containing low levels of reactive oxygen species which are resistant to chemotherapy.[4,5] BCL2 inhibitors have been shown to eradicate AML LSC and sensitize chronic myeloid leukemia LSC to tyrosine kinase inhibitors. Oncogenic dependency on BCL2 was found in AML patients carrying mutations in IDH1 and IDH2.[6,7] A recent study used BH3 profiling to discover that co-inhibition of BCL2 with tyrosine kinase inhibitors facilitated eradication of genetically diverse AML in patient-derived xenograft (PDX) models.[8] We have reported the anti-leukemia potency of venetoclax (ABT-199/GDC-0199), an orally bioavailable BH3 mimetic that selectively binds with high affinity to BCL2, but lacks affinity for BCL-XL and MCL1, in AML models.[9] In a phase II clinical trial, venetoclax monotherapy had clinical activity in patients with relapsed or refractory AML with a tolerable safety profile.[10] However, the inability of venetoclax to inhibit MCL1 causes resistance in leukemia cells that require MCL1 for survival.[11,12]

The RAF/MEK/ERK (MAPK) cascade, a major effector pathway activated in 70%-80% of patients with AML, is activated by upstream mutant proteins such as FLT3, KIT, and RAS.[13-15] The MAPK pathway regulates BCL2 family proteins by stabilizing anti-apoptotic MCL1[11,16] and inactivating pro-apoptotic BIM (BCL2L11).[17] Monotherapy with MEK inhibitors has had limited clinical efficacy.[15] Recently it was shown that MAPK signaling activation contributed to primary resistance to an IDH2 inhibitor[18] and acquired resistance to venetoclax,[19] suggesting that combination regimens that include MEK inhibitors could be efficacious in these patients. Cobimetinib (GDC-0973) is an allosteric MEK inhibitor with antitumor activity in BRAF- and KRAS-mutant tumor cells,[20] and was recently approved to treat patients with metastatic melanoma. Its anti-AML efficacy, particularly in combination with venetoclax, is unknown.

Furthermore, biomarkers predictive of response to this combination in AML are unknown. Suppression of downstream pERK does not predict sensitivity to MEK inhibition.[21] In melanoma, it has been demonstrated that mTORC1/2 and pS6 activities are associated with acquired resistance to MEK inhibitors and suppression of pS6 may serve as a biomarker to predict clinical response to MEK inhibitors.[22,23] The role of pS6 in response to MEK and BCL2 inhibition has not been addressed.

In this study, we evaluated the anti-leukemia effects of concomitant BCL2 and MAPK blockade by venetoclax and cobimetinib in AML cell lines, primary patients' samples, and xenograft murine models. Through the use of reverse-phase protein arrays (RPPA) and RNA sequencing, we identified pharmacodynamic markers that correlated with the efficacy of the combination treatment, in particular activated pS6 (Ser235/236), which discriminated combination-sensitive from -insensitive AML cells. Our data support the rationale for dual inhibition of the BCL2 and MEK pathways.

Methods

Patients' samples, acute myeloid leukemia cell lines, and reagents

Bone marrow and peripheral blood samples were collected from patients with AML or healthy donors after informed con-

sent had been obtained in accordance with the Institutional Review Board of The University of Texas MD Anderson Cancer Center. The cell line culture methodology is described in the *Online Supplementary Methods*.

Assays and other methods

Details of the CellTiter-Glo proliferation assay, colony-forming cell assay, electrochemiluminescent enzyme-linked immunosorbent assay, RPPA, and RNA sequencing are provided in the *Online Supplementary Methods*. Antibody conjugation for mass cytometry staining and the spanning-tree progression analysis of density-normalized events (SPADE) analysis are also explained in detail in the *Online Supplementary Methods*.

Apoptosis in primary acute myeloid leukemia samples

As previously reported,[24] 18 primary AML peripheral blood mononuclear cells or AML PDX samples were cultured in LSC medium. Viable AML CD45^{dim} blast cells were enumerated by using CountBright counting beads (Cat. C36950; Invitrogen, Carlsbad, CA, USA) with concurrent annexin V and DAPI detection on a Gallios Flow Cytometer (Beckman Coulter, Indianapolis, IN, USA). Data analysis and additional details are included in the *Online Supplementary Methods*.

In vivo study of cobimetinib and venetoclax in acute myeloid leukemia xenograft mouse models

The animal studies were performed in accordance with guidelines approved by the Institutional Animal Care and Use Committee at MD Anderson. Nonobese diabetic/severe combined immunodeficient gamma IL3-GM-SF (NSG-SGM3 or NSGS) mice (female, 8-10 weeks old) were purchased from Jackson Laboratory (Bar Harbor, ME, USA). The mice were injected intravenously with OCI-AML3-Luci-GFP (1.0×10^6) cells, which were lentivirally transduced with firefly luciferase. Leukemia engraftment was confirmed 1 week after injection through a noninvasive *in vivo* bioluminescence imaging (BLI) system (Xenogen, Alameda, CA, USA) after injection of a D-luciferin (4 mg/mouse) substrate. Mice were distributed into four groups (11 mice/group) with comparable tumor burden and dosed daily for 4 weeks with one of the following oral preparations: vehicle, cobimetinib (10 mg/kg), venetoclax (100 mg/kg), or cobimetinib plus venetoclax. BLI was performed weekly to determine the extent of engraftment. Survival was monitored as an endpoint. A similar MOLM13 model is described in the *Online Supplementary Methods*.

Statistical analyses

The Student *t*-test was used to analyze the statistical significance of differences between groups, both *in vitro* and *in vivo*. All statistical tests were two-sided, and the results are expressed as the mean ± standard deviation. A *P* value ≤0.05 was considered statistically significant. The RPPA and RNA-sequencing data analysis are described in the *Online Supplementary Methods*.

Results

Cobimetinib and venetoclax demonstrate synergistic anti-leukemia efficacy in acute myeloid leukemia cell lines *in vitro*

To assess the anti-leukemia activity of cobimetinib and venetoclax as single agents or in combination, we studied their effects on cell proliferation of 11 AML cell lines (Table 1). The median inhibitory concentration (IC$_{50}$) values of single agents were determined in a dose-response

manner using CellTiter-Glo (CTG) assays after 72 h of drug treatment. The IC_{50} values of cobimetinib (range, 0.002 μM - 3.0 μM) did not correlate with either the status of RAS mutations or the basal levels of p-ERK1/2 determined by flow cytometry (Table 1). To assess pharmacological interactions between cobimetinib and venetoclax, incremental doses were applied based on the IC_{50} value of each drug. In seven of the 11 cell lines, combination of the agents elicited synergistic growth inhibition based on the Chou-Talalay method of analysis [combination index (CI) <0.8].[25] Cell lines with IC_{50} values below the selected cut-off values (0.3 μM for cobimetinib[20] and 0.1 μM for venetoclax[9]) were defined as sensitive to the single agent. Patterns of response to single agents and the combination were distinct. Notably, while synergy was observed in both venetoclax-resistant (MOLM14, OCI-AML3, NB4) and cobimetinib-resistant cell lines (KG1, MOLM13), the lowest CI value (0.12) was seen in venetoclax-sensitive/cobimetinib-resistant AML cells (KG1) (Figure 1).

Cobimetinib and venetoclax demonstrate on-target suppression of cell proliferation and clonogenic potential of leukemia progenitors in a subset of primary acute myeloid leukemia cells *ex vivo*

The anti-leukemia activities of cobimetinib and venetoclax were examined in 18 primary samples with diverse genetic alterations, collected from patients with AML or spleen from PDX models (Table 2). Primary AML blasts were treated with cobimetinib and venetoclax alone or in combination at 0.1 μM for 5 days in LSC medium to maintain the immature state of the leukemia cells.[24] Cobimetinib alone induced minimal cell death (specific apoptosis, 6.7 ± 5.9%), which was significantly enhanced when the drug was given in combination with venetoclax (27.7 ± 20.2%, P=0.001) (Figure 2A, left). Cobimetinib inhibited cell proliferation in the majority of cases (34.2 ± 23.7%), and this suppression was more pronounced when the drug was combined with venetoclax (60.2 ± 28.8%, P<0.001) (Figure 2A, right). Venetoclax as a single agent reduced viable cell numbers by more than 50% in six cases (33.3%). Three of the four AML samples demonstrating over 50% growth inhibition by the cobimetinib

treatment carried the *FLT3*-ITD and/or D835 point mutation (AML 12, 13, and 17). As previously reported, *IDH*-mutant AML samples were highly sensitive to venetoclax as a single agent (AML 2 and 15). Over 60% (11 of 18) of the patients' samples responded to the combination treatment, including those insensitive to either compound alone (AML 1, 8 and 11). Importantly, induction of apoptosis in AML stem/progenitor CD34+CD38−CD123+ population following the combination treatment was observed in two out of four AML samples tested (*Online Supplementary Figure S1*). The clonogenic potential of myeloid progenitors was significantly suppressed by the combination (82.5 ± 20.0%), as compared to cobimetinib (38.3 ± 14.6%, P=0.01) or venetoclax (41.9 ± 18.6%, P<0.05) alone. Normal progenitor function was minimally affected (Figure 2B and *Online Supplementary Figure S2*).

To test the on-target efficacy of both agents, we developed a 28-parameter mass cytometry [time-of-flight mass spectrometry (CyTOF)] panel comprising antibodies against surface antigens to define AML stem/progenitor fractions and intracellular proteins of the BCL2 family and various signaling pathways[26] (*Online Supplementary Table S1*). The CyTOF study was performed in AML13 (sensitive to the combination) and AML14 (resistant to the combination) samples (Figure 2C). SPADE trees were built and annotated using all cell surface markers (*Online Supplementary Table S1*); the positive markers were included in the heat maps (*Online Supplementary Figure S3*). BCL2 protein levels were significantly enriched in CD34+ stem/progenitor cells compared to CD34− cells and BCL2 was expressed at a higher level in the venetoclax-sensitive sample (AML13) than in the venetoclax-resistant sample (AML14), consistent with our published data9 (Figure 2D). These results support the notion that venetoclax preferentially target LSC in AML. As previously reported, the cancer signaling network relies on the manner in which cancer cells respond to external stimuli rather than their basal phosphorylation state.[27] Therefore, following cobimetinib treatment, we stimulated primary AML cells with granulocyte colony-stimulating factor (G-CSF) or stem cell factor (SCF) to study MEK downstream signaling pathways under conditions mimicking a cytokine-rich bone marrow

Table 1. Cytotoxicity of cobimetinib and venetoclax in acute myeloid leukemia cell lines.

Cell line	Mutations	Cobimetinib IC_{50} (μM)	Venetoclax IC_{50} (μM)	CI value	p-ERK (R-MFI)
MOLM13	*FLT3*-ITD	0.46	0.01	0.49	6.60
MOLM14	*FLT3*-ITD	0.16	1.88	0.36	9.68
MV4;11	*FLT3*-ITD	0.29	0.005	0.99	11.7
TF-1*	*NRAS, TP53*	0.51	10.3	1.51	2.56
OCI-AML3	*NPM1, DNMT3A, NRAS*	0.17	2.90	0.29	8.67
OCI-AML2	*DNMT3A*	0.002	0.04	0.78	3.72
THP1*	*NRAS, TP53*	0.56	39.1	0.54	4.48
KG1*	*ITGB8, SMC2*	3.06	0.03	0.12	3.73
NB4	*PML-RARA*	0.04	0.73	0.30	2.34
U937*	*PTPN11, WT1*	3.00	9.75	0.88	3.30
HL-60	*CDKN2A, TP53, NRAS*	0.45	0.004	0.89	3.83

Half maximal inhibitory concentration (IC_{50}) values were calculated on the basis of the number of viable cells quantified by CTG assay. CI: combination index; R-MFI: relative median fluorescence intensity determined by the ratio of the signal in the antibody-stained cells/autofluorescence of unstained cells; ITD: internal tandem duplication. *Data on gene mutations are from Cancer Cell Line Encyclopedia: http://www.broadinstitute.org/ccle/home

microenvironment. The SPADE trees were colored based on expression levels of CD34. In AML13, annotation 4 (6.5% of total viable cells) represented the leukemia stem/progenitor cell population by phenotypically positive expression of CD34, CD123, CD25, CD135, and CD64. Annotation 8 accounted for 53.4% of total viable cells in AML14, and was highly positive for expression of CD34, CD123, CD117, CD135, and CD64 (*Online Supplementary Figure S3*). In both samples, we observed low basal levels of pERK, which increased following G-CSF stimulation (3.9-fold in AML13 and 5.7-fold increase in AML14). G-CSF-stimulated pERK in both patients' samples was largely inhibited by cobimetinib despite differential responses in proliferation assays (Figure 2C, D), indicating that suppression of pERK does not predict sensitivity to MEK inhibition and is consistent with previous reports.[21] Several studies have shown that suppression of mTORC1 and downstream pathways (especially S6) pre-

dicted sensitivity to MEK inhibition.[21,22] We found that pS6 was highly activated by SCF and effectively suppressed by cobimetinib in the cobimetinib-sensitive AML sample, whereas the cobimetinib-resistant AML sample did not demonstrate a response to SCF. As in this study, we treated cells overnight and transiently stimulated then for 10 min to look into activation of signal transduction pathways (Figure 2). Due to limited exposure to the inhibitors (2 h), we were unable to detect changes in frequencies of AML stem/progenitor cells (*Online Supplementary Figure S4*).

Transcriptomic and proteomic profiles identify pharmacodynamic markers underlying responses to targeted agents

To identify the pharmacodynamic markers underlying the observed drug responses, we treated the 11 AML cell lines (Table 1) with cobimetinib and venetoclax as single
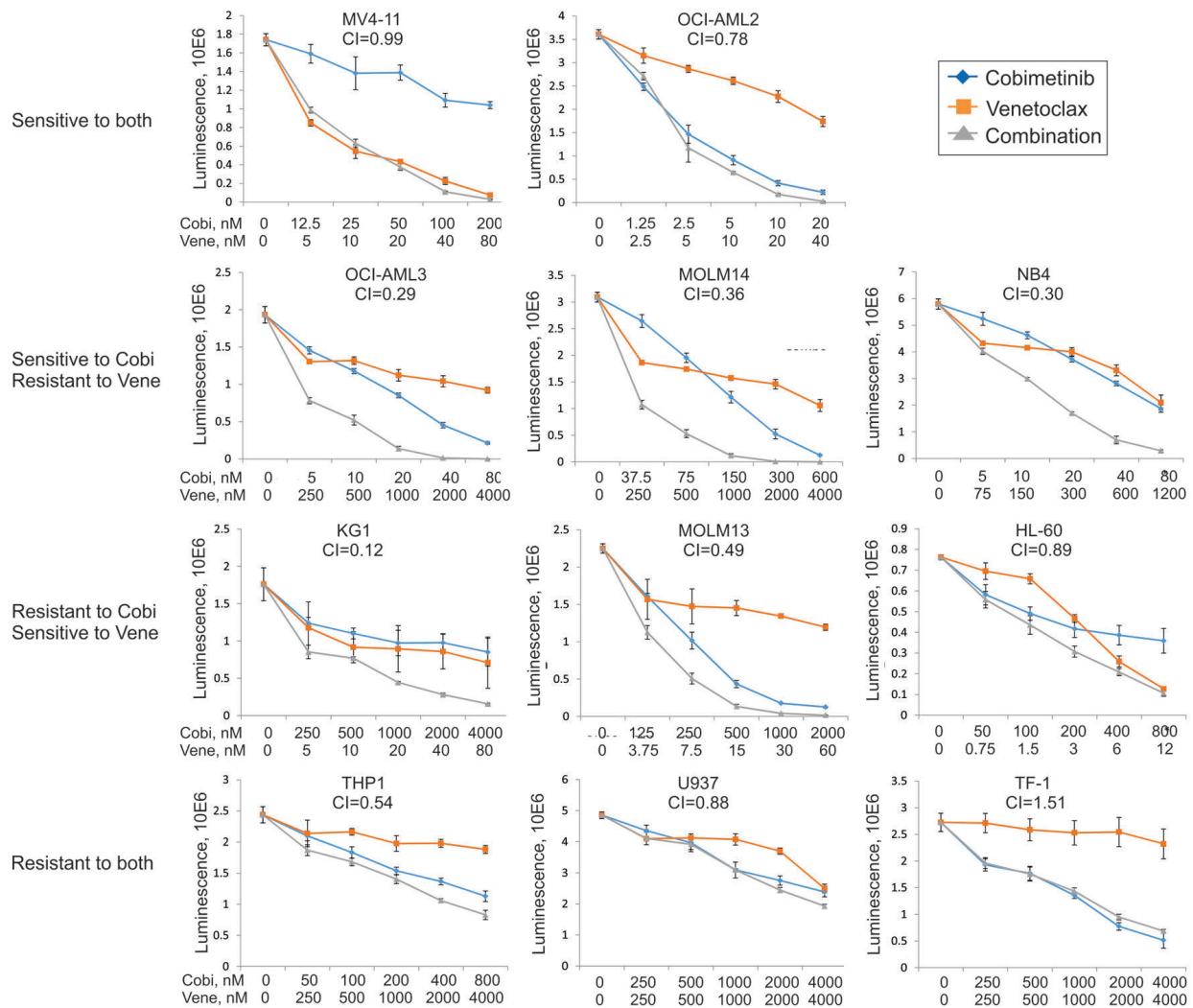
Figure 1. Anti-leukemia efficacy of cobimetinib and venetoclax in acute myeloid leukemia cell lines. Eleven acute myeloid leukemia cell lines were left untreated or treated with cobimetinib or venetoclax as single agents at 0.001, 0.01, 0.1, or 1.0 μM for 72 h. Calcusyn software was used to calculate the median inhibitory concentration (IC$_{50}$) values. Combinations of the two drugs were then tested on the same cell lines at dose ranges of 0.25, 0.5, 1, 2, and 4 times the IC$_{50}$ value of each compound. The combination index of each combination in each cell line was calculated on the basis on the luminescent intensity that correlated with number of viable cells determined by the CellTiter-Glo assay. Responses to treatment were categorized into four patterns: (i) sensitive to both drugs; (ii) sensitive only to cobimetinib and showing synergy for the combination; (iii) sensitive only to venetoclax and showing synergy for the combination; (iv) resistant to both drugs. AML: acute myeloid leukemia; Cobi: cobimetinib; Ven: venetoclax; CI: combination index

agents or in combination for 24 h at doses that were 0.5, 1 or 2 times their IC_{50} values, followed by RPPA and RNA sequencing analysis. As already described, cells with IC_{50} values <0.3 µM for cobimetinib or <0.1 µM for venetoclax were categorized as sensitive and those with IC_{50} values above these cutoffs were considered resistant. For the combination groups, CI values <0.8 were considered synergistic.

Quantification of 90 proteins by RPPA identified several biomarkers that correlated with *in vitro* drug responses. For example, S6 phosphorylation at Ser235/236 was significantly reduced in both cobimetinib-sensitive and -resistant cell lines compared to untreated cells, with sensitive cells displaying higher basal phosphorylation at Ser235/236. Significant pMEK induction was observed in cobimetinib-resistant cell lines (Figure 3A). Several signaling pathways were highly activated under basal condi-

tions in cobimetinib-sensitive cells compared to resistant cells, including pS6 (Ser235/236), pRSK, pERK, p38MAPK and pPTEN (*Online Supplementary Figure S5A*). Proteins indicating responses to venetoclax treatment were largely limited to the caspase-dependent apoptotic cascade (*data not shown*). Higher levels of BAX and BCL2 and lower levels of BIM and pS6 (Ser240/244) correlated with sensitivity to venetoclax (*Online Supplementary Figure S5B*). In cell lines in which cobimetinib and venetoclax had a synergistic effect, several MEK downstream pathways were significantly downregulated and cleaved poly (ADP-ribose) polymerase (PARP) was detected, indicating induction of apoptosis (Figure 3B). These changes were not identified in cell lines in which a synergistic effect did not occur. The heat maps of the complete RPPA datasets are shown in *Online Supplementary Figure S6*.

Western blotting was performed to validate the RPPA

Table 2. Clinical information for primary acute myeloid leukemia patients' samples.

AML#	Status	WBC (x10⁹/L)	Blasts,%	Cytogenetics	Molecular mutations
Samples for 5-day culture					
1	NA	NA	NA	NA	*IKZF1, NOTCH1, BCOR*
2	Relapsed	34.3	95	Complex	*DNMT3A, IDH2, TP53, FLT3-N841*
3	Relapsed	21	96	Complex	*FLT3-ITD, NPM1, WT1, DNMT3A*
4	Relapsed	14.9	98	Complex	*JAK2, MPL, WT1*
5	Relapsed	6.5	94	46,XY,t(9;11)(p22;q23)	*CEBPA, ATM*
6	Relapsed	18.3	57	47,XY,+21	*RUNX1, TET2*
7	Relapsed	19.9	69	NA	*EVI1*
8	*De novo*	13.5	18	46,XX	*EZH2, MPL*
9	*De novo*	20.6	74	NA	NA
10	*De novo*	5.9	21	Complex	*TP53*
11	NA	40	24	Complex	*FLT3-D835*
12	Relapsed	19	94	47,XY,+8	*FLT3-D835, NOTCH1, ASXL1, KIT, TET2*
13	Relapsed	45.8	94	45,XY,der(17;18)	*FLT3*-ITD and *D835*
14	Relapsed	6.4	72	Complex	*EGFR, PTPN11, WT1*
15	Relapsed	5.4	25	47,XY,+8	*RUNX1, ASXL1, IDH1, KRAS, NRAS, TET2*
16	*De novo*	12.7	31	Complex	*RUNX1, TET2, TP53*
17	Relapsed	4.8	89	46,t(X;X)(q22;q26)	*FLT3*-ITD and *D835*
18	Relapsed	4.6	48	Complex	*FLT3*-ITD, *JAK2, RUNX1*
Samples for CFC assays					
19	*De novo*	85.5	51	46,XX	*DNMT3A, IDH2m NPM1, ASXL1*
20	Relapsed	2.4	50	47,XX,+8	*RUNX1, ASXL1, IDH1, TET2, NRAS, KRAS*
21	Relapsed	1.7	82	Complex	*ASXL1, EZH2, IDH1, TET2, RUNX1*
22	Relapsed	5.8	32	Complex	*DNMT3A, IDH1*
Samples for CyTOF (only) study					
23	Relapsed	104.4	3	Complex	*IDH2*
24	Relapsed	163.5	98	Complex	*FLT3*-ITD
25	Relapsed	10.9	10	Complex	*IDH2*
26	Relapsed	5.1	88	Complex	*TP53, ATM*
27	Relapsed	80.1	72	46,XX	No mutations
28	Relapsed	13.1	63	46,XX	*TP53, IDH2*

AML: acute myeloid leukemia; WBC: white blood cell count; NA: not available; ITD: internal duplication; CFC: colony-forming cells; CyTOF: time-of-flight mass spectrometry. For 5-day culture assays, all samples were collected from peripheral blood, except AML #15, which was from bone marrow, and AML #1, #5, and #9, which were from patient-derived xenograft mouse spleens. All the samples for CFC assays were bone marrow.
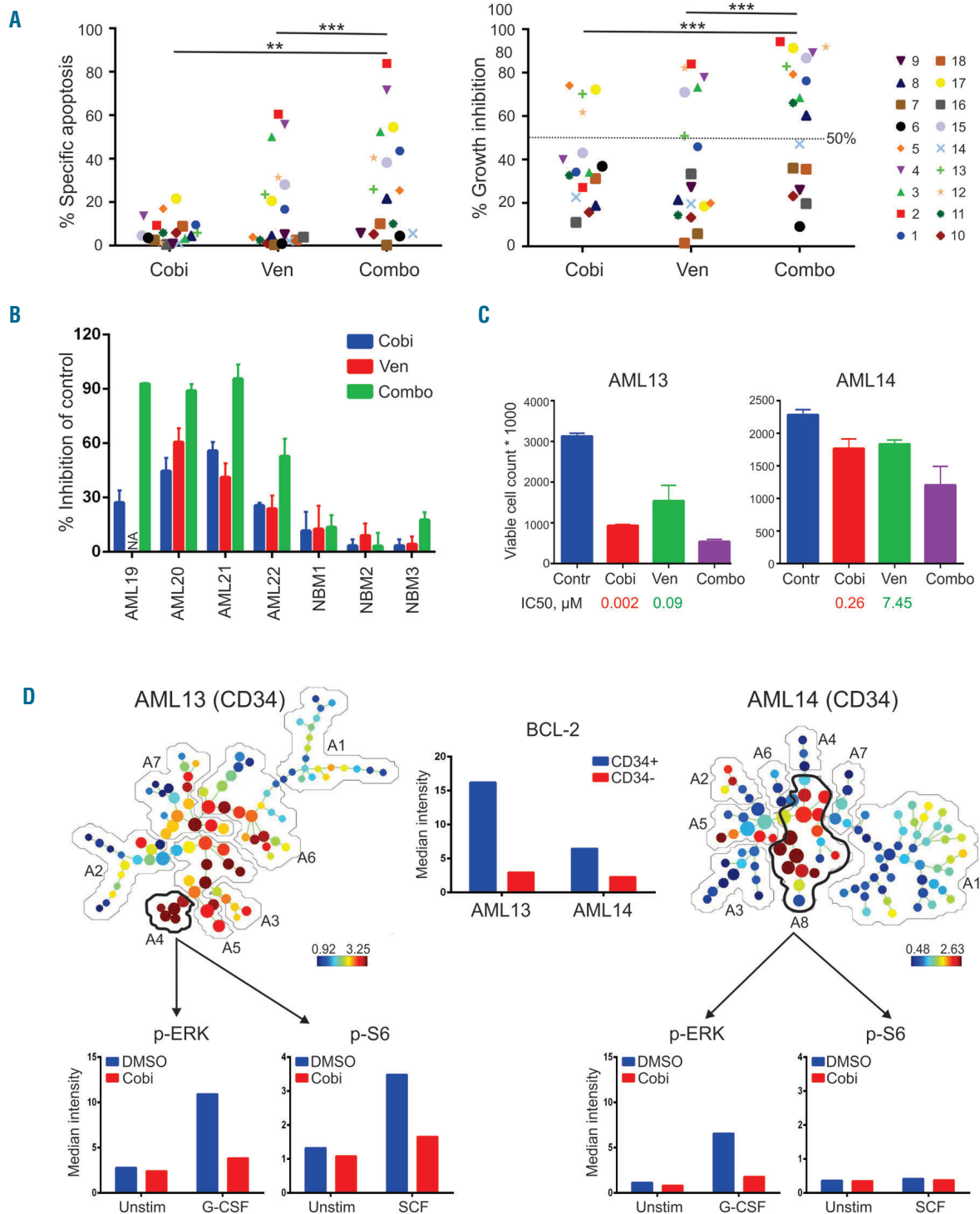
Figure 2. Treatment with cobimetinib and venetoclax causes on-target suppression of cell proliferation and impairs leukemia progenitor function in a subset of primary acute myeloid leukemia cases. (A) Primary acute myeloid leukemia (AML) peripheral blood mononuclear or bone marrow cells from AML cases were cultured in serum-free expansion medium supplemented with BIT 9500 Serum Substitute and cytokines, including stem cell factor (SCF; 100 ng/mL), Flt3 ligand (50 ng/mL), interleukin 3 (IL3; 20 ng/mL), and granulocyte colony-stimulating factor (G-CSF; 20 ng/mL) as well as StemRegenin 1 (SR1; 1 μM). Cells were left untreated or treated with cobimetinib (Cobi) or venetoclax (Van), both at 0.1 μM, as single agents or in combination (Combo). After culture for 5 days, cells were stained with CD45-PE, Annexin-V-APC, and DAPI. Apoptotic leukemia blasts (CD45dimAnnexin-V$^+$) were isolated by flow cytometry. Results are expressed as percentage of specific apoptosis calculated by the formula: 100 × (% apoptosis of treated cells – % apoptosis of control cells)/(100 – % apoptosis of control cells). Percentage of growth inhibition was calculated on the basis of the number of control viable cells (Annexin-V$^-$/DAPI$^-$). **$P<0.01$; ***$P<0.001$. (B) Mononuclear cells collected from AML patients (100,000 cells) or healthy donors (50,000 cells; NBM) were plated in methylcellulose, then treated with venetoclax or cobimetinib (both at 0.1 μM) as single agents or in combination. Colonies were scored on day 14. Data are presented as percentage inhibition compared to control groups. (C) The absolute cell counts of AML13 and AML14 samples as determined in (A) are shown in comparison with those of untreated controls (Contr), with median inhibitory concentration (IC$_{50}$) values indicated for each sample. (D) AML13 and AML14 samples were treated with cobimetinib 1.0 μM overnight followed by 10 min with or without (Unstim) stimulation with SCF or G-CSF (100 ng/mL). Cells were fixed, permeabilized, and processed for time-of-lflight mass spectrometry. Spanning-tree progression analysis of density-normalized events (SPADE) trees were generated by using markers shown in *Online Supplementary Figure S2*. The leukemia stem/progenitor populations were manually annotated and highlighted by analysis of all surface markers. The median intensities of pERK and pS6 in gated populations are shown. BCL2 expression in CD34$^+$ and CD34$^-$ fractions in both samples is shown. DMSO: dimethylsulfoxide.
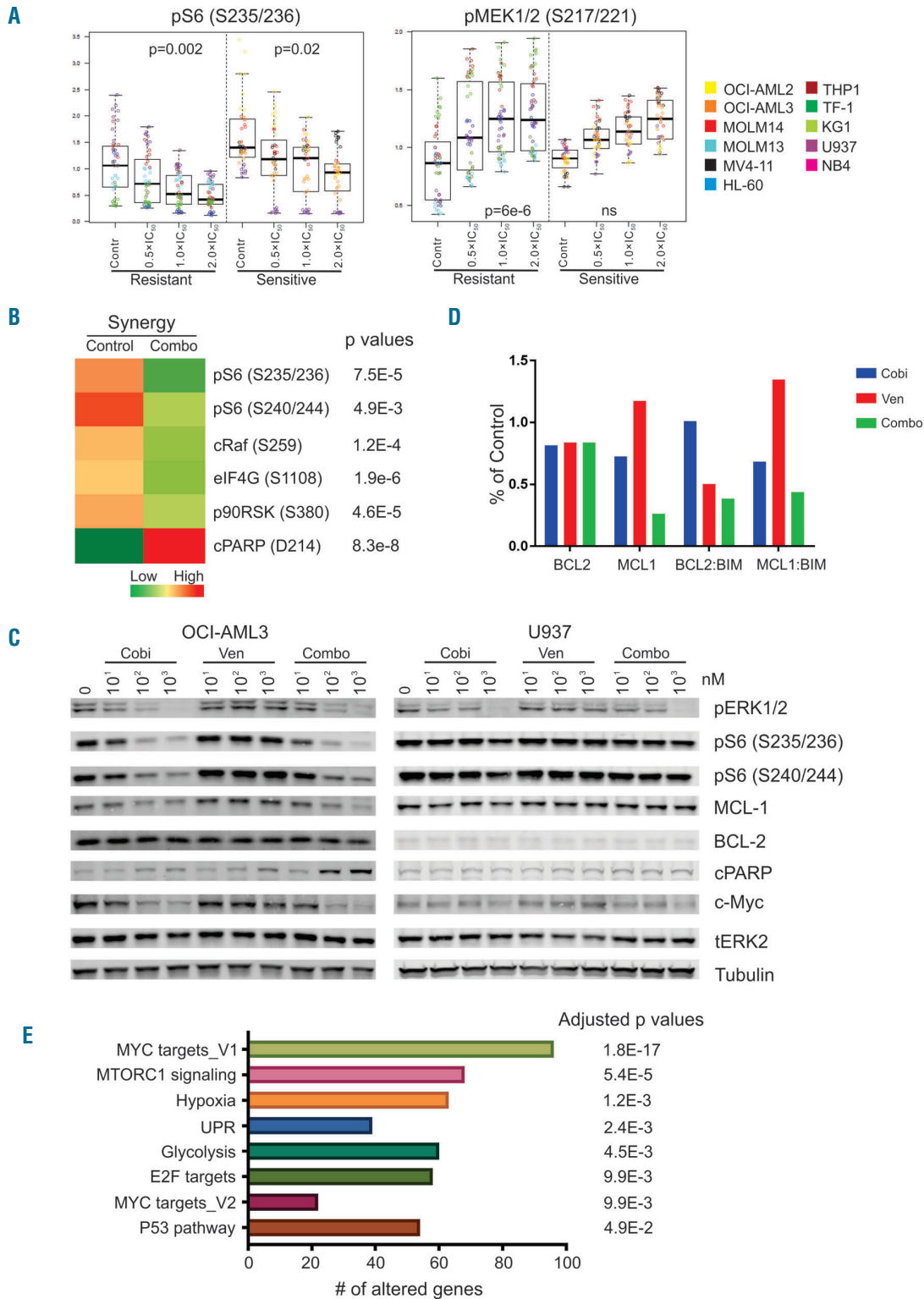
Figure 3. Pharmacodynamic markers of drug response identified through reverse-phase protein arrays and RNA sequencing. Acute myeloid leukemia (AML) cell lines were left untreated or treated with cobimetinib or venetoclax as single agents or in combination at 0.5, 1, or 2 times the median inhibitory concentration (IC_{50}) value of each compound in each cell line for 24 h. Cell pellets were harvested after treatment and subjected to reverse-phase protein array (RPPA) analysis as previously reported. (A) Plots depict proteins differentially expressed between cobimetinib-sensitive and cobimetinib-resistant cells. (B) The mean values of corresponding proteins in cell lines showing synergy to the combination treatment (CI<0.8 as presented in Table 1) are shown in the heatmap. Only the proteins showing significant differences (*P*<0.05) between control and treated groups are shown. C: untreated control; T: treated; S: sensitive; R: resistant; Syn: synergy. (C) Cells were treated with cobimetinib (Cobi), venetoclax (Ven), or a combination (Combo) at 10, 100 and 1000 nM for 4 h and subjected to lysis; proteins were separated and probed with the antibodies indicated. (D) AML cell lines were left untreated (control) or treated with cobimetinib or venetoclax as single agents or in combination at 10 times the median inhibitory concentration (IC_{50}) value of each compound in each cell line for 4 h. Cell pellets were harvested after treatment and subjected to electrochemiluminescent enzyme-linked immunosorbent assay. The levels of BCL2, MCL1, BCL2:BIM and MCL1:BIM complexes were plotted based on percentages of the levels in the control group. (E) AML cells were treated and processed as described above for the RPPA assay. RNA was isolated using the RNeasy kit and sent for mRNA sequencing. The enriched pathways in cell types showing synergy in response to the combination are shown.

data in four cell lines representing different response patterns (Table 1, Figure 3C and *Online Supplementary Figure S5C*). Suppression of pERK by cobimetinib was observed in both sensitive (OCI-AML3 and MV4;11) and resistant (MOLM13 and U937) cells at 0.01 μM, irrespective of response patterns. pS6 (Ser235/236 or Ser240/244) was inhibited by a low dose (0.1 μM) of cobimetinib in sensitive OCI-AML3 cells but not in resistant U937 cells (Figure 3C), consistent with our RPPA findings noted above. These data also indicate direct suppression of mTORC1 signaling by cobimetinib as the Ser240/244 site is regulated exclusively by mTORC1. MYC was downregulated by cobimetinib alone or in combination with venetoclax in OCI-AML3, but not in U937 cells. Cell death characterized by elevated levels of cleaved PARP was observed in the combination group in OCI-AML3 cells, consistent with pro-apoptotic synergy (Figure 3C). To capture the dynamic interactions of pro- and anti-apoptotic BCL2 family members, a Meso Scale Discovery assay was performed in OCI-AML3 cells (Figure 3D). High basal levels of BCL2 and BCL2:BIM complexes were identified. After venetoclax treatment, BCL2:BIM complexes were disrupted and MCL1 protein levels were upregulated, resulting in increased MCL1:BIM complexes. The combination of cobimetinib with venetoclax suppressed both BCL2:BIM and MCL1:BIM complexes, enabling release of free BIM to induce cell death (Figure 3D). In addition, cobimetinib treatment induced total BIM protein levels in MV4;11 cells, thereby priming the cells for death (*Online Supplementary Figure S7*).

To refine our search for potential biomarkers correlating with response to the venetoclax-cobimetinib combination, we performed RNA sequencing and evaluated differential gene expression after exposure to the drugs. The aim was to identify hallmark cancer pathways significantly altered specifically in cells sensitive to the drug combination (Figure 3E and *Online Supplementary Table S2*). Our analysis demonstrated that several downstream pathways, including MYC, E2F and their target genes, were significantly altered after treatment in cells that responded synergistically to the combination. Consistent with western blot data, mTORC1 signaling was also altered in cells showing synergistic responses. Hypoxia and unfolded protein response (UPR) pathways were also significantly enriched, possibly downstream of mTOR/4EBP1/eIF4E signaling, which directs protein synthesis of HIF-1α,[28] and can trigger the UPR.[29] Glycolysis, another enriched pathway, is regulated by the ERK signaling pathway through RNK126-mediated ubiquitination of pyruvate dehydrogenase kinase, which may account for resistance to apoptosis.[30]

The combination of cobimetinib and venetoclax reduces leukemia burden in acute myeloid leukemia models *in vivo*

To test the efficacy of cobimetinib and venetoclax *in vivo*, we induced leukemia in NSGS mice by injecting the animals with genetically engineered OCI-AML3/Luc/GFP cells. Leukemia engraftment was confirmed 1 week after injection using BLI. Mice were randomly distributed into four arms and dosed orally with vehicle, cobimetinib (10 mg/kg), venetoclax (100 mg/kg), or cobimetnib plus venetoclax daily for 28 days. BLI demonstrated that the leukemia burden was significantly reduced in treated groups compared to controls over time (Figure 4A). At

week 5, the tumor reduction was significantly greater in the groups that received single-agent cobimetinib ($P<0.001$) or cobimetnib plus venetoclax ($P<0.001$) than in the control group (Figure 4B). The tumor reduction was greater following combination treatment than following venetoclax ($P<0.05$) or cobimetinib ($P<0.05$) alone. All drug treatments, including combinations, were tolerated *in vivo* based on minimal changes in body weights (*data not shown*).

As a second AML cell line-derived xenograft model, we introduced genetically engineered MOLM3/Luc/GFP cells into NSGS mice and initiated treatment as for the OCI-AML3/Luc/GFP model. Again, BLI demonstrated significantly reduced leukemia burden in the treated groups compared to controls and the reduction was more pronounced in the groups treated with single-agent venetoclax or cobimetinib plus venetoclax (Figure 4C, D). Additionally, human CD45 engraftment and cell counts in both bone marrow and spleen demonstrated a trend toward decreased tumor burden in mice treated with the drug combination compared to that in mice treated with either agent alone (*Online Supplementary Figure S8A, B*). As in the OCI-AML3/Luc xenograft model, all drug treatments were tolerated based on minimal changes in body weights. We performed additional PDX studies in NSG mice using an AML PDX generated from primary sample AML11 (Table 2). The mice were treated with the same doses of drugs as those used in the cell line models. As shown in *Online Supplementary Figure S9*, the combination therapy extended survival in the AML11 PDX model. These data demonstrate that the combination of cobimetinib plus venetoclax potently suppresses leukemia burden in tumor-bearing mice *in vivo* at tolerable doses.

Discussion

Although gain-of-function mutations often represent secondary events in the pathogenesis of AML,[31,32] they are required for AML maintenance and are therefore attractive therapeutic targets.[33] While MEK inhibitors have demonstrated limited activity in AML as single agents,[15,34] preclinical studies with first generation MEK and BCL2 inhibitors demonstrated synergistic induction of apoptosis by suppression of MCL1 following MEK inhibition.[11,35]

In this study, five of the 11 AML cell lines tested were sensitive to cobimetinib, including two that harbored a *FLT3*-ITD mutation (MOLM14 and MV4;11) and one with an *NRAS* mutation (OCI-AML3). Consistent with previous reports, the baseline levels of ERK phosphorylation did not correlate with response to cobimetinib.[21,36] Venetoclax as a single agent had activity in five of the cell lines tested while the combination with cobimetinib was synergistic in seven of the cell lines, including those that were resistant to each agent alone.

To extend our preliminary findings in cell lines, we studied a selection of genetically diverse primary AML patients' samples. Venetoclax induced pronounced apoptosis (>50%) in only three of the samples (16.7%), a rate similar to that of clinical responses to venetoclax monotherapy (19%),[10] possibly reflecting protective properties of the tumor microenvironment, as our culture conditions were cytokine-rich. Cobimetinib induced very limited cell death in all AML samples, consistent with previous reports that MEK inhibitors preferentially suppress

proliferation and promote differentiation, rather than induce death.[33,37,38] Remarkably, over 60% of patients' samples responded to the combination therapy, notably including samples that were insensitive to both agents on their own. Moreover, these responders carried diverse genetic alterations that affect leukemia cell proliferation (*FLT3*, *RAS*), differentiation (*RUNX1*), genomic stability (*NPM1*), and epigenetic modifications (*TET2*, *IDH1* and *IDH2*). Clonogenic assays demonstrated that the combination markedly impaired the colony-forming functions
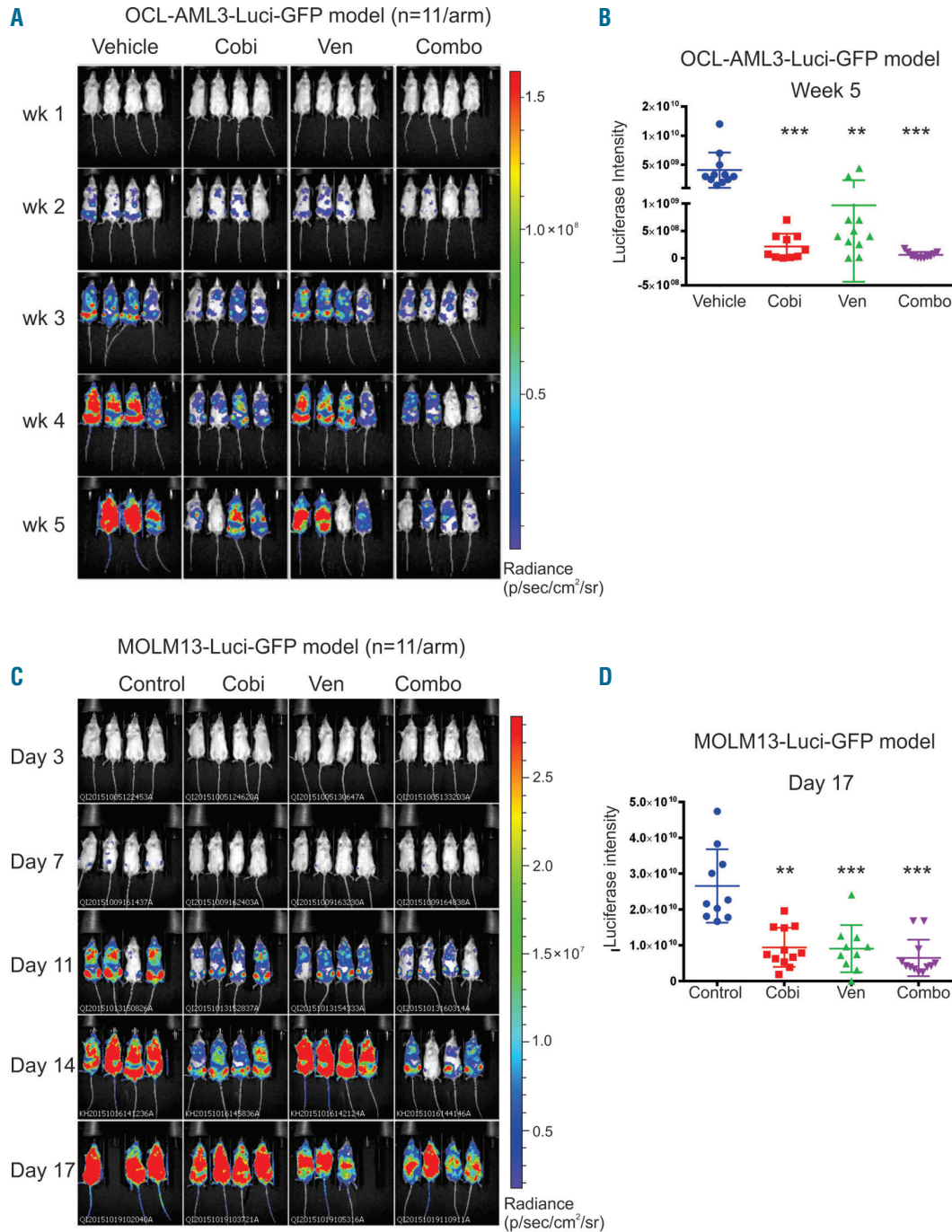
Figure 4. *In vivo* administration of cobimetinib in combination with venetoclax demonstrated anti-leukemia efficacy in acute myeloid leukemia xenograft mouse models. (A) NSGS mice were injected intravenously with OCI-AML3-Luci-GFP cells (1.0×10⁶). Leukemia engraftment was confirmed 1 week later through a noninvasive *in vivo* bioluminescence imaging (BLI) system following injection with a D-luciferin (4 mg/mouse) substrate. Mice were dosed daily with oral vehicle or an orally active form of cobimetinib (Cobi; 10 mg/kg) or venetoclax (Ven; 100 mg/kg) or their combination (Combo) for 4 weeks. BLI data over time are shown. (B) Luciferase intensity [mean ± standard deviation(SD)] at week 5. Human CD45 engraftment in bone marrow and spleen was determined by time-of-flight mass spectrometry (C) BLI data over time from the leukemia model established with MOLM13-Luc-GFP cells (1×10⁶ per animal) in NSGS mice. Mice received treatment as for the OCI-AML3/Luc/GFP model for 14 days. (D) Quantification of BLI signals (mean ± SD) on day 17 in the MOLM13 model. *$P<0.05$; **$P<0.01$; ***$P<0.001$; ****$P<0.0001$.

of AML progenitors, while normal progenitors were only minimally affected.

CyTOF has proven to be a powerful approach for identifying functional proteins in diverse cell populations at single-cell levels.[39] Several groups, including ours, have studied the feasibility of CyTOF in AML.[26,40,41] In this study, we utilized CyTOF combined with SPADE software[42] to investigate the efficacy of cobimetinib and venetoclax in two primary patients' samples: one responder and one non-responder. BCL2 was highly expressed in CD34+ stem/progenitor cells compared to the CD34– cells, underlying the critical need for BCL2 inhibition to eliminate LSC. The venetoclax-sensitive sample displayed a higher level of BCL2 protein than the resistant sample. Cobimetinib inhibited G-CSF-induced pERK irrespective of response status. In line with several studies reporting that suppression of mTORC1 and its downstream pathways (specifically S6) predicted sensitivity to MEK inhibition,[21,22] our data also demonstrated that the pS6 signaling pathway was suppressed in the cobimetinib-responding sample, suggesting that S6 phosphorylation may be a more predictive pharmacodynamic marker for MEK inhibition. However, the latter requires validation in a larger cohort of samples from patients.

The distinct response patterns in AML cell lines and patients' samples led us to search for additional pharmacodynamic markers correlating with drug responses using proteomic and transcriptomic profiling. In line with the findings of an extensive study of MEK inhibition,[20] we observed bypass induction of pMEK signaling upon MEK inhibition, which was more pronounced in cobimetinib-resistant cell lines. Several signaling pathways were highly activated in cobimetinib-sensitive cell lines, including pS6, pERK, p38MAPK, and pPTEN. Lauchle and colleagues demonstrated that leukemia clones with pre-existing resistance to MEK inhibition displayed reduced p38 kinase activity and increased RasGRP1 levels.[13] It was also previously reported that the RSK signaling pathway, which is downstream of MAPK, regulates an mTOR-independent pathway to induce S6 phosphorylation.[43] Western blotting analysis performed to validate the RPPA data showed that S6 phosphorylation at both Ser235/236 and Ser240/244 sites was markedly suppressed in cobimetinib-sensitive OCI-AML3 and MV4-11 cells. In OCI-AML3 cells, the combination treatment resulted in significant cell death characterized by elevated levels of cleaved PARP, which could be attributed to disruption of BCL2:BIM complexes, releasing BIM to trigger apoptosis. We also observed BIM induction in MV4-11 cells, underscoring its critical role in the efficacy of the combination of BCL2 and MEK inhibitors.[37,38,44] Although RPPA data showed no modulation of MCL1 after cobimetinib treatment, both western blot and Meso Scale Discovery assays showed downregulation of MCL1 in OCL-AML3 cells and upregulation of MCL1 after venetoclax treatment. These data suggest that

increased MCL1 levels induced by venetoclax favor the formation of MCL1:BIM complexes were disrupted, freeing BIM to initiate apoptosis. Consistent with these findings, we recently showed that MCL-1 degradation associated with MDM2 inhibition occurs through MEK/ERK suppression and GSK3 activation.[45] The downregulation of MYC levels by cobimetinib also suggests a MEK/ERK-GSK3β link, as ubiquitination and degradation of MYC requires phosphorylation at T58 by GSK3β.[46] Furthermore, RNA sequencing analyses revealed enhanced expression of MYC and E2F target genes in cells demonstrating a synergistic response to the cobimetinib-venetoclax combination. This finding is consistent with a previous report that MEK inhibition sensitized cells to ABT-263-induced apoptosis by promoting a G1 cell cycle arrest.[37] Glycolysis and oxidative phosphorylation (OXPHOS) are known to be regulated by ERK signaling through RNK126-mediated ubiquitination of pyruvate dehydrogenase kinase.[30] Potent antitumor efficacy has been demonstrated in melanoma cells through combined inhibition of BCL2, OXPHOS and MAPK signaling.[47] Alterations in p53 and UPR pathways identified by transcriptome analysis may also account for synergy between MEK and BCL2 inhibition.[48] These proposed mechanisms of actions are summarized in *Online Supplementary Figure S10*. However these models require further validation in controlled mechanistic studies.

The potency of the cobimetinib and venetoclax combination was further demonstrated *in vivo* using models established with OCI-AML3 (resistant to venetoclax) and MOLM13 (resistant to cobimetinib) leukemia cells. Although we observed strong synergistic effects in both cell lines *in vitro*, the combination did not confer significant survival benefits in the *in vivo* models. This may be due to protection against cell death provided by the microenvironment, as we have observed in patients' samples cultured in cytokine-rich medium. Similar to our *in vitro* observations, the OCI-AML3 xenograft model is hypersensitive to cobimetinib, and we found no significant survival differences between animals that received single-agent cobimetinib and those that received the combination. In the very aggressive MOLM13 model, in which untreated mice die 3 weeks after cell injection, the combination reduced but did not eliminate leukemia burden markedly on day 17.

In summary, combinatorial blockade of the MAPK and BCL2 pathways promotes cell death and suppresses proliferation in the majority of primary AML cells. This anti-leukemia efficacy is associated with the simultaneous inhibition of BCL2 by venetoclax and the downregulation of MCL1 mediated by cobimetinib, which together enable the release of the pro-death protein BIM. These preclinical data provided a strong mechanistic rationale for evaluating the combination of cobimetinib with venetoclax in a phase I trial now enrolling elderly patients with relapsed/refractory AML (NCT02670044), and initial data have included objective clinical responses.[49]

References

1. Dohner H, Weisdorf DJ, Bloomfield CD. Acute myeloid leukemia. N Engl J Med. 2015;373(12):1136-1152.

2. Bose P, Vachhani P, Cortes JE. Treatment of relapsed/refractory acute myeloid leukemia. Curr Treat Options Oncol. 2017;18(3):17.

3. Cancer Genome Atlas Research N, Ley TJ, Miller C, et al. Genomic and epigenomic landscapes of adult de novo acute myeloid leukemia. N Engl J Med. 2013;368(22):2059-2074.

4. Lagadinou ED, Sach A, Callahan K, et al. BCL-2 inhibition targets oxidative phosphorylation and selectively eradicates quiescent human leukemia stem cells. Cell Stem Cell.

2013;12(3):329-341.

5. Carter BZ, Mak PY, Mu H, et al. Combined targeting of BCL-2 and BCR-ABL tyrosine kinase eradicates chronic myeloid leukemia stem cells. Sci Transl Med. 2016;8(355):355ra117.

6. Chan SM, Thomas D, Corces-Zimmerman MR, et al. Isocitrate dehydrogenase 1 and 2 mutations induce BCL-2 dependence in acute myeloid leukemia. Nat Med. 2015;21 (2):178-184.

7. Goff DJ, Court Recart A, Sadarangani A, et al. A pan-BCL2 inhibitor renders bone-marrow-resident human leukemia stem cells sensitive to tyrosine kinase inhibition. Cell Stem Cell. 2013;12(3):316-328.

8. Saito Y, Mochizuki Y, Ogahara I, et al. Overcoming mutational complexity in acute myeloid leukemia by inhibition of critical pathways. Sci Transl Med. 2017;9(413).

9. Pan R, Hogdal LJ, Benito JM, et al. Selective BCL-2 inhibition by ABT-199 causes on-target cell death in acute myeloid leukemia. Cancer Discov. 2014;4(3):362-375.

10. Konopleva M, Pollyea DA, Potluri J, et al. Efficacy and biological correlates of response in a phase II study of venetoclax monotherapy in patients with acute myelogenous leukemia. Cancer Discov. 2016;6(10):1106-1117.

11. Konopleva M, Milella M, Ruvolo P, et al. MEK inhibition enhances ABT-737-induced leukemia cell apoptosis via prevention of ERK-activated MCL-1 induction and modulation of MCL-1/BIM complex. Leukemia. 2012;26(4):778-787.

12. Lin KH, Winter PS, Xie A, et al. Targeting MCL-1/BCL-XL forestalls the acquisition of resistance to ABT-199 in acute myeloid leukemia. Sci Rep. 2016;6:27696.

13. Lauchle JO, Kim D, Le DT, et al. Response and resistance to MEK inhibition in leukaemias initiated by hyperactive Ras. Nature. 2009;461(7262):411-414.

14. Smith CC, Shah NP. The role of kinase inhibitors in the treatment of patients with acute myeloid leukemia. Am Soc Clin Oncol Educ Book. 2013;313-318.

15. Jain N, Curran E, Iyengar NM, et al. Phase II study of the oral MEK inhibitor selumetinib in advanced acute myelogenous leukemia: a University of Chicago phase II consortium trial. Clin Cancer Res. 2014;20(2):490-498.

16. Yeh YY, Chen R, Hessler J, et al. Up-regulation of CDK9 kinase activity and Mcl-1 stability contributes to the acquired resistance to cyclin-dependent kinase inhibitors in leukemia. Oncotarget. 2015;6(5):2667-2679.

17. Pei XY, Dai Y, Tenorio S, et al. MEK1/2 inhibitors potentiate UCN-01 lethality in human multiple myeloma cells through a Bim-dependent mechanism. Blood. 2007;110(6):2092-2101.

18. Amatangelo MD, Quek L, Shih A, et al. Enasidenib induces acute myeloid leukemia cell differentiation to promote clinical response. Blood. 2017;130(6):732-741.

19. Zhang Q, Han L, Shi C, et al. Upregulation of MAPK/MCL-1 maintaining mitochondrial oxidative phosphorylation confers acquired resistance to BCL-2 inhibitor venetoclax in AML. Blood. 2016; 128(22):101-101.

20. Hatzivassiliou G, Haling JR, Chen H, et al. Mechanism of MEK inhibition determines efficacy in mutant KRAS- versus BRAF-driven cancers. Nature. 2013;501(7466):232-236.

21. Hirashita Y, Tsukamoto Y, Yanagihara K, et al. Reduced phosphorylation of ribosomal protein S6 is associated with sensitivity to MEK inhibition in gastric cancer cells. Cancer Sci. 2016;107(12):1919-1928.

22. Corcoran RB, Rothenberg SM, Hata AN, et al. TORC1 suppression predicts responsiveness to RAF and MEK inhibition in BRAF-mutant melanoma. Sci Transl Med. 2013;5(196):196ra198.

23. Teh JLF, Cheng PF, Purwin TJ, et al. In vivo E2F reporting reveals efficacious schedules of MEK1/2-CDK4/6 targeting and mTOR-S6 resistance mechanisms. Cancer Discov. 2018;8(5):568-581.

24. Pabst C, Krosl J, Fares I, et al. Identification of small molecules that support human leukemia stem cell activity ex vivo. Nat Methods. 2014;11(4):436-442.

25. Chou TC. Drug combination studies and their synergy quantification using the Chou-Talalay method. Cancer Res. 2010;70(2):440-446.

26. Han L, Qiu P, Zeng Z, et al. Single-cell mass cytometry reveals intracellular survival/proliferative signaling in FLT3-ITD-mutated AML stem/progenitor cells. Cytometry A. 2015;87(4):346-356.

27. Irish JM, Hovland R, Krutzik PO, et al. Single cell profiling of potentiated phospho-protein networks in cancer cells. Cell. 2004;118(2):217-228.

28. Dodd KM, Yang J, Shen MH, Sampson JR, Tee AR. mTORC1 drives HIF-1alpha and VEGF-A signalling via multiple mechanisms involving 4E-BP1, S6K1 and STAT3. Oncogene. 2015;34(17):2239-2250.

29. Croft A, Tay KH, Boyd SC, et al. Oncogenic activation of MEK/ERK primes melanoma cells for adaptation to endoplasmic reticulum stress. J Invest Dermatol. 2014;134(2):488-497.

30. Yoshino S, Hara T, Nakaoka HJ, et al. The ERK signaling target RNF126 regulates anoikis resistance in cancer cells by changing the mitochondrial metabolic flux. Cell Discov. 2016;2:16019.

31. Shlush LI, Zandi S, Mitchell A, et al. Identification of pre-leukaemic haematopoietic stem cells in acute leukaemia. Nature. 2014;506(7488):328-333.

32. Welch JS, Ley TJ, Link DC, et al. The origin and evolution of mutations in acute myeloid leukemia. Cell. 2012;150(2):264-278.

33. Burgess MR, Hwang E, Firestone AJ, et al. Preclinical efficacy of MEK inhibition in Nras-mutant AML. Blood. 2014;124(26):3947-3955.

34. Borthakur G, Popplewell L, Boyiadzis M, et al. Activity of the oral mitogen-activated protein kinase kinase inhibitor trametinib in RAS-mutant relapsed or refractory myeloid malignancies. Cancer. 2016;122(12):1871-1879.

35. Konopleva M, Contractor R, Tsao T, et al. Mechanisms of apoptosis sensitivity and resistance to the BH3 mimetic ABT-737 in acute myeloid leukemia. Cancer Cell. 2006;10(5):375-388.

36. Ricciardi MR, Scerpa MC, Bergamo P, et al. Therapeutic potential of MEK inhibition in acute myelogenous leukemia: rationale for "vertical" and "lateral" combination strategies. J Mol Med (Berl). 2012;90(10):1133-1144.

37. Airiau K, Prouzet-Mauleon V, Rousseau B, et al. Synergistic cooperation between ABT-263 and MEK1/2 inhibitor: effect on apoptosis and proliferation of acute myeloid leukemia cells. Oncotarget. 2016;7(1):845-859.

38. Corcoran RB, Cheng KA, Hata AN, et al. Synthetic lethal interaction of combined BCL-XL and MEK inhibition promotes tumor regressions in KRAS mutant cancer models. Cancer Cell. 2013;23(1):121-128.

39. Bendall SC, Simonds EF, Qiu P, et al. Single-cell mass cytometry of differential immune and drug responses across a human hematopoietic continuum. Science. 2011;332(6030):687-696.

40. Fisher DAC, Malkova O, Engle EK, et al. Mass cytometry analysis reveals hyperactive NF kappa B signaling in myelofibrosis and secondary acute myeloid leukemia. Leukemia. 2017;31(9):1962-1974.

41. Levine JH, Simonds EF, Bendall SC, et al. Data-driven phenotypic dissection of AML reveals progenitor-like cells that correlate with prognosis. Cell. 2015;162(1):184-197.

42. Qiu P, Simonds EF, Bendall SC, et al. Extracting a cellular hierarchy from high-dimensional cytometry data with SPADE. Nat Biotechnol. 2011;29(10):886-891.

43. Roux PP, Shahbazian D, Vu H, et al. RAS/ERK signaling promotes site-specific ribosomal protein S6 phosphorylation via RSK and stimulates cap-dependent translation. J Biol Chem. 2007;282(19):14056-14064.

44. Sale MJ, Cook SJ. The BH3 mimetic ABT-263 synergizes with the MEK1/2 inhibitor selumetinib/AZD6244 to promote BIM-dependent tumour cell death and inhibit acquired resistance. Biochem J. 2013;450(2):285-294.

45. Pan R, Ruvolo V, Mu H, et al. Synthetic lethality of combined Bcl-2 inhibition and p53 activation in AML: mechanisms and superior antileukemic efficacy. Cancer Cell. 2017;32(6):748-760.

46. Tsai WB, Aiba I, Long Y, et al. Activation of Ras/PI3K/ERK pathway induces c-Myc stabilization to upregulate argininosuccinate synthetase, leading to arginine deiminase resistance in melanoma cells. Cancer Res. 2012;72(10):2622-2633.

47. Serasinghe MN, Gelles JD, Li K, et al. Dual suppression of inner and outer mitochondrial membrane functions augments apoptotic responses to oncogenic MAPK inhibition. Cell Death Dis. 2018;9(2):29.

48. Ma Y, Hendershot LM. The role of the unfolded protein response in tumour development: friend or foe? Nat Rev Cancer. 2004;4(12):966-977.

49. Daver N, Pollyea DA, Yee KWL, et al. Preliminary results from a phase Ib study evaluating BCL-2 inhibitor venetoclax in combination with MEK inhibitor cobimetinib or MDM2 inhibitor idasanutlin in patients with relapsed or refractory (R/R) AML. Blood. 2017;130 (Suppl 1):813.

Ferrata Storti Foundation

Phenotype-based drug screening reveals association between venetoclax response and differentiation stage in acute myeloid leukemia

Heikki Kuusanmäki,[1,2] Aino-Maija Leppä,[1] Petri Pölönen,[3] Mika Kontro,[2] Olli Dufva,[2] Debashish Deb,[1] Bhagwan Yadav,[2] Oscar Brück,[2] Ashwini Kumar,[1] Hele Everaus,[4] Bjørn T. Gjertsen,[5] Merja Heinäniemi,[3] Kimmo Porkka,[2] Satu Mustjoki[2,6] and Caroline A. Heckman[1]

[1]Institute for Molecular Medicine Finland, Helsinki Institute of Life Science, University of Helsinki, Helsinki; [2]Hematology Research Unit, Helsinki University Hospital Comprehensive Cancer Center, Helsinki; [3]Institute of Biomedicine, School of Medicine, University of Eastern Finland, Kuopio, Finland; [4]Department of Hematology and Oncology, University of Tartu, Tartu, Estonia; [5]Centre for Cancer Biomarkers, Department of Clinical Science, University of Bergen, Bergen, Norway and [6]Translational Immunology Research Program and Department of Clinical Chemistry and Hematology, University of Helsinki, Helsinki, Finland

Correspondence:

CAROLINE A. HECKMAN
caroline.heckman@helsinki.fi/

HEIKKI KUUSANMÄKI
heikki.kuusanmaki@helsinki.fi

Check the online version for the most updated information on this article, online supplements, and information on authorship & disclosures: www.haematologica.org/content/105/3/708

ABSTRACT

Ex vivo drug testing is a promising approach to identify novel treatment strategies for acute myeloid leukemia (AML). However, accurate blast-specific drug responses cannot be measured with homogeneous "add-mix-measure" cell viability assays. In this study, we implemented a flow cytometry-based approach to simultaneously evaluate the *ex vivo* sensitivity of different cell populations in 34 primary AML samples to seven drugs and 27 rational drug combinations. Our data demonstrate that different cell populations present in AML samples have distinct sensitivity to targeted therapies. Particularly, blast cells of FAB M0/1 AML showed high sensitivity to venetoclax. In contrast, differentiated monocytic cells abundantly present in M4/5 subtypes showed resistance to Bcl-2 inhibition, whereas immature blasts in the same samples were sensitive, highlighting the importance of blast-specific readouts. Accordingly, in the total mononuclear cell fraction the highest *BCL2/MCL1* gene expression ratio was observed in M0/1 and the lowest in M4/5 AML. Of the seven tested drugs, venetoclax had the highest blast-specific toxicity, and combining venetoclax with either MEK inhibitor trametinib or JAK inhibitor ruxolitinib effectively targeted all venetoclax-resistant blasts. In conclusion, we show that *ex vivo* efficacy of targeted agents and particularly Bcl-2 inhibitor venetoclax is influenced by the cell type, and accurate blast-specific drug responses can be assessed with a flow cytometry-based approach.

Introduction

The treatment of AML with high-dose cytarabine and anthracycline-based intensive chemotherapy has remained the standard of care for the last four decades.[1] Despite the increase in overall survival, only 35 to 40% of adult patients under 60 years are cured with chemotherapy and allogeneic stem cell transplantation.[2] A number of novel targeted agents have been investigated in AML, but have usually generated clinical responses only in small patient subsets. Currently, genetic profiling is used for patient stratification and determination of treatment, evident by the recent approvals of midostaurin/gilteritinib and ivosidenib/enasidenib for treating AML patients with *FLT3* or *IDH1/IDH2* mutations, respectively.[3–5] Furthermore, the Bcl-2 inhibitor venetoclax combined with a hypomethylating agent has recently been approved for AML with increased efficacy in patients with *IDH1/2* and *NPM1* mutations.[6,7] However, the majority of AML patients lack actionable mutations and our understanding of the relationship between the cancer genotype, phenotype and drug function remains limited. *Ex vivo* drug testing with primary patient samples

may help to identify novel treatment options and patient subgroups with sensitivity to a specific targeted therapy.

AML is diagnosed when the bone marrow (BM) contains at least 20% of myeloid lineage blast cells, and hematological relapse is defined when the BM exceeds 5% of blasts. The non-blast cells of the AML BM are com-prised of other cell types, mainly lymphocytes and more mature leukemic cells (monocytes, granulocytes) or healthy cells. The BM content and the maturity level of leukemic cells is reflected in the French-American-British (FAB) subtypes.[8] In FAB M0/1 subtypes, the differentiation blockade occurs at the early myeloid progenitor stage,
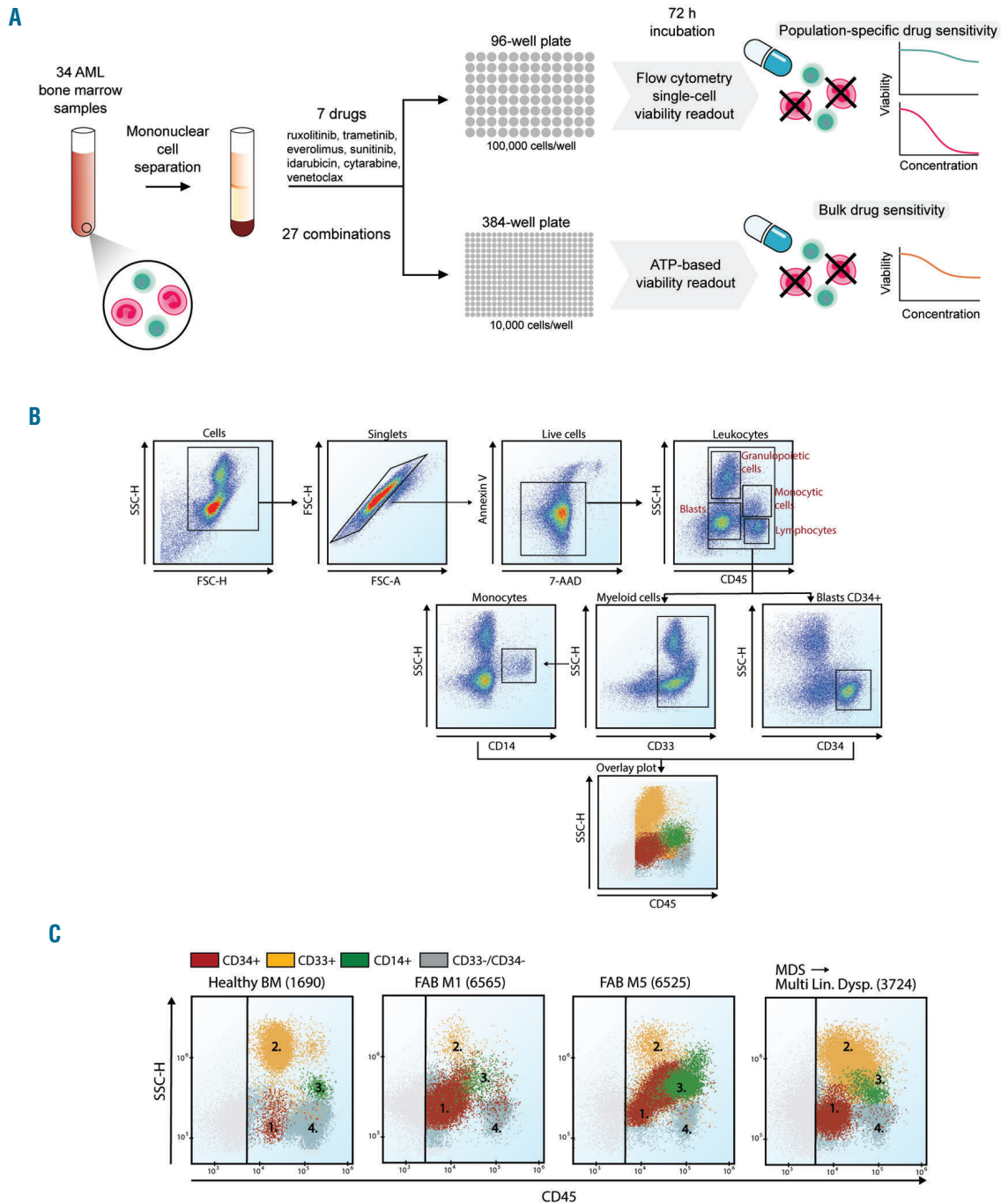
Figure 1. Study outline and gating strategy. (A) Schematic outline of the experimental setup. (B) Gating strategy of cell populations. Dead and apoptotic cells were stained with 7-AAD and Annexin V, respectively, and cells negative to these markers were gated as live cells. CD45^{dim}/SSC^{low} and CD34$^+$ population was used as the standard gate for acute myeloid leukemia (AML) blast cells. For samples with blast cells negative for CD34, CD45^{dim}/SSC^{low} and CD33 positivity was used to identify blasts. Lymphocytes were gated based on CD45^{bright}/SSC^{low} and were confirmed to be CD33 negative. Immature granulocytes (present after Ficoll gradient centrifugation) were gated based on CD45^{dim}/SSC^{high}, CD33$^+$ and CD34$^-$. Monocytes were identified based on CD14 positivity. Clinical immunophenotype data were obtained for all samples to validate the gated cell populations. The illustration shows patient sample 6323 at day 0. (C) Illustration of the immunophenotypic profiles of AML samples with different French-American-British (FAB) subtypes and healthy bone marrow (BM) samples represented by CD45 *versus* SSC plots at day 0.

whereas in FAB M4/5 subtypes the differentiation blockade is "leaky". In addition to immature blasts in FAB M4/5 samples, leukemic cells often show myelomonocytic or monocytic differentiation, respectively. To achieve optimal response in patients, the drugs should target the less differentiated leukemic blasts.[9] However, due to cellular heterogeneity, blast-specific drug responses are challenging to measure with conventional cell viability assays such as CellTiter-Glo (CTG) or tetrazolium reduction assays (MTT/MTS).[10] Although enrichment of blasts is possible,
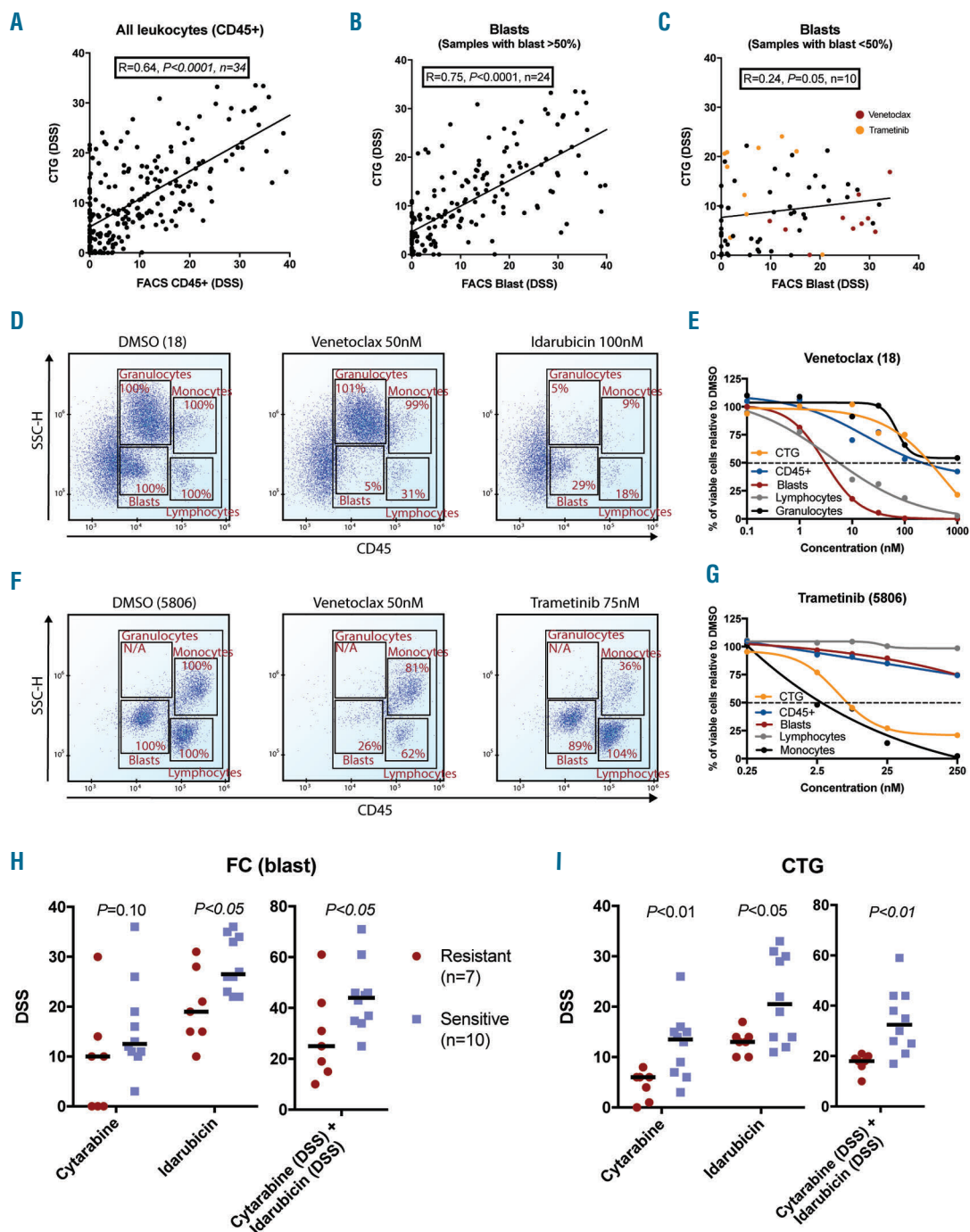
Figure 2. Comparison of flow cytometry (FC) and CellTiter-Glo (CTG) based drug screening approaches. (A) Spearman's correlation between CTG and FC-based cell viability assays with CD45+ leukocytes as the FC readout, or (B) blasts in samples with clinical blast count >50%, or (C) blasts in samples with clinical blast count <50% as the FC readout. (D) Representative FC scatter plots of drug effects on different cell populations in acute myeloid leukemia (AML) sample 18 with low blast count (20%). Absolute cell counts inside the gates were calculated after 72h drug treatment and normalized to the cell counts in the DMSO-treated wells (represented as percentages). (E) Venetoclax dose response curves of different cell populations present in acute monocytic leukemia (FAB M5) sample 18 assessed by FC and overall BM sensitivity with the CTG-based cell viability assay. (F) Representative FC scatter plots of drug effects on patient sample 5806 with FAB M5. (G) Dose response curves of different cell populations after MEK inhibitor trametinib treatment calculated with FC or overall sensitivity calculated with CTG. (H) Comparison of the drug sensitivity score (DSS) values for idarubicin, cytarabine and idarubicin+cytarabine combination in blasts between induction treatment resistant and sensitive patient samples using FC. (I) DSS measured with CTG from the same cohort. *P*-values calculated with Mann-Whitney U test.

this can be time consuming and enrichment might deplete cell populations such as monocytes that secrete cytokines important for blast cell survival and drug responses.[11–13]

To evaluate the *ex vivo* sensitivity of AML patient samples at a cell population level, we applied a multiplexed, 96-well format flow cytometry (FC)-based drug sensitivity assay. We compared this approach with the CTG-based cell viability assay to study potential inconsistencies between these two methods. Furthermore, we aimed to identify drugs and drug combinations that could effectively target leukemic blasts in physiologically relevant concentrations. In addition to standard of care drugs, cytarabine and idarubicin, we selected five Food and Drug Administration approved targeted small molecule inhibitors that have shown AML-selective responses in our earlier studies:[14,15] MEK inhibitor (trametinib), JAK1/2 inhibitor (ruxolitinib), mTORC1 inhibitor (everolimus), FLT3/broad range tyrosine kinase inhibitor (TKI, sunitinib) and Bcl-2 inhibitor (venetoclax). Most importantly, we demonstrate that targeted agents, particularly venetoclax, have different efficacies towards AML cells at distinct stages of myeloid differentiation.

Methods

Methods are described in more detail in the *Online Supplementary Material and Methods*.

Patient samples

BM samples from 34 AML patients and three healthy volunteers were obtained from the Helsinki University Hospital Comprehensive Cancer Center after informed consent (*permit numbers 239/13/03/00/2010, 303/13/03/01/2011, Helsinki University Hospital Ethics Committee*) and in compliance with the Declaration of Helsinki. The patient characteristics are presented in the *Online Supplementary Table S1*.

Preparation of drug plates

The compounds (*Online Supplementary Table S2*) were dispensed on 96-well V-bottom plates (Thermo Fisher Scientific, Carlsbad, CA) and 384-well plates (Corning, Corning, NY, USA) using an acoustic liquid handling device Echo 550 (Labcyte, Sunnyvale, CA). Drug plate layouts and concentrations are presented in *Online Supplementary Figure S1*. BM mononuclear cells (BM-MNC) were isolated using Ficoll-Paque Premium (GE Healthcare, Little Chalfont, Buckinhamshire, UK) density gradient centrifugation. Fresh or frozen BM-MNC were suspended in mononuclear cell

medium (MCM; PromoCell, Heidelberg, Germany) supplemented with 10 μg/mL gentamicin and 2.5 μg/mL amphotericin B and plated in parallel on pre-drugged 96-well plates (100,000 cells/well in 100 μl) for FC analysis and 384-well plates (10,000 cells/well in 25 μl) for CellTiter-Glo® (CTG)-based cell viability assay. The cells were incubated with the drugs for 72 hours at 37°C and 5% CO_2.

FC-based readouts

Following the 72-hour incubation with the drugs, cells were stained with an antibody mix (CD33, CD45, CD14, CD38 and CD34) followed by apoptosis (Annexin-V) and dead (7-AAD) cell staining. A detailed description of the methods is presented in *Online Supplementary Material and Methods* and the gating strategy is illustrated in Figure 1B.

Cell viability analysis using CellTiter-Glo®

Parallel to FC analysis, cell viability was measured with CellTiter-Glo® (CTG; Promega, Madison, WI) in 384-well plates as described earlier.[14] After the 72-hour incubation with the drugs, 25 μL CTG was added to each well. The luminescence signal was measured using a PHERAstar plate reader (BMG LABTECH, Ortenberg, Germany).

Calculation of the drug sensitivity (DSS) and drug combination scores

Ex vivo drug sensitivity of AML and healthy BM cells to the tested drugs was calculated using a DSS as previously described.[16] Drug combination efficacies were calculated as the difference between observed and expected values. The expected value is computed using the Bliss independence model[17] as reference, which assumes that two drugs exhibit their effect independently.[18]

Gene expression and pathway analysis

Publicly available microarray data from the Hemap data set[19,20] (*http://hemap.uta.fi/*) and RNA-seq data (RSEM values) from the TCGA Research Network[21] (*http://cancergenome.nih.gov/*) also included in the Hemap resource were used for gene expression and pathway analysis. Beat AML data[22] was used to assess the correlation between venetoclax drug sensitivity and *BCL2* family and monocytic/granulocytic differentiation marker gene expression. For the analysis of gene expression in healthy hematopoietic cell types Differentiation Map data was used.[23] Detailed methods are described in the *Online Supplementary Material and Methods*.

Statistical analysis

Statistical analysis was conducted with Graph Prism version 7.0 (GraphPad Software, San Diego, CA). Differences between drug responses were analyzed by Mann-Whitney U test, and for multi-

Table 1. Median drug sensitivity score (DSS) and IC50 values of the seven tested drugs against different cell populations.

| | Blasts (n=33) | | Monocytes (n=18) | | Lymphocytes (n=31) | | Granulocytes (n=5) | |
	DSS Median (Range)	IC50 (nM) Median (Range)	DSS Median (Range)	IC50 (nM) Median (Range)	DSS Median (Range)	IC50 (nM) Median (Range)	DSS Median (Range)	IC50 (nM) Median (Range)
Venetoclax	27.1 (0-43)	3.0 (1-1000)	7.1 (0-29)	122.0 (1-1000)	18.1 (9-30)	20.3 (2-84)	5.7 (0.3-9)	113 (11-220)
Idarubicin	22.0 (0-40.0)	28.7 (2-212)	16.1 (6-34)	78.7 (13-390)	16.5 (9-28)	84.0 (18-227)	19.0 (12-24)	41.1 (26-154)
Cytarabine	9.7 (0-36)	894.2 (50-10000)	7.5 (0-23)	1071 (20-10000)	4.8 (0-10)	2550 (43-10000)	9.5 (4-19)	953 (305-1189)
Ruxolitinib	5.0 (0-32)	302.7 (50-3000)	17.2 (0-37)	93.3 (60-2896)	0 (0-8)	2511 (99-10000)	0 (0.0-7)	2476 (246-3 000)
Trametinib	3.0 (0-27)	18.9 (1-250)	25.9 (0-42)	2.4 (1-250)	0 (0-1)	> 250 (7-250)	1.1 (0.0-7)	165 (15-250)
Sunitinib	1.0 (0-17)	321.1 (8-1000)	5.7 (3-22)	223.7 (71-423)	0 (0-4)	> 1000 (6-492)	4.4 (1-11)	352 (92-434)
Everolimus	0.0 (0-19)	55.6 (1-100)	4.6 (0-28)	7.5 (3-28)	0 (0-10)	> 100 (2.5-100)	0 (0.0-3)	> 100 (33-100)

ple *t*-tests *P*-values were adjusted using the Benjamin-Hochberg method (*P*<0.10 used to determine significance). The Kruskal-Wallis test was used when more than two groups were tested and significant comparisons were validated with *post-hoc* analysis (Dunn's test). Statistical dependence between two variables was assessed by Spearman's rank correlation.

Results

Analysis of the AML bone marrow compartment

To measure blast-specific drug responses in mononuclear cell (MNC) enriched BM AML samples, we tested 34 AML samples collected at diagnosis or relapse with seven drugs. Following a 72-hour drug treatment we analyzed the samples by both FC and CTG-based cell viability assays (Figure 1A). With the CTG assay we measured the overall BM-MNC sensitivity, while with the FC analysis the number of viable cells in different cell populations was measured. We used four cell surface markers (CD45,

CD34, CD33, CD14) to identify the major leukocyte populations present in the AML BM: leukemic blasts, immature granulocytes, promonocytes/monocytes and lymphocytes (Figure 1B). In the studied samples, the fraction of blasts out of CD45+ positive leukocytes varied between 17-92% and the lymphocyte population ranged from 1-49% (*Online Supplementary Table S3*). As expected, we observed high numbers of monocytic cells in FAB M4/5 samples, whereas M0/1 samples mainly consisted of blasts and lymphocytes (Figure 1C). After 72-hours in culture, we observed monocytic maturation in several M5 samples,[24] and in many samples the granulopoietic cell population diminished or was completely lost (*Online Supplementary Figure S2*).

FC *versus* homogeneous cell viability assay-based drug sensitivity profiling

In order to determine the correlation between drug sensitivity of the samples measured by FC or CTG-based methods, we converted the cell viability readouts from
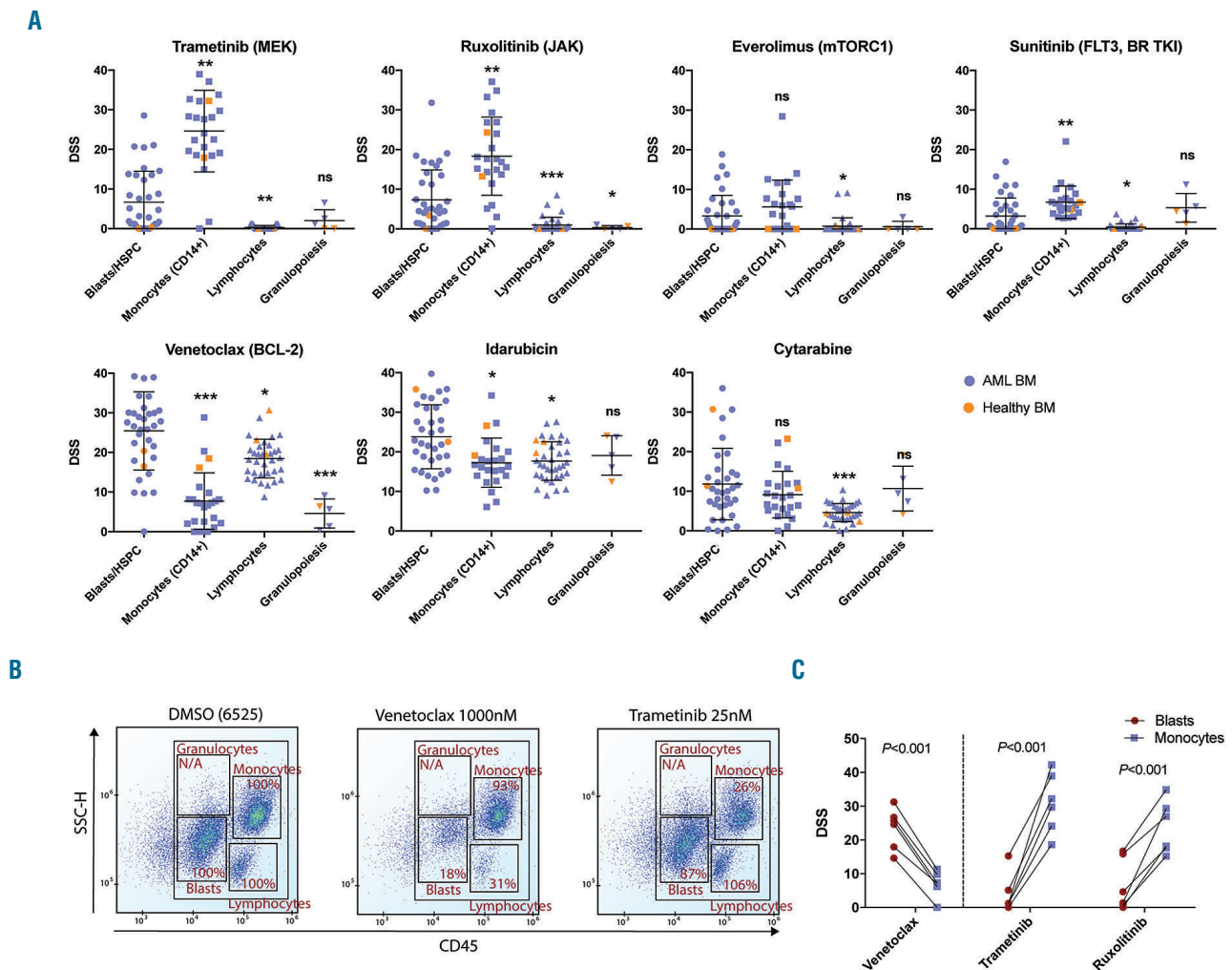
Figure 3. Maturation stage of acute myeloid leukemia (AML) cells affects drug sensitivities. (A) Drug sensitivity score (DSS) values for distinct cell populations in 33 AML samples (blue) and 2-3 healthy controls (orange). Cell population means were compared against blasts with Kruskal-Wallis test (Dunn's test, *P<0.05, **P<0.001, ***P<0.0001). (B) Representative flow cyometric (FC) scatter plots of the effects of venetoclax and trametinib on blasts, monocytic cells (CD14+) and lymphocytes after 72h drug treatment with the indicated concentrations. Absolute cell counts inside the gates were calculated after drug treatment and normalized to the cell counts in the DMSO-treatment wells (represented as percentages). (C) Inter- and intra-patient comparison of the DSS values in blasts and monocytic cell fraction calculated with Mann-Whitney U test. HSPC: healthy hematopoietic stem/progenitor cells.

each assay to DSS (a drug sensitivity metric based on area under the dose-response curve, higher DSS indicates higher sensitivity).[16] We observed a strong correlation between CTG and FC viability derived DSS when all live CD45^{+} leukocytes were used as the FC readout (R=0.64, $P<0.0001$, Figure 2A), and when the blast-specific drug responses were exclusively taken as the FC readout from samples with blast counts over 50% (R=0.75, $P<0.0001$, Figure 2B). However, we observed poor correlation between the FC and CTG results in a sample cohort with blast counts below 50% (R=0.24, $P=0.05$, Figure 2C). The most prominent differences were seen in the response to trametinib and venetoclax (*Online Supplementary Figure S3*). The poor correlation was partly due to highly different drug sensitivities of the non-blast cell populations compared to blasts as demonstrated in two samples with low blast counts (Figure 2D-G). Our data shows that AML BM subpopulations have heterogeneous drug responses that confound the assessment of blast specific drug sensitivities when using homogenous cell viability assays in unsorted BM-MNC samples.

Ex vivo drug screening predicts induction therapy response

Next, we evaluated whether incomplete BM blast clearance at day 14 and day 28 after induction treatment was associated with decreased *ex vivo* drug sensitivity. We evaluated BM samples from 15 patients collected prior to anthracycline+cytarabine induction chemotherapy. Amongst these patients, five had >10% blast cells at day 14 and/or day 28 and were defined as chemoresistant as described in the *Online Supplementary Table S1*. Additionally, we included samples from two patients resistant to induction (collected at the time of resistant disease) in the chemoresistant group. A combined DSS of cytarabine and idarubicin showed significantly lower values for the resistant patients both with FC and ($P<0.05$, 2H) and CTG ($P<0.01$, Figure 2I). Furthermore, we observed a significant difference between responders and non-responders when blast-specific idarubicin response was measured with FC ($P<0.05$, Figure 2H) or total sample sensitivity was measured with CTG ($P<0.05$, Figure 2I). These results are in line with a recent study demonstrating that a similar FC-based platform can predict induction therapy response in a larger AML cohort.[25]

Blasts are highly sensitive to Bcl-2 inhibition whereas monocytes and granulocytes are resistant

Using the FC approach, we were able to evaluate blast-specific drug responses and compare them to other cell types within the same or between samples. Amongst the seven tested drugs, venetoclax (IC50=3.0nM) and idarubicin (IC50=28.7nM) showed the highest toxicity against blasts (Table 1). However, between these two drugs venetoclax showed the most selective efficacy against blasts when compared to other cell populations and healthy CD34^{+} cells (Figure 3A, IC50 values in the *Online Supplementary Figure S4*). Moreover, venetoclax was also effective against CD34^{+}CD38^{−} cells, which suggests activity against leukemic stem cells (*Online Supplementary Figure 5*). Compared to blasts, monocytic cells (CD14^{+}) were highly resistant to Bcl-2 inhibition ($P<0.001$, Mann-Whitney U test), but sensitive to MEK and JAK inhibition ($P<0.001$, Figure 3A). The phenomenon was clearly observed in samples from patients diagnosed with acute monocytic leukemia (M5) that contained substantial fractions of both cell types (Figure 3B-C).

Overall BM AML sample sensitivity to venetoclax is associated with FAB subtype

To follow-up on our findings, we hypothesized that AML samples with a high monocytic cell content should have a distinct drug response profile when overall BM-MNC sensitivity is measured with the CTG assay. We re-analyzed our earlier published CTG-based drug sensitivity data of 37 AML samples comprised of FAB M1, M2, M4 and M5 samples that were screened with 296 compounds.[14,15] Amongst the 296 compounds, venetoclax showed the largest drug sensitivity difference between M1 and M5 AML ($P<0.001$, *Online Supplementary Table S4*, Figure 4A). Similarly, the CTG-based sensitivity of the AML sample cohort studied here showed a gradual decrease in venetoclax sensitivity from M0 towards M5 subtype (Figure 4B). When we limited our FC analysis to diagnostic samples, a significant but smaller difference in blast-specific venetoclax sensitivity was also associated with FAB subtype ($P<0.05$, Figure 4C). This significance was not observed when we also included relapse and chemorefractory samples in the analysis (Figure 4D) largely due to a high number of chemorefractory M1/2 samples in our cohort that were more resistant to venetoclax ($P<0.001$, Figure 4D-E). Taken together, monocytic cells blur the high blast specific venetoclax effect in Ficoll-enriched M4/5 samples when measured with CTG but FAB subtype still has a significant effect on venetoclax response in blasts in our diagnosis AML sample cohort.

FAB subtype is associated with *BCL2* and *MCL1* gene expression

Anti-apoptotic Mcl-1 and Bcl-2 are considered the most important pro-survival factors in AML.[26,27] Furthermore, their expression and phosphorylation has been shown to be regulated through the Ras/Raf/MEK/ERK, PI3K/PTEN/AKT and JAK/STAT signal transduction pathways in different leukemias.[28–31] To study whether the expression of *BCL2* family members and activity of signal transduction pathways is associated with FAB subtypes, we analyzed gene expression data of MNC of diagnosis AML samples using publicly available microarray and RNA-seq data. *BCL2* was highly expressed in M0/1 AML and gradually decreased towards M5 samples and healthy monocytes (Figure 5A, *Online Supplementary Figure S6*). Notably, *MCL1* showed an opposite trend in expression and was most highly expressed in healthy monocytes (Figure 5A). We also detected higher expression of *BCL2A1, BCL2L11 (BIM), BID* and *JAK2* in M4/5 AML. A more detailed analysis of the healthy myeloid compartment revealed that *BCL2* family expression is highly dependent on differentiation stage, which likely also influences the expression patterns seen between the different FAB subtypes (Figure 5B). Interestingly, high *BCL2* and low *MCL1* expression was also observed in FAB M3 AML and their healthy counterparts, colony forming unit (CFU) granulocytes (Figure 5A-B). High *BCL2/MCL1* expression ratio in CFU granulocytes might explain the neutropenia seen in venetoclax treated patients.

Next, we investigated whether common cytogenetic abnormalities (*RUNX1-RUNX1T1, CBFB-MYH11, MLL, PML-RARA*) or mutations (*FLT3, NPM1, RUNX1, CEBPA*) explain some of the variations we observed in *MCL1*,

BCL2 or *BCL-xL* gene expression within FAB subgroups (*Online Supplementary Figure S7*). AML samples with *RUNX1T1-RUNX1T1* fusions showed significantly different gene expression exclusively in the M2 subgroup while samples with *MLL* or *CBFB-MYH11* fusions showed significantly different gene expression exclusively in the M4 subgroup (Figure 5C, *Online Supplementary Table S5*). Particularly, M4 samples with MLL fusions had high *BCL2* but low *MCL1* expression levels compared to other M4 samples. To assess whether major signal transduction pathways are differentially active in FAB subtypes, we performed gene set enrichment analysis (GSEA). The

analysis revealed significant enrichment of gene sets associated with inflammatory signaling and IL6/JAK/STAT pathway in M4/5 AML (Figure 5D-E, *Online Supplementary Table S6*).

To study whether *ex vivo* venetoclax response is associated with differentiation markers and *BCL2* family expression, we analyzed the published Beat AML data set which includes data from 562 AML patients.[22] Supporting our previous findings, samples that had high expression of monocytic/granulocytic cell markers (CD14, CD11b, CD86, CD68) were resistant to venetoclax (Figure 5F). High *BCL2* expression was associated with venetoclax
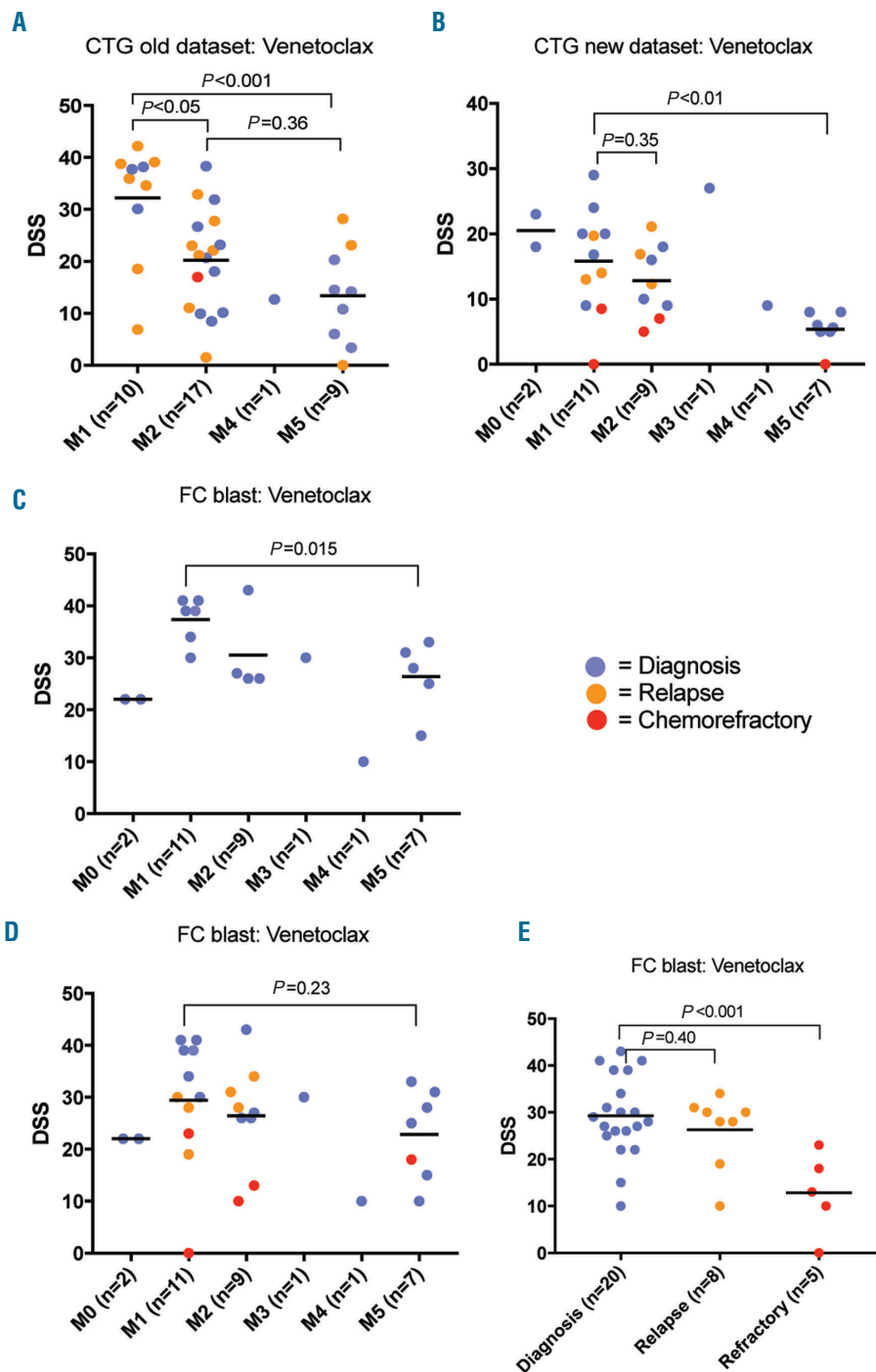
Figure 4. Mononuclear cell (MNC) fraction sensitivity to venetoclax is dependent on FAB subtypes. (A) Venetoclax drug sensitivity score (DSS) values of AML samples with different French-American-British (FAB) subtypes from an earlier published data set, and (B) from the present data set both measuring MNC fraction sensitivity with CTG based cell viability assay. (C) Blast-specific venetoclax sensitivity of diagnosis samples in FAB subgroups measured by FC from the present data set. (D) Blast-specific venetoclax sensitivity in different FAB subgroups measured by FC including chemorefractory and relapse samples. (E) Comparison of venetoclax DSS values between diagnosis, relapse and chemorefractory samples (induction resistant n=3, azacytidine resistant n=2). Black lines represent the mean of each subgroup. *P*-values calculated with the Kruskal-Wallis (and Dunn's) tests. FC: flow cytometric.
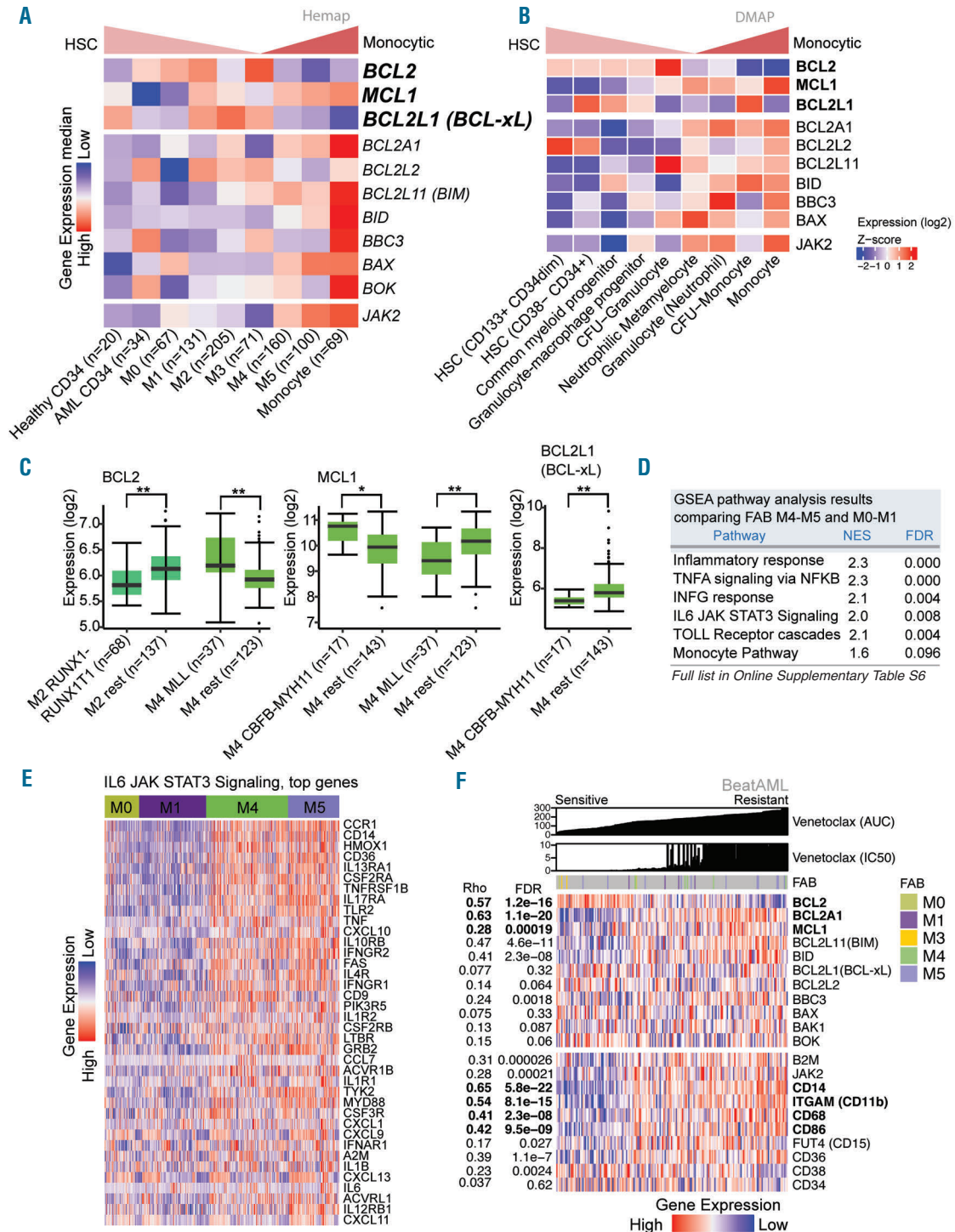
Figure 5. Cell differentiation is associated with low *BCL2* expression and venetoclax *ex vivo* resistance. (A) Heatmap of the median gene expression for each French-British-American (FAB) class and control samples are shown for *BCL2* family genes in the Hemap acute myeloid leukemia (AML) data set. Sample groups are ordered based on the differentiation state between HSC and healthy monocytes. *Z*-scores were used to define high and low expression categories. Z-scores were further discretized to low and high categories, defined as having *Z*-score cutoff over 2 for high and less than -2 for low expression. *P*-values for FAB subgroup comparisons are presented in the *Online Supplementary Table S5*. Similar analysis for TCGA data set is presented in the *Online Supplementary Figure S6*. (B) Heatmap of the median gene expression of *BCL2* family genes for healthy hematopoietic cell types using Differentiation Map data set. (C) Significant *BCL2, MCL1* or *BCL-xL* gene expression differences between samples with *MLL, CBFB-MYH11* or *RUNX1-RUNX1T1* fusion genes when compared to non-fusion gene containing samples in FAB M2 and M4 groups. Values obtained from the Hemap data set. **P*-value<0.05, **P*-value<0.001. (D) Pathway enrichment results with normalized enrichment score (NES) and significance as false discovery rate (FDR) *q*-value are shown for pathways upregulated in M4 and M5 samples when compared to M0 and M1 samples. Pathways consistently enriched in both Hemap and TCGA data sets are shown here, while full results are shown in the *Online Supplementary Table S6*. (E) Heatmap of IL6-JAK-STAT3 signaling pathway leading edge gene expression Z-scores using the Hemap data set. Z-scores were further discretized to low and high categories, defined as having Z-score cutoff over 2 for high and less than -2 for low expression. Samples are ordered based on FAB type. (F) Venetoclax drug response AUC and IC50 profiles, *BCL2* family genes and differentiation marker gene expression value Z-scores and FAB subtypes are shown as a heatmap. Samples are ordered based on drug sensitivity with sensitive samples on the left and resistant on the right. Pearson correlation Rho and FDR value is shown for each gene.

sensitivity whereas high *MCL1* and *BCL2A1* expression was associated with resistance (Figure 5F). These findings were also presented earlier by two different research groups.[32,33]

Taken together, the gene expression data of mononuclear cell enriched AML samples indicate that M4/5 AML have low *BCL2* but high *MCL1* and *BCL2A1* expression and increased inflammatory signaling. Thus, the data support the decreased venetoclax sensitivity we observed with the total mononuclear cell fraction of M4/5 samples.

MEK and JAK inhibitors sensitize venetoclax-resistant blast cells to venetoclax

Next, we studied whether mutations might explain the observed differences in blast specific venetoclax respons-es, but no significant correlation between genetic lesions and venetoclax response in our limited patient cohort was found (*Online Supplementary Table S7*). However, as demonstrated earlier, we detected decreased venetoclax sensitivity in chemorefractory and M5 samples (*Online Supplementary Table S7*, Figure 4A-E). When we divided the AML samples into two subgroups (sensitive DSS 21-43, IC50<20nM and resistant DSS 0-21, IC50>20nM) from the mid-point of the venetoclax response range, we noticed that resistant blasts were sensitive to either MEK and/or JAK inhibitors (Figure 6A). This finding suggests that venetoclax resistant blasts rely on either JAK/STAT and/or MAPK pathways. Furthermore, venetoclax sensitive blasts were enriched for *NPM1* (8 of 25, 32% in sen-
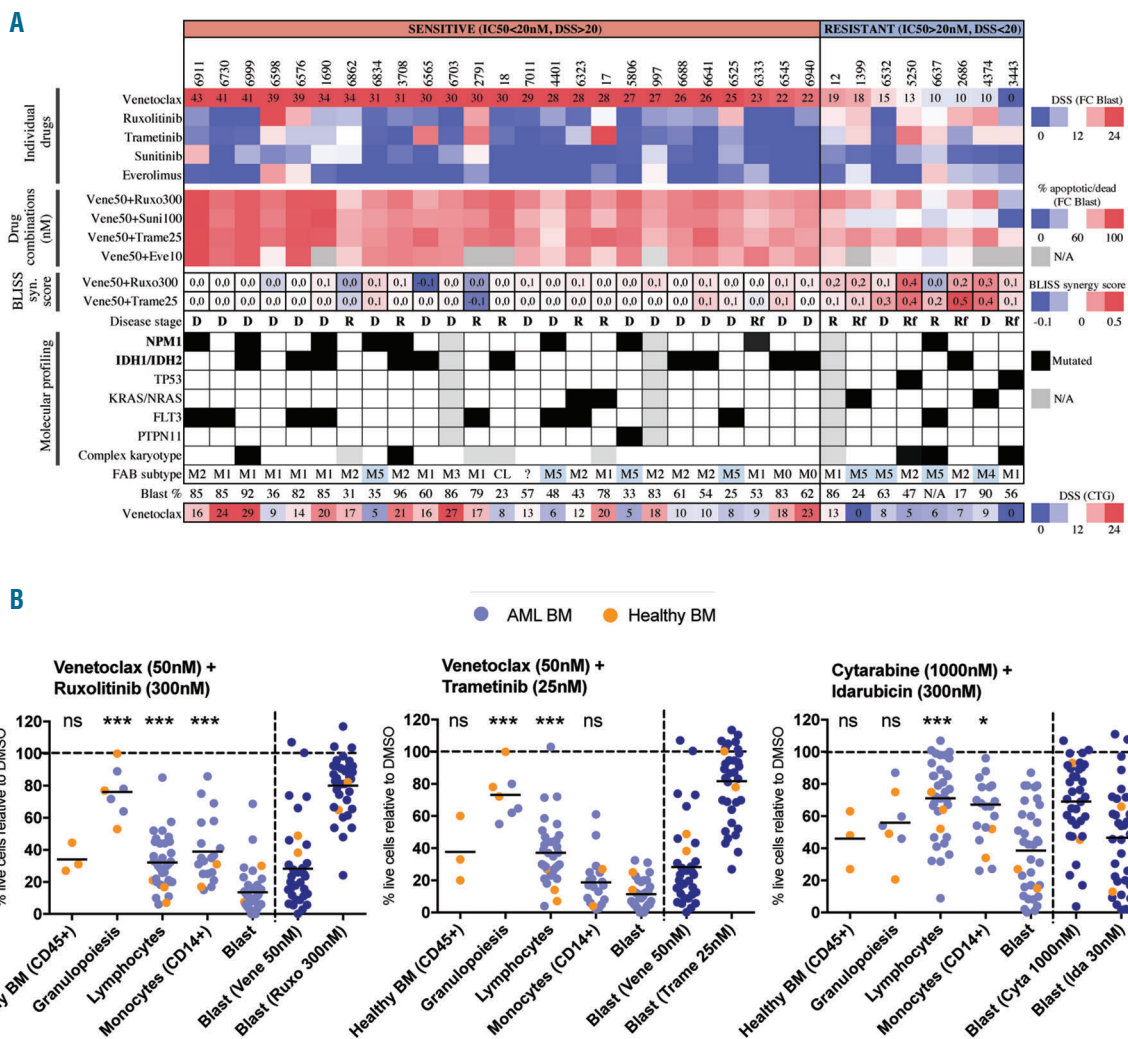
Figure 6. Inhibition of MEK and JAK pathways can overcome venetoclax resistance. (A) Heatmap showing characteristics of venetoclax sensitive (IC50<20nM, DSS>20) and resistant blasts (IC50>50nM, DSS<20) based on single agent venetoclax response measured by flow cytometry (FC) (top row). Blast-specific response of individual drugs is highlighted according to drug sensitivity score (DSS) values with red corresponding to high DSS value and blue to low DSS value. Blast-specific response to venetoclax combinations is highlighted according to percentage of apoptotic/dead cells with red corresponding to high percentage and blue to low percentage of apoptotic/dead cells. The synergistic effect of the drug combination was assessed based on the BLISS synergistic score and is shown in the graph. Other characteristics covered include disease stage, molecular profiling, French-American-British (FAB) subtype with M4 and M5 highlighted blue and FC-determined blast percentage. Overall BM venetoclax sensitivity measured with CellTiter-Glo (CTG) (bottom row) is used to demonstrate how low blast cell percentage affects DSS values when compared to blast-specific DSS values. (B) Dot scatter plots of venetoclax (50nm) + ruxolitinib (300nM), venetoclax (50nM) + trametinib (25nM), and cytarabine (1000nM) + idarubicin (30nM) responses in healthy CD45+ leukocytes, granulopoietic cells, lymphocytes, monocytes and blasts. Orange dots represent healthy BM samples and light blue dots acute myeloid leukemia (AML) samples. Dark blue dots represent single agent toxicity to blasts. Cell population means were compared against blasts with the Kruskal-Wallis test (Dunn's test, *P<0.05, **P<0.001, ***P<0.0001). R: relapse; Rf: refractory; CMML: chronic myelomonocytic leukemia; CL: CMML transitioned to AML.

sitive and 1 of eight, 12.5% in resistant) and *IDH1/IDH2* (10 of 25, 40% in sensitive and 1/8, 12.5% in resistant) mutations supporting the good clinical activity of venetoclax seen in this patient group (Figure 6A, *Online Supplementary Table S7*).

To assess the efficacy and clinical relevancy of 27 drug combinations against blasts, we used concentrations achieved in patients' plasma during treatment. The results demonstrated prominent inter-patient variability with the most synergistic drug combinations when blast-specific drug responses were measured by FC (*Online Supplementary Figure S8*). Of the 27 tested drug combinations, venetoclax plus kinase inhibitors showed the highest average synergistic and blast killing effect (Table 2, higher BLISS score and lower mean % live blasts). Importantly, blasts were highly sensitive to single-agent venetoclax in 76% (25 of 33) of the samples with IC50<20nM. Thus, we did not observe synergy in the majority of the samples with a single venetoclax concentration of 50nM as this concentration alone was sufficient to kill the blasts (Figure 5A). To study the drug combination effect in more detail, we conducted additional drug testing of venetoclax with a more detailed concentration range on four AML samples. We observed that with lower venetoclax concentrations (10nM) a synergistic effect with MEK and/or JAK inhibitors was also detected in samples that were sensitive to single agent 50nM venetoclax treatment (*Online Supplementary Figure S9*).

Importantly, venetoclax (50nM) plus ruxolitinib (300nM) showed high efficacy (apoptosis/death>70%) and synergism in 6 of eight venetoclax resistant samples (Figure 5A-B). Strikingly, by combining venetoclax (50nM) with trametinib (25nM), all venetoclax resistant blasts were effectively targeted (Figure 6A-B). Although the combinations showed substantial toxicity to healthy CD34^{+} cells, they targeted most effectively leukemic blasts (Figure 6B). As a comparison, a drug combination used during induction treatment (cytarabine+idarubicin) showed remarkable inter-patient differences in blast toxicity and it was also toxic to healthy CD34^{+} cells (Figure 6B). Furthermore, the broad-spectrum tyrosine kinase and FLT3 inhibitor sunitinib (100nM) or mTOR inhibitor everolimus (10nM) were not as effective when combined with venetoclax (Figure 6A, Table 2). Our data demonstrate that by simultaneously inhibiting JAK and/or MEK signaling and Bcl-2, blast cells involving chemorefractory AML cells, can be effectively targeted *ex vivo* in physiologically relevant concentrations.

Table 2. Drug combination synergism and combination sensitivity in blasts.

Drug I	Drug II	Drug III	Mean BLISS score*	Mean % of live blasts**
Venetoclax 50nM	Trametinib 25nM		0.083	11.3
Cytarabine 300nM	Trametinib 25nM		0.076	56.7
Trametinib 25nM	Everolimus 10nM		0.075	62.9
Venetoclax 50nM	Ruxolitinib 300nM		0.068	13.4
Idarubicin 10nM	Trametinib 25nM		0.057	51.3
Trametinib 25nM	Ruxolitinib 300nM		0.046	59.7
Venetoclax 50nM	Everolimus 10nM		0.040	18.6
Sunitinib 100nM	Trametinib 25nM		0.034	69.0
Venetoclax 50nM	Sunitinib 100nM		0.030	21.8
Idarubicin 10nM	Ruxolitinib 300nM		0.029	61.8
Venetoclax 50nM	Cytarabine 300nM		0.023	19.6
Sunitinib 100nM	Ruxolitinib 300nM		-0.004	73.3
Sunitinib 100nM	Everolimus 10nM		-0.001	80.8
Everolimus 10nM	Ruxolitinib 300nM		-0.018	73.9
Cytarabine 300nM	Sunitinib 100nM		-0.020	75.9
Idarubicin 10nM	Cytarabine 300nM		-0.026	64.9
Idarubicin 30nM	Cytarabine 1000nM		-0.029	40.1
Idarubicin 10nM	Everolimus 10nM		-0.038	69.5
Cytarabine 300nM	Everolimus 10nM		-0.046	80.1
Everolimus 10nM	Ruxolitinib 300nM	Trametinib 25nM	-0.051	52.4
Cytarabine 300nM	Ruxolitinib 300nM		-0.058	72.2
Sunitinib 100nM	Everolimus 10nM	Ruxolitinib 300nM	-0.067	63.8
Idarubicin 10nM	Ruxolitinib 300nM	Trametinib 25nM	-0.073	39.6
Idarubicin 10nM	Sunitinib 100nM		-0.088	74.7
Cytarabine 300nM	Ruxolitinib 300nM	Everolimus 10nM	-0.123	62.5
Cytarabine 300nM	Ruxolitinib 300nM	Trametinib 25nM	-0.129	54.4
Idarubicin 10nM	Ruxolitinib 300nM	Everolimus 10nM	-0.146	57.3

*Synergism calculated using BLISS score **Normalized to DMSO treated cells.

Discussion

With FC-based drug testing we were able to simultaneously measure drug sensitivities of different cell populations in primary AML BM samples. Monocytic cells abundantly present in FAB M4/5 AML were markedly resistant to the Bcl-2 inhibitor venetoclax, while less differentiated blast cells in the same M4/5 samples or in M0/1/2 samples were sensitive. Accordingly, the overall BM-MNC sensitivity to venetoclax was strongly influenced by FAB subtype. Our study shows that FC-based, phenotypic drug testing can improve the current understanding of *ex vivo* drug effects and may help to identify blast-specific treatments for AML patients.

Along with our previous studies, several other groups have evaluated *ex vivo* drug responses of Ficoll-enriched AML mononuclear cells using high-throughput CTG or MTS based cell viability assays.[14,34–36] While these assays provide fast and robust readouts they fail to accurately measure blast specific drug responses. By using more accurate microscopy based screening, Snijder *et al.* have recently demonstrated that blast specific or relative blast fraction-based readouts increase predictive accuracy to treatment outcome.[37] Similarly, Martinéz-Cuadrón *et al.* showed that a FC-based platform measuring blast specific effect in whole BM without MNC enrichment, predicted clinical response to induction therapy.[25] We also showed earlier that in chronic myeloid leukemia, CD34-depleted cells (mature granulopoietic cells) were insensitive to BCR-ABL-1 inhibitors *ex vivo* whereas CD34+ progenitor cells showed good sensitivity.[38] In accordance, we demonstrate here with a FC-based approach that blasts differ in their drug sensitivities in comparison to other cell populations in the same AML samples. The highest blast-specific efficacy was observed with venetoclax, whereas ruxolitinib and trametinib showed increased activity towards monocytic cells. Importantly, we demonstrate that in samples with a low blast count, the overall mononuclear cell fraction sensitivity does not correlate well with the blast-specific drug sensitivity.

Consistent with our results, earlier studies have shown that primary AML samples are sensitive to venetoclax *ex vivo*.[15,39,40] Most of the studies have used mononuclear cell fractions to assess cell viability and to measure protein and gene expression levels. We observed that mononuclear cells of M0/1 samples that mainly consisted of blasts, were sensitive to venetoclax compared to mononuclear cells of M4/5 samples when using a homogenous CTG-based cell viability assay. Earlier, high *ex vivo* sensitivity to Bcl-2 inhibition has been associated with M3 AML in a study by Niu *et al.*, whereas Pan *et al.* found no associations with FAB subtypes.[39,40] Importantly, both study cohorts lacked comprehensive spectra of different subtypes, with none or only one M0/1 AML case. To support our observation, mononuclear cells of M0/1 samples had a high *BCL2/MCL1* gene expression ratio whereas M4/5 samples had a low ratio. Increased Bcl-2 protein expression has also been reported in M0/1 AML,[41] and increased Mcl-1 expression in M4/5 AML[26] of which the latter has been linked to elevated Mcl-1 expression in differentiating monocytes.[42] Accordingly, we observed high *MCL1* and *BCL2A1* but low *BCL2* expression in healthy monocytic and granulocytic cell populations.

By using a FC-based approach, we observed that several M5 samples contained venetoclax-sensitive blasts and a resistant monocytic cell fraction. This observation raises the question whether drug sensitivity profiling and gene/protein expression studies should focus on the immature blast cells and not the total MNC fraction especially in in M4/5 samples and samples with low blast count. When we compared the FC measured blast-specific venetoclax response between FAB subtypes, we observed a smaller but still significant difference between diagnosis M1 *versus* M5 subgroups. In clinical trials, *NPM1, IDH1/2* and *RUNX1* mutations have shown to be promising biomarkers for venetoclax+HMA treatment.[7,43] Based on a study analyzing genotype and FAB subtype-specific patterns of 4,373 adult *de novo* AML cases,[44] both *IDH1/2* and *RUNX1* mutations are enriched in M0/1/2 AML whereas *NPM1* mutations are common in FAB M1/2/4/5 subtypes. Therefore, patient cohorts with mutated *IDH1/2* or *RUNX1* may be skewed to contain larger numbers of FAB M0/1/2 samples. To identify responders, it might be useful to evaluate the combined genetic and cell phenotype/FAB subtype information in a clinical setting.

With the FC method we also looked for effective combinations, since an overall response rate of only 19% was observed with venetoclax monotherapy in patients with high-risk relapsed/refractory (R/R) AML.[6] In our study, all venetoclax-resistant blasts showed sensitivity to MEK and/or JAK inhibitors suggesting that JAK/STAT and MAPK pathways play a major role in venetoclax resistance. We showed earlier that stromal cell secreted cytokines such as GM-CSF mediate resistance to venetoclax, which can be counteracted by JAK inhibition.[45] Moreover, the MAPK pathway plays a critical role in resistance through the proposed upregulation of *MCL1*.[28] Both of these studies also demonstrated remarkable antileukemic activity in murine xenograft models when inhibiting JAK or MEK kinases together with *Bcl-2*. In agreement with the good synergism between ruxolitinib or trametinib with venetoclax observed here and in a recent study by the Beat AML study group,[46] Kurtz *et al.* additionally showed that several different kinase inhibitors exhibited good synergism with venetoclax in AML samples.[47] However, a recent clinical study with MEK inhibitor cobimetinib and venetoclax in R/R AML was closed due to limited clinical activity demonstrating that *ex vivo* drug screening results might not directly translate into a clinical setting.[48]

Inflammatory pathways are more active in M4/5 AML based on GSEA, consistent with the observed high sensitivity of monocytic cells to ruxolitinib and trametinib. Earlier studies have demonstrated that leukemic cells of patients with M4/5 AML produce IL1/IL6[13] and have a higher proliferative activity in cytokine-free medium.[49] Thus, secreted cytokines and culturing conditions may have a big impact on the drug sensitivity profiles. While further investigation is warranted, results suggest that the JAK/STAT and MEK pathways are more active in differentiated monocytic cells as well as in venetoclax resistant blasts.

In summary, we show that *ex vivo* sensitivity of AML patient samples to venetoclax is associated with cell composition. Furthermore, we demonstrate that FC-based drug screening could be implemented to identify effective targeted drugs and drug combinations against immature blasts, accelerating drug discovery and individualizing therapy for AML patients.

References

1. Tauro S. The blind men and the AML elephant: can we feel the progress? Blood Cancer J. 2016;6(5):e424.
2. Döhner H, Weisdorf DJ, Bloomfield CD. Acute meloid leukemia. N Engl J Med. 2015;373(12):1136-1152.
3. Stone RM, Mandrekar SJ, Sanford BL, et al. Midostaurin plus chemotherapy for acute myeloid leukemia with a FLT3 mutation. N Engl J Med. 2017;377(5):454-464.
4. DiNardo CD, Stein EM, de Botton S, et al. Durable Remissions with ivosidenib in IDH1-mutated relapsed or refractory AML. N Engl J Med. 2018;378(25):2386-2398.
5. Stein EM, DiNardo CD, Pollyea DA, et al. Enasidenib in mutantIDH2relapsed or refractory acute myeloid leukemia. Blood. 2017;130(6):722-731.
6. Konopleva M, Pollyea DA, Potluri J, et al. Efficacy and biological correlates of response in a Phase II Study of venetoclax monotherapy in patients with acute myelogenous leukemia. Cancer Discov. 2016;6(10):1106-1117.
7. DiNardo CD, Pratz K, Pullarkat V, et al. Venetoclax combined with decitabine or azacitidine in treatment-naive, elderly patients with acute myeloid leukemia. Blood. 2019;133(1):7-17.
8. Bennett JM, Catovsky D, Daniel MT, et al. Proposals for the classification of the acute leukaemias. French-American-British (FAB) co-operative group. Br J Haematol. 1976;33(4):451-458.
9. Bonnet D, Dick JE. Human acute myeloid leukemia is organized as a hierarchy that originates from a primitive hematopoietic cell. Nat Med. 1997;3(7):730-737.
10. Riss TL, Moravec RA, Niles AL, et al. Cell viability assays. Eli Lilly & Company and the National Center for Advancing Translational Sciences.
11. Panoskaltsis N, Reid CDL, Knight SC. Quantification and cytokine production of circulating lymphoid and myeloid cells in acute myelogenous leukaemia1. Leukemia. 2003;17(4):716-730.
12. Carey A, Edwards DK, Eide CA, et al. Identification of interleukin-1 by functional screening as a key mediator of cellular expansion and disease progression in acute myeloid leukemia. Cell Rep. 2017;18(13):3204-3218.
13. van der Schoot C, Jansen P, Poorter M, et al. Interleukin-6 and interleukin-1 production in acute leukemia with monocytoid differentiation. Blood. 1989;74(6):2081-2087.
14. Pemovska T, Kontro M, Yadav B, et al. Individualized systems medicine strategy to tailor treatments for patients with chemorefractory acute myeloid leukemia. Cancer Discov. 2013;3(12):1416-1429.
15. Kontro M, Kumar A, Majumder MM, et al. HOX gene expression predicts response to BCL-2 inhibition in acute myeloid leukemia. Leukemia. 2017;31(2):301-309.
16. Yadav B, Pemovska T, Szwajda A, et al. Quantitative scoring of differential drug sensitivity for individually optimized anticancer therapies. Sci Rep. 2014;4:5193.
17. BLISS CI. The toxicity of poisons applied jointly11. Ann Appl Biol. 1939;26(3):585-615.
18. Zhao W, Sachsenmeier K, Zhang L, Sult E, Hollingsworth RE, Yang H. A new bliss independence model to analyze drug combination data. J Biomol Screen. 2014;19(5):817-821.
19. Pölönen P, Mehtonen J, Lin J, et al. Hemap: An interactive online resource for characterizing molecular phenotypes across hematologic malignancies. Cancer Res. 2019;79(10):2466-2479.
20. Mehtonen J, Pölönen P, Häyrynen S, et al. Data-driven characterization of molecular phenotypes across heterogeneous sample collections. Nucleic Acids Res [Epub ahead of print].
21. Network TCGAR. Genomic and epigenomic landscapes of adult de novo acute myeloid leukemia. N Engl J Med. 2013;368(22):2059-2074.
22. Tyner JW, Tognon CE, Bottomly D, et al. Functional genomic landscape of acute myeloid leukaemia. Nature. 2018;562(7728):526-531.
23. Novershtern N, Subramanian A, Lawton LN, et al. Densely interconnected transcriptional circuits control cell states in human hematopoiesis. Cell. 2011;144(2):296-309.
24. Salem M, Delwel R, Mahmoud LA, Clark S, Elbasousy EM, Löwenberg B. Maturation of human acute myeloid leukaemia in vitro: the response to five recombinant haematopoietic factors in a serum-free system. Br J Haematol. 1989;71(3):363-370.
25. Martínez-Cuadrón D, Gil C, Serrano J, et al. A precision medicine test predicts clinical response after idarubicin and cytarabine induction therapy in AML patients. Leuk Res. 2019;76:1-10.
26. Teh T-C, Nguyen N-Y, Moujalled DM, et al. Enhancing venetoclax activity in acute myeloid leukemia by co-targeting MCL1. Leukemia. 2018;32(2):303-312.
27. Glaser SP, Lee EF, Trounson E, et al. Antiapoptotic Mcl-1 is essential for the development and sustained growth of acute myeloid leukemia. Genes Dev. 2012;26(2):120-125.
28. Konopleva M, Milella M, Ruvolo P, et al. MEK inhibition enhances ABT-737-induced leukemia cell apoptosis via prevention of ERK-activated MCL-1 induction and modulation of MCL-1/BIM complex. Leukemia. 2012;26(4):778-787.
29. Wang JM, Chao JR, Chen W, Kuo ML, Yen JJ, Yang-Yen HF. The antiapoptotic gene mcl-1 is up-regulated by the phosphatidylinositol 3-kinase/Akt signaling pathway through a transcription factor complex containing CREB. Mol Cell Biol. 1999;19(9):6195-206.
30. Shenoy AR, Kirschnek S, Häcker G. IL-15 regulates Bcl-2 family members Bim and Mcl-1 through JAK/STAT and PI3K/AKT pathways in T cells. Eur J Immunol. 2014;44(8):2500-2507.
31. Faderl S, Harris D, Van Q, Kantarjian HM, Talpaz M, Estrov Z. Granulocyte-macrophage colony-stimulating factor (GM-CSF) induces antiapoptotic and proapoptotic signals in acute myeloid leukemia. Blood. 2003;102(2):630-637.
32. Zhang H, Wilmot B, Bottomly D, et al. Biomarkers predicting venetoclax sensitivity and strategies for venetoclax combination treatment. Blood. 2018;132(Suppl 1):175.
33. White BS, Khan SA, Ammad-ud-din M, et al. Comparative Analysis of independent ex vivo functional drug screens identifies predictive biomarkers of BCL-2 inhibitor response in AML. Blood. 2018;132(Suppl 1):2763.
34. Tyner JW, Yang WF, Bankhead A, et al. Kinase Pathway Dependence in Primary Human Leukemias Determined by Rapid Inhibitor Screening. Cancer Res. 2013;73(1):285-296.
35. Dietrich S, Oleś M, Lu J, et al. Drug-perturbation-based stratification of blood cancer. J Clin Invest. 2018;128(1):427-445.
36. Swords RT, Azzam D, Al-Ali H, et al. Ex-vivo sensitivity profiling to guide clinical decision making in acute myeloid leukemia: A pilot study. Leuk Res. 2018;64:34-41.
37. Snijder B, Vladimer GI, Krall N, et al. Image-based ex-vivo drug screening for patients with aggressive haematological malignancies: interim results from a single-arm, open-label, pilot study. Lancet Haematol. 2017;4(12):e595-e606.
38. Pietarinen PO, Eide CA, Ayuda-Durán P, et al. Differentiation status of primary chronic myeloid leukemia cells affects sensitivity to BCR-ABL1 inhibitors. Oncotarget. 2017;8(14):22606-22615.
39. Niu X, Wang G, Wang Y, et al. Acute myeloid leukemia cells harboring MLL fusion genes or with the acute promyelocytic leukemia phenotype are sensitive to the Bcl-2-selective inhibitor ABT-199. Leukemia. 2014;28(7):1557-1560.
40. Pan R, Hogdal LJ, Benito JM, et al. Selective

BCL-2 inhibition by ABT-199 causes on-target cell death in acute myeloid leukemia. Cancer Discov. 2014;4(3):362-375.

41. Bogenberger JM, Kornblau SM, Pierceall WE, et al. BCL-2 family proteins as 5-Azacytidine-sensitizing targets and determinants of response in myeloid malignancies. Leukemia. 2014;28(8):1657-1665.

42. Yang T, Kozopas KM, Craig RW. The intracellular distribution and pattern of expression of Mcl-1 overlap with, but are not identical to, those of Bcl-2. J Cell Biol. 1995;128(6):1173-1184.

43. DiNardo CD, Rausch CR, Benton C, et al. Clinical experience with the BCL2-inhibitor venetoclax in combination therapy for relapsed and refractory acute myeloid leukemia and related myeloid malignancies. Am J Hematol. 2018;

93(3):401-407.

44. Rose D, Haferlach T, Schnittger S, Perglerová K, Kern W, Haferlach C. Subtype-specific patterns of molecular mutations in acute myeloid leukemia. Leukemia. 2017;31(1):11-17.

45. Karjalainen R, Pemovska T, Popa M, et al. JAK1/2 and BCL2 inhibitors synergize to counteract bone marrow stromal cell–induced protection of AML. Blood. 2017;130(6):789-802.

46. Kurtz SE, Eide CA, Kaempf A, et al. Dual inhibition of JAK1/2 kinases and BCL2: a promising therapeutic strategy for acute myeloid leukemia. Leukemia. 2018; 32(9):2025-2028.

47. Kurtz SE, Eide CA, Kaempf A, et al. Molecularly targeted drug combinations

demonstrate selective effectiveness for myeloid- and lymphoid-derived hematologic malignancies. Proc Natl Acad Sci U S A. 2017;114(36):E7554-E7563.

48. Daver N, Pollyea DA, Yee KWL, et al. Preliminary results from a Phase Ib study evaluating BCL-2 inhibitor venetoclax in combination with MEK inhibitor cobimetinib or MDM2 inhibitor idasanutlin in patients with relapsed or refractory (R/R) AML. Blood. 2017;130(Suppl 1):813.

49. Lowenberg B, van Putten W, Touw IP, Delwel R, Santini V. Autonomous proliferation of leukemic cells in vitro as a eeterminant of Prognosis in adult acute myeloid leukemia. N Engl J Med. 1993;328(9):614-619.

Mutations associated with a 17-gene leukemia stem cell score and the score's prognostic relevance in the context of the European LeukemiaNet classification of acute myeloid leukemia

Ferrata Storti Foundation

Marius Bill,[1] Deedra Nicolet,[1,2] Jessica Kohlschmidt,[1,2] Christopher J. Walker,[1] Krzysztof Mrózek,[1] Ann-Kathrin Eisfeld,[1] Dimitrios Papaioannou,[1] Xiaoqing Rong-Mullins,[1] Zachary Brannan,[1] Jonathan E. Kolitz,[3] Bayard L. Powell,[4] Kellie J. Archer,[1,5] Adrienne M. Dorrance,[1,6] Andrew J. Carroll,[7] Richard M. Stone,[8] John C. Byrd,[1,6] Ramiro Garzon[1,6] and Clara D. Bloomfield[1,6]

[1]The Ohio State University Comprehensive Cancer Center, Columbus, OH; [2]Alliance Statistics and Data Center, The Ohio State University Comprehensive Cancer Center, Columbus, OH; [3]Monter Cancer Center, Hofstra Northwell School of Medicine, Lake Success, NY; [4]Comprehensive Cancer Center of Wake Forest University, Winston-Salem, NC; [5]College of Public Health, The Ohio State University, Columbus, OH; [6]Division of Hematology, Department of Internal Medicine, The Ohio State University, Columbus, OH; [7]Department of Genetics, University of Alabama at Birmingham, Birmingham, AL and [8]Department of Medical Oncology, Dana-Farber Cancer Institute, Boston, MA, USA

ABSTRACT

Leukemia stem cells (LSC) are more resistant to standard chemotherapy and their persistence during remission can cause relapse, which is still one of the major clinical challenges in the treatment of acute myeloid leukemia (AML). A better understanding of the mutational patterns and the prognostic impact of molecular markers associated with stemness could lead to better clinical management and improve patients' outcomes. We applied a previously described 17-gene expression score comprising genes differently expressed between LSC and leukemic bulk blasts, for 934 adult patients with *de novo* AML, and studied associations of the 17-gene LSC score with clinical data and mutation status of 81 genes recurrently mutated in cancer and leukemia. We found that patients with a high 17-gene score were older and had more mutations. The 17-gene score was found to have a prognostic impact in both younger (aged <60 years) and older (aged ≥60 years) patients with AML. We also analyzed the 17-gene LSC score in the context of the 2017 European LeukemiaNet genetic-risk classification and found that for younger patients the score refined the classification, and identified patients currently classified in the European LeukemiaNet Favorable-risk category who had a worse outcome.

Introduction

Acute myeloid leukemia (AML) is a heterogeneous disease.[1-3] Although many advances have been made in understanding the biology and treatment of AML, the long-term survival rates are still only ~40% for younger adults (aged <60 years), and ~10-15% for older patients (aged ≥60 years).[1-3] One major clinical challenge impeding improved outcome is relapse following achievement of complete remission (CR). It is hypothesized that relapse occurs because of the persistence of leukemia stem cells (LSC) and subsequent outgrowth of the leukemia clone.[4-8] Studies on the clinical relevance of LSC are still rare because no LSC-specific phenotype has been firmly established. Although the percentage of CD34+/CD38−-expressing cells, which were initially assumed to include all LSC, was shown to affect prognosis,[9,10] the use of more permissive immunodeficient mouse models revealed that LSC can also be found in the CD34+/CD38+ and CD34− compartments.[4,7,9,11-15] Instead of using surface markers to identify and quantify the presence

of LSC, in 2011, Eppert *et al.*[4] described a LSC-related gene-expression signature comprising 44 genes that were deregulated in LSC. The derived stem cell-like signature was shown to associate with inferior outcome in adult patients with cytogenetically normal AML.[4,16] Recently, Ng *et al.*[7] used a similar approach to generate a LSC-derived gene-expression signature consisting of 17 genes that also associated with inferior outcome. However, it is still not fully determined whether this signature is associated with clinical characteristics and gene mutations. Moreover, the prognostic value of the 17-gene LSC score in the context of other, well-established risk classifications, for example the one by the European LeukemiaNet (ELN)[1], has not, to our knowledge, been assessed.

We, therefore, derived the 17-gene score from a set of samples from adults with AML and determined associations between the signature and known prognosticators[1,17,18] as well as mutational data of 81 cancer- and leukemia-associated genes.[19] Moreover, we validated the prognostic impact of the 17-gene signature alone and in the context of the 2017 ELN genetic-risk classification.[1]

Methods

Patients and treatment

We investigated 934 adult patients with *de novo* AML (other than acute promyelocytic leukemia), for whom material for molecular analyses was available. Availability of material for analysis was the only criterion for inclusion in our study – we did not select AML patients based on their age, ELN risk group, specific clinical trial they were enrolled onto, etc. Because of differences in the treatment protocols between younger and older patients, we performed outcome analyses separately for these two groups of patients. Within each age group, patients were treated similarly, receiving a cytarabine/anthracycline-based induction on Cancer and Leukemia Group B (CALGB) trials.[20-34] No patient received an allogeneic stem cell transplant in first CR. Details of CALGB treatment protocols are provided in the *Online Supplementary Appendix* and *Online Supplementary Table S1*. There were no significant differences in CR rates, disease-free survival (DFS) or overall survival (OS) for younger patients enrolled onto CALGB 8525, 9222, 9621, 10503, 10603 and 19808 treatment trials (*Online Supplementary Table S2*) nor were there any significant differences in CR rates, DFS or OS among older patients enrolled onto CALBG 9420, 9720, 10201 and 10502 trials (*Online Supplementary Table S3*). CALGB is now part of the Alliance for Clinical Trials in Oncology (Alliance). All patients were enrolled on CALGB 8461 (cytogenetic studies), CALGB 9665 (leukemia tissue bank) and CALGB 20202 (molecular studies) companion protocols. Patients provided written informed consent, and study protocols were in accordance with the Declaration of Helsinki and approved by Institutional Review Boards.

Transcriptome analyses and calculation of the 17-gene leukemia stem cell score

Pretreatment bone marrow and/or blood samples containing ≥20% leukemic blasts were obtained from all patients and mononuclear cells were enriched through Ficoll-Hypaque gradient centrifugation and cryopreserved until use. Total RNA was extracted from patients' samples using the TRIzol method according to the manufacturer's protocol and used for RNA-sequencing analyses (see also the *Online Supplementary Appendix*). RNA-sequencing libraries were prepared using the Illumina (San Diego, CA, USA) TruSeq Stranded Total RNA Sample Prep Kit with Ribo-Zero Gold (n. RS1222201) according to the manufacturer's instructions. Sequencing was performed with Illumina HiSeq systems using the HiSeq version 3 sequencing reagents to an approximate cluster density of 800,000/mm². Image analysis, base calling, error estimation, and quality thresholds were performed using HiSeq Controller software (version 2.2.38) and Real Time Analyzer software (version 1.18.64). Transcript abundance was quantified from the RNA-sequencing data using kallisto,[35] with a reference transcriptome consisting of *Homo sapiens* GRCh38 protein-encoding and non-coding transcripts except rRNA; the strand-specific option of "first read reverse" was chosen. Abundance values are represented in transcripts per million.

The 17-gene LSC score was derived similarly to that in the publication by Ng *et al.*[7] using RNA-sequencing data and the same weights that were published initially for a microarray platform.[7] Briefly, the 17-gene LSC score was calculated as the weighted sum of the normalized expression values of the 17 genes included in the signature: 17-gene LSC score = (*DNMT3B* × 0.0874) + (*ZBTB46* × −0.0347) + (*NYNRIN* × 0.00865) + (*ARHGAP22* × −0.0138) + (*LAPTM4B* × 0.00582) + (*MMRN1* × 0.0258) + (*DPYSL3* × 0.0284) + (*KIAA0125* × 0.0196) + (*CDK6* × −0.0704) + (*CPXM1* × −0.0258) + (*SOCS2* × 0.0271) + (*SMIM24* × −0.0226) + (*EMP1* × 0.0146) + (*NGFRAP1* × 0.0465) + (*CD34* × 0.0338) + (*AKR1C3* × −0.0402) + (*GPR56* × 0.0501).[7] The derived scores were used to divide patients into two groups using the median as the cutoff: a group with a high score (17-gene^high) and a group with a low score (17-gene^low).

Cytogenetic and molecular analyses

Details of the cytogenetic and molecular analyses are provided in the *Online Supplementary Appendix*.

Results

Clinical and cytogenetic characteristics associated with the 17-gene leukemia stem cell score

Pretreatment characteristics of the 934 patients are shown in Table 1. For all patients, we determined the 17-gene LSC score, which indicates a stem cell-like gene-expression profile, and separated them into 17-gene^low and 17-gene^high groups using the median. Comparison between patients with a 17-gene^low and 17-gene^high score showed that the former were younger at diagnosis (median: 46 *vs.* 53 years; *P*<0.001) and had lower platelet counts (median: 50 *vs.* 63x10⁹/L; *P*<0.001). Cytogenetically, there was no difference in the frequency of the presence of cytogenetically normal AML between the groups. Among cytogenetically abnormal patients, those with a 17-gene^low score more frequently had core-binding factor AML (CBF-AML; *P*<0.001), including all patients with t(8;21)(q22;q22) and 88% with inv(16)(p13q22) or t(16;16)(p13;q22). On the other hand, the group with a 17-gene^high score included all patients with inv(3)(q21q26) or t(3;3)(q21;q26) and contained more patients with a complex karyotype than in the 17-gene^low group (*P*<0.001). Most patients with a complex karyotype in the 17-gene^high group had a typical complex karyotype (i.e., complex karyotype with unbalanced chromosome abnormalities leading to loss of material from 5q, 7q and/or 17p), whereas an atypical complex karyotype (i.e., complex karyotype without 5q, 7q and/or 17p abnormalities)[36] was found with a higher frequency among 17-gene^low patients.

Table 1. Comparison of pretreatment clinical and cytogenetic characteristics in 934 patients with acute myeloid leukemia according to low and high 17-gene leukemia stem cell scores.

Characteristic	All patients (n=934)	17-gene^low (n=467)	17-gene^high (n=467)	P
Age, years				
Median	50	46	53	<0.001
Range	17-84	17-82	17-84	
Sex, n (%)				
Female	404 (43)	199 (43)	205 (44)	0.74
Hemoglobin, g/dL				
Median	9.2	9.2	9.1	0.31
Range	2.3-25.1	2.3-25.1	4.2-14.7	
Platelet count, x10⁹/L				
Median	55	50	63	<0.001
Range	4-592	7-433	4-592	
WBC count, x10⁹/L				
Median	24.1	24.1	23.9	0.46
Range	0.4-475.0	0.4-303.6	0.6-475	
% Blood blasts				
Median	54	54	54	0.18
Range	0-99	0-97	0-99	
% Bone marrow blasts				
Median	65	65	66	0.91
Range	0-97	0-97	4-97	
EM involvement, n (%)				
Present	220 (25)	112 (25)	108 (24)	0.88
FAB classification, n (%)				0.18
M0	40 (6)	16 (4)	24 (7)	
M1	150 (22)	82 (23)	68 (21)	
M2	185 (27)	100 (28)	85 (26)	
M4	189 (28)	107 (30)	82 (25)	
M5	113 (17)	52 (15)	61 (19)	
M6	1 (0)	0 (0)	1 (1)	
M7	1 (0)	0 (0)	1 (1)	
ELN group, n (%)				<0.001
Favorable	385 (45)	284 (64)	101 (24)	
t(8;21)	40	40	0	
inv(16)	69	61	8	
NPM1 mut/*FLT3*-ITD wt or low	211	123	88	
CEBPA mut	65	60	5	
Intermediate	188 (22)	69 (16)	119 (28)	
Adverse	291 (34)	89 (20)	202 (48)	
Cytogenetically normal, n (%)				
Present	442 (47)	210 (45)	232 (50)	0.17
CBF, n (%)				<0.001
Present	109 (12)	101 (22)	8 (2)	
t(8;21)	40	40	0	
inv(16)	69	61	8	
KMT2A-rearranged, n (%)				0.65
Present	46 (5)	21 (5)	25 (5)	
t(9;11)	19	9	10	
t(v;11)	27	12	15	
Complex karyotype, n (%)				<0.001
Present	79 (8)	19 (4)	60 (13)	
Typical	53	4	49	
Atypical	26	15	11	
t(6;9), n (%)				1.00
Present	5 (1)	2 (1)	3 (1)	
inv(3), n (%)				<0.001
Present	18 (2)	0	18 (4)	

WBC: white blood cell; EM: extramedullary; FAB: French-American-British; ELN: European LeukemiaNet; mut: mutated; ITD: internal tandem duplication; wt: wild-type; CBF: core-binding factor.

Mutational landscape associated with the 17-gene leukemia stem cell score

To obtain more detailed insights into the mutational patterns associated with the 17-gene LSC signature, we analyzed 81 cancer and leukemia-associated genes.[19] We found that 77 genes were mutated in at least one patient (*Online Supplementary Table S4*). Patients with a 17-gene^low score had fewer mutations compared with patients with a 17-gene^high score (median: 2 *vs.* 3; $P<0.001$). Moreover, 12 gene mutations occurred at significantly different frequencies between patients with 17-gene^low and 17-gene^high scores (Figure 1). Biallelic *CEBPA* ($P<0.001$), *GATA2* ($P=0.008$), and *KIT* ($P<0.001$) mutations were more frequent in the 17-gene^low group of patients (Figure 1A). In contrast, patients with a 17-gene^high score more frequently harbored mutations in *ASXL1* ($P=0.001$), *DNMT3A* ($P<0.001$), *KMT2A* ($P=0.04$), *RUNX1* ($P=0.002$), *SRSF2* ($P=0.02$), *STAG2* ($P=0.009$), *TET2* ($P=0.008$) and *TP53* ($P<0.001$) genes. Additionally, *FLT3*-internal tandem duplications were more frequent in these patients than in
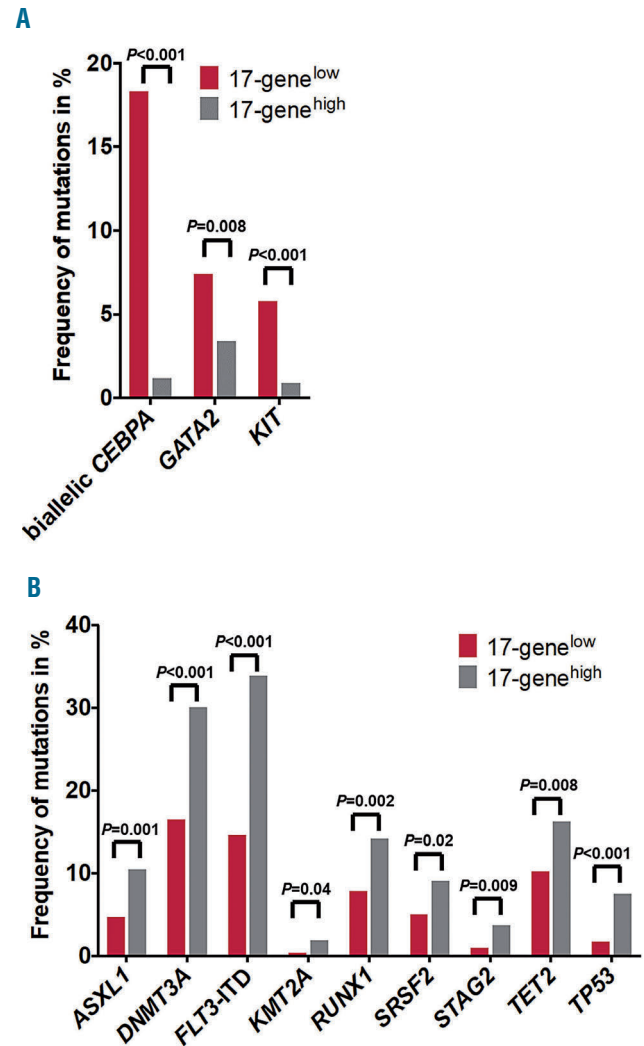
Figure 1. Differences in the frequencies of gene mutations between patients with low and those with high 17-gene leukemic stem cell scores. Mutations that had a significantly higher frequency in the (A) 17-gene^low or (B) 17-gene^high group.

those with a 17-gene[low] score (*P*<0.001) (Figure 1B and *Online Supplementary Table S4*), as previously described by Ng *et al.*[7]

Outcome associated with the 17-gene leukemia stem cell score

All patients were assigned to the 17-gene[low] and 17-gene[high] groups based on the median of the initial analysis of the entire cohort of patients. We kept this initial grouping for all additional sub-analyses that could have potentially re-assigned some patients into different 17-gene score groups. This led to differences in the sizes of the 17-gene[low] and 17-gene[high] score groups in younger and older patients.

Similarly to Ng *et al.*,[7] we found that the 17-gene LSC score was strongly associated with outcome in both the younger (Table 2; Figure 2A, B) and older (Table 2; Figure 2C, D) cohorts of patients. Among younger patients, those with a 17-gene[low] score had higher CR rates (*P*<0.001) (Table 2) and longer DFS (*P*<0.001) (Figure 2A) and OS (*P*<0.001) (Figure 2B). Similar results were found in older patients: CR rates (*P*=0.004) (Table 2), DFS (*P*=0.04), (Figure 2C) and OS (*P*<0.001) (Figure 2D).

Table 2. Comparison of outcomes according to the 17-gene leukemic stem cell score in younger adults (aged <60 years) and older adults (aged ≥60 years) with acute myeloid leukemia.

Endpoint	Younger patients (n=729)			Older patients (n=205)		
	17-gene[low] (n=403)	17-gene[high] (n=326)	*P*	17-gene[low] (n=64)	17-gene[high] (n=141)	*P*
Complete remission, %	87	63	<0.001	72	50	0.004
Disease-free survival			<0.001			0.04
Median, years	2.6	0.7		0.6	0.5	
% disease-free at 3 years	48	26		17	6	
95% confidence interval	43-53	20-32		8-30	2-13	
Overall survival			<0.001			<0.001
Median, years	6.5	1.1		1.1	0.6	
% alive at 3 years	59	27		27	9	
95% confidence interval	54-63	22-321		16-38	5-14	
ELN Favorable-risk group						
Endpoint	17-gene[low] (n=264)	17-gene[high] (n=78)	*P*	17-gene[low] (n=20)	17-gene[high] (n=23)	*P*
Complete remission, %	95	81	<0.001	90	78	0.42
Disease-free survival			0.008			0.09
Median, years	7.7	1.4		1.1	0.6	
% disease-free at 3 years	57	43		39	17	
95% confidence interval	50-63	31-55		17-60	4-37	
Overall survival			<0.001			0.05
Median, years	NR	2.4		2.4	1.1	
% alive at 3 years	68	49		50	17	
95% confidence interval	62-73	37-59		27-69	5-35	
ELN Intermediate-risk group						
Endpoint	17-gene[low] (n=56)	17-gene[high] (n=96)	*P*	17-gene[low] (n=13)	17-gene[high] (n=23)	*P*
Complete remission,%	82	76	0.42	62	43	0.49
Disease-free survival			0.08			0.92
Median, years	1.3	0.7		0.7	0.4	
% disease-free at 3 years	28	25		0	10	
95% confidence interval	16-42	15-35			1-36	
Overall survival			0.03			0.48
Median, years	2.4	1.4		0.9	0.7	
% alive at 3 years	45	28		0	17	
95% confidence interval	31-57	20-37			5-35	
ELN Adverse-risk group						
Endpoint	17-gene[low] (n=67)	17-gene[high] (n=123)	*P*	17-gene[low] (n=22)	17-gene[high] (n=79)	*P*
Complete remission, %	63	41	0.004	59	41	0.15
Disease-free survival			<0.001			0.21
Median, years	1.1	0.6		0.5	0.4	
% disease-free at 3 years	24	6		8	0	
95% confidence interval	12-37	2-15		0-29		
Overall survival			<0.001			0.06
Median, years	1.6	0.7		0.8	0.5	
% alive at 3 years	40	11		18	4	
95% confidence interval	29-52	7-18		6-36	1-10	

NR: not reached.

Next, we tested the prognostic impact of the 17-gene LSC score in multivariable analyses (Table 3). In younger patients, the 17-gene LSC score remained prognostically significant for all clinical endpoints, namely CR, DFS, and OS. In older patients, the score was prognostically significant only for OS, but it was not significant in the final models for achievement of a CR or DFS (Table 3).

Prognostic impact of the 17-gene leukemia stem cell score in the context of the current European LeukemiaNet classification

To test the prognostic value of the 17-gene LSC score in the context of the current 2017 ELN classification, we classified all patients according to the published guidelines into ELN Favorable-, Intermediate- and Adverse-risk groups.[1] In both age cohorts, we found significant differences in the ELN risk-group distribution between patients with 17-gene^{low} and 17-gene^{high} scores ($P<0.001$ for younger and $P=0.009$ for older patients). Among the younger patients, two-thirds with a 17-gene^{low} score were classified as having Favorable-risk, whereas 14% and 17% were classified as having, respectively, Intermediate- and Adverse-risk. On the other hand, younger patients with a 17-gene^{high} score were most frequently classified in the

Adverse-risk group (41%), followed by the Intermediate- (32%) and Favorable-risk (26%) groups. Among the older patients, the majority in both the 17-gene^{low} and 17-gene^{high} score groups were classified in the Adverse-risk group (40% and 63%, respectively) (*Online Supplementary Table S5*), followed by Favorable- (36%) and Intermediate- (24%) risk groups in the 17-gene^{low} group and by equal numbers for Favorable-risk (18%) and Intermediate-risk (18%) groups in the 17-gene^{high} group.

Next, we tested whether the 17-gene LSC score can be used to refine the prognostic impact of the ELN classification. Among younger patients, we found that the 17-gene LSC score could refine the ELN classification for the ELN Favorable- and Adverse-risk groups, but not for the Intermediate-risk group. Younger patients with a 17-gene^{low} score in the ELN Favorable-risk group had higher CR rates ($P<0.001$) (Table 2) and longer DFS ($P=0.008$) (Figure 3A) and OS ($P<0.001$) (Figure 3B) than the 17-gene^{high} patients. Likewise, younger Adverse-risk patients with a 17-gene^{low} score had higher CR rates ($P=0.004$) (Table 2), and longer DFS ($P<0.001$) (Figure 3E) and OS ($P<0.001$) (Figure 3F). On the other hand, among younger patients in the Intermediate-risk group, there was no significant difference in CR rates (Table 2) or DFS ($P=0.08$)
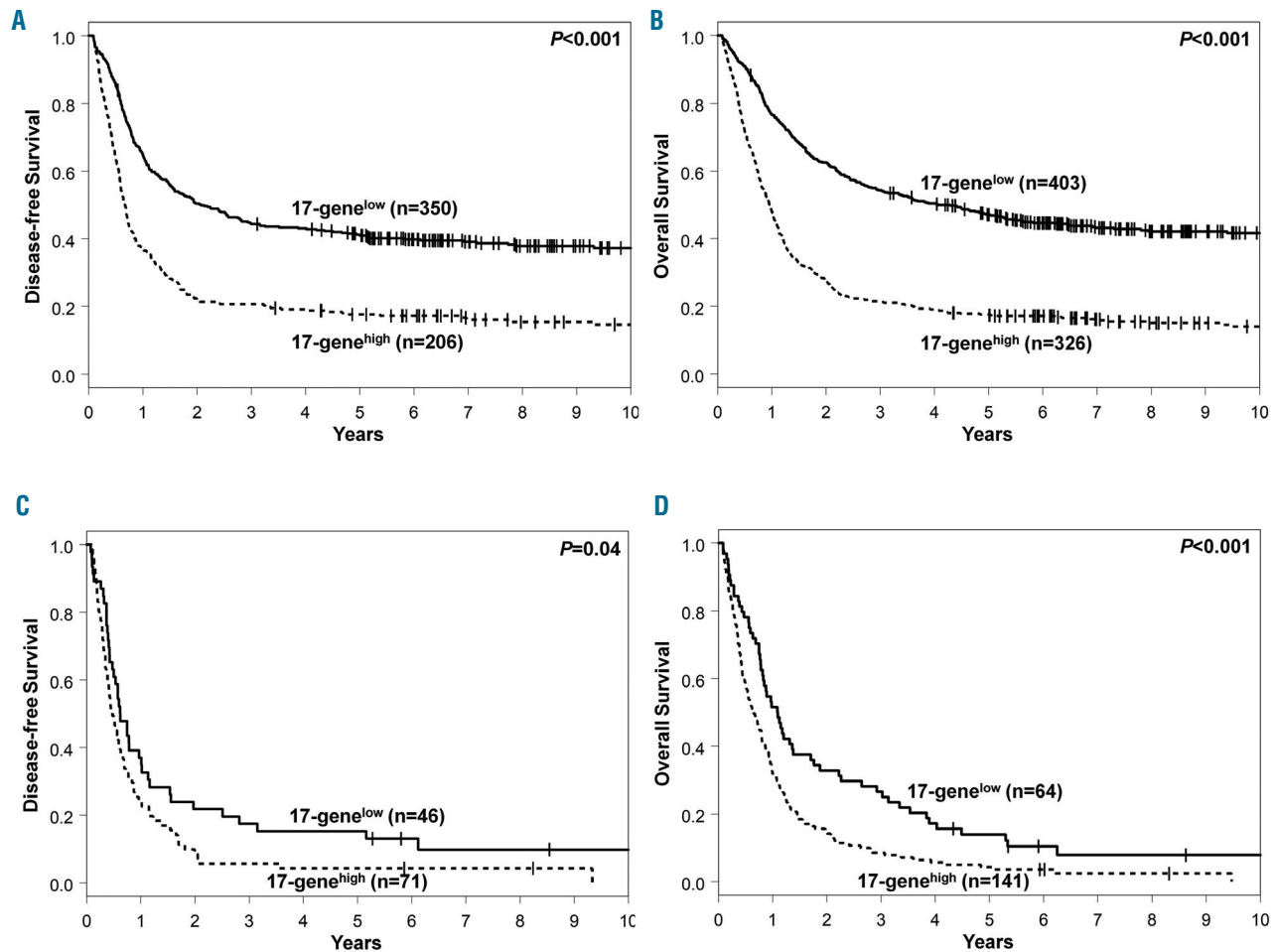
Figure 2. Differences in outcome between patients with low and those with high 17-gene leukemic stem cell scores. (A) Disease-free survival (DFS) and (B) overall survival (OS) of younger adult patients (aged <60 years) according to the 17-gene leukemia stem cell (LSC) score. (C) DFS and (D) OS of older patients (aged ≥60 years) according to the 17-gene LSC score.

(Figure 3C), but those with a 17-gene^low score had longer OS (*P*=0.03) (Figure 3D).

Among older patients, the 17-gene score had almost no impact on outcome after classifying the patients according to the ELN recommendations. We found that only older patients in the Favorable-risk group with a 17-gene^low score had longer OS than those with a 17-gene^high score (*P*=0.05) (*Online Supplementary Figure S1*, Table 2). The 17-gene score showed no prognostic impact in the Adverse- and Intermediate-risk groups.

Discussion

The prognosis of AML patients is still poor, and relapse after achieving a CR is a major clinical challenge.[1-4,7] It is thought that leukemia relapse is caused by the persistence of LSC.[4-7] A better understanding of LSC and their prognostic impact in AML is necessary in order to improve patients' outcomes. However, the lack of a well-established phenotype has thus far impeded studies on the clinical relevance of LSC frequency. Ng *et al.*[7] recently developed a gene-expression signature, consisting of 17 genes that were found to be deregulated in LSC, to quantify the presence of LSC. They showed that the 17-gene LSC signature has a prognostic impact. In our study, we not only validated these data in an independent set of 934 adult patients with *de novo* AML, but also analyzed the prognostic impact of the 17-gene LSC score in the context of the current ELN classification. Moreover, we describe a detailed mutational landscape associated with the 17-gene LSC score.

Whereas the 17-gene score was initially derived using microarray data, Ng *et al.*[7] showed in a relatively small set of patients (n=169) that RNA-sequencing data can also be used to derive the score. We validated this finding in a larger set of 934 AML patients with RNA-sequencing data using the same published weights of the score as Ng *et al.*,[7] and demonstrated the robustness of the 17-gene score. We assigned the score to each patient and classified them into a 17-gene^high or 17-gene^low LSC group for all further analyses, using the median as the cut point.

Clinically, we found that patients with a 17-gene^low score were younger and had lower platelet counts at diagnosis. Similar differences in age were also described by Ng *et al.*[7] Next, we compared cytogenetic findings between the groups of patients with 17-gene^low and 17-gene^high scores and although we did not find any difference in the incidence of cytogenetically normal AML, there was a different distribution of the specific cytogenetic abnormalities

Table 3. Multivariable models for outcome evaluating the 17-gene leukemia stem cell score and known prognosticators in younger (aged <60 years) and older (aged ≥60 years) adults with acute myeloid leukemia.

End point	Variable	Younger patients (n=729)		Older patients (n=205)	
		Odds ratio (95% CI)	*P*	Odds ratio (95% CI)	*P*
Complete remission	17-gene LSC score (high *vs.* low)	0.36 (0.23-0.56)	<0.001	*	*
	ELN 2017		<0.001		
	(Intermediate *vs.* Favorable),	0.48 (0.26-0.86)			
	(Adverse *vs.* Favorable)	0.12 (0.07-0.21)			
	WT1 (mutated *vs.* wild-type)	0.47 (0.24-0.92)	0.03		
	ZRSR2 (mutated *vs.* wild-type)	0.44 (0.19-0.99)	0.05		
	BAALC expression (high *vs.* low)	0.60 (0.39-0.92)	0.02		
	Hemoglobin (continuous)	1.16 (1.03-1.30)	0.01		
		Hazard ratio (95% CI)	*P*	Hazard ratio (95% CI)	*P*
Disease-free survival	17-gene LSC score (high *vs.* low)	1.67 (1.31-2.13)	<0.001	*	*
	ELN 2017		<0.001		
	(Intermediate *vs.* Favorable,	1.84 (1.39-2.42)			
	Adverse *vs.* Favorable)	2.87 (2.16-3.81)			
	DNMT3A (mutated *vs.* wild-type)	1.41 (1.09-1.82)	0.008		
	WT1 (mutated *vs.* wild-type)	1.94 (1.34-2.80)	<0.001		
	Platelets (continuous, 50-unit increase)	0.87 (0.80-0.95)	0.003		
Overall survival	17-gene LSC score (high *vs.* low)	1.88 (1.53-2.31)	<0.001	1.70 (1.19-2.41)	0.003
	ELN 2017		<0.001		
	(Intermediate *vs.* Favorable),	1.77 (1.37-2.29)			
	(Adverse *vs.* Favorable)	2.85 (2.26-3.60)			
	WT1 (mutated *vs.* wild-type)	1.80 (1.33-2.44)	<0.001		
	Age (continuous, 10-year increase)	1.17 (1.07-1.27)	<0.001	1.71 (1.23-2.38)	0.001
	BAALC expression (high *vs.* low)			0.86 (0.77-0.96)	0.007
	Platelets (continuous, 50-unit increase)				

95% CI: 95% confidence interval; ELN: European LeukemiaNet. An odds ratio >1 (<1) corresponds to a higher (lower) odds of achieving a complete remission for higher values of continuous variables and the first level listed of a dichotomous variable. A hazard ratio >1 (<1) corresponds to a higher (lower) risk for higher values of continuous variables and the first level listed of a dichotomous variable. Variables were considered for inclusion in the multivariable models if they had a univariable *P*-value of <0.20. Only markers for which there were at least eight mutated patients in each 17-gene score group (high/low) were included the multivariable modeling. * the 17-gene score does not remain statistically significant in the multivariable model for achievement of a complete remission and disease-free survival in older patients. .

between the groups. Patients with CBF-AML were much more frequently classified in the 17-gene[low] score group, especially those with a t(8;21)(q22;q22) who were never found to have a 17-gene[high] score. As previously reported, patients with CBF-AML had a relatively favorable outcome compared with patients belonging to other cytogenetic subgroups.[37-41] On the other hand, patients in the 17-gene[high] score group more frequently carried cytogenetic

abnormalities associated with adverse outcome, such as a complex karyotype, especially a typical complex karyotype,[36] and inv(3)(q21q26) or t(3;3)(q21;q26).[1,17,36,40-42] Of note, patients with inv(3) or t(3;3) were classified exclusively in the 17-gene[high] score group.

Next, we looked for differences in the mutational patterns of 81 cancer- and leukemia-associated genes[19] between 17-gene[low] and 17-gene[high] score patients. Patients
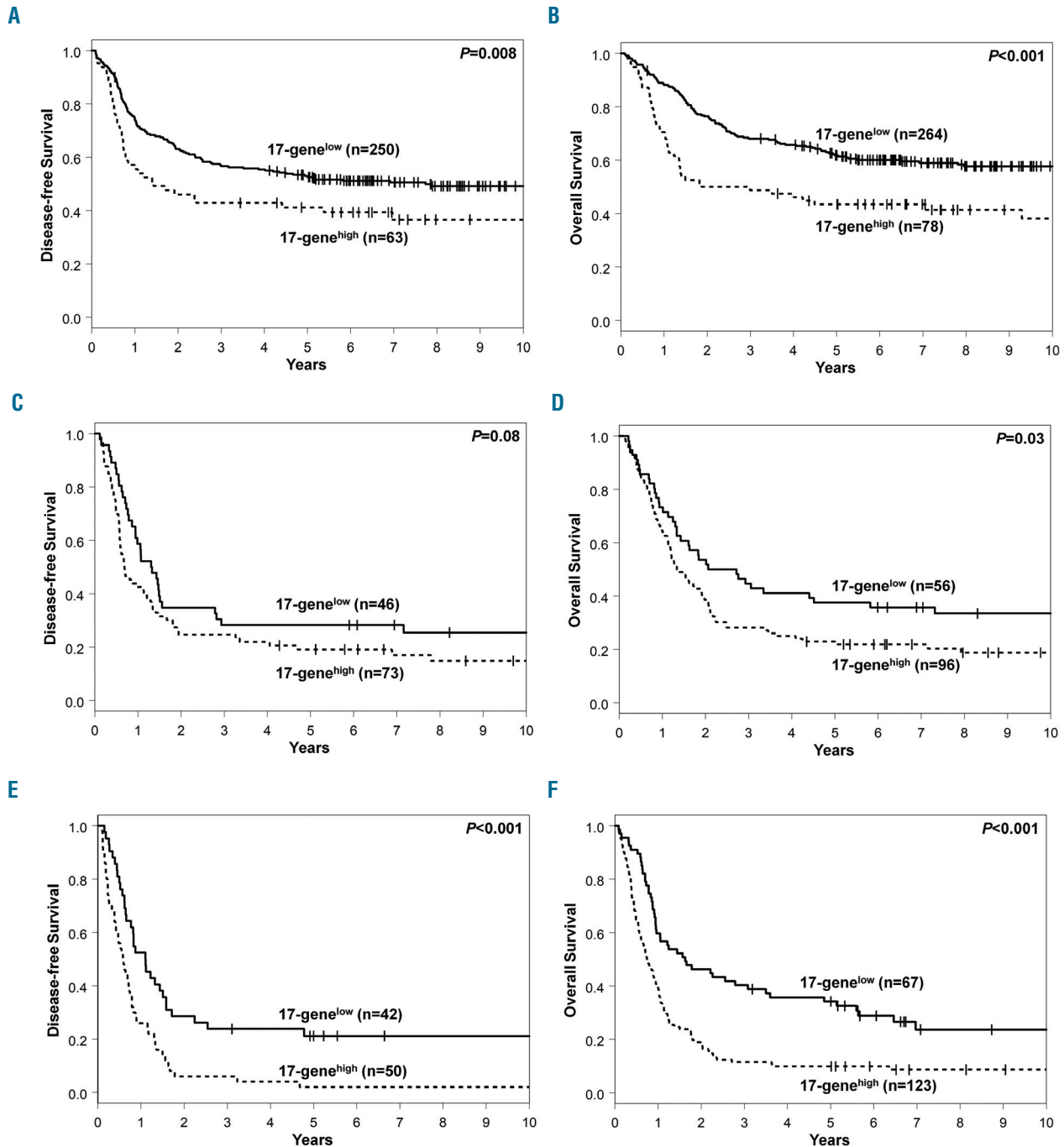
Figure 3. Differences in outcome between younger adult patients (aged <60 years) with low and those with high 17-gene leukemic stem cell scores in the context of the current European LeukemiaNet 2017 classification. (A) Disease-free survival (DFS) and (B) overall survival (OS) of younger patients within the European LeukemiaNet (ELN) Favorable-risk group according to the 17-gene leukemia stem cell (LSC) score. (C) DFS and (D) OS of younger patients within the ELN Intermediate-risk group according to the 17-gene LSC score. (E) DFS and (F) OS of younger patients within the ELN Adverse-risk group according to the 17-gene LSC score.

with a 17-gene[low] score had a lower median number of mutations and only three genes, namely, *GATA2*, *CEBPA* and *KIT*, were found to be mutated more frequently in this group. *GATA2* mutations and biallelic *CEBPA* mutations are known to co-occur,[43] and the higher incidence of *KIT* mutations in 17-gene[low] patients can be at least in part explained by the elevated frequency of CBF-AML in this group, since *KIT* mutations are associated with CBF-AML.[37] Whereas both biallelic *CEBPA* mutations and *GATA2* mutations, which occurred frequently in the 17-gene[low] score group, are associated with a favorable outcome, mutations associated with adverse outcome, such as those in the *RUNX1*, *ASXL1*, and *TP53* genes,[1,2,36,44-50] were more frequently found in patients with a 17-gene[high] score.

We were also interested in characterizing further the prognostic significance of the 17-gene LSC score established by Ng *et al.*[7] We not only validated its prognostic impact in a larger independent cohort of patients, but also asked the question whether the 17-gene LSC score could refine the well-established 2017 ELN classification.[1] This is especially of interest because it appears that some patients classified as ELN Favorable-risk still have a poor outcome. These patients might benefit from other treatment options.[1] When we classified the patients according to the ELN guidelines, we found significant differences in the distribution of patients with 17-gene[low] and 17-gene[high] scores among specific ELN risk groups. In younger patients, the majority of 17-gene[low] score patients were classified as having Favorable-risk, whereas most patients in the 17-gene[high] score group were in the Adverse-risk group.

With regard to clinical outcome, we found that the 17-gene LSC score is capable of refining the ELN classification in younger patients. In the Favorable-risk group, application of the 17-gene LSC score led to the identification of approximately 20% of patients with a 17-gene[high] score who had a worse outcome than patients with a 17-gene[low] score. Prospective studies are needed to test whether these 17-gene[high] score patients might benefit from different induction. A similar ability of the 17-gene LSC score to identify patients with different outcomes was shown for the Adverse-risk group, despite the fact that the outcome of patients in this group is in general poor. The usefulness of the 17-gene LSC score in the ELN Intermediate-risk group seems to be limited, with patients with a 17-gene[low] score having a better OS but not better CR rates or DFS. Likewise, the 17-gene LSC score could not improve the ELN classification in older AML patients, who are known to have a generally poor prognosis.[1-3]

In summary, we found that the 17-gene LSC score is associated with distinct clinical and molecular features. Moreover, we not only validated the prognostic impact of the 17-gene LSC score but also showed for the first time that the score can refine the current 2017 ELN classification, at least in younger patients. This is important because the 17-gene LSC score is associated with well-established prognostic markers that are included in the ELN guidelines. Prospective studies are needed to determine best treatment options for patients currently classified as having Favorable-risk who are identified to have a worse prognosis by the use of the 17-gene LSC score.

References

1. Döhner H, Estey E, Grimwade D, et al. Diagnosis and management of AML in adults: 2017 ELN recommendations from an international expert panel. Blood. 2017;129 (4):424-447.
2. Döhner H, Weisdorf DJ, Bloomfield CD. Acute myeloid leukemia. N Engl J Med. 2015;373(12):1136-1152.
3. Estey EH. Acute myeloid leukemia: 2012 update on diagnosis, risk stratification, and management. Am J Hematol. 2012;87(1):89-99.
4. Eppert K, Takenaka K, Lechman ER, et al. Stem cell gene expression programs influence clinical outcome in human leukemia. Nat Med. 2011;17(9):1086-1093.
5. Dick JE. Stem cell concepts renew cancer research. Blood. 2008;112(13):4793-4807.
6. Dorrance AM, Neviani P, Ferenchak GJ, et al. Targeting leukemia stem cells in vivo with antagomiR-126 nanoparticles in acute myeloid leukemia. Leukemia. 2015;29(11): 2143-2153.
7. Ng SWK, Mitchell A, Kennedy JA, et al. A 17-gene stemness score for rapid determination of risk in acute leukaemia. Nature. 2016;540(7633):433-437.
8. Sagar J, Chaib B, Sales K, Winslet M, Seifalian A. Role of stem cells in cancer therapy and cancer stem cells: a review. Cancer Cell Int. 2007;7:9.
9. Jentzsch M, Bill M, Nicolet D, et al. Prognostic impact of the CD34+/CD38- cell burden in patients with acute myeloid leukemia receiving allogeneic stem cell transplantation. Am J Hematol. 2017;92(4): 388-396.
10. Wang L, Gao L, Xu S, et al. FISH+CD34+CD38- cells detected in newly diagnosed acute myeloid leukemia patients can predict the clinical outcome. J Hematol Oncol. 2013;6(1):85.
11. Heidel FH, Mar BG, Armstrong SA. Self-renewal related signaling in myeloid leukemia stem cells. Int J Hematol. 2011;94(2):109-117.
12. Guan Y, Gerhard B, Hogge DE. Detection, isolation, and stimulation of quiescent primitive leukemic progenitor cells from patients with acute myeloid leukemia (AML). Blood. 2003;101(8):3142-3149.
13. Bonnet D, Dick JE. Human acute myeloid leukemia is organized as a hierarchy that originates from a primitive hematopoietic cell. Nat Med. 1997;3(7):730-737.
14. Sarry J-E, Murphy K, Perry R, et al. Human acute myelogenous leukemia stem cells are rare and heterogeneous when assayed in NOD/SCID/IL2Rγc-deficient mice. J Clin Invest. 2011;121(1):384-395.
15. Raffel S, Falcone M, Kneisel N, et al. BCAT1 restricts αKG levels in AML stem cells leading to IDHmut-like DNA hypermethylation.

Nature. 2017;551(7680):384-388.

16. Metzeler KH, Maharry K, Kohlschmidt J, et al. A stem cell-like gene expression signature associates with inferior outcomes and a distinct microRNA expression profile in adults with primary cytogenetically normal acute myeloid leukemia. Leukemia. 2013;27(10):2023-2031.

17. Grimwade D, Mrózek K. Diagnostic and prognostic value of cytogenetics in acute myeloid leukemia. Hematol Oncol Clin North Am. 2011;25(6):1135-1161.

18. Eisfeld AK, Kohlschmidt J, Mrózek K, et al. Mutation patterns identify adult patients with de novo acute myeloid leukemia aged 60 years or older who respond favorably to standard chemotherapy: an analysis of Alliance studies. Leukemia. 2018;32(6):1338-1348.

19. Eisfeld A-K, Mrózek K, Kohlschmidt J, et al. The mutational oncoprint of recurrent cytogenetic abnormalities in adult patients with de novo acute myeloid leukemia. Leukemia. 2017;31(10):2211-2218.

20. Mayer RJ, Davis RB, Schiffer CA, et al. Intensive postremission chemotherapy in adults with acute myeloid leukemia. N Engl J Med. 1994;331(14):896-903.

21. Schiffer CA, Davis RB, Schulman P, et al. Intensive post remission therapy of acute myeloid leukemia (AML) with cytoxan/etoposide (CY/VP16) and diazaquone/mitoxantrone (AZQ/MITO). Blood. 1991;78(suppl):460 (abstract 1829).

22. Moore JO, Dodge RK, Amrein PC, et al. Granulocyte-colony stimulating factor (filgrastim) accelerates granulocyte recovery after intensive postremission chemotherapy for acute myeloid leukemia with aziridinyl benzoquinone and mitoxantrone: Cancer and Leukemia Group B study 9022. Blood. 1997;89(3):780-788.

23. Cassileth PA, Harrington DP, Appelbaum FR, et al. Chemotherapy compared with autologous or allogeneic bone marrow transplantation in the management of acute myeloid leukemia in first remission. N Engl J Med. 1998;339(23):1649-1656.

24. Moore JO, George SL, Dodge RK, et al. Sequential multiagent chemotherapy is not superior to high-dose cytarabine alone as postremission intensification therapy for acute myeloid leukemia in adults under 60 years of age: Cancer and Leukemia Group B study 9222. Blood. 2005;105(9):3420-3427.

25. Kolitz JE, George SL, Dodge RK, et al. Dose escalation studies of cytarabine, daunorubicin, and etoposide with and without multidrug resistance modulation with PSC-833 in untreated adults with acute myeloid leukemia younger than 60 years: final induction results of Cancer and Leukemia Group B study 9621. J Clin Oncol. 2004;22(21):4290-4301.

26. Marcucci G, Moser B, Blum W, et al. A phase III randomized trial of intensive induction and consolidation chemotherapy ± oblimersen, a pro-apoptotic Bcl-2 antisense oligonucleotide in untreated acute myeloid leukemia patients >60 years old. J Clin Oncol. 2007;25(suppl):360s (abstract 7012).

27. Attar EC, Johnson JL, Amrein PC, et al. Bortezomib added to daunorubicin and cytarabine during induction therapy and to intermediate-dose cytarabine for consolidation in patients with previously untreated acute myeloid leukemia age 60 to 75 years: CALGB (Alliance) study 10502. J Clin Oncol. 2013;31(7):923-929.

28. Blum W, Sanford BL, Klisovic R, et al. Maintenance therapy with decitabine in younger adults with acute myeloid leukemia in first remission: a phase 2 Cancer and Leukemia Group B study (CALGB 10503). Leukemia. 2017;31(1):34-39.

29. Stone RM, Berg DT, George SL, et al. Granulocyte-macrophage colony-stimulating factor after initial chemotherapy for elderly patients with primary acute myelogenous leukemia. N Engl J Med. 1995;332(25):1671-1677.

30. Kolitz JE, George SL, Marcucci G, et al. P-glycoprotein inhibition using valspodar (PSC-833) does not improve outcomes for patients under age 60 years with newly diagnosed acute myeloid leukemia: Cancer and Leukemia Group B study 19808. Blood. 2010;116(9):1413-1421.

31. Lee EJ, George SL, Caligiuri M, et al. Parallel phase I studies of daunorubicin given with cytarabine and etoposide with or without the multidrug resistance modulator PSC-833 in previously untreated patients 60 years of age or older with acute myeloid leukemia: results of Cancer and Leukemia Group B study 9420. J Clin Oncol. 1999;17(9):2831-2839.

32. Baer MR, George SL, Caligiuri MA, et al. Low-dose interleukin-2 immunotherapy does not improve outcome of patients age 60 years and older with acute myeloid leukemia in first complete remission: Cancer and Leukemia Group B study 9720. J Clin Oncol. 2008;26(30):4934-4939.

33. Uy GL, Mandrekar SJ, Laumann K, et al. A phase 2 study incorporating sorafenib into the chemotherapy for older adults with FLT3-mutated acute myeloid leukemia: CALGB 11001. Blood Adv. 2017;1(5):331-340.

34) Roboz GJ, Mandrekar SJ, Desai P, et al. A randomized trial of 10 days of decitabine alone or with bortezomib in previously untreated older patients with acute myeloid leukemia: CALGB 11002 (Alliance). Blood Adv. 2018;2(24):3608-3617.

35. Bray NL, Pimentel H, Melsted P, Pachter L. Near-optimal probabilistic RNA-seq quantification. Nat Biotechnol. 2016;34(5):525-527.

36. Mrózek K, Eisfeld A-K, Kohlschmidt J, et al. Complex karyotype in de novo acute myeloid leukemia: typical and atypical subtypes differ molecularly and clinically. Leukemia. 2019;33(7):1620-1634.

37. Paschka P, Marcucci G, Ruppert AS, et al. Adverse prognostic significance of KIT mutations in adult acute myeloid leukemia with inv(16) and t(8;21): a Cancer and Leukemia Group B study. J Clin Oncol. 2006;24(24):3904-3911.

38. Bloomfield CD, Lawrence D, Byrd JC, et al. Frequency of prolonged remission duration after high-dose cytarabine intensification in acute myeloid leukemia varies by cytogenetic subtype. Cancer Res. 1998;58(18):4173-4179.

39. Byrd JC, Dodge RK, Carroll A, et al. Patients with t(8;21)(q22;q22) and acute myeloid leukemia have superior failure-free and overall survival when repetitive cycles of high-dose cytarabine are administered. J Clin Oncol. 1999;17(12):3767-3775.

40. Byrd JC, Mrózek K, Dodge RK, et al. Pretreatment cytogenetic abnormalities are predictive of induction success, cumulative incidence of relapse, and overall survival in adult patients with de novo acute myeloid leukemia: results from Cancer and Leukemia Group B (CALGB 8461). Blood. 2002;100(13):4325-4336.

41. Grimwade D, Hills RK, Moorman AV, et al. Refinement of cytogenetic classification in acute myeloid leukemia: determination of prognostic significance of rare recurring chromosomal abnormalities among 5876 younger adult patients treated in the United Kingdom Medical Research Council Trials. Blood. 2010;116(3):354-365.

42. Lugthart S, Gröschel S, Beverloo HB, et al. Clinical, molecular and prognostic significance of WHO type inv(3)(q21;q26.2)/t(3;3)(q21;q26.2) and various other 3q abnormalities in acute myeloid leukemia. J Clin Oncol. 2010;28(24):3890-3898.

43. Fasan A, Eder C, Haferlach C, et al. GATA2 mutations are frequent in intermediate-risk karyotype AML with biallelic CEBPA mutations and are associated with favorable prognosis. Leukemia. 2013;27(2):482-485.

44. Gaidzik VI, Bullinger L, Schlenk RF, et al. RUNX1 mutations in acute myeloid leukemia: results from a comprehensive genetic and clinical analysis from the AML study group. J Clin Oncol. 2011;29(10):1364-1372.

45. Mendler JH, Maharry K, Radmacher MD, et al. RUNX1 mutations are associated with poor outcome in younger and older patients with cytogenetically normal acute myeloid leukemia and with distinct gene and microRNA expression signatures. J Clin Oncol. 2012;30(25):3109-3118.

46. Metzeler KH, Becker H, Maharry K, et al. ASXL1 mutations identify a high-risk subgroup of older patients with primary cytogenetically normal AML within the ELN favorable genetic category. Blood. 2011;118(26):6920-6929.

47. Pratcorona M, Abbas S, Sanders MA, et al. Acquired mutations in ASXL1 in acute myeloid leukemia: prevalence and prognostic value. Haematologica. 2012;97(3):388-392.

48. Schnittger S, Eder C, Jeromin S, et al. ASXL1 exon 12 mutations are frequent in AML with intermediate risk karyotype and are independently associated with an adverse outcome. Leukemia. 2013;27(1):82-91.

49. Haferlach C, Dicker F, Herholz H, Schnittger S, Kern W, Haferlach T. Mutations of the TP53 gene in acute myeloid leukemia are strongly associated with a complex aberrant karyotype. Leukemia. 2008;22(8):1539-1541.

50. Bowen D, Groves MJ, Burnett AK, et al. TP53 gene mutation is frequent in patients with acute myeloid leukemia and complex karyotype, and is associated with very poor prognosis. Leukemia. 2009;23(1):203-206.

Ferrata Storti Foundation

CDCA7 finely tunes cytoskeleton dynamics to promote lymphoma migration and invasion

Carla Martín-Cortázar,[1] Yuri Chiodo,[1] Raul Jiménez-P.,[1] Manuel Bernabé,[2] María Luisa Cayuela,[2] Teresa Iglesias[3,4] and Miguel R. Campanero[1,5]

[1]Department of Cancer Biology, Instituto de Investigaciones Biomédicas Alberto Sols, Madrid; [2]Telomerase, Aging and Cancer Group, Research Unit, Department of Surgery, CIBERehd, Instituto Murciano de Investigación Biosanitaria (IMIB), Murcia; [3]Department of Endocrine and Nervous Systems Pathophysiology, Instituto de Investigaciones Biomédicas Alberto Sols, Madrid ; [4]Centro de Investigación Biomédica en Red de Enfermedades Neurodegenerativas (CIBERNED), Madrid and [5]Centro de Investigaciones Biomédicas en Red en Enfermedades Cardiovasculares (CIBERCV), Madrid, Spain

ABSTRACT

Metastases, the major cause of death from cancer, require cells' acquisition of the ability to migrate and involve multiple steps, including local tumor cell invasion and basement membrane penetration. Certain lymphoid tumors are highly metastatic, but the mechanisms of invasion by lymphoma cells are poorly understood. We recently showed that CDCA7, a protein induced by MYC, is overexpressed in lymphoid tumors and that its knockdown decreases lymphoid tumor growth without inhibiting the proliferation of normal cells. Here we show that CDCA7 is critical for invasion and migration of lymphoma cells. Indeed, CDCA7 knockdown in lymphoma cells limited tumor cell invasion in matrigel-coated transwell plates and tumor invasion of neighboring tissues in a mouse xenograft model and in a zebrafish model of cell invasion. CDCA7 silencing markedly inhibited lymphoma cell migration on fibronectin without modifying cell adhesion to this protein. Instead, CDCA7 knockdown markedly disrupted the precise dynamic reorganization of actomyosin and tubulin cytoskeletons required for efficient migration. In particular, CDCA7 silencing impaired tubulin and actomyosin cytoskeleton polarization, increased filamentous actin formation, and induced myosin activation. Of note, inhibitors of actin polymerization, myosin II, or ROCK reestablished the migration capacity of CDCA7-silenced lymphoma cells. Given the critical role of CDCA7 in lymphomagenesis and invasion, therapies aimed at inhibiting its expression or activity might provide significant control of lymphoma growth, invasion, and metastatic dissemination.

Check the online version for the most updated information on this article, online supplements, and information on authorship & disclosures: www.haematologica.org/content/105/3/730

Introduction

Cancer cells acquire molecular alterations relative to their normal counterparts which confer them endless proliferative activity, resistance to death, and the capacity to metastasize, among other traits. Metastases are the major cause of death from cancer and their biological heterogeneity creates a critical obstacle to treatment.[1] Certain lymphoid tumors are highly metastatic, invading the spleen, lymph nodes and central nervous system. Indeed, direct invasion of the central nervous system occurs in 5% of all patients with non-Hodgkin lymphoma.[2] The incidence varies with clinical aggressiveness and can be as high as 27% for very aggressive lymphomas[2] and as high as 70% in the case of acute lymphoblastic leukemia in the absence of central nervous system-directed prophylactic treatment.[3]

Metastases of epithelial cancers involve local tumor cell invasion, basement membrane penetration, intravasation into blood or lymphatic vessels followed by exit from the circulation, and colonization of distant tissues. Most carcinoma cells produce matrix-degrading enzymes to clear a path for tissue invasion. The matrix metalloproteinase (MMP) family, a diverse group of calcium-dependent zinc-con-

taining endopeptidases, is the most common group of extracellular matrix (ECM) proteases involved in tumor invasion and metastasis.[4] MMP-2 and MMP-9, in particular, are highly expressed in metastatic cancer cells and contribute to the progression of tumors and formation of metastases.[5] *Ex vivo* studies suggest that carcinoma cells may also use a protease-independent scheme of invasion, whereby cells either squeeze through existing interstices in the ECM or displace ECM components.[6]

To invade surrounding tissues and vessels, cells must acquire the ability to migrate. Indeed, cell migration is required for the initial scattering of cells, egress from the primary tumor, basement membrane penetration, intravasation, and extravasation. Single carcinoma cells can migrate in mesenchymal or amoeboid manners.[7] Mesenchymal migration involves formation of protrusions and their adhesion to the substrate at the cell front, and loss of adhesion at the opposite end. During directional cell migration, actin polymerization drives protrusion formation, whereas the tension generated by non-muscle myosin II (NM-II) retracts the rear end of the cell.[8] The adhesion of the cell to the ECM at the protrusion end is as important as its dissociation at the opposite end of the cell.[9] The interaction with the substrate is mediated mainly by integrins, which have binding-motifs for ECM proteins. The connection between integrins and the actin cytoskeleton is mediated by actin-binding proteins such as talin, vinculin and α-actinin.[10] NM-II molecules are actin-binding proteins comprised of two heavy chains that have ATPase activity, two regulatory light chains that regulate NM-II activity, and two essential light chains that stabilize the heavy chain structure.[11] A major factor that determines cell migration is the cell's intrinsic contractility capacity,[10] which is modulated through the coordinated regulation of myosin activity and actin polymerization.[9] Myosin activity is exquisitely regulated through phosphorylation by signaling complexes and scaffold proteins to finely tune migration.[10] In particular, phosphorylation of Ser19 in the regulatory light chain induces the ATPase activity of NM-II.[11]

The mechanisms of invasion by lymphoma cells are poorly understood, but various reports suggest that the capacity of normal blood T lymphocytes and the lymphoma T-cell line SupT1 to move through three-dimensional collagen lattices does not require ECM degradation.[7,12] Instead, the motile capacity of these cells might be critical for migration through these gels.[7,13] While various migration modes have been described in normal non-lymphoid cells,[14] normal lymphocytes appear to migrate mainly in an amoeboid fashion. Amoeboid migration is characterized by weak adhesion to the substrate[9,10] and rapid cycles of actin polymerization and actomyosin contraction at the front and rear edges, respectively.[15]

Cell migration also involves the reorganization of the microtubule cytoskeleton. Microtubules are organized around the microtubule-organizing center and, similar to the actin filaments, are polarized.[16] The microtubule-organizing center is reoriented between the nucleus and the leading edge in migrating cells and contributes to directional cell migration.[17] The mechanisms that regulate the reorganization of the tubulin cytoskeleton in migrating lymphocytes do, however, remain unknown.

We recently showed that CDCA7 is a critical mediator of lymphomagenesis.[18] *CDCA7* was identified as a MYC-target gene.[19] Its encoded protein associates with the

Helicase, lymphoid-specific (HELLS) SNF2 family member and is required for nucleosome remodeling by HELLS and for DNA methylation maintenance.[20,21] AKT-mediated phosphorylation of CDCA7 promotes its nuclear exclusion and sequestration to the cytoplasm.[22] *CDCA7* mRNA was found to be deregulated in several tumor types, including lymphoid tumors,[23] and we recently showed that CDCA7 protein is also overexpressed in lymphoid tumors and that its silencing markedly impairs lymphoid tumor growth without inhibiting the proliferation of normal cells.[18]

As lymphoid tumors can be highly invasive,[2,3] we investigated the potential role of CDCA7 in lymphoid tumor invasion. Here we show that CDCA7 is critical for invasion and migration of lymphoma cells and for the reorganization of the tubulin and actomyosin cytoskeletons.

Methods

Details of the Methods can be found in the *Online Supplementary Appendix*.

Lentivirus production, cell transduction, and immunoblotting

Lentiviral particles were produced and cells were transduced, as described elsehwere,[24] employing vectors encoding either a non-targeting short hairpin (sh)RNA or *CDCA7*-targeting shRNA, sh-25 and sh-83. Cell lysates were prepared, resolved in sodium dodecylsulfate polyacrylamide gel electrophoresis, transferred to nitrocellulose membranes, and probed as described previously.[25]

In vitro and *in vivo* migration and invasion assays

In vitro transwell migration and invasion assays were carried out in Boyden chambers using filters (3-μm pore size) coated with fibronectin or a matrigel solution. *In vivo* invasion assays were performed using zebrafish embryos and subcutaneous xengrafts in mice. All animal procedures were approved by the CSIC Ethics Committee (ref. 054/2014 and 634/2017) and by the Madrid Regional authorities (ref. PROEX 31/14 and 215/17).

Results

CDCA7 silencing inhibits lymphoma invasion of adjacent tissues

Subcutaneous inoculation of lymphoma cells in immunodeficient mice gives rise to the formation of solid tumors[26,27] whose growth is impaired upon *CDCA7* knockdown.[18] To further investigate the role of CDCA7 in lymphomagenesis, we screened for histological differences between control- and CDCA7-silenced tumors. We therefore transduced DG-75 Burkitt lymphoma cells with lentivirus encoding *CDCA7*-specific shRNA (sh-25 and sh-83) to knock down CDCA7 expression. Immunoblot analysis showed that both shRNA markedly decreased CDCA7 levels in these cells relative to the levels in control cells transduced with a non-targeting shRNA (sh-Ctl) (Figure 1A). As previously reported,[18] CDCA7 silencing decreased tumor growth (*Online Supplementary Table S1*). Hematoxylin-eosin staining of tumor sections revealed that 100% of tumors formed by control-transduced cells contained muscle or adipose tissue (Figure 1B, C and

Online Supplementary Table S1). These non-lymphoid tissues were extremely disorganized and embedded within the tumor (Figure 1B, C and *Online Supplementary Table S1*), suggesting that lymphoma cells invaded the neighboring fat or muscle. In contrast, only 40% of tumors formed by CDCA7-silenced cells contained non-tumoral tissues and, when present, these tissues showed a rather well-preserved organization (Figure 1B, C and *Online Supplementary Table S1*). These results therefore suggest that while control lymphoma cells readily invade and disorganize adjacent tissues, CDCA7-silenced lymphoma cells hardly invade them. We looked for gene expression profiles of metastatic lymphomas using Genevestigator.[28] While we found gene expression profiling data of more than 1,600 cases of lymphoid tumors, we only found data on four metastatic cases (*Online Supplementary Figure S1*). Of note, CDCA7 levels were high in these cases and in numerous non-metastatic lymphoma/leukemia samples

(*Online Supplementary Figure S1*), suggesting that CDCA7 might be clinically relevant.

CDCA7 silencing restrains lymphoma invasion *in vitro* and *in vivo*

To confirm the contribution of CDCA7 to lymphoma cell invasion, we determined the capacity of CDCA7-silenced cells to invade matrigel-coated transwell plates. CDCA7 knockdown in DG-75 cells transduced with lentivirus encoding sh-Ctl, sh-25 or sh-83 was confirmed by immunoblotting (Figure 2A, left panel). Transduced cells were suspended in serum-free medium and seeded in the top chamber of matrigel-coated transwell plates. We used fetal bovine serum (FBS) as a chemoattractant in the lower chamber of these plates. Quantification of the number of cells capable of crossing the matrigel barrier and reaching the lower chamber showed that the invasive capacity of CDCA7-silenced cells was markedly lower
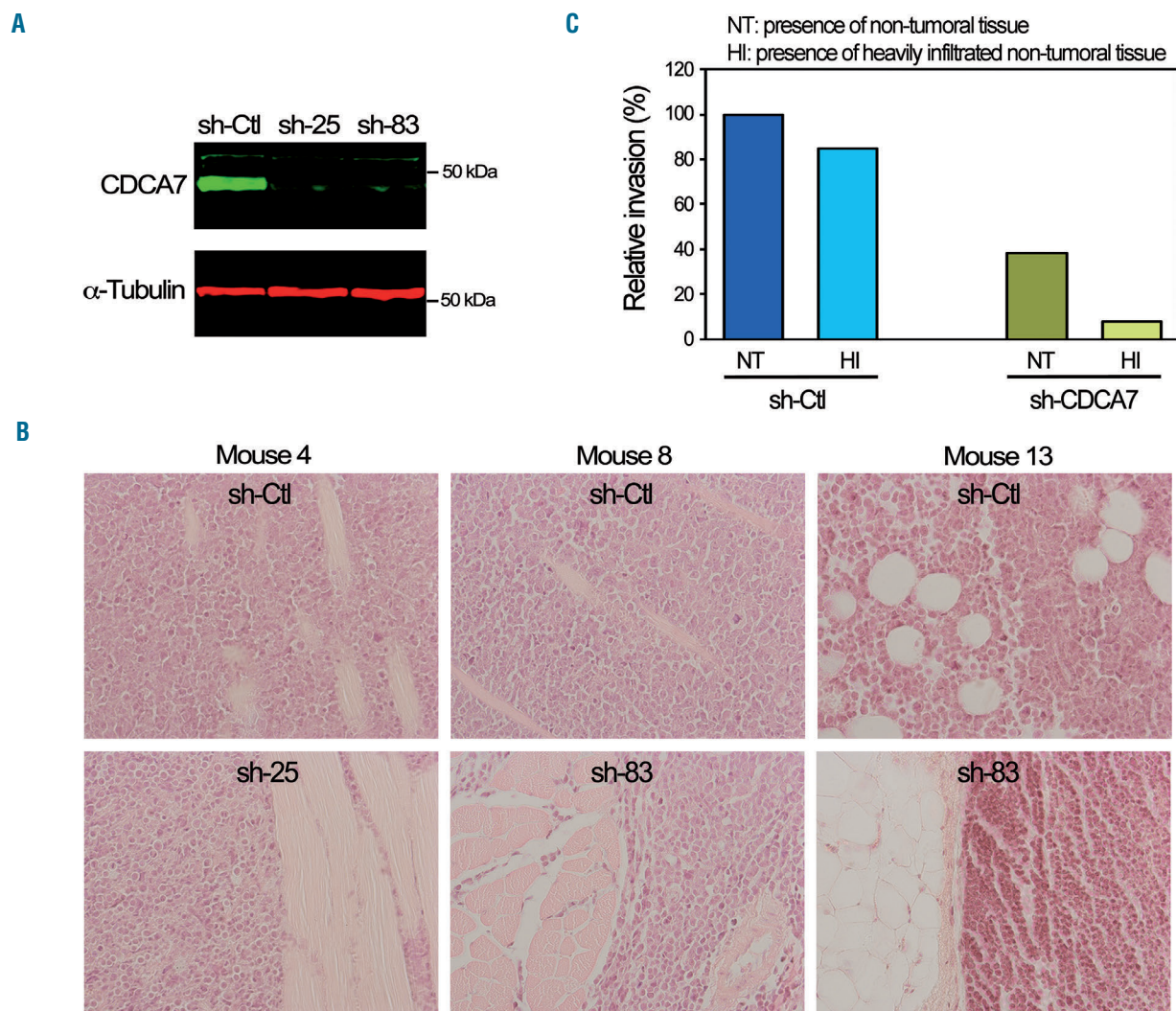
Figure 1. *CDCA7 silencing limits lymphoma dissociation of neighboring tissues.* DG-75 cells were transduced with lentivirus encoding short hairpin (sh) control (Ctl) RNA or the *CDCA7*-specific shRNA, sh-25 and sh-83, and selected in the presence of puromycin for >5 days. (A) Representative CDCA7 and α-tubulin (loading control) immunoblot analysis of these cells. (B, C) Transduced DG-75 cells were inoculated subcutaneously in immunodeficient NOD-SCID mice and tumors grown after 3 weeks were embedded in paraffin. All mice were inoculated with control cells in one flank (n=13) and sh-25 (n=7) or sh-83 (n=6) cells in the opposite flank. (B) Representative images of tumor sections from indicated mice stained with hematoxylin. Massively infiltrated (top panels) and poorly or non-infiltrated muscle and fat tissues (bottom panels) are shown. (C) Percentage of tumor masses with presence of non-tumoral tissues (NT) and percentage of tumor masses with heavily infiltrated non-tumoral tissues (HI). Additional information on these tumors is shown in *Online Supplementary Table S1*.

than that of control-transduced cells (Figure 2B). To determine whether CDCA7 mediates invasion of other lymphoma cells, we transduced BL-2 (Burkitt lymphoma) and Toledo (diffuse large B-cell lymphoma) cells with sh-25 or sh-83 lentivirus. These shRNA readily silenced CDCA7 expression in these cells (Figure 2A, middle and right panels) and sharply decreased their invasive capacity relative to that of control cells (Figure 2B).

As the zebrafish is a robust model for studying the invasive behavior of human tumor cells,[29] we used it to evaluate the contribution of CDCA7 to lymphoma invasion *in vivo*. Transduced DG-75 cells were stained with live dye DiI and microinjected into the yolk sac of zebrafish embryos. The capacity of these cells to escape the yolk sac and migrate to the embryo tail was quantified as the percent of embryos with >5 labeled lymphoma cells in the tail. While control cells were found in the tail of nearly 60% of the embryos, less than 40% of the embryos inoculated with CDCA7-silenced cells showed lymphoma cells in the tail (Figure 3A, B). To assess whether these results could be extended to other lymphomas, we determined the capacity of control and CDCA7-silenced Toledo cells to migrate from the yolk sac to the embryo tail. We found that CDCA7 knockdown markedly decreased the presence of Toledo cells in the tail (Figure 3C, D). Together, our results strongly suggest that CDCA7 is a key mediator of lymphoma invasion.

CDCA7 silencing hinders lymphoma migration

To investigate the mechanisms underlying CDCA7 regulation of cell invasion, we analyzed the expression of *MMP2* and *MMP9*, the major metalloproteinases involved in basement membrane and stromal ECM degradation during invasion.[5] The expression of these metalloproteinases was not detected in DG-75, BL-2, and Toledo cells (*Online Supplementary Figure S2A*), but it was readily detected in breast cancer MCF-7 or colon carcinoma SW480 cells (*Online Supplementary Figure S2B*). Since these results suggest that ECM degradation is not required for lymphoma invasion, we hypothesized that the migratory capacity of lymphoma cells might be critical for invasion. We therefore assessed the contribution of CDCA7 to lymphoma cell migration using fibronectin-coated transwell plates and FBS as a chemoattractant stimulus. BL-2 and Toledo cells attached poorly to fibronectin, but their binding was stimulated in the presence of the TS2/16 monoclonal antibody (*Online Supplementary Figure S3A*), an anti-integrin β1 monoclonal antibody that increases the avidity and affinity of β1 integrins for their ligands.[30] Of note, we could not detect adhesion of DG-75 cells to fibronectin even in the presence of this antibody (*not shown*). As lymphoma cells bind poorly to fibronectin, they reach the lower transwell chamber instead of remaining attached to the fibronectin-coated filter. Quantification of the number of cells in the lower chamber showed that CDCA7 silencing markedly decreased the migratory capacity of DG-75, BL2, and Toledo cells (Figure 4).

Although lymphoma cells bind poorly to fibronectin, the ablation of this binding could formally account for the inhibition of cell migration upon CDCA7 silencing. Alternatively, a sharp increase in binding could also slow down migration. However, we found that CDCA7 knockdown did not substantially affect the binding of lymphoma cells to fibronectin (*Online Supplementary Figure S3A*). Moreover, CDCA7 silencing did not affect the

expression of integrins α4 and β1 (*Online Supplementary Figure S3B, C*), the subunits of the major fibronectin receptor of these cells. Activation of β1 integrin binding activity induces a conformational modification of the β1 subunit that is recognized by the HUTS-21 monoclonal antibody.[31] Staining of lymphoma cells with HUTS-21 showed that CDCA7 silencing did not affect the activity of this fibronectin receptor (*Online Supplementary Figure S3B, C*).
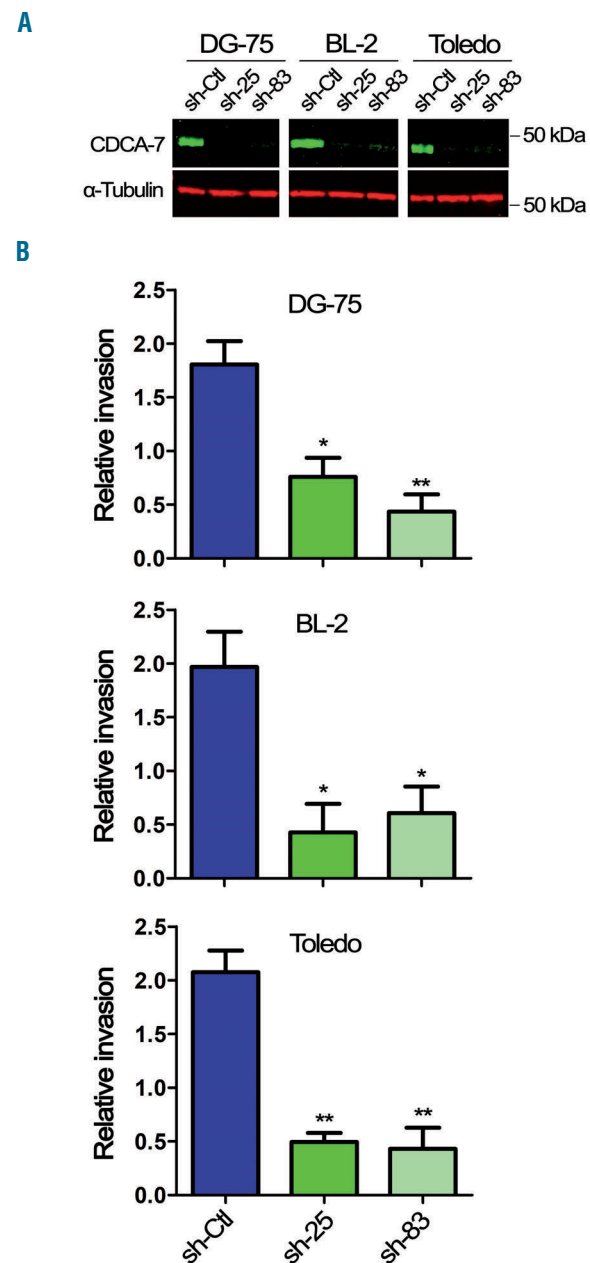
Figure 2. *CDCA7 knockdown inhibits lymphoma invasion in vitro.* (A) Representative CDCA7 and α-tubulin immunoblot analysis of cell lysates from DG-75, BL-2, and Toledo cells lentivirally transduced with the indicated short hairpin (sh) RNA. (B) These cells were seeded on the upper surface of the matrigel-coated polycarbonate membrane of transwell chambers containing 10% fetal bovine serum in the lower chamber. Quantification of the relative invasive capacity is shown as the mean + standard error of mean. of three independent transductions. *$P<0.05$ and **$P<0.01$ (one-way analysis of variance with the Bonferroni post-test).

FBS contains numerous potentially chemoattractant stimuli for lymphoma cells whose receptors could be downregulated upon CDCA7 silencing, thereby accounting for the inhibition of cell migration towards FBS. To challenge this hypothesis, we used the stomal cell-derived factor 1 (SDF1) chemokine as chemoattractant for BL-2 and Toledo cell instead of FBS. SDF1 activated BL-2 and Toledo cells migration in fibronectin-coated transwell plates (*Online Supplementary Figure S4A*) and this migration was markedly inhibited by CDCA7 silencing (*Online Supplementary Figure S4B*). However, the expression of CXCR4, the SDF1 receptor, was not modified in these cells upon CDCA7 silencing, as determined by flow cytometry analysis (*Online Supplementary Figure S5*). CDCA7 knockdown could potentially inhibit migration towards SDF1 by modulating the binding of lymphoma cells to fibronectin. However, SDF1 did not regulate this interaction and CDCA7 silencing also failed to modulate the binding of SDF1-treated lymphoma cells to fibronectin (*Online Supplementary Figure S6*).

Disruption of the tubulin and actomyosin cytoskeletons by CDCA7 silencing

Since cytoskeleton reorganization is critical for cell migration, we next investigated the role of CDCA7 in the reorganization of the microtubule and actomyosin cytoskeletons in lymphoma cells. Confocal microscopic imaging of lymphoma cells stained with fluorescently-labeled phalloidin showed a polarized distribution of filamentous actin (F-actin) in >40% control-transduced Toledo and BL-2 lymphoma cells (Figure 5A-D). CDCA7 silencing reordered F-actin around the cells, decreasing the percentage of cells with polarized distribution of F-actin (Figure 5A-D). In addition, CDCA7 knockdown markedly increased F-actin levels (Figure 5A, B, E). Staining of the microtubule cytoskeleton revealed its marked polarization in control-transduced lymphoma cells and that CDCA7 knockdown elicited its redistribution around the cells (Figure 5A-D). Moreover, while actin and microtubule cytoskeletons were located in opposite ends of most control-transduced cells, their distribution overlapped in CDCA7-silenced cells (Figure 5A, B, F). Of note, we could not assess the polarization of tubulin and actin cytoskeletons in DG-75 cells because these cells did not attach to the fibronectin-coated coverglasses used for these studies.

The actin-binding protein α-actinin is an important organizer of the actomyosin cytoskeleton.[32] Four α-actinin isoforms have been identified (ACTN1-ACTN4), but non-muscle cells express only ACTN1 and ACTN4.[32] Staining of lymphoma cells with a monoclonal antibody specific
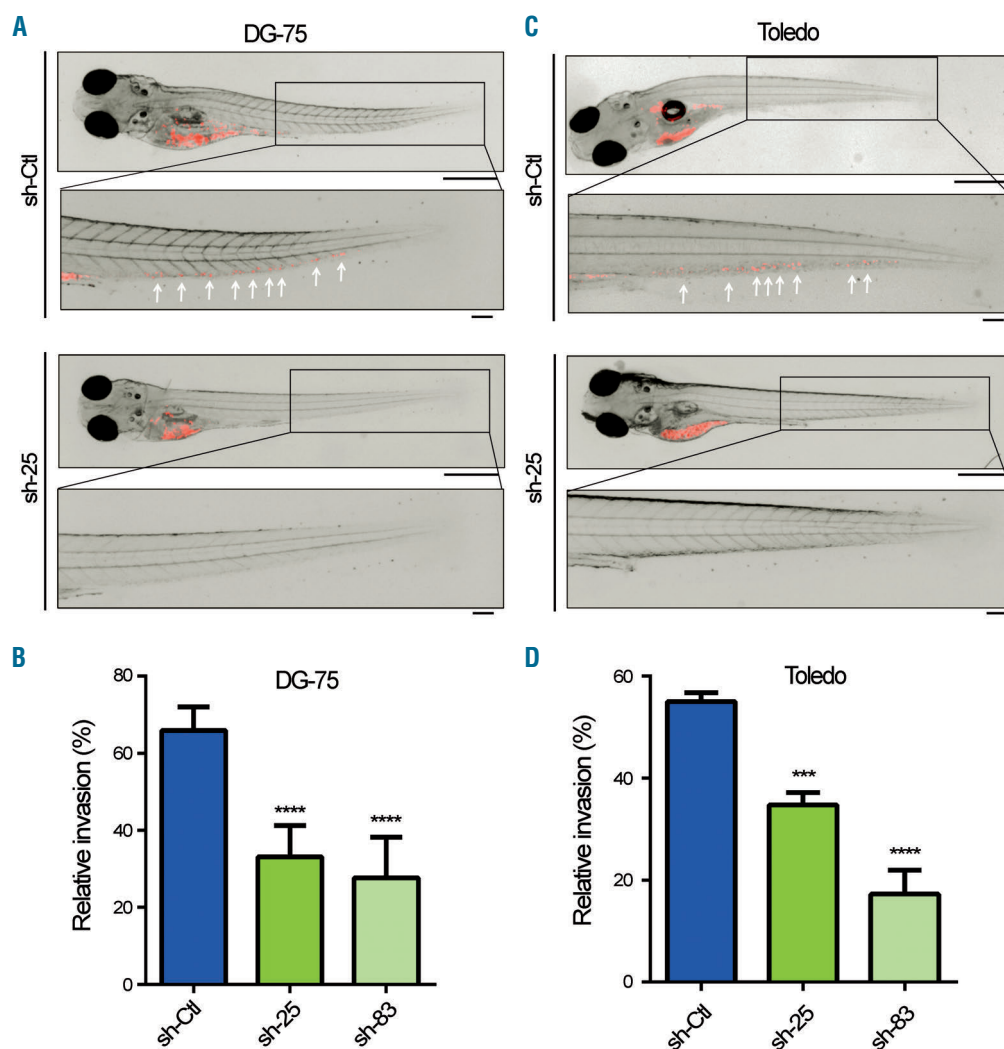
Figure 3. *CDCA7* silencing impairs lymphoma invasion *in vivo*. (A,B) DG-75 and (C,D) Toledo cells lentivirally transduced with short hairpin (sh) control (Ctl) or the CDCA7-specific shRNA, sh25 and sh83, were stained and injected into the yolk sac of zebrafish embryos. Images of representative zebrafish embryos in which sh-Ctl- or sh-25-transduced (A) DG-75 or (C) Toledo cells have invaded (sh-Ctl) or not (sh-25) their caudal region. Long scale bars, 500 μm; short scale bars, 100 μm. Percentage of embryos with >5 (B) DG-75 or (D) Toledo cells in the caudal region shown as the mean + standard error of mean of four independent experiments. ***P<0.001 and ****P<0.0001 (χ² and two-tailed Fisher exact test). More than 100 embryos were examined for each condition, in four independent experiments.

for ACTN1 barely detected its expression in control-transduced cells (Figure 6A-D). However, ACTN1 was readily detected in CDCA7-knockdown cells (Figure 6A-D). In contrast, a polyclonal antibody that reacts with isoforms 1, 2, and 4 showed a similar staining intensity in control and silenced cells (Figure 6A-D). These results suggested that CDCA7 might inhibit ACTN1 expression. However, immunoblot analysis of these cells with the monoclonal antibody revealed similar ACTN1 levels in control and silenced cells (Figure 6E). Together, these data suggest that CDCA7 silencing unmasks the epitope recognized by the ACTN1-specific monoclonal antibody.

Staining of α-actinin with the polyclonal antibody showed a dotted pattern in control-transduced BL-2 and Toledo cells and, contrary to the actin and tubulin cytoskeletons, its distribution was not substantially affected by CDCA7 silencing (*Online Supplementary Figure S7A, B*). As one of the roles of α-actinin is to act as a link between integrins and the actin cytoskeleton, we investigated the distribution of active β1 integrins in lymphoma cells. Similar to α-actinin, active β1 integrin staining showed a dotted pattern in control- and CDCA7-knockdown BL-2 and Toledo cells (*Online Supplementary Figure S7A, B*). The presence of numerous white dots in merged images (*Online Supplementary Figure S7A, B*) strongly suggested that α-actinin and active β1 integrins do indeed colocalize in these cells. Determination of Pearson and Mander coefficients supported this hypothesis (*Online Supplementary Figure S7C, D*).

The actomyosin cytoskeleton is constituted by F-actin in association with numerous proteins, including myosins and tropomyosins (TPM). To investigate whether CDCA7 also regulates the cellular distribution of these proteins, we used fluorescence microscopy analysis. We found that TPM3 showed a polarized distribution in nearly 60% of control-transduced BL-2 and Toledo lymphoma cells, which was markedly decreased upon CDCA7 knockdown (Figure 7A-D).

As phosphorylation of the myosin regulatory light chain (MLC) on Ser19 is a marker of NM-II activation,[11] we investigated the distribution of active myosin in lymphoma cells by immunofluorescence using an antibody that specifically recognizes MLC phosphorylated on that residue (pMLC-S19). Similar to TPM3 and F-actin, pMLC-S19 was located in one pole of nearly 40% of control-

transduced lymphoma cells and its polarized distribution markedly decreased upon CDCA7 silencing (Figure 7A-D). Of note, this redistribution was accompanied by a substantial increase of pMLC-S19 levels in silenced cells (Figure 7A, B, E). MLC phosphorylation can be induced by RhoA kinase (ROCK).[33] To determine whether ROCK-mediated MLC activation contributed to the inhibition of cell migration imposed by CDCA7 knockdown, we treated control and lymphoma cells with the ROCK inhibitor fasudil. We found that fasudil inhibited MLC phosphorylation (*Online Supplementary Figure S8*) and neutralized the inhibition of cell migration in CDCA7-silenced lymphoma cells (Figure 8). Similarly, the NM-II inhibitor blebbistatin restored the migration competency of CDCA7-silenced cells (Figure 8), suggesting that ROCK-mediated NM-II activation hindered cell migration upon CDCA7 knockdown. Given the increase of F-actin in CDCA7-silenced cells, we also investigated the contribution of actin polymerization to the inhibition of lymphoma cell migration. We found that treatment of these cells with the actin polymerization inhibitor cytochalasin D overcame the migratory restraint imposed by CDCA7 silencing (Figure 8). Together, these results strongly support the notion that CDCA7 modulation of myosin activation and actin polymerization is critical for the regulation of cell migration.

Discussion

While the processes and mechanisms involved in carcinoma invasion and the formation of metastases have been extensively characterized, little is known about the molecular mechanisms involved in lymphoma cell invasion. Here we show that CDCA7 is a critical mediator of lymphoma cell invasion *in vivo* and *in vitro* and that *CDCA7* knockdown greatly impairs lymphoma migration, through the regulation of tubulin and actomyosin cytoskeleton dynamics.

Metastases involve breaching of numerous histological barriers to move to distant sites. In the case of epithelial cancers, this process involves not only cell motility but also the proteolytic degradation of ECM molecular components. Among hundreds of proteinase genes, the MMP family has been implicated in carcinoma tumor invasion and metastasis formation.[4] Indeed, MMP are overex-
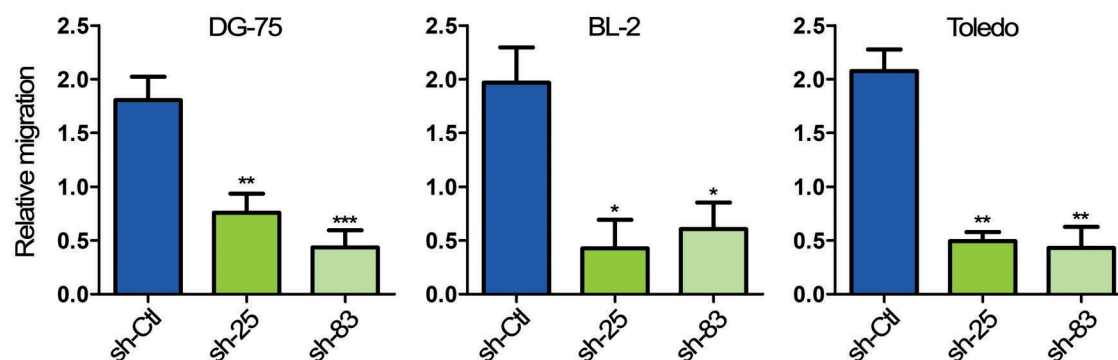
Figure 4. *CDCA7* knockdown markedly inhibits serum-induced lymphoma migration. DG-75, BL-2, and Toledo cells were transduced with lentivirus encoding the indicated short hairpin (sh) RNA and seeded on the upper surface of the fibronectin-coated polycarbonate membrane of transwell chambers containing 10% fetal bovine serum in the lower chamber. Quantification of the relative migration capacity is shown as the mean + standard error of mean of three independent transductions. *P<0.05, **P<0.01 and ***P<0.001 (one-way analysis of variance with the Bonferroni post-test).

pressed in multiple tumors[34] and their overexpression is critical for carcinoma invasion and metastasis formation.[35] MMP2 and MMP9, in particular, degrade type IV collagen, a major component of the basement membrane, and thus facilitate tumor invasion.[4] MMP9 is also required for intravasation, extravasation, and local migration of tumor cells.[36]

Infiltrating non-tumoral lymphocytes often express elevated MMP levels.[37] In fact, the capacity of these cells to penetrate through basement membrane equivalents *in vitro* is facilitated by active MMP2 and MMP9.[38] In addition,

MMP9 was found on the surface of B-cell chronic lymphocytic leukemia cells, where it is a critical regulator of cell migration.[39] MMP2 or MMP9 is also found in some lymphoma cell lines.[40] Nonetheless, none of the lymphoma cells used in our study expresses these MMP, indicating that CDCA7 does not regulate the capacity for invasion of these cells through these proteins. We cannot rule out however that CDCA7 may potentially promote lymphoma invasion through paracrine stimulation of MMP2/9 production by neighboring stromal cells or through the regulation of other MMP. Alternatively,
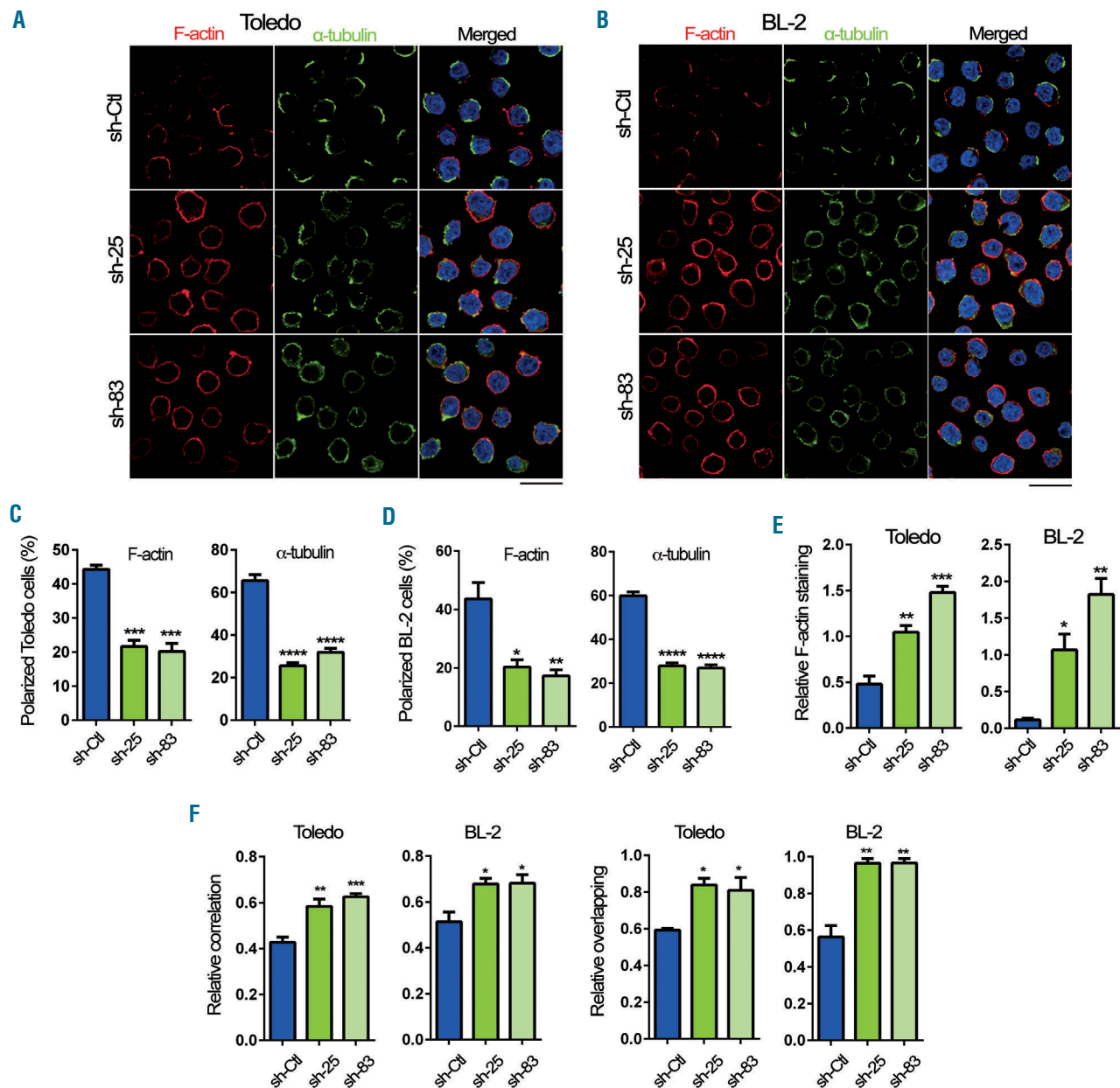
Figure 5. CDCA7 knockdown impairs actin and tubulin cytoskeletons polarization. BL-2 and Toledo cells were transduced with the indicated short hairpin (sh) RNA, seeded on coverslips coated with 2 μg fibronectin, and stimulated with 10 ng/mL stromal cell-derived factor 1 for 15 min. Representative confocal microscopy images (1 section) of (A) Toledo and (B) BL-2 transduced cells stained with anti-α-tubulin, phalloidin (F-actin), and DAPI. Quantification of the percentage of (C) Toledo and (D) BL-2 cells displaying polarized distribution of F-actin and α-tubulin. (E) Quantification of relative F-actin fluorescence intensity and (F) α-tubulin and F-actin colocalization measured as relative correlation (Pearson coefficient) and overlapping (Mander coefficient) of signals. Data are presented as the mean + standard error of mean of three independent experiments. *P<0.05, **P<0.01, ***P<0.001, and ****P<0.0001 (one-way analysis of variance with the Bonferroni post-test). Scale bar, 10 μm.

CDCA7 may regulate the expression or the activity of other enzymes involved in basement membrane degradation, such as heparanases and sulfatases.[41,42]

The histological barriers confronting metastasizing cells vary in ECM composition, organization, and biophysical characteristics. Cells might therefore use different means to negotiate these diverse physical barriers. While, as mentioned above, normal lymphocytes are facilitated in their crossing of basement membrane by MMP,[38] their migration within three-dimensional collagen matrices was insensitive to a protease inhibitor cocktail targeting MMP, serine proteases, cysteine proteases, and cathepsins.[12] In contrast, the invasive behavior of epithelial cancer cells was impaired by pharmacological inhibition of proteas-es.[13] These results suggest that instead of clearing a path for tissue invasion, normal lymphocytes use protease-independent mechanisms to slither through interstices in the stromal ECM. Similarly, ECM degradation is not required for lymphoma cell migration.[43]

The protease-independent fashion of negotiating physical barriers involves the coordinated adoption of an amoeboid type of migration and the use of actomyosin-based mechanical forces to physically displace matrix fibrils.[6] Similar to the mesenchymal type of movement adopted by epithelial cells, amoeboid migration requires dynamic assembly/disassembly of the actomyosin network.[15] However, while mesenchymal migration relies strongly on coordinated cell adhesion to the ECM in the leading
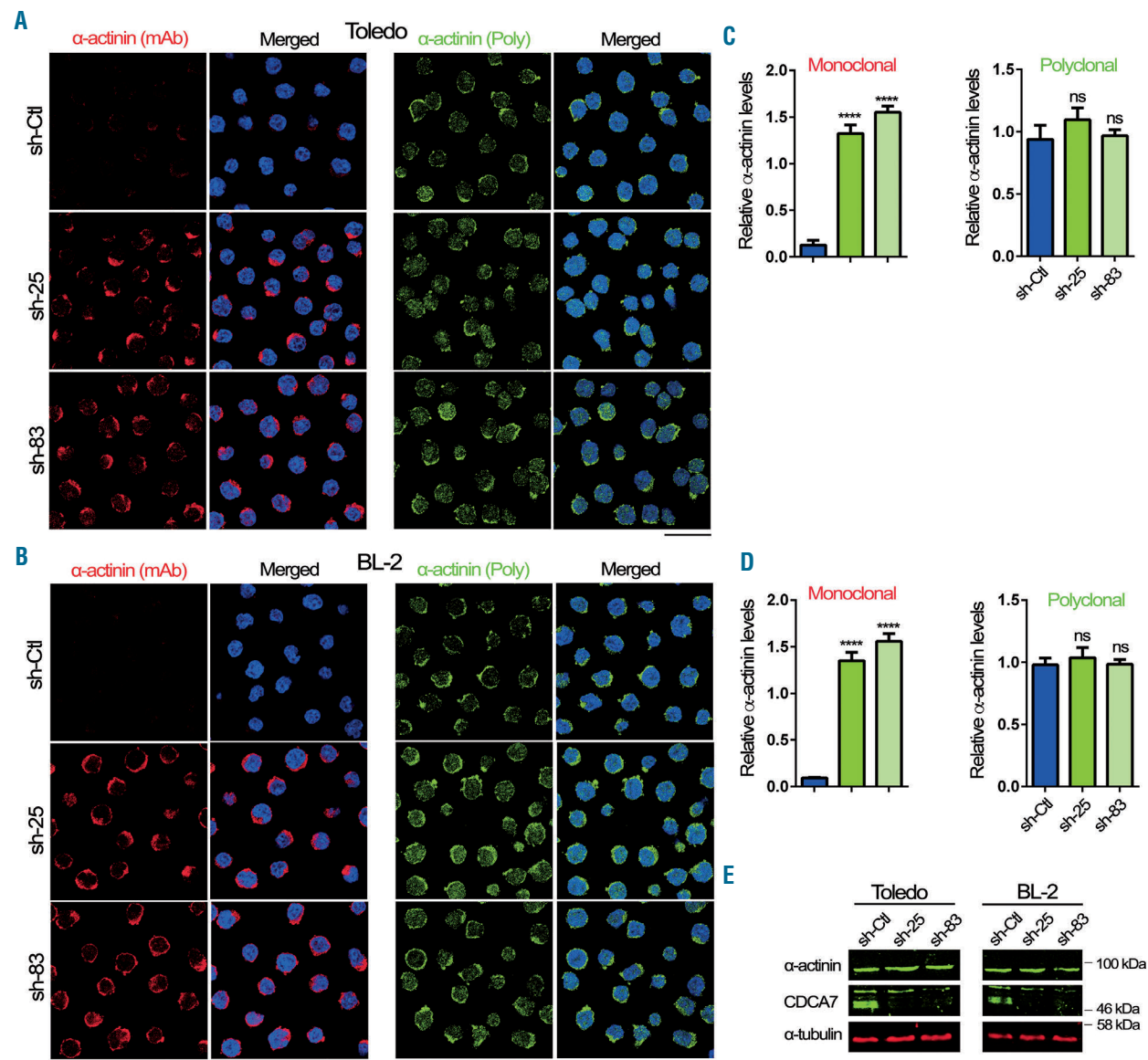
Figure 6. Increased α-actinin staining in *CDCA7*-silenced lymphoma cells. BL-2 and Toledo cells were transduced with the indicated short hairpin (sh) RNA, seeded on coverslips coated with 2 μg fibronectin, and stimulated with 10 ng/mL stromal cell-derived factor 1 for 15 min. Representative confocal microscopy images (1 section) of (A) Toledo and (B) BL-2 transduced cells stained with an anti-α-actinin monoclonal antibody (mAb) and DAPI or an anti-α-actinin polyclonal antibody (Poly) and DAPI. Quantification of relative α-actinin staining with the monoclonal and the polyclonal antibodies in (C) Toledo and (D) BL-2 cells transduced as indicated. ns, non-significant; ****$P<0.0001$ (one-way analysis of variance with the Bonferroni post-test). (E) Representative CDCA7 and α-actinin (probed with the mAb) immunoblot analysis of cell lysates from BL-2 and Toledo cells transduced with the indicated shRNA. Bar, 10 μm.

edge and its detachment at the opposite end of the cell, amoeboid movement is driven by short-lived and relatively weak interactions with the ECM.[7] In amoeboid migration, movement is generated by cortical filamentous actin in the cell front in the absence of focal contacts and stress fibers.[7]

Given that the lymphoma cells used in our study do not express *MMP2* and *MMP9* and bind fibronectin very

weakly, we propose that these cells use an amoeboid type of invasion. In line with a minor role for cell adhesion in the movement of these cells, the inhibition of cell migration and invasion upon CDCA7 silencing was not paralleled by a substantial modification of their binding to fibronectin. Accordingly, the expression and activity of VLA-4, the major fibronectin receptor of these cells, was not affected by CDCA7 knockdown.
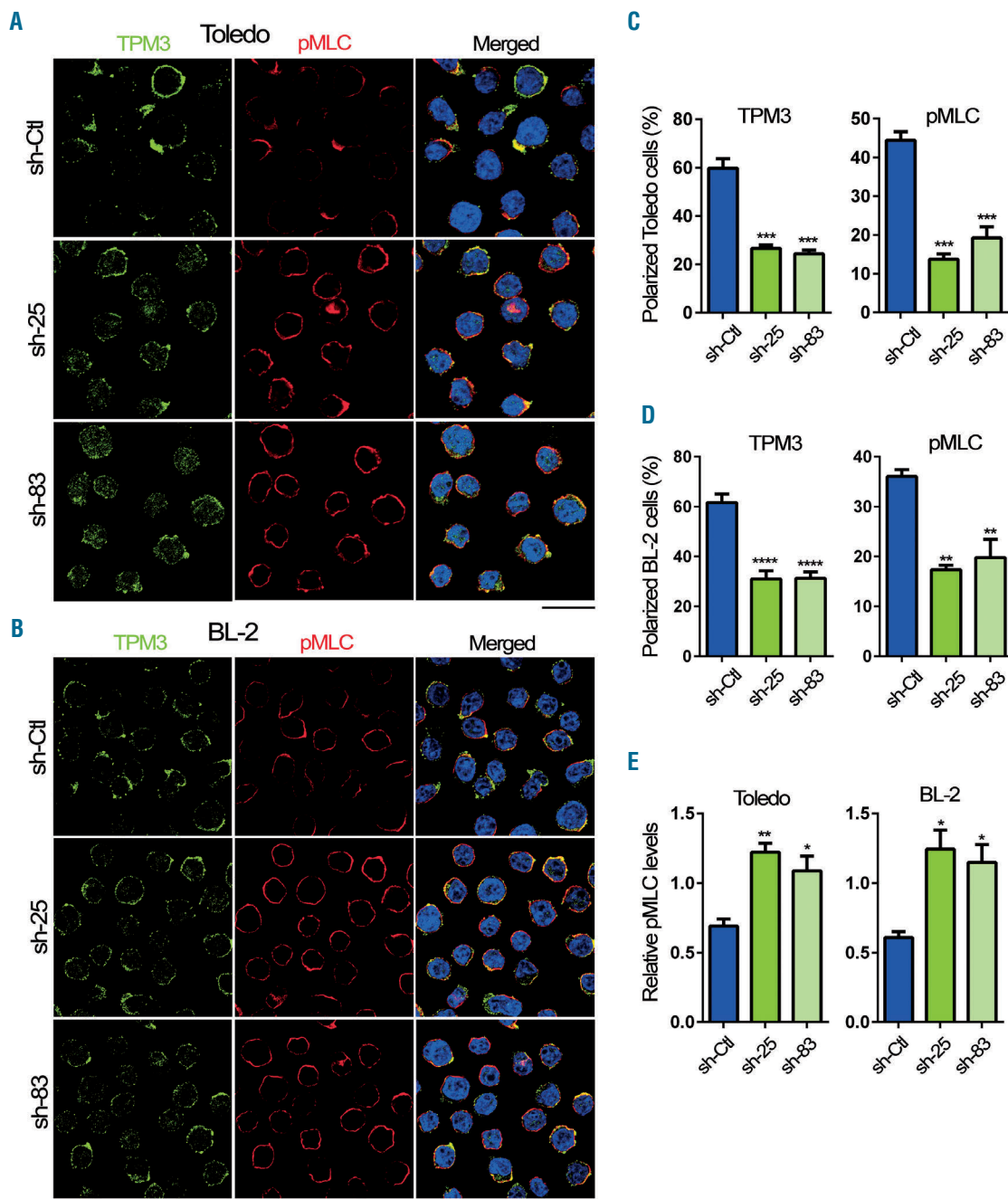
Figure 7. *CDCA7 silencing decreases tropomyosin 3 polarization and promotes myosin light chain phosphorylation.* BL-2 and Toledo cells were transduced with the indicated short hairpin (sh) RNA, seeded on coverslips coated with 2 μg fibronectin, and stimulated with 10 ng/mL stromal cell-derived factor 1 for 15 min. Representative confocal microscopy images (1 section) of (A) Toledo and (B) BL-2 transduced cells stained with anti-tropomyosin 3 (TPM3), anti-phospho-myosin light chain (pMLC) and DAPI. Quantification of the percentage of (C) Toledo and (D) BL-2 cells displaying polarized distribution of TPM3 or pMLC. (E) Quantification of relative pMLC fluorescence intensity. Data are presented as the mean + standard error of mean of three independent experiments. *$P<0.05$, **$P<0.01$, ***$P<0.001$, and ****$P<0.0001$ (one-way analysis of variance with the Bonferroni post-test). Bar, 10 μm.

A recent report described the association of CDCA7 overexpression in the most aggressive breast cancer subtype with metastatic relapse and that CDCA7 mediates breast cancer migration through transcriptional upregulation of the EZH2 epigenetic modifier.[44] However, CDCA7 knockdown did not substantially modify *EZH2* mRNA levels in lymphoma cells (*Online Supplementary Figure S9*), indicating that CDCA7 regulates migration and invasion through distinct mechanisms in breast cancer and lymphoma.

During cell migration, tubulin and actomyosin cytoskeletons are located in opposite ends of the cells, and cell migration involves their constant and coordinated remodeling.[11,16] We propose that CDCA7 is required for the dynamic remodeling of both cytoskeletons and that its absence (as in knockdown cells) elicits depolarization and stabilizes cortical actin filaments, thus preventing the high dynamism of tubulin and actomyosin cytoskeletons required for cell migration. Supporting this hypothesis, we have shown that tubulin and F-actin are grouped in opposite poles of most control lymphoma cells and that both redistribute around the cell in CDCA7-silenced lymphoma cells. Similarly, the polarized distribution of TPM3 and p-MLC observed in most control cells is lost upon CDCA7 knockdown.

In contrast, the dotted distribution of α-actinin was not lost in CDCA7-silenced cells. It should be noted that besides binding to actin filaments, α-actinin associates with a number of signaling molecules, ion channels, transcription factors, and transmembrane receptors, including integrins.[45] It therefore seems likely that α-actinin dissociates from F-actin in CDCA7-silenced cells, remaining associated with integrins or other transmembrane receptors. Indeed, our data support the notion that α-actinin is associated with active integrins in both control- and CDCA7-knockdown cells. Among the four α-actinin isoforms identified, non-muscular cells only express ACTN1 and ACTN4.[46] The staining of lymphoma cells with a monoclonal antibody specific to ACTN1 was markedly increased in CDCA7-silenced cells relative to control cells, raising the possibility that CDCA7 knockdown upregulated ACTN1 expression. However, the staining of these cells with a polyclonal antibody common to ACTN1 and ACTN4 showed no substantial differences between control and silenced cells, and ACTN1 immunoblot analysis revealed similar protein levels in both cell populations. Together these results support the notion that instead of regulating ACTN1 levels, CDCA7 regulates, by unknown mechanisms, ACTN1 conformation or its association with other proteins, thus increasing the exposure of the epitope recognized by the monoclonal antibody. We propose a model whereby CDCA7 is required for the dynamic association/dissociation of integrin-bound α-actinin to/from F-actin. The association of α-actinin to the actomyosin cytoskeleton would mask the epitope recognized by the monoclonal antibody. The absence of CDCA7 would hamper the association of integrin-bound α-actinin to this cytoskeleton, exposing the epitope and, more importantly, altering the cytoskeleton dynamics required for efficient migration. Forced CDCA7 downregulation would also hinder migration through the stabilization of F-actin and myosin activation. Of note, both processes can be activated by ROCK[33] and we show herein that ROCK inhibition
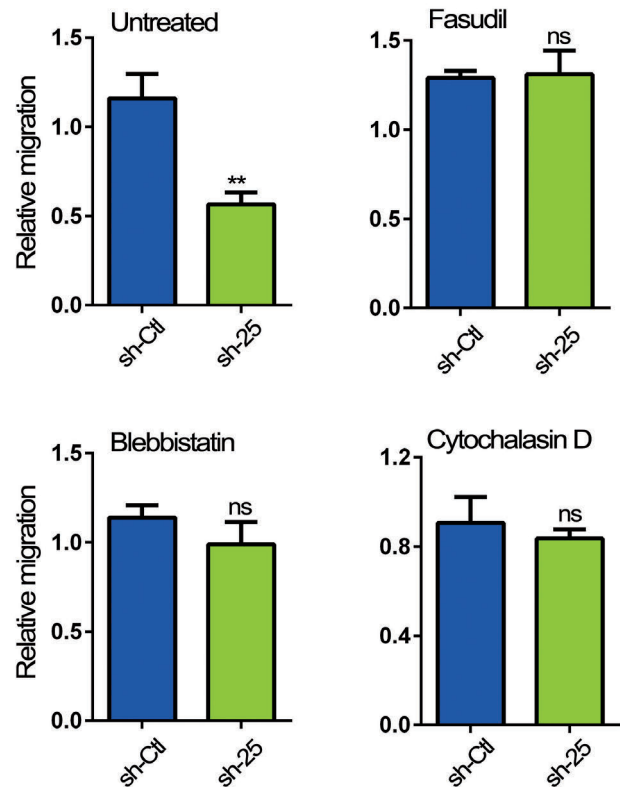
Figure 8. The inhibition of myosin activation or actin polymerization reestablish the migration capacity in CDCA7-silenced cells. Toledo cells were transduced with the indicated short hairpin (sh) RNA, and seeded on the upper surface of the fibronectin-coated polycarbonate membrane of transwell chambers in the presence of 20 μM fasudil, 25 μM blebbistatin, or 0.1 μg/mL cytochalasin D; 10% fetal bovine serum was used in the lower chamber as a chemoattractant. Quantification of the relative migration capacity is shown as the mean + standard error of mean of three independent transductions. **P<0.01; ns, non-significant (one-tailed *t*-test).

re-established the migratory capacity of silenced cells. These results suggest that CDCA7 silencing might induce ROCK activation in lymphoma cells.

We have shown that CDCA7 is critically involved in the anchorage-independent growth of lymphoid tumors and in lymphomagenesis.[18] While CDCA7 is also expressed in normal diploid fibroblasts, its silencing in these cells did not inhibit their anchorage-dependent proliferation.[18] Hence, given the essential role of CDCA7 in lymphoma progression and invasion, treatments that inhibit its expression or its activity represent an attractive strategy for controlling lymphoma growth, invasion, and metastatic dissemination.

References

1. Fidler IJ, Kripke ML. The challenge of targeting metastasis. Cancer Metastasis Rev. 2015;34(4):635-641.
2. Colocci N, Glantz M, Recht L. Prevention and treatment of central nervous system involvement by non-Hodgkin's lymphoma: a review of the literature. Semin Neurol. 2004;24(4):395-404.
3. Kufe DW, Holland JF, Frei E, American Cancer Society. Cancer Medicine. 6th ed. Hamilton, Ont.; Lewiston, NY: BC Decker, 2003.
4. Bonnans C, Chou J, Werb Z. Remodelling the extracellular matrix in development and disease. Nat Rev Mol Cell Biol. 2014;15(12):786-801.
5. Mittal R, Patel AP, Debs LH, et al. Intricate functions of matrix metalloproteinases in physiological and pathological conditions. J Cell Physiol. 2016;231(12):2599-2621.
6. Sabeh F, Shimizu-Hirota R, Weiss SJ. Protease-dependent versus -independent cancer cell invasion programs: three-dimensional amoeboid movement revisited. J Cell Biol. 2009;185(1):11-19.
7. Friedl P, Wolf K. Tumour-cell invasion and migration: diversity and escape mechanisms. Nat Rev Cancer. 2003;3(5):362-374.
8. Ridley AJ. Life at the leading edge. Cell. 2011;145(7):1012-1022.
9. Vicente-Manzanares M, Webb DJ, Horwitz AR. Cell migration at a glance. J Cell Sci. 2005;118(Pt 21):4917-4919.
10. Parsons JT, Horwitz AR, Schwartz MA. Cell adhesion: integrating cytoskeletal dynamics and cellular tension. Nat Rev Mol Cell Biol. 2010;11(9):633-643.
11. Vicente-Manzanares M, Ma X, Adelstein RS, Horwitz AR. Non-muscle myosin II takes centre stage in cell adhesion and migration. Nat Rev Mol Cell Biol. 2009;10(11):778-790.
12. Wolf K, Muller R, Borgmann S, Brocker EB, Friedl P. Amoeboid shape change and contact guidance: T-lymphocyte crawling through fibrillar collagen is independent of matrix remodeling by MMPs and other proteases. Blood. 2003;102(9):3262-3269.
13. Wolf K, Mazo I, Leung H, et al. Compensation mechanism in tumor cell migration: mesenchymal-amoeboid transition after blocking of pericellular proteolysis. J Cell Biol. 2003;160(2):267-277.
14. Michaelis UR. Mechanisms of endothelial cell migration. Cell Mol Life Sci. 2014;71(21):4131-4148.
15. Lammermann T, Sixt M. Mechanical modes of 'amoeboid' cell migration. Curr Opin Cell Biol. 2009;21(5):636-644.
16. Krummel MF, Macara I. Maintenance and modulation of T cell polarity. Nat Immunol. 2006;7(11):1143-1149.
17. Gomes ER, Jani S, Gundersen GG. Nuclear movement regulated by Cdc42, MRCK, myosin, and actin flow establishes MTOC polarization in migrating cells. Cell. 2005;121(3):451-463.
18. Jimenez PR, Martin-Cortazar C, Kourani O, et al. CDCA7 is a critical mediator of lymphomagenesis that selectively regulates anchorage-independent growth. Haematologica. 2018;103(10):1669-1678.
19. Prescott JE, Osthus RC, Lee LA, et al. A novel c-Myc-responsive gene, JPO1, participates in neoplastic transformation. J Biol Chem. 2001;276(51):48276-48284.
20. Jenness C, Giunta S, Muller MM, Kimura H, Muir TW, Funabiki H. HELLS and CDCA7 comprise a bipartite nucleosome remodeling complex defective in ICF syndrome. Proc Natl Acad Sci U S A. 2018;115(5):E876-E885.
21. Thijssen PE, Ito Y, Grillo G, et al. Mutations in CDCA7 and HELLS cause immunodeficiency-centromeric instability-facial anomalies syndrome. Nat Commun. 2015;6:7870.
22. Gill RM, Gabor TV, Couzens AL, Scheid MP. The MYC-associated protein CDCA7 is phosphorylated by AKT to regulate MYC-dependent apoptosis and transformation. Mol Cell Biol. 2013;33(3):498-513.
23. Osthus RC, Karim B, Prescott JE, et al. The Myc target gene JPO1/CDCA7 is frequently overexpressed in human tumors and has limited transforming activity in vivo. Cancer Res. 2005;65(13):5620-5627.
24. Alvaro-Blanco J, Urso K, Chiodo Y, et al. MAZ induces MYB expression during the exit from quiescence via the E2F site in the MYB promoter. Nucleic Acids Res. 2017;45(17):9960-9975.
25. Campanero MR, Herrero A, Calvo V. The histone deacetylase inhibitor trichostatin A induces GADD45 gamma expression via Oct and NF-Y binding sites. Oncogene. 2008;27(9):1263-1272.
26. Molina-Privado I, Jimenez PR, Montes-Moreno S, et al. E2F4 plays a key role in Burkitt lymphoma tumorigenesis. Leukemia. 2012;26(10):2277-2285.
27. Molina-Privado I, Rodriguez-Martinez M, Rebollo P, et al. E2F1 expression is deregulated and plays an oncogenic role in sporadic Burkitt's lymphoma. Cancer Res. 2009;69(9):4052-4058.
28. Hruz T, Laule O, Szabo G, et al. Genevestigator v3: a reference expression database for the meta-analysis of transcriptomes. Adv Bioinformatics. 2008;2008:420747.
29. Chen L, Groenewoud A, Tulotta C, et al. A zebrafish xenograft model for studying human cancer stem cells in distant metastasis and therapy response. Methods Cell Biol. 2017;138:471-496.
30. Arroyo AG, Garcia-Pardo A, Sanchez-Madrid F. A high affinity conformational state on VLA integrin heterodimers induced by an anti-beta 1 chain monoclonal antibody. J Biol Chem. 1993;268(13):9863-9868.
31. Luque A, Gomez M, Puzon W, Takada Y, Sanchez-Madrid F, Cabanas C. Activated conformations of very late activation integrins detected by a group of antibodies (HUTS) specific for a novel regulatory region (355-425) of the common beta 1 chain. J Biol Chem. 1996;271(19):11067-11075.
32. Foley KS, Young PW. The non-muscle functions of actinins: an update. Biochem J. 2014;459(1):1-13.
33. Loirand G, Guerin P, Pacaud P. Rho kinases in cardiovascular physiology and pathophysiology. Circ Res. 2006;98(3):322-334.
34. Rydlova M, Holubec L, Jr., Ludvikova M, Jr., et al. Biological activity and clinical implications of the matrix metalloproteinases. Anticancer Res. 2008;28(2B):1389-1397.
35. Zhong Y, Lu YT, Sun Y, et al. Recent opportunities in matrix metalloproteinase inhibitor drug design for cancer. Expert Opin Drug Discov. 2018;13(1):75-87.
36. Kim J, Yu W, Kovalski K, Ossowski L. Requirement for specific proteases in cancer cell intravasation as revealed by a novel semiquantitative PCR-based assay. Cell. 1998;94(3):353-362.
37. Madri JA, Graesser D. Cell migration in the immune system: the evolving inter-related roles of adhesion molecules and proteinases. Dev Immunol. 2000;7(2-4):103-116.
38. Leppert D, Waubant E, Galardy R, Bunnett NW, Hauser SL. T cell gelatinases mediate basement membrane transmigration in vitro. J Immunol. 1995;154(9):4379-4389.
39. Redondo-Munoz J, Jose Terol M, Garcia-Marco JA, Garcia-Pardo A. Matrix metalloproteinase-9 is up-regulated by CCL21/CCR7 interaction via extracellular signal-regulated kinase-1/2 signaling and is involved in CCL21-driven B-cell chronic lymphocytic leukemia cell invasion and migration. Blood. 2008;111(1):383-386.
40. Vacca A, Ribatti D, Iurlaro M, et al. Human lymphoblastoid cells produce extracellular matrix-degrading enzymes and induce endothelial cell proliferation, migration, morphogenesis, and angiogenesis. Int J Clin Lab Res. 1998;28(1):55-68.
41. Bartlett MR, Underwood PA, Parish CR. Comparative analysis of the ability of leucocytes, endothelial cells and platelets to degrade the subendothelial basement membrane: evidence for cytokine dependence and detection of a novel sulfatase. Immunol Cell Biol. 1995;73(2):113-124.
42. Weissmann M, Arvatz G, Horowitz N, et al. Heparanase-neutralizing antibodies attenuate lymphoma tumor growth and metastasis. Proc Natl Acad Sci U S A. 2016;113(3):704-709.
43. Ivanoff J, Talme T, Sundqvist KG. The role of chemokines and extracellular matrix components in the migration of T lymphocytes into three-dimensional substrata. Immunology. 2005;114(1):53-62.
44. Ye L, Li F, Song Y, et al. Overexpression of CDCA7 predicts poor prognosis and induces EZH2-mediated progression of triple-negative breast cancer. Int J Cancer. 2018;143(10):2602-2613.
45. Otey CA, Carpen O. Alpha-actinin revisited: a fresh look at an old player. Cell Motil Cytoskeleton. 2004;58(2):104-111.
46. Sjoblom B, Salmazo A, Djinovic-Carugo K. Alpha-actinin structure and regulation. Cell Mol Life Sci. 2008;65(17):2688-2701.

A CXCR4-targeted nanocarrier achieves highly selective tumor uptake in diffuse large B-cell lymphoma mouse models

Ferrata Storti Foundation

Aïda Falgàs,[1,2,*] Victor Pallarès,[1,3,*] Ugutz Unzueta,[1,2]
María Virtudes Céspedes,[1,2] Irene Arroyo-Solera,[1,2] María José Moreno,[1]
Alberto Gallardo,[1,4] María Antonia Mangues,[5] Jorge Sierra,[3,6]
Antonio Villaverde,[2,7,8] Esther Vázquez,[2,7,8,*] Ramon Mangues[1,2,6,*]
and Isolda Casanova[1,2,6]

[1]Biomedical Research Institute Sant Pau (IIB-Sant Pau), Hospital de la Santa Creu i Sant Pau; [2]CIBER en Bioingeniería, Biomateriales y Nanomedicina (CIBER-BBN); [3]Department of Hematology, Hospital de la Santa Creu i Sant Pau; [4]Department of Pathology, Hospital de la Santa Creu i Sant Pau; [5]Department of Pharmacy, Hospital de la Santa Creu i Sant Pau; [6]Josep Carreras Research Institute; [7]Institut de Biotecnologia i de Biomedicina, Universitat Autònoma de Barcelona and [8]Departament de Genètica i de Microbiologia, Universitat Autònoma de Barcelona, Barcelona, Spain

*AF and VP contributed equally to this work.

ABSTRACT

One-third of diffuse large B-cell lymphoma patients are refractory to initial treatment or relapse after rituximab plus cyclophosphamide, doxorubicin, vincristine and prednisone chemotherapy. In these patients, CXCR4 overexpression (CXCR4⁺) associates with lower overall and disease-free survival. Nanomedicine pursues active targeting to selectively deliver antitumor agents to cancer cells; a novel approach that promises to revolutionize therapy by dramatically increasing drug concentration in target tumor cells. In this study, we intravenously administered a liganded protein nanocarrier (T22-GFP-H6) targeting CXCR4⁺ lymphoma cells in mouse models to assess its selectivity as a nanocarrier by measuring its tissue biodistribution in cancer and normal cells. No previous protein-based nanocarrier has been described as specifically targeting lymphoma cells. T22-GFP-H6 achieved a highly selective tumor uptake in a CXCR4⁺ lymphoma subcutaneous model, as detected by fluorescent emission. We demonstrated that tumor uptake was CXCR4-dependent because pretreatment with AMD3100, a CXCR4 antagonist, significantly reduced tumor uptake. Moreover, in contrast to CXCR4⁺ subcutaneous models, CXCR4⁻ tumors did not accumulate the nanocarrier. Most importantly, after intravenous injection in a disseminated model, the nanocarrier accumulated and internalized in all clinically relevant organs affected by lymphoma cells with negligible distribution to unaffected tissues. Finally, we obtained antitumor effect without toxicity in a CXCR4⁺ lymphoma model by administration of T22-DITOX-H6, a nanoparticle incorporating a toxin with the same structure as the nanocarrier. Hence, the use of the T22-GFP-H6 nanocarrier could be a good strategy to load and deliver drugs or toxins to treat specifically CXCR4-mediated refractory or relapsed diffuse large B-cell lymphoma without systemic toxicity.

Introduction

Diffuse large B-cell lymphoma (DLBCL) represents 30-33% of all non-Hodgkin lymphomas (NHL).[1] Management of DLBCL has been improved by the addition of rituximab to CHOP (cyclophosphamide, doxorubicin, vincristine and prednisone) chemotherapy. However, despite this advancement, R-CHOP treatment is still associated with high toxicity, relapse and an unacceptably high treatment failure

rate.[2] Relapse after R-CHOP therapy occurs in 40% of patients;[3,4] this is currently managed with salvage chemotherapy. This is followed by high-dose chemotherapy and autologous bone marrow transplant in patients with chemosensitive disease, which, however, leads to long-term disease control in only half of the patients.[5] Moreover, less than 20% of patients treated with an R-CHOP front-line regimen who relapse within one year benefit from salvage autologous hematopoietic cell transplant.[2,6] Thus, novel therapeutic strategies that reduce relapse rates and enhance DLBCL patient survival are urgently needed.

Novel approaches based on selective-drug delivery to cancer cells promise to increase patient benefit by offering both higher cure rates and lower side effects in DLBCL patients. In this regard, we evaluated a previously developed protein nanocarrier as a possible drug carrier to pursue the selective elimination of DLBCL cells over-expressing CXCR4 (CXCR4+), which are responsible for DLBCL relapse and disease progression.[7-9] Thus, the CXCR4-CXCL12 axis is involved in tumor pathogenesis, cancer cell survival, stem cell phenotype, and resistance to chemotherapy.[10,11] In addition, CXCR4 is constitutively over-expressed in NHL cell lines,[12,13] and also in approximately 50% of malignant B-cell lymphocytes derived from DLBCL patients.[8] Interestingly, CXCR4+ DLBCL cell lines show resistance to rituximab but are sensitive to the combination of rituximab with a CXCR4 antagonist.[14,15] Most importantly, we and others reported that CXCR4 overexpression associates with poor progression-free and overall survival in DLBCL patients treated with R-CHOP.[7,8,14]

Our group has developed T22-GFP-H6, a self-assembling protein nanocarrier, which uses the peptidic T22 ligand to target the CXCR4 receptor.[16] This carrier displays a high recirculation time in blood and selectively biodistributes to tumor tissues in solid tumor models, internalizing selectively in CXCR4+ cancer cells, while increasing its tumor uptake compared to the untargeted GFP-H6 counterpart.[17] This nanocarrier is also able to incorporate toxins (e.g. diphtheria toxin catalytic domain) leading to selective elimination of CXCR4+ colorectal cancer cells.[18,19] Nevertheless, no previous protein-based nanocarrier has been described to specifically target cancer cells in hematologic neoplasias. Critical differences between solid cancers and hematologic neoplasias may raise doubts about its use to target CXCR4+ cancer cells in DLBCL models. Thus, the enhanced permeability/retention (EPR) effect, due to abnormal fenestrated vessels and limited lymphatic drainage, allows nanocarrier accumulation in solid tumors. In contrast, DLBCL is a disseminated disease that displays freely circulating lymphoma cells in blood concomitantly with their confinement at specific tumor niches, such as lymph nodes (LN) and bone marrow (BM), in which the EPR effect is unlikely to be present.[20]

Here, we studied whether active targeting of the T22-GFP-H6 nanocarrier leads to its selective uptake in CXCR4+ subcutaneous (SC) DLBCL tumors. We also assessed if this increased uptake associates with specific nanocarrier internalization in CXCR4+ lymphoma cells; issues still be to settled in nanomedicine.[21,22] Importantly, we used a disseminated CXCR4+ DLBCL model (which replicates the organ involvement observed in DLBCL patients[8]) to study nanocarrier accumulation in lymphoma-affected organs (LN and BM) and its capacity to internalize in CXCR4+ lymphoma cells within these organs. Moreover, we evaluated whether T22-DITOX-H6, a nanoparticle incorporating a diphtheria toxin domain that maintains the same structure as the nanocarrier, can selectively eliminate CXCR4+ DLBCL cells in SC tumors. The study goal was to determine whether we could use the nanocarrier to selectively deliver drugs to target CXCR4+ DLBCL cells.

Methods

In vivo experiments

Four-week old female NOD/SCID mice were obtained from Charles River Laboratories. Mice were maintained in specific pathogen-free (SPF) conditions with sterile food and water *ad libitum*. Mouse experiments were approved by the Hospital de la Santa Creu i Sant Pau Animal Ethics Committee.

For SC models, 10 million DLBCL cells were injected in both flanks. Tumor growth was monitored twice a week with a caliper (tumor volume=width^2 x length/2). When tumors reached a volume of 600-800 mm^3, mice received a single intravenous (IV) dose of 200 μg T22-GFP-H6, which contains a fluorescent domain, or buffer (20 mM Tris, 500mM NaCl, pH 8). T22-GFP-H6 design and production have been described in previous studies.[16] Fluorescence intensity (FLI) was measured *ex vivo* at different time points in tumors, plasma, and all organs. A plasma pool was obtained by centrifugation of total blood, obtained by intracardiac puncture (25G), at 600g for ten minutes (min) at 4°C. T22-GFP-H6 biodistribution in SC tumors over time was measured using the area under the curve (AUC). AUC analysis of tumors and normal organs was measured using the GraphPad Prism 6 program. We subcutaneously administered AMD3100 in mice to perform CXCR4 blocking experiments, giving a total of three AMD3100 doses at 10 mg/kg, 1 hour (h) before and 1h and 2h after IV T22-GFP-H6 injection. We used SC tumor models to evaluate the antitumor effect and associated toxicity of T22-DITOX-H6. Mice received a single 25 μg IV dose of T22-DITOX-H6 or buffer when tumors reached a volume of 400-600 mm^3. Animals were euthanized 24h post administration. T22-DITOX-H6 nanoparticle characterization has been published previously.[18]

To generate the disseminated lymphoma model, NOD/SCID mice were intravenously injected with 20x10^6 luminescent Toledo cells (Toledo-Luci) in 200 μL physiological serum. Dissemination was monitored capturing bioluminescence intensity (BLI) twice a week after intraperitoneal injection of firefly D-luciferin. After 27-30 days, animals received a single IV dose of 400 μg T22-GFP-H6 nanocarrier or buffer. Five hours later, FLI was measured *ex vivo* in all organs.

Fluorescence intensity correlates to the amount of accumulated protein in each tissue and is expressed as average radiant efficiency. FLI from experimental mice was calculated subtracting the FLI auto-fluorescence of control mice. The emitted FLI and BLI were measured using the IVIS Spectrum 200 Imaging System (Xenogen). Finally, tumors and all organs were collected, fixed and paraffined to perform histological, immunohistochemical or immunofluorescent evaluations, and were also directly cryopreserved in liquid nitrogen for protein extraction.

Details of methods for cell culture, transfection with Luciferase and CXCR4 plasmids, cell proliferation, flow cytometry, western blot, histopathology, 4′,6-diamidino-2-phenylindole (DAPI) staining, immunohistochemistry (IHC) and immunofluorescence (IF) analyses can be found in the *Online Supplementary Appendix*.

Statistical analysis

In vitro experiments were performed in biological triplicates while *in vivo* experiments were performed in triplicates/quadruplicates. The data for all experiments were reported as mean ±Standard Error of Mean (SEM). All results were analyzed using the Student *t*-test. *P*<0.05 was considered statistically significant. Statistical calculations were performed using SPSS software version.[21]

Results

CXCR4-dependent internalization of T22-GFP-H6 in human CXCR4+ diffuse large B-cell lymphoma cell lines

CXCR4 membrane levels were evaluated in four human DLBCL cell lines by flow cytometry (Figure 1A) and IHC (*Online Supplementary Figure S1*). CXCR4 expression was highest in Toledo cells, followed by U-2932 and RIVA, whereas CXCR4 expression in the SUDHL-2 cell line was undetectable. CXCR4-transfected SUDHL-2 cells (CXCR4+ SUDHL-2) showed average CXCR4 levels.

T22-GFP-H6 nanocarrier internalization correlated with CXCR4 expression. Thus, T22-GFP-H6 internalized the most in Toledo cells, followed by U-2932 and RIVA, whereas it did not internalize in SUDHL-2 (Figure 1B). Moreover, T22-GFP-H6 nanocarrier internalization was CXCR4-dependent. So, after preincubation with CXCR4 antagonist AMD3100, T22-GFP-H6 internalization decreased significantly in Toledo, U-2932 and RIVA cells (Figure 1C). As expected, T22-GFP-H6 did not internalize in SUDHL-2 cells (only background FLI was detected), whereas high internalization was registered in CXCR4+ SUDHL-2 cells. Similarly, AMD3100 preincubation had no effect on nanocarrier internalization in SUDHL-2 cells but led to a significant decrease in CXCR4+ SUDHL-2 cells (Figure 1D). Thus, we showed specific *in vitro* entry of T22-GFP-H6 into CXCR4+ DLBCL cells through the CXCR4 receptor.

Non-cytotoxic effect of T22-GFP-H6 in diffuse large B-cell lymphoma cell lines *in vitro*

After exposure to T22-GFP-H6 (50-500nM range), cell viability for all four evaluated DLBCL cell lines was approximately or above 100% (Figure 1E). Therefore, T22-GFP-H6 nanocarrier has no *in vitro* antineoplastic effect against these DLBCL cell lines.
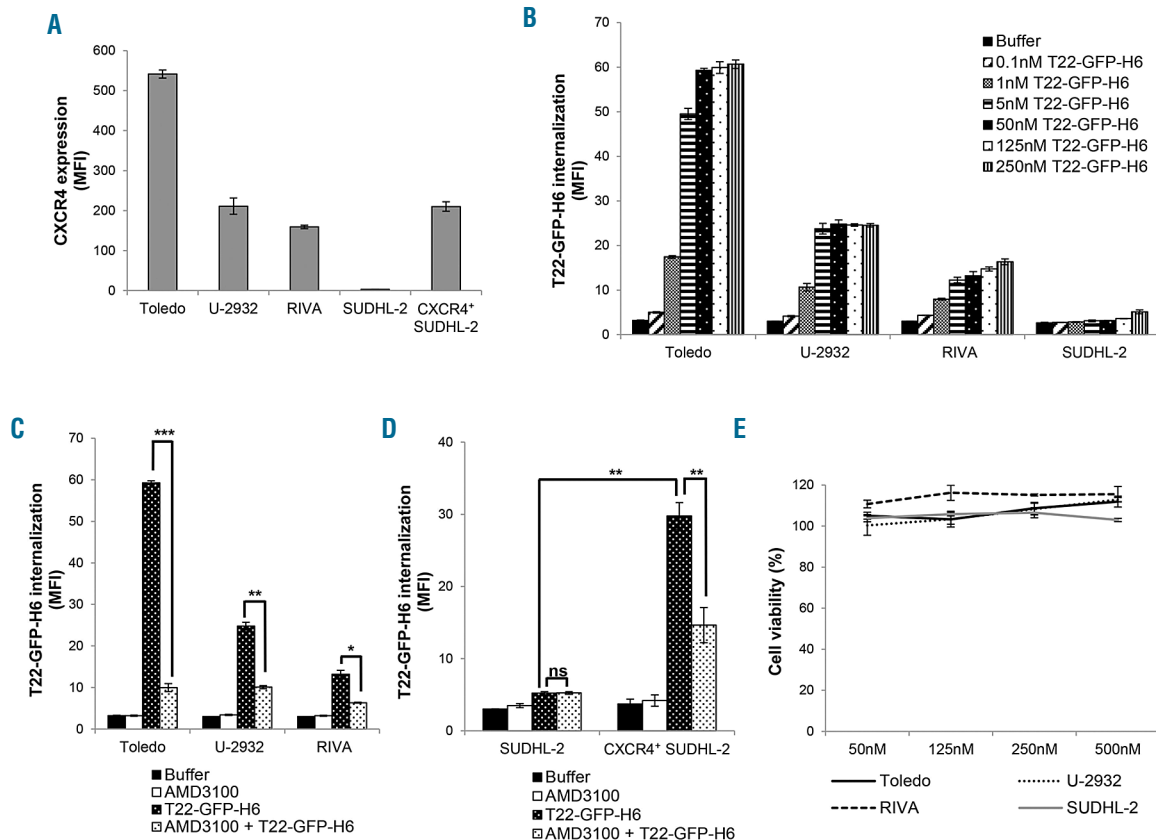
Figure 1. *In vitro* **T22-GFP-H6 nanocarrier internalization in CXCR4+ diffuse large B-cell lymphoma (DLBCL) cell lines and its dependence on the CXCR4 receptor.** (A) CXCR4 membrane expression of different DLBCL cell lines (Toledo, U-2932, RIVA and SUDHL-2) and the SUDHL-2 cell line transfected with a CXCR4 plasmid (CXCR4+ SUDHL-2) measured by flow cytometry. (B) Levels of intracellular fluorescence quantified by flow cytometry in Toledo, U-2932, RIVA and SUDHL-2 cells after 1 hour (h) exposure to T22-GFP-H6 nanocarrier at different concentrations (range: 0.1nM-250nM). (C) T22-GFP-H6 internalization, measured by flow cytometry, in Toledo, U-2932 and RIVA cells after 1h pretreatment with the antagonist AMD3100 (50nM T22-GFP-H6:500nM AMD3100). (D) Competition assays with AMD3100 (250nM T22-GFP-H6: 2500nM AMD3100) in SUDHL-2 cells and CXCR4+ SUDHL-2 cells. (E) Lack of cytotoxicity (measured as percentage of cell viability) after 48h exposure to high concentrations of T22-GFP-H6 nanocarrier (range: 50nM-500nM) in Toledo, U-2932, RIVA and SUDHL-2 cells. *P*<0.05; **P*<0.01; ***P*<0.001; ns: non-significant; MFI: mean fluorescence intensity.

A

SC Toledo tumors

B

C

D

E

F

	T22-GFP-H6 UPTAKE (%)
Spleen	**0.46** ± 0.27
Liver	**5.96** ± 2.83
Kidneys	**1.07** ± 0.45
Heart	**1.17** ± 0.81
Lungs	**4.55** ± 1.20
BM	**0.67** ± 0.51
Tumors	**86.13** ± 4.04
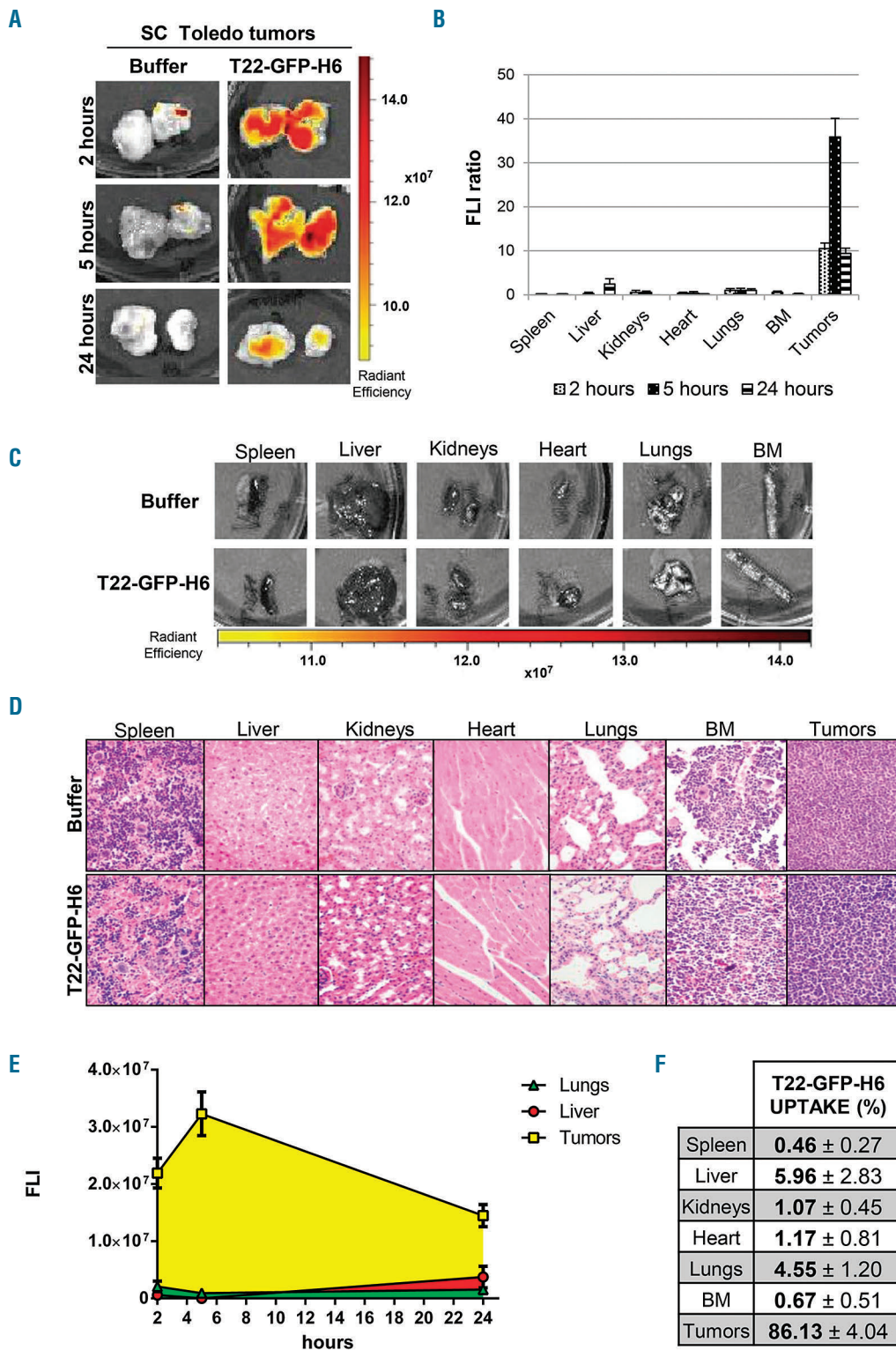
Figure 2. *In vivo* **biodistribution and toxicity assessment of T22-GFP-H6 in the CXCR4+ subcutaneous (SC) Toledo mouse model.** (A) Fluorescence intensity (FLI) detection in SC Toledo tumors at 2, 5 or 24 hours (h) after intravenous (IV) injection of 200 μg of T22-GFP-H6. No fluorescence was detected in buffer-treated mice. (B) Quantification of emitted fluorescence (measured as FLI ratio) at different times (2, 5 and 24h) in SC tumors and normal tissues (liver, spleen, heart, lungs, kidneys and bone marrow). (C) FLI emitted by the nanocarrier in normal tissues 5h after T22-GFP-H6 administration. (D) Hematoxylin & Eosin (H&E) stained tissue sections of normal organs and SC tumors at the 5h FLI peak. (E) Representation of the area under the curve (AUC) of emitted FLI over time (2-24h) registered in tumors, liver and lungs in T22-GFP-H6-treated mice. Notice that the AUC in the organs with an uptake lower than 2% (spleen, kidney, heart and BM) is not visible in this graphic. (F) Percentage of nanocarrier uptake (as measured by the AUC of emitted FLI) registered in each organ studied in relation to the total emitted FLI (sum of AUC in tumors and all studied normal organs) during the 2-24h period and expressed as mean±Standard Error of Mean (SEM). FLI ratio for experimental mice was calculated subtracting the FLI auto-fluorescence of control mice and dividing the FLI signal of each tumor/tissue by the FLI signal of the lungs (organ chosen as reference). Original magnification x400. BM: bone marrow.
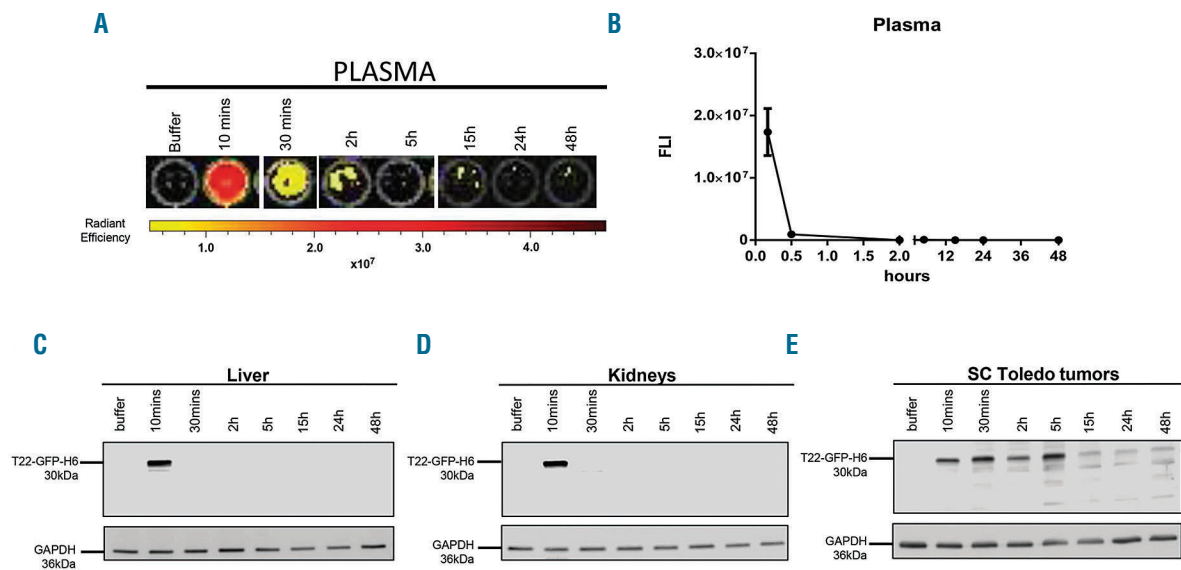
Figure 3. T22-GFP-H6 pharmacokinetics in plasma and clearance in CXCR4+ SC Toledo mouse model. (A) Representative images of fluorescence intensity (FLI) registered in plasma (250 μL) of mice treated with buffer or 200 μg T22-GFP-H6, 10 minutes (min), 30 min, 2 hour (h), 5h, 15h, 24h and 48h after its administration. (B) Graphical representation of FLI quantification in plasma over time. (C and D) Western blot analysis of the fate of the T22-GFP-H6 protein in hepatic and renal tissue in mice treated with buffer or 10 min, 30 min, 2h, 5h, 15h, 24h and 48h after nanocarrier administration. (E) Western blot analysis of the fate and processing of the T22-GFP-H6 protein in subcutaneous (SC) Toledo tumors in mice treated with buffer or 10min, 30min, 2h, 5h, 15h, 24h and 48h after nanocarrier administration. Note the almost complete proteolysis of the full-length protein nanocarrier in tumor tissue, and the absence of proteolysis in liver and kidney. GAPDH was used as a loading control. T22-GFP-H6 was detected with an anti-GFP antibody.

Highly selective T22-GFP-H6 tumor uptake in mice bearing subcutaneous CXCR4+ diffuse large B-cell lymphoma tumors without toxicity

We evaluated T22-GFP-H6 biodistribution in the CXCR4+ SC Toledo mouse model, measuring the fluorescence emitted by the nanocarrier GFP domain, after a single 200 μg IV dose. T22-GFP-H6 accumulated in CXCR4+ SC tumors 2h after injection, reaching a FLI peak 5h post injection, and decreasing considerably after 24h (Figure 2A and B). Tumor uptake 5h post injection was 35.85 times higher than lung uptake, which was taken as a reference among the normal mouse organs because, although almost negligible, it did show the most sustained FLI emission over time (Figure 2B and *Online Supplementary Table S1*). Similar observations were made in all non-tumor organs analyzed (Figure 2B and C). Moreover, we did not observe any histological alteration in Hematoxylin & Eosin (H&E) stained normal organs (Figure 2D).

The quantification of the AUC of emitted FLI over the study period (Figure 2E and *Online Supplementary Table S2*) showed that tumor tissue accumulated 86.13±4.04% of the total FLI detected in all organs, including tumor and non-tumor tissues. In contrast, the liver, which was the non-tumor organ with higher AUC, reached only 5.96±2.83% (Figure 2F). Therefore, T22-GFP-H6 displayed a specific targeting of CXCR4+ SC DLBCL tumors with negligible nanocarrier accumulation in non-tumor bearing organs, which supports a highly selective tumor uptake as compared to normal cells.

After a single T22-GFP-H6 IV administration, measurement of circulating nanocarrier showed a fast biodistribution half-life ($t_{1/2} \approx 20$min) in the blood compartment, followed by a slower elimination phase ($t_{1/2} \approx 75$min), becoming undetectable in plasma at 2h (Figure 3A and B).

The highly unusual T22-GFP-H6 tumor uptake and its low accumulation in the expected non-tumor drug clearance organs (i.e. liver and kidney) triggered the analysis of the nanocarrier fate in these organs by western blot. After a single T22-GFP-H6 dose, we observed the full-length protein (≈30kDa) present in liver and kidney 10min post administration (Figure 3C and D), becoming undetectable over a period which ranged from 30min to 48h. In sharp contrast, we detected full-length T22-GFP-H6 protein in Toledo SC tumors at 10min, 30min, 2h and 5h. Interestingly, faint proteolytic bands appeared over a period which ranged from 30min to 2h, which became more intense at 5h. Over a period which ranged from 15h to 48h, the full-length protein decreased dramatically and the nananocarrier was mostly proteolyzed (Figure 3E). These results, together with the observed FLI AUC in tumor and normal organs, suggest that the proteolytic activity observed in the tumor makes it the main nanocarrier clearance organ.

T22-GFP-H6 and CXCR4 receptor co-localization in the cell membrane followed by its internalization in CXCR4+ diffuse large B-cell lymphoma cells

At the FLI peak (5h) after a single 200μg injection, we observed nanocarrier internalization in 56.2±12.0% of the Toledo cells (green staining with anti-GFP IF) in tumors, whereas all (100%) tumor cells over-expressed CXCR4 (red staining with anti-CXCR4 IF). In buffer-treated tumors, the CXCR4 receptor localized mainly at Toledo cell membrane, while a dot-like staining inside the cell cytosol was observed in the nanocarrier-treated-tumors; a finding consistent with receptor internalization within endocytic vesicles. Merged (yellow) images showed nanocarrier and CXCR4 co-localization in the membrane of Toledo cells in T22-GFP-H6-treated tumors. Once into the cytosol, the CXCR4 and T22-GFP-H6 stained endoso-
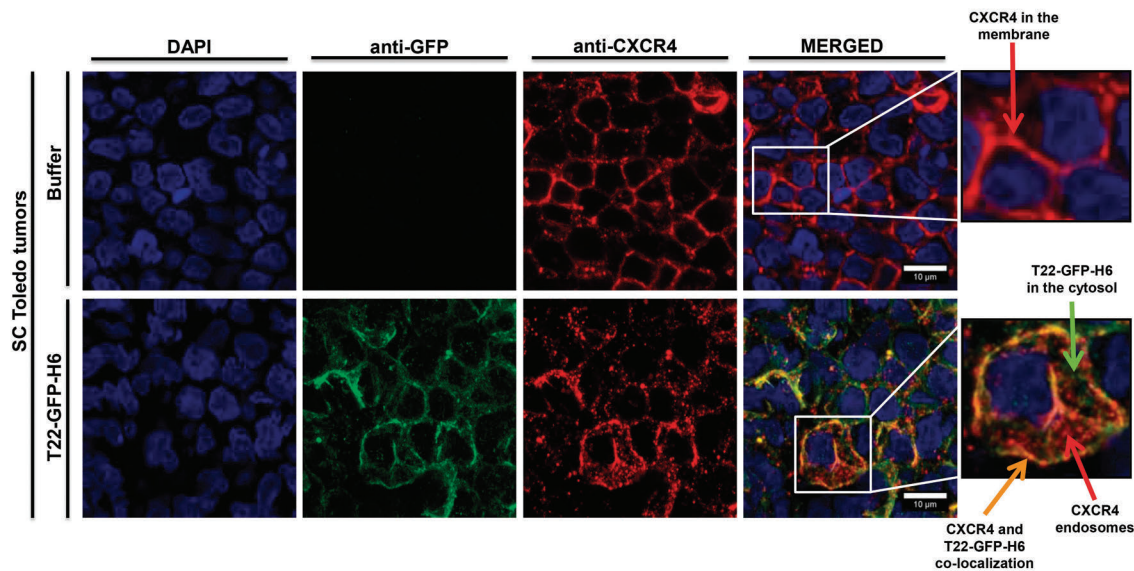
Figure 4. Co-localization of T22-GFP-H6 and CXCR4 receptor in the cell membrane and nanocarrier internalization in CXCR4+ subcutaneous (SC) tumors. Representative immunofluorescence images from SC Toledo tumors of mice treated with T22-GFP-H6 (200 μg, 5h) or buffer. T22-GFP-H6 and CXCR4 co-localization was mainly seen in the cell membrane (yellow dots), whereas internalized nanocarriers were observed in the cell cytosol (green dots) and the endocytic vesicles with the CXCR4 receptor (red dots). DAPI staining (blue), anti-GFP protein (green), anti-CXCR4 receptor (red) and merged images from the three stains. Scale bars=10 μm.

mal vesicles were dissociated (Figure 4). These results suggest that T22-GFP-H6 interacts with the CXCR4 receptor in the cell membrane, where both co-localize and, after internalizing jointly within endosomal vesicles, they are able to release the nanocarrier in the CXCR4+ DLBCL cell cytosol.

Selective CXCR4-dependent T22-GFP-H6 tumor uptake in subcutaneous diffuse large B-cell lymphoma tumors

We also assessed the dependence of nanocarrier tumor uptake on CXCR4 receptor, performing *in vivo* competition assays using the CXCR4 antagonist AMD3100 in mice bearing CXCR4+ Toledo-derived SC tumors (Figure 5A). Five hours after T22-GFP-H6 administration, we registered a peak of nanocarrier accumulation in tumors that reached 3.23±0.38E7. In contrast, the AMD3100 administration prior and after nanocarrier injection blocked nanocarrier uptake in tumors, since the emitted FLI was 10 times lower (0.31±0.52E7) (Figure 5B). Differences between the Toledo tumors treated with T22-GFP-H6 and those treated with AMD3100 plus T22-GFP-H6 were highly significant (Figure 5C). This inhibition of nanocarrier uptake by AMD3100 confirms that tumor uptake depends on the CXCR4-receptor.

Additional support for this selective uptake comes from additional biodistribution assays comparing CXCR4– SUDHL-2 and CXCR4+ SUDHL-2 SC tumor-bearing mice. Five hours after 200 μg T22-GFP-H6 administration, FLI emission from CXCR4+ SUDHL-2 tumors was significantly higher (2.12±0.46E7) than from CXCR4– SUDHL-2 tumors (0.04±0.21E7) (Figure 5C and D).

Consistently, Toledo and CXCR4+ SUDHL-2 tumors showed CXCR4 membrane expression, as measured by IHC, whereas CXCR4– SUDHL-2 tumors did not (Figure 5E); a finding that confirms the specific directioning of T22-GFP-H6 to tumors containing CXCR4+ DLBCL cells.

T22-GFP-H6 biodistributes to all diffuse large B-cell lymphoma-infiltrated organs and internalizes in lymphoma cells in a CXCR4+ diffuse large B-cell lymphoma disseminated mouse model

We evaluated the biodistribution of T22-GFP-H6 *in vivo* in a CXCR4+ Toledo-Luci disseminated DLBCL mouse model, while monitoring lymphoma cell dissemination by measuring BLI levels emitted by the infiltrated organs *in vivo* (Figure 6A). In addition, we precisely identified the organs showing infiltration by Toledo-Luci cells, BM (cranium and hind limbs) and LN (cervical and renal). In some mice (37.5%), we detected residual BLI levels in the spleen and no infiltration was observed in any other organ (Figure 6B). Macroscopic LN (cervical and renal) infiltration was identified in 100% of mice (Figure 6C). H&E staining and anti-CD20 IHC confirmed Toledo-Luci cell infiltration in BM and LN tissue sections. CXCR4 membrane expression was maintained in DLBCL cells located in all infiltrated organs (Figure 6D).

We went on to study T22-GFP-H6 biodistribution after IV injection (400 μg dose) or buffer in mice displaying complete dissemination of Toledo cells (27-30 days post injection). Five hours after nanocarrier injection, we observed high FLI in BM (cranium and hind limbs) and LN (renal and cervical), whereas fluorescence was negligible or undetectable in non-infiltrated organs (Figure 7A and B). Indeed, T22-GFP-H6 was specifically delivered to the DLBCL infiltrated organs since FLI levels in BM and LN were 31.05- and 12.98-fold higher, respectively, in comparison to lungs (the reference organ showing background FLI levels) (Figure 7B and *Online Supplementary Table S3*). Moreover, no histopathological alterations were observed in any tissue analyzed in nanocarrier-treated mice (*data not shown*). IF analysis using anti-GFP showed T22-GFP-H6 (green) in Toledo-Luci cell cytosol in affected BM and LN. In addition, CXCR4 dot-like (red) and nanocarrier (green)

staining co-localized (yellow) on the cell membrane. Moreover, similar to findings in SC Toledo tumors, in the disseminated model, we found a release of the nanocarrier into CXCR4+ DLBCL cell cytosol separated from endocytic vesicles containing the CXCR4 receptor (Figure 7C).

T22-GFP-H6 internalization in CXCR4+ mouse cells

To support the relevance of our CXCR4+ DLBCL models for clinical translation of the tumor (human cells) and non-tumor (mouse cells) biodistribution data, we assessed whether the nanocarrier internalized in mouse cells.
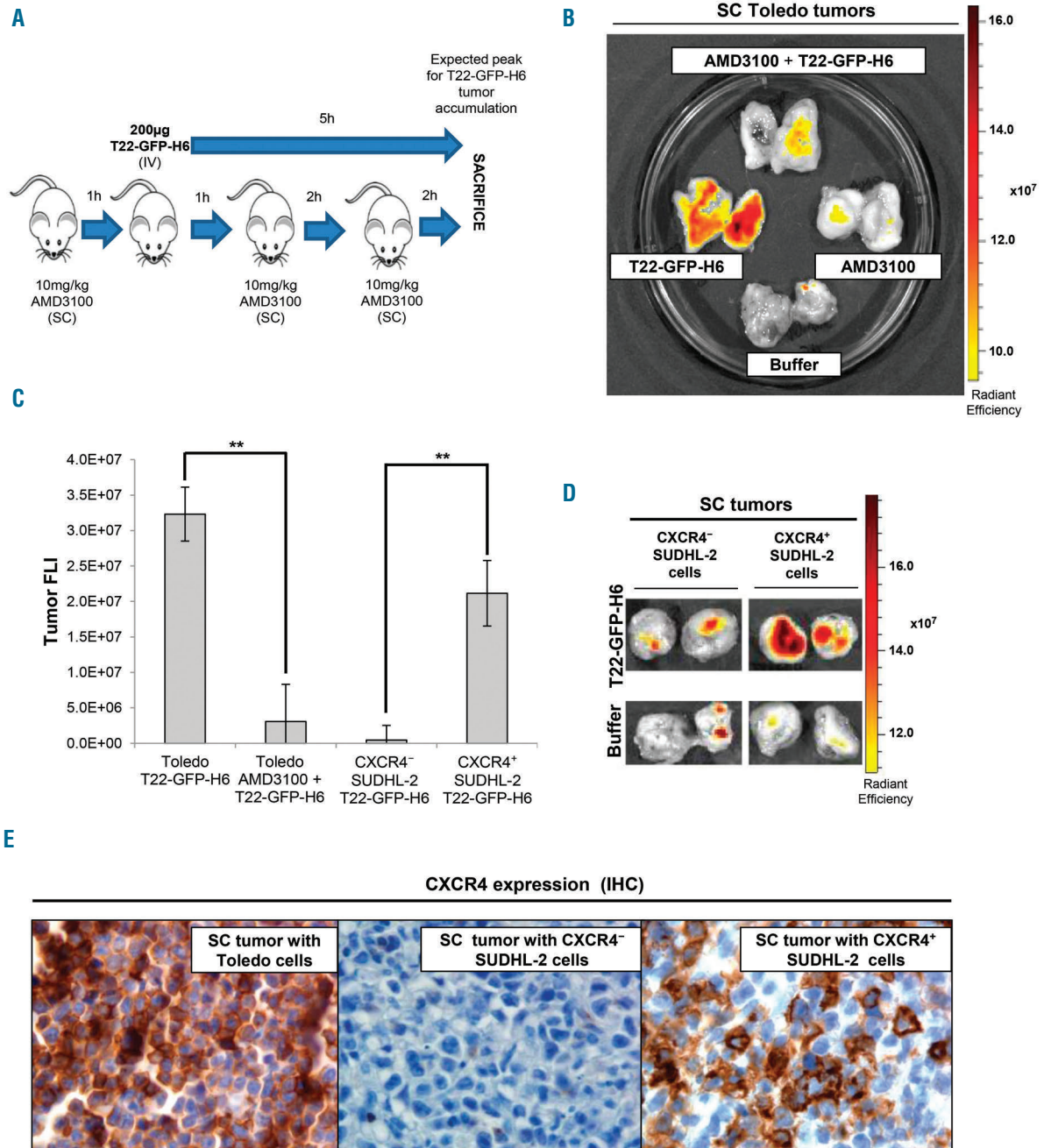
Figure 5. CXCR4-dependent uptake of T22-GFP-H6 nanocarrier in diffuse large B-cell lymphoma (DLBCL) subcutaneous (SC) tumors. (A) For the CXCR4 blocking experiment, mice were injected with a total of three SC doses of AMD3100 at 10 mg/kg. The time point of mice sacrifice was 2 hours (h) after the last AMD3100 SC injection, which corresponds to the 5h fluorescence intensity (FLI) peak after T22-GFP-H6 injection. (B) Representative images of emitted FLI by SC Toledo tumors from buffer, T22-GFP-H6, AMD3100 or AMD3100+T22-GFP-H6 treated animals. (C) FLI levels of SC tumor-bearing-mice of Toledo cells administered with T22-GFP-H6 or AMD3100+T22-GFP-H6 and FLI levels of the tumors in T22-GFP-H6-treated bearing SC CXCR4+ SUDHL-2 tumors or SC CXCR4- SUDHL-2 tumors. (D) A representative image of the FLI in SC tumors of CXCR4- SUDHL-2 and CXCR4+ SUDHL-2 cells after 5h of T22-GFP-H6 or buffer administration. (E) Level of membrane CXCR4 expression detected by immunohistochemistry (IHC) in SC tumors derived from Toledo, CXCR4+ SUDHL-2 and CXCR4- SUDHL-2 cells. **$P<0.01$. Original magnification x1000.

Firstly, we evaluated CXCR4 expression in the mouse B-cell lymphoma WEHI-231 cell line that showed medium CXCR4 membrane expression by flow cytometry and IHC (*Online Supplementary Figure S2A*). Then, we demonstrated intracellular nanocarrier uptake in mouse WEHI-231 cells and its dependence on CXCR4 expression, since it was inhibited by AMD3100 (*Online Supplementary Figure S2B*). Therefore, T22-GFP-H6 internalizes in both CXCR4+ human and CXCR4+ mouse lymphoma cells.

T22-DITOX-H6 antitumor effect and lack of toxicity in a CXCR4+ subcutaneous diffuse large B-cell lymphoma mouse model

Finally, we evaluated whether the therapeutic nanoparticle T22-DITOX-H6, incorporating a toxin domain with known antitumor activity, induced cell death of Toledo cells in SC tumors without damaging normal cells. T22-DITOX-H6 caused apoptosis in lymphoma cells in these tumors since a single IV 25 µg T22-DITOX-H6 dose signif-
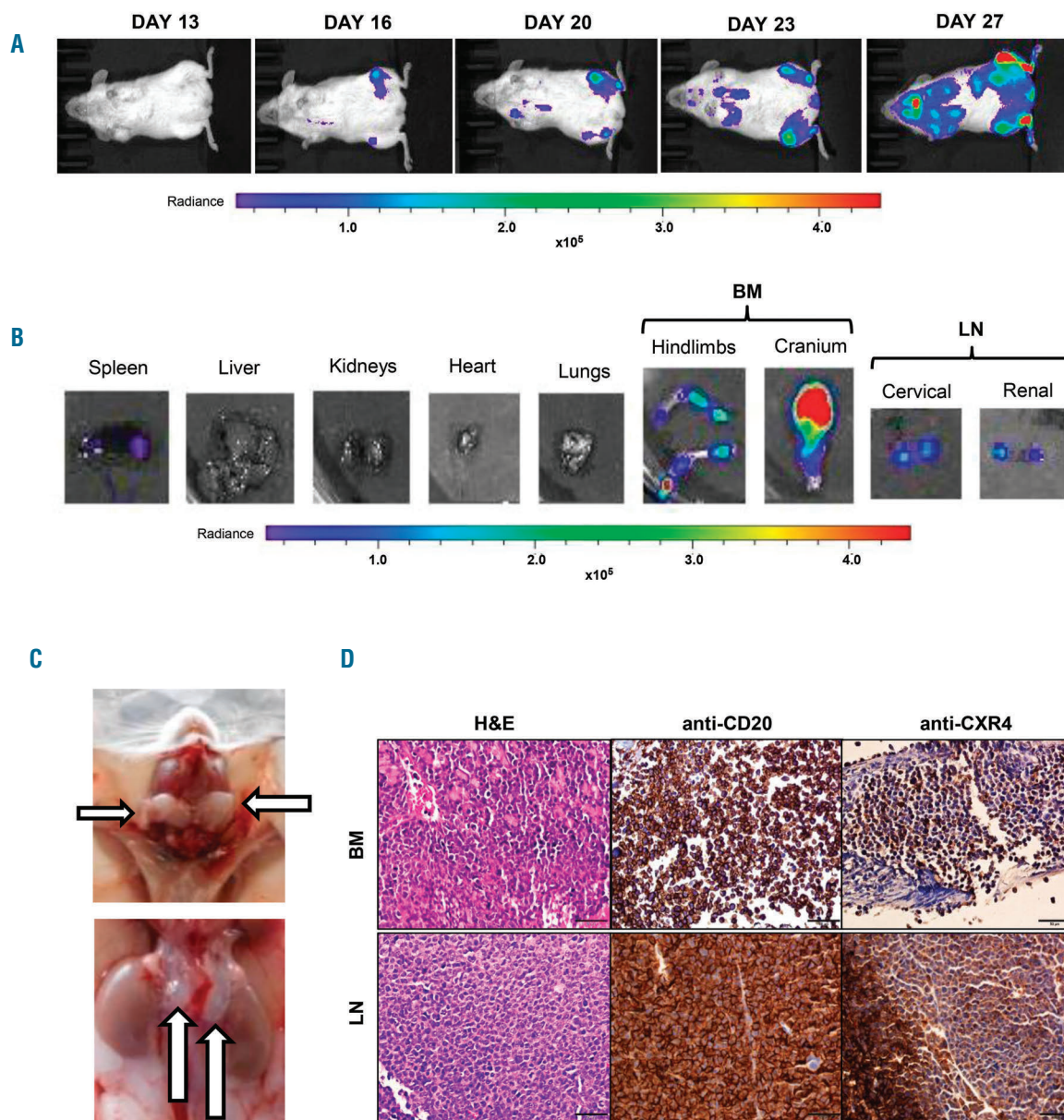
Figure 6. Pattern of organ infiltration in the Toledo-Luci diffuse large B-cell lymphoma (DLBCL) disseminated mouse model. (A) Bioluminescent intensity (BLI) follow up by IVIS Spectrum of mice intravenously injected with Toledo cells transfected with the Luciferase gene (Toledo-Luci cells). (B) *Ex vivo* representative images of the recorded BLI emission in different mouse organs: spleen, liver, kidneys, heart, lungs, hind limbs, cranium, cervical lymph nodes (LN) and renal LN. (C) Macroscopic images showing Toledo-Luci cell infiltration in cervical LN and renal LN. White arrows show the LN location. (D) Hematoxylin & Eosin (H&E) staining, anti-CD20 immunohistochemistry (IHC) for B-cell detection, and anti-CXCR4 IHC in bone marrow (BM) (cranium) and LN (cervical). Original magnification x400. Scale bars=50 µm.

icantly increased the number of apoptotic bodies and cleaved PARP level compared to buffer-treated mice (Figure 8A and B).

We then confirmed CXCR4 expression in hematopoietic cells of the mouse BM (CXCR4+ CD20- staining) (Figure 8C). A direct comparison showed that CXCR4 expression in SC Toledo tumors was significantly (22.87 times) higher than CXCR4 in mouse BM hematopoietic cells (*Online Supplementary Figure S2C and D*). No histopathological alterations (H&E) nor induction of cell death (DAPI stain-
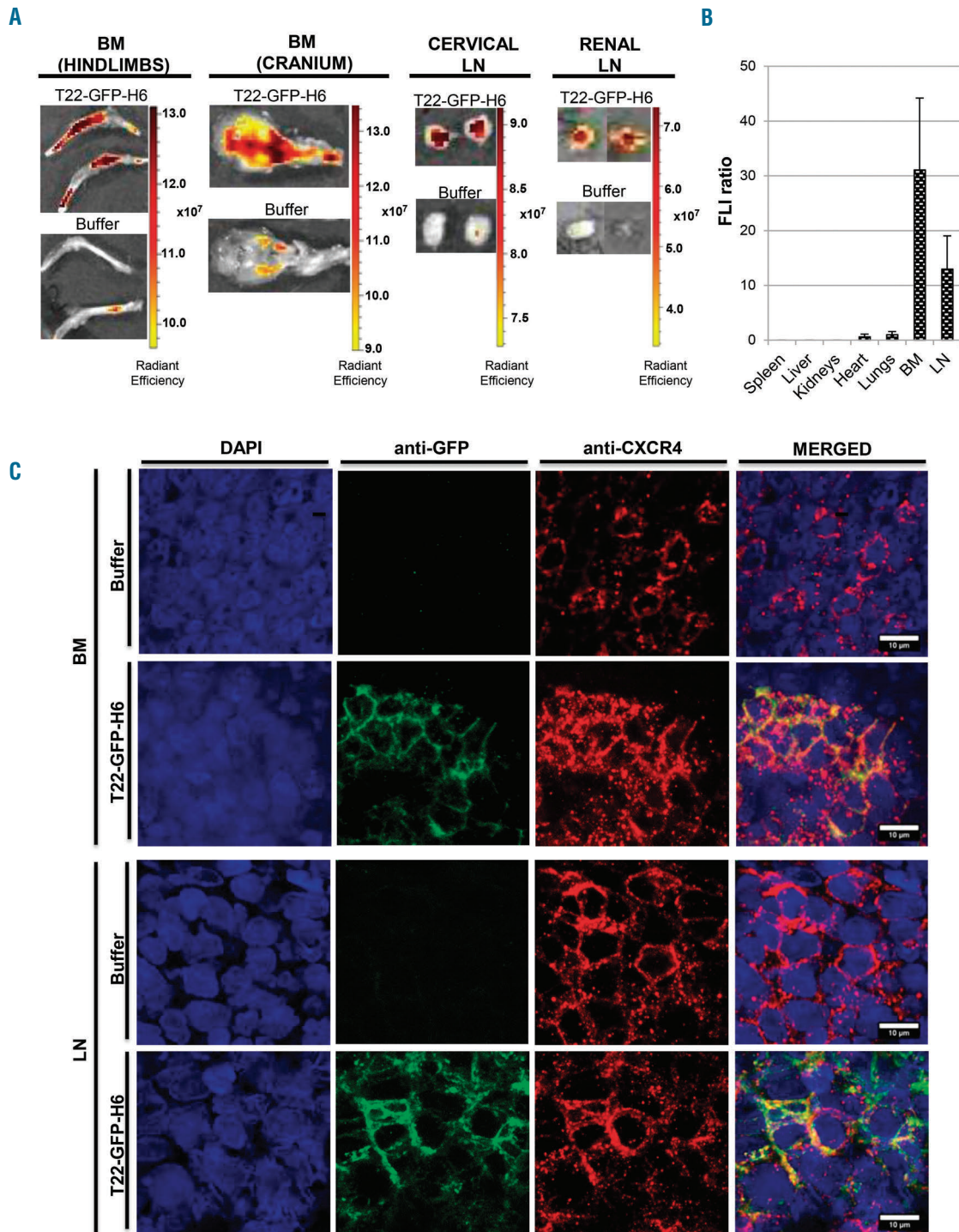
Figure 7. T22-GFP-H6 nanocarrier biodistribution in the Toledo-Luci diffuse large B-cell lymphoma (DLBCL) disseminated mouse model. (A) Level of fluorescence intensity (FLI) emission in bone marrow (BM) (cranium and hind limbs) and lymph nodes (LN) (cervical and renal) 5 hours (h) after the administration of 400 µg T22-GFP-H6 or buffer in a Toledo-Luci disseminated mouse model. (B) Comparison of FLI emission by T22-GFP-H6 accumulated in infiltrated DLBCL organs (BM and LN) as compared to non-DLBCL infiltrated organs (spleen, liver, kidneys, heart and lungs). FLI ratio from experimental mice was calculated subtracting the FLI auto-fluorescence of control mice and dividing the FLI recorded for each tissue by the FLI emitted by the lungs. (C) Representative immunofluorescent images of BM (cranium) and LN (cervical) in nanocarrier-treated mice and buffer-treated mice. Notice that green dots depicting internalized nanocarrier in the cytosol are only observed in T22-GFP-H6 treated animals. DAPI staining (blue), anti-GFP protein (green), anti-CXCR4 receptor (red) and merged images from the three stains. Scale bars=10 µm.

ing) was observed in the BM of T22-DITOX-H6-treated mice (Figure 8C). Lastly, we did not find any macroscopic (*data not shown*) or microscopic (H&E staining) alteration in liver and kidneys (Figure 8D). Our results support the use of the nanocarrier under examination to efficiently deliver antitumor agents to achieve the selective killing of CXCR4^{+} lymphoma cells without inducing toxicity on CXCR4^{+} mouse hematopoietic cells or systemic organs.
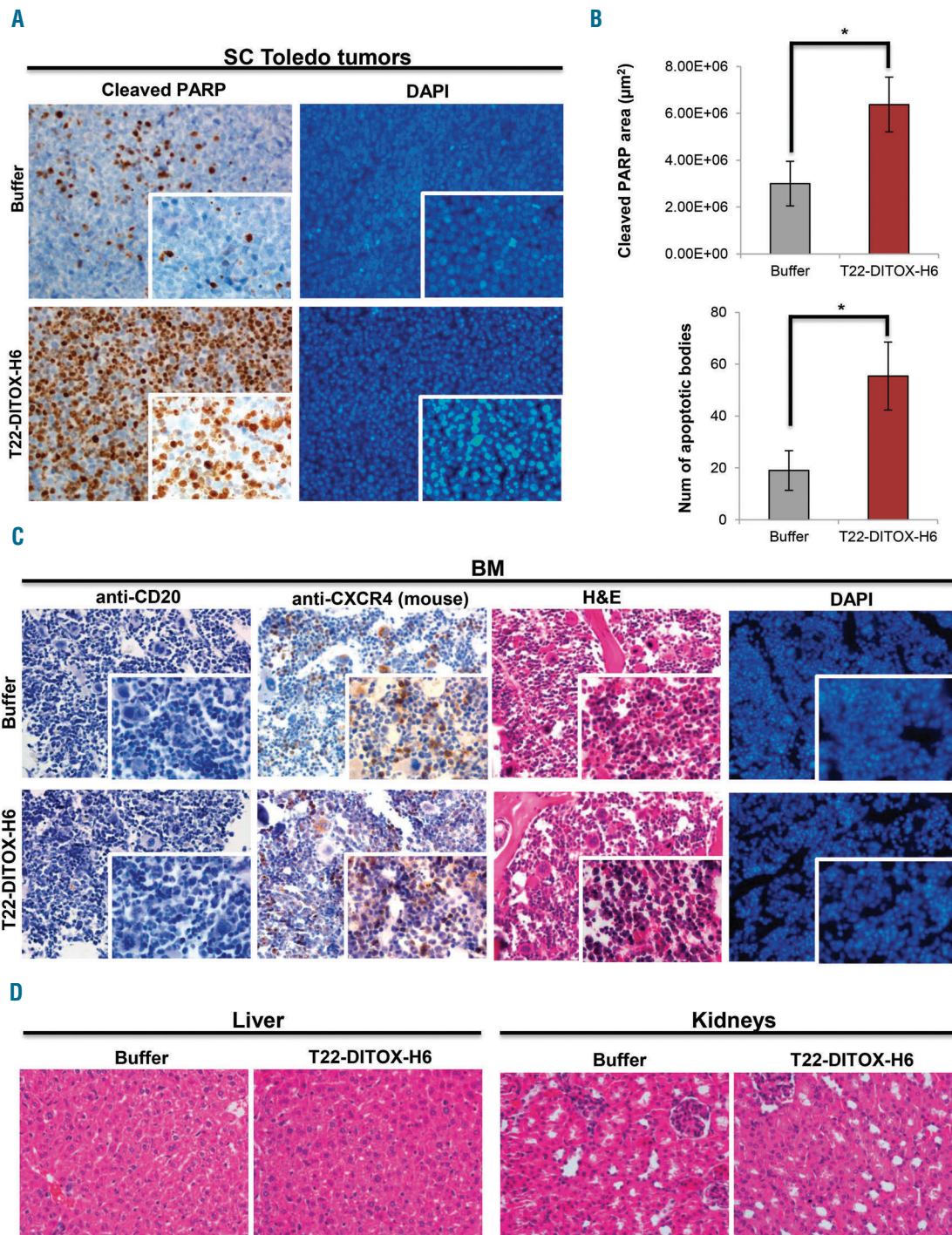
Figure 8. Evaluation of T22-DITOX-H6 antitumor effect and toxicity in a CXCR4^{+} subcutaneous (SC) Toledo mouse model. (A) Apoptosis detection by cleaved Poly(ADP-ribose) polymerase (PARP) immunohistochemistry (IHC) as well as nuclear condensation by 4',6-diamidino-2-phenylindole (DAPI) staining. (B) Mean quantification of cleaved PARP stained area (above) and number of apoptotic bodies by DAPI staining (bottom) in SC Toledo tumors 24 hours (h) after treatment with buffer or a single intravenous (IV) injection of 25 μg T22-DITOX-H6. (C) Lack of T22-DITOX-H6-induced toxicity in mouse bone marrow (BM). Human anti-CD20 and mouse anti-CXCR4 IHC assays were used to identify CXCR4^{+} mouse cells resident in BM. Hematoxylin & Eosin (H&E) and DAPI staining samples were examined to detect possible alterations in cell morphology or cell death induction. (D) Lack of systemic toxicity in liver or kidney by histological analysis of tissue sections H&E 24h after treatment with buffer or 25 μg T22-DITOX-H6. All images were taken at x400 and inserts at x1000. *$P<0.05$.

Discussion

A huge limitation for the clinical translation of nanomedicines in oncology is the fact that only 0.7-5.0% of the administered dose reaches the tumor.[23,24] In contrast, our biodistribution studies show a very high level of T22-GFP-H6 uptake in tumor tissue (86.1% of the total emitted fluorescence) compared to the combined fluorescence emitted by all normal tissues (13.9% of total tumor+non-tumor fluorescence), including the spleen, liver, kidney, heart, lung and BM. We have recently reported a similar finding for the same nanocarrier in a SC colorectal cancer (CRC) model.[25] These data are consistent with the fast biodistribution half-life for the nanocarrier in blood (approx. 20 min) and the detection of the full length protein in the 10min-5h period in SC CXCR4+ DLBCL tumors. Unexpectedly, we found that most of the proteolytic metabolism of T22-GFP-H6 occurs in tumor tissues, whereas clearance in liver or kidney is negligible, being detectable in these organs at 10 min, probably by accessing the fenestrated vessels during a short time period, but being unable to reach their parenchyma. Our data are in dramatic contrast to the reported biodistribution of most nanocarriers studied so far, regardless of whether this was targeted actively or passively.

Nowadays, most nanocarriers that transport medicinal drugs in clinical trials, or that are available on the market, use passive targeting (e.g. liposomal doxorubicin or albumin-paclitaxel). They enhance the drug antitumor effect because its particulate size increases its permeability and retention in the tumor (EPR effect). Nevertheless, 50-80% of these nanocarriers accumulate in the liver.[26] Although still at an initial stage, active nanocarrier targeting is being developed to selectively deliver antitumor drugs to tumor cells through specific surface receptors.[27] Regarding B-cell lymphoma therapy, the use of doxorubicin-loaded mesoporous silica nanoparticles bound to rituximab, for targeting CD20+ B cells, demonstrated a significant increase in doxorubicin tumor uptake and higher inhibition of tumor growth than free doxorubicin.[28] Moreover, additional targeted and non-targeted therapeutic nanoparticles are currently being evaluated for treatment of B-cell malignancies; however, no efficacy data are available yet because Phase I clinical assays to test their tolerability are still ongoing.[29]

The strategy we have used here with the actively targeted T22-GFP-H6 nanocarrier achieves selective and enhanced biodistribution to tumor tissue with no toxicity in the non-tumor organs. One possible explanation for the enhanced T22-GFP-H6 tumor uptake relates to the nature of the nanocarrier material. While our nanocarrier is made of self-assembled proteins, most, if not all, nanocarriers showing limited biodistribution to tumor are either inorganic (gold, silica, iron oxide, quantum dots) or organic (dendrimers, liposomes polymers, hydrogels) rather than protein-based.[23,24] Once administered in blood, non-protein-based nanocarriers are covered by a protein corona that changes the conformation of the nanocarrier surface[30] and undergo intensive phagocytosis by resident macrophages in clearance organs.[31] A completely different protein drug delivery system is represented by the targeted antibody-drug conjugates (ADC), which have lower loading capacity and flexibility for encapsulating various cargos and display a less controllable drug release kinetics compared to nanocarriers.[32] Consequently, in clinical studies, only 0.001-0.01% of the injected antibody dose reaches the tumor;[33] thus, although ADC are standard treatment in some neoplasias, protein nanocarriers could offer an enormous opportunity to improve drug delivery to tumors.

Our results on nanocarrier biodistribution in the SC tumor model demonstrate a specific co-localization of the nanocarrier together with the CXCR4 receptor in the cell membrane followed by their internalization, *via* endocytosis, to reach the cytosol of CXCR4+ DLBCL cells. Once inside the cytosol, the structure of the nanocarrier elicits endosomal escape and delivery of the materials into the cytoplasm, before its ultimate intracellular proteolysis.[16]

Furthermore, the efficacy of a T22-GFP-H6 nanocarrier that targets CXCR4+ DLBCL cells appears to be exclusively dependent on the overexpression of CXCR4 receptor in the membrane of tumor cells. This notion is currently supported by two main findings: on the one hand, T22-GFP-H6 displays a tumor uptake significantly higher than that achieved in the same SC tumor when CXCR4 is inhibited by AMD3100 in the competition assay. On the other hand, T22-GFP-H6 administration to mice bearing CXCR4+ SC SUDHL-2 tumors shows significantly higher uptake than CXCR4- SC SUDHL-2 tumors. Moreover, we confirmed the capacity of T22-GFP-H6 to internalize in CXCR4+ mouse cells, similar to our findings in CXCR4+ human cells. Thus, the high T22-GFP-H6 tumor uptake, and its low uptake in non-tumor organs, is necessarily related to the huge CXCR4 overexpression in DLBCL lymphoma cells and the negligible or low CXCR4 expression in normal organs, including BM mouse hematopoietic cells.

Importantly, in the disseminated CXCR4+ DLBCL mouse model, involving BM and LN, this nanocarrier also shows a high tumor uptake in the organs affected by CXCR4+ lymphoma cells, while displaying low biodistribution to normal tissues (with low or null CXCR4 expression). Unlike low molecular weight drugs that passively diffuse to all cells in the body, the biodistribution of the nanocarrier, or drug-loaded nanocarriers, is limited by their size; thus, it becomes highly dependent on the physiology and anatomy of specific organs in the body. Nanocarriers are unable to access organs irrigated by vessels with continuous endothelia and unable to penetrate membranes, unless they are actively targeted for endocytosis.[34] Our protein nanocarrier can accumulate in the sinusoids of BM and LN infiltrated with tumor cells because they display vascular beds with discontinuous endothelium and 100-200nm fenestrations that allow the transport of macromolecules, including nanocarriers.[35-37] Moreover, as we have showed in the SC mouse model, T22-GFP-H6 also has the capacity to internalize specifically in the CXCR4+ DLBCL cells, here localized in BM and LN in the DLBCL disseminated model. Even though there is no consistent EPR effect in hematologic neoplasias,[20] the structure of the vessels in the sinusoids of the DLBCL niches and the active targeting to CXCR4 allow T22-GFP-H6 accumulation and internalization in the tumor niches that are infiltrated by CXCR4+ DLBCL cells.

Given the high selectivity that T22-GFP-H6 achieves in targeting CXCR4+ DLBCL cells within the tumor, we used the SC CXCR4+ Toledo model to test the antitumor activity of T22-DITOX-H6, a therapeutic nanoparticle derived from this nanocarrier that incorporates the diphtheria cytotoxic domain. This therapeutic nanoparticle induced a high level of apoptotic cell death in tumor tissue without toxicity, since it did not induce any macroscopic or histo-

logical alteration in normal organs, including the BM. The higher levels of CXCR4 expression in DLBCL cells, as compared to normal hematopoietic cells in the BM, were likely responsible for the cytotoxic activity, observed exclusively in tumor cells. These data confirm the capacity of the studied protein nanocarrier to be used as a platform for the delivery of antitumor agents to DLBCL cells. We have previously described also the potential use of T22-GFP-H6 as an antitumor drug delivery agent for the treatment of colorectal cancer and leukemia.[18,38,39] To our knowledge, no protein-based therapeutic nanoparticle has been previously reported as a possible drug carrier for lymphoma therapy.

So far, most research studies for DLBCL therapy targeting CXCR4 are performed with CXCR4 antagonists (e.g. plerixafor or BKT140)[8,10,15] or inverse agonists (e.g. IQS-01.01RS).[40] Our approach differs from these studies since it is not focused on inhibiting signaling downstream of the CXCR4 receptor, but, instead, in delivering high concentrations of potent therapeutic agents to specifically kill CXCR4+ lymphoma cells. The active delivery of the drug-loaded nanocarriers only to CXCR4+ cells should increase the therapeutic index compared to low molecular weight CXCR4 inhibitors, which biodistribute to all tissues independently of their CXCR4 expression.[41,42] In conclusion, specifically eliminating CXCR4+ DLBCL cells could be an effective strategy to enhance the survival and cure rates observed in R-CHOP refractory or relapsed patients.

Acknowledgments

References

1. Campo E, Swerdlow SH, Harris NL, Pileri S, Stein H, Jaffe ES. The 2008 WHO classification of lymphoid neoplasms and beyond: evolving concepts and practical applications. Blood. 2011;117(19):5019–5032.
2. Nowakowski GS, Blum KA, Kahl BS, et al. Beyond RCHOP: A Blueprint for Diffuse Large B Cell Lymphoma Research. J Natl Cancer Inst. 2016;108(12).
3. Cultrera JL, Dalia SM. Diffuse large B-cell lymphoma: current strategies and future directions. Cancer Control J Moffitt Cancer Cent. 2012;19(3):204–213.
4. Feugier P, Van Hoof A, Sebban C, et al. Long-term results of the R-CHOP study in the treatment of elderly patients with diffuse large B-cell lymphoma: a study by the Groupe d'Etude des Lymphomes de l'Adulte. J Clin Oncol. 2005;23(18):4117–4126.
5. Philip T, Guglielmi C, Hagenbeek A, et al. Autologous bone marrow transplantation as compared with salvage chemotherapy in relapses of chemotherapy-sensitive non-Hodgkin's lymphoma. N Engl J Med. 1995;333(23):1540–1545.
6. Gisselbrecht C, Glass B, Mounier N, et al. Salvage regimens with autologous transplantation for relapsed large B-cell lymphoma in the rituximab era. J Clin Oncol. 2010;28(27):4184–4190.
7. Chen J, Xu-Monette ZY, Deng L, et al. Dysregulated CXCR4 expression promotes lymphoma cell survival and independently predicts disease progression in germinal center B-cell-like diffuse large B-cell lymphoma. Oncotarget 2015;6(8):5597–5614.
8. Moreno MJ, Bosch R, Dieguez-Gonzalez R, et al. CXCR4 expression enhances diffuse large B cell lymphoma dissemination and decreases patient survival. J Pathol. 2015;235(3):445–455.
9. Xu Z-Z, Shen J-K, Zhao S-Q, Li J-M. Clinical significance of chemokine receptor CXCR4 and mammalian target of rapamycin (mTOR) expression in patients with diffuse large B-cell lymphoma. Leuk Lymphoma. 2018;59(6):1451–1460.
10. Reinholdt L, Laursen MB, Schmitz A, et al. The CXCR4 antagonist plerixafor enhances the effect of rituximab in diffuse large B-cell lymphoma cell lines. Biomark Res. 2016;4:12.
11. Domanska UM, Kruizinga RC, Nagengast WB, et al. A review on CXCR4/CXCL12 axis in oncology: No place to hide. Eur J Cancer. 2013;49(1):219–230.
12. Bertolini F, Dell'Agnola C, Mancuso P, et al. CXCR4 neutralization, a novel therapeutic approach for non-Hodgkin's lymphoma. Cancer Res. 2002;62(11):3106–3112.
13. Kuhne MR, Mulvey T, Belanger B, et al. BMS-936564/MDX-1338: a fully human anti-CXCR4 antibody induces apoptosis in vitro and shows antitumor activity in vivo in hematologic malignancies. Clin Cancer Res. 2013;19(2):357–366.
14. Reinholdt LR, Laursen MB, Falgreen S, et al. High expression of CXCR4 impairs anti-CD20 monoclonal antibody (Rituximab)-dependent cytotoxicity in diffuse large B-cell lymphoma. Blood. 2015; 126(23):1455–1455.
15. Beider K, Ribakovsky E, Abraham M, et al. Targeting the CD20 and CXCR4 pathways in non-hodgkin lymphoma with rituximab and high-affinity CXCR4 antagonist BKT140. Clin Cancer Res. 2013;19(13):3495–3507.
16. Unzueta U, Céspedes MV, Ferrer-Miralles N, et al. Intracellular CXCR4+ cell targeting with T22-empowered protein-only nanoparticles. Int J Nanomedicine. 2012;7:4533–4544.
17. Céspedes MV, Unzueta U, Tatkiewicz W, et al. In vivo architectonic stability of fully de novo designed protein-only nanoparticles. ACS Nano. 2014;8(5):4166–4176.
18. Sánchez-García L, Serna N, Álamo P, et al. Self-assembling toxin-based nanoparticles as self-delivered antitumoral drugs. J Control Release. 2018;274:81–92.
19. Serna N, Sánchez-García L, Unzueta U, et al. Protein-Based Therapeutic Killing for Cancer Therapies. Trends Biotechnol. 2018;36(3):318–335.
20. Rosenblum D, Joshi N, Tao W, Karp JM, Peer D. Progress and challenges towards targeted delivery of cancer therapeutics. Nat Commun. 2018;9(1):1410.
21. Pirollo KF, Chang EH. Does a targeting ligand influence nanoparticle tumor localization or uptake? Trends Biotechnol. 2008; 26(10):552–558.

22. Lammers T, Kiessling F, Hennink WE, Storm G. Drug targeting to tumors: principles, pitfalls and (pre-) clinical progress. J Control Release. 2012;161(2):175–187.

23. Bae YH, Park K. Targeted drug delivery to tumors: myths, reality and possibility. J Control Release. 2011;153(3):198–205.

24. Wilhelm S, Tavares AJ, Dai Q, et al. Analysis of nanoparticle delivery to tumours. Nat Rev Mater. 2016;1(5):16014.

25. Céspedes MV, Unzueta U, Álamo P, et al. Cancer-specific uptake of a liganded protein nanocarrier targeting aggressive CXCR4+ colorectal cancer models. Nanomedicine. 2016;12(7):1987–1996.

26. Heneweer C, Holland JP, Divilov V, Carlin S, Lewis JS. Magnitude of enhanced permeability and retention effect in tumors with different phenotypes: 89Zr-albumin as a model system. J Nucl Med. 2011;52(4):625–633.

27. Unzueta U, Céspedes MV, Vázquez E, Ferrer-Miralles N, Mangues R, Villaverde A. Towards protein-based viral mimetics for cancer therapies. Trends Biotechnol. 2015;33(5):253–258.

28. Zhou S, Wu D, Yin X, et al. Intracellular pH-responsive and rituximab-conjugated mesoporous silica nanoparticles for targeted drug delivery to lymphoma B cells. J Exp Clin Cancer Res. 2017;36(1):24.

29. Nevala WK, Butterfield JT, Sutor SL, Knauer DJ, Markovic SN. Antibody-targeted paclitaxel loaded nanoparticles for the treatment of CD20+ B-cell lymphoma. Sci Rep. 2017;7:45682.

30. Salvati A, Pitek AS, Monopoli MP, et al. Transferrin-functionalized nanoparticles lose their targeting capabilities when a biomolecule corona adsorbs on the surface. Nat Nanotechnol. 2013;8(2):137–143.

31. Gustafson HH, Holt-Casper D, Grainger DW, Ghandehari H. Nanoparticle uptake: the phagocyte problem. Nano Today. 2015;10(4):487–510.

32. Zhang RX, Li J, Zhang T, et al. Importance of integrating nanotechnology with pharmacology and physiology for innovative drug delivery and therapy – an illustration with firsthand examples. Acta Pharmacol Sin. 2018;39(5):825–844.

33. Gerber H-P, Senter PD, Grewal IS. Antibody drug-conjugates targeting the tumor vasculature: Current and future developments. MAbs. 2009;1(3):247–253.

34. Garnett MC, Kallinteri P. Nanomedicines and nanotoxicology: some physiological principles. Occup Med. 2006;56(5):307–311.

35. Ghitescu L, Robert M. Diversity in unity: the biochemical composition of the endothelial cell surface varies between the vascular beds. Microsc Res Tech. 2002;57(5):381–389.

36. Ribatti D, Vacca A, Nico B, Fanelli M, Roncali L, Dammacco F. Angiogenesis spectrum in the stroma of B-cell non-Hodgkin's lymphomas. An immunohistochemical and ultrastructural study. Eur J Haematol. 1996;56(1–2):45–53.

37. Kobayashi H, Watanabe R, Choyke PL. Improving conventional Enhanced permeability and Retention (EPR) effects; what is the appropriate target? Theranostics. 2013;4(1):81–89.

38. Céspedes MV, Unzueta U, Aviñó A, et al. Selective depletion of metastatic stem cells as therapy for human colorectal cancer. EMBO Mol Med. 2018;10(10).

39. Díaz R, Pallarès V, Cano-Garrido O, et al. Selective CXCR4+ Cancer Cell Targeting and Potent Antineoplastic Effect by a Nanostructured Version of Recombinant Ricin. Small. 2018;14(26):e1800665.

40. Recasens-Zorzo C, Cardesa-Salzmann T, Petazzi P, et al. Pharmacological modulation of CXCR4 cooperates with BET bromodomain inhibition in diffuse large B-cell lymphoma. Haematologica 2019; 104(4):778–788.

41. Aghanejad A. Synthesis and Evaluation of [67Ga]-AMD3100: A Novel Imaging Agent for Targeting the Chemokine Receptor CXCR4. Sci Pharm 2014;82(1):29–42.

42. Zhang X-X, Sun Z, Guo J, et al. Comparison of 18F-labeled CXCR4 antagonist peptides for PET imaging of CXCR4 expression. Mol Imaging Biol 2013; 15(6):758–767.

Highly sensitive and specific *in situ* hybridization assay for quantification of *SOX11* mRNA in mantle cell lymphoma reveals association of *TP53* mutations with negative and low *SOX11* expression

Birgit Federmann, Leonie Frauenfeld, Helga Pertsch, Vanessa Borgmann, Julia Steinhilber, Irina Bonzheim, Falko Fend and Leticia Quintanilla-Martinez

Institute of Pathology and Neuropathology, Comprehensive Cancer Center and University Hospital Tübingen, Eberhard-Karls-University of Tübingen, Tübingen, Germany

ABSTRACT

SOX11 is a valuable marker to identify biologically and clinically relevant groups of mantle cell lymphoma such as cyclin D1 negative and leukemic non-nodal mantle cell lymphoma (MCL). We aimed to establish a sensitive *in situ* hybridization analysis of *SOX11* mRNA allowing its quantification within the histopathological context and compare it with immunohistochemistry and real-time quantitative reverse transcription-PCR (RT-qPCR). Furthermore, *TP53* status was correlated with *SOX11* mRNA levels. Sixty-six cases were investigated; 58 conventional mantle cell lymphomas (cMCL), including six cyclin D1 negative (46 classic, 12 blastoid) and eight leukemic non-nodal mantle cell lymphomas (nnMCL). RNAscope was used for the *in situ* hybridization and the results scored as 0 to 4. MCL cases with SOX11 positivity by immunohistochemistry (IHC) were positive by RNA *in situ* hybridization (RNAscope) but with different scores. RT-qPCR showed a good correlation with the median of the grouped scores but had a wide variation in individual cases. The SOX11 negative leukemic non-nodal mantle cell lymphomas were also negative by RNAscope. *TP53* was mutated in 13/63 (21%) cases, including 5/7 (71%) leukemic non-nodal and 8/56 (14%) cMCL. Interestingly, of the *TP53* mutated cases, nine were in the RNAscope negative/low SOX11 group (9/15; 60%) and four in the high SOX11 group (4/36; 11%) (*P*=0.0007). In conclusion, RNAscope is a reliable method to evaluate *SOX11* mRNA levels. This study demonstrates the broad range of *SOX11* mRNA levels in MCL. An important finding is the significant correlation of *TP53* mutations with negative/low *SOX11* mRNA level both in leukemic nnMCL and cMCL.

Correspondence:

LETICIA QUINTANILLA-MARTINEZ
leticia.quintanilla-fend@med.uni-tuebingen.de

Introduction

MCL is a mature B-cell neoplasm, which accounts for 3-10% of all non-Hodgkin´s lymphomas. The genetic hallmark of MCL is the t(11;14)(q13;q32) chromosomal translocation that juxtaposes the immunoglobulin heavy chain gene (IGH) on 14q32 to the *CCND1* gene on 11q13 leading to a deregulated overexpression of *CCND1* mRNA and cyclin D1 protein, in 95% of the cases.[1,2] The existence of cyclin D1 negative MCL (D1-MCL) was demonstrated by gene expression profile[3] (GEP) and further studies based on real-time quantitative RT-qPCR and fluorescence *in situ* hybridization (FISH) analysis demonstrated that the majority of these cases carry a *CCDN2* translocation[4-7] and few cases have a *CCND3*/IGH or IGK/IGL rearrangement.[8,9] Importantly, cyclin D1 positive and negative MCL have the same morphologic, pathologic, clinical and molecular features and are characterized by the expression of the transcription factor Sex determining region Y-box 11 (SOX11).[10] Due to the positivity of SOX11 in D1-MCL[6,11,12] and the negativity in other mature B-cell neoplasms, the immunohistochemical analysis of SOX11 has become a valuable marker for the identification of the different subsets of MCL.[13] Although MCL has been tra-

ditionally considered an aggressive and incurable disease, an indolent variant has been recognized that presents with leukemic nnMCL, and treatment is usually deferred for months or years.[14,15] Interestingly, nnMCL, in contrast to cMCL, is characterized by a lack of *SOX11* expression, the presence of IGHV mutations and usually low genomic complexity, indicating that these two variants follow different pathways of lymphomagenesis.[15-17] The lack of SOX11 expression in nnMCL is believed to play an important role for the indolent behavior of the disease.[11,14,16,18-20] SOX11 is a transcription factor that belongs to the *SOX* gene family and is widely expressed in embryogenesis, but not in normal hematopoiesis.[21] In MCL, it is controversial whether SOX11 acts as an oncogene or as a tumor suppressor gene. SOX11 has been proposed to act as an oncogene inducing cell proliferation, enforcing PAX5 expression and inhibiting terminal B-cell differentiation into plasma cells *via PRDM1* and *BCL6*.[16,22] Additionally, it has been shown to promote tumor angiogenesis through the PDGFA axis.[23] More recently, in a murine model, it was demonstrated that SOX11 overexpression in B-cells promotes B-cell receptor signaling and results in a disease phenotype similar to MCL.[24] In contrast, it has been shown that SOX11-binding targets could repress proliferation, and therefore, it has been suggested that SOX11 in MCL may act as a tumor suppressor gene.[25] The prognostic relevance of SOX11 in MCL is equally controversially discussed. Although originally it was thought that SOX11 negative cases carried an indolent clinical course, other studies have shown that high SOX11 expression is associated with improved survival in a subset of MCL patients, and low or negative SOX11 expression with poor overall survival.[25-28] Further work identified a group of MCL lacking SOX11 expression with a dismal prognosis.[11] Interestingly, many of these cases were associated with *TP53* mutations. *TP53* mutations are preferentially associated with blastoid morphology (up to 30%),[29] but also occur in both cMCL with classic morphology and nnMCL, and associated with a poor prognosis.[30-32]

SOX11 expression is usually investigated by immunohistochemistry (IHC) in tissue specimens; however, IHC is not a quantitative technique. RNAscope is a relatively new *in situ* hybridization (ISH) technique that allows a highly sensitive visualization of molecular markers in the morphological context by target-specific amplification of signals with suppression of the background.[33] In recent years, some studies have analyzed this technology in different tissues and found it to be a method comparable to immunohistochemistry and RT-qPCR.[34-36]

By integrating *TP53* status and SOX11 expression in the diagnostic workup of MCL the risk stratification could be improved. Given the lack of reliable quantification of IHC and the conflicting results concerning the prognostic role of SOX11, we aimed to establish a sensitive ISH analysis of *SOX11* mRNA allowing its quantification within the histopathological context and to compare it with IHC and RT-qPCR analyses. Furthermore, the *TP53* status was investigated by IHC and next-generation sequencing (NGS) and correlated with *SOX11* mRNA expression levels.

Methods

Patient selection

Sixty-six cases with the diagnosis of MCL were selected from the files of the Institute of Pathology, University of Tübingen. In addition, 12 cases with the diagnosis of small cell B-cell lymphoma (chronic lymphocytic leukemia (CLL), follicular lymphoma (FL) and marginal zone B-cell lymphoma (MZL), four cases each) were used as controls. The study was approved by the local ethics committee (*TÜ-730/2018BO2*).

Histology and immunohistochemistry

Hematoxylin and Eosin (H&E) sections and all immunohistochemical stains were reviewed. BM trephines were formalin-fixed, decalcified in EDTA, and paraffin-embedded (FFPE). Immunohistochemical stains were performed using an automated immunostainer (Ventana Medical Systems, Tuscon, USA), according to the manufacturer´s protocol. The following antibodies were used: SOX11 (MRQ-58) (Medac Diagnostika, Wedel, Germany) and p53 (DO-7) (Novocastra Liquid, Leica Biosystems, Newcastle, UK). SOX11 stain was scored as negative (0%), low (1-10% positive cells) and positive (>10% positive cells). p53 was considered positive when >20% cells were strongly positive.

RNAscope

The mRNA ISH was performed using the RNAscope 2.5 VS reagent kit-RED with custom designed SOX11-RNA, as target (Advanced Cell Diagnostics, ACD, Hayward, CA), according to the manufacturer`s protocol, as previously described[33] (*Online Supplementary Material and Methods*). The RNAscope procedure was performed in the Ventana Discovery XT autostainer for open procedures. Tissue mRNA preservation was assessed by performing RNAscope analysis of mRNA of the housekeeping gene peptidylpropyl isomerase B (PPIB) (*Online Supplementary Figure S1*).

RNAscope scores

The results were scored according to the guidelines described in the manufacturer´s protocol. Briefly, staining score 0 was defined as: no staining or less than 1 dot to every 10 cells (40x magnification), score 1: 1-3 dots/cell (visible at 20-40x magnification), score 2: 4-9 dots/cell, and very few dot clusters (visible at 20-40x magnification), score 3: 10-15 dots/cell, less than 10% positive cells have dot clusters (visible at 20x magnification), and score 4: >15 dots/cell, more than 10% positive cells have dot clusters (visible at 20x magnification). Score 0-1 was considered negative/low, score 2 intermediate, and score 3-4 high SOX11 mRNA expression.

RNA isolation and Real-time quantitative PCR (RT-qPCR)

RNA was isolated using the Maxwell® 16 LEV RNA FFPE Purification Kit and the Maxwell® 16 Instrument (Promega, Madison, WI, USA). RT-qPCR was performed to quantify SOX11 mRNA levels (see *Online Supplementary Material and Methods*). Data were analyzed using the $2^{-\Delta\Delta C_P}$ method and the mean of the SOX11 negative cases was defined as calibrator.

Next generation sequencing of *TP53* gene

NGS was performed using the Ion AmpliSeq™ TP53 Panel (Life Technologies) on the Ion GeneStudio™ S5 Prime System according to the manufacturer`s protocol (see *Online Supplementary Material and Methods*).

Statistical analysis

Statistical analysis was performed with JMP software version 10 (SAS Institute GmbH) using Fisher exact or χ^2 test for comparison of nominal data. Statistical significance was concluded for values of $P<0.05$.

Results

Clinical and Morphological features

Table 1 summarizes the clinical and morphological features. A total of 66 patients with the diagnosis of MCL were included in the study of which 27 were female and 39 males with a median age of 72 years (range 47-91 years). Main biopsy sites were lymph nodes (LN) in 31 cases, bone marrow (BM) in 14 cases, and 21 extranodal sites including one spleen, four tonsils and two intestinal biopsies.

Of the 66 cases, 58 (88%) were classified as cMCL with predominantly nodal involvement, but also BM infiltration. Forty-six of these cases showed a classic morphology (46/58, 79%), and 12 cases (12/58, 21%) were classified as blastoid. Fifty-two cases (52/58; 90%) were cyclin D1 and SOX11 positive, whereas six cases (6/58; 10%) were cyclin D1 negative (four classic and two blastoid) but positive for SOX11. In eight of 66 cases (12%), the diagnosis of nnMCL was made based on peripheral blood and BM involvement without or minimal nodal disease. One case classified as nnMCL presented mainly with splenic involvement. The nnMCL cases were SOX11 negative and cyclin D1 positive. In 63 cases immunohistochemical analysis for p53 was performed. In 11 cases (17%) p53 was strongly expressed in >20% of tumor cells suggesting a TP53 mutation. Forty-seven cases (75%) were considered P53 negative (≤20% of tumor cells). Five cases (8%) were equivocal with weak, heterogeneous staining in the majority of the tumor cells. The proliferation rate assessed with MIB1 showed a low proliferation (<10%) in 10 cases, intermediate proliferation (10-29%) in 34 cases, and high proliferation (>30%) in 19 cases. The 12 cases with blastoid morphology showed a median proliferation rate of 80%. CD5 was analyzed in 65 cases, 54 cases were CD5 positive whereas 11 cases (17%) remained negative.

RNAscope analysis for *SOX11* mRNA

Of the 66 cases analyzed with RNAscope for SOX11 mRNA, 63 cases were informative, whereas two BM biopsies and one lymph node core biopsy were considered not evaluable due to the lack or low expression of the housekeeping gene *PPIB* used as positive control. The poor mRNA preservation in the two BM most probably is secondary to the decalcification process. The interpretation and quantification of RNAscope was easy to perform. The cases were scored according to the quantity of punctate dots, as described above (Figure 1A-E; Table 2). Twenty-two cases were classified as score 4 (cyc D1+ n=18; cyc D1- n=4), 14 cases as score 3 (cyc D1+ n=13; cyc D1- n=1) 12 cases as score 2 (cyc D1+ n=11; cyc D1-, n=1), eight cases as score 1 (cMCL cyc D1+ n=7; nnMCL n=1) and seven cases as score 0 (nnMCL n=7). All small B-cell lymphomas used as controls were negative. Eight of 12 (67%) MCL cases with blastoid morphology and 26 of 44 (59%) MCL with classic morphology showed high SOX11 mRNA expression (score 3 or 4). Interestingly, 5/6 (83%) cases with D1-MCL were in the high SOX11 mRNA expression group. In contrast, 15 (24%) cases had low/negative SOX11 mRNA expression including the 8/8 (100%) nnMCL cases and 7/55 (13%) cMCL cases. The overall correlation between IHC and RNAscope was very good. Two cases that were considered as SOX11 negative by IHC were scored as 1 with RNAscope. One of these cases was a case with primary splenic presentation (Figure

Table 1. Clinical and histological data of the 66 cases.

Diagnosis	n=	Sex female: male	Age median (range)	Morphology classic	blastoid
cMCL	52	18:34	72 (49-91)	42	10
D1-MCL	6	4:2	63 (47-87)	4	2
nnMCL	8	5:3	76 (56-87)	7	1
	66	27:39	72 (47-91)	53	13

cMCL: conventional mantle cell lymphoma; D1-MCL: cyclinD1 negative mantle cell lymphoma; nnMCL: non-nodal leukemic mantle cell lymphoma.

2A) with plasmacytic differentiation (Figure 2B) and kappa immunoglobulin light chain restriction (Figure 2D-E). The SOX11 IHC was equivocal whereas the SOX11 RNAscope demonstrated clear signals corresponding to score 1 (Figure 2F-G). This case was classified as nnMCL with low SOX11 mRNA expression. The remaining seven cases classified as nnMCL in BM were SOX11 negative by IHC and had a score 0 with RNAscope.

SOX11 mRNA analysis with RT-qPCR

In 54 cases, for which material was available, RT-qPCR was performed. The *SOX11* mRNA levels are shown in Figure 1F. The analysis showed a wide range of *SOX11* mRNA levels among the cases. cMCL cases cyclin D1 and SOX11 positive by IHC showed a median level of 30-fold *SOX11* mRNA level compared to the mean of the SOX11 negative cases (range 2-218), whereas the four analyzed D1-MCL cases showed a median *SOX11* mRNA level of 12 (range 8-102). nnMCL negative for SOX11 by IHC showed the lowest *SOX11* mRNA levels (median 1; range 0-1).

Correlation of *SOX11* mRNA levels between RNAscope and RT-qPCR

The correlation of *SOX11* mRNA levels between RNAscope and RT-qPCR was further analyzed (Table 2). A median SOX11 mRNA level of 39-fold (range 3-218) was found for score 4, 23-fold (range 6-119) for score 3, 10-fold (range 2-43) for score 2, seven-fold (range 1-68) for score 1, and 1-fold (range 0-1) for score 0. The correlation between RNAscope and mRNA levels obtained by RT-qPCR analysis showed a significant association between the median of the single groups (P=0.0002) (Figure 1F). However, there was a broad range of *SOX11* mRNA levels, as measured by RT-qPCR in each of the groups. In part, this could be explained by a dilution effect due to the high content of reactive cells in some cases with partial infiltration. This is well demonstrated in a case of D1-MCL with mantle zone growth pattern and partial involvement of the LN (Figure 3A-D). IHC and RNAscope revealed similar patterns and intensities (Figure 3E-F); however, RT-qPCR showed relatively low levels of *SOX11* mRNA.[16] In most cases; however, there was no clear explanation for the variability between RNAscope and RT-qPCR. In the two BM cases with a lack of signals in the RNAscope assay, RT-qPCR detected *SOX11* mRNA and SOX11 was also positive by IHC. This indicates that pre-analytical parameters may differ in their influence on the two mRNA quantification methods. Taken together, although both methods showed an overall good correlation, RNAscope was considered more reliable for the quantification of *SOX11* mRNA in individual cases.

Correlation between *SOX11* and *TP53* status

Table 3 and *Online Supplementary Table S1* summarize the data of the *TP53* mutated group. In thirty-seven cases, all exons of *TP53* were sequenced by NGS including all p53 positive cases (11 cases), the five equivocal cases and 20 p53 negative cases including all remaining blastoid cases. *TP53* mutations were demonstrated in 13 cases; 11 considered p53 positive, and two considered p53 negative; one of these a nnMCL case revealed complete negativity by IHC. The five equivocal and all remaining negative cases were *TP53* wild-type. Although the cut-off for p53 positivity was set on >20%, 10 cases showed strong p53 expression in more than 60% of the tumor cells. *TP53* mutations were identified in eight of 56 cMCL cases (14%), five of them with blastoid morphology (Figure 4). Four of these eight cases were in the group of negative/low *SOX11* expression. In contrast, five of seven evaluable cases (71%) of nnMCL had *TP53* mutations (14% *vs.* 71%; *P*=0.003). Four of these cases were diagnosed in BM and presented with striking lymphocytosis in the peripheral blood (Figure 5). One case had a blastoid morphology. Altogether, nine of the *TP53* mutated cases
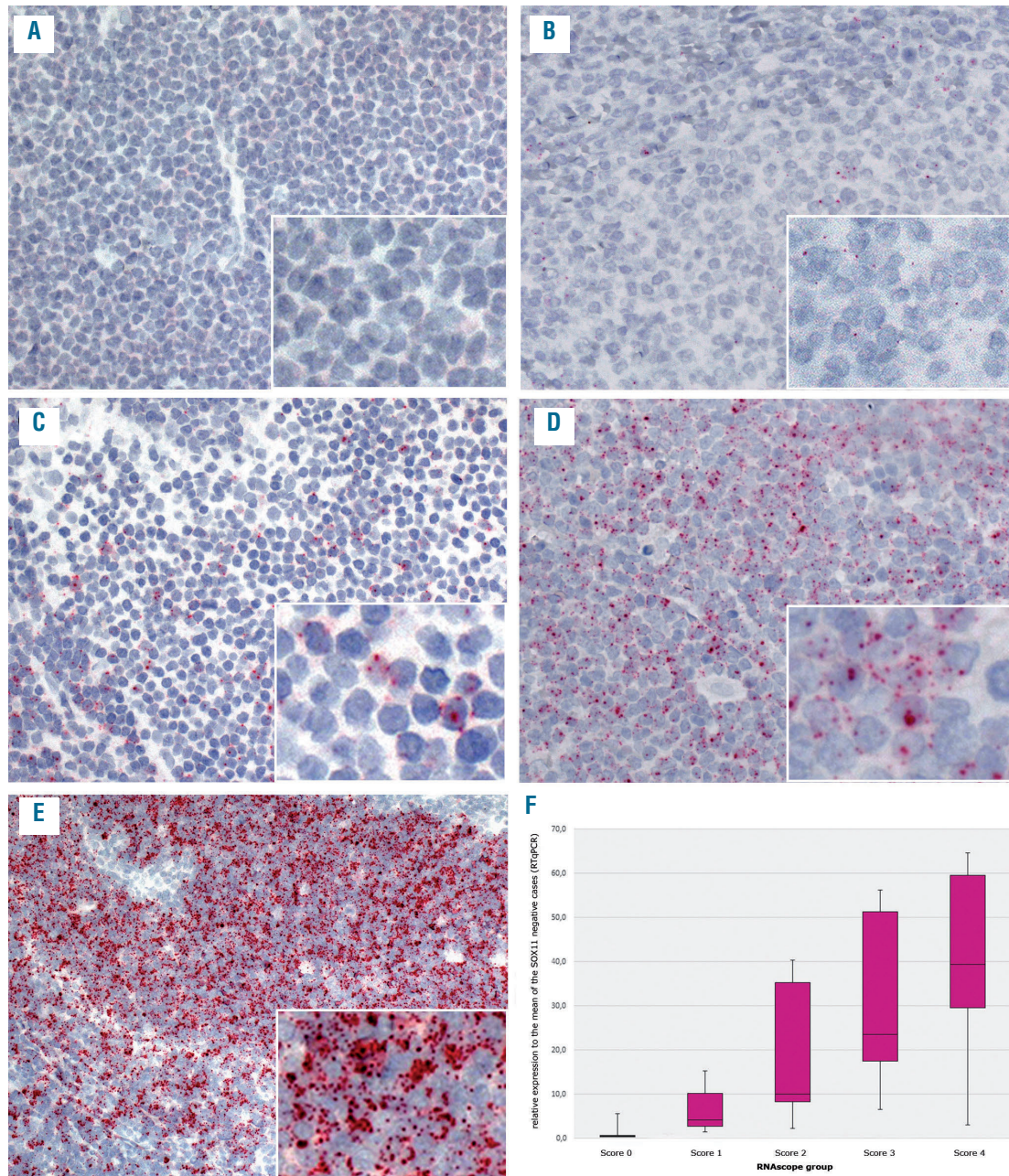
Figure 1. Illustration of the staining pattern in the different RNAscope scores and correlation to the real-time quantitative PCR (RT-qPCR) results, which shows a decrease of SOX11-mRNA levels with decreasing staining scores. (A) score 0, no staining (case #16); (B) score 1, 1-3 dots/cell (case #9); (C) score 2, 4-9 dots/cell, very few clusters (case #5); (D) score 3, 10-15 dots/cell, less than 10% positive cells with dot clusters (case #2); (E) score 4, 15 dots/cell, more than 10% positive cells with dot clusters (case #11); (F) box plot of SOX11 mRNA levels measured by RT-qPCR according to the score groups showing the third quartile and first quartile range of the data and the median for the particular score (*P*=0.0002). A-E original magnification 200x and insert with 400x.

Table 2. SOX11 RNAscope and RT-qPCR analyses in the three MCL subgroups.

Diagnosis	SOX11 mRNA level by RNAscope and RT-qPCR[#]									
	Score 0	RT-qPCR median (range)	Score 1	RT-qPCR median (range)	Score 2	RT-qPCR median (range)	Score 3	RT-qPCR median (range)	Score 4	RT-qPCR median (range)
cMCL	49	0	–	7	7 (4 -68)	11	15 (2-43)	13	24 (6-119)	18	39 (3 -218)
D1-MCL	6	0	–	0	–	1	8.63	1	7.57	4	59+
nnMCL	8	7	1 (0-1)	1	1	0	–	0	–	0	–
Total	**63**	**7**	**1 (0-1)**	**8**	**7 (1-68)**	**12**	**10 (2-43)**	**14**	**23 (6-119)**	**22**	**39 (3 -218)**

cMCL: conventional mantle cell lymphoma; D1-MCL: cyclinD1 negative mantle cell lymphoma; nnMCL: non-nodal leukemic mantle cell lymphoma; real-time quantitative reverse transcription-PCR. #54 cases could be analyzed with RT-qPCR. + mean of the two cases analyzed with RT-qPCR.
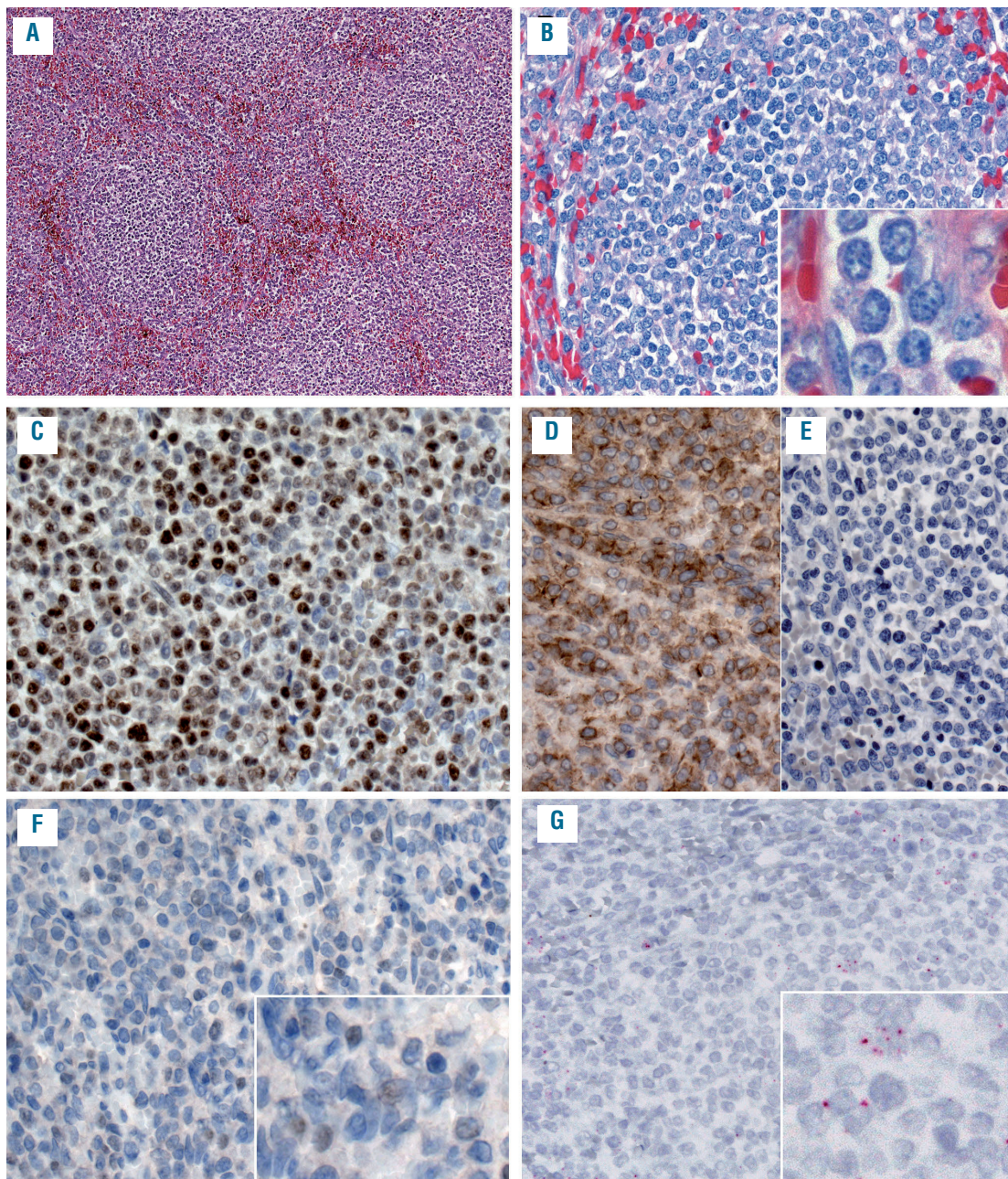
Figure 2. Mantle cell lymphoma (MCL) with splenic involvement and plasmacytoid differentiation (case #9). (A) the spleen is characterized by a nodular infiltration of the white pulp (hematoxylin and eosin); (B) Giemsa stain highlights the cytologic features. The infiltrate is composed of medium-sized cells with a rim of basophilic cytoplasm, dispersed nuclear chromatin and occasional small nucleoli; (C) the cells are positive for cyclin D1; (D) the tumor cells are positive for lambda-stain (D) and negative for kappa (E); (F) the SOX11 immunohistochemistry (IHC) was interpreted as negative at diagnosis, but upon review occasional weakly positive tumor cells could be detected; (G) the SOX11 RNA *in situ* hybridization (RNAscope) shows a score 1 with 1-3 dots/cell. A original magnification 50x, B-G original magnification 200x, insert original magnification 630x.

were in the negative/low SOX11 group (RNAscope 0-1) (9/15; 60%) and four in the high SOX11 group (RNAscope 3-4) (4/36; 11%). This difference was statistically significant (*P*=0.0007). Within the group of cMCL four *TP53* mutated cases where in the low SOX11 group (4/7; 57%) and four in the high SOX11 group (4/36; 11%), and the difference was statistically significant (*P*=0.01) Of the cMCL, the TP53 mutated cases showed the lowest

SOX11 mRNA scores including two cases with blastoid morphology (Figure 4).

Discussion

In this study, we investigated 66 cases of MCL for the expression levels of *SOX11* mRNA with RNAscope ISH
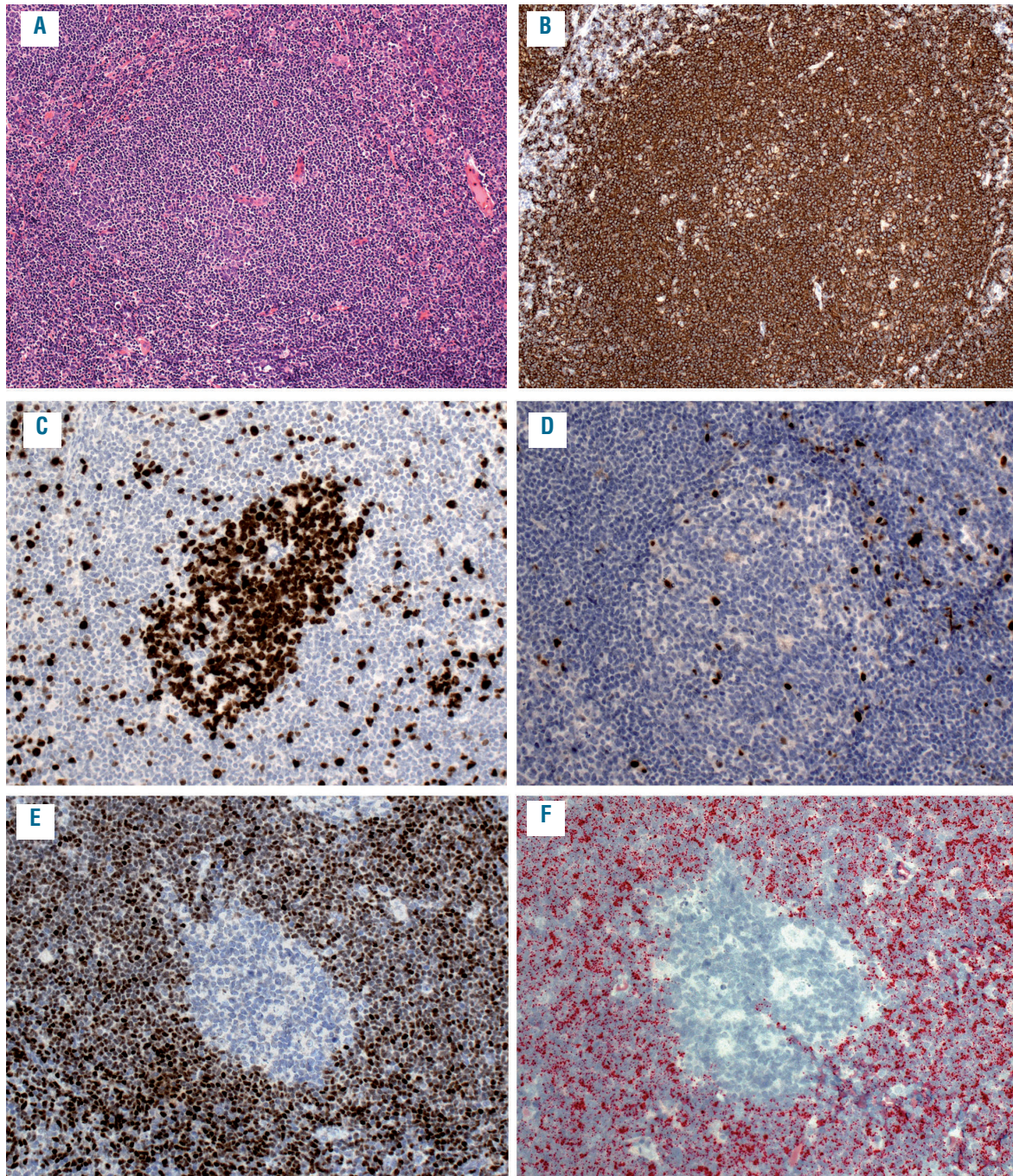
Figure 3. Classical cyclin D1 negative mantle cell lymphoma (D1-MCL) with mantle zone pattern (case #10). (A) the architecture is characterized by the expansion of the follicle mantle zone with tumor cells and a central "naked" germinal center (hematoxylin and eosin), (B) CD20 highlights the expanded mantle area; (C) MIB1 shows a high proliferation in the residual germinal center whereas the proliferation of the tumor cells is 5%; (D) the tumor cells are negative for cyclin D1; (E) the SOX11 stain demonstrates a strong positivity in the tumor cells, while the germinal center cells are negative; (F) the *SOX11* RNA *in situ* hybridization (RNAscope) shows a score 4 with 15 dots/cell and >10% cells with dot clusters. All original magnification 200x.

assay and compared it with IHC and RT-qPCR. Additionally, the TP53 status was investigated and correlated with *SOX11* mRNA levels. We show that RNAscope ISH assay is a reliable method to quantitate SOX11 mRNA levels within the histopathological context. Importantly, and in overall agreement with the RT-qPCR results, we demonstrated that SOX11 mRNA levels show a very broad range in cMCL and confirmed the negative or low mRNA levels in nnMCL cases. An interesting finding of this study was the correlation of *TP53* mutations with low/negative SOX11 mRNA scores in all investigated subtypes of MCL (P=0.0007).

RNAscope is a relatively new ISH technology with a probe design strategy that allows the visualization of RNA expression in the context of preserved tissue morphology.[33,39] In recent years, several studies confirmed the suitability of this method for the quantification of mRNA levels in FFPE tissues; however, *SOX11* has not been investigated.[34,40,41] The diagnostic importance of SOX11 expression for identifying specific subsets of MCL has been confirmed in many studies; however, its relevance as a prognostic marker is controversial. One possible explanation is that IHC, as a predominantly used technique, is not a quantitative method and does not provide reliable information about *SOX11* expression levels. The current gold standard for quantitative gene expression analysis is RT-qPCR.[42] However, this method lacks the morphological context, and in our study, a wide range of SOX11 mRNA level was found that not always correlated with the RNAscope assay. Similar findings were described by Lord *et al.,* who also found a wide range of SOX11 mRNA levels by RT-qPCR and were not able to define a natural cut-off that could stratify cases with low protein expression by IHC.[43] The highly variable SOX11 expression in MCL could indicate that not only the presence or absence of the protein, but also its level may be important for the behavior of the malignant cells. Nevertheless, a similar number of cases, with high expression of *SOX11* mRNA, was found in the group with blastoid morphology when compared with classic morphology (62% *vs.* 59%).

The oncogenic potential of SOX11 has been extensively studied in the last years.[16,22-24,27,44,45] SOX11 has been shown to promote tumor growth *via* the induction of angiogenesis by regulating PDGFA.[23] Recently, it has also been described that SOX11 binds and transcriptionally regulates two genes important for the modulation of microenvironment-tumor interactions, *CXCR4* (C-X-C motif chemokine receptor 4) and *PTK2*, encoding for focal adhesion kinase (FAK).[44] These genes are essential for tumor cell migration and adhesion to stromal cells in the bone marrow.[46] Furthermore, SOX11 has been described to correlate also with high proliferation activity and aggressive behaviour of the disease.[22,47,48] The accurate quantification of SOX11 expression opens the possibility to investigate the potential influence of SOX11 levels, and thus, might help to refine both the biological functions in MCL and to determine whether it can be used as a prognostic marker. The correlation between RNAscope, IHC and RT-qPCR was in general good; however, the automated RNAscope technology, direct visualization in tissue specimens and easy quantification of the signals makes this technology very attractive for diagnosis and research purposes. The

Table 3. Histological, immunohistochemical and molecular data of 13 cases with *TP53* mutation.

Case #	Diagnosis	IHC					RNAscope SOX11 Score	RT-qPCR SOX11 relative expression	TP53		
		SOX11 %	D1	P53 %	CD5	MIB %			mutation	VAF [%]	CADD Score
6	cMCL - classic	<10	+	60	heterogenous	35	1	10	p.R248Q	c.743G>A	77	27.3
42	cMCL - classic	>10	+	3	+	10	4	80	p.L201Afs	c.601_602del	12	19.2
64	cMCL - classic	<10	+	80	+	80	1	1	p.R248W	c.742C>T	7	26.8
									p.P278R	c.833C>G	8	26.4
25	cMCL - blastoid	>10	+	70	+	30	3	21	p.P278S	c.832C>T	38	28.6
34	cMCL - blastoid *	<10	+	30	+	80	1	5	p.R175H	c.524G>A	99	24.1
37	cMCL - blastoid	>10	-	80	+	80	4	NA	p.R282W	c.844C>T	13	25.7
									p.R158H	c.473G>A	6	22.3
									p.R273C	c.817C>T	8	25.3
58	cMCL - blastoid	<10	+	90	heterogenous	80	1	NA	p.R273C	c.817C>T	70	25.3
66	cMCL - blastoid	>10	+	90	+	90	3	NA	p.P278S	c.832C>T	30	28.6
									p.Y220C	c.659A>G	58	29.5
9	nnMCL (spleen)	<10	+	90	-	20	1	0	p.V218G	c.653T>G	77	30
15	nnMCL (BM)	0	+	80	heterogenous	NA	0	1	p.Y205N	c.613T>A	35	24.2
16	nnMCL (BM)	0	+	90	heterogenous	5	0	0	p.V272G	c.815T>G	58	23.4
23	nnMCL (BM)	0	+	-	+	90	0	0	p.R273*	c.815_816insTTGAGGT29		NA
35	nnMCL (BM)	0	+	90	+	80	0	1	p.S127F	c.380C>T	16	27
									p.R248W	c.742C>T	7	26.8

cMCL: conventional mantle cell lymphoma; D1-MCL: cyclinD1 negative mantle cell lymphoma; nnMCL: non-nodal leukemic mantle cell lymphoma; IHC: immunohistochemistry; RT,PCR: real-time quantitative PCR; NGS: next generation sequencing; VAF: variant allelic frequency; NA: not available; * diagnosis of MCL made in pleura effusion; mutations with a CADD algorithm score >15 are considered deleterious.

caveat of any RNA-based technology including RNAscope is that good mRNA preservation is needed, and this depends on good fixation procedures. However, the low dropout rate in our study, with only two decalcified BM specimens not evaluable based on the positive control, documents the robust performance of RNAscope in routine archival tissue specimens.

An intriguing finding in this study was the higher frequency of *TP53* mutations in cases with low/negative SOX11 mRNA levels both in cMCL as well as nnMCL. *TP53* mutations are rarely observed in MCL with classic morphology,[11] but are frequently found in highly proliferative MCL with blastoid morphology (up to 30%), and associated with aggressive clinical course.[29,30,49] A recent study comparing the gene signature of cMCL and nnMCL demonstrated that the incidence of TP53 mutations is similar in both subgroups (36% and 38%, respectively).[50] Nevertheless, an interesting observation was the report of a group of cMCL cases that lacks SOX11 expression, carries *TP53* mutations and has a dismal prognosis.[11] This finding was recently confirmed in a study from the European MCL network that demonstrated that p53 overexpression is preferentially found in SOX11 negative cMCL cases (50% *vs.* 13%).[26] A caveat of the latter study

is that molecular analysis to demonstrate the presence of *TP53* mutations was not performed. Although, p53 stain is a very good surrogate marker of gene mutation when strong, homogeneous staining is considered as positive, a group of cases with negative or low p53 staining due to deletions or frameshift mutations are missed as demonstrated in this study (2/13; 15%). Accordingly, of the *TP53* mutated cases nine were in the negative/low SOX11 mRNA level group and four in the high mRNA level group (60% *vs.* 11%, *P*=0.0007). Our results further confirm previous reports suggesting that TP53 overexpression/mutations frequently occur in SOX11 negative/low cases.[11,26] It is worth mentioning that in the two previous studies only nodal cMCL cases with no previous history of leukemic manifestation were included. Nevertheless, it has been suggested that these cases might correspond to a selected subset of progressed nnMCL tumors.[17,48] However, contrary to the cases reported by Nygren *et al.* and Aukema *et al.*, in this study eight nnMCL cases with typical presentation diagnosed in the BM and one in spleen were included. Although the *TP53* mutated nnMCL cases showed striking lymphocytosis in the peripheral blood, they lacked significant lymphadenopathy and rarely blastoid morphology was observed. The high incidence of nnMCL with
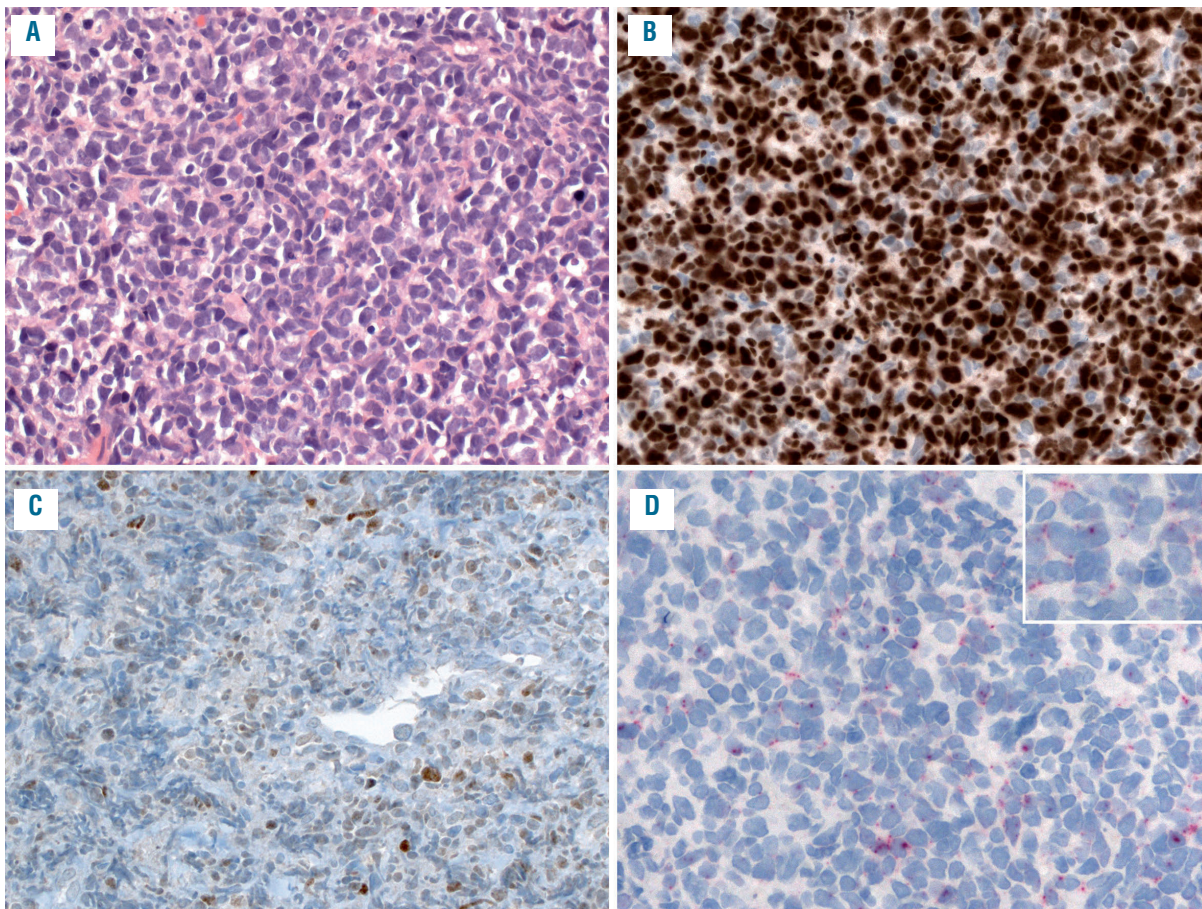
Figure 4. Mantle cell lymphoma (MCL) with blastoid morphology, low *SOX11* expression and *TP53* mutation (case # 58). (A) the infiltrate is characterized by a diffuse, monotonous population of medium-sized to large cells with irregular nuclei, fine chromatin and narrow cytoplasm (hematoxylin and eosin); (B) p53 is strongly positive in the majority of the tumor cells; (C) the SOX11 stain shows a rather weak heterogeneous positivity in the tumor cells (<10%); (D) *SOX11* RNAscope shows a score 1 with 1-3 dots/cell and no dot clusters. All original magnification 200x.

TP53 mutation in this study (5/7; 71%) most probably represents a natural bias since patients with nnMCL will usually seek medical attention only when the disease progresses and becomes symptomatic. Nevertheless, we also confirmed the presence of a group of nodal cMCL with both classic and blastoid morphology with *TP53* mutations and low SOX11 mRNA level. The reason why *TP53* mutations are found preferentially in the negative/low

SOX11 group is not clear. The possible interaction between SOX11 and p53, if any, and the influence of loss of SOX11 in p53 function/mutation have not been explored and warrant further investigation.

In conclusion our data demonstrate that RNAscope ISH assay is a reliable method for the detection and quantification of target RNA and can be used to evaluate SOX11 mRNA expression accurately. This study also revealed a
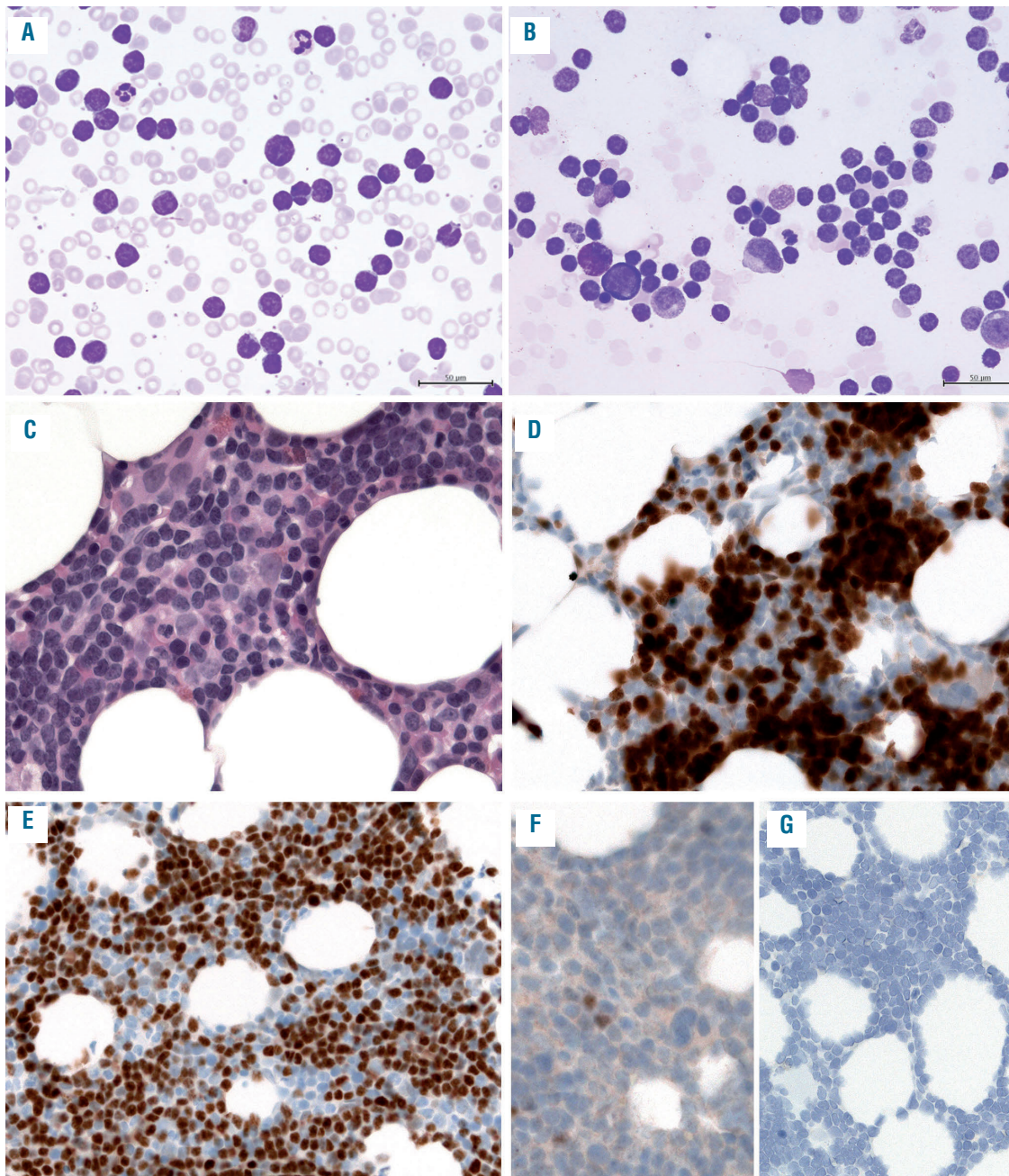
Figure 5. Leukemic non-nodal disease (nnMCL) mantle cell lymphoma (MCL) (case #15). (A-B) The cytology of the peripheral blood (A) and the bone marrow (B) shows a striking increase of small lymphocytes with rather round nuclei, condensed chromatin and scant cytoplasm; (C) Bone marrow biopsy shows a lymphoid infiltrate composed of small lymphocytes with round nuclei and scant cytoplasm (hematoxylin and eosin); (D) the tumor cells are positive for cyclin D1; (E) p53 is positive in 80% of the tumor cells; (F) the SOX11 stain is negative with only isolated positive cells; (G) the *SOX11* RNA *in situ* hybridization (RNAscope) shows a score 0 with no staining. All original magnification 200x.

broad range of SOX11 expression in MCL, indicating that SOX11 expression levels may be relevant for the behaviour of the disease. The association of *TP53* mutations with negative/low SOX11 mRNA expression in different MCL subtypes is an important finding, which needs to be explored in further studies.

References

1. Bosch F, Jares P, Campo E, et al. PRAD-1/cyclin D1 gene overexpression in chronic lymphoproliferative disorders: a highly specific marker of mantle cell lymphoma. Blood. 1994;84(8):2726-2732.
2. Swerdlow SH, Campo, E, Seto M, Müller-Hermelink, H.-K. In: Swerdlow SH, Campo E, Harris, N.L., Jaffe, E.S., Pileri, S.A., Stein, H. et al. eds. Mantle Cell Lymphoma. WHO Classification of Tumours of Hematopoietic and Lymphoid Tissues, Lyon: IARC Press. 2017(Lyon IARC Press):285-290.
3. Rosenwald A, Wright G, Wiestner A, et al. The proliferation gene expression signature is a quantitative integrator of oncogenic events that predicts survival in mantle cell lymphoma. Cancer Cell. 2003;3(2):185-197.
4. Fu K, Weisenburger DD, Greiner TC, et al. Cyclin D1-negative mantle cell lymphoma: a clinicopathologic study based on gene expression profiling. Blood. 2005; 106(13):4315-4321.
5. Quintanilla-Martinez L, Slotta-Huspenina J, Koch I, et al. Differential diagnosis of cyclin D2+ mantle cell lymphoma based on fluorescence in situ hybridization and quantitative real-time-PCR. Haematologica. 2009; 94(11):1595-1618.
6. Salaverria I, Royo C, Carvajal-Cuenca A, et al. CCND2 rearrangements are the most frequent genetic events in cyclin D1(-) mantle cell lymphoma. Blood. 2013;121(8):1394-1402.
7. Gesk S, Klapper W, Martin-Subero JI, et al. A chromosomal translocation in cyclin D1-negative/cyclin D2-positive mantle cell lymphoma fuses the CCND2 gene to the IGK locus. Blood. 2006;108(3):1109-1110.
8. Wlodarska I, Dierickx D, Vanhentenrijk V, et al. Translocations targeting CCND2, CCND3, and MYCN do occur in t(11;14)-negative mantle cell lymphomas. Blood. 2008;111(12):5683-5690.
9. Martin-Garcia D, Navarro A, Valdes-Mas R, et al. CCND2 and CCND3 hijack immunoglobulin light chain enhancers in cyclin D1-negative mantle cell lymphoma. Blood. 2019;133(9):940-951.
10. Ek S, Dictor M, Jerkeman M, et al. Nuclear expression of the non B-cell lineage Sox11 transcription factor identifies mantle cell lymphoma. Blood. 2008;111(2):800-805.
11. Nygren L, Baumgartner Wennerholm S, et al. Prognostic role of SOX11 in a population-based cohort of mantle cell lymphoma. Blood. 2012;119(18):4215-4223.
12. Mozos A, Royo C, Hartmann E, et al. SOX11 expression is highly specific for mantle cell lymphoma and identifies the cyclin D1-negative subtype. Haematologica. 2009;94(11):1555-1562.
13. Sander B, Quintanilla-Martinez L, Ott G, et al. Mantle cell lymphoma--a spectrum from indolent to aggressive disease. Virchows Arch. 2016;468(3):245-257.

14. Fernandez V, Salamero O, Espinet B, et al. Genomic and gene expression profiling defines indolent forms of mantle cell lymphoma. Cancer Res. 2010;70(4):1408-1418.
15. Jares P, Colomer D, Campo E. Genetic and molecular pathogenesis of mantle cell lymphoma: perspectives for new targeted therapeutics. Nat Rev Cancer. 2007;7(10):750-762.
16. Palomero J, Vegliante MC, Eguileor A, et al. SOX11 defines two different subtypes of mantle cell lymphoma through transcriptional regulation of BCL6. Leukemia. 2016;30(7):1596-1599.
17. Bea S, Amador V. Role of SOX11 and genetic events cooperating with cyclin D1 in mantle cell lymphoma. Curr Oncol Rep. 2017;19(6):43.
18. Ribera-Cortada I, Martinez D, Amador V, et al. Plasma cell and terminal B-cell differentiation in mantle cell lymphoma mainly occur in the SOX11-negative subtype. Mod Pathol. 2015;28(11):1435-1447.
19. Wasik AM, Lord M, Wang X, et al. SOXC transcription factors in mantle cell lymphoma: the role of promoter methylation in SOX11 expression. Sci Rep. 2013;3:1400.
20. Navarro A, Clot G, Royo C, et al. Molecular subsets of mantle cell lymphoma defined by the IGHV mutational status and SOX11 expression have distinct biologic and clinical features. Cancer Res. 2012;72(20):5307-5316.
21. Wegner M. All purpose Sox: The many roles of Sox proteins in gene expression. Int J Biochem Cell Biol. 2010;42(3):381-390.
22. Vegliante MC, Palomero J, Perez-Galan P, et al. SOX11 regulates PAX5 expression and blocks terminal B-cell differentiation in aggressive mantle cell lymphoma. Blood. 2013;121(12):2175-2185.
23. Palomero J, Vegliante MC, Rodriguez ML, et al. SOX11 promotes tumor angiogenesis through transcriptional regulation of PDGFA in mantle cell lymphoma. Blood. 2014;124(14):2235-2247.
24. Kuo PY, Jatiani SS, Rahman AH, et al. SOX11 augments BCR signaling to drive MCL-like tumor development. Blood. 2018;131(20):2247-2255.
25. Kuo PY, Leshchenko VV, Fazzari MJ, et al. High-resolution chromatin immunoprecipitation (ChIP) sequencing reveals novel binding targets and prognostic role for SOX11 in mantle cell lymphoma. Oncogene. 2015;34(10):1231-1240.
26. Aukema SM, Hoster E, Rosenwald A, et al. Expression of TP53 is associated with the outcome of MCL independent of MIPI and Ki-67 in trials of the European MCL Network. Blood. 2018;131(4):417-420.
27. Yang W, Wang Y, Yu Z, et al. SOX11 regulates the pro-apoptosis signal pathway and predicts a favorable prognosis of mantle cell lymphoma. Int J Hematol. 2017;106(2):212-220.
28. Wang X, Asplund AC, Porwit A, et al. The subcellular Sox11 distribution pattern iden-

tifies subsets of mantle cell lymphoma: correlation to overall survival. Br J Haematol. 2008;143(2):248-252.
29. Hernandez L, Fest T, Cazorla M, et al. p53 gene mutations and protein overexpression are associated with aggressive variants of mantle cell lymphomas. Blood. 1996;87(8):3351-3359.
30. Slotta-Huspenina J, Koch I, de Leval L, et al. The impact of cyclin D1 mRNA isoforms, morphology and p53 in mantle cell lymphoma: p53 alterations and blastoid morphology are strong predictors of a high proliferation index. Haematologica. 2012;97(9):1422-1430.
31. Royo C, Navarro A, Clot G, et al. Non-nodal type of mantle cell lymphoma is a specific biological and clinical subgroup of the disease. Leukemia. 2012;26(8):1895-1898.
32. Bea S, Valdes-Mas R, Navarro A, et al. Landscape of somatic mutations and clonal evolution in mantle cell lymphoma. Proc Natl Acad Sci U S A. 2013;110(45):18250-18255.
33. Wang F, Flanagan J, Su N, et al. RNAscope: a novel in situ RNA analysis platform for formalin-fixed, paraffin-embedded tissues. J Mol Diagn. 2012;14(1):22-29.
34. Yu X, Guo S, Song W, et al. Estrogen receptor alpha (ERalpha) status evaluation using RNAscope in situ hybridization: a reliable and complementary method for IHC in breast cancer tissues. Hum Pathol. 2017;61: 121-129.
35. Wang H, Wang MX, Su N, et al. RNAscope for in situ detection of transcriptionally active human papillomavirus in head and neck squamous cell carcinoma. J Vis Exp. 2014(85).
36. Roe CJ, Siddiqui MT, Lawson D, et al. RNA In Situ Hybridization for Epstein-Barr virus and cytomegalovirus: comparison with in situ hybridization and immunohistochemistry. Appl Immunohistochem Mol Morphol. 2019;27(2):155-159.
37. Quintanilla-Martinez L, Pittaluga S, Miething C, et al. NPM-ALK-dependent expression of the transcription factor CCAAT/enhancer binding protein beta in ALK-positive anaplastic large cell lymphoma. Blood. 2006;108(6):2029-2036.
38. Schmidt J, Gong S, Marafioti T, et al. Genome-wide analysis of pediatric-type follicular lymphoma reveals low genetic complexity and recurrent alterations of TNFRSF14 gene. Blood. 2016;128(8):1101-1111.
39. Anderson CM, Zhang B, Miller M, et al. Fully automated RNAscope in situ hybridization assays for formalin-fixed paraffin-embedded cells and tissues. J Cell Biochem. 2016;117(10):2201-2208.
40. Schmid E, Klotz M, Steiner-Hahn K, et al. Detection of MET mRNA in gastric cancer in situ. Comparison with immunohistochemistry and sandwich immunoassays. Biotech Histochem. 2017;92(6):425-435.
41. Bingham V, McIlreavey L, Greene C, et al.

RNAscope in situ hybridization confirms mRNA integrity in formalin-fixed, paraffin-embedded cancer tissue samples. Oncotarget. 2017;8(55):93392-93403.

42. Wong ML, Medrano JF. Real-time PCR for mRNA quantitation. BioTechniques. 2005;39(1):75-85.

43. Lord M, Wasik AM, Christensson B, et al. The utility of mRNA analysis in defining SOX11 expression levels in mantle cell lymphoma and reactive lymph nodes. Haematologica. 2015;100(9):e369-372.

44. Balsas P, Palomero J, Eguileor A, et al. SOX11 promotes tumor protective microenvironment interactions through CXCR4 and FAK regulation in mantle cell lymphoma. Blood. 2017;130(4):501-513.

45. Wang X, Bjorklund S, Wasik AM, et al. Gene expression profiling and chromatin immunoprecipitation identify DBN1, SET-MAR and HIG2 as direct targets of SOX11 in mantle cell lymphoma. PloS One. 2010;5(11):e14085.

46. Rudelius M, Rosenfeldt MT, Leich E, et al. Inhibition of focal adhesion kinase overcomes resistance of mantle cell lymphoma to ibrutinib in the bone marrow microenvironment. Haematologica. 2018;103(1):116-125.

47. Ferrando AA. SOX11 is a mantle cell lymphoma oncogene. Blood. 2013;121(12): 2169-2170.

48. Beekman R, Amador V, Campo E. SOX11, a key oncogenic factor in mantle cell lymphoma. Curr Opin Hematol. 2018;25(4): 299-306.

49. Greiner TC, Moynihan MJ, Chan WC, et al. p53 mutations in mantle cell lymphoma are associated with variant cytology and predict a poor prognosis. Blood. 1996;87(10):4302-4310.

50. Clot G, Jares P, Giné E, et al. A gene signature that distinguishes conventional and leukemic nonnodal mantle cell lymphoma helps predict outcome. Blood. 2018;132(4): 413-422.

Clinical characteristics and outcomes of Richter transformation: experience of 204 patients from a single center

Yucai Wang,[1] Marcella A. Tschautscher,[1] Kari G. Rabe,[2] Timothy G. Call,[1] Jose F. Leis,[3] Saad S. Kenderian,[1] Neil E. Kay,[1] Eli Muchtar,[1] Daniel L. Van Dyke,[4] Amber B. Koehler,[1] Susan M. Schwager,[1] Susan L. Slager,[2] Sameer A. Parikh[1] and Wei Ding[1]

[1]Division of Hematology, Mayo Clinic, Rochester, MN; [2]Division of Biomedical Statistics and Informatics, Mayo Clinic, Rochester, MN; [3]Division of Hematology and Medical Oncology, Mayo Clinic, Phoenix, AZ and [4]Division of Laboratory Genetics and Genomics, Mayo Clinic, Rochester, MN, USA

Ferrata Storti Foundation

ABSTRACT

The natural history, prognostication and optimal treatment of Richter transformation developed from chronic lymphocytic leukemia (CLL) are not well defined. We report the clinical characteristics and outcomes of a large series of biopsy-confirmed Richter transformation (diffuse large B-cell lymphoma or high grade B-cell lymphoma, n=204) cases diagnosed from 1993 to 2018. After a median follow up of 67.0 months, the median overall survival (OS) was 12.0 months. Patients who received no prior treatment for CLL had significantly better OS (median 46.3 vs. 7.8 months; P<0.001). Patients with elevated lactate dehydrogenase (median 6.2 vs. 39.9 months; P<0.0001) or TP53 disruption (median 8.3 vs. 12.8 months; P=0.046) had worse OS than those without. Immunoglobulin heavy chain variable region gene mutation, cell of origin, Myc/Bcl-2 double expression and MYC/BCL2/BCL6 double-/triple-hit status were not associated with OS. In multivariable Cox regression, elevated lactate dehydrogenase [Hazard ratio (HR) 2.3, 95% Confidence Interval (CI): 1.3-4.1; P=0.01], prior CLL treatment (HR 2.0, 95%CI: 1.2-3.5; P=0.01), and older age (HR 1.03, 95%CI: 1.01-1.05; P=0.01) were associated with worse OS. Twenty-four (12%) patients underwent stem cell transplant (20 autologous and 4 allogeneic), and had a median post-transplant survival of 55.4 months. In conclusion, the overall outcome of Richter transformation is poor. Richter transformation developed in patients with untreated CLL has significantly better survival. Stem cell transplant may benefit select patients.

Introduction

Richter transformation (RT) refers to the transformation of chronic lymphocytic leukemia (CLL) to an aggressive lymphoma. It was first described by Dr. Maurice Richter in 1928 with a rapidly fatal case of "reticular cell sarcoma of lymph nodes" arising in the background of "lymphatic leukemia".[1] RT presents with diffuse large B-cell lymphoma (DLBCL) in over 90% of the cases, and classical Hodgkin lymphoma in 5% or less. The incidence of DLBCL type of RT is approximately 0.5-1% per year in newly diagnosed CLL patients,[2] and the overall prevalence of RT is about 2-10% in CLL patients according to multiple published studies.[3-5] The reported risk factors associated with RT include: advanced stage, large lymph nodes (> 3 cm), unmutated immunoglobulin heavy chain variable region gene (IGHV), del(17p), TP53 mutation, NOTCH1 mutation, and stereotyped B-cell receptor (BCR).[2,6-11]

Clinically, RT often presents aggressively with rapidly enlarging lymphadenopathy, prominent constitutional symptoms (fevers, night sweats, and unintentional weight loss), elevated LDH, and frequent extranodal tissue involvement.[3] Treatment of RT has been challenging. The standard R-CHOP regimen used for treatment of *de novo* DLBCL has limited efficacy in DLBCL-type RT.[12] Higher intensity chemotherapy does not improve outcomes.[13-18] Stem cell transplant (SCT) has been studied in RT and

appears to be associated with relative long-term survival in select cases.[19-23] Overall, RT has a poor prognosis, with a median survival of only 1-2 years.[3,5]

The landscape of CLL management has changed dramatically with the emergence of several novel targeted agents, such as Bruton's tyrosine kinase (BTK) inhibitors ibrutinib and acalabrutinib, phosphoinositide 3-kinase δ (PI3Kδ) inhibitors idelalisib and duvelisib, and the B-cell lymphoma 2 (BCL-2) inhibitor venetoclax. It is unclear whether these novel agents affect the risk, prognosis and management of RT. In *de novo* DLBCL, the prognostic roles of cell of origin (COO), Myc and Bcl-2 double expression, and *MYC*, *BCL2* and/or *BCL6* gene rearrangements have been well recognized.[24-29] However, the potential impact of these molecular markers on the outcome of DLBCL-type RT has not been well studied.

In this study, we report the clinical characteristics, treatment pattern, and outcomes of a large series of RT patients (n=204) from a single center over more than two decades including the era of novel agents (from 2012 to the present). The potential prognostic impact of prior CLL treatment as well as CLL- and RT-related molecular markers were also explored.

Methods

Patients

This study was approved by the Mayo Clinic Institutional Review Board. All patients were identified from the Mayo Clinic CLL database which includes consecutive CLL patients evaluated in the Division of Hematology at Mayo Clinic, Rochester, MN, USA.[2,30,31] CLL patients who developed biopsy-proven RT between April 1993 and April 2018 were identified from the database. For this study, the focus was RT to DLBCL (including high grade B-cell lymphoma, such as double-/triple-hit lymphoma which is now known as high-grade B-cell lymphoma with *MYC* and *BCL2* and/or *BCL6* rearrangements); transformations to Hodgkin lymphoma or other histology were excluded. Clinical, pathological, and molecular characteristics [*IGHV* mutation, CLL fluorescence *in situ* hybridization (FISH)] and all treatment information during the CLL phase were abstracted from the database. Clinical, pathological and molecular characteristics [CLL FISH, *TP53* somatic mutation, COO by Hans algorithm, Myc/Bcl-2 expression by immunohistochemistry (IHC), *MYC/BCL2/BCL6* rearrangement by FISH, CLL and RT clonal relationship by immunoglobulin gene rearrangement], treatment course, clinical response to treatment as determined by treating physician, and survival information after RT was abstracted by chart review. On IHC, the cut-off value for positivity was 40% for Myc, and 50% for Bcl-2. Our institution started to routinely test for Myc expression by IHC and *MYC* rearrangement by FISH in all DLBCL cases in 2012; therefore, we have missing information on IHC as well as FISH results in patients diagnosed with RT prior to this.

Statistical analysis

The date of RT diagnosis was defined as the date of the biopsy which led to the pathological diagnosis of RT. The time to transformation was defined as the time from CLL diagnosis to RT diagnosis. Overall survival (OS) was defined as the time from RT diagnosis to death from any cause. Time-to-event data were analyzed using the Kaplan-Meier method. Cox proportional hazards models were used to analyze associations between OS and various factors. *P*<0.05 was considered statistically signifi-

Table 1. Clinical characteristics at Richter transformation diagnosis in 204 patients.

	Number (n=204)	%
Year of RT diagnosis		
Prior to 2002	33	16.2
2002-2011	70	34.3
2012-2018	101	49.5
Age (years)		
Median (range)	69 (30-88)	
≤65	69	33.8
>65	135	66.2
Time to transformation (years)		
Median (range)	4.7 (0.0-34.5)	
Prior CLL treatment		
Untreated	69	33.8
Treated with CIT only	108	52.9
Treated with at least one novel agent	27	13.2
Lines of prior CLL therapies		
Median (range)	2 (0-13)	
Bulky disease (≥5 cm)		
No	63	50.4
Yes	62	49.6
Missing	79	
PET SUVmax (n=69)		
Median (range)	13.9 (2.9-30.0)	
LDH (IU/L) (n=175)		
Median (range)	306 (99-9000)	
Ki-67 (n=55)		
Median	80% (10-100%)	
Pathology at transformation		
DLBCL	193	94.6
High grade B-cell lymphoma	11	5.4
Cell of origin		
GCB	31	31.0
Non-GCB	69	69.0
Missing	104	
Myc IHC		
Negative	12	27.9
Positive (≥40%)	31	72.1
Missing	161	
Bcl-2 IHC		
Negative	20	19.4
Positive (≥50%)	83	80.6
Missing	101	
Double expressor		
Negative	29	51.8
Positive	27	48.2
Missing	148	
MYC **FISH**		
Negative	50	73.5
Positive	18	26.5
Missing	136	

continued on the next page

continued from the previous page

BCL2 FISH		
Negative	24	70.6
Positive	10	29.4
Missing	170	
BCL6 FISH		
Negative	27	87.1
Positive	4	12.9
Missing	173	
Double-/triple-hit		
No	58	87.9
Yes	8	12.1
Missing	138	
EBV		
Negative	38	73.1
Positive	14	26.9
Missing	152	
Del(17p) or *TP53* mutation		
Negative	86	65.6
Positive	45	34.4
Missing	73	
CLL and RT clonal relationship		
Unrelated	9	42.9
Related	12	57.1
Missing	180	

RT: Richter transformation; CLL: chronic lymphocytic leukemia; PET: positron emission tomography; SUV: standardized uptake value; LDH: lactate dehydrogenase; DLBCL: diffuse large B-cell lymphoma; GCB: germinal center B-cell-like; IHC: immunohistochemistry; FISH: fluorescence *in situ* hybridization; EBV: Epstein-Barr virus.

cant. All statistical analyses were carried out in SAS 9.4 (SAS Institute, Cary, NC, USA).

Results

Clinical characteristics in the chronic lymphocytic leukemia phase

A total of 204 patients with CLL who developed RT were identified. Baseline characteristics at CLL diagnosis are shown in *Online Supplementary Table S1*. The median age at CLL diagnosis was 62 years (range 22-85), and 148 (72.5%) were male. Seventy-one (71.0%) of 100 patients tested had unmutated *IGHV*. CLL FISH detected del(17p) in 33 (25.4%), del(11q) in 18 (13.8%), and trisomy 12 in 19 (14.6%) of 130 patients. Forty-seven (66.2%) of 71 patients were high or very high risk by CLL-IPI score (≥4).

Clinical characteristics at Richter transofrmation diagnosis

Median time to transformation was 4.7 years (range 0-34.5) (Table 1). Prior to RT, 69 (33.8%) patients received no treatment for CLL, 108 (52.9%) received chemoimmunotherapy (CIT) only, and 27 (13.2%) received at least one novel agent (idelalisib, ibrutinib, or venetoclax) for CLL; 19 patients received CIT previously and developed RT on novel agents (17 ibrutinib, 1 idelalisib, 1 venetoclax), 6 patients received novel agents previously and developed RT on subsequent treatment (1 rituximab-bendamustine, 3 rituximab-corticosteroid, and 2 rituximab

alone), and 2 other patients developed RT on frontline ibrutinib. Median lines of CLL therapy prior to RT was 2 (range 0-13).

Thirty-three patients were diagnosed with RT prior to 2002 (when rituximab was not routinely available), 70 patients were diagnosed between 2002 and 2011, and 101 patients were diagnosed in 2012 or later (when ibrutinib had become available). The median age at RT diagnosis was 69 years (range 30-88). Sixty-two (49.6%) of 125 patients had bulky disease (≥ 5 cm). COO by Hans algorithm was germinal center B-cell-like (GCB) and non-GCB in 31 of 100 (31.0%) and 69 of 100 (69.0%) patients, respectively. Myc and Bcl-2 were positive by IHC in 31 of 43 (72.1%) and 83 of 103 (80.6%) cases, respectively; 27 of 56 (48.2%) were double-expressors. *MYC, BCL2,* and *BCL6* rearrangement was positive by FISH in 18 of 68 (26.5%), 10 of 34 (29.4%), and 4 of 31 (12.9%) cases, respectively; 8 of 66 (12.1%) were double-/triple-hit. Forty-five (34.4%) of 131 patients had del(17p) or *TP53* mutation, i.e. *TP53* disruption. CLL and RT were clonally unrelated in 9 (42.9%) of 21 patients.

Richter transformation treatment and outcome

Pattern of first-line treatment for RT is shown in Table 2. The most commonly used first-line treatment was an R-CHOP-like regimen (n=114, 65.5%). Twelve (6.9%) patients received platinum or high-dose cytarabine containing chemotherapy; 21 (12.1%) patients received other chemotherapy (6 with DA-EPOCH-R-like regimen, 15 with others including ProMACE-CytaBOM, R-CEPP, infusional CDE, R-CVP, R-bendamustine, R-gemcitabine/prednisone, high dose methotrexate-based regimen). Nineteen (10.9%) patients received novel agents: ibrutinib (n=4), venetoclax (n=1), ibrutinib plus venetoclax (n=3), pembrolizumab (n=7), pembrolizumab plus ibrutinib (n=1), CD19 monoclonal antibody (n=1), everolimus (n=1), everolimus plus panobinostat (n=1). Eight (4.6%) patients received palliative therapy defined as rituximab, corticosteroids, radiation therapy, alone or in combination.

Clinical response (assessed by treating physician) to first-line treatment was complete response (CR) in 54 (36.0%), partial response (PR) in 37 (24.0%), stable disease (SD) in 18 (12.0%), and progressive disease (PD) in 42 (28.0%) of 150 patients. The median follow up after RT was 67.0 months, and there were a total of 150 deaths. The median OS after RT diagnosis was 12.0 months (Figure 1A).

Survival by clinical and molecular factors and treatment is summarized in Table 3. The median OS was significantly better in patients who received no CLL treatment than those who received any CLL treatment, with a median OS of 46.3 *versus* 7.8 months (*P*<0.001) (Figure 1B). Among the 69 patients who received no CLL treatment, 31 had concurrent CLL and RT (i.e. RT diagnosis within 3 months of CLL diagnosis), with a median OS of 66.9 months; in the other 38 patients with sequential CLL and RT (median time to transformation 55.5 months), the median OS was 29.4 months (*P*=0.25) (Figure 1C). Among the 135 patients who had received treatment for CLL, patients with only one line of CLL treatment (n=31) had a trend of better OS compared to those with two or more lines of CLL treatment (n=104), with a median OS of 15.3 *versus* 5.8 months (*P*=0.09) (Figure 1D). Patients who received CIT only and those who received at least one novel agent for CLL had a
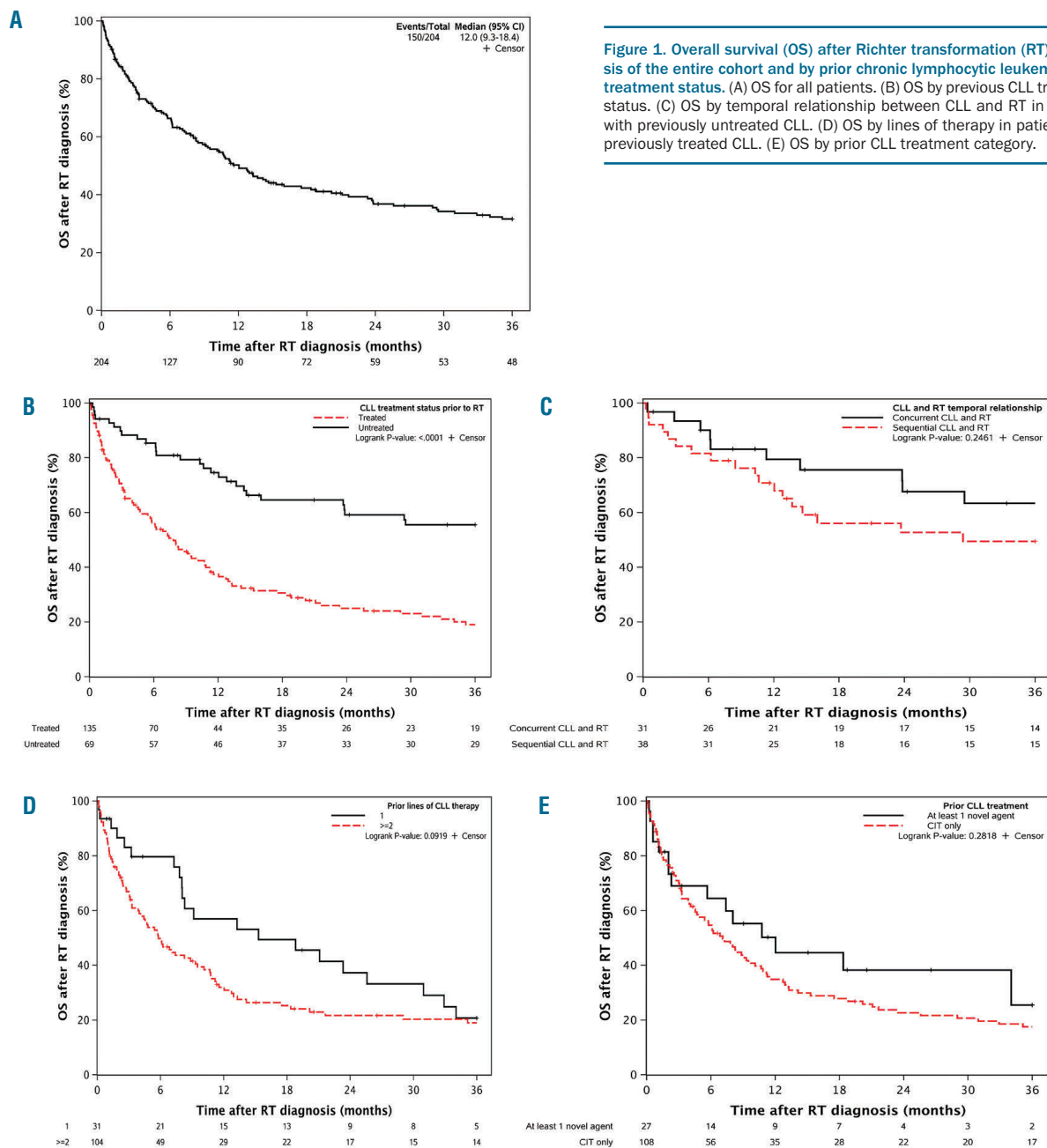
Figure 1. Overall survival (OS) after Richter transformation (RT) diagnosis of the entire cohort and by prior chronic lymphocytic leukemia (CLL) treatment status. (A) OS for all patients. (B) OS by previous CLL treatment status. (C) OS by temporal relationship between CLL and RT in patients with previously untreated CLL. (D) OS by lines of therapy in patients with previously treated CLL. (E) OS by prior CLL treatment category.

median OS of 7.1 and 12.0 months, respectively (*P*=0.28) (Figure 1E).

There was no significant difference in median OS between younger (age≤65) and older (age>65) RT patients, with a median OS of 13.3 *versus* 11.3 months (*P*=0.07) (Figure 2A). Patients with elevated LDH had worse OS compared to those with normal LDH, with a median OS of 6.2 *versus* 39.9 months (*P*<0.0001) (Figure 2B). Bulky disease (nodal size ≥5 cm) was not associated with a worse OS (median OS of 8.0 *vs.* 14.6 months; *P*=0.13) (*Online Supplementary Figure S1*). Patients with *TP53* disruption had a worse OS than those without (median OS 8.3 *vs.* 12.8 months; *P*=0.046) (Figure 2C). Other molecular characteristics, including *IGHV* mutation (*Online Supplementary Figure S2*), DLBCL COO (*Online Supplementary Figure S3*), Myc/Bcl-2 double expression

(Figure 2D), *MYC/BCL2/BCL6* double-/triple-hit status (*Online Supplementary Figure S4*), and CLL and RT clonal relationship (*Online Supplementary Figure S5*) did not impact RT survival.

In a multivariable Cox regression model, we examined the association of age (continuous), LDH (normal *vs.* elevated), prior CLL treatment (untreated *vs.* treated) and *TP53* disruption with RT survival; we found that elevated LDH (HR 2.3, 95%CI: 1.3-4.1; *P*=0.01), prior CLL treatment (HR 2.0, 95%CI: 1.2-3.5; *P*=0.01), and to a lesser extent older age (HR 1.03, 95%CI: 1.01-1.05; *P*=0.01), but not *TP53* disruption (HR 1.3, 95%CI:0.8-2.1; *P*=0.31), were associated with worse OS.

Patients treated with an R-CHOP-like regimen (n=114) had a median OS of 15.3 months (*Online Supplementary Figure S6*). Patients treated with platinum or high-dose
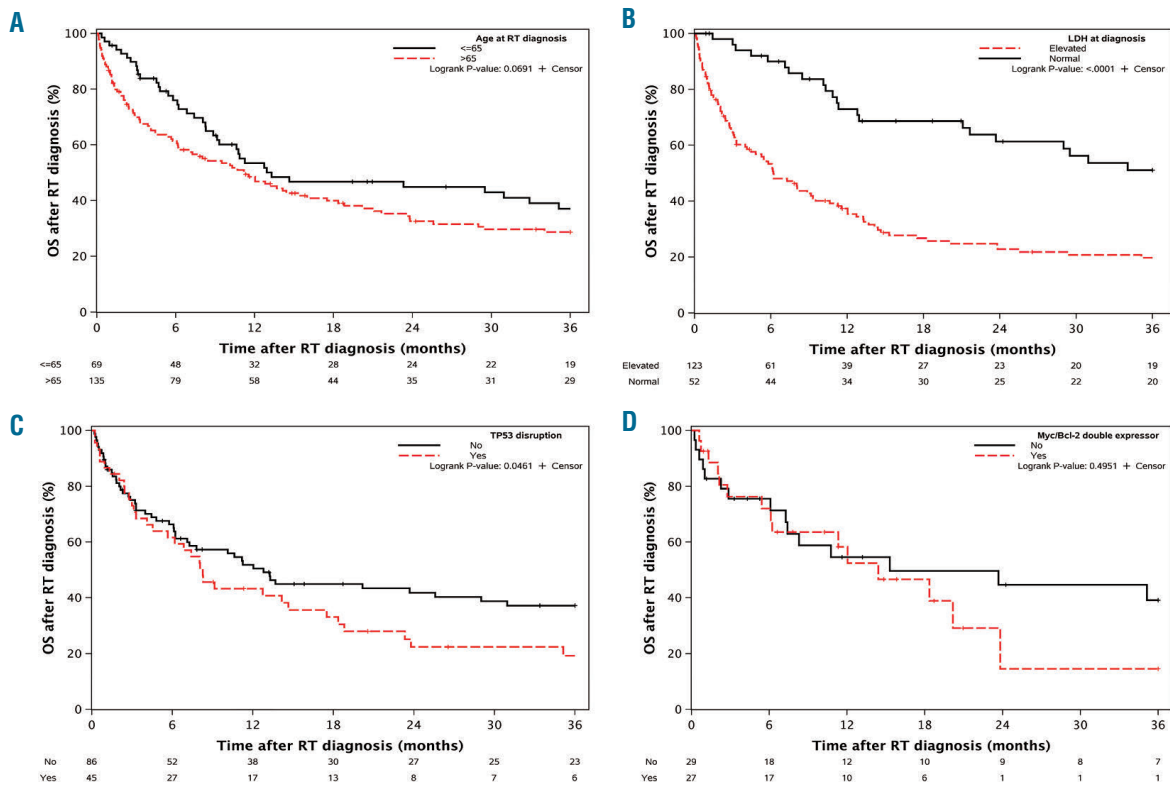
Figure 2. Overall survival (OS) after Richter transformation (RT) diagnosis by clinical and molecular factors. (A) OS by age at RT diagnosis. (B) OS by lactate dehydrogenase (LDH) at RT diagnosis. (C) OS by *TP53* disruption status. (D) OS by Myc and Bcl-2 double expression status.

Table 2. First-line treatment approaches for Richter transformation (RT) in patients with chronic lymphocytic leukemia (CLL).

	All patients (%)	None (%)	Prior CLL treatment Chemoimmunotherapy only (%)	At least one novel agent (%)
R-CHOP-like regimen[1]	114 (65.5%)	49 (81.7%)	60 (66.7%)	5 (20.8%)
Platinum or high dose cytarabine containing chemotherapy[2]	12 (6.9%)	1 (1.7%)	10 (11.1%)	1 (4.2%)
Other chemotherapy[3]	21 (12.1%)	9 (15.0%)	10 (11.1%)	2 (8.3%)
Novel agents[4]	19 (10.9%)	0 (0.0%)	4 (4.4%)	15 (62.5%)
Palliative therapy[5]	8 (4.6%)	1 (1.7%)	6 (6.7%)	1 (4.2%)
Missing	30	9	18	3
Total	204	69	108	27

[1]Predominantly R-CHOP, small numbers of CHOP, MR-CHOP, lenalidomide-R-CHOP. [2]R-ICE, (R-)DHAP, (R-)ESHAP, GDP, R-Hyper-CVAD, CODOX-M-IVAC, OFAR. [3](R-)EPOCH, ProMACE-CytaBOM, (R-)CEPP, infusional CDE, R-CVP, R-bendamustine, R-gemcitabine/prednisone, high-dose MTX-based. [4]Ibrutinib, venetoclax, pembrolizumab, everolimus, CD19 antibody. [5]Rituxiamab, obinutuzumab, corticosteroids, radiation therapy, alone or in combination.

cytarabine containing chemotherapy (n=12) had a median OS of 14.6 months (*P*=0.82 *vs.* R-CHOP-like). Patients treated with other chemotherapy (n=21) had a median OS of 12.8 months (*P*=0.66 *vs.* R-CHOP-like). The 19 patients who received novel agents as first-line RT treatment had a median OS of 10.9 months (*P*=0.12 *vs.* R-CHOP-like). The median OS for patients receiving palliative therapy (n=8) was 6.1 months (*P*=0.01 *vs.* R-CHOP-like).

After achieving PR or better, 24 (11.8%) patients underwent SCT: 20 autologous and 4 allogenic. Details of the clinical characteristics of the 24 patients who underwent SCT are shown in *Online Supplementary Table S2*. The median age at RT diagnosis was 62 years (range 41-73). Ten patients did not receive any prior CLL treatment. Nineteen patients achieved a PR or better with 1-2 lines of

treatment before proceeding to SCT. The median time from RT diagnosis to SCT was 6.8 months (range 3.3-42.3). None of the four allogeneic SCT patients died although the post-SCT follow up was still relatively short for three of them (Figure 3A). Thirteen of the 20 autologous SCT patients had a post-SCT survival greater than two years (Figure 3A). Overall, the 24 SCT patients had a median post-SCT survival of 55.4 months (Figure 3B).

Discussion

To the best of our knowledge, this is the largest series of CLL patients with biopsy-proven DLBCL-type RT with a long follow up. Our results showed that patients with
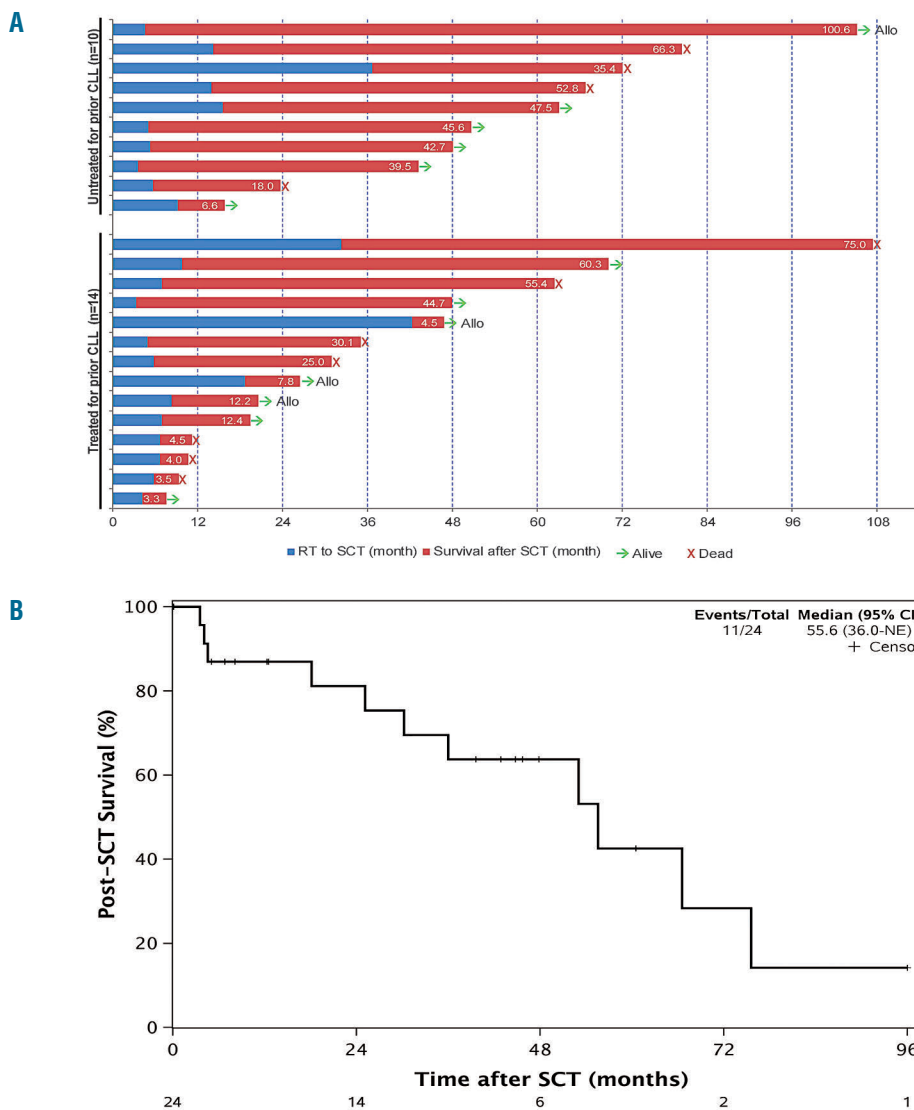
Figure 3. Survival outcomes of the 24 Richter transformation (RT) patients who underwent stem cell transplantation (SCT). (A) Swimmers plot showing time from RT diagnosis to SCT (blue) and post-SCT survival (red; numbers indicate post-SCT survival in months). (B) Post-SCT survival for all patients who underwent SCT. CI: Confidence Interval.

DLBCL-type RT overall had a poor prognosis with a median OS of only 12 months. Patients with RT who received no prior CLL treatment had a significantly better OS, with a median OS of approximately four years.

Our singular finding is that patients who received no prior CLL therapy had a favorable outcome. Further proof of this finding was provided in a prior phase II trial of ofatumumab in combination with CHOP for newly diagnosed RT, where patients who received no prior CLL treatment had significantly better OS (median unreached at 24 months *vs.* approx. 6 months).[32] A recent Danish National CLL Registry study of RT (over 8 years with multiple histologies) also showed similar results, with a median OS of 6.16 year in patients with untreated CLL *versus* 1.49 years in patients with treated CLL.[11] The observed OS differences in these studies may be due to different biology in untreated patients. Further to this finding, RT patients who received only one line of CLL therapy had a trend of better OS compared to those who received two

or more lines of prior CLL therapies in our study, and two other studies also demonstrated that fewer lines of prior CLL therapy was associated with better RT survival,[18,19] supporting the hypothesis that less therapy of CLL may be associated with less chemoresistance of RT. Of note, patients who were diagnosed with CLL and RT within three months (defined as concurrent RT) had a particularly favorable outcome, with a median OS of approximately six years. We suspect that the concurrent RT cases were more likely clonally unrelated (to the CLL) and resemble *de novo* DLBCL. This aspect warrants future studies. Based on our data, patients with concurrent RT may benefit from the typical therapy for *de novo* DLBCL.

TP53 disruption (i.e. del(17p) and/or *TP53* mutation) was associated with a worse prognosis of RT in the univariate analysis, consistent with a number of prior studies.[8,12,18,32-34] Of note, *TP53* disruption was not an independent prognostic factor of OS in the multivariable analysis in our study. Rossi *et al.* showed that *TP53* disrup-

tion was an independent prognostic factor of RT survival.[8] Four other studies did not test for *TP53* somatic mutation and reported inconsistent results regarding the independent prognostic role of del(17p).[8,12,33,34] Given only 27 (13%) of our patients underwent the *TP53* somatic mutation test, we likely underestimated the proportion of RT patients who had *TP53* disruption, and thus might have underestimated the negative impact of this molecular abnormality on RT outcomes in our cohort.

The prognostic roles of COO, double expressor and double-hit status in *de novo* DLBCL have been well established.[24-29] In this study, we found that these molecular markers were not prognostic for RT survival. Indeed, Eyre *et al.* showed that COO and Myc expression status did not influence RT survival in the O-CHOP trial,[32] and Fidai *et al.* showed that *MYC* and/or *BCL2* genetic alterations did not impact RT outcome in a retrospective study.[33] RT and *de novo* DLBCL are likely different diseases given the known distinct genomic abnormalities,[5,35] and the impacts of COO and double expressor/double-hit status may therefore be different. We should note that molecular characterizations of COO and double expressor/double-hit status were incomplete in our dataset, and interpretation of these results should be made with caution.

In terms of other relevant prognostic factors, older age and elevated LDH were associated with worse OS in RT, consistent with the MD Anderson data.[19] Clonal relationship between CLL and RT was reported to be a critical prognostic factor, with a much better outcome in clonally unrelated RT.[8,36] Due to the difficulty of obtaining paired CLL and RT samples (at RT diagnosis) and a lack of universal assessment in our routine clinical practice, we only have a limited number of cases (<5%) in which the CLL and RT clonal relationship was reported. This difficulty is consistent with clinical experiences shared among several different academic centers. While we did not see a statistically significant association of clonal relationship with RT survival, this should not be taken as evidence that goes against prior studies. CLL *IGHV* mutation status was not associated with RT survival in our study. Prior studies were inconsistent regarding the prognostic role of CLL *IGHV* mutation in RT survival, with positive association reported in two studies (one in univariate analysis only, the other with only 16 RT patients)[11,34] but not others.[8,18] It remains unclear whether CLL *IGHV* mutation status is associated with RT outcome.

In our cohort, RT patients who were exposed to at least one novel agent (predominantly ibrutinib) for CLL treatment had a median OS of 10.9 months, similar to those whose CLL were treated with CIT only, and compares favorably to prior data.[37-39] A number of studies have shown that RT that developed on novel agents had poor outcome, with a median OS of approximately 2-3.5 months if developed on ibrutinib[37-39] and approximately 12 months if developed on venetoclax.[40] In these studies, RT was primarily treated with R-CHOP- or R-EPOCH-like regimens. For our RT patients previously exposed to novel agents for CLL, approximately two-thirds were treated with novel agents (e.g. pembrolizumab, ibrutinib and venetoclax, etc.) and only one-third were treated with R-CHOP-like or other chemotherapy at first line. The efficacy of novel agents in treating RT has been reported by a number of studies.[41-46] For example, pembrolizumab demonstrated encouraging efficacy in patients with RT, particularly those with prior exposure of ibrutinib.[43]

Nivolumab in combination with ibrutinib and pembrolizumab in combination with umbralisib and ublituximab also demonstrated encouraging activity in treating RT.[45-47] In addition to the above studies, BTK inhibitors (NCT03899337), PI3K inhibitors (NCT03884998) and/or venetoclax (NCT03054896) based combination regimens (with or without chemotherapy) and other agents such as

Table 3. Median overall survival (OS) after Richter transformation (RT) diagnosis by clinical characteristics at RT diagnosis or first-line treatment approach for RT.

	N	Median (95% CI)	P
Prior CLL treatment			<0.0001
Untreated	69	46.3 (23.8-77.5)	
Treated	135	7.8 (5.8-10.9)	
Temporal relationship between RT and untreated CLL			0.25
Concurrent CLL and RT	31	66.9 (29.5-NE)	
Sequential CLL and RT	38	29.4 (13.7-111.6)	
Lines of prior CLL treatment			0.09
1	31	15.3 (8.1-32.9)	
2 or more	104	5.8 (4.1-10.1)	
Age at RT diagnosis (years)			0.07
≤65	69	13.3 (9.3-39.9)	
>65	135	11.3 (7.1-17.5)	
LDH			<0.001
Normal	52	39.9 (23.7-72.2)	
Elevated	123	6.2 (4.4-10.6)	
Bulky disease (≥ 5 cm)			0.13
No	63	14.6 (11.3-35.1)	
Yes	62	8.0 (4.7-14.4)	
Del(17p)/*TP53* mutation			0.046
No	86	12.8 (7.3-65.5)	
Yes	45	8.3 (5.7-18.4)	
***IGHV* mutation**			0.89
Mutated	29	12.8 (8.3-46.3)	
Unmutated	71	10.6 (6.2-18.4)	
Cell of origin			0.74
GCB	31	34.0 (14.4-NE)	
Non-GCB	69	12.0 (8.0-65.5)	
Myc/Bcl-2 double expressor			0.50
No	29	15.3 (7.4-122.8)	
Yes	27	14.4 (6.2-NE)	
***MYC/BCL2/BCL6* double-/triple-hit**			0.61
No	58	13.3 (9.3-35.1)	
Yes	8	14.4 (2.0-23.8)	
First line treatment for RT			0.08
R-CHOP-like regimen[1]	114	15.3 (10.6-29.5)	
Platinum or high dose cytarabine containing chemotherapy[2]	12	14.6 (11.5-NE)	
Other chemotherapy[3]	21	12.8 (3.2-NE)	
Novel agents[4]	19	10.9 (7.4-34.0)	
Palliative therapy[5]	8	6.1 (0.4-39.9)	

[1]Premoniditly R-CHOP, small numbers of CHOP, MR-CHOP, lenalidomide-R-CHOP. [2]R-ICE, (R-)DHAP, (R-)ESHAP, GDP, R-Hyper-CVAD, CODOX-M-IVAC, OFAR. [3](R-)EPOCH-like, ProMACE-CytaBOM, infusional CDE, (R-)CEPP, R-CVP, R-bendamustine, R-gemcitabine/prednisone, high-dose MTX-based. [4]Ibrutinib, venetoclax, pembrolizumab, everolimus, CD19 antibody. [5]Rituxiamab, obinutuzumab, corticosteroids, radiation therapy, alone or in combination. CLL: chronic lymphocytic leukemia; LDH: lactate dehydrogenase; IGHV: immunoglobulin heavy chain variable region; GCB: germinal center B-cell-like.

immunomodulatory drug lenalidomide (NCT03113695, NCT02005289), engineered anti-CD19 monoclonal antibody MOR208 (NCT02005289), and CD3/CD19 bispecific antibody blinatumumab (NCT03121534, NCT03931642) are actively being tested in clinical trials for RT. Chimeric antigen receptor (CAR) T cells are also showing promise in improving the outcome of RT[48] and are further tested in clinical trials (NCT03484702). Taken together, novel agents (e.g. pembrolizumab/nivolumab, ibrutinib and venetoclax) would seem to be very reasonable choices in patients who develop RT while receiving one of the targeted agents (e.g. ibrutinib, venetoclax, idelalisib) for CLL. However, it is important to note that despite promising results from multiple studies,[41-48] further improvements to increase the efficacy and select optimal patients for different novel agents are clearly needed.

Patients who underwent SCT (n=24, 11.8%) in our cohort overall had a favorable outcome, with a median post-SCT survival of 55.4 months. The role of SCT in RT management has been explored previously.[19-22] In the MD Anderson cohort, 20 (13.5%) of 148 RT patients were able to proceed to SCT (3 autologous, 17 allogeneic), and seven patients who underwent allogeneic SCT for consolidation had a favorable outcome with a 3-year OS of 75%.[19] A retrospective study by the European Group for Blood and Marrow Transplantation (EBMT) showed that post-remission SCT may benefit a subset of RT patients, with a 3-year OS of 59% for autologous SCT and 36% for allogeneic SCT.[20] Two recent single institution studies also reported somewhat favorable outcome of allogenic SCT in RT patients, with a 2-year OS of 44% in one study and a 4-year OS of 50% in the other.[21,22] Collectively, these data suggest that select RT patients can benefit from SCT. One should be aware of the potential selection bias when interpreting the data, e.g. patients need to be relatively young and in good condition to proceed to SCT. For example, 10 of the 24 patients in our SCT cohort received no prior CLL treatment; patients were relatively younger, and most patients achieved a favorable response with 1-2 lines of RT therapy and then went on to SCT. We used substantially more autologous (n=20) than allogeneic (n=4) SCT. While allogeneic SCT target both the CLL and RT clones, an autologous SCT primarily eradicates the RT clone and spares the undesired high non-relapse mortality associated with allogeneic SCT.

Our study shows that RT has poor clinical outcomes in general. However, as a heterogeneous disease, its outcome is influenced significantly by prior CLL therapy status. One reason for the poor survival observed in RT after prior CLL therapy may be the known potential of CLL clones to undergo clonal evolution under the pressure of therapy.[49,50] We propose a newer approach to manage RT based on their prior CLL therapy status. In treatment-naïve patients and patients with clonally unrelated DLBCL, immunochemotherapy, in particular R-CHOP-like regimens, is the preferred approach in treating these RT. In patients exposed to targeted CLL therapies (including kinase inhibitors and BCL-2 inhibitor) or prior chemoimmunotherapies, the management of RT would likely need to incorporate novel agents, immunotherapy, and/or cellular therapy in clinical trials. SCT consolidation should still be considered in RT patients who achieve a good response to therapy. We fully expect that RT biology will continue to evolve with the changing landscape of CLL as management with novel agents are robustly moving to the front line. In support of this, recent data indicated that 70-80% of RT that developed on novel agents had *TP53* disruption and/or complex karyotypes, both of which were prognostic of poor outcomes in RT.[39] It is hoped that our study can provide more valuable information on current management of RT and also point to areas of interest for future clinical trials and biological studies.

References

1. Richter MN. Generalized Reticular Cell Sarcoma of Lymph Nodes Associated with Lymphatic Leukemia. Am J Pathol. 1928; 4(4):285-292.
2. Parikh SA, Rabe KG, Call TG, et al. Diffuse large B-cell lymphoma (Richter syndrome) in patients with chronic lymphocytic leukaemia (CLL): a cohort study of newly diagnosed patients. Br J Haematol. 2013; 162(6):774-782.
3. Parikh SA, Kay NE, Shanafelt TD. How we treat Richter syndrome. Blood. 2014; 123(11):1647-1657.
4. Rossi D, Gaidano G. Richter syndrome: pathogenesis and management. Semin Oncol. 2016;43(2):311-319.
5. Rossi D, Spina V, Gaidano G. Biology and treatment of Richter syndrome. Blood. 2018;131(25):2761-2772.
6. Rossi D, Cerri M, Capello D, et al. Biological and clinical risk factors of chronic lymphocytic leukaemia transformation to Richter syndrome. Br J Haematol. 2008; 142(2):202-215.
7. Rossi D, Spina V, Cerri M, et al. Stereotyped B-cell receptor is an independent risk factor of chronic lymphocytic leukemia transformation to Richter syndrome. Clin Cancer Res. 2009;15(13):4415-4422.
8. Rossi D, Spina V, Deambrogi C, et al. The genetics of Richter syndrome reveals disease heterogeneity and predicts survival after transformation. Blood. 2011;117(12): 3391-3401.
9. Rossi D, Rasi S, Spina V, et al. Different impact of NOTCH1 and SF3B1 mutations on the risk of chronic lymphocytic leukemia transformation to Richter syndrome. Br J Haematol. 2012;158(3):426-429.
10. Rossi D, Rasi S, Fabbri G, et al. Mutations of NOTCH1 are an independent predictor of survival in chronic lymphocytic leukemia. Blood. 2012;119(2):521-529.
11. Ben-Dali Y, Hleuhel MH, Andersen MA, et al. Risk Factors Associated with Richter's Transformation in Patients with Chronic Lymphocytic Leukemia. Blood. 2018; 132(Suppl 1):1697.
12. Langerbeins P, Busch R, Anheier N, et al. Poor efficacy and tolerability of R-CHOP in relapsed/refractory chronic lymphocytic leukemia and Richter transformation. Am J Hematol. 2014;89(12):E239-243.
13. Dabaja BS, O'Brien SM, Kantarjian HM, et al. Fractionated cyclophosphamide, vincristine, liposomal daunorubicin (daunoXome), and dexamethasone (hyperCVXD) regimen in Richter's syndrome. Leuk Lymphoma. 2001;42(3):329-337.
14. Tsimberidou AM, Kantarjian HM, Cortes J, et al. Fractionated cyclophosphamide, vincristine, liposomal daunorubicin, and dexamethasone plus rituximab and granulocyte-macrophage-colony stimulating factor (GM-CSF) alternating with methotrexate and cytarabine plus rituximab and GM-CSF in patients with Richter syndrome or fludarabine-refractory chronic lymphocytic

leukemia. Cancer. 2003;97(7):1711-1720.

15. Tsimberidou AM, Wierda WG, Plunkett W, et al. Phase I-II study of oxaliplatin, fludarabine, cytarabine, and rituximab combination therapy in patients with Richter's syndrome or fludarabine-refractory chronic lymphocytic leukemia. J Clin Oncol. 2008;26(2):196-203.

16. Tsimberidou AM, Wierda WG, Wen S, et al. Phase I-II clinical trial of oxaliplatin, fludarabine, cytarabine, and rituximab therapy in aggressive relapsed/refractory chronic lymphocytic leukemia or Richter syndrome. Clin Lymphoma Myeloma Leuk. 2013;13(5):568-574.

17. Durot E, Michallet A-S, Leprêtre S, Le Q-H, Leblond V, Delmer A. Platinum and high-dose cytarabine-based regimens are efficient in ultra high/high-risk chronic lymphocytic leukemia and Richter's syndrome: results of a French retrospective multicenter study. European Journal of Haematology. 2015;95(2):160-167.

18. Rogers KA, Huang Y, Ruppert AS, et al. A single-institution retrospective cohort study of first-line R-EPOCH chemoimmunotherapy for Richter syndrome demonstrating complex chronic lymphocytic leukaemia karyotype as an adverse prognostic factor. Br J Haematol. 2018;180(2):259-266.

19. Tsimberidou AM, O'Brien S, Khouri I, et al. Clinical outcomes and prognostic factors in patients with Richter's syndrome treated with chemotherapy or chemoimmunotherapy with or without stem-cell transplantation. J Clin Oncol. 2006;24(15):2343-2351.

20. Cwynarski K, van Biezen A, de Wreede L, et al. Autologous and allogeneic stem-cell transplantation for transformed chronic lymphocytic leukemia (Richter's syndrome): a retrospective analysis from the chronic lymphocytic leukemia subcommittee of the chronic leukemia working party and lymphoma working party of the European Group for Blood and Marrow Transplantation. J Clin Oncol. 2012; 30(18):2211-2217.

21. Kharfan-Dabaja MA, Kumar A, Stingo FE, et al. Allogeneic hematopoietic cell transplantation for Richter syndrome: a single-center experience. Clin Lymphoma Myeloma Leuk. 2018;18(1):e35-e39.

22. Bounaix L, Nguyen S, Blaise D, et al. Allogeneic Hematopoietic Stem-Cell Transplantation for Patients with Richter's Syndrome:the SFGM-TC Experience. Blood. 2018;132(Suppl 1):3457.

23. El-Asmar J, Kharfan-Dabaja MA. Hematopoietic cell transplantation for Richter syndrome. Biol Blood Marrow Transplant. 2016;22(11):1938-1944.

24. Alizadeh AA, Eisen MB, Davis RE, et al. Distinct types of diffuse large B-cell lymphoma identified by gene expression profiling. Nature. 2000;403(6769):503-511.

25. Rosenwald A, Wright G, Chan WC, et al. The use of molecular profiling to predict survival after chemotherapy for diffuse large-B-cell lymphoma. N Engl J Med. 2002; 346(25):1937-1947.

26. Hans CP, Weisenburger DD, Greiner TC, et al. Confirmation of the molecular classification of diffuse large B-cell lymphoma by immunohistochemistry using a tissue microarray. Blood. 2004;103(1):275-282.

27. Scott DW, Wright GW, Williams PM, et al. Determining cell-of-origin subtypes of diffuse large B-cell lymphoma using gene expression in formalin-fixed paraffin-embedded tissue. Blood. 2014;123(8):1214-1217.

28. Riedell PA, Smith SM. Double hit and double expressors in lymphoma: Definition and treatment. Cancer. 2018;124(24):4622-4632.

29. Friedberg JW. How I treat double-hit lymphoma. Blood. 2017;130(5):590-596.

30. Shanafelt TD, Jenkins G, Call TG, et al. Validation of a new prognostic index for patients with chronic lymphocytic leukemia. Cancer. 2009;115(2):363-372.

31. Nabhan C, Chaffee KG, Slager SL, et al. Analysis of racial variations in disease characteristics, treatment patterns, and outcomes of patients with chronic lymphocytic leukemia. Am J Hematol. 2016;91(7):677-680.

32. Eyre TA, Clifford R, Bloor A, et al. NCRI phase II study of CHOP in combination with ofatumumab in induction and maintenance in newly diagnosed Richter syndrome. Br J Haematol. 2016;175(1):43-54.

33. Fidai S, Sukhanova M, Chiu BC-H, et al. TP53 Aberrations By FISH in CLL and Complex Karyotype at Transformation Predict for Worse Outcome in Diffuse Large B-Cell Lymphoma - Richter Transformation: A Single Institution Series of 75 DLBCL-RT Cases. Blood. 2018;132(Suppl 1):2984.

34. Fan L, Wang L, Zhang R, et al. Richter transformation in 16 of 149 Chinese patients with chronic lymphocytic leukemia. Leuk Lymphoma. 2012;53(9):1749-1756.

35. Fabbri G, Khiabanian H, Holmes AB, et al. Genetic lesions associated with chronic lymphocytic leukemia transformation to Richter syndrome. J Exp Med. 2013; 210(11):2273-2288.

36. Abrisqueta P, Delgado J, Alcoceba M, et al. Clinical outcome and prognostic factors of patients with Richter's syndrome: retrospective multicenter study of the Spanish Chronic Lymphocytic Leukemia (CLL) Study Group (GELLC). Blood. 2017; 130(Suppl 1):2995.

37. Maddocks KJ, Ruppert AS, Lozanski G, et al. Etiology of Ibrutinib therapy discontinuation and outcomes in patients with chronic lymphocytic leukemia. JAMA Oncol. 2015;1(1):80-87.

38. Jain P, Keating M, Wierda W, et al. Outcomes of patients with chronic lymphocytic leukemia after discontinuing ibrutinib. Blood. 2015;125(13):2062-2067.

39. Davids MS, Huang Y, Rogers KA, et al. Richter's syndrome (RS) in patients with chronic lymphocytic leukemia (CLL) on novel agent therapy. J Clin Oncol. 2017; 35(15_suppl):7505.

40. Anderson MA, Tam C, Lew TE, et al. Clinicopathological features and outcomes of progression of CLL on the BCL2 inhibitor venetoclax. Blood. 2017; 129(25):3362-3370.

41. Tsang M, Shanafelt TD, Call TG, et al. The efficacy of ibrutinib in the treatment of Richter syndrome. Blood. 2015; 125(10):1676-1678.

42. Hillmen P, Schuh A, Eyre TA, et al. Acalabrutinib monotherapy in patients with Richter transformation from the Phase 1/2 ACE-CL-001 clinical study. Blood. 2016;128(22):60.

43. Ding W, LaPlant BR, Call TG, et al. Pembrolizumab in patients with CLL and Richter transformation or with relapsed CLL. Blood. 2017;129(26):3419-3427.

44. Davids MS, Roberts AW, Seymour JF, et al. Phase I First-in-human Study of Venetoclax in patients with relapsed or refractory non-Hodgkin Lymphoma. J Clin Oncol. 2017; 35(8):826-833.

45. Jain N, Ferrajoli A, Basu S, et al. A Phase II Trial of Nivolumab combined with Ibrutinib for patients with Richter transformation. Blood. 2018;132(Suppl 1):296.

46. Mato AR, Svoboda J, Luning Prak ET, et al. Phase I/II Study of Umbralisib (TGR-1202) in Combination with Ublituximab (TG-1101) and Pembrolizumab in patients with relapsed/refractory CLL and Richter's transformation. Blood. 2018;132(Suppl 1):297.

47. Younes A, Brody J, Carpio C, et al. Safety and activity of ibrutinib in combination with nivolumab in patients with relapsed non-Hodgkin lymphoma or chronic lymphocytic leukaemia: a phase 1/2a study. Lancet Haematol. 2019;6(2):e67-e78.

48. Turtle CJ, Hay KA, Hanafi LA, et al. durable molecular Remissions in chronic lymphocytic leukemia treated with CD19-specific chimeric antigen receptor-modified T cells afterfailure of Ibrutinib. J Clin Oncol. 2017; 35(26):3010-3020.

49. Barrio S, Shanafelt TD, Ojha J, et al. Genomic characterization of high-count MBL cases indicates that early detection of driver mutations and subclonal expansion are predictors of adverse clinical outcome. Leukemia. 2017;31(1):170-176.

50. Popp HD, Flach J, Brendel S, et al. Accumulation of DNA damage and alteration of the DNA damage response in monoclonal B-cell lymphocytosis and chronic lymphocytic leukemia. Leuk Lymphoma. 2018;1-10.

The hydroxymethylome of multiple myeloma identifies FAM72D as a 1q21 marker linked to proliferation

Fabrice Chatonnet,[1,2,$] Amandine Pignarre,[1,2,$] Aurélien A. Sérandour,[3-4-5,$] Gersende Caron,[1-2] Stéphane Avner,[6] Nicolas Robert,[7] Alboukadel Kassambara,[8] Audrey Laurent,[6] Maud Bizot,[6] Xabier Agirre,[9] Felipe Prosper,[9] José I. Martin-Subero,[10] Jérôme Moreaux,[7,8] Thierry Fest,[1,2] and Gilles Salbert[6]

[1]Université Rennes 1, Établissement Français du Sang de Bretaggne, Inserm, MICMAC - UMR_S 1236, Rennes, France; [2]Laboratoire d'Hématologie, Pôle de Biologie, Centre Hospitalier Universitaire de Rennes, Rennes, France; [3]CRCINA, INSERM, CNRS, Université d'Angers, Université de Nantes, Nantes, France; [4]Ecole Centrale de Nantes, Nantes, France; [5]Institut de Cancérologie de l'Ouest, Site René-Gauducheau, Saint-Herblain, France; [6]SPARTE, IGDR, CNRS UMR6290, University Rennes 1, Rennes, France; [7]Department of Biological Hematology, CHU Montpellier, Montpellier, France; [8]IGH, CNRS, Univ Montpellier, France; [9]Area de Oncología, Centro de Investigación Médica Aplicada (CIMA), Universidad de Navarra, Pamplona, Spain and [10]IDIBAPS, Barcelona, Spain

[$]FC, AP and AAS are co-first authors.

Correspondence:

GILLES SALBERT
gilles.salbert@univ-rennes1.fr

THIERRY FEST
thierry.fest@univ-rennes1.fr

JÉRÔME MOREAUX
jerome.moreaux@igh.cnrs.fr

Check the online version for the most updated information on this article, online supplements, and information on authorship & disclosures: www.haematologica.org/content/105/3/774

ABSTRACT

Cell identity relies on the cross-talk between genetics and epigenetics and their impact on gene expression. Oxidation of 5-methylcytosine (5mC) into 5-hydroxymethylcytosine (5hmC) is the first step of an active DNA demethylation process occurring mainly at enhancers and gene bodies and, as such, participates in processes governing cell identity in normal and pathological conditions. Although genetic alterations are well documented in multiple myeloma (MM), epigenetic alterations associated with this disease have not yet been thoroughly analyzed. To gain insight into the biology of MM, genome-wide 5hmC profiles were obtained and showed that regions enriched in this modified base overlap with MM enhancers and super enhancers and are close to highly expressed genes. Through the definition of a MM-specific 5hmC signature, we identified FAM72D as a poor prognostic gene located on 1q21, a region amplified in high risk myeloma. We further uncovered that FAM72D functions as part of the FOXM1 transcription factor network controlling cell proliferation and survival and we evidenced an increased sensitivity of cells expressing high levels of FOXM1 and FAM72 to epigenetic drugs targeting histone deacetylases and DNA methyltransferases.

Introduction

MM is a genetically and clinically heterogeneous hematological cancer associated with a limited number of gene translocations into the immunoglobulin heavy chain locus of plasma cells (PC). In particular, CCND1, CCND3, c-MAF, MAFB and MMSET translocations influence prognosis and are used to classify patients into molecular subgroups.[1] Genome sequencing studies have revealed considerable heterogeneity and genomic instability, a complex mutational landscape and a branching pattern of clonal evolution.[2,3] Epigenetic modifications including DNA methylation and histone modifications have been also related to MM pathophysiology.[4-6] Patients with highly proliferative PC can also show genetic instability of the chromosome 1q arm and specially of the pericentromeric region 1q12 and of its immediate neighbor 1q21.[7,8] Amplification of 1q21, and possibly overexpression of genes lying in 1q21, parallel disease progression.[8] However, no causal link between proliferation and 1q21 instability has yet been demonstrated, although overexpression of the histone chaperone gene ANP32E, in 1q21.2 and the cyclin-dependent kinase regulator CKS1B, in 1q21.3, is of poor prognosis in MM.[9] More recently, ILF2, in 1q21.3, was proposed to be involved in the pathogenic role of 1q21 amplification

by increasing DNA damage resistance.[10] Nonetheless, other yet unidentified genes might participate in the pathogenicity of 1q21 gain.

Tumor PC clones show different levels of differentiation,[11] suggesting that MM could originate either from B cells that do not fulfill a complete differentiation program, or from PC that partially dedifferentiate. Cell differentiation relies on the selective engagement of small genomic regions called enhancers which are bound by transcription factors (TF) controlling cell-specific transcriptional programs. As an early step of activation, enhancers undergo active DNA demethylation through iterative oxidation of 5mC into 5hmC, 5-formylcytosine (5fC) and 5-carboxylcytosine (5caC) by Ten-Eleven-Translocation (TET) enzymes and repair by the base excision repair machinery, including the T:G mismatch DNA glycosylase TDG which cleaves 5fC and 5caC.[12] 5hmC has been mapped genome-wide in several cell differentiation models, including *in vitro* differentiation of human naive B cells (NBC) into plasmablasts (PB), where 5hmC accumulates at PC identity genes, as well as in mouse germinal center B cells.[13-15] These studies showed enrichment in 5hmC at poised/active enhancers as well as in the body of highly transcribed genes. Despite the wealth of information on the genetics of MM, the epigenetics of this disease is still poorly described. Nonetheless, a recent genome-wide investigation of active chromatin regions showed that opening of heterochromatin is a hallmark of MM.[16] In addition, interrogation of DNA methylation in MM cells revealed that, despite a global hypomethylation, their genome shows specific hypermethylation of enhancers that normally undergo complete demethylation during B-cell commitment and are bound by B-cell TF.[17] Interestingly, the methylation levels of these enhancers were anti-correlated with expression levels of B-cell-specific TF in MM patients,[17] suggesting that variations in tumor PC differentiation states could indeed be controlled through DNA methylation/demethylation mechanisms guided by specific TF. Here, we investigated the genome-wide distribution of 5hmC in tumor PC and, through the identification of MM-specific hydroxymethylated regions, evidenced new prognosis genes that might contribute to the understanding of this disease.

Methods

Primary multiple myeloma cells

Bone marrow samples were collected after patients' written informed consent in accordance with the Declaration of Helsinki and institutional research board approval from Montpellier University hospital. Patients' MM cells were purified using anti-CD138 MACS microbeads (Miltenyi Biotech, Bergisch Gladbach, Germany). RNA and genomic DNA were extracted using Qiagen kits (Qiagen, Hilden, Germany) and their gene expression profile (GEP) obtained using Affymetrix U133 plus 2.0 microarrays as described.[18] Plasma cell labeling index (PCLI)[19] was investigated using BrdU incorporation and flow cytometry in 101 patients at diagnosis. Correlation between gene expression and PCLI was determined with a Spearman's test. We used publicly available Affymetrix GEP (Gene Expression Omnibus, accession number GSE2658) of a cohort of 345 purified MM cells from previously untreated patients from the University of Arkansas for Medical Sciences (UAMS, Little Rock, AR), termed in the following UAMS-TT2 cohort. These patients were treated with total thera-

py 2 including high-dose melphalan (HDM) and autologous stem cell transplant (ASCT).[20] We also used Affymetrix data from the total therapy 3 cohort (UAMS-TT3; n=158; E-TABM-1138)[21] of 188 relapsed MM patients subsequently treated with bortezomib (GSE9782) from the study by Mulligan *et al.*[22]

FDI-6 treatment of primary MM cells from patients

Bone marrow of patients presenting with previously untreated MM (n=6) at the University Hospital of Montpellier was obtained after patients' written informed consent in accordance with the Declaration of Helsinki and agreement of the Montpellier University Hospital Centre for Biological Resources (*DC-2008-417*). Mononuclear cells were treated with or without graded concentrations of FDI-6 and MM cells cytotoxicity was analyzed using anti-CD138-phycoerythrin monoclonal antibody (Immunotech, Marseille, France) as described previously.[5]

Genome-wide mapping of 5hmC and bioinformatics

5hmC was mapped by selective chemical labeling,[23] coupled or not with exonuclease digestion,[24,25] of 10 μg of sonicated (Bioruptor, Diagenode) genomic DNA from MM patients or from MCF-7 cells. Libraries were obtained using the TruSeq ChIP Sample Prep Kit (Illumina), quantified using the KAPA library quantification kit (KAPA Biosystems) and 50 bp single end sequenced with HiSeq 1500 (Illumina). Reads were mapped to hg19 and processed as described.[25] SCL-exo signal was normalized to the input signal. Principal component analyses (PCA) were run online with Galaxy (*http://deeptools.ie-freiburg.mpg.de/*) with 5hmC signal bined by 10 kb windows. Heatmap clustering of hydroxymethylated CpG was run online (*http://cistrome.org/*).[26] Search for transcription factor binding site (TFBS) motifs surrounding hydroxymethylated CpG used the online Centdist tool[27] in 600 bp windows centered on 5hmCpG. Annotation of 5hmCpG used GREAT.[28] Oxidative bisulfite modification of gDNA and hybridization to Illumina 450K arrays were run as previously described.[29] ChIP-seq data for H3K27ac in primary MM cells[16] were downloaded from the European Nucleotide Archive database (*PRJEB25605*). Data were deposited in the Gene Expression Omnibus database under accession number *GSE124188*.

A detailed description of additional methods is available in the *Online Supplementary Information.*

Results

5hmC-enrichment partly recapitulates the molecular classification of MM

To better understand the relationship between DNA demethylation processes and cell identity in MM, we generated genome-wide maps of 5hmC in MM cells isolated from 11 patients belonging to different molecular subgroups, as well as for three human myeloma cell lines (HMCL), either by SCL-exo[24,25] or SCL-seq[23] (Figure 1A). In parallel, 10 MM samples were processed through the oxidative-bisulfite modification procedure and hybridized to Illumina 450K arrays (oxBS-450K).[29] Annotation of 5hmC positive regions (40,586 CpG for oxBS-450K; 86,591 CpG for SCL-exo; 64,424 regions for SCL-seq) aggregated from all patients included in each procedure was run using GREAT.[28] Results indicated that oxBS-450K did not generate meaningful information whereas SCL-exo and SCL-seq highlighted characteristics of PC biology such as endoplasmic reticulum stress, immune response, but also pathways which could be linked to MM, such as "IRF4 target genes"[30] (*Online*

Supplementary Figure S1A). Based on these annotation data, only SCL-exo and SCL-seq identified regions were further analyzed. Results were first compared to genome-wide 5hmC maps of NBC and PB previously generated by SCL-seq.[14] PCA of the signal showed dispersion of the samples, suggesting variability between tumor hydroxymethylomes. Nonetheless, most MM hydroxymethylomes grouped closer to plasmablasts (PB than to NBC) (Figure 1B). When running PCA only with MM patients from the MMSET, CCND1 and Proliferation groups, 3 clusters were observed (C1 to C3 Figure 1B). These clusters gathered together patients from similar molecular groups, although two patients did not follow this rule (E12097 and E6068), indicating that molecular groups are probably heterogeneous in nature and that 5hmC maps can help refine molecular clustering. We next generated the union of significantly hydroxymethylated CpG ($P<$ $5e^{-2}$) overlapping between samples within each cluster. These 6,385 individual CpG were clusterized according to their 5hmC levels (Figure 1C). The resulting heatmap evidenced two groups of CpG that were selectively more hydroxymethylated either in C1 patients (C'1 cluster) or in C2 patients (C'2 cluster). Analysis of motif enrichment for transcription factor binding sites in C'1 and C'2 and their comparison with motifs found in NBC and PB hydroxymethylated regions suggested that MM cells from C2 patients remain more differentiated than those from C1 patients. Indeed, the BLIMP1 (a major regulator of PC differentiation) motif was significantly enriched in C'2 but not in C'1 regions (*Online Supplementary Figure S1B*). Accordingly, functional annotation through GREAT showed that C'2 regions associated with endoplasmic reticulum stress gene signature or IL-6 signaling, features of mature PC, whereas C'1 regions did not (Figure 1C). Conversely, NOTCH, MYC, Cell Cycle and BCR signaling, which are more characteristic of proliferating and/or undifferentiated B cells, were significantly more associated with C'1 regions than with C'2 regions (Figure 1C). Of note, the SUH and GLI motifs were also selectively enriched in C'1 regions (*Online Supplementary Figure S1B*). Hence, C1 patients from the proliferation group probably have active NOTCH and SHH pathways, both important for proliferation of CD138+ MM cells.[31-32] In addition, the binding motif for MEIS1, a known regulator of hematopoietic progenitor self-renewal,[33] was also selectively enriched in C'1 regions. Collectively, these data indicate that MM cells from the proliferation group have an under-differentiated phenotype and proliferation is likely to rely on a MEIS1/SUH/GLI transcription factor cocktail as well as MYC activity. These results also show that 5hmC is indeed indicative of the biological and clinical traits of patients and could be used to delineate groups with different characteristics.

5mC oxidation targets MM plasma cell enhancers

Investigating the genomic location of high confidence MM 5hmCpG (86,591 CpG, p<1e[-5]) showed that they were mostly distributed in introns and distal intergenic regions and, as previously observed in NBC, PB and mouse activated B cells,[14,15] genes which were close to a 5hmC
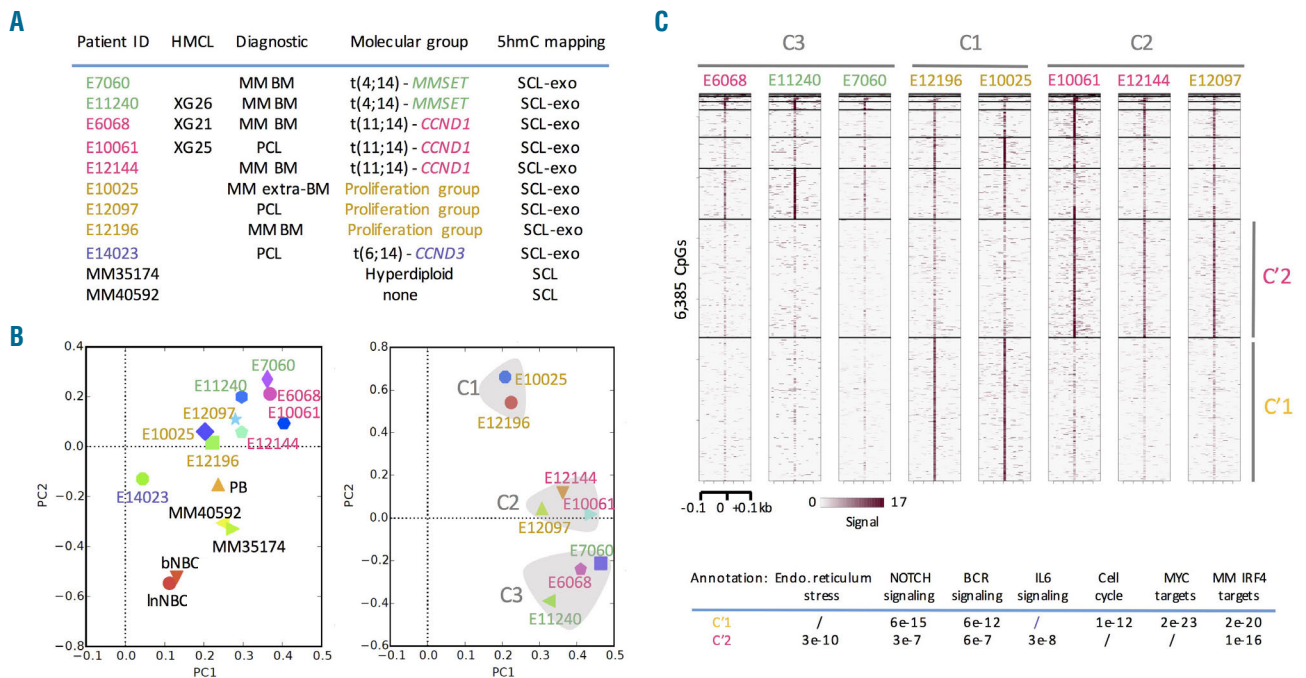
Figure 1. Analysis of the hydroxymethylome of multiple myeloma (MM). (A) Molecular classification of the patient samples analyzed in this study. HMCL indicates the names of cell lines derived from patient samples. The molecular groups are based on Zhan *et al.*[1] MM: multiple myeloma, BM: bone marrow, PCL: plasma cell leukemia. (B) Principal component analysis (PCA) of 5-hydroxymethylcytosine (5hmC) distribution either in all MM patients, compared to naive B cells (NBC) and plasmablast (PM) (left), or in the subset of MM patients from the CCND1, MMSET and proliferation groups. Clusters 1, 2 and 3 (C1, C2 and C3) group samples with similar 5hmC distribution. (C) Heatmap clustering of the SCL-seq signal in C1 to C3 patients at the union of overlapping 5hmCpG and functional annotation with GREAT of genes associated with C'1 and C'2 5-hydroxymethylated CpG(5hmCpG). For each annotation, the corresponding *P* value is indicated.

enriched region showed higher expression than genes which had no such region in their vicinity (Figure 2A). We next considered the presence of these 5hmCpG in regions harboring different chromatin states (ChromHMM) and defined for the lymphoblastoid cell line GM12878 (a cell line used as a model of normal B cells) by the ENCODE consortium. In accordance with a proposed global opening of chromatin in MM cells and as already described for open chromatin regions in MM,[16] and for MM hypomethylated CpG,[17] MM 5hmCpG mainly reside in regions of heterochromatin in GM12878 cells (*Online Supplementary Figure S2A*). During differentiation of NBC into PB, genomic sites undergoing 5mC oxidation often bear histone marks of either commissioned (H3K4me1) or active (both, H3K27ac and H3K4me1) enhancers.[14,15] To investigate the relationship between 5mC oxidation and enhancers in MM, we next analyzed enrichment in H3K4me1 and H3K27ac from NBC, PC and MM cells around 5hmCpG detected in MM patients. Most MM 5hmCpG were found in PC and NBC H3K4me1-premarked genomic sites that become active in MM (Figure 2B). We next investigated the presence of MM 5hmCpG in active enhancers and super-enhancers (SE) identified in the MM1.S HMCL.[34] Most notably, 89.3% (275 of 308) of the active MM1.S SEs and 36% (2949 of 8285) of all active enhancers were enriched in 5hmCpG in MM (*Online Supplementary Figure S2B*), strongly suggesting a role for 5mC oxidation in the control of SE activity. Similar results were obtained when analyzing the overlap

between 5hmCpG and U-266 enhancers and SE defined on the H3K27ac ChIP-seq signal from the Blueprint consortium (*not shown*). However, as exemplified for the KLF13 SE (Figure 2C), the vast majority (98.5%, 271 of 275) of these MM1.S active SE were already marked with 5hmC in PB, indicating that these SE probably maintain a cell-of-origin identity in MM cells. Nonetheless, four SE showed a MM-specific hydroxymethylation profile, including 2 DEPTOR SE, MYC SE and GAS2 SE (Figure 2C). DEPTOR and MYC are known to promote MM cell proliferation and survival[4,35] and, in support of our data, their SE were found to be specifically active in MM cells.[16] GAS2 has not been associated with MM yet but it has been shown to be upregulated and to favor survival in chronic myeloid leukemia cells in correlation with hypomethylation of its promoter region.[36,37] When examined during NBC to PC differentiation (*Online Supplementary Figure S2C*) as well as in patients of the Arkansas MM cohort (*Online Supplementary Figure S2D*), GAS2 mRNA levels were detected in bone marrow plasma cells (BMPC) but found to be higher in MM cells. Furthermore, GAS2 overexpression impacted patient survival (Figure 2C). Since GAS2 inhibits calpain proteases which degrade TET enzymes,[38] it could thus play a central role in sustaining 5mC oxidation levels in MM cells. Overall, this analysis indicates that 5mC oxidation in MM occurs mainly in intronic enhancers and participates in the establishment of a myeloma-specific gene expression program.
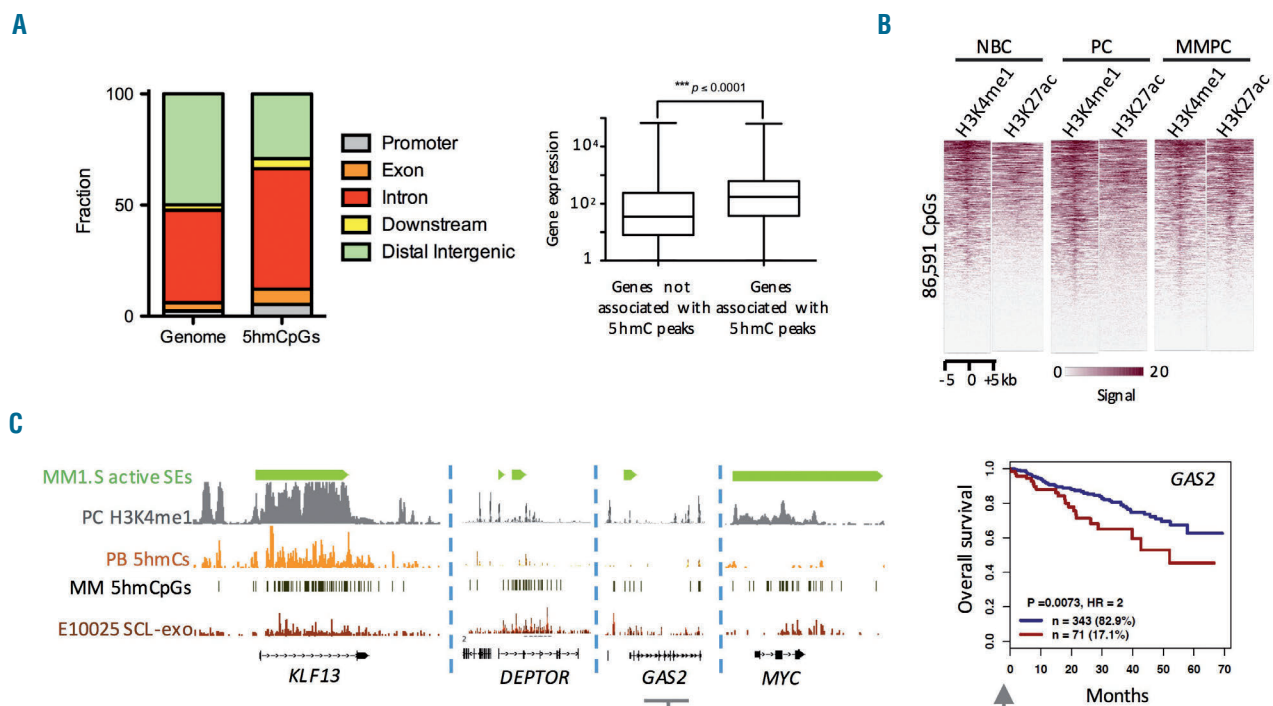
Figure 2. Genomic and epigenomic characterization of sites of 5-methylcytosine (5mC) oxidation in multiple myeloma plasma cells (MMPC). (A) CEAS[31] analysis of the distribution of high confidence multiple myeloma (MM) 5hmCpG (n=86,591) and box plot comparing expression levels of genes associated or not with 5-hydroxymethylcytosine (5hmC) peaks in MM patients. (B) Heatmap representation of H3K4me1 and H3K27ac ChIP-seq signals at MM 5hmCpG. NBC and PC H3K4me1 data were from the Blueprint Consortium (*http://dcc.blueprint-epigenome.eu/#/files*), and MM H3K27ac data were downloaded from the European Nucleotide Archive (*PRJEB*25605). (C) Integrated genome browser (IGB) visualization of H3K4me1 from normal plasma cells (PC H3K4me1), 5hmC from *in vitro* naive B cells (NBC) and plasma cells (PC) differentiated plasmablasts (PB 5hmC), MM 5hmCpG and SCL-exo signal from E10025 at selected super enhancers active in MM1.S cells. The survival of patients from the Arkansas cohort classified as high (n=71) or low (n=343) GAS2 expression is shown on the right.

A MM-specific 5hmC signature identifies prognosis genes

We next delineated a MM-specific 5hmC signature, independently of molecular subgroups, through first calling CpG that were hydroxymethylated ($P<1e^{-5}$) in at least 33% of the myeloma samples and not falling into genomic regions hydroxymethylated in PB ($p<1e^{-2}$), and second by iterative clustering of these CpG according to their hydroxymethylation signal both in MM patients and in PB. Hence, a cluster of 415 CpG uniquely hydroxymethylated in MM was obtained (*Online Supplementary Figure S3A*). A list of 29 genes, including BMP6 and FAM72D (*Online Supplementary Figure S3B*), associating with at least 3 of these hydroxymethylated CpG was next established and investigated for prognostic value in the UAMS-TT2 (n=256) and UAMS-TT3 (n=158) Arkansas cohorts (*http://genomicscape.com/*). Interestingly, around a quarter (7/29) of the 29 genes significantly associated with 5hmCpG were located at 1q21.1 ($P=7.5e^{-4}$) whereas none were at 1q21.2 (Figure 3A and *Online Supplementary Figure S3C-D*). Results showed that among these 29 genes, only six had no prognostic value ($P>0.05$) in both analyzed cohorts (Figure 3A). Others could be classified as either of good (n=4) or of poor (n=7) prognosis in both cohorts, as exemplified for FAM72D (Figure 3B). Investigating the expression of these genes during the differentiation of NBC, poor prognostic genes were mostly expressed in pre-PB, whereas good prognostic genes were mainly expressed in non-proliferating cells (*Online Supplementary Figure S4*). Among the poor prognostic genes located on 1q21.1, *FAM72D* is a gene of unknown function which implication in MM biology has not yet been addressed. Of note, recent duplication events of the ancestral FAM72A gene led to the presence of four highly conserved *FAM72* genes in human (FAM72A ,B , C, D)[39] which cannot be discriminated at the mRNA level (99% identity). Accordingly, "*FAM72*" is used thereafter when referring to expression data. *FAM72* expression levels correlated with 1q21 copy number, which is associated with poor outcome in MM (*Online Supplementary Figure S5A-B*). Importantly, *FAM72* expression levels correlated with 5hmC enrichment at the *FAM72D* locus (*Online Supplementary Figure S5C*) which was not biased by 1q21 amplification (*Online Supplementary Figure S5D*) and was associated with the presence of the enhancer histone modification H3K4me1 in normal plasma cells (*Online Supplementary Figure S5E*). Conversely to *BMP6* (*Online Supplementary Figure S4 and S5F*), expression of FAM72 was found to be higher in proliferative B cells, *i.e.* centroblasts and pre-PB (*Online Supplementary Figure S4*), as well as in the proliferation group (*Online Supplementary Figure S5G*). In accordance with a putative role of *FAM72* in stimulating MM cell proliferation, plasma cell labeling index (PCLI)[19] was significantly correlated with *FAM72*

A

GENE NAME	Localization	Cohort *P* value	
		TT2 (n=256)	TT3 (n=158)
NOTCH2	1p12-1p11.2	6.9e-3	ns
CD160	1q21.1	ns	ns
FAM72D	1q21.1	3.1e-7	2.7e-4
GPR89A	1q21.1	1.5e-4	3.6e-3
NOTCH2NL	1q21.1	ns	ns
PDE4DIP	1q21.1	5.8e-3	8.8e-3
PDZK1	1q21.1	ns	ns
SEC22B	1q21.1	ns	1.9e-3
LINC00152	2p11.2	3.3e-4	0.011
FRG1	4q35.2	ns	0.019
BMP6	6p24.3	2.3e-3	7.3e-5
RSPH10B	7p22.1	0.017	ns
GTF2IRD2	7q11.23	0.045	7.4e-3
GTF2IRD2B	7q11.23	0.047	ns
NCF1C	7q11.23	0.023	0.017
ARHGEF34P	7q35	ns	ns
CTAGE4	7q35	ns	0.015
OR2A20P	7q35	1.3e-3	ns
MIR1204	8q24.21	0.013	0.034
TMEM75	8q24.21	0.027	ns
KIAA1217	10p12.1	6.7e-3	8.3e-5
GOLGA8A	15q13.1	9.1e-3	ns
HERC2P9	15q13.1	ns	ns
EIF3C	16p11.2	3.7e-3	5.7e-3
CDR2	16p12.2	ns	ns
NPIPB5	16p12.2	0.02	7.6e-3
RRN3P3	16p12.2	6.2e-3	ns
USP14	18p11.32	2.9e-6	2.4e-4

B

C

Gene	Correlation (R²)	P-value
FAM72	0.4412	< 0.0001
FOXM1	0.3477	< 0.0001
CKS1B	0.1858	< 0.0001
ANP322	0.0129	0.2879
ILF2	0.0003	0.8744

Figure 3. A multiple myeloma-specific hydroxymethylation signature uncovers new prognostic genes. (A) Genes associated with at least three MM-specific 5hmCpG were analyzed with Genomic-Scape 2.0 for their prognostic value in two cohorts of patients (Arkansas TT2 and TT3). Genes associated with good prognosis are indicated in green and genes associated with poor prognosis in red. The associated *P*-values are also indicated with the same color code. Cutoff was set at *P*=0.05. (B) Overall survival of patients from the TT2 Arkansas cohort expressing low (blue curves) or high (red curves) levels of *FAM72D* (lower panels). (C) Correlations between plasma cell labeling index (PCLI) scores and gene expression values in a cohort of 101 patients.

expression in a cohort of 101 newly diagnosed MM patients (Figure 3C). *PCLI* was also significantly correlated to *FOXM1* and *CKS1B* expression, but at a lower extent. No correlation was found between MM cell proliferation and *ANP32E* or *ILF2* expression (Figure 3C). These data suggest that amplification of the 1q21 region, together with its hydroxymethylation, might affect cell proliferation in MM through enhancing *FAM72* expression.

FAM72D Is involved in MM cell proliferation

Examination of the top-12 FAM72 co-expressed (*P*<0.05) genes during NBC differentiation into PC, highlighted *FOXM1*, a TF known to play a key role in MM cell proliferation[40] (Figure 4A). Furthermore, a strong correlation between *FOXM1* and *FAM72* expression was evidenced in MM samples and derived HMCL (Figure 4A). ChIP-seq data from GM12878 lymphoblastoid cells indicated that *FOXM1* binds to the *FAM72* promoter (*Online Supplementary Figure S6A*), strongly suggesting that this TF directly regulates *FAM72* expression. In support of this hypothesis, *FAM72* hydroxymethylation levels were positively correlated with *FOXM1* expression (*Online Supplementary Figure S6B*). Comparison of *FOXM1* and FAM72 coexpressed genes in patients from the proliferation molecular MM subgroup revealed a significant

overlap (86% of common genes) (*Online Supplementary Figure S6C*). Moreover, *FAM72* coexpressed genes were significantly associated with M phase cell cycle annotations (*Online Supplementary Figure S6D*). *FAM72* was significantly overexpressed in HMCL and MM cells compared to BMPC and monoclonal gammopathy of undetermined significance (MGUS), underlining the link with MM cell proliferation (*Online Supplementary Figure S6E*). Furthermore, gene set enrichment analysis (GSEA) of expression data from patients with high *FAM72* expression and a poor outcome revealed a significant enrichment of genes related to proliferation, overexpressed in proliferating PB compared to mature BMPC and stem cell genes (*Online Supplementary Figure S7*). To study the biological function of *FAM72* overexpression in MM, the XG21 and XG23 HMCL were selected for their low level of endogenous *FAM72* expression (*Online Supplementary Figure S8A-C*). In fetal calf serum (FCS) free medium, *FAM72D* overexpression resulted in significant growth advantage and response to IL-6, a key MM growth factor (Figure 4B). Similar results were obtained with overexpression of *FAM72* in XG23 (*Online Supplementary Figure S8D*). These data support the recent characterization of *FAM72B* as an S/G2-M phase gene whose inactivation reduces cell proliferation in human fibroblasts.[41] To test
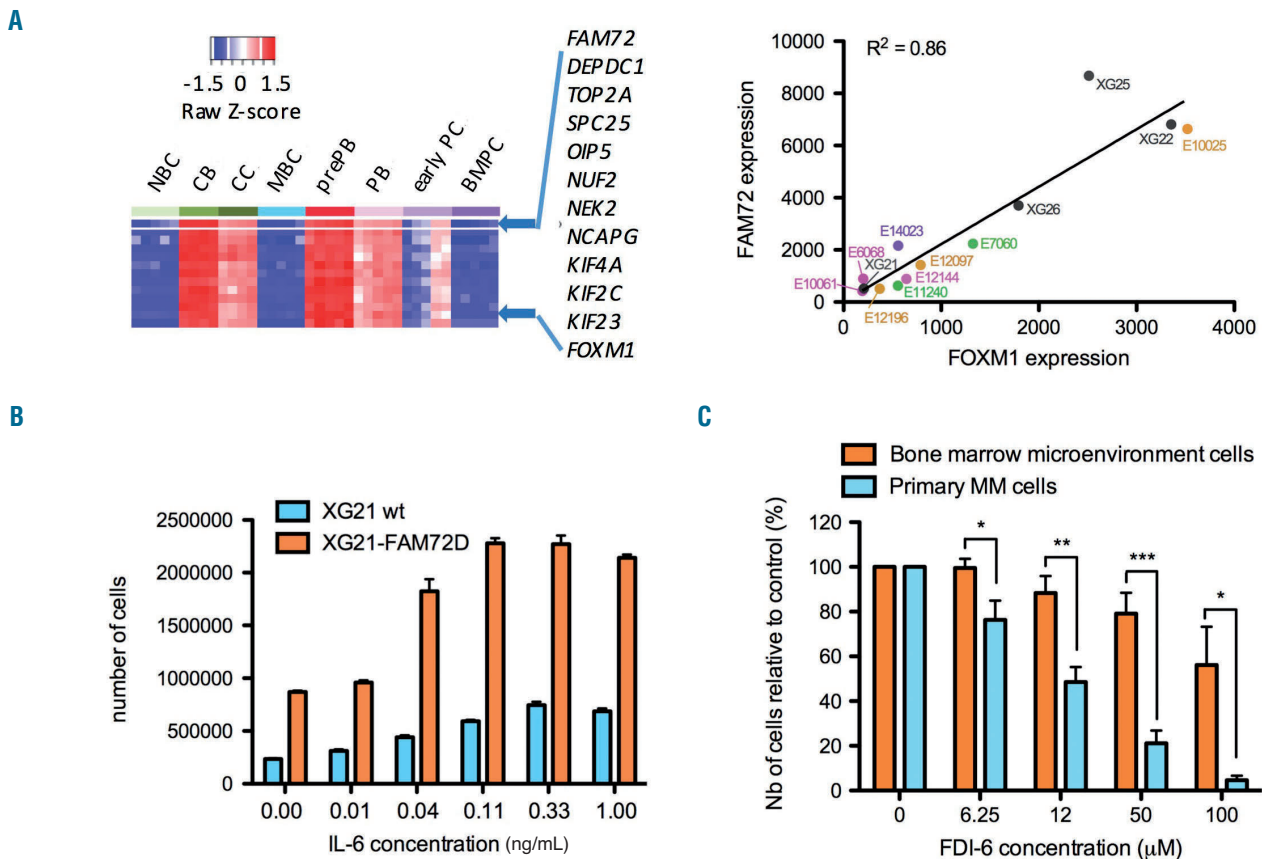
Figure 4. FAM72D regulates cell proliferation in multiple myeloma. (A) Analysis of *FAM72* co-expressed genes during B-cell differentiation in naive B cells (NBC), centroblasts (CB), centrocytes (CC), memory B cells (MBC), pre-plasmablasts (prePB), plasmablasts (PB), early plasma cells (early PC), and bone marrow plasma cells (BMPC). Only the Top-12 co-regulated genes are shown. FOXM1 ranked at position 11. Graph on the right shows the correlation between *FAM72* and *FOXM1* gene expression in the multiple myeloma (MM) patients and derived cell lines for which 5hmCpG were mapped by SCL-exo. (B) Proliferation assay of XG21 (blue bars) and XG21-FAM72D (orange bars) cells in the presence of increasing concentrations of IL-6. (C) Impact of increasing concentrations of the *FOXM1* inhibitor FDI-6 on the *in vitro* growth of bone marrow cells from MM patients (n=6).

for a *FOXM1*-dependency of primary cancer cells as well as derived cell lines, FDI-6, a DNA binding inhibitor of *FOXM1*,[42] was used. Primary MM cells were highly sensitive to *FOXM1* inhibition compared to bone marrow microenvironment cells (Figure 4C). Overexpression of *FAM72D* in *XG21* cells partially counteracted FDI-6-induced cell death (*Online Supplementary Figure S8E*), suggesting that *FAM72D* mediates part of *FOXM1* effects on cell growth and survival.

In order to extend our findings to other cancer types, publicly available data were analyzed (*http://www.cbioportal.org/*,[43] *https://xenabrowser.net/heatmap/*) and indicated (i) that amplification of 1q21 is a highly prevalent event in breast cancer (*Online Supplementary Figure S9A*) and (ii) a higher expression of *FAM72D* within mutated TP53 patients (*Online Supplementary Figure S9B*). In agreement with *FAM72D* genes being targets of *FOXM1*, inhibition of *FOXM1* in MCF-7 breast cancer cells has been shown to significantly reduce *FAM72D, FAM72A* and *FAM72B* expression.[44] Hence, we next generated genome-wide maps of 5hmC in MCF-7 cells and observed that, as in MM cells, the upstream region of *FAM72D* was highly hydroxymethylated (*Online Supplementary Figure S9C*),

suggesting a similar regulation of this gene between MM and breast cancer cells. To investigate a putative function of *FAM72D* in mitosis, *FAM72D* was knocked-down by transfection of siRNAs in MCF-7 cells and mitotic anomalies were analyzed. Data revealed that a reduction in *FAM72D* levels led to a higher occurrence of defects such as misaligned chromosomes, lagging chromatids and micronuclei (*Online Supplementary Figure S9D*), suggesting that *FAM72D* helps maintain mitotic fidelity.

High *FAM72* expression is associated with resistance to bortezomib and sensitivity to histone deacetylase/decitabine inhibitors (HDACi/DNMTi)

Since *FAM72D* expression is associated with a poor outcome in MM, we investigated whether high *FAM72* expression could be related with drug resistance in MM. Correlating *FAM72* gene expression with response to conventional drugs (bortezomib, melphalan, lenalidomide, dexamethasone and panobinostat) in HMCL, we identified that high *FAM72* expression levels are associated with resistance to bortezomib (n=12, *P*=0.049) (Figure 5A). These observations are consistent with the fact that high *FAM72* expression is associated with a poor prognosis in a

Gene	Correlation	*P*-value
FAM72high	- 0.725	0.027
FAM72low	- 0.564	ns
FOXM1high	- 0.315	ns
FOXM1low	- 0.402	ns
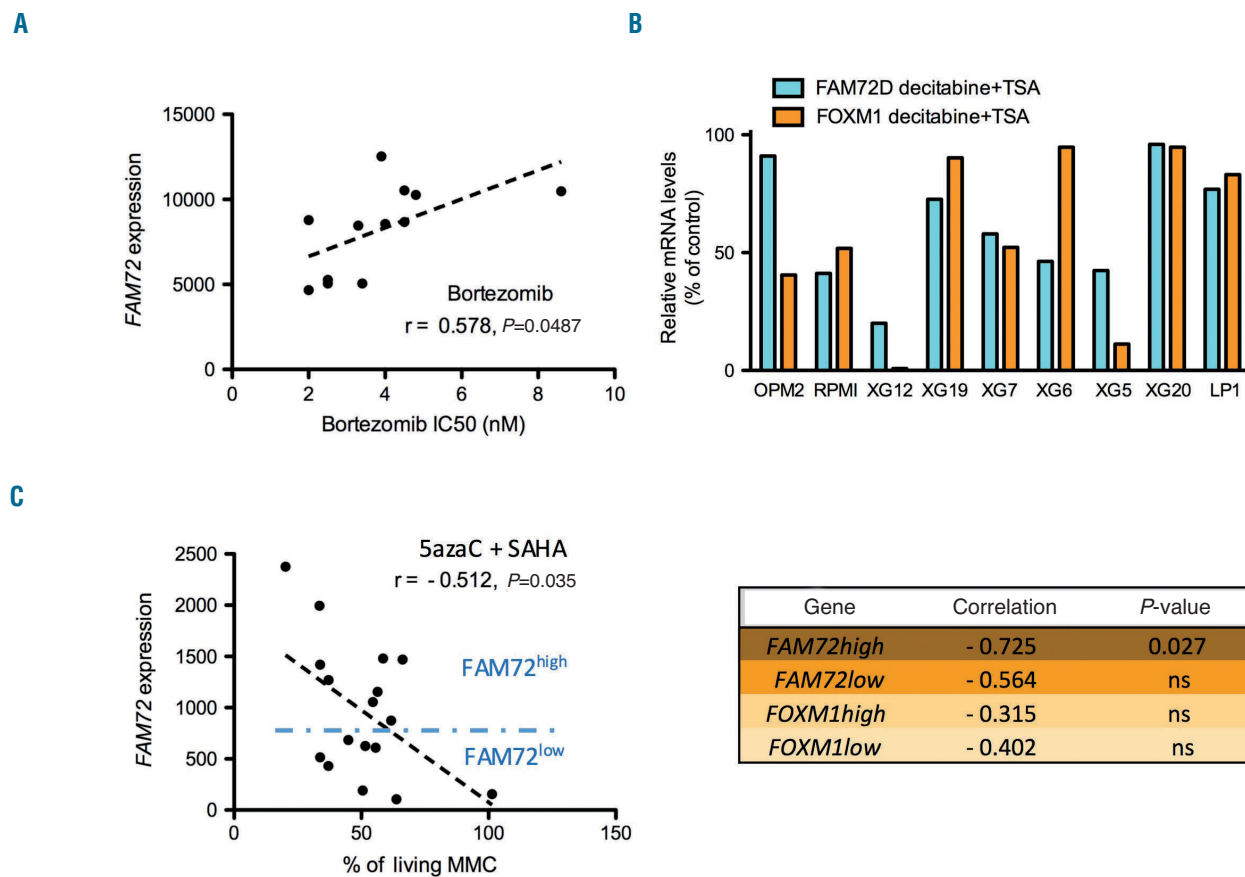
Figure 5. *FAM72* expression levels predict multiple myeloma cell sensitivity to drugs. (A) 12 HMCL were cultured with graded concentrations of Boterzomib for four days and IC50 were calculated with mean values of five experiments determined on sextuplet culture wells. High *FAM72* expression (Affymetrix microarrays) was significantly correlated with resistance to bortezomib. (B) Histone deacetylase/decitabine inhibitors (HDACi/DNMTi) induce a significant downregulation of *FAM72* and *FOXM1* in multiple myeloma (MM). Nine HMCL were treated for seven days with decitabine (DNMTi) and TSA during the last 24 hours and gene expression was assessed using Affymetrix U133P microarrays. (C) *FAM72* expression predicts 5azacitidine/SAHA combination sensitivity of primary myeloma cells of patients. Mononuclear cells from tumor samples of 17 patients with MM were cultured for 4 days in the presence of IL-6 (2 ng/mL) with or without 2 μM 5azacitidine and 300 nM SAHA. At day 4 of culture, the count of viable MMC was determined using CD138 staining by flow cytometry. Samples from Figure 6C and *Online Supplementary Figure S10C* were grouped as *FAM72*high or low and *FOXM*high or low and correlation coefficients between *FAM72* or FOXM1 expression and the percentage of living MM cells were calculated with GraphPad Prism.

cohort of patients at relapse treated by bortezomib mono-therapy (Mulligan cohort, *Online Supplementary Figure S10A*). Conversely, no significant correlation was identified between *FAM72* expression and survival in a cohort of patients at relapse treated by dexamethasone mono-therapy (*Online Supplementary Figure S10B*) and between FAM72 expression and *in vitro* HMCL response to melphalan, lenalidomide or dexamethasone (*not shown*). Of particular interest, high *FAM72* expression tended to be significantly correlated with a better response to panobinostat (n=10, *P*=0.061; *Online Supplementary Figure S10C*), suggesting that HDACi could have a therapeutic interest in *FAM72*^{high} myeloma patients associated with poor survival. Since a combination of both HDACi and DNMTi has been shown to reprogram HMCL cells,[45] we next investigated the ability of the combined DNMTi and HDACi decitabine (5aza-dC) and trichostatin A (TSA) to regulate *FAM72* and *FOXM1* expression in HMCL. Data indicated that the combined treatment reduced, although to different extent, the expression of both genes in a majority of investigated cell lines (Figure 5B). Finally, primary MM cells were treated with a similar combination (5aza-C and the HDACi SAHA) and their resistance to these drugs was inversely correlated to the expression of FAM72 and *FOXM1* (Figure 5C and *Online Supplementary Figure S10D*). When considering *FAM72*^{high}/*FAM72*^{low} and *FOXM1*^{high}/*FOXM1*^{low} expressing cells, only FAM72^{high} samples remained significantly correlated with higher sensitivity to the HDCAi/DNMTi combination (Figure 5C). These results suggest that high-risk patients overexpressing *FAM72* could benefit from treatment by a HDACi/DNMTi combination.

Discussion

Collectively, our data point to a prominent role of DNA demethylation events occurring at 1q21.1, and specially at the *FAM72D* locus, in MM biology and malignancy. One of the most common genetic features in MM linked to high-risk prognosis is the gain (three copies) or amplification (four and more copies) of part or all of the q arm of chromosome 1.[46] Among the partial gains of 1q, 1q21 is particularly detected both in newly diagnosed (30%) and relapse (70%) cases. However, there is still no unifying picture explaining the functional role of the 1q arm amplification and its wide occurrence among high-risk patients. Interestingly, MM-like 1q alterations can be experimentally triggered by inhibiting DNA methylation. Indeed, 5aza-dC treatment of activated B cells leads to a decondensation of the 1q12 pericentromeric chromatin, a process that might enable local rearrangements of the 1q arm.[47] Although DNA methylation levels are generally low in MM cells, residual methylation accumulates at specific sites[17] and can still be erased by active demethylation through TET enzymes. Such mechanisms could play a role in disease progression provided that TET are targeted to the pericentromeric region of chromosome 1 and its adjacent region 1q21. Consistent with this idea, we show that one fourth of the genes associated with MM-specific hydroxymethylated regions lie within the 1q21.1 region. Among them, *FAM72D*, a gene encoding for a protein of unknown function, was shown here to enhance proliferation of MM cells. Whereas most mammals have only one copy of the *FAM72* gene, due to recent duplication events, four genes encode the human FAM72 proteins A to D.[39] The *FAM72* genes are known to be overexpressed in can-
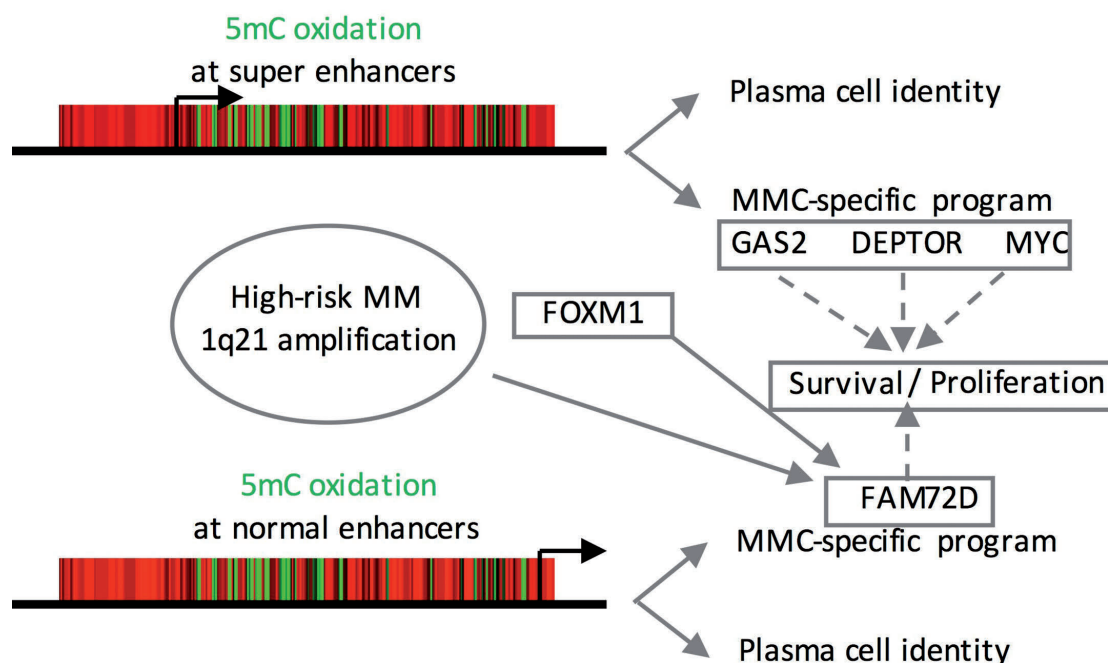
Figure 6. 5-methylcytosine (5mC) oxidation at *FAM72D* enhancer and *GAS2, DEPTOR* and *MYC* super enhancers associate with multiple myeloma. 5mC oxidation in multiple myeloma (MM) cells occurs at super-enhancers (SE) and normal enhancers and as such participates in the establishment of an MM-specific transcription program and the maintenance of plasma cell identity. Several scenarios may lead to *FAM72D* overexpression in MM, including 1q21 gain/amplification, FOXM1 upregulation and DNA demethylation, and might combine in high risk MM to enhance survival and proliferation.

cer and favor tumorigenesis induced by the Epstein-Barr virus-derived latent membrane protein 1.[48,49] *FAM72* genes are highly expressed in *TP53* mutated cancer cells, whose growth has been shown to be dependent on *FAM72D*.[50,51] Interestingly, cancer cell growth dependency on *FAM72D* has also been demonstrated for cells with mutated or copy number variants of p300, p19Arf and CDKI2A,[51] suggesting that *FAM72D* is required for the growth of different cancer types. Corroborating the tumorigenic potential of FAM72 proteins, two insertional mutagenesis screens in mouse identified the mouse *SRGAP2/FAM72A* locus as a driver of chronic myeloid leukemia progression and growth factor-independent leukemogenesis.[52,53] Hence, TET-mediated demethylation of the *FAM72D* upstream region is likely coupled to the proliferation potential of MM cells.

We have defined here a MM-specific hydroxymethylome that favors a survival/proliferation program relying, at least in part, on the cooperative actions of enhancers and super-enhancers controlling *FAM72D, GAS2, DEP-TOR* and *MYC* expression (Figure 6). In accordance with the observation that *FAM72* expression is predictive to the sensitivity of MM cells to different treatments, its evaluation in patients could help to tailor therapy.

References

1. Zhan F, Huang Y, Colla S, et al. The molecular classification of multiple myeloma. Blood. 2006;108(6):2020-2028.
2. Bolli N, Avet-Loiseau H, Wedge DC, et al. Heterogeneity of genomic evolution and mutational profiles in multiple myeloma. Nat Commun. 2014;5:2997.
3. Lohr JG, Stojanov P, Carter SL, et al. Widespread genetic heterogeneity in multiple myeloma: implications for targeted therapy. Cancer Cell. 2014;25(1):91-101.
4. Delmore JE, Issa GC, Lemieux ME, et al. BET bromodomain inhibition as a therapeutic strategy to target c-Myc. Cell. 2011;146(6):904-917.
5. Moreaux J, Reme T, Leonard W, et al. Gene expression-based prediction of myeloma cell sensitivity to histone deacetylase inhibitors. Br J Cancer. 2013;109(3):676-685.
6. Herviou L, Kassambara A, Boireau S, et al. PRC2 targeting is a therapeutic strategy for EZ score defined high risk multiple myeloma patients and overcome resistance to IMiDs. Clin Epigenetics. 2018;10(1):121.
7. Sawyer JR, Tricot G, Mattox S, Jagannath S, Barlogie B. Jumping translocations of chromosome 1q in multiple myeloma: evidence for a mechanism involving decondensation of pericentromeric heterochromatin. Blood. 1998;91(5):1732-1741.
8. Hanamura I, Stewart JP, Huang Y, et al. Frequent gain of chromosome 1q21 in plasma-cell dyscrasias detected by fluorescence in situ hybridization: incidence increases from MGUS to relapsed myeloma and is related to prognosis and disease progression following tandem stem-cell transplantation. Blood. 2006;108(5):1724-1732.
9. Walker BA, Leone PE, Chiecchio L, et al. A compendium of myeloma-associated chromosomal copy number abnormalities and their prognostic value. Blood. 2010;116(15):e56-65.
10. Marchesini M, Ogoti Y, Fiorini E, et al. ILF2 is a regulator of RNA splicing and DNA damage response in 1q21 amplified multiple myeloma. Cancer Cell. 2017;32(1):88-100.
11. Paiva B, Puig N, Cedena MT, et al. Differentiation stage of myeloma plasma cells: biological and clinical significance. Leukemia. 2017;31(2):382-392.
12. Wu X, Zhang Y. TET-mediated active DNA demethylation: mechanism, function and beyond. Nat Rev Genet. 2017;18(9):517-534.
13. Sérandour AA, Avner S, Oger F, et al. Dynamic hydroxymethylation of deoxyribonucleic acid marks differentiation-associated enhancers. Nucleic Acids Res. 2012;40(17):8255-8265.
14. Caron G, Hussein M, Kullis M, et al. Cell-cycle-dependent reconfiguration of the DNA methylome during terminal differentiation of human B cells into plasma cells. Cell Rep. 2015;13(5):1059-1071.
15. Lio C-W, Shukla V, Samaniego-Castruita D, et al. TET enzymes augment activation-induced deaminase (AID) expression via 5-hydroxymethylcytosine modifications at the Aicda superenhancer. Sci Immunol. 2019;4(34).
16. Jin Y, Chen K, De Paepe A, et al. Active enhancer and chromatin accessibility landscapes chart the regulatory network of primary multiple myeloma. Blood. 2018;131(19):2138-2150.
17. Agirre X, Castellano G, Pascual M, et al. Whole-epigenome analysis in multiple myeloma reveals DNA hypermethylation of B cell-specific enhancers. Genome Res. 2015;25(4):478-487.
18. Viziteu E, Klein B, Basbous J, et al. RECQ1 helicase is involved in replication stress survival and drug resistance in multiple myeloma. Leukemia. 2017;31(10):2104-2113.
19. Requirand G, Robert N, Boireau S, et al. BrdU incorporation in multiparameter flow cytometry: A new cell cycle assessment approach in multiple myeloma. Cytometry B Clin Cytom. 2019;96(3):209-214.
20. Barlogie B, Tricot G, Rasmussen E, et al. Total therapy 2 without thalidomide in comparison with total therapy 1: role of intensified induction and posttransplantation consolidation therapies. Blood. 2006;107(7):2633-2638.
21. Pineda-Roman M, Zangari M, Haessler J, et al. Sustained complete remissions in multiple myeloma linked to bortezomib in total therapy 3: comparison with total therapy 2. Br J Haematol. 2008;140(6):625-634.
22. Mulligan G, Mitsiades C, Bryant B, et al. Gene expression profiling and correlation with outcome in clinical trials of the proteasome inhibitor bortezomib. Blood. 2007;109(8):3177-3188.
23. Song CX, Szulwach KE, Fu Y, et al. Selective chemical labeling reveals the genome-wide distribution of 5-hydroxymethylcytosine. Nat Biotechnol. 2011;29(1):68–72.
24. Sérandour AA, Avner S, Mahé EA, et al. Single-CpG resolution mapping of 5-hydroxymethylcytosine by chemical labeling and exonuclease digestion identifies evolutionarily unconserved CpGs as TET targets. Genome Biol. 2016;17:56.
25. Sérandour AA, Avner S, Salbert G. Coupling exonuclease digestion with selective chemical labeling for base-resolution mapping of 5-hydroxymethylcytosine in genomic DNA. Bio Protoc. 2018;8(5):2747.
26. Liu T, Ortiz JA, Taing L, et al. Cistrome: an integrative platform for transcriptional regulation studies. Genome Biol. 2011;12(8):R83.
27. Zhang Z, Chang CW, Goh WL, Sung WK, Cheung E. Centdist: discovery of co-associated factors by motif distribution. Nucleic Acids Res. 2011;39(Web Server issue):W391-399.
28. McLean CY, Bristor D, Hiller M, et al. GREAT improves functional interpretation of cis-regulatory regions. Nat Biotechnol. 2010;28(5):495-501.
29. Stewart SK, Morris TJ, Guilhamon P, et al. oxBS-450K: a method for analysing hydroxymethylation using 450K beadchips. Methods. 2015;72:9-15.
30. Shaffer AL, Emre NC, Lamy L, et al. 2008. IRF4 addiction in multiple myeloma. Nature. 2008;454(7201):226-231.
31. Liu Z, Xu J, He J, et al. A critical role of autocrine sonic hedgehog signaling in human CD138+ myeloma cell survival and drug resistance. Blood. 2014;124(13):2061-2071.
32. Jundt F, Probsting KS, Anagnostopoulos I, et al. Jagged1-induced Notch signaling drives proliferation of multiple myeloma cells.

Blood. 2004;103(9):3511-3515.

33. Cai L, Langer EM, Gill JG, et al. Dual actions of Meis1 inhibit erythroid progenitor development and sustain general hematopoietic cell proliferation. Blood. 2012;120(2):335-346.

34. Lovén J, Hoke HA, Lin CY, et al. Selective inhibition of tumor oncogenes by disruption of super-enhancers. Cell. 2013;153(2):320-334.

35. Peterson TR, Laplante M, Thoreen CC, et al. DEPTOR is an mTOR inhibitor frequently overexpressed in multiple myeloma cells and required for their survival. Cell. 2009;137(5):873-886.

36. Zhou H, Ge Y, Sun L, et al. Growth arrest specific 2 is up-regulated in chronic myeloid leukemia cells and required for their growth. PLoS One. 2014;9(1):e86195.

37. Maupetit-Methouas S, Court F, Bourgne C, et al. DNA methylation profiling reveals a pathological signature that contributes to transcriptional defects of CD34+ CD15- cells in early chronic-phase chronic myeloid leukemia. Mol Oncol. 2018;12(6):814-829.

38. Wang Y, Zhang Y. Regulation of TET protein stability by calpains. Cell Rep. 2014;6(2):278-284.

39. Kutzner A, Pramanik S, Kim PS, Heese K. All-or-(N)One - an epistemological characterization of the human tumorigenic neu-ronal paralogous FAM72 gene loci. Genomics. 2015;106(5):278-285.

40. Gu C, Yang Y, Sompallae R, et al. FOXM1 is a therapeutic target for high-risk multiple myeloma. Leukemia. 2016;30(4):873-882.

41. Giotti B, Chen S-H, Barnett MW, et al. Assembly of a parts list of the human mitotic cell cycle machinery. J Mol Cell Biol. 2018 Nov 17. [Epub ahead of print]

42. Gormally MV, Dexheimer TS, Marsico G, et al. Suppression of the FOXM1 transcriptional programme via novel small molecule inhibition. Nat Commun. 2014;5:5165.

43. Gao J, Aksoy BA, Dogrusoz U, et al. Integrative analysis of complex cancer genomics and clinical profiles using cBioPortal. Sci Signal. 2013;6(269):pl1.

44. Sanders DA, Ross-Ines CS, Beraldi D, Carroll JS, Balasubramanian S. Genome-wide mapping of FOXM1 binding reveals co-binding with estrogen receptor alpha in breast cancer cells. Genome Biol. 2013;14(1):R6.

45. Bruyer A, Maes K, Herviou L, et al. DNMTi/HDACi combined epigenetic targeted treatment induces reprogramming of myeloma cells in the direction of normal plasma cells. Br J Cancer. 2018;118(8):1062-1073.

46. Pawlyn C, Morgan GJ. Evolutionary biology of high-risk multiple myeloma. Nat Rev Cancer. 2017;17(9):543–556.

47. Sawyer JR, Tian E, Heuck CJ, et al. Evidence of an epigenetic origin for high-risk 1q21 copy number alterations in multiple myeloma. Blood. 2015;125(24):3756–3759.

48. Guo C, Zhang X, Fink SP, et al. Ugene, a newly identified protein that is commonly overexpressed in cancer and binds uracil DNA glycosylase. Cancer Res. 2008;68(15):6118-6126.

49. Wang LT, Lin CS, Chai CY, Liu KY, Chen JY, Hsu SH. Functional interaction of Ugene and EBV infection mediates tumorigenic effects. Oncogene. 2011;30(26):2921-2932.

50. Wang X, Sun Q. TP53 mutations, expression and interaction networks in human cancers. Oncotarget. 2017;8(1):624-643.

51. Tshemiak A, Vazquez F, Montgomery PG, et al. Defining a cancer dependency map. Cell. 2017;170(3):564-576.

52. Giotopoulos G, van der Weyden L, Osaki H, et al. A novel mouse model identifies cooperating mutations and therapeutic targets critical for chronic myeloid leukemia progression. J Exp Med. 2015;212(10):1551-1569.

53. Guo Y, Updegraff BL, Park S, et al. Comprehensive Ex vivo transposon mutagenesis identifies genes that promote growth factor independence and leukemogenesis. Cancer Res. 2016;76(4):773-786.

Kinome expression profiling to target new therapeutic avenues in multiple myeloma

Hugues de Boussac,[1] Angélique Bruyer,[1] Michel Jourdan,[1] Anke Maes,[2] Nicolas Robert,[3] Claire Gourzones,[1] Laure Vincent,[4] Anja Seckinger,[5,6] Guillaume Cartron,[4,7,8] Dirk Hose,[5,6] Elke De Bruyne,[2] Alboukadel Kassambara,[1] Philippe Pasero[1] and Jérôme Moreaux[1,3,8]

[1]IGH, CNRS, Université de Montpellier, Montpellier, France; [2]Department of Hematology and Immunology, Myeloma Center Brussels, Vrije Universiteit Brussel, Brussels, Belgium; [3]CHU Montpellier, Laboratory for Monitoring Innovative Therapies, Department of Biological Hematology, Montpellier, France; [4]CHU Montpellier, Department of Clinical Hematology, Montpellier, France; [5]Medizinische Klinik und Poliklinik V, Universitätsklinikum Heidelberg, Heidelberg, Germany; [6]Nationales Centrum für Tumorerkrankungen, Heidelberg , Germany; [7]Université de Montpellier, UMR CNRS 5235, Montpellier, France and [8] Université de Montpellier, UFR de Médecine, Montpellier, France

ABSTRACT

Multiple myeloma (MM) account for approximately 10% of hematological malignancies and is the second most common hematological disorder. Kinases inhibitors are widely used and their efficiency for the treatment of cancers has been demonstrated. Here, in order to identify kinases of potential therapeutic interest for the treatment of MM, we investigated the prognostic impact of the kinome expression profile in large cohorts of patients. We identified 36 kinome-related genes significantly linked with a prognostic value to MM, and built a kinome index based on their expression. The Kinome Index (KI) is linked to prognosis, proliferation, differentiation, and relapse in MM. We then tested inhibitors targeting seven of the identified protein kinases (PBK, SRPK1, CDC7-DBF4, MELK, CHK1, PLK4, MPS1/TTK) in human myeloma cell lines. All tested inhibitors significantly reduced the viability of myeloma cell lines, and we confirmed the potential clinical interest of three of them on primary myeloma cells from patients. In addition, we demonstrated their ability to potentialize the toxicity of conventional treatments, including Melphalan and Lenalidomide. This highlights their potential beneficial effect in myeloma therapy. Three kinases inhibitors (CHK1i, MELKi and PBKi) overcome resistance to Lenalidomide, while CHK1, PBK and DBF4 inhibitors re-sensitize Melphalan resistant cell line to this conventional therapeutic agent. Altogether, we demonstrate that kinase inhibitors could be of therapeutic interest especially in high-risk myeloma patients defined by the KI. CHEK1, MELK, PLK4, SRPK1, CDC7-DBF4, MPS1/TTK and PBK inhibitors could represent new treatment options either alone or in combination with Melphalan or IMiD for refractory/relapsing myeloma patients.

Correspondence:

JEROME MOREAUX,
jerome.moreaux@igh.cnrs.fr

Introduction

MM is the second most common hematological disorder,[1] and is characterized by the clonal accumulation of malignant plasma cells in the bone marrow.[2] MM is a genetically and clinically heterogeneous disease and genome sequencing studies have recently revealed considerable heterogeneity and genomic instability, a complex mutational landscape and a branching pattern of clonal evolution.[3,4]

Novel agents have been developed in MM including the proteasome inhibitors bortezomib and carfilzomib, and the immunomodulatory drugs thalidomide, Lenalidomide and pomalidomide.[5] However, patients invariably relapse after multiple lines of treatment, with shortened intervals in between relapses, and finally

become resistant to any treatment, resulting in loss of clinical control over the disease. It thus remains an unmet need for new therapeutic approaches to improve treatment of MM patients.

Protein kinases are key actors in various cancers where they are involved in proliferation, survival, migration but also drug resistance.[6] Protein kinases have been a potent source of targets for cancer treatment with inhibitors already approved or in clinical evaluation in numbers of malignancies. Kinases represent interesting druggable targets in MM. Indeed, whereas major signaling pathways have been studied in myeloma, they only represent a small proportion of the whole kinome.[7]

In a first study, Tiedemann and colleagues[8] used a high-throughput systematic RNA interference approach to investigate kinome expression in human myeloma cell lines (HMCL) and identified potential new targets for MM therapy. Here, we investigated the kinome expression profiling in large cohorts of MM patients to identify key targets and new synergistic combinations with conventional treatment. We used a list of kinases or kinase-related genes[9] and investigated the prognostic impact of the kinome expression profile in MM. We identified 36 kinases significantly involved in patient's outcome in three independent cohorts and further analyzed the potential impact of selected available kinases inhibitors in HMCL and primary human myeloma cells. We thus provide a list of protein kinases representing potent therapeutic targets for high-risk MM patients and propose new synergistic combinations of kinase inhibitors and conventional MM treatment.

Methods

Gene expression profiling and statistical analyses

We used the gene expression profiling (GEP) from three independent cohorts constituted of MM cells (MMC) purified from untreated patients: the Heidelberg-Montpellier cohort of 206 patients (ArrayExpress public database under accession number E-MTAB-362)[10,11] the UAMS-TT2 cohort of 345 patients from the University of Arkansas for Medical Sciences (UAMS, Little Rock, AR, USA; accession number GSE2658),[12] and the UAMS-TT3 cohort of 158 patients (E-TABM-11,[38] accession number GSE4583).[13] Gene expression data were normalized with the MAS5 algorithm and processing of the data was performed using the webtool genomicscape (http://www.genomicscape.com).[14] STRING webtool (https://string-db.org) was used to evaluate interconnections between genes and analyzed the enriched pathways. Cluster (v2.11) and Tree View were used to visualize gene expression data.[15] Univariate and multivariate analysis of genes prognostic for patients' survival was performed using the Cox proportional hazard model.

Multiple myeloma cell lines

HMCL AMO-1 and OPM2 were purchased from DSMZ (Braunschweig, Germany), XG1 and XG21 were obtained as described.[16] HMCL were cultured in RPMI 1640 medium, 10% foetal calf serum (FCS) (control medium). For XG - IL-6 dependent HMCL, 2 ng/mL IL-6 was added. Cells were cultured in 96-well flat-bottom microtiter plates in the presence of a concentration range of selected compounds: AZD7762/CHK1i and OTSSP167/MELKi (Selleck, euromedex), HITOPK032/PBKi, XL413/CDC7-DBF4i, SRPIN340/SRPK1i (Sigma), AZ3146/MPS1i, Centrinone B/PLK4i (Tocris). Cell Titer Glo Luminescent Assay

(Promega, Madison, WI, USA) was used to assess cell viability, and the 50% inhibition (IC50) was determined using GraphPad Prism software (http://www.graphpad.com/scientific-software/prism/).

The 5T33vv cells originated spontaneously in aging C57BL/KaLwRij mice and have since been propagated in vivo by intravenous transfer of the diseased marrow in young syngeneic mice.[17]

Primary multiple myeloma cells

Bone marrow of patients presenting with previously untreated MM (n=5) at the University Hospital of Montpellier was obtained after patients' written informed consent in accordance with the Declaration of Helsinki and agreement of the Institutional Review Board and the Montpellier University Hospital Centre for Biological Resources (DC-2008-417). Primary myeloma cells of patients were cultured with or without graded concentrations of selected inhibitors and MMC cytotoxicity was evaluated using anti-CD138-Phycoerythrin monoclonal antibody (clone B-A38) and CD38-Allophycocyanin (clone-LS198-4-3) (Beckman-Coulter) as described.[11] In each culture group, viability (trypan blue) and cell counts were assayed and the percentage of CD138+ viable myeloma cells was determined by flow cytometry.

Additional information concerning the methodology are included in the Online Supplementary Materials and Methods.

Results

Identification of 36 kinome-related targets linked to prognosis in three independent MM cohorts

Considering the crucial role played by protein kinases in pathologies, including MM, we first aimed to identify kinome-related genes associated with prognostic value in MM. A list of 661 genes extracted from the literature, representing 661 kinases or kinase-related genes[9] (Online Supplementary Table S1) were thus tested for their prognostic value in the Heidelberg-Montpellier cohort (n=206) using the Maxstat algorithm.[10,11] Among the 661 genes investigated, the expression of 104 demonstrated a significant prognostic value after Benjamini Hochberg multiple testing correction. We searched to validate the prognostic value of the 104 selected kinases in two other independent cohorts of newly diagnosed patients (UAMS-TT212 and UAMS-TT313) and defined a final list of 36 kinases with significant prognostic value in the three cohorts (Figure 1A and Online Supplementary Table S2). Among the 36 kinase or kinase-related genes identified, eight of them were associated with a favorable prognosis (AZU1; CDKN1A; DDR1; HK3; MAP4K2; MERTK; PRKCSH; TESK2), while 28 demonstrated a poor prognostic value (AURKA; BUB1; BUB1B; CDC7; CDKN2C; CDKN3; CHEK1; CKS1B; CKS2; DBF4; DUSP10; HK2; PI4K2B; MAP2K6; MELK; NEK2; NTRK3; PAK2; PBK; PFKP; PLK4; PTPRG; RPRD1A; SRPK1; SRPK2; STK39; TK1; TTK).

Analysis of their involvement in cellular physiology highlighted the cell cycle as the top Kyoto Encyclopedia of Genes and Genomes (KEGG) pathway (Figure 1B), and string network of the 36 genes showed highly interconnected proteins particularly for those with a role in cell cycle (Figure 1C).

Hierarchical clustering underlined a spread expression of the genes among MM patients, except for a cluster composed of 14 kinases related to proliferation/mitosis (CDKN2C; CDC7; CDKN3; BUB1B; MELK; BUB1; AURKA; NEK2; PBK; TTK; CHEK1; PLK4; CKS1B and

A

B

C

String network
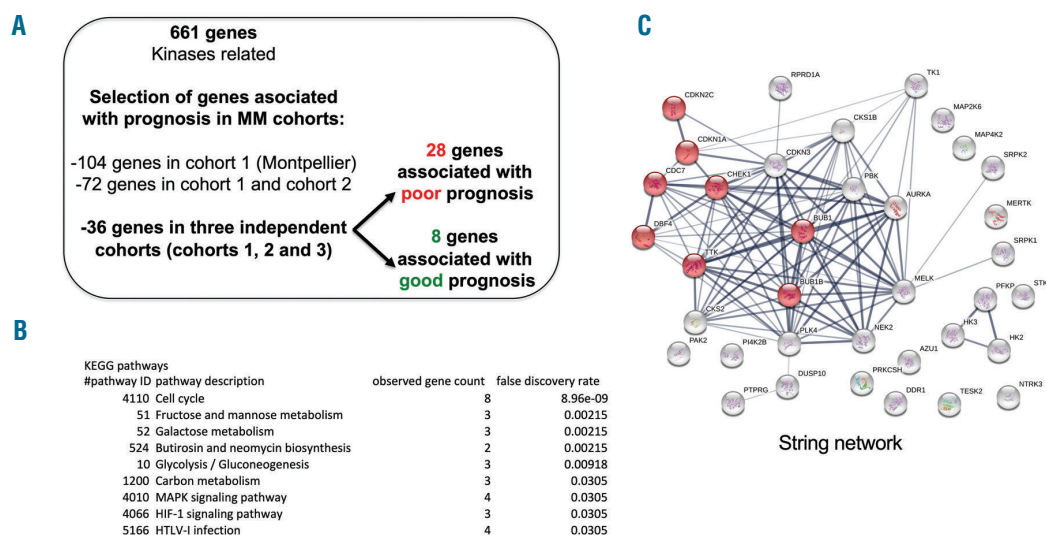
Figure 1. Identification of 36 kinome related probe sets linked to prognosis in three independent cohorts of newly diagnosed multiple myeloma patients. (A) Workflow analysis used to identify kinases with gene expression associated with a prognostic value in muliple myeloma (MM). Cohort 1: HM-Montpellier cohort, Cohort 2: UAMS-TT2, Cohort 3: UAMS-TT3. Poor prognosis means that high gene expression is associated with a significant negative outcome, while good prognosis means that high gene expression is linked to a better outcome (B) Reactome molecular signatures significantly enriched in the kinases related to a poor outcome in MM (C) String network of the 36 identified kinases. Red color represents cell cycle related kinases.

TK1), which exhibited a specific pattern of overexpression in a subgroup of patients (*Online Supplementary Figure S1*). Interestingly 10 of these 14 kinases are part of the CIN-SARC signature, associated with chromosomal instability in many cancer types including multiple myeloma.[19]

Building a Kinome Index (KI) linked to the patient's outcome

We next combined the prognostic information of the 36 identified kinases in a GEP-based a KI. This KI is the sum of the standardized expression value of the 28 kinase genes associated with a poor prognostic value minus the sum of the standardized expression value of the eight genes associated with a favorable prognosis (*Online Supplementary Figure S2*). Maxstat algorithm segregated the HM cohort into two groups with 31% of the patients with a KI>2.1 and 69% of the patients with a KI≤2.1 with a maximum difference in overall survival (OS) (Figure 2A). Patients with KI>2.1 have a median OS of 50.6 months *versus* not reached for patients with KI≤2.1 (*P*=1,7E-05)) and a median event free survival (EFS) of 20.1 months *versus* 40.6 months (*P*=4,5E-05) in the HM cohort (Figure 2B). The prognostic value of the KI was validated in the two additional independent UAMS-TT2 and TT3 cohorts for OS and EFS (*Online Supplementary Figure S3*).

KI is significantly higher in the proliferation (PR) and MAF MM molecular subgroups[20] known to be associated with a poor outcome (*P*<8E-18). Furthermore, higher KI was associated with the proliferating stages of B-cell to plasma-cell differentiation including activated B cells, pre-plasmablasts and plasmablasts compared to non-proliferating memory B cells and mature plasma cells (Figure 2D). This observation corroborates the association of the 36 kinases to cell cycle (Figure 1B) and the PR subgroup (Figure 2C), as well as the well-known association of kinase activation with proliferation. In addition, KI values increased with disease progression from normal bone marrow plasma cells (BMPC) to MM cells with a homoge-

neous index between the different cohorts tested (HM, TT2 and TT3) and HMCL (*P*<0.01) (Figure 2D). Finally, we tested the KI in a cohort of 23 patients with paired samples at diagnosis and relapse, and identified a significant increase of the KI at relapse (*P*=4E-04) (Figure 2E). Altogether these observations further highlight that the selected kinases comprising markers of genomic instability,[19] could represent new potential therapeutic targets for high-risk MM patients.

KI kinases' inhibition leads to MM cell death *in vitro*

According to our *in silico* analysis, the 36 genes demonstrated an outstanding connection with MM physiopathology and prognosis. Thus, we next assessed selected kinases of interest for their individual therapeutic potential on MM cells using specific inhibitors. For that purpose we first excluded the eight genes associated with favorable prognosis, and analysed the 28 remaining kinases for their link with MM in the literature. Three genes whose connections with MM have already been widely studied (more than five references identified in PubMed) (*CKS1B*[21]; *AURKA*[22]; *CDKN2C*)[23] were then also excluded, and we finally selected the seven kinases (*PBK; CHEK1; MPS1/TTK; CDC7-DBF4; MELK; PLK4; SRPK1*) that had commercially available specific inhibitors at the time of the study (Figure 3A). It has to be note that all selected kinases are involved in the mitotic checkpoint (*PBK; MPS1/TTK; MELK; PLK4*) or replicative stress response (*CHK1; CDC7-DBF4; SRPK1*), and the expression of all the selected kinases is individually correlated to high-risk KI-defined MM subgroup (*Online Supplementary Figure S4*).

Then we assessed the kinase inhibitors for their potential anti-myeloma effect on four HMCL (AMO-1, OPM2, XG-1 and XG-21). Remarkably all tested drugs led to a significant decrease in HMCL viability and cell growth, with an IC50 indicated in Figure 3B and *Online Supplementary Figure S5*. We next investigated how the tested drugs impact cell death in the AMO1 HMCL using two drugs
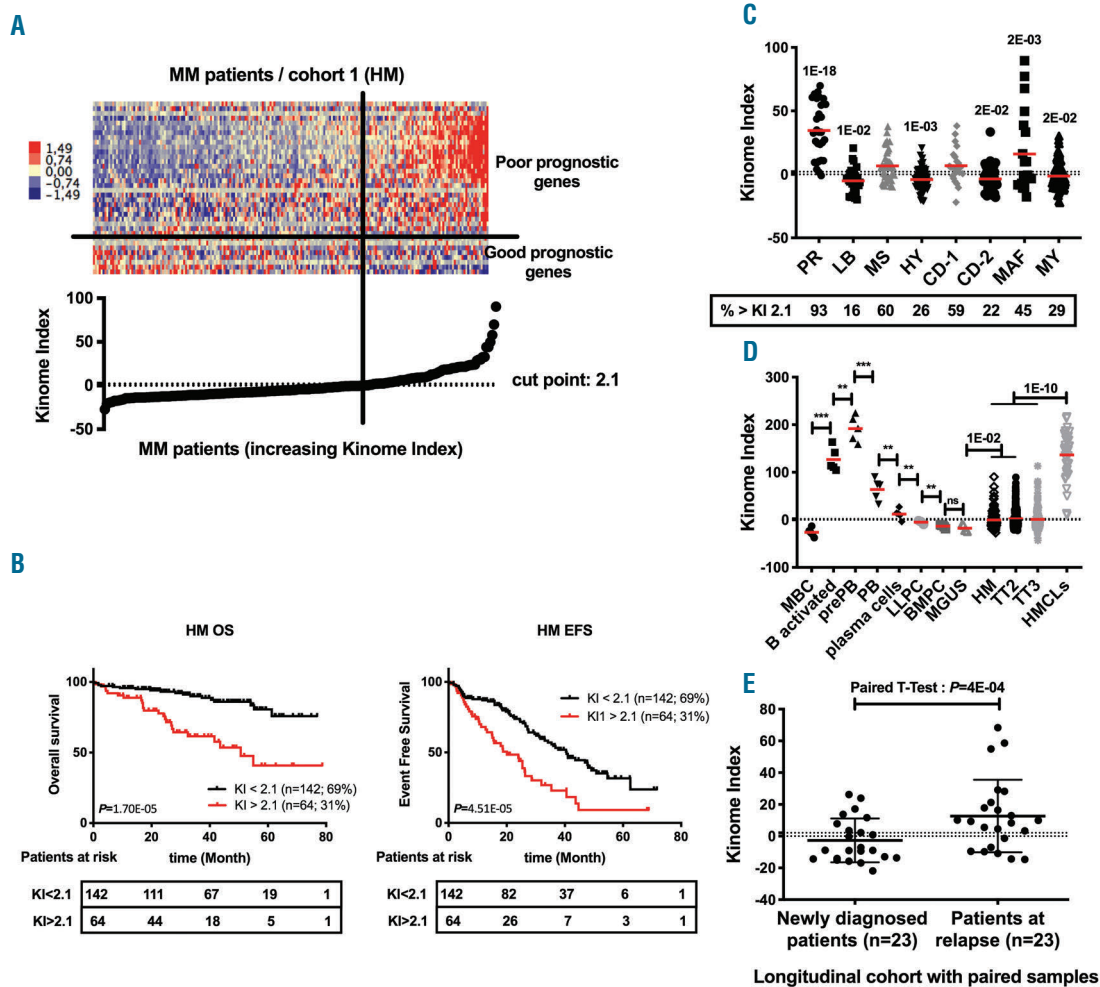
Figure 2. Prognostic value of the Kinome Index in multiple myeloma. (A) Clustergram in the 206 HM cohort's patients (206 patients) of the 36 genes signal used to build the Kinome Index (KI). Signals are displayed from low (deep blue) to high (deep red) expression. (B) Patients of the HM cohort were ranked according to increased KI and a maximum difference in OS was obtained with KI of 2.1 splitting patients into high-risk (31%) and low-risk (69%) groups (OS and EFS). (C) The KI was computed for MMC of patients belonging to the subgroups of the University of Arkansas for Medical Science (UAMS) molecular classification of MM, using UAMS-TT2 cohort. CD1: cyclin D1 and cyclin D3; CD2: cyclin D1 and cyclin D3; HY: hyperdiploid; LB: low bone disease; MF: c-MAF and MAFB; MS: MMSET; MY: myeloid; PR: proliferation; D) KI is increased in Pre-plasmablasts characterized by high proliferation during normal B- to PC-differentiation. MBC: memory B cells (n=5); prePB: pre-plasmablast (n=5); PB: plasmablast (n=5); LLPC: long live plasma cells (n=5); BMPC: bone marrow plasma cells (n=5); HM MM cohort (n=206); TT2 MM cohort (n=345); TT3 MM cohort (n=158); HMCL: human myeloma cell lines (n=44). (E) KI is significantly higher at relapse compared to diagnosis in a cohort of 23 paired patient's samples (paired T-Test). *P*-value: *<0.05; **<0.01; ***<0.001.

concentrations around the calculated IC50. As shown in Figure 3C, all drugs induced apoptosis as measured by the dramatic increase of annexin V and cleaved PARP staining following treatment. Interestingly, this effect was not observed at the lower concentration used, thus confirming our previous observation of a dose-dependent efficacy of the drugs. We then tested the ability of the kinase inhibitors to perturb cell-cycle progression. CHK1i, MELKi and CDC7-DBF4i are associated with a significant blockade of MM cells in S phase, while PLK4i and MPS1i induced a significant accumulation in G0/G1 in AMO1 HMCL (*Online Supplementary Figure S6A-B*). Thus, the different inhibitors tested here induced both apoptosis and deregulate MM cell proliferation. We also investigated the effect of phosphatase receptor type γ (PTPRG) depletion using siRNA. PTPRG was shown to be spiked and mutated in MM.[24] Depletion of PTPRG results in a significant decrease in MM cell growth together with apoptosis induction (*Online Supplementary Figure S15*).

Next, we focused on the three inhibitors that induced MM cells toxicity at nanomolar concentration (CHK1i; MELKi; PLK4i) to validate their therapeutic interest using primary MM cells from patients co-cultured with their bone marrow microenvironment. Remarkably, all three tested drugs significantly reduced the number of tumor cells without toxicity for the bone marrow microenvironment (Figure 4A and *Online Supplementary Figure S6C-E*).

In addition, in order to demonstrate the capability of preclinical studies for the three selected inhibitors, we tested them in 5T33v cells, a murine model of MM.[17] As shown in Figure 4B, CHK1i and MELKi demonstrated similar efficiency while PLK4i was less effective in influencing 5T33vv cell viability compared to human myeloma cells.

A Poor prognostic: 28 genes

B

		AMO1	XG1	XG21	OPM2
CHK1i/AZD7762	IC50 nM	136	95	210	116
	IC20 nM	82	64	139	68
MELKi/OTSSP167	IC50 nM	8.2	12.5	2.2	15.7
	IC20 nM	5.4	7.8	1.0	7.0
PLK4i/Centrinone B	IC50 nM	421	226	1392	340
	IC20 nM	24	4	127	27
PBKi/HI-TOPK	IC50 µM	5.1	4.4	4.1	5.0
	IC20 µM	3.9	2.8	3.1	3.3
CDC7-DBF4i/XL413	IC50 µM	19.9	4.2	30.3	24.5
	IC20 µM	9.4	1.3	13.7	7.0
MPS1i/AZ3146	IC50 µM	2.6	1.2	3.0	1.9
	IC20 µM	1.5	0.8	1.5	1.1
SRPK1i/SRPIN340	IC50 µM	43	30	26	33
	IC20 µM	30	17	15	20

C

Figure 3. Selected kinases inhibition induces human myeloma cell toxicity. (A) Selection of seven kinases for biological investigations based on citation report in Pubmed and the availability of inhibitors. (B) IC50 of the different drugs in four human myeloma cell lines (HMCL), and calculated IC20 for the AMO1 HMCL; C) Kinase inhibitors induce apoptosis (annexin V and PARP cleavage) in AMO1 MM cell line at concentrations close to the calculated IC20 and IC50. Annexin, and PARP cleavage, were monitored by flow cytometry after four days of treatments. Results are representative of four independent experiments. Statistical significance was tested using a Student T-Test for pairs. *P*-value: *<0.05; **<0.01; ***<0.001.

Finally, using a proteome array we examined the pathways involved in apoptosis and cell cycle following treatments in AMO1 cells and in OPM2 cells that are p53 mutated.[25] For all three tested treatments we observed in AMO1, but as expected not in OPM2, an increased p53 phosphorylation on S15 (DNA damage response), S46 (apoptosis) and S392 (growth inhibition) (Figure 4C and *Online Supplementary Figure S7*). Other apoptotic markers including caspase 3 cleavage, p27, cytochrome C, HSP60, TRAIL, BAD and BCL-X were also induced. Upon CHK1i treatment in AMO1, we also observed a decrease in Claspin and Survivin levels, two proteins involved in cell cycle and replication that have been linked to the CHK1 pathway. Indeed Claspin is a co-activator of CHK1,[26,27] whereas Survivin degradation depends on the XAF1/XIAP1[28] a pro-apoptotic complex involved in CHK1 degradation.[29] Those effects were not observed in OPM2 cells although we observed an increase of the pro-apoptotic proteins Diablo and FADD and a decreased in the proliferation related proteins TOR and P70 S6 kinases.[30] Heterogeneity of the cell lines regarding the p53 status

could explain these differences. However, in both tested cell lines anti-, and pro-apoptotic signals were deregulated. Altogether, these data demonstrate the pro-apoptotic and anti-proliferative effects of these three molecules in MM cells and highlight the potential of these kinases as new therapeutic targets in high-risk MM patients.

Conventional MM therapies are potentialized by selected kinase inhibitors

We then investigated the therapeutic interest of combining these kinase inhibitors with therapeutic drugs commonly used in MM (e.g. Melphalan, Lenalidomide, Velcade). Combining sub-lethal IC20 for all the kinase inhibitors with increasing concentrations of standard agents allowed us to identify a significant potentialization of Melphalan toxicity by CHK1, MELK, PBK and CDC7-DBF4 inhibitors in at least two out of the four HMCL investigated. However, no significant effect on the calculated IC50 was noticed for the co-treatment of Melphalan with PLK4, MPS1 and SRPK1 inhibitors with a potential calculated antagonism of the two molecules (Figure 5A
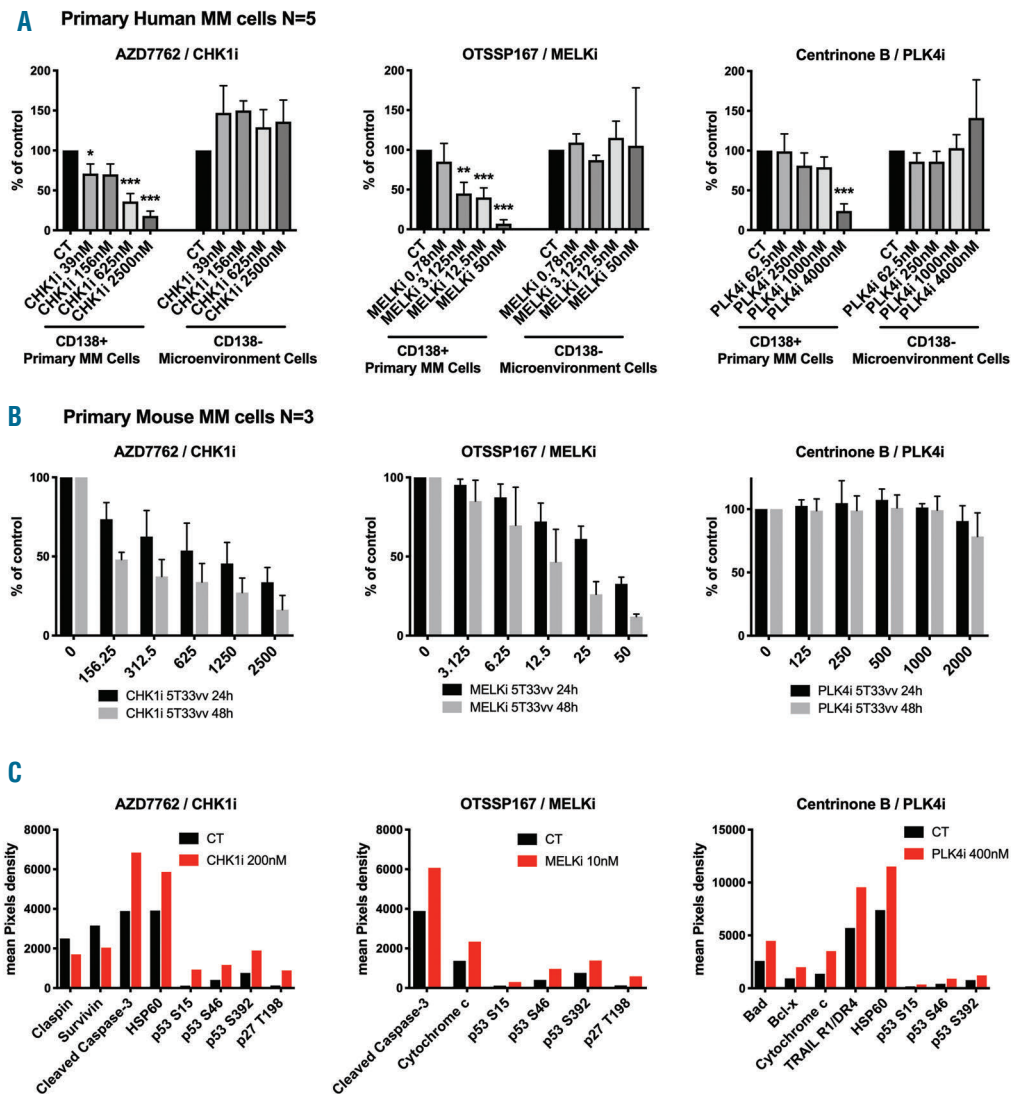
Figure 4. Selected kinases inhibition induces human primary multiple myeloma (MM) cell death and toxicity on 5TMM murine cells. A) Mononuclear cells from five patients with MM were treated or not with CHK1i, MELKi and PLK4i. At day 4 of culture, the viability and total cell counts were assessed and the percentage of CD138+ viable plasma cells and bone marrow non-myeloma cells were determined by flow cytometry. Results are median values of the numbers of myeloma cells in the culture wells. Results were compared with a Student T-Test for pairs. B) Murine myeloma cell (5T33vv) viability was monitored by CTG after 24 and 48 hours treatment with CHK1i, MELKi and PLK4i. Results are representative of three independent experiments C) Apoptosis and Signaling pathways targeted by CHK1i, MELKi and PLK4i. Proteins accumulations were monitored after 48h treatment on AMO1 human myeloma cell lines (HMCL) using proteome profiler array. Relative amount was calculated as the mean of pixel density. *P*-value: *<0.05; **<0.01; ***<0.001.

and *Online Supplementary Figure S8A*). For the immunomodulatory agent Lenalidomide, no significant effect was observed with the tested combinations in two Lenalidomide resistant HMCL: XG1 and XG21. However, the effect of Lenalidomide was significantly potentiated in two other HMCL (AMO1 and OPM2) in combination with the CHK1, MELK or PBK inhibitors. Remarkably, addition of CHK1i, MELKi or PLK4i could overcome Lenalidomide resistance of the AMO1 cell line (Figure 5B and *Online Supplementary Figure S8B*). Conversely, we could not observe any synergy or even additivity for the co-treatment with Velcade, regardless of the cell line tested or the kinase inhibitor used (*Online Supplementary Figure S9A*). Altogether these results demonstrate the therapeutic

interest of CHK1i, MELKi, CDC7-DBF4i and PBKi in combination with Melphalan and IMiDs in MM (*Online Supplementary Figure S9B*).

To characterize the mechanisms involved, we monitored apoptosis after co-treatments of kinases inhibitors with Melphalan or Lenalidomide in AMO1 and OPM2 cells. A sub-lethal dose of Melphalan or Lenalidomide was used in combination with the calculated IC20 of the kinase inhibitors. CHK1i, MELKi and CDC7-DBF4i increased cell death via apoptosis when cells were co-treated with Melphalan or Lenalidomide. In addition, PLK4i co-treatment only potentialized cell death with Lenalidomide (Figure 6A and *Online Supplementary Figure S10A*). As expected from cell growth analyses, SRPK1i and
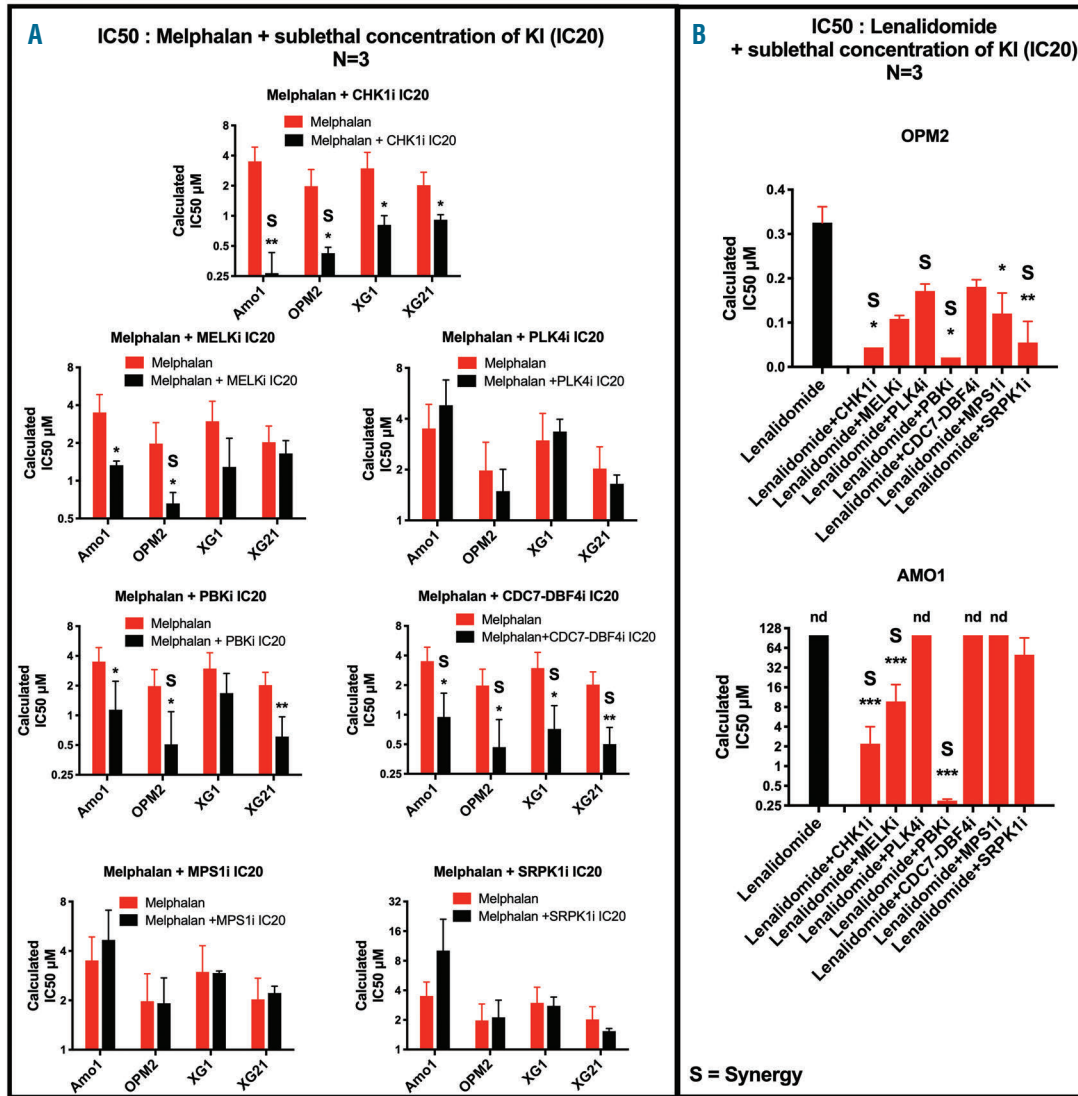
Figure 5. Kinase inhibitors enhance the sensitivity of multiple myeloma cells to conventional treatments. Human myeloma cell lines (HMCL) were cultured for four days in 96-well flat-bottom microtiter plates in RPMI 1640 medium, 10% fetal calf serum, 2 ng/mL IL-6 culture medium (control) and graded Melphalan concentrations (A) or Lenalidomide concentrations (B) in presence or absence of IC20 of CHK1i, MELKi, PBKi, CDC7-DBF4i, SRPKi, MPS1i and PLK4i. IC50 were calculated after viability assessment by CellTiter-Glo® Luminescent Cell Viability Assay. Results are representative of three independent experiments. *P*-value: *<0.05; **<0.01; ***<0.001. S: significant synergy calculated by the method of Chou and Talalay.

MPS1i did not increase cell death (*Online Supplementary Figure S9C and S10A*). Next, we monitored DNA damage by measuring levels of the DNA double-strand break (DSB) marker γH2AX after the different co-treatments. As expected, Melphalan treatment alone, even at the sublethal dose, increased the level of γH2AX, while Lenalidomide did not demonstrate any effect (Figure 6B and *Online Supplementary Figure S10B*). However, among all the combinations tested, only MELKi significantly potentialized Melphalan-induced DNA damage in AMO1 but not in OPM2 cells. Interestingly MELKi, CDC7-DBF4i and SRPK1i alone induced DSB as monitored by γH2AX levels (Figure 6B and *Online Supplementary Figure S9D*) although it should be noted that high concentrations of the CHK1 inhibitor AZD7762 or MELK inhibitor

OTSSP167 induced early DSB that progressively decrease as monitored by measuring γH2AX in AMO1 after 24 and 48 hours of treatment (*Online Supplementary Figure S11*). Thus, the significant potentialization of Melphalan and Lenalidomide toxicity by CHK1i, MELKi, CDC7-DBF4i and SRPK1i appears to be due to an increased induction of apoptosis, and not to an increase of DNA damage or cell cycle deregulation (*Online Supplementary Figure S12*).

According to these results, we investigated the therapeutic interest of kinases inhibitors to overcome Melphalan resistance using Melphalan resistant (Mres) XG7 and XG2 cell lines (Figure 7A and *Online Supplementary Figure S13A*). Interestingly, while no clear differences could be observed for the IC50 of MELKi, CHK1i, PBKi and MPS1i in the Mres and sensitive (WT)
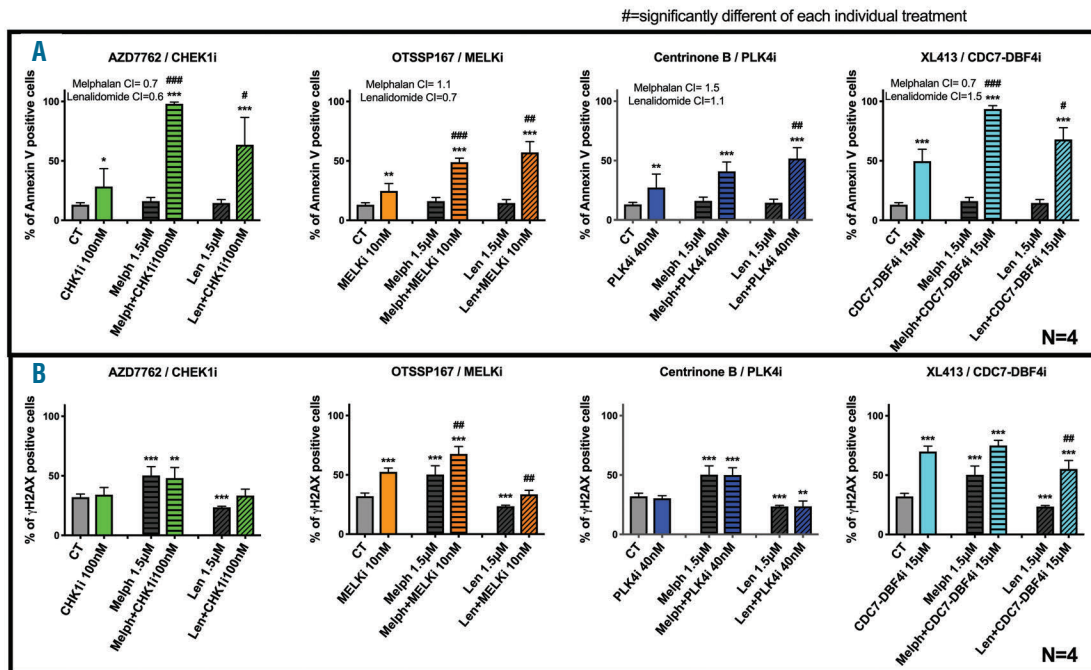
Figure 6. Conventional multiple myeloma therapies are potentialized by selected kinase inhibitors. Co-treatment with selected kinase inhibitors at IC20 and Melphalan or Lenalidomide. (A) Apoptosis induction was analyzed using Annexin V APC staining by flow cytometry. (B) DNA damage induction was analyzed measuring γH2AX levels; Results are representative of four independent experiments. CI: calculated combination index. Statistical significance was tested using a Student T-Test for pairs. *P*-value: *<0.05; **<0.01; ***<0.001. #Significantly different of each individual treatment.

cell lines, PLK4i and CDC7-DBF4i demonstrated a significantly higher toxicity in the XG7 Mres cell line (Figure 7B) but not in XG2 Mres HMCL (*Online Supplementary Figure S13B*). Sublethal IC20 of CHK1i, PBKi and CDC7-DBF4i overcame Melphalan resistance of both cell lines tested (Figure 7C and *Online Supplementary Figure S13C*), while the other inhibitors tested did not show a significant effect. It should however be underlined that the inhibitors alone are active on both resistant and sensitive cell lines as shown in Figure 7B and *Online Supplementary Figure S13B*. Thus, our results highlight the therapeutic interest of CHK1i, MELKi, CDC7-DBF4i and SRPK1i used alone or in combination with conventional therapies, even in case of acquired resistance.

Discussion

Here we identified 36 kinases associated with a prognostic value in three independent cohorts of MM patients, allowing the creation of a kinase-related gene expression profile (GEP) risk score KI. Among them, CHK1, CDC7-DBF4, and MELK were identified as being of therapeutic interest in MM.[31–33] PLK4, SRPK1, MPS1/TTK and PBK represent new therapeutic targets in MM. Using inhibitors of these seven kinases, we validated their therapeutic interest to target MM cells alone or in combination with conventional therapies. In addition, we also highlighted a list of protein kinases for which no inhibitor is currently available and which represent promising new therapeutic targets at least in MM.

Our approach differs from a previous study exploiting a

RNAi library to target the human kinome in six myeloma cell lines.[8] Surprisingly, only one kinase, AURKA, was selected in both studies. This discrepancy could reflect the fact that our study relies on the analysis of primary MM cells from patients and not on HMCL as in previous studies. Since a large number of kinase (135/661) are differentially expressed between primary MM cells and HMCL (*Online Supplementary Table S3*), we believe that our study provides a relevant analysis of the protein kinases important for the survival of MM cells.

Our KI is strikingly enriched in kinases involved in the progression through mitosis (PBK, PLK4, MELK, MPS1) and in the replication stress response (CHK1, CDC7-DBF4, SRPK1). These kinases are also enriched in proliferation[34] and proliferation GEP-based signatures, which represent also powerful risk factors in MM.[10,35] The 36 genes of the KI only have a limited overlap with these signatures indicating that KI does not simply reflect a higher cell proliferation index.

Among the inhibitors against targets validated here (CHK1, MELK, PLK4, SRPK1, CDC7-DBF4, MPS1/TTK and PBK), the CHK1 inhibitor AZD7762 was of particular interest due to its ability to act alone or in combination with other drugs. Our results differ from two earlier studies reporting a limited toxicity of AZD7762 on HMCL at doses equivalent of our calculated IC50, but at high Melphalan concentration, when combined with this drug.[31,36] These discrepancies could reflect differences in culture conditions, as in our hands, the drug sensitivity of HMCL depended exquisitely on the confluency status at seeding and on the treatment protocol. Furthermore, we validated the therapeutic interest of CHK1i using primary

MM cells from patients co-cultured with their bone marrow microenvironment, without detecting significant toxicity on non-myeloma cells. Our observations greatly implement the previous studies, either on the activity of the molecule alone, in combination with Melphalan and IMiD, or to overcome MM drug resistance.

The maternal embryonic leucine zipper kinase (MELK) inhibitor OTSSP167 also demonstrated therapeutic interest. MELK is linked to multiple solid cancer types,[37] and recently two groups showed the potential of this inhibitor in MM.[33,38] In addition to their work, we demonstrated the synergy between OTSSP167 with Melphalan and
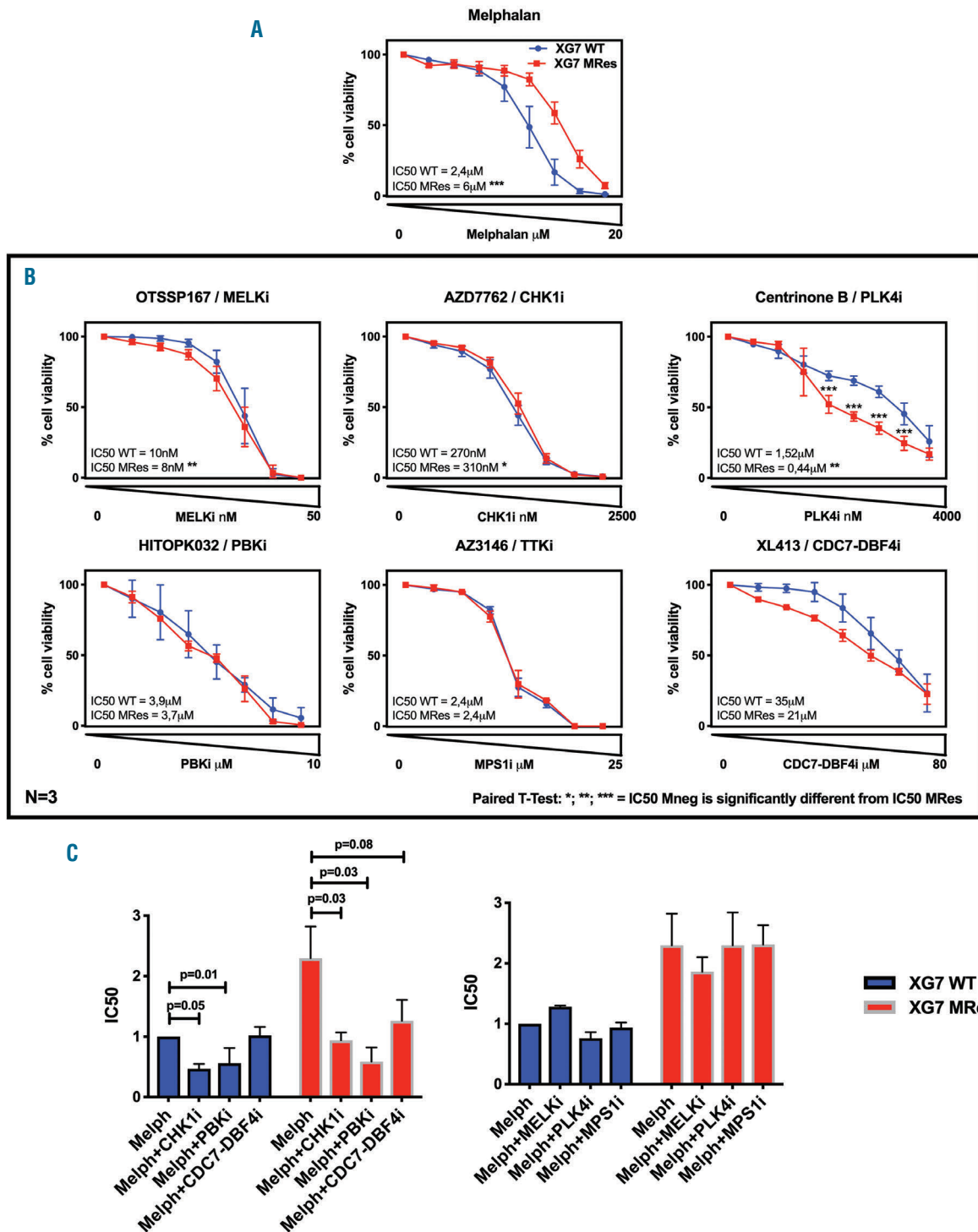
Figure 7. Kinase inhibitors overcome resistance of Melphalan resistant multiple myeloma cells. (A) Dose response curves of XG7 WT and XG7 MRes cell lines. (B) XG7 WT and XG7 MRes HMCL were cultured for 4 days in 96-well flat-bottom microtiter plates in RPMI 1640 medium, 10% fetal calf serum, 2 ng/mL IL-6 culture medium (control) and graded Melphalan concentrations and selected kinase inhibitors at IC20. At day 4 of culture, the viability was assessed by CellTiter-Glo® Luminescent Cell Viability Assay. Data are mean values ±SD of three independent experiments. *P*-value: *<0.05; **<0.01; ***<0.001 using a student T-Test for pairs. Mres: Melphalan resistant; SD: standard deviation. WT: wild-type.

Lenalidomide and its interest to overcome Melphalan drug resistance. Interestingly, OTSSP167 off-targets' BUB1 and TTK/MPS1[39] are also part of our 36 selected kinases, which further highlight the potential of this inhibitor to target MM cells.

Our study represents the first attempt to investigate the therapeutic potential of PLK4, CDC7-DBF4, MPS1, PBK and SRPK1 inhibitors in MM, even though their effect on other cancer cell types has already been established.[40-44] All inhibitors did not demonstrate comparable effects, but they all showed MM cell toxicity when used alone. Furthermore, the toxicity of PLK4i was validated on primary MM cells, and synergy in MM apoptosis induction was also identified for PLK4i and CDC7-DBF4i when combined with Melphalan and Lenalidomide.

Remarkably, all the tested inhibitors (CHK1i, MELKi, PLK4i, SRPK1i, CDC7-DBF4i, MPS1/TTKi and PBKi) demonstrated anti myeloma activity by reducing viability and inducing cellular death of MM cells. Interestingly, a significant correlation between the KI and response to PLK4i was identified (*Online Supplementary Figure S15*). The analysis of the potential mechanisms involved revealed that both cell cycle arrest and apoptosis contributed to the observed phenotype. Both intrinsic and extrinsic apoptosis pathways were involved for AZD7762, OTSSP167 and Centrinone B. Interestingly, these three

inhibitors induced p53 pathway in AMO1, although we believe that the effect of these molecules is not exclusively p53 dependent since they similarly demonstrated significant toxicity in p53 proficient (XG1, OPM2) or p53 deficient (XG21, AMO1) MM cell lines. Though, considering AZD7762, this observation is surprising since several studies noted that CHK1 inhibitors were particularly toxic for p53-deficient cells[45] probably *via* the simultaneous abrogation of the G2 (CHK1) and G1 (p53) checkpoints, and initiation of mitotic catastrophe.[31] However, CHK1 can also suppress death pathways and therefore inhibition of CHK1 can reactivate apoptosis in a p53-independent fashion via caspase 2 activation, mitochondrial outer membrane permeabilization and cytochrome C release.[46] As cytochrome C induction was observed for the three inhibitors tested, this last mechanism could explain the p53-independent effect, which implements considerably its therapeutic interest in MM, where p53 status is highly linked to prognosis.

Here, we demonstrated that low doses of CHK1, MELK, PBK and CDC7-DBF4 inhibitors were able to synergize or even reverse Melphalan resistance. This is very important considering that virtually all MM patients eventually relapse and develop drug resistance. These kinases have all been shown to decrease DNA damage tolerance,[47-50] which could explain this observation. Similarly, CHK1, MELK and

Kinome expression profiling to target new therapeutic avenues in Multiple Myeloma

709 Human MM samples

Gene expression profiles

Kinome Analysis

36 Clinically relevant kinases → **potential therapeutic targets**

Kinome index   Therapeutic marker★

Sensitivity   Resistance

Kinase inhibitors

Targeting MM
7 new kinases related targets (available inhibitors) :
CDC7-DBF4; CHEK1; MELK; MPS1; PBK/TOPK; PLK4; SRPK1

➤ MM cell cytotoxicity

➤ Synergy with Melphalan and IMiD

➤ Overcome resistance to Melphalan and IMiD

Figure 8. Kinome expression profiling to define new therapeutic targets in multiple myeloma. The prognostic impact of the kinome expression was challenged in three independent cohorts of newly-diagnosed multiple myeloma (MM) patients representing 709 patients. 36 clinically relevant genes were selected as potential therapeutic targets, and were used to create a Kinase Index (KI) with a strong prognostic value. Among the 36 selected kinases, we validated seven kinases as new therapeutic targets in MM, as their related inhibitors presented therapeutic interest in MM for personalized treatments.

PBK inhibitors could overcome Lenalidomide resistance. Even if these observations are promising, additional *in vivo* experiments are needed to confirm the potential and elucidate the mechanistic roles of these kinases in Lenalidomide and Melphalan resistance reversion.

The development of the KI could be used to identify high-risk patients that could benefit from treatment with selected kinases inhibitors. Developing the KI, we also identified kinases that have already been linked to MM physiopathology including CKS1B,[21] AURKA,[22] CDKN2C,[23] NEK2[51] and BUB1B.[52] In addition, we also identified a number of kinases (PAK2, HK2, CDC7, BUB1, CKS2, TK1, MAP2K6, NTRK3, STK39, PTPRG, CDKN3, DUSP10, PFKP, SRPK2, RPRD1A, PI4K2B) without a clear or documented connection with MM, but which are considered as potential targets in other cancers. According to the high degree of heterogeneity of the disease, we look forward to the development of new inhibitors targeting these kinases, which could be of therapeutic interest in MM.

To date, no kinase inhibitors have received the approval of the Food and Drug Administration for the treatment of MM.[7] Our study demonstrates that kinase targeting could be of therapeutic interest, especially in high-risk MM patients defined by the KI. Since this index significantly increases at relapse compared to newly diagnosed patients, CHK1, MELK, PLK4, SRPK1, CDC7-DBF4, MPS1/TTK and PBK inhibitors could represent new treatment options alone or in combination with Melphalan or IMiD for refractory/relapsing MM patients.

Funding

References

1. Siegel R, Naishadham D, Jemal A. Cancer statistics, 2012. CA Cancer J Clin. 2012;62(1):10-29.
2. Kyle RA, Rajkumar SV. Multiple myeloma. N Engl J Med. 2004;351(18):1860-1873.
3. Lohr JG, Stojanov P, Carter SL, et al. Widespread genetic heterogeneity in multiple myeloma: implications for targeted therapy. Cancer Cell. 2014;25(1):91-101.
4. Bolli N, Avet-Loiseau H, Wedge DC, et al. Heterogeneity of genomic evolution and mutational profiles in multiple myeloma. Nat Commun. 2014;5:2997.
5. Palumbo A, Rajkumar SV, San Miguel JF, et al. International Myeloma Working Group consensus statement for the management, treatment, and supportive care of patients with myeloma not eligible for standard autologous stem-cell transplantation. J Clin Oncol. 2014;32(6):587-600.
6. Fleuren EDG, Zhang L, Wu J, Daly RJ. The kinome "at large" in cancer. Nat Rev Cancer. 2016;16(2):83-98.
7. Abramson HN. Kinase inhibitors as potential agents in the treatment of multiple myeloma. Oncotarget. 2016;7(49):81926-81968.
8. Tiedemann RE, Zhu YX, Schmidt J, et al. Kinome-wide RNAi studies in human multiple myeloma identify vulnerable kinase targets, including a lymphoid-restricted kinase, GRK6. Blood. 2010;115(8):1594-1604.
9. Sabatier R, Finetti P, Mamessier E, et al. Kinome expression profiling and prognosis of basal breast cancers. Mol Cancer. 2011;10:86.
10. Hose D, Rème T, Hielscher T, et al. Proliferation is a central independent prognostic factor and target for personalized and risk-adapted treatment in multiple myeloma. Haematologica. 2011;96(1):87-95.
11. Moreaux J, Rème T, Leonard W, et al. Development of gene expression-based score to predict sensitivity of multiple myeloma cells to DNA methylation inhibitors. Mol Cancer Ther. 2012; 11(12):2685-2692.
12. Barlogie B, Tricot G, Rasmussen E, et al. Total therapy 2 without thalidomide in comparison with total therapy 1: role of intensified induction and posttransplantation consolidation therapies. Blood. 2006; 107(7):2633-2638.
13. Nair B, van Rhee F, Shaughnessy JD, et al. Superior results of Total Therapy 3 (2003-33) in gene expression profiling-defined low-risk multiple myeloma confirmed in subsequent trial 2006-66 with VRD maintenance. Blood. 2010;115(21):4168-4173.
14. Kassambara A, Rème T, Jourdan M, et al. GenomicScape: an easy-to-use web tool for gene expression data analysis. Application to investigate the molecular events in the differentiation of B cells into plasma cells. PLoS Comput Biol. 2015;11(1):e1004077.
15. Eisen MB, Spellman PT, Brown PO, Botstein D. Cluster analysis and display of genome-wide expression patterns. Proc Natl Acad Sci U S A. 1998;95(25):14863-14868.
16. Zhang XG, Gaillard JP, Robillard N, et al. Reproducible obtaining of human myeloma cell lines as a model for tumor stem cell study in human multiple myeloma. Blood. 1994;83(12):3654-3663.
17. De Bruyne E, Bos TJ, Asosingh K, et al. Epigenetic silencing of the tetraspanin CD9 during disease progression in multiple myeloma cells and correlation with survival. Clin Cancer Res. 2008;14(10):2918-2926.
18. Chou TC, Talalay P. Quantitative analysis of dose-effect relationships: the combined effects of multiple drugs or enzyme inhibitors. Adv Enzyme Regul. 1984;22:27-55.
19. Lesluyes T, Delespaul L, Coindre J-M, Chibon F. The CINSARC signature as a prognostic marker for clinical outcome in multiple neoplasms. Sci Rep. 2017; 7(1):5480.
20. Zhan F, Huang Y, Colla S, et al. The molecular classification of multiple myeloma. Blood. 2006;108(6):2020-2028.
21. Shaughnessy J. Amplification and overexpression of CKS1B at chromosome band 1q21 is associated with reduced levels of p27Kip1 and an aggressive clinical course in multiple myeloma. Hematol Amst Neth. 2005;10 Suppl 1:117-126.
22. Evans R, Naber C, Steffler T, et al. Aurora A kinase RNAi and small molecule inhibition of Aurora kinases with VE-465 induce apoptotic death in multiple myeloma cells. Leuk Lymphoma. 2008;49(3):559-569.
23. Leone PE, Walker BA, Jenner MW, et al. Deletions of CDKN2C in multiple myeloma: biological and clinical implications. Clin Cancer Res. 2008;14(19):6033-6041.
24. Walker BA, Wardell CP, Melchor L, et al. Intraclonal heterogeneity and distinct molecular mechanisms characterize the development of t(4;14) and t(11;14) myeloma. Blood. 2012;120(5):1077-1086.
25. Vikova V, Jourdan M, Robert N, et al. Comprehensive characterization of the mutational landscape in multiple myeloma cell lines reveals potential drivers and pathways associated with tumor progression and drug resistance. Theranostics. 2019; 9(2):540-553.
26. Kumagai A, Dunphy WG. Claspin, a novel protein required for the activation of Chk1 during a DNA replication checkpoint response in Xenopus egg extracts. Mol Cell. 2000;6(4):839-849.
27. Chini CCS, Chen J. Human claspin is required for replication checkpoint control. J Biol Chem. 2003;278(32):30057-30062.
28. Arora V, Cheung HH, Plenchette S, Micali OC, Liston P, Korneluk RG. Degradation of survivin by the X-linked inhibitor of apoptosis (XIAP)-XAF1 complex. J Biol Chem. 2007;282(36):26202-26209.
29. Kim KS, Heo J-I, Choi KJ, Bae S. Enhancement of cellular radiation sensitivity through degradation of Chk1 by the XIAP-XAF1 complex. Cancer Biol Ther. 2014;15(12):1622-1634.
30. Pene F, Claessens Y-E, Muller O, et al. Role of the phosphatidylinositol 3-kinase/Akt and mTOR/P70S6-kinase pathways in the proliferation and apoptosis in multiple myeloma. Oncogene. 2002;21(43):6587-6597.
31. Landau HJ, McNeely SC, Nair JS, et al. The checkpoint kinase inhibitor AZD7762 potentiates chemotherapy-induced apoptosis of p53-mutated multiple myeloma cells. Mol Cancer Ther. 2012;11(8):1781-1788.
32. Natoni A, Coyne MRE, Jacobsen A, et al. Characterization of a dual CDC7/CDK9 inhibitor in multiple myeloma cellular models. Cancers. 2013;5(3):901-918.
33. Bolomsky A, Heuschen R, Schlangen K, et al. Maternal embryonic leucine zipper kinase is a novel target for proliferation-associated high-risk myeloma. Haematologica. 2018;103(2):325-335.
34. Steensma DP, Gertz MA, Greipp PR, et al. A high bone marrow plasma cell labeling index in stable plateau-phase multiple myeloma is a marker for early disease pro-

gression and death. Blood. 2001;97(8): 2522-2523.

35. Decaux O, Lodé L, Magrangeas F, et al. Prediction of survival in multiple myeloma based on gene expression profiles reveals cell cycle and chromosomal instability signatures in high-risk patients and hyperdiploid signatures in low-risk patients: a study of the Intergroupe Francophone du Myélome. J Clin Oncol. 2008;26(29):4798-4805.

36. Pei X-Y, Dai Y, Youssefian LE, et al. Cytokinetically quiescent (G0/G1) human multiple myeloma cells are susceptible to simultaneous inhibition of Chk1 and MEK1/2. Blood. 2011;118(19):5189-5200.

37. Gray D, Jubb AM, Hogue D, et al. Maternal embryonic leucine zipper kinase/murine protein serine-threonine kinase 38 is a promising therapeutic target for multiple cancers. Cancer Res. 2005;65(21):9751-9761.

38. Stefka AT, Park J-H, Matsuo Y, et al. Antimyeloma activity of MELK inhibitor OTS167: effects on drug-resistant myeloma cells and putative myeloma stem cell replenishment of malignant plasma cells. Blood Cancer J. 2016;6(8):e460.

39. Ji W, Arnst C, Tipton AR, et al. OTSSP167 Abrogates mitotic checkpoint through inhibiting multiple mitotic kinases. PloS One. 2016;11(4):e0153518.

40. Liu X. Targeting Polo-Like Kinases: A Promising Therapeutic Approach for cancer treatment. Transl Oncol. 2015;8(3):185-195.

41. Bonte D, Lindvall C, Liu H, Dykema K, Furge K, Weinreich M. Cdc7-Dbf4 kinase overexpression in multiple cancers and tumor cell lines is correlated with p53 inactivation. Neoplasia. 2008;10(9):920-931.

42. Xie Y, Wang A, Lin J, et al. Mps1/TTK: a novel target and biomarker for cancer. J Drug Target. 2017;25(2):112-118.

43. Ohashi T, Komatsu S, Ichikawa D, et al. Overexpression of PBK/TOPK relates to tumour malignant potential and poor outcome of gastric carcinoma. Br J Cancer. 2017;116(2):218-226.

44. Bullock N, Oltean S. The many faces of SRPK1. J Pathol. 2017;241(4):437-440.

45. Ma Z, Yao G, Zhou B, Fan Y, Gao S, Feng X. The Chk1 inhibitor AZD7762 sensitises p53 mutant breast cancer cells to radiation in vitro and in vivo. Mol Med Rep. 2012;6(4):897-903.

46. Meuth M. Chk1 suppressed cell death. Cell Div. 2010;5:21.

47. Blasina A, Hallin J, Chen E, et al. Breaching the DNA damage checkpoint via PF-00477736, a novel small-molecule inhibitor of checkpoint kinase 1. Mol Cancer Ther. 2008;7(8):2394-2404.

48. Beke L, Kig C, Linders JTM, et al. MELK-T1, a small-molecule inhibitor of protein kinase MELK, decreases DNA-damage tolerance in proliferating cancer cells. Biosci Rep. 2015;35(6).

49. Ayllón V, O'connor R. PBK/TOPK promotes tumour cell proliferation through p38 MAPK activity and regulation of the DNA damage response. Oncogene. 2007; 26(24):3451-3461.

50. Sawa M, Masai H. Drug design with Cdc7 kinase: a potential novel cancer therapy target. Drug Des Devel Ther. 2009;2:255-264.

51. Zhou W, Yang Y, Xia J, et al. NEK2 induces drug resistance mainly through activation of efflux drug pumps and is associated with poor prognosis in myeloma and other cancers. Cancer Cell. 2013;23(1):48-62.

52. Yang Y, Gu C, Luo C, Li F, Wang M. BUB1B promotes multiple myeloma cell proliferation through CDC20/CCNB axis. Med Oncol. 2015;32(3):81.

Ferrata Storti Foundation

Long-term eradication of extranodal natural killer/T-cell lymphoma, nasal type, by induced pluripotent stem cell-derived Epstein-Barr virus-specific rejuvenated T cells *in vivo*

Miki Ando,[1,2] Jun Ando,[1] Satoshi Yamazaki,[2] Midori Ishii,[1] Yumi Sakiyama,[2] Sakiko Harada,[1] Tadahiro Honda,[1] Tomoyuki Yamaguchi,[2] Masanori Nojima,[3] Koichi Ohshima,[4] Hiromitsu Nakauchi,[2,5*] and Norio Komatsu[1*]

[1]Department of Hematology, Juntendo University School of Medicine, Tokyo, Japan; [2]Division of Stem Cell Therapy, Center for Stem Cell Biology and Regenerative Medicine, The Institute of Medical Science, The University of Tokyo, Tokyo, Japan; [3]Center for Translational Research, The Institute of Medical Science, The University of Tokyo, Tokyo, Japan; [4]Department of Pathology, School of Medicine, Kurume University, Fukuoka, Japan and [5]Institute for Stem Cell Biology and Regenerative Medicine, Stanford University School of Medicine, Stanford, CA, USA

*HN and NK are co-last authors

ABSTRACT

Functionally rejuvenated induced pluripotent stem cell (iPSC)-derived antigen-specific cytotoxic T lymphocytes (CTL) are expected to be a potent immunotherapy for tumors. When L-asparaginase-containing standard chemotherapy fails in extranodal natural killer/T-cell lymphoma, nasal type (ENKL), no effective salvage therapy exists. The clinical course then is miserable. We demonstrate prolonged and robust eradication of ENKL *in vivo* by Epstein-Barr virus-specific iPSC-derived antigen-specific CTL, with iPSC-derived antigen-specific CTL persisting as central memory T cells in the mouse spleen for at least six months. The anti-tumor response is so strong that any concomitant effect of the programmed cell death 1 (PD-1) blockade is unclear. These results suggest that long-term persistent Epstein-Barr virus-specific iPSC-derived antigen-specific CTL contribute to a continuous anti-tumor effect and offer an effective salvage therapy for relapsed and refractory ENKL.

Introduction

ENKL, a highly aggressive disease, is relatively common in Asia and South America. Necrosis is extensive and dissemination to various sites is rapid. The outcome is miserable.[1,2] Expressing high concentrations of multidrug-resistance P-glycoprotein, ENKL cells resist anthracycline-based standard chemotherapy.[3] L-asparaginase selectively induces apoptosis in ENKL,[4] and the L-asparaginase-containing regimen SMILE (dexamethasone ["steroids"], methotrexate, ifosfamide, L-asparaginase, etoposide) prolongs survival in advanced ENKL.[5,6] However, even with SMILE, 5-year overall survival is 47%.[5] No effective salvage regimen exists. Development of such a regimen is thus an urgent issue.

Antigen-specific CTL therapy can induce durable remission in selected tumors such as melanomas.[7-10] ENKL cells are invariably infected by Epstein-Barr virus (EBV) with type II latency; they express the EBV antigens latent membrane protein (LMP) 1 and LMP2 (LMP1/2). As T cells specific for these antigens are infrequent and often are anergic in the tumor microenvironment, ENKL should be a good target for CTL therapy directed against LMP1 and LMP2.[11-16] However, CTL continuously exposed to viral or tumor antigens become exhausted.[17]

Exploiting fully rejuvenated CTL innovatively overcomes CTL exhaustion. We generated antigen-specific CTL directed against LMP1 and LMP2 from iPSC established from peripheral blood-derived antigen-specific CTL.[18-20] The iPSC-derived CTL have the same antigen specificity as the original CTL. As these redifferentiated CTL have a higher proliferative capacity, younger memory phenotype, and

longer telomeres than the original CTL, iPSC-derived CTL are functionally rejuvenated T cells (rejT).[17] The rejT that we generated have strong anti-tumor effects against EBV-infected lymphoblastoid cells (LCL) *in vivo* and in mice they confer a survival advantage compared to mice treated using original CTL.[19] Hence, rejT therapy directed against LMP1 and LMP2 is expected to be useful as a salvage therapy for ENKL in which SMILE has failed.

Another factor in ENKL prognosis is the PD-1 pathway for immunoevasion.[21-23] EBV-associated lymphoma cells often express the PD-1 ligand (PD-L1).[24-26] The complete remission (CR) rate is high after PD-1 blockade with pembrolizumab in ENKL in which L-asparaginase therapy has failed.[27]

We sought to demonstrate the effectiveness of rejT therapy targeting ENKL. We also investigated additive anti-tumor effects of PD-1 blockade in conjunction with rejT therapy. Both rejT and original CTL showed robust tumor-suppressive effects against ENKL *in vitro* and *in vivo*. However, only LMP2-specific rejT significantly prolonged long-term survival in ENKL-bearing mice. This effect was so strong that any additive anti-tumor effect of PD-1 blockade was overwhelmed. LMP1- and LMP2-specific rejT therapy seems a promising salvage therapy for ENKL refractory to SMILE.

Methods

More detailed information can be found in the *Online Supplementary Data*.

Patients and samples

We reviewed 28 biopsy samples from 24 patients diagnosed with ENKL at the Juntendo University School of Medicine, Department of Hematology, between 2006 and 2017. The use of the material and clinical information was approved by the Research Ethics Committee for the Faculty of Medicine, Juntendo University, and was in accordance with the Declaration of Helsinki.

Immunohistochemical staining

Tissue samples were fixed in formalin and embedded in paraffin. Anti-PD-L1 rabbit monoclonal antibodies (EPR1161[2]; 1:200 dilution; ab174838, Abcam, Cambridge, MA), anti-PD-1 mouse monoclonal antibodies (NAT105; 1:100 dilution; ab52587, Abcam), and anti-CD3 rabbit monoclonal antibodies (SP7; 1:50 dilution; ab16669, Abcam) were used for immunostaining.

Generation of LMP1/2-specific CTL and establishment of T-iPSC

LMP1/2-specific CTL were generated using peripheral blood mononuclear cells (PBMC) obtained from two human leukocyte antigen (HLA)-A*2402-expressing healthy donors and one HLA-A*0201-expressing ENKL patient. Selected clones were transduced with Sendai virus vectors to establish T-iPSC.

T-cell differentiation from T-iPSC

To differentiate human iPSC into hematopoietic cells, small clumps of iPSC were transferred onto C3H10T1/2 cells. Hematopoietic cells collected from iPSC sac contents were transferred onto DL1/4-expressing C3H10T1/2 feeder cells. T-lineage cells were then harvested and stimulated. The antigen specificity of LMP1/2-specific rejT was determined by staining with LMP1/2 tetramer.

Cell lines

ENKL cells (NK-YS and SNK-6 lines) were grown in Iscove's modified Dulbecco's medium supplemented with 10% fetal bovine serum (FBS) and 100 U/mL of interleukin-2 (IL-2) and in NS-A2 (GreenDay) supplemented with 100 U/mL of IL2, respectively.[4,28]

^{51}Cr release assays

Cytotoxic specificity of EBV-CTL and EBV-rejT directed at LMP1/2 antigen was analyzed in a standard 4-hour ^{51}Cr- release assay at different effector : target ratios (E:T; 40:1, 20:1, 10:1 and 5:1) and using a γ counter (PerkinElmer, Waltham, MA).[29] To elucidate whether PD-L1 blockade can enhance the killing potential of EBV-CTL and EBV-rejT against ENKL, NK-YS cells were cultured with 10 µg/mL of anti-PD-L1 antibody (Ultra-LEAF™ purified anti-human CD274, BioLegend) for three days preceding the assay.

Antitumor activity *in vivo* model

To evaluate the antitumor effects of LMP2-CTL and LMP2-rejT against ENKL, cells from an HLA class I-matched ENKL line, NK-YS, that had been transduced with a γ-retroviral vector encoding the fusion protein GFP/FFluc were sorted for GFP expression by flow cytometry. Six-week-old female NOD/Shi-scid, IL-2RγKO Jic (NOG) mice (In-Vivo Science, Tokyo, Japan) were engrafted intraperitoneally with NK-YS (1×10^5 cells/mouse) and tumor growth was monitored using the Xenogen-IVIS Imaging System (Xenogen, Alameda, CA, USA). Once a progressive increase of bioluminescence occurred, usually four days after tumor inoculation, mice were treated intraperitoneally with three once-weekly doses of 5×10^6 LMP2-rejT ± 50 µg of anti-PD-1 Ab or with 5×10^6 original LMP2-CTL ± 50 µg of anti-PD-1 Ab (In VivoMAb anti-h PD-1, BioXCell, West Lebanon, NH, USA).

PCR and sequencing

EBV strain typing of the NK-YS cells in ascites was performed by PCR using LMP2-specific primers 5'-TATGAATCCAGTAT-GCCTGC-3' and 5'-CGCAGTAAGCACTGTCACCG-3' as described[29] to detect LMP2 epitopes that are associated with HLA-A*2402.

Results

Distinct PD-L1 expression was significantly associated with poor prognosis in ENKL

To understand the microenvironment of ENKL cells, ENKL cells and tumor-infiltrating lymphocytes (TIL) were analyzed by immunohistochemical staining for PD-L1 and PD-1 receptor expression respectively. As EBV *in situ* hybridization demonstrated infection in all 28 cases, we initially expected high PD-L1 expression. However, the proportion of ENKL cells (PD-L1 expression ratio, lymphoma cell : macrophage) was 5-10% (+, positive) in only three samples, 2-3% (+/-, weakly positive) in seven, 1% (-/+, slightly positive) in one, and negative in 17 (Figure 1 A-B).

The presence of many PD-1-expressing TIL is associated with favorable overall survival (OS) in patients with diffuse large B-cell lymphoma.[26] It is noteworthy that PD-1$^+$ TIL were rarely observed in ENKL, with only 1% of PD-1$^+$ TIL seen in only two of 28 samples (Figure 1 C-D). Table 1 summarizes the characteristics of patients diagnosed with ENKL in our institute. Three patients whose lymphoma cells expressed PD-L1 (5-10%) were in stage IV

(3 of 3). Of these, two were refractory to initial therapy. They survived for only one month (2 of 3) and 4 months (1 of 3). The lymphoma cells of these three patients did not express LMP1. Statistical analysis showed that distinct PD-L1 expression of ENKL was significantly correlated with poor prognosis (*P*=0.001). Even in advanced-stage disease, PD-L1 expression was significantly associated with poor OS (*P*=0.031) (Figure 1E). Another factor conferring poor OS in ENKL was the lack of LMP1 expression

(*P*=0.009) (Figure 1F). Treatment with SMILE was associated with favorable OS in advanced-stage disease (*P*=0.008) (Figure 1G), whereas plasma EBV DNA positivity did not significantly affect OS in these ENKL patients (*P*=0.181) possibly due to the small number of EBV-DNA negative group (Figure 1H). Table 2 shows the results of cross-tabulation analysis of the correlations between PD-L1 expression and variables including age, sex, clinical stage, EBV DNA titre, SMILE history, CR, and LMP1
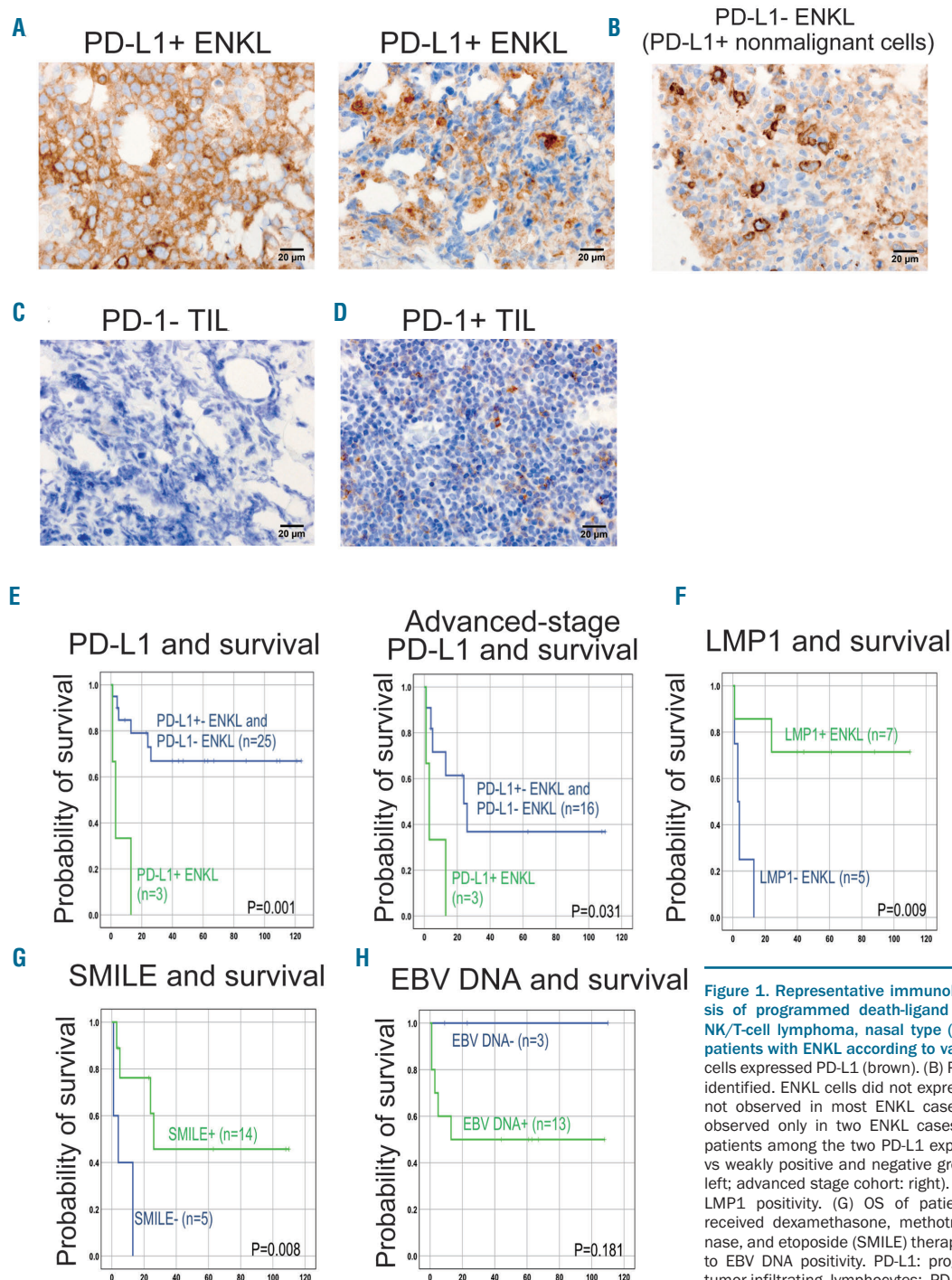
Figure 1. Representative immunohistochemical features, analysis of programmed death-ligand 1 expression in extranodal NK/T-cell lymphoma, nasal type (ENLK), and overall survival in patients with ENKL according to various factors. (A) PD-L1+ ENKL cells expressed PD-L1 (brown). (B) PD-L1+ nonmalignant cells were identified. ENKL cells did not express PD-L1. (C) PD-1+ TILs were not observed in most ENKL cases. (D) PD-1+ TILs (1%) were observed only in two ENKL cases. (E) Overall survival (OS) of patients among the two PD-L1 expressing groups (positive group vs weakly positive and negative groups) (the entire study cohort: left; advanced stage cohort: right). (F) OS of patients according to LMP1 positivity. (G) OS of patients in advanced stage who received dexamethasone, methotrexate, ifosfamide, L-asparaginase, and etoposide (SMILE) therapy. (H) OS of patients according to EBV DNA positivity. PD-L1: programmed death-ligand 1; TIL: tumor-infiltrating lymphocytes; PD-1: programmed cell death 1; LMP: latent membrane protein; EBV: Epstein-Barr virus.

expression. In ENKL cells, lack of LMP1 expression was significantly correlated with PD-L1 expression.

These analyses revealed that distinct PD-L1 expression by ENKL was strongly associated with poor prognosis. CTL therapy directed at LMP1/2 and combined with PD-1/PD-L1 axis blockade is therefore suggested as useful for the treatment of refractory ENKL.

Both LMP1-specific and LMP2-specific rejT showed strong cytotoxicity against ENKL *in vitro*

To examine the cytotoxicity of EBV-specific rejT against ENKL, we first determined the HLA type of the ENKL cell line NK-YS (HLA-A*2402) and SNK6 (HLA-A*02). A*2402- and A*0201-restricted LMP1/2-specific CTL clones were generated from healthy donors expressing A*2402 and an ENKL patient (Pt) (Pt 6) who expresses HLA-A*0201. T-iPSC were established from these clones and were redifferentiated into rejT with antigen specifici-

ties that matched those of the respective clones (Figure 2 A-B). We assayed the cytotoxicity of A*2402-restricted LMP2-rejT (TYGPVFMSL), A*0201-restricted LMP1-rejT (YLQQNWWTL), and A*0201-restricted LMP2-rejT (FLY-ALAL) against HLA-matched ENKL by ^{51}Cr release. Strong killing by A*2402-restricted LMP2-rejT was shown against HLA-A*2402$^+$ NK-YS cells (85.3%, 84.7%, 85.2%, and 83.7%; effector : target [E:T] ratios of 40:1, 20:1, 10:1 and 5:1), but not against HLA-A*2402$^-$ tumors (18.4%, 4.8%, 1.9%, and 2.4%; E:T ratios of 40:1, 20:1, 10:1 and 5:1). A*0201-restricted LMP1-rejTs also demonstrated strong cytotoxic activity against HLA-A*02$^+$ SNK6 cells (72.0%, 69.9%, 70.4%, and 65.1%; E:T ratios of 40:1, 20:1, 10:1 and 5:1), but not against HLA-A*02$^-$ tumors (-2.3%, -1.7%, 1.3%, and 4.8%; E:T ratios of 40:1, 20:1, 10:1 and 5:1). HLA-A*0201-restricted LMP2-rejT exhibited 76.6% and 24.7% killing at E:T ratios of 40:1 and 20:1 against HLA-A*02$^+$ SNK6 cells, with 14.9% and 14.6% killing for

Table 1. Extranodal NK/T-cell lymphoma, nasal type: patient characteristics.

	Age (Years)	Sex	Stage	EBV-DNA (copies/mL)	Treatment	Response to treatment	Survival duration (months)	PD-L1 lymphoma cells	PD-L1 macrophages	PD-1 TILs	LMP1	EBNA2
1	41	F	IVB	1.9x10^3	No treatment	No treatment	1	+	+ +	−	−	−
2	29	M	IVB	2.0x10^6	SMILE	refractory	4	+	+	−	−	−
3	74	M	IVA	2.3x10^2	DEX, VP-16	refractory	1	+	+ −	−	−	−
4	73	F	IVA	2.4x10^1	RT-DeVIC, SMILE	CR	>63	+ −	+ −	−	N.D.	−
5	32	M	IVB	not detected	SMILE, Allo BMT	CR	>24	+ −	+	−	N.D.	N.D.
6	74	M	II A	not detected	RT-DeVIC	CR	>10	+ −	+ +	1 %	N.D.	N.D.
7	53	M	IVA	N.D.	RT-DeVIC, ICE	refractory	24	+ −	+ −	−	+	−
8		M	IVA	8.1x10^2	MILD, Allo BMT, DLI	refractory		+ −	+ −	−	−	−
9	32	M	II A	N.D.	RT-DeVIC	CR	>60	+ −	+	−	N.D.	N.D.
10	32	M	IVB	not detected	SMILE, Auto PBSCT	CR	>110	+ −	+	−	+	N.D.
11	71	F	I B	N.D.	RT-DeVIC	CR	>124	− +	+ −	−	N.D.	N.D.
12	31	M	II A	2.5x10^1	SMILE, RT	CR	>44	−	+ −	−	+	+
13	57	F	II A	1.7x10^2	RT-DeVIC	CR	>61	−	+ −	−	+	−
14	29	M	IVA	N.D.	SMILE, Auto PBSCT	CR	4	−	+ −	−	N.D.	N.D.
15	41	M	IVA	5.3x10^5	RT-DeVIC, MILD	refractory	6	−	+ −	−	N.D.	N.D.
16		M						−	+ −	−	N.D.	N.D.
17		M		9.9x10^2				−	+ −	−	N.D.	N.D.
18	78	M	IVA	1.1x10^4	MILD	unknown	unknown	−	−	−	N.D.	N.D.
19		M	IVA					−	+	−	N.D.	N.D.
20	84	F	IVB	4.5x10^3	RT-DeVIC	unknown	1	−	+	−	+	N.D.
21	46	M	IVB	1.3x10^4	SMILE, Allo BMT	CR	>108	−	+ −	−	N.D.	N.D.
22	32	F	I A	2.3x10^1	RT-DeVIC	CR	>66	−	+ −	−	N.D.	N.D.
23	33	M	IVA	N.D.	SMILE, Auto PBSCT	CR	24	−	+	−	N.D.	−
24	28	M	I A	N.D.	RT-DeVIC	CR	>40	−	+	−	+	−
25	73	M	I A	N.D.	RT-DeVIC	CR	>88	−	+	−	+	−
26	62	F	IVA	N.D.	RT-DeVIC, HD-MTX	refractory	12	−	− +	1 %	N.D.	N.D.
27	71	F	IVB	N.D.	ESHAP, CHOP	refractory	4	−	+ −	−	−	−
28	65	M	I A	N.D.	RT-DeVIC	CR	>120	−	+ +	−	N.D.	N.D.

ENKL: extranodal NK/T cell lymphoma, nasal type; EBV: Epstein-Barr virus; PD-1: programmed cell death 1; PD-L1: programmed death-ligand 1; LMP: latent membrane protein; EBNA: Epstein-Barr nuclear antigen; SMILE: dexamethasone, methotrexate, ifosfamide, L-asparaginase and etoposide; DEX: dexamethasone; VP-16, etoposide; RT: radiation therapy; DeVIC: dexamethasone, etoposide, ifosfamide and carboplatin; Allo BMT: allogenetic bone marrow transplantation; ICE: ifosfamide, carboplatin and etoposide; Auto PBSCT: autologous peripheral blood stem cell transplantation; MILD: methotrexate, ifosfamide, L-asparaginase and dexamethasone; HD-MTX: high dose methotrexate; ESHAP: etoposide, methylprednisolone, high dose cytarabine and cisplatin; CHOP: cyclophosphamide, doxorubicin, vincristine and prednisone; CR: complete remission; N.D., not done.

HLA-A*02⁻ tumors. These results indicated that LMP1-specific and LMP2-specific rejT generated from multiple donors, including an ENKL patient, had strong antigen-specific cytotoxicity against ENKL.

LMP1-specific and LMP2-specific rejT tended to show stronger cytotoxicity against EBV⁺ tumor cells than the original CTL clone *in vitro*

We next compared rejT cytotoxicity against EBV⁺ tumor cells with that of original CTL by ⁵¹Cr release assay. A*2402-restricted LMP2-rejT generated from a healthy donor more efficiently killed autologous EBV-infected LCL (70.4% and 65.4%; E:T ratios of 20:1 and 10:1) compared to the original CTL clone (51.7% and 49.4%; E:T ratios of 20:1 and 10:1). A*0201-restricted LMP1-rejT generated from an ENKL patient showed somewhat stronger cytotoxicity against autologous EBV-infected LCL (90.3%, 90.0%, 77.8%, and 58.8%; E:T ratios of 40:1, 20:1, 10:1 and 5:1) than the original CTL clone (77.8%, 61.9%, and 43.8%; E:T ratios of 20:1, 10:1 and 5:1). The cytotoxicity of A*0201-restricted LMP2-rejT against autologous EBV-infected LCL (44.0% and 34.5%; E:T ratios of 40:1 and 20:1) was almost the same as that of the original CTL clone (40.4% and 33.7%; E:T ratios of 40:1 and 20:1). We further compared PD-1 expression of peripheral blood-derived original EBV-CTL and of rejT from the same LMP2-CTL clone, measured by flow cytometry: values were 15.3% for EBV-CTL and undetectable for rejT (Figure 3B). PD-L1 expression of ENKL cells, measured by flow cytometry, was 57.4% (Figure 3C). Although both LMP2-specific rejT and original LMP2-CTL (PYLFWLAAI) powerfully killed HLA class I-matched NK-YS cells, rejT cytotoxicity tended to be stronger (60.8%, 52.6%, 52.6%, and 40.1%; E:T ratios of 40:1, 20:1, 10:1 and 5:1 specific ⁵¹Cr release, respectively) than that of the original CTL (59.7%, 50%, 40.9%, and 39.8%; E:T ratios of 40:1, 20:1, 10:1 and 5:1 specific ⁵¹Cr release, respectively) (Figure 3D). To elucidate whether PD-L1 blockade can enhance the potential to kill ENKL of the original CTL that express PD-1⁺ and of rejT that do not express PD-1⁻, ENKL cells were cultured with 10 μg/mL of anti-PD-L1 antibody for three days immediately preceding the assay. Anti-PD-L1 antibody did not clearly enhance killing by either PD-1⁺ original CTL or PD-1⁻ rejT (Figure 3D). Our results demonstrated definite cytotoxic activity against EBV-infected tumor

cells *in vitro* for both EBV-specific original CTL and rejT, with cytotoxicity of rejT against ENKL cells stronger than that of original CTL and without killing enhancement in original CTL or rejT cultured with anti-PD-L1 antibody.

Robust anti-ENKL effect and marked survival improvement of LMP2-rejT *in vivo*

ENKL cells express not only PD-L1 but also PD-L2 (Figure 3C). Anti-PD-1 antibody that can block both PD-L1 and PD-L2 was thus potentially more effective than anti-PD-L1 antibody as therapy for ENKL. Using PD-1 blockade to observe whether EBV-specific rejT exert ENKL-suppressive effects *in vivo* and anti-PD-1 antibody has an additive antitumor effect, ENKL cells labeled with retrovirus-derived firefly luciferase were intraperitoneally engrafted into NOG mice (1x10⁵ cells/mouse). Light emission was monitored as an indicator of tumor growth. Four days after tumor inoculation, these mice were divided into two control groups and four treatment groups. No treatment was given in one control group (n=6) and only anti-PD-1 antibody was given in the other (200 μg per dose, three doses) (n=6). The treatment groups consisted of mice treated with original LMP2-CTL (5x10⁶ per dose, three doses) (n=6); mice treated with original LMP2-CTL and anti-PD-1 antibody (5x10⁶ of original CTL and 200 μg of anti-PD-1 antibody per dose, three doses) (n=6); mice treated with LMP2-specific rejT (5x10⁶ per dose, three doses) (n=6); and mice treated with LMP2-specific rejT and anti-PD-1 antibody (5x10⁶ of rejT and 50 μg of anti-PD-1 antibody per dose, three doses) (n=5).

By day 21, bioluminescence had progressively increased in the control-group mice (no treatment, 176.8-fold, range 7.33-326.0; anti-PD-1 Ab, 53.3-fold, range 15.5-101.0) (Figure 4A-B). In contrast, tumor suppressive effects were observed in the original CTL group (6.025-fold, range 1.27-10.4) and in the original CTL with anti-PD-1 Ab group (17.5-fold, range 0.71-51.1), with and even stronger suppressive effects in the rejT group (0.505-fold, range 0.31-0.816) as well as in the rejT with anti-PD-1 Ab group (0.71-fold, range 0.50-1.10). Tumor signals regressed further in the four groups treated with original CTL, original CTL with anti-PD-1 antibody, rejT, or rejT with anti-PD-1 antibody than in the untreated group (original CTL, *P*=0.0001; original CTL with anti-PD-1 antibody, *P*=0.0003; rejT, *P*<0.0001, and rejT with anti-PD-1 anti-

Table 2. PD-L1⁺, PD-L1⁺/⁻, and PD-L1⁻ extranodal NK/T-cell lymphoma nasal type: patient characteristics.

	PD-L1 + N=3		PD-L1 +/- N=8		PD-L1 - N=17		*P* value
	mean/N	SD/%	mean/N	SD/%	mean/N	SD/%	
Age	48.00	23.30	52.43	20.35	52.14	20.12	0.945
Sex	1/3	33.3%	2/8	25.0%	5/17	29.4%	1.000
Advanced	3/3	100.0%	5/8	62.5%	11/17	64.7%	0.566
EBV DNA-positive	3/3	100.0%	2/5	40.0%	8/8	100.0%	0.707
SMILE	1/3	33.3%	5/8	62.5%	9/17	52.9%	1.000
CR	0/3	0.0%	6/8	75.0%	9/17	52.9%	0.590
LMP1	0/3	0.0%	2/3	66.7%	5/6	83.3%	0.038
Observation period (month)	5.67	6.43	57.14	44.69	44.77	41.48	

Programmed death ligand-1 (PD-L1); ENKL: extranodal NK/T-cell lymphoma, nasal type; EBV: Epstein-Barr virus; SMILE: dexamethasone, methotrexate, ifosfamide, L-asparaginase and etoposide; CR: complete remission; PD-L1: programmed death-ligand 1; LMP: latent membrane protein; SD: standard deviation.

body, $P=0.0002$; one-way ANOVA). Treatment enhancement was not clearly observed with concomitant anti-PD1 antibody therapy either in the original CTL group ($P>0.99$, one-way ANOVA) or in the rejT group ($P>0.99$, one-way ANOVA). These three-week observations *in vivo* demonstrated the tumor suppressive effects against ENKL cells of the original CTL treatment, with more pronounced antitumor effects of the rejT treatment.

On long-term observation, original CTL did not prolong survival *versus* no-treatment controls ($P=0.09$). Treatment

with rejT markedly prolonged survival (mean 239 days, 58-296 days) compared to treatment with original CTL ($P=0.03$, mean 74.5 days, 58-140 days), with original CTL with anti-PD-1Ab ($P=0.01$, mean 45.5 days, 34-98 days), and with no treatment ($P=0.01$) (Figure 4C). RejT with anti-PD-1 Ab also significantly improved survival (mean 134 days, 72-204 days) compared to treatment with original CTL with anti-PD-1 Ab ($P=0.008$) and with no treatment ($P=0.004$, mean 58 days, 42-84 days).

No significant survival advantage was observed for the
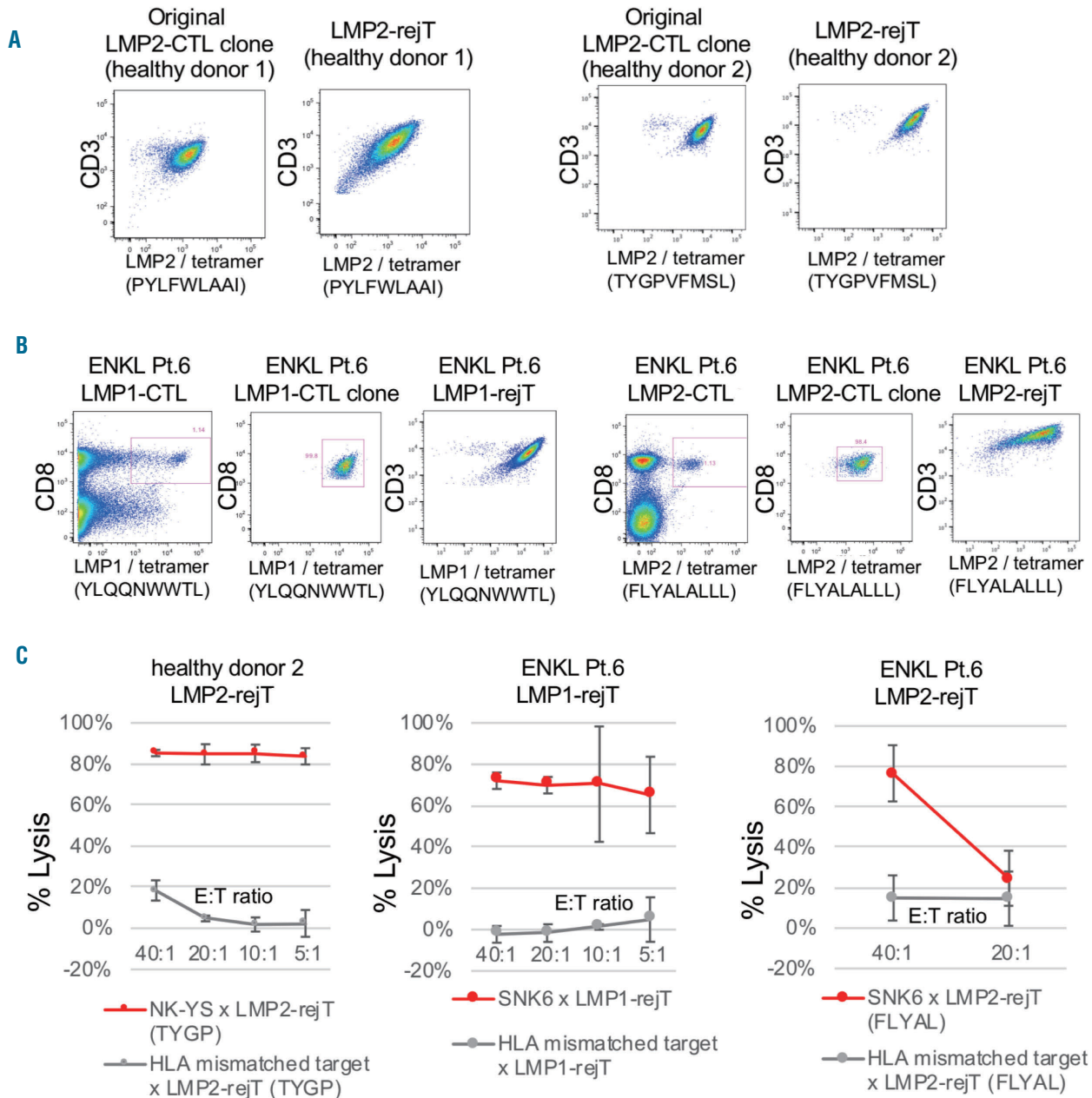
Figure 2. Extranodal NK/T-cell lymphoma, nasal type cell lines are sensitive to killing by induced pluripotent stem cell-derived LMP1- and LMP2-rejT *in vitro*. (A) Flow cytometric EBV LMP2 tetramer analysis of original peripheral blood-derived EBV-CTL and iPSC-derived-EBV-rejT generated from healthy donors. (B) Flow cytometric EBV LMP1 and LMP2 tetramer analysis of original peripheral blood-derived EBV-CTL and iPSC-derived-EBV-rejT generated from an ENKL patient (Pt 6). (C) *In vitro* ^{51}Cr release assay of LMP1- and LMP2-rejT (effectors) against ENKL (targets) and HLA mismatched LCL (control targets). ENKL: extranodal NK/T-cell lymphoma, nasal type; iPSC: induced pluripotent stem cell; LMP: latent membrane protein; rejT: rejuvenated cytotoxic T lymphocytes; EBV: Epstein-Barr virus; Pt: patient; CTL: cytotoxic T lymphocytes; HLA: human leukocyte antigen; LCL: EBV-infected lymphoblastoid cells.
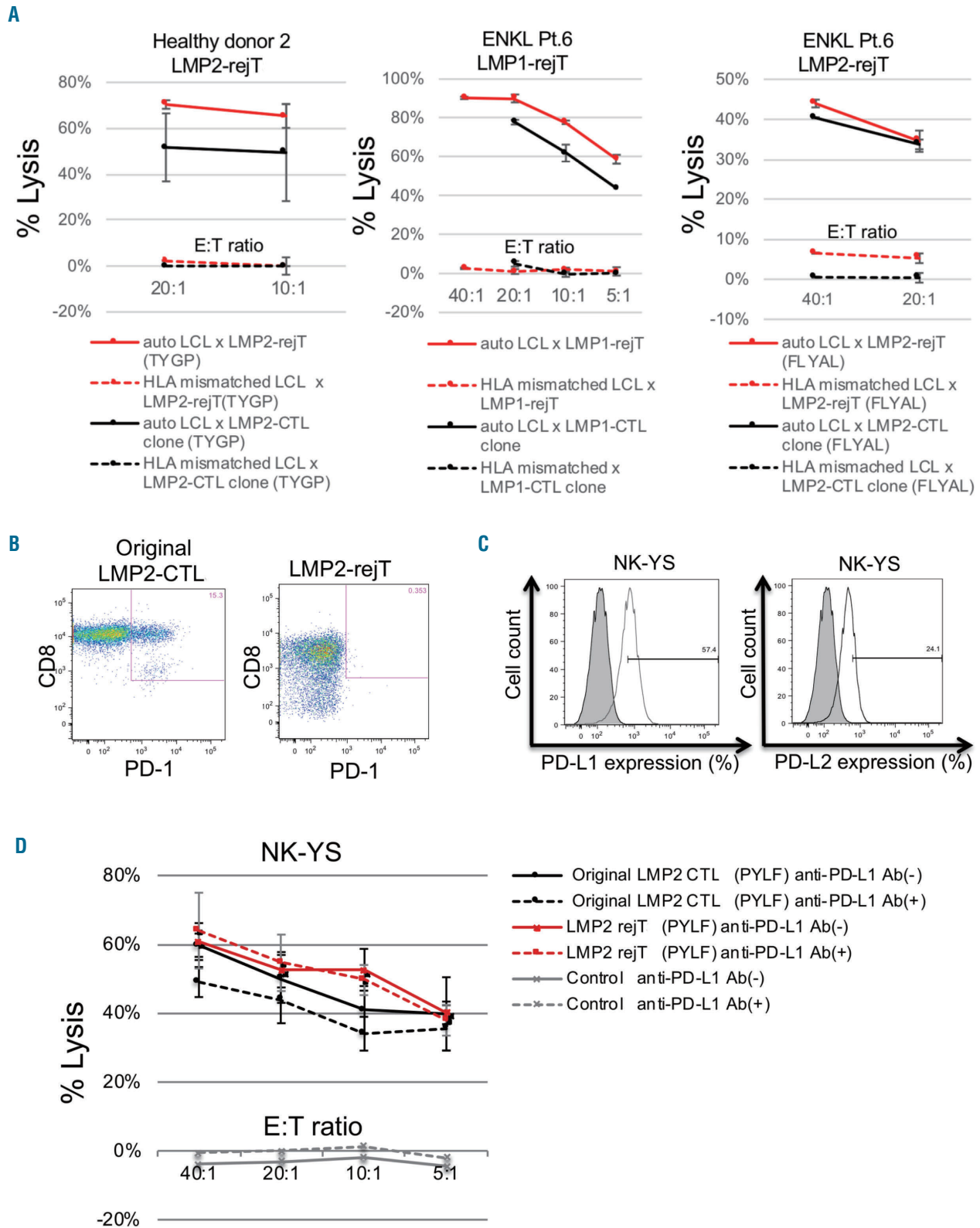
Figure 3. Induced pluripotent stem cell-derived LMP1⁻ and LMP2-rejT show cytotoxicity against Epstein-Barr virus-infected-infected tumors equal to or greater than original cytotixic T lymphocytes *in vitro*. (A) *In vitro* ⁵¹Cr release assay of LMP1- and LMP2-rejT (effectors) and original CTL clones (effectors) against auto LCL (targets) and HLA-mismatched LCL (control targets). (B) Flow cytometric analysis of PD-1 expression of original LMP2-CTLs and iPSC-derived LMP2-rejT. (C) Flow cytometric analysis of PD-L1 and PD-L2 expression on the ENKL cell line NK-YS. (D) *In vitro* ⁵¹Cr release assay of original LMP2-CTL, LMP2-rejT (effectors), and HLA-mismatched T cells (control effector) against ENKL (targets). Anti-PD-L1 Ab(+), ENKL cells were cultured with 10 μg/mL of anti-PD-L1 antibody for three days until the assay was conducted. Anti-PD-L1 Ab(-), ENKL cells were cultured without anti-PD-L1 antibody. Data are presented as mean ± SD and represent at least three independent experiments. E:T ratio: effector : target ratio; iPSC: induced pluripotent stem cell; LMP: latent membrane protein; rejT: rejuvenated cytotoxic T lymphocytes; ENKL: extranodal NK/T-cell lymphoma nasal type; CTL: cytotoxic T lymphocytes; Pt: patient; HLA: human leukocyte antigen; LCL: EBV-infected lymphoblastoid cells; PD-1: programmed cell death 1; PD-L1: programmed death-ligand 1; PD-L2: programmed death-ligand 2; Ab: antibody; SD: standard deviation.

combined use of anti-PD-1 Ab with either original CTL (*P*=0.13) or rejT (*P*=0.37). Collectively, although both original CTL and rejT exhibited strong anti-tumor effects against ENKL during the three-week observation period, only LMP2-rejT, whether or not anti-PD-1 Ab was given, distinctly improved long-term survival in ENKL-bearing mice.

LMP2-rejT treatment completely eliminated ENKL and rejT persisted in long-term survivor mice

We euthanized mice engrafted with ENKL tumors and that had survived 211 days after the fisrt injection of LMP2-rejT ± anti-PD-1 Ab. The heart, lungs, esophagus, stomach, pancreas, liver, colon, kidneys, spleen, and bone
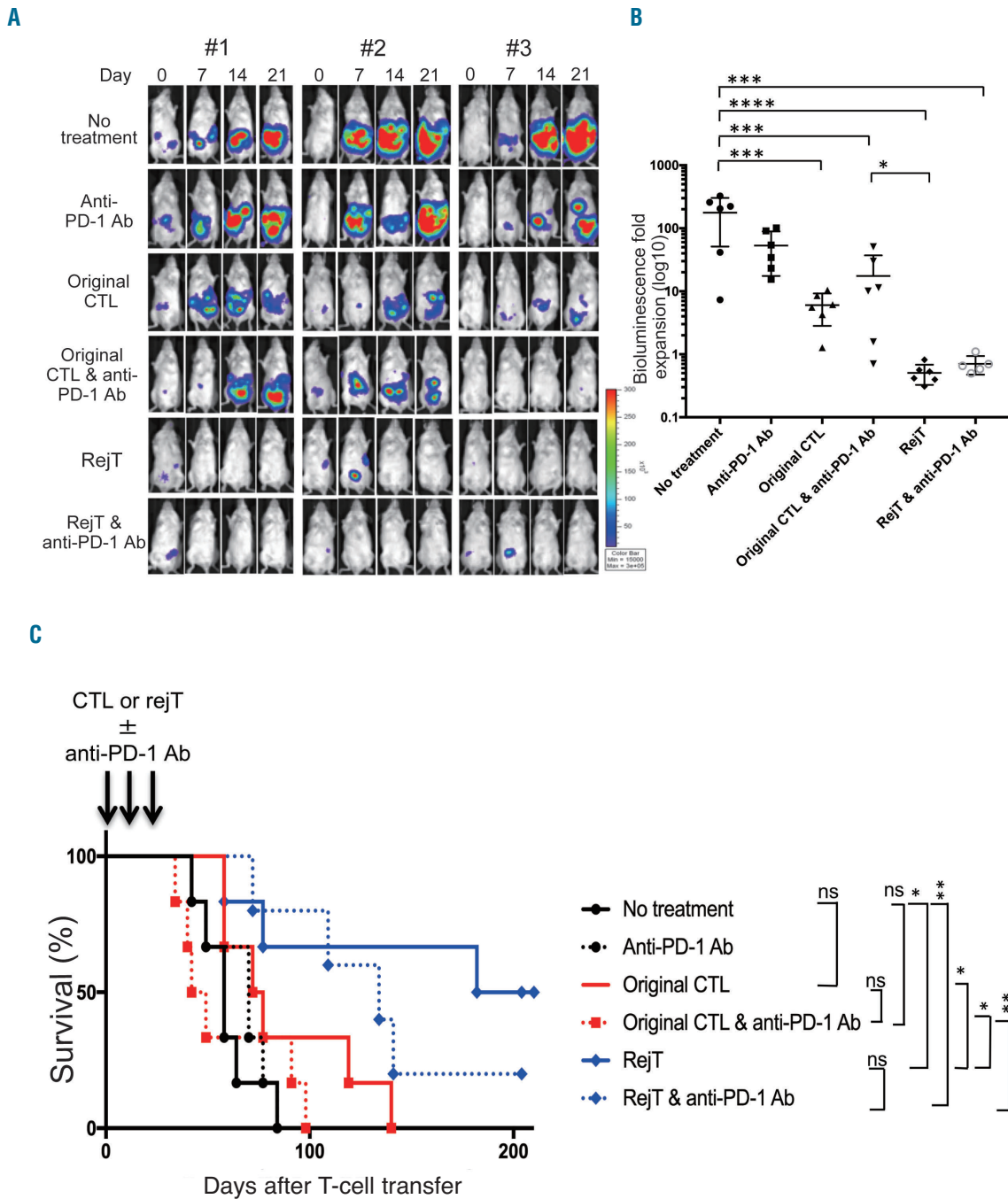
Figure 4. Induced pluripotent stem cell-derived-derived LMP2-rejT display superior anti-extranodal NK/T-cell lymphoma, nasal type activity *in vivo*. (A) Bioluminescence imaging of mice treated either with original LMP2-CTL or LMP2-rejT. FFluc+ENKL-bearing mice were divided into six groups that received no treatment (n=6), anti-PD-1 Ab (n=6), original CTL (n=6), original CTL + anti-PD-1 Ab (n=6), RejT (n=6), or RejT + anti-PD-1 Ab (n=5). Images of three representative mice from each group are shown. (B) Quantification of total tumor growth on day 21 after treatment is represented as log10 signal change. Error bars represent ± SD. ****P<0.0001, ***P<0.001 and *P<0.05 by one-way ANOVA. (C) Kaplan-Meier survival curves representing percentage survival for treated and control mice: tumor only or treated with anti-PD-1 Ab, original CTL, original CTL + anti-PD-1 Ab, RejT, or RejT + anti-PD-1 Ab. **P<0.01 and *P<0.05 by the log-rank test. iPSC: induced pluripotent stem cell; LMP: latent membrane protein; rejT: rejuvenated cytotoxic T lymphocytes; ENKL: extranodal NK/T-cell lymphoma, nasal type; FFluc: firefly luciferase; CTL: cytotoxic T lymphocytes; PD-1: programmed cell death 1; Ab: antibody; SD: standard deviation.

marrow from each mouse were histopathologically examined. All were tumor free in gross and microscopic analysis (Figure 5A, upper row of panels).

After only three rejT injections ENKL tumors were entirely extirpated. By contrast, tissues from a mouse injected with original CTL that died 58 days after the first injection were densely infiltrated by ENKL cells: original

LMP2-CTL could not eradicate ENKL cells *in vivo* long-term. To determine whether injected rejT or original CTL persisted long-term, spleen sections were evaluated immunohistochemically. Spleens of euthanized mice that had been treated with rejT, with or without anti-PD-1 Ab, were well-populated by human CD3^{+} T cells. The spleen of the mouse treated with original CTL and dead at 58
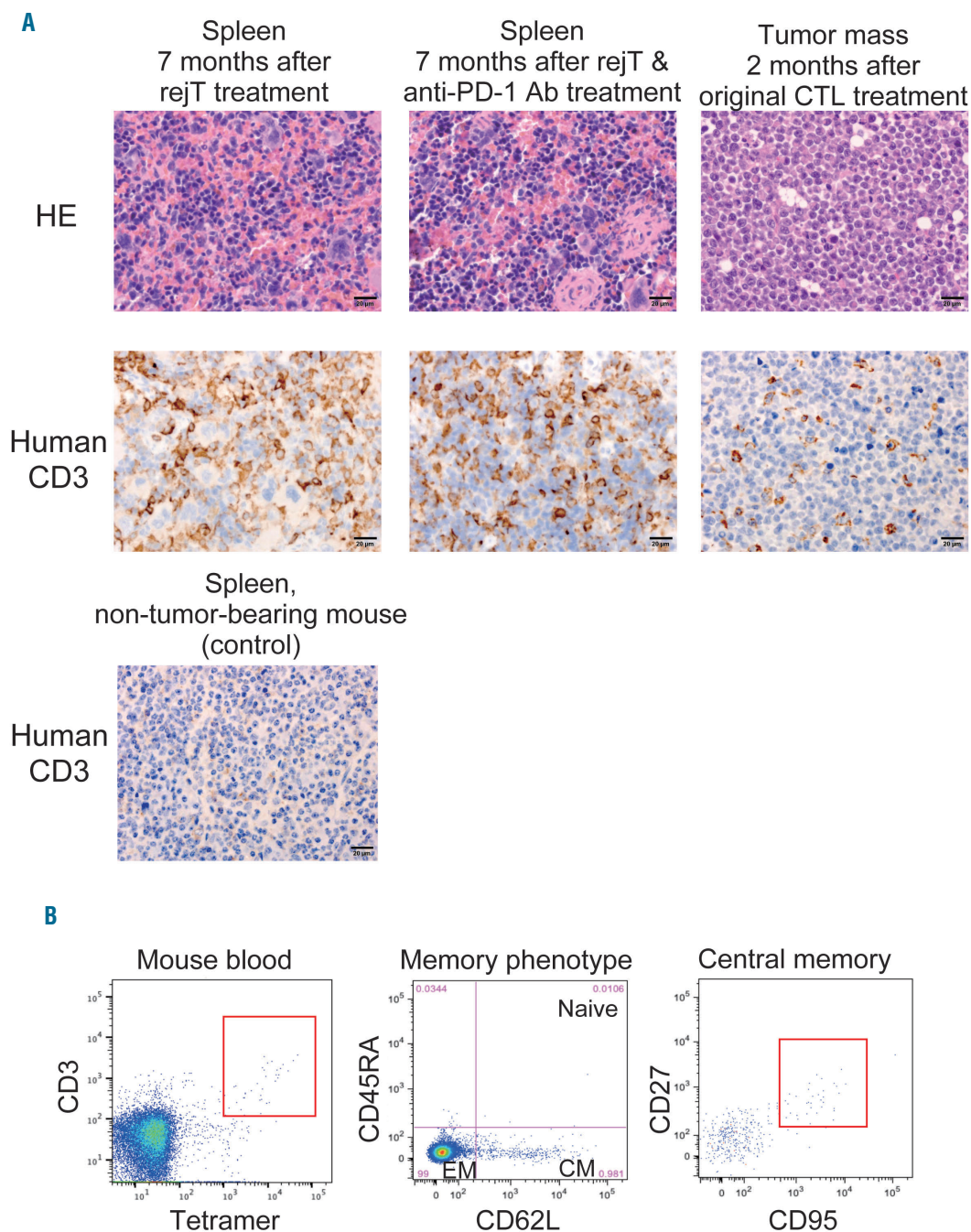
Figure 5. LMP2-rejT persisted in the spleen of long-surviving extranodal NK/T- cell lymphoma, nasal type-bearing mice. (A) Representative HE-stained sections of the spleens of ENKL-bearing mice treated with LMP2-rejT (upper left, center) and tumor mass of ENKL-bearing mice treated with original LMP2-CTL (upper right). Immunohistochemical study shows human CD3^{+} T-cell infiltration of the spleen in ENKL-bearing mice treated with LMP2-rejT (lower left, center) and of tumor mass in ENKL-bearing mice treated with original CTL (lower right). Spleen sections from untreated mice without ENKL were used as negative control. The scale bar represents 20 μm. (B) Flow cytometric analysis of tetramer+CD3^{+} LMP2-rejT population from peripheral blood. Central memory phenotype (CD45RA^{-}, CD62L^{+}, CD27^{+}, CD95^{+}) EBV-rejT are maintained in peripheral blood. LMP: latent membrane protein; rejT: rejuvenated cytotoxic T lymphocyte; ENKL: extranodal NK/T-cell lymphoma, nasal type; HE: hematoxylin and eosin; CTL: cytotoxic T lymphocyte; PD-1: programmed cell death 1; Ab: antibody; EBV: Epstein-Barr virus.

days, by contrast, contained many fewer human CD3^{+} T cells (Figure 5A, lower row of panels). Flow cytometry also was used to detect LMP2-rejT in the peripheral blood of ENKL-bearing mice treated using LMP2-rejT and surviving long-term. LMP2-tetramer – expressing CD3^{+} human T cells were present. Among them were effector memory (CD45RA^{-}, CD62L^{-}) and central memory phenotype T cells (CD45RA^{-}, CD62L^{+}, CD27^{+}, CD95^{+}) (Figure 5B).

Four of six mice that received rejT injections survived 182 to 296 days after treatment. Two relapsed, developing ascites before day 100. Tumor cells in ascitic fluid retained HLA class I expression (Figure 6A) without mutation in LMP2 (Figure 6B). Resistance to LMP2-rejT therapy in ascitic-fluid tumor cells was evaluated by ^{51}Cr release assay. EBV-rejT specific for LMP2 showed robust cytotoxicity (77%, 71.6%, 67.1%, and 51.2%; E:T ratios of 40:1, 20:1, 10:1 and 5:1 specific ^{51}Cr release, respectively) against ENKL cells in ascites (Figure 6C). These findings indicated that mutant ENKL cells did not appear after three rejT treatments and that the tumor cells had not developed resistance to LMP2-rejT therapy.

Discussion

We sought to verify that iPSC-derived rejT therapy specific to LMP1/LMP2 antigen would be an effective salvage therapy for refractory and relapsed ENKL. Although L-asparaginase is a key drug for ENKL[4] and L-asparaginase-containing chemotherapies improve prognosis in advanced ENKL patients,[5,6] tumor in about half of these patients resists L-asparaginase therapy or relapses after remission, resulting in a miserable clinical course. Adoptive T-cell therapy using peripheral blood-derived EBV-specific CTL is clearly effective for EBV-driven lymphoproliferative diseases after hematopoietic stem cell transplantation.[11-14] As these lymphomas develop in immunosuppressive situations and show type III latency, EBV-specific CTL adjuvant therapy can induce durable remissions. However, EBV-associated lymphomas showing type II latency, such as ENKL, Hodgkin lymphoma, and diffuse large B-cell lymphomas, are weakly immunogenic, with lymphoma cells that express only LMP1 and LMP2 antigens.[15] Therefore, EBV-CTL therapy targeting EBV-associated lymphomas with type II latency is more
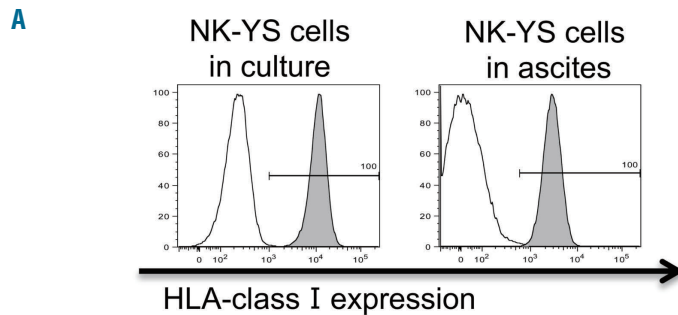
Figure 6. Phenotype of extranodal NK/T-cell lymphoma, nasal type cells in ascites of relapsed mice treated with LMP2-rejT. (A) Flow cytometric analysis of HLA class I (A, B, C) expression on NK-YS cells in ascites. (B) LMP2 sequence of post-rejT NK-YS cells in ascites. (C) In vitro ^{51}Cr release assay of EBV-rejT (effector), and HLA mismatched T cells (control effector) against NK-YS cells in culture and NK-YS cells in ascites (targets). Data are presented as mean ± SD. E:T ratio: effector : target ratio; ENKL: extranodal NK/T-cell lymphoma, nasal type; LMP: latent membrane protein; HLA: human leukocyte antigen; EBV: Epstein-Barr virus; SD: standard deviation.
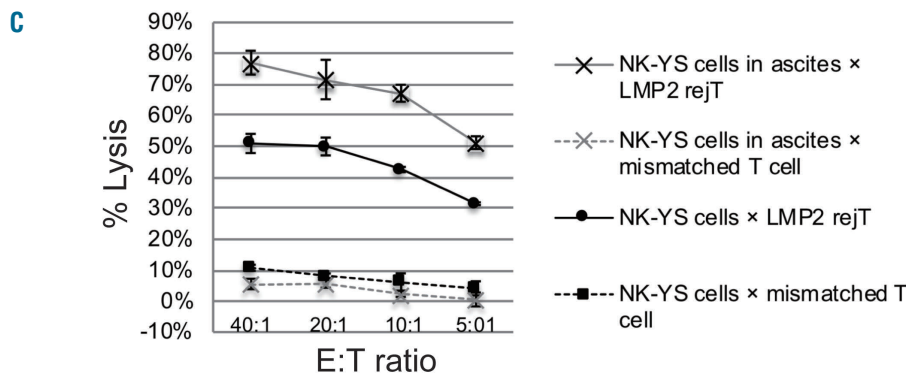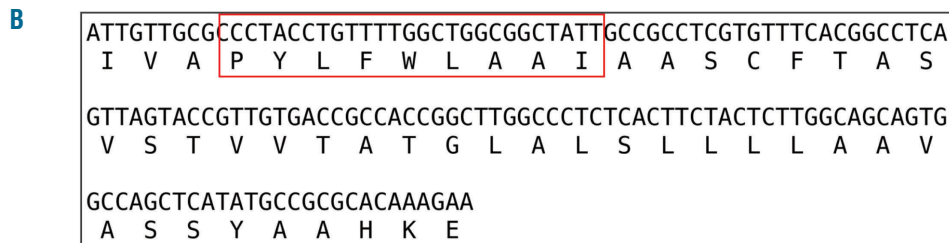
challenging. Bollard and colleagues successfully demonstrated effective control EBV-associated lymphomas with either type II or type III latency using patients' own LMP1- and LMP2-specific T cells: among six NK/T cell lymphoma (EBV-infected) patients whose tumors had relapsed after standard chemotherapies and who had received LMP1 or LMP2-specific CTL, three remained in CR, with responses that were associated with percentages of effector and central memory LMP1-specific T cells in the infused population.[16] Functionally rejT differentiated from T-iPSC include younger phenotypes such as central memory and effector memory phenotypes and have longer telomeres and a stronger proliferation ability (100-fold to 1,000-fold after T-cell stimulation) than original peripheral-blood derived CTL.[18-20,30] Although the original CTL expressed PD-1 strongly, their redifferentiated LMP2-rejT descendants almost lacked PD-1 expression (Figure 3C). CTL generation from heavily treated patients is generally more difficult than from healthy donors because of T-cell exhaustion. Although CTL clones from an ENKL patient showed relatively strong cytotoxicity against EBV-infected autologous LCLs *in vitro* (Figure 3A), the proliferation ability of patient-derived CTL clones was lower than that of healthy donor-derived CTL clones, and much lower than that of rejT. LMP2-rejT had a distinct survival advantage in ENKL-bearing mice over original LMP2-CTL (Figure 4C). Histopathological examination revealed that LMP2-rejT completely eradicated ENKL and that LMP2-rejT persisted in the spleen of long-surviving ENKL-bearing mice, supporting our hypothesis that rejT contribute to ENKL eradication as long-lived memory T cells (Figure 5A). Furthermore, we actually confirmed the presence of central memory phenotype human T cells in the peripheral blood of a long-surviving ENKL-bearing LMP2-rejT treated mouse (Figure 5B). However, neither necrotic lesions nor features of activation of immune cells (which might lead to organ injury) were found in these long-surviving mice, suggesting that long-term persistence of rejT does not reduce safety in this *in vivo* model.

As EBV-associated lymphomas express PD-L1 more strongly than lymphomas without EBV infection,[23-26] we examined PD-L1 expression in ENKL cells. Our statistical analysis demonstrated that PD-L1 expression was clearly related to very poor prognosis in ENKL patients (Figure 2A). Therefore, we anticipated that blockade of PD-1 and PD-L1 engagement would reinforce the efficacy of treatments using EBV-specific CTL expressing PD-1 and possibly EBV-rejT not expressing PD-1 for PD-L1 - expressing ENKL. Contrary to our expectations, we could not observe clear treatment enhancement by anti-PD-1 Ab with either original EBV-CTL or EBV-rejT (Figure 4 B-C), suggesting that PD-1 blockade is not necessarily required in treatment of ENKL with EBV-specific T cells. Anti-PD-1 Ab reportedly had no measurable effect on chimeric antigen receptor (CAR) T-cell expansion, persistence, or circulating cytokine levels when it was administered in combination with CAR T cells and lymphodepletion.[31] In our study, EBV-rejT alone effectively ablated ENKL in tumor-bearing mice, with such strong anti-tumor effects

that any additive beneficial effects of anti-PD-1 Ab were unclear. Of relevance is that toxicities of anti-PD-1 Ab may have impaired survival: disruption of the PD-1/PD-L1 pathway can lead to imbalances in immunologic tolerance, resulting in unchecked autoimmune-like/inflammatory side effects.[32] By contrast, viral-specific antigen-specific CTL therapy is minimally toxic and does not harm healthy tissues.[16] We postulate that also EBV-rejT therapy is free from severe adverse events and suggest that it will be highly effective against ENKL when L-asparaginase therapy has failed.

EBV-rejT still exerted strong cytotoxic effects against tumor cells in ascites from mice with relapse after EBV-rejT therapy. These tumor cells maintained HLA class I expression and harbored no LMP2 mutations (Figure 6). This suggests that EBV-rejT may not fully penetrate all areas of tissue metastasis. We did not administer cytokines such as IL-2, IL-7 and IL-15 to mice to avoid an artificial increase of the activity of ENKL cells *in vivo*, because even without cytokines ENKL cells rapidly proliferated in mice and the tumor signal progressively increased. Using cytokines, the expansion of rejT might be much stronger and the incidence of relapse might decrease. However, it is encouraging that even without cytokines, rejT were well activated by recognizing ENKL cells and showed strong cytotoxic activity against ENKL cells.

Our results collectively suggest that to treat relapsed and refractory ENKL using LMP1- and LMP2-specific rejT will be very useful, as large numbers of functionally rejuvenated LMP1- and LMP2-specific CTL can reliably be obtained from T-iPSC. The greatest advantage of rejT therapy is that once T-iPSC are established from an EBV-CTL clone, therapeutic T cells can be generated from T-iPSC in unlimited numbers. If patient tumor cells strongly express PD-L1, the associated poor prognosis should prompt caregivers to generate patient-specific EBV-rejT targeting LMP1 and LMP2 while SMILE therapy is administered. EBV-rejT can supply a reliable salvage therapy for refractory and relapsed ENKL in which L-asparaginase therapy has failed. To establish banks of T-iPSC directed against a variety of viral antigens and HLA types may ultimately provide effective "off-the-shelf" T-cell adoptive immunotherapy treatments against EKNL. The principle demonstrated here can be extended to other virus-induced tumors and neoantigens.

References

1. Tse E, Kwong YL. How I treat NK/T-cell lymphomas. Blood. 2013;121(25):4997-5005.

2. Oshimi K. Progress in understanding and managing natural killer-cell malignancies. Br J Haematol. 2007;139(4):532-544.

3. Egashira M, Kawamata N, Sugimoto K, Kaneko T, Oshimi K. P-glycoprotein expression on normal and abnormally expanded natural killer cells and inhibition of P-glycoprotein function by cyclosporin A and its analogue, PSC833. Blood. 1999;93(2):599-606.

4. Ando M, Sugimoto K, Kitoh T, et al. Selective apoptosis of natural killer-cell tumours by l-asparaginase. Br J Haematol. 2005;130(6):860-868.

5. Yamaguchi M, Kwong YL, Kim WS, et al. Phase II study of SMILE chemotherapy for newly diagnosed stage IV, relapsed, or refractory extranodal natural killer (NK)/T-cell lymphoma, nasal type: the NK-Cell Tumor Study Group study. J Clin Oncol. 2011;29(33):4410-4416.

6. Kwong YL, Kim WS, Lim ST, et al. SMILE for natural killer/T-cell lymphoma: analysis of safety and efficacy from the Asia Lymphoma Study Group. Blood. 2012;120(15):2973-2980.

7. Rosenberg SA, Packard BS, Aebersold PM, et al. Use of tumor-infiltrating lymphocytes and interleukin-2 in the immunotherapy of patients with metastatic melanoma. A preliminary report. N Engl J Med. 1988;319(25):1676-1680.

8. Dudley ME, Wunderlich JR, Robbins PF, et al. Cancer regression and autoimmunity in patients after clonal repopulation with antitumor lymphocytes. Science. 2002;298(5594):850-854.

9. Dudley ME, Wunderlich JR, Yang JC, et al. Adoptive cell transfer therapy following non-myeloablative but lymphodepleting chemotherapy for the treatment of patients with refractory metastatic melanoma. J Clin Oncol. 2005;23(10):2346-2357.

10. Restifo NP, Dudley ME, Rosenberg SA. Adoptive immunotherapy for cancer: harnessing the T cell response. Nat Rev Immunol. 2012;12(4):269-281.

11. Rooney CM, Smith CA, Ng CY, et al. Infusion of cytotoxic T cells for the prevention and treatment of Epstein-Barr virus-induced lymphoma in allogeneic transplant recipients. Blood. 1998;92(5):1549-1555.

12. Gottschalk S, Edwards OL, Sili U, et al. Generating CTLs against the subdominant Epstein-Barr virus LMP1 antigen for the adoptive immunotherapy of EBV-associated malignancies. Blood. 2003;101(5):1905-1912.

13. Heslop HE, Slobod KS, Pule MA, et al. Long-term outcome of EBV-specific T-cell infusions to prevent or treat EBV-related lymphoproliferative disease in transplant recipients. Blood. 2010;115(5):925-935.

14. Bollard CM, Rooney CM, Heslop HE. T-cell therapy in the treatment of post-transplant lymphoproliferative disease. Nat Rev Clin Oncol. 2012;9(9):510-519.

15. Bollard CM, Gottschalk S, Leen AM, et al. Complete responses of relapsed lymphoma following genetic modification of tumor-antigen presenting cells and T-lymphocyte transfer. Blood. 2007;110(8):2838-2845.

16. Bollard CM, Gottschalk S, Torrano V, et al. Sustained complete responses in patients with lymphoma receiving autologous cytotoxic T lymphocytes targeting Epstein-Barr virus latent membrane proteins. J Clin Oncol. 2014;32(8):798-808.

17. Wherry EJ. T cell exhaustion. Nat Immunol. 2011;12(6):492-499.

18. Nishimura T, Kaneko S, Kawana-Tachikawa A, et al. Generation of rejuvenated antigen-specific T cells by reprogramming to pluripotency and redifferentiation. Cell Stem Cell. 2013;12(1):114-126.

19. Ando M, Nishimura T, Yamazaki S, et al. A safeguard system for induced pluripotent stem cell-derived rejuvenated T cell therapy. Stem Cell Reports. 2015;5(4):597-608.

20. Ando M, Nakauchi H. 'Off-the-shelf' immunotherapy with iPSC-derived rejuvenated cytotoxic T lymphocytes. Exp Hematol. 2017;47:2-12.

21. Okazaki T, Maeda A, Nishimura H, Kurosaki T, Honjo T. PD-1 immunoreceptor inhibits B cell receptor-mediated signaling by recruiting src homology 2-domain-containing tyrosine phosphatase 2 to phosphotyrosine. Proc Natl Acad Sci U S A. 2001;98(24):13866-13871.

22. Okazaki T, Chikuma S, Iwai Y, Fagarasan S, Honjo T. A rheostat for immune responses: the unique properties of PD-1 and their advantages for clinical application. Nat Immunol. 2013;14(12):1212-1218.

23. Ansell SM, Lesokhin AM, Borrello I, et al. PD-1 blockade with nivolumab in relapsed or refractory Hodgkin's lymphoma. N Engl J Med. 2015;372(4):311-319.

24. Yamamoto R, Nishikori M, Kitawaki T, et al. PD-1-PD-1 ligand interaction contributes to immunosuppressive microenvironment of Hodgkin lymphoma. Blood. 2008;111(6):3220-3224.

25. Green MR, Rodig S, Juszczynski P, et al. Constitutive AP-1 activity and EBV infection induce PD-L1 in Hodgkin lymphomas and posttransplant lymphoproliferative disorders: implications for targeted therapy. Clin Cancer Res. 2012;18(6):1611-1618.

26. Kiyasu J, Miyoshi H, Hirata A, et al. Expression of programmed cell death ligand 1 is associated with poor overall survival in patients with diffuse large B-cell lymphoma. Blood. 2015;126(19):2193-2201.

27. Kwong YL, Chan TSY, Tan D, et al. PD1 blockade with pembrolizumab is highly effective in relapsed or refractory NK/T-cell lymphoma failing l-asparaginase. Blood. 2017;129(17):2437-2442.

28. Nagata H, Konno A, Kimura N, et al. Characterization of novel natural killer (NK)-cell and gammadelta T-cell lines established from primary lesions of nasal T/NK-cell lymphomas associated with the Epstein-Barr virus. Blood. 2001;97(3):708-713.

29. Gottschalk S, Ng CY, Perez M, et al. An Epstein-Barr virus deletion mutant associated with fatal lymphoproliferative disease unresponsive to therapy with virus-specific CTLs. Blood. 2001;97(4):835-843.

30. Themeli M, Kloss CC, Ciriello G, et al. Generation of tumor-targeted human T lymphocytes from induced pluripotent stem cells for cancer therapy. Nat Biotechnol. 2013;31(10):928-933.

31. Heczey A, Louis CU, Savoldo B, et al. CAR T Cells Administered in Combination with Lymphodepletion and PD-1 Inhibition to Patients with Neuroblastoma. Mol Ther. 2017;25(9):2214-2224.

32. Naidoo J, Page DB, Li BT, et al. Toxicities of the anti-PD-1 and anti-PD-L1 immune checkpoint antibodies. Ann Oncol. 2016;27(7):1362.

Ferrata Storti Foundation

Atherogenic lipid stress induces platelet hyperactivity through CD36-mediated hyposensitivity to prostacyclin: the role of phosphodiesterase 3A

Martin Berger,[1,2,3] Zaher Raslan,[3*] Ahmed Aburima,[1*] Simbarashe Magwenzi,[1] Katie S. Wraith,[1] Benjamin E.J. Spurgeon,[3] Matthew S. Hindle,[3] Robert Law,[1] Maria Febbraio[4] and Khalid M. Naseem[1,3]

[1]Centre for Cardiovascular and Metabolic Research, Hull York Medical School, University of Hull, Hull, UK; [2]Department of Internal Medicine 1, University Hospital RWTH Aachen, Aachen, Germany; [3]Discovery and Translational Science Department, Leeds Institute of Cardiovascular and Metabolic Medicine, University of Leeds, Leeds, UK and [4]School of Dentistry, University of Alberta, Edmonton, AB, Canada

*ZR and AA contributed equally to this work

ABSTRACT

Prostacyclin (PGI$_2$) controls platelet activation and thrombosis through a cyclic adenosine monophosphate (cAMP) signaling cascade. However, in patients with cardiovascular diseases this protective mechanism fails for reasons that are unclear. Using both pharmacological and genetic approaches we describe a mechanism by which oxidized low density lipoproteins (oxLDL) associated with dyslipidemia promote platelet activation through impaired PGI$_2$ sensitivity and diminished cAMP signaling. In functional assays using human platelets, oxLDL modulated the inhibitory effects of PGI$_2$, but not a phosphodiesterase (PDE)-insensitive cAMP analog, on platelet aggregation, granule secretion and *in vitro* thrombosis. Examination of the mechanism revealed that oxLDL promoted the hydrolysis of cAMP through the phosphorylation and activation of PDE3A, leading to diminished cAMP signaling. PDE3A activation by oxLDL required Src family kinases, Syk and protein kinase C. The effects of oxLDL on platelet function and cAMP signaling were blocked by pharmacological inhibition of CD36, mimicked by CD36-specific oxidized phospholipids and ablated in CD36$^{-/-}$ murine platelets. The injection of oxLDL into wild-type mice strongly promoted FeCl3-induced carotid thrombosis *in vivo*, which was prevented by pharmacological inhibition of PDE3A. Furthermore, blood from dyslipidemic mice was associated with increased oxidative lipid stress, reduced platelet sensitivity to PGI$_2$ *ex vivo* and diminished PKA signaling. In contrast, platelet sensitivity to a PDE-resistant cAMP analog remained normal. Genetic deletion of CD36 protected dyslipidemic animals from PGI$_2$ hyposensitivity and restored PKA signaling. These data suggest that CD36 can translate atherogenic lipid stress into platelet hyperactivity through modulation of inhibitory cAMP signaling.

Correspondence:

KHALID M. NASEEM
k.naseem@leeds.ac.uk

Check the online version for the most updated information on this article, online supplements, and information on authorship & disclosures: www.haematologica.org/content/105/3/808

Introduction

Myocardial infarction (MI) is characterized by platelet-driven atherothrombotic events that lead to acute occlusion of a coronary vessel. Excessive platelet activation is controlled by endothelial derived nitric oxide (NO) and prostacyclin (PGI$_2$),[1] but action of these protective agents is overcome in MI by mechanisms that are yet to be elucidated. A key risk factor for MI is dyslipidemia, which is strongly associated with a pro-thrombotic phenotype linked to atherothrombosis and platelet hyperactivity.[2,3] The blood of high-risk individuals with dyslipidemia is characterized by increased plasma lipid peroxides, with low density lipoproteins (LDL) serving as a highly abundant carriers for these oxidatively-modified lipids.[4-6] Oxidized LDL (oxLDL) are circulating pathological ligands that can enhance thrombosis through

their ability to promote platelet hyperactivity. *In vitro* experimentation demonstrates that these modified lipoproteins can cause direct activation of platelets and also potentiate platelet activation induced by physiological agonists such as thrombin, ADP and epinephrine.[7–10] However, the potential pathophysiological importance of these observations for thrombosis in vivo remain unclear.

The scavenger receptor CD36 has emerged as a potential conduit for transducing plasma lipid stress into platelet hyperactivity and thrombosis, through the recognition of lipoprotein associated molecular patterns (LAMPs). CD36, alone or potentially in combination with Toll-Like Receptor (TLR)[2] and TLR6 drive a complex series of intracellular signaling events that are associated with platelet activation.[11–15] Upon ligation of CD36, Src family kinases constitutively associated with the receptor, drive the activation of Syk, Vav-1, PLCγ2, ERK5 and JNK that are associated with platelet activation.[13,16–18] More recently, data have emerged to suggest that the signaling events promote the generation of reactive oxygen species (ROS).[14,16,17] ROS in turn activate ERK to drive thrombosis directly by platelet hyperactivity and caspase-dependent procoagulant activity.[18,19] Moreover, we found that ROS diminish sensitivity to the nitric oxide (NO)-stimulated cGMP-PKG inhibitory signaling cascade to reduce the threshold for platelet activation.[17] These data suggest that the translation of atherogenic lipid stress by platelet CD36 is functionally linked to both stimulation of activatory signaling pathways and to an as of yet ill-defined modulation of inhibitory pathways.

PGI_2 is the most potent endogenous regulator of platelet function with both genetic and pharmacological modulation of the pathway linked to accelerated thrombosis *in vivo*.[20] PGI_2 activates a cyclic adenosine monophosphate (cAMP) signaling pathway that leads to subsequent activation of protein kinase A (PKA) in platelets and results in the phosphorylation of numerous proteins,[21] linked to the inhibition of Ca^{2+} mobilization, dense granule secretion, spreading, integrin $\alpha_{IIb}\beta_3$ activation and aggregation *in vitro*.[20] To ensure optimal platelet function, cAMP levels are tightly regulated by the hydrolyzing enzymes phosphodiesterase (PDE)2A and 3A. The pharmacological inhibition or genetic ablation of PDE3A in murine and human platelets reduces thrombotic potential.[22,23] Thus, factors that alter platelet inhibition by influencing cAMP synthesis or hydrolysis may be critical modulators of atherothrombosis and potentially lead to a pro-thrombotic phenotype. Given the established link between oxidized lipid stress and excessive platelet activation, the aim of this study was to determine if oxidatively modified lipoproteins could promote platelet hyperactivity through modulation of the PGI_2/cAMP signaling pathway.

Methods

Reagents

Phospho-PKA Substrate (RRXS*/T*) Rabbit mAb and phospho-VASP-Ser[157/239] antibodies were from Cell Signaling Technology (Danvers, USA). PDE3A antibodies were from the MRC Unit (Dundee University, Dundee, UK). Anti-β-Tubulin antibody was from Millipore (Nottingham, UK). BD Phosflow Lyse/Fix Buffer was from BD Biosciences (Oxford, UK). OxPC-E06 mAb was from Avanti Polar Lipids (Alabaster, USA). FITC-labeled Rat Anti-Mouse P-selectin (CD62P) and PE-labeled JON/A antibodies were

from Emfret Analytics (Würzburg, Germany). Alexa-Fluor 647 Goat anti-Rabbit IgG, Alexa-Fluor 488 Succinimidyl Ester and Pacific Blue Succinimidyl Ester were from ThermoFisher Scientific (Waltham, USA). PAR-1 peptide was from Anaspec (Fremont, USA). Anti-CD36 Antibody (FA6-152) was from Abcam (Cambridge, UK). Phosphodiesterase Activity Assay Kit was from Enzo Life Sciences (Exeter, UK). cAMP Biotrack EIA was from GE Healthcare (Buckinghamshire, UK). Horm Collagen was from Nycomed (Munich, Germany). PGI_2 and Cholesterol Assay Kit were from Cayman Chemical (Cambridge, UK). Vena8 Endothelial+ biochips were from Cellix (Hertfordshire, UK). All other reagents were from Sigma-Aldrich (Dorset, UK).

Experimental animals

$CD36^{-/-}$ mice were provided by Prof. Maria Febbraio (University of Alberta, Canada). C57BL/6 were from Charles River (Kent, UK). For high-fat diet studies, male mice were fed a 45% Western diet (Special Diet Services) for 12–16 weeks. Sex/age-matched littermates were fed a normal chow for the duration of the experiments and used as controls. For all remaining experiments, male C57BL/6 and CD36-/- were used at eight weeks of age.

Isolation and oxidation of plasma low density lipoproteins

Low-density lipoproteins (density 1.019–1.063 g/mL) were prepared from fresh human plasma by sequential density ultracentrifugation and oxidised with $CuSO_4$ (10 μmol/L).[14] Separate preparations of LDL were used to repeat the individual experiments.

Platelet aggregation, flow assays, flow cytometric analysis, intravital microscopy, immunoprecipitation, immunoblotting, phosphodiesterase enzyme activity assay and cyclic adenosine monophosphate measurement

Detailed methods are presented in the *Online Supplementary Methods*.

Statistical analysis

Experimental data was analyzed by Graphpad Prism 6 (La Jolla, CA, USA). Data are presented as means±standard error of the mean (SEM) of at least three different experiments. Differences between groups were calculated using Mann-Whitney U Test or Kruskal-Wallis Test for non-parametric testing and statistical significance accepted at $P\leq0.05$.

All studies were approved by the Hull York Medical school Ethics committee and University of Leeds Research Ethics committee.

Results

Oxidized low density lipoproteins cause platelet hyposensitivity to prostacyclin

Treatment of human washed platelets with PGI_2 (20 nM) for one minute (min), at a time point that induces maximal cAMP-mediated signaling[24] reduced thrombin (0.05 U/mL)-induced aggregation from 89.0±4.1 to 9.4±4.4% (*P*<0.01) (Figure 1A). Next, platelets were treated with oxLDL or control native LDL (nLDL) (50 μg/mL) for 2 min prior to the addition of PGI_2 (20 nM) and thrombin (0.05 U/mL). The presence of oxLDL caused a partial recovery in thrombin-stimulated platelet aggregation to 50.0±9.3 (*P*<0.015 *vs.* control), without stimulating aggregation directly (Figure 1A). In contrast, PGI_2-mediated

A

B

C

D

E
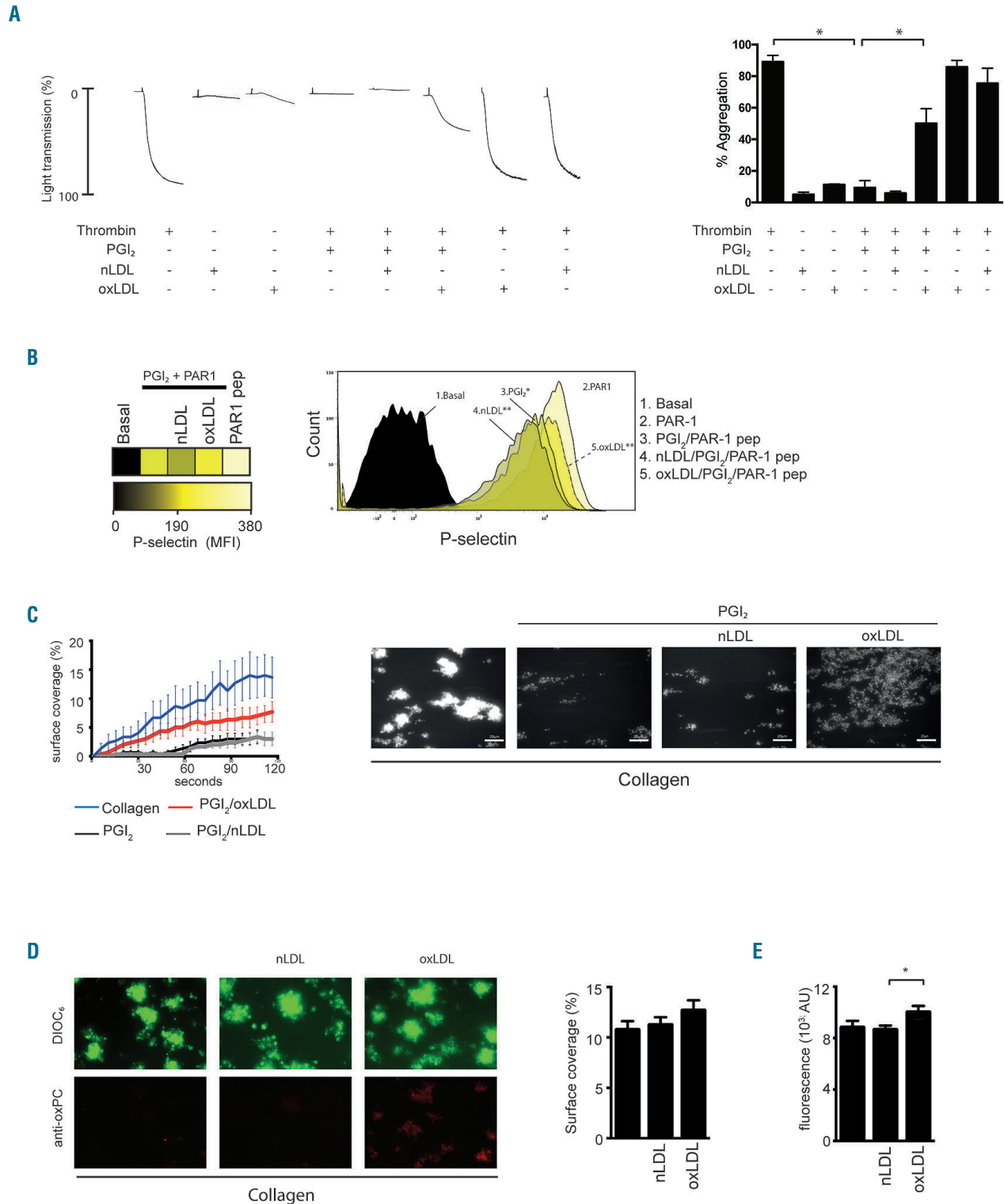
Figure 1. Oxidized low-density lipoproteins (oxLDL) induce prostacyclin (PGI₂) hyposensitivity in platelets. (A) Washed human platelets (2.5 x 10⁸/mL) were treated alone or with control native LDL (nLDL) or oxLDL (50 μg/mL) for 2 minutes (min) followed by a 1 min incubation with PGI₂ (20 nM). Thrombin (0.05U/mL)-stimulated aggregation was then measured under constant stirring (1000 rpm) at 37°C for 4 min. In some cases, platelets were incubated with either thrombin, nLDL or oxLDL alone for 4 min. (Left) Representative aggregation traces. (Right) Percentage aggregation is presented by mean±standard error of mean (SEM) (n= 5). **P<0.01 compared to platelets treated with thrombin and PGI₂, Mann-Whitney U Test. (B) Whole blood was treated as in (A) and activated with PAR-1 peptide (10 ∝M) for 5 min followed by fixation. CD62P expression was assessed by flow cytometry. Representative data of three independent experiments. (Left) Data are presented as heatmap of mean fluorescence intensity (MFI). (Right) Representative histograms. (C) Human whole blood was incubated with PGI₂ (20 nM) for 1 min alone or with control native LDL (nLDL) or oxLDL (50 μg/mL) for 10 min. Blood was perfused over collagen-coated biochips for 2 min at arterial shear 1000s-1 and images of adherent platelets were taken by fluorescence microscopy. (Left) The surface coverage (%) is presented as mean±SEM (n=3) (P<0.05, Mann-Whitney U Test). (Right) Representative fluorescence microscopy images are shown. (D) Whole blood was incubated with nLDL or oxLDL (50 μg/mL) for 10 min and then perfused over collagen-coated surfaces for 2 min at arterial shear 1000s-1. Thrombi were post-stained with anti-oxPC antibody and images were taken by fluorescence microscopy. (Left) Representative of images of 3 independent experiments. Stained with DIOC6 (top panel) or anti-oxPC (bottom panel) (Center) The surface coverage is presented as mean±SEM (n=4, *P<0.05, Mann-Whitney U Test). (Right) Fluorescence (red Channel) is presented as mean±SEM (n=4, *P<0.05, Mann-Whitney U Test).

inhibition was unaffected by nLDL (5.8±1.2%). Similar data were obtained when platelets were stimulated with collagen (*Online Supplementary Figure S1*). Next, the effects of oxLDL in whole blood were examined. Stimulation of whole blood with PAR-1 peptide (10 μM) increased *P*-selectin expression, which was reduced by pre-treatment with PGI$_2$ (20 nM). Consistent with the aggregation experiments, oxLDL reduced inhibitory effects of PGI$_2$ (Figure 1B). Finally, the effects of oxLDL under physiological conditions of arterial flow were examined. Perfusion of whole blood over collagen-coated biochips led to platelet deposition and thrombus formation (Figure 1C), with surface coverage inhibited by PGI$_2$ (20 nM) from 14.9±2.9 to 3.8±1.7% (*P*<0.05). OxLDL, but not nLDL, prevented PGI$_2$-mediated inhibition of platelet deposition (8.1±1.9%; *P*<0.05 compared to PGI$_2$ alone). OxLDL alone caused a small but non-significant increase in thrombosis and was incorporated into the thrombi as evidenced by staining for oxidized lipid epitopes (Figure 1D). These data demonstrate that under a variety of different conditions oxLDL reduces platelet sensitivity to PGI$_2$.

Oxidized low density lipoproteins modulate cyclic adenosine monophosphate signaling through increased phosphodiesterase 3A activity

PGI$_2$ inhibits platelets through the stimulation of cAMP-PKA signaling cascade.[20] Given the reduced platelet sensitivity to PGI$_2$, the direct effect of oxLDL on platelet cAMP metabolism was tested. Incubation with PGI$_2$ caused a significant increase in platelet cAMP concentrations (1814±166 fmol cAMP/1x10^8 platelets; *P*<0.05 *vs.* basal). When platelets were treated with nLDL (50 μg/mL), the ability of the prostanoid to elevate cAMP was unaffected (1885±203 fmol cAMP/1x10^8 platelets), while oxLDL (50 μg/mL) prevented PGI$_2$-induced accumulation of cAMP (481±23 fmol cAMP/1x10^8 platelets; *P*<0.05 compared to PGI$_2$ alone) and also reduced basal cAMP concentrations (not significant) (Figure 2Ai). To determine if oxLDL blocked cAMP synthesis or accelerated cAMP breakdown by phosphodiesterase 3A (PDE3A) and PDE225,[25] the PDE2A inhibitor EHNA (20 μM) and the PDE3A inhibitor milrinone (10 μM) were used. Consistent with previous studies, both inhibitors potentiated cAMP
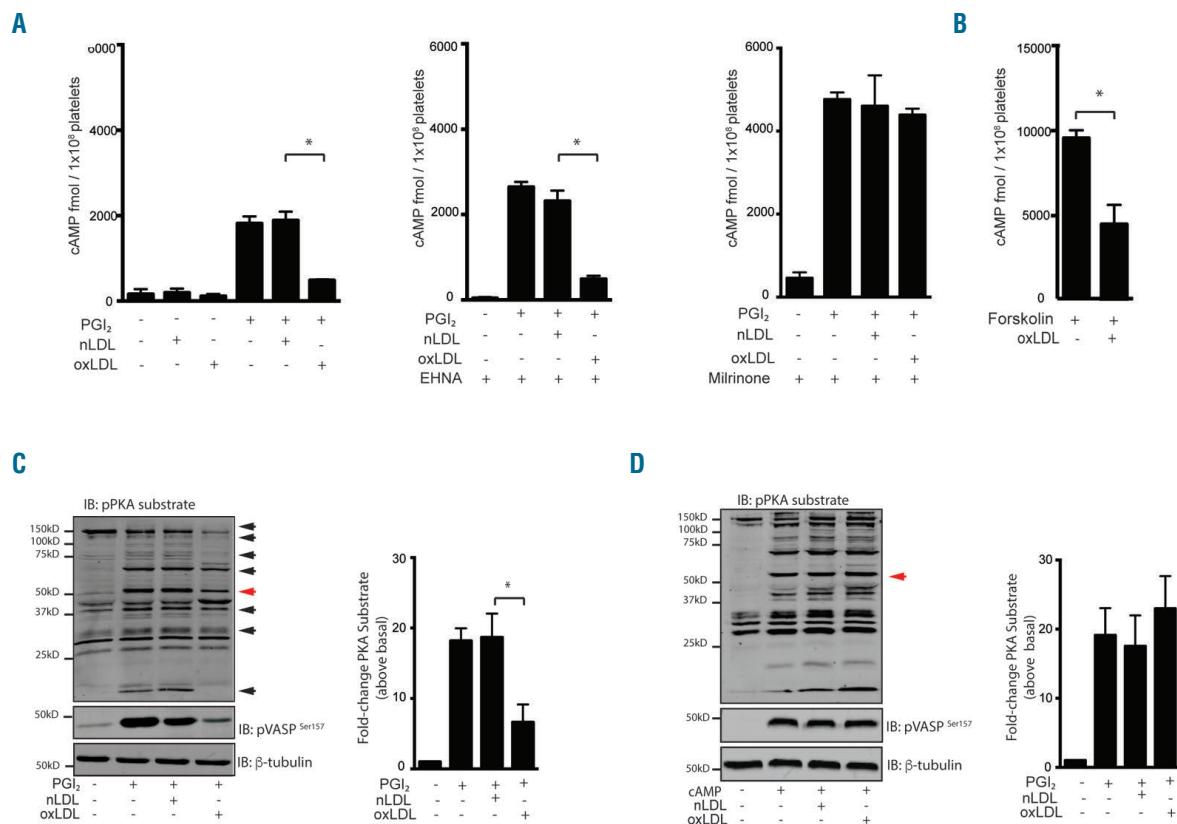
Figure 2. Oxidized low-density lipoproteins modulate cyclic adenosine monophosphate (cAMP) signaling in response to prostacyclin (PGI$_2$). (A) Washed human platelets (2x10^8/mL) incubated with apyrase, indomethacin and EGTA were treated alone or with control native LDL (nLDL) or oxLDL (50 μg/mL) for 2 minutes (min) followed by a 1 min PGI$_2$ (50 nM) incubation. Platelets were lysed and intracellular cAMP concentrations were measured by enzyme immunoassay. (Left) Intracellular cAMP levels presented as mean±standard error of mean (SEM) (n=3, *P*<0.05, Mann-Whitney U Test). (Center) Platelets treated as described under (A) in the presence EHNA (20 μM). Intracellular cAMP levels are presented as mean±SEM (n=3, *P*<0.05, Mann-Whitney U Test) (Right) Platelets treated as described under (A) in the presence of Milrinone (10 μM). Intracellular cAMP levels are presented as mean±SEM (n=3, *P*<0.05, Mann-Whitney U Test). (B) Washed human platelets (2x10^8/mL) were incubated alone or with oxLDL (50 μg/mL) for 2 min followed by a 5-min incubation with Forskolin (10 μM), then lysed and measured as described under (A). Intracellular cAMP concentrations presented as mean±SEM (n=3, *P*<0.05, Mann-Whitney U Test). (C) Washed human platelets (5x10^8/mL) were treated as described under (A), lysed in Laemmli buffer, separated by SDS-PAGE and immunoblotted with anti-phosphoPKA substrate, anti-phosphoVASPser[157] and anti-β tubulin. (Left) Representative blot of three independent experiments. (Right) Densitometry of the representative highlighted band (red) (*P*<0.05, Mann-Whitney U Test). (D) Washed human platelets were treated as described under (A) except that platelets were treated with 8-CPT-cAMP (50 μM) for 5 min and then processed as in (C). (Left) Representative blot of three independent experiments and (Righti) densitometry of the representative highlighted band (red).
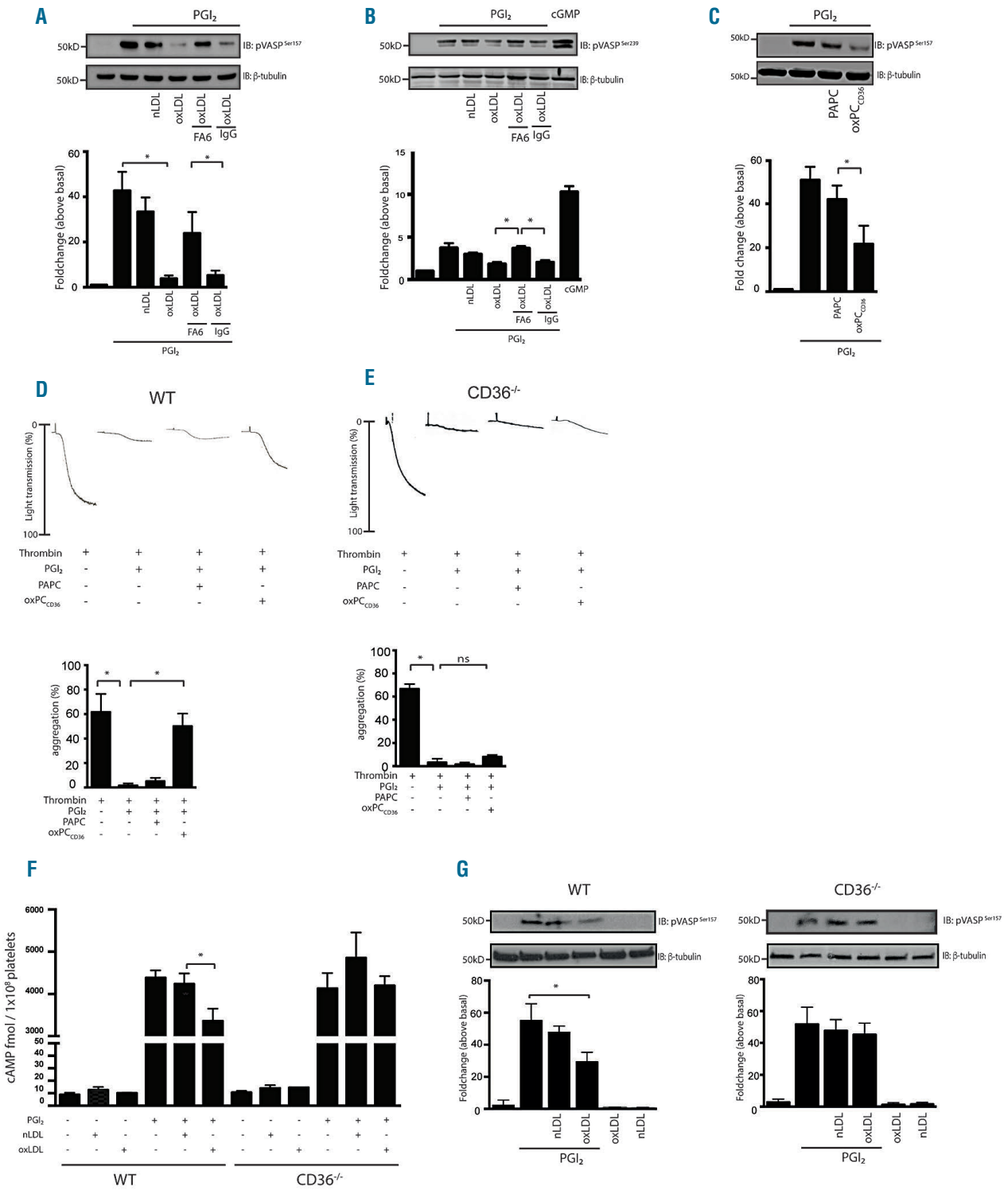
Figure 3. Oxidized low-density lipoproteins (oxLDL) and oxPCCD36 alter prostacyclin (PGI₂) inhibitory signaling *via* CD36. (A) Washed human platelets (5x10⁸/mL) incubated with apyrase, indomethacin and EGTA were incubated with FA6-152 or IgG (1 μg/mL) for 20 minutes (min). Platelets were then incubated alone or with control native LDL (nLDL) or oxLDL (50 μg/mL) for 2 min and subsequently stimulated by PGI₂ (50nM) for 1 min. Treated platelets were lysed in Laemmli buffer, separated by SDS-PAGE and immunoblotted with anti-phosphoVASPser157 or anti-β tubulin. (Top) Representative blot of three independent experiments. (Bottom) Densitometry of pVASPser157 fold-change above basal mean±standard error of mean (SEM) (n=3 *P<0.05, Mann-Whitney U Test). (B) As in (A) except that platelets were probed for pVASPser239. (C) Platelets were treated as in (A) alone or with oxPCCD36 or PAPC (25 μM) for 2 min followed by PGI₂ (50 nM) for 1 min. (Top) Representative blot of three independent experiments and (Bottom) Densitometry of pVASPser157 fold-change above basal, mean±SEM (n=3 *P<0.05, Mann-Whitney U Test). (D) Washed wild-type murine platelets (2.5x10⁸/mL) were treated alone or with oxPCCD36 or PAPC (10 μM) for 2 min followed by a 1 min incubation with PGI₂ (20 nM). Thrombin (0.05 U/mL)-stimulated aggregation was then measured under constant stirring (1000 rpm) at 37°C for 4 min. (Top) Representative aggregation traces and (Bottom) data presented as percentage aggregation, mean±SEM (n=3, P<0.05, Mann-Whitney U Test). (E) As described in (D) for CD36⁻/⁻ platelets. Ns: not significant. (F) Washed murine WT or CD36⁻/⁻ platelets (2x10⁸/ml) were treated alone or with nLDL or oxLDL (50 μg/mL) for 2 min followed by a 1-min PGI₂ (50 nM) incubation. Platelets were lysed, and intracellular cAMP concentrations were measured by enzyme immunoassay. Intracellular cAMP levels are presented as mean±SEM (n=3, *P<0.05, Mann-Whitney U Test). (G) As in (A) except that murine (Left) WT and (Right) CD36-/- platelets were used. Representative blot of three independent experiments. pVASPser157 is presented as beta-tubulin corrected fold-change above basal±SEM (n=3 *P<0.05, Mann-Whitney U Test).
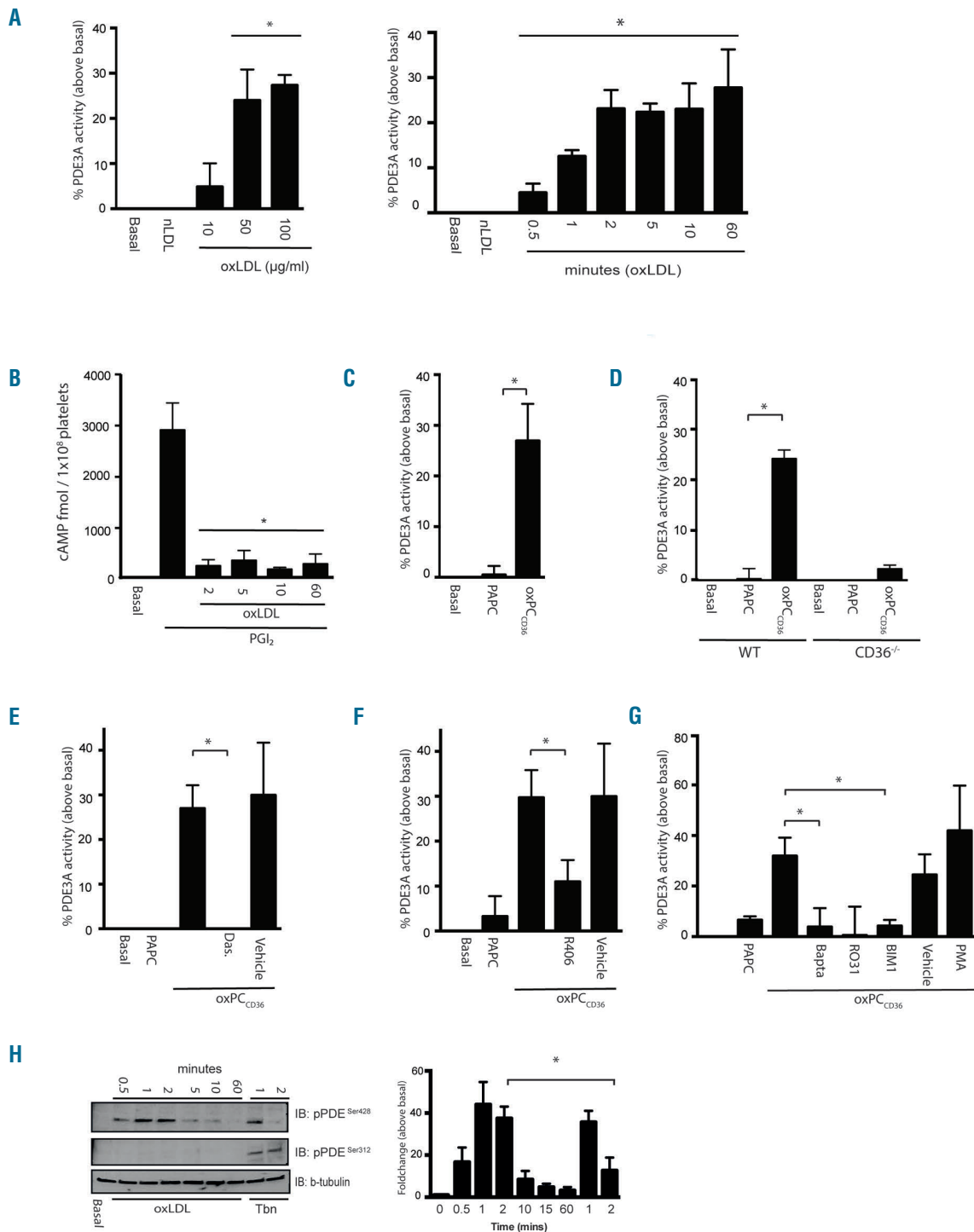
Figure 4. Oxidized low-density lipoproteins (oxLDL) and oxPCCD36 induce sustained phosphodiesterase 3A (PDE3A) activity in a CD36-dependent manner. (A). Washed human platelets ($5x10^8$/mL) incubated with apyrase, indomethacin and EGTA were (Left) incubated with nLDL (50 μg/mL) or oxLDL (10-100 μg/mL) for 2 minutes (min) or (Right) incubated with control native LDL (nLDL) (50 μg/mL) or oxLDL (50 μg/mL) for up to 60 min. Platelets were lysed, PDE3A was immunopre-cipitated and enzyme activity was measured. Data is expressed as % activity above basal activity and presented as mean±standard error of mean (SEM) (*P*<0.05; n=3, Kruskal-Wallis Test). (B) Washed human platelets ($5x10^8$/mL) were incubated with oxLDL (50 μg/mL) followed by PGI$_2$ (50 nM) for 1 min. Platelets were lysed, and intracellular cyclic adenosine monophosphate (cAMP) levels were determined by enzyme immunoassay. Data are presented as mean±SEM (*P*<0.05, n=3, Kruskal-Wallis Test). (C) Washed human platelets ($5x10^8$/mlL) were incubated with oxPCCD36 or PAPC (25 μM) for 2 min, and activity of immuno-precipitated PDE3A measured. Data are expressed as % activity above basal activity and presented as mean±SEM (*P*<0.05; n=3 Mann-Whitney U Test). (D) As in (C), except that PDE3A activity was measured in wild-type (WT) and CD36$^{-/-}$ washed platelets (*P*<0.05; n=3 Mann-Whitney U Test). (E) As in (A) except that human platelets ($5x10^8$/mL) incubated with apyrase, indomethacin and EGTA were then treated with oxPCCD36 or PAPC (25 μM) for 2 min in the presence of absence of dasatinib (10 μM) or vehicle control (DMSO). PDE3A was immunoprecipitated, and enzyme activity was measured. Data are expressed as % activity above basal activity and presented as mean±SEM (*P*<0.05; n=4 Mann-Whitney U Test). (F) As in (A) except that platelets were treated with R406 (1 μM) or vehicle control (DMSO). (G) As in (A), except that platelets were treated with PKC inhibitors (RO31 10μM, BIM1 10μM), PMA (100nM), BAPTA (20 μM) or vehicle control (DMSO). (n=3, *P*<0.05 compared to basal, Kruskal-Wallis Test). (H) Washed human platelets ($5x10^8$/mL) treated with apyrase, indomethacin and EGTA were incubated with or oxLDL (50 μg/mL; 0-60 min) or thrombin (0.1 U/mL; 0-2min). Treated platelets were lysed in Laemmli buffer, separated by SDS-PAGE and immunoblotted with anti-phosphoPDE3Aser[r312], phosphoPDE3Aser[428] or anti-β tubulin. (Left) Representative blot of three independent experiments. (Right) Densitometry for phosphoPDE3Aser[428] is presented as fold-change above basal, mean±SEM (n=3, *P*<0.05, Kruskal-Wallis Test).
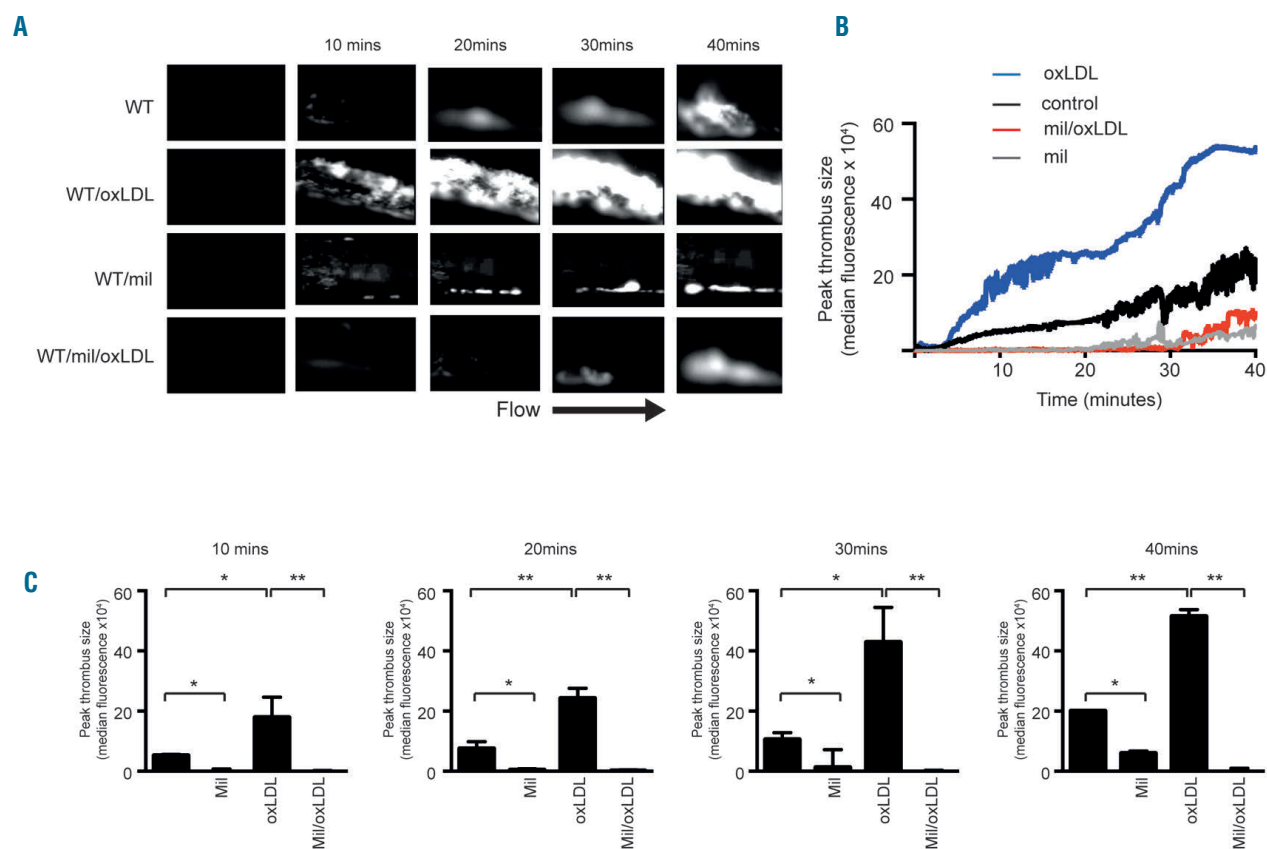
Figure 5. Oxidized low-density lipoproteins induced thrombosis *in vivo* is prevent by inhibition of phosphodiesterase 3A (PDE3A). Intravital microscopy was performed as described in the *Online Supplementary Methods*. (A) Representative fluorescence images of thrombi formed under different conditions are shown over the course of 40 minutes (min) after vascular injury. Black arrow shows the direction of blood flow. (B) Representative median integrated fluorescence signals of Rhodamine G obtained from an individual carotid thrombus under different conditions. (C) Quantified median integrated fluorescence signals from 10, 20, 30 and 40 min after vascular injury taken from five wild-type (WT) mice for each treatment. *$P<0.05$; **$P<0.01$, Kruskal-Wallis Test.

accumulation in response to PGI_2.[26,28] OxLDL reduced cAMP levels in the presence of EHNA (2645±122 to 488±7623 fmol cAMP/1x10^{8} platelets; $P<0.05$), but failed to prevent cAMP accumulation in the presence of milrinone (4761±170 to 4386±15723 fmol cAMP/1x10^{8} platelets; $P<0.05$) (Figure 2Aii and 2Aiii). To confirm that the reduction in cAMP accumulation was not restricted to PGI_2, platelets were stimulated with forskolin, which increases cAMP in a receptor-independent non-compartmentalized mechanism. Forskolin (10 μM)-stimulated elevation in cAMP was prevented by preincubation with oxLDL (9506±526 to 4506±1136 fmol cAMP/2x108 platelets; $P<0.05$) (Figure 2B).

Next, the effects of oxLDL on cAMP signaling were assessed. μ (50 nM) induced robust phosphorylation of a number of PKA substrates with apparent molecular weights of: 150, 100, 75, 70, 50, 37 and 20kDa (Figure 2C upper panel), and specifically vasodilator-stimulated phosphoprotein (VASP) (phosphoVASP-ser157) (Figure 2C middle panel) an established target of PKA signaling.27 These phosphorylation events were diminished by oxLDL (50 μg/mL), but unaffected by nLDL (50 μg/mL) (Figure 2Cii). To further establish that the reduced signaling response was due to enhanced cAMP hydrolysis, the experiment was repeated with 8-CPT-6-Phe-cAMP (50μM), a cell permeable non-hydrolysable (PDE resistant) analog of cAMP

(*Online Supplementary Figure S2*). Using a concentration that produced an equivalent quantity of intracellular cAMP (*Online Supplementary Figure S3*) as μ (50 nM), 8-CPT-6-Phe-cAMP caused robust phosphorylation of PKA substrates, which were unaffected by oxLDL (Figure 2D). These data suggest that oxLDL may regulate platelet sensitivity to μ through modulation of the cAMP-signaling cascade by PDE3A.

CD36 is required for oxidized low-density lipoprotein modulation of cyclic adenosine monophosphate signaling

Previously, we and others have shown that CD36 transduces the effects of oxLDL into platelet hyperactivity.[14,18,28,29] To examine the role of CD36 in linking oxLDL to altered cAMP signaling, we used a three-pronged strategy: (i) the CD36-blocking antibody FA6-152; (ii) the oxidized phospholipid oxPCCD36, a CD36-specific pathological ligand present in oxLDL,[26] and (iii) murine platelets deficient in CD36 (*Online Supplementary Figure S4*). This strategy, particularly the use of oxPCCD36, was used to account for differences in human and murine platelet sensitivity to human oxLDL. PGI_2 induced a robust phosphorylation of both the preferred ser[157] site and the alternative PKA phosphorylation site ser[239] in human platelets,[30] which was reduced significantly by oxLDL. The presence
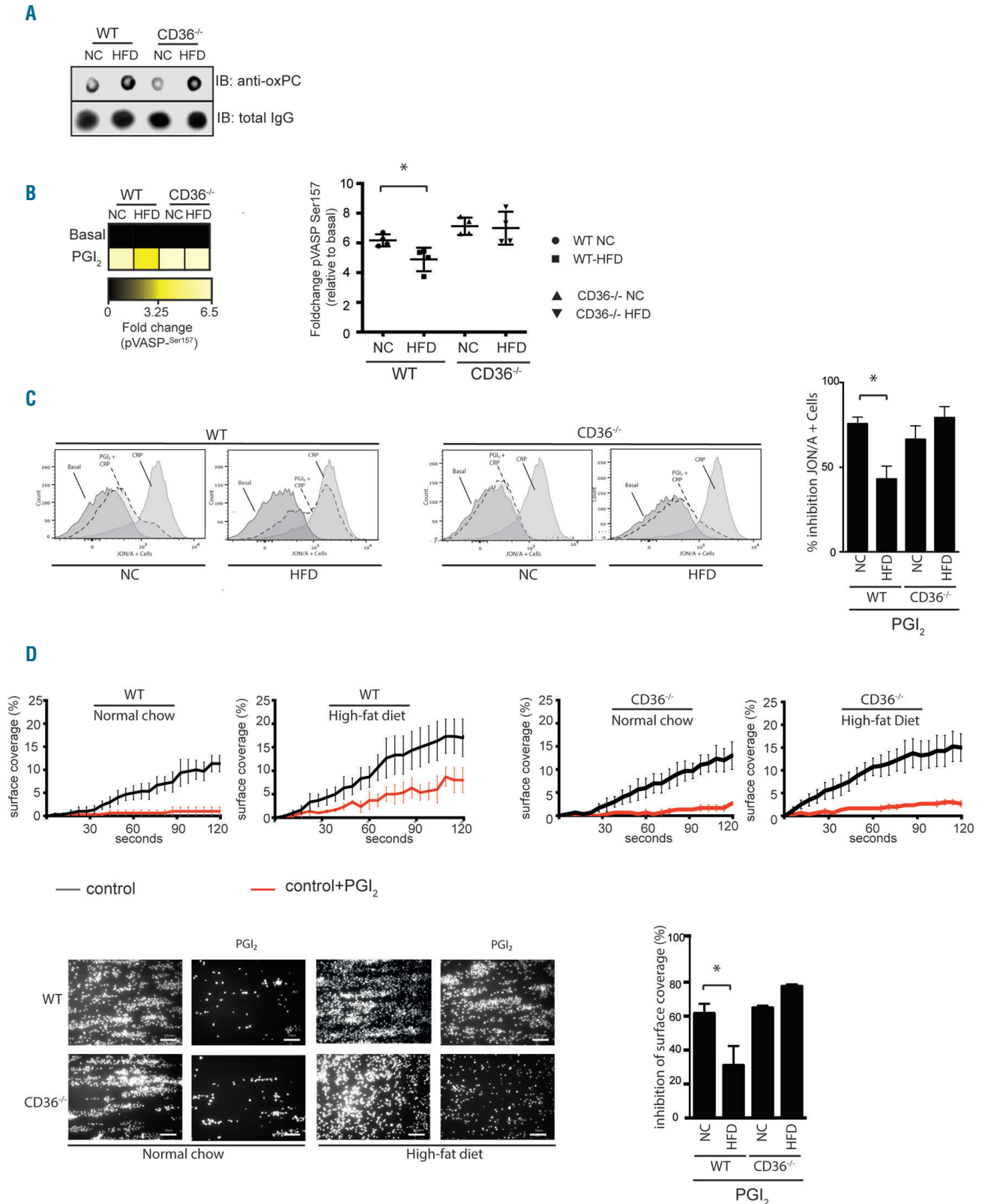
Figure 6. High-fat diet fed mice correlate with increased plasma levels of oxidized phospholipids to reduced prostacyclin (PGI₂) sensitivity *via* CD36. (A) Representative dot blots of mouse plasma probed with anti-oxidized phospholipids (HRP-conjugated-E06) and total-IgG (HRP-conjugated anti-mouse). (B) Whole blood from normal chow and high-fat fed animals were treated with PGI₂ (100nM) for 1 minute (min). Blood was fixed, permeabilized and incubated with anti-pVASPser[157] followed by secondary fluorescent-conjugate (Alexa 647) and analyzed by flow-cytometry. Representative heat map of fold increase in phosphoVASPser[157]. Quantification is presented as fold-change of median fluorescence intensity above basal (n=4, *P<0.05, Mann-Whitney U Test). (C) Whole blood from normal chow and high-fat diet fed animals were treated with PGI₂ (100 nM) for 1 min followed by CRP (10 μg/mL) for 5 min. Blood was fixed and JON/A positive cells were analyzed by flow cytometry. (Left) Representative histograms. (Right) Data presented as percentage inhibition of JON/A binding, mean±standard error of mean (SEM) (n=4 *P<0.05, Mann-Whitney U Test). (D) Whole blood incubated alone or with PGI₂ (20 nM) for 1 min was perfused at arterial shear 1000s⁻¹ for 2 min over a collagen matrix (50 μg/mL). Images of adherent platelets were taken by fluorescence microscopy. (Top) surface coverage (%) presented as a function of time. (Bottom left) Representative images of arterial flow experiments, (Bottom right) Data presented as inhibition of surface coverage (%), mean±SEM (n=5; *P<0.05, Mann-Whitney U Test).
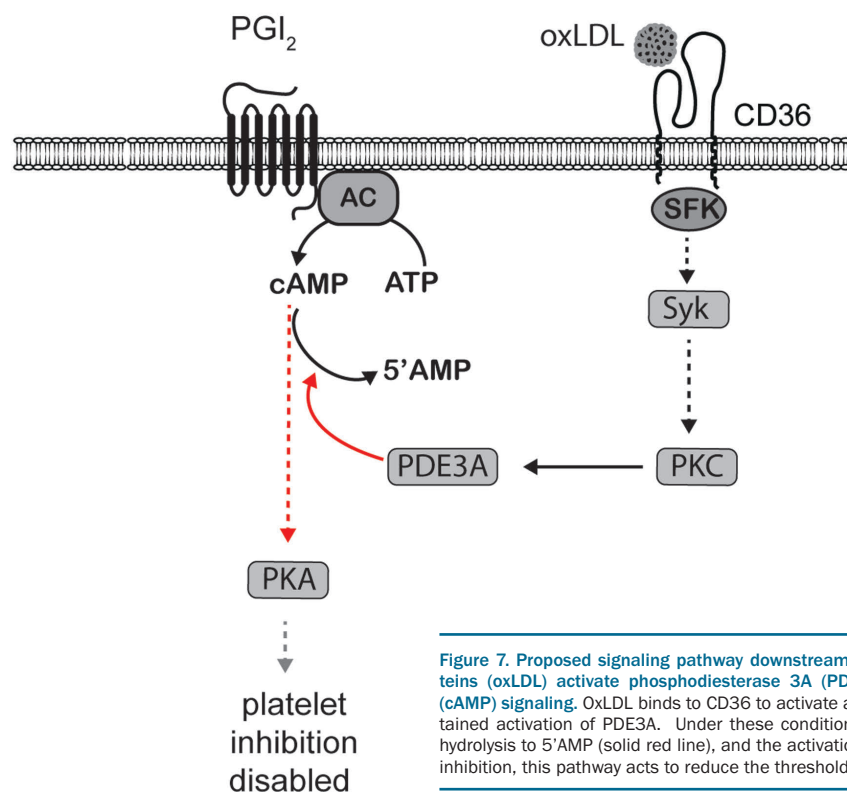
Figure 7. Proposed signaling pathway downstream of CD36 through which oxidized low-density lipoproteins (oxLDL) activate phosphodiesterase 3A (PDE3A) to suppress cyclic adenosine monophosphate (cAMP) signaling. OxLDL binds to CD36 to activate a tyrosine kinase signaling pathway that leads to a sustained activation of PDE3A. Under these conditions cAMP is maintained at low concentrations through hydrolysis to 5'AMP (solid red line), and the activation of PKA is diminished (dashed red line). Through disinhibition, this pathway acts to reduce the threshold for platelet activation and promote thrombosis.

of FA6-152 (1 μg/mL), but not control IgG (1 μg/mL), caused a significant recovery in phosphoVASP-ser157 (Figure 3A and B). OxPCCD36 (25 μM), but not the control lipid, PAPC (25 μM), diminished phospoVASP-ser157 in response to PGI$_2$ (Figure 3C). Thrombin-induced aggregation of wild-type (WT) and CD36$^{-/-}$ platelets was indistinguishable, and and PGI$_2$ (20 nM) caused complete inhibition of aggregation with only shape change remaining (Figure 3D and E). However, in CD36-deficient platelets, oxPCCD36 (25 μM) did not influence the inhibitory effects of PGI$_2$ (Figure 3E). To confirm the mechanism underpinning these observations, we examined cAMP signaling. PGI$_2$ (20 nM) caused a significant increase in cAMP in both WT and CD36$^{-/-}$ platelets (4382±175 and 4128±366 fmol cAMP/1x10^8 platelets). Preincubation with oxLDL, but not nLDL, reduced cAMP accumulation in WT mice (3347±294 fmol cAMP/1x10^8 platelets; *P*<0.05) but not CD36$^{-/-}$ (4196±224fmol cAMP/1x10^8 platelets) (Figure 3F). Furthermore, PGI$_2$-induced phosphoVASP-ser157 (Figure 3G) and ser239 (*Online Supplementary Figure S5*) were reduced by oxLDL in WT but not CD36$^{-/-}$ platelets.

Atherogenic lipid stress induces platelet phosphodiesterase 3A activity through a mechanism that requires CD36, Src kinases and protein kinase C

Our data suggested that ligation of CD36 could activate PDE3A. We tested this directly measuring enzymatic activity of PDE3A immunoprecipitated from platelets treated with either oxLDL or oxPCCD36. PDE activity in the immunoprecipitated samples was blocked by milrinone confirming enzyme activity was due to PDE3A (*Online Supplementary Figure S6*). OxLDL (10-100 μg/mL) caused a concentration-dependent increase in PDE3A activity (Figure 4A, left), which plateaued at 50 μg/mL (24±6.8%; *P*<0.05 compared to basal) and was maintained

at 27.7%±8.5 above basal for up to 60 min (longest time tested) (Figure 4A, right). This was strikingly different from the physiological agonist thrombin which induced a rapid induction of PDE3A activity that peaked at 1 min before returning to basal after 5 min (*Online Supplementary Figure S7*).

To link the sustained activation of PDE3A to decreased cAMP levels, we assessed the cyclic nucleotide concentrations over time. Platelets were incubated with oxLDL for up to 60 min, followed by a 1 min treatment with PGI$_2$ (50 nM) before measuring cAMP concentrations. The preincubation of platelets with oxLDL, but not nLDL (*data not shown*), for up to 60 min significantly blunted PGI$_2$-induced increases in cAMP with concentrations remaining at basal levels for the time course (Figure 4B). To confirm the role of CD36 in the activation of PDE3A, experiments were repeated with oxPCCD36. In human platelets, oxPCCD36 (25 μM), but not PAPC (25 μM), increased PDE3A activity (26.9±7.3%; *P*<0.05 compared to basal and PAPC) (Figure 4C). Critically, oxPCCD36 stimulated activity in WT platelets to 25.4±2.4% (*P*<0.05 compared to basal or PAPC) but not in CD36$^{-/-}$ platelets (Figure 4D).

We previously described a CD36-specific signaling pathway that includes the sequential activation of Src-family kinases (SFK), Syk, PLCγ2 and protein kinase C (PKC)[17] and investigated whether these kinases were involved in the activation of PDE3A. The non-selective SFK inhibitor, dasatinib (10 μM), ablated oxPCCD36-induced PDE3A activation (Figure 4E), while the Syk inhibitor, R406 (1 μM), caused significantly reduced PDE3A activity (Figure 4F). Given that CD36 signaling leads to PKC activation in a SFK manner, and that PDE3A is a target of PKC in platelets,[31] we tested the PKC inhibitors RO318220 (10 μM) and BIM1 (10 μM), and the intracellular Ca^{2+} chelator BAPTA-AM (20 μM) (Figure

4G). These three inhibitors blocked PDE3A activity induced by oxLDL, suggesting a PKC-dependent pathway (*P*<0.05). Platelet PDE3A activation is associated with phosphorylation of key serine residues.[31] We examined two of the most characterised sites, ser[312] (PKA and PKC sensitive) and ser[428] (PKC sensitive). OxLDL led to a time-dependent phosphorylation of ser[428] which peaked at 2 min and was still evident at 10 min, but had no effect on phosphoPDE3Aser[312]. In comparison, thrombin (0.1 U/mL) induced significantly less phosphorylation at ser[428], which peaked at 1 min before returning to basal at 2 min (Figure 4H) but also induced phosphorylation of ser312. These data confirm that oxLDL and its associated oxidized phospholipids require the sequential ligation and activation of CD36, Src, Syk and PKC to activate PDE3A.

Dyslipidemia is associated with platelet prostacyclin hyposensitivity in mice

To demonstrate the functional importance of our observations on dyslipidemia-driven thrombosis, we examined platelet sensitivity to PGI$_2$ in mice fed a Western diet (45%). cAMP signaling, integrin αIIbβ3 activation and thrombosis were assessed in whole blood *ex vivo*, which allowed us to evaluate platelet function and thrombotic potential while avoiding any confounding effects of altered PGI$_2$ synthesis *in vivo* associated with dyslipidemia.[32] Western diet significantly raised cholesterol levels (*Online Supplementary Figure S8*) and the presence of oxidized phospholipids in the plasma (Figure 5A). We then investigated the effect of dyslipidemia on cAMP signaling using multiplexed phosphoflow cytometry to allow the examination of signaling in the physiological conditions of whole blood.[24] Platelets from high-fat fed WT animals produced significantly less phosphoVASP-ser[157] when challenged with PGI$_2$ (100 nM) than normal chow WT mice (4.9±0.4 fold *vs.* 6.2±0.2-fold increase over basal; *P*<0.05) (Figure 5B). The deletion of CD36 protected cAMP signaling in dyslipidemic blood, with phosphoVASP-ser[157] remaining at control levels (Figure 5B). In parallel experiments, blood was stimulated with CRP-XL (10 μg/mL) in the presence and absence of PGI$_2$ (100 nM), and αIIbβ3 activation was measured. In normal chow WT blood, PGI$_2$ caused 75.7±3.9% inhibition of integrin activation (*P*<0.05 compared to absence of PGI$_2$), which was blunted in high-fat fed WT blood (43.1%±7.6 inhibition, *P*<0.05 compared to normal chow) (Figure 5C, left). Conversely, in CD36^{-/-} blood, PGI$_2$ induced inhibition of integrin activation was not significantly different in normal chow and high-fat fed conditions (66.5±8% and 79.3±6.5%, respectively) (Figure 5C, 1st and 2nd left).

When we assessed *ex vivo* thrombosis under flow, normal chow WT blood formed small thrombi on immobilized collagen in a time dependent manner, which was abolished by PGI$_2$ (20 nM) (Figure 5Di). High-fat fed WT blood showed an accelerated thrombotic response with increased surface area (11±3.6% compared to 16.2±4.3% at 2 mins). In addition, dyslipidemia caused significant hyposensitivity to PGI$_2$, with the prostanoid causing 31.7±10.7% inhibition compared 61.6±5.6% with normal chow (*P*<0.05; 2 min) (Figure 5ii and iii). In contrast, accelerated platelet deposition on collagen and platelet hyposensitivity to PGI$_2$ was not detected in CD36^{-/-} high-fat fed blood (Figure 5D). We repeated the experiments with 8-CPT-6-Phe-cAMP. If PDE3A activation was responsible for the increased thrombotic potential associated with reduced sensitivity to PGI$_2$ then CPT-6-Phe-cAMP-mediated inhibition of thrombosis would be unaffected by dyslipidemia. The cAMP analog caused a similar degree of inhibition of thrombosis in all genotypes but critically remained unaffected in the context of dyslipidemia (WT-normal chow, 65.6±11.2%; WT-Western diet, 62.3±7.7%; CD36^{-/-}-normal chow, 70.4±2.0%; CD36^{-/-}-Western diet, 62.3±5% inhibition) (*Online Supplementary Figure S9*). Here we show a physiological role for platelet CD36 in dyslipidemia, where it drives a phenotype of platelet hyperactivity by blocking cAMP-mediated inhibition.

Oxidized low density lipoprotein potentiation of thrombosis *in vivo* is prevented by inhibition of phosphodiesterase 3A

To examine the role of oxLDL in thrombosis *in vivo* we used intravital microscopy following ferric chloride–induced carotid artery injury. Tail-vein injections of oxLDL (2.5 mg/kg[-1] bodyweight)[33,34] into WT mice accelerated post-injury thrombotic response at all time points compared to control PBS injection (Figures 6A-C and *Online Supplementary Videos S1* and *S2*). Next animals were pre-treated with milrinone to explore in principle whether PDE3A inhibition might diminish prothrombotic effects of oxLDL. Consistent with previous studies, modulation of PDE3A activity reduced murine thrombosis (Figure 6A-C).[23] Importantly, the presence of milrinone (10 μmol/L) significantly reduced the ability of oxLDL to promote thrombosis at all time points post injury (*P*<0.05) (*Online Supplementary Video S3*) suggesting the heightened thrombotic response in the presence of oxLDL could be related, at least in part, to changes in PDE3A activity.

Discussion

The presence of oxidized lipid epitopes, including oxLDL, is thought to promote platelet hyperactivity in subjects with obesity, CAD and stroke.[5,6,35] It has been established that oxidative modifications are a hallmark of dyslipidemia and that they stimulate platelet activation directly through a number of distinct receptors.[6,8,13] Interestingly, platelets from patients with CAD and dyslipidemia show a reduced sensitivity to the inhibitory effects of PGI$_2$. These observations, coupled to pharmacological trials indicating that suppression of endothelial PGI$_2$ synthesis increased rate of atherothrombotic events,[36–39] suggest that platelet sensitivity to PGI$_2$ could play an undefined role in the development of atherothrombotic events. Hence, the aim of this study was to investigate whether oxLDL may promote unwanted platelet activation through the modulation of platelet sensitivity to PGI$_2$. Using a combination of pharmacological and genetic approaches, we show that oxidative lipid stress modulates platelet cAMP signaling leading to increased platelet activation. Our key findings include: (i) oxLDL and oxidized phospholipids decrease platelet sensitivity to PGI$_2$, which is coupled to reduced platelet accumulation of cAMP and PKA mediated signaling; (ii) PGI$_2$ hyposensitivity likely occurs *via* sustained activation of the cAMP hydrolysing enzyme PDE3A in response to oxLDL; (iii) the activation of PDE3A by oxLDL requires ligation of CD36; and (iv) that dyslipidemia induces platelet hyposensitivity to PGI$_2$ in a CD36-dependent manner.

In the first instance, we used three increasingly physiological systems to show that exposure of platelets to oxLDL opposes the inhibitory effects of PGI$_2$. In contrast, oxLDL failed to affect platelet inhibition by 8-CPT-6-Phe-cAMP, a PDE-resistant cAMP analog, demonstrating firstly that the PKA signaling was intact and secondly that the effects of the oxidized lipoprotein may regulate cAMP availability. Exploration of the underlying mechanisms demonstrated that OxLDL prevented the accumulation of cAMP in response to both PGI$_2$ and forskolin. Forskolin increases cAMP in a receptor-independent manner, thereby providing evidence that oxLDL did not affect the interaction of PGI$_2$ with the IP receptor or target adenylyl cyclases. This is consistent with previous studies demonstrating that reduced platelet sensitivity to PGI$_2$ in patients with hypercholesterolemia was independent of any changes in cAMP synthesis by adenylyl cyclase.[36] It was therefore possible that oxLDL could either prevent the synthesis of cAMP or accelerate its breakdown. We further found that oxLDL failed to modulate cAMP concentrations in the presence of the PDE3 inhibitor milrinone, but not the PDE2 inhibitor EHNA, suggesting that cAMP hydrolysis by PDE3A was the potential mediator of PGI$_2$ hyposensitivity. A role for PDE3A was confirmed using immunoprecipitation experiments showing that both oxLDL and oxPCCD36 accelerated the hydrolytic activity of PDE3A in both human and murine platelets through ligation of CD36. The activation of PDE3A downstream of CD36 required the activation of Src family kinases, Syk and PKC. This provides further evidence that CD36-SFK-Syk represents a multiprotein complex that transduces extracellular oxidative lipid stress to the intracellular signaling machinery of the platelet. Interestingly, hemostatic agonists such as thrombin and collagen also activate PDE3A through a PKC-dependent mechanism.[31] These agonists are proposed to cause a rapid attenuation of cAMP signaling at sites of vascular injury to promote platelet-mediated hemostasis. However, in contrast to the rapid and short-lived activation of PDE3A activity by thrombin and collagen, oxLDL induced a sustained PDE3A response for up to 60 min (longest time tested). This was linked to a different activatory phosphorylation pattern of PDE3A by oxLDL and could suggest a distinct mechanism of activation induced by short-lived hemostatic agonists from that of oxLDL. Given the sustained activation of platelet PDE3A in the presence of oxidative lipid stress, it is attractive to speculate that PDE3A may be partially activated in dyslipidemic disease states and thereby reduce the threshold for platelet activation by diminution of cAMP. Indeed, gain of function mutations of PDE3 are associated with stroke, underlining its role in vascular pathology.[40] This concept is also supported by observations that inhibition of PDE3A by cilostazol can have beneficial anti-thrombotic effects in high-risk groups characterized a prothrombotic phenotype.[41–43]

The pathophysiological consequences of platelet hyposensitivity to PGI$_2$ and the potential importance of CD36 was explored in a murine model of high-fat feeding-induced dyslipidemia. Interestingly, we found that even mild dyslipidemia was characterized by the presence of oxidized lipid epitopes in the plasma, which was unaffected by the absence of CD36. Whole blood phospho-flow cytometry was used to measure platelet phosphoVASP, as a marker of cAMP signaling, without the need for cell isolation. This demonstrated that mild dyslipidemia was accompanied by reduced cAMP signaling. The functional importance of this blunted cAMP signaling response manifested as diminished platelet sensitivity to the inhibitory effects of PGI$_2$ on integrin activation measured by flow cytometry and *ex vivo* thrombosis. The assessment of thrombosis *ex vivo* was important to demonstrate that hyposensitivity of platelets to PGI$_2$ was a primary platelet defect rather than a response to a dysfunctional endothelium, where altered PGI$_2$ production has been observed in models of dyslipidemia.[32] To support our hypothesis that hyposensitivity to PGI$_2$ was linked to PDE3A activity, we showed that cAMP signaling in dyslipidemia was normal if a PDE-resistant cAMP analog (8-CPT-6-Phe-cAMP) was used, again confirming that PKA signaling downstream of cAMP was functional. Critically, genetic ablation of CD36 protected animals from the loss of PGI$_2$ sensitivity and restored PKA signaling. Infusions of oxLDL into wild-type mice caused a robust potentiation of thrombosis by ferric chloride. However, mice were protected from the prothrombotic effects of oxLDL *in vivo* when PDE3A was pharmacologically inhibited. Using this approach, milrinone did not target only platelets and could therefore have an effect on other PDE3A expressing cells. However, the data are proof of principle that the prothrombotic effects of oxLDL *in vivo*, at least in part, may be prevented by therapeutic strategies based on enhancing or preserving cAMP signaling events in platelets. This element of the work requires further studies focussing on strategies for the specific targeting of PDE3A, and potentially PDE2, in platelets.

Together, our *ex vivo* and *in vitro* data suggest a previously unrecognized mechanism contributing to platelet hyperactivity, where the ligation of CD36 by oxidized lipids modulates cAMP signaling by activating PDE3A leading to PGI$_2$ hyposensitivity. These data may constitute a link to the observed PGI$_2$ hyposensitivity in dyslipidemic high-risk populations and indicate a novel therapeutic strategy to target atherothrombotic risk in certain patient groups. Remarkably, current antiplatelet therapy exclusively targets platelet activatory pathways including cyclo-oxygenases (Aspirin), P2Y12 (Thienopyridines, non-Thienopyridines) or $\alpha_{IIb}\beta_3$ (Tirofiban; Eptifibatide) while platelet inhibitory pathways remain untargeted. Therefore, high-risk populations might remain at increased atherothrombotic risk despite optimal available pharmacological therapy, and impaired platelet inhibition might contribute to the residual cardiovascular risk.

References

1. Mitchell JA, Ali F, Bailey L, Moreno L, Harrington LS. Role of nitric oxide and prostacyclin as vasoactive hormones released by the endothelium. Exp Physiol. 2008;93(1):141-147.

2. Jackson SP. Arterial thrombosis--insidious, unpredictable and deadly. Nat Med. 2011; 17(11):1423-1436.

3. Davì G, Romano M, Mezzetti A, et al. Increased levels of soluble P-selectin in hypercholesterolemic patients. Circulation. 1998;97(10):953-957.

4. Carvalho AC, Colman RW, Lees RS. Platelet function in hyperlipoproteinemia. N Engl J Med. 1974;290(8):434-438.

5. Colas R, Sassolas A, Guichardant M, et al. LDL from obese patients with the metabolic syndrome show increased lipid peroxidation and activate platelets. Diabetogia. 2011;54(11):2931-2940.

6. Chan H-CC, Ke L-YY, Chu C-SS, et al. Highly electronegative LDL from patients with {ST-elevation} myocardial infarction triggers platelet activation and aggregation. Blood. 2013;122(22):3632-3641.

7. Ardlie NG, Selley ML, Simons LA. Platelet activation by oxidatively modified low-density lipoproteins. Atherosclerosis.1989;76(2–3):117-124.

8. Chen R, Chen X, Salomon RG, M, McIntyre T. Platelet activation by low concentrations of intact oxidized LDL particles involves the PAF receptor. Arterioscler. Thromb Vasc Biol. 2009;29(3):363-371.

9. Naseem KM, Goodall AH, Bruckdorfer KR. Differential effects of native and oxidatively modified low-density lipoproteins on platelet function. Platelets. 1997;8(2–3):163–173.

10. van Willigen G, Gorter G, Akkerman JW. LDLs increase the exposure of fibrinogen binding sites on platelets and secretion of dense granules. Arterioscler. Thomb. 1994;14(1):41–46.

11. Podrez EA, Byzova T V, Febbraio M, et al. Platelet CD36 links hyperlipidemia, oxidant stress and a prothrombotic phenotype. Nat Med. 2007;13(9):1086–1095.

12. Korporaal S, Eck M, Adelmeijer J, et al. Platelet Activation by Oxidized Low Density Lipoprotein Is Mediated by Cd36 and Scavenger {Receptor-A}. Arterioscler. Thromb Vasc Biol. 2007;27(11):2476–2483.

13. Chen K, Febbraio M, Li W, Silverstein RL. A Specific CD36-Dependent Signaling Pathway Is Required for Platelet Activation by Oxidized Low-Density Lipoprotein. Circ Res. 2008;102(12):1512–1519.

14. Wraith KS, Magwenzi S, Aburima A, et al. Oxidized low-density lipoproteins induce rapid platelet activation and shape change through tyrosine kinase and Rho kinase-signaling pathways. Blood. 2013; 122(4):580–589.

15. Biswas S, Zimman A, Gao D, Byzova T V, Podrez EA. TLR2 Plays a Key Role in Platelet Hyperreactivity and Accelerated Thrombosis Associated With Hyperlipidemia. Circ Res. 2017;121(8):951–962.

16. Chen K, Li W, Major J, et al. Vav guanine nucleotide exchange factors link hyperlipidemia and a prothrombotic state. Blood. 2011;117(21):5744–5750.

17. Magwenzi S, Woodward C, Wraith KS, et al. Oxidized LDL activates blood platelets through CD36/NOX2-mediated inhibition of the cGMP/protein kinase G signaling cascade. Blood. 2015;125(17):2693–2703.

18. Yang M, Cooley BC, Li W, et al. Platelet CD36 promotes thrombosis by activating redox sensor ERK5 in hyperlipidemic conditions. Blood. 2017;129(21):2917–2927.

19. Yang M, Kholmukhamedov A, Schulte ML, et al. Platelet CD36 signaling through ERK5 promotes caspase-dependent procoagulant activity and fibrin deposition in vivo. Blood Adv. 2018;2(21):2848–2861.

20. Raslan Z, Naseem KM. The control of blood platelets by cAMP signalling. Biochem. J Trans. 2014;42(2):289–294.

21. Beck F, Geiger J, Gambaryan S, et al. Time-resolved characterization of cAMP/PKA-dependent signaling reveals that platelet inhibition is a concerted process involving multiple signaling pathways. 2014;123(5):e1–e10.

22. Beca S, Ahmad F, Shen W, et al. Phosphodiesterase type 3A regulates basal myocardial contractility through interacting with sarcoplasmic reticulum calcium {ATPase} type 2a signaling complexes in mouse heart. Circ Res. 2013;112(2):289–297.

23. Sim DS, Glenn M-S, Furie BC, Furie B, Flaumenhaft R. Initial accumulation of platelets during arterial thrombus formation in vivo is inhibited by elevation of basal cAMP levels. Blood. 2004;103(6):2127–2134.

24. Spurgeon BE, Aburima A, Oberprieler NG, Taskén K, Naseem KM. Multiplexed phosphospecific flow cytometry enables large-scale signaling profiling and drug screening in blood platelets. J Thromb Haemost. 2014;12(10):1733–1743.

25. Haslam RJ, Dickinson NT, Jang EK. Cyclic nucleotides and phosphodiesterases in platelets. Thromb Haemost. 1999; 82(2):412–423.

26. Conti M, Beavo J. Biochemistry and Physiology of Cyclic Nucleotide Phosphodiesterases: Essential Components in Cyclic Nucleotide Signaling. Annu Rev Biochem. 2007;76(1):481–511.

27. Butt E, Abel K, Krieger M, et al. cAMP- and cGMP-dependent protein kinase phosphorylation sites of the focal adhesion vasodilator-stimulated phosphoprotein (VASP) in vitro and in intact human platelets. J Biol Chem. 1994;269(20):14509–14517.

28. Chen K, Febbraio M, Li W, Silverstein RL. A specific CD36-dependent signaling pathway is required for platelet activation by oxidized low-density lipoprotein. Circ Res. 2008;102(12):1512–1519.

29. Podrez E a, Byzova T V, Febbraio M, et al. Platelet CD36 links hyperlipidemia, oxidant stress and a prothrombotic phenotype. Nat Med. 2007;13(9):1086–1095.

30. Butt E, Abel K, Krieger M, Palm D, et al. cAMP-and cGMP-dependent protein kinase phosphorylation sites of the focal adhesion vasodilator-stimulated phosphoprotein (VASP) in vitro and in intact human platelets. J Biol Chem. 1994;269(20):14509-14517.

31. Hunter RW, Carol M, Hers I. Protein Kinase C-mediated Phosphorylation and Activation of PDE3A Regulate {cAMP} Levels in Human Platelets. J Biol Chem. 2009;284(18):12339–12348.

32. Csányi G, Gajda M, Magdalena F-Z, et al. Functional alterations in endothelial NO, PGI₂ and EDHF pathways in aorta in {ApoE/LDLR-/- mice. Prostaglandins Other Lipid Mediat. 2012;98(3–4):107–115.

33. Nakano A, Kawashima H, Miyake Y, et al. 123I–Labeled oxLDL Is Widely Distributed Throughout the Whole Body in Mice. Nucl Med Mol Imaging. 2018;52(2):144-153.

34. Badrnya S, Schrottmaier WC, Kral JB, et al. Platelets mediate oxidized low-density lipoprotein-induced monocyte extravasation and foam cell formation. Arterioscler. Thromb Vasc Biol. 2014;34(3):571–580.

35. Shen M-YY, Chen F-YY, Hsu J-FF, et al. Plasma L5 levels are elevated in ischemic stroke patients and enhance platelet aggregation. Blood. 2016;127(10):1336–1345.

36. Colli S, Lombroso M, Maderna P, Tremoli E, Nicosia S. Effects of PGI₂ on platelet aggregation and adenylate cyclase activity in human type {IIa} hypercholesterolemia. Biochem Pharmacol. 1983;32(13):1989–1993.

37. Sinzinger H, Schernthaner G, Kaliman J. Sensitivity of platelets to prostaglandins in cornary heart disease and angina pectoris. Prostaglandins. 1981;22(5):773–781.

38. Mehta J, Mehta P, Conti CR. Platelet function studies in coronary heart disease. {IX.} Increased platelet prostaglandin generation and abnormal platelet sensitivity to prostacyclin and endoperoxide analog in angina pectoris. Am J Cardiol. 1980;46(6):943–947.

39. Furberg CD, Psaty BM, A FG. Parecoxib, valdecoxib, and cardiovascular risk. Circulation. 2005;111(3):249.

40. Malik R, Chauhan G, Traylor M, et al. Multiancestry genome-wide association study of 520,000 subjects identifies 32 loci associated with stroke and stroke subtypes. Nat Genet. 2018;50(4):524–537.

41. Araki S, Matsuno H, Haneda M, et al. Cilostazol attenuates spontaneous microaggregation of platelets in type 2 diabetic patients with insufficient platelet response to aspirin. Diabetes Care. 2013;36(7):e92-3.

42. Park KW, Kang S-H, Park JJ, et al. Adjunctive Cilostazol Versus Double-Dose Clopidogrel After Drug-Eluting Stent Implantation. JACC Cardiovasc Interv. 2013;6(9):932–942.

43. Angiolillo DJ, Capranzano P, Ferreiro JL, et al. Impact of adjunctive cilostazol therapy on platelet function profiles in patients with and without diabetes mellitus on aspirin and clopidogrel therapy. Thromb Haemost. 2011;106(2):253–262.

Eltrombopag for the treatment of inherited thrombocytopenias: a phase II clinical trial

Carlo Zaninetti,[1,2] Paolo Gresele,[3] Antonella Bertomoro,[4] Catherine Klersy,[5] Erica De Candia,[6,7] Dino Veneri,[8] Serena Barozzi,[1] Tiziana Fierro,[3] Maria Adele Alberelli,[6] Valeria Musella,[5] Patrizia Noris,[1] Fabrizio Fabris,[4] Carlo L. Balduini[1,9] and Alessandro Pecci[1]

[1]Department of Internal Medicine, IRCCS Policlinico San Matteo Foundation and University of Pavia, Pavia; [2]PhD course in Experimental Medicine, University of Pavia, Pavia; [3]Department of Medicine, University of Perugia, Perugia; [4]Department of Medicine, University of Padova, Padova; [5]Service of Clinical Epidemiology & Biometry, IRCCS Policlinico San Matteo Foundation and University of Pavia, Pavia; [6]IRCCS Policlinico Universitario A. Gemelli Foundation, Roma; [7]Institute of Internal Medicine and Geriatrics, Catholic University of the Sacred Heart, Roma; [8]Department of Medicine, Section of Hematology, University of Verona, Verona and [9]Ferrata-Storti Foundation, Pavia, Italy.

ABSTRACT

Patients with inherited thrombocytopenias often require platelet transfusions to raise their platelet count before surgery or other invasive procedures; moreover, subjects with clinically significant spontaneous bleeding may benefit from an enduring improvement of thrombocytopenia. The hypothesis that thrombopoietin-mimetics can increase platelet count in inherited thrombocytopenias is appealing, but evidence is scarce. We conducted a prospective, phase II clinical trial to investigate the efficacy of the oral thrombopoietin-mimetic eltrombopag in different forms of inherited thrombocytopenia. We enrolled 24 patients affected by *MYH9*-related disease, *ANKRD26*-related thrombocytopenia, X-linked thrombocytopenia/Wiskott-Aldrich syndrome, monoallelic Bernard-Soulier syndrome, or *ITGB3*-related thrombocytopenia. The average pre-treatment platelet count was 40.4 x10^9/L. Patients received a 3- to 6-week course of eltrombopag in a dose-escalated manner. Of 23 patients evaluable for response, 11 (47.8%) achieved a major response (platelet count >100 x10^9/L), ten (43.5%) had a minor response (platelet count at least twice the baseline value), and two patients (8.7%) did not respond. The average increase of platelet count compared to baseline was 64.5 x10^9/L (*P*<0.001). Four patients with clinically significant spontaneous bleeding entered a program of long-term eltrombopag administration (16 additional weeks): all of them obtained remission of mucosal hemorrhages, with the remission persisting throughout the treatment period. Treatment was globally well tolerated: five patients reported mild adverse events and one patient a moderate adverse event. In conclusion, eltrombopag was safe and effective in increasing platelet count and reducing bleeding symptoms in different forms of inherited thrombocytopenia. Despite these encouraging results, caution is recommended when using thrombopoietin-mimetics in inherited thrombocytopenias predisposing to leukemia. ClinicalTrials.gov identifier: NCT02422394.

Introduction

Inherited thrombocytopenias are a heterogeneous group of disorders characterized by a reduced number of blood platelets which can result in a bleeding tendency of variable severity. Although inherited thrombocytopenias are rare, recent improvements in the knowledge of these conditions have indicated that, taken together, their prevalence is higher than previously thought. In fact, based on a registry of patients with thrombocytopenia, the prevalence of inherited thrombocytopenias in the Italian population is estimated to be 2.7 cases per 100,000 population.[1]

Most patients with an inherited thrombocytopenia have mild or no spontaneous

bleeding: however, even patients who do not have spontaneous hemorrhages often require platelet transfusions prior to surgery or other invasive procedures because their platelet count is below the safe threshold for the specific procedure.[1-5] Platelet transfusions have several drawbacks, as they expose patients to the risk of acute reactions, transmission of infectious diseases, and alloimmunization with consequent refractoriness to subsequent platelet transfusions.[3,6,7] The last is a particularly critical event in these patients with lifelong thrombocytopenia. Moreover, the availability of platelet units is conditioned by the scarceness of blood donors. Less commonly, some patients with inherited thrombocytopenias have frequent episodes of spontaneous bleeding that affect their quality of life, expose them to the risk of major hemorrhages, and may require frequent hospitalization and/or transfusions. In these subjects, obtaining an enduring increase of platelet count sufficient to stably abolish or reduce spontaneous hemorrhages would be a major achievement.

Thrombopoietin-receptor agonists (TPO-RA) are targeted agents that can stimulate megakaryopoiesis and platelet production through the activation of the thrombopoietin receptor, MPL. These drugs are currently approved for the treatment of a few forms of acquired thrombocytopenia.[8] Although the hypothesis that TPO-RA can increase platelet count also in patients with inherited thrombocytopenias is appealing, the evidence on this topic is very scarce, mainly because of the difficulties in carrying out clinical trials in these orphan diseases. In fact, only one prospective study has been conducted so far: moreover, this study enrolled patients affected with only one of the many forms of inherited thrombocytopenia. In this trial, a short course of the oral TPO-RA eltrombopag was given to 12 patients with thrombocytopenia deriving from mutations in *MYH9* (i.e., *MYH9*-related disease, *MYH9*-RD): 11 patients showed an increase of platelet count.[9] Based on these results, there are anecdotal reports of short-term eltrombopag treatment to prepare *MYH9*-RD patients for major surgery.[10-12] The remaining available clinical information on the effects of TPO-RA in inherited thrombocytopenias derives from single case reports[13-17] and the retrospective investigation of one small case series.[18]

Here we report the results of the second prospective clinical trial on the use of TPO-RA in genetic thrombocytopenias. We investigated the efficacy of eltrombopag in increasing platelet count in patients affected by different forms of inherited thrombocytopenia. Patients received short-term eltrombopag to test whether this treatment can raise platelet count up to safe levels for major surgery. Moreover, in those patients with clinically significant spontaneous bleeding, we also investigated whether prolonged administration of eltrombopag could induce a persistent remission of the spontaneous hemorrhages.

Methods

Patients

Patients were enrolled at five Italian centers (*Online Supplementary Table S1*). The study protocol was approved by the institutional review boards of all centers. Patients or their legal guardians signed written informed consent to participation in the study, which was conducted according to the Declaration of Helsinki. Inclusion and exclusion criteria for this trial are detailed in the *Online Supplementary Methods*.

Study design

This was a phase II, open-label, dose-escalation trial. The study consisted of two parts.

The main aim of part 1 was to test whether, and in which forms of inherited thrombocytopenia, a short-term course of eltrombopag is effective in increasing platelet count above the safe threshold for all types of surgery (100×10^9/L).[4,5] All patients eligible for the study entered part 1. Patients received eltrombopag 50 mg/day for 3 weeks. Patients who obtained a platelet count >100 $\times 10^9$/L by day 21 stopped treatment (as they had achieved the primary endpoint). In the other cases, patients received eltrombopag 75 mg/day for 3 additional weeks.

The main aim of part 2 of the study was to test the efficacy of long-term eltrombopag in achieving an enduring remission of bleeding symptoms in patients with clinically significant spontaneous hemorrhages. Criteria for entering part 2 were the following: patients with spontaneous bleeding at baseline grade ≥2 according to the World Health Organization (WHO) bleeding scale, who completed part 1 without severe side effects and obtained a reduction of bleeding symptoms at the end of part 1. Part 2 consisted of 16 weeks of treatment. Patients were started on eltrombopag 25 mg/day and then re-evaluated every 4 weeks: the eltrombopag dose was adjusted based on bleeding tendency and platelet count according to the schedule reported in *Online Supplementary Figure S1*.

Endpoints and outcome measures

The primary endpoint of part 1 was the achievement of a platelet count >100 $\times 10^9$/L, i.e., a safe level for all types of surgery according to current guidelines.[4,5] Major response was defined as the achievement of the primary endpoint. Minor response was defined as the achievement of a platelet count at least two-fold higher than baseline without reaching the criteria for major response.

The primary endpoint of part 2 was the stable reduction of spontaneous bleeding manifestations according to the WHO bleeding scale during the last 2 weeks of treatment. A major response was defined as a complete remission of hemorrhages. A minor response was defined as a reduction of bleeding according to the WHO bleeding scale without reaching the criteria for a major response.

Secondary endpoints included safety and tolerability of the treatments; dosages of eltrombopag required to achieve the primary endpoints; and improvement of health-related quality of life (HR-QoL) with long-term eltrombopag administration (part 2 only).

Exploratory endpoints included the effects of treatment on serum thrombopoietin levels and on platelet function investigated by light transmission aggregometry and/or flow cytometry.

Investigation of patients

Studies performed to investigate patients at baseline and at each subsequent visit are detailed in the *Online Supplementary Methods*.

Statistical analysis

The statistical analysis was performed as described in the *Online Supplementary Methods*.

Results

Study population

Twenty-four patients were enrolled between April 2015 and May 2017. They consisted of nine patients with *MYH9*-RD; nine with *ANKRD26*-related thrombocytope-

nia (*ANKRD26*-RT);[19] three with thrombocytopenia caused by *WAS* mutations (2 with X-linked thrombocytopenia, XLT, and 1 with Wiskott-Aldrich syndrome, WAS);[20,21] two with monoallelic Bernard-Soulier syndrome (mBSS) caused by the Ala156Val mutation of GPIbα;[22] and one with thrombocytopenia deriving from an *ITGB3* mutation (*ITGB3*-RT).[23] The patients' mean platelet count was 40.4x10⁹/L. Table 1 and *Online Supplementary Table S4* describe the features of the study population at baseline.

Part 1 of the study

Twenty-three patients completed part 1 of the study, whereas one patient with *ANKRD26*-RT discontinued treatment early because of an adverse event (see below). *Primary endpoint*

Responses in part 1 of the study are summarized in Table 2 and detailed in *Online Supplementary Tables S5* and S6. Twenty-one of the 23 evaluable patients [91.3%, 95% confidence interval (95% CI): 72.0-98.9] obtained a response according to the study criteria: 11 patients (47.8%) achieved a major response and ten (43.5%) a minor response. Two patients (8.7%) did not respond (one with *ANKRD26*-RT and the patient with *ITGB3*-RT). Most patients with *MYH9*-RD and the two subjects with mBSS obtained a major response, whereas most patients with *ANKRD26*-RT and the three subjects with XLT/WAS achieved a minor response (Table 2).

The mean platelet count at the end of part 1 of the study was 104.9x10⁹/L (*P*<0.001 compared to baseline). The mean increase in platelet count with respect to baseline

Table 1. Main features of the study population at baseline.

	Overall	*MYH9*-RD	*ANKRD26*-RT	XLT/WAS	mBSS	*ITGB3*-RT
Patients, n.	24	9	9	3	2	1
M/F, n. of patients	14/10	2/7	7/2	3/0	2/0	0/1
Age, years - mean [SD]	41.1 [13.7]	42.9 [14.7]	40.9 [15.1]	29.3 [6.8]	50 [5.7]	45 [-]
Platelet count,[1] x10⁹/L - mean [SD]	40.1 [22.4]	38.2 [22.7]	37.4 [22.2]	26.3 [15.8]	70 [1.4]	62 [-]
Spontaneous bleeding,[2] n. of patients	13	3	7	1	1	1
WHO grade = 1, n.	7	0	7	0	0	0
WHO grade = 2, n.	4	1	0	1	1	1
WHO grade = 3, n.	2	2	0	0	0	0
Previous splenectomy,[3] n. of patients	2	2	0	0	0	0

[1]As evaluated by phase-contrast microscopy in a counting chamber. [2]Spontaneous bleeding during the week preceding the baseline evaluation according to the World Health Organization bleeding scale. [3]Previous splenectomy because of a mistaken diagnosis of immune thrombocytopenia. *MYH9*-RD: *MYH9*-related disease; *ANKRD26*-RT: *ANKRD26*-related thrombocytopenia; XLT/WAS: X-linked thrombocytopenia/Wiskott-Aldrich syndrome; mBSS: monoallelic Bernard-Soulier syndrome; *ITGB3*-RT: *ITGB3*-related thrombocytopenia; n: number; M: male; F: female; SD: standard deviation; WHO: World Health Organization.

Table 2. Responses in part 1 of the study (primary endpoint), overall and according to the different forms of inherited thrombocytopenia.

	Overall	*MYH9*-RD	*ANKRD26*-RT	WAS/XLT	mBSS	*ITGB3*-RT
Evaluable patients, n.	23	9	8	3	2	1
Response[1]						
Any response, % [95% CI]	91.3 [72.0-98.9]	100.0 [66.4-100.0]	87.5 [47.3-99.7]	100.0 [29.2-100.0]	100.0 [15.8-100.0]	0 [0-97.5]
Major response, % [95% CI]	47.8 [26.8-69.4]	77.8 [40.0-97.2]	25.0 [3.2-65.1]	0 [0-70.8]	100.0 [15.8-100.0]	0 [0-97.5]
Minor response, % [95% CI]	43.5 [23.2-65.5]	22.2 [2.8-60.0]	62.5 [24.5-91.5]	100.0 [29.2-100.0]	0 [0-84.2]	0 [0-97.5]
Platelet count[2]						
Baseline, x10⁹/L, mean [SD]	40.4 [22.8]	38.2 [22.7]	38.0 [23.7]	26.3 [15.8]	70.0 [1.4]	62.0 [-]
End of part 1, x10⁹/L, mean [SD]	104.9 [56.7]§	136.3 [68.0]#	75.5 [28.5]§	67.7 [38.4]	150.5 [13.4]	78.0 [-]
Mean increase, x10⁹/L [95% CI]	64.5 [43.7-85.3]	98.1 [53.3-142.9]	37.5 [24.1-50.8]	41.4 [22.1-104.8]	80.5 [27.5-188.5]	16.0 [-]
Mean increase in responders, x10⁹/L [95%CI]	69.5 [48.0-91.1]	98.1 [53.3-142.9]	41.8 [31.7-52.0]	41.4 [22.1-104.8]	80.5 [27.5-188.5]	-
Spontaneous bleeding[3]						
Patients with SB at baseline, n.	12	3	6	1	1	1
Complete remission of SB at end of part 1, % [95% CI]	83.3 [51.6-97.9]	100 [29.2-100]	83.3 [35.9-99.6]	100 [2.5-100]	100 [2.5-100]	0 [0-97.5]
Partial reduction of SB at end of part 1, % [95% CI]	8.3 [0.2-38.5]	0 [0.0-70.8]	0 [0.0-45.9]	0 [0.0-97.5]	0 [0.0-97.5]	100 [2.5-100]

[1]According to predefined study criteria. [2]As evaluated by phase-contrast microscopy in a counting chamber. [3]Spontaneous bleeding during the week preceding evaluation according to the World Health Organization bleeding scale. §*P*<0.001 with respect to baseline. #*P*=0.001 with respect to baseline. *MYH9*-RD: *MYH9*-related disease; *ANKRD26*-RT: *ANKRD26*-related thrombocytopenia; XLT/WAS: X-linked thrombocytopenia/Wiskott-Aldrich syndrome; mBSS: monoallelic Bernard-Soulier syndrome; *ITGB3*-RT: *ITGB3*-related thrombocytopenia; n: number; 95% CI: 95% confidence interval; SD: standard deviation; SB: spontaneous bleeding..

was 64.5x10⁹/L (95% CI: 43.7-85.3) overall, and 69.5x10⁹/L in the 21 responders. Table 2 and Figure 1 report the average increase in platelet count in the responders according to the different forms of inherited thrombocytopenia.

Ten of the 12 patients with spontaneous bleeding at baseline (83.3%) obtained complete remission of bleeding. In particular, all responders (major or minor response) achieved disappearance of bleeding symptoms if present at baseline. Of the two non-responders, the patient with *ANKRD26*-RT did not obtain any improvement of bleeding manifestations, whereas the patient with *ITGB3*-RT experienced a reduction of spontaneous bleeding (WHO grade from 2 to 1) following a slight increase in platelet count (from 62 to 78 x10⁹/L).

Eltrombopag dose

Ten patients (43.5%) achieved a major response with eltrombopag 50 mg/day and stopped therapy (Table 3). These patients were all the individuals with *MYH9*-RD or mBSS who obtained a major response and one subject with *ANKRD26*-RT. Thus, 13 patients (56.5%) switched to the dosage of 75 mg/day. Treatment with the higher dose resulted in the achievement of a better response according to the study criteria in four of these subjects (Table 3).

Exploratory endpoints

In vitro platelet aggregation in response to collagen, ADP, and ristocetin, was studied at the end of treatment in the 11 patients who achieved platelet counts >100x10⁹/L.

Table 3. Doses of eltrombopag administered during part 1 of the study.

	Overall	MYH9-RD	ANKRD26-RT	WAS/XLT	mBSS	ITGB3-RT
Evaluable patients, n.	23	9	8	3	2	1
Major response with 50 mg/day, n. (%)	10 (43.5)	7 (77.8)	1 (12.5)	0	2 (100)	0
Switch to 75 mg/day, n. (%)	13 (56.5)	2 (22.2)	7 (87.5)	3 (100)	0	1
Improvement of response with 75 mg/day¹, n.	4	0	2§	2#	0	0

¹Achievement of a better response according to the study criteria with respect to treatment with 50 mg/day. §One patient achieved a major response, one achieved a minor response. #Both patients achieved minor responses. *MYH9*-RD: *MYH9*-related disease; *ANKRD26*-RT: *ANKRD26*-related thrombocytopenia; XLT/WAS: X-linked thrombocytopenia/Wiskott-Aldrich syndrome; mBSS: monoallelic Bernard-Soulier syndrome; *ITGB3*-RT: *ITGB3*-related thrombocytopenia; n: number.
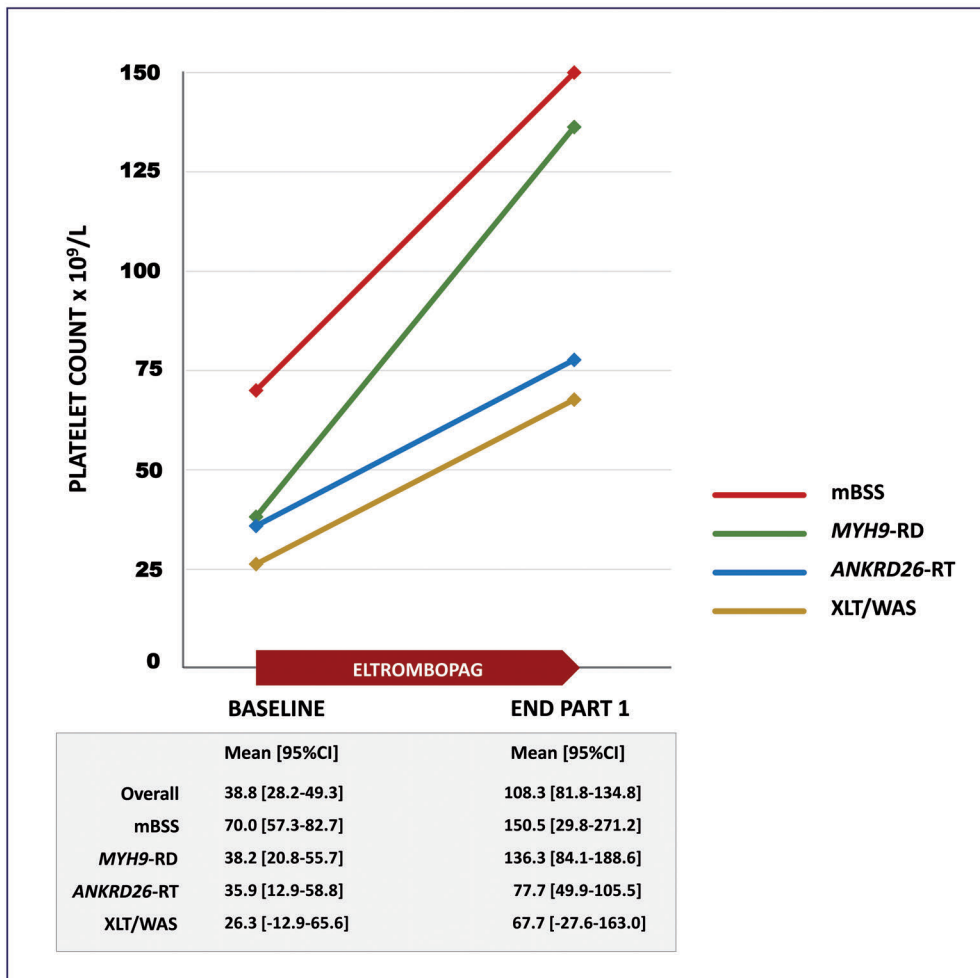
Figure 1. Mean increase in platelet count in the responders in part 1 of the study. Patients are categorized according to the diagnosis of the specific form of inherited thrombocytopenia. mBSS: monoallelic Bernard-Soulier syndrome; *MYH9*-RD: *MYH9*-related disease; . *ANKRD26*-RT: *ANKRD26*-related thrombocytopenia. XLT/WAS: X-linked thrombocytopenia/Wiskott-Aldrich syndrome. Mean values of platelet count at baseline and at the end of part 1 of the treatment along with their 95% confidence intervals (95%CI) are reported in the gray box.

	BASELINE Mean [95%CI]	END PART 1 Mean [95%CI]
Overall	38.8 [28.2-49.3]	108.3 [81.8-134.8]
mBSS	70.0 [57.3-82.7]	150.5 [29.8-271.2]
MYH9-RD	38.2 [20.8-55.7]	136.3 [84.1-188.6]
ANKRD26-RT	35.9 [12.9-58.8]	77.7 [49.9-105.5]
XLT/WAS	26.3 [-12.9-65.6]	67.7 [-27.6-163.0]

Platelet aggregation was normal in all the cases, except for two patients with *MYH9*-RD and one with mBSS who had slightly reduced responses to the lowest ADP dose (*Online Supplementary Table S7*). In 12 patients, platelet activation in response to ADP and TRAP was also assessed through flow cytometry as the induction of surface expression of P-selectin and of the activated form of GPIIb-IIIa.[24] In these subjects, platelet activation at baseline was not significantly different from that of healthy controls. Overall, platelet responsiveness did not change significantly after eltrombopag treatment with respect to baseline in the investigated patients (*Online Supplementary Figure S2*).

The mean serum thrombopoietin level at baseline was 177.8 pg/mL [standard deviation (SD) 125]. Thrombopoietin levels were unchanged at the end of treatment both considering patients overall and stratifying them according to the different disorders or response to treatment (*Online Supplementary Table S8*).

Safety

We recorded seven adverse events in five patients (21%) (Table 4): all the adverse events were grade 1 (mild) according to Common Terminology Criteria for Adverse Events (CTCAE), version 4.0. Four patients reported mild and transient headache and/or diffuse bone pain during the first 2-3 days of treatment. One patient with *ANKRD26*-RT presented with increased plasma creatinine at the assessment after 3 weeks of treatment with 50 mg/day. Although this adverse event was grade 1 (creatinine 1.6 times above baseline), treatment was discontinued according to the study protocol. Further investigations showed that kidney dysfunction was due to urinary retention because of pre-existing benign prostatic hypertrophy and suggested that a causal relationship between eltrombopag administration and the adverse event was unlikely (see Table 4 for details). Results of an ophthalmic assessment at the end of therapy were unchanged in all cases, including the three patients with *MYH9*-RD who had cataracts at baseline.

Table 4. Adverse events recorded during part 1 of the study. All the adverse events were grade 1 according to the Common Terminology Criteria for Adverse Events, version 4.0.

Adverse event	N. of AE	N. of patients (%)	Description
Any adverse event	7	5 (21%)	
Headache	4	4 (17%)	Mild headache that resolved completely after 2 or 3 days. Some patients took low doses of acetaminophen with benefit.
Bone pain	2	2 (8%)	Mild diffuse bone pain that resolved completely after 3 or 4 days. Some patients took low doses of acetaminophen with benefit.
Increased plasma creatinine	1	1 (4%)	Increase 1.6-fold above baseline at the evaluation after 21 days of treatment. Treatment was stopped according to study protocol. Further investigations disclosed that the increased creatinine level was due to urinary retention because of concomitant benign prostatic hypertrophy. Creatinine level continued to increase progressively for 2 months after eltrombopag discontinuation and then completely resolved after specific urologic treatment. Worsening of prostatic hypertrophy has never been reported as an adverse reaction of eltrombopag treatment.[1] Based on the clinical course of the disorder and data from literature, the investigators suggest that a causal relationship between eltrombopag administration and the AE was unlikely.

[1]Eltrombopag (Revolade®) Product information available at *https://www.ema.europa.eu/en/medicines/human/* . N: number; AE: adverse event.

Table 5. Response in part 2 of the study in the four patients enrolled.

Patient ID (patient/family)[1]	1/1	12/10	17/13	22/16
Gender/age, years	F/49	F/45	F/45	M/24
Diagnosis	*MYH9*-RD	*MYH9*-RD	*ITGB3*-RT	WAS
Treatment duration, weeks	16	16	16	8
WHO bleeding score - baseline	3	3	2	2
Bleeding symptoms - baseline	Easy bruising Petechiae Gum bleeding Epistaxis	Easy bruising Gum bleeding Menorrhagia	Easy bruising Menorrhagia	Easy bruising Epistaxis Hematochezia
Platelet count - baseline, x10⁹/L	14	38	62	9
WHO bleeding score - end of part 2[2]	1	1	1	0
Bleeding symptoms - end of part 2	Easy bruising	Easy bruising	Easy bruising	None
Platelet count - end of part 2,[3] x10⁹/L	75	76	70	19
Eltrombopag dose - end of part 2, mg/day	50	25	25	50
Response in part 2[4]	Minor	Minor	Minor	Major

[1]See *Online Supplementary Table S4*. [2]Spontaneous bleeding during the 2 weeks preceding the last on-treatment visit according to the World Health Organization bleeding scale. [3]As evaluated at the last on-treatment visit by phase-contrast microscopy in a counting chamber. [4]According to predefined study criteria. ID: identity; *MYH9*-RD: *MYH9*-related disease; *ITGB3*-RT: *ITGB3*-related thrombocytopenia; WAS: Wiskott-Aldrich syndrome; WHO: World Health Organization.

Part 2 of the study

Six patients met the criteria for enrollment in part 2 of the study. Two of them did not consent to long-term treatment for logistic reasons, as they were not available to undergo the repeated visits planned by the study protocol. Thus, four patients entered part 2 (2 with *MYH9*-RD, 1 with WAS, 1 with *ITGB3*-RT). At baseline all of them had spontaneous mucosal hemorrhages WHO grade 2 or 3 (epistaxis, gum bleeding, menorrhagia, and/or hematochezia) (Table 5).

Primary endpoint

The outcome of part 2 of the study is summarized in Table 5 and Figure 2. Three patients completed the 16 weeks of therapy. All of them obtained a stable remission of mucosal bleeding throughout the treatment period. During eltrombopag administration, they experienced only very mild and occasional easy bruising (WHO grade 1), resulting in a minor response according to the study criteria. Concerning the patient with WAS, treatment was discontinued after 8 weeks because of exacerbation of cutaneous eczema (see below). During treatment, this patient obtained a complete remission of bleeding (WHO grade 0).

Eltrombopag dose and health-related quality of life

Two patients achieved a response with eltrombopag 25 mg/day, whereas two patients required 50 mg/day (Table 5, Figure 2).

The reduction of bleeding symptoms was associated with an overall increase in the scores obtained with the FACT-TH18 and FACIT-F questionnaires (*Online Supplementary Table S9*). The increase was evident in the two *MYH9*-RD patients presenting the highest degree of bleeding tendency at baseline (WHO grade 3), whereas the two other patients obtained mild or no improvements.

Exploratory endpoints

The thrombopoietin levels of the four patients did not change significantly during part 2 of the study. Platelet response to ADP and TRAP was assessed by flow cytometry in the two *MYH9*-RD patients and the WAS patient and did not show any significant changes with long-term eltrombopag (*data not shown*).

Safety

The patient with WAS reported exacerbation of a pre-existing cutaneous eczema, which is a typical manifestation of the genetic disease. For this reason, eltrombopag
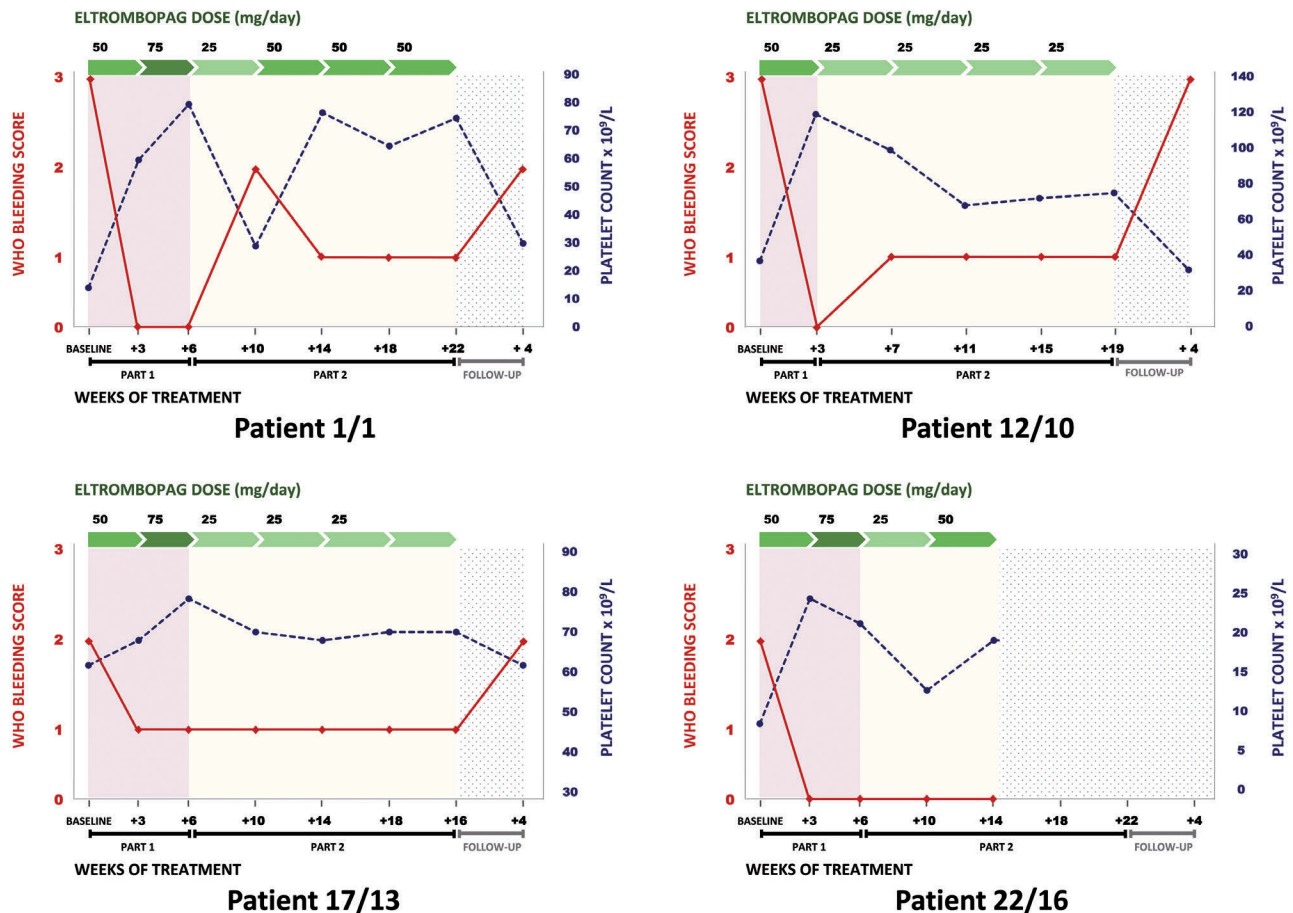
Figure 2. Effects of treatments in part 1 and part 2 of the study in the four individuals who received long-term eltrombopag therapy. The figure summarizes the effects of eltrombopag administration on bleeding symptoms according to the World Health Organization (WHO) bleeding scale and on platelet count. Patients 1/1 and 12/10 have *MYH9*-related disease, patient 17/13 has *ITGB3*-RT, and patient 22/16 has Wiskott-Aldrich syndrome (see Table 5).

was discontinued after 8 weeks of part 2 of the study. The adverse event was grade 2 according to CTCAE version 3.0. The patient described a similar exacerbation of the eczema before enrollment into this study, which occurred without any apparent causes. However, the eczema improved some weeks after eltrombopag discontinuation, supporting a causal relationship with the treatment. No additional adverse events were observed during part 2 therapy. In particular, no occurrence or worsening of cataracts was observed, even in the two patients with *MYH9*-RD who had cataracts at baseline.

Post-treatment assessments

Twenty patients were re-evaluated 30 days after the end of part 1 or 2 (3 patients refused the visit). Post-treatment assessments did not identify any adverse events. The mean platelet count was 47.0×10^9/L (SD 26), similar to that at baseline in the same patients (40.9×10^9/L, SD 23). The bleeding tendency returned to that recorded at baseline in all the cases.

Discussion

TPO-RA represent an appealing hypothesized treatment for the majority of patients with thrombocytopenias of genetic origin. In fact, in most forms of inherited thrombocytopenia, the megakaryocyte response to thrombopoietin is totally or partially preserved:[25,26] TPO-RA can therefore potentially increase platelet production in many of these disorders. Moreover, in most patients with inherited thrombocytopenia platelet function is normal or only partially impaired, so that increasing platelet count is expected to improve hemostasis.[25,27] Patients with an inherited thrombocytopenia may benefit from short-term courses of TPO-RA as well as prolonged treatment. Short-term courses may be given in preparation for elective surgery or other invasive procedures whenever the platelet count is below the safe threshold for the specific procedure. In this context, TPO-RA can replace perioperative platelet transfusions, thus preventing alloimmunization and the other risks of blood derivatives, and provide an option to increase platelet count even in patients refractory to platelet transfusions.[10-12,14,15] On the other hand, patients with clinically significant spontaneous bleeding may benefit from long-term TPO-RA administration to achieve an enduring remission of bleeding symptoms and reduce the risk of major hemorrhages. Despite these premises, clinical evidence on the efficacy and safety of TPO-RA in inherited thrombocytopenias is very scarce.[28]

The only previous prospective study investigated the short-term use of eltrombopag in patients with *MYH9*-RD and showed that most patients responded to treatment without major side effects.[9] The present trial investigates the response to short-term eltrombopag in a wider range of inherited thrombocytopenias, and provides information on the effects of prolonged treatment in those patients with clinically significant spontaneous hemorrhages.

We gave a short-term course of eltrombopag to patients affected with five different disorders: the large majority of them (91.3%) responded to the drug and the mean platelet count at the end of therapy was increased by 64.5×10^9/L compared to baseline ($P<0.001$). However, we observed some differences in the degree of platelet response between the patients with the different forms of inherited thrombocytopenia. Eltrombopag was highly effective in *MYH9*-RD, thus confirming and extending the results of the previous trial.[9] All the *MYH9*-RD patients responded, most of them (78%) reached a platelet count $>100 \times 10^9$/L, and the mean increase in platelet count compared to baseline was 98.1×10^9/L. The two individuals with mBSS also achieved major responses with an increase in platelet count close to that of *MYH9*-RD subjects (80.5×10^9/L). Although seven of the eight evaluable patients with *ANKRD26*-RT responded to eltrombopag, the extent of platelet response was globally lower than that in *MYH9*-RD and mBSS patients: in fact, most *ANKRD26*-RT subjects obtained minor responses and the mean increase in platelet count in responders was 41.8×10^9/L. In the three XLT/WAS patients, results appeared similar to those of *ANKRD26*-RT: these patients reached a minor response with an average rise in platelet count of 41.4×10^9/L. In spite of these differences, we believe that in all the above disorders the response to eltrombopag is highly relevant with regards to the use of the drug in preparation for surgery in clinical practice. In fact, current guidelines define a platelet count of 50×10^9/L as the threshold level recommended for major surgery, with the exception of neurosurgery and posterior eye surgery that require a platelet count of 100×10^9/L.[4,5] In this view, while the response observed in *MYH9*-RD and mBSS appears a very good result, even the extent of the increase in platelet count obtained in *ANKRD26*-RT and XLT/WAS appears sufficient to avoid the use of platelet transfusions to prepare most patients for most surgical procedures.

Finally, we treated only one patient with *ITGB3*-RT, who failed to achieve a platelet response according to the study criteria.

All the patients who responded in part 1 of the study, even those achieving a minor response, had complete remission of bleeding symptoms whenever these were present at baseline. Even one of the two patients classified as non-responders according to the study criteria, experienced the remission of mucosal bleeding following a slight increase in platelet count. Remission of bleeding is consistent with the results of platelet function studies during eltrombopag treatment: since platelet responses to different agonists were normal or only slightly impaired, increasing platelet count was effective in improving hemostasis. Consistent with previous findings in XLT/WAS patients,[18] flow cytometry showed that platelet responsiveness to ADP and TRAP does not change significantly with eltrombopag administration.

Concerning the dosage of eltrombopag, ten of the 11 patients who achieved a major response obtained this result with a dose of 50 mg/day, while one patient required a dose of 75 mg/day. Overall, ten of the 13 patients who were switched from 50 to 75 mg/day obtained a further increase of platelet count with the higher dose: four subjects reached a better response according to the study criteria, while six patients achieved only slightly higher platelet counts. All the patients with *ANKRD26*-RT or XLT/WAS, but one, required the switch to the higher dose, which resulted in a higher platelet count in most cases. These data suggest that 75 mg/day is the most reasonable starting dose for preoperative eltrombopag in patients with either of these two disorders.

Effects of long-term eltrombopag administration were investigated in four patients who had frequent episodes of spontaneous mucosal bleeding. All of them achieved a sta-

ble remission of mucosal hemorrhages and the remission persisted throughout the treatment period. In two patients, the reduction of spontaneous bleeding was associated with a very slight increase of platelet count (around $10x10^9$/L). The same observation was previously made in a patient with WAS who was given long-term treatment with eltrombopag because of severe bleeding symptoms.[17] Two patients achieved remission of bleeding with the dosage of 25 mg/day, suggesting that, in some patients with inherited thrombocytopenia, clinical benefit can be maintained with prolonged administration of relatively low doses of eltrombopag. Interestingly, the two patients with the greatest bleeding tendency at baseline experienced not only stable improvements of HR-QoL related to bleeding, but also an increase of the score measuring the subjective perception of fatigue.

The observation that some patients obtained a significant reduction of bleeding tendency following a very slight increase in platelet count suggests that eltrombopag may improve some discrete platelet functions in addition to raising platelet concentration. As mentioned, overall we did not observe any significant change in platelet GPIIb-IIIa activation or P-selectin expression in response to ADP and TRAP after eltrombopag treatment compared to that at baseline, in 12 investigated patients. However, we cannot exclude that the drug could have improved some other mechanisms of platelet function[29] in some patients, and further investigations are required to explore this hypothesis.

Short-term treatment with eltrombopag was globally well tolerated, with 17% of patients reporting mild and transient headache and/or bone pain at the beginning of treatment. In one ANKRD26-RT patient, we observed a slight increase in plasma creatinine; clinical investigation of this subject suggested that a causal relationship between eltrombopag and this adverse event was unlikely. Regarding long-term treatment, the patient affected with WAS experienced worsening of a pre-existing cutaneous eczema that required eltrombopag discontinuation after 14 weeks. This adverse event had never been described in the previous retrospective reports on WAS patients who received eltrombopag.[17,18] No other adverse events were recorded with long-term therapy.

Eltrombopag has been associated with the occurrence of cataracts in patients with immune thrombocytopenia,[30] and MYH9-RD is a syndromic disorder predisposing to cataracts.[31] Thus, it is noteworthy that none of our MYH9-RD subjects showed development or progression of cataracts, not even the two patients who received long-term therapy and already had cataracts at baseline.

A previous study raised the suspicion that the TPO-RA romiplostim favors progression to myeloid leukemia in patients with myelodysplastic syndromes.[32] Subsequent trials of eltrombopag monotherapy in myelodysplastic syndromes did not reveal any safety issues in this regard;[33-35] however, a trend to an increased risk of disease progression was reported in a study in which eltrombopag was tested in association with azacitidine in intermediate- or high-risk myelodysplastic syndromes.[36] These observations raise concerns about the safety of TPO-RA in ANKRD26-RT, a condition that increases the risk of myeloid malignancies.[37] In the present study, short-term use of eltrombopag did not result in any changes of blood cell parameters or morphology (with the exception of platelet count) in ANKRD26-RT patients. However, further clinical data on this topic are needed, and caution should be used when treating individuals with ANKRD26-RT or other inherited thrombocytopenias predisposing to hematological malignancies[38] with TPO-RA, especially with long-term administration.

In conclusion, this study shows that eltrombopag was effective in increasing platelet count in four different forms of inherited thrombocytopenia, which, taken together, affect more than 55% of patients with genetic thrombocytopenias.[28] In most patients, short-term administration of eltrombopag increased platelet count above the threshold for major surgery recommended by current guidelines,[4,5] indicating that the drug can efficiently replace perioperative platelet transfusions in preparation for surgery or other invasive procedures. Although only four patients received long-term treatment, the results indicate that prolonged eltrombopag therapy can induce persistent remission of spontaneous bleeding. Both short- and long-term treatments were globally well tolerated. Although a greater amount of clinical data on the use of TPO-RA in inherited thrombocytopenias is certainly required, our results suggest that eltrombopag will probably have a central role in the treatment of thrombocytopenias of genetic origin.

References

1. Balduini CL, Pecci A, Noris P. Diagnosis and management of inherited thrombocytopenias. Semin Thromb Hemost. 2013;39(2):161-171.
2. Orsini S, Noris P, Bury L, et al. Bleeding risk of surgery and its prevention in patients with inherited platelet disorders. Haematologica. 2017;102(7):1192-1203.
3. Dupuis A, Gachet C. Inherited platelet disorders: management of the bleeding risk. Transfus Clin Biol. 2018;25(3):228-235.
4. Estcourt LJ, Birchall J, Allard S, et al. Guidelines for the use of platelet transfusions. Br J Haematol. 2017;176(3):365-394.
5. Kaufman RM, Djulbegovic B, Gernsheimer T, et al. Platelet transfusion: a clinical practice guideline from the AABB. Ann Intern Med. 2015;162(3):205-213.
6. Bolton-Maggs PH, Chalmers EA, Collins PW, et al. A review of inherited platelet disorders with guidelines for their management on behalf of the UKHCDO. Br J Haematol. 2006;135(5):603-633.
7. Pecci A. Diagnosis and treatment of inherited thrombocytopenias. Clin Genet. 2016;89(2):141-153.
8. Rodeghiero F, Carli G. Beyond immune thrombocytopenia: the evolving role of thrombopoietin receptor agonists. Ann Hematol. 2017;96(9):1421-1434.

9. Pecci A, Gresele P, Klersy C, et al. Eltrombopag for the treatment of the inherited thrombocytopenia deriving from MYH9 mutations. Blood. 2010;116(26):5832-5837.

10. Pecci A, Barozzi S, d'Amico S, Balduini CL. Short-term eltrombopag for surgical preparation of a patient with inherited thrombocytopenia deriving from MYH9 mutation. Thromb Haemost. 2012;107(6):1188-1189.

11. Favier R, Feriel J, Favier M, Denoyelle F, Martignetti JA. First successful use of eltrombopag before surgery in a child with MYH9-related thrombocytopenia. Pediatrics. 2013;132(3):e793-795.

12. Favier R, De Carne C, Elefant E, Lapusneanu R, Gkalea V, Rigouzzo A. Eltrombopag to treat thrombocytopenia during last month of pregnancy in a woman with MYH9-related disease: a case report. A A Pract. 2018;10(1):10-12.

13. Gröpper S, Althaus K, Najm J, et al. A patient with Fechtner syndrome successfully treated with romiplostim. Thromb Haemost. 2012;107(3):590-591.

14. Fiore M, Saut N, Alessi MC, Viallard JF. Successful use of eltrombopag for surgical preparation in a patient with ANKRD26-related thrombocytopenia. Platelets. 2016;27(8):828-829.

15. Westbury SK, Downes K, Burney C, et al. Phenotype description and response to thrombopoietin receptor agonist in DIAPH1-related disorder. Blood Adv. 2018;2(18):2341-2346.

16. Yamanouchi J, Hato T, Kunishima S, Niiya T, Nakamura H, Yasukawa M. A novel MYH9 mutation in a patient with MYH9 disorders and platelet size-specific effect of romiplostim on macrothrombocytopenia. Ann Hematol. 2015;94(9);1599-1600.

17. Gabelli M, Marzollo A, Notarangelo LD, Basso G, Putti MC. Eltrombopag use in a patient with Wiskott-Aldrich syndrome. Pediatr Blood Cancer. 2017;64(12).

18. Gerrits AJ, Leven EA, Frelinger AL 3rd, et al. Effects of eltrombopag on platelet count and platelet activation in Wiskott-Aldrich syndrome/X-linked thrombocytopenia. Blood. 2015;126(11):1367-1378.

19. Noris P, Perrotta S, Seri M, et al. Mutations in ANKRD26 are responsible for a frequent form of inherited thrombocytopenia: analysis of 78 patients from 21 families. Blood. 2011;117(24):6673-6680.

20. Albert MH, Bittner TC, Nonoyama S, et al. X-linked thrombocytopenia (XLT) due to WAS mutations: clinical characteristics, long-term outcome, and treatment options. Blood. 2010;115(16):3231-3238.

21. Massaad MJ, Ramesh N, Geha RS. Wiskott-Aldrich syndrome: a comprehensive review. Ann N Y Acad Sci. 2013;1285:26-43.

22. Noris P, Perrotta S, Bottega R, et al. Clinical and laboratory features of 103 patients from 42 Italian families with inherited thrombocytopenia derived from the monoallelic Ala156Val mutation of GPIb (Bolzano mutation). Haematologica. 2012;97(1):82-88.

23. Gresele P, Falcinelli E, Giannini S, et al. Dominant inheritance of a novel integrin β3 mutation associated with a hereditary macrothrombocytopenia and platelet dysfunction in two Italian families. Haematologica. 2009;94(5):663-669.

24. Michelson AD, Barnard MR, Krueger LA, Frelinger AL 3rd, Furman MI. Evaluation of platelet function by flow cytometry. Methods. 2000;21(3):259-270.

25. Pecci A. Pathogenesis and management of inherited thrombocytopenias; rationale for the use of thrombopoietin-receptor agonists. Int J Hematol. 2013;98(1):34-47.

26. Pecci A, Balduini CL. Lessons in platelet production from inherited thrombocytopenias. Br J Haematol. 2014;165(2):179-192.

27. Balduini CL, Savoia A, Seri M. Inherited thrombocytopenias frequently diagnosed in adults. J Thromb Haemost. 2013;11(6):1006-1019.

28. Rodeghiero F, Pecci A, Balduini CL. Thrombopoietin receptor agonists in hereditary thrombocytopenias. J Thromb Haemost. 2018;16(9):1700-1710.

29. Daskalakis M, Colucci G, Keller P, et al. Decreased generation of procoagulant platelets detected by flow cytometric analysis in patients with bleeding diathesis. Cytometry B Clin Cytom. 2014;86(6):397-409.

30. Wong RSM, Saleh MN, Khelif A, et al. Safety and efficacy of long-term treatment of chronic/persistent ITP with eltrombopag: final results of the EXTEND study. Blood. 2017;130(23):2527-2536.

31. Pecci A, Klersy C, Gresele P, et al. MYH9-related disease: a novel prognostic model to predict the clinical evolution of the disease based on genotype-phenotype correlations. Hum Mutat. 2014;35(2):236-247.

32. Giagounidis A, Mufti GJ, Fenaux P, et al. Results of a randomized, double-blind study of romiplostim versus placebo in patients with low/intermediate-1-risk myelodysplastic syndrome and thrombocytopenia. Cancer. 2014;120(12):1838-1846.

33. Platzbecker U, Wong RS, Verma A, et al. Safety and tolerability of eltrombopag versus placebo for treatment of thrombocytopenia in patients with advanced myelodysplastic syndromes or acute myeloid leukaemia: a multicentre, randomised, placebo-controlled, double-blind, phase 1/2 trial. Lancet Haematol. 2015;2(10):e417-426.

34. Oliva EN, Alati C, Santini V, et al. Eltrombopag versus placebo for low-risk myelodysplastic syndromes with thrombocytopenia (EQoL-MDS): phase 1 results of a single-blind, randomised, controlled, phase 2 superiority trial. Lancet Haematol. 2017;4(3):e127-e136.

35. Mittelman M, Platzbecker U, Afanasyev B, et al. Eltrombopag for advanced myelodysplastic syndromes or acute myeloid leukaemia and severe thrombocytopenia (ASPIRE): a randomised, placebo-controlled, phase 2 trial. Lancet Haematol. 2018;(1):e34-e43.

36. Dickinson M, Cherif H, Fenaux P, et al. Azacitidine with or without eltrombopag for first-line treatment of intermediate- or high-risk MDS with thrombocytopenia. Blood. 2018;132(25):2629-2638.

37. Noris P, Favier R, Alessi MC, et al. ANKRD26-related thrombocytopenia and myeloid malignancies. Blood. 2013;122(11):1987-1989.

38. Noris P, Pecci A. Hereditary thrombocytopenias: a growing list of disorders. Hematology Am Soc Hematol Educ Program. 2017; 2017(1):385-399.

Next-generation sequencing and recombinant expression characterized aberrant splicing mechanisms and provided correction strategies in factor VII deficiency

Ferrata Storti Foundation

Paolo Ferraresi,[1] Dario Balestra,[1] Caroline Guittard,[2] Delphine Buthiau,[2] Brigitte Pan-Petesh,[3] Iva Maestri,[4] Roula Farah,[5] Mirko Pinotti[1] and Muriel Giansily-Blaizot[2]

[1]Department of Life Sciences and Biotechnology, University of Ferrara, Ferrara, Italy; [2]Department of Biological Haematology, CHU Montpellier, Université Montpellier, Montpellier, France; [3]Haemophilia Centre, CHU Brest, Brest, France; [4]Department of Morphology, Surgery and Experimental Medicine, University of Ferrara, Ferrara, Italy and [5]Department of Pediatrics, Saint George Hospital University Medical Center, Beirut, Lebanon

ABSTRACT

Despite the exhaustive screening of *F7* gene exons and exon-intron boundaries and promoter region, a significant proportion of mutated alleles remains unidentified in patients with coagulation factor VII deficiency. Here, we applied next-generation sequencing to 13 FVII-deficient patients displaying genotype-phenotype discrepancies upon conventional sequencing, and identified six rare intronic variants. Computational analysis predicted splicing effects for three of them, which would strengthen (c.571+78G>A; c.806-329G>A) or create (c.572-392C>G) intronic 5' splice sites (5'ss). In *F7* minigene assays, the c.806-329G>A was ineffective while the c.571+78G>A change led to usage of the +79 cryptic 5'ss with only trace levels of correct transcripts (3% of wild-type), in accordance with factor VII activity levels in homozygotes (1-3% of normal). The c.572-392C>G change led to pseudo-exonization and frame-shift, but also substantial levels of correct transcripts (approx. 70%). However, this variant was associated with the common *F7* polymorphic haplotype, predicted to further decrease factor VII levels; this provided some kind of explanation for the 10% factor VII levels in the homozygous patient. Intriguingly, the effect of the c.571+78G>A and c.572-392C>G changes, and particularly of the former (the most severe and well-represented in our cohort), was counteracted by antisense U7snRNA variants targeting the intronic 5'ss, thus demonstrating their pathogenic role. In conclusion, the combination of next-generation sequencing of the entire *F7* gene with the minigene expression studies elucidated the molecular bases of factor VII deficiency in 10 of 13 patients, thus improving diagnosis and genetic counseling. It also provided a potential therapeutic approach based on antisense molecules that has been successfully exploited in other disorders.

Introduction

The inherited deficiency of factor VII (FVII), the crucial enzyme triggering blood coagulation,[1] is the most common of the rare coagulation disorders transmitted in an autosomal recessive manner. The clinical features are highly variable, ranging from severe (i.e. intracranial or gastro-intestinal hemorrhages) to milder (i.e. epistaxis) or asymptomatic forms,[2] and the relationship with plasma FVII activity (FVII:C) levels is often elusive. On the other hand, molecular genetic studies combined with functional assays and recombinant expression investigations, detailing the residual FVII levels associated with *F7* gene mutations, have clearly helped define genotype and coagulation and clinical phenotype relationships,[3-5] with implications for diagnosis, prognosis and counseling.

Over 220 point-mutations,[6] a few large genomic rearrangements, and six com-

mon variants have been identified in the *F7* gene (*http://f7-db.eahad.org/*). Nevertheless, in spite of an exhaustive direct sequencing of *F7* exons and exon-intron junctions and of the proximal promoter region, a significant proportion of defective alleles has still not been identified. The rate of uncharacterized *F7* disease alleles ranges from 2% to 8%[7-10] in Europe, and a similar estimate (7%) was made in India.[11]

In this context, subtle intronic variations outside the routinely sequenced exon-intron boundaries could have a pathological impact by impairing the splicing process. In fact, precise exon definition during RNA processing requires the interplay among several exonic and intronic splicing regulatory elements,[12] which can be altered by nucleotide changes and lead to aberrant splicing.[4,13-17] Various examples of "deep" intronic changes associated with mis-splicing have been reported in human disorders, including those involved in coagulation.[18-20] It is worth noting that RNA splicing can be modulated for different purposes, including the development of new therapies.[14,20-26] In this context, next-generation sequencing (NGS) could represent a powerful tool to characterize gene defects in patients with unknown alleles; however, only a few studies have been conducted in coagulation factor disorders.[27-29]

Here, we investigated 13 patients with FVII deficiency forms that have not been explained by mutations identified by conventional sequencing and used NGS to identify six rare intronic variations that could be causative. Through expression studies, we demonstrated that two of them lead to aberrant splicing, which explained the residual FVII levels in most patients and, intriguingly, that these can be rescued by an antisense-based correction approach.

Methods

Patients

Since 1997, 400 FVII-deficient patients with FVII coagulant activity (FVII:C) levels <30% were referred to our laboratory for genetic analysis through conventional screening. Among them, 13 (Table 1) showed a genetic profile that, considering the identified mutated alleles[10,30-32] and the major *F7* functional polymorphisms (c.-325_-324insCCTATATCCT, A2 allele; p.Arg413Gln change, M2 allele),[33-37] appeared to be incompatible with the reduced FVII levels. The local Institutional Review Board approved the study and patients provided informed consent.

Measurement of FVII levels

FVII:C and FVII antigen levels were determined by the one-stage method[38] and Enzyme-Linked-Immunoabsorbant-Assay (Diagnostica Stago, Asnière sur Seine, France), respectively.

DNA genotyping and next-generation sequencing

Conventional Sanger technology was exploited to sequence the *F7* exons, including the intronic boundaries and the 5' untranslated region. Large rearrangements were ruled out using semi-quantitative multiplex fluorescent-polymerase chain reaction (SQF-PCR) assays.[39] NGS of the *F7* gene was designed to cover the intronic regions with the exception of the highly repetitive GC-rich region in intron 2 (legacy nomenclature, intron 1b). The probe-capture custom design targeted the 14893-pbF7 gene in two parts: chr13:113759000-113761350 and chr13:113764600-113775100 accounting for a total of 12,850 base-pairs with a gap of 3250 bp. DNA library generation was performed using the Custom SureSelectQXT Target Enrichment system (Agilent, Santa Clara, CA, USA) on a MiSeq platform (Illumina, San Diego, CA, USA). The sequencing data were stored in FASTQ format and analyzed using two bio-informatics

Table 1. Features of the investigated FVII deficient patients.

Proband	Origins	FVII:C (%)	FVII:Ag(%)	Conventional sequencing		Polymorphic pattern c.325_324ins/ p.Arg413Gln	NGS sequencing	
				Mutation	Zygosity		Additional nucleotide change	Zygosity
#17	Maghreb countries	3	uk	p.Met358Ile[10]	het	A1A1/M1M1	c.571+78G>A	het
#19	France	2	<5	p.Met1Val[10]	het	A1A2/M1M2	c.571+78G>A	het
#31	France	<1	19	p.Cys162Tyr[10]	het	A1A1/M1M1	c.64+305G>A and c.806-329G>A	het
#113	France	1	66	p.Arg364Trp[30]	het	A1A1/M1M1	c.571+78G>A and c.291+846C>T	het
#262	France	3	uk	p.Gln160Arg[31]	het	A1A1/M1M1	c.806-329G>A	het
#341	France	16	uk	c.430+1G>A[32]	het	A1A1/M1M1	c.64+305G>A and c.681+132G>T	het
#214	France	1	3	p.Arg58ProfsX92	het	A1A1/M1M1	c.571+78G>A	het
#28	France	13	39	p.Arg59Trp	het	A1A1/M1M1	c.571+78G>A	het
#377	Maghreb countries	23	uk			A2A2/M2M2	c.572-392C>G	het
#284 *	Maghreb countries	20	15			A1A2/M1M2	c.571+78G>A	het
#90 *	Lebanon	<1	uk			A1A1/M1M1	c.571+78G>A	hom
#15	Maghreb countries	3	uk			A1A1/M1M1	c.571+78G>A	hom
#330	France	10	uk			A2A2/M2M2	c.572-392C>G	hom

*Consanguinity. NGS: next-generation sequencing; uk: unknown; A1/A2: decanucleotide insertion c.-325_-324insCCTATATCCT promoter polymorphism rs5742910; M1/M2: p.Arg413Gln polymorphism: rs6046; FVII:C: FVII activity; FVII:Ag: FVII antigen; het: heterozygous; hom: homozygous.

pipelines: SEQUENCE Pilot® module SeqNext, version 4.3.1 (JSI medical systems GmbH, Ettenhein, Germany) and SeqOne® (*https://app.seq.one*). The dataset had a mean coverage of over 300x. For each nucleotide of interest, the sequence depth was at least of 30x and the Phred-based quality score above Q30. Regions that did not reach these criteria were sequenced using Sanger technology (primers available upon request); this also applies to each deleterious variation that was independently checked using Sanger sequencing.

Expression studies with *F7* minigenes

The expression vectors for the c.571+78G>A (pIVS6+78A) and c.572-392C>G (pIVS6-392G) variants were created by site-directed mutagenesis of the pIVS6 wild-type (pIVS6-wt), created by cloning the F7 genomic region spanning exon 5 through exon 7 into the pcDNA3 plasmid.[4] Changes were introduced, as previously described,[40] through the overlapping oligonucleotides 5'GAAGCAGATCAAAAGTAAGCATGGGATC3' and 5'GATCC-CATGCTTACTTTTGATCTGCTTC3' for the c.572-392C>G mutation. For the c.571+78G>A mutation, we exploited the non-overlapping oligonucleotides 5'CTGGACAAAA-GACAGGTGGG AGTGGC3' and 5'TAAGATAATCCG-TAGTGGGACAGGG ACT3' in a slightly modified protocols that implies, after PCR cycles, the addition of T4 polynucleotide kinase and T4 DNA ligase to ensure circulation of the products.

The U7smOPT expression vectors (pU7smOPT) were created as previously described[41] using a standard SP6 reverse oligonucleotide 5'ATTTAGGTGACACTATAG3' and the forward mutagenic oligonucleotides 5'ACAGAGGCCTTTCCGC Acccacctgtcttttgtcca AATTTTTGGAG3'(U7+78A), 5'ACAGAGGCCTTTCCGCAtgaagccactcccacctgAATTTTTGG AG3' (U7+78Ash) and 5'ACAGAGGCCTTTCCGCAcatgcttact tttgatctAATTTTTGGAG3'(U7-392G).

One microgram of the pIVS6 variant, alone or with equimolar amounts of the pU7smOPT variant, was transiently transfected in human embryonic kidney cells (HEK293T) by lipofection in 12-well plates.[13] RNA isolation and reverse transcription[42] were followed by PCR using the forward oligonucleotide *T7bisF* (5'CACTGCTTACTGGCTTATCGAAAT3', in the pcDNA3 T7 region), either unmodified or 5'fluorescently labeled (*T7bisF^FAM*), and the reverse oligonucleotide *F7ex7R* (5'CACAACTGAGCTC-CATTCACCAACA3', in exon 7) or *F7PsExR* (5'TTCAATCAAG-GTCTTGGGCC3', in the pseudo-exon 5b).

Results

Genotyping of FVII deficient patients

Among the 13 selected FVII-deficient patients shown in Table 1, ten had FVII:C levels below 15% and were

expected to have two *F7* pathogenic alleles. However, the conventional sequencing did not reveal any *F7* pathogenic allele for patients #15, #90 and #330, and only one for the remaining seven patients (#17, #19, #28, #31, #113, #214, #262). On the other hand, three patients (#284, #341, #377) presented with FVII:C levels between 15% and 30% but displayed only the c.430+1G>A mutation (#341) or the A2M2 polymorphic haplotype (#284, #377), which points towards the presence of an additional *F7* pathogenic allele for each patient. In this scenario, we had a total of 16 *F7* uncharacterized alleles to be explored using NGS.

As far as the clinical phenotype is concerned, 3 of 13 patients were symptomatic. Patient #19 presented with bruises and frequent epistaxis, patient #90 had post-traumatic oral bleeding, spontaneous hematuria and rectal bleeding, and patient #214 suffered from provoked hematoma and severe menorrhagia resolved by replacement therapy.

Next-generation sequencing, besides confirming the presence of the causative variants identified by the Sanger approach, also revealed several deep intronic substitutions. Among them, only those with a coverage of 30x and observed in databases with a minor allele frequency (MAF) <0.05 were analyzed further. Six deep intronic substitutions matched these criteria (Table 2). The c.571+78G>A change, whose pathogenic effect is supported by its co-segregation with the disease phenotype in the family pedigree of patient #28 (Figure 1), was the most frequent in our series, being present in ten alleles from unrelated patients living in various areas, including France, North Africa and Lebanon (Table 1). NGS data prompted us to analyze an enlarged panel of polymorphic deep intronic variants in both c.571+78G>A homozygotes (#15, #90), who were homozygous for the major A1 and M1 polymorphic alleles. However, they differed on other intronic variants. Patient #15, of Tunisian origin, was homozygous for two variants, c.-402A (rs510317) and c.292-672G (rs12431329), that are quite rare, with a minor allele frequency (MAF) of 0.233 and 0.213, respectively. By contrast, patient #90, living in Lebanon, showed the c.-402G and the c.292-672A variants, and displayed two additional deep intronic polymorphic variants in the homozygous state, the c.64+196G>A (rs2774030) and the c.131-394T>C (rs1745939), with a global frequency of the c.64+196A and c.131-394C alleles of 0.551 and 0.739, respectively. Thus, two different haplotypes associated with the c.571+78G>A mutation could be defined: c.-402A, A1 c.64+196G, c.131-394T, c.292-672G, c.571+78A, M1 (Haplotype 1) and c.-402G, A1,

Table 2. Deep intronic mutations found by next-generation sequencing screening.

Change	Intron	Prediction	Score (wt/mutated)	Position	rs	MAF
c.64+305G>A	1a	Weakening cryptic 3'ss	0.31/0.13	-8	36208414	0.005
c.291+846C>T	2	Strengthening cryptic 3'ss	0.51/0.71	-7	565185989	0.004
c.571+78G>A	5	Strengthening cryptic 5'ss	0.11/0.79	-2	764741909	none
c.572-392C>G	5	Creation of new 5'ss	nd/0.98	+1	none	none
c.681+132G>T	6	Strengthening cryptic 3'ss	0.02/0.12	-8	752129277	none
c.806-329G>A	7	Strengthening cryptic 5'ss	0.79/0.99	+3	none	none

Position of the point mutation is referred to the 5' splice site (5'ss) or 3'ss. RS: reference SNP ID number; MAF: minor allele frequency, based on 1000Genome project (*http://www.internationalgenome.org*). F7 gene reference sequence is NG_009262.1. NNSPLICE 0.9 software (*www.fruitfly.org/seq_tools/splice.html*) was used to predict and calculate the 5'ss or 3'ss of the score. Introns are indicated by legacy nomenclature. wt: wild-type.

c.64+196A, c.131-394C, c.292-672A, c.571+78A, M1 (Haplotype 2). The analysis was also extended to the c.571+78G>A heterozygotes, which revealed that haplotype 1 is compatible with patients of Maghreb origin whereas haplotype 2 is compatible with patients of European origin.

The c.572-392C>G, c.64+305G>A and c.806-329A variants were also relatively frequent as they were found in three, two and two alleles, respectively, whereas the remaining were identified only once.

Computational analysis of splicing regulatory elements

We performed an *in silico* analysis of the six deep-intronic mutations to infer a pathogenic effect on splicing. In principle the nucleotide changes could affect Intronic Splicing regulatory elements such as enhancers (ISE) or Silencers (ISS)[43] or create/strengthen 5' or 3' splice sites (ss). However, regulatory elements generally reside within the first 200 bp of the intron[44] and the main bioinformatics tools (i.e. Human Splicing Finder, *www.umd.be/HSF/*) have been developed to predict exonic elements, which confers prediction of the impact of the investigated changes with an unacceptable degree of speculation. Therefore, we focused the analysis on 5'ss and 3'ss (*www.fruitfly.org/seq_tools/splice.html*), which predicted that the c.64+305G>A, c.291+846C>T, c.681+132G>T nucleotide changes do not appreciably strengthen cryptic splice sites. Concerning the c.571+78G>A, c.572-392C>G and c.806-329G>A variants, the introduction of the nucleotide changes would result in the creation (c.572-392C>G) or remarkable strengthening (c.571+78G>A and c.806-329G>A) of a cryptic 5'ss (Table 2).

In vitro characterization of the splicing variants

Based on the bioinformatics prediction of the impact of these variants on splicing, on the number of affected alleles, on the MAF, and on identification in homozygous conditions, we selected the c.571+78G>A, c.572-392C>G and c.806-329G>A changes for further characterization. Due to the impossibility of investigating *F7* mRNA processing in patients' hepatocytes, the physiological site of *F7* synthesis, or to the unavailability of fresh leukocytes as ectopic source of *F7* mRNA, we exploited the expression of *F7* minigenes (Figure 2A). The transfection of the pIVS6-wt minigene and splicing pattern analysis revealed correct splicing (Figure 2C, transcript 2) but also, albeit to a lesser extent, exon 6 skipping (transcript 1) and usage of the weak cryptic intronic 5'ss at position +79 that leads to partial intron retention (transcript 3G).

The splicing pattern analysis of cells transfected with the pIVS6+78A minigene showed an aberrant transcript (Figure 2C, transcript 3A) that, upon sequencing, indicated the usage of the strengthened intronic 5'ss at position +79 (Figure 2B, transcript 3A). This leads to partial intron retention resulting in a deleted and frame-shifted mRNA harboring a premature nonsense triplet at position p.201, not expected to produce a functional FVII protein. To evaluate the presence of residual FVII levels, the RT-PCR was fluorescently labeled and the amplicons evaluated by denaturing capillary electrophoresis, which ensures high sensitivity. This approach led us to identify very low levels of correct transcripts, which roughly accounted for approximately 3% of the overall transcripts (Figure 3B).

While the splicing analysis of c.806-329G>A construct in pCDNA3 did not reveal any alteration by transient transfection in HEK293T (*Online Supplementary Appendix* and *Online Supplementary Figure S1*) or in Baby Hamster Kidney cells (*data not shown*), the assessment of splicing pattern of cells transfected with the FVII minigene harboring the c.572-392C>G change revealed splicing abnormalities (Figure 2B). In addition to the correctly spliced mRNA, we identified transcripts arising from skipping of
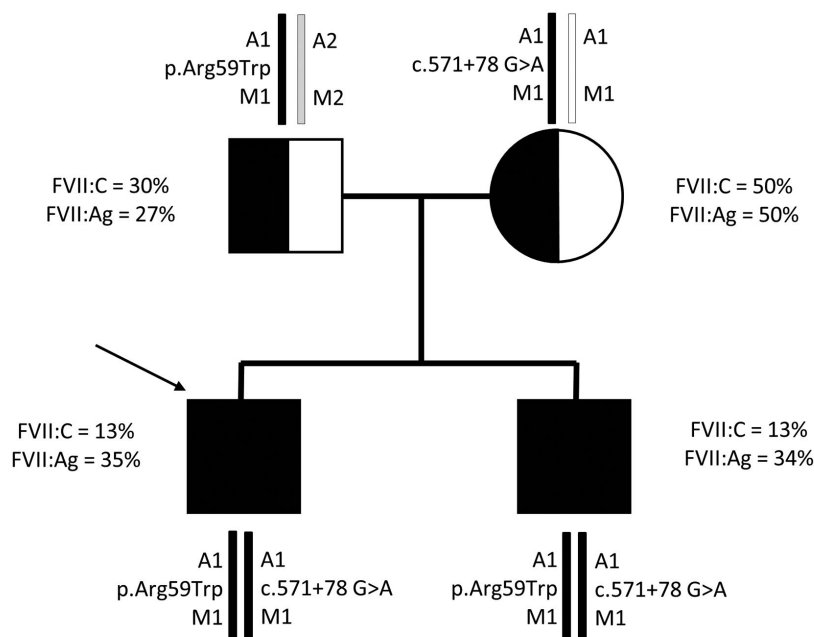
Figure 1. Family pedigree of patient #28. The propositus is indicated by an arrow. Mutation, nucleotide changes, A1A2 (rs5742910), M1M2 (p.Arg413Gln, rs6046) haplotypes, coagulant factor VII (FVII:C) and factor VII antigen (FVII:Ag) are indicated.

exon 6, from usage of the weak cryptic 5'ss at position +79 and, most importantly, from a pseudo-exonization event (transcripts 1, 3G, and 4, respectively). More precisely, this new pseudo-exon 5b originates from the usage of a cryptic 5'ss and of a 282 bp upstream cryptic 3'ss. This finding was further strengthened by a PCR using a primer in the pseudo-exon 5b (F7PsExR), which gave rise to amplified fragments only in cells expressing the pIVS6-392G construct (Figure 2B, lower panel). The inclusion of the pseudo-exon leads to a frame-shifted mRNA with a premature nonsense codon, predicted to encode a dysfunctional FVII protein. Semi-quantitative evaluation of transcripts by fluorescent labeling of amplicons and denaturing capillary electrophoresis revealed that the correct and the aberrant forms are present in the relative proportion of 74% and 26%, respectively (Figure 3C), compared to 90% and 10% in the pIVS6-wt context (Figure 3A).

Overall, these data demonstrate that both mutations exert their detrimental effect by impairing FVII splicing, strengthening the usage of cryptic 5'ss.

Investigation by antisense U7snRNA

Since the observed aberrant splicing is caused by the usage of new 5'ss, we hypothesized that masking them would weaken or abolish their detrimental role. To this purpose, we exploited variants of the U7 small nuclear RNA (U7smOPT)[41] as potent antisense molecules to target the alternative splice sites (Figure 4A).

Co-expression of the c.571+78G>A change with antisense U7smOPT variants resulted in an appreciable rescue of splicing, as evaluated by densitometric analysis of bands upon semi-quantitative PCR. In particular, the proportion of correct transcripts, barely appreciable in untreated conditions, remarkably increased to approximately 9% or to approximately 20% of total transcripts upon co-expression of the pU7+78Ash or pU7+78A, respectively (Figure 4B, bottom).

Concerning the c.572-392G variant, co-expression of pU7-392G, designed on the cryptic 5'ss, resulted in a 3-fold reduction in aberrantly spliced mRNA containing the pseudo-exon 5b and conversely favored (1.3-fold increased) the synthesis of correctly spliced transcripts that rose from approximately 70% to approximately 90% of all forms (Figure 4B, bottom), resembling the proportion observed in the wild-type context.

Overall, these data further demonstrate the causative role of the mutations that create/strengthen cryptic intronic 5'ss.
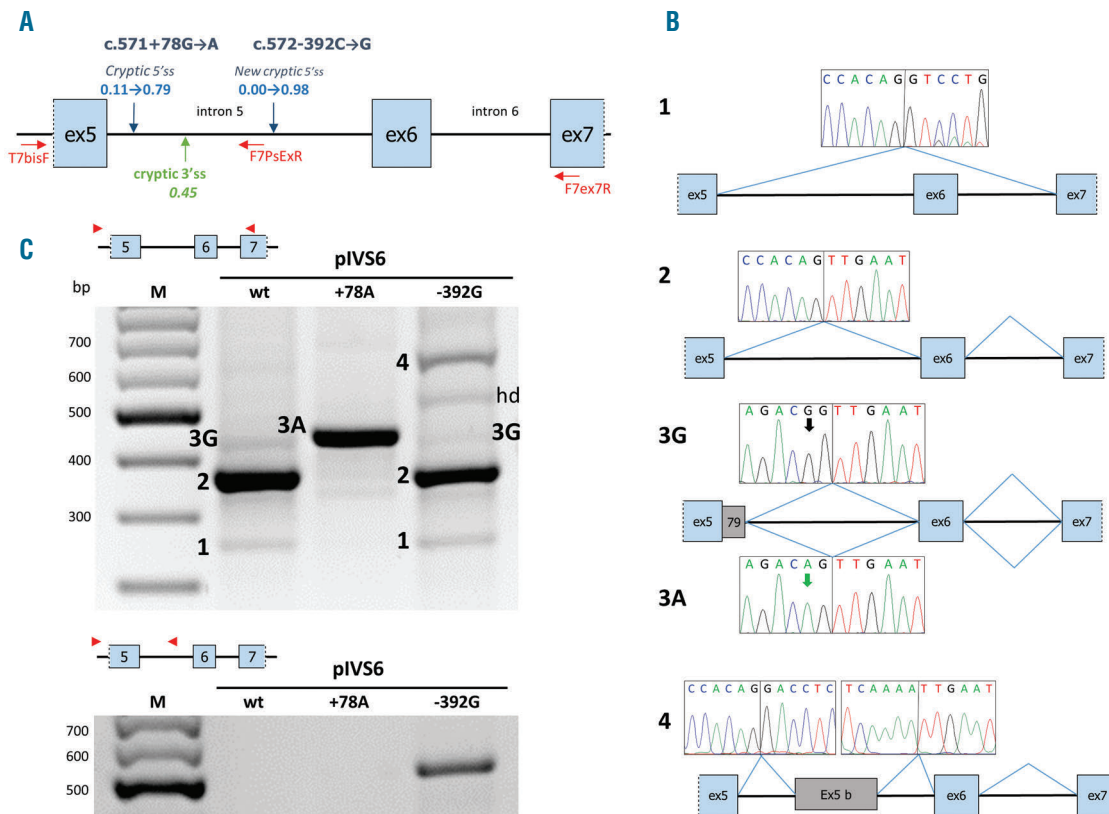
Figure 2. Alternative splicing patterns associated with the c.571+78G>A and c.572-392C>G mutations. (A) Schematic representation of the pIVS6 minigene. Mutations (blue) are reported on top. The presence of cryptic splice sites (5'ss in light blue, 3'ss in green), with related scores are indicated by arrows. Polymerase chain reaction (PCR) oligonucleotides are shown in red. (B) The schematic representation of splicing patterns is reported together with relative sequencing chromatograms of the amplicons, obtained by T7bisF-F7ex7R PCR (see panel A). PCR fragments were cloned before sequencing. (C) Splicing pattern analysis in HEK293T cells transiently transfected with pIVS6 wild type (wt) or with pIVS6 variants c.571+78A (+78A) and c.572-392G (-392G); the PCR with T7bisF-F7ex7R oligonucleotides is reported in the upper panel; PCR with T7bisF-F7psExR oligonucleotides specifically designed to amplify transcripts with the pseudo-exon5b, is reported in the lower panel. M:100 bp ladder; hd: heteroduplex.

Discussion

Uncharacterized *F7* pathogenic alleles are mentioned in all patient databases, and NGS would represent a powerful tool to tackle this; however, so far, this has not been fully explored. Here, we applied this approach in 13 FVII deficient patients who were only partially characterized through conventional sequencing, and identified a panel of deep intronic substitutions as candidates to explain the reduced FVII:C levels in patients. However, as for the numerous deep intronic nucleotide changes identified by NGS and associated with inherited diseases, their pathogenic role requires experimental support.

The evidence for the pathogenicity of deep intronic variations relies on several clinical and molecular observations. The first aspect to consider is their virtual absence in databases. This led us to exclude from our selection the c.64+305G>A and c.291+846C>T variants, with a minor allelic frequency of 0.005 and 0.004, respectively. The same applies to the c.681+132G>T change, reported in dbSnp databases as rs752129277 but with an estimated frequency of <0.0004. Another aspect that could suggest the pathogenicity of the nucleotide changes is their distribution among affected relatives or non-related individu-als. This was the case of the c.571+78G>A, c.572-392C>G and c.806-329G>A changes that occurred in eight, two and two unrelated FVII-deficient patients, respectively. Altogether these elements prompted us to explore the impact of these three variants on the splicing process through the expression of minigenes in eukaryotic cells, a well-proven approach used to dissect splicing abnormalities.[4,13,14,42,45]

Regarding the c.571+78G>A variant, the *in vitro* characterization demonstrated an aberrant splicing profile that was consistent with the FVII:C levels reported in patients. Interestingly, the amount of correctly spliced transcripts (approx. 3%) reflects the FVII:C levels (3% and <1%) in the two c.571+78A homozygotes (patients #15 and #90) (Table 1), which explains the asymptomatic or moderate clinical phenotypes. This finding is also consistent with the observation that the mutation co-segregated with the disease phenotype through the pedigree of patient #28, and the 50% FVII:C levels detected in the heterozygous mother.

It is interesting to note that the c.571+78G>A mutation, albeit absent from databases, occurred in eight apparently unrelated patients in our cohort. The polymorphic analysis in the homozygous patients led us to identify two different haplotypes that suggested two distinct mutational
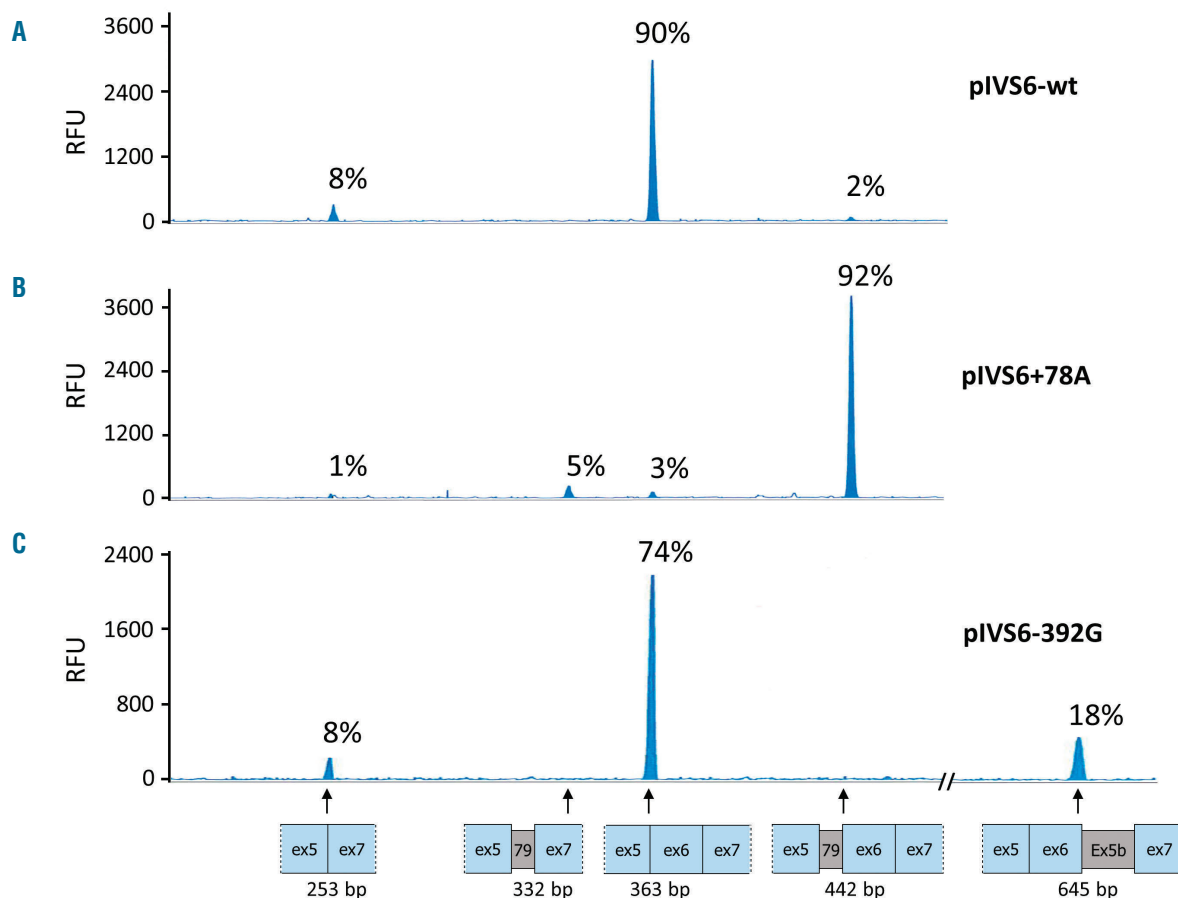
Figure 3. Alternative splicing patterns evaluated by denaturing capillary electrophoresis. Splicing patterns of the pIVS6-wt (A), pIVS6+78A (B) and pIVS6-392G (C) minigenes upon transient transfection in HEK293T cells and evaluated by polymerase chain reaction with T7bisF^Fam-F7ex7R oligonucleotides performed at 28 cycles followed by denaturing capillary electrophoresis. The schematic representation of transcripts (not in scale) is reported below and the amplicons base pairs (bp) are indicated at the bottom. The relative amount of transcripts is indicated by percentages. RFU: relative fluorescence units.

events leading to two subsequent founder effects. In particular, one haplotype was found in patients of Maghreb origin whereas the second one was compatible with genotypes of patients of European and Lebanese origins.

Concerning the c.572-392C>G change, the aberrant splicing profile displayed approximately 70% of correctly spliced transcripts, which is not apparently consistent with the FVII:C levels (10%) observed in homozygous patient #330. However, the mutation was associated with the less frequent A2 and M2 polymorphic alleles, which have been demonstrated to halve the FVII expression when present in the homozygous state.[33-37]

The c.571+78G>A and c.572-392C>G mutations were also found in patients with moderately reduced FVII levels (#28, #377, #284). In patients #377 and #284, this can be explained by the fact that: i) the mutations are present in heterozygous condition; and ii) by the additional contribution of the functional polymorphisms A2 and M2. For patient #28, heterozygous for the c.571+78G>A mutation, the residual expression could arise from the allele bearing the p.Arg59Trp change, which, however, has never been characterized.

In contrast to the c.571+78G>A and c.572-392C>G variants, the *in vitro* splicing analysis did not reveal detrimental

effects on splicing for the c.806-329G>A change. Therefore, we were unable to explain the genotype-phenotype relationship for three patients (#31, #262 and #341) who were not carriers of the c.571+78G>A or c.572-392C>G mutations. Since we have not identified other candidate pathogenic variants besides the mutations previously identified by conventional sequencing, it is tempting to speculate that the genetic defect could be in the unexplored highly repetitive rich GC region of intron 2 or in the 5' or 3' regulatory regions of the *F7* gene.

Knowledge of the alternative splicing patterns and of the mechanisms involved offers the opportunity to design correction strategies that could have therapeutic implications.[20-22] Here, we exploited variants of the U7 small nuclear RNA, the RNA component of the U7 small nuclear ribonucleoprotein that is biologically involved in histone RNA 3' end processing.[46] By changing the Sm consensus sequence of the endogenous U7snRNA, it is possible to express U7snRNA variants (U7smOPT) that no longer modulate histone processing, but can bind to RNA targets though base-pair interaction and efficiently accumulate into nucleus as snRNP.[41] Therefore, by changing the 5' tail of the U7smOPT, it is possible to target a desired RNA sequence and avoid its recognition by splic-
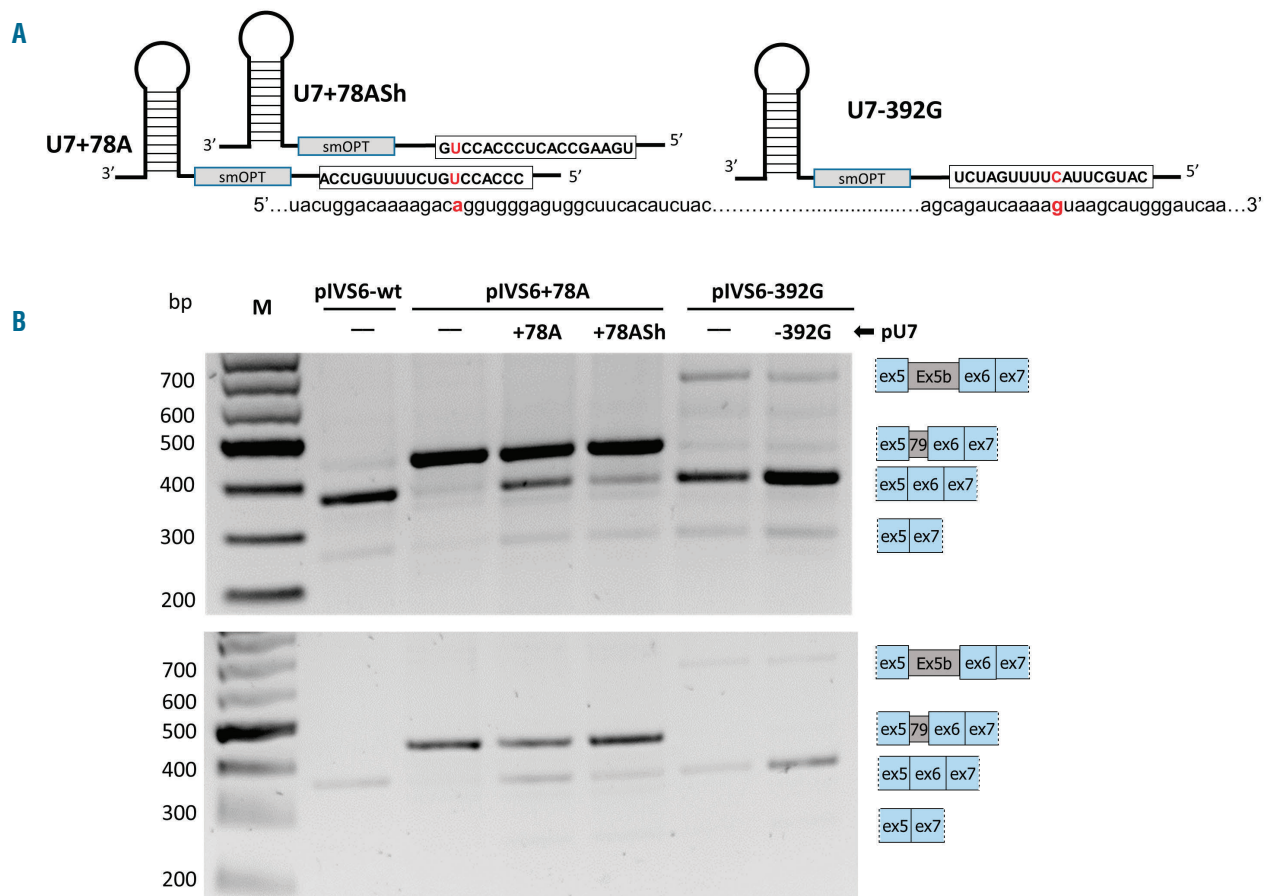
Figure 4. Investigation of aberrant splicing mechanisms by using antisense U7smOPT variants. (A) Schematic representation of engineered U7smOPT exploited in this study. The sequence of intronic mRNA and of the engineered 5'tail of U7smOPT with relative base-pairing is reported. The nucleotide changes identified by next-generation sequencing are indicated in bold and red, as well as the corresponding base in U7smOPT antisense sequence. (B) Splicing pattern analysis in HEK293T cells transiently transfected with pIVS6 wild type (wt) and variants (c.571+78A and c.572-392G) alone or in combination with engineered U7smOPT (pU7). PCR with T7bisF-F7ex7R oligonucleotides performed at 32 cycles (top) or, for semi-quantitative evaluation, at 25 cycles (bottom). M: 100 bp ladder.

ing factors. This opportunity has been exploited to induce both exon skipping for therapeutic purposes[47,48] and to dissect splicing regulatory elements by masking them.[20,22,49] In our study, the observation that antisense U7smOPT variants masking the cryptic 5'ss were able to rescue the splicing pattern further demonstrated the pathogenic role of the nucleotide changes and provided a correction approach that has potential therapeutic implications for the c.571+78A mutation. In fact, if translated into patients, the correct transcripts rescued for this mutation (a well-represented change in our patient cohort and associated with severe forms) would account for FVII levels well beyond the therapeutic threshold.

In conclusion, the combination of NGS of the entire F7 gene with the expression of minigenes elucidated the molecular bases of FVII deficiency in ten out of thirteen FVII deficient patients, thus improving diagnosis and genetic counselling, and provided insight into a potential therapeutic approach based on antisense technology, successfully exploited in other disorders.

References

1. Davie EW, Fujikawa K, Kisiel W. The coagulation cascade: initiation, maintenance, and regulation. Biochemistry. 1991; 30(43):10363-10370.

2. Bernardi F, Dolce A, Pinotti M, et al. Major differences in bleeding symptoms between factor VII deficiency and hemophilia B. J Thromb Haemost. 2009;7(5):774-779.

3. Pinotti M, Etro D, Bindini D, et al. Residual factor VII activity and different hemorrhagic phenotypes in CRM(+) factor VII deficiencies (Gly331Ser and Gly283Ser). Blood. 2002;99(4):1495-1497.

4. Cavallari N, Balestra D, Branchini A, et al. Activation of a cryptic splice site in a potentially lethal coagulation defect accounts for a functional protein variant. Biochim Biophys Acta - Mol Basis Dis. 2012;1822(7):1109-1113.

5. Branchini A, Ferrarese M, Lombardi S, Mari R, Bernardi F, Pinotti M. Differential functional readthrough over homozygous nonsense mutations contributes to the bleeding phenotype in coagulation factor VII deficiency. J Thromb Haemost. 2016;14(10):1994-2000.

6. McVey JH, Boswell E, Mumford AD, Kemball-Cook G, Tuddenham EG. Factor VII deficiency and the FVII mutation database. Hum Mutat. 2001;17(1):3-17.

7. Herrmann FH, Wulff K, Auerswald G, et al. Factor VII deficiency: clinical manifestation of 717 subjects from Europe and Latin America with mutations in the factor 7 gene. Haemophilia. 2009;15(1):267-280.

8. Millar DS, Kemball-Cook G, McVey JH, et al. Molecular analysis of the genotype-phenotype relationship in factor VII deficiency. Hum Genet. 2000;107(4):327-342.

9. Peyvandi F, Jenkins P V, Mannucci PM, et al. Molecular characterisation and three-dimensional structural analysis of mutations in 21 unrelated families with inherited factor VII deficiency. Thromb Haemost. 2000; 84(2):250-257.

10. Giansily-Blaizot M, Aguilar-Martinez P, Biron-Andreani C, Jeanjean P, Igual H, Schved JF. Analysis of the genotypes and phenotypes of 37 unrelated patients with inherited factor VII deficiency. Eur J Hum Genet. 2001;9(2):105-112.

11. Mota L, Shetty S, Idicula-Thomas S, Ghosh K. Phenotypic and genotypic characterization of Factor VII deficiency patients from Western India. Clin Chim Acta. 2009;409(1-2):106-111.

12. De Conti L, Baralle M, Buratti E. Exon and intron definition in pre-mRNA splicing. Wiley Interdiscip Rev RNA. 2013;4(1):49-60.

13. Pinotti M, Toso R, Redaelli R, Berrettini M, Marchetti G, Bernardi F. Molecular mechanisms of FVII deficiency: expression of mutations clustered in the IVS7 donor splice site of factor VII gene. Blood. 1998; 92(5):1646-1651.

14. Balestra D, Barbon E, Scalet D, et al. Regulation of a strong F9 cryptic 5'ss by intrinsic elements and by combination of tailored U1snRNAs with antisense oligonucleotides. Hum Mol Genet. 2015; 24(17):4809-4816.

15. Nuzzo F, Bulato C, Nielsen BI, et al. Characterization of an apparently synonymous F5 mutation causing aberrant splicing and factor V deficiency. Haemophilia. 2015; 21(2):241-248.

16. Donadon I, McVey JH, Garagiola I, et al. Clustered F8 missense mutations cause hemophilia A by combined alteration of splicing and protein biosynthesis and activity. Haematologica. 2018;103(2):344-350.

17. Scalet D, Sacchetto C, Bernardi F, Pinotti M, Van De Graaf SFJ, Balestra D. The somatic FAH C.1061C>A change counteracts the frequent FAH c.1062+5G>A mutation and permits U1snRNA-based splicing correction. J Hum Genet. 2018;63(5):683-686.

18. Castoldi E, Duckers C, Radu C, et al. Homozygous F5 deep-intronic splicing mutation resulting in severe factor V deficiency and undetectable thrombin generation in platelet-rich plasma. J Thromb Haemost. 2011;9(5):959-968.

19. Castaman G, Giacomelli SH, Mancuso ME, et al. Deep intronic variations may cause mild hemophilia A. J Thromb Haemost. 2011;9(8):1541-1548.

20. Nuzzo F, Radu C, Baralle M, et al. Antisense-based RNA therapy of factor V deficiency: In vitro and ex vivo rescue of a F5 deep-intronic splicing mutation. Blood. 2013; 122(23):3825-3831.

21. Goyenvalle A, Vulin A, Fougerousse F, et al. Rescue of dystrophic muscle through U7 snRNA-mediated exon skipping. Science. 2004;306(5702):1796-1799.

22. Meyer K, Marquis J, Trüb J, et al. Rescue of a severe mouse model for spinal muscular atrophy by U7 snRNA-mediated splicing modulation. Hum Mol Genet. 2009; 18(3):546-555.

23. Alanis EF, Pinotti M, Mas AD, et al. An exon-specific U1 small nuclear RNA (snRNA) strategy to correct splicing defects. Hum Mol Genet. 2012;21(11):2389-2398.

24. Balestra D, Scalet D, Pagani F, et al. An exon-specific U1snRNA induces a robust factor IX activity in mice expressing multiple human FIX splicing mutants. Mol Ther - Nucleic Acids. 2016;5(10):e370.

25. Scalet D, Balestra D, Rohban S, et al. Exploring splicing-switching molecules for Seckel syndrome therapy. Biochim Biophys Acta - Mol Basis Dis. 2017;1863(1):15-20.

26. Scalet D, Maestri I, Branchini A, Bernardi F, Pinotti M, Balestra D. Disease-causing variants of the conserved +2T of 5' splice sites can be rescued by engineered U1snRNAs. Hum Mutat. 2018;(October 2018):48-52.

27. Pezeshkpoor B, Zimmer N, Marquardt N, et al. Deep intronic "mutations" cause hemophilia A: Application of next generation sequencing in patients without detectable mutation in F8 cDNA. J Thromb Haemost. 2013;11(9):1679-1687.

28. Bastida JM, del Rey M, Lozano ML, et al. Design and application of a 23-gene panel by next-generation sequencing for inherited coagulation bleeding disorders. Haemophilia. 2016;22(4):590-597.

29. Simeoni I, Stephens JC, Hu F, et al. A high-throughput sequencing test for diagnosing inherited bleeding, thrombotic, and platelet disorders. Blood. 2016;127(23):2791-2803.

30. Matsushita T, Kojima T, Emi N, Takahashi I, Saito H. Impaired human tissue factor-mediated activity in blood clotting factor VIINagoya (Arg304-->Trp). Evidence that a region in the catalytic domain of factor VII is important for the association with tissue factor. J Biol Chem. 1994;269(10):7355-7363.

31. Kavlie A, Orning L, Grindflek A, Stormorken H, Prydz H. Characterization of a factor VII molecule carrying a mutation in the second epidermal growth factor-like domain. Thromb Haemost. 1998;79(6):1136-1143.

32. Arbini AA, Mannucci M, Bauer KA. A Thr359Met mutation in factor VII of a patient with a hereditary deficiency causes defective secretion of the molecule. Blood. 1996;87(12):5085-5094.

33. Bernardi F, Marchetti G, Pinotti M, et al.

Factor VII gene polymorphisms contribute about one third of the factor VII level variation in plasma. Arterioscler Thromb Vasc Biol. 1996;16(1):72-76.

34. Girelli D, Russo C, Ferraresi P, et al. Polymorphisms in the factor VII gene and the risk of myocardial infarction in patients with coronary artery disease. N Engl J Med. 2000;343(11):774-780.

35. Kudaravalli R, Tidd T, Pinotti M, et al. Polymorphic changes in the 5??? flanking region of Factor VII have a combined effect on promoter strength. Thromb Haemost. 2002;88(5):763-767.

36. Bozzini C, Girelli D, Bernardi F, et al. Influence of polymorphisms in the factor VII gene promoter on activated factor VII levels and on the risk of myocardial infarction in advanced coronary atherosclerosis. Thromb Haemost. 2004;92(3):541-549.

37. Sabater-Lleal M, Chillón M, Howard TE, et al. Functional analysis of the genetic variability in the F7 gene promoter. Atherosclerosis. 2007;195(2):262-268.

38. Giansily-Blaizot M, Verdier R, Biron-Adréani C, et al. Analysis of biological phenotypes from 42 patients with inherited fac-tor VII deficiency: Can biological tests predict the bleeding risk? Haematologica. 2004;89(6):704-709.

39. Giansily-Blaizot M, Thorel D, Khau Van Kien P, et al. Characterisation of a large complex intragenic re-arrangement in the FVII gene (F7) avoiding misdiagnosis in inherited factor VII deficiency. Br J Haematol. 2007; 138(3):359-365.

40. Ferrarese M, Testa MF, Balestra D, Bernardi F, Pinotti M, Branchini A. Secretion of wild-type factor IX upon readthrough over F9 pre-peptide nonsense mutations causing hemophilia B. Hum Mutat. 2018;39(5):702–708.

41. Meyer K, Schümperli D. Antisense Derivatives of U7 Small Nuclear RNA as Modulators of Pre-mRNA Splicing. In: Alternative Pre–mRNA Splicing. Wiley-Blackwell; 2012:481-494.

42. Pinotti M, Rizzotto L, Balestra D, et al. U1-snRNA-mediated rescue of mRNA processing in severe factor VII deficiency. Blood. 2008;111(5):2681-2684.

43. Yeo GW, Van Nostrand EL, Liang TY. Discovery and analysis of evolutionarily conserved intronic splicing regulatory ele-ments. PLoS Genet. 2007;3(5):e85.

44. Majewski J, Ott J. Distribution and characterization of regulatory elements in the human genome. Genome Res. 2002; 12(12):1827-1836.

45. Pinotti M, Toso R, Girelli D, et al. Modulation of factor VII levels by intron 7 polymorphisms: population and in vitro studies. Blood. 2000;95(11):3423-3428.

46. Dominski Z, Marzluff WF. Formation of the 3' end of histone mRNA. Gene. 1999; 239(1):1-14.

47. Brun C, Suter D, Pauli C, et al. U7 snRNAs induce correction of mutated dystrophin pre-mRNA by exon skipping. Cell Mol Life Sci. 2003;60(3):557-566.

48. Suter D, Tomasini R, Reber U, Gorman L, Kole R, Schümperli D. Double-target antisense U7 snRNAs promote efficient skipping of an aberrant exon in three human β-thalassemic mutations. Hum Mol Genet. 1999;8(13):2415-2423.

49. Gorman L, Suter D, Emerick V, Schümperli D, Kole R. Stable alteration of pre-mRNA splicing patterns by modified U7 small nuclear RNAs. Proc Natl Acad Sci U S A. 1998;95(9):4929-4934.

Updated meta-analysis on prevention of venous thromboembolism in ambulatory cancer patients

Cecilia Becattini,[1] Melina Verso,[1] Andres Muñoz[2] and Giancarlo Agnelli[1]

[1]Internal and Cardiovascular Medicine – Stroke Unit, University of Perugia, Perugia, Italy and [2]Hospital General Universitario Gregorio Marañón, Madrid, Spain

ABSTRACT

Randomized clinical trials have evaluated the role of anticoagulants in the prevention of venous thromboembolism (VTE) in ambulatory cancer patients treated with chemotherapy. This meta-analysis is aimed at providing an updated evaluation of the efficacy and safety of anticoagulant prophylaxis in this clinical setting. Medline and Scopus were searched to retrieve randomized controlled trials on the prevention of VTE in ambulatory cancer patients. Two groups of trials were identified with VTE or death as the primary outcome, respectively. VTE was the primary outcome of this analysis. Anticoagulant prophylaxis reduced the incidence of VTE in studies in which the primary outcome was VTE [14 studies, 8,226 patients; odds ratio (OR)=0.45; 95% confidence interval (95% CI): 0.36-0.56] or death (8 studies, 3,727 patients; OR=0.61; 95% CI: 0.47-0.81). When these studies were pooled together, VTE was reduced by 49% (95% CI: 0.43-0.61) with no significant increase in major bleeding (OR=1.30, 95% CI: 0.98-1.73). The risk of major bleeding was increased in studies with VTE as the primary outcome (OR=1.43, 95% CI: 1.01-2.04). Similar reductions of VTE were observed in studies with parenteral (OR=0.43, 95% CI: 0.33-0.56) or oral anticoagulants (OR=0.49, 95% CI: 0.33-0.74). The reduction in VTE was confirmed in patients with lung (OR=0.42, 95% CI: 0.26-0.67) or pancreatic cancer (OR=0.26, 95% CI: 0.14-0.48), in estimated high-risk patients, in high-quality studies and with respect to symptomatic VTE. In conclusion, prophylaxis with oral or parenteral anticoagulants reduces the risk of VTE in ambulatory cancer patients, with an acceptable increase in major bleeding.

Introduction

The risk of venous thromboembolism (VTE) is four to seven times higher in patients with cancer than in individuals without this disease.[1,2] The high incidence of cancer-associated thrombosis is probably related to a combination of the intrinsic prothrombotic activity of cancer cells, aggressive chemotherapy treatment, aging of cancer patients, and enhanced VTE detection owing to improvements in imaging technology and frequency of imaging.[3-5] Anti-cancer therapies, either traditional chemotherapy, hormones or biological agents, can potentially increase the risk of VTE up to an annual rate of 15%, depending on the type and combination of agents, or the addition of radiotherapy.[6] Survival of cancer patients has been significantly improved in recent times and this increases the time of risk exposure for VTE in cancer patients.

Based on these epidemiological data, several studies have been conducted aimed at assessing the role of anticoagulants in preventing VTE in ambulatory cancer patients treated with chemotherapy. These studies showed that prophylaxis with anticoagulants reduced the risk of VTE by about 50%, with no significant increase in the risk of major bleeding.[7] However, the use of prophylaxis remains controversial because of concerns over the relatively low incidence of VTE in these patients, the risk-to-benefit ratio, the cost and the inconvenience of prolonged parenteral therapy. As a consequence, antithrombotic prophylaxis is still not recom-

mended in ambulatory cancer patients treated with chemotherapy.[8,9] On this background, the current availability of oral anticoagulants that can be used with no laboratory monitoring reopens the issue of practicality of antithrombotic prophylaxis in ambulatory cancer patients.[10-12] Three clinical trials on the use of new oral anticoagulants for this indication have recently been published.

We performed a meta-analysis of randomized studies to assess the clinical benefit of antithrombotic prophylaxis in ambulatory cancer patients receiving chemotherapy.

Methods

The methods for this meta-analysis are in accordance with "Preferred Reporting Items for Systematic Reviews and Meta-Analyses (PRISMA)" (*http://www.prisma-statement.org/*).[13]

Study objectives and outcomes

The primary objective of this meta-analysis of randomized controlled studies was to assess the efficacy of anticoagulant prophylaxis in preventing VTE in ambulatory cancer patients treated with chemotherapy. The secondary objective was to assess the safety of anticoagulant prophylaxis in these patients.

The primary outcome of the study was objectively confirmed VTE, defined as the composite of pulmonary embolism and/or deep vein thrombosis adjudicated according to the criteria and procedures of the individual studies. The secondary outcome was major bleeding defined according to the criteria of the individual studies. Ancillary outcomes were symptomatic VTE and fatal VTE.

Search strategy and study inclusion criteria

We performed unrestricted searches in MEDLINE and Scopus using the terms "cancer AND venous thromboembolism AND prevention" and "cancer AND venous thromboembolism AND prophylaxis". Studies were independently selected by two authors (CB and MV) using predetermined criteria (detialed in the *Online Supplementary Data*).

Randomized controlled trials on the prevention of VTE in ambulatory cancer patients treated with chemotherapy were included in this meta-analysis and results pooled into two groups: (i) studies with VTE as the primary endpoint; and (ii) studies with death as the primary endpoint.

The kappa statistic was used to assess the agreement between reviewers regarding the studies selected.[14]

Statistical analysis

We determined pooled incidences of study outcomes in patients randomized to anticoagulant prophylaxis or no prophylaxis and the pooled odds ratios (OR) with 95% confidence intervals (95% CI). We planned cumulative and separate analyses for studies with VTE or mortality as the primary outcome.

Sensitivity analyses were performed concerning (i) parenteral or oral anticoagulants; (ii) symptomatic VTE; (iii) fatal VTE; (iv) subgroups of patients based on the primary cancer site (lung, pancreas and breast); (v) patients considered as being at high-risk of VTE; and (vi) high-quality studies.

Study quality was evaluated using the Jadad score and the Cochrane risk assessment tool.[15]

Data were pooled by the Mantel-Haenszel method;[16] results are reported according to a fixed-effects model in the absence of significant heterogeneity and to a random-effects model in the presence of significant heterogeneity.[17,18] The Cochran χ^2 test and

the I^2 test for heterogeneity were used to assess between-study heterogeneity.[16,17] Significant heterogeneity was considered present at $P<0.10$ and $I^2>50\%$.[18]

Correction for zero cells was performed. Publication bias was assessed visually by the use of funnel plots.

Statistical analyses were conducted using Review Manager release 5.3 (The Cochrane Collaboration, Oxford, England) and StatsDirect 3.0.

Results

Overall, 22 papers were found reporting on 23 studies fulfilling the inclusion criteria (flow diagram in *Online Supplementary Figure S1*).[11-12,19-38] After discussion among the authors, a randomized double-blind phase II study with apixaban compared to placebo was included in the analysis despite the main outcome being major bleeding.[10] The reasons for inclusion were high-quality, appropriate study population and the potential to increase the power of the meta-analysis with respect to the efficacy and safety of oral anticoagulants. The main features of included studies are reported in Tables 1 and 2. The primary outcome was VTE in 16 studies and death in eight. The agreement between reviewers regarding study selection was good (kappa statistic: 0.88).

Among the 15 studies with VTE as the primary outcome, eight were double-blind studies with placebo as the comparator.[10-12,19,21-22,24-25] In five studies the comparator was no treatment and in one it was aspirin. One paper was composed of two 'twin-studies', one including patients with breast cancer and the other including patients with lung cancer. With regards to the study populations, these were limited to patients with a single primary site of cancer in eight studies (breast and pancreas in two studies each,[19,24,26-27] acute lymphatic leukemia,[20] multiple myeloma,[23] glioma[22] and lung[24] cancer in one study each) while multiple cancers were included in seven studies. In three studies patients were eligible in the case of an estimated increased risk for VTE assessed by the Khorana score.[11-12,29] The number of study patients varied from a minimum of 34 to a maximum of 3,212. Asymptomatic or incidental VTE accounted for a study outcome event in nine studies.[11-12,24-26,29] All but one of the studies were conducted in adult patients. A systematic assessment of thrombosis by screening tests was scheduled in three studies[12,20,29] and was aimed at the diagnosis of lower limb deep vein thrombosis in two studies and to assess upper-body and cerebral vein thrombosis in one study (Table 1).

Among the studies with death as the primary outcome,[30-38] two were double-blind studies with placebo as the comparator. In seven studies the comparator was no treatment. Patients were eligible in the case of a diagnosis of advanced cancer in four studies.[31,33-34,36] No systematic assessment of thrombosis was scheduled (Table 1).

According to the Jadad scale, nine studies[10-12,19,21-22,24-25] were classified as good quality (*Onlne Supplementary Table S1*).

Efficacy of anticoagulant prophylaxis

In the 14 studies with VTE as the primary outcome and data available for the efficacy analysis (8,226 patients), the pooled incidence of symptomatic or asymptomatic (incidental) VTE was 2% in patients randomized to anticoagulant prophylaxis (95% CI: 2-3; $I^2=85\%$) and 6% in

patients not randomized to anticoagulant prophylaxis (95% CI: 5-7; I²=91%). In these studies, anticoagulant prophylaxis reduced the incidence of VTE (OR=0.45, 95% CI: 0.36-0.56; I²=5%) (Figure 1).

Among studies with VTE as the primary outcome, pro-phylaxis with parenteral anticoagulants (11 studies, 6,700 patients; OR=0.43, 95% CI: 0.33-0.56; I²=0%) and oral agents (3 studies, 1,526 patients; OR=0.49, 95% CI: 0.33-0.74; I²=57%) was associated with the same magnitude of reduction of VTE risk. However, significant heterogeneity

A

Study or Subgroup	Experimental Events	Total	Control Events	Total	Weight	Odds Ratio M-H, Fixed, 95% CI
1.1.1 VTE primary outcome						
Agnelli 2009	11	769	11	381	4.0%	0.49 [0.21, 1.14]
Agnelli 2012	20	1608	55	1604	14.8%	0.35 [0.21, 0.59]
Carrier 2019	12	288	28	275	7.5%	0.38 [0.19, 0.77]
Haas 2012 Topic-2	12	268	22	264	5.8%	0.52 [0.25, 1.06]
Haas 2012 TOPIC-I	7	174	7	177	1.8%	1.02 [0.35, 2.97]
Khorana 2017	6	50	10	48	2.5%	0.52 [0.17, 1.56]
Khorana 2019	25	420	37	421	9.5%	0.66 [0.39, 1.11]
Larocca 2011	2	166	4	176	1.0%	0.52 [0.09, 2.90]
Levine 1994	1	152	7	159	1.9%	0.14 [0.02, 1.18]
Levine 2012	1	93	4	29	1.6%	0.07 [0.01, 0.64]
Maraveyas 2012	7	59	17	62	4.0%	0.36 [0.14, 0.94]
Mitchell 2003	7	25	22	60	2.5%	0.67 [0.24, 1.86]
Pelzer 2015	2	160	15	152	4.1%	0.12 [0.03, 0.51]
Perry 2010	9	99	13	87	3.4%	0.57 [0.23, 1.41]
Subtotal (95% CI)		4331		3895	64.5%	0.45 [0.36, 0.56]
Total events	122		252			

Heterogeneity: Chi² = 13.66, df = 13 (P = 0.40); I² = 5%
Test for overall effect: Z = 6.96 (P < 0.00001)

Study or Subgroup	Experimental Events	Total	Control Events	Total	Weight	Odds Ratio M-H, Fixed, 95% CI
1.1.2 death primary outcome						
Altinbas 2004	0	42	1	42	0.4%	0.33 [0.01, 8.22]
Elit 2012	0	77	0	9		Not estimable
Kakkar 2004	4	190	5	184	1.4%	0.77 [0.20, 2.91]
Klerk 2005	2	148	3	154	0.8%	0.69 [0.11, 4.19]
Lecumberri 2013	0	20	1	18	0.4%	0.28 [0.01, 7.44]
Macbeth 2015	61	1101	107	1101	27.6%	0.54 [0.39, 0.76]
Sideras 2006	4	68	5	70	1.3%	0.81 [0.21, 3.16]
van Doormaal 2011	16	244	15	259	3.7%	1.14 [0.55, 2.36]
Subtotal (95% CI)		1890		1837	35.5%	0.62 [0.47, 0.82]
Total events	87		137			

Heterogeneity: Chi² = 3.94, df = 6 (P = 0.68); I² = 0%
Test for overall effect: Z = 3.36 (P = 0.0008)

Total (95% CI)		6221		5732	100.0%	0.51 [0.43, 0.61]
Total events	209		389			

Heterogeneity: Chi² = 20.21, df = 20 (P = 0.44); I² = 1%
Test for overall effect: Z = 7.56 (P < 0.00001)
Test for subgroup differences: Chi² = 3.27, df = 1 (P = 0.07), I² = 69.5%

B

Study or Subgroup	Experimental Events	Total	Control Events	Total	Weight	Odds Ratio M-H, Fixed, 95% CI
1.1.1 parenteral*						
Agnelli 2009	11	769	11	381	6.1%	0.49 [0.21, 1.14]
Agnelli 2012	20	1608	55	1604	23.0%	0.35 [0.21, 0.59]
Haas 2012 Topic-2	12	268	22	264	9.0%	0.52 [0.25, 1.06]
Haas 2012 TOPIC-I	7	174	7	177	2.8%	1.02 [0.35, 2.97]
Khorana 2017	6	50	10	48	3.8%	0.52 [0.17, 1.56]
Larocca 2011	2	166	4	176	1.6%	0.52 [0.09, 2.90]
Levine 1994	1	152	7	159	2.9%	0.14 [0.02, 1.18]
Maraveyas 2012	7	59	17	62	6.2%	0.36 [0.14, 0.94]
Mitchell 2003	7	25	22	60	3.9%	0.67 [0.24, 1.86]
Pelzer 2015	2	160	15	152	6.4%	0.12 [0.03, 0.51]
Perry 2010	9	99	13	87	5.3%	0.57 [0.23, 1.41]
Subtotal (95% CI)		3530		3170	71.1%	0.43 [0.33, 0.56]
Total events	84		183			

Heterogeneity: Chi² = 8.79, df = 10 (P = 0.55); I² = 0%
Test for overall effect: Z = 6.10 (P < 0.00001)

Study or Subgroup	Experimental Events	Total	Control Events	Total	Weight	Odds Ratio M-H, Fixed, 95% CI
1.1.2 oral						
Carrier 2019	12	288	28	275	11.6%	0.38 [0.19, 0.77]
Khorana 2019	25	420	37	421	14.7%	0.66 [0.39, 1.11]
Levine 2012	1	93	4	29	2.6%	0.07 [0.01, 0.64]
Subtotal (95% CI)		801		725	28.9%	0.49 [0.33, 0.74]
Total events	38		69			

Heterogeneity: Chi² = 4.65, df = 2 (P = 0.10); I² = 57%
Test for overall effect: Z = 3.39 (P = 0.0007)

Total (95% CI)		4331		3895	100.0%	0.45 [0.36, 0.56]
Total events	122		252			

Heterogeneity: Chi² = 13.66, df = 13 (P = 0.40); I² = 5%
Test for overall effect: Z = 6.96 (P < 0.00001)
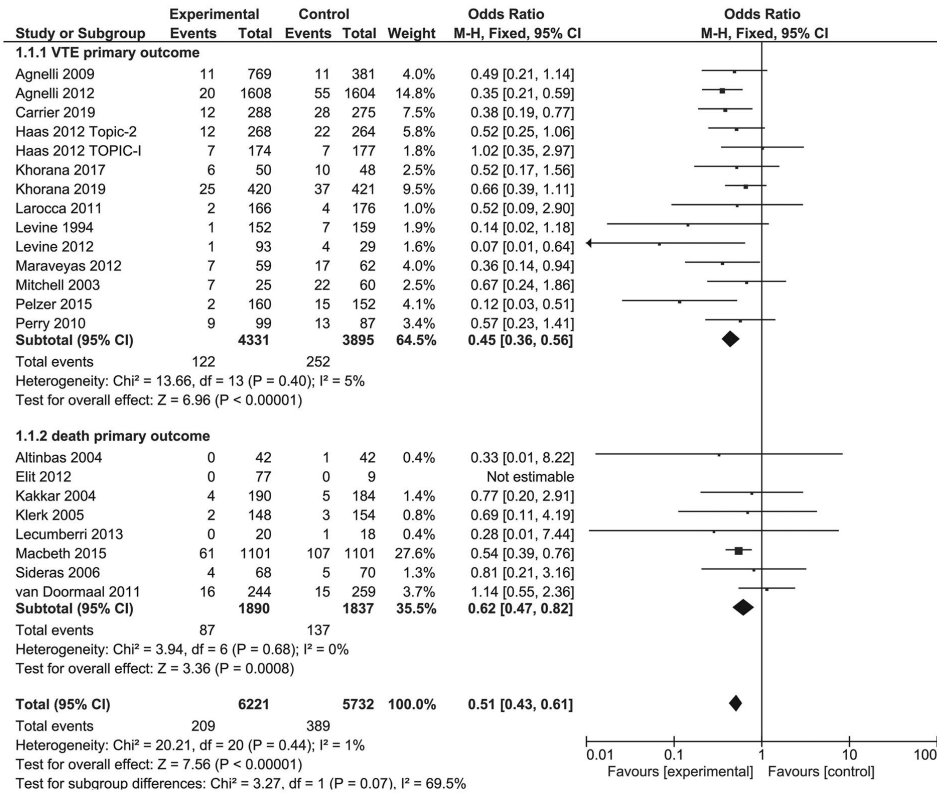Test for subgroup differences: Chi² = 0.33, df = 1 (P = 0.57), I² = 0%

Figure 1. Efficacy of anticoagulant prophylaxis for the prevention of venous thromboembolism in ambulatory cancer patients receiving chemotherapy. (A) Analysis of studies having venous thromboembolism or death as the primary outcome. (B) Analysis of studies with parenteral or oral anti-coagulants. *Warfarin was used for prophyaxis in one study.[19]
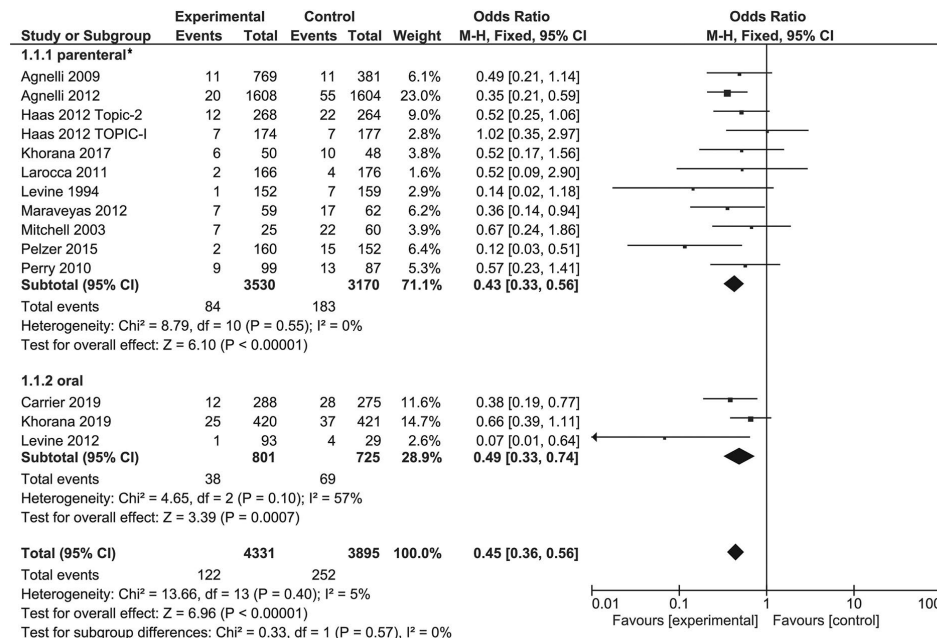
Table 1. Main features of randomized studies on the role of anticoagulants in ambulatory cancer patients receiving chemotherapy with VTE as primary outcome.

Author, year	D-B patients	N. of patients	Eligible cancers	Main inclusion criteria	Study treatments	Primary outcome of prophylaxis	Duration
Levine, 1994[19]	Yes	311	Metastatic breast carcinoma	First-line or second-line CHT for 4 weeks or less	Warfarin (INR 1.3-1.9) vs. Placebo	DVT or PE and arterial thrombosis (myocardial infarction, stroke, or peripheral-artery thrombosis)	6 weeks
Mitchell, 2003[20]	No	85	Newly diagnosed acute lymphoblastic leukemia	Age >6 months and <18 years, at the beginning of the induction CHT, a functioning CVL placed <2 weeks of initiating induction CHT	Antithrombin (plasma levels 3.0 - 4.0 U/mL) vs. No antithrombin	Clinically symptomatic or asymptomatic TE in any location. TE categorized as not clinically significant or clinically significant	4 weeks
Agnelli, 2009[21]	Yes	1150	Metastatic or locally advanced lung, GI, pancreatic, breast, ovarian, or head and neck cancer	Receiving CHT, age> 18 years	Nadroparin (3800 IU o.d.) vs. Placebo	Composite of symptomatic venous or arterial TE	For the duration of CHT (maximum 120 ±10 days)
Perry, 2010[22]	Yes	186	Newly diagnosed, pathologically confirmed WHO grade 3 or grade 4 glioma	Age >18 years	Dalteparin (5000 IU o.d.) vs. Placebo	Symptomatic DVT or PE	6 months
Larocca, 2011[23]	No	342	Newly diagnosed multiple myeloma	Previously untreated patients; age >18 and <65 years	Enoxaparin (40 mg o.d.) vs. ASA (100 mg o.d.)	First objectively confirmed symptomatic DVT, PE, arterial thrombosis, any acute cardiovascular event or sudden, otherwise unexplained death	During the 4 cycles of Rd therapy and the 6 cycles of MPR consolidation
Haas, TOPIC-1 2012[24]	Yes	351	Objectively proven, disseminated metastatic breast carcinoma	Adult patients receiving first- or second-line CHT	Certoparin (3000 IU o.d.) vs. Placebo	First objectively confirmed symptomatic or asymptomatic DVT, symptomatic PE, thrombosis of the jugular or subclavian veins; and superficial thrombophlebitis	6 months
Haas, TOPIC-2 2012[24]	Yes	532	Objectively proven, stage III or IV, non-small cell lung carcinoma	Adult patients receiving first- or second-line CHT	Certoparin (3000 IU o.d.) vs. Placebo	First objectively confirmed symptomatic or asymptomatic DVT, symptomatic PE, thrombosis of the jugular or subclavian veins; and superficial thrombophlebitis	6 months
Agnelli, 2012[25]	Yes	3212	Metastatic or locally advanced cancer of the lung, pancreas, stomach, colon or rectum, bladder, and ovary	Patients >18 years of age and planned to receive a course of CHT	Semuloparin (20 mg o.d.) vs. Placebo	Any symptomatic DVT in lower or upper limbs, any non-fatal PE, or death related to VTE (fatal PE or unexplained death)	3 months, then discontinued when CHT was stopped or regimen changed
Maraveyas, 2012[26]	No	121	Non-resectable, recurrent or metastatic pancreatic adenocarcinoma (histological or cytological diagnosis)	Age >18 years, life expectancy >12 weeks, KPS of 60%; evaluable disease in baseline CT, adequate hematologic function, and bilirubin <1.5 UNL	Dalteparin (200 IU/Kg o.d. for 4 weeks then 150 IU/Kg) vs. No prophylaxis	All types of DVT/PE, all arterial events and all visceral TE	12 weeks
Levine, 2012[10]	Yes	122	Advanced or metastatic lung, breast, colon, rectum, pancreas, stomach, bladder, cancer of unknown origin, ovarian or prostate cancer, myeloma or selected lymphomas	Receiving first-line or second-line CHT; able to begin study medication within 6 weeks of starting CHT; expected course of CHT >90 days; age > 18 years.	Apixaban (5mg, 10 mg or 20 mg o.d.) vs. Placebo	Major bleeding event or a clinically relevant non-major bleeding event	12 weeks
Pelzer, 2015[27]	No	312	Histologically confirmed advanced pancreatic cancer	No previous RT or CHT, KPS of 60%, measurable tumor lesion confirmed by CT or MR <14 days, age >18 years	Enoxaparin (40 mg o.d.) vs. No prophylaxis	First symptomatic VTE	Until disease progression *
Zwicker, 2015[28]	No	34	Adenocarcinoma of pancreas (locally advanced or metastatic), or stomach (unresectable or metastatic), colorectal stage IV, non-small cell lung cancer stage III or IV, relapsed or stage IV ovarian	Histologically confirmed malignancy with no curative therapies, <4 weeks of first or second line CHT, life expectancy >6 months, ECOG ≤ 2; neutrophil count ≥1.0×10^8, platelet count ≥100×10^9/L	Enoxaparin (40 mg o.d.) vs. No enoxaparin	Symptomatic or proximal VTE, based on levels of tissue factor-bearing microparticles	60-day

Author, year	D-B	N. of patients	Eligible cancers	Main inclusion criteria	Study treatments	Primary outcome	Duration of prophylaxis
Khorana, 2017[29]	No	98	Lung, stomach, pancreas, lymphoma, gynecological, genitourinary (excluding prostate)	Histological diagnosis of malignancy, planned initiation of a new systemic CHT regimen (either initial or after progression on CHT), age ≥18 years	Dalteparin (5000 IU o.d.) *vs.* No dalteparin	Symptomatic lower extremity DVT, PE and upper extremity thrombosis, unsuspected DVT and PE detected by lower extremity ultrasonography and CT	12 weeks
Khorana, 2019*[11]	Yes	809	Solid tumor or lymphoma	Age >18 years, Khorana score >2, expected survival >6 months, plan to start a new systemic regimen within 1 week	Rivaroxaban (10 mg o.d.) *vs.* Placebo	Objectively confirmed symptomatic or asymptomatic lower-extremity proximal DVT, symptomatic upper-extremity or distal lower-extremity DVT, symptomatic or incidental PE and VTE–related death	180 (± 3) days
Carrier, 2019[12]	Yes	563	Newly diagnosed cancer or progression of known cancer after complete or partial remission	Initiating a new course of CHT with a minimum treatment intent of 3 months, Khorana score >2, age >18 years	Apixaban (2.5 mg t.d.) *vs.* Placebo	First objectively documented symptomatic or incidentally detected proximal DVT of the lower or upper limbs, any nonfatal symptomatic or incidental PE, and PE–related death	180 days

Enrolled patients underwent bilateral lower-extremity venous duplex compression ultrasonography to exclude pre-existing proximal deep-vein thrombosis based on prior studies in high-risk patients demonstrating a high rate of baseline thrombosis for which prophylactic anticoagulation would be inadequate. CHT: chemotherapy; INR: International Normalized Ratio; DVT: deep vein thrombosis; PE: pulmonary embolism; CVL: central venous line; TE: thromboembolism; GI: gastrointestinal; IU: international units; o.d.: once daily; WHO: World Health Organization; ASA: acetylsalicylic acid; Rd: induction with lenalidomide plus low-dose dexamethasone; MPR: melphalan–prednisone-lenalidomide; VTE: venous thromboembolism; KPS: Karnofsky performance status scale; CT: computed tomography; UNL: upper normal limit; RT: radiotherapy; MR: magnetic resonance; ECOG= Eastern Cooperative Oncology Group; t.d.: twice daily..

was found in the analysis of studies with oral agents, which disappeared after the removal of a dose-ranging study from the analysis.

Anticoagulant prophylaxis reduced symptomatic VTE (OR=0.48, 95% CI: 0.39-0.60) but not fatal VTE (OR=0.52, 95% CI: 0.25-1.08) in studies with VTE as the primary outcome (Table 3; Figure 2).

In the eight studies with death as the primary endpoint, prophylaxis was associated with a reduction of VTE (8 studies, 3,727 patients; OR=0.61, 95% CI: 0.47-0.81; I²=0%)

When all studies were pooled in a single analysis, anticoagulant prophylaxis was confirmed to reduce the incidence of VTE (22 studies, 11,953 patients; OR=0.51, 95% CI: 0.43-0.61; I²=2.4%) (Figure 1) and of symptomatic VTE (17 studies, 10,374 patients; OR=0.49, 95% CI: 0.39-0.61; I²= 0%) with no heterogeneity (Figure 2).

The reduction in the incidence of VTE with the use of anticoagulant prophylaxis was confirmed in patients with lung cancer (3 studies, 1,991 patients; OR=0.42, 95% CI: 0.26-0.67; I²=0%), pancreatic cancer (4 studies, 740 patients; OR=0.26; 95% CI: 0.14-0.48; I²=21%), in patients at estimated high risk according to the Khorana score (5 studies, 2,167 patients; OR=0.48; 95% CI: 0.34-0.68; I²=0%) and in high-quality studies (OR=0.47, 95% CI: 0.36-0.60), all from studies with VTE as the primary outcome (Table 3, Figure 3).

No evidence of publication bias was found in individual comparisons at visual inspection of funnel plots.

Safety of anticoagulant prophylaxis

For the analysis of safety, the results from studies with VTE or death as the primary outcome were pooled in a single analysis. Overall, 24 studies reported on the incidence of major bleeding in patients randomized to anticoagulant prophylaxis or no prophylaxis. The pooled inci-

dence of major bleeding was 2% in patients randomized to prophylaxis or to no prophylaxis, with significant heterogeneity (95% CI: 0.17-0.31; I²>50%). Heterogeneity persisted after removal of outlier studies and disappeared when the analysis was limited to high-quality studies.

Anticoagulant prophylaxis was not associated with an increase in the risk of major bleeding (24 studies, 12,014 patients; OR=1.30, 95% CI: 0.98-1.73; I²=0%) (Figure 4). Similar results were obtained in studies with parenteral anticoagulants (21 studies, 10,713 patients; OR=1.27, 95% CI: 0.93-1.73; I2=0%) or oral anticoagulants (3 studies, 1,494 patients; OR=1.78, 95% CI: 0.83-3.83; I²=0%).

When the analysis was limited to high-quality studies or those with VTE as the primary outcome, the use of anticoagulant prophylaxis was associated with a marginally significant increase in major bleeding (Table 3).

Discussion

This meta-analysis in ambulatory cancer patients treated with chemotherapy shows that anticoagulant prophylaxis, with either oral or parenteral agents, is associated with a 50% reduction in the incidence of VTE and no significant increase in major bleeding. The efficacy of prophylaxis in reducing VTE was consistent in studies with VTE or death as the primary outcome and in all sensitivity analyses.

Anticoagulant prophylaxis is currently used to prevent VTE in patients undergoing major cancer surgery as well as in cancer patients admitted to hospital for an acute illness.[40] Despite the results of individual studies and previous meta-analyses, antithrombotic prophylaxis remained controversial and is still not recommended in ambulatory cancer patients treated with chemotherapy.[8,9] The main concerns regarding the use of antithrombotic prophylaxis

Table 2. Main features of randomized studies on the role of anticoagulants in ambulatory cancer patients receiving chemotherapy with death as the primary outcome.

Author, year	D-B	N. of patients	Main inclusion criteria	Experimental	Duration of follow-up	Duration of prophylaxis	Definition of major bleeding	Study completed
Labeau, 1994[30]	No	277	SCLC	Heparin calcium (initially 500 IU/kg/day then adjusted by clotting times 2-3 times normal value) t.d. (70 patients) or t.i.d. (62 patients) times daily *vs.* No heparin	from randomization to the sixth course of CHT	5 weeks (with 1week stop after the second course of CHT)	Not reported	Yes
Kakkar, 2004[31]	Yes	374	Advanced stage III or IV (locally advanced or metastatic) cancer* of the breast, lung, gastrointestinal tract, pancreas, liver, genitourinary tract, ovary, or uterus; age between 18 and 80 years.	Dalteparin (5,000 IU o.d.) *vs.* Placebo	1 year	1 year or until death	According to standard criteria[39]	Yes
Altinbas, 2004[32]	No	84	SCLC* , ECOG PS < 3; age between 18 and 75 years.	Dalteparin, (5,000 IU o.d.) *vs.* No dalteparin	1 year	18 weeks	Not specified	Yes
Klerk, 2005[33]	Yes	302	Adult patients with metastatic or locally advanced solid tumors*	Nadroparin (BW adjusted**, t.d. during the initial 14 days and o.d. thereafter for another 4 weeks) vs Placebo.	6 weeks	6 weeks	Clinically overt associated with hemoglobin decrease >2 g/dL, requiring >2 transfusion, or retroperitoneal or intracranial.	Yes
Sideras, 2006[34]	Yes	138	Advanced breast cancer failed first-line chemotherapy, advanced prostate cancer failed primary hormonal therapy, advanced lung cancer, or advanced colorectal. ECOG PS <2, life expectancy >12 weeks, age >18 years	Dalteparin (5,000IU o.d.) *vs.* Placebo	13 months	2 years	Not specified	Stopped after first interim analysis
van Doormaal, 2011[35]	No	503	Prostate cancer* <6 m after diagnosis of hormone-refractory state, NSCLC* without clinically significant pleural effusion <3 m after diagnosis of stage IIIB, or locally advanced pancreatic cancer* <3 m after diagnosis	Nadroparin (BW-adjusted therapeutic dose for 2 weeks, and 4 weeks at half therapeutic dose) *vs.* No nadroparin	46 weeks	46 weeks	Overt with hemoglobin decrease >2 g/dL or transfusion >2 units.	Yes
Elit, 2012[36]	No	86	FIGO stage IIB to IV epithelial ovarian cancer*, primary peritoneal or Fallopiantube cancer*; age between 18 and 75 years	Dalteparin (50 IU/kg, 100 IU/kg, or 150 IU/kg) *vs.* No dalteparin	Six 21-day cycles	Within 7 days prior to the cycle 1 of CHT to day 21 of cycle 3	Not specified	Premature interruption slow recruitment
Lecumberri, 2013[37]	No	38	Limited stage SCLC*, ECOG PS ≤2, platelets >100,000/mm³ and absence of active bleeding; age >18 years.	bemiparin (3,500 IU/day) *vs.* No bemiparin	12 months	26 weeks	Associated with hemoglobin decrease >2 g/dL, or transfusion >2 units, involved a critical site, contributed to death, or any clinically relevant bleeding requiring the stop of treatment	Premature interruption slow recruitment
Macbeth, 2015[38]	No	2202	SCLC or NSCLC* <6 weeks of diagnosis; age 18 years or older; ECOG-PS 0-3; able to self-administer LMWH or have it administered to them by a caregiver.	Deltaparin (5,000 IU/day) *vs.* No dalteparin	1 year	24 weeks	Associated with death, occurred at a critical site or resulted in transfusion >2 units, or hemoglobin decrease >2.0 g/dL	The trial did not reach the intended number of outcome events

SCLC: small cell lung cancer; IU: International Units; t.d.: twice daily; t.i.d.:.*ter in die*; CHT: chemotherapy; o.d.: once daily; ECOG: Eastern Cooperative Oncology Group; PS: Performance Status; BW: body weight; NSCLC: non-small cell lung cancer; FIGO: International Federation of Gynecology and Obstetrics; LMWH: low molecular weight heparin. * histologically confirmed; **0.4 mL if body weight <50 kg, 0.6 mL if body weight between 50 and 70 kg, and 0.8 mL if body weight > 70 kg. ° defined according to GCIG-CA125 response criteria.

Table 3. Results of sensitivity analyses.

Sensitivity analyses of efficacy	N of studies; n of patients	OR	95% CI	I²
Symptomatic VTE	12 studies; 7,578 patients	0.48	0.39 -0.60	0%
Fatal VTE	6 studies; 4,705 patients	0.52*	0.25 -1.08	0%
High-risk patients	5 studies**; 2,167 patients	0.48	0.34-0.68	0%
High-quality studies[10-12,19,21-22,24-25]	9 studies; 7,268 patients	0.47	0.36-0.60	15%
Sensitivity analyses of safety	**N of studies; n of patients**	**OR***	**95% CI**	**I squared**
Parenteral anticoagulants[19,21-22,24-25]	21 studies; 10,488 patients	1.27	0.93-1.73	0%
Oral anticoagulants[10-12]	3 studies; 1,526 patients	1.78	0.83-3.83	0%
High-quality studies[10-12,19,21-22,24-25]	9 studies; 7,268 patients	1.50	1.00-2.25	0%
VTE as primary outcome	15 studies; 8,258 patients	1.43	1.01-2.04	0%
Death as primary outcome	9 studies; 4,004 patients	1.16	0.70-1.92	0%

*after correction for zero cells. **This analysis included three studies in full and the subgroups of patients estimated to be at high risk of venous thromboembolism from two additional studies. OR: odds ratio; 95% CI: 95% confidence interval; VTE: venous thromboembolism.

for this specific indication were firstly the relatively low incidence of VTE in these patients. In our analysis, the incidence of VTE in studies in ambulatory cancer patients treated with chemotherapy varied from 2.3% to over 30% without anticoagulant prophylaxis. Such a huge variation is probably related to different study designs concerning populations (single primary site of cancer *vs.* multiple sites, high risk for VTE *vs.* all-comers), anticancer therapies (asparaginase *vs.* others, old *vs.* new regimens) and methods for VTE detection (screening *vs.* symptomatic events). In clinical practice, this heterogeneity is perceived by clinicians as uncertainty concerning the actual need for prophylaxis of VTE in each individual cancer patient. In fact, the risk of VTE correlates with the type of solid or hematologic cancer, the presence of metastatic disease, the use of chemotherapy or radiotherapy, surgery or hospitalization and, according to more recent research, to genetic cancer rearrangements (*ALK* and *ROS1* in lung cancer).[41-43] A clinical model was proposed to categorize ambulatory cancer patients treated with chemotherapy according to their risk of VTE.[44] A meta-analysis of 55 cohorts (34,555 ambulatory cancer patients) recently showed that although this model is able to identify categories of patients at different risk of VTE, most VTE events occur outside the high-risk group.[45] Further studies should be performed to improve the selection of ambulatory cancer patients who are candidates for anticoagulant prophylaxis. Personalized medicine and big data technology could have a role in this process.

The second concern about the use of prophylaxis in cancer patients treated with chemotherapy is the inconvenience of prolonged parenteral therapy. A not negligible number of patients in the context of the selected clinical studies discontinued anticoagulant prophylaxis for reasons other than thrombosis or bleeding (about 30%). Hence, it may be problematic for large numbers of patients to tolerate longer durations of prophylaxis. In this scenario, the availability of oral anticoagulants that can be used with no laboratory monitoring and with the potential for few drug-drug interactions could solve at least the issue of parenteral administration and make prophylaxis acceptable also for extended periods. Three randomized studies have assessed the efficacy and safety of apixaban (2 studies)[10-11] and rivaroxaban (1 study)[12] for the

prevention of VTE in cancer patients and provided promising results. In particular, our meta-analysis found similar risk reductions with parenteral or oral agents. Direct oral anticoagulants could make prophylaxis feasible for ambulatory cancer patients receiving chemotherapy as they will be more acceptable than parenteral agents for those at high risk of VTE.

An additional concern regards the risk-to-benefit ratio of anticoagulant prophylaxis. The pooled incidence of major bleeding was 2% in patients randomized to anticoagulant prophylaxis, with high variability across individual studies as shown by significant heterogeneity. Differences in study populations across individual studies could have had a major role as determinants of heterogeneity. No significant increase in the risk of major bleeding in patients randomized to receive anticoagulant prophylaxis, compared to the risk in controls, was found in this meta-analysis when all studies were pooled together. This finding is reassuring as cancer patients are known to have an increased risk of bleeding, mainly related to the primary site of the cancer, the need for invasive procedures and thrombocytopenia. However, the analysis on risk of major bleeding in high-quality studies and that in studies with VTE as the primary outcome showed a marginally significant increase in the risk of major bleeding by about 50%. Additional evidence on risk factors for major bleeding in ambulatory cancer patients receiving chemotherapy could help decision-making concerning the use of prophylaxis.

Fatal VTE was not significantly reduced by anticoagulant prophylaxis. This result should be considered taking into account the low rates of death deemed to be due to VTE in patients with advanced cancer. Indeed, previous studies failed to show an effect of heparin, given at either therapeutic or prophylactic doses, in improving survival in cancer patients. However, it should be taken into account that a diagnosis of new VTE in cancer patients may affect quality of life and lead to the interruption of anticancer treatment. In this view, preventing VTE can be a relevant clinical goal.

Among the sensitivity analyses, we included one on patients at 'high-risk' of VTE, which confirmed the efficacy of anticoagulant prophylaxis in this setting. The Khorana score was used to identify this population of
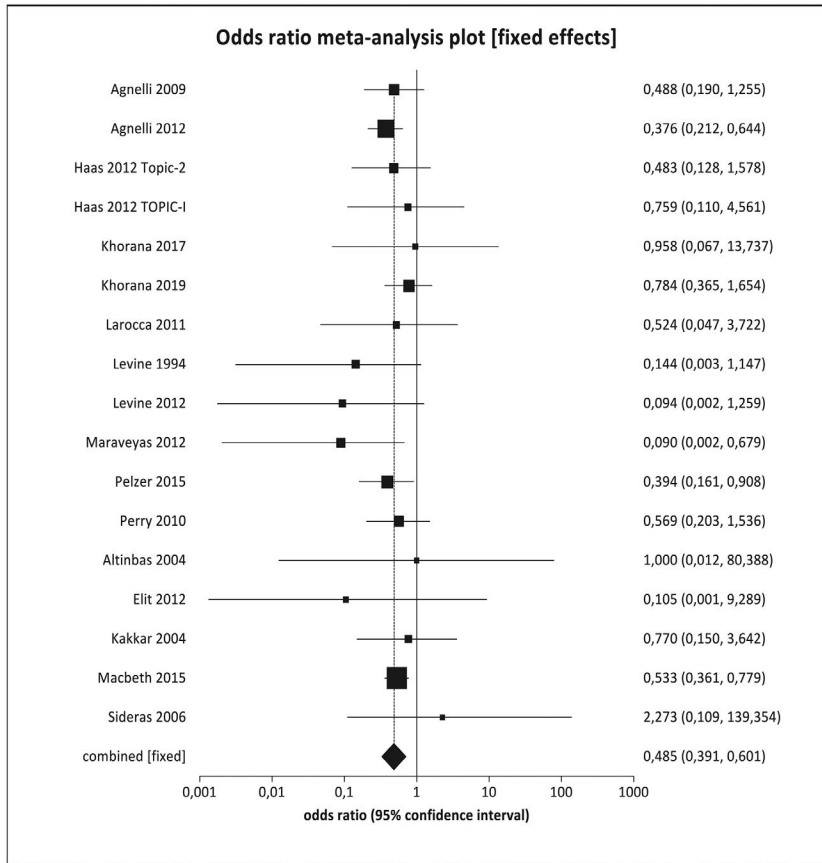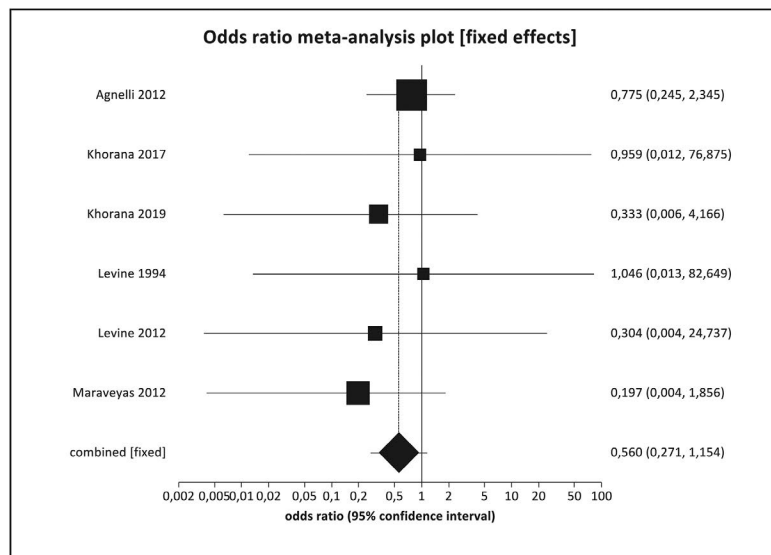
A

B

Figure 2. Efficacy of anticoagulant prophylaxis for the prevention of venous thromboembolism (VTE) in ambulatory cancer patients receiving chemotherapy in studies with VTE as the primary outcome. (A) Efficacy for the prevention of symptomatic VTE. (B) Efficacy for the prevention of fatal VTE.

patients.[44] Even though no consensus exists on the optimal strategy to identify ambulatory cancer patients at high risk of a first VTE,[45] the Khorana approach was followed in the two recent studies.[11,12] While the efficacy of anticoagulant prophylaxis was confirmed in this analysis, the incidence of VTE in the placebo arms in these two trials was 10%. Whether this incidence is high enough to recommend anticoagulant prophylaxis is controversial.

Our study has several limitations in addition to those intrinsic to a meta-analytic approach, which combines heterogeneous datasets. For example, the heterogeneity in the incidence of VTE was not resolved after excluding an outlier study in children receiving asparaginase[20] and was also related to recent studies that specifically included patients at high risk of VTE. The inclusion of screening-detected or incidental VTE in the primary outcome could be a further determinant of heterogeneity. It

should be considered that it has not been determined whether these events have different prognoses.[50] Our analysis cannot answer the issue of the duration of anticoagulant prophylaxis in cancer patients receiving chemotherapy. Thanks to new anticancer treatments, the life expectancy of patients with several types of cancer has increased dramatically. The duration of prophylaxis tested in the studies included in this meta-analysis ranged from a minimum of 4 weeks to a maximum of 6 months for studies having VTE as the primary outcome and to a maximum of 12 months in studies having death as the primary outcome. Whether longer-lasting prophylaxis could be of benefit and maintain the same safety profile remains undefined. Finally, further data are required on the efficacy and safety of anticoagulant prophylaxis in patients receiving newer anticancer therapies, such as immunotherapy or biologics.

Our study also has some strengths. This is a meta-analysis of randomized studies, with results consistent across different sensitivity analyses and no heterogeneity. Moreover, differently from previous meta-analyses, we limited our primary efficacy analysis to randomized clinical trials with VTE as the primary outcome. Even though high-quality trials with death as the primary outcome have been conducted in this setting, our choice was aimed at reducing heterogeneity related to the use of therapeutic regimens of anticoagulants, to the longer duration of anticoagulant treatment and to gaining a more
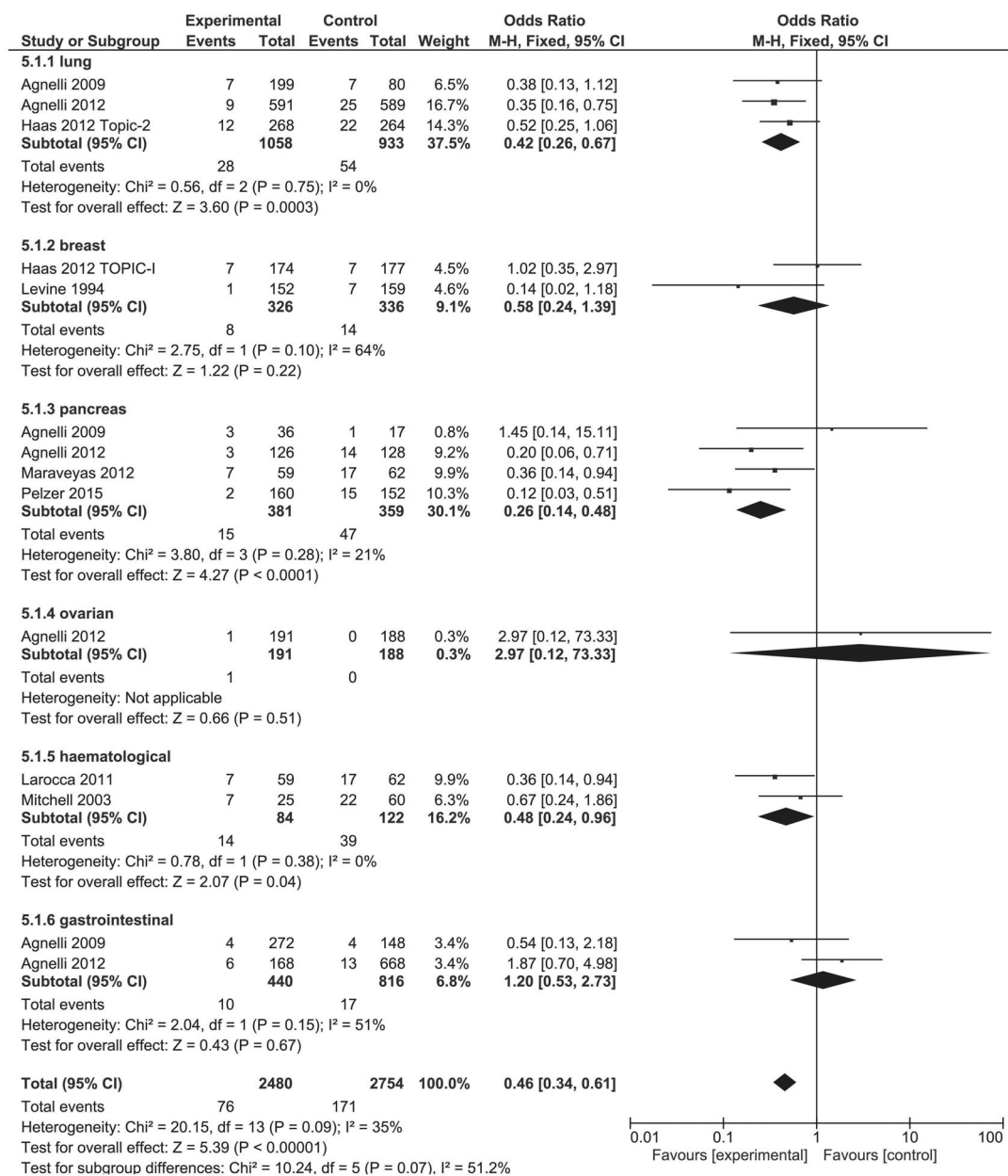

Figure 3. Efficacy of anticoagulant prophylaxis for the prevention of venous thromboembolism in ambulatory cancer patients receiving chemotherapy according to the primary site of cancer.
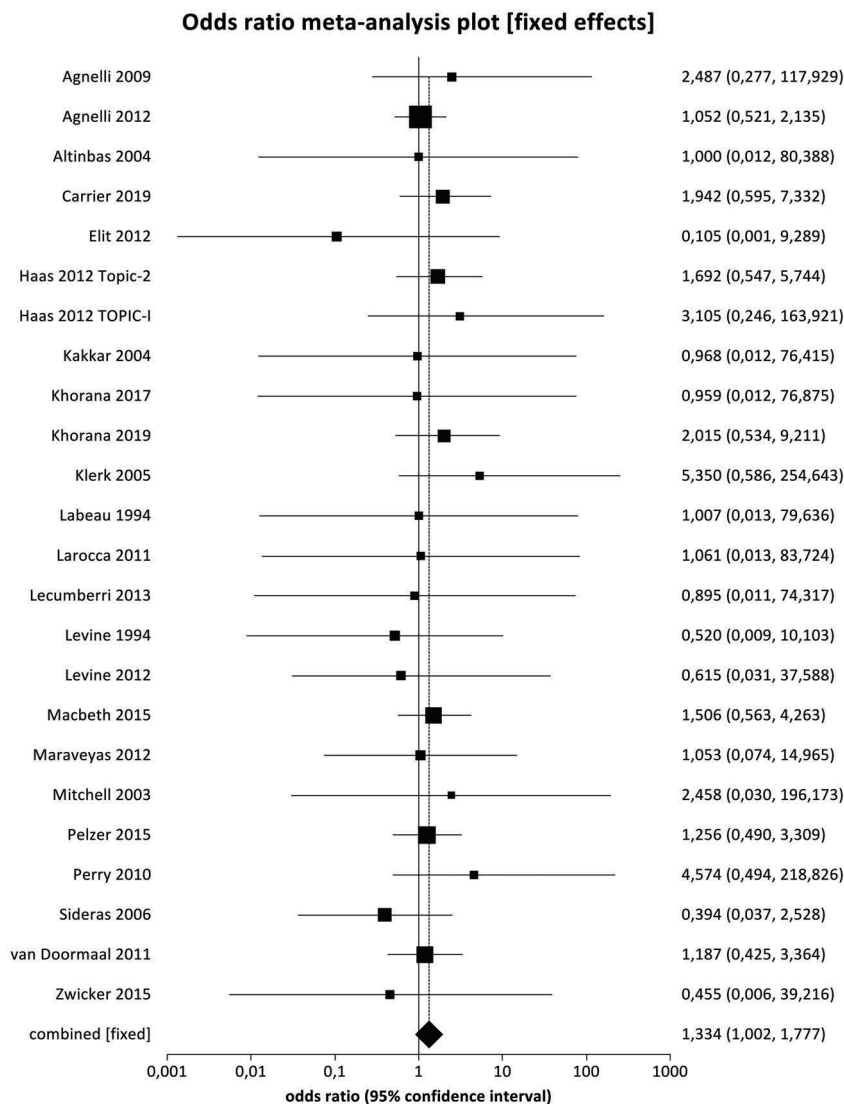
Odds ratio meta-analysis plot [fixed effects]

Study	Odds ratio (95% CI)
Agnelli 2009	2,487 (0,277, 117,929)
Agnelli 2012	1,052 (0,521, 2,135)
Altinbas 2004	1,000 (0,012, 80,388)
Carrier 2019	1,942 (0,595, 7,332)
Elit 2012	0,105 (0,001, 9,289)
Haas 2012 Topic-2	1,692 (0,547, 5,744)
Haas 2012 TOPIC-I	3,105 (0,246, 163,921)
Kakkar 2004	0,968 (0,012, 76,415)
Khorana 2017	0,959 (0,012, 76,875)
Khorana 2019	2,015 (0,534, 9,211)
Klerk 2005	5,350 (0,586, 254,643)
Labeau 1994	1,007 (0,013, 79,636)
Larocca 2011	1,061 (0,013, 83,724)
Lecumberri 2013	0,895 (0,011, 74,317)
Levine 1994	0,520 (0,009, 10,103)
Levine 2012	0,615 (0,031, 37,588)
Macbeth 2015	1,506 (0,563, 4,263)
Maraveyas 2012	1,053 (0,074, 14,965)
Mitchell 2003	2,458 (0,030, 196,173)
Pelzer 2015	1,256 (0,490, 3,309)
Perry 2010	4,574 (0,494, 218,826)
Sideras 2006	0,394 (0,037, 2,528)
van Doormaal 2011	1,187 (0,425, 3,364)
Zwicker 2015	0,455 (0,006, 39,216)
combined [fixed]	1,334 (1,002, 1,777)

odds ratio (95% confidence interval)

Figure 4. Effect of anticoagulant prophylaxis on the incidence of major bleeding in ambulatory cancer patients receiving chemotherapy.

accurate assessment of the incidence of VTE during follow-up. However, the pooled analysis of all the trials with VTE or death as the primary outcome confirmed the efficacy of anticoagulants without heterogeneity. Moreover, to remain on the safe side, the primary safety analysis of major bleeding in our study included all the trials and did not show any safety signal.

In conclusion, we found that anticoagulant prophylaxis is effective and acceptably safe in ambulatory cancer patients treated with chemotherapy. The selection of the most suitable candidates (patients at increased risk of VTE) for anticoagulant prophylaxis among ambulatory cancer patients treated with chemotherapy is a crucial issue and further studies are required to optimize the efficacy of this intervention.

References

1. Heit JA, Silverstein MD, Mohr DN, Petterson TM, O'Fallon WM, Melton LJ III. Risk factors for deep vein thrombosis and pulmonary embolism: a population-based case-control study. Arch Intern Med. 2000;160(6):809-815.
2. Blom JW, Doggen CJM, Osanto S, Rosendaal FR. Malignancies, prothrombotic mutations, and the risk of venous thrombosis. JAMA. 2005;293(6):715-722.
3. Puurunen MK, Gona PN, Larson MG, Murabito JM, Magnani JW, O'Donnell CJ. Epidemiology of venous thromboembolism in the Framingham Heart Study. Thromb Res. 2016;145:27-33.
4. Cohen AT, Katholing A, Rietbrock S, Bamber L, Martinez C. Epidemiology of first and recurrent venous thromboembolism in patients with active cancer. A population-based cohort study. Thromb Haemost. 2017;117(1):57-65.
5. Otten HM, Mathijssen J, ten Cate H, et al. Symptomatic venous thromboembolism in cancer patients treated with chemotherapy: an underestimated phenomenon. Arch Intern Med. 2004;164(2):190-194.
6. Khorana AA, Francis CW, Culakova E, Kuderer NM, Lyman GH. Thromboembolism is a leading cause of death in cancer patients receiving outpatient

chemotherapy. J Thromb Haemost. 2007;5 (3):632-634.

7. Di Nisio M, Porreca E, Candeloro M, De Tursi M, Russi I, Rutjes AW. Primary prophylaxis for venous thromboembolism in ambulatory cancer patients receiving chemotherapy. Cochrane Database Syst Rev. 2016;15(2): CD008500.

8. Farge D, Bounameaux H, Brenner B, et al. International clinical practice guidelines including guidance for direct oral anticoagulants in the treatment and prophylaxis of venous thromboembolism in patients with cancer. Lancet Oncol. 2016;17(10):e452-e466.

9. Lyman GH, Bohlke K, Falanga A. American Society of Clinical Oncology. Venous thromboembolism prophylaxis and treatment in patients with cancer: American Society of Clinical Oncology clinical practice guideline update. J Oncol Pract. 2015;11(3):e442-e444.

10. Levine MN, Gu C, Liebman HA, et al. A randomized phase II trial of apixaban for the prevention of thromboembolism in patients with metastatic cancer. J Thromb Haemost. 2012;10(5):807-814.

11. Carrier M, Abou-Nassar K, Mallick R, et al. Apixaban to prevent venous thromboembolism in patients with cancer. N Engl J Med. 2019;380(8):711-719.

12. Khorana AA, Soff GA, Kakkar AK, et al. Rivaroxaban for thromboprophylaxis in high-risk ambulatory patients with cancer. N Engl J Med. 2019;380(8):720-728.

13. Moher D, Liberati A, Tetzlaff J, Altman DG; PRISMA group. Preferred reporting items for systematic reviews and metaanalyses: the PRISMA statement. PloS Med. 2009;6(7): e1000097.

14. McGinn T, Wyer PC, Newman TB, Keitz S, Leipzig R, For GG; Evidence-based medicine teaching tips working group. Tips for learners of evidence based medicine: 3. Measures of observer variability (kappa statistic). CMAJ. 2004;171(11):1369-1373.

15. Jadad AR, Moore RA, Carroll D, et al. Assessing the quality of reports of randomized clinical trials: Is blinding necessary? Control Clin Trials. 1996;17(1):1-12.

16. Egger M, Smith GD, Altman DG, Chalmers I. Systematic Reviews in Health Care: Meta-Analysis in Context. 2nd ed. London, England. BMJ Books; 2001.

17. Higgins JP, Thompson SG. Quantifying heterogeneity in a meta-analysis. Stat Med. 2002;21(11):1539-1558.

18. Cochran WG. The combination of estimates from different experiments. Biometrics. 1954;10(1):101-129.

19. Levine M, Hirsh J, Gent M, et al. Double-blind randomised trial of a very-low-dose warfarin for prevention of thromboembolism in stage IV breast cancer. Lancet. 1994;343(8902):886-889.

20. Mitchell L, Andrew M, Hanna K, et al. Trend to efficacy and safety using antithrombin concentrate in prevention of thrombosis in children receiving l-asparaginase for acute

lymphoblastic leukemia. Results of the PAARKA study. Thromb Haemost. 2003;90(2):235-244.

21. Agnelli G, Gussoni G, Bianchini C, et al. Nadroparin for the prevention of thromboembolic events in ambulatory patients with metastatic or locally advanced solid cancer receiving chemotherapy: a randomised, placebo-controlled, double-blind study. Lancet Oncol. 2009;10(10):943-949.

22. Perry JR, Julian JA, Laperriere NJ, et al. PRODIGE: a randomized placebo-controlled trial of dalteparin low-molecular-weight heparin thromboprophylaxis in patients with newly diagnosed malignant glioma. J Thromb Haemost. 2010;8(9):1959-1965.

23. Larocca A, Cavallo F, Bringhen S, et al. Aspirin or enoxaparin thromboprophylaxis for patients with newly diagnosed multiple myeloma treated with lenalidomide. Blood. 2012;119(4):933-939.

24. Haas SK, Freund M, Heigener D, et al. Low-molecular-weight heparin versus placebo for the prevention of venous thromboembolism in metastatic breast cancer or stage III/IV lung cancer. Clin Appl Thromb Hemost. 2012;18(2):159-165.

25. Agnelli G, George DJ, Kakkar AK, et al. Semuloparin for thromboprophylaxis in patients receiving chemotherapy for cancer. N Engl J Med. 2012;366(7):601-609.

26. Maraveyas A, Waters J, Roy R, et al. Gemcitabine versus gemcitabine plus dalteparin thromboprophylaxis in pancreatic cancer. Eur J Cancer. 2012;48(9):1283-1292.

27. Pelzer U, Opitz B, Deutschinoff G, et al. Efficacy of prophylactic low-molecular weight heparin for ambulatory patients with advanced pancreatic cancer: outcomes from the CONKO-004 trial. J Clin Oncol. 2015;33(18):2028-2034.

28. Zwicker JI, Liebman HA, Bauer KA, et al. Prediction and prevention of thromboembolic events with enoxaparin in cancer patients with elevated tissue factor-bearing microparticles: a randomized-controlled phase II trial (the Microtec study). Br J Haematol. 2013;160(4):530-537.

29. Khorana AA, Francis CW, Kuderer NM, et al. Dalteparin thromboprophylaxis in cancer patients at high risk for venous thromboembolism: a randomized trial. Thromb Res. 2017;151:89-95.

30. Lebeau B, Chastang C, Brechot JM, et al. Subcutaneous heparin treatment increases survival in small cell lung cancer. "Petites Cellules" Group. Cancer. 1994;74(1):38-45.

31. Kakkar AK, Levine MN, Kadziola Z, et al. Low molecular weight heparin, therapy with dalteparin, and survival in advanced cancer: the fragmin advanced malignancy outcome study (FAMOUS). J Clin Oncol. 2004;22(10):1944-1948.

32. Altinbas M, Coskun HS, Er O, et al. A randomized clinical trial of combination chemotherapy with and without low-molecular-weight heparin in small cell lung can-

cer. J Thromb Haemost. 2004;2(8):1266-1271.

33. Klerk CP, Smorenburg SM, Otten HM, et al. The effect of low molecular weight heparin on survival in patients with advanced malignancy. J Clin Oncol. 2005;23(10):2130-2135.

34. Sideras K, Schaefer PL, Okuno SH, et al. Low-molecular-weight heparin in patients with advanced cancer: a phase 3 clinical trial. Mayo Clin Proc. 2006;81(6):758-767.

35. van Doormaal FF, Di Nisio M, Otten HM, Richel DJ, Prins M, Buller HR. Randomized trial of the effect of the low molecular weight heparin nadroparin on survival in patients with cancer. J Clin Oncol. 2011;29(15):2071-2076.

36. Elit LM, Lee AY, Parpia S, et al. Dalteparin low molecular weight heparin (LMWH) in ovarian cancer: a phase II randomized study. Thromb Res. 2012;130(6):894-900.

37. Lecumberri R, López Vivanco G, Font A, et al. Adjuvant therapy with bemiparin in patients with limited-stage small cell lung cancer: results from the ABEL study. Thromb Res. 2013;132(6):666-670.

38. Macbeth F, Noble S, Evans J, et al. Randomized phase III trial of standard therapy plus low molecular weight heparin in patients with lung cancer: FRAGMATIC trial. J Clin Oncol. 2016;34 (5):488-494.

39. Ansell J, Hirsh J, Dalen J, et al. Managing oral anticoagulant therapy. Chest. 2001;119 (1Suppl):22S-38S.

40. Schünemann HJ, Cushman M, Burnett AE, et al. American Society of Hematology 2018 guidelines for management of venous thromboembolism: prophylaxis for hospitalized and nonhospitalized medical patients. Blood Adv. 2018;2(22):3198-3225.

41. Verso M, Chiari R, Mosca S, et al. Incidence of CT-scan-detected pulmonary embolism in patients with oncogene-addicted, advanced lung adenocarcinoma. Thromb Res. 2015;136(5):924-927.

42. Zugazagoitia J, Biosca M, Oliveira J, et al. Incidence, predictors and prognostic significance of thromboembolic disease in patients with advanced ALK-rearranged non-small cell lung cancer. Eur Respir J. 2018;51(5).

43. Ng TL, Smith DE, Mushtaq R, et al. ROS1 gene rearrangements are associated with an elevated risk of peridiagnosis thromboembolic events. J Thorac Oncol. 2019;14(4): 596-605

44. Khorana AA, Kuderer NM, Culakova E, Lyman GH, Francis CW. Development and validation of a predictive model for chemotherapy-associated thrombosis. Blood. 2008;111(10):4902-4907.

45. Mulder FI, Candeloro M, Kamphuisen PW, et al. The Khorana score for prediction of venous thromboembolism in cancer patients: a systematic review and meta-analysis. Haematologica. 2019;104(6):1277-1287.

50. Khorana AA, O'Connell C, Agnelli G, Liebman HA, Lee AY. Incidental venous thromboembolism in oncology patients. J Thromb Haemost. 2012;10(12):2602-2604.

Radiation exposure from computerized tomography and risk of childhood leukemia: Finnish register-based case-control study of childhood leukemia (FRECCLE)

Atte Nikkilä,[1] Jani Raitanen,[2,3] Olli Lohi[1,4] and Anssi Auvinen[2,3,5]

[1]Faculty of Medicine and Biosciences, University of Tampere; [2]Faculty of Social Sciences, University of Tampere; [3]UKK Institute for Health Promotion Research, Tampere; [4]Tampere Center for Child Health Research, University of Tampere and Tampere University Hospital and [5]STUK – Radiation and Nuclear Safety Authority, Helsinki, Finland

©2020 Ferrata Storti Foundation

With reference to the article Nikkilä A, Raitanen J, Lohi O, Auvinen A. Radiation exposure from computerized tomography and risk of childhood leukemia: Finnish register-based case-control study of childhood leukemia (FRECCLE). Haematologica. 2018;103(11):1873-1880, it has come to the authors' attention that the reported total number of computed tomography (CT) scans in our article was incorrect. The reported numbers were, in fact, the expected numbers prior to the CT scan collection from hospitals. Fortunately, this does not affect the number of CT scans to the study subjects and, thus, all results regarding childhood leukemia remain unchanged.

The errors and their corrections are listed below.

An incorrect sentence appeared in the November 2018 issue, page 1876.

Data on a total of 80,783 pediatric CT scans were obtained and of those, 49 CT scans were performed on the study subjects, excluding the 2-year latency period (Table 1). Half (n=25) were head scans, and 19 were lung scans. Of the CT scans, 36 were performed on 15 (1.4%) cases and 13 scans on 10 (0.3%) controls.

The corrected version of the sentence is published below.

Data on a total of 72,673 pediatric CT scans were obtained and of those, 49 CT scans were performed on the study subjects, excluding the 2-year latency period (Table 1). Half (n=25) were head scans, and 19 were lung scans. Of the CT scans, 36 were performed on 15 (1.4%) cases and 13 scans on 10 (0.3%) controls.

An incorrect version of Table 1 appaered in the November 2018 issue, page 1875.
The corrected version of Table 1 is published below.

Table 1. The collection and availability of electronically stored computed tomography scans.

Hospital	City	Data availability	Number of CT scans
Helsinki University Hospital	Helsinki	1990–2011	28,459
Tampere University Hospital	Tampere	1978–2011	17,077
Oulu University Hospital	Oulu	1993–2011	8,722
Turku University Hospital	Turku	1996–2011	5,806
Kuopio University Hospital	Kuopio	1996–2011	4,115
Central Finland Central Hospital	Jyväskylä	2002–2011	1,635
Satakunta Central Hospital	Pori	1995–2011	2,032
Seinäjoki Central Hospital	Seinäjoki	1999–2011	1,347
Päijänne Tavastia Central Hospital	Lahti	2000–2011	447
North Karelia Central Hospital	Joensuu	1993–2011	3,033
TOTAL			**72,673**

All Finnish university hospitals are listed first and separated slightly are the five chosen central hospitals. The reported numbers represent the data obtained before exclusions or harmonization.

An incorrect version of Figure 2 appeared in the November 2018 issue, page 1875.
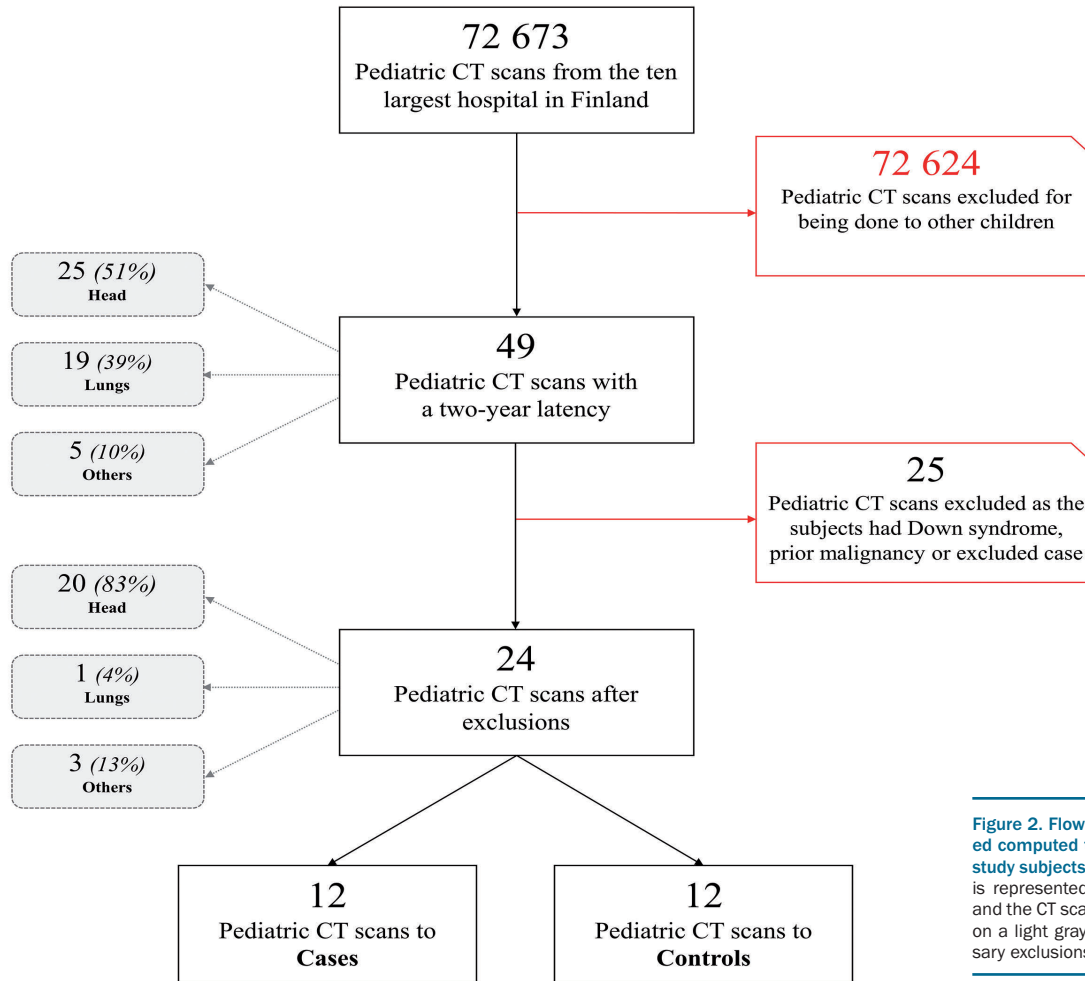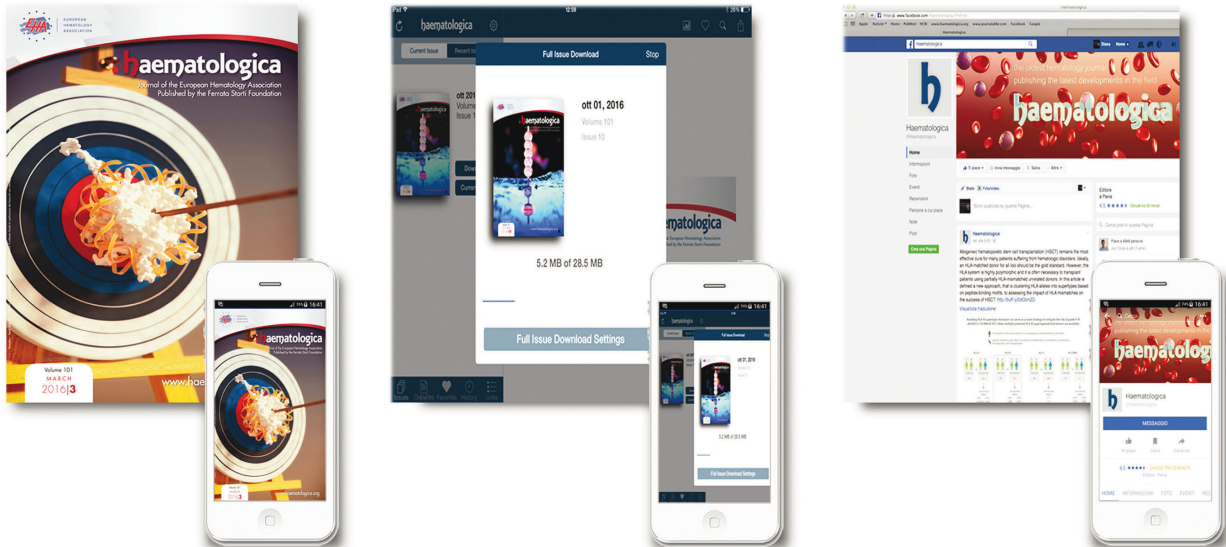*The corrected version of Figure 2 is published below.*

Figure 2. Flow chart linking the collected computed tomography scans to the study subjects The flow of the CT scans is represented on a white background and the CT scans to different body parts on a light gray background. The necessary exclusions are shown in red boxes.

RESEARCH, READ & CONNECT

We reach more than
6 hundred thousand readers each year

The first Hematology Journal in Europe

Impressions YTD

9,621,645

Digital Readers
4,431

Total Audience
554,484

Worldwide rank
7 th

Impact factor
7.570

Total citations
16,255

haematologica